

Special Issue Reprint

---

# Natural Polyphenols in Human Health

Volume II

---

Edited by  
Nour Eddine Es-Safi

[mdpi.com/journal/molecules](https://mdpi.com/journal/molecules)

# **Natural Polyphenols in Human Health-Volume II**



# Natural Polyphenols in Human Health-Volume II

Editor

**Nour Eddine Es-Safi**



Basel • Beijing • Wuhan • Barcelona • Belgrade • Novi Sad • Cluj • Manchester

*Editor*

Nour Eddine Es-Safi  
Mohammed V University in Rabat  
Rabat, Morocco

*Editorial Office*

MDPI  
St. Alban-Anlage 66  
4052 Basel, Switzerland

This is a reprint of articles from the Special Issue published online in the open access journal *Molecules* (ISSN 1420-3049) (available at: [https://www.mdpi.com/journal/molecules/special\\_issues/NPHH](https://www.mdpi.com/journal/molecules/special_issues/NPHH)).

For citation purposes, cite each article independently as indicated on the article page online and as indicated below:

Lastname, A.A.; Lastname, B.B. Article Title. <i>Journal Name</i> <b>Year</b> , <i>Volume Number</i> , Page Range.
--

**Volume II**

**ISBN 978-3-0365-9076-9 (Hbk)**

**ISBN 978-3-0365-9077-6 (PDF)**

**[doi.org/10.3390/books978-3-0365-9077-6](https://doi.org/10.3390/books978-3-0365-9077-6)**

**Set**

**ISBN 978-3-0365-9072-1 (Hbk)**

**ISBN 978-3-0365-9073-8 (PDF)**

# Contents

<b>Marwa M. Saeed, Álvaro Fernández-Ochoa, Fatema R. Saber, Rabab H. Sayed, María de la Luz Cádiz-Gurrea, Amira K. Elmotayam, et al.</b> The Potential Neuroprotective Effect of <i>Cyperus esculentus</i> L. Extract in Scopolamine-Induced Cognitive Impairment in Rats: Extensive Biological and Metabolomics Approaches Reprinted from: <i>Molecules</i> <b>2022</b> , <i>27</i> , 7118, doi:10.3390/molecules27207118 . . . . .	1
<b>Muhammad Ajmal Shah, Ayesha Hamid, Hafiza Ishmal Faheem, Azhar Rasul, Tourki A. S. Baokbah, Muhammad Haris, et al.</b> Uncovering the Anticancer Potential of Polydatin: A Mechanistic Insight Reprinted from: <i>Molecules</i> <b>2022</b> , <i>27</i> , 7175, doi:10.3390/molecules27217175 . . . . .	27
<b>Sang Gu Kang, Gi Baek Lee, Ramachandran Vinayagam, Geum Sook Do, Se Yong Oh, Su Jin Yang, et al.</b> Anti-Inflammatory, Antioxidative, and Nitric Oxide-Scavenging Activities of a Quercetin Nanosuspension with Polyethylene Glycol in LPS-Induced RAW 264.7 Macrophages Reprinted from: <i>Molecules</i> <b>2022</b> , <i>27</i> , 7432, doi:10.3390/molecules27217432 . . . . .	49
<b>Virginia D. Dimaki, Konstantina Zeliou, Fotini Nakka, Michaela Stavreli, Ioannis Bakratsas, Ligeri Papaioannou, et al.</b> Characterization of <i>Sideritis clandestina</i> subsp. <i>peloponnesiaca</i> Polar Glycosides and Phytochemical Comparison to Other Mountain Tea Populations Reprinted from: <i>Molecules</i> <b>2022</b> , <i>27</i> , 7613, doi:10.3390/molecules27217613 . . . . .	71
<b>Hardeep Singh Tuli, Ajay Kumar, Seema Ramniwas, Renuka Coudhary, Diwakar Aggarwal, Manoj Kumar, et al.</b> Ferulic Acid: A Natural Phenol That Inhibits Neoplastic Events through Modulation of Oncogenic Signaling Reprinted from: <i>Molecules</i> <b>2022</b> , <i>27</i> , 7653, doi:10.3390/molecules27217653 . . . . .	91
<b>Graciliana Lopes, Elisabete Gomes, Mariana Barbosa, João Bernardo and Patrícia Valentão</b> Camel Grass Phenolic Compounds: Targeting Inflammation and Neurologically Related Conditions Reprinted from: <i>Molecules</i> <b>2022</b> , <i>27</i> , 7707, doi:10.3390/molecules27227707 . . . . .	109
<b>Mang Sun, Ya Deng, Xining Cao, Lu Xiao, Qian Ding, Fuqing Luo, et al.</b> Effects of Natural Polyphenols on Skin and Hair Health: A Review Reprinted from: <i>Molecules</i> <b>2022</b> , <i>27</i> , 7832, doi:10.3390/molecules27227832 . . . . .	125
<b>Xiaolin Bai, Wenqin Fan, Yingjie Luo, Yipei Liu, Yongmei Zhang and Xun Liao</b> Fast Screening of Protein Tyrosine Phosphatase 1B Inhibitor from <i>Salvia miltiorrhiza</i> Bge by Cell Display-Based Ligand Fishing Reprinted from: <i>Molecules</i> <b>2022</b> , <i>27</i> , 7896, doi:10.3390/molecules27227896 . . . . .	139
<b>Francesco Limongelli, Pasquale Crupi, Maria Lisa Clodoveo, Filomena Corbo and Marilena Muraglia</b> Overview of the Polyphenols in Salicornia: From Recovery to Health-Promoting Effect Reprinted from: <i>Molecules</i> <b>2022</b> , <i>27</i> , 7954, doi:10.3390/molecules27227954 . . . . .	151
<b>Katalin Szabo, Laura Mitrea, Lavinia Florina Călinoiu, Bernadette-Emőke Teleky, Gheorghe Adrian Martău, Diana Plamada, et al.</b> Natural Polyphenol Recovery from Apple-, Cereal-, and Tomato-Processing By-Products and Related Health-Promoting Properties Reprinted from: <i>Molecules</i> <b>2022</b> , <i>27</i> , 7977, doi:10.3390/molecules27227977 . . . . .	171

<b>Sally El Kantar, Hiba N. Rajha, André El Khoury, Mohamed Koubaa, Simon Nachef, Espérance Debs, et al.</b> Phenolic Compounds Recovery from Blood Orange Peels Using a Novel Green Infrared Technology <i>Ired-Irrad</i> <sup>®</sup> , and Their Effect on the Inhibition of <i>Aspergillus flavus</i> Proliferation and Aflatoxin B1 Production Reprinted from: <i>Molecules</i> <b>2022</b> , <i>27</i> , 8061, doi:10.3390/molecules27228061 . . . . .	193
<b>Marisol Villalva, Laura Jaime, María de las Nieves Siles-Sánchez and Susana Santoyo</b> Bioavailability Assessment of Yarrow Phenolic Compounds Using an In Vitro Digestion/Caco-2 Cell Model: Anti-Inflammatory Activity of Basolateral Fraction Reprinted from: <i>Molecules</i> <b>2022</b> , <i>27</i> , 8254, doi:10.3390/molecules27238254 . . . . .	207
<b>Masakatsu Fukuda, Yudai Ogasawara, Hiroyasu Hayashi, Katsuyuki Inoue and Hideaki Sakashita</b> Resveratrol Inhibits Proliferation and Induces Autophagy by Blocking SREBP1 Expression in Oral Cancer Cells Reprinted from: <i>Molecules</i> <b>2022</b> , <i>27</i> , 8250, doi:10.3390/molecules27238250 . . . . .	221
<b>Sara Bautista-Expósito, Albert Vandenberg, Montserrat Dueñas, Elena Peñas, Juana Frias and Cristina Martínez-Villaluenga</b> Selection of Enzymatic Treatments for Upcycling Lentil Hulls into Ingredients Rich in Oligosaccharides and Free Phenolics Reprinted from: <i>Molecules</i> <b>2022</b> , <i>27</i> , 8458, doi:10.3390/molecules27238458 . . . . .	241
<b>Hend Okasha, Tarek Aboushousha, Manuel A. Coimbra, Susana M. Cardoso and Mosad A. Ghareeb</b> Metabolite Profiling of <i>Alocasia gigantea</i> Leaf Extract and Its Potential Anticancer Effect through Autophagy in Hepatocellular Carcinoma Reprinted from: <i>Molecules</i> <b>2022</b> , <i>27</i> , 8504, doi:10.3390/molecules27238504 . . . . .	259
<b>Andrea Ianni, Pierdomenico Ruggeri, Pierangelo Bellio, Francesco Martino, Giuseppe Celenza, Giuseppe Martino and Nicola Franceschini</b> Salvianolic Acid B Strikes Back: New Evidence in the Modulation of Expression and Activity of Matrix Metalloproteinase 9 in MDA-MB-231 Human Breast Cancer Cells Reprinted from: <i>Molecules</i> <b>2022</b> , <i>27</i> , 8514, doi:10.3390/molecules27238514 . . . . .	273
<b>Irene Dini and Lucia Grumetto</b> Recent Advances in Natural Polyphenol Research Reprinted from: <i>Molecules</i> <b>2022</b> , <i>27</i> , 8777, doi:10.3390/molecules27248777 . . . . .	287
<b>Yong-Kang Wang, Si-Yi Hu, Feng-Yi Xiao, Zhan-Bo Dong, Jian-Hui Ye, Xin-Qiang Zheng, et al.</b> Dihydrochalcones in Sweet Tea: Biosynthesis, Distribution and Neuroprotection Function Reprinted from: <i>Molecules</i> <b>2022</b> , <i>27</i> , 8794, doi:10.3390/molecules27248794 . . . . .	309
<b>Juciane Prois Fortes, Fernanda Wouters Franco, Julia Baranzelli, Gustavo Andrade Ugalde, Cristiano Augusto Ballus, Eliseu Rodrigues, et al.</b> Enhancement of the Functional Properties of Mead Aged with Oak ( <i>Quercus</i> ) Chips at Different Toasting Levels Reprinted from: <i>Molecules</i> <b>2023</b> , <i>28</i> , 56, doi:10.3390/molecules28010056 . . . . .	323
<b>Barbara Muñoz-Palazon, Susanna Gorrasi, Aurora Rosa-Masegosa, Marcella Pasqualetti, Martina Braconcini and Massimiliano Fenice</b> Treatment of High-Polyphenol-Content Waters Using Biotechnological Approaches: The Latest Update Reprinted from: <i>Molecules</i> <b>2023</b> , <i>28</i> , 314, doi:10.3390/molecules28010314 . . . . .	335

<b>Maria Stasińska-Jakubas, Barbara Hawrylak-Nowak, Magdalena Wójciak and Sławomir Dresler</b> Comparative Effects of Two Forms of Chitosan on Selected Phytochemical Properties of <i>Plectranthus amboinicus</i> (Lour.) Reprinted from: <i>Molecules</i> <b>2023</b> , <i>28</i> , 376, doi:10.3390/molecules28010376 . . . . .	357
<b>Donatella Aiello, Marcella Barbera, David Bongiorno, Matteo Cammarata, Valentina Censi, Serena Indelicato, et al.</b> Edible Insects an Alternative Nutritional Source of Bioactive Compounds: A Review Reprinted from: <i>Molecules</i> <b>2023</b> , <i>28</i> , 699, doi:10.3390/molecules28020699 . . . . .	373
<b>Julia Baranzelli, Sabrina Somacal, Camila Sant'Anna Monteiro, Renius de Oliveira Mello, Eliseu Rodrigues, Osmar Damian Prestes, et al.</b> Grain Germination Changes the Profile of Phenolic Compounds and Benzoxazinoids in Wheat: A Study on Hard and Soft Cultivars Reprinted from: <i>Molecules</i> <b>2023</b> , <i>28</i> , 721, doi:10.3390/molecules28020721 . . . . .	389
<b>Volkan Aylanc, Samar Larbi, Ricardo Calhelha, Lillian Barros, Feriel Rezouga, María Shantal Rodríguez-Flores, et al.</b> Evaluation of Antioxidant and Anticancer Activity of Mono- and Polyfloral Moroccan Bee Pollen by Characterizing Phenolic and Volatile Compounds Reprinted from: <i>Molecules</i> <b>2023</b> , <i>28</i> , 835, doi:10.3390/molecules28020835 . . . . .	409
<b>Maria Assunta Crescenzi, Gilda D'Urso, Sonia Piacente and Paola Montoro</b> A Comparative UHPLC-Q-Trap-MS/MS-Based Metabolomics Analysis to Distinguish <i>Foeniculum vulgare</i> Cultivars' Antioxidant Extracts Reprinted from: <i>Molecules</i> <b>2023</b> , <i>28</i> , 900, doi:10.3390/molecules28020900 . . . . .	429
<b>El-Sayed Khafagy, Gamal A. Soliman, Ahmad Abdul-Wahhab Shahba, Mohammed F. Aldawsari, Khalid M. Alharthy, Maged S. Abdel-Kader and Hala H. Zaatout</b> Brain Targeting by Intranasal Drug Delivery: Effect of Different Formulations of the Biflavone "Cupressuflavone" from <i>Juniperus sabina</i> L. on the Motor Activity of Rats Reprinted from: <i>Molecules</i> <b>2023</b> , <i>28</i> , 1354, doi:10.3390/molecules28031354 . . . . .	443
<b>Afroditi Michalaki, Haralabos C. Karantonis, Anastasia S. Kritikou, Nikolaos S. Thomaidis and Marilena E. Dasenaki</b> Ultrasound-Assisted Extraction of Total Phenolic Compounds and Antioxidant Activity Evaluation from Oregano ( <i>Origanum vulgare</i> ssp. <i>hirtum</i> ) Using Response Surface Methodology and Identification of Specific Phenolic Compounds with HPLC-PDA and Q-TOF-MS/MS Reprinted from: <i>Molecules</i> <b>2023</b> , <i>28</i> , 2033, doi:10.3390/molecules28052033 . . . . .	459
<b>Claudio Alimenti, Mariacaterina Lianza, Fabiana Antognoni, Laura Giusti, Onelia Bistoni, Luigi Liotta, et al.</b> Characterization and Biological Activities of In Vitro Digested Olive Pomace Polyphenols Evaluated on Ex Vivo Human Immune Blood Cells Reprinted from: <i>Molecules</i> <b>2023</b> , <i>28</i> , 2122, doi:10.3390/molecules28052122 . . . . .	477
<b>Vanessa B. Paula, Letícia M. Estevinho, Susana M. Cardoso and Luís G. Dias</b> Comparative Methods to Evaluate the Antioxidant Capacity of Propolis: An Attempt to Explain the Differences Reprinted from: <i>Molecules</i> <b>2023</b> , <i>28</i> , 4847, doi:10.3390/molecules28124847 . . . . .	499





Article

# The Potential Neuroprotective Effect of *Cyperus esculentus* L. Extract in Scopolamine-Induced Cognitive Impairment in Rats: Extensive Biological and Metabolomics Approaches

Marwa M. Saeed <sup>1,†</sup>, Álvaro Fernández-Ochoa <sup>2,\*</sup>, Fatema R. Saber <sup>3</sup>, Rabab H. Sayed <sup>4,\*</sup>,  
María de la Luz Cádiz-Gurrea <sup>2,\*</sup>, Amira K. Elmotayam <sup>3</sup>, Francisco Javier Leyva-Jiménez <sup>5,6</sup>,  
Antonio Segura-Carretero <sup>2,‡</sup> and Rania I. Nadeem <sup>7,‡</sup>

<sup>1</sup> Lecturer of Pharmacology and Toxicology, Faculty of Pharmacy, Heliopolis University, Cairo 11785, Egypt

<sup>2</sup> Department of Analytical Chemistry, Faculty of Sciences, University of Granada, Avda Fuentenueva s/n, 18071 Granada, Spain

<sup>3</sup> Pharmacognosy Department, Faculty of Pharmacy, Cairo University, Cairo 11562, Egypt

<sup>4</sup> Department of Pharmacology and Toxicology, Faculty of Pharmacy, Cairo University, Cairo 11562, Egypt

<sup>5</sup> Department of Analytical Chemistry and Food Science and Technology, University of Castilla-La Mancha, Ronda de Calatrava, 7, 13071 Ciudad Real, Spain

<sup>6</sup> Regional Institute for Applied Scientific Research (IRICA), Area of Food Science, University of Castilla-La Mancha, Avenida Camilo Jose Cela, 10, 13071 Ciudad Real, Spain

<sup>7</sup> Department of Pharmacology and Toxicology, Faculty of Pharmacy, Heliopolis University, Cairo 11785, Egypt

\* Correspondence: alvaroferochoa@ugr.es (Á.F.-O.); rabab.sayed@pharma.cu.edu.eg (R.H.S.);

mluzcadiz@ugr.es (M.d.L.C.-G.); Tel.: +0020-1001414473 (R.H.S.)

† Those authors contributed equally to the work and are both considered the first coauthors.

‡ Those authors contributed equally to the work and are both considered co-senior authors.

**Citation:** Saeed, M.M.;

Fernández-Ochoa, Á.; Saber, F.R.;

Sayed, R.H.; Cádiz-Gurrea, M.d.L.L.;

Elmotayam, A.K.; Leyva-Jiménez, F.J.;

Segura-Carretero, A.; Nadeem, R.I.

The Potential Neuroprotective Effect

of *Cyperus esculentus* L. Extract in

Scopolamine-Induced Cognitive

Impairment in Rats: Extensive

Biological and Metabolomics

Approaches. *Molecules* **2022**, *27*, 7118.

[https://doi.org/10.3390/](https://doi.org/10.3390/molecules27207118)

[molecules27207118](https://doi.org/10.3390/molecules27207118)

Academic Editor: Nour

Eddine Es-Safi

Received: 26 September 2022

Accepted: 18 October 2022

Published: 21 October 2022

**Publisher's Note:** MDPI stays neutral with regard to jurisdictional claims in published maps and institutional affiliations.



**Copyright:** © 2022 by the authors.

Licensee MDPI, Basel, Switzerland.

This article is an open access article

distributed under the terms and

conditions of the Creative Commons

Attribution (CC BY) license ([https://](https://creativecommons.org/licenses/by/4.0/)

[creativecommons.org/licenses/by/](https://creativecommons.org/licenses/by/4.0/)

[4.0/](https://creativecommons.org/licenses/by/4.0/)).

**Abstract:** The aim of the present study is to investigate the phytochemical composition of tiger nut (TN) (*Cyperus esculentus* L.) and its neuroprotective potential in scopolamine (Scop)-induced cognitive impairment in rats. The UHPLC-ESI-QTOF-MS analysis enabled the putative annotation of 88 metabolites, such as saccharides, amino acids, organic acids, fatty acids, phenolic compounds and flavonoids. Treatment with TN extract restored Scop-induced learning and memory impairments. In parallel, TN extract succeeded in lowering amyloid beta,  $\beta$ -secretase protein expression and acetylcholine esterase (AChE) activity in the hippocampus of rats. TN extract decreased malondialdehyde levels, restored antioxidant levels and reduced proinflammatory cytokines as well as the Bax/Bcl2 ratio. Histopathological analysis demonstrated marked neuroprotection in TN-treated groups. In conclusion, the present study reveals that TN extract attenuates Scop-induced memory impairments by diminishing amyloid beta aggregates, as well as its anti-inflammatory, antioxidant, anti-apoptotic and anti-AChE activities.

**Keywords:** *Cyperus esculentus*; tiger nut; metabolomics; UHPLC-ESI-QTOF-MS/MS; foodomics; scopolamine; memory impairments

## 1. Introduction

Alzheimer's disease (AD) is a progressive neurologic disorder characterized by the presence of senile amyloid-beta ( $A\beta$ ) plaques and neurofibrillary tangles leading to neurodegeneration. It is the most prevalent cause of dementia, accounting for about 60% of cases [1]. It is anticipated that the global burden of AD will rise to reach 106.8 million cases by 2050 [2]. AD patients suffer from a progressive loss of cognitive abilities resulting in memory and learning dysfunctions that are mainly correlated with declines in the cholinergic neurotransmission system [3]. Several factors have been implicated in the pathophysiology of AD including genetic mutations,  $A\beta$  accumulation, hyper-phosphorylation of tau protein, oxidative stress, mitochondrial dysfunction, inflammation and apoptosis. These factors likely act synergistically through complex interactions to promote neurodegeneration [4,5].

Scopolamine (Scop), a muscarinic cholinergic receptor antagonist, has been generally approved to induce memory deficits in experimental animals and to search for and evaluate anti-dementia drugs. Following Scop administration, the cholinergic neurotransmission is blocked and animals exhibit diminished cognitive performance [6]. Additionally, it has been reported that a Scop injection resulted in cognitive impairment together with changes in oxidative stress in the rat brain [7]. Recently, Tang et al., (2019) concluded that Scop is a useful pharmacological model simulating the pathological cellular alterations seen in AD patients and other AD models such as impaired antioxidative defense system, raised oxidative stress, mitochondrial dysfunction, apoptosis and neuroinflammation [3].

Until now, there has been no effective treatment for AD and currently available drugs exhibit minimal effect and poor control on the disease, targeting its late aspects with numerous side effects and fatal complications. These drugs slow down the progression of the disease and relieve the symptoms but at the same time fail to reach a definite cure [8]. Nowadays, there is a worldwide focus on the prospective of using natural herbs as neuroprotective agents.

Tiger nut (TN) (*Cyperus esculentus* L.) is a perennial plant belonging to the family Cyperaceae. The edible part of the plant is the spherical rhizome from the base of the tuber [9]. TN is known by other names such as Zulu nut, chufa (in Spanish), earth chestnut, yellow nutsedge, rush nut as well as ground almond [10]. It is consumed widely in western and eastern Africa and southern Europe, particularly Spain [11]. *Cyperus esculentus* L. is known in Egypt as “habb el ‘aziz” and it is one of the most ancient Egyptian crops [12]. It has been found in jars in pharaonic tombs [13]. TN can be eaten raw, roasted, soaked in water, baked or even as a refreshing drink known in Spain as tiger nut milk or horchata de chufas [9]. Several studies were performed to evaluate the nutritional value of TN and TN-derived products, revealing the benefits of consuming TN for general health and development for all ages. The tubers contain high amounts of carbohydrates and crude fibers. Studies have shown that the tubers are rich in sodium, phosphorus and calcium and show low levels of manganese, zinc, magnesium, copper and iron mineral contents [14]. They also contain vitamins A, C and E, together with several essential amino acids [15]. Further, TN oil is rich in oleic acid, palmitic and linoleic acids [16], which possibly mediate for its biological potential.

Plant phytochemicals vary across different matrices and exhibit a myriad of biological activities [17,18]. The phytochemical investigation of *Cyperus esculentus* L. revealed the presence of flavonoids, sterols, alkaloids, tannins and saponins [19]. These phytochemicals may be responsible for the various biological activities reported on tiger nuts, whether in folk uses or in different studies. The tubers are known to be used as diuretics, tonics, stimulants, emmenagogues and aphrodisiacs [15]. They are used to treat indigestion, flatulence, dysentery and diarrhea [20]. TN is used in the management of several pathophysiological conditions such as: coronary heart disease, hypercholesterolemia, colon cancer, obesity, diabetes, anemia and as an antimicrobial agent. Several reports showed that TN exhibits strong antioxidant activity [21]. This antioxidant activity may contribute to the managing of many oxidative stress-related diseases.

Several studies highlighted the implication of tiger nuts in biological health promotion and novel technological forms of foods in the Mediterranean region, together with the traditional uses of tiger nuts to improve memory and cognitive properties [22]. Nevertheless, the detailed phytochemical composition, or the neuroprotective mechanisms, of *Cyperus esculentus* L. have not been extensively explored. Therefore, our study aimed to investigate the phytochemical composition of *Cyperus esculentus* L., using UPLC-ESI-QTOF-MS analysis. Additionally, the potential neuroprotective effect of different doses of TN in Scop-induced memory deficit was assessed in rats in order to verify the putative mechanisms underlying this effect.

## 2. Results

### 2.1. Metabolite Profiling Using LC/MS

The ethanolic extract of TN was analyzed by UHPLC-ESI-QTOF-MS with the aim to characterize the phytochemical composition that could be responsible for the neuroprotective potential. The base peak chromatogram (BPC) of that analysis is shown in Figure 1. After data processing, 97 potential molecular features were obtained and proposed for annotation. Information on these molecular features (retention time,  $m/z$ , formula molecular,  $m/s$  fragments, relative abundance, etc.) is shown in Table 1. According to the identification guidelines proposed by Sumner et al., [23], 58 compounds were annotated at level 2 by comparing their MS/MS spectra with those present in the databases, 30 solely based on their molecular formula and MS1 spectra (level 3) and 9 molecular features remained as unknowns (level 4).

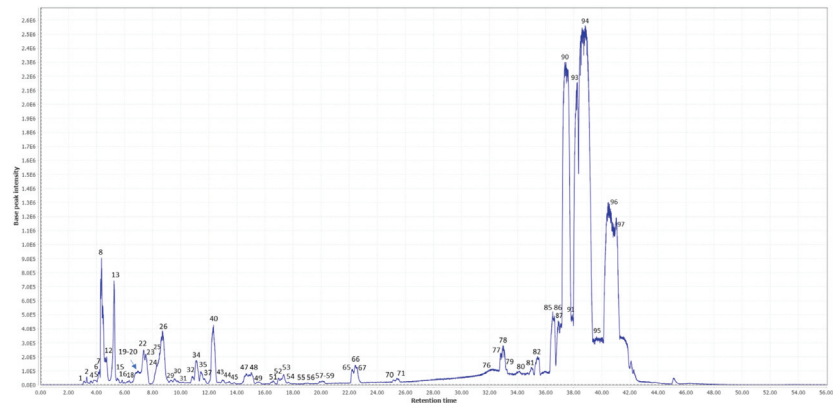


**Figure 1.** Base peak chromatogram (BPC) of the ethanolic extract of TN analyzed by UHPLC-ESI-QTOF-MS. The numbers refer to the dominant compounds in the BPC (see Table 1 for the tentative identity of these compounds).

Among the annotated compounds, phytochemicals belonging to the families of saccharides, amino acids, organic acids, fatty acids, phenolic compounds and flavonoids have been detected. In general, there is a high presence of fatty acids in the phytochemical composition of these matrices according to their relative abundances. This high presence of fatty acids, monounsaturated (e.g., oleic acid, eicosenoic acid, ricinoleic acid), polyunsaturated (e.g., linoleic acid, linolenic acid, docosahexaenoic acid) and saturated (e.g., stearic acid), agrees with previous studies that describe the relevance of fatty acids in *Cyperus Esculentus Lativum* [24]. Several of these fatty acids have been described as having an important role in regulating several processes within the brain and having neuroprotective properties [25]. Oleic acid (OA) has been detected with the highest relative abundance among the 97 compounds. The high concentration of this compound could be of great relevance, given that neuroprotective potential has been demonstrated for this compound. For instance, Song et al., (2019) carried out a study with OA in a rodent model of cerebral ischemia, showing the potential neuroprotective effects of this metabolite [26].

In addition, the presence of monosaccharides and oligosaccharides has also been detected in a high relative abundance. Different families of phenolic compounds have also been characterized, such as phenolic acids (ferulic acid, caffeoylquinic acid, etc.), flavonoids (e.g., apigenin, kaempferol, luteolin, etc.) and glycosylated flavonoids, etc. Although these compounds are found in lower relative concentrations, the neuroprotective potential of many of these compounds has been described in the literature [27–29].

Other families of compounds have also been detected, such as amino acids (tryptophan, arginine, phenylalanine, etc.), vitamins (pantothenic acid), nucleosides (guanosine, uridine,

etc.) or organic acids (quinic acid and citric acid, etc.). Some of these have also been shown to play a role in neurodegenerative processes, such as tryptophan-related metabolites [30]. However, the relative abundance of these metabolites seems minor compared with the fatty acids detected. In any case, according to the literature, many of the annotated metabolites may contribute to the potential neuroprotective effect of this plant matrix, also considering possible synergistic effects between the different phytochemical compounds [31].

## 2.2. Effect of Different Doses of TN on Scop-Induced Behavioral Changes in Rats

In the MWM probe test, Scop-treated rats failed to recall the exact location of the platform, as evidenced by spending significantly less time in the target quadrant than the control rats by approximately 60.75%. On the other hand, the reduced time spent within the target quadrant by Scop-treated rats was significantly reversed by donepezil and TN 50, 100 or 200 mg by approximately 2-fold, 1.3-fold, 1.7-fold and 1.8-fold, respectively, demonstrating that TN ameliorated the Scop-induced deficiency in the memory of the animals ( $F(14, 79) = 57, p < 0.0001$ ) (Figure 2b).

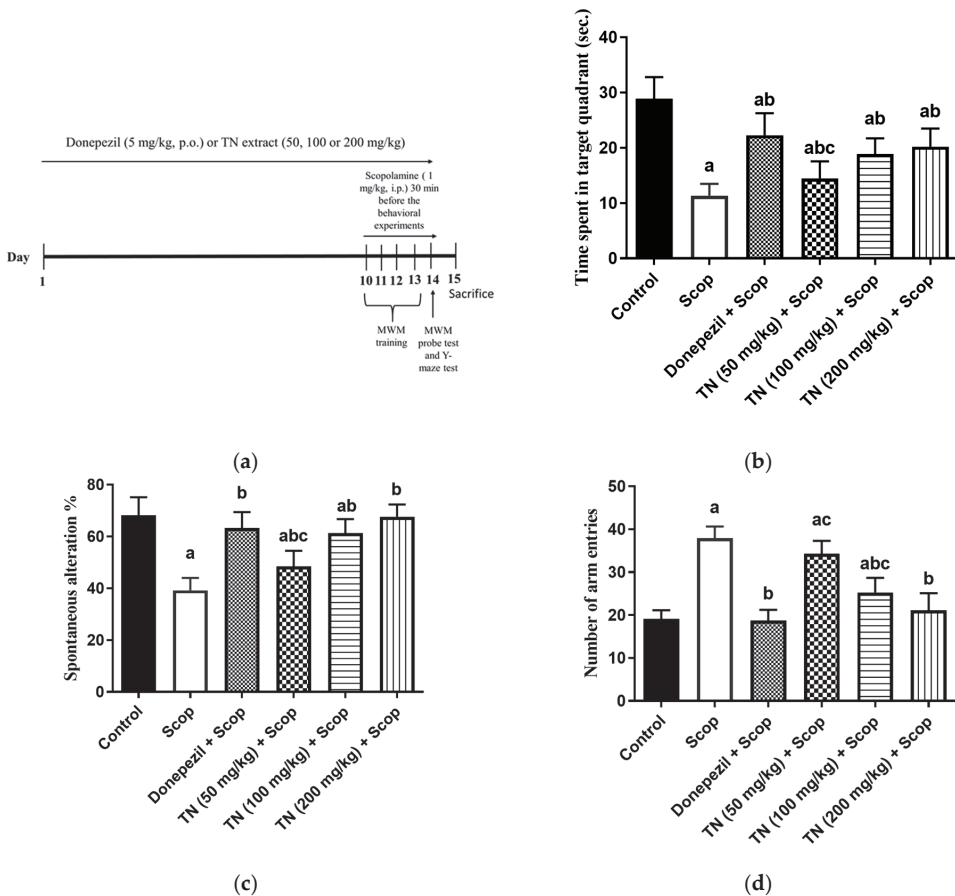


**Figure 2.** Experimental timeline (a). Effect of different doses of TN on the time spent in the target quadrant during the probe trial session in the MWM (b). Percentage of spontaneous alteration (c). Number of arm entries (d) in the Y maze test. Values are expressed as the mean  $\pm$  SD ( $n = 15$ ). Values are statistically significant at  $p < 0.05$  versus the control group,  $p < 0.05$  versus the Scop-treated group and  $p < 0.05$  versus the donepezil-treated group.

Table 1. The metabolite profiling of the ethanolic extract of *C. esculentus* L. rhizomes as analyzed by UHPLC-QTOF-MS.

N°	RT	m/z Experimental	m/z Theoretical	Error (ppm)	Formula	Level of Annotation	Compounds	MS/MS Fragments	Rel. Ab. (%)	REF
1	3.11	201.0249	201.0260	5.47	C <sub>5</sub> H <sub>6</sub> N <sub>4</sub> O <sub>5</sub>	2	2-Oxo-4-hydroxy-4-carboxy-5-ureidomidazole	59/157	0.07	FDB001617
2	3.31	141.0164	141.0188	17.0	C <sub>6</sub> H <sub>6</sub> O <sub>4</sub>	2	Kojic acid	59/141	0.09	HMD032923
3	3.52	131.0821	131.0821	0	C <sub>5</sub> H <sub>12</sub> N <sub>2</sub> O <sub>2</sub>	2	L-ornithine	70	0.03	[32]
4	3.80	173.1040	173.1039	0.58	C <sub>6</sub> H <sub>14</sub> N <sub>4</sub> O <sub>2</sub>	2	Arginine	131	0.1	[33,34]
5	3.82	195.0502	195.0505	1.53	C <sub>6</sub> H <sub>12</sub> O <sub>7</sub>	2	Gluconic acid	75/129/195	0.14	FDB001980
6	4.22	267.0717	267.0716	0.37	C <sub>9</sub> H <sub>16</sub> O <sub>9</sub>	3	xylo-manno-nononic acid γ-lactone	267	0.21	-
7	4.25	191.0553	191.0556	1.57	C <sub>7</sub> H <sub>12</sub> O <sub>6</sub>	2	Quinic acid	85/92/191	0.06	[35]
8	4.36	341.1082	341.1084	0.59	C <sub>12</sub> H <sub>22</sub> O <sub>11</sub>	2	Galactinol dihydrate	59/71/89/101/113/143/161	2.24	[32]
9	4.42	503.1607	503.1612	0.99	C <sub>18</sub> H <sub>32</sub> O <sub>16</sub>	3	Trisaccharide (raffinose)	503	0.17	[32] HMD003213
10	4.50	337.0769	337.0771	0.59	C <sub>12</sub> H <sub>18</sub> O <sub>11</sub>	2	Ascorbyl glucoside isomer I	59/161/277/289	0.03	HMD0253873
11	4.61	115.0031	115.0031	0	C <sub>4</sub> H <sub>4</sub> O <sub>4</sub>	2	Fumaric acid	71/87/99	0.02	[35]
12	4.72	341.1082	341.1084	0.59	C <sub>12</sub> H <sub>22</sub> O <sub>11</sub>	2	Sucrose	59/71/89/101/113/143/161	0.35	[32]
13	5.22	341.1082	341.1084	0.59	C <sub>12</sub> H <sub>22</sub> O <sub>11</sub>	2	Trehalose/maltose	129/143/161/179	1.37	[32]
14	5.30	133.0135	133.0137	1.50	C <sub>4</sub> H <sub>6</sub> O <sub>5</sub>	2	Malic acid	71/89/115/133	0.06	[35]
15	5.47	503.1607	503.1612	0.99	C <sub>18</sub> H <sub>32</sub> O <sub>16</sub>	3	Trisaccharide	503	0.12	[32]
16	5.82	503.1597	503.1612	2.98	C <sub>18</sub> H <sub>32</sub> O <sub>16</sub>	3	Trisaccharide	503	0.05	[32]
17	5.97	337.0763	337.0771	2.37	C <sub>12</sub> H <sub>18</sub> O <sub>11</sub>	2	Ascorbyl glucoside isomer II	59/161/277/289	0.03	HMD0253873
18	6.32	251.0765	251.0780	5.97	C <sub>10</sub> H <sub>12</sub> N <sub>4</sub> O <sub>4</sub>	4	Unknown	251	0.11	-
19	6.61	191.0189	192.0270	0.60	C <sub>6</sub> H <sub>8</sub> O <sub>7</sub>	2	Citric acid	87/111/129/173	0.03	[36]
20	6.76	295.1029	295.1029	0	C <sub>11</sub> H <sub>20</sub> O <sub>9</sub>	3	Aliphatic glucoside derivative	295	0.11	-
21	7.31	243.0621	243.0617	1.64	C <sub>9</sub> H <sub>12</sub> N <sub>2</sub> O <sub>6</sub>	2	Uridine	140/152/200	0.05	[37]
22	7.35	369.1404	369.1397	1.89	C <sub>14</sub> H <sub>26</sub> O <sub>11</sub>	3	Amylose	369	1	HMD003403

Table 1. Cont.

N <sup>o</sup>	RT	m/z Experimental	m/z Theoretical	Error (ppm)	Formula	Level of Annotation	Compounds	MS/MS Fragments	Rel. Ab. (%)	REF
23	7.56	295.1036	295.1029	2.37	C <sub>11</sub> H <sub>20</sub> O <sub>9</sub>	3	Aliphatic glucoside derivative	295	0.07	-
24	8.15	130.0868	130.0868	0	C <sub>6</sub> H <sub>13</sub> NO <sub>2</sub>	3	Leucine	130	1.10	[32,33]
25	8.34	329.0871	329.0873	0.60	C <sub>14</sub> H <sub>18</sub> O <sub>9</sub>	2	Dihydroxy benzoic acid methyl ester hexoside	125/153/167/270	0.06	[35]
26	8.69	413.1654	413.1659	1.21	C <sub>16</sub> H <sub>30</sub> O <sub>12</sub>	3	Glucopyranoside derivate	413	1.42	-
27	8.68	282.0843	282.0838	1.77	C <sub>10</sub> H <sub>13</sub> N <sub>5</sub> O <sub>5</sub>	2	Guanosine	133/150	0.03	FDB003632
28	8.95	493.1546	493.1557	2.23	C <sub>20</sub> H <sub>30</sub> O <sub>14</sub>	2	O-hexosyl-O-methyl-myoinositol-dihydroxy benzoic acid	137/167/209/243/293/331	0.11	[35]
29	9.28	295.1027	295.1029	0.67	C <sub>11</sub> H <sub>20</sub> O <sub>9</sub>	3	Aliphatic glucoside derivative	295	0.11	-
30	9.54	383.1550	383.1553	0.78	C <sub>15</sub> H <sub>28</sub> O <sub>11</sub>	2	Butanediol apiosylglucoside	71/89/161	0.15	HMDB0033063
31	10.53	164.0710	164.0712	1.22	C <sub>9</sub> H <sub>11</sub> NO <sub>2</sub>	2	Phenylalanine	103/147/164	0.03	[32,33]
32	10.84	380.1545	380.1557	3.15	C <sub>15</sub> H <sub>27</sub> NO <sub>10</sub>	4	Unknown	380	0.2	-
33	10.89	218.1026	218.1028	0.91	C <sub>9</sub> H <sub>17</sub> NO <sub>5</sub>	2	Pantothenic acid	71/88/146	0.05	FDB008322
34	11.09	559.2228	559.2238	1.78	C <sub>22</sub> H <sub>40</sub> O <sub>16</sub>	3	Trisaccharide derivative	218	0.62	-
35	11.44	461.1652	461.1659	1.51	C <sub>20</sub> H <sub>30</sub> O <sub>12</sub>	2	Verbascoside	119/137/299	0.32	FDB018766
36	11.56	279.1078	279.1080	0.71	C <sub>11</sub> H <sub>20</sub> O <sub>8</sub>	3	Methyl glucopyranosyloxy butanoate	279	0.16	-
37	11.65	309.1186	309.1186	0	C <sub>12</sub> H <sub>22</sub> O <sub>9</sub>	3	Dideoxy-glucopyranosyl-ribohexose	309	0.15	-
38	11.84	359.0973	359.0978	1.39	C <sub>15</sub> H <sub>20</sub> O <sub>10</sub>	2	Glucosyringic acid	153/197/315/341	0.03	HMDB0303364
39	12.10	397.1657	397.1651	1.51	C <sub>23</sub> H <sub>26</sub> O <sub>6</sub>	2	Kanzonol M	176/161/181	0.02	HMDB0041101
40	12.34	397.1705	397.1710	1.26	C <sub>16</sub> H <sub>30</sub> O <sub>11</sub>	3	Glucopyranoside derivate	397	1.37	-
41	12.35	203.0823	203.0821	0.98	C <sub>11</sub> H <sub>12</sub> N <sub>2</sub> O <sub>2</sub>	2	Tryptophan	116/142	0.06	[32]
42	12.94	193.0504	193.0501	1.55	C <sub>10</sub> H <sub>10</sub> O <sub>4</sub>	2	Ferulic acid	107/134/149	0.05	[35,38]
43	12.98	503.1398	503.1401	0.59	C <sub>21</sub> H <sub>28</sub> O <sub>14</sub>	2	6-Caffeoylsucose	149/161/179/323/341/443	0.12	FDB014172
44	13.45	353.0865	353.0873	2.26	C <sub>16</sub> H <sub>18</sub> O <sub>9</sub>	2	Chlorogenic acid	127/135/191	0.04	FDB002582 [37,39]

Table 1. Cont.

N <sup>o</sup>	RT	m/z Experimental	m/z Theoretical	Error (ppm)	Formula	Level of Annotation	Compounds	MS/MS Fragments	Rel. Ab. (%)	REF
45	13.81	597.2177	597.2183	1.00	C <sub>28</sub> H <sub>38</sub> O <sub>14</sub>	4	Unknown	597	0.05	-
46	14.55	323.1337	323.1342	1.54	C <sub>13</sub> H <sub>24</sub> O <sub>9</sub>	4	Unknown disaccharide	323	0.12	-
47	14.67	293.1232	293.1236	1.36	C <sub>12</sub> H <sub>22</sub> O <sub>8</sub>	2	Ethyl-glucopyranosyl-butanoate isomer I	59/85/101/131	0.3	HMDB0031693
48	15.02	293.1232	293.1236	1.36	C <sub>12</sub> H <sub>22</sub> O <sub>8</sub>	2	Ethyl-glucopyranosyl-butanoate isomer II	59/85/101/131	0.32	HMDB0031693
49	15.54	351.1286	351.1291	1.42	C <sub>14</sub> H <sub>24</sub> O <sub>10</sub>	4	Unknown disaccharide	351	0.08	-
50	15.68	323.0976	323.0978	0.61	C <sub>12</sub> H <sub>20</sub> O <sub>10</sub>	4	Unknown disaccharide	323	0.04	-
51	16.58	609.1462	609.1456	0.98	C <sub>27</sub> H <sub>30</sub> O <sub>16</sub>	2	Luteolin-3',7'-di-O-glucoside	285/447	0.09	[40]
52	16.98	245.0923	245.0926	1.22	C <sub>13</sub> H <sub>14</sub> N <sub>2</sub> O <sub>3</sub>	2	cyclic 6-hydroxymelatonin	74/116/142/159/203/245	0.1	HMDB060810
53	17.32	245.0924	245.0926	0.81	C <sub>13</sub> H <sub>14</sub> N <sub>2</sub> O <sub>3</sub>	2	N-acetyl tryptophan	74/116/142/159/203	0.23	HMDB13713
54	17.67	683.1805	683.1823	2.63	C <sub>30</sub> H <sub>36</sub> O <sub>18</sub>	2	Rosmarinic acid di-O-hexoside	359/521	0.07	[41]
55	19.05	461.1080	461.1084	0.86	C <sub>22</sub> H <sub>22</sub> O <sub>11</sub>	2	Kaempferide 7-glucoside	283/269/299	0.05	HMDB38455
56	19.35	285.0395	285.0399	1.40	C <sub>15</sub> H <sub>10</sub> O <sub>6</sub>	3	Aureusidin	285	0.03	[40]
57	19.88	209.0792	209.0774	8.60	C <sub>6</sub> H <sub>14</sub> N <sub>2</sub> O <sub>6</sub>	4	Unknown	209	0.04	-
58	20.06	209.0790	209.0787	1.43	C <sub>7</sub> H <sub>10</sub> N <sub>6</sub> O <sub>2</sub>	4	Unknown nitrogenous compound	209	0.11	-
59	20.08	287.0560	287.0556	1.39	C <sub>15</sub> H <sub>12</sub> O <sub>6</sub>	2	Dihydrokaempferol	107/135/151/175/229/243	0.06	FDB012431
60	20.21	447.0923	447.0927	0.89	C <sub>21</sub> H <sub>20</sub> O <sub>11</sub>	2	Luteolin-O-glucoside	285	0.04	[40]
61	20.94	299.0488	299.0556	22.7	C <sub>16</sub> H <sub>12</sub> O <sub>6</sub>	3	Luteolin methyl ether	285	0.04	HMDB37339
62	21.27	269.0396	269.0450	20.1	C <sub>15</sub> H <sub>10</sub> O <sub>5</sub>	2	Apigenin	117/269	0.04	[37,40]
63	21.41	299.0556	299.0556	0	C <sub>16</sub> H <sub>12</sub> O <sub>6</sub>	3	Chrysoeriol	284/299	0.02	[34]
64	21.81	271.0555	271.0606	18.8	C <sub>15</sub> H <sub>12</sub> O <sub>5</sub>	2	Naringenin	107/119/151/177/217	0.04	[34]
65	22.22	285.0396	285.0399	1.05	C <sub>15</sub> H <sub>10</sub> O <sub>6</sub>	3	Kaempferol	285	0.23	[38]
66	22.42	285.0397	285.0399	0.70	C <sub>15</sub> H <sub>10</sub> O <sub>6</sub>	2	Luteolin	107/133/151/175	0.52	[36,38,40]
67	23.3	301.0714	301.0712	0.66	C <sub>16</sub> H <sub>14</sub> O <sub>6</sub>	2	Hesperitin	135/151/285	0.03	[42]
68	24.21	299.0556	299.0556	0	C <sub>16</sub> H <sub>12</sub> O <sub>6</sub>	2	Kaempferide	256/284	0.08	[34,43]
69	25.04	209.0815	209.0814	0.48	C <sub>11</sub> H <sub>14</sub> O <sub>4</sub>	3	Methylxanthoylin	209	0.05	HMDB34047
70	25.39	299.0558	299.0556	0.69	C <sub>16</sub> H <sub>12</sub> O <sub>6</sub>	2	Isokaempferide	183/227/255	0.17	HMDB0302564



Table 1. Cont.

N <sup>o</sup>	RT	m/z Experimental	m/z Theoretical	Error (ppm)	Formula	Level of Annotation	Compounds	MS/MS Fragments	Rel. Ab. (%)	REF
71	25.51	313.0713	313.0712	0.31	C <sub>17</sub> H <sub>14</sub> O <sub>6</sub>	2	Cirsimaritin	283/297/313	0.11	HMD/B0250276
72	26.08	329.2324	329.2328	1.21	C <sub>18</sub> H <sub>14</sub> O <sub>5</sub>	2	Trihydroxy-octadecenoic acid	171/211/229/285/311	0.2	FDB002905
73	26.14	351.2144	351.2171	7.68	C <sub>20</sub> H <sub>32</sub> O <sub>5</sub>	4	Unknown	351	0.03	-
74	28.63	373.1291	373.1287	1.07	C <sub>20</sub> H <sub>22</sub> O <sub>7</sub>	3	Isohydroxymatairesinol	373	0.11	HMD/B0301737
75	28.66	339.1235	339.1232	0.88	C <sub>20</sub> H <sub>20</sub> O <sub>5</sub>	3	Prenylharingenin	339	0.09	HMD/B0247465
76	31.09	313.2380	313.2379	0.32	C <sub>18</sub> H <sub>34</sub> O <sub>4</sub>	3	Octadecanedioic acid	313	0.05	HMD/B00782
77	32.44	315.2525	315.2535	3.17	C <sub>18</sub> H <sub>36</sub> O <sub>4</sub>	3	Dihydroxyoctadecanoic acid	315	0.2	HMD/B31008
78	32.95	205.1593	205.1592	0.48	C <sub>14</sub> H <sub>22</sub> O	3	2,4-di-tert-butylphenol	205	1.07	HMD/B13816
79	33.15	295.2272	295.2273	0.33	C <sub>18</sub> H <sub>32</sub> O <sub>3</sub>	3	Hydroxylinoleic acid	277	0.25	HMD/B0247599
80	34.60	199.1698	199.1698	0	C <sub>12</sub> H <sub>24</sub> O <sub>2</sub>	2	Dodecanoic acid	59/155	0.06	FDB030978
81	34.98	299.2592	299.2586	2	C <sub>18</sub> H <sub>36</sub> O <sub>3</sub>	2	Hydroxyoctadecanoic acid	255/269/281/299	0.52	FDB006898
82	35.40	297.2432	297.2430	0.67	C <sub>18</sub> H <sub>34</sub> O <sub>3</sub>	2	Ricinoleic acid	127/183/279	0.8	FDB012640
83	36.03	255.2329	255.2324	1.96	C <sub>16</sub> H <sub>32</sub> O <sub>2</sub>	3	Isopalmitic acid	255	0.18	[32]
84	36.27	281.2480	281.2481	0.35	C <sub>18</sub> H <sub>34</sub> O <sub>2</sub>	3	Elaidic acid	281	0.17	HMD/B00573
85	36.50	277.2162	277.2168	2.16	C <sub>18</sub> H <sub>30</sub> O <sub>2</sub>	2	Linolenic Acid	119	2.27	[32]
86	36.70	227.2007	227.2011	1.76	C <sub>14</sub> H <sub>28</sub> O <sub>2</sub>	2	Myristic acid	209	0.77	[32]
87	36.89	253.2163	253.2168	1.97	C <sub>16</sub> H <sub>30</sub> O <sub>2</sub>	2	Palmitoleic acid	71/253	1.89	[32]
88	36.99	327.2315	327.2324	2.75	C <sub>22</sub> H <sub>32</sub> O <sub>2</sub>	2	DHA	229/283/309	0.92	HMD/B0244316
89	37.38	581.4541	581.4570	4.99	C <sub>38</sub> H <sub>62</sub> O <sub>4</sub>	2	Oxygenated fatty acid derivatives	253/271	0.87	-
90	37.45	279.2337	279.2324	4.65	C <sub>18</sub> H <sub>32</sub> O <sub>2</sub>	2	Linoleic acid	71/261/279	17	[32]
91	37.95	267.2325	267.2324	0.37	C <sub>17</sub> H <sub>32</sub> O <sub>2</sub>	3	Heptadecenoic acid	267	0.35	HMD/B31046
92	38.22	533.4538	533.4570	5.99	C <sub>34</sub> H <sub>62</sub> O <sub>4</sub>	2	Oxygenated fatty acid derivatives	293/533	0.77	-
93	38.26	255.2372	255.2324	18.8	C <sub>16</sub> H <sub>32</sub> O <sub>2</sub>	2	Palmitic acid	237	12	[32]
94	38.32	281.2480	281.2481	0.35	C <sub>18</sub> H <sub>34</sub> O <sub>2</sub>	2	Oleic acid	253/255/267	29.9	[32]
95	39.40	269.2483	269.2481	0.74	C <sub>17</sub> H <sub>34</sub> O <sub>2</sub>	3	Margaric acid	269	0.25	[32]
96	40.46	283.2640	283.2637	1.05	C <sub>18</sub> H <sub>36</sub> O <sub>2</sub>	2	Stearic acid	265	14.5	[32]
97	41.47	309.2792	309.2794	0.65	C <sub>20</sub> H <sub>38</sub> O <sub>2</sub>	3	Condoic acid	309	0.32	[32]

The administration of Scop revealed that short-term memory deficit manifested through a marked drop in the percentage of spontaneous alternation by approximately 42.53%, as well as a significant increment in the locomotor activity (the number of arm entries) by approximately 2-fold in the Y-maze test compared with the control rats. In contrast, compared with Scop, treatment with donepezil and TN 50, 100 or 200 mg significantly mitigated the decline of the spontaneous alternation percentage by approximately 1.6-fold, 1.2-fold, 1.6-fold and 1.7-fold, respectively ( $F(14, 84) = 61.98, p < 0.0001$ ) (Figure 2c). Donepezil and TN 100 or 200 mg also decreased the locomotor activity by approximately 50.61%, 33.37% and 44.29%, respectively ( $F(14, 70) = 99.02, p < 0.0001$ ) (Figure 2d).

### 2.3. Effect of Different Doses of TN on Scop-Induced Alterations in AChE Activity

Rats injected with Scop exhibited a significant rise in hippocampal AChE activity by approximately 0.9-fold compared with the control group. Nevertheless, the administration of donepezil and TN 100 or 200 mg significantly suppressed the AChE activity ( $F(5, 30) = 22.51, p < 0.0001$ ) by approximately 39.01%, 20.85% and 26.74%, respectively, compared with the Scop group values (Figure 3).

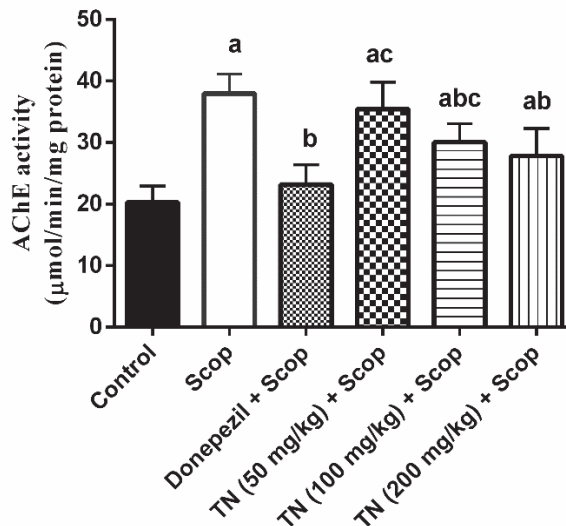


**Figure 3.** Effect of different doses of tiger nut on Scop-induced alterations in AChE activity. Values are expressed as the mean  $\pm$  SD ( $n = 6$ ). Values are statistically significant at  $p < 0.05$  versus the control group,  $p < 0.05$  versus the Scop-treated group and  $p < 0.05$  versus the donepezil-treated group.

### 2.4. Effect of Different Doses of TN on Scop-Induced Oxidative Stress

Scop produced a state of oxidative stress, revealed by the dramatic elevation in the hippocampal MDA level (by  $\approx 2.5$ -fold) along with a significant decline in hippocampal GSH content (by 37.03%) and SOD and CAT activity (by 66.65% and 62.61%, respectively) compared with the control animals. However, donepezil and TN 200 mg treatment ameliorated the Scop-induced increase in MDA levels ( $F(5, 30) = 16.71, p < 0.0001$ ) by approximately 39.04% and 32.79% respectively. Interestingly, compared with the Scop group rats, only donepezil increased the GSH content ( $F(5, 30) = 6.481, p < 0.0003$ ) by approximately 1.4-fold, while donepezil and TN 100 or 200 mg elevated the SOD activity ( $F(5, 30) = 28.82, p < 0.0001$ ) by approximately 2.3-fold, 2.2-fold and 2.5-fold, respectively, as well as the CAT activity ( $F(5, 30) = 12.61, p < 0.0001$ ) by approximately 2.5-fold, 2.7-fold and 2.7-fold, respectively (Figure 4a–d).

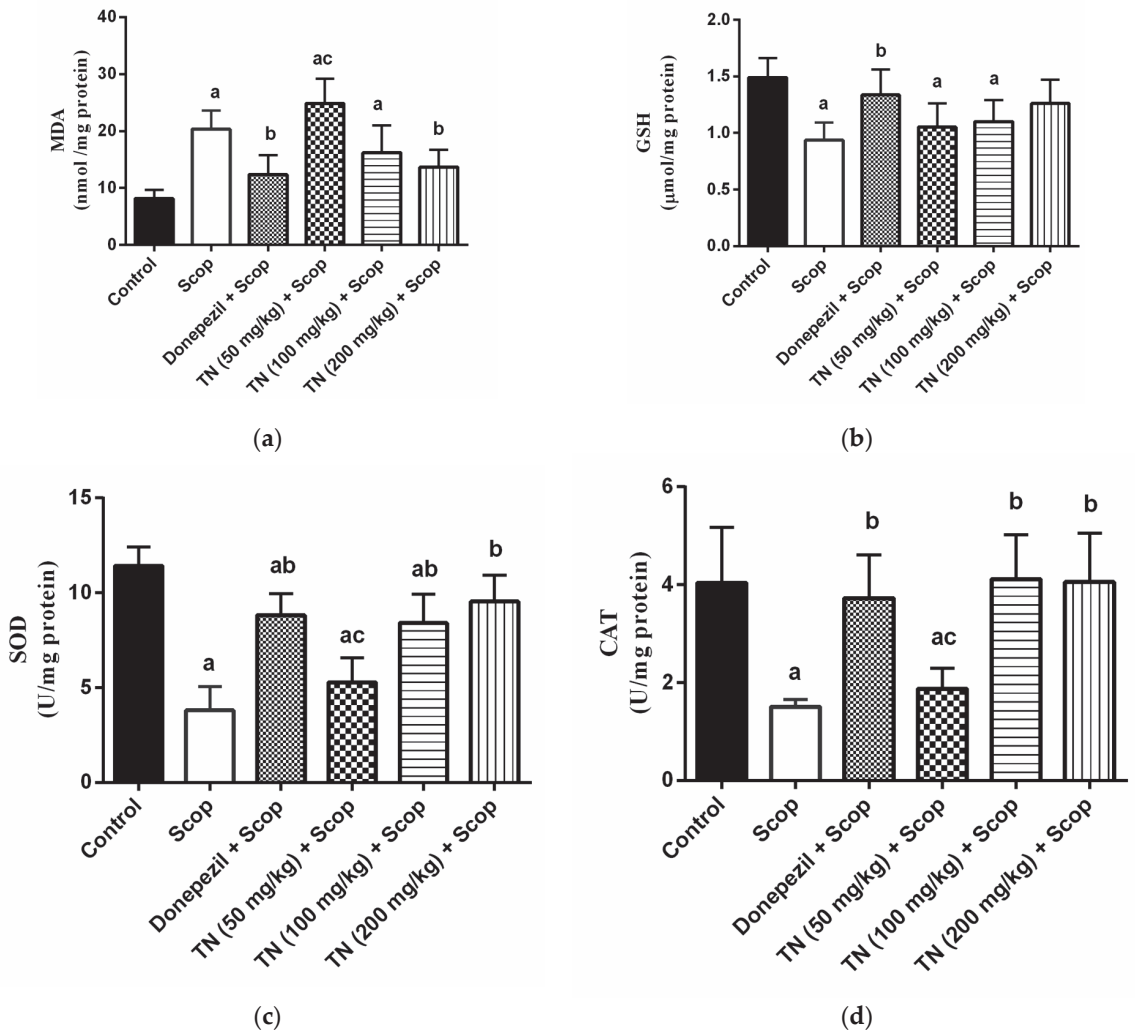


**Figure 4.** Effect of different doses of tiger nut on Scop-induced oxidative stress. (a) MDA, (b) GSH, (c) SOD and (d) CAT. Values are expressed as the mean  $\pm$  SD ( $n = 6$ ). Values are statistically significant at  $p < 0.05$  versus the control group,  $p < 0.05$  versus the Scop-treated group and  $p < 0.05$  versus donepezil-treated group.

#### 2.5. Effect of Different Doses of TN on Scop-Induced Neuroinflammation

As shown in Figure 5a and b, Scop triggered inflammation via elevating the TNF- $\alpha$  and IL-1 $\beta$  levels by 4.7-fold and 3.5-fold, respectively, in comparison with the control rats. On the other hand, treatment with donepezil and TN 50 or 100 or 200 mg induced a marked improvement in Scop-induced neuroinflammation, as evidenced by the decrease in TNF- $\alpha$  levels ( $F(5, 30) = 252.3$ ,  $p < 0.0001$ ) by approximately 33.57%, 90.41%, 64.74% and 50.09%, respectively, and IL-1 $\beta$  levels ( $F(5, 30) = 165.6$ ,  $p < 0.0001$ ) by approximately 34.87%, 86.38%, 72.52% and 52.29%, respectively, of the Scop group values.

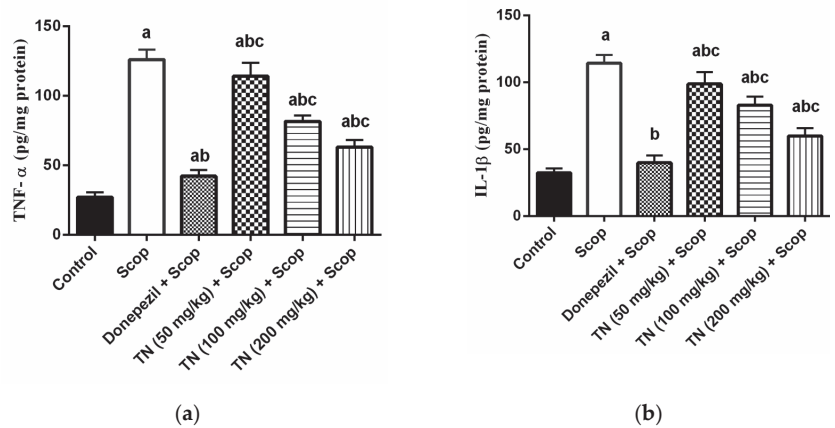


**Figure 5.** Effect of different doses of tiger nut on Scop-induced neuroinflammation. (a) TNF- $\alpha$  and (b) IL-1 $\beta$ . Values are expressed as the mean  $\pm$  SD ( $n = 6$ ). Values are statistically significant at  $p < 0.05$  versus the control group,  $p < 0.05$  versus the Scop-treated group and  $p < 0.05$  versus the donepezil-treated group.

#### 2.6. Effect of Different Doses of TN on Scop-Induced Apoptosis

Scop administration resulted in a dramatic up-regulation of the hippocampal pro-apoptotic Bax mRNA expression and the Bax/Bcl2 ratio by approximately 11.9-fold and 35.8-fold, respectively, along with a significant down-regulation of the hippocampal anti-apoptotic Bcl2 mRNA expression by approximately 34.72% compared with the control group. Donepezil and TN 100 or 200 mg significantly reversed the increase in the Bax mRNA expression ( $F(5, 30) = 77.24$ ,  $p < 0.0001$ ) by approximately 26.39%, 65.20% and 39.49%, respectively, in comparison with the Scop-treated rats. Additionally, treatment with donepezil and TN 50 or 100 or 200 mg attenuated Scop-induced apoptosis, as demonstrated by the increase in the Bcl2 mRNA expression ( $F(5, 30) = 68.25$ ,  $p < 0.0001$ ) by approximately 2.2-fold, 1.4-fold, 1.7-fold and 2.2-fold, respectively, as well as the reduction in the Bax/Bcl2 ratio ( $F(5, 30) = 65.76$ ,  $p < 0.0001$ ) by approximately 11.65%, 62.18%, 36.36% and 17.73%, respectively, of the Scop group values (Figure 6a–c).

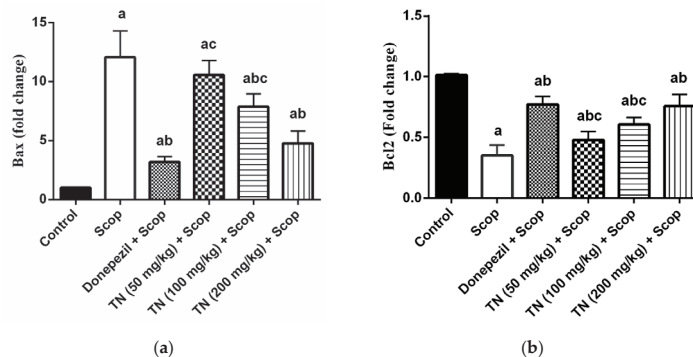


**Figure 6.** Cont.

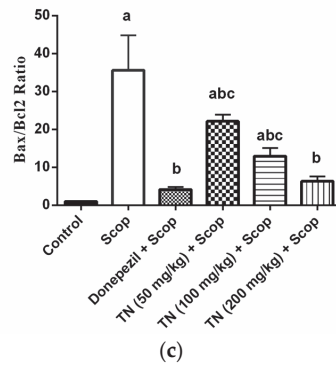


**Figure 6.** Effect of different doses of tiger nut on Scop-induced apoptosis. (a) Bax, (b) Bcl2 and (c) Bax/Bcl2 ratio. Values are expressed as the mean  $\pm$  SD ( $n = 6$ ). Values are statistically significant at  $p < 0.05$  versus the control group,  $p < 0.05$  versus the Scop-treated group and  $p < 0.05$  versus donepezil-treated group.

### 2.7. Effect of Different Doses of TN on Scop-Induced Alterations in A $\beta$ and $\beta$ -Secretase Protein Expression

Scop markedly up-regulated the hippocampal A $\beta$  and  $\beta$ -secretase protein expression by approximately 6-fold compared with the control animals. However, donepezil and TN 50 or 100 or 200 mg significantly ameliorated the increase in both the A $\beta$  protein expression ( $F(5, 30) = 157.1$ ,  $p < 0.0001$ ) reaching approximately 47.79%, 46.88%, 40.74% and 34.54%, respectively, and the  $\beta$ -secretase protein expression ( $F(5, 30) = 313.5$ ,  $p < 0.0001$ ) reaching approximately 37.94%, 36.73%, 40.25% and 28.50%, respectively, in comparison with the Scop-treated rats. (Figure 7a,b).

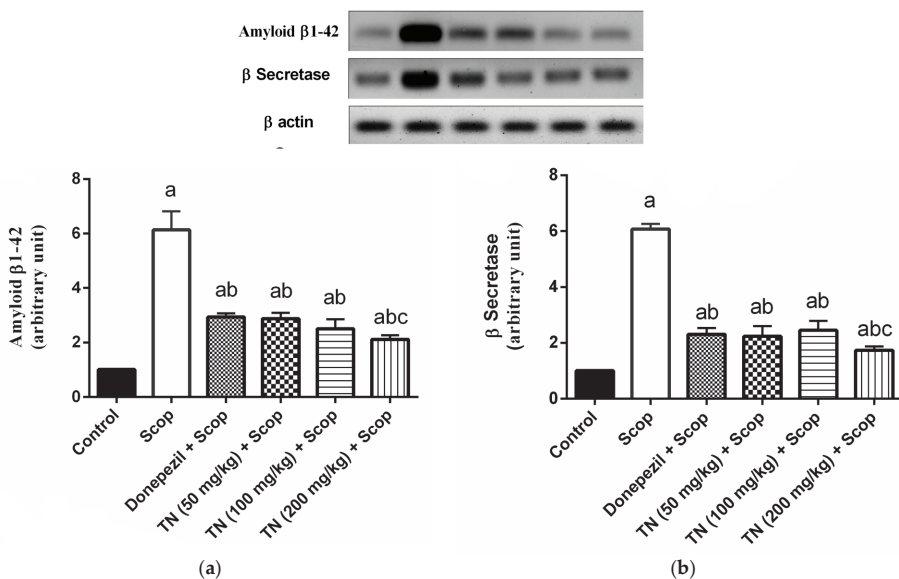
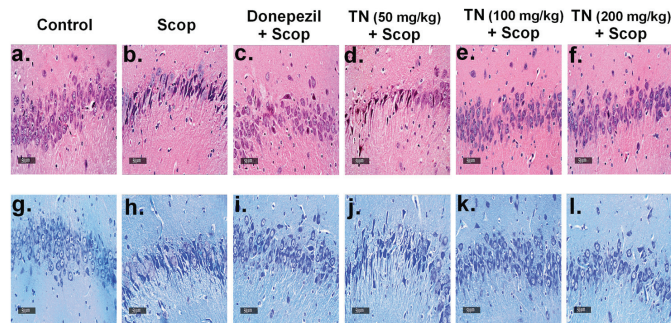


**Figure 7.** Effect of different doses of TN on Scop-induced alterations in (a) A $\beta$  and (b)  $\beta$ -secretase protein expression. Values are expressed as the mean  $\pm$  SD ( $n = 6$ ). Values are statistically significant at  $p < 0.05$  versus the control group,  $p < 0.05$  versus the Scop-treated group and  $p < 0.05$  versus donepezil-treated group. Representative western blots are depicted.

### 2.8. Effect of Different Doses of TN on Scop-Induced Histopathological Alterations and Neuronal Loss

Photomicrographs from the control rats revealed no histopathological alterations, with normal histological features of the hippocampus showing intact pyramidal neurons and intracellular brain matrices (Figure 8a). Additionally, Nissl staining of the control group demonstrated normal intact neurons (Figure 8g,m). On the other hand, Scop-treated rats exhibited severe neuronal necrosis and degeneration, together with mild intracellular edema and extensive gliosis, compared with the control group (Figure 8b). Furthermore, marked neuronal loss was observed by Nissl staining (Figure 8h,m). The administration of donepezil produced significant neuroprotective effects, showing intact neurons with minimal neurodegenerative changes. However, persistent gliosis was observed (Figure 8c). Furthermore, donepezil ameliorated the neuronal loss, as evidenced by the Nissl staining (Figure 8i,m). Interestingly, TN 100 or 200 mg demonstrated marked neuroprotection, resembling donepezil showing intact neurons with minimal neurodegenerative changes, with TN 200 mg presenting diminished gliosis (Figure 8e,f). Furthermore, TN 100 or 200 mg amended the neuronal loss, verified by the Nissl staining (Figure 8k–m). However, TN 50 mg revealed negligible neuroprotective effects, exhibiting almost the same histological alterations seen in the Scop group (Figure 8d), with significant neuronal loss detected by Nissl staining (Figure 8j,m).



m.

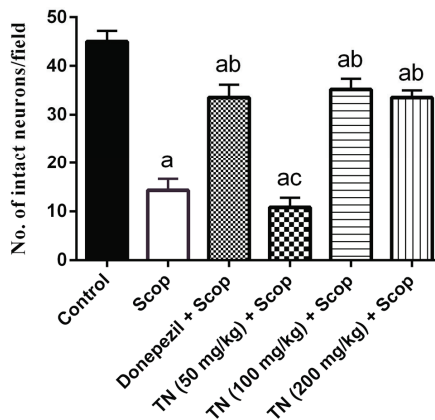


**Figure 8.** Effect of different doses of TN on Scop-induced histopathological alterations and neuronal

loss. (a–f): specimens stained with H&E (400× magnification). (a) The control group showed a normal hippocampal structure; (b) the Scop group showed severe neuronal necrosis and extensive gliosis; (c) the donepezil group showed minimal neurodegenerative changes and persistent gliosis; (d) the TN 50 mg group showed severe neuronal necrosis and extensive gliosis; (e) the TN 100 mg group showed minimal neurodegenerative changes; (f) the TN 200 mg group showed minimal neurodegenerative changes and diminished gliosis. (g–l) Specimens stained with Nissl (400× magnification). (m) Number of Nissl-stained cells (intact neurons). Statistical analysis was carried out using one-way ANOVA followed by the Tukey–Kramer multiple comparison test. Values are expressed as the mean ± SD. Values are statistically significant at  $p < 0.05$  versus the control group,  $p < 0.05$  versus the Scop-treated group and  $p < 0.05$  versus donepezil-treated group.

### 3. Discussion

TN extract offers antioxidant [44,45], anti-inflammatory, neuroprotective [46] and beneficial effects in memory-related disorders [47]. Therefore, the aim of the present study was to investigate the protective effect of TN extract on Scop-induced memory impairment in rats. Scop is a muscarinic cholinergic receptor antagonist, causing cognitive decline by increasing AChE activity, oxidative stress and neuroinflammation in the rat brain, thus developing AD-like symptoms [48,49]

The MWM is the most widely-employed behavioral test for studying hippocampal-spatial learning and reference memory in rodents. Moreover, it is used to recognize drugs capable of reducing or preventing memory loss, i.e., drugs with anti-amnesic properties [50]. Learning is defined as a decline over trials in the latency to locate the sunken platform. [51]. During the acquisition phase, the mean escape latency, which is the time each mouse spent to find the platform, was significantly increased in the Scop group, while treatment with donepezil significantly reversed this alteration. However, treatment with TN (100 and 200 mg/kg) significantly decreased the mean escape latency compared with the Scop group values. In the probe test, the time spent in the target quadrant was measured to indicate the animals' ability to recall the precise location where the platform was previously retained [51]. The Scop-treated rats showed the least time spent in the target quadrant, indicating an impairment in spatial learning and memory. On the other hand, the administration of donepezil restored the time spent in the target quadrant to the control levels. TN extract (100 and 200 mg/Kg) presented the highest time spent in the target quadrant, indicating reestablished memory. The Y-maze is a spontaneous alteration behavioral test, based on the willingness of rodents to explore a completely new environment in order to understand their spatial learning and memory [52]. Alteration behavior is a measure of immediate spatial working memory, a form of short-term memory [53], and the number of arm entries serves as an indicator of locomotor activity [54]. In the present study, the Scop group demonstrated an increase in locomotor activity, as evidenced by a significant increase in the number of arm entries compared with the control group, in addition to a significant decrease in short-term memory performance, as demonstrated by the decreased spontaneous alteration percentage in relation to the control group. The administration of donepezil reversed the high locomotor activity and the low spontaneous alteration percentage. Treatment with TN (100 and 200 mg) showed a greater exploratory drive and that learning and short memory have been restored through the lowering of the locomotor activity and increasing the spontaneous alteration, thus ameliorating the decreased alteration behavior induced by Scop. Improvement in MWM and Y-maze measured parameters by treatment with TN (100 and 200 mg/kg) supported its beneficial effect in reestablishing the rats' spatial learning, memory and exploratory behavior, which may indicate TN's positive effects on postponing neurodegeneration. The fatty acid-enriched profile of TN extract could be associated with ameliorated spatial learning impairment, as tested by MWM. HE et al., [55] reported that maintaining high docosahexaenoic acid (DHA) levels in the brain, either endogenously or supplemented, significantly improved hippocampal neurogenesis, as represented by the higher number of proliferating neurons in addition to neurogenesis. Additionally, the flavonoids also contribute to the neuroprotective effects of tiger nuts.

For instance, luteolin, a major metabolite of TN, has been well-reported for its positive impact on the cognitive functions and spatial learning in an AD-induced-rat model [56]. Luteolin (at 10, 20 mg/kg) reduced the escape latency and the distance traveled in the Morris water maze, while the time spent in the target quadrant notably increased. Several studies have revealed that flavonoids such as luteolin exert this effect via the modulation of brain neurotransmitters acting on the cholinergic and glutamatergic systems [57].

It is well known that AD pathophysiology includes the formation of extracellular senile plaques, which consist of A $\beta$  peptide aggregates [58], that are responsible for cognitive decline, memory loss and significant inflammatory response [59]. Excessive production of the neurotoxic A $\beta$  peptide from the amyloid precursor protein (APP) cleavage is done by  $\beta$ -secretase, which is the rate-limiting enzyme in this process [60]. Therefore, the down-regulation of the  $\beta$ -secretase expression inhibits A $\beta$  generation [61]. In our study, the Scop up-regulated the hippocampal A $\beta$  and  $\beta$ -secretase expression compared with the control group. The administration of donepezil significantly lowered the A $\beta$ 1-42 and  $\beta$ -secretase expression, which correlates with the study of Patel and his colleagues [62]. Interestingly, the A $\beta$ 1-42- and  $\beta$ -secretase-lowering effects of TN at the doses of 50–200 mg were nearly comparable with those of the donepezil-treated group, which may suggest a beneficial effect of TN in decreasing the disease burden.

Furthermore, the accumulation of A $\beta$  plaques can overstimulate microglia, which produce extensive amounts of pro-inflammatory cytokines (TNF- $\alpha$  and IL-1 $\beta$ ), eliciting a cascade of neuroinflammation that mediate neurotoxicity and eventually AD [59]. In the present study, Scop induced a strong inflammatory response through the up-regulation of TNF- $\alpha$  and IL-1 $\beta$  levels in the hippocampus of rats. Treatment with donepezil alleviated the Scop-induced neuroinflammation by diminishing the TNF- $\alpha$  and IL-1 $\beta$  levels, signifying anti-inflammatory properties. These results correlate with previously demonstrated data [63,64]. TN (50, 100 and 200 mg/kg) treatment managed to mitigate Scop-induced neuroinflammation, suggesting the significant anti-inflammatory activity of TN, which was also reported for other *Cyperus* species [46] in a dose-dependent manner. The decrease in the pro-inflammatory cytokines may also prevent the over-activation of the hippocampal cells, thus can diminish A $\beta$  accumulation [59]. This promising neuroprotective effect could be offered by the fatty acids as represented by linolenic acid, with a reported ameliorative effect on A $\beta$ -induced glial-cell-mediated neuroinflammation and cognitive dysfunction in mice [65]. On the other hand, several mechanisms were postulated regarding the potential of flavonoids for decreasing A $\beta$  accumulation [66]. This includes exerting an anti-amyloidogenic activity, interfering with the hyperphosphorylation of tau proteins and  $\beta$ -secretase inhibition [66]. Further, certain flavonoids, such as myricetin, quercetin, catechin and luteolin, are capable of modulating the signaling pathways implicated in neurodegeneration as represented by glycogen synthase kinase-3 $\beta$  (GSK-3 $\beta$ ), phosphatidylinositol-3-kinase/ protein kinase B (PI3K/Akt), tyrosine kinase and the mitogen-activated protein kinase (MAPK) pathways [67–69].

A $\beta$  peptide is documented to be associated with reactive oxygen species' generation, leading to the aggregation of A $\beta$  and plaque formation [70]. Oxidative stress elicits lipid peroxidation, together with decreased GSH and antioxidant enzymes, which leads to cholinergic neuronal damage and cognitive dysfunctions [71]. Oxidative stress is among the fundamental mechanisms of cell damage following the administration of Scop [72]. In our study, Scop produced a state of oxidative stress, revealed by the dramatic elevation in the hippocampal MDA level, a reliable oxidative stress marker, and the significant decline in hippocampal anti-oxidative defenses, which are GSH, SOD and CAT activities. Donepezil succeeded in decreasing hippocampal MDA and in increasing hippocampal GSH, SOD and CAT activity, indicating an increase in antioxidant defenses in the brain. These outcomes were apparently relevant with previous studies [73,74]. However, TN did not enhance antioxidant activity in all its measured parameters, where only TN (200 mg/kg) decreased the elevated hippocampal MDA, while TN (100 and 200 mg/kg) elevated the SOD and CAT activity only. This antioxidant effect is in part due to the flavonoid content. Several



mechanisms of action were assigned for plant flavonoids, to include radical scavenging activity, enhancing the antioxidant enzymes while suppressing the oxidases in addition to metal chelation [75]. In the same context, Moghaddam et al., [76] reported the potential of hesperitin for increasing the antioxidant enzymes, as represented by SOD, CAT, glutathione peroxidase and glutathione reductase, thus resulting in the alleviation of the oxidative stress in the hippocampus.

In the present study, Scop-treated rats showed an increase in hippocampal AChE activity, leading to cognitive impairment and memory loss, as in tune with previously documented data [77], causing amplified acetylcholine degradation and impairment in learning and memory. Donepezil and its metabolites are reversible AChE inhibitors [78]. The administration of donepezil and TN (100 and 200 mg/kg) managed to increase cholinergic activity and to reverse the impairment of cognitive function through the inhibition of hippocampal AChE activity. These results suggest that TN could inhibit cholinergic neuronal loss and cognitive impairment. Long chain polyunsaturated fatty acids (LC-PUFA) constitute an integral part of the brain neuronal composition [79]. Alpha-linolenic acid (ALA, *n*-3) is converted in vivo to eicosapentaenoic acid (EPA) and DHA. Interestingly, the supplementation of DHA has been reported to improve cholinergic transmission in animal models [80]. Additionally, ALA has been recognized as a potential dietary AChE inhibitor [81]. On the other hand, several flavonoids, such as luteolin and naringenin, are able to provoke AChE inhibitory activity as reported both in animal models or in vitro studies [82,83]. This is quite relevant due to the presence of several flavonoids in the extract used, such as luteolin, cirsimaritin, apigenin, kaempferide, naringenin, kaempferol, isokaempferide and various derivatives of these. Flavonoids have the ability to inhibit the activity of cholinesterases, including AChE, butyrylcholinesterase and  $\beta$ -secretase, that are implicated in neuroprotective and cognitive functions. This family of phenolic compounds has shown that they can interact with several signaling protein pathways, such as PI3-kinase/Akt and ERK, and can modulate their actions, leading to biological benefits related to neuroprotection [27,28,83].

Previous persuasive data has proved that apoptotic mechanisms are a part of AD progression that are elicited by oxidative stress and inflammation. Thus, hindering both oxidative stress and inflammation and subsequently preventing apoptosis can account for diminishing neuronal damage and consequent cognitive impairment [84]. In the present study, Scop significantly up-regulated the hippocampal pro-apoptotic protein Bax mRNA level, which causes cell death [85], down-regulated the hippocampal anti-apoptotic Bcl2 mRNA level, which acts as an anti-apoptotic factor [86] and significantly up-regulated the Bax/Bcl2 ratio. Treatment with donepezil significantly reversed Scop-induced effects and managed to diminish the pro-apoptotic Bax mRNA level and the Bax/Bcl2 ratio and to increase the anti-apoptotic Bcl2 mRNA level. These results are consistent with the previous results [87,88]. The administration of TN extract (100 and 200 mg/kg) decreased the Bax mRNA overexpression, while all doses of TN extract (50, 100 and 200 mg/kg) promoted the Bcl2 mRNA expression, thus reducing the Bax/Bcl2 ratio, which indicates an anti-apoptotic effect.

Therefore, these results indicate that TN could ameliorate cognitive and memory dysfunction by diminishing A $\beta$  aggregates, some oxidative stress and inflammation and subsequently modifying neural apoptosis. Similarly, previous reports have demonstrated the inhibitory effect of the total flavonoids of *Scutellaria baicalensis* on neuronal apoptosis, as elicited by amyloid beta-peptide. This effect was evoked by the decreased expression of the pro-apoptotic protein Bax, cytochrome c and caspase-3, concurrent with the increased expression level of Bcl2, in a dose-dependent manner [89]. Regarding the lipid profile, n-3 fatty acids are well documented to maintain a healthy nervous system [90]. In a previous study by Ajami et al., [91], long-term administration (21 days) of a mixture of DHA and EPA supplements before inducing ischemia in the hippocampus of rats, increased the Bcl-2 expression level and decreased the Bax expression 48 h after ischemia, together with a reduced count of neuronal cell loss in the hippocampus.

The histopathological examination of sections from the Scop group revealed neurodegeneration, with extensive gliosis and neuronal loss, while treatment with donepezil showed minimal neurodegeneration and neuronal loss, with less gliosis. Sections from the TN (100 and 200 mg/kg) groups demonstrated marked neuroprotection, as evidenced by intact neurons with minimal neurodegeneration. However, diminished gliosis was obvious with the TN (200 mg/kg) extract.

## 4. Materials and Methods

### 4.1. Plant Material and Extraction

*Cyperus esculentus* L. rhizomes were purchased from a local market “Harraz”, Cairo, Egypt. The identity of the plant was confirmed by staff members at the Egyptian Agricultural Museum. A voucher specimen (20.5.2020.1) was deposited at the herbarium of Pharmacognosy Department, Faculty of Pharmacy, Cairo University, Cairo, Egypt. One Kg of tiger nut rhizomes were extracted by maceration, using ethanol (analytical grade, El-Gomhuria Chemical Company, Cairo, Egypt), being an inexpensive and simple conventional method for the extraction of plant material [92]. The filtered extract was then evaporated using a rotary evaporator and the resultant oily extract was kept in a refrigerator at  $-8\text{ }^{\circ}\text{C}$  for further analysis.

### 4.2. UHPLC-ESI-QTOF-MS Profiling

A solution at a concentration of 10 mg/mL was prepared from the dry extracts for analysis by mass-spectrometry coupled with liquid-chromatography. Specifically, samples were analysed using an ACQUITY UPLC H-Class System (Waters, Milford, MA, USA) coupled with a QTOF-MS (Synapt G2, Waters Corp., Milford, MA, USA). The chemical compounds were separated using a reversed-phase C18 analytical column (Agilent Zorbax Eclipse Plus, 1.8  $\mu\text{m}$ , 4.6  $\times$  150 mm) at 22  $^{\circ}\text{C}$ . The mobile phases were  $\text{H}_2\text{O}$  containing 0.5% of acetic acid and methanol as solvent A and B, respectively. The following mobile phase gradient was used in order to achieve an efficient separation: 0.0 min (A:B 100/0), 15.0 min (A:B 40/60), 33.0 min (A:B 0/100), 46.0 min (A:B 0/100) and 55.0 min (A:B 100/0). The flow rate and the injection volume were 400  $\mu\text{L}/\text{min}$  and 10  $\mu\text{L}$ , respectively. Detection was performed in an electrospray negative-ion mode (ESI-) over a range from 50 to 1200  $m/z$ . The MS acquisition was performed using two parallel scan functions by rapid switching, in which one scan was operated at a low collision energy in the gas cell (4 eV) and the other at an elevated collision energy ( $\text{MS}^E$  energy linear ramp: from 20 to 60 eV). Leucine enkephalin was injected continuously during the analysis for mass calibration at a concentration of 300 ng/mL. Other MS parameters were as follows: capillary voltage 2.2 kV, cone voltage 30 V; desolvation temperature 500  $^{\circ}\text{C}$ ; desolvation gas flow 700 L/h; cone gas flow 50 L/H; source temperature 100  $^{\circ}\text{C}$ ; scan duration 0.1 s, resolution 20000 FWHM.

### 4.3. UHPLC-ESI-QTOF-MS Data Processing

Firstly, the raw data files were transformed to an mzML format using MSConverGUI software [93]. The MS data were processed through the open-source software MZmine 2.53 [94,95]. A noise level of  $1.0 \times 10^3$  was selected. An ADAP chromatogram builder method was used under the following parameters: MS level: 1; min number of scans: 9; group intensity threshold:  $1.0 \times 10^3$ ; min highest intensity:  $1.0 \times 10^4$ ;  $m/z$  tolerance: 10 ppm. After that, the chromatogram was deconvoluted and was performed using the wavelets (ADAP) algorithm and the following parameters: S/N threshold: 50; min feature height:  $5 \times 10^4$ ; coefficient/area threshold: 110; peak duration range: 0.05–0.3 min; RT wavelet range: 0–0.30. An isotopic peak grouper algorithm was also applied ( $m/z$  tolerance: 10 ppm; RT tolerance: 0.02 min, maximum charge: 2). The obtained features were aligned between samples using the “Join Aligner” algorithm, an  $m/z$  tolerance of 10 ppm and a RT tolerance of 0.1 min. The molecular features, which were also detected in blank samples, were removed from the final dataset. Finally, the molecular formulas of the final features were predicted using Sirius 4.4.29 [96], and the biological identities were annotated by

comparing the MS/MS spectra of different databases (e.g., MoNA, Massbank, HMDB, FoodDB, etc.) with the fragments detected in the MS<sup>E</sup> scans.

#### 4.4. Biological Study

##### 4.4.1. Animals

Adult male Wistar rats (4 months old) weighing 150–200 g were provided by the animal facility of the Faculty of Pharmacy Cairo University, Egypt and were housed under controlled environmental conditions of constant temperature ( $22 \pm 2$  °C), relative humidity of  $60 \pm 10\%$ , and a light/dark cycle (12/12-h). The rats were fed with standard chow diet and water was provided ad libitum. The experimental protocol was approved by the Ethics Committee for Animal Experimentation (PT: 3081) and adheres strictly to the recommendations of the National Institutes of Health Guide for Care and Use of Laboratory Animals (2011).

##### 4.4.2. Drugs and Chemicals

Scop hydrobromide trihydrate and tween 80 were purchased from Sigma-Aldrich Co. (St Louis, MO, USA). Donepezil was purchased from Pfizer Pharmaceuticals Company (Cairo, Egypt). Scop was dissolved in a saline solution (0.9% NaCl) and injected intraperitoneally (i.p.) at a volume of 1 mL/kg. Donepezil was dissolved in saline and administrated orally (p.o.) at a volume of 5 mL/kg. All other chemicals were of the highest analytical grade.

##### 4.4.3. Experimental Design

As depicted in Figure 2a, the rats were acclimatized for 1 week and randomly divided into six groups, each containing 15 animals. The whole experimental schedule was followed for 14 consecutive days. Group I: rats received saline i.p. and 1% tween 80 p.o. for 14 days and served as the control group. Group II: rats received 1% tween 80 p.o. for 14 days and Scop (1 mg/kg, i.p.) 30 min before the behavioral experiments on all days of behavioral testing [97]. Group III: rats received donepezil (5 mg/kg, p.o.) dissolved in saline for 14 days [98] and Scop as group II and served as the standard drug group. Group IV: rats received TN extract (50 mg/kg, p.o.) suspended in 1% tween 80 for 14 days and Scop as group II. Group V: rats received TN extract (100 mg/kg, p.o.) for 14 days and Scop as group II. Group VI: rats received TN extract (200 mg/kg, p.o.) for 14 days and Scop as group II. Scop was administrated 1 h after vehicle or treatment administration and 30 min before the behavioral experiments on all days of behavioral testing. On the last day of injection (day 14), neurobehavioral tests were carried out, including the Morris water maze (MWM) and the Y-maze tests.

##### 4.4.4. Behavioral Assessments

###### Morris Water Maze Test

The MWM test is used to evaluate spatial learning and memory in animal models [99,100]. The maze consisted of a stainless-steel circular pool (210 cm in diameter, 51 cm high) divided into four equal quadrants and filled with water ( $26 \pm 2$  °C) to a depth of 35 cm. A black hidden escape platform was placed inside the target quadrant, 2 cm below the water surface. The platform was kept at a fixed position during the time of training. A non-toxic dye was added to make the water opaque so that the platform was made invisible. Memory acquisition trials (120 s/trial) were performed two times a day for four consecutive days, with an interval of at least 15 min between the trials. During each acquisition trial, animals were left free to explore the pool and to search for the hidden platform. Once the rat located the platform, it was left there for an additional 20 s to rest, while if an animal failed to reach the platform within 120 s it was gently guided to it and kept there for 20 s. The mean escape latency was calculated as the time taken by each rat to locate the hidden platform and was used as an index of acquisition or learning. On the fifth day, the rats were subjected to a probe-trial session where the platform was removed from the pool and each rat was

allowed to explore the pool for 60 s. The time spent by each rat in the target quadrant in which the hidden platform was previously placed was taken as an index of retrieval or memory.

#### Y-Maze Test

The Y-maze test is used to measure the spatial working memory in rodents [101]. The maze was composed of 3 identical arms, 40 cm long, 35 cm high and 12 cm wide, positioned at equal angles (labeled A, B and C). The rats were placed in the center of the Y-maze, facing the south arm B, and were allowed to move freely through the maze for a period of 5 min. Spontaneous alternation was examined by visually recording the pattern of entrance into each arm in the maze for each rat. Arm entry was scored when the hind paws of the rat were completely placed in the arm. Consecutive entry into the three arms on an overlapping triplet set was defined as spontaneous alternation, i.e., BCA, ABC or CAB. Accordingly, the alternation percentage was calculated as the number of spontaneous alterations  $\times 100$ /total number of entries.

#### 4.4.5. Brain Processing

Twenty-four hours after the end of the behavioral testing, rats were euthanized by cervical dislocation under light anesthesia and brains were rapidly dissected, washed with ice-cold saline and divided into three sets. In the first set ( $n = 3$ ), the brains were fixed in 10% (*v/v*) formalin for 24 h to perform histopathological staining. In the other sets, the hippocampi were rapidly dissected and stored at  $-80$  °C. The hippocampi from the rats in the second set ( $n = 6$ ) were homogenized in ice-cold physiological saline to prepare a 10% homogenate and used for ELISA and colorimetric assay. The hippocampi from the rats in the third set ( $n = 6$ ) were used for real-time PCR and Western blot analyses.

#### 4.4.6. Biochemical Measurements

##### Acetylcholinesterase Activity

According to the manufacturer's instructions, the hippocampal level of AChE activity was determined using an AChE assay kit (Abcam, Cambridge, UK). The AChE activity assay protocol uses 5,5-dithiobis 2-nitrobenzoic acid (DTNB) to quantify the thiocholine produced from the degradation of acetylthiocholine iodide by AChE. The absorption intensity of the DTNB adduct (412 nm) is proportional to the AChE activity. The results are expressed as U/mg protein.

##### Determination of Oxidative Stress Biomarkers

Malondialdehyde (MDA) was measured in the hippocampal homogenate by determining the thiobarbituric acid reactive substances, according to the method described by [102]. Moreover, the hippocampal glutathione (GSH) content was determined using Ellman's reagent, according to the method described by [103]. The results are expressed as nmol/mg protein and  $\mu\text{mol/mg}$  protein, respectively.

The activity of superoxide dismutase (SOD) and catalase (CAT) were measured colorimetrically in the hippocampal homogenate using commercially available kits (Bio-diagnostic kit, Giza, Egypt) as instructed by the manufacturer. The results are expressed as U/mg protein.

##### Enzyme-Linked Immunosorbent Assay

Hippocampal TNF- $\alpha$  and IL-1 $\beta$  levels were estimated using rat ELISA kits purchased from R&D Systems Inc. (Minneapolis, MN, USA). The procedures were performed according to the manufacturer's instructions. The results are expressed as pg/mg protein.

##### Quantitative Real-Time Polymerase Chain Reaction

Total RNA was extracted from hippocampal tissues using an RNeasy Kit (Qiagen, Valencia, CA, USA) and the purity of the obtained RNA was verified spectrophotometrically

by recording the optical density at 260/280 nm. Equal amounts of RNA were then reverse transcribed into cDNAs using an RT-PCR kit (Fermentas, Waltham, MA, USA) according to the manufacturer's guidelines. Quantitative RT-PCR was performed to assess the expression of the Bax and Bcl2 mRNAs using a SYBR Green PCR Master Mix (Applied Biosystems, Foster City, CA) according to the manufacturer's instructions. Briefly, 1 µg of total RNA was mixed with 50 µM oligo (dT) 20, 50 ng/µL random primers and 10 mM dNTP mix in a total volume of 10 µL. The primer sequences used in the present study are: Bax forward 5'CTGCAGAGGATGATTGCTGA3', Bax reverse: 5'CATCAGCTCGGGCACCTTTAG3', Bcl-2 forward 5'GCTACGAGTGGGATACTGG3', Bcl-2 reverse 5'GTGTGCAGATGCCGTTCA3' and β-actin forward 5'CGTTGACATCCGTAAAGACCTC3' and β-actin 5'reverse TAGGAGCCAGGGCAGTAATCT3'. The thermal cycler protocol consisted of an initial enzyme activation step at 95 °C for 5 min, followed by 40 cycles of 5 s of denaturation at 95 °C and 10 s of annealing/extension at 60 °C. The relative expression of the target gene was obtained using the  $2^{-\Delta\Delta CT}$  formula. All values were normalized to β-actin levels and presented as fold changes.

#### Western Blot Analysis

Hippocampal tissues were homogenized in a lysis buffer and the protein content was measured using a Bradford assay kit (Bio-Rad, USA). Briefly, equal amounts of protein (20 µg) were separated by SDS-PAGE and transferred to polyvinylidene difluoride membranes (Pierce, Rockford, IL) using a Bio-Rad Trans-Blot system. The membranes were blocked with a blocking solution composed of 20 mM Tris-Cl (pH 7.5), 150 mM NaCl, 0.1% Tween 20 and 3% bovine serum albumin and incubated overnight at 4 °C with one of the following primary antibodies (1:1000): Aβ (1–42), β-secretase 1 or β-actin obtained from Thermo Fisher Scientific Inc. (Rockford, IL). The filters were washed and subsequently probed with peroxidase-labeled secondary antibodies. Finally, the band intensity was analyzed using a ChemiDoc imaging system with Image Lab™ software version 5.1 (Bio-Rad Laboratories Inc., Hercules, CA, USA). The results were presented as arbitrary units after normalization to levels of the β-actin protein expression.

#### 4.4.7. Histopathological Examination

The brains were carefully removed, rinsed with ice-cold saline and immediately fixed with 10% neutral buffered formalin for 72 h. Samples were processed and dehydrated in serial grades of ethanol, cleared in xylene, then infiltrated and embedded into Paraplast plus tissue embedding media. Coronal brain sections were processed for paraffin embedding and 4 µm sections were cut by a rotary microtome and mounted on glass slides. Sections were then stained with hematoxylin and eosin (H&E) and examined under a light microscope. Nissl staining was also performed to demonstrate degenerated and intact neurons in the hippocampus. Sections were stained with Cresyl violet dye (1% w/v in water) for 5 min, air dried at room temperature for 1 h and then briefly immersed in alcohol. The average number of intact neurons was quantified from six random non-overlapping fields in the hippocampus in Nissl-stained tissue sections for each sample. All morphological examinations, photographs as well as quantitative analysis were recorded using a Full HD microscopic camera operated by Leica Microsystems (GmbH, Wetzlar, Germany).

#### 4.4.8. Statistical Analysis

The data are presented as the mean ± S.D. Data were analyzed using one-way ANOVA followed by the Tukey–Kramer multiple comparison test. GraphPad Prism software (version 7.04; GraphPad Software, Inc., San Diego, CA, USA) was used to perform the statistical analysis and to present the data. The level of significance was fixed at  $p < 0.05$  for all statistical tests.

## 5. Conclusions

The current study discusses the detailed metabolic profiling of *Cyperus esculentus*, which resulted in the putative annotation of 88 metabolites including saccharides, amino

acids, organic acids, fatty acids, phenolic compounds and flavonoids. In conclusion, it reveals that the TN extract can significantly attenuate Scop-induced memory impairments by diminishing A $\beta$  aggregates, as well as its anti-inflammatory, antioxidant, anti-apoptotic and anti-AChE activities. Therefore, TN may have immense therapeutic and prophylactic potential for the treatment of neurodegenerative cognitive impairment. The presence of polyphenols, especially flavonoids, as well as fatty acids in the TN extract could be correlated with the observed bioactive effects. Nevertheless, future studies are needed to isolate the active ingredient(s) and to reveal the corresponding potential mechanism of action.

**Author Contributions:** Conceptualization, F.R.S. and R.H.S.; methodology, F.R.S., Á.F.-O., M.M.S., R.I.N., A.K.E., M.d.I.L.C.-G., F.J.L.-J. and R.H.S.; software, F.R.S. and Á.F.-O.; validation, F.R.S. and Á.F.-O.; formal analysis, F.R.S. and Á.F.-O.; investigation, F.R.S., Á.F.-O., M.M.S., R.I.N., A.K.E., M.d.I.L.C.-G., F.J.L.-J. and R.H.S.; resources, F.R.S. and A.S.-C.; data curation, F.R.S., Á.F.-O. and M.d.I.L.C.-G.; writing—original draft preparation, F.R.S., Á.F.-O., M.M.S., R.I.N., A.K.E. and R.H.S.; writing—review and editing F.R.S., Á.F.-O. and R.H.S.; visualization, F.R.S. and Á.F.-O.; supervision, F.R.S. and A.S.-C.; project administration, F.R.S. All authors have read and agreed to the published version of the manuscript.

**Funding:** This research received no external funding.

**Institutional Review Board Statement:** The experimental protocol was approved by the Ethics Committee for Animal Experimentation (PT: 3081), in 27/9/2021 and adheres strictly to the recommendations of the National Institutes of Health Guide for Care and Use of Laboratory Animals (2011).

**Informed Consent Statement:** Not applicable.

**Data Availability Statement:** Not Applicable.

**Acknowledgments:** Authors would like to thank Mohamed A. Khattab, Department of Cytology and Histology, Faculty of Veterinary Medicine, Cairo University, for his assistance in performing histopathological analysis. The authors M.d.I.L.C.-G. and Á.F.-O. would like to thank the Regional Ministry of Economy, Knowledge, Enterprise and Universities of Andalusia for the contract for Young Researchers (PAIDI) at the University of Granada. F.-J.L.-J. is thankful to the Spanish Ministry of Science and Innovation for the postdoctoral contract Juan de la Cierva-Formación (FJC2020-044298-I).

**Conflicts of Interest:** The authors declare no conflict of interest.

**Sample Availability:** Not Applicable.

## Abbreviations

A $\beta$ .	amyloid-beta
AD	Alzheimer's disease
AChE	acetylcholinesterase
ALA	alpha-linolenic acid
Bax	Bcl2-associated X protein
Bcl-2	B-cell lymphoma 2
CAT	catalase
DHA	docosahexaenoic acid
DTNB	5,5-dithiobis 2-nitrobenzoic acid
EPA	eicosapentaenoic acid
GSH	glutathione
GSK-3 $\beta$	glycogen synthase kinase-3 $\beta$
IL-1 $\beta$	interleukin 1 beta
LC-PUFA	long chain polyunsaturated fatty acids
MAPK	mitogen-activated protein kinase
MDA	malodialdehyde
MWM	Morris water maze
PI3K/AKT	phosphatidylinositol-3-kinase/protein kinase B
Scop	scopolamine
SOD	superoxide dismutase
TN	tiger nut
TNF- $\alpha$	tumor necrosis factor alpha
UHPLC-ESI-QTOF-MS	ultra performance liquid chromatography with electrospray ionization and quadrupole time-of-flight mass spectrometry

## References

- Fawzi, S.F.; Menze, E.T.; Tadros, M.G. Deferiprone ameliorates memory impairment in Scopolamine-treated rats: The impact of its iron-chelating effect on beta-amyloid disposition. *Behav. Brain. Res.* **2020**, *378*, 112314. [[CrossRef](#)] [[PubMed](#)]
- Thakur, A.K.; Kamboj, P.; Goswami, K.; Ahuja, K.J.J.A.P.R. Pathophysiology and management of Alzheimer's disease: An overview. *J. Anal. Pharm. Res.* **2018**, *9*, 226–235.
- Tang, K.S. The cellular and molecular processes associated with scopolamine-induced memory deficit: A model of Alzheimer's biomarkers. *Life Sci.* **2019**, *233*, 116695. [[CrossRef](#)]
- Aisen, P.S.; Cummings, J.; Jack, C.R.; Morris, J.C.; Sperling, R.; Frölich, L.; Jones, R.W.; Dowsett, S.A.; Matthews, B.R.; Raskin, J.J.A.s.r.; et al. On the path to 2025: Understanding the Alzheimer's disease continuum. *Alzheimer's Res. Ther.* **2017**, *9*, 60.
- Tiwari, S.; Soni, R.J.J.A.D.P. Alzheimer's disease pathology and oxidative stress: Possible therapeutic options. *J. Alzheimers. Dis Park.* **2014**, *4*, 162. [[CrossRef](#)]
- Shabani, S.; Mirshekar, M.A. Diosmin is neuroprotective in a rat model of scopolamine-induced cognitive impairment. *Biomed. Pharmacother.* **2018**, *108*, 1376–1383. [[CrossRef](#)] [[PubMed](#)]
- Fan, Y.; Hu, J.; Li, J.; Yang, Z.; Xin, X.; Wang, J.; Ding, J.; Geng, M. Effect of acidic oligosaccharide sugar chain on scopolamine-induced memory impairment in rats and its related mechanisms. *Neurosci. Lett.* **2005**, *374*, 222–226. [[CrossRef](#)] [[PubMed](#)]
- Kumar, A.; Singh, A.; Ekavali. A review on Alzheimer's disease pathophysiology and its management: An update. *Pharmacol. Rep.* **2015**, *67*, 195–203. [[CrossRef](#)] [[PubMed](#)]
- Gambo, A.; Da' u, A. Tiger nut (*Cyperus esculentus*): Composition, products, uses and health benefits—a review. *Bayero. J. Pure. Appl. Sci.* **2014**, *7*, 56–61. [[CrossRef](#)]
- Oderinde, R.; Tairu, O. Evaluation of the properties of yellow nutsedge (*Cyperus esculentus*) tuber oil. *Food Chem.* **1988**, *28*, 233–237. [[CrossRef](#)]
- Ejoh, R.A.; Djomdi; Ndjouenkeu, R. Characteristics of tigernut (*Cyperus esculentus*) tubers and their performance in the production of a milky drink. *J. Food Process. Preserv.* **2006**, *30*, 145–163. [[CrossRef](#)]
- Tackholm, V. *Students' flora of Egypt*, 2nd ed.; Cairo University Press: Cairo, Egypt, 1974.
- Obadina, A.; Oyawole, O.; Ayoola, A. Quality assessment of gari produced using rotary drier. In *Food Processing: Methods, Techniques and Trends*; VC, B., Ed.; Nova Science Publishers: New York, NY, USA, 2008.
- Arafat, S.M.; Gaafar, A.M.; Basuny, A.M.; Nassef, S.L. Chufa tubers (*Cyperus esculentus* L.): As a new source of food. *World Appl. Sci. J.* **2009**, *7*, 151–156.
- Yu, Y.; Lu, X.; Zhang, T.; Zhao, C.; Guan, S.; Pu, Y.; Gao, F. Tiger Nut (*Cyperus esculentus* L.): Nutrition, Processing, Function and Applications. *Foods* **2022**, *11*, 601. [[CrossRef](#)] [[PubMed](#)]
- Yeboah, S.O.; Mitei, Y.C.; Ngila, J.C.; Wessjohann, L.; Schmidt, J. Compositional and structural studies of the oils from two edible seeds: Tiger nut, *Cyperus esculentum*, and asiato, *Pachira insignis*, from Ghana. *Food Res. Int.* **2012**, *47*, 259–266. [[CrossRef](#)]
- Nofouzi, K.; Mahmudi, R.; Tahapour, K.; Amini, E.; Yousefi, K. *Verbascum speciosum* methanolic extract: Phytochemical components and antibacterial properties. *J. Essent. Oil Bear Plants* **2016**, *19*, 499–505. [[CrossRef](#)]
- Allahyari, S.; Pakbin, B.; Amani, Z.; Mahmoudi, R.; Hamidiyan, G.; Peymani, A.; Qajarbeygi, P.; Mousavi, S. Antiviral activity of *Phoenix dactylifera* extracts against herpes simplex virus type 1: An animal study. *Comp. Clin. Pathol.* **2021**, *30*, 945–951. [[CrossRef](#)]
- Nwosu, L.C.; Edo, G.I.; Ozgor, E. The phytochemical, proximate, pharmacological, GC-MS analysis of *Cyperus esculentus* (Tiger nut): A fully validated approach in health, food and nutrition. *Food Biosci.* **2022**, *46*, 101551. [[CrossRef](#)]
- Sánchez-Zapata, E.; Fernández-López, J.; Angel Pérez-Alvarez, J. Tiger nut (*Cyperus esculentus*) commercialization: Health aspects, composition, properties, and food applications. *Compr. Rev. Food Sci. Food Saf.* **2012**, *11*, 366–377. [[CrossRef](#)]
- Abimbade, S.F.; Oloyede, G.K.; Nwabueze, C.C. Antioxidant and toxicity screenings of extracts obtained from *Cyperus esculentus*. *Acad. Arena* **2014**, *6*, 77–83.
- Saber, F.R.; Mahrous, E.A. Novel Functional Foods From Plants of the Mediterranean Area: Biological, Chemical, Metabolomic Approaches. In *Reference Module in Food Science*; Ferranti, P., Ed.; Elsevier: Amsterdam, The Netherlands, In Press. [[CrossRef](#)]
- Sumner, L.W.; Amberg, A.; Barrett, D.; Beale, M.H.; Beger, R.; Daykin, C.A.; Fan, T.W.-M.; Fiehn, O.; Goodacre, R.; Griffin, J.L. Proposed minimum reporting standards for chemical analysis. *Metabolomics* **2007**, *3*, 211–221. [[CrossRef](#)]
- Jjarotimi, O.S.; Yinusa, M.A.; Adegbembo, P.A.; Adeniyi, M.D. Chemical compositions, functional properties, antioxidative activities, and glycaemic indices of raw and fermented tigernut tubers (*Cyperus esculentus* Lativum) flour. *J. Food Biochem.* **2018**, *42*, e12591. [[CrossRef](#)]
- Bazinnet, R.P.; Layé, S. Polyunsaturated fatty acids and their metabolites in brain function and disease. *Nat. Rev. Neurosci.* **2014**, *15*, 771–785. [[CrossRef](#)]
- Song, J.; Kim, Y.-S.; Lee, D.H.; Lee, S.H.; Park, H.J.; Lee, D.; Kim, H. Neuroprotective effects of oleic acid in rodent models of cerebral ischaemia. *Sci. Rep.* **2019**, *9*, 1–13. [[CrossRef](#)] [[PubMed](#)]
- Ayaz, M.; Sadiq, A.; Junaid, M.; Ullah, F.; Ovais, M.; Ullah, I.; Ahmed, J.; Shahid, M. Flavonoids as prospective neuroprotectants and their therapeutic propensity in aging associated neurological disorders. *Front. Aging. Neurosci.* **2019**, *11*, 155. [[CrossRef](#)] [[PubMed](#)]
- Kempuraj, D.; Thangavel, R.; Kempuraj, D.D.; Ahmed, M.E.; Selvakumar, G.P.; Raikwar, S.P.; Zaheer, S.A.; Iyer, S.S.; Govindarajan, R.; Chandrasekaran, P.N. Neuroprotective effects of flavone luteolin in neuroinflammation and neurotrauma. *Biofactors* **2021**, *47*, 190–197. [[CrossRef](#)] [[PubMed](#)]

29. Szwajgier, D.; Borowiec, K.; Pustelniak, K. The neuroprotective effects of phenolic acids: Molecular mechanism of action. *Nutrients* **2017**, *9*, 477. [[CrossRef](#)]
30. Marim, F.M.; Teixeira, D.C.; Queiroz-Junior, C.M.; Valiate, B.V.S.; Alves-Filho, J.C.; Cunha, T.M.; Dantzer, R.; Teixeira, M.M.; Teixeira, A.L.; Costa, V.V. Inhibition of Tryptophan Catabolism Is Associated With Neuroprotection During Zika Virus Infection. *Front. Immunol.* **2021**, *12*, 702048. [[CrossRef](#)]
31. Wang, J.; Song, Y.; Gao, M.; Bai, X.; Chen, Z. Neuroprotective effect of several phytochemicals and its potential application in the prevention of neurodegenerative diseases. *Geriatrics* **2016**, *1*, 29. [[CrossRef](#)]
32. Aljuhaimi, F.; Şimşek, Ş.; Özcan, M.M. Comparison of chemical properties of taro (*Colocasia esculenta* L.) and tigernut (*Cyperus esculentus*) tuber and oils. *J. Food Process Preserv.* **2018**, *42*, e13534. [[CrossRef](#)]
33. Bosch, L.; Alegria, A.; Farre, R. RP-HPLC determination of tiger nut and orgeat amino acid contents. *Food Sci. Technol. Int.* **2005**, *11*, 33–40. [[CrossRef](#)]
34. Soto Mayer, L. Phytochemical Analysis of the methanolic extract of tigernut, tuber of *Cyperus esculentus*, by ultra-high performance liquid chromatography coupled with electrospray ionization-quadrupole-time of flight-mass spectrometry (UHPLC/ESI-Q-TOF-MS). M.Sc. Thesis, Universidad CEU San pablo, Madrid, 2019.
35. Abd-ElGawad, A.M.; Elshamy, A.I.; Al-Rowaily, S.L.; El-Amier, Y.A. Habitat Affects the Chemical Profile, Allelopathy, and Antioxidant Properties of Essential Oils and Phenolic Enriched Extracts of the Invasive Plant *Heliotropium Curassavicum*. *Plants* **2019**, *8*, 482. [[CrossRef](#)] [[PubMed](#)]
36. Elshamy, A.I.; Farrag, A.R.H.; Ayoub, I.M.; Mahdy, K.A.; Taher, R.F.; Gendy, A.E.-N.G.; Mohamed, T.A.; Al-Rejaie, S.S.; Ei-Amier, Y.A.; Abd-ElGawad, A.M. UPLC-qTOF-MS phytochemical profile and antiulcer potential of *Cyperus conglomeratus* Rottb. alcoholic extract. *Molecules* **2020**, *25*, 4234. [[CrossRef](#)] [[PubMed](#)]
37. Sayed, H.M.; Mohamed, M.H.; Farag, S.F.; Mohamed, G.A.; Omobuwajo, O.R.; Proksch, P. Fructose-amino acid conjugate and other constituents from *Cyperus rotundus* L. *Nat. Prod. Res.* **2008**, *22*, 1487–1497. [[CrossRef](#)] [[PubMed](#)]
38. Sayed, H.M.; Mohamed, M.H.; Farag, S.F.; Mohamed, G.A. Phytochemical and biological investigations of *Cyperus rotundus* L. *Bull. Facult. Pharm. Cairo. Uni.* **2001**, *39*, 195–203.
39. Rocha, F.G.; de Mello Brandenburg, M.; Pawloski, P.L.; da Silva Soley, B.; Costa, S.C.A.; Meinerz, C.C.; Baretta, I.P.; Otuki, M.F.; Cabrini, D.A. Preclinical study of the topical anti-inflammatory activity of *Cyperus rotundus* L. extract (Cyperaceae) in models of skin inflammation. *J. Ethnopharmacol.* **2020**, *254*, 112709. [[CrossRef](#)] [[PubMed](#)]
40. El-Habashy, I.; Mansour, R.; Zahran, M.; El-Hadidi, M.; Saleh, N. Leaf flavonoids of *Cyperus* species in Egypt. *Biochem. Syst. Ecol.* **1989**, *17*, 191–195. [[CrossRef](#)]
41. Uysal, S.; Zengin, G.; Sinan, K.I.; Ak, G.; Ceylan, R.; Mahomoodally, M.F.; Uysal, A.; Sadeer, N.B.; Jekő, J.; Cziáky, Z. Chemical characterization, cytotoxic, antioxidant, antimicrobial, and enzyme inhibitory effects of different extracts from one sage (*Salvia ceratophylla* L.) from Turkey: Open a new window on industrial purposes. *RSC Adv.* **2021**, *11*, 5295–5310. [[CrossRef](#)]
42. Allan, R.; Wells, R.; MacLeod, J. Flavanone quinones from *Cyperus* species. *Tetrahedron Lett.* **1973**, *1*, 7–8. [[CrossRef](#)]
43. Farrag, A.R.H.; Abdallah, H.M.; Khattab, A.R.; Elshamy, A.I.; El Gendy, A.E.-N.G.; Mohamed, T.A.; Farag, M.A.; Efferth, T.; Hegazy, M.-E.F. Antiulcer activity of *Cyperus alternifolius* in relation to its UPLC-MS metabolite fingerprint: A mechanistic study. *Phytomedicine* **2019**, *62*, 152970. [[CrossRef](#)]
44. Innih, S.O.; Eluehike, N.; Francis, B. Effects of aqueous extract of *Cyperus esculentus* (tiger nut) on antioxidant status and hematological indices in the heart of cadmium-induced wistar rats. *Niger. J. Experiment. Clin. Biosci.* **2021**, *9*, 17. [[CrossRef](#)]
45. Sudha, T.S. Evaluation of anticonvulsant and antioxidant properties of *Cyperus esculentus* Linn. in various types of experimentally induced seizures in rats. *Int. J. Green Pharm.* **2021**, *14*(4), 381–387.
46. Hussein, J.S.; Medhat, D.; Abdel-Latif, Y.; Morsy, S.; Gaafar, A.A.; Ibrahim, E.A.; Al-kashef, A.S.; Nooman, M.U. Amelioration of neurotoxicity induced by esfenvalerate: Impact of *Cyperus rotundus* L. tuber extract. *Comparat Clin. Pathol.* **2021**, *30*, 1–10. [[CrossRef](#)]
47. Umukoro, S.; Okoh, L.; Igweze, S.C.; Ajayi, A.M.; Ben-Azu, B. Protective effect of *Cyperus esculentus* (tiger nut) extract against scopolamine-induced memory loss and oxidative stress in mouse brain. *Drug Metab. Person. Ther.* **2020**, *35*(3), 20200112. [[CrossRef](#)]
48. El-Marasy, S.A.; Abd-Elsalam, R.M.; Ahmed-Farid, O.A. Ameliorative effect of silymarin on scopolamine-induced dementia in rats. *Maced. Journal Med. Sci.* **2018**, *6*, 1215. [[CrossRef](#)] [[PubMed](#)]
49. Barai, P.; Raval, N.; Acharya, S.; Borisa, A.; Bhatt, H.; Acharya, N. Neuroprotective effects of bergenin in Alzheimer’s disease: Investigation through molecular docking, in vitro and in vivo studies. *Behav. Brain. Res.* **2019**, *356*, 18–40. [[CrossRef](#)]
50. Kim, M.-S.; Lee, D.Y.; Lee, J.; Kim, H.W.; Sung, S.H.; Han, J.-S.; Jeon, W.K. *Terminalia chebula* extract prevents scopolamine-induced amnesia via cholinergic modulation and anti-oxidative effects in mice. *BMC Complem Altern. Med.* **2018**, *18*, 1–11. [[CrossRef](#)] [[PubMed](#)]
51. Tucker, L.B.; Velosky, A.G.; McCabe, J.T. Applications of the Morris water maze in translational traumatic brain injury research. *Neurosci. Biobehav. Rev.* **2018**, *88*, 187–200. [[CrossRef](#)] [[PubMed](#)]
52. Birla, H.; Keswani, C.; Rai, S.N.; Singh, S.S.; Zahra, W.; Dilmashin, H.; Rathore, A.S.; Singh, S.P. Neuroprotective effects of *Withania somnifera* in BPA induced-cognitive dysfunction and oxidative stress in mice. *Behav. Brain Funct.* **2019**, *15*, 9. [[CrossRef](#)]
53. Sarter, M.; Bodewitz, G.; Stephens, D.N. Attenuation of scopolamine-induced impairment of spontaneous alternation behaviour by antagonist but not inverse agonist and agonist  $\beta$ -carbolines. *Psychopharmacology* **1988**, *94*, 491–495. [[CrossRef](#)]



54. Brinza, I.; Boiangiu, R.S.; Hancianu, M.; Cioanca, O.; Erdogan Orhan, I.; Hritcu, L. Bay Leaf (*Laurus Nobilis*, L.) Incense Improved Scopolamine-Induced Amnesic Rats by Restoring Cholinergic Dysfunction and Brain Antioxidant Status. *Antioxidants* **2021**, *10*, 259. [[CrossRef](#)]
55. He, C.; Qu, X.; Cui, L.; Wang, J.; Kang, J.X. Improved spatial learning performance of fat-1 mice is associated with enhanced neurogenesis and neurogenesis by docosahexaenoic acid. *Proc. Natl. Acad. Sci. USA* **2009**, *106*, 11370–11375. [[CrossRef](#)]
56. Wang, H.; Wang, H.; Cheng, H.; Che, Z. Ameliorating effect of luteolin on memory impairment in an Alzheimer's disease model. *Mol. Med. Rep.* **2016**, *13*, 4215–4220. [[CrossRef](#)] [[PubMed](#)]
57. Bakoyiannis, I.; Daskalopoulou, A.; Pergialiotis, V.; Perrea, D. Phytochemicals and cognitive health: Are flavonoids doing the trick? *Biomed. Pharmacother.* **2019**, *109*, 1488–1497. [[CrossRef](#)]
58. Selkoe, D.J.; Hardy, J. The amyloid hypothesis of Alzheimer's disease at 25 years. *EMBO Mol. Med.* **2016**, *8*, 595–608. [[CrossRef](#)]
59. Wang, W.-Y.; Tan, M.-S.; Yu, J.-T.; Tan, L. Role of pro-inflammatory cytokines released from microglia in Alzheimer's disease. *Annal. Transl. Med.* **2015**, *3*, 136.
60. Das, H.; Sarkar, S.; Paidi, R.K.; Biswas, S.C. Subtle genomic DNA damage induces intraneuronal production of amyloid- $\beta$  (1–42) by increasing  $\beta$ -secretase activity. *FASEB J.* **2021**, *35*, e21569. [[CrossRef](#)]
61. Fourriere, L.; Gleeson, P.A. Amyloid  $\beta$  production along the neuronal secretory pathway: Dangerous liaisons in the Golgi? *Traffic* **2021**, *22*, 319–327. [[CrossRef](#)]
62. Patel, P.; Shah, J.S. Effect of Vitamin D Supplementation on the Progression of Alzheimer's Disease in Rats: A Mechanistic Approach. *Res. Sq. Prepr.* **2021**. [[CrossRef](#)]
63. Djeuzong, E.; Kandeda, A.K.; Djiogue, S.; Stéphanie, L.; Nguedia, D.; Ngueguim, F.; Djientcheu, J.P.; Kouamouo, J.; Dimo, T. Antiamnesic and Neuroprotective Effects of an Aqueous Extract of *Ziziphus jujuba* Mill. (Rhamnaceae) on Scopolamine-Induced Cognitive Impairments in Rats. *Evid-Based Compl. Alt. Med.* **2021**, *2021*, 5577163. [[CrossRef](#)] [[PubMed](#)]
64. Kandeda, A.K.; Nguedia, D.; Ayissi, E.R.; Kouamouo, J.; Dimo, T. *Ziziphus jujuba* (Rhamnaceae) Alleviates Working Memory Impairment and Restores Neurochemical Alterations in the Prefrontal Cortex of D-Galactose-Treated Rats. *Evid-Based Compl. Alt. Med.* **2021**, *2021*, 6610864. [[CrossRef](#)] [[PubMed](#)]
65. Ali, W.; Ikram, M.; Park, H.Y.; Jo, M.G.; Ullah, R.; Ahmad, S.; Abid, N.B.; Kim, M.O. Oral administration of alpha linoleic acid rescues A $\beta$ -induced glia-mediated neuroinflammation and cognitive dysfunction in C57BL/6N mice. *Cells* **2020**, *9*, 667. [[CrossRef](#)]
66. Baptista, F.I.; Henriques, A.G.; Silva, A.M.; Wiltfang, J.; da Cruz e Silva, O.A. Flavonoids as therapeutic compounds targeting key proteins involved in Alzheimer's disease. *ACS Chem. Neurosci.* **2014**, *5*, 83–92. [[CrossRef](#)]
67. Schroeter, H.; Boyd, C.; Spencer, J.P.; Williams, R.J.; Cadenas, E.; Rice-Evans, C. MAPK signaling in neurodegeneration: Influences of flavonoids and of nitric oxide. *Neurobiol. Aging* **2002**, *23*, 861–880. [[CrossRef](#)]
68. Walker, E.H.; Pacold, M.E.; Perisic, O.; Stephens, L.; Hawkins, P.T.; Wymann, M.P.; Williams, R.L. Structural determinants of phosphoinositide 3-kinase inhibition by wortmannin, LY294002, quercetin, myricetin, and staurosporine. *Mol. Cell* **2000**, *6*, 909–919. [[CrossRef](#)]
69. Baier, A.; Szyzka, R. Compounds from Natural Sources as Protein Kinase Inhibitors. *Biomolecules* **2020**, *10*, 1546. [[CrossRef](#)] [[PubMed](#)]
70. Ahmad, W.; Ijaz, B.; Shabbiri, K.; Ahmed, F.; Rehman, S. Oxidative toxicity in diabetes and Alzheimer's disease: Mechanisms behind ROS/RNS generation. *J. Biomed. Sci. Eng.* **2017**, *24*, 1–10. [[CrossRef](#)]
71. Adedayo, B.C.; Jesubowale, O.S.; Adebayo, A.A.; Obboh, G. Effect of *Andrographis paniculata* leaves extract on neurobehavioral and biochemical indices in scopolamine-induced amnesic rats. *J. Food Biochem.* **2021**, *45*, e13280. [[CrossRef](#)]
72. Kouémou, N.E.; Taiwe, G.S.; Moto, F.C.; Pale, S.; Ngoupaye, G.T.; Njapdounk, J.S.; Nkantchoua, G.C.; Pahaye, D.B.; Bum, E.N. Nootropic and neuroprotective effects of *Dichrocephala integrifolia* on scopolamine mouse model of Alzheimer's disease. *Front. Pharmacol.* **2017**, *8*, 847. [[CrossRef](#)]
73. Sun, K.; Bai, Y.; Zhao, R.; Guo, Z.; Su, X.; Li, P.; Yang, P. Neuroprotective effects of matrine on scopolamine-induced amnesia via inhibition of AChE/BuChE and oxidative stress. *Metab. Brain Dis.* **2019**, *34*, 173–181. [[CrossRef](#)]
74. Pattanashetti, L.A.; Patil, B.M.; Hegde, H.V.; Kangle, R.P. Potential ameliorative effect of *Cynodon dactylon* (L.) pers on scopolamine-induced amnesia in rats: Restoration of cholinergic and antioxidant pathways. *Ind. J. Pharmacol.* **2021**, *53*, 50. [[CrossRef](#)]
75. Procházková, D.; Boušová, I.; Wilhelmová, N. Antioxidant and prooxidant properties of flavonoids. *Fitoterapia* **2011**, *82*, 513–523. [[CrossRef](#)]
76. Moghaddam, A.H.; Zare, M. Neuroprotective effect of hesperetin and nano-hesperetin on recognition memory impairment and the elevated oxygen stress in rat model of Alzheimer's disease. *Biomed. Pharmacother.* **2018**, *97*, 1096–1101.
77. Ishola, I.O.; Tota, S.; Adeyemi, O.O.; Agbaje, E.O.; Narender, T.; Shukla, R. Protective effect of *Cnestis ferruginea* and its active constituent on scopolamine-induced memory impairment in mice: A behavioral and biochemical study. *Pharm. Biol.* **2013**, *51*, 825–835. [[CrossRef](#)]
78. Zhao, J.; Ren, T.; Yang, M.; Zhang, Y.; Wang, Q.; Zuo, Z. Reduced systemic exposure and brain uptake of donepezil in rats with scopolamine-induced cognitive impairment. *Xenobiotica* **2020**, *50*, 389–400. [[CrossRef](#)]
79. Bruce, K.D.; Zsombok, A.; Eckel, R.H. Lipid Processing in the Brain: A Key Regulator of Systemic Metabolism. *Front. Endocrinol.* **2017**, *8*, 60. [[CrossRef](#)]

80. Lesa, G.M.; Palfreyman, M.; Hall, D.H.; Clandinin, M.T.; Rudolph, C.; Jorgensen, E.M.; Schiavo, G. Long chain polyunsaturated fatty acids are required for efficient neurotransmission in *C. elegans*. *J. Cell Sci.* **2003**, *116*, 4965–4975. [[CrossRef](#)]
81. Willis, L.M.; Shukitt-Hale, B.; Joseph, J.A. Dietary polyunsaturated fatty acids improve cholinergic transmission in the aged brain. *Genes Nutr.* **2009**, *4*, 309–314. [[CrossRef](#)]
82. Liu, Y.; Fu, X.; Lan, N.; Li, S.; Zhang, J.; Wang, S.; Li, C.; Shang, Y.; Huang, T.; Zhang, L. Luteolin protects against high fat diet-induced cognitive deficits in obesity mice. *Behav. Brain Res.* **2014**, *267*, 178–188. [[CrossRef](#)] [[PubMed](#)]
83. Uriarte-Pueyo, I.; Calvo, M.I. Flavonoids as acetylcholinesterase inhibitors. *Curr. Med. Chem.* **2011**, *18*, 5289–5302. [[CrossRef](#)]
84. Demirci, K.; Nazıroğlu, M.; Övey, İ.S.; Balaban, H. Selenium attenuates apoptosis, inflammation and oxidative stress in the blood and brain of aged rats with scopolamine-induced dementia. *Metab. Brain Dis.* **2017**, *32*, 321–329. [[CrossRef](#)] [[PubMed](#)]
85. Oyama, J.-i.; Maeda, T.; Sasaki, M.; Kozuma, K.; Ochiai, R.; Tokimitsu, I.; Taguchi, S.; Higuchi, Y.; Makino, N. Green tea catechins improve human forearm vascular function and have potent anti-inflammatory and anti-apoptotic effects in smokers. *Internal. Med.* **2010**, *49*, 2553–2559. [[CrossRef](#)]
86. Xu, Y.-Z.; Deng, X.-H.; Bentivoglio, M. Differential response of apoptosis-regulatory Bcl-2 and Bax proteins to an inflammatory challenge in the cerebral cortex and hippocampus of aging mice. *Brain Res. Bull.* **2007**, *74*, 329–335. [[CrossRef](#)]
87. Kim, Y.-J.; Kim, J.-H.; He, M.-T.; Lee, A.-Y.; Cho, E.-J. Apigenin Ameliorates Scopolamine-Induced Cognitive Dysfunction and Neuronal Damage in Mice. *Molecules* **2021**, *26*, 5192. [[CrossRef](#)]
88. Li, D.; Cai, C.; Liao, Y.; Wu, Q.; Ke, H.; Guo, P.; Wang, Q.; Ding, B.; Fang, J.; Fang, S. Systems pharmacology approach uncovers the therapeutic mechanism of medicarpin against scopolamine-induced memory loss. *Phytomedicine* **2021**, *91*, 153662. [[CrossRef](#)]
89. Wang, R.; Shen, X.; Xing, E.; Guan, L.; Xin, L. *Scutellaria baicalensis* stem-leaf total flavonoid reduces neuronal apoptosis induced by amyloid beta-peptide (25–35). *Neural Regen. Res.* **2013**, *8*, 1081.
90. Cutuli, D.; Pagani, M.; Caporali, P.; Galbusera, A.; Laricchiuta, D.; Foti, F.; Neri, C.; Spalletta, G.; Caltagirone, C.; Petrosini, L.; et al. Effects of Omega-3 Fatty Acid Supplementation on Cognitive Functions and Neural Substrates: A Voxel-Based Morphometry Study in Aged Mice. *Front. Aging Neurosci.* **2016**, *8*, 38. [[CrossRef](#)]
91. Ajami, M.; Eghtesadi, S.; Razaz, J.M.; Kalantari, N.; Habibe, R.; Nilforoushzadeh, M.A.; Zarrindast, M.; Pazoki-Toroudi, H. Expression of Bcl-2 and Bax after hippocampal ischemia in DHA+ EPA treated rats. *Neurol. Sci.* **2011**, *32*, 811–818. [[CrossRef](#)]
92. Farooq, S.; Mir, S.A.; Shah, M.A.; Manickavasagan, A. Chapter 2—Extraction techniques. In *Plant Extracts: Applications in the Food Industry*; Mir, S.A., Manickavasagan, A., Shah, M.A., Eds.; Academic Press: Cambridge, MA, USA, 2022; pp. 23–37. [[CrossRef](#)]
93. Adusumilli, R.; Mallick, P. Data conversion with ProteoWizard msConvert. In *Proteomics*, Humana Press: New York, 2017; 339–368. In *Proteomics*; Humana Press: New York, NY, USA, 2017; pp. 339–368.
94. Pluskal, T.; Castillo, S.; Villar-Briones, A.; Orešič, M. MZmine 2: Modular framework for processing, visualizing, and analyzing mass spectrometry-based molecular profile data. *BMC Bioinform.* **2010**, *11*, 1–11. [[CrossRef](#)]
95. Pluskal, T.; Korf, A.; Smirnov, A.; Schmid, R.; Fallon, T.R.; Du, X.; Weng, J.-K. CHAPTER 7 Metabolomics Data Analysis Using MZmine. In *Processing Metabolomics and Proteomics Data with Open Software: A Practical Guide*; The Royal Society of Chemistry: London, UK, 2020; pp. 232–254.
96. Dührkop, K.; Fleischauer, M.; Ludwig, M.; Aksenov, A.A.; Melnik, A.V.; Meusel, M.; Dorrestein, P.C.; Rousu, J.; Böcker, S. SIRIUS 4: Turning tandem mass spectra into metabolite structure information. *Nat. Methods* **2019**, *16*, 299–302. [[CrossRef](#)]
97. Aksoz, E.; Gocmez, S.S.; Sahin, T.D.; Aksit, D.; Aksit, H.; Utkan, T. The protective effect of metformin in scopolamine-induced learning and memory impairment in rats. *Pharmacol. Rep.* **2019**, *71*, 818–825. [[CrossRef](#)] [[PubMed](#)]
98. Ademosun, A.O.; Adebayo, A.A.; Popoola, T.V.; Oboh, G. Shaddock (*Citrus maxima*) peels extract restores cognitive function, cholinergic and purinergic enzyme systems in scopolamine-induced amnesic rats. *Drug Chem. Toxicol.* **2022**, *45*, 1073–1080. [[CrossRef](#)] [[PubMed](#)]
99. Sayed, R.H.; Ghazy, A.H.; Yammany, M.F.E. Recombinant human erythropoietin and interferon-beta-1b protect against 3-nitropropionic acid-induced neurotoxicity in rats: Possible role of JAK/STAT signaling pathway. *Inflammopharmacology* **2022**, *30*, 667–681. [[CrossRef](#)] [[PubMed](#)]
100. Nunez, J. Morris Water Maze Experiment. *J. Vis. Exp.* **2008**, *19*, 897. [[CrossRef](#)]
101. Biggan, S.L.; Beninger, R.J.; Cockhill, J.; Jhamandas, K.; Boegman, R.J. Quisqualate lesions of rat NBM: Selective effects on working memory in a double Y-maze. *Brain Res. Bull.* **1991**, *26*, 613–616. [[CrossRef](#)]
102. Mihara, M.; Uchiyama, M. Determination of malonaldehyde precursor in tissues by thiobarbituric acid test. *Anal. Biochem.* **1978**, *86*, 271–278. [[CrossRef](#)] [[PubMed](#)]
103. Beutler, E.; Duron, O.; Kelly, B.M. Improved method for the determination of blood glutathione. *J. Lab. Clin. Med.* **1963**, *61*, 882–888.



Review

# Uncovering the Anticancer Potential of Polydatin: A Mechanistic Insight

Muhammad Ajmal Shah <sup>1,\*</sup>, Ayesha Hamid <sup>2</sup>, Hafiza Ishmal Faheem <sup>2</sup>, Azhar Rasul <sup>3</sup>, Tourki A. S. Baokbah <sup>4</sup>, Muhammad Haris <sup>5</sup>, Rimsha Yousaf <sup>2</sup>, Uzma Saleem <sup>2</sup>, Shabnoor Iqbal <sup>3</sup>, Maria Silvana Alves <sup>6</sup>, Zahid Khan <sup>7</sup>, Ghulam Hussain <sup>8</sup>, Ifat Alsharfi <sup>9</sup>, Haroon Khan <sup>10</sup> and Philippe Jeandet <sup>11,\*</sup>

<sup>1</sup> Department of Pharmacy, Hazara University, Mansehra 21300, Pakistan

<sup>2</sup> Faculty of Pharmaceutical Sciences, Government College University, Faisalabad 38000, Pakistan

<sup>3</sup> Department of Zoology, Faculty of Life Sciences, Government College University, Faisalabad 38000, Pakistan

<sup>4</sup> Department of Medical Emergency Services, College of Health Sciences-AIQunfudah, Umm Al-Qura University, Makkah 21955, Saudi Arabia

<sup>5</sup> Faculty of Pharmaceutical Sciences, Universiteit Gent, Ghent 9000, Belgium

<sup>6</sup> Laboratory of Cellular and Molecular Bioactivity, Department of Pharmaceutical Sciences, Faculty of Pharmacy, Federal University of Juiz de Fora, Juiz de Fora 36036-900, Brazil

<sup>7</sup> Department of Pharmacognosy, Faculty of Pharmacy, Federal Urdu University of Arts, Science & Technology, Karachi 75300, Pakistan

<sup>8</sup> Department of Physiology, Faculty of Life Sciences, Government College University, Faisalabad 38000, Pakistan

<sup>9</sup> Department of Biology, Jamoum University College, Umm Al-Qura University, Makkah 21955, Saudi Arabia

<sup>10</sup> Department of Pharmacy, Abdul Wali Khan University Mardan, Mardan 23200, Pakistan

<sup>11</sup> Research Unit Induced Resistance and Plant Bioprotection, University of Reims Champagne-Ardenne, USC INRAe 1488, 51100 Reims, France

\* Correspondence: ajmalshah@hu.edu.pk (M.A.S.); philippe.jeandet@univ-reims.fr (P.J.)

**Citation:** Shah, M.A.; Hamid, A.; Faheem, H.I.; Rasul, A.; Baokbah, T.A.S.; Haris, M.; Yousaf, R.; Saleem, U.; Iqbal, S.; Alves, M.S.; et al. Uncovering the Anticancer Potential of Polydatin: A Mechanistic Insight. *Molecules* **2022**, *27*, 7175. <https://doi.org/10.3390/molecules27217175>

Academic Editor: Nour Eddine Es-Safi

Received: 4 August 2022

Accepted: 17 October 2022

Published: 23 October 2022

**Publisher's Note:** MDPI stays neutral with regard to jurisdictional claims in published maps and institutional affiliations.



**Copyright:** © 2022 by the authors. Licensee MDPI, Basel, Switzerland. This article is an open access article distributed under the terms and conditions of the Creative Commons Attribution (CC BY) license (<https://creativecommons.org/licenses/by/4.0/>).

**Abstract:** Polydatin or 3-O-β-D-resveratrol-glucopyranoside (PD), a stilbenoid component of *Polygonum cuspidatum* (Polygonaceae), has a variety of biological roles. In traditional Chinese medicine, *P. cuspidatum* extracts are used for the treatment of infections, inflammation, and cardiovascular disorders. Polydatin possesses a broad range of biological activities including antioxidant, anti-inflammatory, anticancer, and hepatoprotective, neuroprotective, and immunostimulatory effects. Currently, a major proportion of the population is victimized with cervical lung cancer, ovarian cancer and breast cancer. PD has been recognized as a potent anticancer agent. PD could effectively inhibit the migration and proliferation of ovarian cancer cells, as well as the expression of the PI3K protein. The malignancy of lung cancer cells was reduced after PD treatments via targeting caspase 3, arresting cancer cells at the S phase and inhibiting NLRP3 inflammasome by downregulation of the NF-κB pathway. This ceases cell cycle, inhibits VEGF, and counteracts ROS in breast cancer. It also prevents cervical cancer by regulating epithelial-to-mesenchymal transition (EMT), apoptosis, and the C-Myc gene. The objective of this review is thus to unveil the polydatin anticancer potential for the treatment of various tumors, as well as to examine the mechanisms of action of this compound.

**Keywords:** phenol compounds; polydatin; 3-O-β-D-resveratrol-glucopyranoside; breast cancer; cervical cancer; lung cancer; ovarian cancer

## 1. Introduction

Cancer, a multifactorial disease, is a rapidly growing condition in which cells grow abnormally and invade many parts of the body, showing a metastasis behavior. There are many types of cancer known so far [1]. Cancer of the breast, cervix, lungs, and ovaries are the most prevalent types of the disease. About 2.2 million new instances of lung cancer, 2.3 million new cases of breast cancer, and 0.6 million new cases of cervical cancer were detected globally in 2020. The number of new cases of ovarian cancer in 2018 was close

to 0.3 million [2–5]. Totally, 10 million deaths have been estimated in 2020 by cancer and it has become the most prominent cause of mortality. Breast cancer and lung cancer are the leading types of cancer, with increased cases worldwide. Treatment strategies include anticancer drugs, chemotherapy, immunotherapy, and hormonal treatments [6]. Various types of cancers respond to conventional drug therapies such as alkylating drugs, intercalating agents, topoisomerase inhibitors, antimitotic drugs, and antimetabolites as well as kinase inhibitors, but mutations assist the cell to develop resistance. Targeted chemotherapy is effective in some malignancies, but the side effects on normal cells and its high cost have limited its use. Immunotherapy and targeted monoclonal antibodies have also been recognized as successful approaches against specific cancers, but a restricted number of cancers can be totally treated using these curative methods. Unluckily, resistance to cancer therapies, side effects, and high cost continue to be challenging and increase the rate of increased mortality [7].

On the other hand, plants have been employed since ancient times for the extraction of their valuable bioactive compounds to promote the health and well-being of people [8]. Despite the pop up of synthetic therapeutic molecules, natural products are still in use for the mitigation and prevention of diseases [9]. Research is developing a means to find out phytochemicals from natural sources by utilizing different approaches [10]. Polydatin (PD), a compound belonging to the stilbene family [11–13], is extracted from the roots of *Polygonum cuspidatum* (Polygonaceae). PD is very famous in China because of its usage as a painkiller and febrifuge. The trans form of PD is well known for its high therapeutic potential [10]. The anticancer activity of PD is mediated by several mechanisms such as control of reactive oxygen species (ROS) [14] and suppression of the PI3K/AKT pathway [15]. In several investigations, PI3K/AKT inhibitors were found to improve the treatment effectiveness of 2-deoxy-D-glucose (2-DG) and PD [16,17]. Furthermore, PD has attracted a lot of attention because of its positive impact on glucose and lipid management [18]. PD has therefore enhanced 2-DG's anticancer effects via regulating glucose metabolism, blocking the PI3K/AKT, or through other pathways. PD has been investigated to reduce the growth of HeLa cells by causing these cells to enter the S phase, promote cell death, and lower AKT, mTOR PI3K, mRNA expression levels. It was also discovered that PD may limit cervical cancer HeLa cell proliferation and induce apoptosis, and the process could be linked to blockage of the PI3K/AKT/mTOR signaling pathway and gene downstream expression [15]. The anticancer potential of PD has been observed by many researchers by using different cell lines like liver, cervical, and nasopharyngeal cancer cell lines [10]. The objective of this review is thus to unveil PD anticancer potential for the treatment of various tumors, as well as to examine the mechanisms of action of this molecule.

## 2. Polydatin Chemistry and Biosynthesis

PD, also known as piceid (3-*O*- $\beta$ -D-resveratrol glucopyranoside), (*E*)-polydatin, trans-polydatin, (*E*)-piceid, is a monocrystalline substance that was first isolated from the roots and rhizome of *P. cuspidatum* Sieb. It is a stilbene derivative of the phytoalexin resveratrol (3,4',5-trihydroxystilbene), in which the glucoside group linked to position C-3 replaces the hydroxyl group (Figure 1). The trans isomers of stilbenes generally display a higher bioactivity than their cis isomer counterparts (Figure 1) [19]. Previously, scientists scrutinized this compound for its ability to help with heart- and liver-associated disorders [20,21].

The polyketide and phenylpropanoid routes are used to form PD. The first step in the production of PD is the deamination of phenylalanine by phenylalanine ammonia lyase (PAL), which affords cinnamic acid. Cinnamate-4-hydroxylase (C4H) subsequently hydroxylates cinnamic acid to produce *p*-coumaric acid. Coenzyme A (CoA) ligation then takes place through *p*-coumaroyl-CoA ligase activity. Finally, *p*-coumaroyl-CoA and three molecules of malonyl-CoA are combined together by stilbene synthase (STS) to produce resveratrol [22]. Transresveratrol can then be further metabolized to form additional stilbenoids, like polydatin, by the action of glucosyltransferases on resveratrol [23]. In-

terestingly, PD has also been produced on a small scale through microbial resveratrol transformation by the *Bacillus cereus* strain UI 1477 [24]. American pokeweed (*Phytolacca americana* L., Phytolaccaceae) cell suspension cultures have the ability to glucosylate transresveratrol and produce PD, as well [25]. An engineered *Escherichia coli* strain harboring tyrosine ammonia lyase, cinnamoyl/*p*-coumaroyl-coenzyme A ligase and stilbene synthase genes was used to produce PD [26].

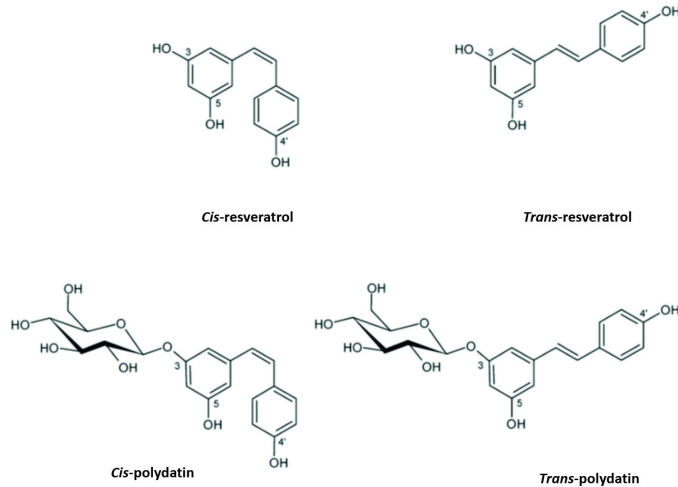


**Figure 1.** Resveratrol and polydatin isomers, trans and cis.

The most common dietary sources of PD are peanuts, dairy products, chocolate, and grapes [27,28]. The greatest PD concentrations were found in cocoa powder (7.14 µg/g), followed by semisweet chocolate baking chips (2.01 µg/g), dark chocolates (1.8 µg/g), milk chocolates (0.44 µg/g), and chocolate syrups (0.35 µg/g). Nevertheless, red wine may contain as much as 29.2 mg/L of PD [19]. The highest concentration of PD in mulberry roots was 3.15 µg/g fresh weight [29]. Since the glucoside content of PD typically exceeds that of the aglycone in red wine and other grape products, it has attracted a lot of interest, much more than resveratrol. The precise wine proportions of glycosylated to aglycone forms are affected by a variety of variables, including fermentation techniques and environmental conditions in the vineyards. Transresveratrol is found in red wine at concentrations of up to 14.3 mg/L and PD in concentrations of up to 29.2 mg/L, or about equal molar levels (60–70 µM) of the aglycone and the glucosylated form; white wine has 100 times less PD than red wine does [30]. In elaborating white wine, just the juice is fermented, whereas in making red wine, both the skins and the seeds are left on the juices until after fermentation is completed, leading to greater concentrations in the final product. Red grape skins typically have a higher PD content than white grape skins, but this can vary widely (from 50 to 200 mg/kg dry weight) across different varieties and vintages of the same variety of grape [31]. Spectrum analysis of eluting peaks from a HPLC system was used to determine the amounts of transpiceid, cispiceid, transresveratrol, and cisresveratrol in 36 different sorts of grape juices. Grape juices mostly included polydatin. The average levels of transpiceid, cispiceid, transresveratrol, and cisresveratrol in red grape juices were 3.38 mg/L, 0.79 mg/L, 0.50 mg/L, and 0.06 mg/L, respectively [32].

The Chinese resident meals guide recommends that adults consume 500 g of vegetables and 200 to 400 g of fruits daily; if we assume according to this recommendation by eating 200 g of celery, 100 g of chili pepper, 200 g of edible amaranth or leaf lettuce, 10 g of black soya beans, and one apple (200 g), then our daily PD intake would range from 100 to

1700 mg. The mulberry may increase our daily PD consumption to 3700 mg. The effective dose of PD intake can be around 2500–5000 mg/day for a 50 kg adult [33].

The presence of PD was first reported in the grape skin. Red, white, and grape juices are the main sources of PD, while *rosé* and effervescent wines mostly contain cisPD. Transresveratrol is more prevalent in grapes, berries, peanuts, and pistachios [34]. PD can also be found in a variety of fruit and vegetable foods, beer, cocoa-containing goods, and chocolate products (Figure 2) [35,36]

The primary source of PD is the roots and rhizomes of *Fallopia japonica*, which have a long history of use in traditional Chinese and Japanese medicines such as analgesics, antipyretics, diuretics, anticancers and expectorants, as well as in the treatment of atherosclerosis [37]. However, this compound is found in a number of other taxa, including *Rosa*, *Rumex*, *Picea*, *Malus*, and species of *Quercus* [38]. Peng et al. [35] used chromatographic techniques to quantify polydatin in fruits and vegetables. The polydatin contents of some vegetables and fruits are summarized in Table 1.

**Table 1.** Polydatin contents in vegetable and fruits samples.

Plant	Plant Organ	Solvent for Extraction	Polydatin Quantity ( $\mu\text{g}/100\text{g}$ )	References
Banana	Fruit	Methanol	1.70 $\mu\text{g}/100\text{g}$	[35]
Lychee	Fruit	Methanol	1.00 $\mu\text{g}/100\text{g}$	[35]
Pomegranate	Fruit	Methanol	7.56 $\mu\text{g}/100\text{g}$	[35]
Waterchestnut	Fruit	Methanol	0.50 $\mu\text{g}/100\text{g}$	[35]
Waxapple	Fruit	Methanol	1.58 $\mu\text{g}/100\text{g}$	[35]
Tomato	Fruit	Methanol	4.22 $\mu\text{g}/100\text{g}$	[35]
Chili pepper	Fruit	Methanol	14.47 $\mu\text{g}/100\text{g}$	[35]
Bell pepper	Fruit	Methanol	36.22 $\mu\text{g}/100\text{g}$	[35]
Grape	Fruit	Methanol	71.54 $\mu\text{g}/100\text{g}$	[35]
Gauva	Fruit	Methanol	0.72 $\mu\text{g}/100\text{g}$	[35]
Lemon	Fruit	Methanol	17.00 $\mu\text{g}/100\text{g}$	[35]
Strawberry	Fruit	Methanol	100 $\mu\text{g}/100\text{g}$	[35]
Orange	Fruit	Methanol	5.31 $\mu\text{g}/100\text{g}$	[35]
Mushroom	Fruit	Methanol	2.16 $\mu\text{g}/100\text{g}$	[35]
Pear	Fruit	Methanol	13.10 $\mu\text{g}/100\text{g}$	[35]
Soya bean	Fruit	Methanol	42.58 $\mu\text{g}/100\text{g}$	[35]
Gallic bulb	Fruit	Methanol	2.00 $\mu\text{g}/100\text{g}$	[35]
Chrysanthemum	Fruit	Methanol	5.20 $\mu\text{g}/100\text{g}$	[35]
Coca	Fruit	Methanol	7.56 $\mu\text{g}/100\text{g}$	[35]
White dammar	Leaves	Diethyl ether	0.22 mg/g	[38]
Peanut	Seeds	Ethanol	0.128 $\mu\text{g}/100\text{g}$	[39]
Cocoa	Seeds	Hexane	7.14 $\mu\text{g}/\text{g}$	[40]
Norway spruce	Phloem	Methanol	16 mg/g	[23]
Norway spruce	Bark	Methanol	1.3 mg/g	[23]

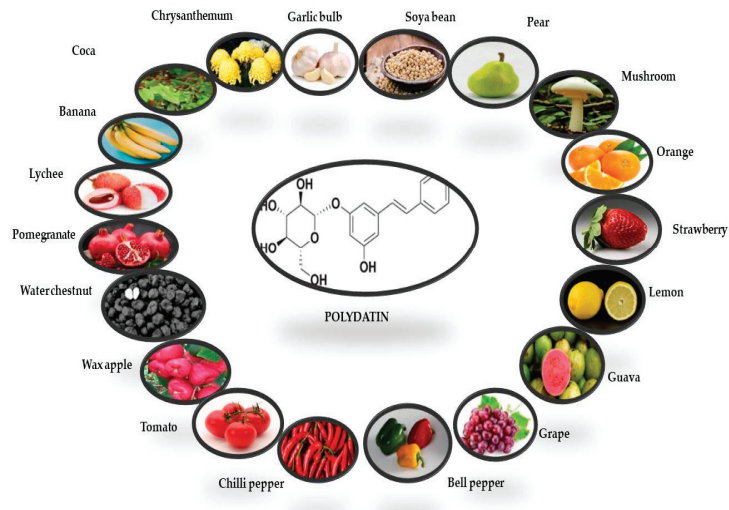


**Figure 2.** Potential dietary sources of polydatin derivative (transisomer). The quantities of PD in each fruit and vegetable have been derived from Peng et al. [35].

### 3. Role of Polydatin in Cancer

PD partly exerts its anticancer activity by enhancing antioxidant activity. PD, like other polyphenols, carries out strong antioxidant activity by neutralizing ROS and boosting the body's natural antioxidant defences. Its chemical structure of a long-conjugated system confers the compound its substantial antioxidant effects. The resistance of PD to enzymatic oxidation was found to be higher than that of resveratrol. It appears that many of the polydatin biological actions are mediated by antioxidant pathways. In vitro, PD displayed  $IC_{50}$  values of 87, 20, and 125  $\mu\text{g}/\text{mL}$  for scavenging of the free radicals ABTS (2,2'-Azino-bis (3-ethylbenzthiazoline-6-sulfonic acid), and DPPH (2,2-Diphenyl-1-(2,4,6-trinitrophenyl)-hydrazyl), and  $\bullet\text{O}_2$ , respectively [41]. The scavenging effect of PD increases in a dose-dependent manner (0.05–2  $\mu\text{M}$ ) in the phenanthroline- $\text{Fe}^{2+}$  system, and PD was shown to exhibit a scavenging activity of hydroxyl radicals more effective than those of resveratrol or vitamin C [42].

The earlier investigations from Yousef et al. [43] have reported that PD reduces ROS generation to protect the cell from oxidative stress. Therefore, oxidative stress was induced with  $\text{H}_2\text{O}_2$  in RINm5F cells, and these latter were treated either with or without PD (20 and 40  $\mu\text{g}/\text{mL}$ , 24 h), intracellular ROS being evaluated by the dichloro-fluorescein (DCF) assay. The mean fluorescence intensity (MFI) of cells treated with  $\text{H}_2\text{O}_2$  was significantly higher compared to cells treated with a negative control dye, suggesting a buildup of ROS. Treatment with PD (40  $\mu\text{g}/\text{mL}$ ) effectively mitigated the formation of ROS due to PD antioxidant properties. [43]. Yousef et al. [43] also depicted pancreatic lipid peroxidation as being significantly reduced in PD-treated diabetic rats as a consequence of an increase in the antioxidant enzymatic activity of catalase (CAT), superoxide dismutase (SOD), and GPx, following oral therapy with PD.

Otherwise, the anticancer activity of PD on tumor growth has been extensively studied in several cell culture and animal tumor models. Oncology has now been recognized as the most important area of concern in the field of cancer research [44]. Various approaches being used currently include chemotherapy, immune therapy, radiotherapy, surgery, drug combination, antibodies, and some others, all of them having their own side effects. Several researchers tried to combine different targeted cancer therapies to increase their effectiveness and more significantly hinder resistance to therapy; unfortunately, clinical trials have not shown satisfactory results [44]. PD has been recognized as a potent anticancer agent,



with the ability to regulate various signaling pathways involved in the progression of several kinds of cancers [45]. The mechanisms by which PD acts in cancer include cell cycle regulation, apoptosis, autophagy, signaling pathways, epithelial-to-mesenchymal transition (EMT), inhibition of inflammation and metastasis, and regulation of enzymes related to oxidative stress [46–48].

#### 4. Anticancer Activity of Polydatin on Liver, Colon, Bone, Breast, Lung, Cervical, and Ovarian Cancer Proliferation

##### 4.1. Liver Cancer

Cancers are the top cause of death for people worldwide, especially those who are 55 and older. Chemotherapy is still the best option for many types of cancer when surgery has been exhausted. Hepatocellular carcinoma (HCC), lung cancer, and breast cancer are just a few examples of the many tumors for which promising results have been obtained from the use of natural substances such as potential medications in recent years [49,50]. Primary HCC is a prevalent secondary malignancy in patients with cirrhosis and other chronic liver disorders. Among cancer-related fatalities, HCC ranks third [51]. Unfortunately, advanced HCC cannot be effectively treated with currently available chemotherapeutic drugs [50,52]. To this end, it is important to have more potent chemicals that might lead to new therapies for treating HCC, especially in its later stages. PD exhibited considerable cytotoxicity in a concentration- and time-dependent manner against HCC (hepatocellular carcinoma) cells at 100  $\mu\text{M}$  and 150  $\mu\text{M}$  concentrations, inducing apoptosis and limited G2/M cell cycle arrest while phosphorylated p-signal transducer and activator of transcription 3 (STAT3), p-Janus kinase 1 and (p)-protein kinase B (AKT) were downregulated [53]. PD may also induce apoptosis by increasing the Bax/Bcl-2 ratio and lowering the Wnt/-catenin signaling in SMMC-7721 and HepG2 cells, both of which are used for the modelling of hepatocellular cancer. Cancer metastasis is thought to be facilitated in large part by the invasion and migration of cancer cells. Treatment with PD inhibited the invasion and migration of HCC cells in two different assays: one measuring invasion and the other measuring wound healing [54]. This suggests that PD may be a useful natural small molecule medication for the treatment of liver cancer at an early stage.

##### 4.2. Colon Cancer

PD inhibited cell differentiation of CaCo-2 human colon cancer cells through inhibition of Hsp27 and vimentin expression (IC<sub>50</sub> values of 72 and 192  $\mu\text{M}$  for exponentially developing and postconfluent cells, respectively). After treatment with PD (240  $\mu\text{M}$ ), the cell cycle arrested at the G1 phase, coinciding with an increase in the cleaved poly-(ADP-ribose) polymerase. Both the total and phosphorylated versions of Akt were decreased though ERK1/2 phosphorylation and p21 expression, which were both enhanced in the CaCo-2 cell line [55]. The growth inhibition of Caco-2 intestinal epithelial cells exerted by PD was concentration-dependent (1–50  $\mu\text{M}$ ) and occurred via cell cycle arrest in the G0/G1 (10–25  $\mu\text{M}$ ) and apoptosis induction. Caco-2 cells treated with 50  $\mu\text{M}$  PD displayed DNA fragmentation, whereas those treated with 100  $\mu\text{M}$  resveratrol underwent apoptosis [56]. Use of flow cytometry and immunoblotting in the investigation by Bae et al. [57] showed that apoptosis was triggered by the disruption of calcium regulation and the expression levels of associated proteins in HT-29 and HCT116 cell lines. Both the MAPK and PI3K/AKT signaling pathways were shown to be downregulated by polydatin. It was also demonstrated that the combination of polydatin and 5-fluorouracil (5-FU) was effective in inhibiting drug resistance in 5-FU-resistant cells. Therefore, the results of this study support further research on PD in order to see whether or not it can be developed as a novel therapeutic agent for the treatment of colon cancer [57]. Polydatin significantly reduced cell growth and increased apoptosis in CRC cell lines [58]. It was shown that miR-382 specifically targets PD-L1. PD ability to upregulate miR-382 enables it to inhibit PD-L1 expression. Furthermore, PD regulates miR-382 to reduce CRC tumor development in vivo, where it suppresses tumor formation and induces death of CRC cells [58]. PD

suppressed cell growth in RPMI 8226 multiple myeloma cells through the mTOR/p70s6k signaling pathway [58]. The  $IC_{50}$  values for PD were 131  $\mu$ M and 93  $\mu$ M at 24 and 48 h, respectively in RPMI 8226 cells. At a concentration of 50  $\mu$ M, PD triggered apoptosis by upregulating caspase-3, caspase-9 and Bax levels and decreasing Bcl-2. The same concentrations also stimulated autophagy by increasing the expression of Beclin 1, Atg5, and LC3II. Phosphorylation of mTOR and p70s6 k was reduced [58].

#### 4.3. Bone Cancer

The child population has a higher incidence of osteosarcoma (OS) than any other primary bone tumor [59]. There are around 3.4 new instances per 1,000,000 persons each year [60,61], with men being more affected than women (5.4 per 100,000 vs. 4.0 per 100,000). Although osteosarcoma can affect any part of the skeleton, it most commonly occurs in the long bones (90%) and the knee (50%). Researches have shown that genetic and epigenetic alterations disrupt the normal differentiation process that begins with mesenchymal stem cells, leading to the development of OS [62]. PD-induced apoptosis was triggered by the downregulation of  $\beta$ -catenin signaling and the upregulated expressions of Bax/Bcl-2 and caspase-3 in MG63 and 143B OS cells at dose-dependent concentrations, and a significantly reduced cell growth was observed [63]. The effect of PD on osteosarcoma cells, both before and after radiation therapy, was described [64]. In these experiments, PD was found to reduce bone cancer progression. Polydatin significantly upregulated cell cycle arrest in S-phase and elevated bone alkaline phosphatase activity in vitro. Pretreatment with PD activated the Wnt/ $\beta$ -catenin pathway and enhanced osteogenic marker expression as well as decreasing tumor cell survival, demonstrating a radiosensitizing effect when combined with radiation therapy for OS [64].

#### 4.4. Breast Cancer

The class of cancer responsible for the highest mortality in women is breast cancer, (BC) which alone causes 25% of death in women as compared to other types of cancers [65]. The most common treatment used for breast cancer is chemotherapy, besides surgical and hormonal treatment [66]. Many factors including dysregulated autophagy, imbalanced apoptosis, changes in gene levels, and certain molecular signaling pathways are the leading causes of BC. These will be discussed one by one.

Uncontrolled cell division is also seen due to a disturbed cell cycle. The cell cycle consists of four major phases which are controlled by certain cyclin-dependent kinases (CDKs) and their partners, cyclins [67]. Sometimes, these CDKs and cyclins are upregulated or overexpressed leading to BC pathogenesis [68]. Upregulation of CDK2 and overexpression of cyclins E and B1 are observed in BC [69,70]. So, cell cycle arrest can be targeted for preventing BC progression. A transcription factor called Creb, which regulates many genes, plays a role in cell survival and multiplication [71]. Current research has also hypothesized that Creb is involved in the metastasis of cancerous cells, which means that its level is significantly increased in people suffering from BC [72]. Cyclin D1 plays a crucial role in the continuation of the cell cycle (Figure 3). To synthesize DNA, Cyclin D1 is required in a significant amount during the gap phase [73]. It is also necessary in the G2 phase for the continuation of the cell cycle [74]. It has been found that the phosphorylation process of Creb is compromised when treating BC cells with PD. So, the tumor-suppressing effect of PD appears to be due to its interference with Creb phosphorylation, which puts a lid on Cyclin D1 and thus terminates the cell cycle [75] (Figure 3).

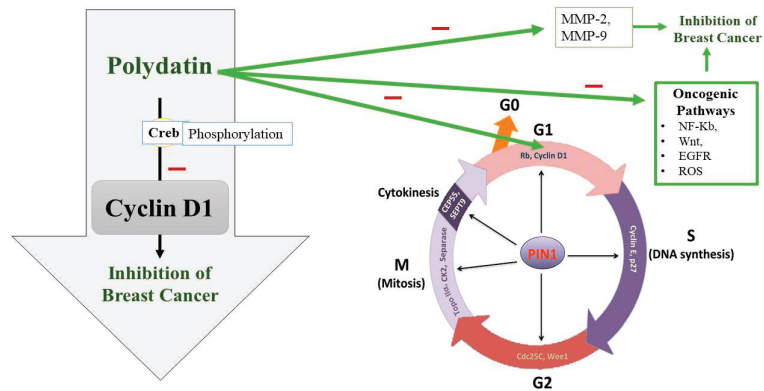


**Figure 3.** Polydatin (PD) potential to inhibit the G1 phase of the cell cycle along with other oncogenic pathways. PD appears to interfere with Creb phosphorylation, which downregulates Cyclin D1 and thus terminates the cell cycle at G1 phase and in turn inhibits breast cancer growth. PIN1: peptidyl-prolyl cis/trans isomerase, CEP55: Centrosomal protein 55, CK2: casein kinase 2, Rb: the retinoblastoma protein.

Another major factor responsible for breast cancer is the matrix metalloproteinase (MMP) as it disrupts ECM. MMP is responsible for blood supply to cancerous cells, and its activity is modulated via NF- $\kappa$ B [76]. MMP-2 and MMP-9 are known to disturb the extracellular matrix and also play a significant role in metastasis [77]. Moreover, a direct relationship has been found between the levels of vascular endothelial growth factor (VEGF) and the development of cancer. PD is known to counteract all these factors contributing to BC [78,79], as shown in Table 2. Zhang et al. [80] investigated the anticancer activity of PD on the breast cancer cell lines 4T1 and MCF-7 and observed that, compared to the control group, PD at 100  $\mu$ mol/L substantially suppressed cell growth and migration. Rising levels of the autocrine vascular VEGF are seen as a characteristic of cancer invasion in vitro. The results of Zhang et al. [80] showed that, as compared to the control, PD along with 2-Deoxy-D-glucose significantly suppressed MMP9, MMP2, and VEGF expression. Another major regulator of tumor progression is programmed cell death and apoptosis, which is utilized as a target for BC. Certain caspases like caspase-3,9 and apoptosis-related proteins such as Bcl-2 and Bax should be targeted [80,81]. Research has confirmed that by regulating proapoptotic and antiapoptotic proteins, PD causes cancer cell death [80]. Mitochondrial dysfunction and ROS production are also responsible for malignancy. ROS production is most commonly seen in triple-negative breast cancer (TNBC), thus it can be used as a target in the treatment of TNBC [82]. Certain signaling pathways which are oncogenic are upregulated by the overproduction of ROS like NF- $\kappa$ B, Wnt, MMPs, and EGFR [83–85]. ROS are involved in the upregulation of the PI3K/Akt pathway, which ultimately leads to prosurvival signaling. PD also acts as a free radical scavenger [86]. PD treatment thus balances the levels of free radicals within the body and also blocks the prosurvival signaling pathway [87,88] (Figure 4). The energy-making process of cancerous cells is aerobic glycolysis, which is required for their proliferation and migration [89]. To fulfill their energy demands, cancer cells require high levels of glucose, so glycolysis is one of the novel emerging targets of PD [90,91]. Hexokinase 2 (HK2) is an enzyme markedly expressed in cancerous cell glycolysis and which is targeted by PD [92]; PD decreases the levels of this enzyme. Uncontrolled expression of the hypoxia-inducible factor 1 $\alpha$  (HIF1 $\alpha$ ) is also a hallmark of cancer which prevents apoptosis. HIF1 $\alpha$  was also found to be impaired by PD [93–95]. In one study, the anticancer activity of PD was observed by giving it with D-glucose, using MCF-7, 4T1 cell lines. It was found that proliferation and metastasis was reduced. It was also demonstrated that its antioxidant activity was a major contributor in

the treatment of BC because of its ability to reduce ROS, and also by targeting PI3K/Akt pathway that is linked with ROS production [80] (Figure 3).

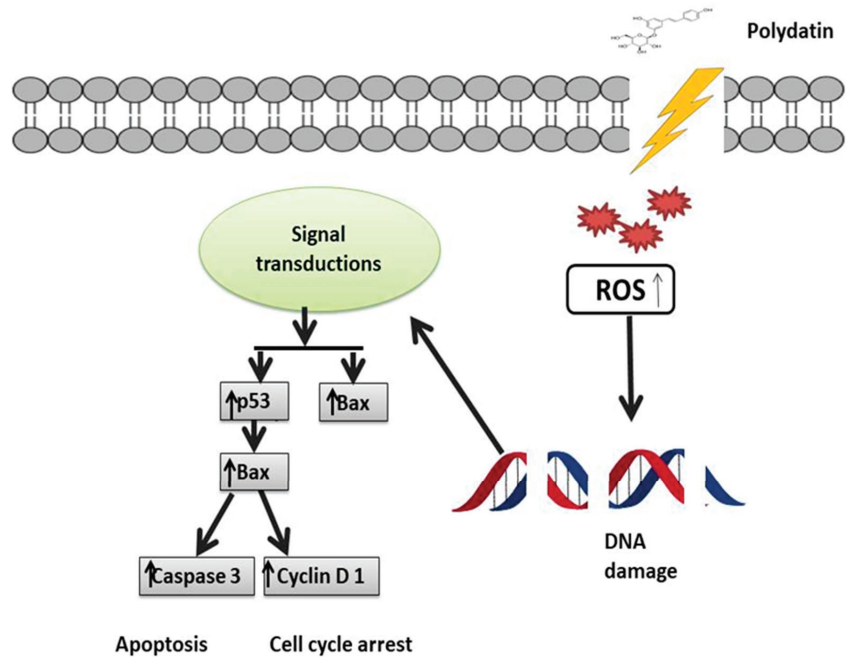


**Figure 4.** Mechanistic illustration of polydatin activity in the treatment of breast cancer through p53 activation. Activation of p53 leads to activation of p21 and Bax, which in turn leads to cell cycle arrest and apoptosis. ↑ Upregulation, ↓ Downregulation.

#### 4.5. Cervical Cancer

The fourth major reason for death among women is cervical cancer, which is more prevalent in developed countries [96]. Research has revealed that cervical cancer has a link to human papillomavirus (HPV). Smoking, HPV, early sexual activity, and genetic modifications lead to cervical cancer [97,98]. Undoubtedly, treatment options are available, but their outcomes are still uncertain, and there is a need to find other therapeutic alternatives [99–101]. PD is known to have anticancer potential and it can target some major factors involved in cervical cancer development [102–104]. The cell cycle is under the control of CDKs and cyclins, whose dysregulation leads to uncontrolled cellular multiplication [76]. Research has confirmed that PD causes cell cycle termination at the G0/G1 phase, upregulation of p21 and p27, and also induces repression of CDK4 and cyclin D1 [105]. One major factor affecting cell movement and invasion is EMT, which is controlled by several signaling pathways like NF- $\kappa$ B, MAPK, and other transcription factors [76]. During EMT, structural changes are seen in epithelial cells whose polarity is lost. Some proteins are linked with EMT, from which some are overexpressed and some are downregulated, leading to metastasis. The expression of these proteins is actually targeted by PD to prevent cell invasion, as shown in Table 2. PD causes upregulation of E-cadherin expression and downregulation of Snail and Slug expressions, thus impairing cell metastasis in cervical cancer as the switch from E-cadherin to N-cadherin, which plays a major role in the invasiveness of cancer [105–107]. Snail and Slug expressions also play a major role in cancer metastasis [108]. It is well-known that proto-oncogenes are involved in all the major types of cancers. The *c-Myc* gene is one of these specific genes which has been identified in cervical cancer. Along with cyclins and CDKs, the cell cycle is also

affected by the expression of the *c-Myc* gene [109] so that its expression can be targeted in treating cervical cancer. *C-Myc* overexpression is seen as a sign of cervical cancer [110]. *C-Myc* gene underexpression has been reported in CaSki and C33A cells after PD exposure, suggesting its possible use for ameliorating cervical cancer treatment [111,112]. A lot of proteins regulate the cell cycle whose expression is controlled by *c-Myc* by altering signaling pathways [113,114]. Downregulation of the *c-Myc* gene by PD will impair the overexpression of these proteins. Actually, the mechanism behind the regulation of the cell cycle by *c-Myc* is responsible for the downregulation of the expression of both *p21* and *p27* [115,116]. Both are tumor-suppressant genes that arrest the cell cycle during the gap and the synthesis phases. It is known that a particular CDK interacts with a particular cyclin, allowing the continuation of the cell cycle [117]. The CDK4-Cyclin D1 interaction causes cell proliferation but *p21* has the ability to stop the cell cycle by preventing this association [118] (Figure 5). The same effect is seen with *p21* and *p27* and CDK2-Cyclin E1 combinations, CDK2-Cyclin E1 also being a major contributor to cell cycle progress. PD was found to downregulate both *p21* and *p27* in cervical cancerous cells, thus stopping cell cycle progression [119]. The *c-Myc* gene also increases Snail and Slug expression, thus inhibiting N-cadherin, promoting E-cadherin, and leading to the prevention of the survival of cancer cells [120] (Figure 5). The anticancer potential of PD was observed on HeLa cell lines, and it was found that this stilbene decreases mRNA and protein expression levels of PI3K, AKT, mTOR, leading to apoptosis. It also causes cell death in cervical cancer by targeting the ROS/PI3K/AKT/mTOR pathway [121]. Another study was conducted by using female nude mice. PD (100 mg/kg) was given by injection and the results showed that the tumor size was small and its progression was also reduced [105] (Figure 5).

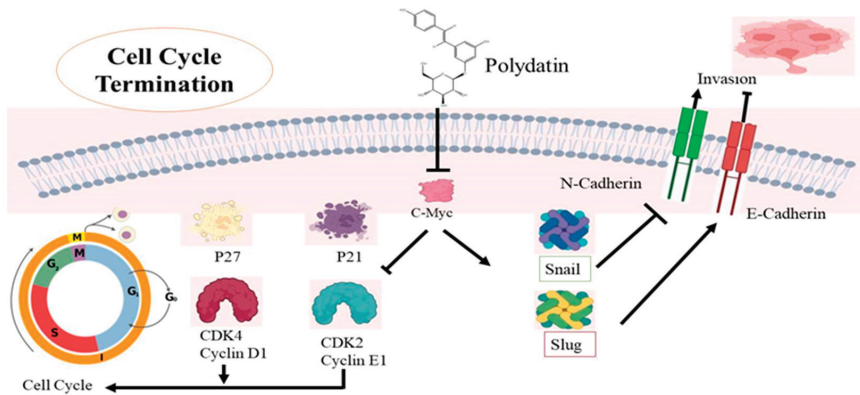


**Figure 5.** The mechanistic approach of polydatin (PD) activity in terminating cell cycle in cervical cancer cells. PD causes the downregulation of the *c-Myc* gene, which alters two mechanisms involved in cervical cancer. PD causes upregulation of *p21* and *p27*, and also induces repression of *CDK4* and *cyclin D1* as well as *CDK2* and *cyclin E1*; their dysregulation ultimately terminates the G<sub>0</sub>/G<sub>1</sub> phase of the cell cycle. In the second pathway, PD causes Snail and Slug expressions, leading to upregulation of E-cadherin expression and downregulation of N-cadherin, and thus impairing cell metastasis in cervical cancer.

Table 2. Anticancer activity of polydatin on different types of cancer.

Cancer Type	Cell Line	Type of Study	Concentrations of PD	Molecular Targets	Mechanism of Action	References
Breast cancer	MDA-MB-231 MCF-7	In vitro	2, 4, 6 $\mu$ M	$\uparrow$ p38 $\uparrow$ JUN $\uparrow$ ERK $\uparrow$ AKT	Promotes apoptosis by MAPK/ERK & P13K/AKT pathways	[122]
	4T1 MCF-7	In vitro	5.53 mmol/L 8.67 mmol/L	$\downarrow$ p-P13K/PI3K $\downarrow$ p-AKT/AKT	Inhibits P13K/AKT pathways	[80]
Cervical cancer	CaSki C33A	In vitro	0.1, 10,100, 500 $\mu$ M	$\uparrow$ p21 $\uparrow$ p27 $\downarrow$ Cdk4 $\downarrow$ Cdk2 Cyclin D1 $\downarrow$ Cyclin E1	Inhibits growth promoter proteins and cell cycle arrest	[105]
	HeLa	In vitro	50, 100, 150 $\mu$ mol/L	$\downarrow$ PI3K $\downarrow$ AKT $\downarrow$ mTOR P70S6K $\downarrow$ c-Myc	Induced apoptosis by suppression of PI3K/AKT/mTOR signaling	[15]
Lung cancer	A549 NCI-H1975	In vitro	6 $\mu$ mol/L	$\downarrow$ Bcl 2 $\uparrow$ Bax $\uparrow$ Cyclin D1	Cell cycle arrest and apoptotic pathway	[123]
	A549 and H1299 cells	In vitro		$\downarrow$ NLRP3 $\downarrow$ ASC $\uparrow$ pro-caspase-1 $\uparrow$ NF- $\kappa$ B $\uparrow$ p56	Promotes apoptosis and <i>NLRP3 inflammasome inhibition by NF-<math>\kappa</math>B</i>	[20]
Ovarian cancer	OVCAR-3, A2780, and HO-8910	In vitro	50 $\mu$ M	$\uparrow$ P13K $\uparrow$ AKT	AKT signaling	[124]
	SKOV-3 and OVCAR-8	In vitro	5, 10, 50, 100 $\mu$ M	$\downarrow$ Her-2 $\downarrow$ EGFR $\downarrow$ VEGF $\downarrow$ ERK $\uparrow$ PARP-1	Down/upregulation of various cell signaling molecules	[125]
Liver cancer	HCC cells	In vitro	100 $\mu$ M 150 $\mu$ M	$\downarrow$ G2/M Phase $\downarrow$ STAT3 $\downarrow$ AKT $\downarrow$ JAK1	Cell cycle arrest JAK1/STAT3 and P13K/AKT signaling	[53]
	HepG2 SMMC-7721	In vitro	1, 3, 10, 30, and 100 $\mu$ M	$\downarrow$ $\beta$ -catenin $\downarrow$ Bcl 2 $\uparrow$ Bax $\uparrow$ Caspase-3 $\uparrow$ Caspase-9	Apoptotic pathway	[80]
	HepG2	In Vitro	(10, 30, and 100 $\mu$ M)	$\downarrow$ Bcl 2 $\uparrow$ Bax $\downarrow$ Wnt	Wnt signaling Apoptotic pathway	[54]
Colon carcinoma	CaCo-2	In vitro	1–50 $\mu$ M	$\downarrow$ DNA synthesis $\downarrow$ G0/G1	Cell cycle arrest	[56]
	Caco-2	In vitro	100 240 $\mu$ M	$\downarrow$ AKT $\uparrow$ PARP $\downarrow$ Erk-1 $\downarrow$ Erk-2	Regulation of Akt/PKB signaling	[55]

Table 2. Cont.

Cancer Type	Cell Line	Type of Study	Concentrations of PD	Molecular Targets	Mechanism of Action	References
Human myeloma cells	RPMI 8226	In vitro	50, 100, 200 $\mu\text{mol/L}$	↑ Caspase-3 ↑ Caspase-9 ↑ Bax ↓ mTOR/p70s6k	Apoptotic pathway	[58]
Osteosarcoma cells	143B MG63	In vitro	10, 30, 100 $\mu\text{M}$	↑ Caspase -3 ↓ Bcl 2 ↑ Bax ↓ $\beta$ -catenin	Regulation of Apoptotic pathway	[63]
Lukemia cells	MOLT-4	In vitro	1, 4 or 20 $\mu\text{M}$	↓ Cyclin D1 ↓ CYCLIN B1 ↓ Bcl2	Cell cycle arrest and apoptotic pathway	[126]
Nasal carcinoma	CNE	In vitro	5, 10, 20 $\mu\text{M}$	↓ AKT ↑ Endoplasmic Reticulum stress ↑ Caspase 3 ↑ Caspase 4 ↑ Caspase 9	Regulation of apoptotic pathway molecules	[127]
Laryngeal cancer	AMC-HN-8 cells	In vitro	2, 4, 6 $\mu\text{M}$	↓ PDGF-B ↓ Ki67 ↓ Bcl 2 ↑ Bax ↓ Akt	Regulation of apoptotic pathway and Akt signaling molecules	[128]

NF-KB: Nuclear Factor kappa-light-chain-enhancer of activated B cells, Wnt: Wingless/Integrated, EGFR: Epidermal growth factor receptor, MMP: Matrix metalloproteinase, VEGF: Vascular endothelial growth factor, ROS: Reactive oxygen species, EMT: Epithelial-to-mesenchymal transition, Bcl-2: B-cell lymphoma 2, Bax: BCL2 associated X apoptosis regulator, NLRP3: NLR family pyrin domain containing 3, PI3K: Phosphatidylinositol 3-kinase, PD: Polydatin, Akt: Serine/threonine kinase 1, mTOR: Mammalian target of rapamycin, ERK: Extracellular signal-regulated kinase, PARP: poly adenosine diphosphate-ribose polymerase. ↑ Upregulation, ↓ Downregulation.

#### 4.6. Lung Cancer

Lung cancer, a growing health problem worldwide was found to be the most common type of cancer compared to other cancers [129]. Its prevalence and increase in mortality are strongly related to the history of smoking [130]. Many treatments such as targeted chemotherapies, radiotherapies, and surgery are used to cure lung cancer but despite advancements in these therapies, lung cancer still remains antagonistic in nature with poor survival rate. Chemotherapy is used recurrently against lung cancer in progressive stages but with deleterious consequences for patients [131]. Lung cancer cells treated with doses till 6  $\mu\text{M}$  PD, showed a dose-dependent reduction in Bcl-2 and cyclin D1 levels as well as an increase in Bax, leading to cell cycle arrest at the S phase. Interestingly, the human non-cancerous nasopharyngeal cell line exhibited lower cytotoxicity when exposed to PD. This was also corroborated by several researchers [132]. A recent study found that PD is advantageous for lung cancer inhibition [132]. The initiation of apoptosis in lung cancer cells is considered a good anticancer target [133,134]. In cancer cells, the antiapoptotic protein Bcl-2 is not capable of forming heterodimeric complexes with the proapoptotic protein Bax, resulting in high Bax levels. Increased Bax/Bcl-2 ratios upregulate the release of cytochrome C from mitochondria into the cytosol, leading to caspase-3 stimulation and apoptosis activation [135,136]. Research has revealed that 6  $\mu\text{mol/L}$  of PD activates apoptosis in A549 lung cancer cell lines by impairing Bcl-2 levels and upregulating Bax levels [132] (Table 2). On the other hand, cell cycle arrest of the cancer cells is considered to be a potential target against cancer progression [137,138] (Figure 6). Cyclin D1 expression should be high for the normal initiation of DNA synthesis, while cyclin D1 levels should be

low during the S phase [139]. Overincrease in cyclin D1 expression has been reported in many cancers including lung cancer [140,141]. In recent in vitro studies, PD has been found to hamper lung cancer cell (A549 and NCI-H1975 cells) progression by decreasing cyclin D1 levels and arresting cells at the S phase [132] (Table 2). PD also exerts some antioxidant and anti-inflammatory activities by inhibiting secretion of inflammatory oxidative factors or by increasing the scavenging of free oxygen radicals [142]. In recent studies, NLRP3 (NLR family pyrin domain containing protein 3) inflammasome has been observed to take part in inflammation related to cancer and tumor progression. Thus, suppression of the NLRP3 inflammasome might also be an effective strategy in the treatment of lung cancer [143]. NF- $\kappa$ B pathway has been revealed to be the significant marker in NLRP3 inflammasome activation. Increased levels of TNF- $\alpha$  activates the NF- $\kappa$ B pathway which then upregulates the IL-1 $\beta$  and IL-18 levels, causing the activation of NLRP3 inflammasome. PD (50  $\mu$ M) has been shown to attenuate the multiplication and metastasis of human A549 and H1299 cell lines through suppression of the NLRP3 inflammasome by suppression of the NF- $\kappa$ B pathway [20] (Figure 6).

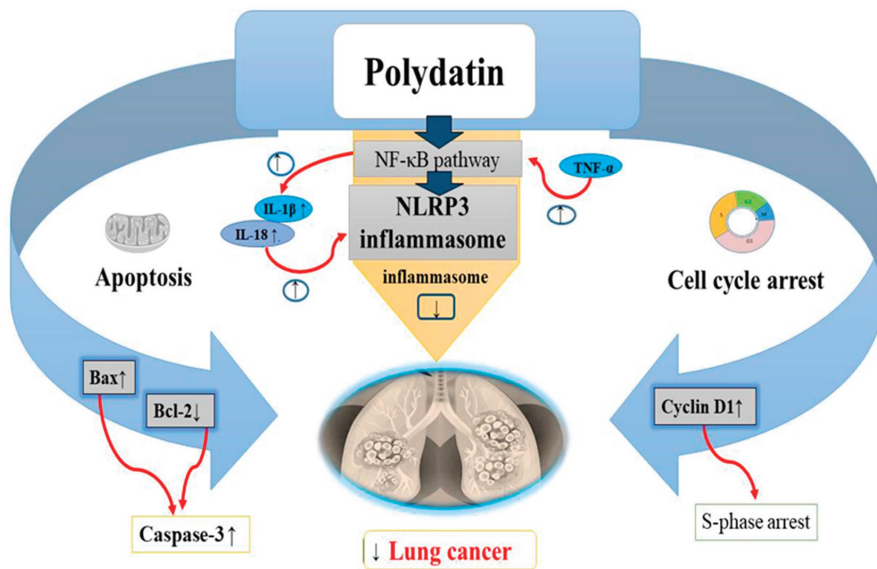


**Figure 6.** Anticancer effects of polydatin on lung cancer via the apoptotic pathway by increasing BAX levels, decreasing Bcl-2 levels and increasing caspase-3 levels, induction of cell cycle arrest at S phase by decreasing the cyclin D1 levels, and inhibition of the NLRP3 inflammasome by suppressing the NF- $\kappa$ B pathway in tumor cells. Upregulation  $\uparrow$  Downregulation  $\downarrow$ .

#### 4.7. Ovarian Cancer

Ovarian cancer is the most frequent cause of death among women within gynecological cancers worldwide [144]. Researchers have discovered in recent years that Chinese medicine displays a significant anticancer activity with fewer side effects as compared to synthetic drugs. PD ought to enhance ovarian cancer cell susceptibility to radiations, limit cell growth, and promote apoptosis. It has been found that PD has the potential to facilitate cancer cell apoptosis [145] (Table 2). PI3K signaling controls cell growth, death, and survival [146]. PD triggered apoptosis in cancer cells, namely ovarian cancer cells, and protected against inflammatory damage through the phosphoinositide, 3-kinase/protein kinase B/mammalian target of rapamycin (mTOR) pathway [75,147]. PD was able to successfully limit the growth of the ovarian cancer cell lines OVCAR-3, A2780 and HO-8910. There was a decrease in proliferation, migration and invasion after treatment with PD in



the cancer cell lines OVCAR-3, A2780, and HO-8910 [124]. In addition, PD inhibited PI3K, which in turn increased extracellular signaling and regulated ERK phosphorylation, thus inhibiting cancer cell growth [124] (Figure 7). The anticancer effect of PD was demonstrated by the downregulation of tumor suppressor genes via inhibition of the PI3K/Akt signaling and upregulation of bone morphogenetic protein 7 (BMP7) [127]. Inhibiting the proliferation, migration, and invasion of ovarian cancer cells is one of the main PD's effects [148]. PD prevents ovarian cancer cell proliferation, migration and invasion by inhibiting the expression of the PI3K protein, which is the cornerstone of ovarian cancer treatment. By decreasing EGFR phosphorylation and production of ERK and VEGF, PD inhibited the cellular aggregation of ovarian cancer cell lines in three dimensions. At concentrations of 5–100  $\mu\text{M}$ , PD was shown to suppress growth of the ovarian cancer cell lines SKOV-3 and OVCAR-8 by decreasing EGFR phosphorylation levels, which in turn increases the likelihood of the cells committing suicide. [149]. Earlier investigations utilising polydatin have suggested that this compound suppresses PI3K protein expression and blocks growth, migration and invasion of OVCAR-3, A2780 and HO-8910 cells. It appears that PI3K is the target of PD, since increasing PI3K protein expression greatly attenuates the inhibitory impact of PD on proliferation, migration and invasiveness of OVCAR-3, A2780 and HO-8910 cell lines. Experimental evidence supports the possible use of PD in the treatment of ovarian cancers because of its ability to suppress the growth, migration, and invasion of these cell lines by downregulating PI3K protein expression [124].

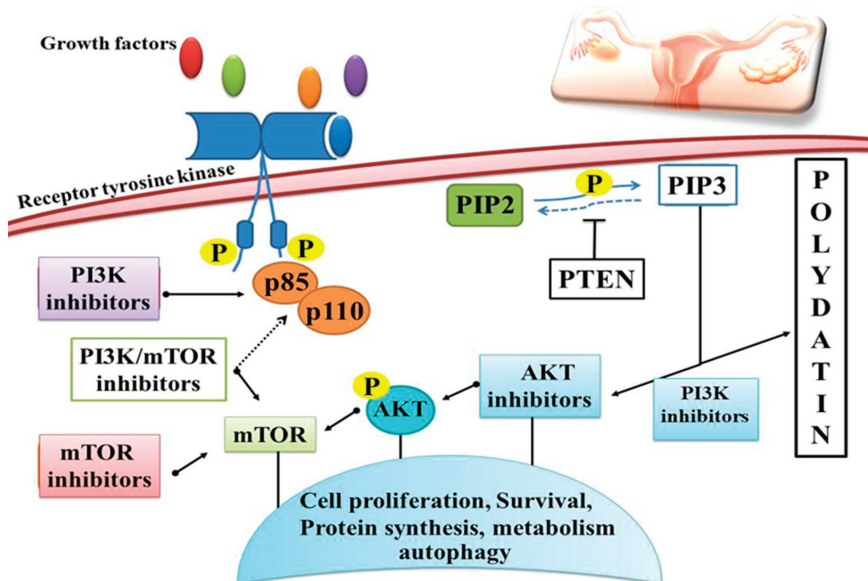


**Figure 7.** Schematic overview of polydatin activity on the PI3K/AKT/mTOR signaling pathway with different strategies for inhibition. PD induces apoptosis in cancer cells through the PI3K/Akt/mTOR signaling pathway and protects against inflammatory damage, as well as inhibiting cell proliferation, survival and protein synthesis through protein phosphorylation.

PD inhibited OVCAR-8 and SKOV-3 cell growth in a dose-dependent manner. A growth rate decrease was achieved by triggering apoptosis through the cleavage of poly (ADP-ribose) polymerase (PARP-1) at PD concentrations of 50 and 100  $\mu\text{M}$ . In the SKOV-3 line, PD inhibited Her-2 and EGFR phosphorylation and Erk expression, as well as the VEGF, when used at greater dosages, and stimulated Erk activation in the OVCAR-8 cell line. Results of this investigation showed that PD has the potential to block the formation of 3D cell aggregates in ovarian cancer cell lines by influencing a variety of signaling

molecules. However, more experiments for the *in vivo* testing of resveratrol and PD are needed to determine their potential therapeutic values [125]. Several other cancer cell lines were shown to be significantly inhibited by PD (Table 2).

### 5. Underlying Polydatin Anticancer Mechanisms of Action

PD has been studied extensively for its potential as a chemopreventive agent and chemotherapeutic treatment for halting or reversing carcinogenesis at multiple stages. PD, like other phytochemicals, can act as a suppressive agent on multiple impaired signaling pathways; as such, it has been classified as a functionally pleiotropic agent, capable of expressing its activity on multiple targets in cancer cells while causing only mild side effects in healthy cells. Important cellular changes include increased oxidative stress, overproduction of growth-regulatory hormones, accelerated transition of cells through cell cycle checkpoints, abnormal cell proliferation, genome instability, abnormal response to signals or other stimulators of programmed cell death, uncontrolled neoangiogenesis, and altered host immune responses. In addition, oxidative stress-related damage (including DNA damage, protein oxidation, and lipid peroxidation) is mitigated by antioxidant, anti-inflammatory, and immunomodulatory activities, which also boost immune oncosurveillance [150]. PD inhibits the monooxygenase cytochrome P450 isoenzyme CYP1 A1, the enzyme deputed to the liver metabolism of xenobiotics, and hence it can also function as a cancer-blocking agent by preventing the transformation of procarcinogens into carcinogens [151].

One of the primary functions of phytochemicals is to inhibit growth-signaling activity. A transmembrane tyrosine kinase is activated by ligands; the epidermal growth factor (EGF), and its related receptor (EGF-R) represent two of the resveratrol's primary targets. Overexpression of EGF-R is a hallmark of malignant tumors with aggressive characteristics because it stimulates cell growth and proliferation [152]. Resveratrol, acetyl-resveratrol and polydatin showed dose-dependent antigrowth activities against 3D cell aggregates of EGF-R/Her-2-positive and -negative ovarian cancer cell lines [125]. The phosphorylation of Her-2 and EGF-R, as well as the expression of extracellular-signal-regulated kinases (ERK) and VEGF, were all significantly reduced when resveratrol, PD and acetyl-resveratrol were tested at high concentrations on the positive ovarian cell line [125].

PD and its analogues displayed an interactive effect with TRAIL (tumor necrosis factor-related apoptosis-inducing ligand) and triggered apoptosis (programmed cell death). Particularly resistant to TRAIL are androgen-dependent LNCaP cells in prostate cancer; however, PD downregulated the PI3K/AKT pathway to make these cells more responsive to TRAIL-mediated apoptosis. Treatment of LNCaP cells with PD induced ROS production, mitochondrial membrane potential decreases, and translocation of the Bcl2-like protein 4, also known as Bcl-2-associated X protein (Bax), and p53 tumor suppressor protein. Proteins such as cytochrome c CASP-3 and CASP-9, apoptosis-inducing factor (AIF), the second mitochondria-derived activator of caspase/direct inhibitor of apoptosis-binding protein with low pI (Smac/DIABLO), and protein high-temperature requirement serine protease A2 (HtrA2), also known as Omi, are among the proapoptotic proteins released by mitochondria in relation to PD analogues [153] (Figure 8).

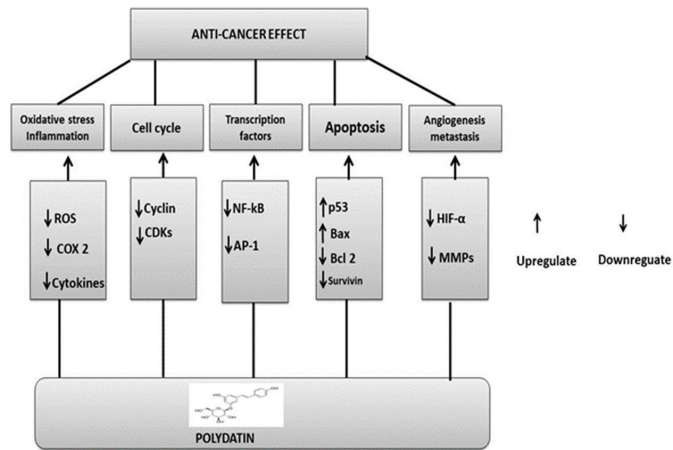


**Figure 8.** Polydatin anticancer mechanisms: upregulation or downregulation of various pathways.

## 6. Concluding Remarks

Currently, phytomedicine is gaining the attention of researchers and nutritionists due to its diversified pharmacological activities. The data collected showed the anticancer activities of PD. So, it would be valuable to investigate the in-depth mechanisms of PD activities. In recent years, PD has gained attention as a promising anticancer drug due to its potential to modulate many signaling pathways associated with cancer development. PD's anticancer effects arise from the fact that it boosts antioxidant activity. Due to its long-conjugated chemical structure, this molecule displays powerful antioxidant properties. PD may trigger apoptosis by raising the Bax/Bcl-2 ratio and decreasing Wnt/catenin signaling to kill cancer cells. It also targets cell cycle arrest to inhibit the development of BC. Among the several oncogenic pathways involved in BC the cell cycle arrest is linked to PD's apparent interference with Creb phosphorylation, which in turn downregulates Cyclin D1. PD therapy also restores the body's natural equilibrium of free radicals. Tumor size and rate of cancer progression were both significantly decreased after intravenous administration of PD. Furthermore, it was shown that PI3K levels are decreased in PD-treated patients. PD also protects against inflammatory damage and inhibits cell proliferation, survival, and protein synthesis by targeting the PI3K/Akt/mTOR signaling pathway, which is activated in cancer cells. Liver xenobiotic metabolism is mostly carried out by the monooxygenase cytochrome P450 isoenzyme CYP1 A1, which is inhibited by PD. As a blocking agent, it can stop procarcinogens from becoming carcinogenic. In this review, we have thus emphasized the anticancer activity of PD and its underlying pharmacological modes of action. The anticancer effect of PD should also be investigated through thorough preclinical trials. There is thus a need for carefully monitored human studies to determine its therapeutic efficacy.

**Author Contributions:** Conceptualization: M.A.S., H.K. and P.J.; Methodology: M.S.A., A.H., H.I.F., A.R., M.H. and R.Y. Project administration: M.S.A. and P.J.; Supervision: M.S.A. and P.J.; Writing—original draft: M.A.S., A.H., H.I.F., A.R., M.H., R.Y. and P.J.; Data curation: A.H., A.R., M.H., U.S., M.S.A. and G.H.; Investigation: H.I.F., T.A.S.B., R.Y., U.S., S.I., G.H. and H.K.; Writing—review & editing: T.A.S.B., U.S., S.I., Z.K., G.H., I.A. and H.K.; Formal analysis: T.A.S.B. and M.S.A. Validation: T.A.S.B., U.S. and M.S.A. All authors have read and agreed to the published version of the manuscript.

**Funding:** This research received no external funding.

**Institutional Review Board Statement:** Not applicable.

**Informed Consent Statement:** Not applicable.

**Conflicts of Interest:** The authors declare no conflict of interest.

## References

- National Cancer Institute. What Is Cancer. Available online: <https://www.cancer.gov/about-cancer/understanding/what-is-cancer> (accessed on 5 May 2021).
- WHO Cancer Prevalence. Available online: <https://www.who.int/news-room/fact-sheets/detail/breast-cancer#:~:text=In%202020%2C%20there%20were%202.3,the%20world's%20most%20prevalent%20cancer> (accessed on 26 March 2021).
- WHO, Cervical Cancer Prevalence. Available online: <https://www.who.int/news-room/fact-sheets/detail/cervical-cancer> (accessed on 22 February 2022).
- Medscape, Non Small Lung Cancer. Available online: <https://emedicine.medscape.com/article/279960-overview> (accessed on 19 August 2022).
- SEER Cancer Stat Facts: Ovarian Cancer. National Cancer Institute. Bethesda, MD, USA. Available online: <https://seer.cancer.gov/statfacts/html/ovary.html> (accessed on 3 August 2022).
- Breast Cancer: Types of Treatment. Available online: <https://www.cancer.net/cancer-types/breast-cancer/types-treatment> (accessed on 19 October 2021).
- Meegan, M.J.; O'Boyle, N.M. Special Issue "Anticancer Drugs". *Pharmaceuticals* **2019**, *12*, 134. [[CrossRef](#)] [[PubMed](#)]
- Sarfraz, A.; Javeed, M.; Shah, M.A.; Hussain, G.; Shafiq, N.; Sarfraz, I.; Riaz, A.; Sadiqa, A.; Zara, R.; Zafar, S. Biochanin A: A novel bioactive multifunctional compound from nature. *Sci. Total Environ.* **2020**, *722*, 137907. [[CrossRef](#)] [[PubMed](#)]
- Veresham, C. Natural products derived from plants as a source of drugs. *J. Adv. Pharm. Technol. Res.* **2012**, *3*, 200. [[CrossRef](#)] [[PubMed](#)]
- Du, Q.-H.; Peng, C.; Zhang, H. Polydatin: A review of pharmacology and pharmacokinetics. *Pharm Biol* **2013**, *51*, 1347–1354. [[CrossRef](#)]
- Jeandet, P.; Delaunoy, B.; Conreux, A.; Donnez, D.; Nuzzo, V.; Cordelier, S.; Clément, C.; Courot, E. Biosynthesis, metabolism, molecular engineering, and biological functions of stilbene phytoalexins in plants. *Biofactors* **2010**, *36*, 331–341. [[CrossRef](#)]
- Jeandet, P.; Vannozzi, A.; Sobarzo-Sánchez, E.; Uddin, M.S.; Bru, R.; Martínez-Márquez, A.; Clément, C.; Cordelier, S.; Manayi, A.; Nabavi, S.F. Phytostilbenes as agrochemicals: Biosynthesis, bioactivity, metabolic engineering and biotechnology. *Nat. Prod. Rep.* **2021**, *38*, 1282–1329. [[CrossRef](#)]
- Jeandet, P.; Sobarzo-Sánchez, E.; Uddin, M.S.; Bru, R.; Clément, C.; Jacquard, C.; Nabavi, S.F.; Khayatkashani, M.; Batiha, G.E.-S.; Khan, H. Resveratrol and cyclodextrins, an easy alliance: Applications in nanomedicine, green chemistry and biotechnology. *Biotechnol Adv.* **2021**, *53*, 107844. [[CrossRef](#)]
- Quan, Z.; Gu, J.; Dong, P.; Lu, J.; Wu, X.; Wu, W.; Fei, X.; Li, S.; Wang, Y.; Wang, J. Reactive oxygen species-mediated endoplasmic reticulum stress and mitochondrial dysfunction contribute to cirsimaritin-induced apoptosis in human gallbladder carcinoma GBC-SD cells. *Cancer Lett.* **2010**, *295*, 252–259. [[CrossRef](#)]
- Pan, J.-H.; Wang, H.-B.; Du, X.-F.; Liu, J.-Y.; Zhang, D.-J. Polydatin induces human cervical cancer cell apoptosis via PI3K/AKT/mTOR signaling pathway. *Zhongguo Zhongyao Zazhi—China J. Chin. Mater. Med.* **2017**, *42*, 2345–2349.
- DeSalvo, J.; Kuznetsov, J.N.; Du, J.; Leclerc, G.M.; Leclerc, G.J.; Lampidis, T.J.; Barredo, J.C. Inhibition of Akt potentiates 2-DG-Induced apoptosis via downregulation of UPR in acute lymphoblastic leukemia. *Mol. Cancer Res.* **2012**, *10*, 969–978. [[CrossRef](#)]
- Estañ, M.C.; Calviño, E.; de Blas, E.; del Carmen Boyano-Adán, M.; Mena, M.L.; Gómez-Gómez, M.; Rial, E.; Aller, P. 2-Deoxy-D-glucose cooperates with arsenic trioxide to induce apoptosis in leukemia cells: Involvement of IGF-1R-regulated Akt/mTOR, MEK/ERK and LKB-1/AMPK signaling pathways. *Biochem. Pharmacol.* **2012**, *84*, 1604–1616. [[CrossRef](#)] [[PubMed](#)]
- Xie, X.; Peng, J.; Huang, K.; Huang, J.; Shen, X.; Liu, P.; Huang, H. Polydatin ameliorates experimental diabetes-induced fibronectin through inhibiting the activation of NF- $\kappa$ B signaling pathway in rat glomerular mesangial cells. *Mol. Cell. Endocrinol.* **2012**, *362*, 183–193. [[CrossRef](#)] [[PubMed](#)]
- Mikulski, D.; Molski, M. Quantitative structure–antioxidant activity relationship of trans-resveratrol oligomers, trans-4, 4'-dihydroxystilbene dimer, trans-resveratrol-3-O-glucuronide, glucosides: Trans-piceid, cis-piceid, trans-astringin and trans-resveratrol-4'-O- $\beta$ -D-glucopyranoside. *Eur. J. Med. Chem.* **2010**, *45*, 2366–2380.
- Zou, J.; Yang, Y.; Yang, Y.; Liu, X. Polydatin suppresses proliferation and metastasis of non-small cell lung cancer cells by inhibiting NLRP3 inflammasome activation via NF- $\kappa$ B pathway. *Biomed. Pharm.* **2018**, *108*, 130–136. [[CrossRef](#)] [[PubMed](#)]
- Xing, W.-W.; Wu, J.-Z.; Jia, M.; Du, J.; Zhang, H.; Qin, L.-P. Effects of polydatin from *Polygonum cuspidatum* on lipid profile in hyperlipidemic rabbits. *Biomed. Pharm.* **2009**, *63*, 457–462. [[CrossRef](#)] [[PubMed](#)]
- Choi, O.; Lee, J.K.; Kang, S.-Y.; Pandey, R.P.; Sohng, J.-K.; Ahn, J.S.; Hong, Y.-S. Construction of artificial biosynthetic pathways for resveratrol glucoside derivatives. *J. Microbiol. Biotechnol.* **2014**, *24*, 614–618. [[CrossRef](#)]
- Kiselev, K.V.; Grigorochuk, V.P.; Ogneva, Z.V.; Suprun, A.; Dubrovina, A. Stilbene biosynthesis in the needles of spruce *Picea jezoensis*. *Phytochemistry* **2016**, *131*, 57–67. [[CrossRef](#)]
- Cichewicz, R.H.; Kouzi, S.A. Biotransformation of resveratrol to piceid by *Bacillus cereus*. *J. Nat. Prod.* **1998**, *61*, 1313–1314. [[CrossRef](#)]
- Ozaki, S.-i.; Imai, H.; Iwakiri, T.; Sato, T.; Shimoda, K.; Nakayama, T.; Hamada, H. Regioselective glucosidation of trans-resveratrol in *Escherichia coli* expressing glucosyltransferase from *Phytolacca americana*. *Biotechnol. Lett.* **2012**, *34*, 475–481. [[CrossRef](#)]
- Choi, O.; Wu, C.-Z.; Kang, S.-Y.; Ahn, J.S.; Uhm, T.-B.; Hong, Y.-S. Biosynthesis of plant-specific phenylpropanoids by construction of an artificial biosynthetic pathway in *Escherichia coli*. *J. Ind. Microbiol. Biotechnol.* **2011**, *38*, 1657–1665. [[CrossRef](#)]

27. Regev-Shoshani, G.; Shoseyov, O.; Bilkis, I.; Kerem, Z. Glycosylation of resveratrol protects it from enzymic oxidation. *Biochem. J.* **2003**, *374*, 157–163. [[CrossRef](#)] [[PubMed](#)]
28. Zhao, G.; Jiang, K.; Wu, H.; Qiu, C.; Deng, G.; Peng, X. Polydatin reduces *Staphylococcus aureus* lipoteichoic acid-induced injury by attenuating reactive oxygen species generation and TLR 2-NF  $\kappa$ B signalling. *J. Cell. Mol. Med.* **2017**, *21*, 2796–2808. [[CrossRef](#)] [[PubMed](#)]
29. Li, Z.; Chen, X.; Liu, G.; Li, J.; Zhang, J.; Cao, Y.; Miao, J. Antioxidant activity and mechanism of resveratrol and polydatin isolated from mulberry (*Morus alba* L.). *Molecules* **2021**, *26*, 7574. [[CrossRef](#)]
30. Galeano-Díaz, T.; Durán-Merás, I.; Airado-Rodríguez, D. Isocratic chromatography of resveratrol and piceid after previous generation of fluorescent photoproducts: Wine analysis without sample preparation. *J. Sep. Sci.* **2007**, *30*, 3110–3119. [[CrossRef](#)] [[PubMed](#)]
31. Kammerer, D.; Claus, A.; Carle, R.; Schieber, A. Polyphenol screening of pomace from red and white grape varieties (*Vitis vinifera* L.) by HPLC-DAD-MS/MS. *J. Agric. Food Chem.* **2004**, *52*, 4360–4367. [[CrossRef](#)] [[PubMed](#)]
32. Romero-Perez, A.I.; Ibern-Gomez, M.; Lamuela-Raventos, R.M.; de La Torre-Boronat, M.C. Piceid, the major resveratrol derivative in grape juices. *J. Agric. Food Chem.* **1999**, *47*, 1533–1536. [[CrossRef](#)]
33. Peng, X.L.; Qu, W.; Wang, L.Z.; Huang, B.Q.; Ying, C.J.; Sun, X.F.; Hao, L.P. Resveratrol ameliorates high glucose and high-fat/sucrose diet-induced vascular hyperpermeability involving Cav-1/eNOS regulation. *PLoS ONE* **2014**, *9*, e113716. [[CrossRef](#)]
34. Zamora-Ros, R.; Andres-Lacueva, C.; Lamuela-Raventós, R.M.; Berenguer, T.; Jakszyn, P.; Martínez, C.; Sanchez, M.J.; Navarro, C.; Chirlaque, M.D.; Tormo, M.-J. Concentrations of resveratrol and derivatives in foods and estimation of dietary intake in a Spanish population: European Prospective Investigation into Cancer and Nutrition (EPIC)-Spain cohort. *Br. J. Nutr.* **2008**, *100*, 188–196. [[CrossRef](#)]
35. Peng, X.L.; Xu, J.; Sun, X.F.; Ying, C.J.; Hao, L.P. Analysis of trans-resveratrol and trans-piceid in vegetable foods using high-performance liquid chromatography. *Int. J. Food Sci. Nutr.* **2015**, *66*, 729–735. [[CrossRef](#)]
36. Chiva-Blanch, G.; Urpi-Sarda, M.; Rotchés-Ribalta, M.; Zamora-Ros, R.; Llorach, R.; Lamuela-Raventós, R.M.; Estruch, R.; Andrés-Lacueva, C. Determination of resveratrol and piceid in beer matrices by solid-phase extraction and liquid chromatography–tandem mass spectrometry. *J. Chromatogr. A* **2011**, *1218*, 698–705. [[CrossRef](#)]
37. Jensen, J.S.; Wertz, C.F.; O'Neill, V.A. Preformulation stability of trans-resveratrol and trans-resveratrol glucoside (piceid). *J. Agric. Food Chem.* **2010**, *58*, 1685–1690. [[CrossRef](#)] [[PubMed](#)]
38. Şöhretöğlü, D.; Baran, M.Y.; Arroo, R.; Kuruüzüm-Uz, A. Recent advances in chemistry, therapeutic properties and sources of polydatin. *Phytochem. Rev.* **2018**, *17*, 973–1005. [[CrossRef](#)]
39. Ibern-Gomez, M.; Roig-Perez, S.; Lamuela-Raventos, R.M.; de la Torre-Boronat, M.C. Resveratrol and piceid levels in natural and blended peanut butters. *J. Agric. Food Chem.* **2000**, *48*, 6352–6354. [[CrossRef](#)] [[PubMed](#)]
40. Hurst, W.J.; Glineski, J.A.; Miller, K.B.; Apgar, J.; Davey, M.H.; Stuart, D.A. Survey of the trans-resveratrol and trans-piceid content of cocoa-containing and chocolate products. *J. Agric. Food Chem.* **2008**, *56*, 8374–8378. [[CrossRef](#)]
41. Xu, L.-Q.; Xie, Y.-L.; Gui, S.-H.; Zhang, X.; Mo, Z.-Z.; Sun, C.-Y.; Li, C.-L.; Luo, D.-D.; Zhang, Z.-B.; Su, Z.-R. Polydatin attenuates d-galactose-induced liver and brain damage through its anti-oxidative, anti-inflammatory and anti-apoptotic effects in mice. *Food Funct.* **2016**, *7*, 4545–4555. [[CrossRef](#)]
42. Su, D.; Cheng, Y.; Liu, M.; Liu, D.; Cui, H.; Zhang, B.; Zhou, S.; Yang, T.; Mei, Q. Comparison of piceid and resveratrol in antioxidation and antiproliferation activities in vitro. *PLoS ONE* **2013**, *8*, e54505. [[CrossRef](#)]
43. Yousef, A.I.; Shawki, H.H.; El-Shahawy, A.A.; El-Twab, S.M.A.; Abdel-Moneim, A.; Oishi, H. Polydatin mitigates pancreatic  $\beta$ -cell damage through its antioxidant activity. *Biomed. Pharmacother.* **2021**, *133*, 111027. [[CrossRef](#)]
44. Aggarwal, S. Targeted cancer therapies. *Nat. Rev. Drug Discov.* **2010**, *9*, 427. [[CrossRef](#)]
45. Zhang, H.; Park, S.; Huang, H.; Kim, E.; Yi, J.; Choi, S.-K.; Ryoo, Z.; Kim, M. Anticancer effects and potential mechanisms of ginsenoside Rh2 in various cancer types. *Oncol. Rep.* **2021**, *45*, 1–10. [[CrossRef](#)]
46. Wang, B.; Zhang, Y.; Mao, Z.; Yu, D.; Gao, C. Toxicity of ZnO nanoparticles to macrophages due to cell uptake and intracellular release of zinc ions. *J. Nanosci. Nanotechnol.* **2014**, *14*, 5688–5696. [[CrossRef](#)]
47. Hong, C.; Wang, D.; Liang, J.; Guo, Y.; Zhu, Y.; Xia, J.; Qin, J.; Zhan, H.; Wang, J. Novel ginsenoside-based multifunctional liposomal delivery system for combination therapy of gastric cancer. *Theranostics* **2019**, *9*, 4437. [[CrossRef](#)] [[PubMed](#)]
48. Yao, H.; Wan, J.Y.; Zeng, J.; Huang, W.H.; Sava-Segal, C.; Li, L.; Niu, X.; Wang, Q.; Wang, C.Z.; Yuan, C.S. Effects of compound K, an enteric microbiome metabolite of ginseng, in the treatment of inflammation associated colon cancer. *Oncol. Lett.* **2018**, *15*, 8339–8348. [[CrossRef](#)] [[PubMed](#)]
49. Wu, L.-S.; Jia, M.; Chen, L.; Zhu, B.; Dong, H.-X.; Si, J.-P.; Peng, W.; Han, T. Cytotoxic and antifungal constituents isolated from the metabolites of endophytic fungus DO14 from *Dendrobium officinale*. *Molecules* **2015**, *21*, 14. [[CrossRef](#)] [[PubMed](#)]
50. Newman, D.J.; Cragg, G.M. Natural products as sources of new drugs over the nearly four decades from 01/1981 to 09/2019. *J. Nat. Prod.* **2020**, *83*, 770–803. [[CrossRef](#)]
51. Trautwein, C.; Friedman, S.L.; Schuppan, D.; Pinzani, M. Hepatic fibrosis: Concept to treatment. *J. Hepatol.* **2015**, *62*, S15–S24. [[CrossRef](#)]
52. Nakamoto, Y. Promising new strategies for hepatocellular carcinoma. *Hepatol. Res.* **2017**, *47*, 251–265. [[CrossRef](#)]
53. Jiang, J.; Chen, Y.; Dong, T.; Yue, M.; Zhang, Y.; An, T.; Zhang, J.; Liu, P.; Yang, X. Polydatin inhibits hepatocellular carcinoma via the AKT/STAT3-FOXO1 signaling pathway. *Oncol. Lett.* **2019**, *17*, 4505–4513. [[CrossRef](#)]

54. Jiao, Y.; Wu, Y.; Du, D. Polydatin inhibits cell proliferation, invasion and migration, and induces cell apoptosis in hepatocellular carcinoma. *Braz. J. Med. Biol. Res.* **2018**, *51*. [[CrossRef](#)]
55. De Maria, S.; Scognamiglio, I.; Lombardi, A.; Amodio, N.; Caraglia, M.; Carteni, M.; Ravagnan, G.; Stiuso, P. Polydatin, a natural precursor of resveratrol, induces cell cycle arrest and differentiation of human colorectal Caco-2 cell. *J. Transl. Med.* **2013**, *11*, 1–11. [[CrossRef](#)]
56. Storniolo, C.E.; Quifer-Rada, P.; Lamuela-Raventos, R.M.; Moreno, J.J. Piceid presents antiproliferative effects in intestinal epithelial Caco-2 cells, effects unrelated to resveratrol release. *Food Funct.* **2014**, *5*, 2137–2144. [[CrossRef](#)]
57. Bae, H.; Lee, W.; Song, J.; Hong, T.; Kim, M.H.; Ham, J.; Song, G.; Lim, W. Polydatin Counteracts 5-Fluorouracil Resistance by Enhancing Apoptosis via Calcium Influx in Colon Cancer. *Antioxidants* **2021**, *10*, 1477. [[CrossRef](#)] [[PubMed](#)]
58. Yang, B.; Zhao, S. Polydatin regulates proliferation, apoptosis and autophagy in multiple myeloma cells through mTOR/p70s6k pathway. *Onco Targets.* **2017**, *10*, 935. [[CrossRef](#)] [[PubMed](#)]
59. Taran, S.J.; Taran, R.; Malipatil, N.B. Pediatric osteosarcoma: An updated review. *Indian J. Med. Paediatr. Oncol.* **2017**, *38*, 33–43. [[CrossRef](#)]
60. Misaghi, A.; Goldin, A.; Awad, M.; Kulidjian, A.A. Osteosarcoma: A comprehensive review. *Sicot-J* **2018**, *4*, 12. [[CrossRef](#)] [[PubMed](#)]
61. Han, X.; Wang, W.; He, J.; Jiang, L.; Li, X. Osteopontin as a biomarker for osteosarcoma therapy and prognosis. *Oncol. Lett.* **2019**, *17*, 2592–2598. [[CrossRef](#)] [[PubMed](#)]
62. Gibbs, C.P.; Kukekov, V.G.; Reith, J.D.; Tchigrinova, O.; Suslov, O.N.; Scott, E.W.; Ghivizzani, S.C.; Ignatova, T.N.; Steindler, D.A. Stem-like cells in bone sarcomas: Implications for tumorigenesis. *Neoplasia* **2005**, *7*, 967–976. [[CrossRef](#)] [[PubMed](#)]
63. Xu, G.; Kuang, G.; Jiang, W.; Jiang, R.; Jiang, D. Polydatin promotes apoptosis through upregulation the ratio of Bax/Bcl-2 and inhibits proliferation by attenuating the  $\beta$ -catenin signaling in human osteosarcoma cells. *Am. J. Transl. Res.* **2016**, *8*, 922.
64. Luce, A.; Lama, S.; Millan, P.C.; Iтро, A.; Sangiovanni, A.; Caputo, C.; Ferranti, P.; Cappabianca, S.; Caraglia, M.; Stiuso, P. Polydatin Induces Differentiation and Radiation Sensitivity in Human Osteosarcoma Cells and Parallel Secretion through Lipid Metabolite Secretion. *Oxid. Med. Cell. Longev.* **2021**, *2021*, 3337013. [[CrossRef](#)]
65. United States Cancer Statistics (USCS). Prevention, Global Cancer Statistics. 2012. 2019. Available online: <https://www.cdc.gov/cancer/uscs/index.htm> (accessed on 3 August 2022).
66. Ginsburg, O.; Yip, C.H.; Brooks, A.; Cabanes, A.; Caleffi, M.; Dunstan Yataco, J.A.; Gyawali, B.; McCormack, V.; McLaughlin de Anderson, M.; Mehrotra, R. Breast cancer early detection: A phased approach to implementation. *Cancer* **2020**, *126*, 2379–2393. [[CrossRef](#)]
67. Schwartz, G.K.; Shah, M.A. Targeting the cell cycle: A new approach to cancer therapy. *J. Clin. Oncol.* **2005**, *23*, 9408–9421. [[CrossRef](#)] [[PubMed](#)]
68. Ding, L.; Cao, J.; Lin, W.; Chen, H.; Xiong, X.; Ao, H.; Yu, M.; Lin, J.; Cui, Q. The roles of cyclin-dependent kinases in cell-cycle progression and therapeutic strategies in human breast cancer. *Int. J. Mol. Sci.* **2020**, *21*, 1960. [[CrossRef](#)] [[PubMed](#)]
69. Lin, Z.P.; Zhu, Y.-L.; Ratner, E.S. Targeting cyclin-dependent kinases for treatment of gynecologic cancers. *Front. Oncol.* **2018**, *8*, 300. [[CrossRef](#)] [[PubMed](#)]
70. Kuo, S.-H.; Wei, M.-F.; Lee, Y.-H.; Yang, W.-C.; Yang, S.-Y.; Lin, J.-C.; Huang, C.-S. MAP3K1 Expression Is Associated with Progression and Poor Prognosis of Hormone Receptor-Positive, HER2-Negative Early-Stage Breast Cancer. 2020. Available online: <https://assets.researchsquare.com/files/rs-53956/v1/20512c99-6481-480b-9d9e-37881a993bb9.pdf?c=1631849978> (accessed on 3 August 2022).
71. Mayr, B.; Montminy, M. Transcriptional regulation by the phosphorylation-dependent factor CREB. *Nat. Rev. Mol. Cell Biol.* **2001**, *2*, 599–609. [[CrossRef](#)] [[PubMed](#)]
72. Chhabra, A.; Fernando, H.; Watkins, G.; Mansel, R.E.; Jiang, W.G. Expression of transcription factor CREB1 in human breast cancer and its correlation with prognosis. *Oncol. Rep.* **2007**, *18*, 953–958. [[CrossRef](#)]
73. Zhang, X.; Odom, D.T.; Koo, S.-H.; Conkright, M.D.; Canetti, G.; Best, J.; Chen, H.; Jenner, R.; Herbolsheimer, E.; Jacobsen, E. Genome-wide analysis of cAMP-response element binding protein occupancy, phosphorylation, and target gene activation in human tissues. *Proc. Natl. Acad. Sci.* **2005**, *102*, 4459–4464. [[CrossRef](#)]
74. Alao, J.P. The regulation of cyclin D1 degradation: Roles in cancer development and the potential for therapeutic invention. *Mol. Cancer* **2007**, *6*, 1–16. [[CrossRef](#)]
75. Hartmann, N.B.; Rist, S.; Bodin, J.; Jensen, L.H.; Schmidt, S.N.; Mayer, P.; Meibom, A.; Baun, A. Microplastics as vectors for environmental contaminants: Exploring sorption, desorption, and transfer to biota. *Integr. Environ. Assess. Manag.* **2017**, *13*, 488–493. [[CrossRef](#)]
76. Jin, Y.; Huynh, D.T.N.; Nguyen, T.L.L.; Jeon, H.; Heo, K.S. Therapeutic effects of ginsenosides on breast cancer growth and metastasis. *Arch. Pharmacol. Res.* **2020**, *43*, 773–787. [[CrossRef](#)]
77. Orgaz, J.L.; Pandya, P.; Dalmeida, R.; Karagiannis, P.; Sanchez-Laorden, B.; Viros, A.; Albregues, J.; Nestle, F.O.; Ridley, A.J.; Gaggioli, C. Diverse matrix metalloproteinase functions regulate cancer amoeboid migration. *Nat. Commun.* **2014**, *5*, 1–13. [[CrossRef](#)]
78. Chabottaux, V.; Noel, A. Breast cancer progression: Insights into multifaceted matrix metalloproteinases. *Clin. Exp. Metastasis* **2007**, *24*, 647–656. [[CrossRef](#)] [[PubMed](#)]

79. Lu, K.V.; Chang, J.P.; Parachoniak, C.A.; Pandika, M.M.; Aghi, M.K.; Meyronet, D.; Isachenko, N.; Fouse, S.D.; Phillips, J.J.; Cheresch, D.A. VEGF inhibits tumor cell invasion and mesenchymal transition through a MET/VEGFR2 complex. *Cancer Cell* **2012**, *22*, 21–35. [[CrossRef](#)] [[PubMed](#)]
80. Zhang, T.; Zhu, X.; Wu, H.; Jiang, K.; Zhao, G.; Shaukat, A.; Deng, G.; Qiu, C. Targeting the ROS/PI3K/AKT/HIF-1 $\alpha$ /HK2 axis of breast cancer cells: Combined administration of Polydatin and 2-Deoxy-d-glucose. *J. Cell. Mol. Med.* **2019**, *23*, 3711–3723. [[CrossRef](#)] [[PubMed](#)]
81. Jung, J.; Song, D.Y.; Hwang, J.J.; Park, H.J.; Lee, J.S.; Song, S.Y.; Jeong, S.-Y.; Choi, E.K. Induction of p53-mediated senescence is essential for the eventual anticancer therapeutic effect of RH1. *Arch. Pharm Res.* **2019**, *42*, 815–823. [[CrossRef](#)] [[PubMed](#)]
82. Sarmiento-Salinas, F.L.; Delgado-Magallón, A.; Montes-Alvarado, J.B.; Ramírez-Ramírez, D.; Flores-Alonso, J.C.; Cortés-Hernández, P.; Reyes-Leyva, J.; Herrera-Camacho, I.; Anaya-Ruiz, M.; Pelayo, R. Breast cancer subtypes present a differential production of reactive oxygen species (ROS) and susceptibility to antioxidant treatment. *Front. Oncol.* **2019**, *9*, 480. [[CrossRef](#)] [[PubMed](#)]
83. Morgan, M.J.; Liu, Z.-G. Crosstalk of reactive oxygen species and NF- $\kappa$ B signaling. *Cell Res.* **2011**, *21*, 103–115. [[CrossRef](#)]
84. de Sá Junior, P.L.; Câmara, D.A.D.; Porcacchia, A.S.; Fonseca, P.M.M.; Jorge, S.D.; Araldi, R.P.; Ferreira, A.K. The roles of ROS in cancer heterogeneity and therapy. *Oxidative Med. Cell. Longev.* **2017**, *2017*, 2467940. [[CrossRef](#)]
85. Kubli, S.P.; Bassi, C.; Roux, C.; Wakeham, A.; Göbl, C.; Zhou, W.; Jafari, S.M.; Snow, B.; Jones, L.; Palomero, L. AhR controls redox homeostasis and shapes the tumor microenvironment in BRCA1-associated breast cancer. *Proc. Natl. Acad. Sci. USA* **2019**, *116*, 3604–3613. [[CrossRef](#)]
86. Han, B.; Liu, W.; Li, J.; Wang, J.; Zhao, D.; Xu, R.; Lin, Z. Catalytic hydrodechlorination of triclosan using a new class of anion-exchange-resin supported palladium catalysts. *Water Res.* **2017**, *120*, 199–210. [[CrossRef](#)]
87. Chen, L.; Lan, Z.; Lin, Q.; Mi, X.; He, Y.; Wei, L.; Lin, Y.; Zhang, Y.; Deng, X. Polydatin ameliorates renal injury by attenuating oxidative stress-related inflammatory responses in fructose-induced urate nephropathic mice. *Food Chem. Toxicol.* **2013**, *52*, 28–35. [[CrossRef](#)]
88. Checker, R.; Gambhir, L.; Sharma, D.; Kumar, M.; Sandur, S.K. Plumbagin induces apoptosis in lymphoma cells via oxidative stress mediated glutathionylation and inhibition of mitogen-activated protein kinase phosphatases (MKP1/2). *Cancer Lett.* **2015**, *357*, 265–278. [[CrossRef](#)]
89. Vander Heiden, M.G.; Cantley, L.C.; Thompson, C.B. Understanding the Warburg effect: The metabolic requirements of cell proliferation. *Science* **2009**, *324*, 1029–1033. [[CrossRef](#)] [[PubMed](#)]
90. Dwarakanath, B. Cytotoxicity, radiosensitization, and chemosensitization of tumor cells by 2-deoxy-D-glucose in vitro. *J. Cancer Res. Ther.* **2009**, *5*, 27. [[CrossRef](#)] [[PubMed](#)]
91. Zhang, D.; Li, J.; Wang, F.; Hu, J.; Wang, S.; Sun, Y. 2-Deoxy-D-glucose targeting of glucose metabolism in cancer cells as a potential therapy. *Cancer Lett.* **2014**, *355*, 176–183. [[CrossRef](#)] [[PubMed](#)]
92. Wolf, A.; Agnihotri, S.; Micallef, J.; Mukherjee, J.; Sabha, N.; Cairns, R.; Hawkins, C.; Guha, A. Hexokinase 2 is a key mediator of aerobic glycolysis and promotes tumor growth in human glioblastoma multiforme. *J. Exp. Med.* **2011**, *208*, 313–326. [[CrossRef](#)] [[PubMed](#)]
93. Shafae, A.; Dastyar, D.Z.; Islamian, J.P.; Hatamian, M. Inhibition of tumor energy pathways for targeted esophagus cancer therapy. *Metabolism* **2015**, *64*, 1193–1198. [[CrossRef](#)]
94. Palazon, A.; Tyrakis, P.A.; Macias, D.; Veliça, P.; Rundqvist, H.; Fitzpatrick, S.; Vojnovic, N.; Phan, A.T.; Loman, N.; Hedenfalk, I. An HIF-1 $\alpha$ /VEGF-A axis in cytotoxic T cells regulates tumor progression. *Cancer Cell* **2017**, *32*, 669–683.e5. [[CrossRef](#)]
95. Li, S.; Li, J.; Dai, W.; Zhang, Q.; Feng, J.; Wu, L.; Liu, T.; Yu, Q.; Xu, S.; Wang, W. Genistein suppresses aerobic glycolysis and induces hepatocellular carcinoma cell death. *Br. J. Cancer* **2017**, *117*, 1518–1528. [[CrossRef](#)]
96. Bray, F.; Ferlay, J.; Soerjomataram, I.; Siegel, R.L.; Torre, L.A.; Jemal, A. Global cancer statistics 2018: GLOBOCAN estimates of incidence and mortality worldwide for 36 cancers in 185 countries. *CA A Cancer J. Clin.* **2018**, *68*, 394–424. [[CrossRef](#)]
97. Torre, L.A.; Bray, F.; Siegel, R.L.; Ferlay, J.; Lortet-Tieulent, J.; Jemal, A. Global cancer statistics, 2012. *CA A Cancer J. Clin.* **2015**, *65*, 87–108. [[CrossRef](#)]
98. Vaccarella, S.; Laversanne, M.; Ferlay, J.; Bray, F. Cervical cancer in Africa, Latin America and the Caribbean and Asia: Regional inequalities and changing trends. *Int. J. Can.* **2017**, *141*, 1997–2001. [[CrossRef](#)] [[PubMed](#)]
99. Hu, Z.; Ma, D. The precision prevention and therapy of HPV-related cervical cancer: New concepts and clinical implications. *Can. Med.* **2018**, *7*, 5217–5236. [[CrossRef](#)] [[PubMed](#)]
100. Den Boon, J.A.; Pyeon, D.; Wang, S.S.; Horswill, M.; Schiffman, M.; Sherman, M.; Zuna, R.E.; Wang, Z.; Hewitt, S.M.; Pearson, R. Molecular transitions from papillomavirus infection to cervical precancer and cancer: Role of stromal estrogen receptor signaling. *Proc. Natl. Acad. Sci. USA* **2015**, *112*, E3255–E3264. [[CrossRef](#)] [[PubMed](#)]
101. Marquina, G.; Manzano, A.; Casado, A. Targeted agents in cervical cancer: Beyond bevacizumab. *Curr. Oncol. Rep.* **2018**, *20*, 1–10. [[CrossRef](#)] [[PubMed](#)]
102. Wen, W.; Lowe, G.; Roberts, C.M.; Finlay, J.; Han, E.S.; Glackin, C.A.; Dellinger, T.H. Pterostilbene suppresses ovarian cancer growth via induction of apoptosis and blockade of cell cycle progression involving inhibition of the STAT3 pathway. *Int. J. Mol. Sci.* **2018**, *19*, 1983. [[CrossRef](#)]

103. Yu, H.; Pan, C.; Zhao, S.; Wang, Z.; Zhang, H.; Wu, W. Resveratrol inhibits tumor necrosis factor- $\alpha$ -mediated matrix metalloproteinase-9 expression and invasion of human hepatocellular carcinoma cells. *Biomed. Pharmacother.* **2008**, *62*, 366–372. [[CrossRef](#)]
104. Ma, Z.; Yang, Y.; Di, S.; Feng, X.; Liu, D.; Jiang, S.; Hu, W.; Qin, Z.; Li, Y.; Lv, J. Pterostilbene exerts anticancer activity on non-small-cell lung cancer via activating endoplasmic reticulum stress. *Sci. Rep.* **2017**, *7*, 1–14. [[CrossRef](#)]
105. Bai, L.; Ma, Y.; Wang, X.; Feng, Q.; Zhang, Z.; Wang, S.; Zhang, H.; Lu, X.; Xu, Y.; Zhao, E. Polydatin inhibits cell viability, migration, and invasion through suppressing the c-Myc expression in human cervical cancer. *Front. Cell Dev. Biol.* **2021**, *9*, 587218. [[CrossRef](#)]
106. Nishioka, R.; Itoh, S.; Gui, T.; Gai, Z.; Oikawa, K.; Kawai, M.; Tani, M.; Yamaue, H.; Muragaki, Y. SNAIL induces epithelial-to-mesenchymal transition in a human pancreatic cancer cell line (BxPC3) and promotes distant metastasis and invasiveness in vivo. *Exp. Mol. Pathol.* **2010**, *89*, 149–157. [[CrossRef](#)]
107. Cercelaru, L.; Stepan, A.E.; Mărgăritescu, C.; Osman, A.; Popa, I.-C.; Florescu, M.M.; Simionescu, C.E.; Mărgăritescu, O.C. E-cadherin,  $\beta$ -catenin and Snail immunorexpression in laryngeal squamous cell carcinoma. *Rom. J. Morphol. Embryol.* **2017**, *58*, 761–766.
108. Dhasarathy, A.; Phadke, D.; Mav, D.; Shah, R.R.; Wade, P.A. The transcription factors Snail and Slug activate the transforming growth factor-beta signaling pathway in breast cancer. *PLoS ONE* **2011**, *6*, e26514. [[CrossRef](#)] [[PubMed](#)]
109. Huang, H.; Guo, W.-J.; Yao, R.-X. Advances research on C-MYC proto-oncogene in multiple myeloma-review. *Zhongguo Shi Yan Xue Ye Xue Za Zhi* **2016**, *24*, 1248–1251. [[PubMed](#)]
110. Wu, S.-H.; Zeng, X.-F.; Wang, P.; Zhou, Y.; Lin, W. The Expression and Significance of c-myc and beat1 in Cervical Cancer. *Djournal Sichuan Univ.* **2018**, *49*, 725–730.
111. Gao, K.; Eurasian, M.; Zhang, J.; Wei, Y.; Zheng, Q.; Ye, H.; Li, L. Can genomic amplification of human telomerase gene and C-MYC in liquid-based cytological specimens be used as a method for opportunistic cervical cancer screening? *Gynecol. Obstet. Investig.* **2015**, *80*, 153–163. [[CrossRef](#)] [[PubMed](#)]
112. Zhao, E.; Ding, J.; Xia, Y.; Liu, M.; Ye, B.; Choi, J.-H.; Yan, C.; Dong, Z.; Huang, S.; Zha, Y. KDM4C and ATF4 cooperate in transcriptional control of amino acid metabolism. *Cell Rep.* **2016**, *14*, 506–519. [[CrossRef](#)] [[PubMed](#)]
113. Nowak, D.G.; Cho, H.; Herzka, T.; Watrud, K.; DeMarco, D.V.; Wang, V.M.; Senturk, S.; Fellmann, C.; Ding, D.; Beinortas, T. MYC drives Pten/Trp53-deficient proliferation and metastasis due to IL6 secretion and AKT suppression via PHLPP2. *Cancer Discov.* **2015**, *5*, 636–651. [[CrossRef](#)] [[PubMed](#)]
114. Chen, H.; Liu, H.; Qing, G. Targeting oncogenic Myc as a strategy for cancer treatment. *Signal. Transduct. Target. Ther.* **2018**, *3*, 1–7. [[CrossRef](#)] [[PubMed](#)]
115. Musgrove, E.A.; Lee, C.; Sutherland, R.L. Progestins both stimulate and inhibit breast cancer cell cycle progression while increasing expression of transforming growth factor alpha, epidermal growth factor receptor, c-fos, and c-myc genes. *Mol. Cell. Biol.* **1991**, *11*, 5032–5043.
116. García-Gutiérrez, L.; Delgado, M.D.; León, J. MYC oncogene contributions to release of cell cycle brakes. *Genes* **2019**, *10*, 244. [[CrossRef](#)]
117. Finn, R.S.; Aleshin, A.; Slamon, D.J. Targeting the cyclin-dependent kinases (CDK) 4/6 in estrogen receptor-positive breast cancers. *Breast Cancer Res.* **2016**, *18*, 1–11. [[CrossRef](#)]
118. Thomasova, D.; Anders, H.-J. Cell cycle control in the kidney. *Nephrol. Dial. Transplant.* **2015**, *30*, 1622–1630. [[CrossRef](#)] [[PubMed](#)]
119. Karimian, A.; Ahmadi, Y.; Yousefi, B. Multiple functions of p21 in cell cycle, apoptosis and transcriptional regulation after DNA damage. *Dna Repair* **2016**, *42*, 63–71. [[CrossRef](#)] [[PubMed](#)]
120. Aleem, E.; Kiyokawa, H.; Kaldis, P. Cdc2-cyclin E complexes regulate the G1/S phase transition. *Nat. Cell Biol.* **2005**, *7*, 831–836. [[CrossRef](#)]
121. Hsiao, Y.-H.; Lin, C.-W.; Wang, P.-H.; Hsin, M.-C.; Yang, S.-F. The potential of Chinese herbal medicines in the treatment of cervical cancer. *Integr. Cancer Ther.* **2019**, *18*, 1534735419861693. [[CrossRef](#)] [[PubMed](#)]
122. Chen, S.; Tao, J.; Zhong, F.; Jiao, Y.; Xu, J.; Shen, Q.; Wang, H.; Fan, S.; Zhang, Y. Polydatin down-regulates the phosphorylation level of Creb and induces apoptosis in human breast cancer cell. *PLoS ONE* **2017**, *12*, e0176501. [[CrossRef](#)]
123. Zhang, Y.; Zhuang, Z.; Meng, Q.; Jiao, Y.; Xu, J.; Fan, S. Polydatin inhibits growth of lung cancer cells by inducing apoptosis and causing cell cycle arrest. *Oncol Lett* **2014**, *7*, 295–301. [[CrossRef](#)] [[PubMed](#)]
124. Zhang, X. Effects of polydatin on the proliferation, migration, and invasion of ovarian cancer. *Biocell* **2019**, *43*, 313. [[CrossRef](#)]
125. Hogg, S.J.; Chitcholtan, K.; Hassan, W.; Sykes, P.H.; Garrill, A. Resveratrol, acetyl-resveratrol, and polydatin exhibit antigrowth activity against 3D cell aggregates of the SKOV-3 and OVCAR-8 ovarian cancer cell lines. *Obs. Gynecol. Int.* **2015**, 2015. [[CrossRef](#)]
126. Cao, W.J.; Wu, K.; Wang, C.; Wan, D.M. Polydatin-induced cell apoptosis and cell cycle arrest are potentiated by Janus kinase 2 inhibition in leukemia cells. *Mol. Med. Rep.* **2016**, *13*, 3297–3302. [[CrossRef](#)]
127. Liu, H.; Zhao, S.; Zhang, Y.; Wu, J.; Peng, H.; Fan, J.; Liao, J. Reactive oxygen species-mediated endoplasmic reticulum stress and mitochondrial dysfunction contribute to polydatin-induced apoptosis in human nasopharyngeal carcinoma CNE cells. *J. Cell. Biochem.* **2011**, *112*, 3695–3703. [[CrossRef](#)]
128. Li, H.; Shi, B.; Li, Y.; Yin, F. Polydatin inhibits cell proliferation and induces apoptosis in laryngeal cancer and HeLa cells via suppression of the PDGF/AKT signaling pathway. *J. Biochem. Mol. Toxicol.* **2017**, *31*, e21900. [[CrossRef](#)] [[PubMed](#)]



129. Spiro, S.G.; Tanner, N.T.; Silvestri, G.A.; Janes, S.M.; Lim, E.; Vansteenkiste, J.F.; Pirker, R. Lung cancer: Progress in diagnosis, staging and therapy. *Respirology* **2010**, *15*, 44–50. [[CrossRef](#)] [[PubMed](#)]
130. Lemjabbar-Alaoui, H.; Hassan, O.U.; Yang, Y.-W.; Buchanan, P. Lung cancer: Biology and treatment options. *Biochim. Biophys. Acta (Bba)—Rev. Cancer* **2015**, *1856*, 189–210. [[CrossRef](#)] [[PubMed](#)]
131. Luan, J.; Duan, H.; Liu, Q.; Yagasaki, K.; Zhang, G. Inhibitory effects of norcantharidin against human lung cancer cell growth and migration. *Cytotechnology* **2010**, *62*, 349–355. [[CrossRef](#)]
132. Jiang, T.; Tian, F.; Zheng, H.; Whitman, S.A.; Lin, Y.; Zhang, Z.; Zhang, N.; Zhang, D.D. Nrf2 suppresses lupus nephritis through inhibition of oxidative injury and the NF- $\kappa$ B-mediated inflammatory response. *Kidney Int.* **2014**, *85*, 333–343. [[CrossRef](#)]
133. Neto, C.C.; Amoroso, J.W.; Liberty, A.M. Anticancer activities of cranberry phytochemicals: An update. *Mol. Nutr. Food Res.* **2008**, *52*, S18–S27. [[CrossRef](#)]
134. Verma, N.; Tiku, A.B. Polydatin-induced direct and bystander effects in a549 lung cancer cell line. *Nutr. Cancer* **2022**, *74*, 237–249. [[CrossRef](#)]
135. Yang, J.; Liu, X.; Bhalla, K.; Kim, C.N.; Ibrado, A.M.; Cai, J.; Peng, T.-I.; Jones, D.P.; Wang, X. Prevention of apoptosis by Bcl-2: Release of cytochrome c from mitochondria blocked. *Science* **1997**, *275*, 1129–1132. [[CrossRef](#)]
136. Kluck, R.M.; Bossy-Wetzell, E.; Green, D.R.; Newmeyer, D.D. The release of cytochrome c from mitochondria: A primary site for Bcl-2 regulation of apoptosis. *Science* **1997**, *275*, 1132–1136. [[CrossRef](#)]
137. Graña, X.; Reddy, E.P. Cell cycle control in mammalian cells: Role of cyclins, cyclin dependent kinases (CDKs), growth suppressor genes and cyclin-dependent kinase inhibitors (CKIs). *Oncogene* **1995**, *11*, 211–220.
138. Pavletich, N.P. Mechanisms of cyclin-dependent kinase regulation: Structures of Cdks, their cyclin activators, and Cip and INK4 inhibitors. *J. Mol. Biol.* **1999**, *287*, 821–828. [[CrossRef](#)] [[PubMed](#)]
139. Yang, K.; Hitomi, M.; Stacey, D.W. Variations in cyclin D1 levels through the cell cycle determine the proliferative fate of a cell. *Cell Div.* **2006**, *1*, 1–8. [[CrossRef](#)] [[PubMed](#)]
140. Molenaar, J.J.; Ebus, M.E.; Koster, J.; van Sluis, P.; van Noesel, C.J.; Versteeg, R.; Caron, H.N. Cyclin D1 and CDK4 activity contribute to the undifferentiated phenotype in neuroblastoma. *Cancer Res.* **2008**, *68*, 2599–2609. [[CrossRef](#)] [[PubMed](#)]
141. Hall, M.; Peters, G. Genetic alterations of cyclins, cyclin-dependent kinases, and Cdk inhibitors in human cancer. *Adv. Cancer Res.* **1996**, *68*, 67–108.
142. Liu, Y.-L.; Chen, B.-Y.; Nie, J.; Zhao, G.-H.; Zhuo, J.-Y.; Yuan, J.; Li, Y.-C.; Wang, L.-L.; Chen, Z.-W. Polydatin prevents bleomycin-induced pulmonary fibrosis by inhibiting the TGF- $\beta$ /Smad/ERK signaling pathway. *Exp. Ther. Med.* **2020**, *20*, 1. [[CrossRef](#)]
143. Wang, Y.; Kong, H.; Zeng, X.; Liu, W.; Wang, Z.; Yan, X.; Wang, H.; Xie, W. Activation of NLRP3 inflammasome enhances the proliferation and migration of A549 lung cancer cells. *Oncol. Rep.* **2016**, *35*, 2053–2064. [[CrossRef](#)]
144. Howlader, N.; Noone, A.-M.; Krapcho, M.; Garshell, J.; Neyman, N.; Altekruse, S.; Kosary, C.; Yu, M.; Ruhl, J.; Tatalovich, Z. *SEER cancer statistics review, 1975–2010*. *Natl. Cancer Inst.* **2014**.
145. Bast, R.C.; Hennessy, B.; Mills, G.B. The biology of ovarian cancer: New opportunities for translation. *Nat. Rev. Cancer* **2009**, *9*, 415–428. [[CrossRef](#)]
146. Cheaib, B.; Auguste, A.; Leary, A. The PI3K/Akt/mTOR pathway in ovarian cancer: Therapeutic opportunities and challenges. *Chin. J. Cancer* **2015**, *34*, 4–16. [[CrossRef](#)]
147. Leary, A.; Auclin, E.; Pautier, P.; Lhomme, C. The PI3K/Akt/mTOR pathway in ovarian cancer: Biological rationale and therapeutic opportunities. *Ovarian Cancer—A Clin. Transl. Update* **2013**, 275–302.
148. Mabuchi, S.; Kuroda, H.; Takahashi, R.; Sasano, T. The PI3K/AKT/mTOR pathway as a therapeutic target in ovarian cancer. *Gynecol. Oncol.* **2015**, *137*, 173–179. [[CrossRef](#)] [[PubMed](#)]
149. Ye, P.; Wu, H.; Jiang, Y.; Xiao, X.; Song, D.; Xu, N.; Ma, X.; Zeng, J.; Guo, Y. Old dog, new tricks: Polydatin as a multitarget agent for current diseases. *Phytother. Res.* **2022**, *36*, 214–230. [[CrossRef](#)] [[PubMed](#)]
150. Varoni, E.M.; Lo Faro, A.F.; Sharifi-Rad, J.; Iriti, M. Anticancer molecular mechanisms of resveratrol. *Front. Nutr.* **2016**, *3*, 8. [[CrossRef](#)]
151. Diaz-Gerevini, G.T.; Repossi, G.; Dain, A.; Tarres, M.C.; Das, U.N.; Eynard, A.R. Beneficial action of resveratrol: How and why? *Nutrition* **2016**, *32*, 174–178. [[CrossRef](#)] [[PubMed](#)]
152. Kubota, T.; Uemura, Y.; Kobayashi, M.; Taguchi, H. Combined effects of resveratrol and paclitaxel on lung cancer cells. *Anticancer Res.* **2003**, *23*, 4039–4046.
153. Shankar, S.; Chen, Q.; Siddiqui, I.; Sarva, K.; Srivastava, R.K. Sensitization of TRAIL-resistant LNCaP cells by resveratrol (3,4',5-tri-hydroxystilbene): Molecular mechanisms and therapeutic potential. *J. Mol. Signal.* **2007**, *2*, 1–17. [[CrossRef](#)]

## Article

# Anti-Inflammatory, Antioxidative, and Nitric Oxide-Scavenging Activities of a Quercetin Nanosuspension with Polyethylene Glycol in LPS-Induced RAW 264.7 Macrophages

Sang Gu Kang<sup>1,\*</sup>, Gi Baek Lee<sup>1,†</sup>, Ramachandran Vinayagam<sup>1</sup>, Geum Sook Do<sup>2</sup>, Se Yong Oh<sup>3</sup>,  
Su Jin Yang<sup>3</sup>, Jun Bum Kwon<sup>3</sup> and Mahendra Singh<sup>1,\*</sup>

<sup>1</sup> Department of Biotechnology, Institute of Biotechnology, Life and Applied Sciences, Yeungnam University, Gyeongsan 38541, Korea

<sup>2</sup> Department of Biology, College of Natural Sciences, Kyungpook National University, Buk-gu, Daegu 41566, Korea

<sup>3</sup> Nova M Healthcare Co., Ltd., 16-53, Jisiksaneop 4-ro, Gyeongsan 38408, Korea

\* Correspondence: kangsg@ynu.ac.kr (S.G.K.); m.singh2685@gmail.com (M.S.)

† These authors contributed equally to this work.

**Abstract:** Quercetin (Qu) is a dietary antioxidant and a member of flavonoids in the plant polyphenol family. Qu has a high ability to scavenge reactive oxygen species (ROS) and reactive nitrogen species (RNS) molecules; hence, exhibiting beneficial effects in preventing obesity, diabetes, cancer, cardiovascular diseases, and inflammation. However, quercetin has low bioavailability due to poor water solubility, low absorption, and rapid excretion from the body. To address these issues, the usage of Qu nanosuspensions can improve physical stability, solubility, and pharmacokinetics. Therefore, we developed a Qu and polyethylene glycol nanosuspension (Qu-PEG NS) and confirmed its interaction by Fourier transform infrared analysis. Qu-PEG NS did not show cytotoxicity to HaCaT and RAW 264.7 cells. Furthermore, Qu-PEG NS effectively reduced the nitrogen oxide (NO) production in lipopolysaccharide (LPS)-induced inflammatory RAW 264.7 cells. Additionally, Qu-PEG NS effectively lowered the levels of COX-2, NF- $\kappa$ B p65, and IL-1 $\beta$  in the LPS-induced inflammatory RAW 264.7 cells. Specifically, Qu-PEG NS exhibited anti-inflammatory properties by scavenging the ROS and RNS and mediated the inhibition of NF- $\kappa$ B signaling pathways. In addition, Qu-PEG NS had a high antioxidant effect and antibacterial activity against *Escherichia coli* and *Bacillus cereus*. Therefore, the developed novel nanosuspension showed comparable antioxidant, anti-inflammatory, and antibacterial functions and may also improve solubility and physical stability compared to raw quercetin.

**Keywords:** quercetin; nanosuspension; antioxidant properties; flavonoids; LPS-induced inflammation; NO-scavenging activity

**Citation:** Kang, S.G.; Lee, G.B.; Vinayagam, R.; Do, G.S.; Oh, S.Y.; Yang, S.J.; Kwon, J.B.; Singh, M. Anti-Inflammatory, Antioxidative, and Nitric Oxide-Scavenging Activities of a Quercetin Nanosuspension with Polyethylene Glycol in LPS-Induced RAW 264.7 Macrophages. *Molecules* **2022**, *27*, 7432. <https://doi.org/10.3390/molecules27217432>

Academic Editor: Nour Eddine Es-Safi

Received: 7 October 2022

Accepted: 27 October 2022

Published: 1 November 2022

**Publisher's Note:** MDPI stays neutral with regard to jurisdictional claims in published maps and institutional affiliations.



**Copyright:** © 2022 by the authors. Licensee MDPI, Basel, Switzerland. This article is an open access article distributed under the terms and conditions of the Creative Commons Attribution (CC BY) license (<https://creativecommons.org/licenses/by/4.0/>).

## 1. Introduction

Inflammation is a complex biological response of body tissues against infection by pathogens, injury, or irritants, such as toxins and UV, and a repair system for damaged tissues [1]. During the inflammatory phase, macrophages secrete cytokines and chemokines, process antigens in acute immune responses and phagocytosis, and play an essential role in wound healing [2]. Macrophages in the inflammation phase regulate inflammation through the production of various inflammatory mediators, including prostaglandins, such as cyclooxygenase 2 (COX 2), nitric oxide (NO), tumor necrosis factor- $\alpha$  (TNF- $\alpha$ ), interleukin-6 (IL-6), and interleukin-1 $\beta$  (IL-1 $\beta$ ) [3]. Thus, COX-2, TNF- $\alpha$ , IL-6, and IL-1 $\beta$  of cytokines are biomarkers for inflammation responses [4].

Hence, inflammation is the cause of many diseases, and a variety of drugs (steroids and nonsteroidal anti-inflammatory drugs) are utilized to treat it. Hence, phytochemicals,

such as polyphenols (e.g., salicylic acid and derivatives, acetylsalicylic acid (aspirin)), are commonly utilized to treat inflammation. In addition, plant polyphenols extracted from medicinal plants and their synthetic derivatives have been historically used for treating inflammatory diseases [5]. Recently, many medicinal plants enriched with polyphenols have been established for anti-inflammatory disease treatments, including *Eucalyptus globules*, *Thymus vulgaris* [6], *Mentha longifolia* [7], *Pycnocycla spinosa* [8], *Echium amoenum* (borage), and *Mitrephora sirikitiae* [9,10].

Moreover, reactive oxygen (ROS) and reactive nitrogen species (RNS) are products of metabolism that use oxygen in living cells and are highly reactive to cellular and mitochondrial membranes and lead to cell damage. ROS are the derivatives of oxygen, such as superoxide radicals ( $O_2^{\bullet-}$ ), hydroxyl radicals ( $OH^{\bullet}$ ), singlet oxygen ( $^1O_2$ ), and hydrogen peroxide ( $H_2O_2$ ). RNS are nitric oxide ( $^{\bullet}NO$ ), peroxynitrite ( $ONOO^-$ ), and other harmful chemical agents [11]. Excess ROS can oxidize biomolecules and modify proteins and genes, which can lead to the progression of inflammatory diseases [12]. Therefore, rapid clearance of ROS and RNS by antioxidants is essential to prevent the occurrence of inflammation. For rapid clearance of oxidative stresses, plant polyphenols are excellent scavengers for free radicals, such as ROS and RNS. Thus, the antioxidant-rich flavonoids of polyphenols found in vegetables and fruits lower inflammation and reduce the risk of cardiovascular and brain disease. In addition, flavonoids have the advantage of being less toxic and can be prescribed for an extended duration. Therefore, various plant-derived flavonoids use as drugs have been reported as a modulator for chronic inflammation caused by virus infection and other diseases, such as human papillomavirus [13,14], hepatitis virus [15], SARS-CoV-2 [16,17], autoimmune disease [18,19], type 2 diabetes [20,21], cardiovascular diseases [22], Alzheimer's disease [23], Parkinson's disease [24], and cancer [25]. The therapeutic effect of these flavonoids and polyphenols is to inhibit the function of the enzymes as ligands that attach to the specific sites of the enzymes. For example, the catechins of flavonoids have been demonstrated to inhibit tyrosinase by binding to the enzyme's active site in molecular docking and inhibition assays [26]. Therefore, flavonoids and polyphenols are of great value in the development of disease treatments.

Quercetin (Qu) (3,3',4',5,7-pentahydroxy-2-phenylchromen-4-one), a plant flavonol of polyphenols, is found in grains, fruits, and vegetables and in higher levels in capers, buckwheat seeds, radish, onions, apples, red leaf lettuce, and asparagus [27–29]. Qu has been used as an immuno-protective and anti-inflammatory activity [30], antioxidant, antidiabetic, anticarcinogenic agent [31–33], antimicrobial activity [34], and ability to prevent various chronic disorders [35]. Hence, it can be taken as a supplement with the daily consumption of a nutraceutical with doses ranging from 10 to 125 mg/serving [36]. However, because quercetin possesses poor water solubility, low absorption, and fast excretion, it has shown relatively short bioavailability compared to the other nutraceutical polyphenolics [37,38]. Indeed, low bioavailability of Qu in human plasma has been observed after oral administration of Qu [38]. In addition, the low solubility and fast excretion of Qu results in minimal absorption in the gastrointestinal tract. In addition, quercetin is metabolized and lost by the gut microbiome before absorption in the gastrointestinal tract [17]. To overcome these factors, nanosuspension technology can improve the efficacy of drugs by changing the solubility, bioavailability, and pharmacokinetics [38].

Therefore, we proposed a novel Qu nanosuspension to improve solubility, physical stability, biosafety, and bioavailability. Furthermore, the Qu nanosuspensions were examined for their physicochemical characteristics, particle size, differential scanning calorimetry, cytotoxicity, anti-inflammatory, antibacterial, and antioxidant effects. The chemical structures of quercetin and polyethylene glycol are shown in the Figure 1.

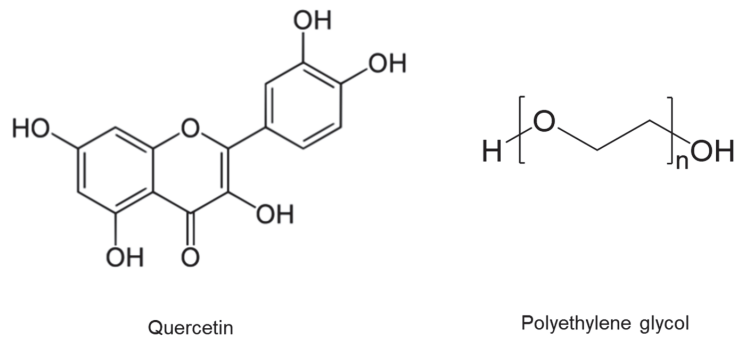


**Figure 1.** Chemical structures of quercetin and polyethylene glycol.

## 2. Results and Discussion

### 2.1. Preparation of Nanosuspension and Physical Observation

The solubility of Qu in water is relatively low (about 60 mg/L). However, Qu is soluble in organic solvents, such as ethanol, dimethyl formamide (DMF), methanol, or acetone [39]. For the preparation of Qu nanosuspension, PEG 8000 was selected as a suitable material because of its high-water solubility, excellent stability at room temperature, and non-hygroscopic properties. In addition, Qu precipitates in aqueous acidic solutions while being soluble in aqueous alkaline solutions. By taking advantage of Qu's poor solubility in acidic aqueous solutions, the same nanoprecipitation process was employed to produce the Qu-PEG nanosuspension. When 1 M HCl was added to the alkaline solution, Qu precipitated with the PEG 8000. The principle of nanosuspension predicted that the precipitated quercetin molecules interact with and are entrapped within the PEG 8000 molecules, resulting in the formation of quercetin nanosuspension (Qu-PEG NS). To prevent Qu from degrading, the nanoprecipitation was performed right after Qu was solubilized [40]. Hence, the final pH of nanosuspension was kept at 6–7 to prevent the Qu degradation. The final product was sonicated, lyophilized, and stored in a light-resistant air-tight container for further use.

Three different Qu-PEG NS samples were prepared (Table 1). The samples showed the different characteristics in their lyophilized form. The Qu-PEG NS1 was a completely dry and free-flowing powder. However, Qu-PEG NS2 had some lumps and was not dry. Qu-PEG NS3 had more lumps than Qu-PEG NS2 and was not completely dry under set conditions. This may be due the high quantity of PEG. In comparison to pure quercetin, Qu-PEG NS1 had better powder characteristics. Furthermore, the agglomeration was not observed in Qu-PEG NS1 as compared to Qu, as shown in Figure 2. The color of lyophilized formulations was found to be different than pure quercetin and Qu-PEG NS1 showed a red-orange color with respect to pure quercetin (yellow) (Figure 2).

**Table 1.** The composition ratio of nanosuspension formulation.

Formulation	Ratio (Quercetin: PEG8000)
Qu-PEG NS1	2:1
Qu-PEG NS2	1:1
Qu-PEG NS3	1:2

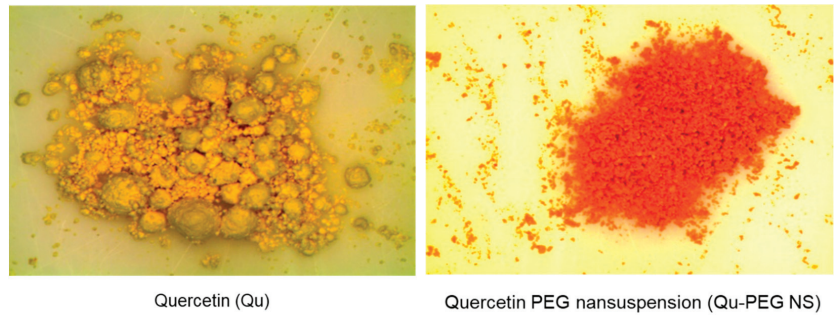


**Figure 2.** Stereomicroscopy photographs of quercetin (Qu) and quercetin with PEG nanosuspension 1 (Qu-PEG NS).

Previously, several formulation technologies for nanosuspension have been developed, i.e., nanocrystals using high-pressure homogenization [41], nanosuspensions by high-pressure homogenization [42], and nanosuspension by a solvent displacement method followed by solvent evaporation [43]. In this study, quercetin nanosuspension was successfully developed to improve the solubility and stability of natural quercetin molecules using an acid-base nanoprecipitation method (Figure 2 and Table 1).

### 2.2. Determination of Content Uniformity

Approximately  $94.6 \pm 1.78\%$  of the quercetin was found to be present in the freeze-dried formulation (Qu-PEG NS). The loss that may have occurred during preparation and lyophilization could be responsible for the loss of quercetin content [44].

### 2.3. ATR-FTIR Analysis

In conjunction with conventional infrared spectroscopy, attenuated total reflection (ATR) sampling allows materials to be directly viewed in solid or liquid conditions without needing further preparation. Hence, attenuated total reflectance-Fourier transform infrared (ATR-FTIR) assessment was performed to examine the interaction between the components used in the formation of nanosuspensions. The ATR-FTIR spectra of the components and their nanosuspensions (Qu-PEG NS) are shown in Figure 3.

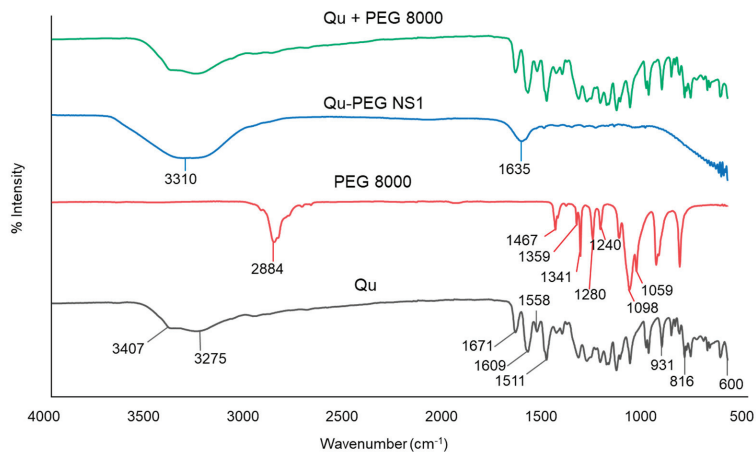


**Figure 3.** Attenuated total reflectance-Fourier transform infrared (ATR-FTIR) calculation of Qu, PEG 8000, Qu-PEG NS, and Qu + PEG 8000.

Pure Qu has three distinct peaks at 1671, 1609, and 1511  $\text{cm}^{-1}$ , which correspond to the compound's benzene ring and  $\text{-C=O}$  group. The FTIR spectrum of pure Qu showed evidence of stretching OH groups at 3407 and 3275  $\text{cm}^{-1}$  and bending OH groups of the phenol at 1350  $\text{cm}^{-1}$ . At 1671  $\text{cm}^{-1}$ , the C-O aryl ketonic stretch absorption was visible. Stretch bands for the C-C aromatic ring were observed at 1609, 1558, and 1511  $\text{cm}^{-1}$ . Furthermore, peaks at 931, 816, and 600  $\text{cm}^{-1}$  indicate the out-of-plane bending bands. Moreover, bands at 1243, 1199, and 1161  $\text{cm}^{-1}$  reveal the C-O stretching in the aryl ether ring, the C-O stretching in phenol, the C-CO-C stretching and bending in ketone, respectively. The FTIR spectrum for pure Qu is shown in Figure 3, where its characteristic groups were detected as previously reported [45].

The spectra of PEG 8000 exhibited peaks at 1467, 1359, 1341, 1280, and 1240  $\text{cm}^{-1}$ , indicating alkyl CH deforming, as well as 1113  $\text{cm}^{-1}$  for C-O-C stretching, 1060  $\text{cm}^{-1}$  for C-OH stretching, and 2884  $\text{cm}^{-1}$  for alkyl CH stretching (Figure 3), which were found similar to previously reported findings [46]. In the spectrum of PEG 8000, both trans-planar and helical structures are characteristic bands. The peaks at 1341  $\text{cm}^{-1}$  ( $\text{CH}_2$  wagging), 1240  $\text{cm}^{-1}$  ( $\text{CH}_2$  twisting), and 960  $\text{cm}^{-1}$  ( $\text{CH}_2$  rocking) were found due to the trans-planar structure. Meanwhile, the bands of the helical structure were found at 1359  $\text{cm}^{-1}$  ( $\text{CH}_2$  wagging), 1279 and 1240  $\text{cm}^{-1}$  ( $\text{CH}_2$  twisting), 960 and 841  $\text{cm}^{-1}$  ( $\text{CH}_2$  rocking), and 1059  $\text{cm}^{-1}$  (coupled C-O and C-C stretching), as previously reported [47]. Other bands in PEG 8000 at 1146, 1097, and 1059  $\text{cm}^{-1}$  can be assigned to ether groups. The physical mixture (Qu + PEG8000) showed peaks similar to Qu (Figure 3), indicating no interaction between Qu and PEG 8000. Additionally, it was observed that Qu-PEG NS indicated the broadening of peaks and showed peaks at 3310  $\text{cm}^{-1}$  and 1635  $\text{cm}^{-1}$ ; hence, this indicates that the interaction between Qu and PEG 8000 occurred, as shown in Figure 3. A previous study also demonstrated that quercetin-PEG interaction in a solid dispersion system is indicated by the broadening and shifting of the hydroxyl vibration band of PEG from 3800 to 3000  $\text{cm}^{-1}$  [48].

#### 2.4. DSC Analysis

DSC is a thermal analysis apparatus that computes the heat flow and temperature association with material conversions as a function of temperature and time. Figure 4A,B show the thermal behavior of pure Qu against the thermogram of Qu-PEG NS. It is visible that the thermogram of pure Qu revealed an endothermic peak corresponding to a swift and sharp disintegration at 324.97 °C. As seen from the DSC thermogram of the Qu-PEG NS, the peak of Qu at 324.97 °C was reduced and shifted to 211.58 °C (Figure 4A,B). An endothermic peak for Qu at 324.97 °C reveals that it exists in crystalline form. According to a previous study, quercetin's melting point was found to be 326 °C [49] and our finding also indicates an almost similar melting point. The endothermic peak disappearance in the prepared Qu-PEG NS suggests that Qu may be molecularly diffused or be interacting with the PEG matrix. Furthermore, this endothermic peak drop suggests that Qu-PEG NS could be amorphous [50,51]. Non-crystalline substances are known as amorphous forms since they have no long-range arrangement. Furthermore, amorphous materials display an apparent second-order phase transition so-called "glass transition temperature," or  $T_g$ , when examined using conventional thermal analytical techniques, such as differential scanning calorimetry (DSC). In this method, the temperature range is significantly below the melting point of the crystalline material. Hence, ' $T_g$ ' is one of a few distinguishing characteristics of an amorphous material that can be utilized to predict its suitability and stability to determine if it is appropriate for use in dosage forms [52].

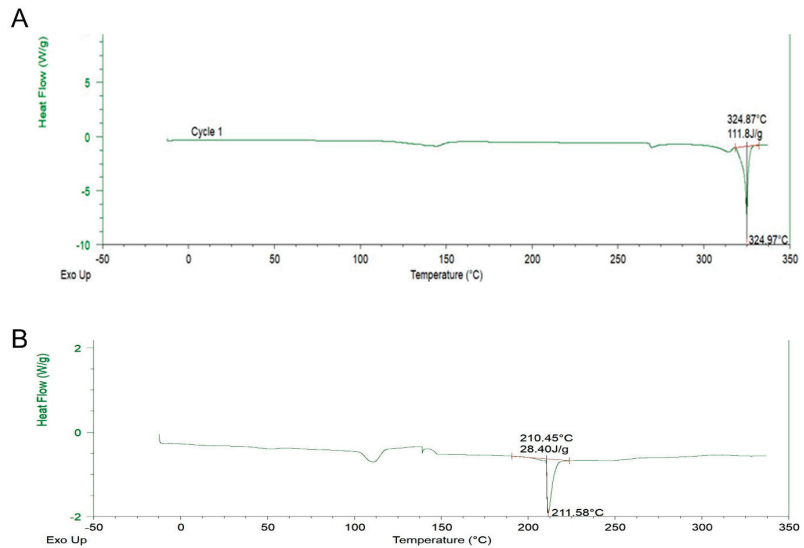


**Figure 4.** Differential scanning calorimeter (DSC) thermograms of (A) Qu and (B) Qu-PEG NS.

### 2.5. Particle Size Measurements

The particle sizes of nanosuspensions without and with lyophilization were measured (Figure 5). All lyophilized nanosuspensions increased as compared to non-lyophilized samples. Liquid nanosuspensions showed particle sizes of 261.2 to 415.5 nm while lyophilized samples showed particle sizes in the 271.1 to 422.6 nm range. The Qu-PEG NS3 showed a smaller particle size than Qu-PEG NS1 and Qu-PEG NS2. This may be due to the increased solubility of quercetin due to the addition of higher amounts of PEG 8000. The quercetin PEG nanosuspension Sample 1 (Qu-PEG NS1) (Figure 5) was selected and named Qu-PEG NS for further study due to its free-flowing properties and particle size, which can be considerable for activity. The solid particles in nanosuspensions typically have a particle-size distribution of less than one micron, with an average particle size of 200–600 nm [53]. In this experiment, we also agreed that the nanosuspension modifies the drug's pharmacokinetics with efficacy and safety by improving low solubility and bioavailability.

### 2.6. Antioxidant Activity

The hydrogen-donating ability of antioxidants is essential for predicting the physiological function of substances. The antioxidant function of the Qu-PEG NS was investigated to predict its physiological function (Figure 6). At a concentration of 250 µg per ml, the Qu-PEG NS displayed 74.80% of DPPH radical-scavenging activity, whereas ascorbic acid and Qu showed 82.20% and 76.40%, respectively (Figure 6A). The Qu-PEG NS showed an apparent ability to function as a free radical scavenger for DPPH inhibition, comparable to ascorbic acid, which is recognized as a free radical scavenger. The free-radical-scavenging activity of Qu-PEG NS may be attributed to the free-radical-scavenging activity of its central substance, quercetin. The antioxidant effect of quercetin is due to the phenolic hydroxyl group of quercetin. Phenolic hydroxyl groups in plant phenolic compounds can provide hydrogen to reduce free radicals and prevent the oxidation of proteins, lipids, and DNA [41]. Thus, Qu-PEG NS exhibited the same antioxidant capacity as Qu, because the amount of free hydroxyl groups contained in Qu-PEG NS is directly related to the scavenging ability of flavonoids, such as quercetin. It has been found that quercetin shows concentration-dependent antioxidant activity and, at higher concentrations (10 µg/mL), exhibits a plateau phase [54]. Our results also showed the plateau phase at a higher concentration, as shown in Figure 6A. Similarly, amylose–quercetin complexes [55] and

electrospun zein nanofibrous encapsulating quercetin–cyclodextrin inclusion complex [56] showed the antioxidant activity against a DPPH radical agent.

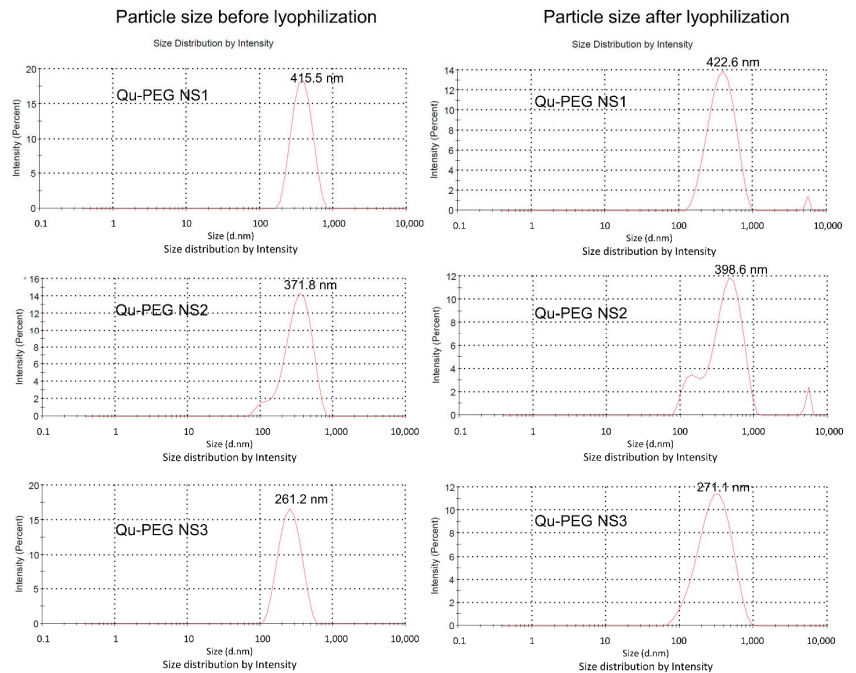


Figure 5. Particle-size distribution of nanosuspensions before and after lyophilization.

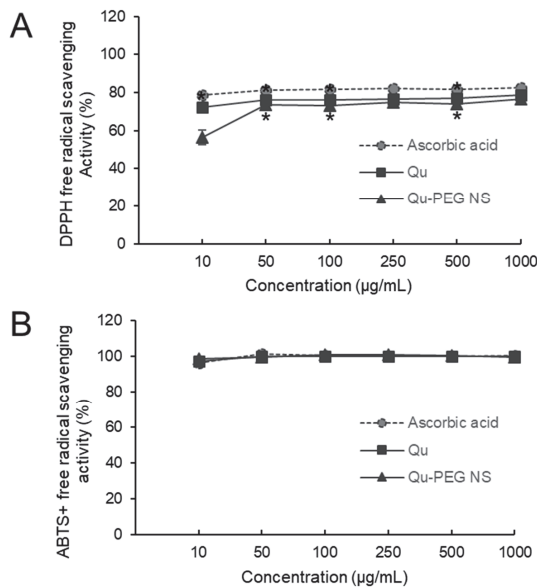


Figure 6. Effect of Qu and Qu-PEG NS on (A) DPPH and (B) ABTS free radical scavenging, \*  $p < 0.05$  indicates significant difference as compared to control.



Moreover, we also employed the ABTS assay to establish the synthetic complex's anti-radical capability. After reacting with ABTS for 12–14 h in the dark, potassium persulphate produced the blue chromophore known as ABTS. Qu-PEG NS effectively scavenged ABTS radicals, such as a powerful antioxidant ascorbic acid (Figure 6B). Moreover, the ABTS radical-scavenging abilities of Qu-PEG NS and Qu were almost the same. Thus, although the physical composition of Qu-PEG NS differs from that of pure Qu, and Qu-PEG NS has almost the same physiological properties as Qu, that may be because it retains the powerful antioxidant function of Qu substances. Previous studies also confirmed that Qu and its formulations had favorable DPPH and ABTS antioxidant activity [57–60]. Likewise, bovine serum albumin nanoparticle promoted the stability of quercetin and decreased ( $p < 0.05$ ) the ABTS radical-scavenging activity of Qu [61].

Additionally, Qu is widely known for its potent anti-free-radical properties and for acting as a chelating agent to inactivate the metal iron that is responsible for the production of reactive oxygen species [62]. Therefore, Qu shows antioxidant or pro-oxidant effects depending on the concentration, which is known as hormetic characteristic of Qu (biphasic dose response), where a low dose of Qu exhibits an antioxidant effect and a high dose shows a pro-oxidant effect [63,64]. Because of the hormetic properties, it is a strong candidate for investigations on cancer prevention [65]. Furthermore, it has been found that Qu is a significant and effective antioxidant and can be thought of as a powerful anticancer agent [63].

Additionally, ROS' oxidative damage to intracellular organelles and macromolecules causes inflammation, leading to various diseases, such as heart disease, diabetes, Alzheimer's disease, Parkinson's disease, and cancer [12,66,67]. Therefore, we predicted that Qu-PEG NS and Qu scavenge free radicals from the cells, thus inhibiting inflammation, which helps to prevent the occurrence of chronic diseases occurrence.

### 2.7. Cell Viability of Qu and Qu-PEG NS on RAW 264.7 Cells

The commonly used MTS assay is an essential parameter to determine the degree of toxicity and to measure cell viability for new substances. HaCaT and RAW 264.7 cells were treated with Qu and prepared nanosuspension to measure cell viability by MTS assay (Figure 7A,B). The cell viability on HaCaT cells was performed with Qu and Qu-PEG NS at 5, 10, 50, and 100  $\mu\text{g}/\text{mL}$  concentrations (Figure 7A). HaCaT cells treated with Qu and Qu-PEG NS at a concentration of 10  $\mu\text{g}/\text{mL}$  showed cell viability of 85.2% and 89.4% compared to control cells that were not treated with anything. When the concentration of the test sample was increased by 10 folds (100  $\mu\text{g}/\text{mL}$ ), the survival rate was slightly lower in Qu-PEG NS (76.9%), while pure quercetin showed a significant difference in cell cytotoxicity (63.8%) at a high concentration. Therefore, Qu-PEG NS had a safer function for cells than the original native Qu molecules.

In addition, we measured the cell viability of Qu and Qu-PEG NS in RAW 264.7 cells with LPS treatment and DMSO to investigate their function on inflammation. Qu showed cell viability of 79.1% and 54.7% at concentrations of 10 and 100  $\mu\text{g}/\text{mL}$ , respectively (Figure 6B), while the Qu-PEG NS showed cell viability of 80.8% and 74.8% at concentrations of 10 and 100  $\mu\text{g}/\text{mL}$ , respectively. For the results of the MTS assay, the Qu and Qu-PEG NS did not show serious cytotoxicity to HaCaT and RAW 264.7 cells. Therefore, two molecules may not have caused toxicity to mouse and human normal cells. In addition, Qu-PEG NS showed less cytotoxicity than Qu at the 100  $\mu\text{g}/\text{mL}$  concentration (Figure 7), suggesting that prepared nanosuspension is more biocompatible than the pure Qu molecules. When a material exhibits the anticipated favorable tissue response, clinically significant performance is called to be a biocompatible material. The other factors are cytotoxicity, mutagenicity, genotoxicity, carcinogenicity, and immunogenicity, which check the biocompatibility of the prepared material. In this study, the cytotoxicity study was performed and nanosuspension showed less cytotoxicity than the pure Qu. Hence, the prepared nanosuspension can be more biocompatible than the pure Qu.

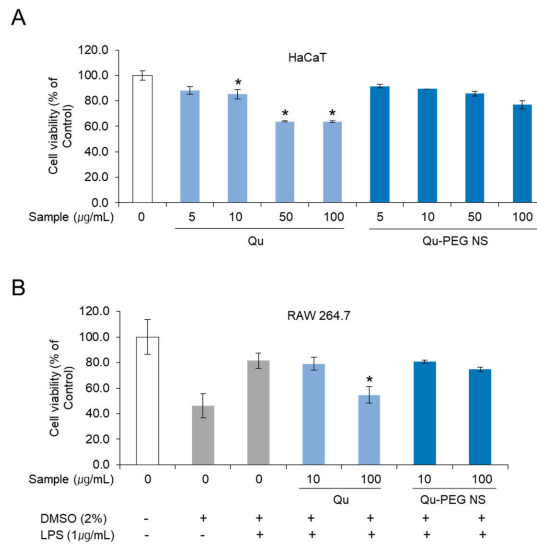


**Figure 7.** MTS analysis of (A) HaCaT and (B) RAW 264.7 cell viability treated with Quercetin and Qu-PEG NS. The cells were pre-treated with different concentrations of quercetin. Qu-PEG NS was then treated with LPS (1 µg/mL) for 48 h. Results are the mean ± S.D. of samples. \*  $p < 0.05$  indicates a significant difference from the Qu-PEG NS.

2.8. The Effect of Qu and Qu-PEG NS on NO Production by RAW 264.7 Cells

Nitric oxide (NO) is a highly reactive free radical and an important secondary messenger that mediates the inflammatory response [68]. Furthermore, LPS increases the NO production in macrophages and triggers an inflammatory response [69]. Hence, we investigated the effects of Qu-PEG NS and Qu on lowering the NO production in LPS-induced macrophages. The RAW 264.5 cells were pre-treated with 10 or 100 µg/mL of Qu, Qu-PEG NS, and catechin for 48 h. Then, the RAW 264.7 cells stimulated inflammation by treatment of LPS (1 µg/mL) for 24 h and were assayed for NO levels (Figure 8). Macrophages are one of the main cell types that demonstrate the NF-κB activation in inflammatory disorders and one of the leading NO generators in vivo [70,71].

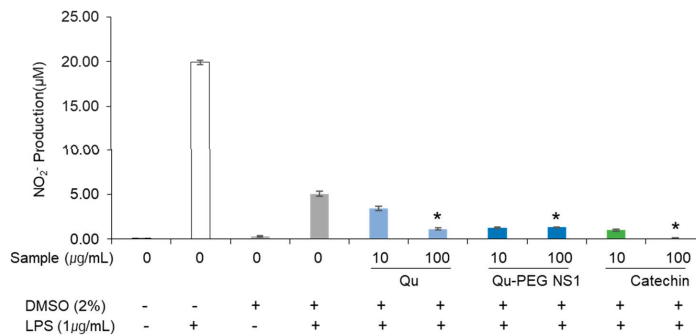


**Figure 8.** Effects of Qu and Qu-PEG NS on NO production by RAW 264.7 cells in the presence of LPS. Results are the mean ± SD of test samples, \*  $p < 0.05$  indicates a significant difference from the control at a concentration of 100 µg/mL.

Findings were confirmed that NO synthesis in RAW 264.7 cells induced the inflammatory response by LPS treatment (Figure 8). As compared to LPS treatment alone, RAW 264.7

cells treated with Qu, Qu-PEG NS, and catechins along with LPS showed a reduction in the NO production. Therefore, Qu and Qu-PEG NS dramatically reduced the NO production of macrophage cells in inflammatory conditions (Figure 8). LPS enhances the NO synthesis during the inflammatory response by activating NF- $\kappa$ B and up-regulating inducible nitric oxide synthase (iNOX) [72]. Hence, we prove the anti-inflammatory properties by considering this reduction in NO generation in inflammatory macrophage cells by Qu and nanosuspension.

### 2.9. Differentiation of RAW 264.7 Cells with Qu and Qu-PEG NS in the Presence of LPS

Macrophages represent monocytes, which are highly differentiated cellular phenotypes that coordinate host inflammatory responses and wound healing. Monocyte cells exist in a gradient along this maturation pathway, depending on the external environment, from immature to mature phenotype [73]. The degree of change from the immature to mature phenotype of monocytes treated with nanosuspension was measured (Figure 9). The RAW 264.7 cells are monocytic progenitors and have a smaller, rounded phenotype with less cytoplasmic expansion before LPS treatment, as shown in Figure 9. After treatment with LPS, cells were matured to macrophages after 48 h. As a result of the morphological transformation experiment, LPS promotes adhesion, growth, and proliferation of monocytic cells to mature and spread the culture surface. This indicates that LPS was modified to induce an inflammatory response in the immature RAW 264.7 cells. The RAW 264.7 cells were incubated with relative amounts of Qu or Qu-PEG NS with 1  $\mu$ g/mL of LPS and recorded by phase contrast microscopy (Figure 8). After 24 h of Qu and Qu-PEG NS treatment, RAW 264.7 cells had many untransformed monocytes. On the other hand, 24 h after treatment with Qu and Qu-PEG NS with LPS, RAW 264.7 cells became mature macrophages. This indicates that LPS matures macrophages due to an inflammatory response. Therefore, macrophages treated with Qu or Qu-PEG NS remained immature monocytes until LPS treatment (24 h) because the quercetin and its nanosuspension did not induce an inflammatory response. LPS is a gram-negative bacterial cell wall component and causes inflammatory bone loss by converting macrophages into osteoclasts [74]. Furthermore, LPS induces the production of various cytokines and mediators, such as tumor necrosis factor (TNF)- $\alpha$ , interleukin (IL)-1, and prostaglandin E2 (PGE2), in macrophages and plays a vital role in the maturation of macrophages [36]. Here, we confirmed that LPS-induced RAW 264.7 cells were transformed into macrophages which involves in the inflammatory response. Since Qu and Qu-PEG NS were decreased the NO production (Figure 8). Hence, they lowered the inflammatory response in LPS-induced inflammatory RAW 264.7 cells.

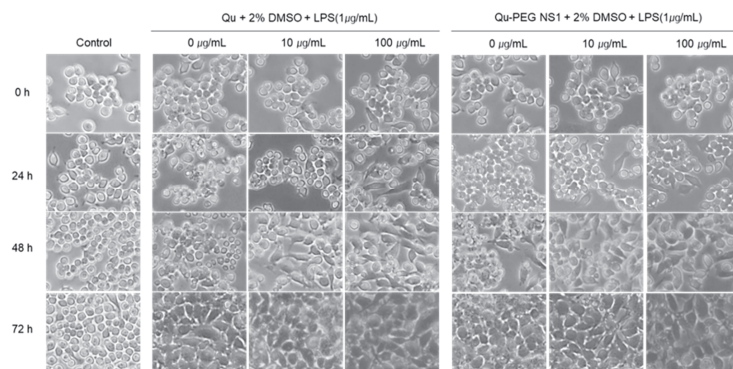


**Figure 9.** The morphological changes in LPS-induced RAW 264.7 cells treated with Qu and Qu-PEG NS. The RAW 264.7 cells were incubated with Qu or Qu-PEG NS for 24 h (24 h) and then LPS was added and grown (48 h and 72 h). Phase contrast microscopy was used to capture the images of RAW 264.7 (150 $\times$  magnification).

### 2.10. Effect of Qu and Qu-PEG NS on Inflammatory Proteins in LPS-Induced RAW 264.7 Cells

Cytokines, including TNF- $\alpha$ , IL-6, and IL-1 $\beta$ , are pro-inflammatory [75]. Furthermore, IFN- $\gamma$  and/or LPS-stimulated macrophages that have produced TNF- $\alpha$  are synergistically induced to produce NO [76]. Numerous physiological reactions are induced by TNF- $\alpha$ , including septic shock, cachexia, inflammation, and cytotoxicity [77]. In addition to controlling the expression of pro-inflammatory cytokines and enzymes, including iNOS, COX-2, TNF- $\alpha$ , and IL-6, NF- $\kappa$ B is a recognized biomarker of cellular inflammation responses [78].

Therefore, we analyzed the inflammation-related effects of Qu and Qu-PEG NS by increasing or decreasing inflammatory biomarkers, such as IL-1 $\beta$ , COX-2, and TNF- $\alpha$ -activated NF- $\kappa$ B (p65), by Western blot analysis (Figure 10).

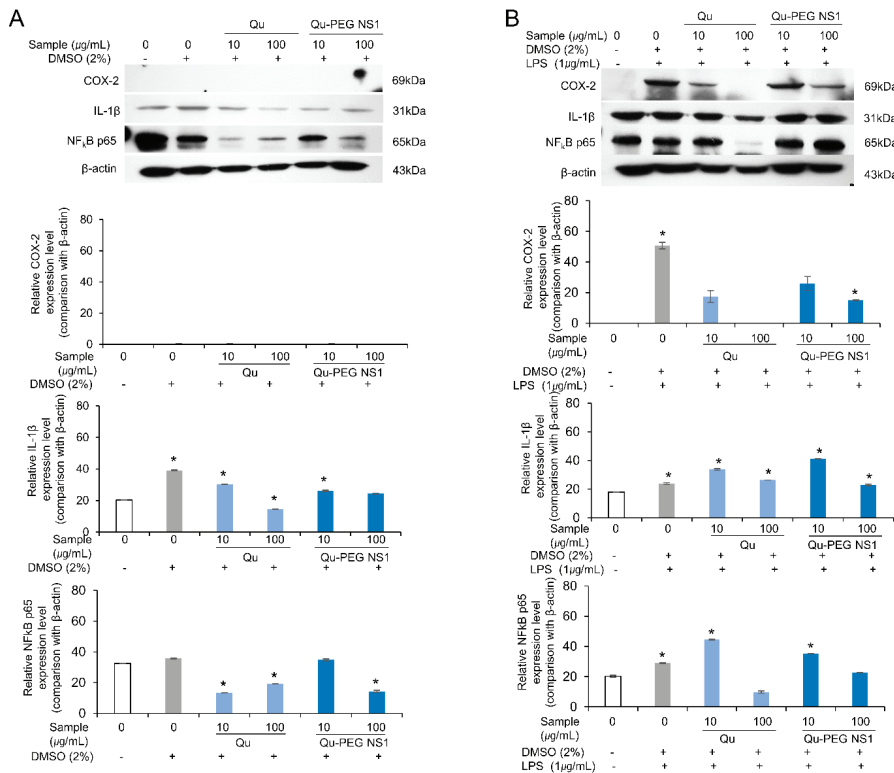


**Figure 10.** Effects of Qu and Qu-PEG NS on RAW 264.7 cells (A) in the absence of LPS and (B) in the presence of LPS on the expression of COX-2, IL-1 $\beta$ , and TNF- $\alpha$ -activated NF- $\kappa$ B (p65) as biomarkers of inflammation. The  $\beta$ -actin was employed as base level of protein expression. \*  $p < 0.05$  indicates a significant difference.

In the absence of LPS, the COX-2 protein was not expressed, while IL-1 $\beta$  and NF- $\kappa$ B were constitutively expressed (Figure 10A). However, when Qu and Qu-PEG NS were used, the IL-1 $\beta$  and NF- $\kappa$ B were significantly down-regulated compared to  $\beta$ -actin (Figure 10A). While in the presence of LPS, the RAW 264.7 cells induced the COX-2 protein, indicating inflammation (Figure 10B). Furthermore, expression of COX-2, IL-1 $\beta$ , and NF- $\kappa$ B were markedly up-regulated by LPS. However, pretreatment with Qu and Qu-PEG NS of 100  $\mu$ g/mL significantly reduced the levels of COX-2, IL-1 $\beta$ , and NF- $\kappa$ B as compared to  $\beta$ -actin level (Figure 10B).

When LPS stimulates the cells, NF- $\kappa$ B is transferred to the nucleus to regulate gene expression [79]. Here, the reduction in NF- $\kappa$ B may result in down-regulation of COX-2,

IL-1 $\beta$ , and NO production levels, indicating an anti-inflammatory effect (Figures 8 and 10). Additionally, it has been previously observed that quercetin successfully inhibited Nod-like receptor family pyrin domain-containing 3 (NLRP3) of the inflammasome family [29]. Inflammasomes are cytoplasmic multiprotein oligomers that generate active forms of cytokines IL-1 $\beta$  and IL-18 to activate the inflammatory response [80]. Therefore, by weakening the inflammasome function, quercetin is a potential treatment for severe inflammation, such as SARS-CoV-2-induced cytokine storm and Alzheimer's disease, and life-threatening diseases, such as atherosclerosis and cardiac arrhythmias. Generally, ROS-induced transcription factors, including NF $\kappa$ B, and pro-inflammatory factors, such as COX-2, TNF- $\alpha$ , IL-6, and IL-1 $\beta$ , lead to the onset of inflammation [8]. As with our experimental results, a high antioxidant effect of quercetin and epigallocatechin gallate (EGCG) reduces ROS production to inhibit thioredoxin-interacting protein (TXNIP)-NLRP3 inflammasome and decrease IL-1 $\beta$  production [81]. The possible mechanisms of inflammation by LPS and anti-inflammatory action by Qu and Qu-PEG NS are summarized in Figure 11. A possible mechanism of anti-inflammation of Qu and Qu-PEG NS may be due to high antioxidant ability, which could be responsible for reducing the activation of NLRP3 inflammasome, thereby reducing cytokines. In addition, Qu and Qu-PEG NS have a high ROS-/RNS-scavenging ability that inhibits the NF- $\kappa$ B pathway to reduce iNOS, COX-2, and lipoygenase expression levels, leading to anti-inflammatory action.

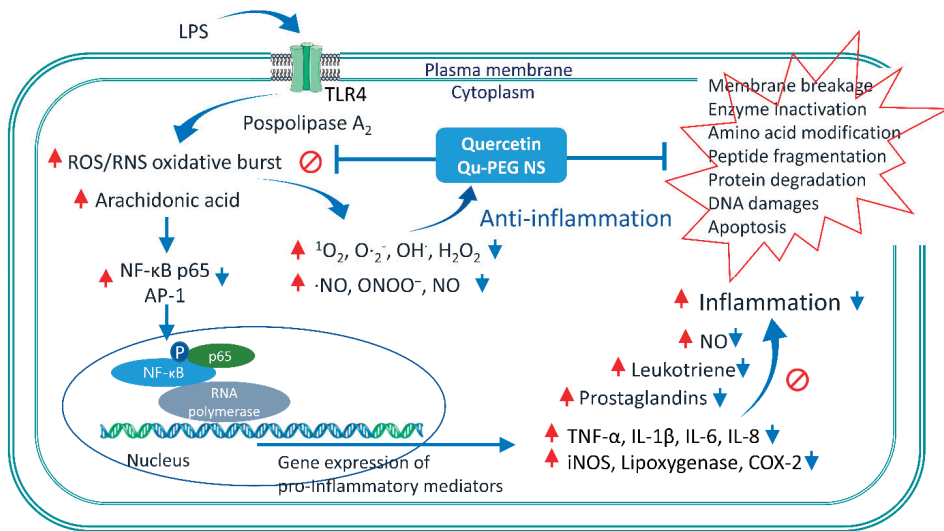


**Figure 11.** Schematic representation of the mechanism of Qu and Qu-PEG NS anti-inflammation effects in LPS-induced inflammatory RAW 264.7 cells. In this study, the Qu and Qu-PEG NS quench ROS and RNS, which may be responsible for inhibiting the active NF- $\kappa$ B transcription factor and suppression iNOS, Cox-2, and pro-inflammatory mediator protein levels, including TNF $\alpha$ , IL-1 $\beta$ , IL-6, and IL-8. Furthermore, the attenuation of NF- $\kappa$ B activity accompanies the inhibition effects of Qu and Qu-PEG NS by preventing NF- $\kappa$ B translocation from the cytoplasm to the nucleus. Red arrows indicate for inflammation pathway by LPS. Blue arrows indicate the anti-inflammation pathway by Qu or Qu-PEG NS molecules. Abbreviations: Activator protein 1 (AP-1), Cytochrome c oxidase subunit 2 (COX-2), inducible nitric oxide synthases (iNOS), Interleukin 1 beta (IL-1 $\beta$ ), Interleukin 6 (IL-6), Interleukin 8 (IL-8) Nuclear factor kappa-light-chain-enhancer of activated B cells (NF- $\kappa$ B), Nuclear factor NF-kappa-B p65 subunit (NF- $\kappa$ B p65), reactive nitrogen species (RNS), reactive oxygen species (ROS), toll-like receptor 4 (TLR4), lipopolysaccharide (LPS), tumor necrosis factor alpha (TNF- $\alpha$ ).

### 2.11. Antibacterial Activity

Pathogenic bacteria can infect humans and cause fatal diseases. The current significant issue of modern medicine is the development of drugs for drug-resistant bacteria. Though antibiotics are the first line of protection against bacterial illness, the evolution of pathogenic drug resistance has encouraged the design of highly efficient and new antimicrobial medications [82]. Antimicrobial resistance is a global problem because it induces antibiotic resistance and a rise in healthcare expenses [83]. Hence, effective antibacterial materials are considerably required. Even though many species from the *Bacillus* and *Escherichia* genera are beneficial for food fermentations, probiotics, and industrial purposes [84,85], many of these species are also referred to as pathogens. *B. cereus* is a facultative, anaerobic, gram-positive, and spore-forming soil, plant, and food bacterium, which has been associated with the development of foodborne diseases, including severe nausea, vomiting, and diarrhea [86]. Additionally, *E. coli* is a facultative, anaerobic, gram-negative, rod-shaped, coliform bacteria typically detected in mammals' gastrointestinal tract [87]. While most *E. coli* strains are not harmful to humans, others, such as *E. coli* O157:H7 has been linked to severe food poisoning [88]. Therefore, the anti-microbial activity of Qu-PEG NS against these bacteria has emphasized the potential non-antibiotic treatments. Hence, in this investigation, we used colony-forming unit (CFU) methods to assess the antibacterial activity of and Qu-PEG NS at different concentrations against *B. cereus* and *E. coli*. As shown in Figure 12, the CFU of *B. cereus* was reduced to  $171 \times 10^6$  when treated with Qu-PEG NS (0.1 mg/mL) while 0.5 mg/mL and 1 mg/mL did not show any growth in the number of bacteria as compared to  $342 \times 10^6$  CFU/mL for the untreated control. However, Qu showed  $139 \times 10^6$  CFU/mL,  $109 \times 10^6$  CFU/mL, and  $42 \times 10^6$  CFU/mL at concentrations of 0.1, 0.5, and 1.0 mg/mL, respectively. The Qu-PEG NS treatments (0.5, 1.0 mg/mL) also significantly inhibited *B. cereus* growth compared to Qu and control (Figure 12).

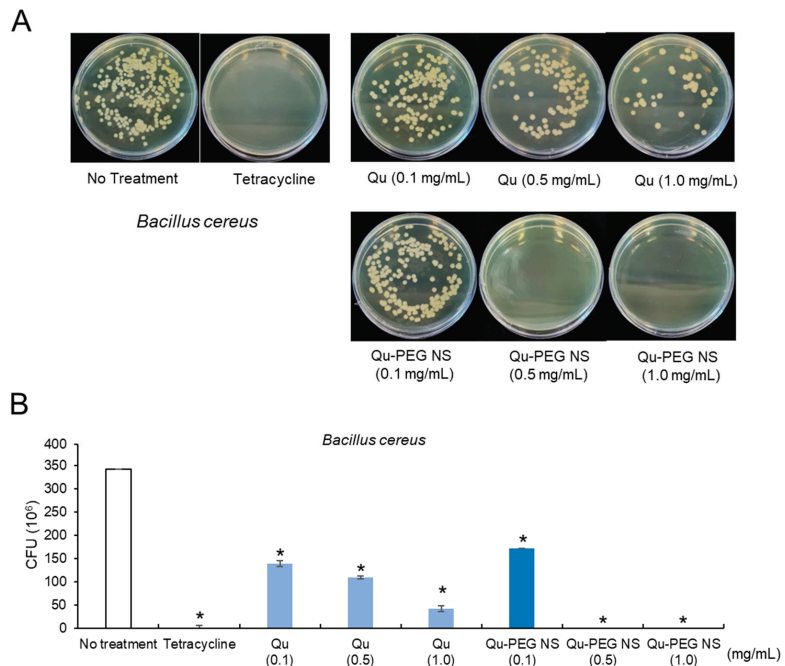


**Figure 12.** Antibacterial activity of Qu and Qu-PEG NS against *B. cereus* (A) Colony forming on growth medium and (B) Number of colonies forming units, \*  $p < 0.05$  significant difference compared to control.

*E. coli* treated with 0.1 and 0.5 mg/mL of Qu-PEG NS showed a CFU of  $126 \times 10^7$  CFU/mL and  $40 \times 10^7$  CFU/mL, respectively (Figure 13). The 1.0 mg/mL treatment of Qu and Qu-PEG NS did not produce any colonies compared to  $129 \times 10^7$  CFU/mL for the untreated control. The antimicrobial activity of Qu and Qu-PEG NS may be due to microbial cell lysis by precipitation of membrane proteins of bacteria [89]. At a dosage of 0.5 mg/mL, the Qu-PEG NS was found to be more efficient against gram-positive bacteria, such as *B. cereus*, compared to gram-negative bacteria. This result may be related to the possibility that the nanosuspension can easily adhere to the bacterial membrane and induce cell lysis through protein precipitation. Thus, Qu-PEG NS can be used as a non-antibiotic antimicrobial agent against gram-positive bacterial infections.

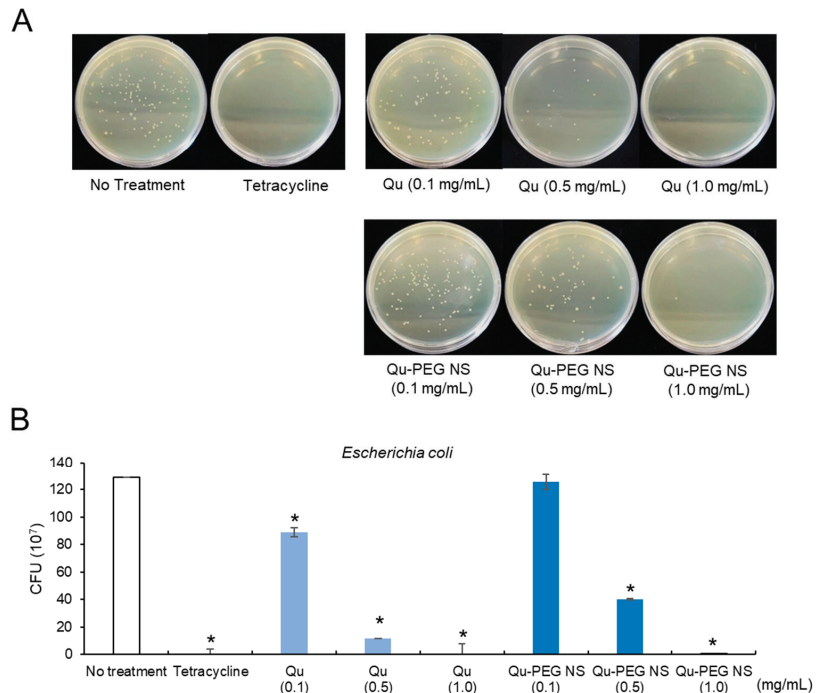


**Figure 13.** Antibacterial activity of Qu and Qu-PEG NS against *E. coli* (A) Colony forming on growth medium and (B) Number of colonies forming units, \*  $p < 0.05$  significant difference compared to control.

### 3. Materials and Methods

#### 3.1. Chemicals and Cell Culture

HaCaT and RAW 264.7 (KTCC No. 40071) cells were taken from the Korea Cellular Bank (KTCC, Seoul, Korea). Penicillin (100 units/mL)/streptomycin (100 g/mL) and fetal bovine serum (FBS), 0.25% trypsin-EDTA, Cell Titer 96 Aqueous one solution cell proliferation assay kit (Prommega, Madison, WI, USA), lipopolysaccharide (Sigma Aldrich, St. Louis, MO, USA), Halt Protease Inhibitor Cocktail, EDTA-Free (Thermo Scientific, Waltham, MA, USA), Goat Anti-Rabbit IgG antibody (HRP) (GeneTex, Irvine, CA, USA), m-IgGκ BP-HRP (Santa Cruz Biotechnology, Dallas, TX, USA), M-PER<sup>®</sup> Mammalian Protein Extraction Reagent (Thermo Scientific Waltham, MA, USA), Western Enhanced Buffer (NEOSCIENCE, Seoul, Korea), Super Signal<sup>®</sup> West Pico Chemical Substrate (Thermo Scientific Waltham, MA, USA), PVDF membrane (Sigma Aldrich, St. Louis, MO, USA), phosphate buffer saline (PBS) (Welgene, Gyeongsan, Republic of Korea; Sigma, St. Louis,

MO, USA), sodium hydroxide, hydrochloric acid, polyethylene glycol 8000, quercetin, and other reagents (Sigma Aldrich) were used.

### 3.2. Preparation of Nanosuspension

Nanosuspension was prepared by the acid-base nanoprecipitation method. First, a mixture of quercetin and polyethylene glycol 8000 (0.6 g) was weighed in different ratios such as 2:1, 1:1, and 1:2. The weighed quantity of combinations was dissolved separately in 20 mL of 0.2 N NaOH solution at room temperature using a magnetic stirrer (Dathan scientific, MSH-20D) at 500 rpm to form a clear solution. Then, 3.5 mL of 1M HCl was added under continuous magnetic stirring at 1500 rpm for 15 min to obtain the precipitated quercetin suspension. Furthermore, the prepared suspension pH was adjusted to 6–7 with 0.1 N NaOH or 0.1M HCl. Then, the formulation was sonicated with a probe sonicator (Vibra cell sonicator, 750-watt model) for 20 min at 35% amplitude at room temperature to formulate nanosuspensions. Then, the prepared nanosuspensions were frozen at  $-70\text{ }^{\circ}\text{C}$  for 24 h and lyophilized at  $-60\text{ }^{\circ}\text{C}$  for 48 h. The lyophilized samples were stored in an air-tight container for further evaluation.

#### 3.2.1. Physical Observation and Determination of Content Uniformity

The Qu and lyophilized nanosuspensions (Qu-PEG NS1, Qu-PEG NS2, and Qu-PEG NS3) were examined for agglomeration and color using stereomicroscopy. The samples were scattered on a glass slide and focused and the photomicrographs were taken.

The amount of quercetin in the freeze-dried product was determined by dissolving 10 mg of lyophilized nanosuspension in 10 mL of methanol. After 15 min of probe sonication and filtering with a 0.22  $\mu\text{m}$  membrane filter, the absorbance of quercetin was measured spectrophotometrically at 370 nm. The concentration of quercetin was calculated using the regression equation ( $y = 0.0673x + 0.0375$ ,  $r^2 = 1$ ), which was obtained by preparing the standard curve of quercetin in methanol (where 'y' is the absorbance of the test sample and 'x' is the concentration to be determined). Among the three types of nanosuspension in Table 1, Qu-PEG NS1 was selected and named Qu-PEG NS to investigate the physiological activity properties.

#### 3.2.2. Analytical Characterization

Attenuated total reflectance-Fourier transform infrared (ATR-FTIR) spectroscopy was recorded on a Perkin Elmer (Waltham, MA, USA) in the infrared region ( $4000$  and  $600\text{ cm}^{-1}$ ) and analyzed by transmittance technique at a spectral resolution of  $1\text{ cm}^{-1}$ .

The DSC curves of the different samples were recorded on a differential scanning calorimeter (Perkin Elmer Inc., Waltham, MA, USA) calibrated with indium. The thermal behavior was studied by heating samples in aluminum crimped pans under nitrogen gas flow. The samples were heated from  $-10\text{ }^{\circ}\text{C}$  to  $340\text{ }^{\circ}\text{C}$  at  $10\text{ }^{\circ}\text{C}/\text{min}$  to obtain the thermogram.

#### 3.2.3. Particle Size Measurements

Quercetin nanosuspensions were analyzed for particle size by photon correlation spectroscopy (PCS) using a Zetasizer Nano ZS (Zen 3600, Malvern Instruments, Worcester-shire, United Kingdom). The instrument scientifically and instinctively adjusts to the test sample by altering the intensity of the laser and the attenuator of the photomultiplier, thus confirming the reproducibility of the experimental measurement conditions.

### 3.3. Determination of Antioxidant Capacity

The DPPH $\cdot$  free-radical-scavenging activity with Qu and Qu-PEG NS was evaluated in contrast to ascorbic acid [87]. In brief, 200  $\mu\text{L}$  of the 10, 50, 100, 250, 500, and 1000  $\mu\text{g}/\text{mL}$  NQS1 solution and 100  $\mu\text{L}$  of the 0.2 mM DPPH solution in ethanol were combined. The mixture was then left to react for 30 min at room temperature before the absorbance at



517 nm was recorded using an ELISA reader. Equations (1) and (2) were used to determine the DPPH<sup>•</sup> free-radical-scavenging activity.

$$\text{DPPH scavenging activity \%} = [1 - \text{Absorbance sample}/\text{Absorbance control}] \times 100 \quad (1)$$

As previously reported, the ABTS<sup>+</sup> radical-cation-scavenging method was performed [40]. To generate ABTS<sup>+</sup> radicals, 7 mM ABTS and 2.5 mM potassium persulfate were combined in an equal volume and left at room temperature in the dark for 24 h. Then, using an ELISA reader (Infinite™ F200, Männedorf, Switzerland), the absorbance of this solution was measured at 734 nm after being diluted twice with ethanol. An ELISA reader was used to measure the absorbance at 734 nm to check the scavenging activity of Qu and Qu-PEG NS in an equal volume (150 µL) of ABTS solution and with different concentrations of test samples, i.e., 10, 50, 100, 250, 500, and 1000 µg/mL of Qu and Qu-PEG NS. The reaction was allowed to proceed for 6 min at room temperature. ABTS scavenging activity was calculated by the following equation.

$$\text{ABTS scavenging activity \%} = [1 - \text{Absorbance sample}/\text{Absorbance control}] \times 100 \quad (2)$$

### 3.4. Nitric Oxide (NO) Production Measurement

After treatment with LPS, NO production assay was performed to measure the effect of Qu and Qu-PEG NS on NO production from RAW 264.7 cells. The RAW 264.7 cells were uniformly dispensed in 24 wells at a density of  $2 \times 10^5$  cells/well and then each test solution was applied at a concentration of 10 or 100 µg/mL and incubated for 48 h. Furthermore, cells were treated with LPS (1 µg/mL) and incubated for 96 h (LPS treatment for 48 h). After that, 50 µL of the cell supernatant was collected and reacted with 50 µL of the sulfanilamide solution (1% sulfanilamide in 5% phosphoric acid) for 10 min. Then, 50 µL of the NED solution (0.1% N-1-naphthylethylenediamine) was used to react for 10 min, and the absorbance was measured at 548 nm by utilizing an ELISA reader. A standard curve of sodium nitrite was utilized to calculate the NO concentration.

### 3.5. Measurement of Cell Viability of Qu and Qu-PEG NS

Cytotoxicity and proliferation rates of Qu and Qu-PEG NS on HaCaT and RAW 264.7 cells were measured after the treatment with lipopolysaccharide (LPS, 1 µg/mL). Testing procedures were performed as previously reported, with some modifications to detect cell cytotoxicity [90]. The HaCaT and RAW 264.7 cells were evenly distributed in a 96-well plate at a density of  $1 \times 10^4$  cells/well to measure cytotoxicity and proliferation. After 24 h, each sample was treated with a solution containing 10 or 100 µg/mL and incubated for 96 h. The impact of concentration-specific therapy on cell proliferation was examined using the Cell Titer 96 Aqueous one solution cell proliferation assay kit. All the media were taken out after incubation and then 20 µL of DMEM medium and 100 µL of 3-(4,5-dimethylthiazol-2-yl)-5-(3-carboxymethoxyphenyl)-2-(4-sulfophenyl)-2H-tetrazol inner salt (MTS) solution were added. The sample optical density was measured with an ELISA reader using a 96-well plate (Infinite™ F200, Switzerland). The absorbance at 390 nm, 37 °C, and 3 °C was measured. As a control, a culture solution without any treatment was employed.

### 3.6. Anti-Inflammatory Activity of LPS-Induced RAW 264.7 Cells with Qu and Qu-PEG NS

In a 100 mm petri plate, macrophages (RAW 264.7 cells) were cultured at a density of  $4.5 \times 10^7$  cells/plate for 24 h. Afterward, cells were rinsed with PBS and treated with various concentrations (10 and 100 µg/mL) of quercetin and nano-quercetin and incubated for 48 h, followed by cells being exposed to LPS (1 µg/mL) and further incubated for 96 h to induce the inflammation. Then, the protein was extracted from the sample-treated RAW 264.7 cells using M-PER® Mammalian Protein Extraction Reagent and Halt Protease Inhibitor Cocktail, EDTA-Free, and the protein content was assessed.

Proteins extracted from treated RAW 264.7 cells were used for Western blot analysis. Briefly, 30 µg of protein was separated by electrophoresis using 7.5% sodium dodecyl sulfate-polyacrylamide gel (SDS-PAGE) and afterward transferred to PVDF membrane (polyvinylidene fluoride) and blocked with Western Enhanced Buffer (NEOSCIENCE, Seoul, Korea). The primary antibodies were employed in a ratio of 1:2000 and 1:1000. The secondary antibodies were Goat Anti-Rabbit IgG antibody (HRP) (GeneTex, Alton Pkwy Irvine, CA, USA) and m-IgGκ BP-HRP (Santa Cruz Biotechnology, Dallas, TX, USA). The primary antibodies COX-2, IL-1β NFκB p65, and β-actin were purchased from GeneTex or Santa Cruz Biotechnology. The secondary antibodies were labelled in the ratio of 1:10,000. After completing the second antibody reaction, a Super Signal® West Pico Chemical Substrate (Thermo Scientific, Waltham, MA, USA) solution was applied to a PVDF membrane (Sigma Aldrich, St. Louis, MI, USA), made photosensitive to film in a darkroom, and developed. The relative strength of a specific protein band was determined utilizing an Image J® analyzer (National Institutes of Health, Bethesda, MD, USA).

### 3.7. Antimicrobial Activity

*Bacillus cereus* (ATCC 14579) and *Escherichia coli* (ATCC 15597) were purchased from the ATCC (American Type Culture Collection, Manassas, VI, USA) and assessed for the antibacterial activity with Qu and Qu-PEG NS (0.1 and 1.0 mg/mL). Bacterial culture was performed in LB (Luria–Bertani) media for 12 h at 37 °C with shaking at 120 rpm. Tetracycline was used as a positive control. Bacteria ( $10^4$  cells/mL) were then collected and washed with PBS (pH 6.8). These cells were then added to fresh LB media with varied sample concentrations and cultured at 37 °C for another 12 h with shaking. The sample-treated bacterial cultures were serially diluted from  $10^{-5}$  to  $10^{-7}$  and then plated on LB agar plates and incubated at 32 °C for 12 h. The antibacterial activity of the Qu and Qu-PEG NS was determined by colony counting on the culture plates.

### 3.8. Statistical Analysis

All experiments were repeated three times and an average ± standard deviation represented statistical analysis. The student's t-test method was used (GraphPad 8 trial version) and  $p < 0.05$  indicated a statistically significant difference.

## 4. Conclusions

According to physicochemical characterization and the acid-base condition of the synthesis, we addressed the development of nanosuspensions. In addition, this study observed that prepared nanosuspension showed favorable biosafety against cell line studies. Furthermore, the nanosuspension significantly protected RAW 264.7 cells by regulating NO overproduction and ROS levels. Moreover, nanosuspension showed suitable anti-inflammatory activity by reducing the COX-2, IL-1β and NF-κB levels along with antibacterial activity. Hence, it can be concluded that the prepared nanosuspension possesses considerable antioxidant, anti-inflammatory, and antibacterial activity, which may help to prevent the occurrence of chronic diseases.

**Author Contributions:** Conceptualization and writing original draft preparation: M.S. and S.G.K.; project administration: S.G.K. and J.B.K.; methodology: M.S., G.B.L. and S.G.K.; data curation: M.S., G.S.D., G.B.L., R.V., S.Y.O. and S.J.Y.; writing, review and editing: M.S., R.V., G.S.D. and S.G.K.; supervision: S.G.K. All authors have read and agreed to the published version of the manuscript.

**Funding:** This research received no external funding.

**Institutional Review Board Statement:** Not applicable.

**Informed Consent Statement:** Not applicable.

**Data Availability Statement:** Not applicable.

**Acknowledgments:** This manuscript is the result of a study on the “Leaders in Industry-University Cooperation 3.0” Project, supported by the Ministry of Education and National Research Foundation of Korea (1345356171). The authors thank the Core Research Support Center for Natural Products and Medical Materials at Yeungnam University, Gyeongsan, the Republic of Korea, for technical support regarding physicochemical analysis using the FTIR (PerkinElmer, Inc., Waltham, USA) Differential scanning calorimeter (DSC) (Perkin Elmer) and the Zetasizer Nano ZS (Malvern Panalytical Ltd. Malvern, UK).

**Conflicts of Interest:** The authors declare no conflict of interest.

## References

- Dunster, J.L. The macrophage and its role in inflammation and tissue repair: Mathematical and systems biology approaches. *Wiley Interdiscip. Rev. Syst. Biol. Med.* **2016**, *8*, 87–99. [[CrossRef](#)] [[PubMed](#)]
- Nahrendorf, M.; Hoyer, F.F.; Meerwaldt, A.E.; van Leent, M.M.T.; Senders, M.L.; Calcagno, C.; Robson, P.M.; Soultanidis, G.; Pérez-Medina, C.; Teunissen, A.J.P. Imaging cardiovascular and lung macrophages with the positron emission tomography sensor <sup>64</sup>Cu-macrin in mice, rabbits, and pigs. *Circ. Cardiovasc. Imaging* **2020**, *13*, e010586. [[CrossRef](#)] [[PubMed](#)]
- Jiang, Z.; Zhu, L. Update on the role of alternatively activated macrophages in asthma. *J. Asthma Allergy* **2016**, *9*, 101. [[CrossRef](#)]
- Sadeghi-Aliabadi, H.; Aliasgharluo, M.; Fattahi, A.; Mirian, M.; Ghannadian, M. In vitro cytotoxic evaluation of some synthesized COX-2 inhibitor derivatives against a panel of human cancer cell lines. *Res. Pharm. Sci.* **2013**, *8*, 298. [[PubMed](#)]
- Amirghofran, Z. Herbal medicines for immunosuppression. *Iran. J. Allergy Asthma Immunol.* **2012**, *11*, 111–119.
- Vigo, E.; Cepeda, A.; Perez-Fernandez, R.; Gualillo, O. In-vitro anti-inflammatory effect of Eucalyptus globulus and Thymus vulgaris: Nitric oxide inhibition in J774A. 1 murine macrophages. *J. Pharm. Pharmacol.* **2004**, *56*, 257–263. [[CrossRef](#)]
- Karimian, P.; Kavooosi, G.; Amirghofran, Z. Anti-inflammatory effect of Mentha longifolia in lipopolysaccharide-stimulated macrophages: Reduction of nitric oxide production through inhibition of inducible nitric oxide synthase. *J. Immunotoxicol.* **2013**, *10*, 393–400. [[CrossRef](#)]
- Minaiyan, M.; Asghari, G.; Sadraei, H.; Feili, E. Anti-inflammatory effect of Pycnocyclus spinosa extract and its component isoacetovanillone on acetic acid induced colitis in rats. *Res. Pharm. Sci.* **2015**, *10*, 345.
- Naseri, N.; Kalantar, K.; Amirghofran, Z. Anti-inflammatory activity of Echinum amoenum extract on macrophages mediated by inhibition of inflammatory mediators and cytokines expression. *Res. Pharm. Sci.* **2018**, *13*, 73.
- Mangmool, S.; Limpichai, C.; Han, K.K.; Reutrakul, V.; Anantachoke, N. Anti-inflammatory effects of Mitrephora sirikitiae leaf extract and isolated lignans in RAW 264.7 cells. *Molecules* **2022**, *27*, 3313. [[CrossRef](#)]
- Dröge, W. Free radicals in the physiological control of cell function. *Physiol. Rev.* **2002**, *82*, 47–95. [[CrossRef](#)] [[PubMed](#)]
- Chatterjee, S. Oxidative stress, inflammation, and disease. In *Oxidative Stress and Biomaterials*; Elsevier: Amsterdam, The Netherlands, 2016; pp. 35–58.
- Fernandes, J.V.; Fernandes, T.A.A.d.M.; De Azevedo, J.C.V.; Cobucci, R.N.O.; De Carvalho, M.G.F.; Andrade, V.S.; De Araujo, J.M.G. Link between chronic inflammation and human papillomavirus-induced carcinogenesis. *Oncol. Lett.* **2015**, *9*, 1015–1026. [[CrossRef](#)] [[PubMed](#)]
- Massa, S.; Pagliarello, R.; Paolini, F.; Venuti, A. Natural Bioactives: Back to the Future in the Fight against Human Papillomavirus? A Narrative Review. *J. Clin. Med.* **2022**, *11*, 1465. [[CrossRef](#)] [[PubMed](#)]
- Fried, M.W.; Navarro, V.J.; Afdhal, N.; Belle, S.H.; Wahed, A.S.; Hawke, R.L.; Doo, E.; Meyers, C.M.; Reddy, K.R. Effect of silymarin (milk thistle) on liver disease in patients with chronic hepatitis C unsuccessfully treated with interferon therapy: A randomized controlled trial. *JAMA* **2012**, *308*, 274–282. [[CrossRef](#)]
- Bharadwaj, S.; Dubey, A.; Yadava, U.; Mishra, S.K.; Kang, S.G.; Dwivedi, V.D. Exploration of natural compounds with anti-SARS-CoV-2 activity via inhibition of SARS-CoV-2 Mpro. *Brief. Bioinform.* **2021**, *22*, 1361–1377. [[CrossRef](#)]
- Jang, M.; Park, R.; Park, Y.-I.; Cha, Y.-E.; Yamamoto, A.; Lee, J.I.; Park, J. EGCG, a green tea polyphenol, inhibits human coronavirus replication in vitro. *Biochem. Biophys. Res. Commun.* **2021**, *547*, 23–28. [[CrossRef](#)]
- Khan, H.; Sureda, A.; Belwal, T.; Çetinkaya, S.; Süntar, İ.; Tejada, S.; Devkota, H.P.; Ullah, H.; Aschner, M. Polyphenols in the treatment of autoimmune diseases. *Autoimmun. Rev.* **2019**, *18*, 647–657. [[CrossRef](#)]
- Mueller, A.-L.; Brockmueller, A.; Kunnumakkara, A.B.; Shakibaei, M. Modulation of Inflammation by Plant-Derived Nutraceuticals in Tendinitis. *Nutrients* **2022**, *14*, 2030. [[CrossRef](#)]
- Reis, C.E.G.; Dórea, J.G.; da Costa, T.H.M. Effects of coffee consumption on glucose metabolism: A systematic review of clinical trials. *J. Tradit. Complement. Med.* **2019**, *9*, 184–191. [[CrossRef](#)]
- Van Dam, R.M.; Willett, W.C.; Manson, J.E.; Hu, F.B. Coffee, caffeine, and risk of type 2 diabetes: A prospective cohort study in younger and middle-aged US women. *Diabetes Care* **2006**, *29*, 398–403. [[CrossRef](#)]
- Szczepańska, E.; Białek-Dratwa, A.; Janota, B.; Kowalski, O. Dietary Therapy in Prevention of Cardiovascular Disease (CVD)—Tradition or Modernity? A Review of the Latest Approaches to Nutrition in CVD. *Nutrients* **2022**, *14*, 2649. [[CrossRef](#)]
- Mohamed, H.E.; Asker, M.E.; Younis, N.N.; Shaheen, M.A.; Eissa, R.G. Modulation of brain insulin signaling in Alzheimer’s disease: New insight on the protective role of green coffee bean extract. *Nutr. Neurosci.* **2020**, *23*, 27–36. [[CrossRef](#)] [[PubMed](#)]

24. Pacifici, F.; Salimei, C.; Pastore, D.; Malatesta, G.; Ricordi, C.; Donadel, G.; Bellia, A.; Rovella, V.; Tafani, M.; Garaci, E. The Protective Effect of a Unique Mix of Polyphenols and Micronutrients against Neurodegeneration Induced by an In Vitro Model of Parkinson's Disease. *Int. J. Mol. Sci.* **2022**, *23*, 3110. [[CrossRef](#)]
25. Maleki Dana, P.; Sadoughi, F.; Asemi, Z.; Yousefi, B. The role of polyphenols in overcoming cancer drug resistance: A comprehensive review. *Cell. Mol. Biol. Lett.* **2022**, *27*, 1. [[CrossRef](#)]
26. Lee, K.E.; Bharadwaj, S.; Sahoo, A.K.; Yadava, U.; Kang, S.G. Determination of tyrosinase-cyanidin-3-O-glucoside and (-/+)-catechin binding modes reveal mechanistic differences in tyrosinase inhibition. *Sci. Rep.* **2021**, *11*, 24494. [[CrossRef](#)]
27. Di Petrillo, A.; Orrù, G.; Fais, A.; Fantini, M.C. Quercetin and its derivatives as antiviral potentials: A comprehensive review. *Phytother. Res.* **2022**, *36*, 266–278. [[CrossRef](#)] [[PubMed](#)]
28. Nishimuro, H.; Ohnishi, H.; Sato, M.; Ohnishi-Kameyama, M.; Matsunaga, I.; Naito, S.; Ippoushi, K.; Oike, H.; Nagata, T.; Akasaka, H. Estimated daily intake and seasonal food sources of quercetin in Japan. *Nutrients* **2015**, *7*, 2345–2358. [[CrossRef](#)] [[PubMed](#)]
29. Yang, D.; Wang, T.; Long, M.; Li, P. Quercetin: Its main pharmacological activity and potential application in clinical medicine. *Oxidative Med. Cell. Longev.* **2020**, *2020*, 8825387. [[CrossRef](#)] [[PubMed](#)]
30. Saeedi-Boroujeni, A.; Mahmoudian-Sani, M.-R. Anti-inflammatory potential of Quercetin in COVID-19 treatment. *J. Inflamm.* **2021**, *18*, 3. [[CrossRef](#)] [[PubMed](#)]
31. Carrasco-Pozo, C.; Tan, K.N.; Reyes-Farias, M.; De La Jara, N.; Ngo, S.T.; Garcia-Diaz, D.F.; Llanos, P.; Cires, M.J.; Borges, K. The deleterious effect of cholesterol and protection by quercetin on mitochondrial bioenergetics of pancreatic  $\beta$ -cells, glycemic control and inflammation: In vitro and in vivo studies. *Redox Biol.* **2016**, *9*, 229–243. [[CrossRef](#)]
32. Carullo, G.; Cappello, A.R.; Frattaruolo, L.; Badolato, M.; Armentano, B.; Aiello, F. Quercetin and derivatives: Useful tools in inflammation and pain management. *Future Med. Chem.* **2017**, *9*, 79–93. [[CrossRef](#)] [[PubMed](#)]
33. Rauf, A.; Imran, M.; Khan, I.A.; ur-Rehman, M.; Gilani, S.A.; Mehmood, Z.; Mubarak, M.S. Anticancer potential of quercetin: A comprehensive review. *Phytother. Res.* **2018**, *32*, 2109–2130. [[CrossRef](#)] [[PubMed](#)]
34. Farhadi, F.; Khameneh, B.; Iranshahi, M.; Iranshahi, M. Antibacterial activity of flavonoids and their structure–activity relationship: An update review. *Phytother. Res.* **2019**, *33*, 13–40. [[CrossRef](#)]
35. Aguirre, L.; Arias, N.; Teresa Macarulla, M.; Gracia, A.; P Portillo, M. Beneficial effects of quercetin on obesity and diabetes. *Open Nutraceuticals J.* **2011**, *4*, 189–198.
36. Lesjak, M.; Beara, I.; Simin, N.; Pintač, D.; Majkić, T.; Bekvalac, K.; Orčić, D.; Mimica-Dukić, N. Antioxidant and anti-inflammatory activities of quercetin and its derivatives. *J. Funct. Foods* **2018**, *40*, 68–75. [[CrossRef](#)]
37. Li, Y.; Yao, J.; Han, C.; Yang, J.; Chaudhry, M.T.; Wang, S.; Liu, H.; Yin, Y. Quercetin, inflammation and immunity. *Nutrients* **2016**, *8*, 167. [[CrossRef](#)]
38. Alizadeh, S.R.; Ebrahimzadeh, M.A. O-Glycoside quercetin derivatives: Biological activities, mechanisms of action, and structure–activity relationship for drug design, a review. *Phytother. Res.* **2022**, *36*, 778–807. [[CrossRef](#)]
39. Chebil, L.; Humeau, C.; Anthoni, J.; Dehez, F.; Engasser, J.-M.; Ghoul, M. Solubility of flavonoids in organic solvents. *J. Chem. Eng. Data* **2007**, *52*, 1552–1556. [[CrossRef](#)]
40. Jurasekova, Z.; Domingo, C.; García-Ramos, J.V.; Sánchez-Cortés, S. Effect of pH on the chemical modification of quercetin and structurally related flavonoids characterized by optical (UV-visible and Raman) spectroscopy. *Phys. Chem. Chem. Phys.* **2014**, *16*, 12802–12811. [[CrossRef](#)]
41. Sahoo, N.G.; Kakran, M.; Shaal, L.A.; Li, L.; Müller, R.H.; Pal, M.; Tan, L.P. Preparation and characterization of quercetin nanocrystals. *J. Pharm. Sci.* **2011**, *100*, 2379–2390. [[CrossRef](#)]
42. Karadag, A.; Ozcelik, B.; Huang, Q. Quercetin nanosuspensions produced by high-pressure homogenization. *J. Agric. Food Chem.* **2014**, *62*, 1852–1859. [[CrossRef](#)]
43. Pessoa, L.Z.d.S.; Duarte, J.L.; Ferreira, R.M.d.A.; Oliveira, A.E.M.d.F.M.; Cruz, R.A.S.; Faustino, S.M.M.; Carvalho, J.C.T.; Fernandes, C.P.; Souto, R.N.P.; Araújo, R.S. Nanosuspension of quercetin: Preparation, characterization and effects against *Aedes aegypti* larvae. *Rev. Bras. De Farmacogn.* **2018**, *28*, 618–625. [[CrossRef](#)]
44. Kattabooinaa, S.; Chandrasekhar, P.; Balaji, S. Drug nanocrystals: A novel formulation approach for poorly soluble drugs. *Int. J. Pharmtech Res.* **2009**, *1*, 682–694.
45. Kuzniarz, A. Infrared spectrum analysis of some flavonoids. *Acta Pol. Pharm. -Drug Res.* **2014**, *58*, 415–420.
46. Alemdar, A.; Güngör, N.; Ece, O.I.; Atici, O. The rheological properties and characterization of bentonite dispersions in the presence of non-ionic polymer PEG. *J. Mater. Sci.* **2005**, *40*, 171–177. [[CrossRef](#)]
47. Ilie, C.; Stinga, G.; Iovescu, A.; Purcar, V.; Anghel, D.F.; Donescu, D. The influence of nonionic surfactants on the carbopol-peg interpolymer complexes. *Rev. Roum. Chim.* **2010**, *55*, 409–417.
48. Otto, D.P.; Otto, A.; de Villiers, M.M. Experimental and mesoscale computational dynamics studies of the relationship between solubility and release of quercetin from PEG solid dispersions. *Int. J. Pharm.* **2013**, *456*, 282–292. [[CrossRef](#)] [[PubMed](#)]
49. Li, B.; Konecke, S.; Harich, K.; Wegiel, L.; Taylor, L.S.; Edgar, K.J. Solid dispersion of quercetin in cellulose derivative matrices influences both solubility and stability. *Carbohydr. Polym.* **2013**, *92*, 2033–2040. [[CrossRef](#)] [[PubMed](#)]
50. Kakran, M.; Sahoo, N.G.; Li, L. Dissolution enhancement of quercetin through nanofabrication, complexation, and solid dispersion. *Colloids Surf. B Biointerfaces* **2011**, *88*, 121–130. [[CrossRef](#)]

51. Biswal, S.; Sahoo, J.; Murthy, P.N.; Giradkar, R.P.; Avari, J.G. Enhancement of dissolution rate of gliclazide using solid dispersions with polyethylene glycol 6000. *Aaps Pharmscitech* **2008**, *9*, 563–570. [[CrossRef](#)] [[PubMed](#)]
52. Hancock, B.C.; Zografi, G. Characteristics and significance of the amorphous state in pharmaceutical systems. *J. Pharm. Sci.* **1997**, *86*, 1–12. [[CrossRef](#)] [[PubMed](#)]
53. Chingunpituk, J. Nanosuspension technology for drug delivery. *Walailak J. Sci. Technol. (WJST)* **2007**, *4*, 139–153.
54. Casagrande, R.; Georgetti, S.R.; Verri Jr, W.A.; Borin, M.F.; Lopez, R.F.V.; Fonseca, M.J.V. In vitro evaluation of quercetin cutaneous absorption from topical formulations and its functional stability by antioxidant activity. *Int. J. Pharm.* **2007**, *328*, 183–190. [[CrossRef](#)] [[PubMed](#)]
55. Lv, R.; Qi, L.; Zou, Y.; Zou, J.; Luo, Z.; Shao, P.; Tamer, T.M. Preparation and structural properties of amylose complexes with quercetin and their preliminary evaluation in delivery application. *Int. J. Food Prop.* **2019**, *22*, 1445–1462. [[CrossRef](#)]
56. Aytac, Z.; Ipek, S.; Durgun, E.; Uyar, T. Antioxidant electrospun zein nanofibrous web encapsulating quercetin/cyclodextrin inclusion complex. *J. Mater. Sci.* **2018**, *53*, 1527–1539. [[CrossRef](#)]
57. Ozgen, M.; Reese, R.N.; Tulio, A.Z.; Scheerens, J.C.; Miller, A.R. Modified 2, 2-azino-bis-3-ethylbenzothiazoline-6-sulfonic acid (ABTS) method to measure antioxidant capacity of selected small fruits and comparison to ferric reducing antioxidant power (FRAP) and 2, 2'-diphenyl-1-picrylhydrazyl (DPPH) methods. *J. Agric. Food Chem.* **2006**, *54*, 1151–1157. [[CrossRef](#)]
58. Ghanta, S.; Banerjee, A.; Poddar, A.; Chattopadhyay, S. Oxidative DNA damage preventive activity and antioxidant potential of *Stevia rebaudiana* (Bertoni) Bertoni, a natural sweetener. *J. Agric. Food Chem.* **2007**, *55*, 10962–10967. [[CrossRef](#)] [[PubMed](#)]
59. Barbosa, A.I.; Costa Lima, S.A.; Reis, S. Application of pH-responsive fucoidan/chitosan nanoparticles to improve oral quercetin delivery. *Molecules* **2019**, *24*, 346. [[CrossRef](#)]
60. Esposito, L.; Barbosa, A.I.; Moniz, T.; Costa Lima, S.; Costa, P.; Celia, C.; Reis, S. Design and characterization of sodium alginate and poly (vinyl) alcohol hydrogels for enhanced skin delivery of quercetin. *Pharmaceutics* **2020**, *12*, 1149. [[CrossRef](#)]
61. Fang, R.; Hao, R.; Wu, X.; Li, Q.; Leng, X.; Jing, H. Bovine serum albumin nanoparticle promotes the stability of quercetin in simulated intestinal fluid. *J. Agric. Food Chem.* **2011**, *59*, 6292–6298. [[CrossRef](#)] [[PubMed](#)]
62. Murota, K.; Mitsukuni, Y.; Ichikawa, M.; Tsushida, T.; Miyamoto, S.; Terao, J. Quercetin-4'-glucoside is more potent than quercetin-3-glucoside in protection of rat intestinal mucosa homogenates against iron ion-induced lipid peroxidation. *J. Agric. Food Chem.* **2004**, *52*, 1907–1912. [[CrossRef](#)] [[PubMed](#)]
63. Nam, J.-S.; Sharma, A.R.; Nguyen, L.T.; Chakraborty, C.; Sharma, G.; Lee, S.-S. Application of bioactive quercetin in oncology: From nutrition to nanomedicine. *Molecules* **2016**, *21*, 108. [[CrossRef](#)]
64. Salehi, B.; Machin, L.; Monzote, L.; Sharifi-Rad, J.; Ezzat, S.M.; Salem, M.A.; Merghany, R.M.; El Mahdy, N.M.; Kiliç, C.S.; Sytar, O. Therapeutic potential of quercetin: New insights and perspectives for human health. *ACS Omega* **2020**, *5*, 11849–11872. [[CrossRef](#)] [[PubMed](#)]
65. Vargas, A.J.; Burd, R. Hormesis and synergy: Pathways and mechanisms of quercetin in cancer prevention and management. *Nutr. Rev.* **2010**, *68*, 418–428. [[CrossRef](#)] [[PubMed](#)]
66. Umeno, A.; Biju, V.; Yoshida, Y. In vivo ROS production and use of oxidative stress-derived biomarkers to detect the onset of diseases such as Alzheimer's disease, Parkinson's disease, and diabetes. *Free. Radic. Res.* **2017**, *51*, 413–427. [[CrossRef](#)] [[PubMed](#)]
67. Toyokuni, S. Molecular mechanisms of oxidative stress-induced carcinogenesis: From epidemiology to oxygenomics. *IUBMB Life* **2008**, *60*, 441–447. [[CrossRef](#)]
68. McCafferty, D.M. Peroxynitrite and inflammatory bowel disease. *Gut* **2000**, *46*, 436–439. [[CrossRef](#)]
69. Vane, J.R.; Mitchell, J.A.; Appleton, I.; Tomlinson, A.; Bishop-Bailey, D.; Croxtall, J.; Willoughby, D.A. Inducible isoforms of cyclooxygenase and nitric-oxide synthase in inflammation. *Proc. Natl. Acad. Sci. USA* **1994**, *91*, 2046–2050. [[CrossRef](#)]
70. MacMacking, J.; Xie, Q.; Nathan, C. Nitric oxide and macrophages function. *Annu. Rev. Immunol.* **1997**, *15*, 323–350. [[CrossRef](#)]
71. Wang, Z.; Jiang, W.; Zhang, Z.; Qian, M.; Du, B. Nitidine chloride inhibits LPS-induced inflammatory cytokines production via MAPK and NF-kappaB pathway in RAW 264.7 cells. *J. Ethnopharmacol.* **2012**, *144*, 145–150. [[CrossRef](#)]
72. Jones, E.; Adcock, I.M.; Ahmed, B.Y.; Punchard, N.A. Modulation of LPS stimulated NF-kappaB mediated Nitric Oxide production by PKCε and JAK2 in RAW macrophages. *J. Inflamm.* **2007**, *4*, 23. [[CrossRef](#)]
73. Burke, B.; Lewis, C.E. *The macrophage*; Oxford University Press: New York, NY, USA, 2002.
74. Islam, S.; Hassan, F.; Tumurkhuu, G.; Dagvadorj, J.; Koide, N.; Naiki, Y.; Mori, I.; Yoshida, T.; Yokochi, T. Bacterial lipopolysaccharide induces osteoclast formation in RAW 264.7 macrophage cells. *Biochem. Biophys. Res. Commun.* **2007**, *360*, 346–351. [[CrossRef](#)]
75. Deleuran, B.W.; Chu, C.Q.; Field, M.; Brennan, F.M.; Mitchell, T.; Feldmann, M.; Maini, R.N. Localization of tumor necrosis factor receptors in the synovial tissue and cartilage-pannus junction in patients with rheumatoid arthritis. Implications for local actions of tumor necrosis factor α. *Arthritis Rheum. Off. J. Am. Coll. Rheumatol.* **1992**, *35*, 1170–1178. [[CrossRef](#)] [[PubMed](#)]
76. Jun, C.-D.; Choi, B.-M.; Kim, H.-M.; Chung, H.-T. Involvement of protein kinase C during taxol-induced activation of murine peritoneal macrophages. *J. Immunol.* **1995**, *154*, 6541–6547. [[PubMed](#)]
77. Aggarwal, B.B. Tumor necrosis factors: Developments during the last decade. *Eur. Cytokine Netw.* **1996**, *7*, 93–124. [[PubMed](#)]
78. Baeuerle, P.A.; Baltimore, D. NF-κB: Ten years after. *Cell* **1996**, *87*, 13–20. [[CrossRef](#)]
79. Gupta, S.C.; Sundaram, C.; Reuter, S.; Aggarwal, B.B. Inhibiting NF-κB activation by small molecules as a therapeutic strategy. *Biochim. Et Biophys. Acta (BBA)-Gene Regul. Mech.* **2010**, *1799*, 775–787. [[CrossRef](#)]

80. Broz, P.; Dixit, V.M. Inflammasomes: Mechanism of assembly, regulation and signalling. *Nat. Rev. Immunol.* **2016**, *16*, 407–420. [[CrossRef](#)]
81. Wu, J.; Xu, X.; Li, Y.; Kou, J.; Huang, F.; Liu, B.; Liu, K. Quercetin, luteolin and epigallocatechin gallate alleviate TXNIP and NLRP3-mediated inflammation and apoptosis with regulation of AMPK in endothelial cells. *Eur. J. Pharmacol.* **2014**, *745*, 59–68. [[CrossRef](#)]
82. Lamikanra, A.; Crowe, J.L.; Lijek, R.S.; Odetoyn, B.W.; Wain, J.; Aboderin, A.O.; Okeke, I.N. Rapid evolution of fluoroquinolone-resistant *Escherichia coli* in Nigeria is temporally associated with fluoroquinolone use. *BMC Infect. Dis.* **2011**, *11*, 312. [[CrossRef](#)]
83. Chen, S.; Wang, H.; Katzianer, D.S.; Zhong, Z.; Zhu, J. LysR family activator-regulated major facilitator superfamily transporters are involved in *Vibrio cholerae* antimicrobial compound resistance and intestinal colonisation. *Int. J. Antimicrob. Agents* **2013**, *41*, 188–192. [[CrossRef](#)] [[PubMed](#)]
84. Chmielewska, A.; Szajewska, H. Systematic review of randomised controlled trials: Probiotics for functional constipation. *World J. Gastroenterol. WJG* **2010**, *16*, 69–75. [[PubMed](#)]
85. Song, D.; Ibrahim, S.; Hayek, S. Recent application of probiotics in food and agricultural science. In *Probiotics*; IntechOpen: London, UK, 2012; Volume 10, pp. 1–34.
86. Stefnors Arnesen, L.P.; Fagerlund, A.; Granum, P.E. From soil to gut: *Bacillus cereus* and its food poisoning toxins. *FEMS Microbiol. Rev.* **2008**, *32*, 579–606. [[CrossRef](#)]
87. Singh, M.; Lee, K.E.; Vinayagam, R.; Kang, S.G. Antioxidant and antibacterial profiling of pomegranate-pericarp extract functionalized-zinc oxide nanocomposite. *Biotechnol. Bioprocess Eng.* **2021**, *26*, 728–737. [[CrossRef](#)]
88. Croxen, M.A.; Law, R.J.; Scholz, R.; Keeney, K.M.; Wlodarska, M.; Finlay, B.B. Recent advances in understanding enteric pathogenic *Escherichia coli*. *Clin. Microbiol. Rev.* **2013**, *26*, 822–880. [[CrossRef](#)]
89. Dike, C.S.; Orish, C.N.; Nwokocho, C.R.; Sikoki, F.D.; Babatunde, B.B.; Frazzoli, C.; Orisakwe, O.E. Phytowaste as nutraceuticals in boosting public health. *Clin. Phytoscience* **2021**, *7*, 24. [[CrossRef](#)]
90. Adan, A.; Kiraz, Y.; Baran, Y. Cell proliferation and cytotoxicity assays. *Curr. Pharm. Biotechnol.* **2016**, *17*, 1213–1221. [[CrossRef](#)] [[PubMed](#)]



## Article

# Characterization of *Sideritis clandestina* subsp. *peloponnesiaca* Polar Glycosides and Phytochemical Comparison to Other Mountain Tea Populations

Virginia D. Dimaki<sup>1</sup>, Konstantina Zeliou<sup>1</sup>, Fotini Nakka<sup>1</sup>, Michaela Stavreli<sup>1</sup>, Ioannis Bakratsas<sup>1</sup>, Ligeri Papaioannou<sup>1,2</sup>, Gregoris Iatrou<sup>2</sup> and Fotini N. Lamari<sup>1,\*</sup>

<sup>1</sup> Laboratory of Pharmacognosy & Chemistry of Natural Products, Department of Pharmacy, University of Patras, 26504 Patras, Greece

<sup>2</sup> Division of Plant Biology, Department of Biology, University of Patras, 26504 Patras, Greece

\* Correspondence: flam@upatras.gr; Tel.: +30-2610962335

**Abstract:** *Sideritis clandestina* (Bory & Chaub.) Hayek subsp. *peloponnesiaca* (Boiss. & Heldr.) Baden (SCP) is endemic to the mountains of the Northern Peloponnese (Greece). This and other *Sideritis* taxa, collectively known as mountain tea, are widely ingested as beverages for refreshment or medicinal purposes. We describe a methodology for the characterization of SCP. Four iridoid glycosides (monomelittoside, melittoside, ajugoside, and 7-O-acetyl-8-epiloganic acid), two phenolic acid glycosides (vanillic and salicylic acid glycosides), and three caffeoyl ester glycosides (chlorogenic acid, verbascoside, and isoverbascoside) were isolated from SCP for the first time. We used ultrasound-assisted extraction of 3 g of plant material to produce petroleum ether and aqueous extracts, which we then analyzed using GC/MS and LC/MS. This was applied to eight samples from four different taxa. In total, 70 volatile and 27 polar metabolites were determined. The *S. clandestina* samples had a lower phenolic content and weaker antioxidant properties than *S. raeseri* and *S. scardica*. However, *S. clandestina* ssp. *clandestina* seemed to be the most aromatic taxon, with almost double the number of volatiles as the others. This study could contribute to authentication and chemotaxonomic studies of *Sideritis* taxa.

**Keywords:** mountain tea; Lamiaceae; iridoids; phenylethanoids; metabolomics; ultrasound-assisted extraction; flavonoids; melittoside; ajugoside; verbascoside

**Citation:** Dimaki, V.D.; Zeliou, K.; Nakka, F.; Stavreli, M.; Bakratsas, I.; Papaioannou, L.; Iatrou, G.; Lamari, F.N. Characterization of *Sideritis clandestina* subsp. *peloponnesiaca* Polar Glycosides and Phytochemical Comparison to Other Mountain Tea Populations. *Molecules* **2022**, *27*, 7613. <https://doi.org/10.3390/molecules27217613>

Academic Editor: Nour Eddine Es-Safi

Received: 27 September 2022

Accepted: 4 November 2022

Published: 6 November 2022

**Publisher's Note:** MDPI stays neutral with regard to jurisdictional claims in published maps and institutional affiliations.



**Copyright:** © 2022 by the authors. Licensee MDPI, Basel, Switzerland. This article is an open access article distributed under the terms and conditions of the Creative Commons Attribution (CC BY) license (<https://creativecommons.org/licenses/by/4.0/>).

## 1. Introduction

The genus *Sideritis* (Lamiaceae family) comprises more than 150 species worldwide [1]. They are annual or perennial xerophytic and thermophytic shrubs growing in mountain areas. Most of the *Sideritis* species are consumed as infusions of exquisite aroma and taste and are widely known as mountain tea. In traditional medicine, infusions and decoctions of its aerial parts are used as a remedy for cough, common cold, pain, asthma, gastrointestinal disorders, and mild anxiety. Meanwhile, the increasing number of studies on their bioactivity is confirming those actions and is revealing numerous bioactive phytoconstituents [2,3]. The commercial demand for large quantities of mountain tea as a raw material for the production of beverages, cosmetics, herbal drugs, and food supplements, and the research findings on its beneficial health properties, intensify the efforts of cultivation, plant breeding, and authentication of the plant material.

Their taxonomical classification is difficult due to their tendency to hybridize, and many chemotaxonomic approaches have been adopted [1,4–7]. Apart from the chemovariability that derives not only from the genotype but also from the location, the time of collection, the environmental conditions, and cultivation practices, there is an intrinsic difficulty in those phytochemical studies since the genus *Sideritis* is a rich source of secondary



metabolites [1]. For most of the *Sideritis* taxa, their phytochemistry is largely unknown and new natural products are discovered annually.

Most studies have focused on essential oil chemistry, but *Sideritis* taxa have a relatively low content of essential oil; the monoterpenes  $\alpha$ -pinene and  $\beta$ -pinene are usually present in high concentrations in the majority of *Sideritis* taxa [1]. Regarding the non-volatiles, quinic acid derivatives, flavonoids and their glucosides, phenylpropanoid glucosides such as verbascoside and isoverbascoside, and some iridoids, with melittoside being the most usual one, were present in all studied *Sideritis* plants [4,6,8].

*Sideritis clandestina* (Bory & Chaub.) Hayek is a variable hemicryptophytic species endemic on the mountains of the Peloponnese, prospering at altitudes of 1600–2300 m. Taxonomically, two subspecies can be recognized: *S. clandestina* (Bory & Chaub.) Hayek subsp. *peloponnesiaca* (Boiss. & Heldr.) Baden (SCP), endemic to the mountains of Central and Northern Peloponnese, and *S. clandestina* (Bory & Chaub.) Hayek subsp. *clandestina* (SCC), which prospers in the southern mountains, on Taygetos and Parnon [9] (pp. 84–91). The variability of the species is expressed by synonyms that have been given in previous times to several populations of the species.

Synonyms of SCP are *Sideritis peloponnesiaca* Boiss. & Heldr., *Sideritis theezans* subsp. *peloponnesiaca* (Boiss. & Heldr.) Bornm., and *Sideritis clandestina* subsp. *cyllenea* (Boiss.) Papan. & Kokkini, whereas synonyms of SCC are *Phlomis clandestina* Bory & Chaub., *Sideritis cretica* Sm., *Sideritis syriaca* Bory & Chaub., and *Sideritis theezans* Boiss. & Heldr. [9] (pp. 84–91). There are studies on their essential-oil composition [10–13]. We have previously demonstrated that SCP and SCC tea consumption enhances the antioxidant defense of the adult rodent brain in a region-specific manner [14,15] and that SCC confers anxiolysis to rodents [15]. The LC/MS characterization of SCC infusion showed the presence of 17 compounds, including quinic acid and melittoside derivatives, martynoside and  $\beta$ -hydroxyverbascoside, and apigenin and isoscutellarein glycosides [15]. However, several peaks in the SCC extract could not be characterized, and there has not been any analysis of SCP. In 2017, we evaluated several distillation and extraction methods and reached the conclusion that petroleum ether ultrasound-assisted extraction of a small amount of plant material after acidic pretreatment could facilitate a thorough determination of volatiles in SCP and other *Sideritis* taxa [16].

With the aim of characterizing the phytochemical profile of SCP for the first time, we proceeded to the fractionation and isolation of pure polar glycosides from SCP and developed a methodology of metabolomic fingerprinting to compare with similar taxa and contribute to the authentication and chemotaxonomic efforts. In particular, in order to record both volatiles and polar metabolites from a small amount of plant material, we revisited the extraction method developed earlier [16] and analyzed both aqueous and petroleum ether extracts. We applied this methodology to SCP, SCC, and two other *Sideritis* taxa, i.e., *Sideritis raeseri* Boiss. & Heldr. and *Sideritis scardica* Griseb. *S. raeseri* is a variable species occurring in the southern and western part of the Balkan Peninsula. In Greece, two subspecies can be recognized: subsp. *raeseri* (SR) in Northern Greece up to Sterea Hellas (recently collected from the mountain Gaidourorahi in the Northern Peloponnese) and subsp. *attica* (Heldr.) Papanic. & Kokkini in a few mountains of Sterea Hellas (Pateras, Kitheron, Parnis), whereas *S. scardica* (SS) prospers in the Southern Balkan Peninsula, including Northern Greece, and is cultivated in Southern Greece. In order to compare those taxa, we also applied colorimetric assays to evaluate the antioxidant properties of the aqueous extracts.

## 2. Results and Discussion

### 2.1. Isolation of Polar Glycosides from SCP

To facilitate the characterization of SCP metabolites and the qualitative analysis of the aqueous extracts, we proceeded with the isolation of polar compounds from SCP methanolic extract, and the isolated compounds were used as reference compounds. To the best of our knowledge, it is the first time the isolation of nine polar metabolites from SCP

species is reported (Figure 1). The molecular structures of the isolated compounds were determined mainly with  $^1\text{H-NMR}$  spectra in comparison with literature data, as well as UV and MS spectra. The small quantities and the poor solubility of the compounds did not give us the proper results from  $^{13}\text{C-NMR}$  and 2D experiments in all cases.

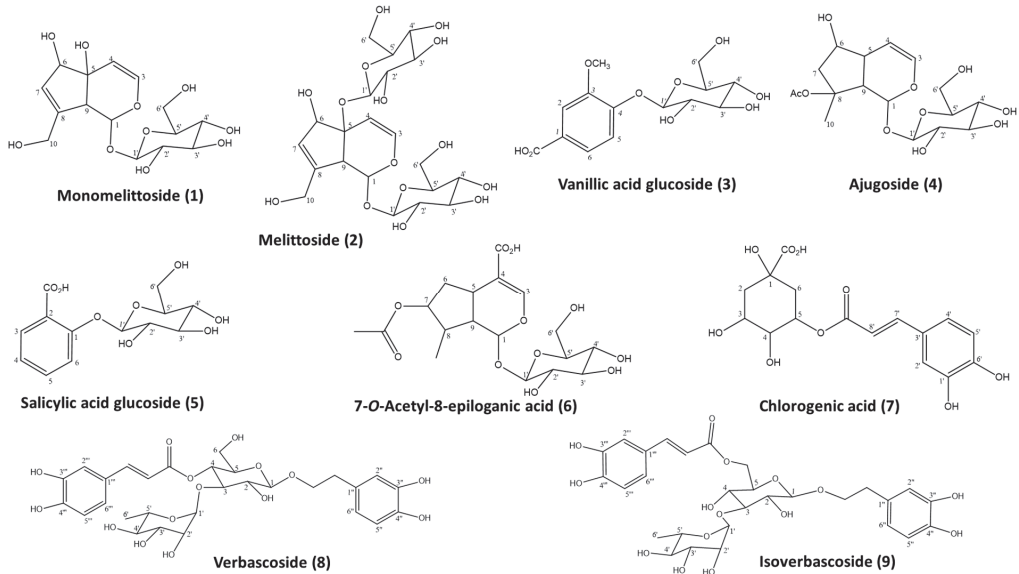


**Figure 1.** Structures of isolated iridoid, phenylpropanoid, and phenolic acid glycosides.

Monomelittoside (**1**) with the molecular structure  $\text{C}_{15}\text{H}_{22}\text{O}_{10}$  and a molecular weight (M.W.) of 362 was isolated as a pale white solid. The  $^1\text{H-NMR}$ , MS, and UV-vis spectra are presented in Table S1 and Figures S1–S3, and are in accordance with previous studies [17]. It is the first time this iridoid glycoside was isolated from SCP; it has previously been isolated from *S. perfoliata* subsp. *perfoliata* and *S. sipylea* [18,19].

Melittoside (**2**) was isolated as a white amorphous powder and its molecular structure  $\text{C}_{21}\text{H}_{32}\text{O}_{15}$  was determined by  $^1\text{H-}$  &  $^{13}\text{C-NMR}$ , MS, and UV-vis spectra (Table S2 and Figures S4–S7), which agreed with a previous reference [17]. This is an iridoid glycoside that bears two glucose units at C-1 and C-5 linked via O-glycosidic bonds and its presence in several *Sideritis* taxa has been reported earlier [1,15,20–22]; this is the first report of its occurrence in SCP.

Vanillic acid glucoside (**3**),  $\text{C}_{14}\text{H}_{18}\text{O}_9$  and M.W. of 330, was isolated as light grey powder and the structure was determined with  $^1\text{H-NMR}$ , MS, and UV spectra (Table S3 and Figures S8–S10) in accordance with Yu et al. [23]. Vanillic acid presence in *Sideritis* taxa has been reported earlier [24,25] but not of its glucoside.

Ajugoside (**4**),  $\text{C}_{17}\text{H}_{26}\text{O}_{10}$  and M.W. of 390, was isolated as a pale white powder, and the  $^1\text{H-NMR}$ , MS, and UV spectra (Table S4, Figures S11–S13) were in accordance with published data [26]. This iridoid has been isolated from several *Sideritis* taxa like *S. perfoliata* subsp. *perfoliata* [1,27].

Compound (**5**) was isolated as pale viscous solid and it was ascribed to salicylic acid glucoside (**5**),  $\text{C}_{13}\text{H}_{16}\text{O}_8$ , according to  $^1\text{H-NMR}$ , MS, UV spectra (Table S5 and Figures S14–S16), and literature data [28,29].

A 7-O-acetyl-8-*epi*-loganic acid (**6**)  $\text{C}_{18}\text{H}_{25}\text{O}_{11}$  (M.W. 418) was isolated as a brown sticky solid, and the structure was determined by  $^1\text{H-NMR}$ , MS, and UV-vis spectra (Table S6 and Figures S17–S19), which was in accordance with Hanoglu et al. [30].

Chlorogenic acid (**7**)  $\text{C}_{16}\text{H}_{18}\text{O}_9$  (M.W. 354) was isolated as a white amorphous powder and the structure was elucidated from spectroscopic data ( $^1\text{H-NMR}$ , MS, and UV-vis spectra

in Table S7 and Figures S20–S22) that agreed with the literature [31]. It has been previously isolated from several Mediterranean *Sideritis* taxa [1].

The phenylethanoid glycoside isomers verbascoside (8) and isoverbascoside (9)  $C_{29}H_{36}O_{15}$  were isolated as an amorphous powder and elucidated using 1D NMR ( $^1H$ ,  $^{13}C$ , and APT), 2D NMR (HSQC, HMBC, COSY, and ROSEY), and MS spectra in accordance with previous studies [32,33]. The spectroscopic data for verbascoside (8) are presented in Table S8 and Figures S23–S30 and those for isoverbascoside (9) are presented in Table S9 and Figures S31–S38. References to their occurrence in other *Sideritis* taxa are provided in the comprehensive review by Fraga in 2012 [1].

## 2.2. Qualitative and Quantitative Analysis of Polar Compounds in the Aqueous Extracts by LC/MS Analysis

The acidic pretreatment combined with ultrasound-assisted extraction was previously developed by us and applied to the analysis of volatiles in the petroleum ether extracts [16], but at that time we did not use the aqueous extracts. In this work, we extend the applications of the UAE extraction of a small quantity of plant material (3 g) and describe the characterization of the aqueous extracts, as well. Two biological samples of SCP, SCC, SR, and SS were extracted, and the final yields of the acidic extraction were 30.11%, 35.00%, 39.14%, and 30.29%, respectively. The LC-ESI-MS analysis of the extracts (see Figure S39) combined with the use of the isolated compounds 1–9 and rutin as standards, allowed the identification and quantification of most of the components, 27 in total, classifying them into several phytochemical groups: iridoid, quinic acid, phenylpropanoid, and glycosylated flavonoid derivatives (Table 1). Among these groups, flavonoids were the most prevalent one. The results are congruent with many previous studies [6,8,22,34–37]. The quantitation was performed with a common glycosylated flavonoid, rutin, as an external standard and not with the identified/isolated compounds; the non-commercially available compounds were not isolated in satisfactory amounts, and we did not isolate any flavonoids. The results are expressed as mg rutin equivalents/100 g dry plant material. Despite the anticipated lack of accuracy stemming from the use of a standard that is not present in *Sideritis*, this methodological approach offers the advantage of broad applicability in all laboratories, since rutin is cheap and commercially available.

The highest concentration of polar metabolites was found in the SR extract, followed by SS, whereas SCP had the lowest. Flavonoids were abundant in all four taxa (53.49–170.82 mg/100 g dry plant material in the order SS > SR > SCC and SCP), followed by phenylpropanoids (50.98–164.70 mg/100 g in the order SR > SS > SCC > SCP). Hypolaetin glycosylated derivatives (compounds C14, C19, C20, C21, C23, C24, and C25) had the strongest presence, especially in SR and SS samples (108.02 and 96.73 mg/100 g of dry plant material, respectively). Herein, the distinction between isoscutellarein and luteolin glycosylated derivatives was not feasible in all cases.

**Table 1.** List of polar metabolites and their concentrations (mg rutin equivalents/100 g of dry plant material, average values  $\pm$  standard deviation) in *Sideritis claudeslina* subsp. *peloponnesiaca* (SCP), *Sideritis claudeslina* subsp. *claudeslina* (SCC), *Sideritis raeseri* (SR), and *Sideritis scardica* (SS) aqueous extracts (2 biological samples,  $n = 2$  for each sample).

a/a	$t_R$ (min)	Components	M.W.	[M+H] <sup>−</sup>	Other Negative Ions	SCP	SCC	SR	SS
C1	6.96	Melittoside *	524	523	583 [M+Hac-H] <sup>−</sup> 1070 [2M+Na-H] <sup>−</sup>	19.18 $\pm$ 2.95	15.52 $\pm$ 0.49	15.49 $\pm$ 3.01	n.d.
C2	12.00	Unknown	374	373	747 [2M-H] <sup>−</sup> 769 [2M+2H+Na] <sup>−</sup>	n.d.	21.17 $\pm$ 4.89	n.d.	n.d.
C3	13.30	Unknown	374	373	747 [2M-H] <sup>−</sup> 769 [2M+2H+Na] <sup>−</sup>	n.d.	28.57 $\pm$ 6.87	n.d.	n.d.
C4	17.65	Unknown	488	487	975 [2M-H] <sup>−</sup>	9.20 $\pm$ 5.28	29.19 $\pm$ 3.55	n.d.	29.66 $\pm$ 0.99
C5	18.20	Unknown	376	375	751 [2M-H] <sup>−</sup> 773 [2M+2H+Na] <sup>−</sup>	n.d.	7.57 $\pm$ 5.71	n.d.	n.d.
C6	18.80	Chlorogenic acid *	354	353	191 (quinic acid) 375 [M+Na-2H] <sup>−</sup> 707 [2M-H] <sup>−</sup> 729 [2M+2H+Na] <sup>−</sup>	33.23 $\pm$ 7.45	56.81 $\pm$ 11.81	61.21 $\pm$ 2.57	65.65 $\pm$ 8.96
C7	22.85	$\beta$ -Hydroxyverbascoside isomer [34]	640	639	661 [M+Na-2H] <sup>−</sup>	8.55 $\pm$ 3.05	11.45 $\pm$ 3.56	n.q.	16.80 $\pm$ 6.95
C8	23.65	$\beta$ -Hydroxyverbascoside isomer [34]	640	639	661 [M+Na-2H] <sup>−</sup>	9.20 $\pm$ 4.14	15.48 $\pm$ 3.81	9.78 $\pm$ 0.32	19.34 $\pm$ 6.79
C9	24.81	7-O-Acetyl-8-epi-loganic acid *	418	417	835 [2M-H] <sup>−</sup> 857 [2M+Na-2H] <sup>−</sup>	7.29 $\pm$ 4.68	n.d.	11.76 $\pm$ 0.17	n.d.
C10	25.57	Ajugoside *	390		449 [M+Hac-H] <sup>−</sup> 779 [2M-H] <sup>−</sup>	n.q.	n.d.	27.62 $\pm$ 3.84	n.d.
C11	28.60	Forsythoside B or Lavandulofolioside [34,35]	756	755	377 [M-2H] <sup>−2</sup> 1512 [2M-H] <sup>−</sup>	n.d.	n.q.	29.42 $\pm$ 3.56	n.d.
C12	30.00	All-Glc-ISC [8]	610	609	1220 [2M-H] <sup>−</sup>	n.d.	n.d.	n.d.	25.46 $\pm$ 1.34
C13	30.30	Verbascoside *	624	623	311 [M-2H] <sup>−2</sup> 1248 [2M-H] <sup>−</sup>	n.q.	23.31 $\pm$ 10.52	52.53 $\pm$ 5.22	39.05 $\pm$ 2.31
C14	31.80	All-Glc-HYP [8]	626	625	1251 [2M-H] <sup>−</sup>	8.59 $\pm$ 0.94	n.d.	18.13 $\pm$ 4.01	28.79 $\pm$ 1.44

Table 1. Cont.

a/a #	t <sub>R</sub> (min)	Components	M.W.	[M-H] <sup>-</sup>	Other Negative Ions	SCP	SCC	SR	SS
C15 #	34.78	Allylsonoside/ Forsythoside B or lavandulifolioside [6,8,22,37]	770/756	769/755		n.d.	n.d.	11.58 ± 0.63	n.d.
C16 #	35.60	Leucoseptoside isomer/ Isoverbascoside* [8,37]	638/624	637/623		n.d.	n.d.	n.q.	7.57 ± 1.39
C17	36.40	AcO-All-Glc-ISC or AcO-All-Glc-LUT [8,37]	652	652	325 [M-2H] <sup>-2</sup>	n.d.	n.d.	n.d.	14.82 ± 0.82
C18	36.90	All-Glc-LUT [8]	610	609	1219 [2M+H] <sup>-</sup>	15.86 ± 4.56	18.29 ± 0.44	16.36 ± 5.71	20.72 ± 3.95
C19	37.00	AcO-All-Glc-HYP [6,8]	668	667		n.d.	n.d.	9.44 ± 2.08	7.51 ± 0.04
C20	38.50	All-Glc-HYP-Me [6,8]	640	639	1279 [2M+H] <sup>-</sup>	11.82 ± 1.60	10.33 ± 1.43	15.29 ± 3.24	11.28 ± 1.69
C21	39.30	AcO-All-Glc-HYP [6]	668	667	1335 [2M+H] <sup>-</sup>	n.q.	n.d.	28.71 ± 0.59	38.55 ± 1.21
C22	44.50	AcO-All-Glc-ISC or AcO-All-Glc-LUT [8,35,37]	652	651	1303 [2M+H] <sup>-</sup>	9.07 ± 3.21	11.42 ± 1.78	16.25 ± 0.29	13.09 ± 0.58
C23	44.90	AcO-All-Glc-HYP-Me [35,37]	682	681	1364 [2M+H] <sup>-</sup>	7.25 ± 0.66	7.16 ± 0.88	12.85 ± 0.55	n.q.
C24	45.80	AcO-All-Glc-HYP [8,35,37]	668	667	1336 [2M+H] <sup>-</sup>	n.q.	n.d.	11.71 ± 0.65	n.q.
C25	48.45	(AcO) <sub>2</sub> -All-Glc-HYP [8,35,36]	710	709	1419 [2M+H] <sup>-</sup>	n.q.	n.d.	11.90 ± 2.00	10.60 ± 0.29
C26	49.09	AcO-All-Glc-ISC-Me [8,35,36]	666	665	1332 [2M+H] <sup>-</sup> 1354 [2M-2H+Na] <sup>-</sup>	n.d.	6.29 ± 0.44	n.d.	n.d.
C27 #	49.95	(AcO) <sub>2</sub> -All-Glc-ISC/ (AcO) <sub>2</sub> -All-Glc-HYP-Me [8,35,37]	694/724	693/723	733.7 [M+Hac-H] <sup>-</sup> 1388 [2M+H] <sup>-</sup> 1448 [2M+H] <sup>-</sup>	6.30 ± 1.12	n.q.	13.11 ± 1.68	n.q.
Total						145.55	262.56	373.12	348.90

\* Reference compounds have been used for the identification. # Those peaks were a mixture of two compounds that co-eluted. Abbreviations: n.q.: not quantified, n.d.: not detected, AcO: O-acetyl, All: allyl, Glc: glucoside, HYP: hypolaetin, ISC: isoscutellarein, LUT: luteolin, Me: methyl, Hac: acetic acid.

Among the four taxa, the most abundant constituent was chlorogenic acid and was followed by the phenylpropanoid verbascoside, which was detected in all samples but quantified in three of them (SCC, SR, and SS samples). Chlorogenic acid, verbascoside, and isoverbascoside presence in SR and SS was reported earlier [8,34,38].

It is noteworthy to comment on the presence of the iridoids melittoside, acetyl-8-epi-loganic acid, and ajugoside. To the best of our knowledge, it is the first time that melittoside, acetyl-8-epi-loganic acid and ajugoside have been determined in SCP and SR taxa; acetyl-8-epi-loganic acid has been identified and isolated only from *Sideritis cypria* [21,30] and ajugoside from *Sideritis perfoliata*, *Sideritis romana*, and *Sideritis cypria* [21,27,39]. Melittoside was previously reported by Vasilopoulou et al. [15] in an SCC aqueous extract but it was not isolated, and was isolated from SS by Koleva et al. [20]. Finally, four unknown compounds were quantified in relatively high concentrations, mainly in SCC extract. Altogether, the highest concentration of iridoids was determined in SR followed by SCP and SCC (43.11, 26.47, and 15.52 mg/100 g of dry plant material, respectively), whereas they were not detected in SS.

### 2.3. Determination of Total Phenolics, Flavonoid Content, and Antioxidant Capacity (DPPH and FRAP) in Aqueous Extracts

The total phenolic content (TPC), total flavonoid content (TFC), and antioxidant capacity (FRAP and DPPH) of the aqueous extracts of the four *Sideritis* taxa from the Peloponnese were determined by colorimetric assays and the results are given in Table 2. The SR samples had the highest phenolic content, followed by SS, whereas the polyphenolic composition of SCC and SCP was 63% and 74% lower, respectively, in comparison to SR. The same pattern was observed for the total flavonoid content, where flavonoid composition was significantly higher in the SR samples, followed by SS, whereas SCC and SCP had the lowest flavonoid content (not significantly different between SCC and SCP). These results are in accordance with the LC/MS characterization in Section 2.2.

**Table 2.** Total phenolics (TPC), total flavonoids (TFC), and antioxidant properties (DPPH radical scavenging activity and ferric ion reducing power (FRAP)) of the *Sideritis* aqueous extracts. The results are expressed as average values  $\pm$  standard deviation (SD) of triplicate analysis ( $n = 2$  biological samples per taxon). Significant differences among group means were determined by ANOVA and post-hoc Tukey's test ( $\alpha = 0.05$ ) and are indicated with different letters in superscript. The same letter indicates no statistically significant differences across rows at the confidence level of 95%.

	TPC (mg GAE/g) <sup>1</sup>	TFC (mg QE/g) <sup>2</sup>	FRAP Assay (mmol Fe <sup>II</sup> /g) <sup>3</sup>	DPPH Assay IC <sub>50</sub> (mg/mL) <sup>4</sup>
SCP	3.19 $\pm$ 0.44 <sup>d</sup>	2.40 $\pm$ 0.41 <sup>c</sup>	19.48 $\pm$ 0.88 <sup>d</sup>	5.44 $\pm$ 0.63 <sup>a</sup>
SCC	4.62 $\pm$ 0.67 <sup>c</sup>	2.94 $\pm$ 0.43 <sup>c</sup>	39.94 $\pm$ 5.82 <sup>c</sup>	3.11 $\pm$ 0.59 <sup>b</sup>
SR	12.38 $\pm$ 1.23 <sup>a</sup>	10.67 $\pm$ 1.20 <sup>a</sup>	94.89 $\pm$ 7.41 <sup>a</sup>	1.79 $\pm$ 0.19 <sup>c</sup>
SS	9.53 $\pm$ 1.69 <sup>b</sup>	9.18 $\pm$ 1.43 <sup>b</sup>	78.41 $\pm$ 11.09 <sup>b</sup>	1.73 $\pm$ 0.31 <sup>c</sup>

<sup>1</sup> Expressed as mg of gallic acid (GAE) per g of dry plant material. <sup>2</sup> Expressed as mg of quercetin (QE) per g of dry plant material. <sup>3</sup> Expressed as mmol Fe<sup>II</sup> per g of dry plant material. <sup>4</sup> Expressed as IC<sub>50</sub> values corresponding to the aqueous extract concentration (mg of dry plant material/mL) causing 50% inhibition of DPPH radical.

A very high and significant correlation was observed between total phenolic content and total flavonoid content (Table 3). These findings are consistent with the results of the LC/MS analysis, since the majority of the detected phenolics were flavonoids, especially in the SR extracts, which were the richest taxa in flavonoids.

**Table 3.** Pearson’s correlation matrix of all values of total phenolic content (TPC), total flavonoid content (TFC), FRAP values, and the IC<sub>50</sub> DPPH.

	TPC	TFC	FRAP	DPPH IC <sub>50</sub>
TPC	1			
TFC	0.982 **	1		
FRAP	0.987 **	0.981 **	1	
DPPH IC <sub>50</sub>	−0.853 **	−0.849 **	−0.919 **	1

\*\*  $p < 0.01$ .

Previous comparisons among *Sideritis* species also found that *S. scardica* samples had higher TPC than *S. raeseri* [5]. Overall, the values of total phenolics and total flavonoids herein were comparatively equal [40] or lower in comparison with previous studies [4,5,14,34,40] and the differences could be attributed to the extraction method, as well. The high content of total phenols and flavonoids of SR was depicted in its high antioxidant activity in both FRAP and DPPH assays. SS extract also exhibited high antioxidant properties but lower than SR in the case of FRAP. The IC<sub>50</sub> values of SR and SS were much lower than those described in the study of Karapandzova et al. [41]. SCC displayed stronger antioxidant activities in comparison to SCP, but both were lower than SR and SS extracts. Finally, according to Pearson’s correlation matrix, FRAP was very highly and significantly correlated to phenolics and flavonoids, and DPPH was highly and significantly correlated to phenolics, flavonoids, and FRAP.

#### 2.4. GC/MS Determination of Volatile Compounds in Petroleum Ether Extracts

The acidic pretreatment along with the ultrasound-assisted extraction with petroleum ether afforded significantly high yields for all studied samples; 1.92%, 0.70%, 2.58%, and 0.75% for SCP, SCC, SR, and SS, respectively. These high values can be justified by the fact that organic solvents also extract compounds such as fatty acids, esters, and hydrocarbons along with the essential oil (EO), in contrast to distillation, in which only volatile compounds are obtained. These results agree with earlier observations [16,42].

Seventy (70) compounds in total were identified in all extracts (Table 4). Specifically, 31, 50, 24, and 39 compounds were identified in SCP, SCC, SR, and SS, respectively. Among the identified compounds, only 13 were in common among all taxa: monoterpenes  $\alpha$ -pinene, sabinene,  $\beta$ -pinene, *o*-cymene, sylvestrene, linalool and 1,8-cineole; sesquiterpenes  $\alpha$ -copaene,  $\beta$ -bourbonene,  $\beta$ -elemene,  $\beta$ -caryophyllene, and caryophyllene oxide; and the alkane nonane.  $\alpha$ -Pinene was found in relatively high percentages (18.26% to 20.40%) in almost all samples except for SR (2.64%). The percentage of the identified compounds varied among extracts, and it was more than 78% in all samples (82.88%, 78.75%, 79.97%, and 89.20% of the total extract content in SCP, SCC, SR, and SS, respectively). Not only the number but also the concentration of volatiles was the highest in SCC extract (41.31 mg/100 g plant material); it was approximately two-fold higher than the other samples.

All samples were characterized by the presence of hydrocarbons that ranged from 53.85% in SR to 73.00% in SS, whereas oxygenated compounds were detected in lower percentages (9.94–41.09%). Monoterpene hydrocarbons were the dominant group in all samples (12.68–44.71%) (Figure 2). Oxygenated monoterpenes were in a high percentage in SCC (24.26%). SCC also contained the highest content of oxygenated sesquiterpenes. Diterpenes were detected only in SCC, SCP, and SS extracts and in very low amounts (<2.04%). The SR extract was characterized by the highest content in alkanes (34.84%) and non-terpene oxygenated compounds (12.65%), outweighing monoterpenes (18.24%) and sesquiterpenes (14.24%).

**Table 4.** Percentages and concentrations of volatile components identified in petroleum ether extracts of *Sideritis clandestina* subsp. *peloponnesiaca* (SCP), *Sideritis clandestina* subsp. *clandestina* (SCC), *Sideritis raeseri* subsp. *raeseri* (SR), and *Sideritis scardica* (SS) (2 biological samples, n = 2 for each sample). The percentages are expressed as normalized peak areas (peak area of component/peak area of internal standard). Concentrations are expressed as mg  $\alpha$ -pinene equivalents/100 g dry plant material (average  $\pm$  standard deviation).

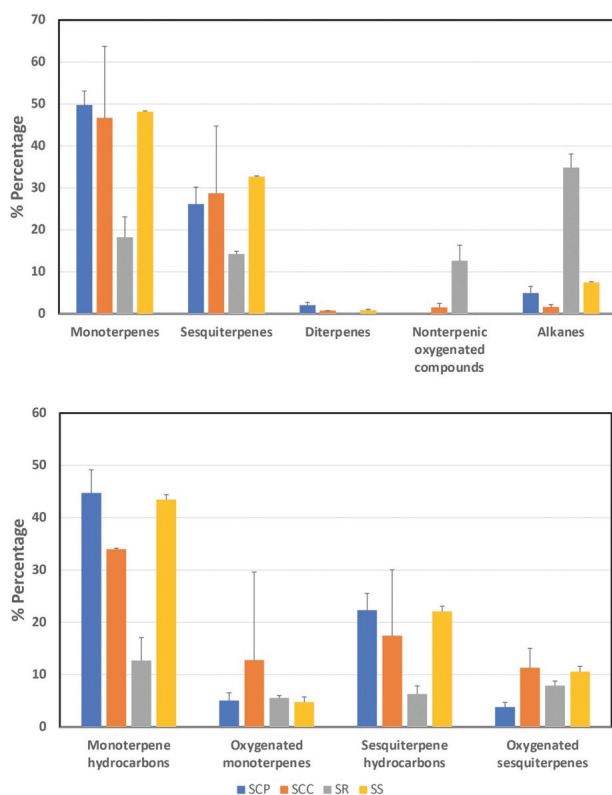
No	RI <sub>cal</sub> <sup>1</sup>	RI <sub>lit</sub> <sup>2</sup>	Components	SCP		SCC		SR		SS	
				%	mg/100 g	%	mg/100 g	%	mg/100 g	%	mg/100 g
1	901	900	Nonane	4.26	1.11 $\pm$ 0.35	1.17	0.52 $\pm$ 0.03 *	11.25	2.13 $\pm$ 0.03	7.48	1.31 $\pm$ 0.17
2	923	924	$\alpha$ -Thujene	0.74	0.32 $\pm$ 0.02	0.29	0.17 $\pm$ 0.03	n.d.	n.d.	n.q.	n.q.
3	929	932	$\alpha$ -Pinene	20.01	4.70 $\pm$ 0.29	20.40	8.31 $\pm$ 0.57	2.64	0.54 $\pm$ 0.15	18.26	3.18 $\pm$ 0.42 *
4	969	969	Sabinene	1.61	0.51 $\pm$ 0.06	0.73	0.35 $\pm$ 0.07	n.q.	n.q.	6.44	1.13 $\pm$ 0.06
5	971	974	$\beta$ -Pinene	7.73	1.91 $\pm$ 0.21	6.47	2.68 $\pm$ 0.02	3.89	0.78 $\pm$ 0.26	6.04	1.06 $\pm$ 0.01
6	979	974	1-Octen-3-ol	n.d.	n.d.	0.43	0.23 $\pm$ 0.01	n.d.	n.d.	n.d.	n.d.
7	991	988	$\beta$ -Myrcene	5.86	1.48 $\pm$ 0.25	n.d.	n.d.	n.d.	n.d.	2.28	0.41 $\pm$ 0.08
8	1000	1000	<i>n</i> -Decane	0.69	0.30 $\pm$ 0.07	n.d.	n.d.	23.59	4.42 $\pm$ 0.32	n.d.	n.d.
9	1002	1002	$\alpha$ -Phellandrene	0.74	0.31 $\pm$ 0.02	1.02	0.47 $\pm$ 0.17	n.d.	n.d.	n.d.	n.d.
10	1007	1008	3-Carene	0.87	0.34 $\pm$ 0.05	1.44	0.64 $\pm$ 0.18	0.56	0.15 $\pm$ 0.01 *	n.d.	n.d.
11	1014	1014	$\alpha$ -Terpinene	0.57	0.28 $\pm$ 0.05	n.d.	n.d.	n.d.	n.d.	1.69	0.30 $\pm$ 0.07
12	1022	1022	$\alpha$ -Cymene	0.94	0.36 $\pm$ 0.09	0.37	0.20 $\pm$ 0.05	2.83	0.58 $\pm$ 0.38	1.75	0.31 $\pm$ 0.16
13	1025	1025	Sylvestrene	5.52	1.41 $\pm$ 0.24	3.10	1.31 $\pm$ 0.41	1.39	0.31 $\pm$ 0.06	4.76	0.85 $\pm$ 0.29
14	1027	1026	1,8-Cineole	1.30	0.46 $\pm$ 0.33	0.58	0.28 $\pm$ 0.17	n.q.	n.q.	n.q.	n.q.
15	1046	1053	<i>trans</i> -Decahydro-naphthalene	0.31	0.22 $\pm$ 0.03	n.d.	n.d.	1.65	0.35 $\pm$ 0.03	1.50	0.27 $\pm$ 0.01
16	1056	1054	$\gamma$ -Terpinene	n.d.	n.d.	n.d.	n.d.	n.q.	n.q.	0.72	0.14 $\pm$ 0.01
17	1085	1086	Terpinolene	n.d.	n.d.	0.17	0.12 $\pm$ 0.01 *	n.d.	n.d.	n.d.	n.d.
18	1101	1095	Linalool	3.73	1.02 $\pm$ 0.24	13.90	5.57 $\pm$ 0.11 *	n.q.	n.q.	3.59	0.63 $\pm$ 0.14
19	1138	1141	Camphor	n.d.	n.d.	2.68	1.12 $\pm$ 0.05 *	n.d.	n.d.	n.d.	n.d.
20	1151	1155	Isoborneol	n.d.	n.d.	0.41	0.22 $\pm$ 0.01 *	n.d.	n.d.	n.d.	n.d.
21	1160	1165	Borneol	n.d.	n.d.	1.48	0.64 $\pm$ 0.02 *	n.d.	n.d.	n.d.	n.d.
22	1174	1174	Terpinen-4-ol	n.d.	n.d.	0.72	0.34 $\pm$ 0.01 *	n.d.	n.d.	n.d.	n.d.
23	1187	1186	$\alpha$ -Terpineol	n.d.	n.d.	0.72	0.34 $\pm$ 0.06	n.d.	n.d.	0.69	0.13 $\pm$ 0.01
24	1200	1200	<i>n</i> -Dodecane	n.d.	n.d.	0.45	0.24 $\pm$ 0.09	n.d.	n.d.	n.d.	n.d.
25	1260	1254	Linalool acetate	n.d.	n.d.	3.76	1.55 $\pm$ 0.15 *	n.d.	n.d.	n.d.	n.d.
26	1332 #	1324	Bicycloelemene	3.49	0.95 $\pm$ 0.22	0.71	0.34 $\pm$ 0.16	n.d.	n.d.	n.d.	n.d.
27	1355	1356	Eugenol	n.d.	n.d.	n.d.	n.d.	3.43	0.69 $\pm$ 0.15	0.47	0.10 $\pm$ 0.03
28	1360	1369	Cyclosativene	n.d.	n.d.	n.d.	n.d.	n.d.	n.d.	0.75	0.15 $\pm$ 0.02
29	1370	1370	$\alpha$ -Copaene	n.q.	n.q.	0.93	0.44 $\pm$ 0.08 *	n.q.	n.q.	4.05	0.72 $\pm$ 0.14
30	1378	1387	$\beta$ -Bourbonene	0.62	0.29 $\pm$ 0.06	0.33	0.19 $\pm$ 0.01 *	0.91	0.22 $\pm$ 0.01 *	1.60	0.30 $\pm$ 0.12
31	1388	1389	$\beta$ -Elemene	n.q.	n.q.	0.22	0.14 $\pm$ 0.01 *	n.q.	n.q.	0.32	0.07 $\pm$ 0.01 *
32	1413	1417	$\beta$ -Caryophyllene	3.82	1.03 $\pm$ 0.22	4.86	2.04 $\pm$ 1.12	4.28	0.84 $\pm$ 0.08	4.33	0.77 $\pm$ 0.24
33	1423	1430	$\beta$ -Copaene	n.d.	n.d.	n.d.	n.d.	n.d.	n.d.	0.39	0.08 $\pm$ 0.02
34	1444	1451	<i>trans</i> -Muuroloa,3,5-diene	n.d.	n.d.	0.25	0.15 $\pm$ 0.01 *	n.d.	n.d.	n.d.	n.d.
35	1446	1452	$\alpha$ -Humulene	n.d.	n.d.	0.28	0.17 $\pm$ 0.02 *	n.d.	n.d.	n.d.	n.d.
36	1456	1456	$\beta$ -Farnesene	n.d.	n.d.	0.92	0.43 $\pm$ 0.03 <sup>§</sup> *	n.d.	n.d.	1.10	0.21 $\pm$ 0.15
37	1457	1464	$\alpha$ -Acoradiene	0.54	0.27 $\pm$ 0.04	n.d.	<sup>§</sup> *	n.d.	n.d.	n.d.	n.d.
38	1461 #	1464	9-epi-(E)- $\beta$ -Caryophyllene	n.d.	n.d.	3.12	1.33 $\pm$ 0.57	n.d.	n.d.	n.d.	n.d.
39	1474	1478	$\gamma$ -Muuroloa	n.d.	n.d.	1.89	0.83 $\pm$ 0.97	n.d.	n.d.	n.d.	n.d.
40	1474	1480	Germacrene D	5.28	1.37 $\pm$ 0.28	n.d.	n.d.	1.35	0.30 $\pm$ 0.06	2.60	0.47 $\pm$ 0.15
41	1477	1481	$\gamma$ -Curcumene	0.71	0.30 $\pm$ 0.02	0.38	0.21 $\pm$ 0.01 *	n.d.	n.d.	n.d.	n.d.
42	1480	1480	$\alpha$ -Curcumene	0.87	0.35 $\pm$ 0.06	0.44	0.23 $\pm$ 0.03 *	n.d.	n.d.	0.64	0.12 $\pm$ 0.07
43	1490	1493	epi-Cubebol	n.d.	n.d.	n.d.	n.d.	n.d.	n.d.	0.90	0.17 $\pm$ 0.01
44	1490	1500	Bicyclogermacrene	6.01	1.54 $\pm$ 0.54	1.35	0.61 $\pm$ 0.33	n.d.	n.d.	n.q.	n.q.
45	1493	1493	$\alpha$ -Zingiberene	1.03	0.38 $\pm$ 0.06	0.70	0.34 $\pm$ 0.02 *	n.d.	n.d.	n.d.	n.d.
46	1506	1505	$\beta$ -Bisabolene	n.d.	n.d.	1.55	0.68 $\pm$ 0.16	0.48	0.14 $\pm$ 0.01 *	n.d.	n.d.
47	1509	1514	$\beta$ -Curcumene	n.d.	n.d.	0.60	0.30 $\pm$ 0.03 *	n.d.	n.d.	n.d.	n.d.
48	1510	1514	Cubebol	n.d.	n.d.	0.62	0.31 $\pm$ 0.04 *	n.d.	n.d.	1.23	0.23 $\pm$ 0.03
49	1518	1528	<i>cis</i> -Calamene	n.d.	n.d.	0.93	0.43 $\pm$ 0.03 *	n.d.	n.d.	1.39	0.26 $\pm$ 0.10
50	1518	1522	$\delta$ -Cadinene	n.d.	n.d.	0.38	0.21 $\pm$ 0.01 *	n.d.	n.d.	4.75	0.84 $\pm$ 0.08
51	1519 #	1522	Dihydroactinidiolide	n.d.	n.d.	n.d.	n.d.	2.13	0.44 $\pm$ 0.03	n.d.	n.d.
52	1526	1534	<i>trans</i> -Cadina-(1Z)-diene	n.d.	n.d.	1.58	0.70 $\pm$ 0.01 *	n.d.	n.d.	0.34	0.08 $\pm$ 0.01 *
53	1543	1549	Elemol	n.d.	n.d.	n.d.	n.d.	n.d.	n.d.	0.95	0.18 $\pm$ 0.11
54	1568	1578	Spathulenol	2.06	0.62 $\pm$ 0.12	0.31	0.18 $\pm$ 0.08	n.d.	n.d.	n.d.	n.d.
55	1572	1583	Caryophyllene oxide	n.q.	n.q.	1.29	0.58 $\pm$ 0.07	4.17	0.82 $\pm$ 0.13	2.63	0.48 $\pm$ 0.12
56	1583	1590	Globulol	n.d.	n.d.	0.17	0.12 $\pm$ 0.02 *	n.d.	n.d.	1.74	0.31 $\pm$ 0.10
57	1621	1628	1-epi-Cubebol	n.d.	n.d.	n.d.	n.d.	n.d.	n.d.	0.72	0.14 $\pm$ 0.03
58	1621	1631	Muuroloa-4,10(14)-dien-1 $\beta$ -ol	n.d.	n.d.	n.d.	n.d.	n.d.	n.d.	0.57	0.11 $\pm$ 0.02
59	1634	1642	$\alpha$ -epi-Muuroloa	n.d.	n.d.	n.d.	n.d.	n.d.	n.d.	0.37	0.08 $\pm$ 0.01 *
60	1654	1666/1668	14-Hydroxy-(Z)-caryophyllene/14-Hydroxy-9-epi-(E)-caryophyllene	n.d.	n.d.	0.17	0.12 $\pm$ 0.01 *	n.d.	n.d.	n.d.	n.d.
61	1660	1668	<i>trans</i> -Calamene-10-ol	n.d.	n.d.	n.d.	n.d.	n.d.	n.d.	0.81	0.16 $\pm$ 0.04
62	1660	1675	Valeranone	n.d.	n.d.	0.78	0.36 $\pm$ 0.02 *	n.d.	n.d.	n.d.	n.d.
63	1677	1683	$\alpha$ -epi-Bisabolol	n.d.	n.d.	3.42	1.45 $\pm$ 0.19	n.d.	n.d.	n.d.	n.d.
64	1677	1685	Germacrene-4(15),5,10(14)-trien-1-a-ol	n.d.	n.d.	n.d.	n.d.	n.d.	n.d.	0.67	0.13 $\pm$ 0.04
65	1678	1685	$\alpha$ -Bisabolol	1.75	0.56 $\pm$ 0.19	5.42	2.26 $\pm$ 0.66	3.75	0.74 $\pm$ 0.02	n.d.	n.d.
66	1754	1759	Benzyl benzoate	n.d.	n.d.	n.d.	n.d.	1.56	0.34 $\pm$ 0.01	n.d.	n.d.



Table 4. Cont.

No	RI <sub>cal</sub> <sup>1</sup>	RI <sub>lit</sub> <sup>2</sup>	Components	SCP		SCC		SR		SS	
				%	mg/100 g	%	mg/100 g	%	mg/100 g	%	mg/100 g
67	1975	1997	Kaur-15-ene	1.26	0.42 ± 0.08	0.74	0.35 ± 0.01	n.d.	n.d.	n.d.	n.d.
68	1979	1960	Hexadecanoic acid	n.d.	n.d.	n.d.	n.d.	11.09	2.09 ± 0.58	n.d.	n.d.
69	1995	1987/2009	Manool oxide/ 13- <i>epi</i> -Manool oxide	1.10	0.40 ± 0.07	n.d.	n.d.	n.d.	n.d.	0.86	0.16 ± 0.01
70	2066 <sup>#</sup>	2060	Oleyl alcohol	n.d.	n.d.	1.10	0.51 ± 0.40	n.d.	n.d.	n.d.	n.d.
Total				82.88	23.05 ± 2.78	78.75	41.31 ± 0.79	79.97	15.64 ± 0.41	89.20	16.01 ± 0.67
Number of compounds				31		50		24		38	

Note: n.q.: not quantified, n.d.: not detected. <sup>1</sup> Retention index on HP-5MS (non-polar column). <sup>2</sup> Literature retention index on the non-polar column as reported in [43] except those with <sup>#</sup>, which are reported in König et al. [44]. \* These compounds were detected only in one biological sample. <sup>§</sup> These compounds did not separate, and the values refer to both compounds.



**Figure 2.** The content of each volatile category in the petroleum ether extracts of the four *Sideritis* taxa (2 biological samples per taxon, n = 2). The values of the percentage of peak areas (average ± standard deviation) are presented.

In detail, in SCP the main components were the monoterpenes  $\alpha$ -pinene (20.01%),  $\beta$ -pinene (7.73%),  $\beta$ -myrcene (5.86%), and sylvestrene (5.52%), as well as the sesquiterpenes bicyclogermacrene (6.01%) and germacrene D (5.28%) (Table 4). These results are quite consistent with previous studies concerning the high amounts of  $\alpha$ -pinene and  $\beta$ -pinene [12,16].

In SCC extract,  $\alpha$ -pinene (20.40%), linalool (13.90%), and  $\beta$ -pinene (6.47%) had the highest percentages. Other quantitatively important compounds were  $\alpha$ -bisabolol (5.42%) and  $\beta$ -caryophyllene (4.86%). These results are consistent with previous studies [10–12].

In the study of Ntalli et al. [13], the major compounds in the essential oil of *S. clandestina* were  $\beta$ -pinene (8.3%),  $\alpha$ -pinene (4.3%), and  $\beta$ -bisabolol (5.7%), as well as spathulenol (5.0%) (found in very low concentrations in our study). Comparing our results of *S. clandestina* to the literature [10–13], it is noteworthy to mention the absence of monoterpene sylvestrene, which was found in a significant amount (3.10%) in the present study, and also the consistency in the presence of  $\alpha$ -pinene and  $\beta$ -pinene that characterizes the EO of most *Sideritis* species. It is interesting to note that the comparison of our SCC and SCP extracts revealed some qualitative and quantitative dissimilarities (Table 4); more compounds were detected in SCC, the total concentration of the volatiles was 77% higher, and the oxygenated monoterpenes were six-fold higher in comparison to SCP (10.07 over 1.48 mg/100 g plant material, respectively). Linalool and  $\alpha$ -bisabolol were three-fold higher, whereas linalool acetate and epi- $\alpha$ -bisabolol were detected only in SCC in considerable concentrations.

As far as SR extract is concerned, the hydrocarbons *n*-decane (23.59%), nonane (11.25%), and hexadecanoic acid (11.09%) were the prevalent compounds (Table 4). Other quantitatively important volatiles were  $\beta$ -caryophyllene (4.28%), caryophyllene oxide (4.17%),  $\alpha$ -bisabolol (3.75%), and eugenol (3.43%). According to Qazimi et al. [42], the *n*-hexane extracts of different populations of SR collected from Albania and North Macedonia showed up with a similar chemical load. The extracts consisted mainly of hydrocarbons, and the components *n*-decane, nonane, and hexadecanoic acid were present in different amounts. Comparing our results with previous studies using mainly hydrodistillation, significant dissimilarities in the chemical composition were observed. The analysis of SR Eos originating from Greece, North Macedonia, and Albania [45] indicated that they were rich in monoterpenes, whereas no alkanes were detected;  $\alpha$ -pinene and  $\beta$ -pinene were found in very high amounts. The strong presence of monoterpenes is also supported in previous studies, and different compounds are reported as the main constituents [10,11,16,46,47]. On the contrary, Romanucci et al. [48] supported that most SR Eos consisted of sesquiterpenes, representing 60–70% of the total EO content, with bicyclogermacrene being the main sesquiterpene, along with spathulenol and  $\beta$ -caryophyllene, whereas monoterpenes were found in very low amounts. Kostadinova et al. [49] also supported that sesquiterpenes were in high concentrations, indicating germacrene, elemol acetate, and  $\alpha$ -cadinol as the prevalent compounds.  $\beta$ -Caryophyllene was also found in high concentrations in two Greek populations of cultivated SR [5]), whereas  $\alpha$ -bisabolol and bicyclogermacrene were found in the population originating from Florina. Observations of great variety in essential-oil composition of close Greek SR populations (both from Kozani) have been made by Kloukina et al. [50]. This nonuniformity of the chemical composition among our results and those previously investigated could be attributed to the differences in the plant material used (we used leaves and flowers in a specific ratio and not stems), in addition to the extraction method of the volatiles (ultrasound-assisted extraction); in most other studies EOs were obtained with distillation. Furthermore, the genotypes, the site of collection, and the climatic conditions, which differ from year to year, could also be the reason for the qualitative and quantitative disparity [51].

The analysis of the SS extract revealed that the prevalent compounds were  $\alpha$ -pinene (18.95%), nonane (7.48%), sabinene (6.44%), and  $\beta$ -pinene (6.04%) (Table 4). The high values of  $\alpha$ -pinene and  $\beta$ -pinene agree with many previous studies [50–54]. However, some chemical variations were observed between our results and those of previous studies. According to Kouklina et al. [50], the analysis of the EO of SS cultivation from Chromio Kozani indicated *m*-camphorene (10.3%) as one of the main constituents, whereas the EO of an SS cultivation from Metamorfofis Kozani was rich in sesquiterpenes (45.9%) and not in monoterpenes (31.2%). Different chemical profiles have also been found among four different Greek cultivated populations of SS despite the same cultivation conditions [5]. Todorova et al. [55] reported that  $\beta$ -caryophyllene (18.8%) and nerolidol (12.1%) were the major compounds of an SS wild population originating from North Macedonia, along with  $\beta$ -farnesene (6.6%) and germacrene D (6.6%), whereas Kostadinova et al. [49] found that octadecenol and  $\alpha$ -cadinol had a very strong presence in SS from North Macedonia. These

discrepancies could be attributed to the different cultivation and environmental conditions such as altitude [50,54].

### 3. Materials and Methods

#### 3.1. Plant Material

*Sideritis raeseri* Boiss. & Heldr. Subsp. *raeseri*, *Sideritis clandestina* subsp. *peloponnesiaca* (Boiss. & Heldr.) Baden, and *Sideritis clandestina* Bory & Chaub. Hayek subsp. *clandestina* were collected from the mountains Gaidourorahi (38°02'10.9" N–22°13'08.9" E), Dourdouvana (37°54'95.6" N–22°15'03.7" E), and Parnonas (37°12'55.5" N–22°38'14.5" E), whereas *Sideritis scardica* Griseb. Was collected from commercial cultivation. All plants were harvested during the summer (July) of 2016. Their aerial parts were air dried and voucher specimens were authenticated by Prof. Gregoris Iatrou (UPA 15685 for *S. raeseri* Gaidourorahi; UPA 15690 for *S. clandestina* subsp. *peloponnesiaca* Dourdouvana; UPA 31153 for *S. clandestina* subsp. *clandestina*).

#### 3.2. Isolation of Polar Compounds from SCP Extracts

The dried and macerated aerial parts of SCP (943 g) were successively extracted with a total volume of 10 L petroleum ether, 7.5 L of ethyl acetate, and 7 L of methanol. In detail, the plant was extracted five times with each solvent at room temperature; the solvent was replaced every day with a fresh one and the extraction procedure lasted 15 days. The dried methanol extract was redissolved in methanol and processed with activated charcoal to remove chlorophylls. After two hours, the extract was decolorized and filtered through celite under vacuum. The filtrate was dried in a rotary evaporator, lyophilized, and weighed (11.44 g).

The aqueous fraction was further processed, and 0.451 g were submitted to solid-phase extraction (SPE). The cartridges used were octadecyl C<sub>18</sub> (500 mg/3 mL) Strata™-X 33 µm from Phenomenex (Torrance, CA, USA). They were conditioned with 3 mL of methanol and equilibrated with 3 mL of water. The sample was diluted in 3 mL 1% acetic acid aqueous solution and the elution was performed with 1% acetic acid aqueous solution (A) and methanol (B). Gradient elution was performed as follows: 85% A, 65% A, 60% A, 50% A, and 0% A. The SPE procedure afforded Fraction 1 (210 mg), Fraction 2 (28.8 mg), Fraction 3 (16.4 mg), Fraction 4 (15.5 mg), and Fraction 5 (19.4 mg). Fractions 1–3 were subjected to RP-HPLC (HPLC-DAD 1260 Infinity II) from Agilent Technologies Inc. (Santa Clara, CA, USA) using a semi-preparative column C-18 (250 × 10 mm, 5 µm, 100 Å, Phenomenex), the flow rate was 1.5 mL/min, and the detection wavelengths were set at 210/254/280/330 nm. The HPLC isolation afforded compounds 1–7.

Compounds 1 (2.4 mg,  $t_R = 15.18$  min) and 2 (11.5 mg,  $t_R = 15.4$  min) were isolated from Fraction 1. The mobile phase consisted of 0.2% formic acid aqueous solution (A) and acetonitrile (B). The gradient conditions were 95–65% A (0–30 min), 65–95% A (30–31 min), and 95% A (31–38 min). The concentration of the sample was 4 mg/mL and the injection volume was 70 µL.

Compounds 3 (0.6 mg,  $t_R = 15.85$  min), 4 (1.2 mg,  $t_R = 19.65$  min), and 5 (2.1 mg,  $t_R = 26.03$  min) were isolated from Fraction 2. The mobile phase consisted of 0.2% formic acid aqueous solution (A) and methanol (B). The gradient conditions were as follows: 76% A (0–7 min), 76–60% A (7–22 min), 60% A (22–24 min), 60–76% A (24–26 min), and 76% A (26–31 min). The concentration of the sample was 4 mg/mL and the injection volume was 50 µL.

Compounds 6 (4.9 mg,  $t_R = 17.79$ ) and 7 (1.2 mg,  $t_R = 28.13$ ) were isolated from Fraction 3. The mobile phase consisted of 0.2% formic acid aqueous solution (A) and methanol (B). The gradient was as follows: 65% A (0–12 min), 65–45% A (12–29 min), 45–65% A (29–30 min), and 65% A (30–33 min). The concentration of the sample was 3.6 mg/mL and the injection volume was 50 µL.

Compounds 8 (5.5 mg,  $t_R = 7.42$  min)–9 (4.2 mg,  $t_R = 10.07$  min) were isolated from ethyl acetate fraction. Specifically, 21.5 mg of the ethyl acetate fraction were loaded on a preparative

TLC plate coated with silica gel GF<sub>254</sub> (1 mm) from Macherey-Nagel GmbH & Co. KG (Dueren, Germany). The chromatogram was developed with EtOAc:CH<sub>2</sub>Cl<sub>2</sub>:HCOOH:AcOH:H<sub>2</sub>O (100:25:10:10:11, v/v/v/v/v) and examined under a UV lamp (254 and 365 nm). The fluorescent band was scraped out and extracted with methanol. The diluted mixture was centrifuged at 7000 rpm for 10 min and the supernatant was submitted to RP-HPLC on a semi-preparative column C-18. The detection wavelengths were set at 235, 268, and 330 nm. The mobile phase consisted of 0.2% formic acid aqueous solution (A) and methanol (B) and the gradient was as follows: 50–45% A (0–4 min), 45% A (4–9 min), 45–10% A (9–20 min), 10% A (20–23 min), 10–50% A (23–28 min), and 50% A (28–35 min) at a flow rate of 1.3 mg/mL.

NMR spectra (<sup>1</sup>H, <sup>13</sup>C and 2D) were recorded on a Bruker 600 MHz (600 MHz for <sup>1</sup>H, 150.9 MHz for <sup>13</sup>C) Avance III HD Ascend TM spectrometer at the Center of Instrumental Analysis, University of Patras, Greece. The chemical shifts (δ) are reported in parts per million (ppm) and the residual solvent signal was used as an internal standard. HPLC-DAD 1260 Infinity II (Agilent Technologies Inc., Santa Clara, CA, USA) equipped with the software OpenLab 3.2 was used for the isolation of glycosides. Analysis of extracts and glycosides was performed in a single quadrupole LC/MS system of LC/MSD1260 Infinity II (Agilent Technologies, Inc.) equipped with OpenLab 3.2. software from Agilent Technologies Inc.

### 3.3. Determination of Polar and Volatile Metabolites in Different *Sideritis* Samples

#### 3.3.1. Extraction

The extraction protocol was described in our previous work [16], namely, ultrasound-assisted extraction with pretreatment in citrate buffer (UAE-A). In detail, three (3) grams of plant material (flowers and leaves in a ratio of 2:5, in small pieces) were incubated in 90 mL of 0.05 M citrate buffer pH 4.8 for 75 min in a water bath at 37 °C. The aqueous buffer was removed, and the plant material was further extracted with 80 mL of petroleum ether in an ultrasonic bath for 30 min. Each extraction step was performed twice. The aqueous buffer was collected, extracted with petroleum ether, dried (lyophilized), weighed, and stored at −20 °C until use. The organic layers were merged, washed with saturated sodium chloride solution, dried over anhydrous sodium sulphate, filtered, and concentrated under vacuum. The petroleum ether extracts were submitted to a nitrogen flow for about 10 min (until the petroleum ether was evaporated). After measuring their volume, they were stored in clear glass vials at −20 °C until use. The experiments were performed twice for each sample.

#### 3.3.2. Gas Chromatography–Mass Spectrometry (GC/MS)

Analysis was carried out in an Agilent 6890N GC apparatus coupled to an Agilent 5975 B mass spectrometer with a non-polar column HP-5MS (30 m × 0.25 mm × 0.25 μm film thickness) using electron impact (70 eV) ionization mode. Helium was used as a carrier gas and the flow rate for the HP-5MS column was 1 mL/min; the injected volume was 1 μL in splitless mode. The injector temperature was set to 280 °C and the source temp to 230 °C. Specifically, the initial oven temperature was 50 °C for 4 min, which was then ramped up 2 °C/min<sup>−1</sup> to 92 °C, 4 °C/min<sup>−1</sup> to 108 °C, 2 °C/min<sup>−1</sup> to 130 °C, 1 °C/min<sup>−1</sup> to 150 °C, 5 °C/min<sup>−1</sup> to 180 °C, and finally 15 °C/min<sup>−1</sup> to 270 °C. Qualitative analysis was based on a comparison of the obtained MS spectra to literature data and of the retention indices (RI) on apolar columns [43,56]. RI values were calculated based on a series of linear alkanes, C8–C20 and C21–C40, using the Van den Dool and Kratz equation.

Quantification was performed as described in our previous published work [16]. Data were expressed in two forms: (a) as a percentage of peak area divided by that of the internal standard and (b) as milligrams of α-pinene equivalents per 100 g of dry plant material. The procedure yields were expressed in milliliters per 100 g of dry material since the extracts were all liquid at ambient temperature. Only the compounds for which the peak area exceeded 0.1% of total peak area are presented.

### 3.3.3. Liquid Chromatography–Mass Spectrometry (LC/MS)

The single quadrupole LC/MS system of LC/MSD1260 Infinity II (Agilent Technologies, Inc., Santa Clara, CA, USA) was used in this study. The system was equipped with an ESI ion source and the mass range was  $m/z$  100–1600 in full scan mode. Nitrogen was used as the gas for ionization. Working conditions were in ESI negative mode and separation was performed on a Poroshell 120 EC 18 column ( $4.6 \times 100$  mm,  $2.7 \mu\text{m}$ ) (Agilent Technologies, Inc.). The mobile phase consisted of 0.1% acetic acid in water (A) and methanol (B). Separation was carried out in 65 min under the following conditions: 0–8 min 15% B; 8–13 min 15–35% B; 13–18 min 35% B; 18–19 min 35–40% B; 19–27 min 40% B; 27–28 min 40–45% B; 28–35 min 45% B; 35–45 min 45–75% B; 45–55 min 75% B; 55–59 min 75–15% B; 59–65 min 15% B. The flow rate was 0.3 mL/min and the injection volume was 10  $\mu\text{L}$ . The samples were prepared by diluting the dry aqueous extracts in methanol, and their final concentration was 10 mg/mL.

The identification of the compounds was based on comparison of their retention time and their obtained mass spectra to the literature. Furthermore, six reference compounds were used (melittoside, ajugoside, 7-*O*-acetyl-8-epi-loganic acid, chlorogenic acid, verbascoside, isoverbascoside) that were isolated in our laboratory. Rutin (HPLC > 99%) from Extrasynthese (Genay, France) was used for the quantification. The calibration curve was established for eight concentrations (2–16  $\mu\text{g/mL}$ ) through the equation  $y = 126832x + 81400$  ( $R^2 = 0.9951$ ). The lower limit of quantitation (LLOQ) was 0.772  $\mu\text{g/mL}$  and the lower limit of detection (LLOD) was 0.232  $\mu\text{g/mL}$ .

The experiments were performed in duplicate for each sample and the results are expressed in mg rutin equivalents per 100 g of dry plant material. The procedure yields are expressed as g of lyophilized extract per 100 g of dry plant material.

### 3.4. Determination of Total Phenolics, Flavonoids Content, and Antioxidant Capacity (DPPH and FRAP) in Aqueous Buffer Extracts

Total phenolics, total flavonoids, and antioxidant capacity were measured in the aqueous extracts (in triplicate, twice) with methods adapted for 96-well plates, and the absorbance was measured in a UV/vis microplate reader (Sunrise, Tecan Austria) against blanks.

Total phenolic content was determined with the Folin–Ciocalteu reagent method [57,58] at 620 nm and is expressed as mg of gallic acid equivalents (GAE) per g of dry weight (D.W.) of plant material.

Total flavonoid content was determined with the aluminum chloride ( $\text{AlCl}_3$ ) method [59] at 405 nm and the results are expressed as mg of quercetin equivalents (QE) per g of D.W. of plant material. In detail, 75  $\mu\text{L}$  of ddH<sub>2</sub>O were mixed with 5  $\mu\text{L}$  of  $\text{CH}_3\text{COOH}$  1M, 16  $\mu\text{L}$  extract or standard (quercetin) in ethanol 60% (*v/v*), 40  $\mu\text{L}$  ethanol 95% (*v/v*), and 5  $\mu\text{L}$  of  $\text{AlCl}_3$  10% *w/v* incubated at RT for 45 min.

The antioxidant activity was evaluated with two different assays—ferric reducing antioxidant power (FRAP) and 2,2-diphenyl-1-picrylhydrazyl (DPPH) radical scavenging activity. The FRAP method [60] measures the ability of antioxidants to reduce the  $[\text{Fe}_{\text{III}}(\text{TPTZ})_2]^{3+}$  to  $[\text{Fe}_{\text{II}}(\text{TPTZ})_2]^{2+}$ . In detail, 80  $\mu\text{L}$  of FRAP solution (15 mL of a solution of 10 mM 2,4,6-tri(2-pyridyl)-s-triazine (TPTZ) in 40 mM HCl, 15 mL of 20 mM  $\text{FeCl}_3 \cdot 6\text{H}_2\text{O}$ , and 75 mL of 300 mM acetate buffer solution, pH 3.6), were mixed with 55  $\mu\text{L}$  of acetate buffer and 60  $\mu\text{L}$  extract or standard ( $\text{FeSO}_4 \cdot 7\text{H}_2\text{O}$ ) and incubated at room temperature for 5 min. Absorbance was measured at 592 nm and the results are expressed as mmol  $\text{Fe}^{2+}$  per g of D.W.

In addition, the antioxidant activity was determined with the 2,2-diphenyl-1-picrylhydrazyl (DPPH) method [61,62], which measures the ability of antioxidants to scavenge the stable organic nitrogen radical DPPH $\bullet$ . Absorbance was measured at 540 nm and the results are expressed as  $\text{IC}_{50}$  g of D.W. of plant material. In detail, 195  $\mu\text{L}$  of 0.1 mM DPPH (in methanol) were mixed with 5  $\mu\text{L}$  of extract or BHT (butylated hydroxytoluene) used as standard (both diluted in methanol 50% *v/v*) and incubated at RT for 30 min.

### 3.5. Statistical Analysis

Averages and standard deviation were calculated using replicates from all samples. The data were tested for normality with the Shapiro–Wilk test ( $\alpha > 0.01$ ) and for homogeneity of variance with the Levene test. ANOVA and the post-hoc Tukey test ( $\alpha = 0.05$ ) were performed at a significance level. Pearson’s correlation was performed for all variable pairs at a significance level of 95% ( $\alpha = 0.05$ ) and  $r > 0.90$ ,  $r > 0.70$ ,  $r > 0.50$ , and  $r > 0.30$  were interpreted as very high, high, moderate, and low coefficients, respectively. SPSS version 25.0 (IBM Corp., Armonk, NY, USA) was used for data analysis.

## 4. Conclusions

This study contributes to the phytochemical characterization of *Sideritis clandestina* and suggests a methodology for the comparison of its volatile and polar metabolite composition to other *Sideritis* taxa. *Sideritis* plants have been used daily in Balkan countries as aromatic infusions/decoctions that not only provide sensory pleasure but also various health benefits, e.g., sedation and alleviation of common-cold symptoms. In the last decade, the pursuit of producing novel and unique herbal products of high added value amid the economic crisis has highlighted the potential of mountain tea, especially in the light of studies of its health benefits and of the European Medicines Agency’s approval for its use in traditional herbal medicinal products for the relief of cough associated with a cold and for the relief of mild stomach and gut discomfort. Beverages, cosmetics, and food supplements using *Sideritis* plant material were introduced to the market. In official documents and in the market, the term “mountain tea” or “ironwort” describes many species of *Sideritis* and, in many cases, there are no special references to the particular taxa used, as there is still a lack of studies describing the phytochemical characterization of each taxon. The amount of material collected from nature is controlled by agronomical decisions (no more than 2 kg per person are allowed), and uprooting is prohibited. Most of the mountain-tea material on the market comes from the cultivations of SR and SS in open and covered fields that have increased in recent years. *S. clandestina* taxa are endemic in the Peloponnese, not cultivated, and were recently assigned as critically endangered and threatened [63].

We herein describe the phytochemical characterization of *S. clandestina* subsp. *peloponnesiaca* (SCP) for the first time. Four iridoid glycosides, two phenolic glycosides, and three caffeoyl ester derivatives (chlorogenic acid, verbascoside, and isoverbacoside) were isolated from SCP for the first time; vanillic acid and salicylic glycosides are not common in *Sideritis* taxa. We herein optimized a methodology previously developed by us (ultrasound-assisted extraction of samples with petroleum ether after acidic pretreatment) to determine both volatile and polar metabolites using plant samples as small as 3 g. The isolation of those nine compounds from SCP greatly helped the LC/MS identification of polar metabolites in the aqueous extracts. Regarding aqueous extracts, *S. raeseri* and *S. scardica* had higher phenolic and flavonoid content and therefore antioxidant properties than the *S. clandestina* samples. SCC seemed to be the most aromatic taxon with almost twice the amount of volatiles as the others. In total, 27 polar and 70 volatile metabolites were determined. This methodology could be applied to chemotaxonomic studies after testing larger numbers of samples, the selection of genotypes during breeding efforts for the development of varieties, and certainly the authentication of new final herbal products.

**Supplementary Materials:** The following supporting information can be downloaded at: <https://www.mdpi.com/article/10.3390/molecules27217613/s1>, Figure S1.  $^1\text{H-NMR}$  spectrum of monomelittoside (1) ( $^1\text{H-NMR}$ :600 MHz;  $\text{D}_2\text{O}$ ). Figure S2. MS spectrum of monomelittoside (1) in negative mode. The major ions were 407  $[\text{M}+\text{FA-H}]^-$ , 361  $[\text{M-H}]^-$ , and 723  $[\text{2M-H}]^-$ . Figure S3. UV-vis spectrum of monomelittoside (1) showing a  $\lambda_{\text{max}}$  of 210 nm. Figure S4.  $^1\text{H-NMR}$  spectrum of melittoside (2) ( $^1\text{H-NMR}$ :600 MHz;  $\text{D}_2\text{O}$ ). Figure S5.  $^{13}\text{C-NMR}$  spectrum of melittoside (2) ( $^{13}\text{C-NMR}$ :150 MHz;  $\text{D}_2\text{O}$ ). Figure S6. MS spectrum of melittoside (2) in negative mode. The major ions were 523  $[\text{M-H}]^-$ , 583  $[\text{M}+\text{Hac-H}]^-$ , and 1047  $[\text{2M-H}]^-$ . Figure S7. UV-vis spectrum of melittoside (2) showing a maximum absorbance at 210 nm. Figure S8.  $^1\text{H-NMR}$  spectrum of vanillic acid glucoside (3) ( $^1\text{H-NMR}$ :600 MHz;  $\text{D}_2\text{O}$ ). Figure S9. MS spectrum of vanillic acid glucoside (3) in negative mode.

The major ions were 659 [2M-H]<sup>−</sup> and 329 [M-H]<sup>−</sup>. Figure S10. UV spectrum of vanillic acid glucoside (3). Maximum absorbance at 210, 254, and 290 nm. Figure S11. <sup>1</sup>H-NMR spectrum of ajugoside (4) (<sup>1</sup>H-NMR:600 MHz; D<sub>2</sub>O). Figure S12. MS spectrum of ajugoside (4) in negative mode. The major ions were 449 [M+Hac-H]<sup>−</sup> and 779 [2M-H]<sup>−</sup>. Figure S13. UV-vis spectrum of ajugoside (4). Maximum absorbance at 200 nm. Figure S14. <sup>1</sup>H-NMR spectrum of salicylic acid glucoside (5) (<sup>1</sup>H-NMR:600 MHz; D<sub>2</sub>O). Figure S15. MS spectrum of salicylic acid glucoside (5) in negative mode. The major ions of 299 and 599 correspond to [M-H]<sup>−</sup> and [2M-H]<sup>−</sup>, respectively. Figure S16. UV-vis spectrum of salicylic acid glucoside (5) having maximum absorbance at 230 and 286 nm. Figure S17 <sup>1</sup>H-NMR spectrum of 7-O-acetyl-8-epi-loganic acid (6) (<sup>1</sup>H-NMR:600 MHz; D<sub>2</sub>O). Figure S18. MS spectrum of 7-O-acetyl-8-epi-loganic acid (6) in negative mode. The major ions were 417 [M-H]<sup>−</sup> and 835 [2M-H]<sup>−</sup>. Figure S19. UV spectrum of 7-O-acetyl-8-epi-loganic acid (6) with maximum absorbance at 236 nm. Figure S20. <sup>1</sup>H-NMR spectrum of chlorogenic acid (7) (<sup>1</sup>H-NMR:600 MHz; CD<sub>3</sub>OD). Figure S21. MS spectrum of chlorogenic acid (7) in negative mode. The major ions of 707 and 353 correspond to [2M-H]<sup>−</sup> and [M-H]<sup>−</sup>, respectively, whereas the ion of m/z = 191 is a fragment corresponding to quinic acid. Figure S22. UV-vis spectrum of chlorogenic acid (7) showing maximum absorbance at 330 nm. Figure S23. <sup>1</sup>H-NMR spectrum of verbascoside (8) (<sup>1</sup>H-NMR:600 MHz; D<sub>2</sub>O). Figure S24. <sup>13</sup>C-NMR spectrum of verbascoside (8) (<sup>13</sup>C-NMR:150 MHz; D<sub>2</sub>O). Figure S25. HSQC-NMR spectrum of verbascoside (8) (D<sub>2</sub>O). Figure S26. HMBC-NMR spectrum of verbascoside (8) (D<sub>2</sub>O). Figure S27. COSY-NMR spectrum of verbascoside (8) (D<sub>2</sub>O). Figure S28. ROESY-NMR spectrum of verbascoside (8) (D<sub>2</sub>O). Figure S29. MS spectrum of verbascoside (8) in negative mode with the sole ion of 623 [M-H]<sup>−</sup>. Figure S30. UV spectrum of verbascoside (8) showing maximum absorbance at 210 and 330 nm. Figure S31. <sup>1</sup>H-NMR spectrum of isoverbascoside (9) (<sup>1</sup>H-NMR:600 MHz; D<sub>2</sub>O). Figure S32. <sup>13</sup>C-NMR spectrum of isoverbascoside (9) (<sup>13</sup>C-NMR:150 MHz; D<sub>2</sub>O). Figure S33. HSQC-NMR spectrum of isoverbascoside (9) (D<sub>2</sub>O). Figure S34. HMBC-NMR spectrum of isoverbascoside (9) (D<sub>2</sub>O). Figure S35. COSY-NMR spectrum of isoverbascoside (9) (D<sub>2</sub>O). Figure S36. ROESY-NMR spectrum of isoverbascoside (9) (D<sub>2</sub>O). Figure S37. MS spectrum of isoverbascoside (9) in negative mode with the main ion of 623 [M-H]<sup>−</sup>. Figure S38. UV-vis spectrum of isoverbascoside (9) showing absorbance maxima at 210 and 330 nm. Figure S39. Total ion chromatogram (TIC) in negative mode of *Sideritis clandestina* subsp. *peloponnesiaca* (SCP) aqueous extract. Table S1. <sup>1</sup>H-NMR (600 MHz) data of monomelitioside (1) in D<sub>2</sub>O. Table S2. <sup>1</sup>H-NMR (600 MHz) and <sup>13</sup>C-NMR (150 MHz) data of melitioside (2) in D<sub>2</sub>O. Table S3. <sup>1</sup>H-NMR (600 MHz) data of vanillic acid glucoside (3) in D<sub>2</sub>O. Table S4. <sup>1</sup>H-NMR (600 MHz) data of ajugoside (4) in D<sub>2</sub>O. Table S5. <sup>1</sup>H-NMR data of salicylic acid glucoside (5) (D<sub>2</sub>O). Table S6. <sup>1</sup>H-NMR data of 7-O-acetyl-8-epi-loganic acid (6) (D<sub>2</sub>O). Table S7. <sup>1</sup>H-NMR data of chlorogenic acid (7) (CD<sub>3</sub>OD). Table S8. <sup>1</sup>H-NMR, <sup>13</sup>C-NMR and APT-NMR data of verbascoside (8) (D<sub>2</sub>O). Table S9. <sup>1</sup>H-NMR, <sup>13</sup>C-NMR and APT-NMR data of isoverbascoside (9) (D<sub>2</sub>O).

**Author Contributions:** Conceptualization, G.I. and F.N.L.; formal analysis, V.D.D., K.Z., F.N. and M.S.; funding acquisition, G.I. and F.N.L.; investigation, V.D.D., F.N., M.S., I.B. and L.P.; methodology, V.D.D. and F.N.L.; project administration, F.N.L.; resources, G.I. and F.N.L.; supervision, V.D.D., K.Z. and F.N.L.; validation, V.D.D. and K.Z.; writing—original draft, V.D.D. and K.Z.; writing—review and editing, G.I. and F.N.L. All authors have read and agreed to the published version of the manuscript.

**Funding:** This project had been partly funded by the Operational Program “Competitiveness, Entrepreneurship and Innovation” under the call “RESEARCH-CREATE-INNOVATE” (project code: T1EDK 00353).

**Institutional Review Board Statement:** Not applicable.

**Informed Consent Statement:** Not applicable.

**Data Availability Statement:** Data will be made available on request.

**Conflicts of Interest:** The authors declare no conflict of interest.

## References

1. Fraga, B.M. Phytochemistry and Chemotaxonomy of *Sideritis* Species from the Mediterranean Region. *Phytochemistry* **2012**, *76*, 7–24. [[CrossRef](#)] [[PubMed](#)]
2. González-Burgos, E.; Carretero, M.E.; Gómez-Serranillos, M.P. *Sideritis* spp.: Uses, Chemical Composition and Pharmacological Activities—A Review. *J. Ethnopharmacol.* **2011**, *135*, 209–225. [[CrossRef](#)] [[PubMed](#)]

3. Aneva, I.; Zhelev, P.; Kozuharova, E.; Danova, K.; Nabavi, S.F.; Behzad, S. Genus *Sideritis*, Section *Empedoclia* in Southeastern Europe and Turkey—Studies in Ethnopharmacology and Recent Progress of Biological Activities. *DARU J. Pharm. Sci.* **2019**, *27*, 407–421. [[CrossRef](#)]
4. Ibraliu, A.; Trendafilova, A.B.; Anđelković, B.; Qazimi, B.; Godevac, D.; Bebeci, E.; Stefkov, G.; Zdunic, G.; Aneva, I.; Pasho, I.; et al. Comparative Study of Balkan *Sideritis* Species from Albania, Bulgaria and Macedonia. *Eur. J. Med. Plants* **2015**, *5*, 328–340. [[CrossRef](#)]
5. Triikka, F.; Michailidou, S.; Makris, A.M.; Argiriou, A. Biochemical Fingerprint of Greek *Sideritis* spp.: Implications for Potential Drug Discovery and Advanced Breeding Strategies. *Med. Aromat. Plants* **2019**, *8*, 1–11. [[CrossRef](#)]
6. Stanoeva, J.P.; Stefova, M.; Stefkov, G.; Kulevanova, S.; Alipieva, K.; Bankova, V.; Aneva, I.; Evstatieva, L.N. Chemotaxonomic Contribution to the *Sideritis* Species Dilemma on the Balkans. *Biochem. Syst. Ecol.* **2015**, *61*, 477–487. [[CrossRef](#)]
7. Pappas, C.S.; Xagoraris, M.; Kimbaris, A.; Korakis, G.; Tarantilis, P.A. Chemometric-Infrared Spectroscopic Model for the Taxonomy of Medicinal Herbs—The Case of Perennial *Sideritis* Species. *Biomed. J. Sci. Tech. Res.* **2020**, *32*, 24707–24712. [[CrossRef](#)]
8. Petreska, J.; Stefova, M.; Ferreres, F.; Moreno, D.A.; Tomás-Barberán, F.A.; Stefkov, G.; Kulevanova, S.; Gil-Izquierdo, A. Potential Bioactive Phenolics of Macedonian *Sideritis* Species Used for Medicinal “Mountain Tea”. *Food Chem.* **2011**, *125*, 13–20. [[CrossRef](#)]
9. Strid, A.; Tan, K. *Mountain Flora of Greece*; Cambridge University Press: Cambridge, UK; New York, NY, USA, 1986; ISBN 978-0-521-25737-4.
10. Koedam, A. Volatile Oil Composition of Greek Mountain Tea (*Sideritis* spp.). *J. Sci. Food Agric.* **1986**, *37*, 681–684. [[CrossRef](#)]
11. Aligiannis, N.; Kalpoutzakis, E.; Chinou, I.B.; Mitakou, S.; Gikas, E.; Tsarbopoulos, A. Composition and Antimicrobial Activity of the Essential Oils of Five Taxa of *Sideritis* from Greece. *J. Agric. Food Chem.* **2001**, *49*, 811–815. [[CrossRef](#)]
12. Koutsaviti, A.; Bazos, I.; Milenkovi, M.; Pavlovi, M. Antimicrobial Activity and Essential Oil Composition of Five *Sideritis* Taxa of *Empedoclia* and *Hesiodia* Sect. from Greece. *Rec. Nat. Prod.* **2013**, *7*, 6–14.
13. Ntalli, N.G.; Ferrari, F.; Giannakou, I.; Menkissoglu-Spiroudi, U. Phytochemistry and Nematicidal Activity of the Essential Oils from 8 Greek Lamiaceae Aromatic Plants and 13 Terpene Components. *J. Agric. Food Chem.* **2010**, *58*, 7856–7863. [[CrossRef](#)] [[PubMed](#)]
14. Linardaki, Z.I.; Vasilopoulou, C.G.; Constantinou, C.; Iatrou, G.; Lamari, F.N.; Margarit, M. Differential Antioxidant Effects of Consuming Tea from *Sideritis Clandestina* subsp. *Peloponnesiaca* on Cerebral Regions of Adult Mice. *J. Med. Food* **2011**, *14*, 1060–1064. [[CrossRef](#)]
15. Vasilopoulou, C.G.; Kontogianni, V.G.; Linardaki, Z.I.; Iatrou, G.; Lamari, F.N.; Nerantzaki, A.A.; Gerathanassis, I.P.; Tzakos, A.G.; Margarit, M. Phytochemical Composition of “Mountain Tea” from *Sideritis Clandestina* Subsp. *Clandestina* and Evaluation of Its Behavioral and Oxidant/Antioxidant Effects on Adult Mice. *Eur. J. Nutr.* **2013**, *52*, 107–116. [[CrossRef](#)]
16. Dimaki, V.D.; Iatrou, G.; Lamari, F.N. Effect of Acidic and Enzymatic Pretreatment on the Analysis of Mountain Tea (*Sideritis* spp.) Volatiles via Distillation and Ultrasound-Assisted Extraction. *J. Chromatogr. A* **2017**, *1524*, 290–297. [[CrossRef](#)] [[PubMed](#)]
17. Serrilli, A.M.; Ramunno, A.; Piccioni, F.; Serafini, M.; Ballero, M.; Bianco, A. Monoterpenoids from *Stachys Glutinosa* L. *Nat. Prod. Res.* **2006**, *20*, 648–652. [[CrossRef](#)] [[PubMed](#)]
18. Chrysargyris, A.; Kloukina, C.; Vassiliou, R.; Tomou, E.-M.; Skaltsa, H.; Tzortzakis, N. Cultivation Strategy to Improve Chemical Profile and Anti-Oxidant Activity of *Sideritis Perfoliata* L. Subsp. *Perfoliata*. *Ind. Crops Prod.* **2019**, *140*, 111694. [[CrossRef](#)]
19. Tomou, E.-M.; Lytra, K.; Chrysargyris, A.; Christofi, M.-D.; Miltiadous, P.; Corongiu, G.L.; Tziouvelis, M.; Tzortzakis, N.; Skaltsa, H. Polar Constituents, Biological Effects and Nutritional Value of *Sideritis Sipylea* Boiss. *Nat. Prod. Res.* **2022**, *36*, 4200–4204. [[CrossRef](#)]
20. Koleva, I.I.; Linssen, J.P.; van Beek, T.A.; Evstatieva, L.N.; Kortenska, V.; Handjieva, N. Antioxidant Activity Screening of Extracts from *Sideritis* Species (Labiatae) Grown in Bulgaria. *J. Sci. Food Agric.* **2003**, *83*, 809–819. [[CrossRef](#)]
21. Lytra, K.; Tomou, E.; Chrysargyris, A.; Christofi, M.; Miltiadous, P.; Tzortzakis, N.; Skaltsa, H. Bio-Guided Investigation of *Sideritis Cypria* Methanol Extract Driven by In Vitro Antioxidant and Cytotoxic Assays. *Chem. Biodivers.* **2021**, *18*, e2000966. [[CrossRef](#)]
22. Axiotis, E.; Petrakis, E.A.; Halabalaki, M.; Mitakou, S. Phytochemical Profile and Biological Activity of Endemic *Sideritis Sipylea* Boiss. in North Aegean Greek Islands. *Molecules* **2020**, *25*, 2022. [[CrossRef](#)]
23. Yu, H.; Yang, G.; Sato, M.; Yamaguchi, T.; Nakano, T.; Xi, Y. Antioxidant Activities of Aqueous Extract from *Stevia Rebaudiana* Stem Waste to Inhibit Fish Oil Oxidation and Identification of Its Phenolic Compounds. *Food Chem.* **2017**, *232*, 379–386. [[CrossRef](#)]
24. Sarikurkc, C.; Ozer, M.S.; Istifli, E.S.; Sahinler, S.S.; Tepe, B. Chromatographic Profile and Antioxidant and Enzyme Inhibitory Activity of *Sideritis Leptoclada*: An Endemic Plant from Turkey. *S. Afr. J. Bot.* **2021**, *143*, 393–405. [[CrossRef](#)]
25. Özkan, G. Comparison of Antioxidant Phenolics of Ethanolic Extracts and Aqueous Infusions from *Sideritis* Species. *Asian J. Chem.* **2009**, *21*, 1024–1028.
26. Venditti, A.; Frezza, C.; Lorenzetti, L.; Maggi, F.; Serafini, M.; Bianco, A. Reassessment of the Polar Fraction of *Stachys Alopeucuros* (L.) Benth. Subsp. *Divulsa* (Ten.) Grande (Lamiaceae) from the Monti Sibillini National Park and Its Potential Pharmacologic Uses. *J. Intercult. Ethnopharmacol.* **2017**, *6*, 144–153. [[CrossRef](#)] [[PubMed](#)]
27. Charami, M.-T.; Lazari, D.; Karioti, A.; Skaltsa, H.; Hadjipavlou-Litina, D.; Souleles, C. Antioxidant and Antiinflammatory Activities of *Sideritis Perfoliata* subsp. *Perfoliata* (Lamiaceae). *Phytother. Res.* **2008**, *22*, 450–454. [[CrossRef](#)]
28. Mendoza, D.; Arias, J.P.; Cuaspad, O.; Esturau-Escofet, N.; Hernández-Espino, C.C.; de San Miguel, E.R.; Arias, M. 1H-NMR-Based Metabolomic of Plant Cell Suspension Cultures of *Thevetia Peruviana* Treated with Salicylic Acid and Methyl Jasmonate. *Ind. Crops Prod.* **2019**, *135*, 217–229. [[CrossRef](#)]



29. Wang, D.; Wang, X.; Fayvush, G.; Tamanyan, K.; Khutsishvili, M.; Atha, D.; Borris, R.P. Phytochemical Investigations of *Aethionema Armenum* Boiss. (Brassicaceae). *Biochem. Syst. Ecol.* **2018**, *81*, 37–41. [[CrossRef](#)]
30. Hanoğlu, D.Y.; Hanoğlu, A.; Yusufoglu, H.; Demirci, B.; Başer, K.H.C.; Çaliş, İ.; Yavuz, D.Ö. Phytochemical Investigation of Endemic *Sideritis Cypria* Post. *Rec. Nat. Prod.* **2019**, *14*, 105–115. [[CrossRef](#)]
31. Garayev, E.; Di Giorgio, C.; Herbette, G.; Mabrouki, F.; Chiffolleau, P.; Roux, D.; Sallanon, H.; Ollivier, E.; Elias, R.; Baghdikian, B. Bioassay-Guided Isolation and UHPLC-DAD-ESI-MS/MS Quantification of Potential Anti-Inflammatory Phenolic Compounds from Flowers of *Inula montana* L. *J. Ethnopharmacol.* **2018**, *226*, 176–184. [[CrossRef](#)] [[PubMed](#)]
32. Li, L.; Tsao, R.; Liu, Z.; Liu, S.; Yang, R.; Young, J.C.; Zhu, H.; Deng, Z.; Xie, M.; Fu, Z. Isolation and Purification of Acteoside and Isoacteoside from *Plantago Psyllium* L. by High-Speed Counter-Current Chromatography. *J. Chromatogr. A* **2005**, *1063*, 161–169. [[CrossRef](#)]
33. Owen, R.W.; Haubner, R.; Mier, W.; Giacosa, A.; Hull, W.E.; Spiegelhalder, B.; Bartsch, H. Isolation, Structure Elucidation and Antioxidant Potential of the Major Phenolic and Flavonoid Compounds in Brined Olive Drupes. *Food Chem. Toxicol.* **2003**, *41*, 703–717. [[CrossRef](#)]
34. Pljevljakušić, D.; Šavikin, K.; Janković, T.; Zdunić, G.; Ristić, M.; Godjevac, D.; Konić-Ristić, A. Chemical Properties of the Cultivated *Sideritis Raeseri* Boiss. & Heldr. Subsp. *Raeseri*. *Food Chem.* **2011**, *124*, 226–233. [[CrossRef](#)]
35. Stanoeva, J.P.; Bagashovska, D.; Stefova, M. Characterization of Urinary Bioactive Phenolic Metabolites Excreted after Consumption of a Cup of Mountain Tea (*Sideritis scardica*) Using Liquid Chromatography Tandem Mass Spectrometry. *Maced. J. Chem. Chem. Eng.* **2012**, *31*, 229–243. [[CrossRef](#)]
36. Menkovi, N.; Godevac, D.; Šavikin, K.; Zdunić, G.; Milosavljević, S.; Bojadži, A.; Avramoski, O. Bioactive Compounds of Endemic Species *Sideritis Raeseri* Subsp. *Raeseri* Grown in National Park Galičica. *Rec. Nat. Prod.* **2013**, *7*, 161–168.
37. Petreska Stanoeva, J.; Stefova, M. Assay of Urinary Excretion of Polyphenols after Ingestion of a Cup of Mountain Tea (*Sideritis scardica*) Measured by HPLC-DAD-ESI-MS/MS. *J. Agric. Food Chem.* **2013**, *61*, 10488–10497. [[CrossRef](#)] [[PubMed](#)]
38. Petreska, J.; Stefova, M.; Ferreres, F.; Moreno, D.A.; Tomás-Barberán, F.A.; Stefkov, G.; Kulevanova, S.; Gil-Izquierdo, A. Dietary Burden of Phenolics per Serving of “Mountain Tea” (*Sideritis*) from Macedonia and Correlation to Antioxidant Activity. *Nat. Prod. Commun.* **2011**, *6*, 1305–1314. [[CrossRef](#)]
39. Venditti, A.; Bianco, A.; Frezza, C.; Serafini, M.; Giacomello, G.; Giuliani, C.; Bramucci, M.; Quassinti, L.; Lupidi, G.; Lucarini, D.; et al. Secondary Metabolites, Glandular Trichomes and Biological Activity of *Sideritis montana* L. subsp. *Montana* from Central Italy. *Chem. Biodivers.* **2016**, *13*, 1380–1390. [[CrossRef](#)]
40. Alipieva, K.; Petreska, J.; Gil-Izquierdo, Á.; Stefova, M.; Evstatieva, L.; Bankova, V. Influence of the Extraction Method on the Yield of Flavonoids and Phenolics from *Sideritis* spp. (Pirin Mountain Tea). *Nat. Prod. Commun.* **2010**, *5*, 51–54. [[CrossRef](#)]
41. Karapandzova, M.; Qazimi, B.; Stefkov, G.; Bačeva, K.; Stafilov, T.; Panovska, T.K.; Kulevanova, S. Chemical Characterization, Mineral Content and Radical Scavenging Activity of *Sideritis scardica* and *S. raeseri* from R. Macedonia and R. Albania. *Nat. Prod. Commun.* **2013**, *8*, 639–644. [[CrossRef](#)]
42. Qazimi, B.; Karapandzova, M.; Stefkov, G.; Kulevanova, S. Chemical Composition of Ultrasonic-Assisted n-Hexane Extracts of *Sideritis scardica* Griseb. and *Sideritis raeseri* Boiss. & Heldr. (Lamiaceae) from Macedonia and Albania. *Maced. Pharm. Bull.* **2011**, *56*, 45–56. [[CrossRef](#)]
43. Adams, R.P. *Identification of Essential Oil Components by Gas Chromatography/Mass Spectroscopy*, 4th ed.; Allured Pub. Corp: Carol Stream, IL, USA, 2007; ISBN 978-1-932633-21-4.
44. König, W.A.; Joulain, D.; Hochmuth, D.H. Available online: [https://massfinder.com/wiki/Terpenoids\\_Library](https://massfinder.com/wiki/Terpenoids_Library) (accessed on 25 May 2021).
45. Qazimi, B.; Stefkov, G.; Karapandzova, M.; Cvetkovikj, I.; Kulevanova, S. Aroma Compounds of Mountain Tea (*Sideritis scardica* and *S. raeseri*) from Western Balkan. *Nat. Prod. Commun.* **2014**, *9*, 1369–1372. [[CrossRef](#)] [[PubMed](#)]
46. Hodaj-Çeliku, E.; Tsiftoglou, O.; Shuka, L.; Abazi, S.; Hadjipavlou-Litina, D.; Lazari, D. Antioxidant Activity and Chemical Composition of Essential Oils of Some Aromatic and Medicinal Plants from Albania. *Nat. Prod. Commun.* **2017**, *12*, 785–790. [[CrossRef](#)] [[PubMed](#)]
47. Tzakou, O. The Essential Oil of *Sideritis raeseri* Boiss. et Heldr. Ssp. *Attica* (Heldr.) Pap. et Kok. *J. Essent. Oil Res.* **2002**, *14*, 376–377. [[CrossRef](#)]
48. Romanucci, V.; Di Fabio, G.; D’Alonzo, D.; Guaragna, A.; Scapagnini, G.; Zarrelli, A. Traditional Uses, Chemical Composition and Biological Activities of *Sideritis raeseri* Boiss. & Heldr.: Uses, Composition and Activities of *S. raeseri*. *J. Sci. Food Agric.* **2017**, *97*, 373–383. [[CrossRef](#)]
49. Kostadinova, E.; Nikolova, D.; Alipieva, K.; Stefova, M.; Stefkov, G.; Evstatieva, L.; Matevski, V.; Bankova, V. Chemical Constituents of the Essential Oils of *Sideritis Scardica* Griseb. and *Sideritis raeseri* Boiss and Heldr. from Bulgaria and Macedonia. *Nat. Prod. Res.* **2007**, *21*, 819–823. [[CrossRef](#)]
50. Kloukina, C.; Tomou, E.-M.; Skaltsa, H. Essential oil composition of two Greek cultivated *Sideritis* spp. *Nat. Volatiles Essent. Oils* **2019**, *6*, 16–23.
51. Trendafilova, A.B.; Todorova, M.N.; Evstatieva, L.N.; Antonova, D.V. Variability in the Essential-Oil Composition of *Sideritis scardica* Griseb. from Native Bulgarian Populations. *Chem. Biodivers.* **2013**, *10*, 484–492. [[CrossRef](#)]
52. Baser, K.H.C.; Kirimer, N.; Tümen, G. Essential Oil of *Sideritis Scardica* Griseb. Subsp. *Scardica*. *J. Essent. Oil Res.* **1997**, *9*, 205–207. [[CrossRef](#)]

53. Komaitis, M.E.; Melissari-Panagiotou, E.; Infanti-Papatragianni, N. Constituents of the Essential Oil of *Sideritis scardica*. In *Developments in Food Science*; Elsevier: Amsterdam, The Netherlands, 1992; Volume 28, pp. 411–415. ISBN 978-0-444-88558-6.
54. Todorova, M.; Trendafilova, A.; Evstatieva, L.; Antonova, D. Volatile Components in *Sideritis scardica* Griseb. Cultivar. *Proc. Bulg. Acad. Sci.* **2013**, *66*, 507–512. [[CrossRef](#)]
55. Todorova, M.N.; Christov, R.C.; Evstatieva, L.N. Essential Oil Composition of Three *Sideritis* Species from Bulgaria. *J. Essent. Oil Res.* **2000**, *12*, 418–420. [[CrossRef](#)]
56. National Institute of Standards and Technology (NIST) WebBook. Available online: <http://webbook.nist.gov/chemistry/> (accessed on 20 April 2021).
57. Singleton, V.L.; Rossi, J.A. Colorimetry of Total Phenolics with Phosphomolybdic-Phosphotungstic Acid Reagents. *Am. J. Enol. Vitic.* **1965**, *16*, 144–158.
58. Zeliou, K.; Papasotiropoulos, V.; Manoussopoulos, Y.; Lamari, F.N. Physical and Chemical Quality Characteristics and Antioxidant Properties of Strawberry Cultivars (*Fragaria* × *Ananassa* Duch.) in Greece: Assessment of Their Sensory Impact: Quality Factors Determining Sensory Characteristics of Strawberry Cultivars in Greece. *J. Sci. Food Agric.* **2018**, *98*, 4065–4073. [[CrossRef](#)]
59. Chang, C.-C.; Yang, M.-H.; Wen, H.-M.; Chern, J.-C. Estimation of Total Flavonoid Content in Propolis by Two Complementary Colorimetric Methods. *J. Food Drug Anal.* **2002**, *10*, 178–182.
60. Benzie, I.F.F.; Strain, J.J. The Ferric Reducing Ability of Plasma (FRAP) as a Measure of “Antioxidant Power”: The FRAP Assay. *Anal. Biochem.* **1996**, *239*, 70–76. [[CrossRef](#)]
61. Blois, M.S. Antioxidant Determinations by the Use of a Stable Free Radical. *Nature* **1958**, *181*, 1199–1200. [[CrossRef](#)]
62. Brand-Williams, W.; Cuvelier, M.E.; Berset, C. Use of a Free Radical Method to Evaluate Antioxidant Activity. *LWT—Food Sci. Technol.* **1995**, *28*, 25–30. [[CrossRef](#)]
63. Kougioumoutzis, K.; Kokkoris, I.P.; Panitsa, M.; Strid, A.; Dimopoulos, P. Extinction Risk Assessment of the Greek Endemic Flora. *Biology* **2021**, *10*, 195. [[CrossRef](#)]



Review

# Ferulic Acid: A Natural Phenol That Inhibits Neoplastic Events through Modulation of Oncogenic Signaling

Hardeep Singh Tuli <sup>1</sup>, Ajay Kumar <sup>2</sup>, Seema Ramniwas <sup>3</sup>, Renuka Coudhary <sup>1</sup>, Diwakar Aggarwal <sup>1</sup>, Manoj Kumar <sup>4</sup>, Ujjawal Sharma <sup>5</sup>, Nidarshana Chaturvedi Parashar <sup>1</sup>, Shafiu Haque <sup>6</sup> and Katrin Sak <sup>7,\*</sup>

- <sup>1</sup> Department of Biotechnology, Maharishi Markandeshwar Engineering College, Maharishi Markandeshwar (Deemed to be University), Mullana-Ambala 133207, India
  - <sup>2</sup> Punjab Biotechnology Incubator (PBTI), Phase VIII, Mohali 160071, India
  - <sup>3</sup> University Centre for Research and Development, University Institute of Pharmaceutical Sciences, Chandigarh University, Gharuan, Mohali 140413, India
  - <sup>4</sup> Department of Chemistry, Maharishi Markandeshwar University, Sadopur-Ambala 134007, India
  - <sup>5</sup> Department of Human Genetics and Molecular Medicine, Central University of Punjab, Bhatinda 151001, India
  - <sup>6</sup> Research and Scientific Studies Unit, College of Nursing and Allied Health Sciences, Jazan University, Jazan 45142, Saudi Arabia
  - <sup>7</sup> NGO Praeventio, 50407 Tartu, Estonia
- \* Correspondence: katrin.sak.001@mail.ee

**Abstract:** Despite the immense therapeutic advances in the field of health sciences, cancer is still to be found among the global leading causes of morbidity and mortality. Ethnomedicinally, natural bioactive compounds isolated from various plant sources have been used for the treatment of several cancer types and have gained notable attention. Ferulic acid, a natural compound derived from various seeds, nuts, leaves, and fruits, exhibits a variety of pharmacological effects in cancer, including its proapoptotic, cell-cycle-arresting, anti-metastatic, and anti-inflammatory activities. This review study presents a thorough overview of the molecular targets and cellular signaling pathways modulated by ferulic acid in diverse malignancies, showing high potential for this phenolic acid to be developed as a candidate agent for novel anticancer therapeutics. In addition, current investigations to develop promising synergistic formulations are also discussed.

**Keywords:** ferulic acid; apoptosis and cell cycle arrest; anti-angiogenesis; anti-metastasis; synergism

**Citation:** Singh Tuli, H.; Kumar, A.; Ramniwas, S.; Coudhary, R.; Aggarwal, D.; Kumar, M.; Sharma, U.; Chaturvedi Parashar, N.; Haque, S.; Sak, K. Ferulic Acid: A Natural Phenol That Inhibits Neoplastic Events through Modulation of Oncogenic Signaling. *Molecules* **2022**, *27*, 7653. <https://doi.org/10.3390/molecules27217653>

Academic Editor: Nour Eddine Es-Safi

Received: 15 October 2022  
Accepted: 3 November 2022  
Published: 7 November 2022

**Publisher's Note:** MDPI stays neutral with regard to jurisdictional claims in published maps and institutional affiliations.



**Copyright:** © 2022 by the authors. Licensee MDPI, Basel, Switzerland. This article is an open access article distributed under the terms and conditions of the Creative Commons Attribution (CC BY) license (<https://creativecommons.org/licenses/by/4.0/>).

## 1. Introduction

Over the past few decades, it has become more and more popular to study the role of natural plant-derived compounds in a wide range of models for chronic diseases, especially against different types of human cancers [1]. One reason for this is the continuously raising incidence of these aging-related disorders all over the world [2]. On the other hand, as there are no curative treatment options frequently available, findings regarding new safe and efficient therapeutics are increasingly genuine. It is indeed well known that plants are able to synthesize a large spectrum of structurally unrelated molecules, many of which have been demonstrated to reveal diverse bioactivities in human experimental systems [3]. As a result, some specific compounds, such as alkaloids vincristine and vinblastine and terpenoid paclitaxel, have been developed in chemotherapeutics, commonly used in the clinical settings today, whereas several others are currently under clinical trials as adjunctive therapies against different cancer types [3].

The most widespread class of compounds among the huge diversity of phytochemicals constitutes phenolic agents, further divided into polyphenols with flavonoids and tannins, and simple phenols, including phenolic acids [4]. Ferulic acid is a hydroxycinnamic acid ubiquitously occurring in the plant kingdom and is derived from various vegetable sources, such as leaves, fruits, seeds, and nuts [5]. A number of studies have described the diverse

bioactivities of this phenolic acid, and especially its anticancer potential. This natural compound can exert anti-inflammatory, antiproliferative, proapoptotic, antiangiogenic, and/or antimetastatic effects in various experimental models of malignancies, including lung cancer [6], colorectal cancer [7], liver cancer [8], breast cancer [9], cervical cancer [10], osteosarcoma [11] and glioblastoma [12]. In doing so, ferulic acid is able to attack multiple molecular targets and alter several cellular signaling pathways, which ultimately results in the inhibition of malignant development and tumor growth [13].

In this review article, the current knowledge regarding the anticancer potential of ferulic acid is compiled and systematically presented, and it is then analyzed in addition to the role of this phytochemical on the resistance mechanisms of conventional chemotherapeutic drugs. Moreover, the co-effects of ferulic acid, along with other therapeutic modalities, are discussed, presenting synergistic combinations that are most valuable for further studies. Considering the generally low bioavailability characteristic for natural phenolics, nanotechnological possibilities to improve the targeted delivery of ferulic acid to the tumoral sites are discussed. In this way, relying on the complex picture, further steps can be readily planned for applications of the anticancer properties of ferulic acid in the fight against cancer.

## 2. Sources, Chemistry, and Structural Activity Relationship of Ferulic Acid

Chemically, ferulic acid is 4-hydroxy-3-methoxycinnamic acid or (*E*)-3-(4-hydroxy-3-methoxyphenyl) acrylic acid, occurring in two isomeric forms, i.e., *cis* and *trans*. It is found naturally in various plants such as citrus fruits, wheat, spinach, sugar beets, cereals, sugarcane bagasse, neem, and pineapples [14]. It has also been reported in Chinese medicine herbs, including *Angelica sinensis*, *Cimicifuga heracleifolia*, and *Lignsticum chuangxiang*. Ferulic acid can be synthesized in a laboratory through the condensation of vanillin with malonic acid in the presence of piperidine. However, this reaction takes three weeks to complete, but the yield is found to be high with a mixture of *trans*- and *cis*-isomers. Nevertheless, Da and Xu successfully reduced this reaction time to 2 h by utilizing benzylamine as a catalyst and methylbenzene as the solvent at 85–95 °C [15].

It has been reported that the biological activity of ferulic acid can be altered by creating its derivatives. A series of such derivatives of ferulic acid with  $\beta$ -amino alcohol has been previously reported (Figure 1) [16]. The chemical structure of ferulic acid has the presence of benzene rings with a carboxylic group. Hydroxyl groups present at C1 and C9 are considered to be the main sources of antioxidant character. The double bond presented between C2-C3 is known to be responsible for effective bio-activity [17]. Furthermore, the carboxylic group of ferulic acid provides an easily made ester, which is in turn responsible for cholesterol-lowering activity [15].

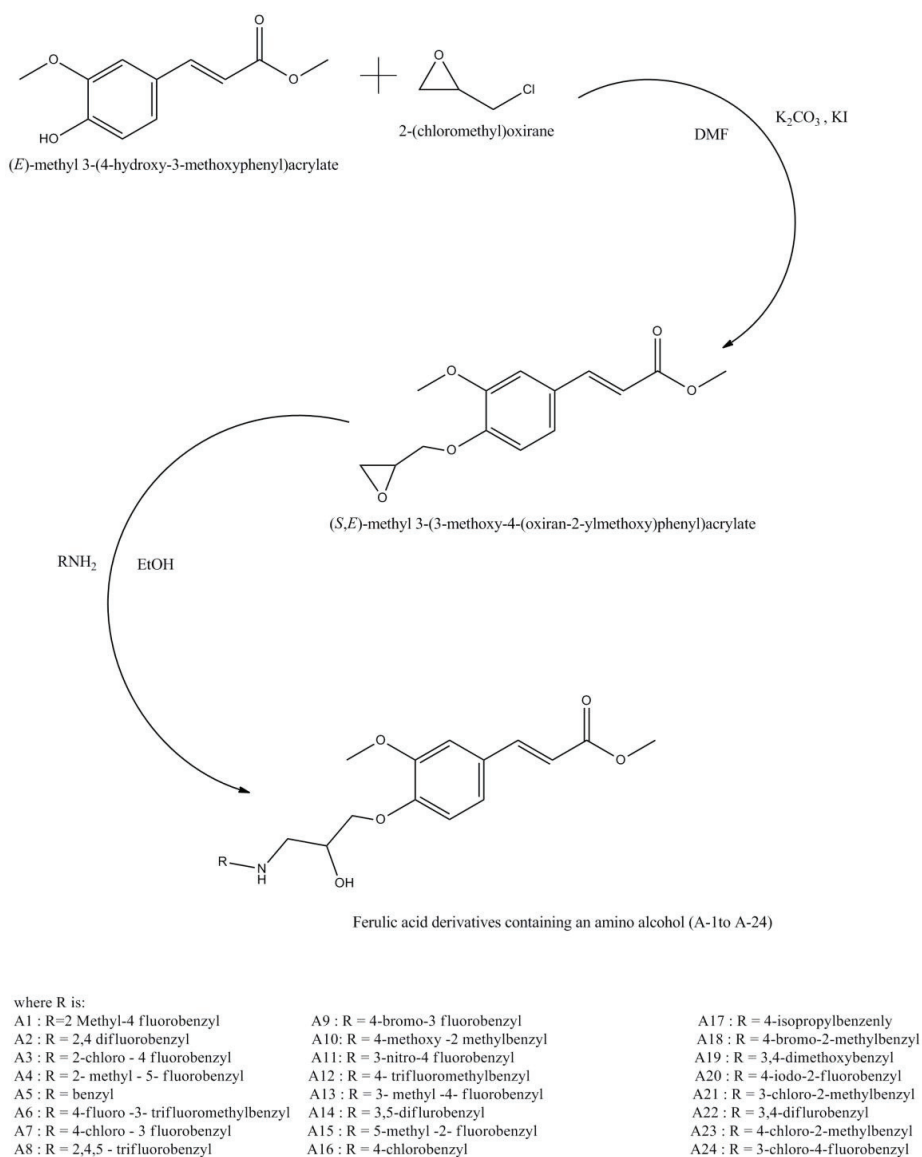


**Figure 1.** Chemical structure of ferulic acid and synthetic routes of its derivatives.

### 3. In Vivo Pharmacokinetics of Ferulic Acid

In rodents and humans, the absorption and metabolism of ferulic acid has been widely studied and reported. Polyphenolic compounds are mostly consumed as simple phenolic acids. It has been reported that, in the stomach, the rate of absorption of ferulic acid is relatively faster than other phenolic compounds, and that it can be absorbed along the entire gastrointestinal tract [18]. The metabolism of ferulic acid mainly occurs in the liver, and forms conjugated products with glucuronides, sulfate, and sulfoglucuronide [19]. In humans, ferulic acid is excreted in urine as 3-hydroxyphenyl and 3-methoxy-4-hydroxyphenyl derivatives of phenyl propionic acid, hydracrylic acid, and glycine conjugates after metabolism. In rats, ferulic acid itself is partly excreted as glucuronide, as revealed in

feeding studies. However, 3-hydroxy phenylpropionic acid is excreted by rats as a major urinary metabolite after the intraperitoneal administration of ferulic acid [20]. After a single administration, the distribution of ferulic acid in the body is substantial. For example, distribution of ferulic acid is ~4% in the gastric mucosa after oral administration; it is 10% in the blood pool, kidney, and liver, and distribution in other tissues is 53% [18]. Due to the low toxicity of ferulic acid, it has been reported to be a relatively safer molecule. The LD<sub>50</sub> value is lower for female rats (2113 mg kg<sup>-1</sup> body weight) in comparison to male rats (2445 mg kg<sup>-1</sup> body weight) [21].

#### 4. Cellular Mechanism of Ferulic Acid in Cancer

##### 4.1. Induction of Apoptosis and Cell Cycle Arrest

Programed cell death, apoptosis, is one of the most preferred target pathways for inhibition of proliferation and growth of the tumor by anticancer therapies. Chemo-preventive phytochemicals are known to mediate apoptosis either via intrinsic (mitochondrial) or extrinsic mechanisms (death receptor). It has been discovered that these compounds upregulate apoptotic protein and downregulate anti-apoptotic protein (Figure 2). For instance, by upregulating the tumor suppressor and apoptotic genes Bcl-2-associated X protein (BAX), BCL-2 interacting killer (BIK), tumor suppressor p53 (p53), and cytochrome complex (CYCS) and downregulating the expression of the antiapoptotic protein B-cell lymphoma 2 (Bcl-2), ferulic acid causes apoptosis in prostate cancer cells [22]. Furthermore, Luo et al. observed that reduced levels of Myeloid cell leukemia 1 (Mcl-1) and Bcl-2, and increased Bax levels after ferulic acid treatment resulted in apoptosis in human cervical cancer cell lines (HeLa and Caski) [23]. Caspase (CASP)-8, Fas-ligand (FASL), and Poly (ADP-ribose) polymerase (PARP) are three extrinsic mechanisms of apoptotic cell death that are associated with the expression of molecular proteins. According to Kampa et al., FAS/FASLG caused the human breast cancer cell line (T47D) to undergo apoptosis [24]. Ferulic acid treatment leads to the induction of apoptosis via elevated expressions of the apoptotic proteins CASP1, CASP2, CASP8, FASLG, FAS, and TNFR-associated death domain (TRADD) in the prostate cancer cell line (LNCaP) [25]. Through regulation of p53, Bax, caspase-3, and growth arrest and DNA-damage (GADD45), treatment with ferulic acid has been shown to begin apoptosis in non-small cell lung cancer cells (NCI-H460) [26]. According to Grasso et al., free ferulic acid significantly reduced the levels of Bcl-2 and Master Regulator of Cell Cycle proteins (c-Myc) expression along with caspase-3 and PARP-1 cleavage, which activated the apoptotic pathway [27]. DNA fragmentation, which is the hallmark of apoptosis, was determined in Caski cells after ferulic acid treatment [28]. Ferulic acid reduced the phosphorylation of protein kinase B (Akt) and Phosphoinositide 3-kinase (PI3K) in Caski cells. In osteosarcoma cells, ferulic acid augmented the Bax expression, decreased the Bcl-2 expression, and then increased the activity of caspase-3, and induced death by blocking the PI3K/Akt pathway [28].

Cyclins (CCN), cyclin-dependent kinase (CDKI) inhibitors, and cyclin-dependent kinases (CDK) are known to arrest cell cycle progression. By upregulating CDKN1A (P21) protein expression and downregulating CCND1 and phosphorylated retinoblastoma protein (RB) levels in the endothelial cells (ECV304), ferulic acid produced cell cycle arrest in the G<sub>0</sub>/G<sub>1</sub> phase [29]. Ferulic acid treatment inhibited PI3K/Akt pathway and induced G<sub>0</sub>/G<sub>1</sub> phase arrest via downregulation of expression of cell cycle-related proteins CDK2, CDK4, and CDK6 in osteosarcoma cells [30]. In HeLa and Caski cells, Gao et al. demonstrated that ferulic acid caused cell death and G<sub>0</sub>/G<sub>1</sub> phase arrest by increasing the cell cycle-related proteins, such as p53 and p21 expression, and by lowering CCND1 and CCNE levels [31]. According to Janick et al., ferulic acid led to an arrest of the cell cycle in the S phase and had an antiproliferative effect on colon cancer cells (Caco-2) [32]. Due to the decreased expression of genes that were crucial for cell cycle arrest in the G<sub>1</sub>/S phase in prostate cancer cells, ferulic acid may prevent cell cycle progression. The Transcription Factor 4 (E2F4) gene expression that was much higher in the ferulic acid-treated cells

caused arrest of the cell cycle at the G<sub>0</sub>/G<sub>1</sub> stages in prostate cancer cells (PC-3) due to downregulation of transcription by creating a complex with RB1 [25].

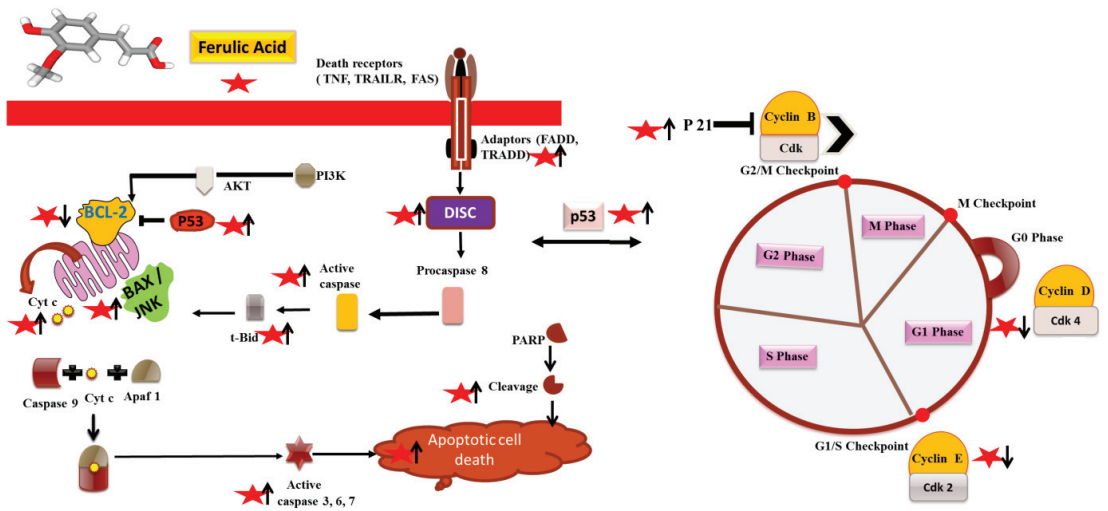


**Figure 2.** Molecular targets of ferulic acid in signaling processes leading to cell cycle arrest and apoptosis. Bcl-2-associated X protein (BAX), BCL-2 antagonist/killer (BAK), tumor suppressor p53 (p53) and cytochrome complex (CYCS), B-cell lymphoma 2 (Bcl-2), Poly (ADP-ribose) polymerase (PARP), Fas-ligand (FASL), and TNFR-associated death domain (TRADD).

In addition, ferulic acid is also known to induce autophagy in cancer cells. It is a natural breakdown of the cell to eliminate malfunctioning components through a lysosome-dependent controlled mechanism. For instance, using hepatocellular carcinoma (HepG2) cells, Wang et al. in 2022 determined that proliferative ability was decreased by ferulic acid by elevating the levels of the apoptosis and autophagy biomarkers, including beclin-1, Light chain (LC3-I/LC3-II), PTEN-induced putative kinase 1 (PINK-1), and Parkin [33]. Similar to this, utilizing the ferulic acid derivative tributyltin(IV) ferulate (TBT-F) on colon cancer cells (HCT116, HT-29 and Caco-2) led to an increase in autophagy-related proteins, such as LC3-II, and receptors of autophagy (p62) [34]. Therefore, genes or proteins involved in apoptosis and cell cycle regulation are significant in the development of anticancer drugs, and research on these genes for cancer therapies has been constantly growing.

#### 4.2. Antiangiogenic Action of Ferulic Acid

There are two main hallmarks of cancer progression: uninhibited angiogenesis and development of vascular architecture [35]. Angiogenesis is the process of creating new blood vessels from previous ones and is essential for transporting oxygen, nutrients, and growth hormones to distant organs for the development of cells, playing an important role in cancer progression [36]. Through the release of chemical signals that promote angiogenesis, tumors maintain blood supply by regulating both positive (angiogenic) and negative (anti-angiogenic) endogenous factors, such as adult endothelial cells (ECs). Angiogenesis is crucial for the development of numerous illnesses, as well as for regular physiological processes like the formation of an embryo, the healing of wounds, and the menstrual cycle. It is generally recognized that angiogenesis is dysregulated in a number of diseases, including psoriasis, diabetic retinopathy, malignant tumors, rheumatoid arthritis, and age-related macular degeneration (AMD). An imbalance between numerous pro-angiogenic and anti-angiogenic factors is important for angiogenesis [37]. Angiogenesis process is initiated by pro-angiogenic signals, inflammation, ischemia, hypoxia, and other variables that act on cytokines, as well as angiogenic factors like vascular endothelial growth factor (VEGF) or



fibroblast growth factor (FGF) in tumor cells, urokinase-type plasminogen activator (uPA), and adrenomedullin (ADM) [38]. As a result, stopping angiogenesis is an effective therapeutic strategy for the management of a number of illnesses, including cancer. Despite being widely available, anti-angiogenic medications like bevacizumab, pegaptanib, ranibizumab, sunitinib, sorafenib, regorafenib, and axitinib also have serious side effects, such as cardiovascular toxicity, bleeding risk, intraocular inflammation, ocular hemorrhage, and retinal detachment [39]. In order to complement and integrate with current therapies, innovative and efficient treatments that precisely target angiogenesis and have fewer side effects need to be researched, developed, and tested [40]. Among the broad spectrum of botanicals, ferulic acid is one of the potent constituents found in many vegetables and has numerous pharmacological activities, such as anti-cancer, anti-inflammation, neuroprotective, anti-coagulation, and anti-angiogenesis [41]. In a normal cellular microenvironment using human umbilical vein endothelial cells (HUVECs), Lin et al. [42] determined that ferulic acid significantly augmented angiogenesis by increasing VEGF, platelet-derived growth factor (PDGF), and hypoxic-induced factor (HIF) 1 $\alpha$  expression via mitogen-activated protein kinase and PI3K pathways. Whereas, Yang et al., 2015 [43], reported that ferulic acid reduced the growth of melanoma cells (A375, CHL-1 and SK-MEL-2) via suppressing FGF1, leading to the activation of FGFR1 and PI3K-Akt signaling. In addition, ferulic acid showed anticancer potential by suppressing angiogenesis and causing inhibition of melanoma growth in a xenograft model [44]. Researchers have reported that ferulic acid significantly revealed antiangiogenic properties in a chorioallantoic membrane (CAM) model of chicken eggs through downregulation of VEGF-2 and cyclooxygenase (COX-2) expression. Therefore, anti-angiogenic mechanisms can be considered promising for the future design of novel therapeutics.

#### 4.3. Inhibition of Metastasis and Invasion

Another main hallmark of malignant tumors is believed to be invasion and metastasis that lead to clinical death [45]. Tumor invasion and metastasis mechanisms involve the detachment of cancer cells from the main tumor, migration, angiogenesis, and proliferation to distant tissues [46]. Beyond the boundaries of the healthy tissue from which they originate, cancer cells can enter the bloodstream, travel to distant organs, and ultimately cause the development of secondary tumors, known as metastases. Matrix metalloproteinases (MMPs) play a significant role in the growth of malignancies by disrupting natural invasion barriers [47]. The zinc-dependent endopeptidases MMP-2 and MMP-9 are associated with tumor invasion and metastasis due to their capacity to remodel tissue by degrading the basement membrane and extracellular matrix, thereby triggering angiogenesis (Figure 3) [48]. Therefore, the largest problem in cancer chemotherapy has been preventing the phenomenon of invasion and metastasis. Many natural constituents such as polyphenols, terpenoids, flavonoids, alkaloids, steroids, and saponins have the potential to be anti-invasive and anti-metastatic. Zhang et, 2016 [49], reported that ferulic acid showed antimetastatic potential against breast cancer cells (MDA-MB-231) by upregulating caspase-3 and downregulating epithelial-mesenchymal transition (EMT). Ferulic acid oral dose significantly reduced the tumor volume in MDA-MB-231 xenografts in female BALB/c nude mice, and showed no toxicity at a dose of 100 mg/kg body weight of animals. El-Gogary et al., 2022 [50], investigated that nanoencapsulated ferulic acid exhibited anticancer potential in colorectal cancer cell lines (HCT-116 and Caco2), and ferulic acid lipid encapsulated nanoparticles showed significant antioxidant, apoptotic, anti-angiogenic, and anti-inflammatory properties in vivo through downregulation of cyclin D1, Insulin-like growth factor (IGF II), and VEGF and modulation of BAX/Bcl-2. Therefore, inhibition of cancer migration from one site to another can significantly increase patients' survival rates, and researchers are currently exploring anti-metastatic drugs from plant origins.

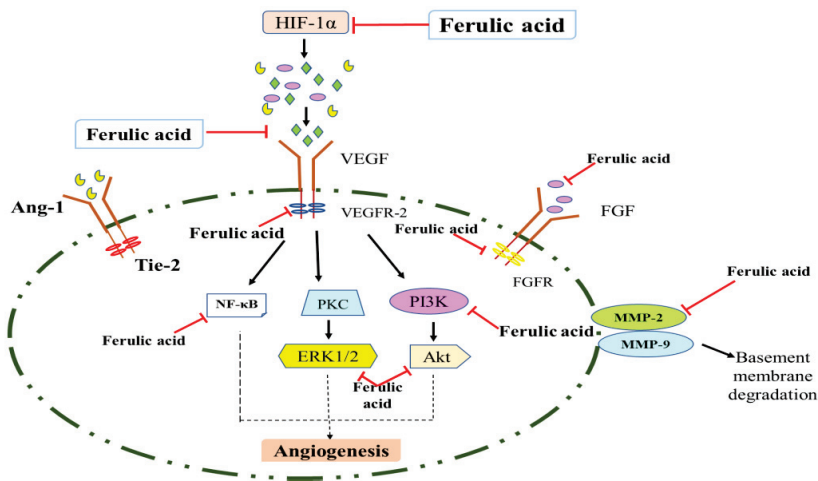


**Figure 3.** Major signaling pathways targeted by ferulic acid in angiogenesis and metastasis processes. Vascular endothelial growth factor (VEGF), Angiopoietin-1 (Ang1), Tyrosine-protein kinase (Tie-2), Hypoxic-inducible factor (HIF) 1 $\alpha$ , Protein kinase B (Akt), Phosphoinositide 3-kinase (PI3K), protein kinase (PKC), Nuclear factor kappa light chain enhancer of activated B cells (NF- $\kappa$ B), Extracellular signal-regulated kinase (ERK), Matrix metalloproteinases (MMPs).

#### 4.4. Anti-Inflammatory Mechanisms

For the emergence and spread of chronic illnesses, inflammatory and immune responses act as key regulators. Activated inflammatory cells mediate chronic and acute inflammation through a multi-step process [41]. In several *in vitro* and *in vivo* models, it has been reported that ferulic acid possesses anti-inflammatory action. *In vitro* inflammation is widely studied in LPS-treated murine macrophages (Raw 264.7) [19]. The overproduction of inflammatory mediators (reactive oxygen species (ROS), nitric oxide (NO), pro-inflammatory cytokines, and prostaglandin E2 (PGE2)) generated by activated inducible nitric oxide synthase (iNOS) and COX is centrally managed by the macrophages generated by the immune system [51]. Ferulic acid acts as an antioxidant and decreases macrophage inflammatory protein-2 (MIP-2) production [52]. Ferulic acid and its derivatives also inhibit the expression of inflammatory mediators, such as iNOS, NO production, prostaglandin E2, and tumor necrosis factor- $\alpha$  (TNF $\alpha$ ) in cells stimulated by the bacterial endotoxin lipopolysaccharide [53–55]. A recent study showed that ferulic acid isolated from corn also inhibited the iNOS expression and NO production in lipopolysaccharide (LPS)-stimulated Raw 264.7 cells [56]. In addition to this, it has been reported that ferulic acid derivative feruloyl-myoinositol leads to the suppression of cyclooxygenase-2 promoter activity in human colon cancer (DLD-1) cells via  $\beta$ -galactosidase reporter gene assay system [57]. In a concentration-dependent manner, ferulic acid leads to the inhibition of chemokine superfamily member (murine MIP-2) as studied in LPS-stimulated macrophages (RAW 264.7) cells. The anti-inflammatory response of ferulic acid (20 mg/kg) was studied *in vivo* also in rats, showing reduction of the expression of cyclooxygenase-2 and nuclear factor kappa light chain enhancer of activated B cells (NF- $\kappa$ B) in lung and liver, which was increased by nicotine treatment [58]. These findings suggest that ferulic acid has anti-inflammatory mechanisms against inflammatory diseases (Figure 4).

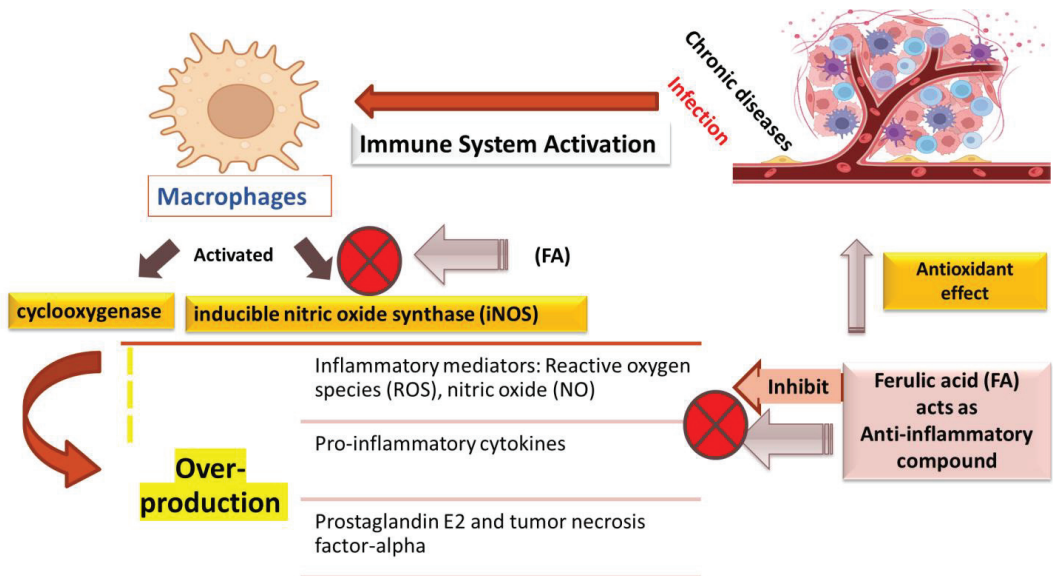


Figure 4. Anti-inflammatory targets of ferulic acid.

### 5. Synergistic Interactions of Ferulic Acid in Cancer

The use of diverse synergistic chemo-preventive techniques with improved sensitivity in combination with known chemotherapeutic medications has received a lot of attention. Evidence has suggested that synergisms provide maximum therapeutic efficacy, minimal side effects, and overcome drug resistance [59]. When given in combination with  $\delta$ -tocotrienol, ferulic acid was reported to synergistically inhibit telomerase activity in human colorectal adenocarcinoma cells (DLD-1) by synergistically down-regulating the expression of human telomerase reverse transcriptase (hTERT), the catalytic subunit of the enzyme, suggesting that ferulic acid might augment the anti-cancer activity of  $\delta$ -T3 [60]. Additionally, the combination of  $\delta$ -tocotrienol and ferulic acid has also been investigated, showing synergistic inhibitory effects and preventing the spread of different forms of cancer cells, including prostate cancer (DU-145), breast cancer (MCF-7), and pancreatic cancer (PANC-1) cells. Synergistic therapy has been found to be more effective and remarkably reduced cell proliferation, as compared to  $\delta$ -tocotrienol and ferulic acid alone [61]. Moreover, the compound has also been demonstrated to exert anti-proliferative/pro-apoptotic effects and to decrease the metastatic or angiogenic properties of different cancer cells when given in combination with unsaturated tocotrienols (TTs) [62]. Furthermore, recent studies have shown the concerted pro-apoptotic effects of ferulic acid and nanostructured lipid carrier in glioblastoma cells, thus increasing its bioavailability in the glioblastoma cells by escalating the effects on protein expression levels and on the activation of the apoptotic pathway more conspicuously when the cells were exposed to ferulic acid loaded in nanostructured lipid carriers (NLCs), as compared to free ferulic acid [63]. In addition, the combinatorial therapy of ferulic acid and cisplatin has also been reported to synergistically inhibit cellular proliferation in human leukemia cancer cell lines, and the synergized growth inhibitory effect with cisplatin was shown to be probably associated with the G2/M arrest in the cell cycle progression, thus indicating ferulic acid to be a better modulating agent on human malignant cell lines [64]. Furthermore, the combined effect of ferulic acid and gemcitabine on apoptosis and metastasis was also investigated, and the expression of various genes involved in apoptosis and metastasis was found to be increased with a higher fold change compared to the single treatment of gemcitabine in human prostate cancer cell (PC-3) lines [65]. Additionally, ferulic acid in combination with PARP inhibitors has been

reported to sensitize breast cancer cells, thus serving as an effective combination chemotherapeutic agent as a natural bioactive compound [66]. Furthermore, the potential role of a combination formula of ferulic acid and aspirin was also explored for pancreatic cancer chemoprevention, utilizing a new chitosan-coated solid lipid nanoparticles (c-SLN) drug delivery system encapsulating the natural compound and the drug; the results were found to be promising [67]. Moreover, a study including two different polyphenols, curcumin, and ferulic acid as adjuvant chemotherapeutics was carried out, evaluating chemoresistance and cisplatin-induced ototoxicity against chemotherapeutic regimens, such as cisplatin, for different types of cancers. The use of adjuvants was found to be an effective tool for cancer therapy targeting ROS-modulated pathways [68]. Furthermore, a combination of caffeic and ferulic acid lipophilic derivatives also showed increased cytotoxicity toward human breast cancer cell lines, and thus could be applicable for chemopreventive and/or chemotherapeutic purposes [69]. From the above discussion, it can be determined that this bioactive natural substance has the potential to have synergistic effects on growth inhibition, apoptosis induction, and anticarcinogenic properties, and it may prove to be a promising alternative approach for boosting therapeutic potency and lowering systemic toxicity of chemotherapeutic drugs [70].

## 6. Safety Studies

As a natural plant-derived compound, ferulic acid is considered to be generally safe. Although several investigations have confirmed this assumption, systematic studies on its safety are still required before the development of ferulic acid as a therapeutic tool [71]. Actually, *trans*-ferulic acid-4- $\beta$ -glucoside revealed no apparent toxicity in mice models, inducing no significant alterations in the body weight and blood biochemical parameters of animals [72]. Additionally, topical applications of ferulic acid did not cause any skin irritation in nude mice, representing an efficient and safe route for using ferulic acid against photodamage [73]. However, a long-term treatment with ferulic acid was still demonstrated to cause some nephrodamaging effects in the model of doxorubicin-induced chronic kidney disease in rats [74], suggesting that further studies on the safety of this phenolic acid are needed to determine the values of no-observed-adverse-effect-level (NOAEL) in health risk assessments. Tables 1 and 2 represent an overview of ferulic acid anticancer effects.

Table 1. Anticancer effects of ferulic acid based on in vitro studies.

Type of Cancer	Cell Lines	Effects	Mechanisms	Concentration	References
Melanoma	Murine B16	-	↓ melanin production, ↓ tyrosinase activity, ↓ casein kinase 2 (CK2), ↑ p-tyrosinase	25 and 50 µM	[75]
	A375, CHL-1, SK-MEL-2, B16F10	Anti-angiogenic	↓ proliferation, migration and tube formation, ↓ fibroblast growth factor 1 (FGF1), ↓ FGFR1, ↓ PI3K, ↓ protein kinase B (Akt) signaling, ↓ PI3K-Akt pathway, ↑ (HUVVEC) Growth, ↓ VEGF-A, FGF1, FGF2, PDGF-α, PDGF-β and phosphatidylinositol-glycan biosynthesis class f protein (PIGF)	0, 2.5, 5, 10, 20, 30, 40 µM	[43]
Sarcoma	S180	Ameliorating oxidative stress injury	↓ diosbulbin B-induced liver injury, ↓ ALT and AST activities, Ferulic acid reverses diosbulbin B-decreased CuZn-SOD and CAT enzymatic activities and mRNA expression	-	[76]
Osteosarcoma	143B and MG63	Induces apoptosis	↓ proliferation, ↑ G0/G1 phase arrest, ↓ CDK 2, CDK 4, CDK 6, ↑ Bax, ↓ Bcl-2, ↑ caspase-3 activity, ↓ PI3K/Akt activation	0,10,30,100 and 150 µM	[77]
Thyroid	TT cells	Induces apoptosis	↓ invasion, migration and colony formation, ↓ URG4/URGCP (upregulated gene-4/upregulator of cell proliferation), ↓ CCND1, CDK4, CDK6, BCL2, MMP2, and MMP9, ↑ p53, PARP, PUMA, NOXA, BAX, BID, CASP3, CASP9 and TIMP1	50, 75, 100, 150, 200, 300, 400, 500, 750 µM and 1 mM	[78]
Breast	MDA-MB 231	Induces apoptosis	↓ proliferation, ↑ apoptotic cells, ↓ percentages of cells in G0/G1 phases by TQ, ↓ in %ages of cells in the S phase by FA	Thymoquinone (TQ) and Ferulic Acid (FA) 25 µM TQ + 250 µM FA, 50 µM TQ + 350 µM FA, 50 µM TQ + 450 µM FA, 100 µM TQ + 350 µM FA, 100 µM TQ + 450 µM FA)	[79]
	MCF7 and 4T1	Induces apoptosis	↓ viability, structural changes in cancer cells as compared to normal cells, ↑ apoptosis, ↑ lipid peroxidation, ↑ mitochondrial damage, ↑ cell death	FA-Nanosponges 5, 10, 20, 40, 80, 125, 250, 500, 750, and 1000 µM	[80]
	MDA-MB-231	-	↓ S phase, ↑ antiproliferative effects, ↑ sensitivity to UV treatment	0–10 µM	[81]
MCF-7, MDAMB-231 and HS578T	MDA-MB-231	Induces apoptosis and inhibits metastasis	↓ viability, ↑ apoptosis, ↓ metastatic potential, reversal of epithelial-mesenchymal transition (EMT), ↑ caspase-3, ↓ migration across the wound edges, ↓ vimentin, ↑ E-cadherin	3, 10, 30 and 100 µM	[49]
	MCF-7, MDAMB-231 and HS578T	Induces apoptosis	↓ proliferation, ↑ cytotoxicity, ↑ p53, ↑ Bax, ↑ caspase-9	0–75 µM	[82]

Table 1. Contd.

Type of Cancer	Cell Lines	Effects	Mechanisms	Concentration	References
Lung	A549	Induces apoptosis	↓ proliferation, ↓ oxidative stress, ↓ GSH, ↑ Keap1, ↓ Nrf2 nuclear level, ↑ apoptotic population, ↓ p-p38 MAPK level, ↓ activation of Akt/MAPK, ↓ p-STAT3, ↓ Cox-2, ↓ MMP-9 and VEGF, ↓ PECAM1, ↑ arrest at G2/M phase, ↑ p53 and p21 protein, ↓ Cdc25C, ↑ active caspase 9,3, ↑ Bax, ↓ Bcl-2, ↑ radiation sensitivity	ferulic acid –10–400 μM, Gamma radiation 5, 7.5, 10 and 15 Gy (60 Co)	[83]
	A549	Inhibits metastasis	↓ Proliferation, ↑ G0/G1 phase (cell cycle arrest), ↓ migration and invasion, ↓ Bcl-2, ↑ Bax, ↑ Bax/Bcl-2 ratio, ↓ MMP-2 and MMP-9, ↓ p-ERK and p-p38, it increased JNK expression, ↓ p-AKT, p-mTOR, p-MEK, and p-ERK	Ferulic acid derivative FXS-3 0.2–50 μM	[84]
Hepatocellular	HepG2	Induces apoptosis	↓ proliferation, ↓ oxidative stress, ↓ GSH, ↑ Keap1, ↓ Nrf2 nuclear level, ↑ apoptotic population, ↓ p-p38 MAPK level, ↓ activation of Akt/MAPK, ↓ p-STAT3, ↓ Cox-2, ↓ MMP-9 and VEGF, ↓ PECAM1, ↑ arrest at G2/M phase, ↑ p53 and p21 protein, ↓ Cdc25C, ↑ active caspase 9,3, ↑ Bax, ↓ Bcl-2, ↑ radiation sensitivity	ferulic acid -10–400 μM, Gamma radiation 5, 7.5, 10 and 15 Gy (60 Co)	[83]
	Huh-7 and HepG2	Induces apoptosis	↓ viability, ↑ structural changes, ↑ ROS, ↓ MMP, ↑ DNA damage, ↓ percent of cells in G0/G and G2/M, ↑ S phase, ↑ γH2AX, ↑ Bax, Bad, cleaved caspase 3	ZnONPs with ferulic acid (ZnONPs-FAC) 0.05, 0.1, 1, 5, 10 and 20 μg/ml	[85]
Pancreatic	MIA PaCa-2	Induces apoptosis	↓ cell viability and colony formation, ↑ p53, Bax, PTEN caspase 3 and 9	150 μM, 200 μM, 300 μM, 400 μM, 500 μM, 750 μM and 1 mM	[86]
	HeLa and Caski	Induces apoptosis	↓ viability, ↑ DNA condensation, ↑ apoptosis, ↑ pro-caspase-3, pro-caspase-8, pro-caspase-9 and PARP, ↓ Bcl-2 and Mcl-1, ↑ Bax and ROS, ↓ p-Akt and p-P13K	4–20 μM	[28]
Cervical	HeLa and Caski	Induction of cell cycle arrest and autophagy	↓ invasion, ↓ MMP-9, ↑ arrest in G0/G1 phase, ↑ p53 and p21, ↓ Cyclin D1 and Cyclin E, ↓ LC3-II, Beclin1 and Atg12-Atg5	0, 0.5, 1.0, 1.5 and 2.0 mM	[32]
	HeLa	-	↓ Cell viability	ferulic acid nanohybrids 1, 5, 10, 20, 30, 40, and 50 μM	[87]
	HeLa and ME-180	Enhances radiation effects by increasing lipid peroxidative markers	↓ viability ↓ GSH, ↑ TBARS, CD and LHO, ↓ SOD, CAT and GPx, ↑ DNA damage, ↑ intracellular ROS levels (results by ferulic acid + irradiation in comparison with radiation or ferulic acid treatment alone)	ferulic acid (1, 5, 10, 20, 30 and 40 μg/mL) + radiation (2, 4, 6, 8, 10, 12 and 15 Gy)	[88]

Table 1. Cont.

Type of Cancer	Cell Lines	Effects	Mechanisms	Concentration	References
Prostate	PC-3	Induces apoptosis	↓ proliferation, ↑ ATR, ATM, CDKN1A, CDKN1B, E2F4, RB1, and TP53 (Gene expression), ↓ CCND1, CCND2, CCND3, CDK2, CDK4, and CDK6 (gene expression) ↓ CDK4 and BCL2 (protein expression), ↓ invasion and colony formation	20, 30, 50, 75, 100, 150, 200, 250, 300, 350, 500, 750, 900 $\mu$ M, 1, 2 mM	[25]
	LNCaP	Induces apoptosis	↓ proliferation, ↑ CASP1, CASP2, CASP8, CYCS, FAS, FASLG, and TRADD (gene expression), ↓ BCL2 and XIAP (gene expression), ↓ CDK4 and BCL2 (protein expression), ↓ invasion and colony formation	20, 30, 50, 75, 100, 150, 200, 250, 300, 350, 500, 750, 900, 1000 and 2000 $\mu$ M	[25]
Colorectal	HCT-116 and HT-29	Induces apoptosis	↑ antiproliferative effects, ↑ arrest at the G1 phase, ↓ S phase, ↑ Early apoptotic cells, ↑ Caspase 3, 8, and 9 activity	0,0.25,0.5,1.0 and 1.5 mM	[89]
	HCT116	Induces apoptosis	↓ proliferation, ↑ p15 (mRNA level)	Ferulic acid-bound resveratrol-0, 0.625, 1.25, 2.5, 5, 10 and 20 $\mu$ M	[90]

Table 2. Representation of anticancer activities of ferulic acid in vivo models.

Type of Cancer	Animal Models	Effects	Mechanisms	Dosage	Duration	References
Melanoma	Female C57BL/6 mice xenografted with B16F10 cells	Inhibited tumor angiogenesis	↓ tumor volume and weight, ↓ p-FGFR1Y1 positive cells, ↓ FGFR1, ↓ p-Akt, ↓ p-PI3K	0, 10, 30, 50 mg/kg	30 days	[91]
Sarcoma	ICR male mice transplanted with S180 cells	-	↑ diosbulbin B-induced anti-tumor activity	ferulic acid 8 mg/kg + DB 32 mg/kg	-	[92]
Colon	Male BALB/c mice xenografted with CT 26 cells	Inhibited tumor growth	↑ tumor regression, ↑ cleaved caspase 3, ↑ tumor shrinkage, ↑ damage in tumor cell parenchyma, ↑ shrinkage in tissues, ↑ nuclear fragmentation, ↑ apoptotic body formation at the neoplastic region	ferulic acid 50 mg/kg + 2 Gy dose of radiation	27 days	[86]

Table 2. Cont.

Type of Cancer	Animal Models	Effects	Mechanisms	Dosage	Duration	References
Breast	Female BALB/c nude xenografted with MDA-MB-231	Inhibited tumor metastasis	↓ toxicity, ↓ tumor volumes and weights, ↓ proliferation (Ki67 staining), ↑ apoptosis (active caspase-3 staining), ↓ tumor nodules on the surface of the lungs and liver	100 mg/kg	28 days	[84]
Lung	C57BL/6 mice transplanted with A549 cells	Inhibited tumor metastasis	↓ tumor volume, ↓ pulmonary metastatic nodules, ↓ pulmonary tumor metastasis	FXS-3 at 25–100 mg/kg	27 days	[93]
Hepatocellular	Wistar albino rat	Inhibited tumor metastasis	↓ nodular formation, ↓ GST-P + ive, ↓ Ki67 and 8-OHdG positivity, ↓ ALT, AST, ALP, γ-GT and TBARS (liver marker enzymes)	ZnONPs with ferulic acid (ZnONPs-FAC) 3.6 µg/mL, µg/ml	-	[88]
Pancreatic	SCID mice	Inhibited tumor growth ↓↑	↓ tumor volume, ↓ PCNA and MKI67, and ↑ p-RB, ↑ p21, ↑ p-ERK1/2	75 mg/kg	35 days	[94]



## 7. Conclusions and Future Perspectives

The evidence presented in this review study clearly suggests that ferulic acid can be considered a possible option for the development of novel anticancer agents due to its capacity to disrupt cancer cell signaling. Several studies have reported the anti-neoplastic role of ferulic acid in various cancer cells, including brain cancer, breast cancer, gastric cancer, prostate cancer, cervical cancer, and colorectal cancer. Together, it can be established that this bioactive natural substance may have effects on tumor growth inhibition, apoptosis induction, suppression of angiogenesis, and metastasis, and may prove to be one of the most promising alternatives to current chemotherapeutic treatment methods for increasing therapeutic potency and lowering systemic toxicity. However, ferulic acid stability and limited solubility in aqueous media continue to be key obstacles to its bioavailability, preclinical efficacy, and clinical use. In this context, ferulic acid-loaded nano-therapeutic strategies, such as ionic gelation methods, can play an important role in overcoming these problems. For instance, chitosan-based nano-formulations can improve the stability of ferulic acid by modulating the hydrophobic interactions. Furthermore, investigations on synergistic combinations between ferulic acid and conventional anticancer drugs must be continued to find a more efficient dosage regimen for the treatment of diverse types of malignancies, inducing lower adverse side effects. Overall, ferulic acid presents a promising natural agent for supplementing the current anticancer arsenal with improved life expectancy and quality of life for patients.

**Author Contributions:** H.S.T., A.K., S.R., R.C., D.A., M.K., U.S., N.C.P. and S.H.—writing of the manuscript; K.S. writing and proof reading. All authors have read and agreed to the published version of the manuscript.

**Funding:** This research received no external funding.

**Institutional Review Board Statement:** Not applicable.

**Informed Consent Statement:** Not applicable.

**Data Availability Statement:** Not applicable.

**Acknowledgments:** Authors would like to acknowledge Maharishi Markandeshwar (Deemed to Be University), Mullana for providing necessary facilities.

**Conflicts of Interest:** The authors declare no conflict of interest.

## References

1. Samtiya, M.; Aluko, R.E.; Dhewa, T.; Moreno-Rojas, J.M. Potential Health Benefits of Plant Food-Derived Bioactive Components: An Overview. *Foods* **2021**, *10*, 839. [[CrossRef](#)] [[PubMed](#)]
2. Sung, H.; Ferlay, J.; Siegel, R.L.; Laversanne, M.; Soerjomataram, I.; Jemal, A.; Bray, F. Global Cancer Statistics 2020: GLOBOCAN Estimates of Incidence and Mortality Worldwide for 36 Cancers in 185 Countries. *CA Cancer J. Clin.* **2021**, *71*, 209–249. [[CrossRef](#)] [[PubMed](#)]
3. Sak, K. Anticancer Action of Plant Products: Changing Stereotyped Attitudes. *Explor Target. Antitumor Ther.* **2022**, *3*, 423–427. [[CrossRef](#)] [[PubMed](#)]
4. Alara, O.R.; Abdurahman, N.H.; Ukaegbu, C.I. Extraction of Phenolic Compounds: A Review. *Curr. Res. Food Sci.* **2021**, *4*, 200–214. [[CrossRef](#)] [[PubMed](#)]
5. Sova, M.; Saso, L. Natural Sources, Pharmacokinetics, Biological Activities and Health Benefits of Hydroxycinnamic Acids and Their Metabolites. *Nutrients* **2020**, *12*, 2190. [[CrossRef](#)]
6. Choudhari, A.S.; Mandave, P.C.; Deshpande, M.; Ranjekar, P.; Prakash, O. Phytochemicals in Cancer Treatment: From Preclinical Studies to Clinical Practice. *Front. Pharmacol.* **2020**, *10*, 1614. [[CrossRef](#)]
7. Haque, A.; Brazeau, D.; Amin, A.R. Perspectives on Natural Compounds in Chemoprevention and Treatment of Cancer: An Update with New Promising Compounds. *Eur. J. Cancer* **2021**, *149*, 165–183. [[CrossRef](#)]
8. Ramasamy, K.; Agarwal, R. Multitargeted Therapy of Cancer by Silymarin. *Cancer Lett.* **2008**, *269*, 352–362. [[CrossRef](#)]
9. Helmy, S.A.; El-Mofty, S.; el Gayar, A.M.; El-Sherbiny, I.M.; El-Far, Y.M. Novel Doxorubicin / Folate-Targeted Trans-Ferulic Acid-Loaded PLGA Nanoparticles Combination: In-Vivo Superiority over Standard Chemotherapeutic Regimen for Breast Cancer Treatment. *Biomed. Pharmacother.* **2022**, *145*, 112376. [[CrossRef](#)]
10. Abotaleb, M.; Liskova, A.; Kubatka, P.; Büsselberg, D. Therapeutic Potential of Plant Phenolic Acids in the Treatment of Cancer. *Biomolecules* **2020**, *10*, 221. [[CrossRef](#)]

11. Ceci, C.; Lactal, P.; Tentori, L.; de Martino, M.; Miano, R.; Graziani, G. Experimental Evidence of the Antitumor, Antimetastatic and Antiangiogenic Activity of Ellagic Acid. *Nutrients* **2018**, *10*, 1756. [[CrossRef](#)] [[PubMed](#)]
12. Vengoji, R.; Macha, M.A.; Batra, S.K.; Shonka, N.A. Natural Products: A Hope for Glioblastoma Patients. *Oncotarget* **2018**, *9*, 22194–22219. [[CrossRef](#)] [[PubMed](#)]
13. Talib, W.H.; Awajan, D.; Hamed, R.A.; Azzam, A.O.; Mahmod, A.I.; AL-Yasari, I.H. Combination Anticancer Therapies Using Selected Phytochemicals. *Molecules* **2022**, *27*, 5452. [[CrossRef](#)]
14. Tilay, A.; Bule, M.; Kishenkumar, J.; Annapure, U. Preparation of Ferulic Acid from Agricultural Wastes: Its Improved Extraction and Purification. *J. Agric. Food Chem.* **2008**, *56*, 7644–7648. [[CrossRef](#)] [[PubMed](#)]
15. Ou, S.; Kwok, K.-C. Ferulic Acid: Pharmaceutical Functions, Preparation and Applications in Foods. *J. Sci. Food Agric.* **2004**, *84*, 1261–1269. [[CrossRef](#)]
16. Dai, A.; Huang, Y.; Yu, L.; Zheng, Z.; Wu, J. Design, Synthesis, and Bioactivity of Ferulic Acid Derivatives Containing an  $\beta$ -Amino Alcohol. *BMC Chem.* **2022**, *16*, 34. [[CrossRef](#)]
17. Das, A.; Baidya, R.; Chakraborty, T.; Samanta, A.K.; Roy, S. Pharmacological Basis and New Insights of Taxifolin: A Comprehensive Review. *Biomed. Pharmacother.* **2021**, *142*, 112004. [[CrossRef](#)]
18. Zhao, Z.; Moghadasian, M.H. Chemistry, Natural Sources, Dietary Intake and Pharmacokinetic Properties of Ferulic Acid: A Review. *Food Chem.* **2008**, *109*, 691–702. [[CrossRef](#)]
19. Alam, M.A. Anti-Hypertensive Effect of Cereal Antioxidant Ferulic Acid and Its Mechanism of Action. *Front. Nutr.* **2019**, *6*, 121. [[CrossRef](#)]
20. Clifford, M.N.; King, L.J.; Kerimi, A.; Pereira-Caro, M.G.; Williamson, G. Metabolism of Phenolics in Coffee and Plant-Based Foods by Canonical Pathways: An Assessment of the Role of Fatty Acid  $\beta$ -Oxidation to Generate Biologically-Active and -Inactive Intermediates. *Crit. Rev. Food Sci. Nutr.* **2022**, 1–58. [[CrossRef](#)]
21. Tada, Y.; Tayama, K.; Aoki, N. Acute Oral Toxicity of Ferulic Acid, Natural Food Additive, in Rats. *Ann. Rep. Tokyo Metr. Lab. PH* **1999**, *50*, 311–313.
22. Ramadan, M.A.; Shawkey, A.E.; Rabeh, M.A.; Abdellatif, A.O. Expression of P53, BAX, and BCL-2 in Human Malignant Melanoma and Squamous Cell Carcinoma Cells after Tea Tree Oil Treatment in Vitro. *Cytotechnology* **2019**, *71*, 461–473. [[CrossRef](#)] [[PubMed](#)]
23. Zhang, X.; Wu, Q.; Yang, S. Ferulic Acid Promoting Apoptosis in Human Osteosarcoma Cell Lines. *Pak. J. Med. Sci.* **2017**, *33*, 127–131. [[CrossRef](#)] [[PubMed](#)]
24. Kampa, M.; Alexaki, V.-I.; Notas, G.; Nifli, A.-P.; Nistikaki, A.; Hatzoglou, A.; Bakogeorgou, E.; Kouimtoglou, E.; Blekas, G.; Boskou, D.; et al. Antiproliferative and Apoptotic Effects of Selective Phenolic Acids on T47D Human Breast Cancer Cells: Potential Mechanisms of Action. *Breast Cancer Res.* **2004**, *6*, R63. [[CrossRef](#)]
25. Eroglu, C.; Seçme, M.; Baçcı, G.; Dodurga, Y. Assessment of the Anticancer Mechanism of Ferulic Acid via Cell Cycle and Apoptotic Pathways in Human Prostate Cancer Cell Lines. *Tumor Biology* **2015**, *36*, 9437–9446. [[CrossRef](#)]
26. Bandugula, V.R. 2-Deoxy-d-Glucose and Ferulic Acid Modulates Radiation Response Signaling in Non-Small Cell Lung Cancer Cells. *Tumor Biol.* **2013**, *34*, 251–259. [[CrossRef](#)]
27. Grasso, R.; Dell’Albani, P.; Carbone, C.; Spatuzza, M.; Bonfanti, R.; Sposito, G.; Puglisi, G.; Musumeci, F.; Scordino, A.; Campisi, A. Synergic Pro-Apoptotic Effects of Ferulic Acid and Nanostructured Lipid Carrier in Glioblastoma Cells Assessed through Molecular and Delayed Luminescence Studies. *Sci. Rep.* **2020**, *10*, 4680. [[CrossRef](#)]
28. Luo, L.; Zhu, S.; Tong, Y.; Peng, S. Ferulic Acid Induces Apoptosis of HeLa and Caski Cervical Carcinoma Cells by Down-Regulating the Phosphatidylinositol 3-Kinase (PI3K)/Akt Signaling Pathway. *Med. Sci. Monit.* **2020**, *26*, e920095. [[CrossRef](#)]
29. Hou, Y.; Yang, J.; Zhao, G.; Yuan, Y. Ferulic Acid Inhibits Endothelial Cell Proliferation through NO Down-Regulating ERK1/2 Pathway. *J. Cell Biochem.* **2004**, *93*, 1203–1209. [[CrossRef](#)]
30. Wu, X.; Hu, Z.; Zhou, J.; Liu, J.; Ren, P.; Huang, X. Ferulic Acid Alleviates Atherosclerotic Plaques by Inhibiting VSMC Proliferation Through the NO/P21 Signaling Pathway. *J. Cardiovasc. Transl. Res.* **2022**, *15*, 865–875. [[CrossRef](#)]
31. Gao, J.; Yu, H.; Guo, W.; Kong, Y.; Gu, L.; Li, Q.; Yang, S.; Zhang, Y.; Wang, Y. The Anticancer Effects of Ferulic Acid Is Associated with Induction of Cell Cycle Arrest and Autophagy in Cervical Cancer Cells. *Cancer Cell Int.* **2018**, *18*, 102. [[CrossRef](#)] [[PubMed](#)]
32. Janicke, B.; Hegardt, C.; Krogh, M.; Önnings, G.; Åkesson, B.; Cirenajwis, H.M.; Oredsson, S.M. The Antiproliferative Effect of Dietary Fiber Phenolic Compounds Ferulic Acid and *p*-Coumaric Acid on the Cell Cycle of Caco-2 Cells. *Nutr. Cancer* **2011**, *63*, 611–622. [[CrossRef](#)] [[PubMed](#)]
33. Wang, J.; Lai, X.; Yuan, D.; Liu, Y.; Wang, J.; Liang, Y. Effects of Ferulic Acid, a Major Component of Rice Bran, on Proliferation, Apoptosis, and Autophagy of HepG2 Cells. *Food Res. Int.* **2022**, *161*, 111816. [[CrossRef](#)] [[PubMed](#)]
34. Pellerito, C.; Emanuele, S.; Ferrante, F.; Celesia, A.; Giuliano, M.; Fiore, T. Tributyltin(IV) Ferulate, a Novel Synthetic Ferulic Acid Derivative, Induces Autophagic Cell Death in Colon Cancer Cells: From Chemical Synthesis to Biochemical Effects. *J. Inorg. Biochem.* **2020**, *205*, 110999. [[CrossRef](#)]
35. McDaniel, J.T.; Nuhu, K.; Ruiz, J.; Alorbi, G. Social Determinants of Cancer Incidence and Mortality around the World: An Ecological Study. *Glob. Health Promot.* **2019**, *26*, 41–49. [[CrossRef](#)]
36. Nishida, N.; Yano, H.; Nishida, T.; Kamura, T.; Kojiro, M. Angiogenesis in Cancer. *Vasc. Health Risk Manag.* **2006**, *2*, 213–219. [[CrossRef](#)]
37. Lopes-Coelho, F.; Martins, F.; Pereira, S.A.; Serpa, J. Anti-Angiogenic Therapy: Current Challenges and Future Perspectives. *Int. J. Mol. Sci.* **2021**, *22*, 3765. [[CrossRef](#)]

38. Waltham, M.; Burnand, K.G.; Collins, M.; Smith, A. Vascular Endothelial Growth Factor and Basic Fibroblast Growth Factor Are Found in Resolving Venous Thrombi. *J. Vasc. Surg.* **2000**, *32*, 988–996. [[CrossRef](#)]
39. Chen, L.-T.; Oh, D.-Y.; Ryu, M.-H.; Yeh, K.-H.; Yeo, W.; Carlesi, R.; Cheng, R.; Kim, J.; Orlando, M.; Kang, Y.-K. Anti-Angiogenic Therapy in Patients with Advanced Gastric and Gastroesophageal Junction Cancer: A Systematic Review. *Cancer Res. Treat.* **2017**, *49*, 851–868. [[CrossRef](#)]
40. Sagar, S.M.; Yance, D.; Wong, R.K. Natural Health Products That Inhibit Angiogenesis: A Potential Source for Investigational New Agents to Treat Cancer-Part 1. *Curr. Oncol.* **2006**, *13*, 14–26. [[CrossRef](#)]
41. Srinivasan, M.; Sudheer, A.R.; Menon, V.P. Ferulic Acid: Therapeutic Potential Through Its Antioxidant Property. *J. Clin. Biochem. Nutr.* **2007**, *40*, 92–100. [[CrossRef](#)] [[PubMed](#)]
42. Lin, C.-M.; Chiu, J.-H.; Wu, I.-H.; Wang, B.-W.; Pan, C.-M.; Chen, Y.-H. Ferulic Acid Augments Angiogenesis via VEGF, PDGF and HIF-1 $\alpha$ . *J. Nutr. Biochem.* **2010**, *21*, 627–633. [[CrossRef](#)] [[PubMed](#)]
43. Yang, G.-W.; Jiang, J.-S.; Lu, W.-Q. Ferulic Acid Exerts Anti-Angiogenic and Anti-Tumor Activity by Targeting Fibroblast Growth Factor Receptor 1-Mediated Angiogenesis. *Int. J. Mol. Sci.* **2015**, *16*, 24011–24031. [[CrossRef](#)]
44. EKOWATI, J.; HAMID, I.S.; DIYAH, N.W.; SISWANDONO, S. Ferulic Acid Prevents Angiogenesis Through Cyclooxygenase-2 and Vascular Endothelial Growth Factor in the Chick Embryo Chorioallantoic Membrane Model. *Turk. J. Pharm. Sci.* **2020**, *17*, 424–431. [[CrossRef](#)] [[PubMed](#)]
45. Fares, J.; Fares, M.Y.; Khachfe, H.H.; Salhab, H.A.; Fares, Y. Molecular Principles of Metastasis: A Hallmark of Cancer Revisited. *Signal. Transduct. Target Ther.* **2020**, *5*, 28. [[CrossRef](#)] [[PubMed](#)]
46. Jiang, Y.-L.; Liu, Z.-P. Natural Products as Anti-Invasive and Anti-Metastatic Agents. *Curr. Med. Chem.* **2011**, *18*, 808–829. [[CrossRef](#)] [[PubMed](#)]
47. Groblewska, M.; Siewko, M.; Mroczo, B.; Szmikowski, M. The Role of Matrix Metalloproteinases (MMPs) and Their Inhibitors (TIMPs) in the Development of Esophageal Cancer. *Folia Histochem. Cytobiol.* **2012**, *50*, 12–19. [[CrossRef](#)] [[PubMed](#)]
48. Bauvois, B. New Facets of Matrix Metalloproteinases MMP-2 and MMP-9 as Cell Surface Transducers: Outside-in Signaling and Relationship to Tumor Progression. *Biochim. Biophys. Acta* **2012**, *1825*, 29–36. [[CrossRef](#)]
49. Zhang, X.; Lin, D.; Jiang, R.; Li, H.; Wan, J.; Li, H. Ferulic Acid Exerts Antitumor Activity and Inhibits Metastasis in Breast Cancer Cells by Regulating Epithelial to Mesenchymal Transition. *Oncol. Rep.* **2016**, *36*, 271–278. [[CrossRef](#)]
50. El-Gogary, R.I.; Nasr, M.; Rahsed, L.A.; Hamzawy, M.A. Ferulic Acid Nanocapsules as a Promising Treatment Modality for Colorectal Cancer: Preparation and in Vitro/in Vivo Appraisal. *Life Sci.* **2022**, *298*, 120500. [[CrossRef](#)]
51. Walsh, L.J. Mast Cells and Oral Inflammation. *Crit. Rev. Oral Biol. Med.* **2003**, *14*, 188–198. [[CrossRef](#)] [[PubMed](#)]
52. Sakai, S.; Kawamata, H.; Kogure, T.; Mantani, N.; Terasawa, K.; Umatake, M.; Ochiai, H. Inhibitory Effect of Ferulic Acid and Isoferulic Acid on the Production of Macrophage Inflammatory Protein-2 in Response to Respiratory Syncytial Virus Infection in RAW264.7 Cells. *Mediat. Inflamm.* **1999**, *8*, 173–175. [[CrossRef](#)] [[PubMed](#)]
53. Tetsuka, T.; Baier, L.D.; Morrison, A.R. Antioxidants Inhibit Interleukin-1-Induced Cyclooxygenase and Nitric-Oxide Synthase Expression in Rat Mesangial Cells. Evidence for Post-Transcriptional Regulation. *J. Biol. Chem.* **1996**, *271*, 11689–11693. [[CrossRef](#)] [[PubMed](#)]
54. Otu, L.; Kong, L.-Y.; Zhang, X.-M.; Niwa, M. Oxidation of Ferulic Acid by *Momordica charantia* Peroxidase and Related Anti-Inflammation Activity Changes. *Biol. Pharm. Bull.* **2003**, *26*, 1511–1516. [[CrossRef](#)] [[PubMed](#)]
55. Ohnishi, M.; Matuo, T.; Tsuno, T.; Hosoda, A.; Nomura, E.; Taniguchi, H.; Sasaki, H.; Morishita, H. Antioxidant Activity and Hypoglycemic Effect of Ferulic Acid in STZ-Induced Diabetic Mice and KK-Ay Mice. *Biofactors* **2015**, *21*, 315–319. [[CrossRef](#)]
56. Kim, E.O.; Min, K.J.; Kwon, T.K.; Um, B.H.; Moreau, R.A.; Choi, S.W. Anti-Inflammatory Activity of Hydroxycinnamic Acid Derivatives Isolated from Corn Bran in Lipopolysaccharide-Stimulated Raw 264.7 Macrophages. *Food Chem. Toxicol.* **2012**, *50*, 1309–1316. [[CrossRef](#)]
57. Hosoda, A.; Ozaki, Y.; Kashiwada, A.; Mutoh, M.; Wakabayashi, K.; Mizuno, K.; Nomura, E.; Taniguchi, H. Syntheses of Ferulic Acid Derivatives and Their Suppressive Effects on Cyclooxygenase-2 Promoter Activity. *Bioorg. Med. Chem.* **2002**, *10*, 1189–1196. [[CrossRef](#)]
58. Sudheer, A.R.; Muthukumar, S.; Devipriya, N.; Devaraj, H.; Menon, V.P. Influence of Ferulic Acid on Nicotine-Induced Lipid Peroxidation, DNA Damage and Inflammation in Experimental Rats as Compared to N-Acetylcysteine. *Toxicology* **2008**, *243*, 317–329. [[CrossRef](#)]
59. Tuli, H.S.; Kashyap, D.; Sharma, A.K.; Sandhu, S.S. Molecular Aspects of Melatonin (MLT)-Mediated Therapeutic Effects. *Life Sci.* **2015**, *135*, 147–157. [[CrossRef](#)]
60. Eitsuka, T.; Tatewaki, N.; Nishida, H.; Nakagawa, K.; Miyazawa, T. A Combination of  $\delta$ -Tocotrienol and Ferulic Acid Synergistically Inhibits Telomerase Activity in DLD-1 Human Colorectal Adenocarcinoma Cells. *J. Nutr. Sci. Vitaminol.* **2016**, *62*, 281–287. [[CrossRef](#)]
61. Eitsuka, T.; Tatewaki, N.; Nishida, H.; Kurata, T.; Nakagawa, K.; Miyazawa, T. Synergistic Inhibition of Cancer Cell Proliferation with a Combination of  $\delta$ -Tocotrienol and Ferulic Acid. *Biochem. Biophys. Res. Commun.* **2014**, *453*, 606–611. [[CrossRef](#)] [[PubMed](#)]
62. Montagnani Marelli, M.; Marzagalli, M.; Fontana, F.; Raimondi, M.; Moretti, R.M.; Limonta, P. Anticancer Properties of Tocotrienols: A Review of Cellular Mechanisms and Molecular Targets. *J. Cell Physiol.* **2019**, *234*, 1147–1164. [[CrossRef](#)] [[PubMed](#)]
63. Ju, J.; Picinich, S.C.; Yang, Z.; Zhao, Y.; Suh, N.; Kong, A.-N.; Yang, C.S. Cancer-Preventive Activities of Tocopherols and Tocotrienols. *Carcinogenesis* **2010**, *31*, 533–542. [[CrossRef](#)] [[PubMed](#)]

64. Indap, M.A.; Radhika, S.; Motiwale, L.; Rao, K.V.K. Inhibitory Effect of Cinnamoyl Compounds against Human Malignant Cell Line. *Indian J. Exp. Biol.* **2006**, *44*, 216–220.
65. Eroglu, C.; Avci, E.; Secme, M.; Dodurga, Y. The Combination Effect of Ferulic Acid and Gemcitabine on Expression of Genes Related Apoptosis and Metastasis in PC-3 Prostate Cancer Cells. *Eur. J. Biol.* **2018**, *77*, 32–37. [[CrossRef](#)]
66. Choi, Y.E.; Park, E. Ferulic Acid in Combination with PARP Inhibitor Sensitizes Breast Cancer Cells as Chemotherapeutic Strategy. *Biochem. Biophys. Res. Commun.* **2015**, *458*, 520–524. [[CrossRef](#)]
67. Sadoughi, F.; Mansournia, M.A.; Mirhashemi, S.M. The Potential Role of Chitosan-based Nanoparticles as Drug Delivery Systems in Pancreatic Cancer. *IUBMB Life* **2020**, *72*, 872–883. [[CrossRef](#)]
68. Paciello, F.; Fetoni, A.R.; Mezzogori, D.; Rolesi, R.; di Pino, A.; Paludetti, G.; Grassi, C.; Troiani, D. The Dual Role of Curcumin and Ferulic Acid in Counteracting Chemoresistance and Cisplatin-Induced Ototoxicity. *Sci. Rep.* **2020**, *10*, 1063. [[CrossRef](#)]
69. Predarska, I.; Saoud, M.; Drača, D.; Morgan, I.; Komazec, T.; Eichhorn, T.; Mihajlović, E.; Dunderović, D.; Mijatović, S.; Maksimović-Ivanić, D.; et al. Mesoporous Silica Nanoparticles Enhance the Anticancer Efficacy of Platinum(IV)-Phenolate Conjugates in Breast Cancer Cell Lines. *Nanomaterials* **2022**, *12*, 3767. [[CrossRef](#)]
70. Raina, K.; Agarwal, R. Combinatorial Strategies for Cancer Eradication by Silibinin and Cytotoxic Agents: Efficacy and Mechanisms. *Acta Pharmacol. Sin.* **2007**, *28*, 1466–1475. [[CrossRef](#)]
71. Mancuso, C.; Santangelo, R. Ferulic Acid: Pharmacological and Toxicological Aspects. *Food Chem. Toxicol.* **2014**, *65*, 185–195. [[CrossRef](#)] [[PubMed](#)]
72. Xue, C.; Lu, H.; Liu, Y.; Zhang, J.; Wang, J.; Luo, W.; Zhang, W.; Chen, J. Trans-Ferulic Acid-4- $\beta$ -Glucoside Alleviates Cold-Induced Oxidative Stress and Promotes Cold Tolerance. *Int. J. Mol. Sci.* **2018**, *19*, 2321. [[CrossRef](#)] [[PubMed](#)]
73. Zhang, L.-W.; Al-Suwayeh, S.A.; Hsieh, P.-W.; Fang, J.-Y. A Comparison of Skin Delivery of Ferulic Acid and Its Derivatives: Evaluation of Their Efficacy and Safety. *Int. J. Pharm.* **2010**, *399*, 44–51. [[CrossRef](#)] [[PubMed](#)]
74. Peng, C.-C.; Hsieh, C.-L.; Wang, H.-E.; Chung, J.-Y.; Chen, K.-C.; Peng, R.Y. Ferulic Acid Is Nephrodamaging While Gallic Acid Is Renal Protective in Long Term Treatment of Chronic Kidney Disease. *Clin. Nutr.* **2012**, *31*, 405–414. [[CrossRef](#)] [[PubMed](#)]
75. Maruyama, H.; Kawakami, F.; Lwin, T.-T.; Imai, M.; Shamsa, F. Biochemical Characterization of Ferulic Acid and Caffeic Acid Which Effectively Inhibit Melanin Synthesis via Different Mechanisms in B16 Melanoma Cells. *Biol. Pharm. Bull.* **2018**, *41*, 806–810. [[CrossRef](#)] [[PubMed](#)]
76. Pandi, A.; Raghu, M.H.; Chandrashekar, N.; Kalappan, V.M. Cardioprotective Effects of Ferulic Acid against Various Drugs and Toxic Agents. *Beni Suef Univ. J. Basic Appl. Sci.* **2022**, *11*, 92. [[CrossRef](#)]
77. Wang, T.; Gong, X.; Jiang, R.; Li, H.; Du, W.; Kuang, G. Ferulic Acid Inhibits Proliferation and Promotes Apoptosis via Blockage of PI3K/Akt Pathway in Osteosarcoma Cell. *Am. J. Transl. Res.* **2016**, *8*, 968–980.
78. Dodurga, Y.; Eroğlu, C.; Seçme, M.; Elmas, L.; Avci, Ç.B.; Şatiroğlu-Tufan, N.L. Anti-Proliferative and Anti-Invasive Effects of Ferulic Acid in TT Medullary Thyroid Cancer Cells Interacting with URG4/URGCP. *Tumour Biol.* **2016**, *37*, 1933–1940. [[CrossRef](#)]
79. Al-Mutairi, A.; Rahman, A.; Rao, M.S. Low Doses of Thymoquinone and Ferulic Acid in Combination Effectively Inhibit Proliferation of Cultured MDA-MB 231 Breast Adenocarcinoma Cells. *Nutr. Cancer* **2021**, *73*, 282–289. [[CrossRef](#)]
80. Rezaei, A.; Varshosaz, J.; Fesharaki, M.; Farhang, A.; Jafari, S.M. Improving the Solubility and in Vitro Cytotoxicity (Anticancer Activity) of Ferulic Acid by Loading It into Cyclodextrin Nanosponges. *Int. J. Nanomed.* **2019**, *14*, 4589–4599. [[CrossRef](#)]
81. Park, E. Data on Cell Cycle in Breast Cancer Cell Line, MDA-MB-231 with Ferulic Acid Treatment. *Data Brief.* **2016**, *7*, 107–110. [[CrossRef](#)] [[PubMed](#)]
82. Serafim, T.L.; Carvalho, F.S.; Marques, M.P.M.; Calheiros, R.; Silva, T.; Garrido, J.; Milhazes, N.; Borges, F.; Roleira, F.; Silva, E.T.; et al. Lipophilic Caffeic and Ferulic Acid Derivatives Presenting Cytotoxicity against Human Breast Cancer Cells. *Chem. Res. Toxicol.* **2011**, *24*, 763–774. [[CrossRef](#)] [[PubMed](#)]
83. Das, U.; Manna, K.; Adhikary, A.; Mishra, S.; das Saha, K.; Sharma, R.D.; Majumder, B.; Dey, S. Ferulic Acid Enhances the Radiation Sensitivity of Lung and Liver Carcinoma Cells by Collapsing Redox Homeostasis: Mechanistic Involvement of Akt/P38 MAPK Signalling Pathway. *Free Radic. Res.* **2019**, *53*, 944–967. [[CrossRef](#)]
84. Cao, Y.; Zhang, H.; Tang, J.; Wang, R. Ferulic Acid Mitigates Growth and Invasion of Esophageal Squamous Cell Carcinoma through Inducing Ferroptotic Cell Death. *Dis. Markers* **2022**, *2022*, 1–19. [[CrossRef](#)] [[PubMed](#)]
85. Ezhuthupurakkal, P.B.; Ariraman, S.; Arumugam, S.; Subramaniam, N.; Muthuvel, S.K.; Kumpati, P.; Rajamani, B.; Chinnasamy, T. Anticancer Potential of ZnO Nanoparticle-Ferulic Acid Conjugate on Huh-7 and HepG2 Cells and Diethyl Nitrosamine Induced Hepatocellular Cancer on Wistar Albino Rat. *Nanomedicine* **2018**, *14*, 415–428. [[CrossRef](#)] [[PubMed](#)]
86. Fahrioğlu, U.; Dodurga, Y.; Elmas, L.; Seçme, M. Ferulic Acid Decreases Cell Viability and Colony Formation While Inhibiting Migration of MIA PaCa-2 Human Pancreatic Cancer Cells in Vitro. *Gene* **2016**, *576*, 476–482. [[CrossRef](#)] [[PubMed](#)]
87. Kim, H.-J.; Ryu, K.; Kang, J.-H.; Choi, A.-J.; Kim, T.; Oh, J.-M. Anticancer Activity of Ferulic Acid-Inorganic Nanohybrids Synthesized via Two Different Hybridization Routes, Reconstruction and Exfoliation-Reassembly. *Sci. World J.* **2013**, *2013*, 421967. [[CrossRef](#)]
88. Karthikeyan, S.; Kanimozhi, G.; Prasad, N.R.; Mahalakshmi, R. Radiosensitizing Effect of Ferulic Acid on Human Cervical Carcinoma Cells in Vitro. *Toxicol. In Vitro* **2011**, *25*, 1366–1375. [[CrossRef](#)]
89. Luo, Y.; Wang, C.-Z.; Sawadogo, R.; Yuan, J.; Zeng, J.; Xu, M.; Tan, T.; Yuan, C.-S. 4-Vinylguaiaicol, an Active Metabolite of Ferulic Acid by Enteric Microbiota and Probiotics, Possesses Significant Activities against Drug-Resistant Human Colorectal Cancer Cells. *ACS Omega* **2021**, *6*, 4551–4561. [[CrossRef](#)]

90. Sawata, Y.; Matsukawa, T.; Doi, S.; Tsunoda, T.; Arikawa, N.; Matsunaga, N.; Ohnuki, K.; Shirasawa, S.; Kotake, Y. A Novel Compound, Ferulic Acid-Bound Resveratrol, Induces the Tumor Suppressor Gene P15 and Inhibits the Three-Dimensional Proliferation of Colorectal Cancer Cells. *Mol. Cell Biochem.* **2019**, *462*, 25–31. [[CrossRef](#)]
91. Potez, M.; Trappetti, V.; Bouchet, A.; Fernandez-Palomo, C.; Güç, E.; Kilariski, W.W.; Hlushchuk, R.; Laissue, J.; Djonov, V. Characterization of a B16-F10 Melanoma Model Locally Implanted into the Ear Pinnae of C57BL/6 Mice. *PLoS ONE* **2018**, *13*, e0206693. [[CrossRef](#)]
92. Wang, J.; Sheng, Y.; Ji, L.; Wang, Z. Ferulic Acid Prevents Liver Injury and Increases the Anti-Tumor Effect of Diosbulbin B in Vivo. *J. Zhejiang Univ. Sci. B* **2014**, *15*, 540–547. [[CrossRef](#)] [[PubMed](#)]
93. Yue, S.-J.; Zhang, P.-X.; Zhu, Y.; Li, N.-G.; Chen, Y.-Y.; Li, J.-J.; Zhang, S.; Jin, R.-Y.; Yan, H.; Shi, X.-Q.; et al. A Ferulic Acid Derivative FXS-3 Inhibits Proliferation and Metastasis of Human Lung Cancer A549 Cells via Positive JNK Signaling Pathway and Negative ERK/P38, AKT/MTOR and MEK/ERK Signaling Pathways. *Molecules* **2019**, *24*, 2165. [[CrossRef](#)] [[PubMed](#)]
94. Thakkar, A.; Chenreddy, S.; Wang, J.; Prabhu, S. Ferulic Acid Combined with Aspirin Demonstrates Chemopreventive Potential towards Pancreatic Cancer When Delivered Using Chitosan-Coated Solid-Lipid Nanoparticles. *Cell Biosci.* **2015**, *5*, 46. [[CrossRef](#)] [[PubMed](#)]

Article

# Camel Grass Phenolic Compounds: Targeting Inflammation and Neurologically Related Conditions

Graciliana Lopes <sup>†,‡</sup>, Elisabete Gomes <sup>†</sup>, Mariana Barbosa <sup>§</sup>, João Bernardo and Patrícia Valentão <sup>\*</sup>

REQUIMTE/LAQV, Laboratory of Pharmacognosy, Department of Chemistry, Faculty of Pharmacy, University of Porto, Rua de Jorge Viterbo Ferreira, n° 228, 4050-313 Porto, Portugal

<sup>\*</sup> Correspondence: valentao@ff.up.pt<sup>†</sup> These authors contributed equally to this work.<sup>‡</sup> Current address: Interdisciplinary Centre of Marine and Environmental Research (CIIMAR), 4450-208 Matosinhos, Portugal.<sup>§</sup> Current address: Applied Biomolecular Sciences Unit (UCIBIO), Department of Life Sciences, NOVA School of Science and Technology (FCT NOVA), University of Lisbon, 1649-004 Lisboa, Portugal.

**Abstract:** Background: The use of plants for therapeutic purposes has been supported by growing scientific evidence. Methods: This work consisted of (i) characterizing the phenolic compounds present in both aqueous and hydroethanol (1:1, *v/v*) extracts of camel grass, by hyphenated liquid chromatographic techniques, (ii) evaluating their anti-inflammatory, antioxidant, and neuromodulation potential, through *in vitro* cell and cell-free models, and (iii) establishing a relationship between the chemical profiles of the extracts and their biological activities. Results: Several caffeic acid and flavonoid derivatives were determined in both extracts. The extracts displayed scavenging capacity against the physiologically relevant nitric oxide ( $\bullet\text{NO}$ ) and superoxide anion ( $\text{O}_2^{\bullet-}$ ) radicals, significantly reduced NO production in lipopolysaccharide (LPS)-stimulated macrophages (RAW 264.7), and inhibited the activity of hyaluronidase (HAase), acetylcholinesterase (AChE) and butyrylcholinesterase (BChE). Some of these bioactivities were found to be related with the chemical profile of the extracts, namely with 3-caffeoylquinic, 4-caffeoylquinic, chlorogenic, and *p*-coumaric acids, as well as with luteolin and apigenin derivatives. Conclusions: This study reports, for the first time, the potential medicinal properties of aqueous and hydroethanol extracts of camel grass in the RAW 264.7 cell model of inflammation, and in neurologically related conditions.

**Keywords:** *Cymbopogon schoenanthus*; hyaluronidase; acetylcholinesterase; neurodegeneration; oxidative stress; phenolic compounds

**Citation:** Lopes, G.; Gomes, E.; Barbosa, M.; Bernardo, J.; Valentão, P. Camel Grass Phenolic Compounds: Targeting Inflammation and Neurologically Related Conditions. *Molecules* **2022**, *27*, 7707. <https://doi.org/10.3390/molecules27227707>

Academic Editor: Nour Eddine Es-Safi

Received: 12 October 2022

Accepted: 6 November 2022

Published: 9 November 2022

**Publisher's Note:** MDPI stays neutral with regard to jurisdictional claims in published maps and institutional affiliations.



**Copyright:** © 2022 by the authors. Licensee MDPI, Basel, Switzerland. This article is an open access article distributed under the terms and conditions of the Creative Commons Attribution (CC BY) license (<https://creativecommons.org/licenses/by/4.0/>).

## 1. Introduction

Since the dawn of humanity, plants have been used in the prophylaxis, relief, and treatment of diseases with several etiological origins. Despite being intrinsically linked to popular wisdom, the medicinal use of plants is abandoning its empiric framework and becoming increasingly supported by scientific evidence [1]. As important sources of new bioactive compounds with promising pharmacological effects, several plant species have been recognized by the World Health Organization for their medicinal properties [2].

Inflammation is one of the main healthcare concerns for which medicinal plants are well-documented [3]. As part of the organism response to cell and tissues injury, inflammation is characterized by the release of several systemic mediators that act together for damage repair. When the cause of inflammation persists, or when the defence mechanisms are deregulated, inflammation can become chronic [4]. Nitric oxide (NO) plays an important role in many physiologic processes, not only as a signalling molecule, but also as neurotransmitter and participant in platelet aggregation inhibition. Under physiologic conditions, NO acts as an anti-inflammatory mediator; however, at higher concentrations, it induces and exacerbates inflammation, leading to tissue damage [5]. This mediator is

produced from L-arginine, by the action of a family of nitric oxide synthase (NOS) enzymes. Of them, the inducible nitric oxide synthase (iNOS) isoform, originally expressed in macrophages in response to inflammatory *stimuli*, is crucial in the inflammatory process due to its capacity to increase NO production [5]. Thus, compounds able to inhibit NO overproduction, or to scavenge the reactive species formed during the inflammatory process, are interesting for the resolution of inflammatory frames [4,6].

The appropriate regulation of reactive species is essential for organism homeostasis. Thus, antioxidants play an essential role in the prevention of various pathologies. Reactive nitrogen species (RNS) and reactive oxygen species (ROS) can accumulate, resulting in the oxidation of cellular components and cellular destruction [7]. Apart from its role in inflammation, oxidative stress underlies other pathologies. The progression of neurodegeneration is a classic example; brain structures supporting memory are particularly sensitive to the oxidative status, due to their high demand for oxygen [8]. Most cognitive and behavioural changes are postulated to be caused by deficient brain cholinergic pathways. This can help explain why the enhancement of cholinergic transmission, by extending the availability of acetylcholine (ACh) in the synaptic cleft, can improve the symptoms associated with neurodegeneration. Moreover, the inhibition of acetylcholinesterase (AChE) and butyrylcholinesterase (BChE), enzymes responsible for the hydrolysis of ACh following synaptic release, has thus been suggested as a promising strategy to avoid the progression of dementia [9]. In this regard, diverse medicinal species traditionally used to treat neurological diseases have been evaluated for their cholinesterase inhibitory activity to support their ethnopharmacological applications [9,10].

*Cymbopogon* species have been used in traditional medicine worldwide, lemon grass (*Cymbopogon citratus* (DC.) Stapf) being the most widely distributed and well-studied one [11–13]. Camel grass (*Cymbopogon schoenanthus* (L.) Spreng.), on the other hand, has been scarcely explored regarding its chemical profile and pharmacological activities [14–16]. Besides the over-studied volatile extracts of *Cymbopogon* spp., identified as essential oils, non-volatile extracts are gaining researchers' attention for their promising pharmacological applications and lower toxicity [17]. Among the specialized metabolites present in non-volatile extracts of *Cymbopogon* spp., phenolic compounds are likely the most notable ones. In particular, hydroxycinnamic acids and flavonoids can be highlighted for their marked antioxidant and anti-inflammatory properties and capacity to inhibit key enzymes involved in several pathologic processes [18–22].

The aims of this work were to establish the phenolic profiles of aqueous and hydroethanol extracts of camel grass and to evaluate their toxicity, anti-inflammatory and antioxidant potential, together with their effect on enzymes engaged in the neurodegenerative process. In addition to contributing to the enrichment of scientific knowledge on the chemistry of phenols of this still understudied species of the genus *Cymbopogon*, the present work highlights the potential medicinal properties of aqueous and hydroethanol extracts of *C. schoenanthus* in the RAW 264.7 cell model of inflammation, and in neurologically related conditions, for the first time.

## 2. Results and Discussion

The genus *Cymbopogon* is widely known for its high content in essential oils. Though the pharmacological applications of its volatile extracts are well-exploited, other extracts and species from this same genus remain underexplored [12]. Likewise, preliminary *in vitro* data on the potential toxicity of extracts are scarce to non-existent. Therefore, this work focused on the antioxidant, anti-inflammatory and neuromodulating capacity of aqueous and hydroethanol extracts of camel grass, which are among the biological properties most reported in traditional medicine for this genus. Moreover, the toxicity of the extracts was screened in different cell lines, and the effect of the extraction method and solvent composition on their chemical profile and biological activity was also considered. Additionally, a relationship between the biological activities and the phenolic profile was established.

### 2.1. Phenolic Profile

HPLC-DAD analysis of camel grass extracts revealed similar qualitative compositions, regardless of the extraction solvent and procedure. Figure 1 displays the HPLC-DAD chromatogram obtained with the aqueous extract.

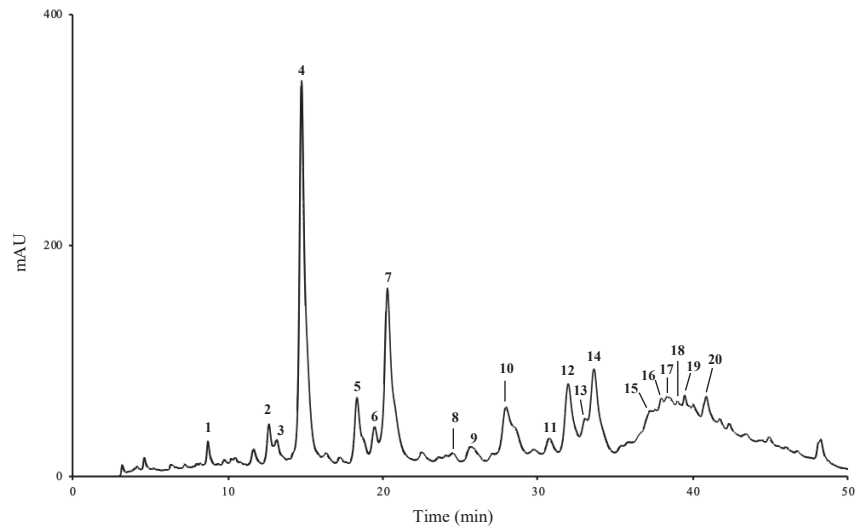


**Figure 1.** HPLC-DAD chromatogram of camel grass aqueous extract, recorded at 320 nm. 1: 3-*O*-caffeoylquinic acid; 2: 4-*O*-caffeoylquinic acid; 4: chlorogenic acid; 7: *p*-coumaric acid; 9: ferulic acid; 12: isoorientin; 13: luteolin glycoside; 14: luteolin-3',7-di-*O*-glucoside; 3, 5, 6 and 8: caffeic acid derivatives; 10, 11, 15–20: apigenin glycosides.

On the other hand, the concentrations of the identified compounds varied according to the nature of the extracting solvent (Table 1). The aqueous extract was significantly richer in phenolic compounds (1.85 mg/g dry plant) than the hydroethanol extract (0.95 mg/g dry plant) ( $p < 0.05$ ). This demonstrates that the infusion process was much more effective in extracting phenolic compounds than the ultrasound-assisted extraction procedure used to obtain the hydroethanol extract ( $p < 0.05$ ). Ultrasound is known for enhancing the rate of mass transfer of analytes to the solvent. Nevertheless, the hydroethanol extracts, obtained with sonication, presented a lower amount of phenols than the extracts obtained by infusion, confirming that the effect of the solvent is more decisive than the extraction method.

Regarding the major subclasses of phenolic compounds determined in camel grass extracts, flavonoid derivatives clearly dominated, when compared to hydroxycinnamic acids, in both aqueous (1.02 vs. 0.83 mg/g of dry plant) and hydroethanol extract (0.62 vs. 0.33 mg/g of dry plant) (Table 1). Among hydroxycinnamic acids, chlorogenic acid (4) was the major compound in the aqueous extract, while *p*-coumaric acid (7) was the most representative compound in the hydroethanol extract. Among flavonoid derivatives, luteolin-3',7-di-*O*-glucoside (14) was the phenolic found at the highest concentration in both extracts (Table 1).

Studies reporting the chemical profile of camel grass are almost exclusively dedicated to its essential oils. To our knowledge, few studies have reported the phenolic composition of non-volatile extracts of this species. The works by the groups of Khadri [15], Musa [23] and Abu-Serie [24] explored different biological activities of aqueous and methanol (80%) extracts. However, the phenolic profile of the extract was not established, and the total phenolic content was quantified through the non-specific Folin-Ciocalteu colorimetric method. Ben Othman and colleagues [16] determined the phenolic composition of an ethanol extract (70%) of camel grass. In the HPLC-DAD analysis, the authors identified seven phenolic



compounds, namely quercetin-3-*O*-rhamnoside, resorcinol, and *trans*-cinnamic, caffeic, 2,5-dihydroxybenzoic, ferulic and gallic acids, the flavonoid being the most representative compound. Najja and co-workers [25] also characterized an ethanol extract (70%) of camel grass by HPLC-DAD, reporting the presence of the same compounds, quercetin-3-*O*-rhamnoside being also the most abundant. Rocchetti and co-workers [26] analysed the phenolic profile of an aqueous extract by triple-TOF mass spectrometry, having found several flavonoids and phenolic acids: kaempferol, quercetin, luteolin and apigenin glycosides were the most representative among the flavonoids, while caffeic, ferulic and coumaric acids predominated among the phenolic acids. These results are in line with those obtained in the study herein. In this work, ferulic acid (9) was the only compound that had been previously reported. As far as we are aware, 3-caffeoylquinic (1), 4-caffeoylquinic (2) and chlorogenic (4) acids are being reported here for the first time in camel grass.

**Table 1.** Quantification of the phenolic compounds identified in camel grass extracts <sup>1</sup>.

	Compounds	Rt (min)	Aqueous Extract	Hydroethanol Extract
<b>Hydroxycinnamic acids</b>				
1	3-Caffeoylquinic acid	8.66	0.03 ± < 0.01	0.08 ± < 0.01
2	4-Caffeoylquinic acid	12.57	0.04 ± < 0.01	0.01 ± < 0.01
3	Caffeic acid derivative	13.09	0.02 ± < 0.01	0.01 ± < 0.01
4	Chlorogenic acid	14.66	0.49 ± 0.04	0.02 ± 0.01
5	Caffeic acid derivative	18.22	0.04 ± > 0.01	nq
6	Caffeic acid derivative	19.33	0.02 ± > 0.01	nq
7	<i>p</i> -Coumaric acid	20.21	0.18 ± 0.01	0.16 ± < 0.01
8	Caffeic acid derivative	24.45	0.00 ± < 0.01	nq
9	Ferulic acid	25.51	0.01 ± < 0.01	0.05 ± 0.01
	<b>Σ</b>		<b>0.83<sup>a</sup> ± 0.05</b>	<b>0.33<sup>b</sup> ± 0.02</b>
<b>Flavonoids</b>				
10	Apigenin glycoside	28.50	0.06 ± < 0.01	0.03 ± < 0.01
11	Apigenin glycoside	30.60	0.01 ± < 0.01	nq
12	Isoorientin	31.81	0.13 ± 0.01	0.08 ± 0.01
13	Luteolin glycoside	32.89	0.07 ± 0.01	nq
14	Luteolin-3',7-di- <i>O</i> -glucoside	33.46	0.31 ± 0.03	0.22 ± 0.01
15	Apigenin glycoside	37.10	0.09 ± 0.01	0.03 ± 0.02
16	Apigenin glycoside	37.91	0.03 ± < 0.01	0.06 ± 0.01
17	Apigenin glycoside	38.27	0.07 ± 0.01	0.06 ± 0.01
18	Apigenin glycoside	38.96	0.09 ± 0.01	0.04 ± 0.01
19	Apigenin glycoside	39.90	0.05 ± 0.01	0.03 ± 0.01
20	Apigenin glycoside	40.73	0.11 ± 0.01	0.07 ± 0.01
	<b>Σ</b>		<b>1.02<sup>a</sup> ± 0.1</b>	<b>0.62<sup>b</sup> ± 0.09</b>
	<b>Total</b>		<b>1.85<sup>a</sup> ± 0.15</b>	<b>0.95<sup>b</sup> ± 0.11</b>

<sup>1</sup> Values are expressed in mg/g of dry plant, as mean ± SD of four determinations; nq—not quantified. Different superscript letters in each row indicate statistical differences at *p* < 0.05 (two-tailed unpaired *t*-test).

Unlike camel grass, lemon grass is, by far, the most well-documented species within the genus. Figueirinha and collaborators [19] determined the composition of lemon grass aqueous extracts, having reported the presence of two classes of phenolic compounds: hydroxycinnamic acids, namely caffeic acid, its derivatives, and *p*-coumaric acid, and flavonoids, mainly 6-C and 8-C glycosyl flavones, derivatives of luteolin and apigenin, which is in accordance with our results (Figure 1, Table 1). As herein, other surveys performed with different extracts from the aerial parts of lemon grass [27] reported chlorogenic acid as the major compound in aqueous extracts, together with two luteolin glycosides, and luteolin derivatives as the most representative of a methanol:water extract. Similar results were later obtained by Campos et al. [28]. More recently, Roriz and colleagues focused on the antioxidant compounds of different plants, having found luteolin derivatives as the major compounds in lemon grass [29,30]. This is in accordance with our findings, in

which luteolin glycoside corresponded to ca. 28 and 32% of the total phenolic compounds identified in the aqueous and hydroethanol extracts, respectively.

## 2.2. Antioxidant Activity

Camel grass extracts were screened for their antioxidant capacity against  $\bullet\text{NO}$  and  $\text{O}_2^{\bullet-}$ . The two extracts were able to scavenge both reactive species in a dose-dependent manner (Figure 2, Table 2). When comparing the  $\text{IC}_{50}$  values obtained, the aqueous extract was significantly more efficient than the hydroethanol one against  $\bullet\text{NO}$  ( $p < 0.05$ ), while no significant differences were observed regarding the  $\text{O}_2^{\bullet-}$  scavenging ability of both extracts (Table 2). The results obtained for  $\bullet\text{NO}$  scavenging were less promising than those obtained with the reference standard quercetin ( $\text{IC}_{50} = 58.1 \mu\text{g}/\text{mL}$ ); however, regarding  $\text{O}_2^{\bullet-}$ , the results were quite remarkable, being of the same order of magnitude of the reference standard ( $\text{IC}_{50} = 24.6 \mu\text{g}/\text{mL}$ ).

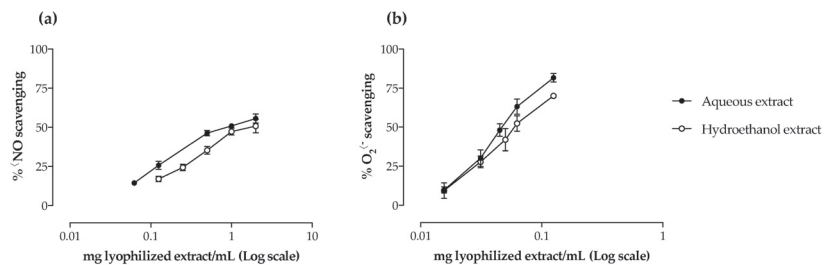


**Figure 2.** Scavenging effect of camel grass extracts against nitric oxide ( $\bullet\text{NO}$ ) (a) and superoxide anion ( $\text{O}_2^{\bullet-}$ ) (b) radicals generated in a cell-free system. Results are expressed as percentage of the respective control (mean  $\pm$  SD of at least three determinations, each performed in triplicate).

**Table 2.**  $\text{IC}_{50}$  values (mg lyophilized extract/mL) obtained for the antioxidant, anti-inflammatory and enzyme inhibitory capacity of camel grass extracts <sup>1</sup>.

	Aqueous Extract	Hydroethanol Extract
$\bullet\text{NO}$ scavenging	$0.93 \pm 0.19^a$	$1.27 \pm 0.20^b$
$\text{O}_2^{\bullet-}$ scavenging	$0.05 \pm < 0.01$	$0.06 \pm 0.01$
NO reduction in RAW 264.7 cells	$1.32 \pm 0.17$	$1.38 \pm 0.04$
HAase	$1.40 \pm 0.07^a$	$2.57 \pm 0.17^b$
AChE <sup>2</sup>	$1.49 \pm 0.17$	$1.69 \pm 0.21$
BChE <sup>2</sup>	$0.68 \pm 0.02^a$	$0.82 \pm 0.12^b$

<sup>1</sup> Values are expressed as mean  $\pm$  SD of at least three independent determinations, each performed in triplicate. Different superscript letters in each row indicate statistical differences at  $p < 0.05$  (two-tailed unpaired *t*-test). <sup>2</sup> Values correspond to 25% inhibition. AChE, acetylcholinesterase; BChE, butyrylcholinesterase; HAase, hyaluronidase;  $\bullet\text{NO}$ , nitric oxide radical; NO, nitric oxide,  $\text{O}_2^{\bullet-}$ , superoxide anion radical.

Antioxidants have been implicated in the prevention of various diseases by protecting the organism against cell damage caused by oxidative stress [31]. Although the total amount of phenolic compounds was significantly different between the two extracts tested ( $p < 0.05$ ) (Table 1), their  $\bullet\text{NO}$  scavenging capacity seemed to rely on the presence of certain compounds. For instance, a negative correlation was observed between the  $\text{IC}_{50}$  values and 4-caffeoylquinic acid (**2**) ( $-0.816$ ,  $p < 0.05$ ) and the apigenin glycoside (**15**) ( $-0.828$ ,  $p < 0.05$ ), while a positive correlation was found for the apigenin glycoside (**16**) ( $0.889$ ,  $p < 0.05$ ) (Table 3). With regard to  $\text{O}_2^{\bullet-}$ , data analysis demonstrated that the total amount of phenolic compounds was negatively correlated with the radical scavenging capacity of the extracts ( $-0.814$ ,  $p < 0.05$ ), mainly due to flavonoids (Table 3).

**Table 3.** Correlation between the biological activities and the chemical profile of camel grass extracts <sup>1,2</sup>.

	Compounds	Antioxidant Activity		Enzyme Inhibition	
		$\bullet$ NO Scavenging	$O_2^{\bullet-}$ Scavenging	HAase	AChE
<b>Hydroxycinnamic acids</b>					
1	3-Caffeoylquinic acid			0.981 **	
2	4-Caffeoylquinic acid	−0.816 *		−0.944 **	
3	Caffeic acid derivative		−0.872 *	−0.827 *	
4	Chlorogenic acid			−0.978 **	
5	Caffeic acid derivative			−0.974 **	
6	Caffeic acid derivative			−0.952 **	
8	Caffeic acid derivative				−0.998 *
9	Ferulic acid		0.904 *	0.961 **	
	$\Sigma$			−0.989 **	
<b>Flavonoids</b>					
10	Apigenin glycoside		−0.888 *	0.965 **	
12	Isoorientin			−0.932 **	
13	Luteolin glycoside				−0.998 *
14	Luteolin-3',7-di-O-glucoside			−0.864 *	
15	Apigenin glycoside	−0.828 *		−0.898 **	
16	Apigenin glycoside	0.889 *		0.896 **	
17	Apigenin glycoside		−0.928 **		
18	Apigenin glycoside		−0.871 **	−0.930 **	
19	Apigenin glycoside		−0.940 **	−0.896 **	
20	Apigenin glycoside		−0.941 *	−0.868 *	
	$\Sigma$			−0.965 **	
	<b>Total</b>		−0.814 *	−0.974 **	

<sup>1</sup> Significance levels set at \*  $p < 0.05$  and \*\*  $p < 0.01$ . <sup>2</sup>  $\bullet$ NO, nitric oxide radical;  $O_2^{\bullet-}$ , superoxide anion radical; HAase, hyaluronidase; AChE, acetylcholinesterase.

As far as we know, the evaluation of the antioxidant capacity of camel grass non-volatile extracts was limited to the studies conducted by the groups of Khadri [15] and Rocchetti [26]. The first assessed the effect of an aqueous extract against the non-physiological 1,1-diphenyl-2-picryl-hydrazyl radical (DPPH $\bullet$ ) and concluded that the antioxidant activity was positively correlated with the phenolic content [15]. The correlation between phenolics and the antioxidant potential of the extracts was corroborated by Rocchetti et al., through the Trolox equivalent antioxidant capacity (TEAC), who also found that flavonoids were strongly correlated with TEAC values [26]. To our knowledge, this is the first work reporting the antioxidant potential of camel grass extracts against free radicals with biological importance ( $\bullet$ NO and  $O_2^{\bullet-}$ ) and the first one to establish a relationship between their radical scavenging capacity and their phenolic profile.

Contrary to camel grass, several studies reported the antioxidant potential of non-volatile extracts from species of the same genus, namely lemon grass [19,27]. Cheel and collaborators [27] evaluated the antioxidant potential of several lemon grass extracts, including methanol, methanol:water (7:3 and 1:1, *v/v*), infusion and decoction, against DPPH $\bullet$  and  $O_2^{\bullet-}$  and reported a positive correlation between the antioxidant activity and the phenolics content. Our results are in accordance with these, as a higher phenolic content led to lower IC<sub>50</sub> value (Tables 1–3). In another work [19], caffeic and *p*-coumaric acids and apigenin and luteolin derivatives were determined and correlated with the free radical scavenging capacity of the extracts. In accordance with the present study, those authors also suggested that flavonoids, the major subclass of identified compounds, were responsible for the antioxidant potential of the extracts [19].

### 2.3. Anti-Inflammatory Potential

The anti-inflammatory potential of camel grass extracts was assessed by a model of macrophages challenged with lipopolysaccharide (LPS). Both extracts were able to reduce cellular NO production in a dose-dependent manner, and no cytotoxicity was observed under the range of concentrations tested (0.19–1.5 mg lyophilized extract/mL) (Figure 3). Despite being less effective than the reference drug dexamethasone ( $IC_{50} = 34.6 \mu\text{g/mL}$ ), at the highest concentration tested (1.5 mg lyophilized extract/mL), the co-incubation with camel grass extracts reduced NO released by stimulated macrophages by more than 50%, in comparison to the untreated control (Figure 3). However, no correlation was found between the total phenolic content and the reduction of NO released by RAW 264.7 cells.

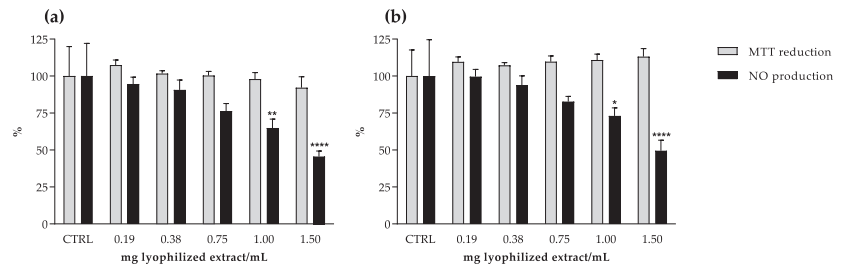


**Figure 3.** Effect of camel grass aqueous (a) and hydroethanol (b) extracts on thiazolyl blue tetrazolium bromide (MTT) reduction and nitric oxide (NO) production in lipopolysaccharide (LPS)-stimulated RAW 264.7 cells. Results are expressed as percentage of the respective control (CTRL) (mean  $\pm$  SD of four determinations, each performed in triplicate). \*  $p < 0.05$ ; \*\*  $p < 0.01$ ; \*\*\*\*  $p < 0.0001$  (ANOVA, Tukey HSD multiple comparison test).

Inflammation is one of the conditions for which traditional medicine recommends the use of species of *Cymbopogon* genus [12]. To our knowledge, there are no previous reports concerning the anti-inflammatory potential of camel grass in macrophages upon LPS stimulation.

Although no significant differences were found between the  $IC_{50}$  values, the extract with higher content of both flavonoids and hydroxycinnamic acids displayed a tendency to be more active (Tables 1 and 2). This is in accordance with previous studies conducted with macrophages that attributed the anti-inflammatory activity of *Cymbopogon* spp. extracts to their flavonoid content [6,32]. Additionally, even with little expression when compared to essential oils, some authors have explored the anti-inflammatory potential of non-volatile extracts of *Cymbopogon* spp., namely those of lemon grass [18,20,21]. A study conducted with LPS-stimulated RAW 264.7 cells treated with a lemon grass aqueous extract suggested phenolic compounds as the main contributors to the reduction in iNOS expression and NO production [21]. The anti-inflammatory activity of some compounds isolated from lemon grass was further assessed in the same cell model, revealing that luteolin glucosides were partly responsible for the anti-inflammatory properties of the extracts [20]. These observations are in accordance with our results: treatment with the aqueous extract, richer in luteolin glycosides, seemed to have a stronger effect regarding NO reduction in the cell system (Tables 1 and 2). Another cell model was used to evaluate the anti-inflammatory potential of an infusion of lemon grass, as well as its polyphenol fractions, on the NO produced by LPS-stimulated dendritic cells [18]. The authors demonstrated that the infusion significantly inhibited NO production and iNOS expression; the strongest anti-inflammatory effects were observed for the flavonoid-rich fraction, again indicating luteolin glycosides as the main contributors to the effects. A recent work evaluated the anti-inflammatory capacity of camel grass aqueous and ethanol (50% v/v) extracts by assessing the inhibition of the active NF- $\kappa$ B pathway in an HT-29 cell line. The authors found that only the aqueous extract was able to significantly inhibit the pro-inflammatory gene expression but did not report a correlation with the phenolic compounds identified [26]. Regarding

phenolic acids, Francisco and co-workers reported the contribution of chlorogenic acid to the anti-inflammatory activity displayed by a lemon grass infusion [33]. The authors tested the main phenolic acid in the extract, chlorogenic acid, and found that it maintained the phosphorylation levels of I $\kappa$ B $\alpha$ , as the extract did. The inhibition of p65 translocation to the nucleus by lemon grass extract was also observed, which was consistent with the NF- $\kappa$ B inhibition, suggesting the anti-inflammatory potential of the extract by inhibition of NF- $\kappa$ B activation. Chlorogenic acid is the most representative hydroxycinnamic of the extracts evaluated herein. Consequently, it may also contribute to the anti-inflammatory activity observed in our study.

The mechanisms behind inflammation are complex, accounting for a huge number of mediators and enzymes that may be directly or indirectly involved in the process. High and low molecular weight forms of hyaluronic acid (HA) exhibit opposite effects on cell behaviour. High molecular weight HA inhibits endothelial cell growth, is increased at sites of inflammation, and often correlates with leukocyte adhesion and migration. Studies on activated macrophages have shown that HA fragments induce the expression of chemokine genes, such as macrophage inflammatory proteins (MIP) with a crucial role in initiating and maintaining the inflammatory response [34]. Hyaluronidase (HAase) is an enzyme responsible for the degradation of HA; thus, its inhibition can result in a favourable environment to overcome inflammation.

Both extracts demonstrated capacity to inhibit the HAase-mediated degradation of HA in a dose-dependent manner (Figure 4a). At the highest tested concentrations (3.0 and 2.5 mg lyophilized extract/mL for hydroethanol and aqueous extract, respectively), the extracts almost completely inhibited the enzymatic activity (Figure 4a). The aqueous extract was more effective ( $p < 0.05$ ), presenting an IC<sub>50</sub> value of about half of that obtained for the hydroethanol extract (Table 2), and in the same order of magnitude of the reference drug disodium cromoglicate (1.10 mg/mL).

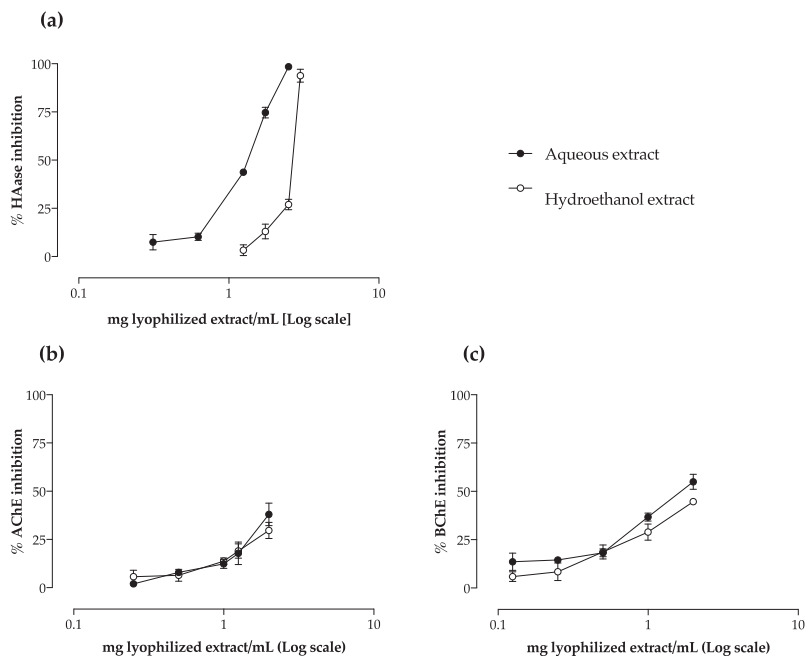


**Figure 4.** Effect of camel grass extracts on hyaluronidase (HAase) (a), acetylcholinesterase (AChE) (b), and butyrylcholinesterase (BChE) (c) activity. Results are expressed as percentage of control (mean  $\pm$  SD of, at least, three determinations).

Regarding HAase inhibition, a clear correlation was observed, not only concerning individual compounds, but also considering the total amount within each subclass (Table S1). Strong negative correlations were found for hydroxycinnamic acids ( $-0.989$ ,  $p < 0.01$ ) and flavonoids ( $-0.965$ ,  $p < 0.01$ ), which easily explains the significantly lower  $IC_{50}$  value obtained with the aqueous extract (Tables 2 and 3). To the best of our knowledge, this is the first report devoted to the evaluation of the effect of *Cymbopogon* spp. on HAase.

#### 2.4. Effect on AChE and BChE Activity

Camel grass extracts showed a dose-dependent behaviour concerning their capacity to inhibit AChE and BChE (Figure 4b,c). Both extracts displayed a stronger capacity to inhibit BChE than AChE (Table 2): the aqueous extract was the most effective to impair butyrylcholine hydrolysis, being the only one to inhibit half of the enzyme activity ( $IC_{50}$  value of 1.76 mg lyophilized extract/mL against BChE).

The neuromodulator properties of *Cymbopogon* spp. have been mostly attributed to their essential oils [35,36]. Adaramoye and Azeez [37] evaluated the capacity of a methanol extract of lemon grass to inhibit AChE, but found no differences compared to the untreated control. Khadri and colleagues [15] evaluated the effect of different camel grass extracts on AChE inhibition and verified that the inhibitory activity increased with the solvent polarity. These previous results are in accordance with our work; even with no statistical differences found, the  $IC_{25}$  obtained with the aqueous extract was lower than that of the hydroethanol extract (Table 2). However, both extracts still presented higher  $IC_{25}$  values than that of the control drug galantamine (0.86 mg/mL). Regarding BChE, the strongest inhibition was also obtained with the aqueous extract (Table 2), with a promising  $IC_{25}$  value about 3 times lower than that of the reference standard galantamine ( $IC_{25} = 1.81$  mg/mL). However, no correlation with the chemical profile was observed, suggesting that this biological activity may result from a synergism between all the compounds. To our knowledge, this is the first work reporting the BChE inhibitory activity of camel grass.

The disabled concentration of neurotransmitters in the synaptic cleft is associated with the impairment of cognitive functions and the progressive loss of memory. In this way, the consumption of non-volatile extracts of *Cymbopogon* species can be seen as a promising non-pharmacological approach to increase neurotransmitter concentrations, contributing to reduce the adverse symptoms of neurodegenerative diseases. Moreover, the severe side effects associated with the currently commercialized cholinesterase inhibitors, namely related to hepatotoxicity and gastrointestinal disorders [10], may be overcome with inhibitors from natural sources, such as camel grass extracts. In fact, cell viability assays conducted with the human gastric adenocarcinoma (AGS) and liver hepatocellular carcinoma (HepG2) cell lines exposed for 24 h to the different extracts revealed no toxicity under the tested concentrations, relative to the respective control ( $p > 0.05$ ) (Figure 5).

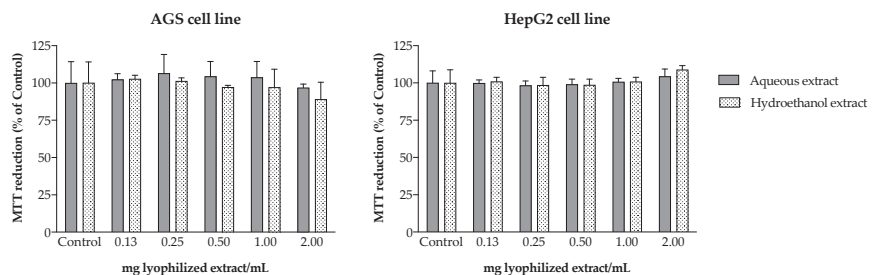


**Figure 5.** Effect of camel grass extracts on MTT reduction in AGS and HepG2 cells. Results are expressed as percentage of untreated control (mean  $\pm$  SD of four determinations performed in triplicate).

This preliminary *in vitro* toxicological screening encourage the consumption of camel grass extracts under the effective concentrations found in the present work.

### 3. Materials and Methods

#### 3.1. Standards and Reagents

Thiazolyl blue tetrazolium bromide (MTT),  $\beta$ -nicotinamide adenine dinucleotide reduced form (NADH), sodium nitroprusside dehydrate (SNP), sulphanilamide, naphthylethylene-diamine, ethanol, LPS from *Salmonella enterica*, formic acid, nitrotetrazolium blue chloride (NBT), phenazinemetosulfate (PMS), dimethyl sulfoxide (DMSO), sodium chloride (NaCl), sodium formate, HAase from bovine testes (type IV-S), hyaluronic acid (HA) sodium salt from *Streptococcus equi*, bovine serum albumin (BSA), AChE, acetylthiocholine iodine, BChE, S-butyrylthiocholine chloride, dexamethasone ( $\geq 97\%$ ), galantamine hydrobromide from *Lycoris* sp. ( $\geq 94\%$ ) and disodium cromoglycate (DSCG) ( $\geq 95\%$ ) were purchased from Sigma-Aldrich (St. Louis, MO, USA). Acetic acid (glacial), HPLC-grade methanol, acetonitrile, disodium tetraborate and 4-dimethylaminobenzaldehyde (DMAB) were from Merck (Darmstadt, Germany). Dulbecco's Modified Eagle Medium (DMEM), Dulbecco's phosphate buffered saline (DPBS), heat-inactivated foetal bovine serum (FBS) and Pen Strep solution (Penicillin 5000 units/mL and Streptomycin 5000 mg/mL) were from Gibco (Invitrogen, Paisley, UK). Murine macrophage-like cell line RAW 264.7, human hepatoma cell line and human gastric adenocarcinoma cell line AGS were from the American Type Culture Collection (LGC Standards S.L.U., Barcelona, Spain). 3-Caffeoylquinic acid (HPLC)  $\geq 98\%$ , 4-caffeoylquinic acid (HPLC)  $\geq 98\%$ , caffeic acid (HPLC)  $\geq 98\%$ , chlorogenic acid (HPLC)  $\geq 98\%$ , *p*-coumaric acid (HPLC)  $\geq 98\%$ , ferulic acid (HPLC)  $\geq 98\%$ , isoorientin (HPLC)  $\geq 98\%$ , luteolin-3',7-di-O-glucoside (HPLC)  $\geq 98\%$  and vitexin (HPLC)  $\geq 98\%$  were purchased from Extrasynthèse (Genay, France). Water was purified using a Milli-Q water purification system (Millipore, Bedford, MA, USA).

#### 3.2. Plant Material and Extract Preparation

Camel grass (aerial parts) was obtained from the herbalist "Dermapelle" (São Paulo, Brazil) ([www.dermapelle.com.br](http://www.dermapelle.com.br), accessed on 5 November 2022). Plant identification was attested according to eFloras (2008), and a voucher specimen was deposited at the herbarium of the Laboratory of Pharmacognosy, Faculty of Pharmacy, Porto University. After powdering (particle size  $< 910 \mu\text{m}$ ), two different extracts were prepared.

**Aqueous extract:** 300 mL of boiling water were added to 3 g of powdered plant material. The mixture was left at room temperature for 15 min, after which the resulting extract was filtered by cotton and subsequently by Buchner funnel. The filtrate was left to cool to room temperature, frozen and kept at  $-20 \text{ }^\circ\text{C}$  prior to lyophilization in a Virtis SP Scientific Sentry 2.0 apparatus (Gardiner, NY, USA).

**Hydroethanol extract:** 300 mL of a water:ethanol (1:1 *v/v*) mixture were added to 3 g of powdered plant material, and the mixture was subjected to sonication for 30 min. The resulting extract was filtered, following the same procedure used for the aqueous extract. The organic phase was evaporated to dryness under reduced pressure, at  $35 \text{ }^\circ\text{C}$ . The remaining aqueous solution was treated as described above.

The extraction yields were ca. 10.4 and 14.1% for aqueous and hydroethanol extract, respectively. The dried extracts were kept in a desiccator until analyses.

#### 3.3. HPLC-DAD Analysis

The analysis was performed on an analytical HPLC unit (Gilson, Lewis Center, OH, USA). Lyophilized extracts were dissolved in ultrapure water (30 mg/mL for the infusion and 20 mg/mL for the hydroethanol extract) and filtered through a  $0.45 \mu\text{m}$  pore membrane. Twenty microliters of the resulting solution were analysed using a Spherisorb ODS2 column ( $4.6 \times 250 \text{ mm}$ ,  $5 \mu\text{m}$  particle size; Waters, Ireland). A column heater (Column-Thermostat model Jetstream 2 Plus, Hockenheim, Germany) was used to keep temperature at  $25 \text{ }^\circ\text{C}$  during the analyses. The solvent system consisted in methanol (A) and water:formic acid

(95:5 *v/v*) (B), starting with 5% A and installing a gradient to obtain 15% A at 3 min, 25% A at 22 min, 30% A at 30 min, 45% A at 33 min, 55% A at 38 min, 75% A at 46 min, and 100% A from 48 to 50 min. The solvent flow rate was 0.9 mL/min. Spectral data from peaks were accumulated in the range of 190–600 nm. Data were processed with Clarity chromatography software (DataApex, Prague, Czech Republic). Compounds were identified by comparing their retention times and UV-Vis spectra with those of authentic standards. Phenolic compound quantification was achieved by measuring the absorbance recorded in the chromatograms relative to external standards: hydroxycinnamic acids (1–9) were determined at 320 nm, and flavonoids (10–20) at 350 nm.

Caffeic acid derivatives (3, 5, 6, and 8) were tentatively identified by comparing their UV spectra with that of caffeic acid, and quantified as caffeic acid; apigenin glycosides (10, 11, 15–20) were tentatively identified by comparing their UV spectra with that of vitexin (apigenin 8-C-glucoside), and quantified as vitexin; the luteolin glycoside (13) was tentatively identified by comparing its UV spectrum with that of isoorientin (luteolin 6-C-glucoside, 12), and quantified as isoorientin. The other compounds were quantified as themselves. Calibration curves, limit of detection (LOD) and limit of quantification (LOQ) are shown in Table S1.

#### 3.4. Superoxide Anion Radical ( $O_2^{\bullet-}$ ) Scavenging Assay

The anti-radical capacity of lemon grass extracts was evaluated as before [38]. Three independent assays were performed in triplicate. Quercetin was used as positive control.

#### 3.5. Nitric Oxide Radical ( $^{\bullet}NO$ ) Scavenging Assay

$^{\bullet}NO$  was generated from SNP dehydrate and determined as previously described [39]. Four independent assays were performed in duplicate. Quercetin was used as positive control.

#### 3.6. HAase Inhibition Assay

The assay was performed following the protocol proposed by our group [40]. DSCG was used as positive control. Three independent assays were performed in duplicate.

#### 3.7. AChE and BChE Inhibition Assays

The capacity to inhibit cholinesterase was determined based on Ellman's method and following a previously proposed procedure [41]. Galantamine was used as positive control. At least three independent assays were performed in triplicate.

#### 3.8. Cell Culture and Treatments

The murine macrophage cell line RAW 264.7, the human hepatoma cell line HepG2 and the human gastric adenocarcinoma cell line AGS were grown at 37 °C, in DMEM supplemented with GlutaMAX™-I, 10% FBS, 100 U/L penicillin and 100 µg/mL streptomycin, in a humidified atmosphere of 5% CO<sub>2</sub>. Cells were inoculated in 96-well plates and cultured until confluence. Camel grass lyophilized extracts were dissolved in DMEM, sterilized by filtration through a 0.22 µm pore membrane and stored at –20 °C until use. Five dilutions of the extracts were prepared in supplemented DMEM immediately before cell exposure. To determine the effect of the extracts on NO production by RAW 264.7 cells, a 2 h pre-treatment with different extract concentrations or vehicle was undertaken, followed by the addition of 1 µg/mL LPS (or vehicle) and a further incubation for 22 h at 37 °C in a humidified atmosphere of 5% CO<sub>2</sub>. The effect on NO production was also evaluated in the absence of LPS, in order to observe possible changes in NO basal levels. No LPS was added to the negative controls. Four independent assays were performed in duplicate.



### 3.9. Toxicity to RAW 264.7 Cells

Cytotoxicity of camel grass extracts was assessed by the MTT assay, as previously described by Barbosa et al. [39]. DMSO (20%) was used as positive control.

### 3.10. NO Release by RAW 264.7 Cells

After the incubation period, the nitrite accumulated in the culture medium was determined using the Griess reaction, as previously reported [39]. Dexamethasone was used as positive control. Four independent experiments were performed in duplicate.

### 3.11. Toxicity to AGS and HepG2 Cells

The human gastric cell line AGS was used as model to assess the camel grass extracts' gastric toxicity. Cells were seeded at a density of 15,000 cells/well in 96-well plates and, after confluence, incubated with the extracts for 24 h (37 °C). The human hepatoma cell line HepG2 was used to predict the toxicity of the extracts to human liver. Cells were seeded at a density of 10,000 cells/well into 96-well plates and, after confluence, incubated with the extracts for 24 h at 37 °C. The MTT assay was conducted for both cell lines, following the conditions described before. DMSO (20%) was used as positive control.

### 3.12. Statistical Analysis

Statistical analysis was performed using IBM SPSS STATISTICS software, version 24.0, IBM Corporation, New York, NY, USA (2011). Data were analysed for normality and homogeneity of variance by Kolmogorov–Smirnov and Leven's tests and then submitted to one-way ANOVA, using a Tukey's HSD (honest significant difference) as post hoc test for cell assays, or to a two-tailed unpaired t-test to compare the total content of phenolic compounds and the IC<sub>50</sub> values of the bioactivity assays. IC<sub>50</sub> values (expressed in mg of lyophilized extract/mL), concerning both cell-free and cell assays were presented as mean ± SD of at least three independent experiments. A Pearson correlation test was used to compare normalized expression data between the chemical profile and the biological activities of camel grass extracts.

## 4. Conclusions

The biological activities of camel grass extracts explored herein provided evidence that supports the use of this species in traditional medicine, encouraging its consumption as a non-pharmacological measure for the treatment and relief of inflammation and neurodegeneration-associated conditions. Some of these bioactivities are intimately related with the chemical profile. In fact, the consumption of aqueous extract seems to be advantageous compared to the hydroethanol one, as it is effective in lower doses and can be directly consumed without the need for technological manipulation. As demonstrated herein, camel grass constitutes a natural source of compounds with promising antioxidant and anti-inflammatory potential that can act in several mediators and enzymes related to the inflammatory process. Due to their capacity to inhibit key enzymes involved in the process of neurodegeneration, bioactive extracts can also be promising as a natural alternative to synthetic neuromodulators that influence mood and memory, and their incorporation in new functional foods may create new added-value products.

**Supplementary Materials:** The following supporting information can be downloaded at: <https://www.mdpi.com/article/10.3390/molecules27227707/s1>, Table S1: Calibration curves of authentic standards used for quantification of different phenolic compounds.

**Author Contributions:** Methodology, E.G., G.L., M.B. and J.B.; investigation, G.L. and E.G.; writing—original draft preparation, G.L. and E.G.; writing—review and editing, M.B., J.B. and P.V.; supervision, P.V.; funding acquisition, P.V. All authors have read and agreed to the published version of the manuscript.

**Funding:** This research was funded by FCT/MEC, Fundação para a Ciência e Tecnologia/Ministério da Educação e Ciência, grant number UID/QUI/50006/2013, and by the European Union (FEDER under the Partnership Agreement PT2020), from Norte Portugal Regional Operational Programme, grant number NORTE-01-0145-FEDER-000024.

**Institutional Review Board Statement:** Not applicable.

**Informed Consent Statement:** Not applicable.

**Data Availability Statement:** Not applicable.

**Acknowledgments:** G.L. thanks FCT for her work contract through the Scientific Employment Stimulus-Individual Call (CEECIND/01768/2021). M.B. thanks ProDGNE project (EJPRD/0001/2020) for her work contract through the European Union's Horizon 2020 research and innovation programme under the EJP RD COFUND-EJP N 825575.

**Conflicts of Interest:** The authors declare no conflict of interest. The funders had no role in the design of the study, in the collection, analyses, or interpretation of data, in the writing of the manuscript or in the decision to publish the results.

## References

- Palhares, R.M.; Gonçalves Drummond, M.; dos Santos Alves Figueiredo Brasil, B.; Pereira Cosenza, G.; das Graças Lins Brandão, M.; Oliveira, G. Medicinal plants recommended by the world health organization: DNA barcode identification associated with chemical analyses guarantees their quality. *PLoS ONE* **2015**, *10*, e0127866.
- Bodeker, G.; Ong, C.-K. *WHO Global Atlas of Traditional, Complementary and Alternative Medicine*; World Health Organization: Geneva, Switzerland, 2005; Volume 1.
- Calixto, J.B.; Campos, M.M.; Otuki, M.F.; Santos, A.R. Anti-inflammatory compounds of plant origin. Part II. Modulation of pro-inflammatory cytokines, chemokines and adhesion molecules. *Planta Med.* **2004**, *70*, 93–103. [[PubMed](#)]
- Barbosa, M.; Lopes, G.; Andrade, P.B.; Valentão, P. Bioprospecting of brown seaweeds for biotechnological applications: Phlorotannin actions in inflammation and allergy network. *Trends Food Sci. Technol.* **2019**, *86*, 153–171. [[CrossRef](#)]
- Coleman, J.W. Nitric oxide in immunity and inflammation. *Int. Immunopharmacol.* **2001**, *1*, 1397–1406. [[CrossRef](#)]
- Kim, H.K.; Cheon, B.S.; Kim, Y.H.; Kim, S.Y.; Kim, H.P. Effects of naturally occurring flavonoids on nitric oxide production in the macrophage cell line RAW 264.7 and their structure–activity relationships. *Biochem. Pharmacol.* **1999**, *58*, 759–765. [[CrossRef](#)]
- Abot, A.; Fried, S.; Cani, P.D.; Knauf, C. Reactive oxygen species/reactive nitrogen species as messengers in the gut: Impact on physiology and metabolic disorders. *Antioxid. Redox Signal.* **2022**, *37*, 394–415. [[CrossRef](#)]
- Jivad, N.; Rabiei, Z. A review study on medicinal plants used in the treatment of learning and memory impairments. *Asian Pac. J. Trop. Biomed.* **2014**, *4*, 780–789. [[CrossRef](#)]
- Shah, A.; Dar, T.; Dar, P.; Ganie, S.; Kamal, M. A current perspective on the inhibition of cholinesterase by natural and synthetic inhibitors. *Curr. Drug Metab.* **2017**, *18*, 96–111. [[CrossRef](#)]
- Suganthi, N.; Pandian, S.K.; Devi, K.P. Cholinesterase inhibitors from plants: Possible treatment strategy for neurological disorders—a review. *Int. J. Biomed Pharm. Sci.* **2009**, *3*, 87–103.
- Shah, G.; Shri, R.; Panchal, V.; Sharma, N.; Singh, B.; Mann, A. Scientific basis for the therapeutic use of *Cymbopogon citratus*, stapf (Lemon grass). *J. Adv. Pharm. Technol. Res.* **2011**, *2*, 3. [[CrossRef](#)]
- Avoseh, O.; Oyedeji, O.; Rungqu, P.; Nkeh-Chungag, B.; Oyedeji, A. *Cymbopogon* species; ethnopharmacology, phytochemistry and the pharmacological importance. *Molecules* **2015**, *20*, 7438–7453. [[CrossRef](#)] [[PubMed](#)]
- Oladeji, O.S.; Adelowo, F.E.; Ayodele, D.T.; Odelade, K.A. Phytochemistry and pharmacological activities of *Cymbopogon citratus*: A review. *Sci. Afr.* **2019**, *6*, e00137. [[CrossRef](#)]
- Pavlović, I.; Omar, E.; Drobac, M.; Radenković, M.; Branković, S.; Kovačević, N. Chemical composition and spasmolytic activity of *Cymbopogon schoenanthus* (L.) Spreng. (Poaceae) essential oil from Sudan. *Arch. Biol. Sci.* **2017**, *69*, 409–415. [[CrossRef](#)]
- Khadri, A.; Neffati, M.; Smiti, S.; Falé, P.; Lino, A.R.L.; Serralheiro, M.L.M.; Araújo, M.E.M. Antioxidant, anti-acetylcholinesterase and antimicrobial activities of *Cymbopogon schoenanthus* L. Spreng (lemon grass) from Tunisia. *LWT-Food Sci. Technol.* **2010**, *43*, 331–336. [[CrossRef](#)]
- Ben Othman, M.; Han, J.; El Omri, A.; Ksouri, R.; Neffati, M.; Isoda, H. Antistress effects of the ethanolic extract from *Cymbopogon schoenanthus* growing wild in Tunisia. *Evid. Based Complement. Altern. Med.* **2013**, *2013*, 737401. [[CrossRef](#)]
- Raut, J.S.; Karuppayil, S.M. A status review on the medicinal properties of essential oils. *Ind. Crops Prod.* **2014**, *62*, 250–264. [[CrossRef](#)]
- Figueirinha, A.; Cruz, M.T.; Francisco, V.; Lopes, M.C.; Batista, M.T. Anti-inflammatory activity of *Cymbopogon citratus* leaf infusion in lipopolysaccharide-stimulated dendritic cells: Contribution of the polyphenols. *J. Med. Food* **2010**, *13*, 681–690. [[CrossRef](#)]

19. Figueirinha, A.; Paranhos, A.; Pérez-Alonso, J.J.; Santos-Buelga, C.; Batista, M.T. *Cymbopogon citratus* leaves: Characterization of flavonoids by HPLC–PDA–ESI/MS/MS and an approach to their potential as a source of bioactive polyphenols. *Food Chem.* **2008**, *110*, 718–728. [[CrossRef](#)]
20. Francisco, V.; Figueirinha, A.; Costa, G.; Liberal, J.; Lopes, M.C.; García-Rodríguez, C.; Geraldés, C.F.; Cruz, M.T.; Batista, M.T. Chemical characterization and anti-inflammatory activity of luteolin glycosides isolated from lemongrass. *J. Funct. Foods* **2014**, *10*, 436–443. [[CrossRef](#)]
21. Francisco, V.; Figueirinha, A.; Neves, B.M.; García-Rodríguez, C.; Lopes, M.C.; Cruz, M.T.; Batista, M.T. *Cymbopogon citratus* as source of new and safe anti-inflammatory drugs: Bio-guided assay using lipopolysaccharide-stimulated macrophages. *J. Ethnopharmacol.* **2011**, *133*, 818–827. [[CrossRef](#)]
22. Sousa, R.; Figueirinha, A.; Batista, M.T.; Pina, M.E. Formulation effects in the antioxidant activity of extract from the leaves of *Cymbopogon citratus* (Dc) stapf. *Molecules* **2021**, *26*, 4518. [[CrossRef](#)]
23. Musa, H.A.A.; Ahmed, E.; Osman, G.; Ali, H.; Müller, J. Microbial load and phytochemicals stability of camel hay (*Cymbopogon schoenanthus* L.) leaves as affected by gamma irradiation. *Agric. Biol. J. N. Am.* **2010**, *1*, 662–670.
24. Abu-Serie, M.M.; Habashy, N.H.; Maher, A.M. *In vitro* anti-nephrotoxic potential of Ammi visnaga, Petroselinum crispum, Hordeum vulgare, and *Cymbopogon schoenanthus* seed or leaf extracts by suppressing the necrotic mediators, oxidative stress and inflammation. *BMC Complement. Altern. Med.* **2019**, *19*, 1–16. [[CrossRef](#)]
25. Najjaa, H.; Abdelkarim, B.A.; Doria, E.; Boubakri, A.; Trabelsi, N.; Falleh, H.; Tlili, H.; Neffati, M. Phenolic composition of some Tunisian medicinal plants associated with anti-proliferative effect on human breast cancer MCF-7 cells. *EuroBiotech J.* **2020**, *4*, 104–112. [[CrossRef](#)]
26. Rocchetti, G.; Alcántara, C.; Bäuerl, C.; García-Pérez, J.V.; Lorenzo, J.M.; Lucini, L.; Collado, M.C.; Barba, F.J. Bacterial growth and biological properties of *Cymbopogon schoenanthus* and *Ziziphus lotus* are modulated by extraction conditions. *Food Res. Int.* **2020**, *136*, 109534. [[CrossRef](#)]
27. Cheel, J.; Theoduloz, C.; Rodríguez, J.; Schmeda-Hirschmann, G. Free radical scavengers and antioxidants from Lemongrass (*Cymbopogon citratus* (DC.) Stapf.). *J. Agric. Food Chem.* **2005**, *53*, 2511–2517. [[CrossRef](#)]
28. Campos, J.; Schmeda-Hirschmann, G.; Leiva, E.; Guzmán, L.; Orrego, R.; Fernández, P.; González, M.; Radojkovic, C.; Zuñiga, F.; Lamperti, L. Lemon grass (*Cymbopogon citratus* (DC) Stapf) polyphenols protect human umbilical vein endothelial cell (HUVECs) from oxidative damage induced by high glucose, hydrogen peroxide and oxidised low-density lipoprotein. *Food Chem.* **2014**, *151*, 175–181. [[CrossRef](#)]
29. Roriz, C.L.; Barros, L.; Carvalho, A.M.; Santos-Buelga, C.; Ferreira, I.C. *Pterospartum tridentatum*, *Gomphrena globosa* and *Cymbopogon citratus*: A phytochemical study focused on antioxidant compounds. *Food Res. Int.* **2014**, *62*, 684–693. [[CrossRef](#)]
30. Roriz, C.L.; Barros, L.; Carvalho, A.M.; Santos-Buelga, C.; Ferreira, I.C. Scientific validation of synergistic antioxidant effects in commercialised mixtures of *Cymbopogon citratus* and *Pterospartum tridentatum* or *Gomphrena globosa* for infusions preparation. *Food Chem.* **2015**, *185*, 16–24. [[CrossRef](#)]
31. Reuter, S.; Gupta, S.C.; Chaturvedi, M.M.; Aggarwal, B.B. Oxidative stress, inflammation, and cancer: How are they linked? *Free Radic. Biol. Med.* **2010**, *49*, 1603–1616. [[CrossRef](#)]
32. González, R.; Ballester, I.; López-Posadas, R.; Suárez, M.; Zarzuelo, A.; Martínez-Augustin, O.; Medina, F.S.D. Effects of flavonoids and other polyphenols on inflammation. *Crit. Rev. Food Sci. Nutr.* **2011**, *51*, 331–362. [[CrossRef](#)]
33. Francisco, V.; Costa, G.; Figueirinha, A.; Marques, C.; Pereira, P.; Neves, B.M.; Lopes, M.C.; García-Rodríguez, C.; Cruz, M.T.; Batista, M.T. Anti-inflammatory activity of *Cymbopogon citratus* leaves infusion via proteasome and nuclear factor- $\kappa$ B pathway inhibition: Contribution of chlorogenic acid. *J. Ethnopharmacol.* **2013**, *148*, 126–134. [[CrossRef](#)]
34. Girish, K.; Kemparaju, K. The magic glue hyaluronan and its eraser hyaluronidase: A biological overview. *Life Sci.* **2007**, *80*, 1921–1943. [[CrossRef](#)]
35. Khadri, A.; Serralheiro, M.; Nogueira, J.; Neffati, M.; Smiti, S.; Araújo, M. Antioxidant and antiacetylcholinesterase activities of essential oils from *Cymbopogon schoenanthus* L. Spreng. Determination of chemical composition by GC–mass spectrometry and <sup>13</sup>C NMR. *Food Chem.* **2008**, *109*, 630–637. [[CrossRef](#)]
36. Goes, T.C.; Ursulino, F.R.C.; Almeida-Souza, T.H.; Alves, P.B.; Teixeira-Silva, F. Effect of lemongrass aroma on experimental anxiety in humans. *J. Altern. Complement. Med.* **2015**, *21*, 766–773. [[CrossRef](#)]
37. Adaramoye, O.A.; Azeez, F.A. Evaluation of antioxidant and acetylcholinesterase-inhibitory properties of methanol extracts of *Nauclealatifolia*, *Cymbopogon citratus* and *Cocos nucifera*: An *in vitro* study. *Br. J. Med. Med. Res.* **2014**, *4*, 2156–2170. [[CrossRef](#)]
38. Lopes, G.; Barbosa, M.; Andrade, P.B.; Valentão, P. Phlorotannins from Fucales: Potential to control hyperglycemia and diabetes-related vascular complications. *J. Appl. Phycol.* **2019**, *31*, 3143–3152. [[CrossRef](#)]
39. Barbosa, M.; Lopes, G.; Ferreres, F.; Andrade, P.B.; Pereira, D.M.; Gil-Izquierdo, Á.; Valentão, P. Phlorotannin extracts from Fucales: Marine polyphenols as bioregulators engaged in inflammation-related mediators and enzymes. *Algal Res.* **2017**, *28*, 1–8. [[CrossRef](#)]

40. Favas, R.; Morone, J.; Martins, R.; Vasconcelos, V.; Lopes, G. Cyanobacteria Secondary Metabolites as Biotechnological Ingredients in Natural Anti-Aging Cosmetics: Potential to Overcome Hyperpigmentation, Loss of Skin Density and UV Radiation-Deleterious Effects. *Mar. Drugs* **2022**, *20*, 183. [[CrossRef](#)]
41. Bernardo, J.; Ferreres, F.; Gil-Izquierdo, Á.; Valentao, P.; Andrade, P.B. Medicinal species as MTDLs: *Turnera diffusa* Willd. Ex Schult inhibits CNS enzymes and delays glutamate excitotoxicity in SH-SY5Y cells via oxidative damage. *Food Chem. Toxicol.* **2017**, *106*, 466–476. [[CrossRef](#)]



Review

# Effects of Natural Polyphenols on Skin and Hair Health: A Review

Mang Sun <sup>1</sup>, Ya Deng <sup>1</sup>, Xining Cao <sup>1</sup>, Lu Xiao <sup>1</sup>, Qian Ding <sup>1</sup>, Fuqing Luo <sup>1</sup>, Peng Huang <sup>1</sup>, Yuanyuan Gao <sup>2</sup>, Mengqi Liu <sup>3</sup> and Hengguang Zhao <sup>1,\*</sup>

<sup>1</sup> Department of Dermatology, The Second Affiliated Hospital of Chongqing Medical University, Chongqing 400010, China

<sup>2</sup> Department of Dermatology, Daping Hospital, The Army Medical University, Chongqing 400042, China

<sup>3</sup> Bioengineering College, Chongqing University, Chongqing 400030, China

\* Correspondence: zhao@cqmu.edu.cn

**Abstract:** The skin is the largest organ of the body and plays multiple essential roles, ranging from regulating temperature, preventing infections, to ultimately affecting human health. A hair follicle is a complex cutaneous appendage. Skin diseases and hair loss have a significant effect on the quality of life and psychosocial adjustment of individuals. However, the available traditional drugs for treating skin and hair diseases may have some insufficiencies; therefore, a growing number of researchers are interested in natural materials that could achieve satisfactory results and minimize adverse effects. Natural polyphenols, named for the multiple phenolic hydroxyl groups in their structures, are promising candidates and continue to be of scientific interest due to their multifunctional biological properties and safety. Polyphenols have a wide range of pharmacological effects. In addition to the most common effect, antioxidation, polyphenols have anti-inflammatory, bacteriostatic, antitumor, and other biological effects associated with reduced risk of a number of chronic diseases. Various polyphenols have also shown efficacy against different types of skin and hair diseases, both in vitro and in vivo, via different mechanisms. Thus, this paper reviews the research progress in natural polyphenols for the protection of skin and hair health, especially focusing on their potential therapeutic mechanisms against skin and hair disorders. A deep understanding of natural polyphenols provides a new perspective for the safe treatment of skin diseases and hair loss.

**Keywords:** polyphenols; skin; hair; human health

**Citation:** Sun, M.; Deng, Y.; Cao, X.; Xiao, L.; Ding, Q.; Luo, F.; Huang, P.; Gao, Y.; Liu, M.; Zhao, H. Effects of Natural Polyphenols on Skin and Hair Health: A Review. *Molecules* **2022**, *27*, 7832. <https://doi.org/10.3390/molecules27227832>

Academic Editor: Nour Eddine Es-Safi

Received: 13 October 2022

Accepted: 11 November 2022

Published: 14 November 2022

**Publisher's Note:** MDPI stays neutral with regard to jurisdictional claims in published maps and institutional affiliations.



**Copyright:** © 2022 by the authors. Licensee MDPI, Basel, Switzerland. This article is an open access article distributed under the terms and conditions of the Creative Commons Attribution (CC BY) license (<https://creativecommons.org/licenses/by/4.0/>).

## 1. Introduction

The skin is the largest organ, with a complicated structure and multiple physical functions, thus providing a barrier against outside hazards. In addition, the skin is also involved in regulating the hydroelectrolytic balance and immune response of individual organisms. Due to the extensive distribution and functional diversity of the skin, skin diseases are among the most common disorders. A hair follicle is a complex cutaneous appendage. Studies have shown that hair loss has a significant effect on the quality of life and psychosocial adjustment of people. Hair loss can lead to social anxiety, symptoms of depression and anxiety, low self-confidence, and dissatisfaction with life [1]. Many factors are related to skin and hair diseases, including genetics, local infections, endocrine disorders, and mental stress. People have used various drugs and remedies to treat skin and hair diseases according to their different pathogeneses. However, the available drugs for treating skin and hair diseases still have many drawbacks. Considering the occurrence and complexity of skin and hair diseases, as well as the adverse effects of available drugs, research investigating novel remedies and less dangerous natural materials has increased in recent years.

Polyphenols, which are widely found in plants, play an increasingly important role in protecting human health. Polyphenolic compounds are chemical substances commonly

found in fruits, vegetables, and cereals. They are named for the multiple phenolic hydroxyl groups in their structures. In recent years, along with developments in science and technology that have enabled structure identification, over 1000 kinds of polyphenols have been identified, and their pharmacological activities have been extensively studied. According to their different chemical constitutions, polyphenols are mainly classified into four groups, including phenolic acids, flavonoids, stilbenes, and lignans (Figure 1). Phenolic acids can be further identified as hydroxybenzoic and hydroxycinnamic acids. Some well-known polyphenols include resveratrol, quercetin, curcumin, epigallocatechin gallate, catechin, hesperetin, cyanidin, procyanidin, caffeic acid, and genistein [2]. Polyphenols have a wide range of pharmacological effects. In addition to the most common effect, antioxidation, polyphenols have anti-inflammatory, bacteriostatic, antitumor, and other biological effects associated with reduced risk of a number of chronic diseases, including cardiovascular disease and cancer [3–6]. Various polyphenols have also shown efficacy against different types of skin and hair diseases, both in vitro and in vivo, via different mechanisms [7–9]. Herein, we primarily focused on the effects and mechanisms of polyphenols related to skin and hair health.

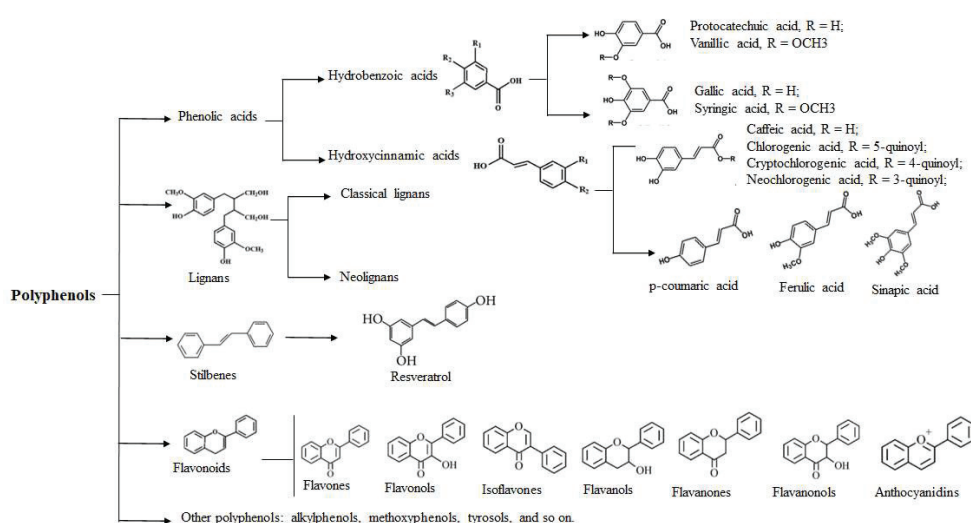


**Figure 1.** Main classification and basic chemical structures of polyphenols.

## 2. Roles of Polyphenols in Skin Health

### 2.1. Anti-Inflammatory Effects of Natural Polyphenols

Inflammatory skin diseases encompass a wide spectrum of skin disorders and affect people of all ages and skin types. The majority of chronic inflammatory skin diseases manifest a relapsing and remitting course throughout life, including atopic dermatitis, psoriasis vulgaris, lichen planus, and so on. These diseases are associated with complex multifactorial etiologies in which genetic and environmental factors interact both in the genesis and development of the disease. Specifically, signaling molecules released from the injured stratum corneum initiate a cytokine cascade, triggering an inflammatory response, which then contributes to the pathogenesis of a variety of dermatoses [10]. Glucocorticoids and biological agents are now commonly used to manage inflammatory skin diseases via different mechanisms, but systemic corticosteroids and immunosuppressives can only be used for short-term treatment because of their serious adverse effects, including growth inhibition, hematopoietic suppression, glaucoma, hypertension, hyperglycemia, osteoporosis, myopathy, cataracts, infection, and thin or easily bruised skin [11]. Biological therapies have revolutionized moderate-to-severe inflammatory dermatosis treatment, focusing on

inhibiting selective key pathways of inflammation, including interleukin-4 (IL-4), IL-13, IL-31, IL-12/23, IL-17, thymic stromal lymphopoietin (TSLP), and tumor necrosis factor (TNF- $\alpha$ ) [12]. Side effects of biological agents remain unavoidable, for instance, associated serious bacterial, viral, and fungal infections, including active hepatitis B virus, reactivation of latent tuberculosis infection, and increased risk of *Candida* infections, as well as worsening of pre-existing inflammatory bowel disease and, rarely, new-onset ulcerative colitis [13–16].

Many polyphenols, especially flavonoids, possess potent anti-inflammatory properties and can regulate immunity [17–21]. Several natural polyphenols have been well studied for their beneficial effects in autoimmune inflammatory diseases. Some polyphenols, such as resveratrol, chlorogenic acid, caffeic acid, pelargonin, and ferulic acid, modulate pro-inflammatory gene expression and cytokine production, thus impacting immune cell populations [22,23]. The non-flavonoid curcumin was shown to downregulate the expression of TNF, IL-1, adhesion molecule-like vascular cell adhesion molecule-1 (VCAM-1), and intercellular adhesion molecule-1 (ICAM-1) in human umbilical vein endothelial cells and inflammatory mediators such as prostaglandins and leukotrienes. Topical application of green tea polyphenols (GTPs) and epigallocatechin-3-gallate (EGCG) resulted in inhibited production of prostaglandin metabolites, including prostaglandin D2 (PGD2), prostaglandin E2 (PGE2), and prostaglandin F2 $\alpha$  (PGF2 $\alpha$ ) [24]. Resveratrol can induce endothelial nitric oxide synthase (eNOS), inhibit cyclooxygenase (COX), and inactivate peroxisome proliferator-activated receptor gamma (PPAR $\gamma$ ) in vitro and in vivo [25,26]. What's more, curcumin downregulated signal transducer and activator of transcription 3 (STAT3) and nuclear factor kappa-light-chain-enhancer of activated B cells (NF- $\kappa$ B) and reduced the expression of toll-like receptor-2 (TLR-2) and -4 while upregulating PPAR $\gamma$  in an in vivo study [27,28]. Caffeic acid phenethyl ester suppresses LPS-mediated TLR-4 and NF- $\kappa$ B activation in macrophages. Quercetin was also confirmed to inhibit leukotriene biosynthesis in human polymorphonuclear leukocytes [29].

Based on their anti-inflammatory and immunomodulatory effects, natural polyphenols are used to treat a variety of skin diseases. Vitiligo is a common skin disorder characterized by hypopigmentation. *Ginkgo biloba* is known to be a rich source of polyphenolics. *G. biloba* extract was associated with the progression of vitiligo by reducing depigmentation and promoting repigmentation [30,31]. Carnosic acid is a natural benzenediol abietane diterpene found in rosemary. Carnosol was able to reduce levels of neutrophils, inflammatory cytokines (IL-1 $\beta$  and TNF- $\alpha$ ), COX-2, and iNOS in mice blood [32,33]. Animals with atopic dermatitis topically treated with carnosol showed obvious skin lesion reductions [34]. Artichoke polyphenols, as potential anti-inflammatory agents, can improve the vasodilatation and microcirculation of endothelial cells by inhibiting nitric oxide (NO) production in both macrophages and endothelial cells. Moreover, artichoke polyphenols can improve skin elasticity and roughness by inhibiting vascular aging, thus acting as a protective ingredient for both lymphatic and endothelial cells. These effects could be the direct result of their antioxidant or anti-inflammatory properties and indirect result via modulation of molecular pathways that improve the expression of genes involved in anti-aging mechanisms [35].

## 2.2. Antioxidant Properties of Natural Polyphenols

Human life is dependent upon oxygen. Occasionally, oxygen becomes mutagenic and toxic. Oxidative stress plays a very important role in human dermal diseases and skin aging [36,37]. Overproduction of reactive oxygen species (ROS) can damage the membranes, lipids, proteins, RNA, and DNA of cells. The traditional view is that the antioxidant activity of a polyphenol is positively correlated with its number of phenolic hydroxyl groups. As excellent antioxidants, the phenolic hydroxyl groups of polyphenols can decrease levels of free radicals by providing electrons and can also be used as free radical scavengers or metal-chelating agents (chelating metals with redox activity, such as copper and iron) to inhibit or eliminate the formation of free radicals, thereby destroying the progress of free radical chain peroxidation [38].



The skin is directly and frequently exposed to ultraviolet (UV) rays from the sun (UVA: 320–400 nm and UVB: 280–320 nm) [39,40]. UV radiation is involved in the pathogenesis of severe skin conditions, including photoaging of the skin, immune disorders, and skin cancer [41,42]. Many plants are rich in antioxidants because they must survive continual UV radiation exposure. For example, a marine algal polyphenol isolated from the brown alga *Ecklonia cava* was confirmed to have an inhibitory effect on melanogenesis and a protective property against photo-oxidative stress induced by UVB. Intracellular ROS induced by UVB radiation was reduced by the addition of the marine algal polyphenol and cell viability was dose-dependently increased. Moreover, the marine algal polyphenol demonstrated strong protective properties against UVB radiation-induced DNA damage, including damaged tail intensity and morphological changes in fibroblasts [43]. Clove is another kind of plant that is widely used in Chinese medicine and also used in the cosmetics industry. Cloves are rich in natural polyphenols such as ferric acid. Our previous study proved that cloves can decrease UVB damage through their influence on  $\text{Na}^+\text{-K}^+\text{-ATPase}$ , which led to a reduction in oxidation and inflammation in mice, thereby inhibiting skin injury and protecting the skin [44]. The above studies demonstrate that many natural polyphenols contribute to the prevention of UVB skin damage and inhibit photodamage to the skin. They are very promising for future research and applications.

Estrogen deficiency is associated with deteriorating skin health as it affects internal structural balance, dermal cellular mechanisms, and other biological functions. The effects of estrogen deficiency include loss of elastin, collagen, fibroblast dysfunction, increased vascular and matrix metalloproteinase activity, and extracellular and cellular degradation, leading to wrinkles, atrophy, dryness, impaired wound healing/barrier function, and reduced antioxidant capacity. Several studies have examined polyphenolic phytochemicals, also known as phytoestrogens, which act as estrogen receptor modulators (SERMs) and possess  $\text{ER}\beta$ -agonist properties [45]. The resveratrol compound extracted from grapes has been known for its anti-aging effects for over a decade [22,46]. Recently, an increasing number of studies have reported the benefits of resveratrol on the skin, including its antioxidant properties, which are achieved through activation of nuclear factor erythroid 2-related factor 2 (Nrf2) by reducing the expression of nuclear factor kappa-B (NF- $\kappa$ B) and activating protein 1 (AP-1), fibroblast proliferation by increasing type I, II, and III collagen expression through activation of sirtuin 1 (SIRT 1, anti-aging factor), and inhibition of melanogenesis [45–47]. In preliminary studies, human skin benefited from several types of resveratrol analogs, the most potent of which was 4'-acetoxyresveratrol (4AR) [45,48], which increased human genetic expression of the antioxidant superoxide dismutase (SOD) [45]. Equol is a relatively new phytochemical found in food sources and plants [45,49,50]. It is classified as a phytoestrogen with selective SERM properties and binds to  $\text{ER}\beta$  in keratinocytes [49–51]. Equol exhibits skin-protecting antioxidant properties. In a clinical investigation involving a 12-week single-center study with 59 female subjects, equol significantly improved skin characteristics, including hydration and firmness, which suggested that equol may be effective in treating estrogen-deficient skin [52].

Along with their antioxidant properties, some natural polyphenols have potential whitening effects and prominent protective effects against cell damage and skin aging, which may be used in the cosmeceutical and pharmaceutical industries (Table 1) [44,53–56].

**Table 1.** Several marketed formulations based on polyphenols as anti-aging cosmeceuticals.

Plant	Compounds	Bioactivity
Blackberry	Anthocyanins	$\downarrow$ IL-6, $\downarrow$ TNF- $\alpha$ , $\downarrow$ ERK1/2, $\downarrow$ P38, $\downarrow$ JNK1/2, $\downarrow$ MKK4, $\downarrow$ PGE2, $\downarrow$ iNOS, $\downarrow$ NF- $\kappa$ B, $\downarrow$ I $\kappa$ - $\beta$ a
Cacao bean	Flavonoids	$\downarrow$ Wrinkle formation, $\uparrow$ Collagen level, $\downarrow$ MMP-1, $\downarrow$ AP-1 expression
Strawberry	Phenolic	$\downarrow$ ROS, $\downarrow$ NF- $\kappa$ $\beta$ , $\downarrow$ I $\kappa$ - $\beta$ a phosphorylation, $\downarrow$ TNF- $\alpha$ , $\downarrow$ IL-6, $\downarrow$ IL-1 $\beta$ , $\uparrow$ Nrf2, $\uparrow$ CAT, $\uparrow$ HO-1

Table 1. Cont.

Plant	Compounds	Bioactivity
Black rice	Flavonoids	↓ROS, ↓MMP-1, ↓MMP-3, ↓Procollagen type 1, ↓p-cfos, ↓p-cjun, ↓p-p38, ↓p-JNK
Grape	Flavonoids Phenolics Anthocyanins Resveratrol	↑Nrf2, ↑HO-1, ↓MMP-1, ↓MMP-9
Tea	EGCG	↑Erk, ↑Akt, ↑Bcl-2/Bax
Clove	Eugenol Gallic acid	↓Skin wrinkle, ↓Skin Thickness, ↓ROS, ↓MMP-1, ↓MMP-3, ↓IL-6, ↓p-c-fos, ↓p-c-jun, ↑NF-κB, ↑Ik-βa, ↑Nrf2, ↑HO-1, ↑NQO-1, ↑Skin hydration, ↑p-Smad2/3, ↑TGF-β1

### 2.3. Anti-Allergic Effects of Natural Polyphenols

It is said that allergic diseases are prevalent in approximately 40% of the general population and will rapidly increase to 50% [57,58]. The skin is very often the target organ involved in allergic reactions, including urticaria, angioedema, atopic dermatitis, contact dermatitis, and vasculitis. This may be associated with many immunologically competent cells, such as mast cells, lymphocytes, eosinophils, neutrophils, and Langerhans cells, especially antigen-presenting Langerhans cells [59]. As an alternative to conventional treatments with corticosteroids and antihistamines, polyphenols also exhibit anti-allergic effects, including inhibiting the production of proinflammatory cytokines and leukocytes, as well as histamine release [60]. Polyphenols have also been shown to regulate the balance of Th1/Th2 and inhibit the formation of antigen-specific IgE antibodies. Two main mechanisms may be involved in this process. Firstly, polyphenols may affect the allergen-IgE complex formation [61]. Secondly, polyphenols may affect the binding of this complex to its receptors (FcεRI) on basophils and mast cells [62]. For instance, the ingestion of tannins extracted from apples has been proven to prevent food allergies, which may be associated with the increased proportion of  $\gamma\delta$  TCR T cells in intestinal intraepithelial lymphocytes [63]. EGCG has a strong suppressive effect on the migratory and adhesive abilities of peripheral blood B cells. This suppressive effect is mediated by the binding of EGCG to CD11b on B cells, and the consequent suppression of B-cell extravasation to the extravascular space. Because of the important role played by B cells in humoral immunity, EGCG is a promising drug for the prevention and/or treatment of skin allergic diseases [64]. Overall, polyphenols hold promise as anti-allergy agents capable of influencing multiple biological pathways and immune cell functions involved in the allergic immune response, and thus deserve further investigation.

### 2.4. Antimicrobial Activity of Polyphenols

Antibiotic therapy has been a fundamental treatment for skin diseases for many years; however, the adverse reactions caused by medications end up making the treatment unpleasant, in addition to cases of decreased sensitivity to antibiotics. Natural products are becoming increasingly common in dermatology due to the increased resistance of bacteria to synthetic antibiotics and the active principle of medicinal plants becoming new options as antiseptics and antimicrobials. It is believed that flavonoids, such as caffeic acid (CA), benzoic acid, and cinnamic acid, appear to act on the membrane or cell wall of the microorganism, causing functional and structural destruction [65]. Natural polyphenols can play dynamic roles as antimicrobials against bacteria, fungi, and viruses. Pomegranate, a kind of fruit from the Persian region, is rich in polyphenols of varying content during different stages of maturation. Due to its characteristics, pomegranate has medicinal purposes and is used to treat strep throat, hoarseness, and fever, and also has antiviral and antiseptic uses. Pomegranate polyphenols revealed antimicrobial activity when assayed against *Pseudomonas aeruginosa*, *Escherichia coli*, *Candida albicans*, methicillin-resistant *Staphylococcus aureus* (MRSA), *Cryptococcus neoformans*, *Mycobacterium intracellulare*, and *Aspergillus*

*fumigatus* [66]. *Micrococcus luteus* is a kind of non-pathogenic skin commensal bacterium, although it can act as an opportunistic pathogen and cause serious infections, especially for patients with catheters and comorbidities. Pomegranate polyphenols showed antimicrobial activity against *M. luteus* via inhibition of biofilm formation. Grape seed polyphenols have shown effective antimicrobial properties and were efficiently used against Gram-positive bacteria (*Bacillus cereus*, *Staphylococcus aureus*, *Bacillus coagulans*, and *Bacillus subtilis*), but they were more effective against Gram-negative bacteria, such as *P. aeruginosa* or *E. coli* [67]. *Schinus terebinthifolius* Raddi was found to enhance microbial inhibition against the tested strains, especially against Gram-negative bacteria [68]. Its potential use as an alternative to overcome bacterial resistance can be expected. Phlorotannins, polyphenols extracted from brown seaweeds, are recognized for their antimicrobial biological capacity. Phlorotannins were more effective against Gram-positive bacteria, with *Staphylococcus epidermidis* being the most susceptible species [69]. Resveratrol has been shown to inhibit 80% of the growth of dermatophytes of *Trichophyton mentagrophytes*, in particular, and was demonstrated to be an apoptosis inducer in the human pathogenic fungus *C. albicans* by activating metacaspase and promoting cytochrome c release [70]. Pro-anthocyanidins are common natural polyphenols, which were shown to reduce the adherence properties of *C. albicans* by attenuating the inflammatory response and interfering with NF- $\kappa$ B and p65 activation and the phosphorylation of specific signal intracellular kinases [71]. Although the underlying molecular mechanisms of the antimicrobial properties of polyphenols remain poorly understood, existing research results may turn many polyphenols into potent and novel pharmacological alternatives for the treatment of a wide range of microbial infections.

### 2.5. Polyphenols as Anticancer Agents for Skin

Chemotherapy, immunotherapy, radiotherapy, and targeted therapy are included in the current management of metastatic and/or non-metastatic skin cancer. The above methods are highly toxic, expensive, and, in some cases, ineffective due to the development of resistance, especially in metastatic cancer [72]. Thus, it is important to propose new effective therapeutic strategies or drugs which are more affordable and safer. Accumulating evidence from the last decade indicates that promising anticancer natural compounds, such as EGCG, resveratrol, and curcumin, among others, may be extracted from plants [73–76]. Polyphenols may exert these anticancer effects via a variety of mechanisms, including removal of carcinogenic agents, modulation of cancer cell signaling and cell cycle progression, promotion of apoptosis, and modulation of enzymatic activities. Tea polyphenols are abundant in green tea leaves, accounting for ca. 30% of dry leaf weight, and are also collectively referred to as catechins. The biological bioactivities of tea polyphenols, with EGCG as the primary contributor, have been well documented and include anticancer effects and reduced risk of degenerative diseases. Tea polyphenols can reduce UV-induced mouse skin carcinogenesis in terms of tumor incidence and multiplicity [77]. Tea polyphenols provided protection against 7,12-dimethyl benz(a)anthracene-induced mouse skin tumorigenesis. A population-based case-control study indicated that strong (hot) black tea had independent potentially protective effects against skin squamous cell carcinoma [78]. Pre-clinical trials have examined the anticancer properties of resveratrol in skin [79]. The underlying anticancer mechanisms of resveratrol have been shown to be due to the induction of apoptosis, antioxidant systems, amelioration of inflammation, and cell cycle suppression in mouse skin carcinogenesis models [80–82]. Curcumin extracted from *Curcuma longa* L. was also indicated to have anticancer biological activities [83].

Several signaling pathways are involved in the mechanism of polyphenols against skin cancer metastasis, including NF- $\kappa$ B, epidermal growth factor receptor/mitogen activated protein kinase (EGFR/MAPK), and phosphatidylinositide 3- kinases/protein kinase B (PI3K/Akt) [83,84]. Carnosic acid has been shown to play an important protective role against melanoma. This secondary metabolite inhibited the adhesion and proliferation of B16F10 melanoma cells in a dose-dependent manner via inhibition of the expression of cell migration markers (uPA, MMP-9, VCAM-1, and TIMP-1) and phosphorylation of signaling

molecules (FAK, Sr, and Akt) [85]. A series of studies have demonstrated that various polyphenol-rich fruits and vegetables are particularly effective in protecting against colon cancer development. In general, the anticancer effects of polyphenols are a comprehensive reflection of their anti-inflammatory and antioxidant properties, as well as other effects (Figure 2).

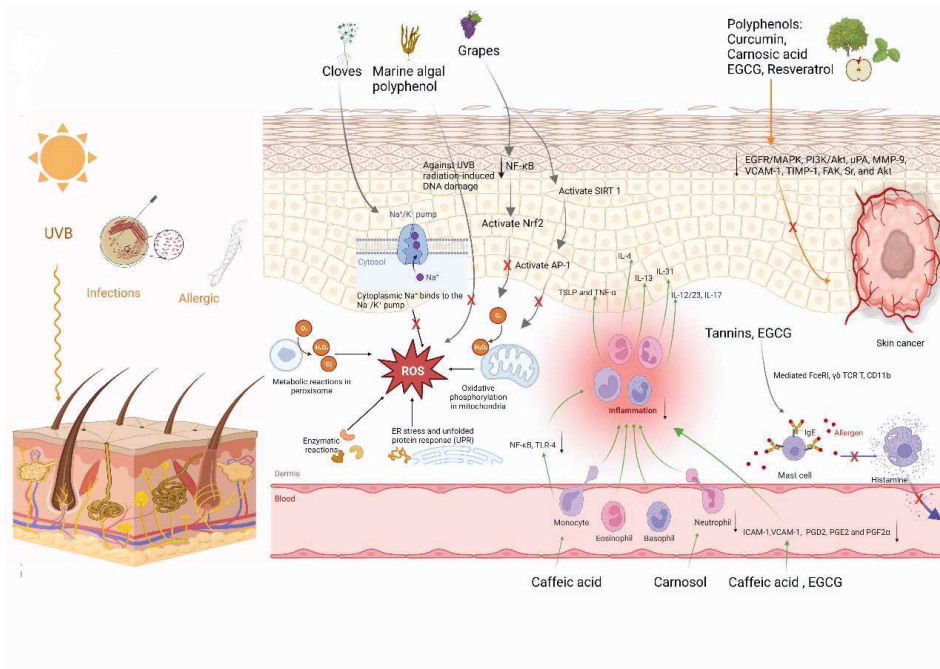


**Figure 2.** Overview of different mechanisms of several natural polyphenols on skin health.

### 3. Roles of Polyphenols in Hair Health

#### 3.1. Effects of Polyphenols on Hair Growth

Alopecia is characterized by the loss of some or all hair. Millions of individuals have suffered due to hair loss resulting from a variety of reasons, including the primary genetic cause, social, psychological, and mental stress, local infection, and endocrine disorders. Hair disorders may considerably impact the social and psychological well-being of an individual. Androgenetic alopecia (AGA) and alopecia areata (AA) are the most common types of hair disorder. AGA affects approximately 50% of men and women. AA occurs in 2% of the population. In general, hair loss may affect up to 70% of men and 50% of women at some point in their lifetime [86]. AGA is associated with high 5- $\alpha$ -reductase activity, elevated 5- $\alpha$ -dihydrotestosterone (DHT), and dysregulated transforming growth factor- $\beta$  (TGF- $\beta$ ) signaling [87]. Identification of lymphocytic infiltrates in AA lesions gave rise to the hypothesis that there is an autoimmune attack on hair follicles (HFs), which is likely a consequence of loss of immune privilege mediated by immune T cells [88].

It was reported that EGCG might be useful in the prevention or treatment of AGA by selectively inhibiting 5- $\alpha$ -reductase activity [89]. EGCG promoted hair growth in hair follicles in ex vivo culture and the proliferation of cultured dermal papilla cells (DPCs). The growth stimulation of DPCs by EGCG in vitro may be mediated through the upregulation of phosphorylated Erk and Akt and by an increase in the ratio of Bcl-2/Bax [90]. Resveratrol and fisetin regulated the genetic expression of cytokines, such as insulin-like growth factor-1 (IGF-1) and keratinocyte growth factor-2 (KGF), which activate the  $\beta$ -catenin pathway,

and TGF- $\beta$ 1, which plays an important role in maintaining the niche of hair follicle stem cells, and were thus thought to play roles in promoting hair growth. Resveratrol and fisetin induced a shift from telogen to anagen in the hair follicle by inducing proliferation of hair follicle bulge stem cells, thus promoting hair growth [91]. Procyanidin has been found to decrease the expression of protein kinase C (PKC) in hair epithelial cells and stimulate anagen induction [92]. Additionally, it is also posited that procyanidin and flavonoids may counteract TGF- $\beta$ -induced cell death by inhibiting 5- $\alpha$ -reductase, antioxidant-related mechanisms, and upregulating the expression of anti-apoptotic factors, such as Bcl-xL [92]. Oligomeric procyanidins have also shown remarkable hair growth stimulant effects in vitro and in vivo, being able to promote hair epithelial cell growth and anagen induction of the hair cycle [93]. In particular, procyanidins B2 and B3 show evidence of protective action against apoptosis in hair epithelial cell cultures, thereby restricting catagen induction in the hair cycle [94]. All of the above phenolics are expected to play important roles in the treatment of human AGA and AA (Figure 3).

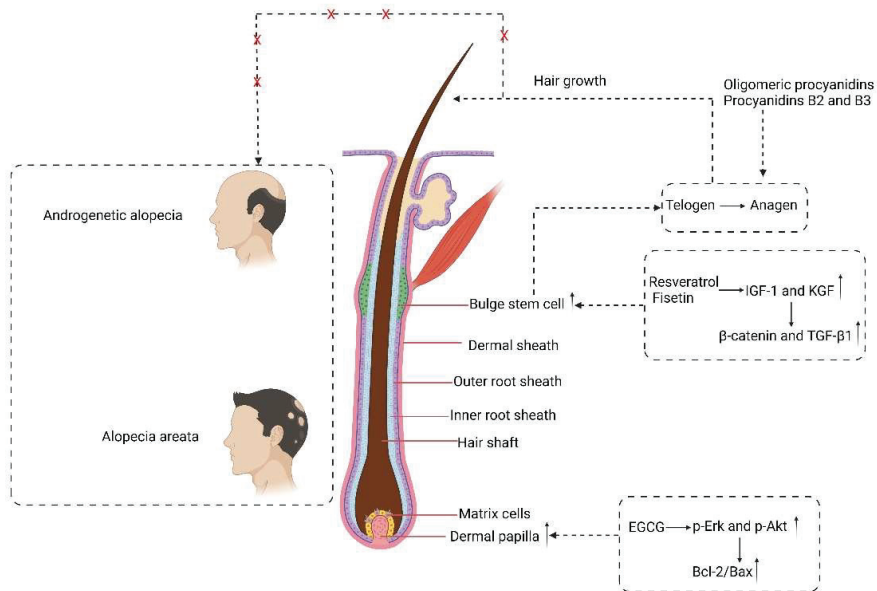


**Figure 3.** Mechanisms of natural polyphenols in the treatment of human AGA and AA.

### 3.2. Effects of Polyphenols on Hair Pigmentation

Hair pigmentation is determined by the degree and distribution of melanin in the cortex. Photodamage to hair (photobleaching) may be caused by UVA, UVB, and visible radiation, and the effects of different wavelength ranges vary. UVB and UVA radiation interact negatively with hair proteins, while visible light promotes melanin granule degradation. *Punica granatum L.* hydroalcoholic extract reduced photodamage of hair exposed to UVA radiation [95]. In addition, natural polyphenols, including tannins, present high antioxidant activity and could be used to reduce fading of natural hair color.

Hair dyeing is a common method used to recolor hair. Traditional commercial permanent hair dyeing products usually contain p-phenylenediamine (PPD) or PPD-derived compounds and hydrogen peroxide as key ingredients. These components are reportedly toxic, allergenic, mutagenic, and potentially carcinogenic to people. Recently, a method using metal—phenolic networks (MPNs), such as tannic acid (TA)-based MPNs and gallic acid (GA)-composed MPNs, reportedly dyed natural gray hair without potentially toxic chemicals and protected the dyed hair against repeated shampoo washing [96].

#### 4. Summary and Remaining Problems

Polyphenols are ubiquitously found in plants and therefore consumed in relatively high quantities in the human diet. Polyphenolic extracts are attractive ingredients for pharmaceuticals and cosmetics due to their beneficial and multifunctional biological properties and abundant availability in various dietary sources. However, similar to conventional drugs, natural polyphenols can be toxic if they accumulate beyond acceptable levels in the human body. Moreover, some studies reported polyphenols consumed in whole foods; thus, we do not know whether the results are due to interactions between polyphenols and other ingredients, and further research is needed to focus on the isolated forms of natural polyphenols. Indeed, studies investigating the beneficial effects of polyphenols, and the magnitude of the effects, must consider interfering matrix effects, enzymatic interactions, reactions with other foods, and genetic or gender characteristics [97]. In addition, most of the clinical studies exploring isolated forms of polyphenols were short-term studies; long-term health and adverse effects should be elucidated in future studies [98–100]. The effects of polyphenols on skin and hair are primarily determined by their physicochemical properties. Therefore, it is important to assess the effectiveness of polyphenolic compounds against skin and hair diseases applied systemically and/or topically. Despite the fact that polyphenols are multi-potent compounds that can be used in the treatment of a wide spectrum of diseases, including skin and hair diseases, some properties may limit their efficient use in therapy, such as low water solubility and poor stability. Improving the percutaneous absorption of plant polyphenols is a direction of future research.

**Author Contributions:** M.S. created the plot of the manuscript and first draft with the help of Y.D., X.C., L.X., Q.D., F.L., P.H., Y.G., M.L. and H.Z. critically edited and revised the manuscript. All authors have read and agreed to the published version of the manuscript.

**Funding:** This work was funded by the National Natural Science Foundation of China to Hengguang Zhao (No. 82173440).

**Institutional Review Board Statement:** Not applicable.

**Informed Consent Statement:** Not applicable.

**Data Availability Statement:** Not applicable.

**Acknowledgments:** The authors want to dedicate this manuscript to the 130th year celebration of The Second Affiliated Hospital of Chongqing Medical University, China. The figures were created using Biorender.com (accessed on 11 October 2022).

**Conflicts of Interest:** The authors declare no conflict of interest.

**Sample Availability:** Samples of the compounds are not available from the authors.

#### References

1. Dua, P.; Heiland, M.F.; Kracen, A.C.; Deshields, T.L. Cancer-related hair loss: A selective review of the alopecia research literature. *Psycho-Oncol.* **2017**, *26*, 438–443. [[CrossRef](#)] [[PubMed](#)]
2. Vauzour, D.; Rodriguez-Mateos, A.; Corona, G.; Oruna-Concha, M.J.; Spencer, J.P. Polyphenols and human health: Prevention of disease and mechanisms of action. *Nutrients* **2010**, *2*, 1106–1131. [[CrossRef](#)] [[PubMed](#)]
3. Brimson, J.M.; Prasanth, M.I.; Malar, D.S.; Sharika, R.; Sivamaruthi, B.S.; Kesika, P.; Chaiyasut, C.; Tencomnao, T.; Prasansuklab, A. Role of Herbal Teas in Regulating Cellular Homeostasis and Autophagy and Their Implications in Regulating Overall Health. *Nutrients* **2021**, *13*, 2162. [[CrossRef](#)]
4. Zhang, M.; Wang, R.; Tian, J.; Song, M.; Zhao, R.; Liu, K.; Zhu, F.; Shim, J.H.; Dong, Z.; Lee, M.H. Targeting LIMK1 with luteolin inhibits the growth of lung cancer in vitro and in vivo. *J. Cell. Mol. Med.* **2021**, *25*, 5560–5571. [[CrossRef](#)]
5. Yoo, H.S.; Won, S.B.; Kwon, Y.H. Luteolin Induces Apoptosis and Autophagy in HCT116 Colon Cancer Cells via p53-Dependent Pathway. *Nutr. Cancer* **2022**, *74*, 677–686. [[CrossRef](#)] [[PubMed](#)]
6. Malar, D.S.; Prasanth, M.I.; Brimson, J.M.; Sharika, R.; Sivamaruthi, B.S.; Chaiyasut, C.; Tencomnao, T. Neuroprotective Properties of Green Tea (*Camellia sinensis*) in Parkinson's Disease: A Review. *Molecules* **2020**, *25*, 3926. [[CrossRef](#)] [[PubMed](#)]
7. Piccolo, M.; Ferraro, M.G.; Maione, F.; Maisto, M.; Stornaiuolo, M.; Tenore, G.C.; Santamaria, R.; Irace, C.; Novellino, E. Induction of Hair Keratins Expression by an Annurca Apple-Based Nutraceutical Formulation in Human Follicular Cells. *Nutrients* **2019**, *11*, 3041. [[CrossRef](#)]

8. Sajadimajd, S.; Bahramsoltani, R.; Iranpanah, A.; Kumar Patra, J.; Das, G.; Gouda, S.; Rahimi, R.; Rezaei-amiri, E.; Cao, H.; Giampieri, F.; et al. Advances on Natural Polyphenols as Anticancer Agents for Skin Cancer. *Pharmacol. Res.* **2020**, *151*, 104584. [[CrossRef](#)]
9. Ratz-Lyko, A.; Arct, J.; Majewski, S.; Pytkowska, K. Influence of polyphenols on the physiological processes in the skin. *Phytother. Res.* **2015**, *29*, 509–517. [[CrossRef](#)]
10. Elias, P.M.; Wood, L.C.; Feingold, K.R. Epidermal pathogenesis of inflammatory dermatoses. *Am. J. Contact Dermat.* **1999**, *10*, 119–126.
11. Passali, D.; Spinosi, M.C.; Crisanti, A.; Bellussi, L.M. Mometasone furoate nasal spray: A systematic review. *Multidiscip. Respir. Med.* **2016**, *11*, 18. [[CrossRef](#)] [[PubMed](#)]
12. Michalak-Stoma, A.; Pietrzak, A.; Szepietowski, J.C.; Zalewska-Janowska, A.; Paszkowski, T.; Chodorowska, G. Cytokine network in psoriasis revisited. *Eur. Cytokine Netw.* **2011**, *22*, 160–168. [[CrossRef](#)] [[PubMed](#)]
13. van de Kerkhof, P.C.; Griffiths, C.E.; Reich, K.; Leonardi, C.L.; Blauvelt, A.; Tsai, T.F.; Gong, Y.; Huang, J.; Papavassilis, C.; Fox, T. Secukinumab long-term safety experience: A pooled analysis of 10 phase II and III clinical studies in patients with moderate to severe plaque psoriasis. *J. Am. Acad. Dermatol.* **2016**, *75*, 83–98.e84. [[CrossRef](#)] [[PubMed](#)]
14. Strober, B.; Leonardi, C.; Papp, K.A.; Mrowietz, U.; Ohtsuki, M.; Bissonnette, R.; Ferris, L.K.; Paul, C.; Lebwohl, M.; Braun, D.K.; et al. Short- and long-term safety outcomes with ixekizumab from 7 clinical trials in psoriasis: Etanercept comparisons and integrated data. *J. Am. Acad. Dermatol.* **2017**, *76*, 432–440.e417. [[CrossRef](#)] [[PubMed](#)]
15. Farahnik, B.; Beroukhi, K.; Abrouk, M.; Nakamura, M.; Zhu, T.H.; Singh, R.; Lee, K.; Bhutani, T.; Koo, J. Brodalumab for the Treatment of Psoriasis: A Review of Phase III Trials. *Dermatol. Ther.* **2016**, *6*, 111–124. [[CrossRef](#)]
16. Targan, S.R.; Feagan, B.; Vermeire, S.; Panaccione, R.; Melmed, G.Y.; Landers, C.; Li, D.; Russell, C.; Newmark, R.; Zhang, N.; et al. A Randomized, Double-Blind, Placebo-Controlled Phase 2 Study of Brodalumab in Patients with Moderate-to-Severe Crohn's Disease. *Am. J. Gastroenterol.* **2016**, *111*, 1599–1607. [[CrossRef](#)]
17. Bucio-Noble, D.; Kautto, L.; Krisp, C.; Ball, M.S.; Molloy, M.P. Polyphenol extracts from dried sugarcane inhibit inflammatory mediators in an in vitro colon cancer model. *J. Proteom.* **2018**, *177*, 1–10. [[CrossRef](#)]
18. Jantan, I.; Ahmad, W.; Bukhari, S.N. Plant-derived immunomodulators: An insight on their preclinical evaluation and clinical trials. *Front. Plant Sci.* **2015**, *6*, 655. [[CrossRef](#)]
19. Middleton, E., Jr. Effect of plant flavonoids on immune and inflammatory cell function. *Adv. Exp. Med. Biol.* **1998**, *439*, 175–182. [[CrossRef](#)]
20. Wei, B.L.; Weng, J.R.; Chiu, P.H.; Hung, C.F.; Wang, J.P.; Lin, C.N. Antiinflammatory flavonoids from *Artocarpus heterophyllus* and *Artocarpus communis*. *J. Agric. Food Chem.* **2005**, *53*, 3867–3871. [[CrossRef](#)]
21. Rengasamy, K.R.R.; Khan, H.; Gowrishankar, S.; Lagoa, R.J.L.; Mahomoodally, F.M.; Khan, Z.; Suroowan, S.; Tewari, D.; Zengin, G.; Hassan, S.T.S.; et al. The role of flavonoids in autoimmune diseases: Therapeutic updates. *Pharmacol. Ther.* **2019**, *194*, 107–131. [[CrossRef](#)] [[PubMed](#)]
22. Wen, S.; Zhang, J.; Yang, B.; Elias, P.M.; Man, M.Q. Role of Resveratrol in Regulating Cutaneous Functions. *Evid.-Based Complement. Altern. Med.* **2020**, *2020*, 2416837. [[CrossRef](#)] [[PubMed](#)]
23. Karasawa, K.; Uzuhashi, Y.; Hirota, M.; Otani, H. A matured fruit extract of date palm tree (*Phoenix dactylifera* L.) stimulates the cellular immune system in mice. *J. Agric. Food Chem.* **2011**, *59*, 11287–11293. [[CrossRef](#)] [[PubMed](#)]
24. Katiyar, S.K.; Matsui, M.S.; Elmets, C.A.; Mukhtar, H. Polyphenolic antioxidant (-)-epigallocatechin-3-gallate from green tea reduces UVB-induced inflammatory responses and infiltration of leukocytes in human skin. *Photochem. Photobiol.* **1999**, *69*, 148–153. [[CrossRef](#)]
25. Speciale, A.; Chirafisi, J.; Saija, A.; Cimino, F. Nutritional antioxidants and adaptive cell responses: An update. *Curr. Mol. Med.* **2011**, *11*, 770–789. [[CrossRef](#)]
26. Biasutto, L.; Mattarei, A.; Zoratti, M. Resveratrol and health: The starting point. *Chembiochem* **2012**, *13*, 1256–1259. [[CrossRef](#)]
27. Marchiani, A.; Rozzo, C.; Fadda, A.; Delogu, G.; Ruzza, P. Curcumin and curcumin-like molecules: From spice to drugs. *Curr. Med. Chem.* **2014**, *21*, 204–222. [[CrossRef](#)]
28. Noorafshan, A.; Ashkani-Esfahani, S. A review of therapeutic effects of curcumin. *Curr. Pharm. Des.* **2013**, *19*, 2032–2046.
29. Akyol, S.; Ozturk, G.; Ginis, Z.; Armutcu, F.; Yigitoglu, M.R.; Akyol, O. In vivo and in vitro antineoplastic actions of caffeic acid phenethyl ester (CAPE): Therapeutic perspectives. *Nutr. Cancer* **2013**, *65*, 515–526. [[CrossRef](#)]
30. Szczurko, O.; Shear, N.; Taddio, A.; Boon, H. Ginkgo biloba for the treatment of vitiligo vulgaris: An open label pilot clinical trial. *BMC Complement. Altern. Med.* **2011**, *11*, 21. [[CrossRef](#)]
31. Qa'adan, F.; Nahrstedt, A.; Schmidt, M.; Mansoor, K. Polyphenols from Ginkgo biloba. *Sci. Pharm.* **2010**, *78*, 897–907. [[CrossRef](#)] [[PubMed](#)]
32. Lim, S.J.; Kim, M.; Randy, A.; Nam, E.J.; Nho, C.W. Effects of *Hovenia dulcis* Thunb. extract and methyl vanillate on atopic dermatitis-like skin lesions and TNF- $\alpha$ /IFN- $\gamma$ -induced chemokines production in HaCaT cells. *J. Pharm. Pharmacol.* **2016**, *68*, 1465–1479. [[CrossRef](#)]
33. Boos, A.C.; Hagl, B.; Schlesinger, A.; Halm, B.E.; Ballenberger, N.; Pinarci, M.; Heinz, V.; Kreiling, D.; Spielberger, B.D.; Schimke-Marques, L.F.; et al. Atopic dermatitis, STAT3- and DOCK8-hyper-IgE syndromes differ in IgE-based sensitization pattern. *Allergy* **2014**, *69*, 943–953. [[CrossRef](#)]

34. Lee, D.Y.; Hwang, C.J.; Choi, J.Y.; Park, M.H.; Song, M.J.; Oh, K.W.; Son, D.J.; Lee, S.H.; Han, S.B.; Hong, J.T. Inhibitory Effect of Carnosol on Phthalic Anhydride-Induced Atopic Dermatitis via Inhibition of STAT3. *Biomol. Ther.* **2017**, *25*, 535–544. [[CrossRef](#)]
35. D'Antuono, I.; Carola, A.; Sena, L.M.; Linsalata, V.; Cardinali, A.; Logrieco, A.F.; Colucci, M.G.; Apone, F. Artichoke Polyphenols Produce Skin Anti-Age Effects by Improving Endothelial Cell Integrity and Functionality. *Molecules* **2018**, *23*, 2729. [[CrossRef](#)] [[PubMed](#)]
36. Natarajan, V.T.; Ganju, P.; Ramkumar, A.; Grover, R.; Gokhale, R.S. Multifaceted pathways protect human skin from UV radiation. *Nat. Chem. Biol.* **2014**, *10*, 542–551. [[CrossRef](#)] [[PubMed](#)]
37. Makrantonaki, E.; Zouboulis, C.C. Androgens and ageing of the skin. *Curr. Opin. Endocrinol. Diabetes Obes.* **2009**, *16*, 240–245. [[CrossRef](#)]
38. Fraga, C.G.; Galleano, M.; Verstraeten, S.V.; Oteiza, P.I. Basic biochemical mechanisms behind the health benefits of polyphenols. *Mol. Asp. Med.* **2010**, *31*, 435–445. [[CrossRef](#)]
39. Matsumura, Y.; Ananthaswamy, H.N. Toxic effects of ultraviolet radiation on the skin. *Toxicol. Appl. Pharmacol.* **2004**, *195*, 298–308. [[CrossRef](#)] [[PubMed](#)]
40. Yin, L.; Morita, A.; Tsuji, T. Alterations of extracellular matrix induced by tobacco smoke extract. *Arch. Dermatol. Res.* **2000**, *292*, 188–194. [[CrossRef](#)]
41. Kondo, S. The roles of cytokines in photoaging. *J. Dermatol. Sci.* **2000**, *23* (Suppl. 1), S30–S36. [[CrossRef](#)]
42. Pallela, R.; Na-Young, Y.; Kim, S.K. Anti-photoaging and photoprotective compounds derived from marine organisms. *Mar. Drugs* **2010**, *8*, 1189–1202. [[CrossRef](#)] [[PubMed](#)]
43. Heo, S.J.; Ko, S.C.; Cha, S.H.; Kang, D.H.; Park, H.S.; Choi, Y.U.; Kim, D.; Jung, W.K.; Jeon, Y.J. Effect of phlorotannins isolated from *Ecklonia cava* on melanogenesis and their protective effect against photo-oxidative stress induced by UV-B radiation. *Toxicol. In Vitro* **2009**, *23*, 1123–1130. [[CrossRef](#)] [[PubMed](#)]
44. Gao, X.; Luo, F.; Zhao, H. Cloves Regulate Na(+)-K(+)-ATPase to Exert Antioxidant Effect and Inhibit UVB Light-Induced Skin Damage in Mice. *Oxidative Med. Cell. Longev.* **2021**, *2021*, 5197919. [[CrossRef](#)]
45. Lephart, E.D. Resveratrol, 4' Acetoxy Resveratrol, R-equol, Racemic Equol or S-equol as Cosmeceuticals to Improve Dermal Health. *Int. J. Mol. Sci.* **2017**, *18*, 1193. [[CrossRef](#)]
46. Ratz-Lyko, A.; Arct, J. Resveratrol as an active ingredient for cosmetic and dermatological applications: A review. *J. Cosmet. Laser Ther.* **2019**, *21*, 84–90. [[CrossRef](#)]
47. Liu, T.; Li, N.; Yan, Y.Q.; Liu, Y.; Xiong, K.; Liu, Y.; Xia, Q.M.; Zhang, H.; Liu, Z.D. Recent advances in the anti-aging effects of phytoestrogens on collagen, water content, and oxidative stress. *Phytother. Res.* **2020**, *34*, 435–447. [[CrossRef](#)]
48. Lephart, E.D.; Acerson, M.J.; Andrus, M.B. Synthesis and skin gene analysis of 4'-acetoxy-resveratrol (4AR), therapeutic potential for dermal applications. *Bioorganic Med. Chem. Lett.* **2016**, *26*, 3258–3262. [[CrossRef](#)]
49. Gopaul, R.; Knaggs, H.E.; Lephart, E.D. Biochemical investigation and gene analysis of equol: A plant and soy-derived isoflavonoid with antiaging and antioxidant properties with potential human skin applications. *BioFactors* **2012**, *38*, 44–52. [[CrossRef](#)]
50. Lephart, E.D. Skin aging and oxidative stress: Equol's anti-aging effects via biochemical and molecular mechanisms. *Ageing Res. Rev.* **2016**, *31*, 36–54. [[CrossRef](#)]
51. Lephart, E.D. Protective effects of equol and their polyphenolic isomers against dermal aging: Microarray/protein evidence with clinical implications and unique delivery into human skin. *Pharm. Biol.* **2013**, *51*, 1393–1400. [[CrossRef](#)] [[PubMed](#)]
52. Yoshikata, R.; Myint, K.Z.Y.; Ohta, H.; Ishigaki, Y. Effects of an equol-containing supplement on advanced glycation end products, visceral fat and climacteric symptoms in postmenopausal women: A randomized controlled trial. *PLoS ONE* **2021**, *16*, e0257332. [[CrossRef](#)] [[PubMed](#)]
53. Divya, S.P.; Wang, X.; Pratheeshkumar, P.; Son, Y.O.; Roy, R.V.; Kim, D.; Dai, J.; Hitron, J.A.; Wang, L.; Asha, P.; et al. Blackberry extract inhibits UVB-induced oxidative damage and inflammation through MAP kinases and NF- $\kappa$ B signaling pathways in SKH-1 mice skin. *Toxicol. Appl. Pharmacol.* **2015**, *284*, 92–99. [[CrossRef](#)]
54. Hwang, E.; Lin, P.; Ngo, H.T.T.; Yi, T.H. Clove attenuates UVB-induced photodamage and repairs skin barrier function in hairless mice. *Food Funct.* **2018**, *9*, 4936–4947. [[CrossRef](#)]
55. Verma, A.; Kushwaha, H.N.; Srivastava, A.K.; Srivastava, S.; Jamal, N.; Srivastava, K.; Ray, R.S. Piperine attenuates UV-R induced cell damage in human keratinocytes via NF- $\kappa$ B, Bax/Bcl-2 pathway: An application for photoprotection. *J. Photochem. Photobiology. B Biol.* **2017**, *172*, 139–148. [[CrossRef](#)]
56. Hernandez, D.F.; Cervantes, E.L.; Luna-Vital, D.A.; Mojica, L. Food-derived bioactive compounds with anti-aging potential for nutricosmetic and cosmeceutical products. *Crit. Rev. Food Sci. Nutr.* **2021**, *61*, 3740–3755. [[CrossRef](#)]
57. Strózek, J.; Samoliński, B.K.; Klak, A.; Gawińska-Druzba, E.; Izdebski, R.; Krzych-Fałta, E.; Raciborski, F. The indirect costs of allergic diseases. *Int. J. Occup. Med. Environ. Health* **2019**, *32*, 281–290. [[CrossRef](#)]
58. Canonica, G.W.; Cox, L.; Pawankar, R.; Baena-Cagnani, C.E.; Blaiss, M.; Bonini, S.; Bousquet, J.; Calderón, M.; Compalati, E.; Durham, S.R.; et al. Sublingual immunotherapy: World Allergy Organization position paper 2013 update. *World Allergy Organ. J.* **2014**, *7*, 6. [[CrossRef](#)] [[PubMed](#)]
59. Ding, S.; Jiang, H.; Fang, J. Regulation of Immune Function by Polyphenols. *J. Immunol. Res.* **2018**, *2018*, 1264074. [[CrossRef](#)]
60. Di Meo, F.; Lemaire, V.; Cornil, J.; Lazzaroni, R.; Duroux, J.L.; Olivier, Y.; Trouillas, P. Free radical scavenging by natural polyphenols: Atom versus electron transfer. *J. Phys. Chem. A* **2013**, *117*, 2082–2092. [[CrossRef](#)]



61. Persia, F.A.; Mariani, M.L.; Fogal, T.H.; Penissi, A.B. Hydroxytyrosol and oleuropein of olive oil inhibit mast cell degranulation induced by immune and non-immune pathways. *Phytomedicine* **2014**, *21*, 1400–1405. [[CrossRef](#)]
62. Choi, Y.H.; Yan, G.H. Silibinin attenuates mast cell-mediated anaphylaxis-like reactions. *Biol. Pharm. Bull.* **2009**, *32*, 868–875. [[CrossRef](#)]
63. Sato, Y.; Akiyama, H.; Matsuoka, H.; Sakata, K.; Nakamura, R.; Ishikawa, S.; Inakuma, T.; Totsuka, M.; Sugita-Konishi, Y.; Ebisawa, M.; et al. Dietary carotenoids inhibit oral sensitization and the development of food allergy. *J. Agric. Food Chem.* **2010**, *58*, 7180–7186. [[CrossRef](#)] [[PubMed](#)]
64. Kawai, K.; Tsuno, N.H.; Kitayama, J.; Sunami, E.; Takahashi, K.; Nagawa, H. Catechin inhibits adhesion and migration of peripheral blood B cells by blocking CD11b. *Immunopharmacol. Immunotoxicol.* **2011**, *33*, 391–397. [[CrossRef](#)] [[PubMed](#)]
65. Carolina Oliveira Dos Santos, L.; Spagnol, C.M.; Guillot, A.J.; Melero, A.; Corrêa, M.A. Caffeic acid skin absorption: Delivery of microparticles to hair follicles. *Saudi Pharm. J.* **2019**, *27*, 791–797. [[CrossRef](#)] [[PubMed](#)]
66. Reddy, M.K.; Gupta, S.K.; Jacob, M.R.; Khan, S.I.; Ferreira, D. Antioxidant, antimalarial and antimicrobial activities of tannin-rich fractions, ellagitannins and phenolic acids from *Punica granatum* L. *Planta Med.* **2007**, *73*, 461–467. [[CrossRef](#)]
67. Mayer, R.; Stecher, G.; Wuerzner, R.; Silva, R.C.; Sultana, T.; Trojer, L.; Feuerstein, I.; Krieg, C.; Abel, G.; Popp, M.; et al. Proanthocyanidins: Target compounds as antibacterial agents. *J. Agric. Food Chem.* **2008**, *56*, 6959–6966. [[CrossRef](#)]
68. Celiksoy, V.; Moses, R.L.; Sloan, A.J.; Moseley, R.; Heard, C.M. Synergistic In Vitro Antimicrobial Activity of Pomegranate Rind Extract and Zinc (II) against *Micrococcus luteus* under Planktonic and Biofilm Conditions. *Pharmaceutics* **2021**, *13*, 851. [[CrossRef](#)]
69. Lopes, G.; Sousa, C.; Silva, L.R.; Pinto, E.; Andrade, P.B.; Bernardo, J.; Mougá, T.; Valentão, P. Can phlorotannins purified extracts constitute a novel pharmacological alternative for microbial infections with associated inflammatory conditions? *PLoS ONE* **2012**, *7*, e31145. [[CrossRef](#)]
70. Jung, H.J.; Hwang, I.A.; Sung, W.S.; Kang, H.; Kang, B.S.; Seu, Y.B.; Lee, D.G. Fungicidal effect of resveratrol on human infectious fungi. *Arch. Pharmacol. Res.* **2005**, *28*, 557–560. [[CrossRef](#)]
71. Simonetti, G.; Brasili, E.; Pasqua, G. Antifungal Activity of Phenolic and Polyphenolic Compounds from Different Matrices of *Vitis vinifera* L. against Human Pathogens. *Molecules* **2020**, *25*, 3748. [[CrossRef](#)] [[PubMed](#)]
72. Simões, M.C.F.; Sousa, J.J.S.; Pais, A. Skin cancer and new treatment perspectives: A review. *Cancer Lett.* **2015**, *357*, 8–42. [[CrossRef](#)] [[PubMed](#)]
73. Curti, V.; Di Lorenzo, A.; Dacrema, M.; Xiao, J.; Nabavi, S.M.; Daglia, M. In vitro polyphenol effects on apoptosis: An update of literature data. *Semin. Cancer Biol.* **2017**, *46*, 119–131. [[CrossRef](#)] [[PubMed](#)]
74. Shi, J.; Liu, F.; Zhang, W.; Liu, X.; Lin, B.; Tang, X. Epigallocatechin-3-gallate inhibits nicotine-induced migration and invasion by the suppression of angiogenesis and epithelial-mesenchymal transition in non-small cell lung cancer cells. *Oncol. Rep.* **2015**, *33*, 2972–2980. [[CrossRef](#)] [[PubMed](#)]
75. Xiao, J. Dietary flavonoid aglycones and their glycosides: Which show better biological significance? *Crit. Rev. Food Sci. Nutr.* **2017**, *57*, 1874–1905. [[CrossRef](#)]
76. Khan, H.; Reale, M.; Ullah, H.; Sureda, A.; Tejada, S.; Wang, Y.; Zhang, Z.J.; Xiao, J. Anti-cancer effects of polyphenols via targeting p53 signaling pathway: Updates and future directions. *Biotechnol. Adv.* **2020**, *38*, 107385. [[CrossRef](#)]
77. Kalra, N.; Prasad, S.; Shukla, Y. Antioxidant potential of black tea against 7,12-dimethylbenz(a)anthracene- induced oxidative stress in Swiss albino mice. *J. Environ. Pathol. Toxicol. Oncol.* **2005**, *24*, 105–114. [[CrossRef](#)]
78. Hakim, I.A.; Harris, R.B. Joint effects of citrus peel use and black tea intake on the risk of squamous cell carcinoma of the skin. *BMC Dermatol.* **2001**, *1*, 3. [[CrossRef](#)]
79. Bishayee, A. Cancer prevention and treatment with resveratrol: From rodent studies to clinical trials. *Cancer Prev. Res.* **2009**, *2*, 409–418. [[CrossRef](#)]
80. Afaq, F.; Adhami, V.M.; Ahmad, N. Prevention of short-term ultraviolet B radiation-mediated damages by resveratrol in SKH-1 hairless mice. *Toxicol. Appl. Pharmacol.* **2003**, *186*, 28–37. [[CrossRef](#)]
81. Reagan-Shaw, S.; Afaq, F.; Aziz, M.H.; Ahmad, N. Modulations of critical cell cycle regulatory events during chemoprevention of ultraviolet B-mediated responses by resveratrol in SKH-1 hairless mouse skin. *Oncogene* **2004**, *23*, 5151–5160. [[CrossRef](#)] [[PubMed](#)]
82. Aziz, M.H.; Reagan-Shaw, S.; Wu, J.; Longley, B.J.; Ahmad, N. Chemoprevention of skin cancer by grape constituent resveratrol: Relevance to human disease? *FASEB J.* **2005**, *19*, 1193–1195. [[CrossRef](#)] [[PubMed](#)]
83. Kunnumakkara, A.B.; Anand, P.; Aggarwal, B.B. Curcumin inhibits proliferation, invasion, angiogenesis and metastasis of different cancers through interaction with multiple cell signaling proteins. *Cancer Lett.* **2008**, *269*, 199–225. [[CrossRef](#)]
84. Balasubramanian, S.; Efimova, T.; Eckert, R.L. Green tea polyphenol stimulates a Ras, MEK1, MEK3, and p38 cascade to increase activator protein 1 factor-dependent involucrin gene expression in normal human keratinocytes. *J. Biol. Chem.* **2002**, *277*, 1828–1836. [[CrossRef](#)]
85. Park, S.Y.; Song, H.; Sung, M.K.; Kang, Y.H.; Lee, K.W.; Park, J.H. Carnosic acid inhibits the epithelial-mesenchymal transition in B16F10 melanoma cells: A possible mechanism for the inhibition of cell migration. *Int. J. Mol. Sci.* **2014**, *15*, 12698–12713. [[CrossRef](#)] [[PubMed](#)]
86. Aljuffali, I.A.; Sung, C.T.; Shen, F.M.; Huang, C.T.; Fang, J.Y. Squarticles as a lipid nanocarrier for delivering diphenylprone and minoxidil to hair follicles and human dermal papilla cells. *AAPS J.* **2014**, *16*, 140–150. [[CrossRef](#)] [[PubMed](#)]

87. Inui, S.; Fukuzato, Y.; Nakajima, T.; Yoshikawa, K.; Itami, S. Androgen-inducible TGF-beta1 from balding dermal papilla cells inhibits epithelial cell growth: A clue to understand paradoxical effects of androgen on human hair growth. *FASEB J.* **2002**, *16*, 1967–1969. [[CrossRef](#)] [[PubMed](#)]
88. Paus, R.; Bulfone-Paus, S.; Bertolini, M. Hair Follicle Immune Privilege Revisited: The Key to Alopecia Areata Management. *J. Investig. Dermatol. Symp. Proc.* **2018**, *19*, S12–S17. [[CrossRef](#)] [[PubMed](#)]
89. Shen, Y.L.; Li, X.Q.; Pan, R.R.; Yue, W.; Zhang, L.J.; Zhang, H. Medicinal Plants for the Treatment of Hair Loss and the Suggested Mechanisms. *Curr. Pharm. Des.* **2018**, *24*, 3090–3100. [[CrossRef](#)]
90. Kwon, O.S.; Han, J.H.; Yoo, H.G.; Chung, J.H.; Cho, K.H.; Eun, H.C.; Kim, K.H. Human hair growth enhancement in vitro by green tea epigallocatechin-3-gallate (EGCG). *Phytomedicine* **2007**, *14*, 551–555. [[CrossRef](#)]
91. Kubo, C.; Ogawa, M.; Uehara, N.; Katakura, Y. Fisetin Promotes Hair Growth by Augmenting TERT Expression. *Front. Cell Dev. Biol.* **2020**, *8*, 566617. [[CrossRef](#)] [[PubMed](#)]
92. Loing, E.; Lachance, R.; Ollier, V.; Hocquaux, M. A new strategy to modulate alopecia using a combination of two specific and unique ingredients. *J. Cosmet. Sci.* **2013**, *64*, 45–58. [[PubMed](#)]
93. Kamimura, A.; Takahashi, T. Procyanidin B-2, extracted from apples, promotes hair growth: A laboratory study. *Br. J. Dermatol.* **2002**, *146*, 41–51. [[CrossRef](#)] [[PubMed](#)]
94. Kamimura, A.; Takahashi, T.; Morohashi, M.; Takano, Y. Procyanidin oligomers counteract TGF-beta1- and TGF-beta2-induced apoptosis in hair epithelial cells: An insight into their mechanisms. *Ski. Pharmacol. Physiol.* **2006**, *19*, 259–265. [[CrossRef](#)]
95. Dario, M.F.; Pahl, R.; de Castro, J.R.; de Lima, F.S.; Kaneko, T.M.; Pinto, C.A.; Baby, A.R.; Velasco, M.V. Efficacy of *Punica granatum* L. hydroalcoholic extract on properties of dyed hair exposed to UVA radiation. *J. Photochem. Photobiol. B Biol.* **2013**, *120*, 142–147. [[CrossRef](#)] [[PubMed](#)]
96. Geng, H.; Zhuang, L.; Li, M.; Liu, H.; Caruso, F.; Hao, J.; Cui, J. Interfacial Assembly of Metal-Phenolic Networks for Hair Dyeing. *ACS Appl. Mater. Interfaces* **2020**, *12*, 29826–29834. [[CrossRef](#)] [[PubMed](#)]
97. Bertelli, A.; Biagi, M.; Corsini, M.; Bainsi, G.; Cappellucci, G.; Miraldi, E. Polyphenols: From Theory to Practice. *Foods* **2021**, *10*, 2595. [[CrossRef](#)]
98. Vittala Murthy, N.T.; Paul, S.K.; Chauhan, H.; Singh, S. Polymeric Nanoparticles for Transdermal Delivery of Polyphenols. *Curr. Drug Deliv.* **2022**, *19*, 182–191. [[CrossRef](#)]
99. Cristiano, M.C.; Barone, A.; Mancuso, A.; Torella, D.; Paolino, D. Rutin-Loaded Nanovesicles for Improved Stability and Enhanced Topical Efficacy of Natural Compound. *J. Funct. Biomater.* **2021**, *12*, 74. [[CrossRef](#)]
100. Li, Q.; Duan, M.; Liu, L.; Chen, X.; Fu, Y.; Li, J.; Zhao, T.; McClements, D.J. Impact of Polyphenol Interactions with Titanium Dioxide Nanoparticles on Their Bioavailability and Antioxidant Activity. *J. Agric. Food Chem.* **2021**, *69*, 9661–9670. [[CrossRef](#)]



Article

# Fast Screening of Protein Tyrosine Phosphatase 1B Inhibitor from *Salvia miltiorrhiza* Bge by Cell Display-Based Ligand Fishing

Xiaolin Bai<sup>1,2</sup>, Wenqin Fan<sup>1,2</sup>, Yingjie Luo<sup>3</sup>, Yipei Liu<sup>4</sup>, Yongmei Zhang<sup>1,\*</sup> and Xun Liao<sup>1,\*</sup><sup>1</sup> Chinese Academy of Sciences, Chengdu Institute of Biology, Chengdu 610041, China<sup>2</sup> University of Chinese Academy of Sciences, Beijing 100049, China<sup>3</sup> Department of Molecular Science, The University of Western Australia, Perth, WA 6000, Australia<sup>4</sup> Polus International College, Chengdu 610103, China

\* Correspondence: zhangym@cib.ac.cn (Y.Z.); liaoxun@cib.ac.cn (X.L.);

Tel.: +86-28-82890756 (Y.Z.); +86-28-828290402 (X.L.)

**Abstract:** *Salvia miltiorrhiza* Bge is a medicinal plant (Chinese name “Danshen”) widely used for the treatment of hyperglycemia in traditional Chinese medicine. Protein tyrosine phosphatase 1B (PTP1B) has been recognized as a potential target for insulin sensitizing for the treatment of diabetes. In this work, PTP1B was displayed at the surface of *E. coli* cells (EC-PTP1B) to be used as a bait for fishing of the enzyme’s inhibitors present in the aqueous extract of *S. miltiorrhiza*. Salvianolic acid B, a polyphenolic compound, was fished out by EC-PTP1B, which was found to inhibit PTP1B with an IC<sub>50</sub> value of 23.35 μM. The inhibitory mechanism of salvianolic acid B was further investigated by enzyme kinetic experiments and molecular docking, indicating salvianolic acid B was a non-competitive inhibitor for PTP1B (with K<sub>i</sub> and K<sub>is</sub> values of 31.71 μM and 20.08 μM, respectively) and its binding energy was −7.89 kcal/mol. It is interesting that in the comparative work using a traditional ligand fishing bait of PTP1B-immobilized magnetic nanoparticles (MNPs-PTP1B), no ligands were extracted at all. This study not only discovered a new PTP1B inhibitor from *S. miltiorrhiza* which is significant to understand the chemical basis for the hypoglycemic activity of this plant, but also indicated the effectiveness of cell display-based ligand fishing in screening of active compounds from complex herbal extracts.

**Keywords:** immobilized PTP1B; drug screening; cell surface display; salvianolic acid B; traditional Chinese medicine

**Citation:** Bai, X.; Fan, W.; Luo, Y.; Liu, Y.; Zhang, Y.; Liao, X. Fast Screening of Protein Tyrosine Phosphatase 1B Inhibitor from *Salvia miltiorrhiza* Bge by Cell Display-Based Ligand Fishing. *Molecules* **2022**, *27*, 7896. <https://doi.org/10.3390/molecules27227896>

Academic Editor: Nour Eddine Es-Safi

Received: 13 October 2022

Accepted: 8 November 2022

Published: 15 November 2022

**Publisher’s Note:** MDPI stays neutral with regard to jurisdictional claims in published maps and institutional affiliations.



**Copyright:** © 2022 by the authors. Licensee MDPI, Basel, Switzerland. This article is an open access article distributed under the terms and conditions of the Creative Commons Attribution (CC BY) license (<https://creativecommons.org/licenses/by/4.0/>).

## 1. Introduction

Protein tyrosine phosphatase 1B (PTP1B) is a member of the protein tyrosine phosphatase family, which is mainly localized on the surface of the endoplasmic reticulum [1]. The functional balance of PTP1B and protein tyrosine kinases (PTKs) is crucial to regulate the phosphorylation of tyrosine [2]. Excessive accumulation of PTP1B causes various diseases including type 2 diabetes, obesity, and breast cancer [3–5]. It is a negative modulator of insulin signaling and has been recognized as a potential target for insulin sensitizing for the treatment of diabetes. Up till now, several PTP1B inhibitors have been reported as leading compounds for the above-mentioned diseases, but most of them failed in clinical trials because of poor clinical efficacy, severe side effects, and drastic weight loss [6]. Therefore, it is of great significance to discover novel PTP1B inhibitors for development of new drugs.

Traditional Chinese medicine (TCM) has been used to fight diseases for thousands of years, and is a precious pool for discovery and development of new drugs. *Salvia miltiorrhiza* Bge is a famous medicinal plant used in TCM for the treatment of a wide variety of diseases such as diabetes, cardiovascular disease, Alzheimer’s disease, and liver disease [7]. Specifically, it is one of the major ingredients in anti-diabetes Chinese herbal formulas [8].

Both *S. miltiorrhiza* and some major compounds in this plant such as cryptotanshinone, tanshinol, and dehydrodanshenol A have been reported to possess a strong inhibitory effect on PTP1B [9,10].

Ligand fishing has been quickly developed over the past decade for screening bioactive natural products. By using the target protein immobilized on certain solid phases as solid-phase extraction adsorbents, active compounds present in complex plant extracts can be specifically extracted via the high affinity interaction between the protein and its ligands [11]. Various solid phases for this purpose have been reported including magnetic nanoparticles (MNPs), halloysite nanotubes (HNTx) [12], hollow fibers [13], cellular membrane [14], and capillary electrophoresis (CE) [15]. While a variety of instrumentation techniques such as high performance liquid chromatography/mass spectrometry (HPLC-MS) [11], matrix-assisted laser desorption ionization time-of-flight mass spectrometry (MALDI-TOF-MS) [16], ultrafiltration liquid chromatography/mass spectrometry (UF-LC-MS) [17], and lab-on-chip were used to identify the fished out active compounds [18]. However, those methods have a common drawback in that the natural conformation of target proteins cannot be maintained during the immobilization process, which usually causes false results. Very recently, we displayed PTP1B on the surface of *Escherichia coli* cells to obtain a recombinant bacteria (EC-PTP1B) and used it as a new bait for ligand fishing, which exhibited promising potential to overcome such shortcomings [19].

In this work, the EC-PTP1B was applied to screen PTP1B inhibitors present in *S. miltiorrhiza* Bge in comparison with the conventional ligand fishing bait of magnetic nanoparticle immobilized PTP1B (MNPs-PTP1B). The stability and enzymatic activity of PTP1B in the forms of free PTP1B, MNPs-PTP1B, and EC-PTP1B were first compared, and the enzyme's ligand fished out was investigated for its inhibitory mechanism by enzyme kinetics and molecular docking experiments. The schematic illustration of this experimental procedure was shown in Figure 1.

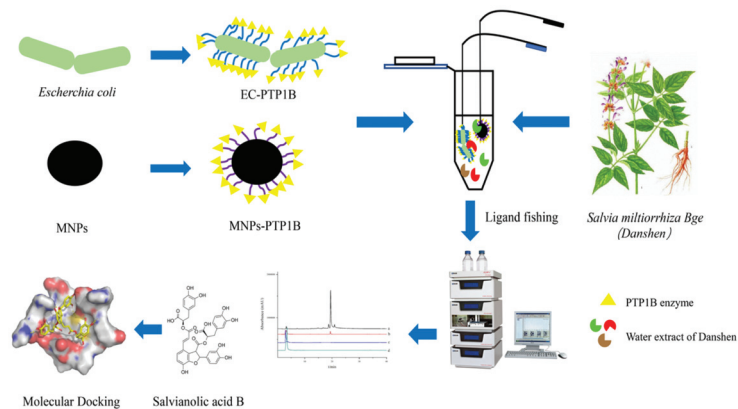


**Figure 1.** Flow chart of screening PTP1B inhibitors from *S. miltiorrhiza* extract.

## 2. Results and Discussion

### 2.1. Characterization of the Immobilized-PTP1Bs

The PTP1B was immobilized on carboxyl terminated magnetic beads for the first time in this study. FT-IR was used to confirm chemical composition of MNPs-SiO<sub>2</sub>, MNPs-COOH, and MNPs-PTP1B. As shown in Figure 2, the stretching vibration of Fe-O and asymmetric vibration of Si-O-Si of MNPs-SiO<sub>2</sub> (black line) were observed around 591 cm<sup>-1</sup> and 1021 cm<sup>-1</sup>, respectively. For MNPs-COOH (red line), the absorption peaks at 1553 cm<sup>-1</sup> and 1636 cm<sup>-1</sup> were ascribable to stretching vibration of C = O and bending vibration of N-H, indicating that NH<sub>2</sub> and COOH groups had been successfully coated on MNPs. In addition, it is obvious that the peaks at 1553 cm<sup>-1</sup> and 1636 cm<sup>-1</sup> for MNPs-PTP1B

(blue line) were stronger than those for MNPs-COOH, demonstrating that PTP1B was successfully immobilized on the surface of MNPs. The ratio of PTP1B immobilized versus MNPs was about 89  $\mu\text{g}/\text{mg}$  measured by Bradford assay.

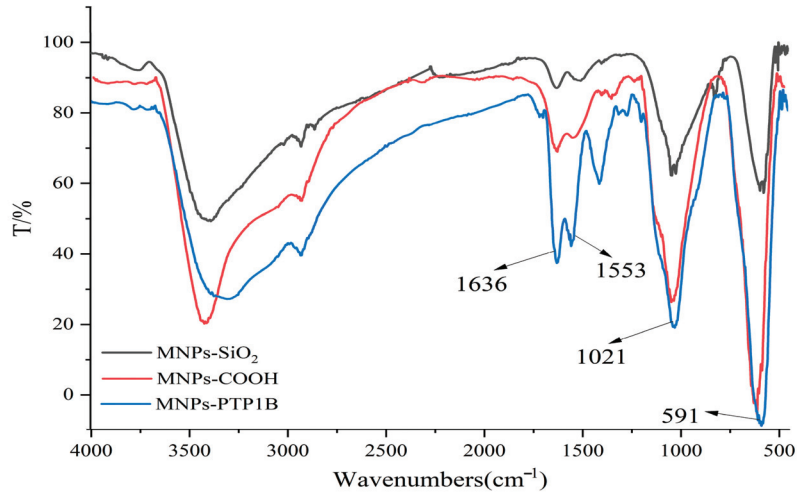


**Figure 2.** FT-IR spectra of MNPs-SiO<sub>2</sub>, MNPs-COOH, and MNPs-PTP1B.

### 2.2. Effects of pH and Temperature on the Activity of Free PTP1B, MNPs-PTP1B, and EC-PTP1B

The influence of pH on free PTP1B, MNPs-PTP1B, and EC-PTP1B was compared at a temperature of 37 °C in Figure 3a. It was found that the optimum pH values for them were all 7.0. In the pH range of 6.0–7.0, the enzymatic activity of MNPs-PTP1B was weaker than those of free PTP1B and EC-PTP1B, which might be due to the reduction of PTP1B active centers resulting from the covalent immobilization [20]. On the other hand, the MNPs-PTP1B and EC-PTP1B exhibited higher activity than the free one when the pH value was higher than 8.5, indicating that immobilized enzymes are more resistant to extreme pH conditions via restricting changes in enzyme conformation [21].

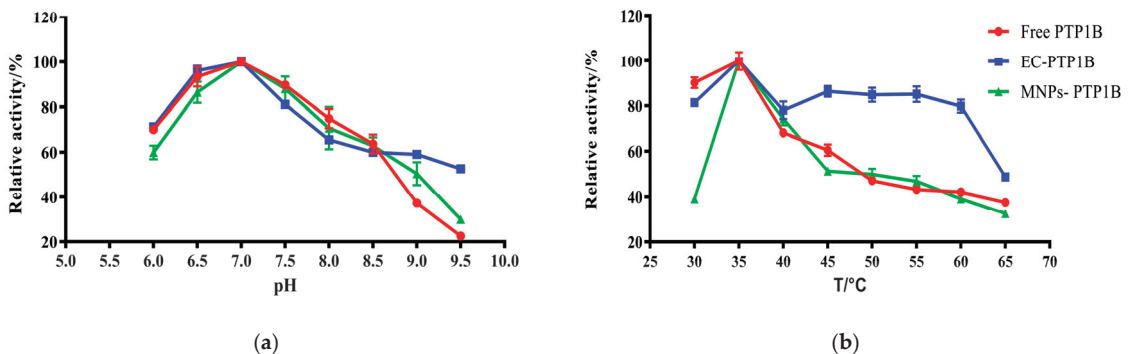


**Figure 3.** Effect of pH (a) and temperature (b) on the activity of free PTP1B, MNPs-PTP1B, and displayed PTP1B cells.

The effect of temperature (30–65 °C) on the activity of the three types of enzymes is illustrated in Figure 3b. All of them exhibited the highest enzymatic activity at 35 °C, whereas EC-PTP1B was more stable than the other two. It is well known that free enzymes are unstable once added into an in vitro reaction solution. In our case, *E. coli* can provide

a natural and intact cell membrane which is similar to the biological environment for the enzyme immobilized onto it [22], leading to the significant higher stability of EC-PTP1B at a high temperature.

### 2.3. Storage Stability of Free PTP1B, MNPs-PTP1B, and EC-PTP1B

Storage stability is an important parameter for the practical application of the immobilized enzyme. We compared the storage stability of free PTP1B, MNPs-PTP1B, and EC-PTP1B at 4 °C for 15 days. As shown in Figure 4, the activity of EC-PTP1B was maintained during the first six days compared to the sharp drop of the other two. The decrease of activity of all three types of enzymes started from day 7, while EC-PTP1B was still much more stable than the other two by maintaining around 50% of the initial activity until day 10 in comparison to 30% and 5% of MNPs-PTP1B and the free enzyme, respectively. It was reported that the interaction between two proteins which were co-expressed by *E. coli* was much stronger and stable than that between protein and non-biological materials [23–25], which might lead to the excellent storage stability of EC-PTP1B. Further, MNPs-PTP1B exhibited higher storage stability than the free PTP1B, which might result from the covalent bonding between the MNPs and the enzyme that not only maintained the conformational stability of enzyme, but also avoided the undesirable aggregation of the free enzyme [26].

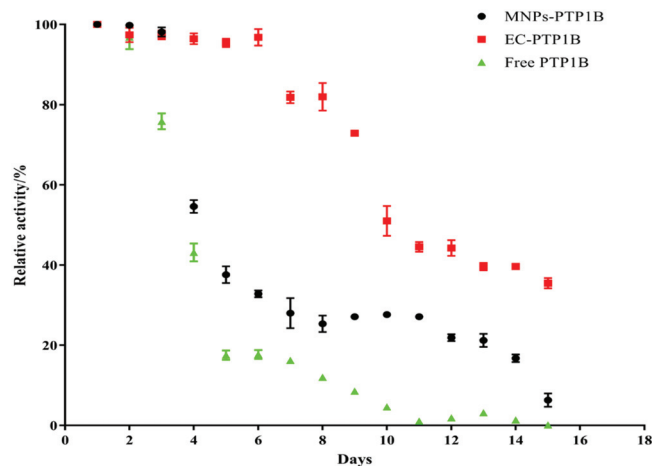


**Figure 4.** Stability of free PTP1B, MNPs-PTP1B, and EC-PTP1B.

### 2.4. Ligand Fishing from the Standard Mixture by MNPs-PTP1B and EC-PTP1B

The selectivity of ligand fishing by EC-PTP1B and MNPs-PTP1B was compared using the standard mixture containing one ligand (rutin) and two non-ligands (4-hydroxycinnamic and coumarin) of the enzyme. As shown in Figure 5, only EC-PTP1B extracted the positive compound rutin, indicating that EC-PTP1B was efficient for fishing the enzyme ligand. MNPs-PTP1B as a traditional ligand fishing bait was supposed to fish out rutin, however, it failed this time. It might be explained by the destruction of the natural conformation and active centers of PTP1B resulting from the covalent binding of the enzyme to MNPs.

### 2.5. Ligand Fish and Analysis of Aqueous Extract of *S. miltiorrhiza*

Several PTP1B inhibitors have been reported from methanol extract of *S. miltiorrhiza*, such as grandifolia F, ferruginol, tanshinone IIA, tanshinol B, and isocryptotanshinone [9,27]. However, there is no report on the aqueous extract of this plant. Since traditional herbs are basically consumed in the form of decoction with water; the aqueous extract is supposed to be more important as far as pharmacological significance is concerned. As shown in Figure 6, there was one compound fished out by EC-PTP1B, but none was fished

out by MNPs-PTP1B. It is the same interesting result as in Section 2.4. As mentioned above, this may be explained by the natural conformation as well as active centers of protein displayed at the surface of *E. coli* being well preserved, making it capable of interacting with its ligands in the aqueous extract. In contrast, the covalent binding of PTP1B to the MNPs probably destroyed the two factors, resulting in the unsuccessful fishing of the enzyme ligand.

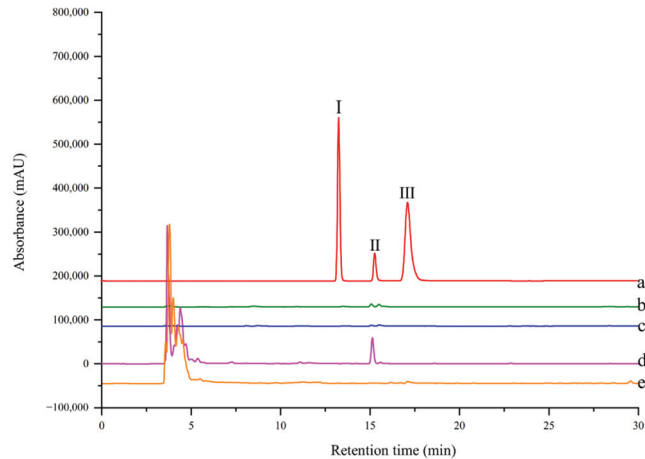


**Figure 5.** HPLC chromatogram from a model mixture before and after ligand fishing (a) the model mixture: two non-binders (0.05 mg/mL 4-hydroxycinnamic (I) and 0.05 mg/mL coumarin (III)) and one binder (0.05 mg/mL rutin (II)). (b) the compounds obtained by ligand fishing using MNPs-PTP1B. (c) the compounds obtained by ligand fishing using MNPs. (d) the compounds obtained by ligand fishing using EC-PTP1B. (e) the compounds obtained by ligand fishing using control cells (*E. coli* cells expressing only ice nuclein protein).

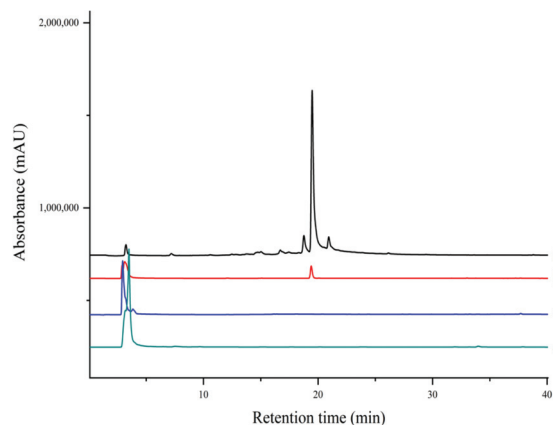


**Figure 6.** HPLC chromatograms of extract and ligand fishing of (a) *S. multiorrhiza* aqueous extract, (b) ligand fishing by EC-PTP1B, (c) ligand fishing by the control cells (*E. coli* cells expressing only ice nuclein protein), and (d) ligand fishing by MNPs-PTP1B.

The compound fished out by EC-PTP1B was identified as salvianolic acid B using HPLC-MS/MS and NMR in Supplementary Materials (Table S1 [28] and Figures S1–S3).



The molecular formula of  $C_{36}H_{30}O_{16}$  was deduced by HRMS ( $m/z$  718.1534  $[M + Na]^+$ , calcd. for 741.1432), and its retention time was identical to the standard compound.

## 2.6. Inhibitory Mechanism of Salvianolic Acid B against PTP1B

Salvianolic acid B is one of the major polyphenolic ingredients in *S. miltiorrhiza* possessing various biological activities such as neuroprotection, anti-inflammatory, antithrombotic, and anticancer activity [7,29–31]. We found for the first time the PTP1B inhibitory activity of salvianolic acid B with  $IC_{50}$  of  $23.35 \pm 4.48 \mu M$  in Supplementary Materials (Figure S4) compared to  $9.93 \pm 2.74 \mu M$  of the positive control sodium orthovanadate [32]. The inhibitory mechanism of salvianolic acid B was investigated by the Lineweaver-Burk plot method. As shown in Figure 7, when the concentration of salvianolic acid B increased, the value of  $V_{max}$  decreased while  $K_m$  remained unchanged, suggesting the inhibitor did not interfere with the binding of *p*NPp to the enzyme and it was a non-competitive inhibitor for PTP1B. As a result,  $K_i$  and  $K_{is}$  values were  $31.71 \mu M$  and  $20.08 \mu M$  for salvianolic acid B, respectively. Recently, various natural compounds were found to possess PTP1B-inhibitory activity, such as shikonin, garcinone E, and kuraridin [33–35]. The  $IC_{50}$  of them including salvianolic acid B found in this work are between 0 and  $50 \mu M$ . Their inhibitory mechanism is worth investigating in the future.

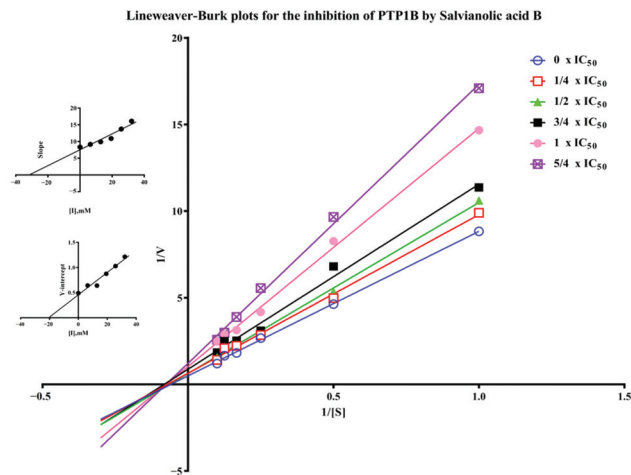


**Figure 7.** Lineweaver-Burk plots for the inhibition of PTP1B by salvianolic acid B. (Insets) Replots of the slopes and Y-intercept of the Lineweaver–Burk plots.

## 2.7. Molecular Docking Study

Molecular docking is a widely accepted tool for exploring the interaction between drug candidates and proteins in computer-aided drug discovery and design [36]. Pymol 2.1 software was used for this purpose in this work. The results displayed that the binding energy of salvianolic acid B was  $-7.89$  kcal/mol. The 2D and 3D computational binding results between salvianolic acid B and PTP1B are illustrated in Figure 8a,b,c. The rich benzene rings of salvianolic acid B were found to form hydrogen bonds with the amino acid residues of Asp-48, Lys-36, Met-258, Asp-29, Arg-254, His-25, and Arg-24. Based on the above observation, salvianolic acid B exhibited good performance in binding with active centers of the enzyme with a high docking score, suggesting its potential inhibitory effect on the enzyme.

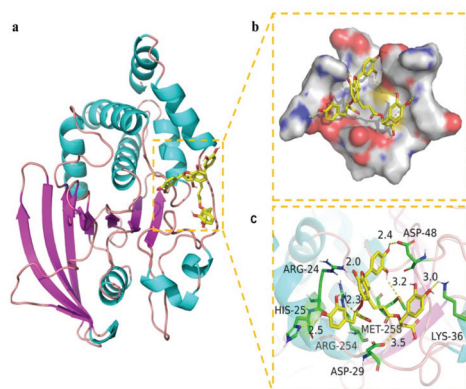


**Figure 8.** Binding mode of salvianolic acid B to PTP1B. (a) The 3D structure of the complex. (b) The surface of active site. (c) The detail binding mode of the complex. The backbone of protein was rendered in tube and colored in bright blue. Salvianolic acid B compound was rendered in yellow. The yellow dash represents hydrogen bond distance.

### 3. Materials and Methods

#### 3.1. Chemicals and Materials

PTP1B (human, recombinant) was purchased from Sangon Company (Shanghai, China). The rhizomes of *Salvia miltiorrhiza* Bge were generously presented by the Wansheng Agricultural Company of Zhongjiang County (Sichuan, China). A voucher specimen (2019-07) was deposited in the herbarium of Chengdu Institute of Biology, Chinese Academy of Science. Salvianolic acid B was obtained from Lemeitian Medicine (Chengdu, China). Sodium Orthovanadate ( $\text{Na}_3\text{VO}_4$ ), and para-nitrophenyl phosphate (*p*NPP) were purchased from Macklin Company (Shanghai, China). Tetraethyl orthosilicate (TEOS) and 3-aminopropyltrimethoxysilane (APTMS) were obtained from TCI (Tokyo, Japan). Ferric chloride hexahydrate ( $\text{FeCl}_3 \cdot 6\text{H}_2\text{O}$ ), Iron(II) chloride tetrahydrate ( $\text{FeCl}_2 \cdot 4\text{H}_2\text{O}$ ), 4-Morpholineethanesulfonic acid (MES), Hydrochloric acid (HCl), and sodium hydroxide (NaOH) were purchased from Tianjing Kermel Chemical Reagent (Tianjing, China). Acetonitrile and Methanol (HPLC-grade) were obtained from J&K Technology (Beijing, China). Deionized water (18.5 M $\Omega$ ) was prepared from the Chengdu Youpu Equipment Company (Chengdu, China). The 96-well microtiter plates were purchased from Bioland Technology company (Hangzhou, China).

#### 3.2. Apparatus

The High-performance liquid chromatography (HPLC) system includes two LC-20AD pumps (Shimadzu, Japan), an SPD-20A UV-Vis detector, a thermostat column, and an Agilent ZORBAX SB-C18 column (5  $\mu\text{m}$ , 4.6  $\times$  250 mm). The elution system consists of water with 0.1% formic acid (mobile phase A) and methanol (mobile phase B), and the flow rate was 0.8 mL/min during the following gradient: 0.00–35.00 min, 30–100% mobile phase B; 35.00–40.00 min 100 mobile phase B. The 1D NMR spectra were recorded in  $\text{CD}_3\text{OD}$  using a Bruker DRX-600 spectrometer (Bruker, Rheinstetten, Germany) with tetramethylsilane (TMS) as the internal standard. Cells were cultured in a constant temperature incubator shaker (Zhicheng Analytical Instrument, Shanghai, China). The ligand fishing process was completed by a high-speed centrifuge (DLABsci Instrument, Beijing, China) and a vortex oscillator (Crystal Instrument, HYQ-3110, USA). HPLC-MS/MS analysis was performed on a Waters ACQUITY system coupled with a XEVO TQ MS triple-quadrupole mass spectrometer (Waters, Milford, PA, USA). A microplate reader (ThermoFisher, Multiskan GO, USA) was used for enzymatic activity assay. A Shimadzu 8030 LC-MS (Shimadzu, Japan) was used for compound identification.

### 3.3. Preparation of PTP1B Immobilized Magnetic Nanoparticles (MNPs-PTP1B)

Firstly, carboxyl terminated magnetic nanoparticles (MNPs) were synthesized according to the same protocol as in our previous work [37,38]. Briefly, 0.7455 g  $\text{FeCl}_2 \cdot 4\text{H}_2\text{O}$  and 2.0271 g  $\text{FeCl}_3 \cdot 6\text{H}_2\text{O}$  were added in 250 mL ddH<sub>2</sub>O under pH = 9–10 to react for 30 min. The obtained MNPs were coated with a layer of silica using 400  $\mu\text{L}$  TEOS in 150 mL of ethanol for 5 h at 35 °C (pH = 9), which were then modified with amino groups by adding 2 mL APTES in 100 mL 95% ethanol for 24 h at 35 °C. Finally, 0.5 g MNPs-SiO<sub>2</sub>-NH<sub>2</sub> beads were terminated with carboxyl group by adding 3 g butanedioic anhydride in 30 mL dimethyl formamide for 3 h at room temperature. The above products, i.e., MNPs-SiO<sub>2</sub>, MNPs-SiO<sub>2</sub>-NH<sub>2</sub>, and MNPs-SiO<sub>2</sub>-NH<sub>2</sub>-COOH were characterized by FT-IR. Secondly, PTP1B was covalently immobilized on the carboxyl terminated MNPs as follows. Briefly, 5 mg EDC and 7 mg NHS were used to activate 20 mg of MNPs-COOH beads for 30 min at room temperature, and 0.5 mg/mL PTP1B was incubated with the activated beads in a 5 mL Eppendorf tube (13.7 mM NaCl, 2.7 mM KCl, 10 mM Na<sub>2</sub>HPO<sub>4</sub>·12H<sub>2</sub>O, 1.76 mM KH<sub>2</sub>PO<sub>4</sub>, pH = 7.4) at room temperature over 24 h. The prepared MNPs-PTP1B was suspended in PBS buffer and stored at 4 °C before use. In our study, protein content was measured using bovine serum albumin (BSA) as a standard by the Coomassie brilliant blue G-250 method which was commonly used to quantify the content of protein [39]. The bond PTP1B of MNP was determined by the difference between the initial and residual protein concentrations.

### 3.4. Preparation of PTP1B Displayed Cells (EC-PTP1B)

The *E. coli* cells, which harbored vector pETInaK-N/PTPN1 (as EC-PTP1B) and pMDInaK-N (as control cells), were obtained from our previous study and stored in a storage buffer with 50% glycerol at −20 °C [19]. Both cells were resuscitated and grown in an LB-Kan+ medium (5 g yeast extract, 10 g tryptone, 10 g NaCl, and 50 mg kanamycin dissolved in 1 L ddH<sub>2</sub>O, pH = 7.4) by shaking (200 rpm) at 37 °C until OD<sub>600</sub> = 0.6. The expression of the PTP1B enzyme on the *E. coli* surface was induced with 0.5 mM isopropyl- $\beta$ -thiogalactopyranoside (IPTG) at 25 °C for 24 h. After that, displayed cells were washed with PBS buffer and stored in a 50-mL centrifuge tube with 20 mL PBS buffer at 4 °C.

### 3.5. Comparison of the Activity and Stability of the Free and Immobilized PTP1B

The enzymatic activity of PTP1B was assayed using 4-nitrophenyl phosphate (*p*NPP) as a substrate according to a previously reported method with a slight modification [19]. Briefly, the *p*NPP (10 mM, 100  $\mu\text{L}$ ) in reaction buffer (25 mM Tris/HCL, 150 mM NaCl, 5 mM MgCl<sub>2</sub> and 4 mM DTT, pH = 8.5) was mixed with the enzyme solution (100  $\mu\text{L}$ ) in an Eppendorf tube incubated at 37 °C for 30 min. The reaction was then terminated by the addition of NaOH (0.1 M, 100  $\mu\text{L}$ ), and the product *p*NP was transferred to a 96-well plate to be measured using a microplate reader at 405 nm. All experiments were carried out in triplicate and data shown as mean  $\pm$  SD.

To compare the enzymatic activity of the three forms of PTP1B, the following five groups of enzyme or control were assayed: (1) free PTP1B enzyme; (2) EC-PTP1B; (3) control cells; (4) MNPs-PTP1B; (5) control MNPs. For MNPs-PTP1B and the control MNPs, 20 mg of each was firstly suspended in 3 mL reaction buffer, from which 100  $\mu\text{L}$  was added to the substrate to start the reaction. After completion of the reaction, the supernatant was collected after magnetic separation and its absorbance was read at 405 nm using a microplate reader. For the other three groups, the free PTP1B was diluted to a concentration of 10  $\mu\text{g}/\text{mL}$ , and the EC-PTP1B and control cells were dissolved in reaction buffer to OD<sub>600</sub> = 0.5 before starting the enzymatic reaction, while the remaining process was the same as described with MNPs-PTP1B.

To compare the stability of the three forms of PTP1B, the effect of various temperatures on the activity of the three forms of PTP1B at pH = 7.5 was first investigated. In the meantime, the influence of pH (ranging from 6.0 to 9.0) on the enzymes' activity was also evaluated. Secondly, the enzymatic activity of the three forms of PTP1B was tested on 16 consecutive days to evaluate their storage stability.

### 3.6. Validation of Ligand Fishing by MNPs-PTP1B and EC-PTP1B

#### 3.6.1. Preparation of the Standard Mixture

Coumarin and 4-hydroxycinnamic (both are non-PTP1B inhibitors), and rutin (PTP1B inhibitor) were mixed to prepare a standard mixture for validating the selectivity of MNPs-PTP1B and EC-PTP1B for ligand fishing. All the compounds were dissolved in PBS buffer at a concentration of 0.05 mg/mL.

#### 3.6.2. Ligand Fishing from the Standard Mixture by MNPs-PTP1B and EC-PTP1B

MNPs-PTP1B (20 mg) was incubated with 1 mL of the standard mixture at 37 °C for 30 min. After the magnetic separation, the MNPs-PTP1B were washed with 3 mL PBS buffer thrice before 1 mL 50% acetonitrile was added to desorb the ligand. The supernatant after magnetic separation was collected and filtered with a 0.22 µm membrane for HPLC analysis. In the meantime, MNPs were used for ligand fishing following the same procedure as a control for this experiment.

A total of 1 mL EC-PTP1B ( $OD_{600} = 0.5$ ) was incubated with 1 mL standard mixture at 37 °C for 4 h. Then, the mixture was centrifuged for 15 min (4500 rpm) to remove the supernatant. The EC-PTP1B was washed with PBS buffer thrice before 1 mL of 50% acetonitrile was added to desorb the ligand. After centrifugation, the supernatant containing the ligand was collected and filtered with a 0.22 µm membrane for the following analysis. In parallel, the control cells ( $OD_{600} = 0.5$ ) were used as bait for ligand fishing following the same procedure.

### 3.7. Ligand Fishing of PTP1B Inhibitor from *S. miltiorrhiza*

#### 3.7.1. Extraction of *S. miltiorrhiza*

Firstly, 50 g of powdered rhizome of the plant was refluxed twice in 500 mL water in a round bottom flask for 2 h. The aqueous solutions were combined to be concentrated in a rotary evaporator. Because herbs are generally boiled to prepare the decoction and PTP1B of EC-PTP1B or MNP-PTP1B is stable in PBS buffer, the extract was dissolved in PBS buffer to a concentration of 1.0 mg/mL and stored at 4 °C before use.

#### 3.7.2. Ligand Fishing by MNPs-PTP1B and EC-PTP1B

MNPs-PTP1B (20 mg) and EC-PTP1B ( $OD_{600} = 0.5$ ) were incubated with 1 mL extract of *S. miltiorrhiza* at 37 °C for 30 min and 4 h, respectively. The following steps were the same as described in Section 3.6.2 for the corresponding fishing bait. Similarly, MNPs and EC-PTP1B were used as the control in this experiment.

### 3.8. Inhibitory Assay and Kinetic Study of the Enzyme's Ligand Salvianolic Acid B

The PTP1B inhibitory activity of salvianolic acid B was tested as described in 2.5 with sodium orthovanadate as a positive control. A series of concentrations of salvianolic acid B (50 µL) was incubated with 50 µL 10 mM pNPP at 37 °C for 30 min before 100 µL NaOH was added to end the reaction. The inhibition effect on PTP1B was calculated by the formula: inhibition % =  $(A_{\text{blank control}} - A_{\text{sample}}) / A_{\text{blank control}} \times 100\%$ , where  $A_{\text{blank control}}$  and  $A_{\text{sample}}$  stands for the absorbance of the blank control and sample.

For the enzyme kinetic study of salvianolic acid B, the inhibition mode and kinetic constants were calculated by the Lineweaver-Burk plot, and six lines were represented by different concentrations of salvianolic acid B (0,  $1/4 \times IC_{50}$ ,  $1/2 \times IC_{50}$ ,  $3/4 \times IC_{50}$ ,  $1 \times IC_{50}$ , and  $5/4 \times IC_{50}$ ) with a series of increasing concentrations of pNPP (1, 2, 4, 6, 8, and 10 mM). The reaction rate was recorded in the first 20 min after the reaction was triggered by pNPP.

### 3.9. Molecular Docking Study

Molecular docking was conducted to verify the mode of interaction between the ligand and enzyme. The X-ray crystal structure of PTP1B (PDB ID: 1QXK) was obtained from the RCSB PDB protein data bank, and the resultant structure was processed with the

help of Maestro 11.9 software after removing the crystal water, adding a hydrogen atom, repairing incomplete peptide bonds, and minimizing the protein energy. The 3D structure of salvianolic acid B was downloaded from PubChem database. Glide functionalities provided in Schrödinger Maestro software (Schrödinger, Cambridge, MA, USA) were used for the molecular docking [40,41].

#### 4. Conclusions

In this study, ligand fishing methods were employed for screening PTP1B inhibitors based on two functional adsorbents, i.e., MNPs-PTP1B and EC-PTP1B. MNPs-PTP1B was synthesized via covalent binding of PTP1B and carboxyl terminated MNPs for the first time. The storage stability as well as the pH and thermo durability of the two adsorbents were investigated. Both were more stable than the free enzyme, while EC-PTP1B exhibited significant improvement over the MNPs-PTP1B. When applied in the ligand fishing of aqueous extract of *S. miltiorrhiza*, it was interesting to find that only EC-PTP1B fished out an active polyphenolic compound of salvianolic acid B, which was found to be a non-competitive inhibitor of PTP1B with  $IC_{50}$  of 23.35  $\mu$ M. This result indicated that enzymes displayed on the surface of *E. coli* is superior to covalently immobilized ones in terms of ligand fishing due to the maintenance of the natural conformation of the enzyme, thus providing a powerful tool for screening active compounds from complex medicinal plant extracts.

**Supplementary Materials:** The following supporting information can be downloaded at: <https://www.mdpi.com/article/10.3390/molecules27227896/s1>, Table S1: NMR spectroscopic data ( $CD_3OD$ ) for salvianolic acid B; Figure S1:  $^{13}C$  NMR (150 MHz,  $CD_3OD$ ) spectrum of salvianolic acid B; Figure S2:  $^1H$  NMR (600 MHz,  $CD_3OD$ ) spectrum of salvianolic acid B; Figure S3: MS spectrum of salvianolic acid B (positive ion mode); Figure S4:  $IC_{50}$  plot of salvianolic acid B and its chemical structure.

**Author Contributions:** Conceptualization, X.L. and Y.Z.; methodology, X.B. and W.F.; software, X.B.; validation, X.B. and X.L.; formal analysis, X.B. and X.L.; investigation, X.B.; resources, Y.L. (Yipei Liu); data curation, X.B., W.F., and Y.L. (Yingjie Luo); writing—original draft preparation, X.B.; writing—review and editing, Y.L. (Yingjie Luo), X.L., and Y.L. (Yingjie Luo); visualization, W.F. and Y.L. (Yipei Liu); supervision, X.L. and Y.Z.; project administration, X.L. and Y.Z. All authors have read and agreed to the published version of the manuscript.

**Funding:** The research was funded by the Chinese Academy of Sciences, grant number KFJ-BRP-008, the Ministry of Science and Technology of China, grant number E0117G1001.

**Institutional Review Board Statement:** Not applicable.

**Informed Consent Statement:** Not applicable.

**Data Availability Statement:** All data are available upon reasonable request.

**Conflicts of Interest:** The authors declare no conflict of interest.

#### References

1. Cook, W.S.; Unger, R.H. Protein tyrosine phosphatase 1B. *Infect. Immun.* **2002**, *2*, 385–387. [CrossRef]
2. Stanford, S.M.; Aleman Muench, G.R.; Bartok, B.; Sacchetti, C.; Kiosses, W.B.; Sharma, J.; Maestre, M.F.; Bottini, M.; Mustelin, T.; Boyle, D.L. TGF $\beta$  responsive tyrosine phosphatase promotes rheumatoid synovial fibroblast invasiveness. *Ann. Rheum. Dis.* **2016**, *75*, 295–302. [CrossRef] [PubMed]
3. St-Pierre, J.; Tremblay, M.L. Modulation of leptin resistance by protein tyrosine phosphatases. *Cell Metab.* **2012**, *15*, 292–297. [CrossRef] [PubMed]
4. Tonks, N.K.; Muthuswamy, S.K. A brake becomes an accelerator: PTP1B-A new therapeutic target for breast cancer. *Cancer Cell* **2007**, *11*, 214–216. [CrossRef] [PubMed]
5. Zhang, S.; Zhang, Z.Y. PTP1B as a drug target: Recent developments in PTP1B inhibitor discovery. *Drug Discov. Today* **2007**, *12*, 373–381. [CrossRef]
6. Proenca, C.; Ribeiro, D.; Freitas, M.; Carvalho, F.; Fernandes, E. A comprehensive review on the antidiabetic activity of flavonoids targeting PTP1B and DPP-4: A structure-activity relationship analysis. *Crit. Rev. Food Sci. Nutr.* **2021**, *62*, 4095–4151. [CrossRef]

7. Zhan, Z. Advances in biosynthesis and regulation of the active ingredient of *Salvia miltiorrhiza* based on multi-omics approach. *Acta Pharm. Sin.* **2020**, *55*, 2892–2903.
8. Ma, R.F.; Zhu, R.Y.; Wang, L.L.; Guo, Y.B.; Liu, C.Y.; Liu, H.X.; Liu, F.W.; Li, H.J.; Li, Y.; Fu, M.; et al. Diabetic osteoporosis: A review of its traditional chinese medicinal use and clinical and preclinical research. *Evid.-Based Complement. Altern. Med.* **2016**, *2016*, 3218313. [[CrossRef](#)]
9. Kim, D.H.; Paudel, P.; Yu, T.; Thi Men, N.; Kim, J.A.; Jung, H.A.; Yokozawa, T.; Choi, J.S. Characterization of the inhibitory activity of natural tanshinones from *Salvia miltiorrhiza* roots on protein tyrosine phosphatase 1B. *Chem.-Biol. Interact.* **2017**, *278*, 65–73. [[CrossRef](#)]
10. Kim, Y.H.; Kim, B.Y.; Seog, A.J. Screening of the inhibitory activity of medicinal plants against protein tyrosine phosphatase 1B. *Korean J. Pharmacogn.* **2004**, *35*, 16–21.
11. Zhu, Y.T.; Jia, Y.W.; Liu, Y.M.; Liang, J.; Ding, L.S.; Liao, X. Lipase ligands in *Nelumbo nucifera* leaves and study of their binding mechanism. *J. Agric. Food Chem.* **2014**, *62*, 10679–10686. [[CrossRef](#)]
12. Wang, H.B.; Zhao, X.P.; Wang, S.F.; Tao, S.; Ai, N.; Wang, Y. Fabrication of enzyme-immobilized halloysite nanotubes for affinity enrichment of lipase inhibitors from complex mixtures. *J. Chromatogr. A* **2015**, *1392*, 20–27. [[CrossRef](#)] [[PubMed](#)]
13. Tao, Y.; Zhang, Y.F.; Wang, Y.; Cheng, Y.Y. Hollow fiber based affinity selection combined with high performance liquid chromatography-mass spectroscopy for rapid screening lipase inhibitors from lotus leaf. *Anal. Chim. Acta* **2013**, *785*, 75–81. [[CrossRef](#)]
14. Hou, X.F.; Zhou, M.Z.; Jiang, Q.; Wang, S.C.; He, L.C. A vascular smooth muscle/cell membrane chromatography-offline-gas chromatography/mass spectrometry method for recognition, separation and identification of active components from traditional Chinese medicines. *J. Chromatogr. A* **2009**, *1216*, 7081–7087. [[CrossRef](#)]
15. Wen, Y.Y.; Li, J.H.; Ma, J.P.; Chen, L.X. Recent advances in enrichment techniques for trace analysis in capillary electrophoresis. *Electrophoresis* **2012**, *33*, 2933–2952. [[CrossRef](#)]
16. Ji, L.Y.; Wu, J.H.; Luo, Q.; Li, X.C.; Zheng, W.; Zhai, G.J.; Wang, F.Y.; Lu, S.; Feng, Y.Q.; Liu, J.N.; et al. Quantitative mass spectrometry combined with separation and enrichment of phosphopeptides by titania coated magnetic mesoporous silica microspheres for screening of protein kinase inhibitors. *Anal. Chem.* **2012**, *84*, 2284–2291. [[CrossRef](#)] [[PubMed](#)]
17. Song, H.P.; Chen, J.; Hong, J.Y.; Hao, H.; Qi, L.W.; Lu, J.; Fu, Y.; Wu, B.; Yang, H.; Li, P. A strategy for screening of high-quality enzyme inhibitors from herbal medicines based on ultrafiltration LC-MS and in silico molecular docking. *Chem. Commun.* **2015**, *51*, 1494–1497. [[CrossRef](#)]
18. Mark, D.; Haeberle, S.; Roth, G.; von Stetten, F.; Zengerle, R. Microfluidic lab-on-a-chip platforms: Requirements, characteristics and applications. *Chem. Soc. Rev.* **2010**, *39*, 1153–1182. [[CrossRef](#)] [[PubMed](#)]
19. Yuan, Y.C.; Bai, X.L.; Liu, Y.M.; Tang, X.Y.; Yuan, H.; Liao, X. Ligand fishing based on cell surface display of enzymes for inhibitor screening. *Anal. Chim. Acta* **2021**, *1156*, 338359. [[CrossRef](#)] [[PubMed](#)]
20. Stano, J.; Siekel, P.; Micieta, K.; Blanarikova, V.; Korenova, M.; Bergerova, E.; Nemeč, P. Identification and determination of the intra- and extracellular aminopeptidase activity by synthetic L-Ala-, L-Tyr-, and L-Phe-beta-naphthylamide. *Pharmazie* **2008**, *63*, 909–912. [[PubMed](#)]
21. Cui, C.; Tao, Y.F.; Li, L.L.; Chen, B.Q.; Tan, T.W. Improving the activity and stability of *Yarrowia lipolytica* lipase Lip2 by immobilization on polyethyleneimine-coated polyurethane foam. *J. Mol. Catal. B Enzym.* **2013**, *91*, 59–66. [[CrossRef](#)]
22. Yao, Y.F.; Ding, Q.B.; Ou, L. Biosynthesis of (deoxy)guanosine-5'-triphosphate by GMP kinase and acetate kinase fixed on the surface of *E. coli*. *Enzym. Microb. Technol.* **2019**, *122*, 82–89. [[CrossRef](#)]
23. Francisco, J.A.; Stathopoulos, C.; Warren, R.A.J.; Kilburn, D.G.; Georgiou, G. Specific adhesion and hydrolysis of cellulose by intact *Escherichia coli* expressing surface anchored cellulase or cellulose binding domains. *Biotechnology* **1993**, *11*, 491–495.
24. Wang, A.A.; Mulchandani, A.; Chen, W. Whole-cell immobilization using cell surface-exposed cellulose-binding domain. *Biotechnol. Prog.* **2001**, *17*, 407–411. [[CrossRef](#)]
25. Wang, A.J.A.; Mulchandani, A.; Chen, W. Specific adhesion to cellulose and hydrolysis of organophosphate nerve agents by a genetically engineered *Escherichia coli* strain with a surface-expressed cellulose-binding domain and organophosphorus hydrolase. *Appl. Environ. Microbiol.* **2002**, *68*, 1684–1689. [[CrossRef](#)] [[PubMed](#)]
26. Colak, U.; Gencer, N. Immobilization of paraoxonase onto chitosan and its characterization. *Artif. Cells Blood Substit. Biotechnol.* **2012**, *40*, 290–295. [[CrossRef](#)]
27. Han, Y.M.; Oh, H.; Na, M.K.; Kim, B.S.; Oh, W.K.; Kim, B.Y.; Jeong, D.G.; Ryu, S.E.; Sok, D.E.; Ahn, J.S. PTP1B inhibitory effect of abietane diterpenes isolated from *Salvia miltiorrhiza*. *Biol. Pharm. Bull.* **2005**, *28*, 1795–1797. [[CrossRef](#)] [[PubMed](#)]
28. Sun, Y.S.; Zhu, H.F.; Wang, J.H.; Liu, Z.B.; Bi, J.J. Isolation and purification of salvianolic acid A and salvianolic acid B from *Salvia miltiorrhiza* by high-speed counter-current chromatography and comparison of their antioxidant activity. *J. Chromatogr. B Anal. Technol. Biomed. Life Sci.* **2009**, *877*, 733–737. [[CrossRef](#)]
29. Wu, J.Z.; Ardah, M.; Haikal, C.; Svanbergsson, A.; Diepenbroek, M.; Vaikath, N.N.; Li, W.; Wang, Z.Y.; Outeiro, T.F.; El-Agnaf, O.M.; et al. Dihydromyricetin and salvianolic acid B inhibit alpha-synuclein aggregation and enhance chaperone-mediated autophagy. *Transl. Neurodegener.* **2019**, *8*, 18. [[CrossRef](#)] [[PubMed](#)]
30. Jiang, P.; Guo, Y.J.; Dang, R.L.; Yang, M.Q.; Liao, D.H.; Li, H.D.; Sun, Z.; Feng, Q.Y.; Xu, P.F. Salvianolic acid B protects against lipopolysaccharide-induced behavioral deficits and neuroinflammatory response: Involvement of autophagy and NLRP3 inflammasome. *J. Neuroinflamm.* **2017**, *14*, 239. [[CrossRef](#)] [[PubMed](#)]

31. Chen, R.; Zhu, C.Q.; Xu, L.; Gu, Y.; Ren, S.J.; Bai, H.; Zhou, Q.; Liu, X.; Lu, S.F.; Bi, X.L.; et al. An injectable peptide hydrogel with excellent self-healing ability to continuously release salvianolic acid B for myocardial infarction. *Biomaterials* **2021**, *274*, 120855. [[CrossRef](#)]
32. Ha, M.T.; Shrestha, S.; Tran, T.H.; Kim, J.A.; Woo, M.H.; Choi, J.S.; Min, B.S. Inhibition of PTP1B by farnesylated 2-arylbenzofurans isolated from *Morus alba* root bark: Unraveling the mechanism of inhibition based on in vitro and in silico studies. *Arch. Pharmacol Res.* **2020**, *43*, 961–975. [[CrossRef](#)]
33. Saeed, M.; Shoab, A.; Tasleem, M.; Alabdallah, N.M.; Alam, M.J.; El Asmar, Z.; Jamal, Q.M.S.; Bardakci, F.; Alqahtani, S.S.; Ansari, I.A.; et al. Assessment of antidiabetic activity of the shikonin by allosteric inhibition of protein-tyrosine phosphatase 1B (PTP1B) using state of art: An in silico and in vitro tactics. *Molecules* **2021**, *26*, 3996. [[CrossRef](#)] [[PubMed](#)]
34. Hu, Y.; Li, J.X.; Chang, A.K.; Li, Y.N.; Tao, X.; Liu, W.B.; Wang, Z.N.; Su, W.P.; Li, Z.H.; Liang, X. Screening and tissue distribution of protein tyrosine phosphatase 1B inhibitors in mice following oral administration of *Garcinia mangostana* L. ethanolic extract. *Food Chem.* **2021**, *357*, 129759. [[CrossRef](#)] [[PubMed](#)]
35. Sasaki, T.; Li, W.; Higai, K.; Tran Hong, Q.; Kim, Y.H.; Koike, K. Protein tyrosine phosphatase 1B inhibitory activity of lavandulyl flavonoids from roots of *Sophora flavescens*. *Planta Med.* **2014**, *80*, 557–560. [[CrossRef](#)]
36. Banchi, L.; Fingerhuth, M.; Babej, T.; Ing, C.; Arrazola, J.M. Molecular docking with gaussian boson sampling. *Sci. Adv.* **2020**, *6*, eaax1950. [[CrossRef](#)] [[PubMed](#)]
37. Chen, Z.M.; Liu, L.L.; Wu, X.D.; Yang, R.C. Synthesis of Fe<sub>3</sub>O<sub>4</sub>/P(St-AA) nanoparticles for enhancement of stability of the immobilized lipases. *RSC Adv.* **2016**, *6*, 108583–108589. [[CrossRef](#)]
38. Liu, B.; Wang, D.; Huang, W.; Yu, M.; Yao, A. Fabrication of nanocomposite particles with superparamagnetic and luminescent functionalities. *Mater. Res. Bull.* **2008**, *43*, 2904–2911. [[CrossRef](#)]
39. Bradford, M.M. Rapid and sensitive method for the quantitation of microgram quantities of protein utilizing the principle of protein-dye binding. *Anal. Biochem.* **1976**, *72*, 248–254. [[CrossRef](#)]
40. Rajeswari, M.; Santhi, N.; Bhuvanawari, V. Pharmacophore and virtual screening of JAK3 inhibitors. *Bioinformation* **2014**, *10*, 157–163. [[CrossRef](#)] [[PubMed](#)]
41. Fazi, R.; Tintori, C.; Brai, A.; Botta, L.; Selvaraj, M.; Garbelli, A.; Maga, G.; Botta, M. Homology model-based virtual screening for the identification of human helicase DDX3 inhibitors. *J. Chem. Inf. Model.* **2015**, *55*, 2443–2454. [[CrossRef](#)] [[PubMed](#)]

Review

# Overview of the Polyphenols in Salicornia: From Recovery to Health-Promoting Effect

Francesco Limongelli <sup>1</sup>, Pasquale Crupi <sup>2,\*</sup>, Maria Lisa Clodoveo <sup>2</sup>, Filomena Corbo <sup>3</sup> and Marilena Muraglia <sup>3</sup>

<sup>1</sup> Dipartimento di Scienze del Suolo e Degli Alimenti, Università degli Studi di Bari, Campus Universitario E. Quagliarello Via Orabona 4, 70125 Bari, Italy

<sup>2</sup> Dipartimento Interdisciplinare di Medicina, Università degli Studi Aldo Moro Bari, Piazza Giulio Cesare 11, 70124 Bari, Italy

<sup>3</sup> Dipartimento di Farmacia-Scienze del Farmaco, Università degli Studi di Bari, Campus Universitario E. Quagliarello Via Orabona 4, 70125 Bari, Italy

\* Correspondence: pasquale.crupi@uniba.it or pasquale.crupi@crea.gov.it

**Abstract:** Nowadays, there has been considerable attention paid toward the recovery of waste plant matrices as possible sources of functional compounds with healthy properties. In this regard, we focus our attention on Salicornia, a halophyte plant that grows abundantly on the coasts of the Mediterranean area. Salicornia is used not only as a seasoned vegetable but also in traditional medicine for its beneficial effects in protecting against diseases such as obesity, diabetes, and cancer. In numerous research studies, Salicornia consumption has been highly suggested due to its high level of bioactive molecules, among which, polyphenols are prevalent. The antioxidant and antiradical activity of polyphenols makes Salicornia a functional food candidate with potential beneficial activities for human health. Therefore, this review provides specific and compiled information for optimizing and developing new extraction processes for the recovery of bioactive compounds from Salicornia; focusing particular attention on polyphenols and their health benefits.

**Keywords:** Salicornia; extraction technologies; phenolic acids; flavonoids; lignans

**Citation:** Limongelli, F.; Crupi, P.; Clodoveo, M.L.; Corbo, F.; Muraglia, M. Overview of the Polyphenols in Salicornia: From Recovery to Health-Promoting Effect. *Molecules* **2022**, *27*, 7954. <https://doi.org/10.3390/molecules27227954>

Academic Editor: Nour Eddine Es-Safi

Received: 18 October 2022

Accepted: 15 November 2022

Published: 17 November 2022

**Publisher's Note:** MDPI stays neutral with regard to jurisdictional claims in published maps and institutional affiliations.



**Copyright:** © 2022 by the authors. Licensee MDPI, Basel, Switzerland. This article is an open access article distributed under the terms and conditions of the Creative Commons Attribution (CC BY) license (<https://creativecommons.org/licenses/by/4.0/>).

## 1. Introduction






Recently, the use of natural substances as a health resource has become increasingly popular, especially the recovery of antioxidants, minerals, pigments, polymer, and oils from fresh vegetable matrices and agro-industrial by-products. Furthermore, nutraceutical extracts from food plants are finding success due to their nutritional and functional properties [1,2].

Salicornia is a halophyte plant that grows in saltwater around much of the Mediterranean coast as well as in the coastal regions of East Asia. The most-studied species of Salicornia, illustrated in Table 1, are the following:

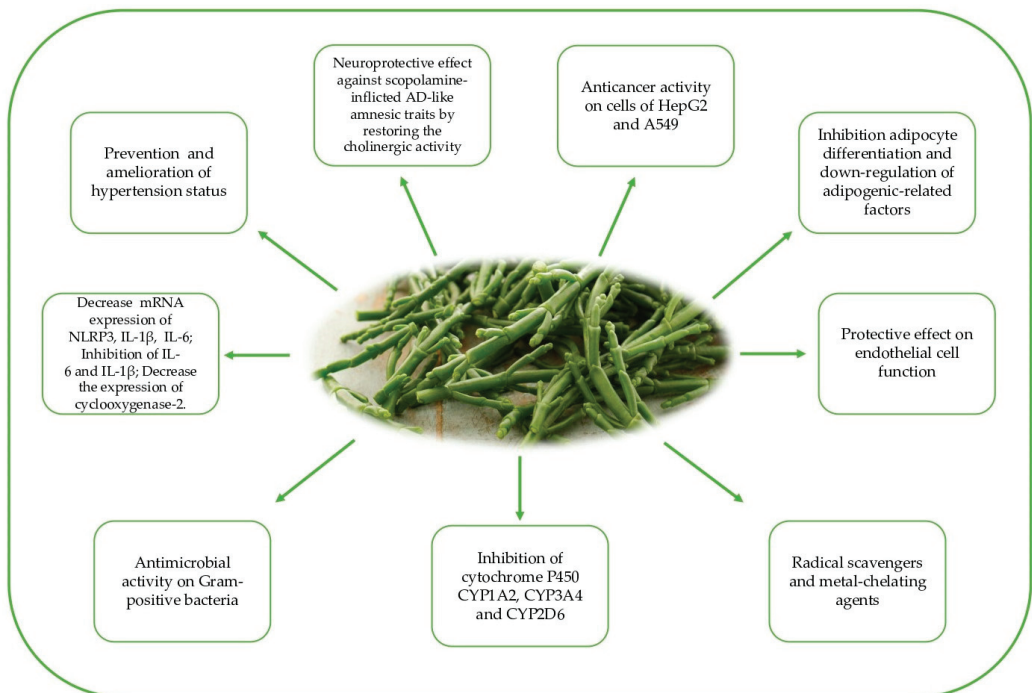
- *S. europea*, the common glasswort, appears as a relatively small plant, having bright green stems characterized by small leaves and fleshy fruits that contain a single seed. It is present in Britain, France, and Ireland [3];
- *S. bigelovii*, the dwarf saltwort Salicornia, is located in USA and Mexico and can be distinguished from other species by its acute and sharply mucronate leaf and bract tips [4];
- *S. ramosissima*, also known as purple glasswort, is situated in France and Iberia and has stems up to 30 cm high, highly branched, green or purple depending on their youth [5];
- *S. herbacea*, the dwarf glasswort, is diffused in Korea and Italy and has fleshy, erect stems and opposite leaves, similar in appearance to flattened scales on the stems [6];
- *S. brachiata*, also named umari keerai, is located in India [7].



**Table 1.** Characteristics of the main *Salicornia* plants.

					
<b>Botanical name</b>	<i>S. bigelovii</i>	<i>S. brachiata</i>	<i>S. europaea</i>	<i>S. ramosissima</i>	<i>S. herbacea</i>
<b>Common names</b>	Dwarf saltwort	Umari Keerai	Common glasswort	Purple glasswort	Dwarf glasswort
<b>Geographical range</b>	USA, Mexico	India	Britain, France, Ireland	France, Iberia	South Korea
<b>References</b>	[4]	[7]	[3]	[5]	[6]

*Salicornia* has long been used in traditional Eastern medicine to treat intestinal disorders (diarrhea and constipation) and inflammatory disorders, including nephropathies, hepatitis, diabetes, and cancer (Figure 1). Furthermore, the effects of *Salicornia* extract on pain were recently evaluated by performing a placebo-controlled study to investigate its analgesic and antipruritic effects, e.g., the effects on neurogenic inflammation at 24 and 48 h after the topical application of *S. ramosissima* in healthy subjects [8]. The collected results represent a starting point both for the evaluation of the antinociceptive potential of the bioactive compounds of *Salicornia* and for overcoming the limits derived from its pharmaceutical synthesis in this sector [9].

**Figure 1.** Health biological effects of *Salicornia*.

It is acknowledged that saline stress leads to the production of reactive oxygen species (ROS) that damage cell membranes and enzymatic activity in plants [10]. *Salicornia* is one of the most salt-tolerant species and is, therefore, equipped with a powerful antioxidant system (including enzymes and antioxidant compounds) capable of extinguishing and

resisting ROS, and is also responsible for its therapeutic effect against the aforementioned chronic diseases. Therefore, the medicinal qualities of this plant have aroused the interest of the scientific community, spurring investigation of its phytochemical composition. Phytochemicals found in *Salicornia*, such as tungtunmadic acid, quercetin, chlorogenic acid, and their glycosides, contain many hydroxyl groups that make them highly electrophilic; this feature is fundamental because it induces the stimulation of antioxidant enzymes and exerts a radical scavenging activity, thus protecting cells from the damage provoked by ROS [11].

Nowadays, there is a growing interest in the valorization of such food plants and their eventual by-products for the recovery and/or biotransformation in various industrial applications, such as food supplements, cosmetics, and the pharmaceutical industry [12]. For this reason, more cost-effective and sustainable extraction methods to obtain nutraceutical extracts have been developed in the last few years [13,14]. Different extraction techniques have been used to isolate phytochemicals in *Salicornia* extracts, ranging from the more traditional (such as solid–liquid extraction by maceration) to non-conventional emerging technologies (such as microwave and ultrasound-assisted extraction and supercritical fluid extraction) in order to favor mass transfer, shorten extraction times, and/or reduce solvent requirements. Moreover, the technological parameters (i.e., particle size, solvent type and composition, solid-to-solvent ratio, extraction temperature and pressure, extraction time, and pH) affecting the extractability of bioactive compounds have been carefully optimized [15].

This review deals with an overview of the principal phytochemicals (especially polyphenols) identified in *Salicornia* that have shown health benefits, as well as the most widespread extraction methods (including green processes) employed for their recovery.

## 2. Principal Phytochemicals (Especially Polyphenols) Identified in *Salicornia*

Several studies on the characterization of *Salicornia* extracts by analytical techniques (i.e., HPLC-UV, HPLC-MS, GC-MS, etc.) have reported the presence of vitamins, amino acids, minerals, sterols, fatty acids, saponins, oxalates, phenolic acids, flavonoids, and lignans [16,17].

*Salicornia* has shown high levels of vitamin C; the content of ascorbic and dehydroascorbic acids is more than 100 mg/100 g. *S. bigelovii* shows a high amount of  $\beta$ -carotene (15.9 mg/100 g of fresh weight (fw)), which is a good source of vitamin A [10,18]. Lima et al., 2020 have reported a high content of the soluble fat vitamin E,  $\alpha$ -Tocopherol (241  $\mu$ g/100 g fw), and vitamin B<sub>2</sub> and B<sub>5</sub> (with a relative content of 4.14% in 0.5 g) in *S. ramosissima* and *S. bigelovi*, respectively [19,20].

Significant contents of important amino acids, such as aspartic acid (140.1 and 165.5 mg/100 g fw), glutamic acid (160.5 and 182.3 mg/100 g fw), and isoleucine (107.5 and 94.7 mg/100 g fw) were quantified in stems and roots of *S. herbacea*. While, six amino acids, including glutamic and aspartic acids, which were present at the highest concentration, were found in *S. bigelovii* [16,18].

Na<sup>+</sup> and K<sup>+</sup> were the most abundant minerals in the *Salicornia* species; indeed, especially *S. bigelovi* and *S. europea* could be used as a salt substitute due to their protective effect on vascular dysfunction and hypertension. Recent studies proved that a high intake of salt increased blood pressure in rats, while intake of *Salicornia*, with the same quantity of sodium, had a low effect on blood pressure [21,22]. Up to 1421.2 and 173.3 mg/100 g of Na<sup>+</sup> and K<sup>+</sup>, respectively, were found in *S. europea* leaves. In addition, important amounts of other minerals were also identified mainly in stems and roots of *S. herbacea* and *S. europea*, such as Ca<sup>2+</sup> (158.8 mg/100 g), K<sup>+</sup> (740.1 mg/100 g), Mg<sup>2+</sup> (52.2 mg/100 g), and Fe<sup>2+</sup> (3.25 mg/100 g) [23,24]. Moreover, the presence of selenium, an essential micronutrient with a significant antioxidant effect, was found in *S. brachiata* [25].

Sterols have been identified in *S. herbacea* and *S. europea* extracts. The main sterols contained are stigmasterol and ergosterol. Stigmasterol (0.47 mg/kg) shows hypoglycemic, antioxidant, antitumor, antimutagenic, and anti-inflammatory properties while ergosterol

(0.31 mg/kg) is an important source of vitamin D and possesses potent NF- $\kappa$ B inhibitory activities [11,26]. Another sterol identified is the  $\beta$ -sitosterol, the predominant phytosterol in the human diet, with neuroprotective and anti-diabetic effects [27,28].

Salicornia shows also a relevant amount of saturated and polyunsaturated fatty acids, including stearic acid, linolenic acid, linoleic acid, and palmitic acid, especially found in *S. herbacea*, *S. europea*, and *S. brachiata* species [29,30]. Linolenic acid is the most representative polyunsaturated fatty acid mainly found in Salicornia leaves at concentrations around 4 mg/g [31]. This compound is used in the prevention and treatment of many common diseases such as arthritis, eczema, and premenstrual syndrome [31,32]. Linoleic acid, mostly contained in leaves (2.18 mg/g), is an essential fatty acid whose consumption is fundamental to good health. It exhibited high antioxidant and antiproliferative activities toward HepG2 and A549 cells, as shown by Wang et al., 2013 [11].

Saponins were identified in *S. herbacea* and *bigelovii* extracts with antioxidant and antifungal effects. Among these, new noroleanane and nortriterpene saponins were isolated. Nevertheless, saponins could exhibit toxicity due to tissue necrotic and gut permeability alteration, which can compromise the immune system [30]. Similarly, oxalates, which were revealed in high content, are anti-nutrients that should be removed to justify usage of Salicornia as a 'sea vegetable' [30].

Other identified aliphatic compounds are octacosanol and tetracosanol, two aliphatic alcohols isolated from *S. europea* and *ramosissima*. Tetracosanol has a significant role in diabetes therapy for its  $\alpha$ -amylase ability, while Octacosanol has been known for its ability to lower total cholesterol levels [30,33].

However, despite the significant amount of the aforementioned nutrients present in Salicornia tissues, major attention has been devoted to their phenolics content, which ranges from 1.2 to 2 mg GAE/g fw [34], due to the related health benefits and bioactivity [35]. Phenolic compounds, characterized by aromatic rings with one or more hydroxyl groups, include several structurally different classes; those found in Salicornia extracts at different concentration levels are mainly phenolic acids, flavonoids, and lignans [28] (Figure 2).

### 2.1. Phenolic Acids

Phenolic acids are a class of polyphenols very abundant in the human diet, as they are contained in vegetables, fruits, and whole grains. The daily intake of phenolic acids should be around 200 mg/day [36]. Phenolic acids are types of aromatic acid compounds derivatives of benzoic and cinnamic acids. They exhibit high antioxidant activity and thus possess health protective effects, such as antimicrobial, anticancer, anti-inflammatory, and anti-mutagenic. [37]

Salicornia has been shown to possess a high content of phenolic acids, including chlorogenic, tungtungmadic, ferulic, protocatechuic, caffeic, salicylic, syringic, and coumaric acids [23,38].

Chlorogenic acid, an ester of caffeic acid, is found in many plants, including Salicornia, with a content of 0.84 mg/g of dry weight (dw) from ethanolic extract of *S. europea* [39]. Furthermore, various chlorogenic acid derivatives, such as dicaffeoylquinic acids, have been also identified in Salicornia. For instance, four new dicaffeoylquinic acid derivatives, specifically 3-caffeoyl-5-dihydrocaffeoylquinic acid ( $75.6 \pm 2.3$  mg/100 g fw), 3-caffeoyl-5-dihydrocaffeoylquinic acid methyl ester ( $69.3 \pm 1.4$   $\mu$ g/100 g fw), 3-caffeoyl-4-dihydrocaffeoylquinic acid methyl ester ( $71.9 \pm 1.9$   $\mu$ g/100 g fw), and 3,5-dihydrocaffeoylquinic acid methyl ester ( $171.9 \pm 1.5$   $\mu$ g/100 g fw), as well as 3-caffeoylquinic acid and 3-caffeoylquinic acid methyl ester, were isolated from the aerial parts of *S. herbacea*. The antioxidant activity of these compounds was examined by measuring the cholesteryl ester hydroperoxide (CE-OOH) content, produced by oxidation in healthy human plasma, during rat blood plasma oxidation induced by copper ions. CE-OOH accumulates in atherosclerotic plaques, and for this reason, it has been used as an index of lipid peroxidation to evaluate the inhibitory effect of antioxidants on lipids oxidized in blood plasma. The caffeoylquinic acid derivatives considerably inhibited CE-OOH. In particular, the

dicafeoylquinic acid derivatives showed a relatively higher ability to inhibit CE-OOH formation rather than monocaffeoylquinic acid derivatives and caffeic acid. Moreover, this important activity is demonstrated by their significant scavenging effects, as shown by the DPPH assay performed. DPPH radical-scavenging activities and metal-chelating effects of caffeoylquinic acid derivatives were proportionally correlated with the number of catechol groups. Therefore, the dicafeoylquinic acid derivatives, isolated from *S. herbacea*, containing a catechol group may act as excellent radical scavengers and metal-chelating agents [40].

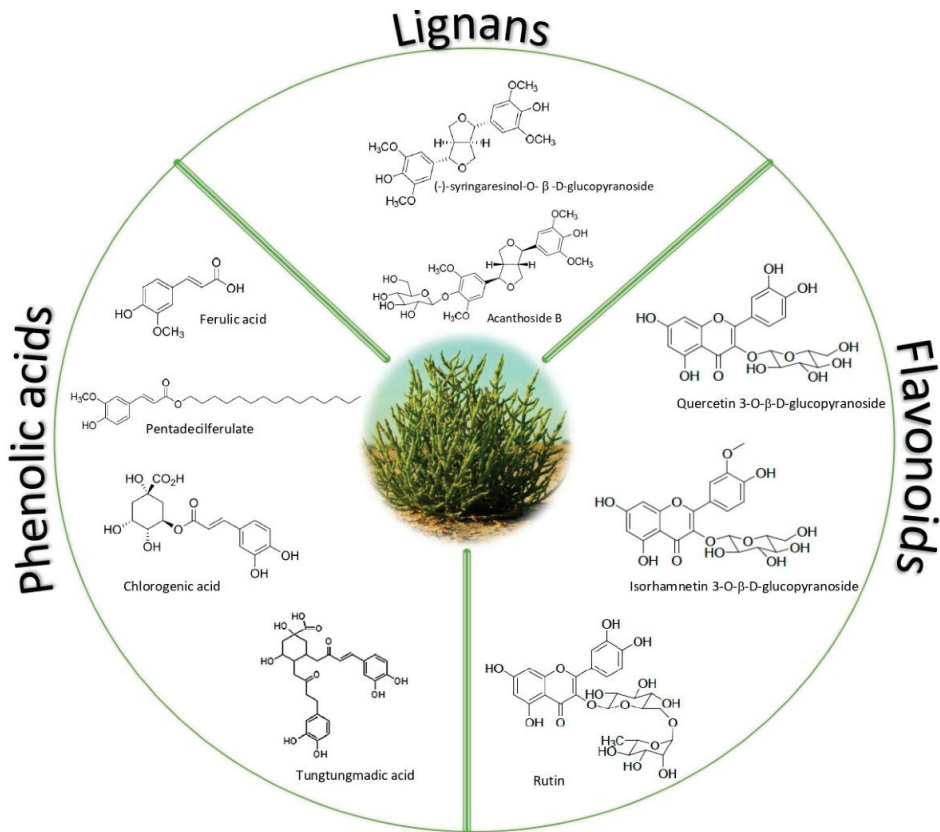


**Figure 2.** Classes of polyphenols revealed in *Salicornia*.

3-caffeoyl-4-dicafeoylquinic acid (CDCQ), known as tungtungmadic acid, has been isolated from *S. herbacea*. It is a natural chlorogenic acid derivative with high antioxidative activity in free radical scavenging assay and in the iron-induced liver microsomal lipid peroxidation test. In addition, it shows a significant effect in protecting the plasmid DNA against strand breakage induced by  $\text{Fe}^{3+}$ -nitrilotriacetic acid-hydrogen peroxide [38].

CDCQ antioxidant, anti-inflammatory, and anticancer effects were demonstrated on nitric oxide (NO) production and eNOS phosphorylation in endothelial cells. CDCQ induced eNOS phosphorylation and NO production by the phosphorylation of PKA, CaMKII, CaMKK $\beta$ , and AMPK in endothelial cells. Furthermore, CDCQ exhibited activities on the L-type  $\text{Ca}^{2+}$  channel (LTCC), present in the membrane of endothelial cells, and mediated signaling by increasing intracellular  $\text{Ca}^{2+}$  influx (Figure 3) [41]. Overall, CDCQ exercises a significant protective effect on endothelial cell function, which is important for modulating hemostasis, blood flow, and vascular health [42,43].

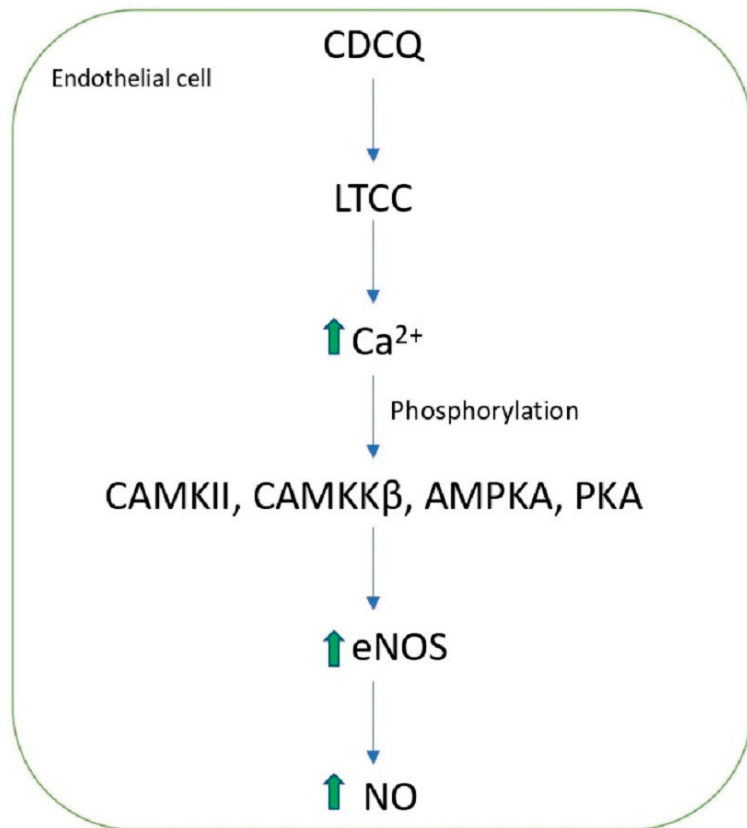


**Figure 3.** 3-caffeoyl-4-dicaffeoylquinic acid (CDCQ) mechanism on eNos and NO in endothelial cells.

Ferulic acid is abundant in plants and it is mainly conjugated with mono- and oligosaccharides and lipids. *trans*-ferulic acid (TFA) was the most abundant component identified in desalted *S. europaea* powder (DSP), exhibiting significant biological effects. When administered to rats with HFD-induced obesity, DSP reduced body weight gain, abdominal fat mass, and serum lipid profiles. Furthermore, it inhibited adipogenesis and adipocyte differentiation by down-regulating the adipocyte-specific transcriptional regulators SREBP1, FAS, C/EBP $\alpha$ , and PPAR $\alpha$ . Therefore, these results show that DSP and, in particular, TFA could protect against HFD-induced obesity [44].

Another research examined the biological effects of *trans*-ferulic ( $2.60 \pm 0.33$  mg/g) and *p*-coumaric ( $3.19 \pm 0.47$  mg/g) acids isolated from *S. europaea*. Notably, the two acids contained in the *Salicornia* extracts were investigated for their effect on vascular dysfunction and hypertension. *p*-coumaric acid and *trans*-ferulic acid-induced vasorelaxation in a dose-dependent manner in the coronary artery on vascular dysfunction induced by high salt content [21].

Wang et al., 2013, isolated (from *S. herbacea*) for the first time the pentadecylferulate, an alkyl ester of ferulic acid. This compound showed higher antioxidant activity than ascorbic acid and other ferulic acid derivatives in the DPPH assay, probably due to its structure characterized by a long-chain alkane (15-carbon) moiety. In addition, it showed anticancer activity in cells of hepatocarcinoma HepG2 and pulmonary adenocarcinoma A549 [11].

Various extracts of *S. europaea* collected from two different regions of Tunisia were evaluated for their antimicrobial activity, using the agar well diffusion method. The two different ethanolic extracts exhibited a high total phenolic content (TPC,  $43.1 \pm 0.2$  and

32.1 ± 0.3 mg GAE/g dw) with a rich composition in phenolic acids, including gallic acid (0.8 mg/g dw), chlorogenic acid (0.22 mg/g dw), vanillic acid (0.69 mg/g dw), caffeic acid (0.28 mg/g dw), and coumaric acid (0.32 mg/g dw), but also in catechin hydrate (1.17 mg/g dw) and rutin hydrate (10.05 mg/g dw). Because of the structural difference in their lipid layer, Gram-positive bacteria were significantly more sensitive to the two extracts and showed more inhibition zones compared to Gram-negative bacteria [24]. Thus, a synergistic or additive effect of the phenolic acids with the other compounds could be hypothesized for the antimicrobial activity of *S. europaea* extracts [24,45]. Another study [46] confirmed the antimicrobial activity of other halophyte plants, such as *S. brachiata*, whose extracts were also very efficient against Gram-positive bacteria.

The effect of *S. ramosissima* ethanolic extract was evaluated on carbon tetrachloride (CCl<sub>4</sub>)-induced testicular damage in a mouse model. The phytochemical composition of the extract showed the presence of known phenolic and aliphatic compounds, such as ethyl linolenate (0.44 mg/g dw), sitostanol (0.09 mg/g dw), octadecyl (0.12 mg/g dw) and eicosanyl (0.09 mg/g dw) (E)-ferulates, ethyl (E)-2-hydroxycinnamate (0.06 mg/g dw), and scopoletin (0.09 mg/g dw). The results of the histopathological analysis showed that the treatment with the ethanolic extract prior to CCl<sub>4</sub> administration significantly prevented the architectural disorder of seminiferous epithelium and germ cell exfoliation. Therefore, the nature of the extracted compounds suggests a significant therapeutic value on the male reproductive system, especially due to the antioxidant action of its constituents, besides other therapeutic and nutritional effects of certain compounds isolated [47].

## 2.2. Flavonoids

Flavonoids are the most important phytochemical compounds present in many plants, fruits, and vegetables, which confer many health benefits, including anticancer, antioxidant, anti-inflammatory, antiviral, neuroprotective, and cardioprotective effects [48]. Their chemical structure, in particular the presence of hydroxy groups, influences their bioavailability and biological activity [49,50]. Flavonoids possess a basic 15-carbon flavone skeleton with two benzene (A-B) rings connected by a three-carbon pyran ring. The position of the catechol B-ring and the number of hydroxy groups on the B-ring influence their antioxidant capacity [51,52].

Rutin, isorhamnetin, quercetin, quercetin 3-O-β-D-glucopyranoside, isorhamnetin 3-O-β-D-glucopyranoside, noreugenin, and isoquercitrin are the most prevalent compounds in *Salicornia*. These compounds, especially quercetin, rutin, and isorhamnetin 3-O-β-D-glucopyranoside, have relevant anti-diabetic, cardiovascular protection, and anticancer activity due to their antioxidant potential [53,54]. Isorhamnetin 3-O-β-D-glucopyranoside, isolated from *S. herbacea*, exhibited scavenging intracellular radical activity in the cellular system, as well as in the cell-free system. Moreover, it participated in the modulation of cellular redox status due to the induction of cellular GSH levels and other antioxidant enzymes. Therefore, this compound showed a relevant effect in the prevention of radical-mediated cellular damage and could be developed as a candidate for potential use as a natural antioxidant related to oxidative stress [55]. Significant content (up to 57.52% of total compounds) of flavonoids and flavonoid glycosides have been revealed in *S. bigelovii* and *S. europaea* extracts. Other studies reported in the literature have isolated rutin hydrate (10.05 mg/g dw) and catechin hydrate (1.17 mg/g dw) from *S. europaea* [24,39,56].

Kim et al., 2011 isolated a novel flavonoid glycoside, isoquercitrin 6''-O-methyloxalate from *S. herbacea*; this compound, along with quercetin 3-O-β-D-glucopyranoside, exhibited a relevant antioxidant activity compared to other flavonoids compounds that presented substitutions on catechol group of B ring [57]. Therefore, the catechol group of the B ring has an important effect on the pharmaceutical property of the molecule. In particular, it influences the antioxidant activity of flavonoids as reported by previous studies [58].

The flavonol glycosides, isoquercitrin 6''-O-methyloxalate, isorhamnetin 3-O-β-D-glucopyranoside, and quercetin 3-O-β-D-glucopyranoside from *S. herbacea* extract have been examined in macrophages and trophoblasts to test their inflammatory properties. Pre-

treatment and delayed treatment of these compounds in bone marrow-derived macrophages (BMDMs) reduced the activity of NLRP3 inflammasome induced by lipopolysaccharide (LPS) and adenosine triphosphate stimulation and downregulated interleukin (IL)-1 $\beta$  production. In addition, the extract decreased the mRNA expression of NLRP3, IL-1 $\beta$ , and IL-6 in the LPS-stimulated human trophoblast cell line inhibiting the production of IL-6 and IL-1 $\beta$  and decreasing the expression of cyclooxygenase-2 [59].

Other interesting flavonoids have been isolated from *S. Europea* such as luteolin (0.019 mg/g dw), kaempferol (108.1–247.6 mg/100 g dw) [60], and its glucoside derivative [29]. Like previous molecules, these compounds also have antioxidant, anti-inflammatory, antiapoptotic, and cardioprotective activities [61].

Another study explored the effects of the ethyl acetate fraction of desalted *S. europea* extract on atherosclerotic events in vascular smooth muscle cells (VSMCs) and vascular neointima formation. The major abundant components were five phenolic acids and four flavonols, including protocatechuic acid (8.4 mg/g), chlorogenic (14.1 mg/g), caffeic acid (9.5 mg/g), *p*-coumaric acid (6.8 mg/g), ferulic acid (8.2 mg/g), quercetin-3O-b-D-glucopyranoside (3.4 mg/g), isorhamnetin-3O-b-D-glucopyranoside (16.2 mg/g), quercetin (2.5 mg/g), and isorhamnetin (18.4 mg/g). The study demonstrated that the extract suppressed the platelet-derived growth factor (PDGF)-BB-induced migration and proliferation of VSMCs and increase mitogen-activated protein kinases (MAPK) and extracellular signal-regulated kinase (ERK)1/2 phosphorylation in VSMCs, consequently leading to the reduction of neointimal hyperplasia (Figure 4) [62].

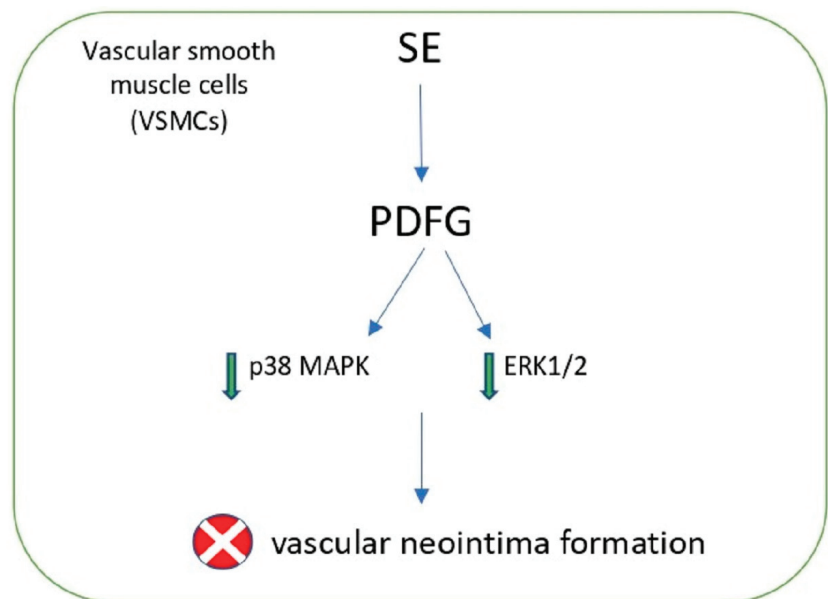


**Figure 4.** Neointima formation inhibition of *Salicornia* extract (SE) in VSMCs.

Essaidi et al., 2013 highlighted how *S. herbacea* methanol extract was a potent inhibitor of cytochrome P450 CYP1A2, CYP3A4, and CYP2D6, related to the activation of carcinogens, due to its phenolic composition characterized by the presence of many phenolic acids and flavonoids, such as chlorogenic acid, caffeic acid, syringic acid, *p*-coumaric acid, sinapic acid, ferulic acid, salicylic acid, myricetin, quercetin, and kampferol [63,64]. It is demonstrated that flavonols and flavonoids, in general, such as quercetin and kaempferol have a 3-OH and phenolic hydroxyl (eOH) group with inhibitory activity on CYP2D6, CYP1A2, and CYP3A4 [65].

### 2.3. Lignans

Lignans are a class of natural compounds widely produced by various plant species. Recent studies have demonstrated that lignans provide very important biological and pharmacological properties, including immunosuppressive, anti-inflammatory, cardiovascular, antioxidant, antitumor, and antiviral effects. In fact, they are found in many plants used in Eastern medicine [66,67]. Lignans contain a core scaffold that is formed by two or more phenylpropanoid units and monomers such as cinnamic acid, cinnamyl alcohol, propenyl benzene, and allyl benzene [68].

Syringaresinol 4-O- $\beta$ -D-glucopyranoside, erythro-1-(4-O- $\beta$ -D-glucopyranosyl-3,5-dimethoxyphenyl)-2-syringaresinoxyl-propane-1,3-diol, and longifloroside B have been the main lignans isolated from *S. europaea*. Notably, syringaresinol 4-O- $\beta$ -D-glucopyranoside has shown interesting biological activities including DPPH radical scavenging activity, antiestrogenic activity against MCF-7 cells, and antitumor activity against the A549 cancer cell line [69]. This compound has been found to modulate lipid and glucose metabolism in HepG2 cells and C2C12 myotubes [70]. In addition, other lignans such as (-)-syringaresinol and episyngaresinol-4''O- $\beta$ -D-glucopyranoside were isolated from *S. europaea*. In particular, (-)-syringaresinol (4.25 mg/Kg dw) has been found to possess antiplatelet aggregation, DPPH radical scavenging, nitric oxide (NO) inhibition, and P-glycoprotein inhibition activities [28].

Acanthoside B is another important lignan, extracted from *S. europaea*, which has exhibited negligible toxicity and showed a dose-dependent nitric oxide inhibitory potential in Lipopolysaccharide (LPS)-stimulated BV-2 microglial cells. Furthermore, it has attenuated scopolamine-inflicted AD-like amnesic traits by restoring the cholinergic activity, suppressing neuroinflammation, and activating the TrkB/CREB/BDNF pathway in mice. For these effects, acanthoside B could be a potential drug candidate for the treatment of neurodegenerative diseases (Figure 5) [71].

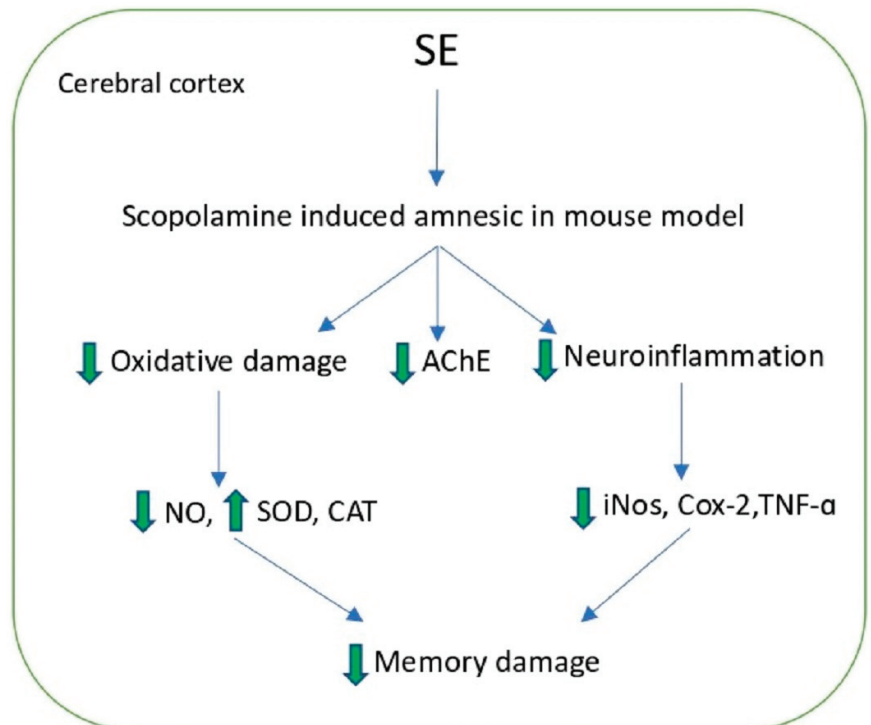


**Figure 5.** Ameliorative effect of Salicornia extract (SE) on Scopolamine induced amnesic.



### 3. Comparison of Extraction Methods of Polyphenols from *Salicornia*

Extraction from plants is generally the crucial step for both the isolation and exploitation of their bioactive compounds [72]. The bioactive compounds can be extracted from fresh or dried plant samples firstly pre-treated by milling, grinding, and homogenization. Furthermore, the fundamental parameters affecting the extraction yield, such as extraction time and temperature, solvent-to-solid ratio, number of repetitions, as well as the choice of extraction solvents, can be opportunely optimized [13,73]. Ideally, an extraction method should be quantitative, non-destructive, and time-saving; moreover, it should be chosen based on the chemical composition and purity degree of the extract one wishes to obtain [74].

Conventional solid-liquid extraction by maceration in organic solvents has been traditionally used to extract phenolic compounds from vegetable matrices. The main disadvantages of this process include the length of time needed in solid–solvent contact to reach equilibrium and the overall use of high temperatures which, although can favor the solid-liquid mass transfer of the compounds, frequently provokes a decrease in the extraction efficiency due to thermosensitivity of polyphenols [75]. As a consequence, in order to solve these limitations, new techniques have been developed in recent years for the extraction of bioactive compounds from plant materials, including ultrasound-assisted extraction, microwave-assisted extraction, enzyme-assisted extraction, and supercritical fluid extraction [76].

#### 3.1. Maceration

Maceration is a traditional method, based on the soaking of plant materials in a solvent for the recovery of bioactive compounds. It uses organic solvents, such as methanol, acetone, and ethyl acetate, which are toxic to human health and the environment because some residues may remain in the final extract. Moreover, this method is associated with high solvents volumes and extraction times that generate a large amount of waste and low extraction yields. Another disadvantage is the high temperature that sometimes leads to the loss of polyphenols caused by hydrolysis and/or oxidation during the process [77,78].

There are many reports on the investigation of the parameters affecting the profile and yield of polyphenols from *Salicornia* by maceration. Extraction with the sample added to boiling distilled water for 5 min has shown a phenolic composition of *S. ramosissima* extracts that are mainly characterized by the presence of myricetin, gallic acid, catechin, rutin, kaempferol-3-O-glucoside, and quercetin-3-O-galactoside [79].

Other studies have performed maceration at room temperature with a longer extraction time (16–24 h) [58,80]. This technique ensured the recovery of many phenolic compounds that could be degraded at high temperatures. Extraction with methanol from aerial parts of *S. herbacea* has identified four new dicaffeoylquinic acid derivatives and some flavonoid glucosides [40].

Modulating the polarity of the extraction solvents allows for the obtainment of a different type/range of polyphenols. High amounts of phenolic compounds are mainly found in extractions with a polar solvent. Ethanol extracts of *S. europea* have shown the presence of nine polyphenols including phenolic acids (i.e., chlorogenic acid or gallic acid) and flavonoids (i.e., rutin hydrate and catechin hydrate) [24]. While *S. herbacea* extraction with 80% acetone at room temperature for 24 h has allowed recovering pentadecyl ferulate in high yield [11].

Five phenolic acids, including protocatechuic acid, chlorogenic acid, caffeic acid, *p*-coumaric acid, and ferulic acid, together with quercetin-3-O- $\beta$ -D-glucopyranoside, isorhamnetin-3-O- $\beta$ -D-glucopyranoside, quercetin, and isorhamnetin, were identified in *S. europea* extracts obtained by a vacuum extractor at 100 °C for 5 h and subjected to ethanol precipitation for removing the high molecular polysaccharides and proteins [63].

Ferreira et al., (2018) executed extraction with fresh aerial parts (1.2 kg) of *S. ramosissima*, chopped into small pieces, and extracted with ethanol (5 L) three times at room temperature for 24 h using an overhead stirrer [47].

Another study performed an extraction on *S. ramosissima* biowaste using a thermostatic water bath. The powdered samples (2.5 g) were mixed with distilled water (25 mL) and extracted at different times and temperatures with a constant agitation of 200 rpm. The best extraction conditions were fixed at 80 °C in 10 min. Hydroxycinnamic acids, flavonols, and isoflavones, known for their excellent scavenging ability against ROS, have been extracted and isolated from *S. ramosissima* by-product which could be considered a useful source of antioxidant and neuroprotective compounds with interesting applications in the food, nutraceutical, and cosmetic industries [81].

### 3.2. Microwave-Assisted Extraction

Microwave-assisted extraction (MAE) is one of the most advanced methods currently used in plant extraction and is based on the effect of microwaves with a frequency between 0.3 to 300 GHz. Depending on the polarity of the solvent and the presence of ions in the solvent (methanol, ethanol, water, or their mixtures, having high or medium absorbance capacity of microwaves, are generally used), dielectric heating and ionic conduction can occur simultaneously in causing the swelling and rupturing the plant cell, thus facilitating the extraction of polyphenols [82].

The advantages of this method are mainly quick heating and extraction efficiency, lower solvent requirements, short extraction time, and a clean process. On the other hand, MAE is usually performed at higher temperatures (>80 °C), thus its application in the isolation of antioxidants has to be carefully assessed [83].

The only report dealing with the application of this technology to the extraction of polyphenols from *Salicornia* was that of Silva et al. (2021) who performed a MAE achieving better antioxidant and antiradical activities (65.56 mol FSE/g dw and 17.74 g AAE/g dw for FRAP and ABTS assays, respectively) rather than conventional extraction [79].

### 3.3. Ultrasound-Assisted Extraction

Ultrasound-assisted extraction (UAE) uses ultrasounds that enhance the extraction rate by increasing the mass transfer and possible rupture of cell walls due to the well-known “cavitation effect”, leading to higher product yields without modifying the extract composition [82].

Moreover, UAE allows for a reduction of processing time, thermal degradation losses, solvent, and energy consumption, and is compatible with any solvent including water and other generally recognized as safe (GRAS) solvents [84].

The influence of extraction time, temperature, solvent concentration, solid-to-liquid ratio, particle size, ultrasound power, and frequency on the polyphenols recovery from *Salicornia* were investigated in many studies.

Several researchers have performed extractions at 50 °C for different time periods in order to select the most suitable extraction time to recover the highest level of phenolic substances [46]. Even though an extraction time of 20 min has been shown as the best condition to recover quantities of antioxidant compounds from *Salicornia* matrix [85]. Regarding solvent type and concentration, different preferences appear in the literature, from 40% to 80% ethanol, for the best recovery of phenolic acids, phenolic alcohols, and flavonoids. The presence of water reduces solution viscosity and increases the plant swelling promoting a higher yield [86,87]. The effect of extraction time (1, 9, 30, 51, and 60 min) and power of ultrasonic waves (100, 150, 275, 400, and 450 W) parameters on the extraction of polyphenols from *Salicornia* were also investigated by recent reports. The highest content of phenolic compounds, ranging between 16.3 and 20.0 mg GAE/g dw, and overall antioxidant activity were obtained by extracting *S. ambigua* or *S. neei* samples (250 mg) with 15 mL of ethanol 80% in an ultrasound bath setting the ultrasound power and extraction time at 275 W and 30 min, respectively. Conversely, a longer extraction time led to lower contents of polyphenols, indeed lower extraction yield of gallic acid was found with an extraction time of 50 min [88,89].

Fifteen hydroxycinnamic acids (i.e., neochlorogenic, chlorogenic, *p*-coumaric, ferulic, and caffeic glycosides acids) together with caffeoylquinic dimers, such as 3,5-dicaffeoylquinic and 4,5-dicaffeoylquinic acids, and nine flavonoids (quercetin glycosides and apigenin glycoside) were extracted from *S. ramosissima* by adding 100 mL of ethanol:water (80:20, *v/v*) solution to 10 g of the fresh plant in an ultrasonic water bath at 40 kHz and 220 W for 60 min at  $25 \pm 3$  °C [90].

Kim et al. 2009 performed the extraction from *S. herbacea* powder (5 g) by sonication but by changing the solvent composition and the extraction temperature with a constant working frequency of 40 kHz. A linear gain of total phenolic content with increasing ethanol concentration and decreasing extraction temperature was observed; indeed, the maximum phenolic content (50.36 mg GAE/g) was recovered at an ethanol concentration of 76.82% and extraction temperature of 50 °C, while the lowest phenolic content (33.09 mg GAE/g) was revealed at an ethanol concentration of 50% and extraction temperature of 40 °C [91].

Finally, Wang et al. recently applied an efficient association/combination of extractive methods. *S. bigelovii* samples were extracted by maceration using 16 mL of 60% ethanol for 3 h at 60 °C, followed by a 200 W ultrasonic extraction for 40 min. This technique has provided a high recovery of flavonoids, including rutin (20.23%), noreugenin (15.26%), isoquercitrin (7.13%), quercetin (2.54%), camellianin A (5.91%), and 7-O- $\beta$ -D-glucopyranosyl-methoxychromone (1.04%) [20].

### 3.4. Supercritical Fluid Extraction

Supercritical Fluid Extraction (SFE) is another fast and efficient green method usually adopted for the extraction of natural compounds from plants. SFE employs supercritical fluids having low viscosity and high diffusivity, which, at the critical point (a specific temperature and pressure), diffuse into the solid matrix like gas and dissolve active materials like a liquid. These characteristics enhance diffusion and mass transfer while reducing extraction time [92]. The most widespread supercritical fluid in plant extractions is CO<sub>2</sub>, which has a very low critical temperature (31 °C) and can be easily removed, allowing rapid and selective extraction [93]. However, due to the apolarity of CO<sub>2</sub>, a co-solvent, such as water, ethanol, and methanol, is frequently used to allow the extraction of more polar compounds [94].

In this context, some researchers, carrying out the extraction of *S. europea* at constant extraction temperature (50 °C) and pressure (300 bar) with CO<sub>2</sub> flow of 2 L min<sup>-1</sup> and different ethanol concentrations (10, 20 or 40% *v/v*, respectively), have observed that both total phenolic compound (TPC), total extract yield (TEY), and antioxidant indices (ABTS and FRAP) were directly influenced by the ethanol percentage used in the SFE technique. Indeed, the values of TPC (0.29 vs. 0.15 mg GAEs g<sup>-1</sup> dw), TEY (16.30 vs. 11.01 mg g<sup>-1</sup> dw), ABTS (1.16 vs. 0.71 mg Tes g<sup>-1</sup> dw), and FRAP (10.22 vs. 5.22  $\mu$ mol FeSO<sub>4</sub> g<sup>-1</sup> dw) at 20% of ethanol were almost double than those at 10% [82,95]. The number of cycles (one cycle included 10 min of static condition and 10 min of dynamic phase) operated at the previous condition was crucial for yield: eight cycles were the optimal extraction condition to obtain a rich chemical profile [87].

Other studies use SFE for oil extraction from the matrix. This method allows for the extraction and analysis of the fatty acid profile of *Salicornia* oil. As shown by Adewale Folayan et al. (2019), high amounts of saturated and unsaturated fatty acids were obtained, such as myristic acid, palmitic acid, linoleic, and linolenic acid [96].

### 3.5. Enzyme-Assisted Extraction

Enzyme-assisted extraction (EAE) is a green extraction technology determined by numerous factors, including pH, temperature, treatment time, and enzyme selection. In particular, pH and temperature monitoring are essential to ensure optimal enzyme activity. The choice of the right enzyme allows the extraction of specific compounds from the matrix. For example, pectinase improved the extraction of polyphenols and phenols that are difficult to extract due to their high/low molecular weight [97]. Pectinase hydrolyses

pectin macromolecules that constitute the cell membrane, exposing entrapped polyphenols to the solvent. Other types of enzymes generally used in the extraction are cellulase and hemicellulase, which participate in breaking down the cell wall [98]. EAE of *Salicornia* is often combined with other extraction techniques, as described in various studies. Indeed, extracts with high phenolics content (particularly, procatechuic, caffeic, and ferulic acids, and quercetin and isorhamnetin) and significant radical scavenging activity was obtained by coupling EAE and UAE through two steps: firstly, *Salicornia* was suspended in ionic water and treated with vscozime (i.e., cellulolytic enzyme mixture) for 12 h at 40 °C; subsequently, it was extracted by ultrasound with ethanol for 3 h [99]. Isorhamnetin and acanthoside B were extracted from *S. europaea* by treating the matrix with pectinase and cellulase at 50 °C for 15 h and subsequently by refluxing twice with 50% ethanol for 3 h [100].

Definitely, the main polyphenols present in the different types of *Salicornia*, together with their quantities, their extraction technologies, and the health benefits aforementioned, are summarized in Table 2.

**Table 2.** Extraction methods, quantities, and health-promoting effects of *Salicornia* polyphenols.

Polyphenolic Compounds	<i>Salicornia</i> Species	Extraction Method	Experimental Condition	Amount	Biological Activity	Ref.
Chlorogenic acid	<i>S. europaea</i> , <i>S. ramosissima</i> <i>S. herbacea</i>	CE	EtOH	0.22 mg/g	Antihypertensive	[24]
		CE	H <sub>2</sub> O, 100 °C, 5 h	14.1 mg/g dw	Antimicrobial	[62]
		UAE	80% EtOH, 25 °C, 1 h	53.19 µg/g fw	Reduction of neointimal hyperplasia	[90]
		CE	H <sub>2</sub> O, 100 °C, 5 min	0.0758 mg/g dw		[79]
		MAE	72–94 °C, 300 W, 5–10 min	0.0342 mg/g dw		
Caffeoyl-5-dihydrocaffeoylquinic acid	<i>S. herbacea</i>	CE	MeOH, rt, 24 h	75.6 ± 2.3 mg/100 g fw	Inhibiting CE-OOH formation	[40]
3-caffeoyl-5-dihydrocaffeoylquinic acid methyl ester	<i>S. herbacea</i>	CE	MeOH, rt, 24 h	69 ± 1.4 µg/100 g fw	Inhibiting CE-OOH formation	[40]
3-caffeoyl-4-dihydrocaffeoylquinic acid methyl ester	<i>S. herbacea</i>	CE	MeOH, rt, 24 h	71.9 ± 1.9 µg/100 g fw	Inhibiting CE-OOH formation	[40]
3,5-dihydrocaffeoylquinic acid methyl ester	<i>S. herbacea</i>	CE	MeOH, rt, 24 h	171.9 ± 1.5 µg/100 g fw	Inhibiting CE-OOH formation	[40]
3-caffeoylquinic acid	<i>S. herbacea</i>	CE	MeOH, rt, 24 h		Inhibiting CE-OOH formation	[40]
3-caffeoylquinic acid methyl ester	<i>S. herbacea</i>	CE	MeOH, rt, 24 h		Inhibiting CE-OOH formation	[40]
3-caffeoyl-4-dicafeoylquinic acid (tungtungmadic acid)	<i>S. herbacea</i>	CE	80% MeOH, rt	8 mg/kg dw	Protective effect on endothelial cell function	[43,63]
3,5-dicafeoylquinic acid	<i>S. ramosissima</i>	UAE	80% EtOH, 1 h, 25 °C	25.83 mg/g fw	Antiproliferative	[90]
		CE	H <sub>2</sub> O, 5 min, 100 °C	0.0259 mg/g dw	Antihypertensive	[79]
		MAE	300 W, 5–10 min, 72–9 °C,	0.0280 mg/g dw		
4,5-dicafeoylquinic acid	<i>S. ramosissima</i>	UAE	80% EtOH, 1 h, 25 °C	11.75 mg/g fw	Antiproliferative Antihypertensive	[90]
<i>trans</i> -Ferulic acid	<i>S. europaea</i> , <i>S. ramosissima</i> , <i>S. herbacea</i>	EAE	H <sub>2</sub> O, 37 °C, 6 h	2.60 ± 0.33 µg/g		[21]
		CE	H <sub>2</sub> O, 100 °C, 5 h	8.2 mg/g dw	Antidiabetic	[62]
		UAE	80% EtOH, 1 h, 25 °C	4.21 mg/g fw	Antihypertensive	[99]
		EAE + UAE	12 h, 40 °C and EtOH, 3 h	8.45 mg% dw	Inhibitor of CYP450	[63]
		CE	MeOH, rt, 72 h	0.1346 mg/g dw		[79]
		MAE	H <sub>2</sub> O, 100 °C, 5 min 300 W, 72–94 °C, 5–10 min	0.0578 mg/g dw		
<i>p</i> -Coumaric acid	<i>S. europaea</i> , <i>S. ramosissima</i> <i>S. herbacea</i>	CE	H <sub>2</sub> O, 100 °C, 5 h	3.19 mg/g dw		[21]
		UAE	80% EtOH, 25 °C, 1 h	0.32 mg/g dw	Antihypertensive	[62]
		CE	MeOH, rt, 72 h	2.75 mg/g fw	Inhibitor of CYP450	[63]
		CE	H <sub>2</sub> O, 100 °C, 5 min	0.0483 mg/g dw		[79]
		MAE	300 W, 72–94 °C, 5–10 min	0.0349 mg/g dw		
Pentadecylferulate	<i>S. herbacea</i>	CE	80% acetone, rt, 24 h.		Anticancer	[11]
Caffeic acid	<i>S. europaea</i> , <i>S. ramosissima</i> <i>S. herbacea</i>	CE	EtOH	0.28 mg/g dw		[24]
		CE	H <sub>2</sub> O, 100 °C, 5 h	9.5 mg/g dw	Antibacterial	[62]
		EAE + UAE	12 h, 40 °C + EtOH, 3 h	6.87 mg% dw	Inhibitor of CYP450	[99]
		CE	H <sub>2</sub> O, 100 °C, 5 min	0.0144 mg/g dw		[79]
		MAE	300 W, 72–94 °C, 5–10 min	0.0032 mg/g dw		

Table 2. Cont.

Polyphenolic Compounds	Salicornia Species	Extraction Method	Experimental Condition	Amount	Biological Activity	Ref.
Gallic acid	<i>S. europaea</i>	CE	EtOH	0.8 mg/g dw	Antibacterial Inhibitor of CYP450	[24] [79]
		CE	H <sub>2</sub> O, 100 °C, 5 min	0.21 mg/g dw		
		MAE	300 W, 72–94 °C, 5–10 min	0.15 mg/g dw		
Protocatechuic acid	<i>S. europaea</i> , <i>S. ramosissima</i> <i>S. herbacea</i>	CE	H <sub>2</sub> O, 100 °C, 5 h	8.4 mg/g dw	Amelioration and prevention of vascular diseases.	[62] [99] [79]
		EAE + UAE	12 h, 40 °C + EtOH, 3 h	1.54 mg% dw		
		CE	H <sub>2</sub> O, 100 °C, 5 min	0.1275 mg/g dw		
Rutin hydrate	<i>S. europaea</i> , <i>S. ramosissima</i>	CE	EtOH	10.05 mg/g dw	Antibacterial	[24] [79]
		CE	H <sub>2</sub> O, 100 °C, 5 min	0.0999 mg/g dw		
		MAE	300 W, 72–94 °C, 5–10 min	0.0781 mg/g dw		
Catechin hydrate	<i>S. europaea</i> , <i>S. ramosissima</i>	CE	EtOH	1.17 mg/g dw	Antibacterial	[24] [79]
		CE	H <sub>2</sub> O, 100 °C, 5 min	0.1116 mg/g dw		
		MAE	300 W, 72–94 °C, 5–10 min	0.0046 mg/g dw		
Isoquercitrin 6"-O-methylxalate	<i>S. herbacea</i>	CE	MeOH, rt, 24 h	0.47 mg/kg fw	Anti-inflammatory	[57]
Isorhamnetin 3-O-β-D- glucopyranoside	<i>S. herbacea</i>	CE	H <sub>2</sub> O, 100 °C, 5 h	16.2 mg/g dw	Anti-inflammatory Amelioration and prevention of vascular diseases.	[62] [57]
		CE	MeOH, rt, 24 h	1.25 mg/kg fw		
Quercetin 3-O-β-D- glucopyranoside	<i>S. herbacea</i>	CE	H <sub>2</sub> O, 100 °C, 5 h	3.4 mg/g dw	Amelioration and prevention of vascular diseases.	[62] [57]
		CE	MeOH, rt, 24 h	2.15 mg/kg fw		
Kaempferol	<i>S. europaea</i> , <i>S. ramosissima</i> <i>S. herbacea</i>	UAE	80% EtOH, 25 °C, 1 h,	108.1–24.6 mg/10 g dw	Inhibitor of CYP450	[90] [79] [63]
		CE	H <sub>2</sub> O, 100 °C, 5 min	10.90 mg/g		
		MAE	300 W, 72–94 °C, 5–10 min	0.0052 mg/g dw		
		CE	MeOH, rt, 24 h	0.0047 mg/g dw		
Quercetin	<i>S. europaea</i> , <i>S. ramosissima</i> <i>S. herbacea</i>	CE	H <sub>2</sub> O, 100 °C, 5 h	2.5 mg/g dw	Inhibitor of CYP450 Amelioration and prevention of vascular diseases.	[62] [99] [79]
		EAE + UAE	12 h, 40 °C + EtOH, 3 h	12.63 mg% dw		
		CE	H <sub>2</sub> O, 100 °C, 5 min	0.0340 mg/g dw		
		MAE	300 W, 72–94 °C, 5–10 min	0.0284 mg/g dw		
Isorhamnetin	<i>S. europaea</i> <i>S. herbacea</i>	CE	H <sub>2</sub> O, 100 °C, 5 h	18.4 mg/g dw	Amelioration and prevention of vascular diseases.	[62] [99]
		EAE + UAE	12 h, 40 °C + EtOH, 3 h	6.65 mg% dw		
Acanthoside B	<i>S. europaea</i>	EAE + CE	50 °C, 15 h + 50% EtOH, 3 h	2.40 mg/g	Neuroprotective	[100]

CE: conventional extraction; UAE: Ultrasound assisted extraction; MAE: Microwave assisted extraction; EAE: Enzyme assisted extraction; dw: dry weight; fw: fresh weight; rt: room temperature; CYP450: Cytochrome P450 System.

#### 4. Conclusions

Nowadays, evidence supporting the health effects of natural resources has led the scientific community to better understand the phytochemical composition of innovative health food diet products with the aim of obtaining bioactive compounds capable of reducing oxidative stress and related inflammatory disorders [101]. To this end, scientific evidence supports the beneficial effects of *Salicornia*, a halophytic plant of the Mediterranean basin and the coastal regions of East Asia, on gastrointestinal disorders, diabetes, hypertension, inflammation, vascular diseases, and oxidative stress. Focusing our attention on *S. herbacea*, *S. ramosissima*, and *S. europaea*, the scientific studies collected in this review highlight the interesting content of phenolic compounds from 1.2 to 2 mg/GAE in *Salicornia*. Most of the research reviewed here supports the contribution of *Salicornia* in protecting cells from ROS-induced damage. Beneficial effects have been described, such as antitumor, antihypertensive, antibacterial, neuroprotective, and antidiabetic activities. In addition, a significant improvement in vascular disease was observed. Furthermore, in this review, a knowledge base for the selection of extraction procedures adopted for the recovery of polyphenols from *Salicornia* has been collected. The knowledge that emerged on the extraction methods adopted to extract polyphenols from *Salicornia* suggests the development and implementation of eco-friendly procedures to enhance the extraction of polyphenols through the adoption of sustainable extraction methods with higher yields.

Overall, the present work provides strong evidence that *Salicornia* polyphenols are involved in several pathways that contribute to both antioxidant and antiradical activities

by candidating *Salicornia* for the development of nutraceuticals and food supplements with a wide variety of health-beneficial effects.

**Author Contributions:** Conceptualization, M.L.C. and F.C.; methodology, F.L. and P.C.; writing—original draft preparation, F.L. and P.C.; writing—review and editing, M.M. and P.C.; supervision, M.M.; project administration, M.L.C.; funding acquisition, F.C. All authors have read and agreed to the published version of the manuscript.

**Funding:** This research was funded by PON REACT EU XXXVII Doctoral School in Food and Soil Science.

**Institutional Review Board Statement:** Not applicable.

**Informed Consent Statement:** Not applicable.

**Data Availability Statement:** Not applicable.

**Acknowledgments:** Special thanks to Sestre srl, Nutraceutical supplements, Via Oberdan, 9 76015 Trinitapoli (BT) Italy for the technical support.

**Conflicts of Interest:** The authors declare no conflict of interest.

**Sample Availability:** Not available.

## References

1. Corbo, F.; Brunetti, G.; Crupi, P.; Bortolotti, S.; Storlino, G.; Piacente, L.; Carocci, A.; Catalano, A.; Milani, G.; Colaianni, G.; et al. Effects of Sweet Cherry Polyphenols on Enhanced Osteoclastogenesis Associated With Childhood Obesity. *Front. Immunol.* **2019**, *10*, 1001. [[CrossRef](#)] [[PubMed](#)]
2. De Santis, S.; Liso, M.; Verna, G.; Curci, F.; Milani, G.; Faienza, M.F.; Franchini, C.; Moschetta, A.; Chieppa, M.; Clodoveo, M.L.; et al. Extra Virgin Olive Oil Extracts Modulate the Inflammatory Ability of Murine Dendritic Cells Based on Their Polyphenols Pattern: Correlation between Chemical Composition and Biological Function. *Antioxidants* **2021**, *10*, 1016. [[CrossRef](#)]
3. Zhang, L.Q.; Niu, Y.D.; Huridu, H.; Hao, J.F.; Qi, Z.; Hasi, A. *Salicornia europaea* L. Na<sup>+</sup>/H<sup>+</sup> antiporter gene improves salt tolerance in transgenic alfalfa (*Medicago sativa* L.). *Genet. Mol. Res.* **2014**, *13*, 5350–5360. [[CrossRef](#)]
4. Zhang, S.; Wei, M.; Cao, C.; Ju, Y.; Deng, Y.; Ye, T.; Xia, Z.; Chen, M. Effect and mechanism of *Salicornia bigelovii* Torr. plant salt on blood pressure in SD rats. *Food Funct.* **2015**, *6*, 920–926. [[CrossRef](#)]
5. Isca, V.M.; Seca, A.M.; Pinto, D.C.; Silva, H.; Silva, A.M. Lipophilic profile of the edible halophyte *Salicornia ramosissima*. *Food Chem.* **2014**, *165*, 330–336. [[CrossRef](#)]
6. Cho, H.D.; Lee, J.H.; Jeong, J.H.; Kim, J.Y.; Yee, S.T.; Park, S.K.; Lee, M.K.; Seo, K.I. Production of novel vinegar having antioxidant and anti-fatigue activities from *Salicornia herbacea* L. *J. Sci. Food. Agric.* **2015**, *96*, 1085–1092. [[CrossRef](#)] [[PubMed](#)]
7. Jha, B.; Singh, N.P.; Mishra, A. Proteome profiling of seed storage proteins reveals the nutritional potential of *Salicornia brachiata* Roxb.; an extreme halophyte. *J. Agric. Food Chem.* **2012**, *60*, 4320–4326. [[CrossRef](#)] [[PubMed](#)]
8. Giordano, R.; Aliotta, G.E.; Johannesen, A.S.; Voetmann-Jensen, D.; Laustsen, F.H.; Andersen, L.A.; Rezai, A.; Fredsgaard, M.; Vecchio, S.L.; Arendt-Nielsen, L.; et al. Effects of *Salicornia*-Based Skin Cream Application on Healthy Humans' Experimental Model of Pain and Itching. *Pharmaceuticals* **2022**, *15*, 150. [[CrossRef](#)] [[PubMed](#)]
9. Carocci, A.; Lentini, G.; Catalano, A.; Cavalluzzi, M.M.; Bruno, C.; Muraglia, M.; Franchini, C. Chiral Aryloxyalkylamines: Selective 5-HT<sub>1B</sub>/1D Activation and Analgesic Activity. *ChemMedChem* **2010**, *5*, 696–704. [[CrossRef](#)] [[PubMed](#)]
10. Loconsole, D.; Cristiano, G.; De Lucia, B. Glassworts: From Wild Salt Marsh Species to Sustainable Edible Crops. *Agriculture* **2019**, *9*, 14. [[CrossRef](#)]
11. Wang, X.; Zhang, M.; Zhao, Y.; Wang, H.; Liu, T.; Xin, Z. Pentadecyl ferulate, a potent antioxidant and antiproliferative agent from the halophyte *Salicornia herbacea*. *Food Chem.* **2013**, *141*, 2066–2074. [[CrossRef](#)]
12. Mallamaci, R.; Budriesi, R.; Clodoveo, M.L.; Biotti, G.; Micucci, M.; Ragusa, A.; Curci, F.; Muraglia, M.; Corbo, F.; Franchini, C. Olive Tree in Circular Economy as a Source of Secondary Metabolites Active for Human and Animal Health Beyond Oxidative Stress and Inflammation. *Molecules* **2021**, *26*, 1072. [[CrossRef](#)]
13. Faienza, M.F.; Corbo, F.; Carocci, A.; Catalano, A.; Clodoveo, M.L.; Grano, M.; Wang, D.Q.; D'Amato, G.; Muraglia, M.; Franchini, C.; et al. Novel insights in health-promoting properties of sweet cherries. *J. Funct. Foods* **2020**, *69*, 103945. [[CrossRef](#)]
14. Clodoveo, M.L.; Crupi, P.; Corbo, F. Optimization of a Green Extraction of Polyphenols from Sweet Cherry (*Prunus avium* L.) Pulp. *Processes* **2022**, *10*, 1657. [[CrossRef](#)]
15. Clodoveo, M.L.; Crupi, P.; Annunziato, A.; Corbo, F. Innovative extraction technologies for development of functional ingredients based on polyphenols from olive leaves. *Foods* **2021**, *11*, 103. [[CrossRef](#)] [[PubMed](#)]
16. Cárdenas-Pérez, S.; Piernik, A.; Chanona-Pérez, J.J.; Grigore, M.N.; Perea-Flores, M.J. An overview of the emerging trends of the *Salicornia* L. genus as a sustainable crop. *Environ. Exp. Bot.* **2021**, *191*, 104606. [[CrossRef](#)]

17. Wang, H.; Xu, Z.; Li, X.; Sun, J.; Yao, D.; Jiang, H.; Zhou, T.; Liu, Y.; Li, J.; Wang, C.; et al. Extraction, preliminary characterization and antioxidant properties of polysaccharides from the testa of *Salicornia herbacea*. *Carbohydr. Polym.* **2017**, *176*, 99–106. [[CrossRef](#)] [[PubMed](#)]
18. Lu, D.; Zhang, M.; Wang, S.; Cai, J.; Zhou, X.; Zhu, C. Nutritional characterization and changes in quality of *Salicornia bigelovii* Torr. during storage. *LWT-Food Sci. Technol.* **2010**, *43*, 519–524. [[CrossRef](#)]
19. Lima, A.R.; Castaneda-Loaiza, V.; Salazar, M.; Nunes, C.; Quintas, C.; Gama, F.; Barreira, L. Influence of cultivation salinity in the nutritional composition, antioxidant capacity and microbial quality of *Salicornia ramossissima* commercially produced in soilless systems. *Food Chem.* **2020**, *333*, 127525. [[CrossRef](#)]
20. Wang, D.; Wang, Y.; Dong, G.; Shang, Y.; Lyu, Y.; Li, F.; Yu, X. The chemical composition analysis of dwarf saltwort (*Salicornia bigelovii* Torr.) and its preservative effects on snakehead fish fillets. *J. Food Process. Preserv.* **2022**, *46*, e16433. [[CrossRef](#)]
21. Panth, N.; Park, S.H.; Kim, H.J.; Kim, D.H.; Oak, M.H. Protective effect of *Salicornia europaea* extracts on high salt intake-induced vascular dysfunction and hypertension. *Int. J. Mol. Sci.* **2016**, *17*, 1176. [[CrossRef](#)] [[PubMed](#)]
22. Feng, J.; Wang, J.; Fan, P.; Jia, W.; Nie, L.; Jiang, P.; Li, Y. High-throughput deep sequencing reveals that microRNAs play important roles in salt tolerance of euhalophyte *Salicornia europaea*. *BMC Plant Biol.* **2015**, *15*, 63. [[CrossRef](#)] [[PubMed](#)]
23. Lee, S.J.; Jeong, E.M.; Ki, A.Y.; Oh, K.S.; Kwon, J.; Jeong, J.H.; Chung, N.J. Oxidative defense metabolites induced by salinity stress in roots of *Salicornia herbacea*. *J. Plant Physiol.* **2016**, *206*, 133–142. [[CrossRef](#)]
24. Rahmani, R.; Arbi, K.E.; Aydi, S.S.; Hzami, A.; Tlahig, S.; Najar, R.; Debouba, M. Biochemical composition and biological activities of *Salicornia europaea* L. from southern Tunisia. *J. Food Meas. Charact.* **2022**, *16*, 4833–4846. [[CrossRef](#)]
25. Mishra, A.; Patel, M.K.; Jha, B. Non-targeted metabolomics and scavenging activity of reactive oxygen species reveal the potential of *Salicornia brachiata* as a functional food. *J. Funct. Foods* **2015**, *13*, 21–31. [[CrossRef](#)]
26. Kaur, N.; Chaudhary, J.; Jain, A.; Kishore, L. Stigmasterol: A comprehensive review. *Int. J. Pharm. Sci. Res.* **2011**, *2*, 2259.
27. Saeidnia, S.; Manayi, A.; Gohari, A.R.; Abdollahi, M. The story of beta-sitosterol-a review. *Eur. J. Med. Plants* **2014**, *4*, 590. [[CrossRef](#)]
28. Kim, S.; Lee, E.Y.; Hillman, P.F.; Ko, J.; Yang, I.; Nam, S.J. Chemical structure and biological activities of secondary metabolites from *Salicornia europaea* L. *Molecules* **2021**, *26*, 2252. [[CrossRef](#)]
29. Lyu, H.; Ma, X.; Guan, F.; Chen, Y.; Wang, Q.; Feng, X. 30-Noroleanane triterpenoid saponins from *Salicornia europaea* Linn. and their chemotaxonomic significance. *Biochem. Syst. Ecol.* **2018**, *78*, 106–109. [[CrossRef](#)]
30. Patel, S. *Salicornia*: Evaluating the halophytic extremophile as a food and a pharmaceutical candidate. *3 Biotech* **2016**, *6*, 104. [[CrossRef](#)]
31. Elsebaie, E.M.; Elsanat, S.Y.; Gouda, M.S.; Elnemr, K.M. Oil and fatty acids composition in glasswort (*Salicornia fruticosa*) seeds. *J. App. Chem.* **2013**, *4*, 2278–5736.
32. Baker, E.J.; Miles, E.A.; Burdge, G.C.; Yaqoob, P.; Calder, P.C. Metabolism and functional effects of plant-derived omega-3 fatty acids in humans. *Prog. Lipid Res.* **2016**, *64*, 30–56. [[CrossRef](#)] [[PubMed](#)]
33. Liu, Y.W.; Zuo, P.Y.; Zha, X.N.; Chen, X.L.; Zhang, R.; He, X.X.; Liu, C.Y. Octacosanol enhances the proliferation and migration of human umbilical vein endothelial cells via activation of the PI3K/Akt and MAPK/Erk pathways. *Lipids* **2015**, *50*, 241–251. [[CrossRef](#)]
34. Ventura, Y.; Wuddineh, W.A.; Shpigel, M.; Samocha, T.M.; Klim, B.C.; Cohen, S.; Sagi, M. Effects of day length on flowering and yield production of *Salicornia* and *Sarcocornia* species. *Sci. Hort.* **2011**, *130*, 510–516. [[CrossRef](#)]
35. Rana, A.; Samtiya, M.; Dhewa, T.; Mishra, V.; Aluko, R.E. Health benefits of polyphenols: A concise review. *J. Food Biochem.* **2022**, *46*, e14264. [[CrossRef](#)]
36. Lorenzo, C.; Colombo, F.; Biella, S.; Stockley, C.; Restani, P. Polyphenols and human health: The role of bioavailability. *Nutrients* **2021**, *13*, 273. [[CrossRef](#)]
37. Kumar, N.; Goel, N. Phenolic acids: Natural versatile molecules with promising therapeutic applications. *Biotechnol. Rep.* **2019**, *24*, e00370. [[CrossRef](#)]
38. Gouda, M.S.; Elsebaie, E.M. Glasswort (*Salicornia* spp) as a source of bioactive compounds and its health benefits: A review. *Alex J. Sci. Technol.* **2016**, *13*, 1–7.
39. Petropoulos, S.A.; Karkanis, A.; Martins, N.; Ferreira, I.C. Edible halophytes of the Mediterranean basin: Potential candidates for novel food products. *Trends Food Sci. Technol.* **2018**, *74*, 69–84. [[CrossRef](#)]
40. Cho, J.Y.; Kim, J.Y.; Lee, Y.G.; Lee, H.J.; Shim, H.J.; Lee, J.H.; Moon, J.H. Four new dicaffeoylquinic acid derivatives from glasswort (*Salicornia herbacea* L.) and their antioxidative activity. *Molecules* **2016**, *21*, 1097. [[CrossRef](#)]
41. Zhao, Y.; Wang, J.; Balleve, O.; Luo, H.; Zhang, W. Antihypertensive effects and mechanisms of chlorogenic acids. *Hypertens. Res.* **2012**, *35*, 370–374. [[CrossRef](#)] [[PubMed](#)]
42. Heo, K.S.; Berk, B.C.; Abe, J.I. Disturbed flow-induced endothelial proatherogenic signaling via regulating post-translational modifications and epigenetic events. *Antioxid. Redox Signal.* **2016**, *25*, 435–450. [[CrossRef](#)]
43. Lee, G.H.; Lee, S.Y.; Zheng, C.; Pham, H.T.; Kim, C.Y.; Kim, M.Y.; Jeong, H.G. Effect of 3-caffeoyl, 4-dihydrocaffeoylquinic acid from *Salicornia herbacea* on endothelial nitric oxide synthase activation via calcium signaling pathway. *Toxicol. Res.* **2022**, *38*, 355–364. [[CrossRef](#)] [[PubMed](#)]

44. Rahman, M.M.; Kim, M.J.; Kim, J.H.; Kim, S.H.; Go, H.K.; Kweon, M.H.; Kim, D.H. Desalted *Salicornia europaea* powder and its active constituent, trans-ferulic acid, exert anti-obesity effects by suppressing adipogenic-related factors. *Pharm. Biol.* **2018**, *56*, 183–191. [[CrossRef](#)]
45. Adamczak, A.; Ożarowski, M.; Karpiński, T.M. Antibacterial activity of some flavonoids and organic acids widely distributed in plants. *J. Clin. Med.* **2019**, *9*, 109. [[CrossRef](#)]
46. Padalino, L.; Costa, C.; Del Nobile, M.A.; Conte, A. Extract of *Salicornia europaea* in fresh pasta to enhance phenolic compounds and antioxidant activity. *Int. J. Food Sci. Technol.* **2019**, *54*, 3051–3057. [[CrossRef](#)]
47. Ferreira, D.; Isca, V.M.; Leal, P.; Seca, A.M.; Silva, H.; de Lourdes Pereira, M.; Pinto, D.C. *Salicornia ramosissima*: Secondary metabolites and protective effect against acute testicular toxicity. *Arab. J. Chem.* **2018**, *11*, 70–80. [[CrossRef](#)]
48. Ullah, A.; Munir, S.; Badshah, S.L.; Khan, N.; Ghani, L.; Poulson, B.G.; Jaremko, M. Important flavonoids and their role as a therapeutic agent. *Molecules* **2020**, *25*, 5243. [[CrossRef](#)]
49. Maleki, S.J.; Crespo, J.F.; Cabanillas, B. Anti-inflammatory effects of flavonoids. *Food Chem.* **2019**, *299*, 125124. [[CrossRef](#)]
50. Šamec, D.; Karalija, E.; Šola, I.; Vujčić Bok, V.; Salopek-Sondi, B. The role of polyphenols in abiotic stress response: The influence of molecular structure. *Plants* **2021**, *10*, 118. [[CrossRef](#)]
51. D’Amelia, V.; Aversano, R.; Chiaiese, P.; Carputo, D. The antioxidant properties of plant flavonoids: Their exploitation by molecular plant breeding. *Phytochem. Rev.* **2018**, *17*, 611–625. [[CrossRef](#)]
52. Dias, M.C.; Pinto, D.C.; Silva, A.M. 2021 Plant flavonoids: Chemical characteristics and biological activity. *Molecules* **2021**, *26*, 5377. [[CrossRef](#)]
53. David, A.V.A.; Arulmoli, R.; Parasuraman, S. Overviews of biological importance of quercetin: A bioactive flavonoid. *Pharmacogn. Rev.* **2016**, *10*, 84.
54. Ganeshpurkar, A.; Saluja, A.K. The pharmacological potential of rutin. *Saudi Pharm. J.* **2017**, *25*, 149–164. [[CrossRef](#)]
55. Kong, C.S.; Kim, J.A.; Qian, Z.J.; Kim, Y.A.; Im Lee, J.; Kim, S.K.; Seo, Y. Protective effect of isorhamnetin 3-O-β-D-glucopyranoside from *Salicornia herbacea* against oxidation-induced cell damage. *Food Chem. Toxicol.* **2009**, *47*, 1914–1920. [[CrossRef](#)]
56. Cybulska, I.; Zembrzaska, J.; Brudecki, G.; Thomsen, M.H. Optimizing Methods to Characterize Caffeic, Ferulic, and Chlorogenic Acids in *Salicornia sinus-persica* and *Salicornia bigelovii* Extracts by Tandem Mass Spectrometry (LC-MS/MS). *Bioresources* **2021**, *16*, 5508–5523. [[CrossRef](#)]
57. Kim, J.Y.; Cho, J.Y.; Ma, Y.K.; Park, K.Y.; Lee, S.H.; Ham, K.S.; Moon, J.H. Dicafeoylquinic acid derivatives and flavonoid glucosides from glasswort (*Salicornia herbacea* L.) and their antioxidative activity. *Food Chem.* **2011**, *125*, 55–62. [[CrossRef](#)]
58. Masuoka, N.; Matsuda, M.; Kubo, I. Characterisation of the antioxidant activity of flavonoids. *Food Chem.* **2012**, *131*, 541–545. [[CrossRef](#)]
59. Noh, E.J.; Lee, J.Y.; Park, S.Y.; Park, J.H.; Cho, J.Y.; Kim, Y.M.; Lee, S.K. *Salicornia herbacea* Aqueous Extracts Regulate NLRP3 Inflammasome Activation in Macrophages and Trophoblasts. *J. Med. Food* **2022**, *25*, 503–512. [[CrossRef](#)]
60. Kim, J.Y.; Cho, J.Y.; Moon, J.H.; Choi, G.C.; Lee, K.D.; Ham, K.S.; Kim, S.J. Change of phenylpropanoic acid and flavonol contents at different growth stage of glasswort (*Salicornia herbacea* L.). *Food Sci. Biotechnol.* **2014**, *23*, 685–691. [[CrossRef](#)]
61. Luo, Y.; Shang, P.; Li, D. Luteolin: A flavonoid that has multiple cardio-protective effects and its molecular mechanisms. *Front. Pharmacol.* **2017**, *8*, 692. [[CrossRef](#)] [[PubMed](#)]
62. Won, K.J.; Lee, K.P.; Baek, S.; Cui, L.; Kweon, M.H.; Jung, S.H.; Kim, B. Desalted *Salicornia europaea* extract attenuated vascular neointima formation by inhibiting the MAPK pathway-mediated migration and proliferation in vascular smooth muscle cells. *Biomed. Pharmacother.* **2017**, *94*, 430–438. [[CrossRef](#)]
63. Essaidi, I.; Brahmi, Z.; Snoussi, A.; Koubaier, H.B.H.; Casabianca, H.; Abe, N.; Bouzouita, N. Phytochemical investigation of Tunisian *Salicornia herbacea* L.; antioxidant, antimicrobial and cytochrome P450 (CYPs) inhibitory activities of its methanol extract. *Food Control.* **2013**, *32*, 125–133. [[CrossRef](#)]
64. Pandit, A.; Sachdeva, T.; Bafna, P. Drug-induced hepatotoxicity: A review. *J. Appl. Pharm. Sci.* **2012**, *02*, 233–243. [[CrossRef](#)]
65. Greenblatt, D.J.; Zhao, Y.; Hanley, M.J.; Chen, C.; Harmatz, J.S.; Cancalon, P.F.; Gmitter Jr, F.G. Mechanism-based inhibition of human cytochrome P450-3A activity by grapefruit hybrids having low furanocoumarin content. *Xenobiotica* **2012**, *42*, 1163–1169. [[CrossRef](#)] [[PubMed](#)]
66. Polat Kose, L.; Gulcin, I. Evaluation of the antioxidant and antiradical properties of some phyto and mammalian lignans. *Molecules* **2021**, *26*, 7099. [[CrossRef](#)] [[PubMed](#)]
67. Köse, L.P.; Gulcin, I. Inhibition effects of some lignans on carbonic anhydrase, acetylcholinesterase and butyrylcholinesterase enzymes. *Rec. Nat. Prod.* **2017**, *11*, 558–561. [[CrossRef](#)]
68. Zálesák, F.; Bon, D.J.Y.D.; Pospíšil, J. Lignans and Neolignans: Plant secondary metabolites as a reservoir of biologically active substances. *Pharmacol. Res.* **2019**, *146*, 104284. [[CrossRef](#)]
69. Wang, X.Y.; Feng, X.; Wang, M.; Chen, Y.; Dong, Y.F.; Zhao, Y.Y.; Sun, H. Studies on the chemical constituents of *Salicornia europaea*. *Zhong Yao Cai Zhongyao Cai J. Chin. Med. Mater.* **2011**, *34*, 67–69.
70. Wang, S.; Wu, C.; Li, X.; Zhou, Y.; Zhang, Q.; Ma, F.; Guo, P. Syringaresinol-4-O-β-D-glucoside alters lipid and glucose metabolism in HepG2 cells and C2C12 myotubes. *Acta Pharm. Sin. B* **2017**, *7*, 453–460. [[CrossRef](#)]
71. Karthivashan, G.; Kweon, M.H.; Park, S.Y.; Kim, J.S.; Kim, D.H.; Ganesan, P.; Choi, D.K. Cognitive-enhancing and ameliorative effects of acanthoside B in a scopolamine-induced amnesic mouse model through regulation of oxidative/inflammatory/cholinergic systems and activation of the TrkB/CREB/BDNF pathway. *Food Chem. Toxicol.* **2019**, *129*, 444–457. [[CrossRef](#)] [[PubMed](#)]



72. Clodoveo, M.L.; Crupi, P.; Muraglia, M.; Corbo, F. Ultrasound Assisted Extraction of Polyphenols from Ripe Carob Pods (*Ceratonia siliqua* L.): Combined Designs for Screening and Optimizing the Processing Parameters. *Foods* **2022**, *11*, 284. [CrossRef] [PubMed]
73. Vuong, Q.V.; Hirun, S.; Roach, P.D.; Bowyer, M.C.; Phillips, P.A.; Scarlett, C.J. Effect of extraction conditions on total phenolic compounds and antioxidant activities of Carica papaya leaf aqueous extracts. *J. Herb. Med.* **2013**, *3*, 104–111. [CrossRef]
74. Crupi, P.; Dipalmo, T.; Clodoveo, M.L.; Toci, A.T.; Coletta, A. Seedless table grape residues as a source of polyphenols: Comparison and optimization of non-conventional extraction techniques. *Eur. Food Res. Technol.* **2018**, *244*, 1091–1100. [CrossRef]
75. Jovanović, A.; Petrović, P.; Đorđević, V.; Zdunić, G.; Šavikin, K.; Bugarski, B. Polyphenols extraction from plant sources. *Lek. Sirovine* **2017**, *37*, 45–49. [CrossRef]
76. Panja, P. Green extraction methods of food polyphenols from vegetable materials. *Curr. Opin. Food Sci.* **2018**, *23*, 173–182. [CrossRef]
77. Saini, A.; Panesar, P.S. Beneficiation of food processing by-products through extraction of bioactive compounds using neoteric solvents. *LWT* **2020**, *134*, 110263. [CrossRef]
78. Naviglio, D.; Scarano, P.; Ciaravolo, M.; Gallo, M. Rapid Solid-Liquid Dynamic Extraction (RSLDE): A powerful and greener alternative to the latest solid-liquid extraction techniques. *Foods* **2019**, *8*, 245. [CrossRef]
79. Silva, A.M.; Lago, J.P.; Pinto, D.; Moreira, M.M.; Grosso, C.; Cruz Fernandes, V.; Rodrigues, F. Salicornia ramosissima bioactive composition and safety: Eco-friendly extractions approach (microwave-assisted extraction vs. conventional maceration). *Appl. Sci.* **2021**, *11*, 4744. [CrossRef]
80. Ko, Y.C.; Choi, H.S.; Kim, S.L.; Yun, B.S.; Lee, D.S. Anti-Inflammatory Effects of (9Z, 11E)-13-Oxooctadeca-9, 11-dienoic Acid (13-KODE) Derived from Salicornia herbacea L. on Lipopolysaccharide-Stimulated Murine Macrophage via NF-κB and MAPK Inhibition and Nrf2/HO-1 Signaling Activation. *Antioxidants* **2022**, *11*, 180. [CrossRef]
81. Pinto, D.; Reis, J.; Silva, A.M.; Salazar, M.; Dall'Acqua, S.; Delerue-Matos, C.; Rodrigues, F. Valorisation of Salicornia ramosissima biowaste by a green approach—An optimizing study using response surface methodology. *Sustain. Chem. Pharm.* **2021**, *24*, 100548. [CrossRef]
82. Vinatoru, M.; Mason, T.J.; Calinescu, I. Ultrasonically assisted extraction (UAE) and microwave assisted extraction (MAE) of functional compounds from plant materials. *TrAC Trends Anal. Chem.* **2017**, *97*, 159–178. [CrossRef]
83. Markhali, F.S.; Teixeira, J.A.; Rocha, C.M. Olive tree leaves—A source of valuable active compounds. *Processes* **2020**, *8*, 1177. [CrossRef]
84. Chemat, F.; Rombaut, N.; Sicaire, A.G.; Meullemiestre, A.; Fabiano-Tixier, A.S.; Abert-Vian, M. Ultrasound assisted extraction of food and natural products. Mechanisms, techniques, combinations, protocols and applications. A review. *Ultrason. Sonochemistry* **2017**, *34*, 540–560. [CrossRef] [PubMed]
85. Cristina, C.; Lucia, P.; Sara, S.; Francesco, S.; Nobile Matteo Alessandro, D.; Amalia, C. Study of the efficacy of two extraction techniques from Crithmum maritimum and Salicornia europaea. *J. Food Nutr. Res.* **2018**, *6*, 456–463. [CrossRef]
86. Magiera, S.; Sobik, A. Ionic liquid-based ultrasound-assisted extraction coupled with liquid chromatography to determine isoflavones in soy foods. *J. Food Compos. Anal.* **2017**, *57*, 94–101. [CrossRef]
87. Sicaire, A.G.; Vian, M.A.; Fine, F.; Carré, P.; Tostain, S.; Chemat, F. Ultrasound induced green solvent extraction of oil from oleaginous seeds. *Ultrason. Sonochemistry* **2016**, *31*, 319–329. [CrossRef]
88. Souza, M.M.; Silva, B.D.; Costa, C.S.; Badiale-Furlong, E. Free phenolic compounds extraction from Brazilian halophytes, soybean and rice bran by ultrasound-assisted and orbital shaker methods. *An. Da Acad. Bras. Ciências* **2018**, *90*, 3363–3372. [CrossRef]
89. Faria, G.Y.Y.; Souza, M.M.; Oliveira, J.R.M.; Costa, C.S.B.; Collares, M.P.; Prentice, C. Effect of ultrasound-assisted cold plasma pretreatment to obtain sea asparagus extract and its application in Italian salami. *Food Res. Int.* **2020**, *137*, 109435. [CrossRef]
90. Oliveira-Alves, S.C.; Andrade, F.; Prazeres, I.; Silva, A.B.; Capelo, J.; Duarte, B.; Bronze, M.R. Impact of drying processes on the nutritional composition, volatile profile, phytochemical content and bioactivity of Salicornia ramosissima J. woods. *Antioxidants* **2021**, *10*, 1312. [CrossRef]
91. Kim, H.J.; Lee, J.H. Optimization of ultrasound-assisted extraction of phenolic compounds from Salicornia herbacea powder. *Prev. Nutr. Food Sci.* **2009**, *14*, 129–133. [CrossRef]
92. Uwineza, P.A.; Waśkiewicz, A. Recent advances in supercritical fluid extraction of natural bioactive compounds from natural plant materials. *Molecules* **2020**, *25*, 3847. [CrossRef] [PubMed]
93. Xynos, N.; Papaefstathiou, G.; Psychis, M.; Argyropoulou, A.; Aligiannis, N.; Skaltsounis, A.L. Development of a green extraction procedure with super/subcritical fluids to produce extracts enriched in oleuropein from olive leaves. *J. Supercrit. Fluids* **2012**, *67*, 89–93. [CrossRef]
94. Gallego, R.; Bueno, M.; Herrero, M. Sub-and supercritical fluid extraction of bioactive compounds from plants, food-by-products, seaweeds and microalgae—An update. *TrAC Trends Anal. Chem.* **2019**, *116*, 198–213. [CrossRef]
95. Heffernan, N.; Smyth, T.J.; FitzGerald, R.J.; Vila-Soler, A.; Mendiola, J.; Ibáñez, E.; Brunton, N.P. Comparison of extraction methods for selected carotenoids from macroalgae and the assessment of their seasonal/spatial variation. *Innov. Food Sci. Emerg. Technol.* **2016**, *37*, 221–228. [CrossRef]
96. Folan, A.J.; Anawe, P.A.L.; Ayeni, A.O. Synthesis and characterization of *Salicornia bigelovii* and *Salicornia brachiata* halophytic plants oil extracted by supercritical CO<sub>2</sub> modified with ethanol for biodiesel production via enzymatic transesterification reaction using immobilized *Candida antarctica* lipase catalyst in tert-butyl alcohol (TBA) solvent. *Cogent Eng.* **2019**, *6*, 1625847.

97. Domínguez-Rodríguez, G.; Marina, M.L.; Plaza, M. Enzyme-assisted extraction of bioactive non-extractable polyphenols from sweet cherry (*Prunus avium* L.) pomace. *Food Chem.* **2021**, *339*, 128086. [[CrossRef](#)]
98. Akyüz, A.; Ersus, S. Optimization of enzyme assisted extraction of protein from the sugar beet (*Beta vulgaris* L.) leaves for alternative plant protein concentrate production. *Food Chem.* **2021**, *335*, 127673. [[CrossRef](#)]
99. Oh, J.H.; Kim, E.O.; Lee, S.K.; Woo, M.H.; Choi, S.W. Antioxidant activities of the ethanol extract of hamcho (*Salicornia herbacea* L.) cake prepared by enzymatic treatment. *Food Sci. Biotechnol.* **2007**, *16*, 90–98.
100. Karthivashan, G.; Park, S.Y.; Kweon, M.H.; Kim, J.; Haque, M.; Cho, D.Y.; Choi, D.K. Ameliorative potential of desalted *Salicornia europaea* L. extract in multifaceted Alzheimer's-like scopolamine-induced amnesic mice model. *Sci. Rep.* **2018**, *8*, 7174. [[CrossRef](#)]
101. Clodoveo, M.L.; Muraglia, M.; Crupi, P.; Hbaieb, R.H.; De Santis, S.; Desantis, A.; Corbo, F. The Tower of Babel of Pharma-Food Study on Extra Virgin Olive Oil Polyphenols. *Foods* **2022**, *11*, 1915. [[CrossRef](#)] [[PubMed](#)]



Review

# Natural Polyphenol Recovery from Apple-, Cereal-, and Tomato-Processing By-Products and Related Health-Promoting Properties

Katalin Szabo <sup>1,2</sup>, Laura Mitrea <sup>1,2</sup>, Lavinia Florina Călinoiu <sup>2</sup>, Bernadette-Emőke Teleky <sup>2</sup>, Gheorghe Adrian Martău <sup>2</sup>, Diana Plamada <sup>2</sup>, Mihaela Stefana Pascuta <sup>2</sup>, Silvia-Amalia Nemeș <sup>2</sup>, Rodica-Anita Varvara <sup>2</sup> and Dan Cristian Vodnar <sup>2,\*</sup>

<sup>1</sup> Institute of Life Sciences, University of Agricultural Sciences and Veterinary Medicine, 400372 Cluj-Napoca, Romania

<sup>2</sup> Department of Food Science and Technology, University of Agricultural Sciences and Veterinary Medicine, 400372 Cluj-Napoca, Romania

\* Correspondence: dan.vodnar@usamvcluj.ro

**Abstract:** Polyphenols of plant origin are a broad family of secondary metabolites that range from basic phenolic acids to more complex compounds such as stilbenes, flavonoids, and tannins, all of which have several phenol units in their structure. Considerable health benefits, such as having prebiotic potential and cardio-protective and weight control effects, have been linked to diets based on polyphenol-enriched foods and plant-based products, indicating the potential role of these substances in the prevention or treatment of numerous pathologies. The most representative phenolic compounds in apple pomace are phloridzin, chlorogenic acid, and epicatechin, with major health implications in diabetes, cancer, and cardiovascular and neurocognitive diseases. The cereal by-products are rich in flavonoids (cyanidin 3-glucoside) and phenolic acids (ferulic acid), all with significant results in reducing the incidence of noncommunicable diseases. Quercetin, naringenin, and rutin are the predominant phenolic molecules in tomato by-products, having important antioxidant and antimicrobial activities. The present understanding of the functionality of polyphenols in health outcomes, specifically, noncommunicable illnesses, is summarized in this review, focusing on the applicability of this evidence in three extensive agrifood industries (apple, cereal, and tomato processing). Moreover, the reintegration of by-products into the food chain via functional food products and personalized nutrition (e.g., 3D food printing) is detailed, supporting a novel direction to be explored within the circular economy concept.

**Citation:** Szabo, K.; Mitrea, L.; Călinoiu, L.F.; Teleky, B.-E.; Martău, G.A.; Plamada, D.; Pascuta, M.S.; Nemeș, S.-A.; Varvara, R.-A.; Vodnar, D.C. Natural Polyphenol Recovery from Apple-, Cereal-, and Tomato-Processing By-Products and Related Health-Promoting Properties. *Molecules* **2022**, *27*, 7977. <https://doi.org/10.3390/molecules27227977>

Academic Editor: Nour Eddine Es-Safi

Received: 14 October 2022

Accepted: 11 November 2022

Published: 17 November 2022

**Publisher's Note:** MDPI stays neutral with regard to jurisdictional claims in published maps and institutional affiliations.



**Copyright:** © 2022 by the authors. Licensee MDPI, Basel, Switzerland. This article is an open access article distributed under the terms and conditions of the Creative Commons Attribution (CC BY) license (<https://creativecommons.org/licenses/by/4.0/>).

**Keywords:** agro-industrial by-products; biological activity; circular economy; health effects; re-integration; waste management; phenolic compounds

## 1. Introduction

By-products of agro-industrial provenance and food waste are severe global concerns, particularly in many developed countries [1]. Food consumption has increased as a consequence of urbanization, population expansion, and economic growth, and it remains a consistent issue worldwide in the long run [2,3]. The most bothersome sectors are the wheat flour production, apple juice production, and tomato-processing industries, which generate massive amounts of residues, as a result of the extensive yearly processed tonnage (Figure 1). On the other hand, the low cost and straightforward availability of this residual biomass shelter the economic prospects of its potentially valuable components [4].

In general, cereal grains are the world's main food source, contributing up to 300 million tons (Mt) of food products yearly according to FAOSTAT (<http://www.fao.org/> accessed on 10 October 2022) [5]. The primary cereals produced are maize, wheat, rice, barley, and oat crops, from which maize is mainly submerged as flour, animal feed, and

substrate in ethanol production [6], while wheat is consumed worldwide mostly in the form of flour [7].

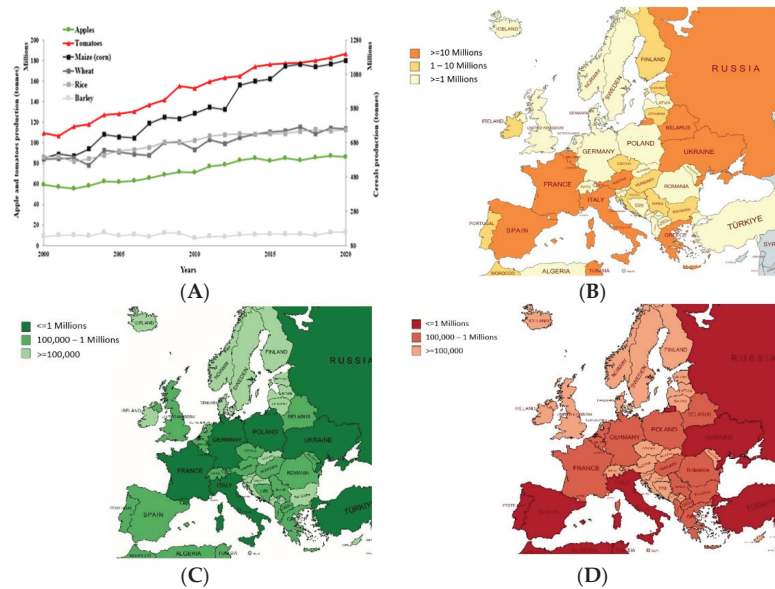


**Figure 1.** Production of cereal, apples, and tomatoes (tons) in Europe. (A) Evolution of world cereal, apple, and tomato production over the last two decades; (B) production of wheat (tons) in Europe for every country in 2020; (C) production of apples (tons) in Europe for every country in 2020; (D) production of tomatoes (tons) in Europe for every country in 2020 (<http://www.fao.org/faostat>, accessed on 22 April 2022).

Maize (*Zea mays* L.), cultivated globally, is the prime cereal grown in the world [8]. As presented in Figure 1A, its production increased by more than 50% in the last 20 years and is the most significant starch supply, and subsequently, it is one of the main organic by-product generators in the world [6]. In Europe, cereal production increased more than four times from 2000 to 2020, with the highest production in Western and Eastern Europe (Figure 1B). According to a recent study, in Europe, these cereal by-products, via integration with foodstuffs, could replace as many as 8.8 Mt of edible grains [9].

Wheat (*Triticum aestivum* L.) is one of the world's most prominent cereals. According to FAOSTAT, the global output in 2020 was over 760 million tons (Mt), up from 580 Mt in 2000, showing a 30.97% increase in wheat production over the last two decades, and the global output is expected to increase gradually in the future [10]. In agreement with the European Flour Millers' Report (2016), more than 45 Mt of wheat and oats is processed annually in Europe, creating over 6.5 Mt of by-products, which are predominantly used for animal nutrition [11]. By-products such as bran are a rich source of beneficial phytochemicals such as dietary fibers, minerals, vitamins, polyphenols, and phytosterols, known for their health-promoting properties [7,11–13]. Phenolic acids are among these components since they are categorized as bioactive phytochemicals and have a significant impact on human health [14].

Apple (*Malus domestica* sp.) is one of the most widespread fruits on the global scale. In 2020, the global output was over 86 Mt, up from just over 59 Mt in 2000, indicating an incremental tendency of apple production, with 46.19% in the last two decades [5]. China is the leading contributor to overall production with 46.85%, followed by the USA with 5.38%, and Turkey with 4.97%, and from Europe, the main contributor is Poland with 4.11%, as shown in Figure 1C. Furthermore, the worldwide output is predicted to rise steadily in the future [15,16].

The resulting by-product of apple pressing/processing, which derives from juice, cider, wine, distilled spirits, and vinegar production, as well as the formulation of jellies, is known as apple pomace (AP). Solid pomace makes up to 20–35% of the apple fruit's fresh weight and is composed of a mixture of pulp, peel, core, seed, and calyx. Approximately 95.5% of the solid waste is produced by epi-mesocarp [17]. Dietary fiber, which makes up around 65% of the dry weight of AP, is the main component from a nutritional point of view, and the majority of dietary fiber in all pomace is insoluble. Apple seeds include significant amounts of proteins and lipids, up to 49.5 and 24%, respectively. Additionally, hemicellulose is the second-most significant fiber in AP (19.9–32.2%), and cellulose accounts for a crucial part, comprising 43% of the pomace [18]. The by-products of the seed and peel are rich in phenolic chemicals, primarily chlorogenic acid and phloridzin [19].

Tomatoes (*Solanum lycopersicum* L.) are considered one of the world's most popular vegetables but are classified as a fruit. In Europe, it was first domesticated in Spain [20], and the main producers are represented in Figure 1D. The global output of tomatoes increased to 186 Mt in 2020, up from just over 109 Mt in 2000 [5]. According to FAOSTAT, a substantial increase in tomato production can be observed in the last two decades, precisely above 70%. The major producers are China with 34.67%, followed by India with 11.01%, Turkey with 7.07%, and the USA with 6.54% of global tomato crop production. Additionally, the global output is expected to increase gradually in the future [2]. More than one-third of the tomatoes are processed due to their perishable nature, and considerable amounts of by-products are generated via juice, sauces, ketchup, or puree production, among other meals. The removal of tomato peels, seeds, and tiny amounts of pulp can add between 5 and 30% to the cost of the primary products, and the by-products are a source of environmental discomfort due to their high moisture content, which favors bacterial growth and carbon dioxide emission [21]. The scientific literature confirms the presence of health-promoting compounds such as carotenoids, polyphenols, tocopherols, terpenes, and sterols in industrial tomatoes and their by-products, and endorses their extraction and revalorization in functional food products, as the bioactive substances resist to industrial processes [22,23].

Polyphenols are secondary metabolites that contain one or more hydroxyl groups, being one of the largest classes of valuable bioactive compounds for supporting human health [24,25]. Phenols are essentially made up of a hydroxyl group (-OH) linked directly to an aromatic hydrocarbon group, whereas polyphenols are larger polymers of 12 phenolic hydroxyl groups linked to five-to-seven aromatic rings [26,27]. Based on recent trends regarding healthier lifestyles and an increase in the consumption of foodstuffs derived from natural resources without any environmental drawbacks, the reintegration of by-products generated by the food industry is an important topic [28,29].

Green alternatives to lessen environmental pollution and waste generation include renewable biomaterials, and wheat-, apple-, and tomato-processing by-products can be framed into this category. In recent years, innovative and inventive applications of these by-products have contributed to the steady advancement of bioeconomy and biotechnology through the extraction and/or revalorization of natural phenolic compounds [30].

The use of agro-industrial derivatives might provide an additional source of income, and it could reduce by-product disposal and improve the nutritional profile of functional food items at the same time. Utilizing grain, tomato, and apple by-products from industrial production may provide a generous supply of nutrients, and their repurposing might represent a substantial source of revenue. Therefore, the objective of the current literature review is to highlight the primary phenolic components linked to human health, which can be found in the by-products of these three major agrifood industries (apple, cereal, and tomato processing), and to encourage their recovery and, accordingly, reintegration into the food chain using circular economy principles. Nonetheless, based on the findings of this study, it is projected that the food-processing industries could better manage their by-products and waste (e.g., through the incorporation of by-products into food formulations to boost the nutritional value), therefore avoiding a major environmental concern.

## 2. Polyphenols in Apple-Processing By-Products

Apples are one of the most consumed fruits worldwide, both in industry and at the individual population level [31]. Approximately 11 million metric tons of apples is produced and used annually in the apple-processing industry and alcoholic beverage production in Europe [32]. Apple pomace is one of the most widely produced agrifood wastes, with an annual production rate of about 4 million tons worldwide [33]. The recovery rate for this by-product, however, is modest. Pomace is frequently discarded and dumped in landfills as waste, which causes environmental issues and presents a potential risk to public health [3,34].

The amount of pomace resulting after apple processing can be reused in biotechnological routes as a substrate for the production of different compounds, such as flavoring compounds, pigments, fuel, and citric acid, or as raw materials for the extraction of fibers and phenolic compounds [35–38].

From a nutritional point of view, apple pomace is a by-product rich in fibers, vitamins, minerals, phenolic compounds, and pigments [19]. All these macronutrients have a significant role in the human organism through their effects on metabolism. Therefore, apple pomace has attracted researchers' consideration, as well as stakeholders' attention, by virtue of its valuable composition and by presenting suitable properties for further sustainable use [39].

The nutritional profile of apple pomace is mainly represented by phenolic compounds, carbohydrates, and fibers, as presented in table Table 1. These constituents can help treat gastrointestinal disorders, decrease serum triglycerides and LDL-cholesterol, and regulate glycemia [40,41]. All these effects in the human organism can be explained through their high concentration of the beneficial compounds mentioned above, primarily exerting anti-inflammatory and antioxidant roles [42].

**Table 1.** The nutritional and polyphenolic profile of apple pomace <sup>1</sup> [43].

Composition	Amount (% DW)
Total sugar	45.1 ± 5.3
Total dietary fiber	26.5 ± 0.8
Insoluble fiber	18.4 ± 0.4
Soluble fiber	8.2 ± 0.5
Total phenolic content (mg EGA/100 g AP)	289.1 ± 24.2
Fat	3.8 ± 0.2
Protein <sup>2</sup>	3.8 ± 0.0
Polyphenolic profile	(mg/100 g dry matter)
Quercetin-3- <i>O</i> -galactoside	22.55 ± 0.34
Quercetin-3- <i>O</i> -xyloside	13.91 ± 0.03
Quercetin-3- <i>O</i> -rhamnoside	19.21 ± 0.00
Chlorogenic acid	20.55 ± 0.12
<i>p</i> -coumaroylquinic acid	0.16 ± 0.03
Catechin	1.44 ± 0.02
Procyanidin B2	2.61 ± 0.00
Phloretin-2- <i>O</i> -xylosyl-glucoside	1.48 ± 0.14
Phlorizin	15.52 ± 0.00

<sup>1</sup> Values represent mean ± standard deviation, based on [43]; <sup>2</sup> nitrogen to protein conversion factor was 5.7.

In addition to the benefits, the consumption of apple pomace may raise questions associated with toxicity when it comes to its applicability in the food industry [44], with seeds representing 4–5% of the apple pomace [45]. Apple seeds contain a plant toxin called cyanogenic glycoside amygdalin, which can interact with digestive enzymes, resulting in the release of hydrogen cyanide. This toxin can cause different symptoms, from mild symptoms such as dizziness to severe symptoms such as paralysis and coma [46]. However, to reach poisoning levels, the ingested quantity must be significantly high; more exactly, between 83–500 apple seeds are needed to reach the poisoning level, or the person must

consume more than 800 g of apple pomace [33,47]. Studies on apple seed oil have confirmed the safety of its use, as the limit was found to be below the toxicity level [48].

Phenolic compounds are concentrated mainly in the core, seeds, peel, calyx, and stem, as well as in smaller amounts in the pulp, highlighting how apple pomace can be valorized through its high amount of antioxidant compounds. As shown in Figure 2, the total phenolic content of seeds has a higher value compared with the pulp, followed by the peel, both being part of apple pomace.

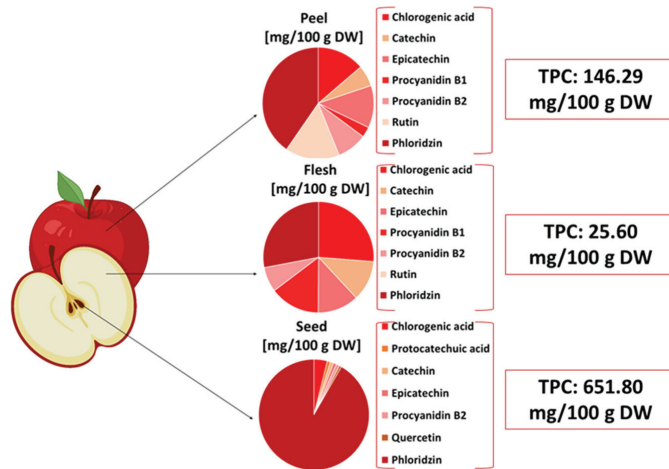


**Figure 2.** Distribution of phenolic compounds in apple fruit, according to Feng et al. [49]. TPC—total phenolic content; DW—dry weight.

The predominant phenolic compound families in apple pomace are dihydrochalcones, procyanidins, flavan-3-ol monomers, flavonols, anthocyanidins, and hydroxycinnamic acids. The most representative compounds are phlorizin from the dihydrochalcones family, chlorogenic acid from the hydroxycinnamic acids family, and epicatechin from the flavan-3-ol monomer family [50].

One of the representative phenolic compounds in apples and, remarkably, apple pomace, is phlorizin (Figure 3A). As the main compound from the dihydrochalcone family, the amount of phlorizin in apple pomace is approximately 1.6 mg/g dry weight, highlighted in a study by Lavelli et al. on the stability of phenolic compounds in apple pomace [51]. Phlorizin is used as a marker of apple varieties and is mainly concentrated in apple seeds. This polyphenol is also used as a reliable marker for spotting the presence of apples, a less expensive alternative compared with the reported fruits [52].

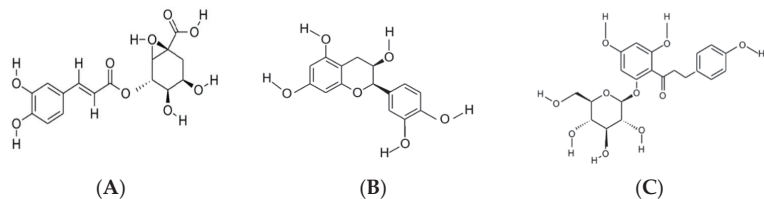


**Figure 3.** The chemical structure of the predominant phenolic compounds identified in apple pomace: chlorogenic acid (A); epicatechin (B); phlorizin (C). Source: ChemDraw Software.

Nevertheless, it also acts as a strong antioxidant, anti-inflammatory, and antimicrobial compound [53,54]. Regarding its benefits, phlorizin exerts several health benefits, mainly in diabetes, due to its ability to alter the glucose absorbed and excreted. A recent



study illustrated that the intestine and kidney's sodium/glucose cotransporters are specifically and competitively inhibited by phlorizin. In addition, postprandial hyperglycemia therapy in diabetes and other associated illnesses, such as obesity, may benefit from this characteristic [55]. A study conducted on streptozotocin-induced diabetic mice showed that a diet containing 0.5% phlorizin significantly improves the exacerbated elevations in blood glucose levels [56,57]. Another health benefit can be seen in colitis, where it acts as a protective compound for the intestinal brush border [58].

Chlorogenic acid (Figure 3B) is representative in the peel and flesh of apples compared with their seeds. Chlorogenic acid is a powerful antioxidant known for counteracting pathologies caused by oxidative processes [59,60]. A study conducted on the improvement of mood and cognition in the elderly showed enhanced results after the administration of enriched decaffeinated coffee with chlorogenic acid, displaying that the consumption of products containing chlorogenic acid can help in the treatment of neuro-cognitive diseases [61]. Besides the benefits mentioned previously, chlorogenic acid can also confer positive effects by lowering blood pressure, confirmed in a randomized trial involving healthy volunteers after the administration of 400 mg chlorogenic acid in 400 mL low-nitrate water. This effect can be explained by the ability of phenolic compounds to increase nitric oxide, which improves cardiovascular health [62].

The third phenolic compound found in apple pomace in smaller amounts is epicatechin (Figure 3C). Besides all its fulfilled roles (e.g., antioxidation, anti-inflammation), epicatechin can exert its role in diabetes, cancer, and cardiovascular disease, acting as a neuroprotective compound, and it improves muscle performance [63]. Cilleros et al. showed, in an *in vitro* study, the effect of epicatechin in regulating glucose uptake and bolstering the insulin signaling pathway [64]. A study conducted on human monocytic cells (THP1 cells) showed similar results regarding the beneficial effects of epicatechin in diabetes through the attenuation of high-glucose-induced inflammation [65].

### 3. Polyphenols in Cereal-Processing By-Products

Rice, wheat, barley, and corn are the most prevalent cereals globally, accounting for more than 90% of total cereal consumption [8]. By-products from the grain processing food industry include bran, straw, germ, and spent brewery grain [8,14]. Recent scientific studies confirm that the by-products of grain milling contain a wide range of beneficial components that support human health. These components, illustrated in Figure 4, include dietary fiber, vitamins, minerals, phytosterols, and polyphenols [66].

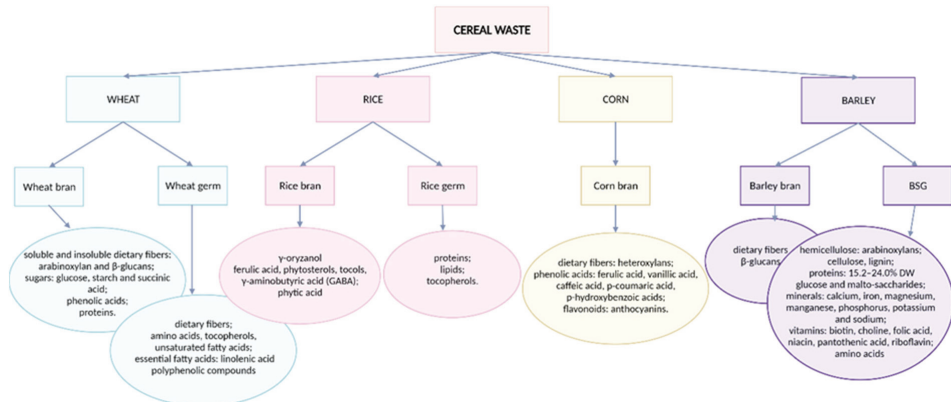


**Figure 4.** The most common cereals and their primary bioactive compounds.

The most common polyphenols in cereal by-products are flavonoids and phenolic acids, categorized into two large classes: hydroxybenzoic acids and hydroxycinnamic

acids [67]. Gallic, vanillic, p-hydroxybenzoic, protocatechuic, syringic, and salicylic acids are all hydroxybenzoic acids with a C6-C1 structure. Hydroxycinnamic acids, on the other hand, have a C6-C3 structure comprising caffeic, ferulic, p-coumaric, chlorogenic, and syringic acids [68].

Most of the phytochemicals found in cereal grains are identified in the bran fraction and are primarily bound to dietary fiber components, such as cellulose, hemicellulose, and lignin. In cereal by-products, a smaller amount of phenolic acid is present in a free form, and a larger amount is present in a bound form. In corn, for example, the free phenolic fraction ranges between 1 and 5 mg/100 g DW, while the bound fraction ranges between 150 and 300 mg/100 g DW [69]. The common phytochemical composition of cereal bran is presented in Table 2.

**Table 2.** Chemical composition of cereal bran.

Compound	Amount (% DW)				References
	Wheat Bran	Rice Bran	Oat Bran	Corn Bran	
Water	12.1	8.72-	29.4–31.2	4	[70–73]
Protein	13.2–18.4	10–16	5.9–6.7	9.5–10.1	[71,74,75]
Fat	3.5–3.9	15–22	6.47	1.92–6.41	[74,76–78]
Total carbohydrates	56.8	34.1–52.3	66.22	78.05–79.7	[74,76–78]
Starch	13.8–24.9	18.19–32.45	2.5–16.3	27.7–28.2	[70,72]
Cellulose	10.5–14.8	15.8	3.4	23–23.1	[72,79]
Hemicellulose	35.5–39.2	31.3	35%	26.1–27	[72,79,80]
Lignin	8.3–12.5	11.6	11.22	2.2–6.5	[72,79]
Total arabinoxylans	10.9–26.0	4.8–5.1	3	17.5–17.7	[70,79,81]
Total $\beta$ -glucan	2.1–2.5	0.04–0.21	5.4–8.5	-	[79,81]
Phenolic acids	1.1	1.57	0.7–1	2.2–2.7	[71,74,82]
Ferulic acid	0.02–1.5	0.004	1.76	1.5–1.9	[70,82,83]
Phytic acid	4.2–5.4	50.68 *	-	-	[74]
Ash	3.4–8.1	10.65	10.3–10.9	4	[71,73]

\* Phytic acid content of rice bran is expressed as mg/g DW.

Ferulic acid is primarily found in cereal by-products with values over 1000  $\mu\text{g/g}$  DW [69]. Wheat bran contains 90% ferulic acid, while oat bran contains 75% ferulic acid [84]. The metabolism of phenylalanine and tyrosine is responsible for their widespread presence in plant-based sources. Ferulic acid may be found in cereals in several forms, including free ferulic acid,  $\gamma$ -oryzanol, ferulic acid monoesters, and certain triterpene alcohols [84]. Ferulic acid is covalently linked to cell wall molecules, such as lignin, polysaccharides, long-chain fatty acids, and flavonoids via ester, ether, and amide bonds [85,86]. Because of the position of the hydrogen atom in the hydroxyl group of ferulic acid, it reacts with a free radical to produce an antioxidant effect [69,87].

Cereal bran is also rich in vanillic, syringic, salicylic, caffeic, and p-coumaric acids [68]. Vanillic acid (4-hydroxy-3-methoxybenzoic acid) is a hydroxybenzoic acid, a major component of vanilla flavor, which is used in the food industry for flavoring and preserving applications, along with the beverage, pharmaceutical, cosmetic, and tobacco industries [88].

Another predominant phenolic acid found in cereal bran is p-coumaric acid, which is the most available form of cinnamic acid and the most common cinnamic acid isomer in nature [89]. Coumaric acid, like the vast majority of phenolic acids, is found in lower concentrations in the endosperm of grains, with significantly increased concentrations in the peripheral tissues. Barley (230  $\mu\text{g/g}$ ), wheat (166  $\mu\text{g/g}$ ), oats (165  $\mu\text{g/g}$ ), and corn (2555  $\mu\text{g/g}$ ) have the highest levels of p-coumaric acid in their pericarp fractions [89].

Generally, phenolic acids have powerful biological effects such as antioxidant activity, antibacterial activity, anticancer properties, and anti-inflammatory effects, along with flavonoids. Flavonoids derived from grain-processing by-products contain antioxidant and anti-inflammatory functional groups. Flavonoid glycosides, such as cyanidin 3-glucoside, have been found to provide antioxidant and anti-inflammatory effects, and their gastrointestinal absorption rate is high. These chemicals' bioavailability is poor, ranging from 1–100 nmol/L of the total plasma concentration [87]. However, bounded polyphenols can be released in the colon by intestinal bacteria and certain enzymes, resulting in bioavailable phenolic metabolites with possible health advantages.

A study conducted on the effects of phenolic compounds on the large intestine's modulation showed that chlorogenic acid was converted into caffeic acid during the first stage of microbial biotransformation (dehydroxylation, dehydrogenation, or ester hydrolysis), and the primary metabolites found included di- and mono-hydroxylated phenylpropionic acids, m-coumaric, and hippuric acid [90].

An *in vivo* study conducted by Nuria Mateo Anson and colleagues [91] investigated how processed bran from whole wheat bread modifies the bioavailability of phenolic acids and exerts antioxidant and anti-inflammatory effects by examining postprandial plasma. The results showed a two- to three-fold increase in the bioavailability of ferulic acid, vanillic acid, sinapic acid, and 3,4-dimethoxybenzoic acid after eating bioprocessed bread. Furthermore, the ratio of pro-anti-inflammatory cytokines was significantly lower [92]. Another study examined the impact of regulated ferulic acid intake on lipid profiles, oxidative stress, and inflammatory activity in hyperlipidemic individuals. The improvement of the lipid profile, oxidation of LDL-cholesterol, decrease in oxidative stress, and reduction in inflammation were noticed after the consumption of 1000 mg of ferulic acid daily [93]. Thus, a diet rich in phenolic compounds can help prevent illnesses caused by oxidative stress and inflammation, as well as relieve symptoms associated with chronic diseases, including cardiovascular disease, obesity, and metabolic syndrome.

#### 4. Polyphenols in Tomato-Processing By-Products

Tomatoes are highly appreciated and consumed for their appetizing taste and various shapes and colors, as well as for their antioxidant properties and chemoprotective and cardioprotective effects. Tomato-based food products such as juices, ketchup, sauces, paste, and puree generate large quantities of wet solid by-products with harmful environmental consequences; however, paradoxically, these solid wastes are a promising source of health-promoting compounds, such as carotenoids and polyphenols [2,22,94,95]. The main tomato-processing by-products are peels and seeds, together with small amounts of pulp. For instance, the seeds account for 10% of the fruit and 60% of the total waste [96].

Tomatoes contain various phytochemicals and bioactive compounds that are able to endure industrial treatments and still remain in the tomato waste [97]. Therefore, the valorization of tomato by-products could be a valuable source of natural bioactive molecules for human health. Their reintegration into the food chain may be achieved by using them as natural additives in food production and/or nutraceuticals [2]. Bioactive compounds found in tomato by-products are carotenoids, polyphenols, vitamins, proteins, and high-quality fatty acids [95,98,99]. Among these active molecules, polyphenols have antioxidant and anti-inflammatory properties that play an essential role in human health [25]. The primary phenolic compounds found in tomato by-products are flavonols and phenolic acids, illustrated in Figure 5, with quercetin, naringenin, and rutin being the predominant molecules [100].

Tomato peels contain a significantly higher level of phenolic compounds in comparison with the seeds and pulp; 83% of the flavonols in tomatoes are present in the peels [101]. As an example, a higher level of polyphenol content in tomato peel by-products (33.5 mg TAE/100 g dried peel) was reported by Sarkar and Kaul (2014) compared with tomato seed by-products (20.11 mg TAE/100 g meal) [94]. However, the profile of polyphenol contents found in tomato by-products is dependent on several factors, such as the fruit

varieties [99], the geographical origin of the fruits [101], and the extraction methods used on the target compound [102]. Some examples regarding the total phenolic content in tomato by-products considering location and extraction method, as well as their antimicrobial and antioxidant activity, are provided in Table 3. Given the fact that tomato-processing by-products are most abundant in carotenoids as primary bioactive molecules, the antioxidant activity and antimicrobial effects might be attributed to the synergistic antioxidative effects of lycopene with other bioactive compounds to enhance their overall antioxidant activity [103].

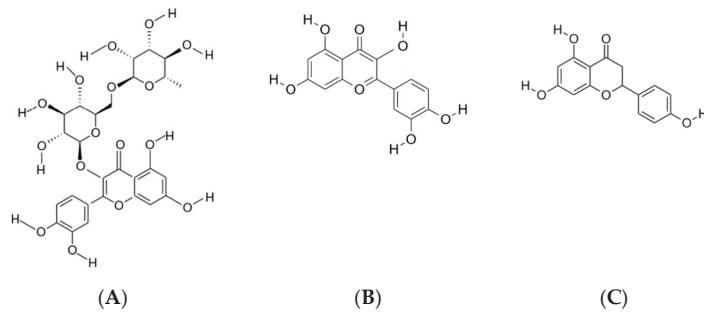


**Figure 5.** The chemical structure of the predominant phenolic compounds identified in tomato-processing by-products: rutin (A); quercetin (B); naringenin (C). Source: ChemDraw Software.

**Table 3.** Total phenolic content and antimicrobial and antioxidant activity considering the localization and extraction methods.

Geographical Origin	Tomato By-Products	Extraction Method	Total Phenolic Content	Antioxidant Activity	Antimicrobial Activity	Reference
India	Peels Seeds		33.5 mg TAE/100 g 20.11 mg TAE/100 g meal	21.0% inhibition/g 34.0% inhibition/g	-	[94]
Romania	Seeds and peels of 10 varieties of tomato Peels of 10 varieties of tomato		111.9 to 407.7 mg/100 g DW 35 to 157 mg/100 g DW	Mean value of 489.9 ± 41.5 μmol TE/100 g Mean value of 201 ± 44 μmol TE/100 g	Gram-positive and Gram-negative bacteria	[99] [95]
Portugal	Whole tomato	Solvent extraction	408.89 ± 12.11 and 277.24 ± 11.29 mg GAE/100 g DM (fresh and after 6 months of frozen storage); 310.33 ± 10.38 and 283.64 ± 11.84 mg GAE/100 g DW (before and after 6 months of powder storage)	ABTS (694.07 ± 45.00 and 558.73 ± 29.06 mg TE/100 g in fresh and after 6 months of frozen storage); 350.15 ± 14.37 and 407.56 ± 25.93 mg TE/100 g before and after 6 months of powder storage) ORAC (3165.18 ± 77.48 mg TE/100 g, 3285.77 ± 271.25 mg TE/100 g 1771.66 ± 31.25 mg TE/100 g in fresh and after 1 to 6 months of frozen storage; 1581.76 ± 124.90 TE/100 g, 1610.74 ± 46.51 mg TE/100 g and 1229.74 ± 38.52 mg TE/100 g before and after 2 to 6 months of powder storage) DPPH (418.79 ± 30.92, 648.06 ± 55.38, 388.53 ± 27.18 mg TE/100 g in fresh and after 3 to 6 months of frozen storage; 117.78 ± 4.99 to 130.44 ± 3.51 mg TE/100 g before and after 6 months of powder storage)	<i>Enterobacteriaceae</i> , <i>Bacillus cereus</i> spp., yeasts, and molds	[104]
Spain	Peels fiber	Enzyme hydrolysis Maceration Ultrasonic assistance (5 to 15 min)	291.14 ± 11.1 to 353.15 ± 19.6 mg GAE/kg 749.84 ± 15.55 mg GAE/kg 985.78 ± 112.93 to 1056.18 ± 67.9 mg GAE/kg	3.90 μmol TEAC/g	-	[105]

DW—dry weight; GAE—gallic acid equivalents.

The antioxidant and antimicrobial capacity of polyphenols has attracted increasing interest. These compounds have the ability to scavenge free radicals and reactive oxygen species, which are known to be involved in the development of cardiovascular diseases and several cancers [106]. For a more thorough study regarding the mechanism of action of polyphenols, Zhang and Tsao (2016) critically reviewed their biological activities, including antioxidative stress activity, anti-inflammatory effects, etc. [107].

The antioxidant capacity of tomato by-products can be divided between the hydrophilic and the lipophilic fractions. The antioxidant activity generated by polyphenols

is attributed to the hydrophilic fraction since these molecules are soluble in water. The entrapment of polyphenols in the major insoluble fraction of tomato peels, formed mainly by hemicelluloses, leads to low antioxidant activity. The antioxidant activity of tomato peel fiber was found to be 3.90  $\mu\text{mol TE/g}$  for the hydrophilic extract, lower than expected [105]. The mean value of the antioxidant activity of ten varieties of tomato by-products was found to be about 4.90  $\mu\text{mol TE/g}$ , with the highest value being 5.74  $\mu\text{mol TE/g}$ . Furthermore, little to any correlation has been found between the total phenolic content and antioxidant activity [99]. However, antioxidant activity might not always correlate with the number of phenols; it could be connected to the mutual interactions between all hydrophilic antioxidants and other constituents of the tomato by-products [95].

Even though tomato peels and seeds have relatively modest antioxidant activities, it is necessary to consider other remarkable attributes of these by-products, such as the antimicrobial capacity of polyphenols. Due to their hydrophobicity, phenolic compounds such as flavonols are capable of penetrating the cell phospholipid membranes of bacteria, able to exert their antibacterial activity inside the cell [108]. Gram-negative bacteria have cell walls surrounded by external membranes, which have high lipopolysaccharide contents. This makes Gram-negative bacteria less sensitive to the action of bioactive compounds such as polyphenols. This phenomenon was proved when the phenolic extracts of ten varieties of tomato by-products were tested against seven bacterial strains. The Gram-positive bacteria showed a higher sensitivity to the extract compared with the Gram-negative bacteria. All extracts were effective against *Staphylococcus aureus*, especially the Tiny Tim tomato variety, with a higher amount of flavonol glycosides and isochlorogenic acid. The Mirsini extract presented moderate antibacterial activity against Gram-negative bacteria (*Pseudomonas aeruginosa*, *Salmonella typhimurium*, *Klebsiella pneumoniae*, and *Escherichia coli*) [99].

The microbial contamination of soil can also influence the antimicrobial activity of fresh tomato by-products. When the Portuguese national microbiological guidelines for ready-to-eat foods were considered, unwashed and impure tomato by-products showed unsatisfactory *Enterobacteriaceae*, yeast, and *Bacillus cereus* spp. microbial counts for these food products. Washed and disinfected tomato by-products maintained these bacteria within satisfactory limits. Thus, tomato by-products have antimicrobial potential and can be used in food formulations or for cooking also considering their carotenoid content as natural food colorants. Furthermore, 6 months of frozen storage causes no substantial variation in microbial counts. Storing dry tomato by-products at room temperature slightly decreases the microbial counts of tested microorganisms [109]. Therefore, tomato by-products may control microbiological growth and may play an important role in the prevention of foodborne diseases.

## 5. Health-Promoting Properties of Polyphenol-Rich Diets

Since ancient times, the consumption of fresh vegetables, various green leaves, seeds, and fruits has promoted an optimal health state in the human organism without people knowing the exact mechanism of action. Polyphenols have contributed significantly to the enhancement of health status in humans over time, mainly due to their antioxidant properties, prebiotic potential, and, in some cases, their antimicrobial effects [25,110]. Based on their antioxidant effects, the polyphenolic structures are involved in the stimulation of the immune response against the progression of degenerative disorders such as metabolic syndrome, neurological affections, and different types of cancer. In addition, diets rich in polyphenols have been proven to sustain the optimal functioning of the immune system, as they enhance the activation of the NF- $\kappa$ B signaling pathway in macrophages that intervene in the management of inflammation processes [111]. Furthermore, multiple associations have been made between polyphenols and protective effects against chronic diseases based on chronic inflammation, and substantial evidence highlights the precautionary consequences of a polyphenol-rich dietary pattern [112–114].

The generous number of scientific reports available in recent years point out the strong antioxidant potential of vegetable-based polyphenols manifested through their antidiabetic, anti-obesity, anti-inflammatory, anticancer, hepatoprotective, cardioprotective, nephroprotective, neuroprotective, and osteoprotective effects, confirmed through various *in vitro* and *in vivo* studies [112]. In the same line, Condezo-Hoyos et al. highlighted, through a systematic review, the role of polyphenol-rich diets in clinical trials. The main results of the investigation showed substantial differences considering the consumption of 2564 mg of polyphenols (including hydroxycinnamic acids) per day [115].

Apples are among the most polyphenol-abundant fruits that are broadly consumed worldwide. Both the peels and pulp of apple fruits are rich in polyphenols, such as catechins, quercetin, rutin, phloridzin, phloretin, and chlorogenic acid, which are confirmed to exert positive effects, especially in reducing the evolution of neurodegenerative disorders [31]. At the same time, *in vitro* studies conducted on mice have proved that polyphenols extracted from apples have a protective effect on damaged gastrointestinal mucosa induced by drugs [31]. In addition, plenty of *in vitro* studies and clinical trials demonstrate the positive biological effects of polyphenol-rich foods such as apples on human and animal health, especially by stimulating the immune system. Diets consisting of moderate apple consumption maintain the general health state and accelerate the immune system's response to pathogenic threats [116]. Due to the lower water percentage in apple by-products, the phenolic content increases compared with fresh fruit. Additionally, the exterior layer of the apple contains enzymatic and nonenzymatic antioxidants as a consequence of outer environment exposure, which is valuable for homeostasis maintenance [117].

In addition, cereal bran represents a valuable source of polyphenolic compounds. Bran derived from wheat, corn, rice, barley, sorghum, rye, oat, and millet has been proven to contain high concentrations of phenolics, flavonoids, and anthocyanins, which can inhibit the oxidation of human low-density lipoprotein (LDL) cholesterol. Moreover, the bioactive compounds found in cereal bran have great biological potential in the prevention of chronic disease development, such as cardiovascular disease, diabetes, and cancer [118].

In the same line, tomato-processing by-products contain different concentrations of polyphenolic compounds, mainly phenolic acids and flavonoids, which have been validated to be involved in decreasing triglyceride levels and regulating lipid metabolism. Nonetheless, tomato peel-derived polyphenols have shown anticarcinogenic, anti-inflammatory, anti-aggregation, and vasodilating effects *in vitro* and in clinical studies [119,120].

### 5.1. The Prebiotic Potential of Phenolic Compounds

Phenolic compounds may play an important role in the gut microbiota's health state, acting as a prebiotic substrate for a diversity of probiotic strains [25,121]. In addition, polyphenols are considered prebiotics in the consensus document of the International Scientific Association for Probiotics and Prebiotics (ISAPP) [122]. Polyphenols such as catechin, gallic, vanillic, ferulic, and protocatechuic acids selectively stimulate probiotic strains and inhibit pathogenic ones. A study conducted by Pacheco-Ordaz et al. [123] investigated the effect of the five abovementioned polyphenols on the development of two probiotic strains, *Lactobacillus rhamnosus* GG ATCC 53103 and *Lactobacillus acidophilus* NR-RLB 4495, and two pathogens, *Escherichia coli* 0157:H7 ATCC 43890 and *Salmonella enterica* serovar Typhimurium ATCC 14028. The authors observed that the combination of phenols allows for the selective growth of probiotics and inhibits the development of pathogenic bacteria [123].

Apple pomace, composed especially of seeds and peel, contains the more significant part of phenolic compounds, primarily phloridzin, chlorogenic acid, and soluble/insoluble fibers. These contribute to the diminished glycemic index and amended mineral bioavailability [124]. Besides improving the nutritional quality of food products, their applicability in food fortification promotes the viability and fermentation period of lactic acid bacteria, which can further upgrade sourdough quality [3].

### 5.2. Cardioprotective Effects of Polyphenols

The imbalance between free radical accumulation and antioxidant activity is one of the critical indicators contributing to the high prevalence of cardiovascular disease. This noncommunicable illness is the primary cause of mortality worldwide [125]. The current pandemic also highlighted the importance of nutrition and a healthy lifestyle regarding the immune system and the prevention of certain chronic diseases, particularly cardiovascular disease [126].

Diets comprising polyphenols extracted from apples, cereals' bran, tomato peels showed positive activity close-connected to the well-functioning of the cardiovascular system [31]. For instance, in vivo studies on mice with cardiovascular disorders, treated with polyphenolic extracts from apple peels, showed improved results considering blood pressure, endothelial function, lipid homeostasis, and insulin resistance compared with the control group [127].

A double-blind, placebo-controlled investigation on 24 hyperlipidemic adults found that taking 1000 mg of ferulic acid daily for six weeks resulted in a significant reduction in total cholesterol (8.1%), LDL-cholesterol (9.3%), triglyceride (12.1%), and significantly increased HDL-cholesterol (4.3%) compared with placebo subjects [73]. Additionally, studies have demonstrated that regular whole grain consumption lowers the chance of developing particular illnesses, including type 2 diabetes, cardiovascular diseases, metabolic syndrome, and obesity [72,103,104]. Particular attention has been paid to the use of polyphenols in the prevention of cardiovascular-associated diseases, as these represent one of the main causes of increased mortality worldwide [105]. Moreover, ferulic acid, which abounds in wheat and oat brans, has good cardioprotective potential, as it maintains blood pressure, cholesterol, and glycemia at their optimal levels [128]. Furthermore, phenolic compounds found in tomato peels and seeds influence the cardiovascular system, mainly through their antithrombotic activity, imprinting ischemic injury prevention at the same time [129].

### 5.3. Polyphenols in Weight-Control Diets

Gut homeostasis is perturbed by obesity and overweightness, and it consequently enhances the ratio of *Firmicutes/Bacteroidetes*, which accelerate adiposity [130]. Studies conducted on polyphenols extracted from apples showed the positive impact of these compounds on weight loss and on the microbial communities of the guts of obese individuals [131]. Moreover, studies conducted on the effect of phenolic acids extracted from grain bran showed their output in reducing obesity risk and attenuating insulin resistance, thus contributing to maintaining a balanced body weight [132]. Polysaccharides, such as arabinoxylans and xylooligosaccharides extracted from cereal by-products, have a prebiotic effect, which also contributes to various metabolic dysfunctions and decreases blood cholesterol and glucose [133,134].

Polyphenols have shown a positive impact on the control of blood glucose levels, thus resulting in their positive attributes in the management of metabolic-related afflictions, such as diabetes [135]. In a systematic review performed by Coe and Ryan, several randomized clinical trials studying the effect of polyphenols in connection with carbohydrates on acute postprandial glycemic and insulin responses were analyzed. The results of the study pointed out that polyphenol-rich sources diminished the peak and early-phase glycemic response and also maintained the glycemic response in the later digestion phases. In addition, the polyphenol intake exhibited the mitigation of the insulin response, in particular, when they were consumed with bread, thus sustaining the beneficial properties in diminishing type 2 diabetes incidence [135].

## 6. Applicability of Recovered Polyphenols from Apple-, Cereal-, and Tomato-Processing By-Products in Functional Food Products in the Food Chain

The present concept of functional foods is the result of the gradual recognition that healthy diets derive from eating nutritious foods and from the identification of the mechanisms by which foods modulate metabolism and health. Some groups of foods, in addition

to their nutritional properties, have supplementary properties for health. These types of foods are called functional foods and may be defined as any food that has a positive impact on an individual's health, physical performance, or state of mind, in addition to its nutritious value.

### 6.1. Apple-Processing-Derived By-Products

The by-products of apple processing can be efficiently integrated into various foodstuffs, as specified in Table 4. Due to high fiber content, such as pectin and starch, which increases the viscosity of the products, these by-products can be integrated efficiently into functional food products, such as jellies, jams, or other foodstuffs [30]. In addition, due to several favorable health-related effects, the integration of AP is becoming more and more popular in various forms and applications [3,136].

One of the most efficient methods of preserving and integrating AP is drying and grinding it to obtain a powder, namely, AP flour. As indicated by Martau et al., 2021, the fortification of sourdough with 5 or 10% AP flour improved the microorganism's viability due to high sugar content and enhanced the flavor of the sourdough [137]. Another study indicated an increased dietary fiber content after the inclusion of AP flour in wheat and rye crispbreads, from 9.39 to 15.89 g/100g and 15.8 to 19.89 g/100, respectively [138]. Besides, no browning reaction could be observed in the final products even if the AP flour contained increased reducing sugar content. The same results could be observed in other studies, as shown in Table 4.

AP can also be applied to snacks or yogurts through extrusion and freeze-drying or even to pork meat to prepare salami products [139–141]. The main phenolic compound, phlorizin, has also been efficiently integrated into chewing gums, which can be dissolved after 5 min of chewing, thus contributing to administering bioactive compounds [142].

On another note, from apple by-products, several other important compounds can be obtained, such as pectin, via extraction and various organic chemicals (e.g., butanol, propionic acid, bio-succinic acid) using fermentation processes [143]. In addition, from the extracted pectin, efficient biofilm solutions can be produced, which can be further applied in the production of active packaging that can be additionally enriched with AP-derived antioxidants [144]. Introducing these bioactive compounds results in biodegradable, water-soluble packages that improve the quality and shelf-life of wrapped foodstuffs.

### 6.2. Cereal-Processing-Derived By-Products

By-products belonging to the cereal industry mainly include rice, corn, wheat, barley, and other cereals used in the production of bakery products and alcoholic beverages. Cereal grains comprise one of the primary assets of human food, and recently, their manufacturing has expanded; the by-products originating from these resources have also increased [28,145]. The direct derivatives of these cereals are bran, germ, husk, hulls, and brewery wastes (brewer's spent disposal) [133]. These comprise diverse, major compounds with significant health effects [14,134].

The need for gluten-free diets, especially in humans with Celiac disease, has grown steadily, and finding products with enhanced nutritional properties is of foremost importance [146]. The integration of by-products can contribute to the improvement of gluten-free products. A recent study improved the nutritional content of rice muffins through the integration of sweet corn cob flour. This increased the fiber and ferulic content of the final product [147]. Another efficient method is the integration of oat proteins, which are usually removed through processing and can be efficiently integrated into various functional food products [148,149].

Several other kinds of cereal, native to their respective countries, contain important functional and nutritional properties. One of these is quinoa, a pseudo-cereal that originates from the Andean region. This cereal can also be efficiently used in the production of gluten-free products, especially after sourdough fermentation [150]. Through fermentation, the overall characteristics of the final foodstuff obtained from cereal by-products are improved,



through prolonged shelf life, improved texture, flavor, diminished antinutrients, and growth in phytochemicals [151,152].

### 6.3. Tomato-Processing-Derived By-Products

Tomatoes are consumed in high quantities worldwide; thus, the by-products originating from this vegetable are consistent. Various studies have handled the reutilization of this by-product, as it contains essential amounts of organic acids, sugars, antioxidants, fibers, vitamins, proteins, and oils that are crucial to the effective functioning of the human body [22,153].

The main compounds recovered from tomato-industry-derived by-products are carotenoids, which can be efficiently integrated into various functional food products. They contribute to the sensory properties and shelf life and increase the bioactive ingredients [97,154,155]. Several studies tackle the troubles that are encountered through their inclusion in food products, such as their hydrophobic nature. A recent study by Szabo et al., 2022, efficiently incorporated these carotenoids in microcapsules that improved bioaccessibility through in vitro digestion model [2]. In a recent study, tomato by-products were integrated with various vegetable oils [154]. These extracts decreased the viscosity in the cases of hempseed and grapeseed oils and increased the viscosity in the case of flaxseed oil. This variation in viscosity can be attributed to the fact that the enrichment increased the thermal motion of the oil molecules and decreased the intermolecular resilience. These oils can be easily integrated with functional foods and are an efficient delivery system for these carotenoid extracts.

A high portion of tomato by-products is composed of seeds (5–10%), from which tomato seed oil can be extracted. These seeds consist of proteins (34%), lipids (30%), and fibers [129], as well as unsaturated fatty acids (palmitic, oleic, and linoleic acid). Generally, the proportion of oil extraction from tomato seeds ranges between 10 and 35% DW, depending on the extraction method [156].

**Table 4.** Examples of the reintegration of apple-, cereal-, and tomato-processing by-products in functional food products.

	Food Product	Effect On Food Product	Ref.	
Apple	AP flour (5, 10%)	Bakery product—sourdough	+ cell viability; ↑ organic acid content (malic, oxalic, and citric acid)	[3]
	AP flour (5, 10, 15%)	Cereal crispbread	↑ total dietary fiber; ↑ hardness and crispiness	[139]
	Apple peel powder	Muffin	↑ dietary fiber; ↑ bioactive compounds; + color and texture; + organoleptic characteristics (12%)	[157]
	AP flour (2.5, 5, 7, 10%)	Pasta	↓ carbohydrate content; ↑ fiber, protein, fat, and ash content; ↑ swelling index, cooking water absorption, and cooking loss; ↓ optimum cooking time; ↓ texture and structure of pasta (10%)	[32]
	AP (2, 3, 6, 9%)	Freeze-dried snacks	↑ AP; ↓ lightness coefficient; ↑ cutting force; ↑ organoleptic properties (2%); ↓ water activity	[158]
	AP 20%	GF corn snacks	↑x36 chlorogenic acid; ↑x4 cryptochlorogenic acid; ↑x6 catechin; ↑x3 procyanidin; ↑x8 epicatechin; ↑x25 phlorizin; ↑x3 total soluble and insoluble dietary fiber; ↑ organoleptic scores	[159]
	AP powder	Yogurt	↓ sensory profile; ↑ protein and fat content; ↑ rheological attributes	[141]
	Freeze-dried AP powder (0.5, 1%)	Set-type yogurt	↑ gelation pH; ↓ fermentation time (1%); firmer and consistent yogurt (cold storage); stable structure (0.5%); stabilizer and texturizer	[43]
	Dried AP (7, 14%)	Italian salami	↓ fat and calories; ↑ fiber and phenol content	[140]
	Defatted apple seed flour	Chewing gum	↑ phlorizin content (52–67% and 75–83% of the total phenolics)	[143]
Cereal	WB & BF	Bread	↑ dietary fibers content ↑ alveograph profile ↑ volume of bread	[160]
	SCC (10, 20, and 30%)	GF rice muffin	↑ dietary fibers and ferulic acid content; ↑ nutritional value; + height, color, and texture (20% SCC)	[147]
	BRF	Buns and muffins	↑ dietary fibers, iron, zinc, and calcium; ↑ antioxidant capacity and phytonutrient content; ↓ carbohydrates and sensory acceptability; moderate glycemic index and glycemic load; ↑ shelf life	[161]
	OPC & OPI	Yogurt	↑ nutritional benefits (OPI); ↑ product quality and sustainability (OPC); ↑ nutritional (OPC)	[149]
	BMG + PBD (1:1)	Cereal composite bar	+ essential minerals and fiber; ↑ sensorial evaluation; antifungal properties	[162]
	BSG	Yogurt	↑ viscosity and shear stress; ↓ fermentation time; maintained flow behavior and stability	[163]
	BRG+PFPF+WP	GF breakfast cereals	Average acceptance; + total, soluble, and insoluble dietary fiber; ↑ darkness, protein, and carbohydrate content; ↓ expansion and consumer acceptance	[164]

Table 4. Cont.

	Food Product	Effect On Food Product	Ref.	
Tomato	PH	Gel-based foods	↑ textural and sensory characteristics; syneresis and fat loss during cooking avoidance; ↑ gelling properties	[165]
	CT	Hemp, flaxseed, grapeseed oil	↑ oil quality; ↑ viscosity (flaxseed oil); ↓ viscosity (hemp and grapeseed oil); intense color	[154]
	TBPP	biofilms	↑ aesthetic impact and coloring; ↓ transparency	[166]
	TBPP	biofilms	↑ physical properties (diameter, thickness, density, weight); ↑ antimicrobial effect; ↑ total phenolic content	[155]
	TPP	GF ready to cook snack	↑ fiber, mineral, and lycopene content; ↑ antioxidant activity; ↓ oil uptake	[167]
	TPF	Spreadable cheese	↑ spreadability; ↑ antioxidant activity and phenolic content; ↑ fibers	[168]
	TBP	Passata	↑ total dietary fiber; ↑ lycopene and polyphenols	[169]
	TPP (5, 10, 15, 20, 25%)	cookies	↓ lightness values; ↑ redness and yellowness; acceptable by consumers (5%)	[170]
	TPF (15%)	pasta	↑ carotenoids and dietary fiber; ↓ sensory scores for elasticity, odor, and firmness	[171]

Food manufacturing through 3D-printing technology is an innovative method of delivering personalized food, meeting our nutritional needs and expectations regarding taste, texture, color, and other aspects [172]. In addition, personalized, 3D-printed food products are promising in the prevention of different noncommunicable diseases due to the possibility of enhancing them with bioactive compounds (e.g., polyphenols, dietary fibers, proteins, etc.) [173].

As for future perspectives, bioactive compounds, such as polyphenols, vitamins, and/or proteins found in food processing by-products, could be easily integrated into functional foods by associating 3D-printed food with molecular gastronomy [174]. Alongside a facile integration of recovered polyphenols, the inner biological activities and nutritional profile can be enhanced, obtaining fortified nourishment [175]. In addition, delivering fortified foods via 3D printing is a sustainable approach to food-waste management, according to circular economy principles [174].

## 7. Conclusions

All things considered, apple-, cereal-, and tomato-processing by-products are a valuable source of phenolic compounds that can be safely reintegrated with the food chain within recommended parameters. Apple pomace possesses a significant number of beneficial effects for the human body, most of them offered by their antioxidant and anti-inflammatory properties. The three main compounds identified in apple pomace—phlorizin, chlorogenic acid, and epicatechin—can act upon metabolic diseases, being important pillars in the prevention and treatment of the ailment.

Studies demonstrate that regular whole grain consumption lowers the chance of developing noncommunicable diseases, the cause for these health effects being the synergy between the polyphenols and dietary fibers found in the outer layers of the grains, which are unfortunately discarded as by-products.

It is necessary to consider the remarkable antimicrobial capacity of polyphenols derived from tomato by-products, with a focus on flavonol glycosides and isochlorogenic acid against *Staphylococcus aureus*.

In addition to altering the composition of the gut microbiota, which is closely linked with health benefits, gut bacteria also metabolize polyphenols to create bioactive chemicals that have therapeutic effects. Polyphenols such as catechin, gallic, vanillic, ferulic, and protocatechuic acids selectively stimulate probiotic strains and inhibit pathogenic ones.

In light of this, polyphenols seem to be promising candidates for use in both functional food products and personalized nutrition (e.g., 3D-printed food). To fully take advantage of their outstanding qualities, various pharmacokinetic concerns, such as decreased intestinal absorption and bioavailability and quick metabolic alterations, should be considered.

**Author Contributions:** Conceptualization, K.S.; validation, K.S. and D.C.V.; investigation, R.-A.V., B.-E.T., M.S.P., D.P., S.-A.N., L.M., L.F.C. and G.A.M.; writing—original draft preparation, R.-A.V., B.-E.T., K.S., D.P., S.-A.N., L.M., M.S.P., L.F.C. and G.A.M.; writing—review and editing, K.S.; visualization, K.S.; supervision, D.C.V.; project administration, K.S. All authors have read and agreed to the published version of the manuscript.

**Funding:** This research was funded by “Unitatea Executiva pentru Finantarea Invatamantului Superior a Cercetarii Dezvoltarii si Inovarii” (UEFISCDI), Grant No. PN-III-P1-1.1-PD-2021-0672.

**Institutional Review Board Statement:** Not applicable.

**Informed Consent Statement:** Not applicable.

**Data Availability Statement:** Not applicable.

**Conflicts of Interest:** The authors declare no conflict of interest.

**Sample Availability:** Samples of the compounds are available from the authors.

## References

- Gu, B.; Zhang, X.; Bai, X.; Fu, B.; Chen, D. Four steps to food security for swelling cities. *Nature* **2019**, *566*, 31–33. [[CrossRef](#)] [[PubMed](#)]
- Szabo, K.; Teleky, E.B.; Ranga, F.; Simon, E.; Pop, L.O.; Babalau-Fuss, V.; Kapsalis, N.; Cristian, D. Bioaccessibility of microencapsulated carotenoids, recovered from tomato processing industrial by-products, using in vitro digestion model. *LWT* **2021**, *152*, 112285. [[CrossRef](#)]
- Martău, G.A.; Teleky, B.E.; Ranga, F.; Pop, I.D.; Vodnar, D.C. Apple Pomace as a Sustainable Substrate in Sourdough Fermentation. *Front. Microbiol.* **2021**, *12*, 3850. [[CrossRef](#)] [[PubMed](#)]
- Iriondo-Dehond, M.; Miguel, E.; Del Castillo, M.D. Food byproducts as sustainable ingredients for innovative and healthy dairy foods. *Nutrients* **2018**, *10*, 1358. [[CrossRef](#)]
- Food and Agriculture Organization. Available online: <https://www.fao.org/home/en> (accessed on 10 October 2022).
- Zhang, R.; Ma, S.; Li, L.; Zhang, M.; Tian, S.; Wang, D.; Liu, K.; Liu, H.; Zhu, W.; Wang, X. Grain & Oil Science and Technology Comprehensive utilization of corn starch processing by-products: A review. *Grain Oil Sci. Technol.* **2021**, *4*, 89–107.
- Deroover, L.; Tie, Y.; Verspreet, J.; Courtin, C.M.; Verbeke, K. Modifying wheat bran to improve its health benefits. *Crit. Rev. Food Sci. Nutr.* **2020**, *60*, 1104–1122. [[CrossRef](#)]
- Fărcaș, A.C.; Socaci, S.A.; Nemeș, S.A.; Pop, O.L.; Coldea, T.E.; Fogarasi, M.; Biriș-Dorhoi, E.S. An Update Regarding the Bioactive Compound of Cereal By-Products: Health Benefits and Potential Applications. *Nutrients* **2022**, *14*, 3470. [[CrossRef](#)]
- Sandström, V.; Chrysafi, A.; Lamminen, M.; Troell, M.; Jalava, M.; Piipponen, J.; Siebert, S.; Van Hal, O.; Virkki, V.; Kummu, M. Food system by-products upcycled in livestock and aquaculture feeds can increase global food supply. *Nat. Food* **2022**, *3*, 729–740. [[CrossRef](#)]
- Vodnar, D.C.; Calinoiub, L.F.; Mitrea, L.; Precup, G.; Bindea, M.; Pacurar, A.M.; Szabo, K.; Stefanescu, B.E. *A New Generation of Probiotic Functional Beverages Using Bioactive Compounds from Agro-Industrial Waste*; Academic Press: Cambridge, MA, USA, 2019; ISBN 9780128163979.
- Călinoiu, L.F.; Vodnar, D.C. Thermal processing for the release of phenolic compounds from wheat and oat bran. *Biomolecules* **2020**, *10*, 21. [[CrossRef](#)]
- Călinoiu, L.F.; Vodnar, D.C. Whole Grains and Phenolic Acids: A Review on Bioactivity, Functionality, Health Benefits and Bioavailability. *Nutrients* **2018**, *10*, 1615. [[CrossRef](#)]
- Martău, G.A.; Unger, P.; Schneider, R.; Venus, J.; Vodnar, D.C.; López-Gómez, J.P. Integration of solid state and submerged fermentations for the valorization of organic municipal solid waste. *J. Fungi* **2021**, *7*, 766. [[CrossRef](#)] [[PubMed](#)]
- Florina, L.; Adriana-florinela, C.; Vodnar, D.C. Solid-State Yeast Fermented Wheat and Oat Bran as A Route for Delivery of Antioxidants. *Antioxidants* **2019**, *8*, 372.
- Purić, M.; Rabrenović, B.; Rac, V.; Pezo, L.; Tomašević, I.; Demin, M. Application of defatted apple seed cakes as a by-product for the enrichment of wheat bread. *LWT* **2020**, *130*, 109391. [[CrossRef](#)]
- Spengler, R.N. Origins of the apple: The role of megafaunal mutualism in the domestication of *Malus* and rosaceous trees. *Front. Plant Sci.* **2019**, *10*, 617. [[CrossRef](#)] [[PubMed](#)]
- Giovanetti Canteri, M.H.; Nogueira, A.; de Oliveira Petkowicz, C.L.; Wosiacki, G. Characterization of Apple Pectin—A Chromatographic Approach. *Chromatogr. Most Versatile Method Chem. Anal.* **2012**. [[CrossRef](#)]
- Rupasinghe, H.P.V.; Wang, L.; Huber, G.M.; Pitts, N.L. Effect of baking on dietary fibre and phenolics of muffins incorporated with apple skin powder. *Food Chem.* **2008**, *107*, 1217–1224. [[CrossRef](#)]
- Rabetafika, H.N.; Bchir, B.; Blecker, C.; Richel, A. Fractionation of apple by-products as source of new ingredients: Current situation and perspectives. *Trends Food Sci. Technol.* **2014**, *40*, 99–114. [[CrossRef](#)]

20. Laranjeira, T.; Costa, A.; Faria-Silva, C.; Ribeiro, D.; Ferreira, M.P.; Sim, S.; Ascenso, A. Sustainable Valorization of Tomato By-Products to Obtain Bioactive Compounds: Their Potential in Inflammation and Cancer Management. *Molecules* **2022**, *27*, 1701. [[CrossRef](#)]
21. Kumar, R.; Hyun, S.; Keum, Y. An updated review on use of tomato pomace and crustacean processing waste to recover commercially vital carotenoids. *Food Res. Int.* **2018**, *108*, 516–529.
22. Szabo, K.; Cătoi, A.-F.; Vodnar, D.C. Bioactive Compounds Extracted from Tomato Processing by-Products as a Source of Valuable Nutrients. *Plant Foods Hum. Nutr.* **2018**, *73*, 268–277. [[CrossRef](#)]
23. Strati, I.F.; Oreopoulou, V. Recovery of carotenoids from tomato processing by-products—A review. *Food Res. Int.* **2014**, *65*, 311–321. [[CrossRef](#)]
24. Wang, D.; Wang, T.; Zhang, Z.; Li, Z.; Guo, Y.; Zhao, G.; Wu, L. Recent advances in the effects of dietary polyphenols on inflammation in vivo: Potential molecular mechanisms, receptor targets, safety issues, and uses of nanodelivery system and polyphenol polymers. *Curr. Opin. Food Sci.* **2022**, *48*, 100921. [[CrossRef](#)]
25. Plamada, D.; Vodnar, D.C. Polyphenols—Gut Microbiota Interrelationship: A Transition to a New Generation of Prebiotics. *Nutrients* **2022**, *14*, 137. [[CrossRef](#)] [[PubMed](#)]
26. Martins, N.; Ferreira, I.C.F.R. Wastes and by-products: Upcoming sources of carotenoids for biotechnological purposes and health-related applications. *Trends Food Sci. Technol.* **2017**, *62*, 33–48. [[CrossRef](#)]
27. Ding, Y.; Morozova, K.; Scampicchio, M.; Ferrentino, G. Non-Extractable polyphenols from food by-products: Current knowledge on recovery, characterisation, and potential applications. *Processes* **2020**, *8*, 925. [[CrossRef](#)]
28. Čolović, D.; Rakita, S.; Banjac, V.; Đuragić, O.; Čabarkapa, I. Plant food by-products as feed: Characteristics, possibilities, environmental benefits, and negative sides. *Food Rev. Int.* **2019**, *35*, 363–389. [[CrossRef](#)]
29. Precup, G.; Mitrea, L.; Călinoiu, L.F.; Martău, A.G.; Nemeș, A.; Emoke Teleky, B.; Coman, V.; Vodnar, D.C. Food processing by-products and molecular gastronomy. *Gastron. Food Sci.* **2021**, *8*, 137–163.
30. Coman, V.; Teleky, B.-E.; Mitrea, L.; Martău, G.A.; Szabo, K.; Călinoiu, L.-F.; Vodnar, D.C. *Bioactive Potential of Fruit and Vegetable Wastes*; Academic Press: Cambridge, MA, USA, 2020; Volume 91, ISBN 9780128204702.
31. Francini, A.; Sebastiani, L. Phenolic compounds in apple (*Malus x domestica* borkh.): Compounds characterization and stability during postharvest and after processing. *Antioxidants* **2013**, *2*, 181–193. [[CrossRef](#)]
32. Bchir, B.; Karoui, R.; Danthine, S.; Blecker, C.; Besbes, S.; Attia, H. Date, Apple, and Pear By-Products as Functional Ingredients in Pasta: Cooking Quality Attributes and Physicochemical, Rheological, and Sensorial Properties. *Foods* **2022**, *11*, 1393. [[CrossRef](#)]
33. Gołębiewska, E.; Kalinowska, M.; Yildiz, G. Sustainable Use of Apple Pomace (AP) in Different Industrial Sectors. *Materials* **2022**, *15*, 1788. [[CrossRef](#)]
34. Lyu, F.; Luiz, S.F.; Azeredo, D.R.P.; Cruz, A.G.; Ajlouni, S.; Ranadheera, C.S. Apple pomace as a functional and healthy ingredient in food products: A review. *Processes* **2020**, *8*, 319. [[CrossRef](#)]
35. Ricci, A.; Cirlini, M.; Guido, A.; Liberatore, C.M.; Ganino, T.; Lazzi, C.; Chiancone, B. From byproduct to resource: Fermented apple pomace as beer flavoring. *Foods* **2019**, *8*, 309. [[CrossRef](#)] [[PubMed](#)]
36. Le Deun, E.; Van Der Werf, R.; Le Bail, G.; Le Quééré, J.M.; Guyot, S. HPLC-DAD-MS Profiling of Polyphenols Responsible for the Yellow-Orange Color in Apple Juices of Different French Cider Apple Varieties. *J. Agric. Food Chem.* **2015**, *63*, 7675–7684. [[CrossRef](#)] [[PubMed](#)]
37. Molinuevo-Salces, B.; Riaño, B.; Hijosa-Valsero, M.; González-García, I.; Paniagua-García, A.I.; Hernández, D.; Garita-Cambronero, J.; Díez-Antolínez, R.; García-González, M.C. Valorization of apple pomaces for biofuel production: A biorefinery approach. *Biomass Bioenergy* **2020**, *142*, 105785. [[CrossRef](#)]
38. Shojaosadati, S.A.; Babaepour, V. Citric acid production from apple pomace in multi-layer packed bed solid-state bioreactor. *Process Biochem.* **2002**, *37*, 909–914. [[CrossRef](#)]
39. Sato, M.F.; Vieira, R.G.; Zardo, D.M.; Falcão, L.D.; Nogueira, A.; Wosiacki, G. Apple pomace from eleven cultivars: An approach to identify sources of bioactive compounds. *Acta Sci. Agron.* **2010**, *32*, 29–35.
40. Kasprzak-Drozd, K.; Oniszczuk, T.; Stasiak, M.; Oniszczuk, A. Beneficial effects of phenolic compounds on gut microbiota and metabolic syndrome. *Int. J. Mol. Sci.* **2021**, *22*, 3715. [[CrossRef](#)]
41. Sergeant, T.; Piront, N.; Meurice, J.; Toussaint, O.; Schneider, Y.J. Anti-inflammatory effects of dietary phenolic compounds in an in vitro model of inflamed human intestinal epithelium. *Chem. Biol. Interact.* **2010**, *188*, 659–667. [[CrossRef](#)]
42. Skinner, R.C.; Gigliotti, J.C.; Ku, K.M.; Tou, J.C. A comprehensive analysis of the composition, health benefits, and safety of apple pomace. *Nutr. Rev.* **2018**, *76*, 893–909. [[CrossRef](#)]
43. Wang, X.; Kristo, E.; LaPointe, G. The effect of apple pomace on the texture, rheology and microstructure of set type yogurt. *Food Hydrocoll.* **2019**, *91*, 83–91. [[CrossRef](#)]
44. Gumul, D.; Ziobro, R.; Korus, J.; Kruczek, M. Apple pomace as a source of bioactive polyphenol compounds in gluten-free breads. *Antioxidants* **2021**, *10*, 807. [[CrossRef](#)] [[PubMed](#)]
45. Walia, M.; Rawat, K.; Bhushan, S.; Padwad, Y.S.; Singh, B. Fatty acid composition, physicochemical properties, antioxidant and cytotoxic activity of apple seed oil obtained from apple pomace. *J. Sci. Food Agric.* **2014**, *94*, 929–934. [[CrossRef](#)] [[PubMed](#)]
46. Bolaninwa, I.F.; Orfila, C.; Morgan, M.R.A. Determination of amygdalin in apple seeds, fresh apples and processed apple juices. *Food Chem.* **2015**, *170*, 437–442. [[CrossRef](#)] [[PubMed](#)]

47. Opyd, P.M.; Jurgoński, A.; Juśkiewicz, J.; Milala, J.; Zduńczyk, Z.; Król, B. Nutritional and health-related effects of a diet containing apple seed meal in rats: The case of amygdalin. *Nutrients* **2017**, *9*, 1091. [[CrossRef](#)] [[PubMed](#)]
48. Montañés, F.; Catchpole, O.J.; Tallon, S.; Mitchell, K.A.; Scott, D.; Webby, R.F. Extraction of apple seed oil by supercritical carbon dioxide at pressures up to 1300 bar. *J. Supercrit. Fluids* **2018**, *141*, 128–136. [[CrossRef](#)]
49. Feng, S.; Yi, J.; Li, X.; Wu, X.; Zhao, Y.; Ma, Y.; Bi, J. Systematic Review of Phenolic Compounds in Apple Fruits: Compositions, Distribution, Absorption, Metabolism, and Processing Stability. *J. Agric. Food Chem.* **2021**, *69*, 7–27. [[CrossRef](#)]
50. Pollini, L.; Cossignani, L.; Juan, C.; Mañes, J. Extraction of phenolic compounds from fresh apple pomace by different non-conventional techniques. *Molecules* **2021**, *26*, 4272. [[CrossRef](#)]
51. Lavelli, V.; Corti, S. Phloridzin and other phytochemicals in apple pomace: Stability evaluation upon dehydration and storage of dried product. *Food Chem.* **2011**, *129*, 1578–1583. [[CrossRef](#)]
52. Hrubá, M.; Baxant, J.; Čížková, H.; Smutná, V.; Kovařík, F.; Ševčík, R.; Hanušová, K.; Rajchl, A. Phloridzin as a marker for evaluation of fruit product's authenticity. *Czech J. Food Sci.* **2021**, *39*, 49–57. [[CrossRef](#)]
53. Rana, S.; Gupta, S.; Rana, A.; Bhushan, S. Functional properties, phenolic constituents and antioxidant potential of industrial apple pomace for utilization as active food ingredient. *Food Sci. Hum. Wellness* **2015**, *4*, 180–187. [[CrossRef](#)]
54. Táborský, J.; Sus, J.; Lachman, J.; Šebková, B.; Adamcová, A.; Šatinský, D. Dynamics of phloridzin and related compounds in four cultivars of apple trees during the vegetation period. *Molecules* **2021**, *26*, 3816. [[CrossRef](#)] [[PubMed](#)]
55. Najafian, M.; Jahromi, M.Z.; Nowroznejhad, M.J.; Khajeaian, P.; Kargar, M.M.; Sadeghi, M.; Arasteh, A. Phloridzin reduces blood glucose levels and improves lipids metabolism in streptozotocin-induced diabetic rats. *Mol. Biol. Rep.* **2012**, *39*, 5299–5306. [[CrossRef](#)] [[PubMed](#)]
56. Kamdi, S.P.; Badwaik, H.R.; Raval, A.; Ajazuddin; Nakhate, K.T. Ameliorative potential of phloridzin in type 2 diabetes-induced memory deficits in rats. *Eur. J. Pharmacol.* **2021**, *913*, 174645. [[CrossRef](#)] [[PubMed](#)]
57. Masumoto, S.; Akimoto, Y.; Oike, H.; Kobori, M. Dietary Phloridzin Reduces Blood Glucose Levels and Reverses Sglt1 Expression in the Small Intestine in Streptozotocin-Induced Diabetic Mice. *J. Agric. Food Chem.* **2009**, *57*, 4651–4656. [[CrossRef](#)]
58. Lu, Y.Y.; Liang, J.; Chen, S.X.; Wang, B.X.; Yuan, H.; Li, C.T.; Wu, Y.Y.; Wu, Y.F.; Shi, X.G.; Gao, J.; et al. Phloridzin alleviate colitis in mice by protecting the intestinal brush border and improving the expression of sodium glycogen transporter 1. *J. Funct. Foods* **2018**, *45*, 348–354. [[CrossRef](#)]
59. Fang, Y.Z.; Yang, S.; Wu, G. Free radicals, antioxidants, and nutrition. *Nutrition* **2002**, *18*, 872–879. [[CrossRef](#)]
60. Upadhyay, R.; Mohan Rao, L.J. An Outlook on Chlorogenic Acids—Occurrence, Chemistry, Technology, and Biological Activities. *Crit. Rev. Food Sci. Nutr.* **2013**, *53*, 968–984. [[CrossRef](#)]
61. Cropley, V.; Croft, R.; Silber, B.; Neale, C.; Scholey, A.; Stough, C.; Schmitt, J. Does coffee enriched with chlorogenic acids improve mood and cognition after acute administration in healthy elderly? A pilot study. *Psychopharmacology* **2012**, *219*, 737–749. [[CrossRef](#)]
62. Mubarak, A.; Catherine, P.B.; Liu, A.H.; Considine, M.J.; Rich, L.; Mas, E.; Croft, K.D.; Hodgson, J.M. Acute effects of chlorogenic acid on nitric oxide status, endothelial function and blood pressure in healthy volunteers: A randomised trial. *J. Agric. Food Chem.* **2012**, *60*, 9130–9136. [[CrossRef](#)]
63. Qu, Z.; Liu, A.; Li, P.; Liu, C.; Xiao, W.; Huang, J.; Liu, Z.; Zhang, S. Advances in physiological functions and mechanisms of (-)-epicatechin. *Crit. Rev. Food Sci. Nutr.* **2021**, *61*, 211–233. [[CrossRef](#)]
64. Cilleros, D.Á.; Martín, M.Á.; Ramos, S. (-)-Epicatechin and the colonic 2,3-dihydroxybenzoic acid metabolite regulate glucose uptake, glucose production, and improve insulin signalling in renal NRK-52E cells. *Mol. Nutr. Food Res.* **2018**, *62*, 1700470.
65. Cordero-Herrera, I.; Chen, X.; Ramos, S.; Devaraj, S. (-)-Epicatechin attenuates high-glucose-induced inflammation by epigenetic modulation in human monocytes. *Eur. J. Nutr.* **2017**, *56*, 1369–1373. [[CrossRef](#)] [[PubMed](#)]
66. Luithui, Y.; Baghya Nisha, R.; Meera, M.S. Cereal by-products as an important functional ingredient: Effect of processing. *J. Food Sci. Technol.* **2019**, *56*, 1–11. [[CrossRef](#)] [[PubMed](#)]
67. Fărcaș, A.; Dretcanu, G.; Pop, T.D.; Enaru, B.; Socaci, S.; Diaconeasa, Z. Cereal processing by-products as rich sources of phenolic compounds and their potential bioactivities. *Nutrients* **2021**, *13*, 3934. [[CrossRef](#)] [[PubMed](#)]
68. Roasa, J.; De Villa, R.; Mine, Y.; Tsao, R. Phenolics of cereal, pulse and oilseed processing by-products and potential effects of solid-state fermentation on their bioaccessibility, bioavailability and health benefits: A review. *Trends Food Sci. Technol.* **2021**, *116*, 954–974. [[CrossRef](#)]
69. Tylewicz, U.; Nowacka, M.; Martín-García, B.; Wiktor, A.; Gómez Caravaca, A.M. *Target Sources of Polyphenols in Different Food Products and Their Processing By-Products*; Elsevier: Amsterdam, The Netherlands, 2018; ISBN 9780128135723.
70. Apprich, S.; Tirpanalan, Ö.; Hell, J.; Reisinger, M.; Böhmendorfer, S.; Siebenhandl-Ehn, S.; Novalin, S.; Kneifel, W. Wheat bran-based biorefinery 2: Valorization of products. *LWT* **2014**, *56*, 222–231. [[CrossRef](#)]
71. Bannikova, A.; Zyainitdinov, D.; Evteev, A.; Drevko, Y.; Evdokimov, I. Microencapsulation of polyphenols and xylooligosaccharides from oat bran in whey protein-maltodextrin complex coacervates: In-vitro evaluation and controlled release. *Bioact. Carbohydr. Diet. Fibre* **2020**, *23*, 100236. [[CrossRef](#)]
72. Zhuang, X.; Yin, T.; Han, W.; Zhang, X. *Nutritional Ingredients and Active Compositions of Defatted Rice Bran*; Elsevier Inc.: Amsterdam, The Netherlands, 2019; ISBN 9780128128282.
73. Yadav, M.P.; Moreau, R.A.; Hicks, K.B. Phenolic acids, lipids, and proteins associated with purified corn fiber arabinoxylans. *J. Agric. Food Chem.* **2007**, *55*, 943–947. [[CrossRef](#)]

74. Moongngarm, A.; Daomukda, N.; Khumpika, S. Chemical Compositions, Phytochemicals, and Antioxidant Capacity of Rice Bran, Rice Bran Layer, and Rice Germ. *APCBEE Procedia* **2012**, *2*, 73–79. [[CrossRef](#)]
75. Yue, Z.; Sun, L.L.; Sun, S.N.; Cao, X.F.; Wen, J.L.; Zhu, M.Q. Structure of corn bran hemicelluloses isolated with aqueous ethanol solutions and their potential to produce furfural. *Carbohydr. Polym.* **2022**, *288*, 119420. [[CrossRef](#)]
76. Feng, S.; Wang, L.; Shao, P.; Lu, B.; Chen, Y.; Sun, P. Simultaneous analysis of free phytosterols and phytosterol glycosides in rice bran by SPE/GC–MS. *Food Chem.* **2022**, *387*, 132742. [[CrossRef](#)] [[PubMed](#)]
77. Duță, D.E.; Culețu, A.; Mohan, G. *Reutilization of Cereal Processing By-Products in Bread Making*; Woodhead Publishing Series in Food Science; Woodhead Publishing: Sawston, UK, 2018; ISBN 9780081022146.
78. Moreau, R.A.; Hicks, K.B. The composition of corn oil obtained by the alcohol extraction of ground corn. *JAOCs J. Am. Oil Chem. Soc.* **2005**, *82*, 809–815. [[CrossRef](#)]
79. Arzami, A.N.; Ho, T.M.; Mikkonen, K.S. Valorization of cereal by-product hemicelluloses: Fractionation and purity considerations. *Food Res. Int.* **2022**, *151*, 110818. [[CrossRef](#)] [[PubMed](#)]
80. Schmitz, E.; Nordberg Karlsson, E.; Adlercreutz, P. Warming weather changes the chemical composition of oat hulls. *Plant Biol.* **2020**, *22*, 1086–1091. [[CrossRef](#)] [[PubMed](#)]
81. Li, S.; Chen, H.; Cheng, W.; Yang, K.; Cai, L.; He, L.; Du, L.; Liu, Y.; Liu, A.; Zeng, Z.; et al. Impact of arabinoxylan on characteristics, stability and lipid oxidation of oil-in-water emulsions: Arabinoxylan from wheat bran, corn bran, rice bran, and rye bran. *Food Chem.* **2021**, *358*, 129813. [[CrossRef](#)]
82. Ndolo, V.U.; Beta, T. Comparative studies on composition and distribution of phenolic acids in cereal grain botanical fractions. *Cereal Chem.* **2014**, *91*, 522–530. [[CrossRef](#)]
83. Martín-Diana, A.B.; García-Casas, M.J.; Martínez-Villaluenga, C.; Frías, J.; Peñas, E.; Rico, D. Wheat and oat brans as sources of polyphenol compounds for development of antioxidant nutraceutical ingredients. *Foods* **2021**, *10*, 115. [[CrossRef](#)]
84. Yin, Z.N.; Wu, W.J.; Sun, C.Z.; Liu, H.F.; Chen, W.B.; Zhan, Q.P.; Lei, Z.G.; Xin, X.; Ma, J.J.; Yao, K.; et al. Antioxidant and Anti-inflammatory Capacity of Ferulic Acid Released from Wheat Bran by Solid-state Fermentation of *Aspergillus niger*. *Biomed. Environ. Sci.* **2019**, *32*, 11–21.
85. Long, L.; Wu, L.; Lin, Q.; Ding, S. Highly Efficient Extraction of Ferulic Acid from Cereal Brans by a New Type A Feruloyl Esterase from *Eupenicillium parvum* in Combination with Dilute Phosphoric Acid Pretreatment. *Appl. Biochem. Biotechnol.* **2020**, *190*, 1561–1578. [[CrossRef](#)]
86. Upadhyay, P.; Singh, N.K.; Tupe, R.; Odenath, A.; Lali, A. Biotransformation of corn bran derived ferulic acid to vanillic acid using engineered *Pseudomonas putida* KT2440. *Prep. Biochem. Biotechnol.* **2020**, *50*, 341–348. [[CrossRef](#)]
87. Ed Nignpense, B.; Francis, N.; Blanchard, C.; Santhakumar, A.B. Bioaccessibility and bioactivity of cereal polyphenols: A review. *Foods* **2021**, *10*, 1595. [[CrossRef](#)] [[PubMed](#)]
88. Martău, G.A.; Călinoiu, L.F.; Vodnar, D.C. Bio-vanillin: Towards a sustainable industrial production. *Trends Food Sci. Technol.* **2021**, *109*, 579–592. [[CrossRef](#)]
89. Boz, H. p-Coumaric acid in cereals: Presence, antioxidant and antimicrobial effects. *Int. J. Food Sci. Technol.* **2015**, *50*, 2323–2328. [[CrossRef](#)]
90. Mosele, J.I.; Macià, A.; Motilva, M.J. Metabolic and microbial modulation of the large intestine ecosystem by non-absorbed diet phenolic compounds: A review. *Molecules* **2015**, *20*, 17429–17468. [[CrossRef](#)] [[PubMed](#)]
91. Anson, N.M.; Aura, A.M.; Selinheimo, E.; Mattila, I.; Poutanen, K.; Van Den Berg, R.; Havenaar, R.; Bast, A.; Haenen, G.R.M.M. Bio-processing of wheat bran in whole wheat bread increases the bioavailability of phenolic acids in men and exerts antiinflammatory effects ex vivo1-3. *J. Nutr.* **2011**, *141*, 137–143. [[CrossRef](#)]
92. Hamadou, M.; Martin Alain, M.M.; Obadias, F.V.; Hashmi, M.Z.; Başaran, B.; Jean Paul, B.; Samuel René, M. Consumption of underutilised grain legumes and the prevention of type II diabetes and cardiometabolic diseases: Evidence from field investigation and physicochemical analyses. *Environ. Chall.* **2022**, *9*, 100621. [[CrossRef](#)]
93. Bumrungpert, A.; Lilitchan, S.; Tuntipopipat, S.; Tirawanchai, N.; Komindr, S. Ferulic acid supplementation improves lipid profiles, oxidative stress, and inflammatory status in hyperlipidemic subjects: A randomized, double-blind, placebo-controlled clinical trial. *Nutrients* **2018**, *10*, 713. [[CrossRef](#)]
94. Sarkar, A.; Kaul, P. Evaluation of tomato processing by-products: A comparative study in a pilot scale setup. *J. Food Process Eng.* **2014**, *37*, 299–307. [[CrossRef](#)]
95. Szabo, K.; Diaconeasa, Z.; Cătoi, A.-F.; Vodnar, D.C. Screening of ten tomato varieties processing waste for bioactive components and their related antioxidant and antimicrobial activities. *Antioxidants* **2019**, *8*, 292. [[CrossRef](#)]
96. Schieber, A. By-Products of Plant Food Processing as a Source of Valuable Compounds. *Ref. Modul. Food Sci.* **2019**, *12*, 401–413.
97. Szabo, K.; Dulf, F.V.; Eleni, P.; Boukouvalas, C.; Krokida, M.; Kapsalis, N.; Rusu, A.V.; Socol, C.T.; Vodnar, D.C. Evaluation of the Bioactive Compounds Found in Tomato Seed Oil and Tomato Peels Influenced by Industrial Heat Treatments. *Foods* **2021**, *10*, 110. [[CrossRef](#)] [[PubMed](#)]
98. Popescu, M.; Iancu, P.; Plesu, V.; Todasca, M.C.; Isopencu, G.O.; Bildea, C.S. Valuable Natural Antioxidant Products Recovered from Tomatoes by Green Extraction. *Molecules* **2022**, *27*, 4191. [[CrossRef](#)] [[PubMed](#)]
99. Szabo, K.; Dulf, F.V.; Diaconeasa, Z.; Vodnar, D.C. Antimicrobial and antioxidant properties of tomato processing byproducts and their correlation with the biochemical composition. *LWT—Food Sci. Technol.* **2019**, *116*, 108558. [[CrossRef](#)]

100. Cruz-Carrión, Á.; Calani, L.; de Azua, M.J.R.; Mena, P.; Del Rio, D.; Suárez, M.; Arola-Arnal, A. (Poly)phenolic composition of tomatoes from different growing locations and their absorption in rats: A comparative study. *Food Chem.* **2022**, *388*, 132984. [[CrossRef](#)] [[PubMed](#)]
101. Shahidi, F.; Varatharajan, V.; Oh, W.Y.; Peng, H. Phenolic compounds in agri-food by-products, their bioavailability and health effects. *J. Food Bioact.* **2019**, *5*, 57–119. [[CrossRef](#)]
102. Ebrahimi, P.; Lante, A. Environmentally Friendly Techniques for the Recovery of Polyphenols from Food By-Products and Their Impact on Polyphenol Oxidase: A Critical Review. *Appl. Sci.* **2022**, *12*, 1923. [[CrossRef](#)]
103. Shixian, Q.; Dai, Y.; Kakuda, Y.; Shi, J.; Mittal, G.; Yeung, D.; Jiang, Y. Synergistic anti-oxidative effects of lycopene with other bioactive compounds. *Food Rev. Int.* **2005**, *21*, 295–311. [[CrossRef](#)]
104. Ara, H.; Santos, D.; Campos, D.A.; Ratinho, M.; Rodrigues, I.M.; Pintado, M.E. Development of Frozen Pulps and Powders from Carrot and Tomato by-Products: Impact of Processing and Storage Time on Bioactive and Biological Properties. *Horticulturae* **2021**, *7*, 185.
105. Navarro-González, I.; García-Valverde, V.; García-Alonso, J.; Periago, M.J. Chemical profile, functional and antioxidant properties of tomato peel fiber. *Food Res. Int.* **2011**, *44*, 1528–1535. [[CrossRef](#)]
106. Venturi, F.; Sanmartin, C.; Taglieri, I.; Andrich, G.; Zinnai, A. A simplified method to estimate Sc-CO<sub>2</sub> extraction of bioactive compounds from different matrices: Chili pepper vs. tomato by-products. *Appl. Sci.* **2017**, *7*, 361. [[CrossRef](#)]
107. Zhang, H.; Tsao, R. Dietary polyphenols, oxidative stress and antioxidant and anti-inflammatory effects. *Curr. Opin. Food Sci.* **2016**, *8*, 33–42. [[CrossRef](#)]
108. Daglia, M. Polyphenols as antimicrobial agents. *Curr. Opin. Biotechnol.* **2012**, *23*, 174–181. [[CrossRef](#)]
109. Araújo-Rodrigues, H.; Santos, D.; Campos, D.A.; Guerreiro, S.; Ratinho, M.; Rodrigues, I.M.; Pintado, M.E. Impact of processing approach and storage time on bioactive and biological properties of rocket, spinach and watercress byproducts. *Foods* **2021**, *10*, 2301. [[CrossRef](#)]
110. Nemes, S.; Mitrea, L.; Adrian, G.; Szabo, K.; Mihai, M.; Vodnar, D.C.; Cris, G. Microencapsulation and Bioaccessibility of Phenolic Compounds of Vaccinium Leaf Extracts. *Antioxidants* **2022**, *11*, 674.
111. Petroff, O.A.C. Book Review: GABA and Glutamate in the Human Brain. *Neurosci.* **2002**, *8*, 562–573. [[CrossRef](#)]
112. Pattern, H.P.D.; Del Bo, C.; Bernardi, S.; Marino, M.; Porrini, M.; Tucci, M.; Guglielmetti, S.; Cherubini, A.; Carrieri, B.; Kirkup, B.; et al. Systematic Review on Polyphenol Intake and Health Outcomes: Is there Sufficient Evidence to define a health-promoting polyphenol-rich dietary pattern. *Nutrients* **2019**, *11*, 1355.
113. Ganesan, K.; Xu, B. Polyphenol-Rich Dry Common Beans (*Phaseolus vulgaris* L.) and Their Health Benefits. *Int. J. Mol. Sci.* **2017**, *18*, 2331. [[CrossRef](#)]
114. Mitrea, L.; Nemes, S.-A.; Szabo, K.; Teleky, B.-E.; Vodnar, D.-C. Guts Imbalance Imbalances the Brain: A Review of Gut Microbiota Association with Neurological and Psychiatric Disorders. *Front. Med.* **2022**, *9*, 813204. [[CrossRef](#)]
115. Condezo-hoyos, L.; Gazi, C.; Jara, P. Design of polyphenol-rich diets in clinical trials: A systematic review. *Food Res. Int.* **2021**, *149*, 110655. [[CrossRef](#)]
116. Bergmann, H.; Triebel, S.; Kahle, K.; Richling, E. The Metabolic Fate of Apple Polyphenols in Humans. *Curr. Nutr. Food Sci.* **2010**, *6*, 19–35. [[CrossRef](#)]
117. Barreira, J.C.M.; Arraibi, A.A.; Ferreira, I.C.F.R. Bioactive and functional compounds in apple pomace from juice and cider manufacturing: Potential use in dermal formulations. *Trends Food Sci. Technol.* **2019**, *90*, 76–87. [[CrossRef](#)]
118. Hung, P. Van Critical Reviews in Food Science and Nutrition Phenolic compounds of cereals and their antioxidant capacity. *Crit. Rev. Food Sci. Nutr.* **2014**, *56*, 25–35. [[CrossRef](#)]
119. Lourenzi, E.; Novelli, B.; Okoshi, K.; Polit, M.; Paulino, B.; Muzio, D.; Guimara, J.F.C. Influence of rutin treatment on biochemical alterations in experimental diabetes. *Biomed. Pharmacother.* **2010**, *64*, 214–219.
120. Elbadrawy, E.; Sello, A. Evaluation of nutritional value and antioxidant activity of tomato peel extracts. *Arab. J. Chem.* **2011**, *9*, S1010–S1018. [[CrossRef](#)]
121. De Souza, E.L.; Mariano, T.; De Albuquerque, R. Potential interactions among phenolic compounds and probiotics for mutual boosting of their health-promoting properties and food functionalities—A review. *Crit. Rev. Food Sci. Nutr.* **2019**, *59*, 1645–1659. [[CrossRef](#)]
122. Moorthy, M.; Chaiyakunapruk, N.; Anne, S.; Palanisamy, U.D. Trends in Food Science & Technology Prebiotic potential of polyphenols, its effect on gut microbiota and anthropometric / clinical markers: A systematic review of randomised controlled trials. *Trends Food Sci. Technol.* **2020**, *99*, 634–649.
123. Pacheco-Ordaz, R.; Wall-Medrano, A.; Goñi, M.G.; Ramos-Clamont-Montfort, G.; Ayala-Zavala, J.F.; González-Aguilar, G.A. Effect of phenolic compounds on the growth of selected probiotic and pathogenic bacteria. *Lett. Appl. Microbiol.* **2018**, *66*, 25–31. [[CrossRef](#)]
124. Gobetti, M.; De Angelis, M.; Di Cagno, R.; Polo, A.; Rizzello, C.G. The sourdough fermentation is the powerful process to exploit the potential of legumes, pseudo-cereals and milling by-products in baking industry. *Crit. Rev. Food Sci. Nutr.* **2020**, *60*, 2158–2173. [[CrossRef](#)]
125. Nishiga, M.; Wang, D.W.; Han, Y.; Lewis, D.B.; Wu, J.C. COVID-19 and cardiovascular disease: From basic mechanisms to clinical perspectives. *Nat. Rev. Cardiol.* **2020**, *17*, 543–558. [[CrossRef](#)]

126. Vodnar, D.C.; Mitrea, L.; Teleky, B.E.; Szabo, K.; Călinoiu, L.F.; Nemeş, S.A.; Martău, G.A. Coronavirus Disease (COVID-19) Caused by (SARS-CoV-2) Infections: A Real Challenge for Human Gut Microbiota. *Front. Cell. Infect. Microbiol.* **2020**, *10*, 575559. [[CrossRef](#)]
127. Tian, J.; Wu, X.; Zhang, M.; Zhou, Z.; Liu, Y. Comparative study on the effects of apple peel polyphenols and apple flesh polyphenols on cardiovascular risk factors in mice. *Clin. Exp. Hypertens.* **2017**, *40*, 65–72. [[CrossRef](#)] [[PubMed](#)]
128. Alam, A. Anti-hypertensive Effect of Cereal Antioxidant Ferulic Acid and Its Mechanism of Action. *Front. Nutr.* **2019**, *6*, 121. [[CrossRef](#)]
129. Kumar, M.; Chandran, D.; Tomar, M.; Bhuyan, D.J.; Grasso, S.; Sá, A.G.A.; Carciofi, B.A.M.; Dhupal, S.; Singh, S.; Senapathy, M.; et al. Valorization Potential of Tomato (*Solanum lycopersicum* L.) Seed: Nutraceutical Quality, Food Properties, Safety Aspects, and Application as a Health-Promoting Ingredient in Foods. *Horticulturae* **2022**, *8*, 265. [[CrossRef](#)]
130. Magne, F.; Gotteland, M.; Gauthier, L.; Zazueta, A.; Pesoa, S.; Navarrete, P.; Balamurugan, R. The firmicutes/bacteroidetes ratio: A relevant marker of gut dysbiosis in obese patients? *Nutrients* **2020**, *12*, 1474. [[CrossRef](#)]
131. Rastmanesh, R. Chemico-Biological Interactions High polyphenol, low probiotic diet for weight loss because of intestinal microbiota interaction. *Chem. Biol. Interact.* **2011**, *189*, 1–8. [[CrossRef](#)]
132. Patel, S. Cereal bran fortified-functional foods for obesity and diabetes management: Triumphs, hurdles and possibilities. *J. Funct. Foods* **2015**, *14*, 255–269. [[CrossRef](#)]
133. Dapčević-Hadnadev, T.; Hadnadev, M.; Pojić, M. *The Healthy Components of Cereal By-Products and Their Functional Properties*; Woodhead Publishing Series in Food Science; Woodhead Publishing: Sawston, UK, 2018; ISBN 9780081022146.
134. Precup, G.; Pocol, C.B. Awareness, Knowledge, and Interest about Prebiotics—A Study among Romanian Consumers. *Int. J. Environ. Res. Public Health* **2022**, *19*, 1208. [[CrossRef](#)]
135. Coe, S.; Ryan, L. Impact of polyphenol-rich sources on acute postprandial glycaemia: A systematic review. *J. Nutr. Sci.* **2016**, *5*, 1–11. [[CrossRef](#)]
136. O’Shea, N.; Ktenioudaki, A.; Smyth, T.P.; McLoughlin, P.; Doran, L.; Auty, M.A.E.; Arendt, E.; Gallagher, E. Physicochemical assessment of two fruit by-products as functional ingredients: Apple and orange pomace. *J. Food Eng.* **2015**, *153*, 89–95. [[CrossRef](#)]
137. Allaqaband, S.; Dar, A.H.; Patel, U.; Kumar, N.; Alabdallah, N.M.; Kumar, P.; Pandey, V.K.; Kovács, B. Utilization of Fruit Seed-Based Bioactive Compounds for Formulating the Nutraceuticals and Functional Food: A Review. *Front. Nutr.* **2022**, *9*, 902554. [[CrossRef](#)]
138. Muntean, M.V.; Fărcaş, A.C.; Medeleanu, M.; Salanță, L.C.; Borşa, A. A Sustainable Approach for the Development of Innovative Products from Fruit and Vegetable By-Products. *Sustainability* **2022**, *14*, 10862. [[CrossRef](#)]
139. Konrade, D.; Klava, D.; Gramatina, I. Cereal Crispbread Improvement with Dietary Fibre from Apple By-Products. *CBU Int. Conf. Proc.* **2017**, *5*, 1143–1148. [[CrossRef](#)]
140. Grispoldi, L.; Ianni, F.; Blasi, F.; Pollini, L.; Crotti, S.; Cruciani, D.; Cenci-Goga, B.T.; Cossignani, L. Apple Pomace as Valuable Food Ingredient for Enhancing Nutritional and Antioxidant Properties of Italian Salami. *Antioxidants* **2022**, *11*, 1221. [[CrossRef](#)]
141. Ahmed, M.; Ali, A.; Sarfraz, A.; Hong, Q.; Boran, H. Effect of Freeze-Drying on Apple Pomace and Pomegranate Peel Powders Used as a Source of Bioactive Ingredients for the Development of Functional Yogurt. *J. Food Qual.* **2022**, *2022*, 3327401. [[CrossRef](#)]
142. Karwacka, M.; Ciurzyńska, A.; Galus, S.; Janowicz, M. Freeze-dried snacks obtained from frozen vegetable by-products and apple pomace—Selected properties, energy consumption and carbon footprint. *Innov. Food Sci. Emerg. Technol.* **2022**, *77*, 102949. [[CrossRef](#)]
143. Gunes, R.; Palabiyik, I.; Toker, O.S.; Konar, N.; Kurultay, S. Incorporation of defatted apple seeds in chewing gum system and phloridzin dissolution kinetics. *J. Food Eng.* **2019**, *255*, 9–14. [[CrossRef](#)]
144. Awasthi, M.K.; Ferreira, J.A.; Sirohi, R.; Sarsaiya, S.; Khoshnevisan, B.; Baladi, S.; Sindhu, R.; Binod, P.; Pandey, A.; Juneja, A.; et al. A critical review on the development stage of biorefinery systems towards the management of apple processing-derived waste. *Renew. Sustain. Energy Rev.* **2021**, *143*, 110972. [[CrossRef](#)]
145. Antioxidants, P.; Mitrea, L.; Plamada, D.; Nemes, S.A.; Lavinia-Florina, C.; Pascuta, M.S.; Varvara, R.; Szabo, K. Development of Pectin and Poly ( vinyl alcohol )-Based Active Packaging Enriched with Itaconic Acid and Apple. *Antioxidants* **2022**, *11*, 1729.
146. Majzoobi, M.; Poor, Z.V.; Jamalian, J.; Farahnaky, A. Improvement of the quality of gluten-free sponge cake using different levels and particle sizes of carrot powder. *Int. J. Food Sci. Technol.* **2016**, *51*, 1369–1377. [[CrossRef](#)]
147. Lau, T.; Clayton, T.; Harbourne, N.; Rodriguez-Garcia, J.; Oruna-Concha, M.J. Sweet corn cob as a functional ingredient in bakery products. *Food Chem. X* **2022**, *13*, 100180. [[CrossRef](#)]
148. Kumar, L.; Sehrawat, R.; Kong, Y. Oat proteins: A perspective on functional properties. *LWT* **2021**, *152*, 112307. [[CrossRef](#)]
149. Brückner-Gühmann, M.; Benthin, A.; Drusch, S. Enrichment of yoghurt with oat protein fractions: Structure formation, textural properties and sensory evaluation. *Food Hydrocoll.* **2019**, *86*, 146–153. [[CrossRef](#)]
150. Chi, M.S.; Adriana, P.; Man, S.M.; Vodnar, D.C.; Teleky, B.; Pop, C.R.; Stan, L.; Borsai, O.; Kadar, C.B.; Urcan, A.C. Quinoa Sourdough Fermented with *Lactobacillus plantarum* ATCC 8014 Designed for Gluten-Free Muffins—A Powerful Tool to Enhance Bioactive Compounds. *Appl. Sci.* **2020**, *10*, 7140. [[CrossRef](#)]
151. Verni, M.; Rizzello, C.G.; Coda, R. Fermentation biotechnology applied to cereal industry by-products: Nutritional and functional insights. *Front. Nutr.* **2019**, *6*, 42. [[CrossRef](#)] [[PubMed](#)]
152. Teleky, B.E.; Martău, G.A.; Ranga, F.; Pop, I.D.; Vodnar, D.C. Biofunctional soy-based sourdough for improved rheological properties during storage. *Sci. Rep.* **2022**, *12*, 17535. [[CrossRef](#)] [[PubMed](#)]



153. Campbell, J.K.; Canene-Adams, K.; Lindshield, B.L.; Boileau, T.W.-M.; Clinton, S.K.; Erdman, J.W.J. Tomato phytochemicals and prostate cancer risk. *J. Nutr.* **2004**, *134*, 3486S–3492S. [[CrossRef](#)]
154. Szabo, K.; Teleky, B.; Ranga, F.; Roman, I.; Khaoula, H.; Boudaya, E.; Ltaief, A.B.; Aouani, W.; Thiamrat, M.; Vodnar, D.C. Carotenoid Recovery from Tomato Processing By-Products through Green Chemistry. *Molecules* **2022**, *27*, 3771. [[CrossRef](#)]
155. Szabo, K.; Teleky, B.E.; Mitrea, L.; Călinoiu, L.F.; Martău, G.A.; Simon, E.; Varvara, R.A.; Vodnar, D.C. Active packaging-poly (vinyl alcohol) films enriched with tomato by-products extract. *Coatings* **2020**, *10*, 141. [[CrossRef](#)]
156. PA Silva, Y.; Borba, B.C.; Pereira, V.A.; Reis, M.G.; Caliari, M.; Brooks, M.S.L.; Ferreira, T.A. Characterization of tomato processing by-product for use as a potential functional food ingredient: Nutritional composition, antioxidant activity and bioactive compounds. *Int. J. Food Sci. Nutr.* **2019**, *70*, 150–160. [[CrossRef](#)]
157. Kaur, M.; Kaur, M.; Kaur, H. Apple peel as a source of dietary fiber and antioxidants: Effect on batter rheology and nutritional composition, textural and sensory quality attributes of muffins. *J. Food Meas. Charact.* **2022**, *16*, 2411–2421. [[CrossRef](#)]
158. Ciuzyńska, A.; Popkowicz, P.; Galus, S.; Janowicz, M. Innovative Freeze-Dried Snacks with Sodium Alginate and Fruit Pomace (Only Apple or Only Chokeberry) Obtained within the Framework of Sustainable Production. *Molecules* **2022**, *27*, 3095. [[CrossRef](#)] [[PubMed](#)]
159. Gumul, D.; Ziobro, R.; Kruczek, M.; Rosicka-Kaczmarek, J. Fruit Waste as a Matrix of Health-Promoting Compounds in the Production of Corn Snacks. *Int. J. Food Sci.* **2022**, *2022*, 7341118. [[CrossRef](#)] [[PubMed](#)]
160. Chaari, F.; Zouari-Ellouzi, S.; Belguith-Fendri, L.; Yosra, M.; Ellouz-Chaabouni, S.; Ellouz-Ghorbel, R. Valorization of Cereal by Products Extracted Fibre and Potential use in Breadmaking. *Chem. Afr.* **2022**. [[CrossRef](#)]
161. Barbhai, M.D.; Hymavathi, T.V.; Kuna, A.; Mulinti, S.; Voliveru, S.R. Quality assessment of nutri-cereal bran rich fraction enriched buns and muffins. *J. Food Sci. Technol.* **2022**, *59*, 2231–2242. [[CrossRef](#)]
162. Khojah, E.Y.; Badr, A.N.; Mohamed, D.A.; Abdel-Razek, A.G. Bioactives of Pomegranate By-Products and Barley Malt Grass Engage in Cereal Composite Bar to Achieve Antimycotic and Anti-Aflatoxigenic Attributes. *Foods* **2022**, *11*, 119. [[CrossRef](#)]
163. Naibaho, J.; Butula, N.; Jonuzi, E.; Korzeniowska, M.; Laaksonen, O.; Föste, M.; Kütt, M.L.; Yang, B. Potential of brewers' spent grain in yogurt fermentation and evaluation of its impact in rheological behaviour, consistency, microstructural properties and acidity profile during the refrigerated storage. *Food Hydrocoll.* **2022**, *125*, 107412. [[CrossRef](#)]
164. Alonso dos Santos, P.; Caliari, M.; Soares Soares Júnior, M.; Soares Silva, K.; Fleury Viana, L.; Gonçalves Caixeta Garcia, L.; Siqueira de Lima, M. Use of agricultural by-products in extruded gluten-free breakfast cereals. *Food Chem.* **2019**, *297*, 124956. [[CrossRef](#)]
165. Nogueiro, A.T.; Marta Igual, M.; Pagán, M.J. Developing psyllium fibre gel-based foods: Physicochemical, nutritional, optical and mechanical properties. *Food Hydrocoll.* **2022**, *122*, 107108. [[CrossRef](#)]
166. Mitrea, L.; Călinoiu, L.-F.F.; Martău, G.-A.; Szabo, K.; Teleky, B.-E.E.; Mureşan, V.; Rusu, A.-V.V.; Socol, C.-T.T.; Vodnar, D.-C.C.; Mărtău, G.A.; et al. Poly(vinyl alcohol)-based biofilms plasticized with polyols and colored with pigments extracted from tomato by-products. *Polymers* **2020**, *12*, 532. [[CrossRef](#)]
167. Rehal, J.K.; Aggarwal, P.; Dhaliwal, I.; Sharma, M.; Kaushik, P. A Tomato Pomace Enriched Gluten-Free Ready-to-Cook Snack's Nutritional Profile, Quality, and Shelf Life Evaluation. *Horticulturae* **2022**, *8*, 403. [[CrossRef](#)]
168. Lucera, A.; Costa, C.; Marinelli, V.; Saccotelli, M.A.; Alessandro, M.; Nobile, D.; Conte, A. Fruit and Vegetable By-Products to Fortify Spreadable Cheese. *Antioxidants* **2018**, *7*, 61. [[CrossRef](#)] [[PubMed](#)]
169. Sandei, L.; Stingone, C.; Vitelli, R.; Cocconi, E.; Zanotti, A.; Zoni, C. Processing tomato by-products re-use, secondary raw material for tomato product with new functionality. *Acta Hortic.* **2019**, *1233*, 255–260. [[CrossRef](#)]
170. Ahmad Bhat, M.; Ahsan, H. Physico-Chemical Characteristics of Cookies Prepared with Tomato Pomace Powder. *J. Food Process. Technol.* **2016**, *7*, 543. [[CrossRef](#)]
171. Padalino, L.; Conte, A.; Lecce, L.; Likyova, D.; Sicari, V.; Pellicanò, T.M.; Poiana, M.; Del Nobile, M.A. Functional pasta with tomato by-product as a source of antioxidant compounds and dietary fibre. *Czech J. Food Sci.* **2017**, *35*, 48–56.
172. Dankar, I.; Haddarah, A.; Omar, F.E.; Sepulcre, F.; Pujolà, M. 3D printing technology: The new era for food customization and elaboration. *Trends Food Sci. Technol.* **2018**, *75*, 231–242. [[CrossRef](#)]
173. Sehrawat, N.; Yadav, M.; Singh, M.; Kumar, V.; Ruchi, V. Seminars in Cancer Biology Probiotics in microbiome ecological balance providing a therapeutic window against cancer. *Semin. Cancer Biol.* **2021**, *70*, 24–36. [[CrossRef](#)]
174. Varvara, R.A.; Szabo, K.; Vodnar, D.C. 3D food printing: Principles of obtaining digitally-designed nourishment. *Nutrients* **2021**, *13*, 3617. [[CrossRef](#)]
175. Oliveira, S.M.; Gruppi, A.; Vieira, M.V.; Matos, G.S.; Spigno, G.; Pastrana, L.M.; Teixeira, A.C.; Fuci, P. How additive manufacturing can boost the bioactivity of baked functional foods. *J. Food Eng.* **2021**, *294*, 110394. [[CrossRef](#)]

## Article

# Phenolic Compounds Recovery from Blood Orange Peels Using a Novel Green Infrared Technology *Ired-Irrad*<sup>®</sup>, and Their Effect on the Inhibition of *Aspergillus flavus* Proliferation and Aflatoxin B1 Production

Sally El Kantar <sup>1</sup>, Hiba N. Rajha <sup>2,3</sup>, André El Khoury <sup>2</sup>, Mohamed Koubaa <sup>1,\*</sup>, Simon Nachef <sup>4</sup>, Espérance Debs <sup>5</sup>, Richard G. Maroun <sup>2</sup> and Nicolas Louka <sup>2</sup>

- <sup>1</sup> Université de Technologie de Compiègne, ESCOM, TIMR (Integrated Transformations of Renewable Matter), Centre de Recherche Royallieu, CS 60319, 60203 Compiègne Cedex, France
  - <sup>2</sup> Centre d'Analyses et de Recherche, Unité de Recherche Technologies et Valorisation Agro-Alimentaire, Faculté des Sciences, Université Saint-Joseph de Beyrouth, Riad El Solh, P.O. Box 17-5208, Beirut 1104 2020, Lebanon
  - <sup>3</sup> Ecole Supérieure d'Ingénieurs de Beyrouth (ESIB), Université Saint-Joseph de Beyrouth, CST Mkalles Mar Roukos, Riad El Solh, P.O. Box 11-514, Beirut 1107 2050, Lebanon
  - <sup>4</sup> Techno Heat Society, Al Firdaws Street, Sabtiyeh, Beirut 1100, Lebanon
  - <sup>5</sup> Department of Biology, Faculty of Arts and Sciences, University of Balamand, P.O. Box 100, Tripoli 1300, Lebanon
- \* Correspondence: m.koubaa@escom.fr; Tel.: +33-344238841

**Citation:** El Kantar, S.; Rajha, H.N.; El Khoury, A.; Koubaa, M.; Nachef, S.; Debs, E.; Maroun, R.G.; Louka, N. Phenolic Compounds Recovery from Blood Orange Peels Using a Novel Green Infrared Technology *Ired-Irrad*<sup>®</sup>, and Their Effect on the Inhibition of *Aspergillus flavus* Proliferation and Aflatoxin B1 Production. *Molecules* **2022**, *27*, 8061. <https://doi.org/10.3390/molecules27228061>

Academic Editor: Nour Eddine Es-Safi

Received: 19 October 2022

Accepted: 17 November 2022

Published: 20 November 2022

**Publisher's Note:** MDPI stays neutral with regard to jurisdictional claims in published maps and institutional affiliations.



**Copyright:** © 2022 by the authors. Licensee MDPI, Basel, Switzerland. This article is an open access article distributed under the terms and conditions of the Creative Commons Attribution (CC BY) license (<https://creativecommons.org/licenses/by/4.0/>).

**Abstract:** The intensification of total phenolic compound (TPC) extraction from blood orange peels was optimized using a novel green infrared-assisted extraction technique (IRAE, *Ired-Irrad*<sup>®</sup>) and compared to the conventional extraction using a water bath (WB). Response surface methodology (RSM) allowed for the optimization of ethanol concentration (E), time (t), and temperature (T) in terms of extracted TPC and their antiradical activity, for both WB extraction and IRAE. Using WB extraction, the multiple response optimums as obtained after 4 h at 73 °C and using 79% ethanol/water were 1.67 g GAE/100 g for TPC and 59% as DPPH inhibition percentage. IRAE increased the extraction of TPC by 18% using 52% ethanol/water after less than 1 h at 79 °C. This novel technology has the advantage of being easily scalable for industrial usage. HPLC analysis showed that IRAE enhanced the recovery of gallic acid, resveratrol, quercetin, caffeic acid, and hesperidin. IR extracts exhibited high bioactivity by inhibiting the production of Aflatoxin B1 by 98.9%.

**Keywords:** blood orange peels; phenolic compounds; infrared-assisted extraction; optimization; Aflatoxin B1

## 1. Introduction

Phenolic compounds are plant secondary metabolites, known for their antioxidant, antimicrobial, anticarcinogenic and anti-inflammatory activities [1,2]. In food industries, they prevent the rancidity of oils and fats [3], and can inhibit fungal growth and subsequent mycotoxin production in stored grains [4].

Aflatoxins are toxic secondary metabolites especially produced by two filamentous fungi *Aspergillus flavus* and *Aspergillus parasiticus* [5,6]. Under favorable conditions of humidity and temperature, these fungi grow on foods and feeds like corn, peanuts, cottonseed and cereals, resulting in aflatoxins production [7]. Aflatoxin B1 (AFB1), the most potent and toxic one, is a mutagenic, carcinogenic, teratogenic and immunodepressive agent. Humans and animals are exposed to AFB1 through ingestion, skin contact and inhalation [8]. Pesticides are usually used to protect crops from the development of fungi. However synthetic fungicide residues also have toxic effects, and pathogens can develop

resistance to it. For these reasons, interest in the use of natural antimicrobials such as essential oils and phenolic compounds is growing [9].

*Citrus* (*Rutaceae* family) is an important world fruit crop [10]. Its health benefits are mainly related to the presence of bioactive compounds, such as polyphenols, vitamin C and carotenoids [11,12]. After consuming citrus fruits as fresh produce or juice, a large number of peels are generated and generally discarded as waste [13], used as animal feed or for fuel production [14]. The extraction of total phenolic compounds (TPC) from citrus peels is attracting more and more attention due to their biological virtues as natural antioxidants and antimicrobials [15]. Conventional methods such as water bath (WB) extraction, were used for the valorization of citrus peels by the extraction of bioactive compounds [16]. Nonetheless, researchers have been focusing on developing innovative extraction techniques for industries that can be more efficient and energy-saving [17,18]. Extraction techniques such as ultrasound [19], microwave [20,21], instantaneous controlled pressure drop [22,23], supercritical CO<sub>2</sub> [24], pulsed electric field [25,26] and Intensification of Vaporization by Decompression to the Vacuum (IVDV) [27] were previously used to intensify the extraction of bioactive compounds from agro-industrial residues and by-products. These extraction processes can improve mass transfer, decrease the extraction time and temperature and reduce solvent use. They can also improve the recovery of bioactive compounds from by-products with lower energy consumption.

The green extraction process is based on the discovery and the design of techniques to reduce energy and solvent consumption [28]. In this sense, infrared-assisted extraction (IRAE) technology is a novel, simple and low-cost extraction method that can be scalable to industrial level. IR radiation is characterized by its high penetration ability and has found many applications in health care and industrial treatment [29].

To the best of our knowledge, IR was not previously tested for the extraction of polyphenols from blood orange peels. The objective of this work is to test the efficiency of this novel green technology for the recovery of high TPC yields from blood orange peels and to investigate the potential use of the obtained extracts as antifungal and anti-mycotoxigenic agents. The optimization of TPC extraction was conducted by a conventional WB extraction and a novel method of IRAE. The optimal ethanol concentration, time, and temperature were determined by response surface methodology (RSM) for the two techniques. Chemical characterization of the extracted TPC was also explored.

## 2. Results and Discussion

Time (t), temperature (T) and ethanol percentage (E) were optimized for WB and IR extraction of TPC from blood orange peels using RSM. The latter is an effective statistical optimization method. It allows the evaluation of multiple parameters and their interactions with a reduced number of experiments. Tables 1 and 2 show the experimental design, where factors are presented in their real and coded values, with their responses TPC and inhibition % of DPPH, for the conventional WB extraction and IRAE. For WB extraction, TPC ranged from 1.20 to 1.67 g GAE/100 g DM, and inhibition percentage from 37.6% to 58.7%. While for IRAE, TPC ranged from 0.95 to 1.90 g GAE/100 g DM (14% increase compared to WB) and inhibition percentage from 34.7% to 56.4%. The obtained results are comparable to those obtained in a previous study where the yields of polyphenols extracted from orange peels ranged between 0.30 and 1.70 g GAE/100 g DM with DPPH inhibition percentages values between 30% and 50% [30].

**Table 1.** RSM central composite design for three parameters (real and coded values) of five levels and the experimental responses (TPC and inhibition % of DPPH) of **WB** extraction from blood orange peels.

	Run	Ethanol (%)	Time (h)	Temperature (°C)	TPC (g	Inhibition %
		Real [Coded] Value	Real [Coded] Value	Real [Coded] Value	GAE/100 g DM)	of DPPH
Factorial Design	1	50 [−1]	2 [−1]	40 [−1]	1.36	46.04
	2	80 [+1]	2 [−1]	40 [−1]	1.20	42.45
	3	50 [−1]	4 [+1]	40 [−1]	1.37	44.24
	4	80 [+1]	4 [+1]	40 [−1]	1.33	43.50
	5	50 [−1]	2 [−1]	70 [+1]	1.48	50.52
	6	80 [+1]	2 [−1]	70 [+1]	1.55	55.01
	7	50 [−1]	4 [+1]	70 [+1]	1.54	52.17
	8	80 [+1]	4 [+1]	70 [+1]	1.67	55.75
Center Points	9	65 [0]	3 [0]	55 [0]	1.40	45.59
	10	65 [0]	3 [0]	55 [0]	1.38	44.69
	11	65 [0]	3 [0]	55 [0]	1.50	46.49
	12	65 [0]	3 [0]	55 [0]	1.46	46.93
	13	65 [0]	3 [0]	55 [0]	1.44	45.29
	14	65 [0]	3 [0]	55 [0]	1.47	49.77
Star Points	15	39.8 [− $\alpha$ ]	3 [0]	55 [0]	1.33	48.88
	16	90.2 [+ $\alpha$ ]	3 [0]	55 [0]	1.24	48.06
	17	65 [0]	1.3 [− $\alpha$ ]	55 [0]	1.48	51.27
	18	65 [0]	4.7 [+ $\alpha$ ]	55 [0]	1.50	53.29
	19	65 [0]	3 [0]	29.8 [− $\alpha$ ]	1.28	37.64
	20	65 [0]	3 [0]	80.2 [+ $\alpha$ ]	1.58	58.74

**Table 2.** RSM central composite design of three parameters (real and coded values) of five levels and the experimental responses (TPC and inhibition % of DPPH) of **IRAE** from blood orange peels.

	Run	Ethanol (%)	Time (h)	Temperature (°C)	TPC (g	Inhibition %
		Real [Coded] Value	Real [Coded] Value	Real [Coded] Value	GAE/100 g DM)	of DPPH
Factorial Design	1	15 [−1]	0.5 [−1]	40 [−1]	0.95	34.75
	2	55 [+1]	0.5 [−1]	40 [−1]	1.22	36.06
	3	15 [−1]	1.5 [+1]	40 [−1]	1.12	47.54
	4	55 [+1]	1.5 [+1]	40 [−1]	1.30	42.95
	5	15 [−1]	0.5 [−1]	70 [+1]	1.18	42.79
	6	55 [+1]	0.5 [−1]	70 [+1]	1.79	54.10
	7	15 [−1]	1.5 [+1]	70 [+1]	1.19	44.26
	8	55 [+1]	1.5 [+1]	70 [+1]	1.60	56.39
Center Points	9	35 [0]	1 [0]	55 [0]	1.39	54.10
	10	35 [0]	1 [0]	55 [0]	1.47	55.90
	11	35 [0]	1 [0]	55 [0]	1.34	48.85
	12	35 [0]	1 [0]	55 [0]	1.50	52.95
	13	35 [0]	1 [0]	55 [0]	1.48	47.38
	14	35 [0]	1 [0]	55 [0]	1.48	52.62
Star Points	15	1.36 [− $\alpha$ ]	1 [0]	55 [0]	1.17	39.34
	16	68.6 [+ $\alpha$ ]	1 [0]	55 [0]	1.52	45.74
	17	35 [0]	0.16 [− $\alpha$ ]	55 [0]	1.27	46.39
	18	35 [0]	1.84 [+ $\alpha$ ]	55 [0]	1.34	51.64
	19	35 [0]	1 [0]	29.8 [− $\alpha$ ]	1.21	36.39
	20	35 [0]	1 [0]	80.2 [+ $\alpha$ ]	1.90	55.57

In both extraction techniques, the multivariate second-degree regression analysis indicates high values for  $R^2$  coefficients (>90%) (Table 3). This means that all of the models have low residual errors when trying to predict the values of either TPC or inhibition % of DPPH, using the independent variables.

**Table 3.** The second order regression equation for TPC and inhibition % of DPPH of each extraction technique and the R-squared of each equation.

Extraction Technique	R <sup>2</sup> (Percent)	Equation
WB	90.45	TPC = 1.55 + 0.01E − 0.24t − 0.01T − 0.0002E <sup>2</sup> + 0.002Et + 0.0002ET + 0.02t <sup>2</sup> + 0.0002tT + 0.00002T <sup>2</sup>
	93.26	Inhibition % of DPPH = 87.46 − 0.69E − 13.03t − 0.35T + 0.002E <sup>2</sup> + 0.02Et + 0.007ET + 1.81t <sup>2</sup> + 0.03tT + 0.002T <sup>2</sup>
IRAE	91.08	TPC = 0.22 + 0.01E + 1.12t + 0.002T − 0.0001E <sup>2</sup> − 0.004Et + 0.0002ET − 0.28t <sup>2</sup> − 0.007tT + 0.00007T <sup>2</sup>
	92.24	Inhibition % of DPPH = −15.95 + 0.17E + 30.92t + 1.31T − 0.009E <sup>2</sup> − 0.06Et + 0.01ET − 4.69t <sup>2</sup> − 0.27tT − 0.01T <sup>2</sup>

### 2.1. Water Bath Extraction

Pareto charts (Figure 1a) show the positive or negative effects of temperature, time, and ethanol concentration on the extraction of TPC from blood orange peels using WB. The parameters that have the most significant effects (with a confidence level above 95%) correspond to the histograms that cross the vertical line. According to Figure 1a, the temperature had a significant linear positive effect on TPC extraction within the studied domain. The estimated response surface plot, in its three-dimensional illustration, and considering its shape, gives valuable data about the significance of each parameter (Figure 1c). The increase in temperature permitted a higher diffusivity of TPC and improved their transfer into the solvent [31]. Additionally, high temperatures weaken the membrane structure of the cells, which improves the extraction of biomolecules from the peels [14]. TPC are positively affected by the interaction between ethanol and temperature (ET). The increase in ethanol percentage combined with the increase in temperature improved the diffusivity and solubility of TPC in their solvent. Thus, a synergetic effect between ethanol and temperature enhanced the extraction of TPC. However, the TPC content was negatively affected by the quadratic effect of ethanol (E<sup>2</sup>). The increase in ethanol percentage up to a certain value, reduces the dielectric constant of the solvent, which enhances the solubility of TPC and improves their extraction [32]. This is similar to a previous result concerning the effect of ethanol on the extraction of phenolic compounds from flaxseed extracts where the yield of TPC decreased for an ethanol percentage higher than 60% [33]. Higher ethanol concentration may modify the polarity of the solvent and could dehydrate and collapse the plant cells, making difficult the diffusion of biomolecules from the plant matrix to the solvent [34]. In addition, some TPC are soluble in the aqueous phase, whereas others are soluble in organic solvents, which explains the need to use a mixture of ethanol and water to extract higher yields of TPC. The insert in Figure 1a presents the evolution of TPC as a function of ethanol-water percentage and demonstrates that the optimum value of TPC is reached with an intermediate ethanol-water percentage.

Figure 1b,d presents the Pareto chart and the estimated response surface plot for the antiradical activity. The same as for TPC, the DPPH inhibition % was positively affected by the temperature and by the interaction between ethanol percentage and temperature. Studies have shown a correlation between the presence of TPC in extracts and the scavenging activity against the DPPH radical [35,36]. The insert in Figure 1b shows the effect of ethanol percentage on the inhibition % of DPPH at 40 °C (dashed line) and 70 °C (solid line). The observed difference is due to the interaction effect between temperature and ethanol percentage. At 70 °C, a higher amount of TPC is extracted compared to 40 °C, which explains the greater inhibition % of DPPH obtained at this temperature.

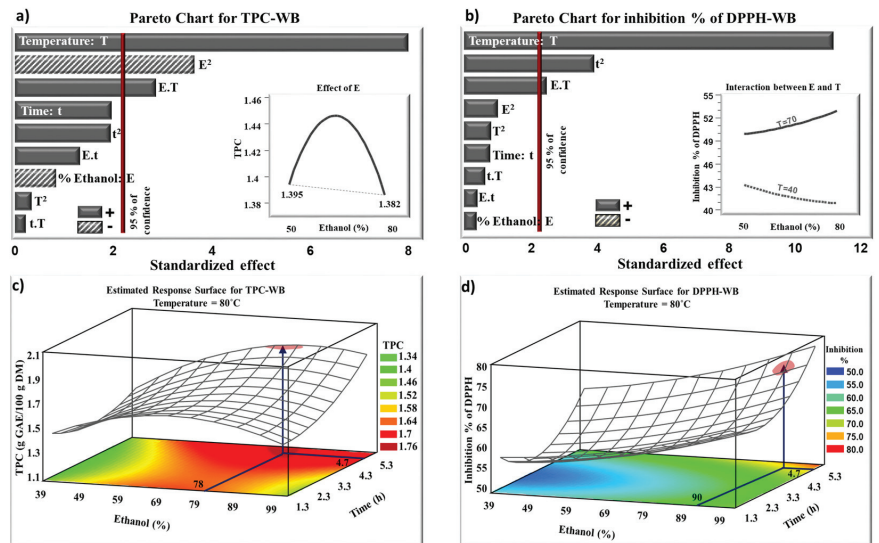


**Figure 1.** Standardized Pareto charts for TPC (a) and the inhibition % of DPPH (b). Estimated response surface for TPC (c) and the inhibition % of DPPH (d). The TPC extracts were obtained after WB extraction.

## 2.2. Infrared-Assisted Extraction

Figure 2a shows the Pareto chart obtained by IRAE. As in WB extraction, TPC solubility increased with temperature, thus facilitating TPC diffusion out of the cells. For the same temperature of 80 °C, the extraction of TPC increased by 20% with IRAE (35% ethanol for 1 h), compared to the conventional WB extraction (65% ethanol for 3 h). This could be associated with cell bursting occurring during IR heating. Ethanol also had positive linear effect on TPC extraction. It acts on the polarity of the medium, which permits to solubilize lipophilic TPC. IR waves are efficiently absorbed by the solvent, which leads to efficient heating and improves the cells rupture for a better extraction of TPC [29,37]. The extraction of TPC with IR is negatively affected by the quadratic effect of time ( $t^2$ ). A short period of time was not sufficient for the extraction of TPC. However, longer extraction times could lead to the degradation and oxidation of the extracted TPC, which explains the negative quadratic effect of this parameter [38]. The insert in Figure 2a shows the evolution of TPC as a function of ethanol-water percentage. A maximum value of TPC was obtained when 50% ethanol-water was used as a solvent. Therefore, the use of IR could lead to a reduction in ethanol percentage. Figure 2c presents the evolution of TPC as a function of ethanol percentage and time at a fixed temperature (80 °C). The optimum value of TPC (2.1 g GAE/100 g DM) was obtained after 0.6 h of extraction with 55% ethanol-water. This value was higher than that obtained after 4.7 h of WB extraction (1.78 g GAE/100 g DM) using 78% ethanol-water at the same temperature.

Figure 2b,d shows that temperature, time, and ethanol had linear positive effects on the inhibition percentage of DPPH. The inhibition percentage increased from 34% to 56% when the ethanol percentage, the treatment duration, and the temperature increased from 15%, 0.5 h, and 40 °C to 55%, 1.5 h, and 70 °C, respectively. However, the quadratic effects of ethanol ( $E^2$ ) and temperature ( $T^2$ ) had negative effects on the inhibition % of DPPH. At high temperatures, the stability of TPC may be negatively affected. Moreover, a possible thermal degradation of TPC already released at low temperatures may have occurred [39]. The insert in Figure 2b presents the evolution of the inhibition % of DPPH as function of ethanol percentage at two different temperatures. The maximum value of 58% inhibition of DPPH was obtained with 50% ethanol-water at 70 °C. A conjugated effect between the increase in ethanol percentage and temperature was observed. The increase

in ethanol percentage up to 50% at 70 °C significantly improved the inhibition % of the free radical DPPH. Therefore, the interaction between ethanol and temperature positively affects the antiradical activity of the extracted TPC. A similar behavior was observed with WB (Figure 1b). However, a higher percentage of ethanol-water (80%) is required during WB extraction to obtain only 53% of DPPH inhibition at the same temperature (70 °C).

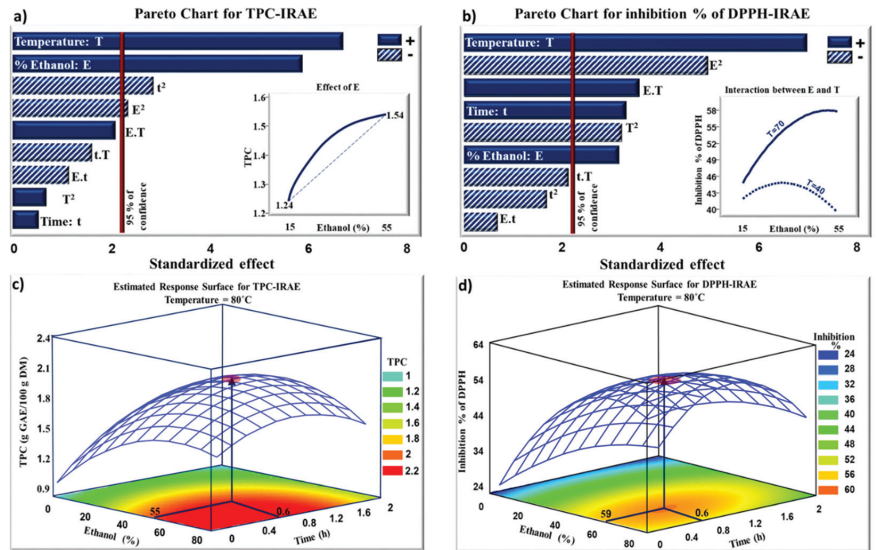


**Figure 2.** Standardized Pareto charts for TPC (a) and the inhibition % of DPPH (b). Estimated response surface for TPC (c) and the inhibition % of DPPH (d). The TPC extracts were obtained after IRAE.

### 2.3. Multiple Response Optimization: Comparison between the Optimums Obtained with Water Bath Extraction and Infrared-Assisted Extraction

The optimization of the TPC and the inhibition % of DPPH were conducted separately and the parameters giving the highest quantity of TPC, and the highest inhibition levels of the free radical DPPH were determined. It is important to keep a balance between the concentrations of the TPC and their bioactivity. This is why it is necessary to show the two responses (TPC and inhibition % of DPPH) simultaneously as affected by the combination of the experimental parameters (E, t, T). The simultaneous optimums obtained with the conventional WB extraction (Figure 3a), for both TPC and inhibition % were 1.78 g GAE/100 g DM and 63.5%, respectively. These optimums were found with 83% of ethanol, during 4.7 h at 80 °C. However, IRAE allowed the extraction of 18% more polyphenols (2.1 g GAE/100 g DM) with an inhibition percentage of DPPH of 60%, with 57% of ethanol at 80 °C and for a treatment duration (0.6 h) 7.8 times lower than the WB extraction (Figure 3b).

It is noteworthy to mention that the optimums for TPC and DPPH inhibition converge at the same point and are obtained at close conditions with IRAE, which was not the case with WB. The exactitude of the model was confirmed by repeating the optimal conditions for the optimization of TPC and inhibition percentage for both WB extraction and IRAE (Table 4).

IRAE intensifies the extraction of TPC with shorter time and lower solvent consumption. This result was already shown on the extraction of TPC from grape seeds [37], and pomegranate peels [40]. The efficiency of IRAE compared to conventional extraction technique was also observed in olive leaves where the yield of TPC was improved by more than 30% using IRAE as compared to water bath extraction [41]. In IRAE, the solvent mixture is heated directly, while in conventional WB extraction, a certain period of time is required

to heat the container before the heat is transferred to the solution [42]. The efficiency of IRAE can be due to the IR radiation that could stimulate the vibrations in molecules in diverse modes like extending, bending, rocking, and rotating [43]. These vibrations lead to the release of TPC molecules and to an increase in the interactions between the solvent and the active compounds [44], allowing an efficient extraction of TPC from orange peels.

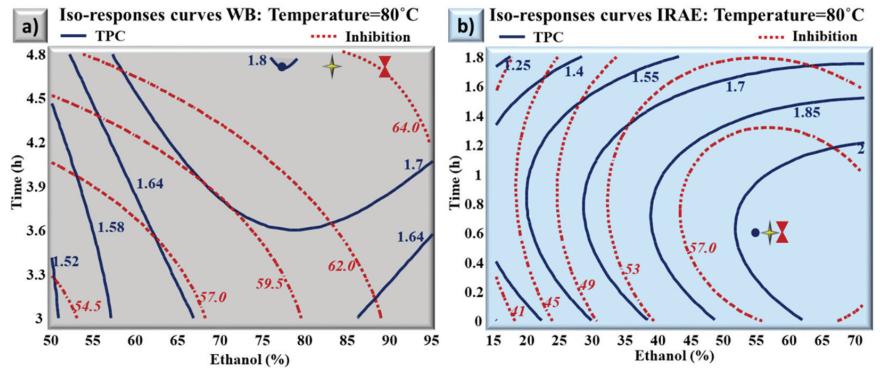


**Figure 3.** Overlapping for TPC and inhibition percentage of DPPH contour plots in case of WB extraction (a) and IRAE (b) as obtained at the optimal temperatures for the two responses simultaneously. The blue circle, red hourglass and the four-pointed star represent the optimum of TPC, the optimum of DPPH, and the multiple optimum, respectively.

**Table 4.** Predicted and experimental results for TPC and inhibition %, at the multiple optimum conditions for WB extraction and IRAE.

Extraction Technique (Optimal Conditions)	Multiple Optimum	Predicted Values	Experimental Values
WB (T = 80 °C t = 4.7 h E = 83%)	TPC g GAE/100 g DM	1.78	1.77 ± 0.040
	Inhibition %	63.5	61.7 ± 0.32
IRAE (T = 80 °C t = 0.6 h E = 57%)	TPC g GAE/100 g DM	2.1	2.2 ± 0.043
	Inhibition %	60	61.5 ± 0.24

#### 2.4. Concentrations and Diversity of Phenolic Compounds Extracted from Orange Peels

HPLC analysis were conducted on the multiple response optimums obtained with WB and IRAE. Table 5 shows the concentration and diversity of the TPC at the optimal points. IRAE selectively extracted caffeic acid and improved the extraction of gallic acid, resveratrol, quercetin and hesperidin by 4.7, 22.6, 17.6, and 24%, respectively, compared to WB extraction. The most remarkable improvement was observed in hesperidin, the principal flavonoid found in orange peels [26], and has an inhibitory effect on food fungal contaminants such as *Aspergillus* species and mycotoxin production [45]. However, the bioactivity of the extracts could be attributed to the synergetic effects of the extracted TPC. Phenolic quantity depends on the method of extraction and higher TPC yields were obtained with IRAE, which seems to be a promising new technique that intensifies the extraction of bioactive compounds with less time and solvent consumption.



**Table 5.** TPC (mg/100 g DM) obtained in the simultaneous optimums after WB extraction and IRAE.

Phenolic Compound (mg/100 g DM)	WB	IRAE
Gallic acid	2.33 ± 0.20	2.44 ± 0.042
Resveratrol	28.46 ± 2.16	34.89 ± 0.54
Quercetin	5.50 ± 0.79	6.47 ± 0.58
Caffeic acid	nd	0.16 ± 0.050
Hesperidin	286.67 ± 0.60	355.60 ± 0.89

### 2.5. Antifungal Activity

The activities of the extracts obtained at the multiple optimums by WB extraction and IRAE against the growth of *A. flavus* and the production of AFB1 were studied. Figure 4 shows that TPC extracts obtained from WB extraction and IRAE slightly inhibited the growth of *A. flavus* by 11.8% and 15.8%, respectively. However, the inhibition of aflatoxin production was greater than the inhibition of the growth of the fungus. Both TPC extracts obtained from WB extraction and IRAE inhibited AFB1 production by 99.4% and 98.9%, respectively.

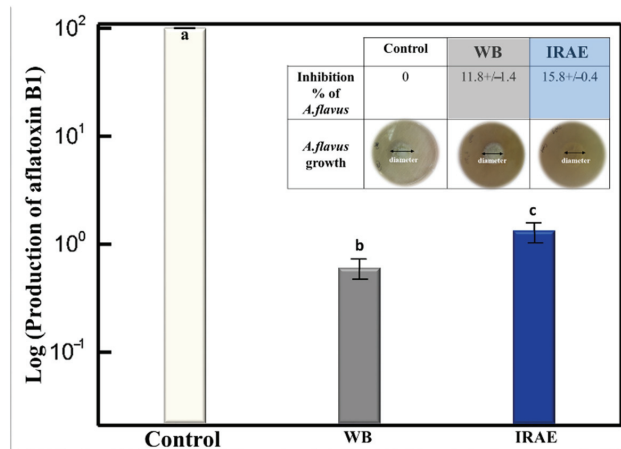


**Figure 4.** Effect of the simultaneous optimum level of extracts obtained after WB extraction and IRAE on the production of Aflatoxin B1 yield (letters a, b and c indicate significant statistical difference between means). The insert shows the inhibition growth of *A. flavus* by simultaneous optimums extracts obtained after WB extraction and IRAE.

AFB1 is synthesized by enzymes encoded within a large cluster of 27 genes. Mycotoxin production is governed by complex environmental signals and different cellular pathways [46]. TPC may inhibit the production of AFB1 by acting at one of the three levels: altering the environmental and physiological signals perceived by the fungi, down regulating the gene expression of the cluster or blocking the activity of certain enzymes involved in the biosynthesis of AFB1 [47].

Extracts from plants or spices, including TPC and essential oils have demonstrated fungicidal and/or anti-toxicogenic properties. In some cases, extracts inhibit the fungal growth and the production of mycotoxin. In other cases, the growth of the fungi is not affected but the production of mycotoxin is partially or totally halted. A variety of flavonoids in tea leaves inhibited the production of AFB1 without affecting the mycelial growth of *A. flavus*. They decreased the production of AFB1 by 99.6%. The inhibition of aflatoxin was attributed to the down-regulations of transcription of genes involved in aflatoxin biosynthesis [48]. Extracts of the plant *Garcinia indica* inhibited the growth of *A. flavus* and the subsequent production of AFB1 [4]. Eugenol (0.5 mM), the active compound of many

essential oils, slightly affected the fungal growth but totally inhibited the production of AFB1. It has been demonstrated that all cluster genes were strongly down regulated in the presence of eugenol. Nineteen out of 27 genes were completely inhibited and the others had 10- to 20-fold reductions in their expression levels [46]. In our case, TPC from blood orange peels are specific inhibitors of AFB1 biosynthesis rather than inhibitors of the fungal growth. This is specifically interesting since the presence of *A. flavus* that cannot produce AFB1 will avoid the contamination of foods with other microbial agents' producers of other toxins, and will not imbalance the fungal ecology in the field. TPC extracts from orange peels have therefore shown their high potential in the development of anti-aflatoxin agents for food preservation.

### 3. Materials and Methods

#### 3.1. Raw Material

Blood orange (*Citrus sinensis*) peels were provided by Balkis Company (Ansariyeh, South Lebanon) and stored at  $-20\text{ }^{\circ}\text{C}$  until use. Orange peels were manually cut into equal squares of  $1 \times 1\text{ cm}^2$ . The moisture content, measured by drying fresh peels at  $105\text{ }^{\circ}\text{C}$  to constant weight, was about 76% wet basis.

#### 3.2. Extraction Techniques

Intervals of variation in the parameters, notably the percentage of ethanol and the treatment time, were chosen differently for the WB and the IRAE, based on previous studies [30,40,41]. These studies, along with preliminary trials, have proven that the optimal intervals, in terms of TPC yield, for these two techniques are completely distinct. In order to reach the optimal ranges for the WB technique, a higher percentage of ethanol and a longer treatment time than IRAE are required. Within this perspective, the ranges of variation in these two parameters have been established in the following paragraphs.

##### 3.2.1. Water Bath Extraction

Water bath extraction of TPC from blood orange peels was performed with a liquid to solid ratio of 8. Ethanol concentration varied between 40% and 90%, extraction time varied between 1.3 h and 4.7 h, and temperature varied between  $30\text{ }^{\circ}\text{C}$  and  $80\text{ }^{\circ}\text{C}$ . These values were selected based on preliminary studies, and were optimized by RSM.

##### 3.2.2. Infrared-Assisted Extraction

The infrared-assisted-extraction apparatus, *Ired-Irrad*<sup>®</sup> (Patent 2017/11-11296L) was used in this purpose. Orange peels were introduced in a round bottom flask with ethanol-water (liquid to solid ratio 8). The flask was placed 1 cm from a ceramic infrared transmitter with a power varying between 70 and 170 W for the irradiation/heating process, linked to a PID control for temperature adjustment. Both the temperature and the voltage can be monitored.

Ethanol concentration varied between 1% and 68%, treatment duration between 0.2 h and 1.8 h and temperature between  $29\text{ }^{\circ}\text{C}$  and  $80\text{ }^{\circ}\text{C}$  for the IRAE. The optimal conditions for extracting a maximal yield of TPC with the maximum antiradical activity were determined. Extracts were obtained by centrifugation at 6000 rpm for 15 min using a Heraeus Primo R Centrifuge (Thermo Scientific<sup>™</sup> Heraeus<sup>™</sup>, Hanau, Germany). Supernatants were collected and stored at  $-20\text{ }^{\circ}\text{C}$  until use.

#### 3.3. Experimental Designs

Response Surface Methodology (RSM) was used for the optimization of TPC extraction from orange peels by two different techniques. Independent variables were ethanol-water concentration (%), time (t) and temperature (T). The three variables were coded at 5 levels  $\{-\alpha, -1, 0, +1, +\alpha\}$ . The central composite design ( $2^3 + \text{star}$ ) resulted of twenty experimental points including six repetitions at the central level. Considering three parameters and two

responses, experimental data were fitted to obtain a second-degree regression Equation (1) as follows:

$$Y = \beta_1 + \beta_2E + \beta_3t + \beta_4T + \beta_5E^2 + \beta_6t^2 + \beta_7T^2 + \beta_8Et + \beta_9ET + \beta_{10}tT \quad (1)$$

where Y is the predicted response parameter (TPC or DPPH);  $\beta_1$  is the mean value of responses at the central point of the experiment;  $\beta_2$ ,  $\beta_3$ , and  $\beta_4$  are the linear coefficients;  $\beta_5$ ,  $\beta_6$ , and  $\beta_7$  are the quadratic coefficients;  $\beta_8$ ,  $\beta_9$ , and  $\beta_{10}$  are the interaction coefficients; E is the solvent mixture; t is the treatment time; and T is the treatment temperature. Experimental design and statistical analysis of the results were carried out using STATGRAPHICS® Centurion XV for windows.

The experimental protocol is depicted in Figure 5.

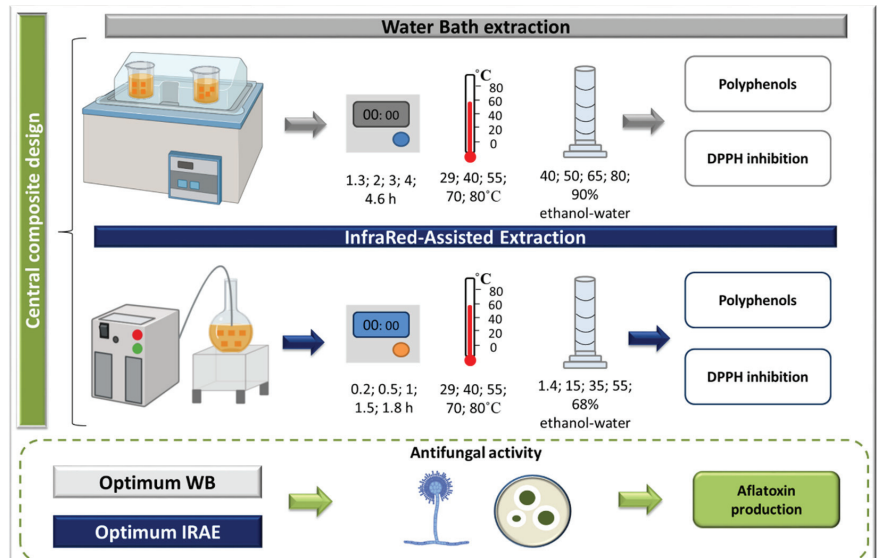


**Figure 5.** Optimization of TPC extraction from blood orange peels using WB and IRAE. The antifungal activity of the extracts obtained was assessed at optimal conditions.

### 3.4. Analysis

#### 3.4.1. Total Phenolic Compounds (TPC)

The amount of total TPC extracted from blood orange peels was determined by the Folin-Ciocalteu colorimetric method [49]. In this method, 1 mL of ten-fold diluted Folin-Ciocalteu reagent (Scharlau, Spain) was added to 0.2 mL of extract. Then, 0.8 mL of sodium carbonate ( $\text{Na}_2\text{CO}_3$ ) (75 g/L) (BDH, England) were added. The mixture was incubated at 60 °C for 10 min, and then cooled to room temperature. The absorbance was measured at 750 nm by the UV-Vis spectrophotometer (UV-9200, UK). Gallic acid (Sigma-Aldrich, St-Quentin Fallavier, France) was used for the calibration curve. The results were expressed as g of gallic acid equivalent (GAE) per 100 g of dry matter (g GAE/100 g DM).

#### 3.4.2. Antiradical Activity

The free radical scavenging activity was determined by the capacity of the extracted TPC to reduce the free radical, 2,2-diphenyl-1-picrylhydrazyl: DPPH [50]. This method is based on the reduction of the free radical DPPH by phenolic extracts. First, 1.45 mL of DPPH (0.06 mM) (Sigma-Aldrich, St-Quentin Fallavier, France) free radical were added to 50  $\mu\text{L}$  of orange peels extracts or Trolox (control) (Sigma-Aldrich, St-Quentin Fallavier, France). After 30 min of incubation at room temperature, the absorbance was measured at

515 nm. The inhibition percentage of the DPPH free radical was calculated according to Equation (2):

$$\text{Inhibition Percentage} = [(\text{absorbance of control} - \text{absorbance of sample}) / \text{absorbance of control}] \times 100 \quad (2)$$

### 3.4.3. High Performance Liquid Chromatography Analyses

Gallic acid, resveratrol, quercetin, caffeic acid and hesperidin (Sigma-Aldrich, St-Quentin Fallavier, France) were used as standards in high performance liquid chromatography (HPLC) analyses, to identify the TPC in the simultaneous optimums obtained after WB extraction and IRAE. Ultimate 3000 (Dionex, Idtsein, Germany) liquid chromatography apparatus coupled to a diode array detector was used. Before analyses, the samples and standards were filtered through 0.2  $\mu\text{m}$  syringe filters (VWR, Rosny-sous-Bois, France). The chromatography column C18 capillary column 100  $\times$  4.6 mm (Hypersil Gold, Thermo Scientific, MA, USA), was used for all experiments. The temperature of the column was maintained at 40  $^{\circ}\text{C}$ . Water-formic acid solution (95:5) (solvent A) and acetonitrile (solvent B) (HPLC grade, Sigma-Aldrich, St-Quentin Fallavier, France) were used as solvents. A flow rate of 1 mL/min was applied. The HPLC applied method was as follows: 2%–6% of solvent B in 25 min, 6%–15% of solvent B in 15 min, 15%–20% of solvent B in 12 min and 20%–40% of solvent B in 18 min. The injection volume of the sample was 20  $\mu\text{L}$ .

### 3.4.4. Antifungal Activity

Simultaneous optimums of TPC extracts from orange peels obtained after WB extraction and IRAE were tested against the growth of a toxinogenic fungi *A. flavus* and the toxin secretion of AFB1 from this fungus. *A. flavus* strain NRRL 62477 was used for this purpose.

After the growth of *A. flavus* strain on Czapek yeast extract agar medium (CYA) at 30  $^{\circ}\text{C}$  for 7 days, a spore suspension was prepared. The surface of the prepared culture was scrapped with a sterile Pasteur pipette (Chase Scientific Glass, Inc., Rockwood, TN, USA) and 8 mL of Tween 80 solution (0.005%) were added. A Neubauer hemocytometer (Superior, Marienfeld, Lauda-Konigshofen, Germany) was used to count the spores. The concentration of spores was adjusted to  $10^6$  spore/mL and spore suspension was then kept at 4  $^{\circ}\text{C}$  for further use.

A rotavapor was used to evaporate ethanol and concentrate the TPC tested samples. TPC (250  $\mu\text{g}$ ) obtained from each WB and IR extract were added to CYA medium. A final volume of 20 mL was poured in petri dishes. For the control culture, 20 mL of CYA were poured in the dish without TPC extracts. Then, 10  $\mu\text{L}$  of the previously prepared spore solution ( $10^6$  spores/mL) were added in the center of each petri dish. The assays were made in triplicate and all the dishes were left 4 days in the incubator at 28  $^{\circ}\text{C}$ . After this incubation period, the growth inhibition of *A. flavus* was determined. The diameters of the cultures were measured and compared to the negative control. The *A. flavus* inhibition percentage was calculated according to Equation (3):

$$\text{Inhibition Percentage} = [(\text{initial diameter} - \text{diameter after incubation}) / \text{initial diameter}] \times 100 \quad (3)$$

### 3.4.5. AFB1 Extraction and HPLC Analysis

After 7 days of incubation at 28  $^{\circ}\text{C}$  on (CYA) medium, 3 agar plugs (0.5 cm diameter) were removed from different points of the colony for each culture, weighted and placed into 3 mL microtubes. One milliliter of HPLC grade methanol was added to each tube, then the mixture was incubated and shaken for 60 min at room temperature. The mixture was centrifugated for 15 min at 13,000 r.p.m (round per minute). Then, the supernatant phase was recuperated and diluted with 11 mL phosphate buffer. The diluted extract was injected into Aflaprep immunoaffinity columns (R-Biopharm, Glasgow, Scotland) using a syringe for purification. An elution was done by adding 1.5 mL of methanol/acetic acid (98:2, v/v) followed by 1.5 mL of HPLC grade water and the total volume was filtered through 0.45  $\mu\text{m}$  filters (Sartorius Stedim Biotech<sup>TM</sup>, PA, USA) then stored at 4  $^{\circ}\text{C}$  before quantification. Aflatoxin B1 quantification was done with a Water Alliance HPLC system

using an Utisphere ODB column, C18 (150 × 4.6 mm, 5 µm, 120 Å) (Interchim, Montluçon, France) at 30 °C.

#### 3.4.6. Statistical Analysis

All experiments and measurements were conducted in triplicates. Mean values were calculated and standard deviations were expressed. Significance of the obtained results was evaluated by *p*-value ( $p < 0.05$ ; 95% of confidence level) using analysis of variance (ANOVA) and LSD tests (Least Significant Difference). These statistical analysis and tests were achieved using the software STATGRAPHICS® Centurion XV.

### 4. Conclusions

Our study aimed at valorizing blood orange peels using a simple and low-cost extraction method, *Ired-Irrad*®, that has the potential to improve the extraction of TPC. A central composite design optimized the process. Based on the response surface methodology, the optimal TPC extraction parameters were 79 °C for 37 min with an ethanol percentage of 64%. Under these optimized conditions, the experimental yield of TPC and their inhibition percentage matched closely with the predicted results, and TPC yields were 18% higher than those obtained with the conventional solid-liquid extraction. The bioactivity of the extracted TPC was tested on the inhibition of the growth of *A. flavus* and the production of Aflatoxin B1 by the same fungus. Extracted TPC have the potential to be used as natural inhibitors of the carcinogenic Aflatoxin B1 production by *A. flavus*. IR blood orange peels extracts represent an alternative strategy to the use of pesticides to control crop contamination. They can be commercially exploited and applied to food systems. It will be interesting to study the molecular mechanism responsible for the inhibition of Aflatoxin B1 by TPC extracted from blood orange peels.

### 5. Patent

The *Ired-Irrad*®, an infrared irradiation apparatus, was designed and patented in collaboration between Faculty of Sciences at USJ and Faculty of Arts and Sciences at University of Balamand. Lebanese patent 2017/11-11296L, granted on 29 November 2017.

**Author Contributions:** Conceptualization, S.E.K., N.L. and H.N.R.; methodology, S.E.K., H.N.R. and A.E.K.; software, N.L.; validation, N.L., A.E.K. and H.N.R.; formal analysis, S.E.K., H.N.R. and N.L.; resources, S.N.; data curation, S.E.K. and N.L.; writing—original draft preparation, S.E.K.; writing—review and editing, N.L., M.K. and E.D.; supervision, N.L. and R.G.M.; funding acquisition, N.L. All authors have read and agreed to the published version of the manuscript.

**Funding:** This research was jointly funded by the Lebanese National Council for Scientific Research and the Research Council at Saint Joseph University of Beirut (USJ) (CNRS-L/XFS92).

**Institutional Review Board Statement:** Not applicable.

**Informed Consent Statement:** Not applicable.

**Data Availability Statement:** Not applicable.

**Conflicts of Interest:** The authors declare no conflict of interest.

**Sample Availability:** Not available.

### References

1. Ahmad, S.; Zeb, A.; Ayaz, M.; Murkovic, M. Characterization of phenolic compounds using UPLC–HRMS and HPLC–DAD and anti-cholinesterase and anti-oxidant activities of *Trifolium repens* L. leaves. *Eur. Food Res. Technol.* **2019**, *246*, 485–496. [CrossRef]
2. Chacar, S.; Itani, T.; Hajal, J.; Saliba, Y.; Louka, N.; Faivre, J.-F.; Maroun, R.; Fares, N. The Impact of Long-Term Intake of Phenolic Compounds-Rich Grape Pomace on Rat Gut Microbiota. *J. Food Sci.* **2017**, *83*, 246–251. [CrossRef] [PubMed]
3. Rehman, Z.U. Citrus peel extract—A natural source of antioxidant. *Food Chem.* **2006**, *99*, 450–454. [CrossRef]
4. Selvi, A.T.; Joseph, G.; Jayaprakasha, G. Inhibition of growth and aflatoxin production in *Aspergillus flavus* by *Garcinia indica* extract and its antioxidant activity. *Food Microbiol.* **2003**, *20*, 455–460. [CrossRef]

5. Elaridi, J.; Bassil, M.; Kharma, J.A.; Daou, F.; Hassan, H.F. Analysis of Aflatoxin M1 in Breast Milk and Its Association with Nutritional and Socioeconomic Status of Lactating Mothers in Lebanon. *J. Food Prot.* **2017**, *80*, 1737–1741. [[CrossRef](#)] [[PubMed](#)]
6. Elaridi, J.; Dimassi, H.; Hassan, H. Aflatoxin M1 and ochratoxin A in baby formulae marketed in Lebanon: Occurrence and safety evaluation. *Food Control* **2019**, *106*, 106680. [[CrossRef](#)]
7. Gizachew, D.; Chang, C.-H.; Szonyi, B.; De La Torre, S.; Ting, W.-T.E. Aflatoxin B1 (AFB1) production by *Aspergillus flavus* and *Aspergillus parasiticus* on ground Nyjer seeds: The effect of water activity and temperature. *Int. J. Food Microbiol.* **2019**, *296*, 8–13. [[CrossRef](#)] [[PubMed](#)]
8. Khoury, A.E.; Rizk, T.; Lteif, R.; Azouri, H.; Delia, M.-L.; Lebrihi, A. Fungal contamination and Aflatoxin B1 and Ochratoxin A in Lebanese wine–grapes and musts. *Food Chem. Toxicol.* **2008**, *46*, 2244–2250. [[CrossRef](#)]
9. Bluma, R.; Amaiden, M.; Daghero, J.; Etcheverry, M. Control of *Aspergillus* section *Flavigrowth* and aflatoxin accumulation by plant essential oils. *J. Appl. Microbiol.* **2008**, *105*, 203–214. [[CrossRef](#)]
10. Sdiri, S.; Cuenca, J.; Navarro, P.; Salvador, A.; Bermejo, A. New triploids late-maturing mandarins as a rich source of antioxidant compounds. *Eur. Food Res. Technol.* **2009**, *246*, 225–237. [[CrossRef](#)]
11. Guimarães, R.; Barros, L.; Barreira, J.C.; Sousa, M.J.; Carvalho, A.M.; Ferreira, I.C. Targeting excessive free radicals with peels and juices of citrus fruits: Grapefruit, lemon, lime and orange. *Food Chem. Toxicol.* **2010**, *48*, 99–106. [[CrossRef](#)] [[PubMed](#)]
12. Maksoud, S.; Abdel-Massih, R.M.; Rajha, H.N.; Louka, N.; Chemat, F.; Barba, F.J.; Debs, E. *Citrus aurantium* L. Active Constituents, Biological Effects and Extraction Methods. An Updated Review. *Molecules* **2021**, *26*, 5832. [[CrossRef](#)] [[PubMed](#)]
13. Londoño-Londoño, J.; de Lima, V.R.; Lara, O.; Gil, A.; Pasa, T.B.C.; Arango, G.J.; Pineda, J.R.R. Clean recovery of antioxidant flavonoids from citrus peel: Optimizing an aqueous ultrasound-assisted extraction method. *Food Chem.* **2010**, *119*, 81–87. [[CrossRef](#)]
14. Li, B.B.; Smith, B.; Hossain, M.M. Extraction of phenolics from citrus peels II. Enzyme-assisted extraction method. *Sep. Purif. Technol.* **2006**, *48*, 189–196. [[CrossRef](#)]
15. Nakajima, V.M.; Macedo, G.A.; Macedo, J.A. Citrus bioactive phenolics: Role in the obesity treatment. *LWT* **2014**, *59*, 1205–1212. [[CrossRef](#)]
16. Lou, S.-N.; Lai, Y.-C.; Hsu, Y.-S.; Ho, C.-T. Phenolic content, antioxidant activity and effective compounds of kumquat extracted by different solvents. *Food Chem.* **2016**, *197*, 1–6. [[CrossRef](#)]
17. Sharma, K.; Mahato, N.; Cho, M.H.; Lee, Y.R. Converting citrus wastes into value-added products: Economic and environmentally friendly approaches. *Nutrition* **2016**, *34*, 29–46. [[CrossRef](#)]
18. Maroun, R.G.; Rajha, H.N.; Vorobiev, E.; Louka, N. Emerging Technologies for the Recovery of Valuable Compounds From Grape Processing By-Products. In *Handbook of Grape Processing By-Products Sustainable Solutions*; Galanakis, C.M., Ed.; Academic Press (Elsevier): Amsterdam, the Netherlands, 2017. [[CrossRef](#)]
19. Sillero, L.; Prado, R.; Labidi, J. Simultaneous microwave-ultrasound assisted extraction of bioactive compounds from bark. *Chem. Eng. Process. Process Intensif.* **2020**, *156*, 108100. [[CrossRef](#)]
20. Vázquez, M.B.; Andreatta, A.; Martini, R.; Montoya, S.N.; Cabrera, J.; Comini, L. Optimization of pretreatment with microwaves prior the pressurized hot water extraction of anthraquinones from *Heterophyllaea pustulata*, using Doehlert experimental design. *Chem. Eng. Process. Process Intensif.* **2020**, *155*, 108055. [[CrossRef](#)]
21. Miccio, M.; Pierri, R.; Cuccurullo, G.; Metallo, A.; Brachi, P. Process intensification of tomato residues drying by microwave heating: Experiments and simulation. *Chem. Eng. Process. Process Intensif.* **2020**, *156*, 108082. [[CrossRef](#)]
22. Rezzoug, S.-A.; Louka, N. Thermomechanical process intensification for oil extraction from orange peels. *Innov. Food Sci. Emerg. Technol.* **2009**, *10*, 530–536. [[CrossRef](#)]
23. Rezzoug, S.A.; Baghdadi, M.W.; Louka, N.; Boutekdjiret, C.; Allaf, K. Study of a new extraction process: Controlled instantaneous decompression. Application to the extraction of essential oil from rosemary leaves. *Flavour Fragr. J.* **1998**, *13*, 251–258. [[CrossRef](#)]
24. Diaz-Reinoso, B.; Moure, A.; Domínguez, H. Ethanol-modified supercritical CO<sub>2</sub> extraction of chestnut burs antioxidants. *Chem. Eng. Process. Process Intensif.* **2020**, *156*, 108092. [[CrossRef](#)]
25. Fratianne, A.; Niro, S.; Messia, M.C.; Panfili, G.; Marra, F.; Cinquanta, L. Evaluation of carotenoids and furosine content in air dried carrots and parsnips pre-treated with pulsed electric field (PEF). *Eur. Food Res. Technol.* **2019**, *245*, 2529–2537. [[CrossRef](#)]
26. EL Kantar, S.; Boussetta, N.; Lebovka, N.; Foucart, F.; Rajha, H.N.; Maroun, R.G.; Louka, N.; Vorobiev, E. Pulsed electric field treatment of citrus fruits: Improvement of juice and polyphenols extraction. *Innov. Food Sci. Emerg. Technol.* **2018**, *46*, 153–161. [[CrossRef](#)]
27. Abi-Khattar, A.-M.; Rajha, H.N.; Abdel-Massih, R.M.; Habchi, R.; Maroun, R.G.; Debs, E.; Louka, N. “Intensification of Vaporization by Decompression to the Vacuum” (IVDV), a novel technology applied as a pretreatment to improve polyphenols extraction from olive leaves. *Food Chem.* **2020**, *342*, 128236. [[CrossRef](#)]
28. Chemat, F.; Rombaut, N.; Meullemiestre, A.; Turk, M.; Perino, S.; Fabiano-Tixier, A.-S.; Abert-Vian, M. Review of Green Food Processing techniques. Preservation, transformation, and extraction. *Innov. Food Sci. Emerg. Technol.* **2017**, *41*, 357–377. [[CrossRef](#)]
29. Qu, Y.; Li, C.; Zhang, C.; Zeng, R.; Fu, C. Optimization of infrared-assisted extraction of *Bletilla striata* polysaccharides based on response surface methodology and their antioxidant activities. *Carbohydr. Polym.* **2016**, *148*, 345–353. [[CrossRef](#)]
30. El Kantar, S.; Rajha, H.N.; Maroun, R.G.; Louka, N. Intensification of polyphenols extraction from orange peels using infrared as a novel and energy saving pretreatment. *J. Food Sci.* **2020**, *85*, 414–420. [[CrossRef](#)]

31. D'Alessandro, L.G.; Kriaa, K.; Nikov, I.; Dimitrov, K. Ultrasound assisted extraction of polyphenols from black chokeberry. *Sep. Purif. Technol.* **2012**, *93*, 42–47. [[CrossRef](#)]
32. Garcia-Castello, E.M.; Rodriguez-Lopez, A.D.; Mayor, L.; Ballesteros, R.; Conidi, C.; Cassano, A. Optimization of conventional and ultrasound assisted extraction of flavonoids from grapefruit (*Citrus paradisi* L.) solid wastes. *LWT* **2015**, *64*, 1114–1122. [[CrossRef](#)]
33. Waszkowiak, K.; Gliszczynska-Świgło, A. Binary ethanol–water solvents affect phenolic profile and antioxidant capacity of flaxseed extracts. *Eur. Food Res. Technol.* **2015**, *242*, 777–786. [[CrossRef](#)]
34. Librán, C.M.; Mayor, L.; Garcia-Castello, E.M.; Vidal-Brotons, D. Polyphenol extraction from grape wastes: Solvent and pH effect. *Agric. Sci.* **2013**, *04*, 56–62. [[CrossRef](#)]
35. Hegazy, A.E.; Ibrahim, M.I. Antioxidant Activities of Orange Peel Extracts. *World Appl. Sci. J.* **2012**, *18*, 684–688. [[CrossRef](#)]
36. Lagha-Benamrouche, S.; Madani, K. Phenolic contents and antioxidant activity of orange varieties (*Citrus sinensis* L. and *Citrus aurantium* L.) cultivated in Algeria: Peels and leaves. *Ind. Crop. Prod.* **2013**, *50*, 723–730. [[CrossRef](#)]
37. Cai, Y.; Yu, Y.; Duan, G.; Li, Y. Study on infrared-assisted extraction coupled with high performance liquid chromatography (HPLC) for determination of catechin, epicatechin, and procyanidin B2 in grape seeds. *Food Chem.* **2011**, *127*, 1872–1877. [[CrossRef](#)]
38. Rajha, H.N.; Chacar, S.; Afif, C.; Vorobiev, E.; Louka, N.; Maroun, R.G.  $\beta$ -Cyclodextrin-Assisted Extraction of Polyphenols from Vine Shoot Cultivars. *J. Agric. Food Chem.* **2015**, *63*, 3387–3393. [[CrossRef](#)]
39. Rajha, H.N.; El Darra, N.; Vorobiev, E.; Louka, N.; Maroun, R.G. An Environment Friendly, Low-Cost Extraction Process of Phenolic Compounds from Grape Byproducts. Optimization by Multi-Response Surface Methodology. *Food Nutr. Sci.* **2013**, *04*, 650–659. [[CrossRef](#)]
40. Rajha, H.N.; Abi-Khattar, A.-M.; El Kantar, S.; Boussetta, N.; Lebovka, N.; Maroun, R.G.; Louka, N.; Vorobiev, E. Comparison of aqueous extraction efficiency and biological activities of polyphenols from pomegranate peels assisted by infrared, ultrasound, pulsed electric fields and high-voltage electrical discharges. *Innov. Food Sci. Emerg. Technol.* **2019**, *58*, 102212. [[CrossRef](#)]
41. Abi-Khattar, A.-M.; Rajha, H.N.; Abdel-Massih, R.M.; Maroun, R.G.; Louka, N.; Debs, E. Intensification of Polyphenol Extraction from Olive Leaves Using Ired-Irrad®, an Environmentally-Friendly Innovative Technology. *Antioxidants* **2019**, *8*, 227. [[CrossRef](#)]
42. Chen, Y.; Duan, G.; Xie, M.; Chen, B.; Li, Y. Infrared-assisted extraction coupled with high-performance liquid chromatography for simultaneous determination of eight active compounds in *Radix Salviae miltiorrhizae*. *J. Sep. Sci.* **2010**, *33*, 2888–2897. [[CrossRef](#)] [[PubMed](#)]
43. Wang, S.; Zhang, L.; Yang, P.; Chen, G. Infrared-assisted tryptic proteolysis for peptide mapping. *PROTEOMICS* **2008**, *8*, 2579–2582. [[CrossRef](#)]
44. Chen, Q.; Liu, T.; Chen, G. Highly Efficient Proteolysis Accelerated by Electromagnetic Waves for Peptide Mapping. *Curr. Genom.* **2011**, *12*, 380–390. [[CrossRef](#)] [[PubMed](#)]
45. Iranshahi, M.; Rezaee, R.; Parhiz, H.; Roohbakhsh, A.; Soltani, F. Protective effects of flavonoids against microbes and toxins: The cases of hesperidin and hesperetin. *Life Sci.* **2015**, *137*, 125–132. [[CrossRef](#)] [[PubMed](#)]
46. Caceres, I.; El Khoury, R.; Medina; Lippi, Y.; Naylies, C.; Atoui, A.; El Khoury, A.; Oswald, I.P.; Bailly, J.-D.; Puel, O. Deciphering the Anti-Aflatoxinogenic Properties of Eugenol Using a Large-Scale q-PCR Approach. *Toxins* **2016**, *8*, 123. [[CrossRef](#)]
47. Holmes, R.A.; Boston, R.S.; Payne, G.A. Diverse inhibitors of aflatoxin biosynthesis. *Appl. Microbiol. Biotechnol.* **2008**, *78*, 559–572. [[CrossRef](#)]
48. Mo, H.Z.; Zhang, H.; Wu, Q.H.; Bin Hu, L. Inhibitory effects of tea extract on aflatoxin production by *Aspergillus flavus*. *Lett. Appl. Microbiol.* **2013**, *56*, 462–466. [[CrossRef](#)]
49. Singleton, V.L.; Orthofer, R.; Lamuela-Raventós, R.M. Analysis of total phenols and other oxidation substrates and antioxidants by means of Folin-Ciocalteu reagent. In *Methods in Enzymology*; Academic Press: Cambridge, MA, USA, 1999; Volume 299, pp. 152–178.
50. Brand-Williams, W.; Cuvelier, M.E.; Berset, C. Use of a free radical method to evaluate antioxidant activity. *LWT Food Sci. Technol.* **1995**, *28*, 25–30. [[CrossRef](#)]

Article

# Bioavailability Assessment of Yarrow Phenolic Compounds Using an In Vitro Digestion/Caco-2 Cell Model: Anti-Inflammatory Activity of Basolateral Fraction

Marisol Villalva, Laura Jaime, María de las Nieves Siles-Sánchez and Susana Santoyo \*

Institute of Food Science Research (CIAL), Universidad Autónoma de Madrid (CEI UAM+CSIC),  
28049 Madrid, Spain

\* Correspondence: susana.santoyo@uam.es; Tel.: +34-91-001-79-26

**Abstract:** In this study, a combined in vitro digestion/Caco-2 model was performed with the aim to determine the phenolic compounds bioavailability of two yarrow extracts. HPLC-PAD characterisation indicated that the main components in both extracts were 3,5-dicaffeoylquinic acid (DCQA) and luteolin-7-*O*-glucoside. Analyses after the simulated digestion process revealed that phenolic composition was not affected during the oral phase, whereas gastric and intestinal phases represented critical steps for some individual phenolics, especially intestinal step. The transition from gastric medium to intestinal environment caused an important degradation of 3,5-DCQA (63–67% loss), whereas 3,4-DCQA and 4,5-DCQA increased significantly, suggesting an isomeric transformation within these caffeic acid derivatives. However, an approx. 90% of luteolin-7-*O*-glucoside was recovered after intestinal step. At the end of Caco-2 absorption experiments, casticin, diosmetin and centaureidin represented the most abundant compounds in the basolateral fraction. Moreover, this fraction presented anti-inflammatory activity since was able to inhibit the secretion of IL-1 $\beta$  and IL-6 pro-inflammatory cytokines. Thus, the presence in the basolateral fraction of flavonoid-aglycones from yarrow, could be related with the observed anti-inflammatory activity from yarrow extract.

**Keywords:** *Achillea millefolium*; bioaccessibility; Caco-2 absorption; in vitro digestion; phenolic compounds

**Citation:** Villalva, M.; Jaime, L.; Siles-Sánchez, M.d.l.N.; Santoyo, S. Bioavailability Assessment of Yarrow Phenolic Compounds Using an In Vitro Digestion/Caco-2 Cell Model: Anti-Inflammatory Activity of Basolateral Fraction. *Molecules* **2022**, *27*, 8254. <https://doi.org/10.3390/molecules27238254>

Academic Editor: Nour Eddine Es-Safi

Received: 14 October 2022

Accepted: 22 November 2022

Published: 26 November 2022

**Publisher's Note:** MDPI stays neutral with regard to jurisdictional claims in published maps and institutional affiliations.



**Copyright:** © 2022 by the authors. Licensee MDPI, Basel, Switzerland. This article is an open access article distributed under the terms and conditions of the Creative Commons Attribution (CC BY) license (<https://creativecommons.org/licenses/by/4.0/>).

## 1. Introduction

*Achillea millefolium* L. (yarrow) is a flowering plant traditionally used in the treatment of digestive and hepatobiliary disorders, inflammation, and diabetes [1]. Recent reports indicated that *Achillea* genus presented important biological activities, such as antioxidant, anti-inflammatory and antitumor activities [2]. Most health benefits of aqueous and alcoholic yarrow extracts have been associated with its composition in phenolic compounds, mainly phenolic acids (caffeic acid derivatives), and flavonoids (luteolin, apigenin and quercetin derivatives) [1,3]. Thus, Trumbeckaite et al. [4] related the antioxidant properties of an *Achillea millefolium* hydroalcoholic extract with the presence of luteolin and chlorogenic acid in the extract, and in a lesser extent with rutin and luteolin-7-*O*-glucoside. Pereira et al. [5] also reported that an *A. millefolium* hydroethanolic extract, containing 3,5-*O*-dicaffeoylquinic acid, 5-*O*-caffeoylquinic acid, luteolin-*O*-acetylhexoside and apigenin-*O*-acetylhexoside as main phenolic compounds, inhibited the growth of human tumour cell lines. Furthermore, both essential oils and hydroethanolic yarrow extracts have demonstrated anti-inflammatory properties, causing the inhibition of nitric oxide (NO) production and IL-8 secretion in vitro [6,7].

Nevertheless, after oral consumption, phenolic compounds must be bioavailable in order to perform their potential health benefits. The bioavailability is dependent upon the stability of the compound during gastrointestinal digestion, its release from the food-matrix and the efficiency of its intestinal absorption. In yarrow, the assessment of mineral and



vitamins bioaccessibility has been performed [8], but studies for phenolic compounds are still scarce. The stability of phenolic compounds during the gastrointestinal digestion is strongly influenced by their chemical structure, since phenolics present a different sensitivity to pH variations and digestive enzymes activity [9,10]. Moreover, the stability of phenolic compounds under gastrointestinal conditions highly depends on the nature of the matrix in which these compounds are included [11]. Thereby, Lingua et al. [12] reported that phenolic acids and quercetin were the most resistant polyphenols in white grape after a simulated digestion. However, Ortega-Vidal et al. [13] indicated that caffeoylquinic acids in herbal infusions were highly reduced by gastrointestinal digestion (approx. 10% remain). Moreover, Spínola et al. [14] carried out extracts of *Rumex maderensis* and reported that the degradation of different phenolic classes after digestion varied within morphological parts employed (leaves, flowers, and stems). Thus, flavanols were the most stable compounds, although in flowers presented a reduction of 29.7% against 40.4% in stems. Hydroxycinnamic acids from leaves and flowers, presented a similar degradation rate (approx. 56.5%), meanwhile in stems extracts hydroxycinnamic acids were very unstable (71.8% reduction).

After gastrointestinal digestion, the intestinal absorption of phenolic compounds has also been reported to be highly influenced by the phenolic compounds chemical structure. Bowles et al. [15] studied the intestinal transport across Caco-2 cell monolayer of nine phenolic acids found in an aqueous extract of *Athrixia phylicoides*, concluding that *p*-coumaric acid presented the highest transport. Besides, Wu et al. [16] reported that the absorption of caffeic acid was higher than chlorogenic acid in the Caco-2 model as well as in rat jejunum. Therefore, the use of an *in vitro* digestion/Caco-2 cell culture model has been proposed by several authors as an economical and useful alternative to the *in vivo* analysis, in order to investigate the bioavailability of phenolic compounds [12,17].

Concerning phenolic compounds extraction, several studies proposed the ultrasound-assisted extraction (UAE) as an adequate technique to obtain phenolic compounds from vegetal matrices [18,19]. In this regard, UAE has been reported to reduce extraction time and solvent consumption, as well as to maximizing the recoveries of bioactive compounds [20]. However, sometimes it is difficult to obtain highly concentrated extracts using only UAE, due to complexity of vegetable raw materials. Therefore, the use of adsorption resins (e.g., XAD-2, XAD-7, XAD-16 and Oasis HLB) has been successfully employed as a tool for selective enrichment of phenolic compounds from plant material [21,22]. The aim of this work was to study the bioavailability of yarrow phenolic compounds, by using a combined *in vitro* digestion/Caco-2 cell model. In addition, the influence of phenolics compounds concentration in the matrix on their bioavailability was also determined. Besides, the biological activity of Caco-2 basolateral fraction, in terms of anti-inflammatory activity was measured.

## 2. Results and Discussions

### 2.1. Influence of *In Vitro* Gastrointestinal Steps on Phenolic Composition and Antioxidant Activity of the Extracts

Phenolic compounds identification of yarrow extract (YE) and yarrow phenolic enriched-extract (EE) was performed by HPLC-PAD-ESI-QTOF-MS allowing the identification of 49 phenolic compounds (Table S1). These results were in accordance with similar reported YE composition [23]. The quantitative analysis in both extracts (YE and EE) before and after the three-steps digestion process (oral, gastric, and intestinal) were shown in Tables 1 and 2, respectively. As can be observed, both extracts presented a similar behaviour during the gastrointestinal process. In general, the phenolic composition of both yarrow extracts was not affected during the oral phase, whereas gastric and intestinal phases, especially intestinal one, resulted as critical steps for some individual phenolic compounds. Figure S1 shows the base peak chromatogram of the EE before and after intestinal digestion, where the major differences can be observed.

**Table 1.** Phenolic composition (mg/g extract) of yarrow extract (YE) before and after oral, gastric and intestinal digestion steps.

Compound	Undigested YE	Oral	Gastric	Intestinal
Neochlorogenic acid	0.24 ± 0.11 <sup>b</sup>	0.21 ± 0.06 <sup>b</sup>	0.29 ± 0.09 <sup>b</sup>	0.56 ± 0.07 <sup>a</sup>
Protocatechuic acid	0.13 ± 0.10 <sup>b</sup>	0.12 ± 0.07 <sup>b</sup>	0.13 ± 0.08 <sup>b</sup>	0.47 ± 0.12 <sup>a</sup>
Caftaric acid isomer	0.08 ± 0.03 <sup>a</sup>	0.08 ± 0.04 <sup>a</sup>	0.06 ± 0.03 <sup>ab</sup>	0.04 ± 0.03 <sup>b</sup>
Caftaric acid	0.07 ± 0.03 <sup>a</sup>	0.07 ± 0.04 <sup>a</sup>	0.18 ± 0.09 <sup>a</sup>	0.13 ± 0.07
Caffeoylquinic acid isomer I	0.39 ± 0.09 <sup>a</sup>	0.39 ± 0.08 <sup>a</sup>	0.24 ± 0.08 <sup>ab</sup>	0.22 ± 0.06 <sup>b</sup>
Chlorogenic acid	5.67 ± 0.25 <sup>a</sup>	5.02 ± 0.21 <sup>ab</sup>	5.90 ± 0.30 <sup>a</sup>	4.75 ± 0.20 <sup>b</sup>
Cryptochlorogenic acid	0.13 ± 0.05 <sup>b</sup>	0.10 ± 0.03 <sup>b</sup>	0.17 ± 0.04 <sup>b</sup>	0.75 ± 0.12 <sup>a</sup>
Vicenin 2	2.11 ± 0.10 <sup>bc</sup>	2.02 ± 0.10 <sup>c</sup>	2.45 ± 0.15 <sup>a</sup>	2.24 ± 0.10 <sup>ab</sup>
Caffeoylquinic acid isomer II	0.10 ± 0.03 <sup>a</sup>	0.12 ± 0.04 <sup>a</sup>	0.10 ± 0.02 <sup>a</sup>	0.10 ± 0.03 <sup>a</sup>
Apigenin hexoside-pentoside I	0.46 ± 0.06 <sup>a</sup>	0.48 ± 0.05 <sup>a</sup>	0.49 ± 0.06 <sup>a</sup>	0.43 ± 0.06 <sup>a</sup>
Caffeic acid	0.34 ± 0.04 <sup>a</sup>	0.36 ± 0.06 <sup>a</sup>	0.40 ± 0.05 <sup>a</sup>	0.42 ± 0.06 <sup>a</sup>
Schaftoside isomer	1.34 ± 0.10 <sup>a</sup>	1.32 ± 0.09 <sup>a</sup>	1.43 ± 0.10 <sup>a</sup>	1.43 ± 0.12 <sup>a</sup>
Schaftoside	1.77 ± 0.18 <sup>ab</sup>	1.61 ± 0.15 <sup>b</sup>	2.14 ± 0.19 <sup>a</sup>	2.01 ± 0.16 <sup>a</sup>
Homoorientin	2.10 ± 0.19 <sup>a</sup>	1.94 ± 0.12 <sup>a</sup>	2.20 ± 0.15 <sup>a</sup>	1.89 ± 0.12 <sup>a</sup>
Apigenin hexoside-pentoside II	1.04 ± 0.11 <sup>a</sup>	0.97 ± 0.09 <sup>a</sup>	1.04 ± 0.10 <sup>a</sup>	0.98 ± 0.08 <sup>a</sup>
Luteolin dihexoside I	2.60 ± 0.18 <sup>ab</sup>	2.32 ± 0.12 <sup>b</sup>	2.77 ± 0.11 <sup>a</sup>	2.52 ± 0.11 <sup>b</sup>
6-hydroxyluteolin-7-O-glucoside	2.03 ± 0.12 <sup>b</sup>	1.97 ± 0.08 <sup>b</sup>	2.34 ± 0.12 <sup>a</sup>	1.74 ± 0.09 <sup>c</sup>
Apigenin dihexoside	0.15 ± 0.09 <sup>a</sup>	0.16 ± 0.06 <sup>a</sup>	0.21 ± 0.07 <sup>a</sup>	0.16 ± 0.04 <sup>a</sup>
Quercetin hexoside	1.33 ± 0.13 <sup>a</sup>	1.31 ± 0.08 <sup>a</sup>	1.10 ± 0.10 <sup>a</sup>	0.25 ± 0.07 <sup>b</sup>
Luteolin dihexoside II	0.23 ± 0.04 <sup>a</sup>	0.23 ± 0.06 <sup>a</sup>	0.27 ± 0.07 <sup>a</sup>	0.24 ± 0.04 <sup>a</sup>
Rutin	1.06 ± 0.07 <sup>a</sup>	1.08 ± 0.09 <sup>a</sup>	1.16 ± 0.07 <sup>a</sup>	1.02 ± 0.09 <sup>a</sup>
Apigenin hexoside	0.50 ± 0.04 <sup>a</sup>	0.47 ± 0.07 <sup>a</sup>	0.57 ± 0.06 <sup>a</sup>	0.52 ± 0.06 <sup>a</sup>
Vitexin	0.67 ± 0.07 <sup>a</sup>	0.61 ± 0.09 <sup>a</sup>	0.72 ± 0.08 <sup>a</sup>	0.64 ± 0.07 <sup>a</sup>
Apigenin hexoside-deoxyhexoside	0.40 ± 0.05 <sup>a</sup>	0.42 ± 0.04 <sup>a</sup>	0.25 ± 0.04 <sup>b</sup>	0.22 ± 0.03 <sup>b</sup>
Apigenin derivative	2.52 ± 0.12 <sup>b</sup>	2.49 ± 0.09 <sup>b</sup>	2.54 ± 0.10 <sup>b</sup>	2.72 ± 0.11 <sup>a</sup>
Luteolin-7-O-glucoside	8.29 ± 0.28 <sup>a</sup>	8.12 ± 0.32 <sup>a</sup>	6.70 ± 0.25 <sup>c</sup>	7.24 ± 0.33 <sup>b</sup>
Luteolin-7-O-glucuronide	0.72 ± 0.09 <sup>a</sup>	0.69 ± 0.08 <sup>ab</sup>	0.57 ± 0.05 <sup>b</sup>	0.69 ± 0.07 <sup>ab</sup>
Quercetin hexuronide	0.15 ± 0.03 <sup>b</sup>	0.12 ± 0.05 <sup>b</sup>	0.25 ± 0.03 <sup>a</sup>	0.20 ± 0.04 <sup>ab</sup>
3,4-Dicaffeoylquinic acid	1.49 ± 0.10 <sup>b</sup>	1.37 ± 0.08 <sup>b</sup>	1.42 ± 0.08 <sup>b</sup>	6.26 ± 0.27 <sup>a</sup>
Isorhamnetin hexoside I	1.59 ± 0.12 <sup>a</sup>	1.49 ± 0.09 <sup>a</sup>	1.00 ± 0.07 <sup>b</sup>	1.00 ± 0.06 <sup>b</sup>
1,5-Dicaffeoylquinic acid	1.65 ± 0.11 <sup>a</sup>	1.66 ± 0.10 <sup>a</sup>	1.49 ± 0.07 <sup>ab</sup>	1.37 ± 0.08 <sup>b</sup>
3,5-Dicaffeoylquinic acid	23.8 ± 1.81 <sup>a</sup>	22.9 ± 1.13 <sup>a</sup>	18.8 ± 0.90 <sup>b</sup>	8.77 ± 0.11 <sup>c</sup>
Apigenin-7-O-glucoside	2.27 ± 0.10 <sup>a</sup>	2.15 ± 0.07 <sup>ab</sup>	2.01 ± 0.08 <sup>b</sup>	1.81 ± 0.09 <sup>c</sup>
Luteolin-O-malonylglucoside	0.53 ± 0.04 <sup>a</sup>	0.52 ± 0.03 <sup>a</sup>	0.50 ± 0.04 <sup>ab</sup>	0.44 ± 0.03 <sup>b</sup>
4,5-Dicaffeoylquinic acid	4.25 ± 0.20 <sup>b</sup>	4.05 ± 0.18 <sup>b</sup>	3.61 ± 0.12 <sup>c</sup>	11.5 ± 0.51 <sup>a</sup>
Isorhamnetin hexoside II	0.62 ± 0.06 <sup>b</sup>	0.60 ± 0.04 <sup>b</sup>	0.50 ± 0.04 <sup>c</sup>	1.35 ± 0.10 <sup>a</sup>
Dicaffeoylquinic acid isomer	0.06 ± 0.01 <sup>b</sup>	0.05 ± 0.02 <sup>b</sup>	0.06 ± 0.02 <sup>b</sup>	0.10 ± 0.01 <sup>a</sup>
Feruloylcaffeoylquinic acid	0.14 ± 0.03 <sup>a</sup>	0.12 ± 0.02 <sup>a</sup>	0.07 ± 0.02 <sup>b</sup>	0.11 ± 0.03 <sup>ab</sup>
Tricaffeoylquinic acid	0.36 ± 0.06 <sup>a</sup>	0.31 ± 0.04 <sup>ab</sup>	0.09 ± 0.01 <sup>c</sup>	0.25 ± 0.04 <sup>b</sup>
Luteolin	1.90 ± 0.10 <sup>a</sup>	1.94 ± 0.11 <sup>a</sup>	0.95 ± 0.08 <sup>c</sup>	1.32 ± 0.10 <sup>b</sup>
Quercetin	0.63 ± 0.05 <sup>a</sup>	0.60 ± 0.07 <sup>a</sup>	0.29 ± 0.06 <sup>b</sup>	0.16 ± 0.04 <sup>c</sup>
Methoxyquercetin	0.36 ± 0.03 <sup>a</sup>	0.34 ± 0.04 <sup>ab</sup>	0.26 ± 0.04 <sup>b</sup>	0.32 ± 0.04 <sup>ab</sup>
Apigenin	0.56 ± 0.05 <sup>a</sup>	0.58 ± 0.04 <sup>a</sup>	0.18 ± 0.02 <sup>c</sup>	0.38 ± 0.05 <sup>b</sup>
Diosmetin	0.40 ± 0.05 <sup>a</sup>	0.38 ± 0.04 <sup>a</sup>	0.22 ± 0.03 <sup>c</sup>	0.29 ± 0.04 <sup>b</sup>
Trihydroxy dimethoxyflavone	0.27 ± 0.02 <sup>a</sup>	0.29 ± 0.02 <sup>a</sup>	0.13 ± 0.01 <sup>c</sup>	0.20 ± 0.02 <sup>b</sup>
Centaureidin	2.02 ± 0.12 <sup>a</sup>	2.07 ± 0.09 <sup>a</sup>	1.22 ± 0.05 <sup>c</sup>	1.76 ± 0.08 <sup>b</sup>
Methoxyacacetin	0.25 ± 0.03 <sup>a</sup>	0.26 ± 0.02 <sup>a</sup>	0.09 ± 0.02 <sup>c</sup>	0.16 ± 0.02 <sup>b</sup>
Dihydroxy trimethoxyflavone	0.44 ± 0.05 <sup>a</sup>	0.46 ± 0.06 <sup>a</sup>	0.17 ± 0.03 <sup>c</sup>	0.31 ± 0.05 <sup>b</sup>
Casticin	2.93 ± 0.10 <sup>a</sup>	2.92 ± 0.11 <sup>a</sup>	1.45 ± 0.09 <sup>c</sup>	2.31 ± 0.10 <sup>b</sup>

<sup>a, b, c</sup> Different letters denote statistical differences within a line according to Fisher's least significant difference (LSD) procedure ( $p < 0.05$ ).

**Table 2.** Phenolic compounds (mg/g extract) of yarrow enriched-extract (EE) before and after oral, gastric and intestinal digestion steps.

Compound	Undigested-EE	Oral	Gastric	Intestinal
Neochlorogenic acid	0.15 ± 0.03 <sup>c</sup>	0.15 ± 0.02 <sup>c</sup>	0.22 ± 0.04 <sup>b</sup>	0.86 ± 0.06 <sup>a</sup>
Protocatechuic acid	0.13 ± 0.02 <sup>b</sup>	0.13 ± 0.03 <sup>b</sup>	0.14 ± 0.03 <sup>b</sup>	0.74 ± 0.07 <sup>a</sup>
Caftaric acid isomer	0.15 ± 0.02 <sup>a</sup>	0.13 ± 0.02 <sup>a</sup>	0.05 ± 0.01 <sup>b</sup>	0.05 ± 0.02 <sup>b</sup>
Caftaric acid	0.19 ± 0.06 <sup>b</sup>	0.18 ± 0.05 <sup>b</sup>	0.30 ± 0.08 <sup>a</sup>	0.30 ± 0.06 <sup>a</sup>
Caffeoylquinic acid isomer I	0.46 ± 0.07 <sup>a</sup>	0.42 ± 0.06 <sup>a</sup>	0.48 ± 0.07 <sup>a</sup>	0.39 ± 0.06 <sup>a</sup>
Chlorogenic acid	7.60 ± 0.35 <sup>a</sup>	7.46 ± 0.21 <sup>a</sup>	7.49 ± 0.01 <sup>a</sup>	6.28 ± 0.25 <sup>b</sup>
Cryptochlorogenic acid	0.12 ± 0.01 <sup>b</sup>	0.14 ± 0.02 <sup>b</sup>	0.15 ± 0.02 <sup>b</sup>	1.11 ± 0.07 <sup>a</sup>
Vicenin 2	3.20 ± 0.12 <sup>b</sup>	3.22 ± 0.10 <sup>b</sup>	3.37 ± 0.10 <sup>a</sup>	3.49 ± 0.11 <sup>a</sup>
Caffeoylquinic acid isomer II	0.22 ± 0.02 <sup>a</sup>	0.24 ± 0.02 <sup>a</sup>	0.27 ± 0.03 <sup>a</sup>	0.28 ± 0.02 <sup>a</sup>
Apigenin hexoside-pentoside I	0.76 ± 0.04 <sup>b</sup>	0.77 ± 0.05 <sup>b</sup>	0.96 ± 0.08 <sup>a</sup>	0.80 ± 0.07 <sup>ab</sup>
Caffeic acid	0.90 ± 0.06 <sup>a</sup>	0.91 ± 0.06 <sup>a</sup>	0.90 ± 0.04 <sup>a</sup>	0.94 ± 0.05 <sup>a</sup>
Schaftoside isomer	2.33 ± 0.14 <sup>b</sup>	2.29 ± 0.11 <sup>b</sup>	2.62 ± 0.12 <sup>a</sup>	2.77 ± 0.10 <sup>a</sup>
Schaftosin	3.64 ± 0.10 <sup>b</sup>	3.57 ± 0.11 <sup>b</sup>	4.02 ± 0.15 <sup>a</sup>	3.92 ± 0.12 <sup>a</sup>
Homoorientin	6.31 ± 0.21 <sup>a</sup>	6.03 ± 0.16 <sup>a</sup>	6.36 ± 0.18 <sup>a</sup>	5.50 ± 0.13 <sup>b</sup>
Apigenin hexoside-pentoside II	1.90 ± 0.10 <sup>a</sup>	1.76 ± 0.09 <sup>a</sup>	1.88 ± 0.08 <sup>a</sup>	1.87 ± 0.09 <sup>a</sup>
Luteolin dihexoside I	7.68 ± 0.19 <sup>a</sup>	7.35 ± 0.12 <sup>b</sup>	7.20 ± 0.10 <sup>b</sup>	7.56 ± 0.11 <sup>ab</sup>
6-hydroxyluteolin-7-O-glucoside	6.46 ± 0.20 <sup>a</sup>	6.25 ± 0.16 <sup>a</sup>	6.58 ± 0.21 <sup>a</sup>	5.26 ± 0.18 <sup>b</sup>
Apigenin dihexoside	0.44 ± 0.08	0.41 ± 0.06	0.52 ± 0.06	0.42 ± 0.04
Quercetin hexoside	4.10 ± 0.20 <sup>a</sup>	4.00 ± 0.14 <sup>a</sup>	3.37 ± 0.15 <sup>b</sup>	0.96 ± 0.10 <sup>c</sup>
Luteolin dihexoside II	0.63 ± 0.05 <sup>b</sup>	0.66 ± 0.04 <sup>b</sup>	0.78 ± 0.06 <sup>a</sup>	0.69 ± 0.04 <sup>ab</sup>
Rutin	2.86 ± 0.11 <sup>b</sup>	3.19 ± 0.12 <sup>a</sup>	3.30 ± 0.10 <sup>a</sup>	3.00 ± 0.13 <sup>ab</sup>
Apigenin hexoside	1.75 ± 0.08 <sup>b</sup>	2.06 ± 0.10 <sup>a</sup>	2.25 ± 0.11 <sup>a</sup>	2.24 ± 0.10 <sup>a</sup>
Vitexin	2.51 ± 0.10 <sup>a</sup>	2.44 ± 0.09 <sup>a</sup>	2.52 ± 0.10 <sup>a</sup>	2.42 ± 0.08 <sup>a</sup>
Apigenin hexoside- deoxyhexoside	0.85 ± 0.04 <sup>a</sup>	0.89 ± 0.05 <sup>a</sup>	0.72 ± 0.04 <sup>b</sup>	0.56 ± 0.03 <sup>c</sup>
Apigenin derivative	6.44 ± 0.21 <sup>c</sup>	6.80 ± 0.22 <sup>c</sup>	7.60 ± 0.21 <sup>b</sup>	8.23 ± 0.30 <sup>a</sup>
Luteolin-7-O-glucoside	24.2 ± 1.30 <sup>a</sup>	23.6 ± 1.12 <sup>a</sup>	19.5 ± 1.06 <sup>c</sup>	21.8 ± 1.02 <sup>b</sup>
Luteolin-7-O-glucuronide	1.57 ± 0.08 <sup>a</sup>	1.45 ± 0.07 <sup>a</sup>	1.06 ± 0.06 <sup>c</sup>	1.17 ± 0.09 <sup>b</sup>
Quercetin hexuronide	0.95 ± 0.06 <sup>a</sup>	0.88 ± 0.05 <sup>a</sup>	0.87 ± 0.04 <sup>a</sup>	0.97 ± 0.02 <sup>a</sup>
3,4-Dicaffeoylquinic acid	3.78 ± 0.18 <sup>b</sup>	3.73 ± 0.12 <sup>b</sup>	3.80 ± 0.10 <sup>b</sup>	20.9 ± 1.22 <sup>a</sup>
Isorhamnetin hexoside I	3.36 ± 0.10 <sup>a</sup>	3.39 ± 0.09 <sup>a</sup>	3.57 ± 0.11 <sup>a</sup>	3.50 ± 0.12 <sup>a</sup>
1,5-Dicaffeoylquinic acid	4.29 ± 0.27 <sup>ab</sup>	4.75 ± 0.21 <sup>a</sup>	4.10 ± 0.12 <sup>b</sup>	3.62 ± 0.14 <sup>c</sup>
3,5-Dicaffeoylquinic acid	72.4 ± 2.92 <sup>a</sup>	72.5 ± 1.91 <sup>a</sup>	60.4 ± 2.10 <sup>b</sup>	24.2 ± 1.33 <sup>c</sup>
Apigenin-7-O-glucoside	7.30 ± 0.33 <sup>a</sup>	7.11 ± 0.21 <sup>a</sup>	7.00 ± 0.18 <sup>a</sup>	6.28 ± 0.15 <sup>b</sup>
Luteolin-O-malonylglucoside	1.08 ± 0.08 <sup>a</sup>	1.05 ± 0.05 <sup>a</sup>	1.08 ± 0.07 <sup>a</sup>	1.09 ± 0.08 <sup>a</sup>
4,5-Dicaffeoylquinic acid	13.3 ± 0.87 <sup>b</sup>	12.6 ± 0.63 <sup>b</sup>	10.5 ± 0.51 <sup>c</sup>	36.9 ± 1.21 <sup>a</sup>
Isorhamnetin hexoside II	1.57 ± 0.10 <sup>b</sup>	1.61 ± 0.09 <sup>b</sup>	1.27 ± 0.07 <sup>c</sup>	1.73 ± 0.09 <sup>a</sup>
Dicaffeoylquinic acid isomer	0.26 ± 0.04 <sup>a</sup>	0.28 ± 0.05 <sup>a</sup>	0.23 ± 0.03 <sup>a</sup>	0.23 ± 0.05 <sup>a</sup>
Feruloylcaffeoylquinic acid	0.29 ± 0.05 <sup>a</sup>	0.30 ± 0.06 <sup>a</sup>	0.15 ± 0.03 <sup>b</sup>	0.25 ± 0.04 <sup>a</sup>
Tricaffeoylquinic acid	0.86 ± 0.08 <sup>a</sup>	0.79 ± 0.06 <sup>a</sup>	0.15 ± 0.02 <sup>c</sup>	0.60 ± 0.06 <sup>b</sup>
Luteolin	3.33 ± 0.15 <sup>a</sup>	3.17 ± 0.11 <sup>a</sup>	1.78 ± 0.09 <sup>c</sup>	2.57 ± 0.10 <sup>b</sup>
Quercetin	0.89 ± 0.06 <sup>a</sup>	0.86 ± 0.06 <sup>a</sup>	0.50 ± 0.09 <sup>b</sup>	0.35 ± 0.05 <sup>c</sup>
Methoxyquercetin	0.83 ± 0.08 <sup>a</sup>	0.80 ± 0.07 <sup>a</sup>	0.61 ± 0.06 <sup>b</sup>	0.75 ± 0.07 <sup>a</sup>
Apigenin	0.39 ± 0.04 <sup>a</sup>	0.39 ± 0.05 <sup>ab</sup>	0.12 ± 0.01 <sup>c</sup>	0.31 ± 0.03 <sup>b</sup>
Diosmetin	0.24 ± 0.02 <sup>a</sup>	0.24 ± 0.03 <sup>a</sup>	0.16 ± 0.03 <sup>b</sup>	0.23 ± 0.03 <sup>a</sup>
Trihydroxy dimethoxyflavone	0.35 ± 0.03 <sup>a</sup>	0.35 ± 0.04 <sup>a</sup>	0.18 ± 0.02 <sup>b</sup>	0.31 ± 0.03 <sup>a</sup>
Centaureidin	3.34 ± 0.14 <sup>a</sup>	3.30 ± 0.15 <sup>a</sup>	2.09 ± 0.13 <sup>c</sup>	2.93 ± 0.17 <sup>b</sup>
Methoxyacacetin	0.23 ± 0.03 <sup>a</sup>	0.23 ± 0.02 <sup>a</sup>	0.06 ± 0.01 <sup>c</sup>	0.20 ± 0.02 <sup>a</sup>
Dihydroxy trimethoxyflavone	0.34 ± 0.04 <sup>a</sup>	0.32 ± 0.05 <sup>a</sup>	0.16 ± 0.02 <sup>c</sup>	0.20 ± 0.03 <sup>b</sup>
Casticin	4.18 ± 0.17 <sup>a</sup>	4.02 ± 0.14 <sup>a</sup>	2.27 ± 0.11 <sup>c</sup>	3.62 ± 0.12 <sup>b</sup>

<sup>a, b, c</sup> Different letters denote statistical differences within a line according to Fisher's least significant difference (LSD) procedure ( $p < 0.05$ ).

Chlorogenic acid (CGA), the most abundant mono-caffeoylquinic acid in both extracts, was stable under oral and gastric conditions, but showed a loss of about 17% at the end of the intestinal step. However, it should be highlighted the higher quantity of neochlorogenic and cryptochlorogenic acids measured after intestinal step, whose increase could be attributed to CGA isomerization. This behaviour was also found by Bouayed et al. [24], who reported that CGA was stable to gastric conditions but degraded (between 23–41%) during intestinal digestion, with partial isomerisation to neochlorogenic and cryptochlorogenic acids. Yu et al. [25] also reported an important bioaccessibility (68.39–91.34%) after digestion process for chlorogenic acid obtained from mulberry leaves.

With respect to dicaffeoylquinic acids (DCQAs), these compounds seem to be stable under oral conditions in both extracts. Gastric conditions mainly affected 3,5- and 4,5-DCQAs with a significant loss of approx. 20%. The transition from gastric medium to intestinal environment caused an important degradation of 3,5-DCQA (63–67% loss), whereas 3,4-DCQA and 4,5-DCQA significantly increased their quantity after intestinal step. This increment could be related with isomerization processes among different DCQAs at intestinal pH. Moreover, at the end of the intestinal step, the sum of all DCQAs represented the 90% of these compounds in the undigested extract. D'Antuono et al. [26] previously described that 3,5-DCQA (pure individual compound) gastrointestinal digestion produced a higher isomerization effect with the presence of 3,4-DCQA and 4,5-DCQA.

Both extracts, YE and EE, also presented an important quantity of flavonoids, either in glycosylated or in aglycone form. Among the glycosylated forms, luteolin-7-*O*-glucoside, the most abundant compound within flavonoids group, was stable to oral digestion but gastric conditions produced a decrease of approx. 20%. However, this compound increased up to 87–90% at the end of intestinal step. Gutiérrez-Grijalva et al. [27] also found that in digestion process, the quantity of luteolin-7-*O*-glucoside decreased after gastric step but increased at the end of intestinal step. They indicated that the loss of luteolin-7-*O*-glucoside after gastric phase could be related, in addition to pH changes, to a possible interaction between the compound and gastric enzymes that render it undetectable in chromatographic analysis. Regarding aglycones, luteolin was also stable to oral step but hardly affected by gastric conditions (approx. 50% loss). Moreover, luteolin registered an increased when intestinal phase ended. This behaviour was observed in other aglycones such as casticin and centaureidin. According with previous results, this effect could be also related with possible interactions between digestive enzymes and phenolics, as was detected for luteolin-7-*O*-glucoside.

Digestion effect on total phenolic content (TPC) and antioxidant activity for both extracts is shown in Table 3. During digestion process, the amount of TPC only decreased slightly for both extracts (between 7–13%). Regarding antioxidant activity, this was not significantly affected during oral phase, however, stomach and intestinal phases resulted in critical steps for this activity (26–40% decrease). This loss of antioxidant activity could be related with the losses registered in some phenolic compounds, such as luteolin and its glycosylated derivatives, since these compounds have been reported to present an important antioxidant activity [28]. However, the isomerization effect occurred in some compounds (i.e., CGA and DCQAs) could also be related. Shang et al. [29] indicated that among DCQA isomers from a *L. fischeri* leaves ethanolic extract, 3,5-DCQA presented the highest radical scavenging activity.

**Table 3.** Total phenolic content (TPC) and antioxidant activity (TEAC value) of yarrow ultrasound-assisted extract (YE) and yarrow enriched-extract (EE) after oral, gastric, and intestinal digestion.

		Undigested	Oral	Gastric	Intestinal
TPC <sup>1</sup>	YE	105 ± 3 <sup>a</sup>	96 ± 3 <sup>b</sup>	87 ± 2 <sup>c</sup>	91 ± 2 <sup>b</sup>
	EE	224 ± 3 <sup>a</sup>	214 ± 2 <sup>b</sup>	201 ± 3 <sup>d</sup>	208 ± 3 <sup>c</sup>
TEAC value <sup>2</sup>	YE	0.36 ± 0.01 <sup>a</sup>	0.35 ± 0.01 <sup>a</sup>	0.20 ± 0.01 <sup>b</sup>	0.22 ± 0.04 <sup>b</sup>
	EE	1.12 ± 0.06 <sup>a</sup>	1.06 ± 0.03 <sup>a</sup>	0.75 ± 0.06 <sup>b</sup>	0.83 ± 0.04 <sup>b</sup>

<sup>1</sup> TPC = mg GAE/g extract. <sup>2</sup> TEAC value = mmol Trolox/g extract. <sup>a,b,c,d</sup> Different letters denote statistical differences within a same line, according to Fisher's least significant difference (LSD) procedure ( $p < 0.05$ ).

## 2.2. Caco-2 Cells Transport Experiments

In order to investigate the potential bioavailability of digested yarrow phenolic compounds, their intestinal uptake was evaluated using Caco-2 cells monolayers at 2, 4 and 6 h. Due to EE digested extract presented a 2–3 fold superior concentration of phenolic compounds, this extract was selected to carry out the transport experiments. The cytotoxicity assays, performed by the MTT method, indicated that 40 µL/mL of digested EE was the maximum concentration that did not affect the cell viability during 6 h (data not shown). Thus, the concentration of EE phenolic compounds detected in the apical compartment, cellular monolayer, and basolateral compartment after 2, 4 and 6 h of transport experiments are shown in Table 4. After 2 h of incubation, 11 phenolic compounds were identified in the cell monolayer, mainly flavonoid aglycones (casticin, diosmetin and centaureidin) and DCQAs isomers (3,4-DCQA and 3,5-DCQA). The concentration of those compounds in cell monolayer decreased after 4 and 6 h of experiment. Regarding the basolateral compartment, after 2 h of incubation, casticin was the main compound, followed by 3,4 and 3,5-DCQAs. Data obtained after 4 h showed an increase in casticin, diosmetin and centaureidin concentration in the basolateral compartment, meanwhile the amount of 3,5-DCQA remains constant and 3,4-DCQA slightly decreased. Successively, an increment in the quantity of casticin, diosmetin and centaureidin continued until 6 h of experiment, while neither 3,4 nor 3,5-DCQAs were detected at that time.

Casticin (a methoxylated flavonol) was the most abundant compound in the basolateral fraction (after 6 h, a 41.7% from digested extract). The apparent permeability coefficients ( $P_{app}$ ) for casticin presented a maximum value at 2 h ( $P_{app} = 16.7 \pm 0.1 \times 10^{-6} \text{ cm s}^{-1}$ ) in comparison with 4 h and 6 h ( $P_{app} = 10.9 \pm 0.1 \times 10^{-6}$  and  $10.2 \pm 0.3 \times 10^{-6} \text{ cm s}^{-1}$ , respectively). These results suggested that casticin permeability was time-dependent and transported across the Caco-2 monolayers with a faster rate at a shorter incubation time. In spite of in vitro studies of casticin's permeability are still scarce; Piazzini et al. [30] reported a casticin's  $P_{app}$  value of  $8.1 \pm 0.9 \times 10^{-6} \text{ cm s}^{-1}$  across Caco-2 cells, after 4 h incubation with a *Vitex agnus-castus* extract.

Diosmetin's uptake also increased with incubation time. Surprisingly, the sum of diosmetin amount in cell monolayer and basolateral fraction (at 2, 4 or 6 h), was higher than the concentration of this compound initially placed in the apical side ( $0.84 \pm 0.1 \text{ mg/L}$  of digested extract). Thus, considering that diosmetin is the 4'-methyl derivative of luteolin, the detected increment could be originated from the metabolism of luteolin (aglycone) and/or luteolin glycosylated-derivatives presented in the digested extract. The occurrence of diosmetin as a principal methylated metabolite from luteolin was reported in rats [31].

Centaureidin represented the third most abundant compound in the basolateral fraction after 6 h. This methylated flavonol, also showed a time-dependent absorption through Caco-2 cell monolayer, being more rapidly transported at earlier incubation time ( $P_{app}$  at 2 h =  $7.0 \pm 0.4 \times 10^{-6} \text{ cm s}^{-1}$ ). To the best of our knowledge, no previous studies had been reported for centaureidin's in vitro absorption. In general, a passive transcellular diffusion through Caco-2 monolayer could be related with casticin, diosmetin and centaureidin absorption. Nevertheless, interactions of diosmetin with selected transporters such as mul-

tidrug resistance-associated protein isoform 1 (MRP1) and monocarboxylate transporter isoform 1 (MCT1), also expressed in Caco-2 cells, have been previously described [32].

**Table 4.** Phenolic compounds (mg/L of digested extract) detected in the apical compartment, Caco-2 cell monolayer and basolateral compartment at 2, 4 and 6 h incubation with digested yarrow enriched-extract (EE).

Compounds	Apical Compartment			Cell Monolayer			Basolateral Compartment		
	2 h	4 h	6 h	2 h	4 h	6 h	2 h	4 h	6 h
Apigenin derivative	18.50 ± 0.04 <sup>a</sup>	18.30 ± 0.07 <sup>b</sup>	17.70 ± 0.10 <sup>c</sup>	0.37 ± 0.0 <sup>a</sup>	0.37 ± 0.01 <sup>a</sup>	0.36 ± 0.01 <sup>a</sup>	0.45 ± 0.01 <sup>a</sup>	0.46 ± 0.01 <sup>a</sup>	0.42 ± 0.01 <sup>b</sup>
Luteolin-7-O-glucoside	41.64 ± 0.10 <sup>a</sup>	40.98 ± 0.30 <sup>a</sup>	39.77 ± 0.04 <sup>b</sup>	0.39 ± 0.02 <sup>a</sup>	0.36 ± 0.01 <sup>a</sup>	0.28 ± 0.01 <sup>b</sup>	0.25 ± 0.01 <sup>a</sup>	0.24 ± 0.01 <sup>a</sup>	0.21 ± 0.01 <sup>b</sup>
3,4-Dicaffeoyl-quinic acid	14.85 ± 0.10 <sup>a</sup>	12.09 ± 0.10 <sup>b</sup>	9.18 ± 0.05 <sup>c</sup>	0.68 ± 0.01 <sup>a</sup>	0.66 ± 0.02 <sup>a</sup>	n.d.	0.76 ± 0.01 <sup>a</sup>	0.71 ± 0.01 <sup>b</sup>	n.d.
3,5-Dicaffeoyl-quinic acid	4.95 ± 0.12 <sup>a</sup>	4.26 ± 0.05 <sup>b</sup>	2.99 ± 0.07 <sup>c</sup>	0.75 ± 0.01	n.d.	n.d.	0.71 ± 0.01 <sup>a</sup>	0.70 ± 0.01 <sup>a</sup>	n.d.
Apigenin 7-O-glucoside	13.34 ± 0.06 <sup>a</sup>	12.06 ± 0.08 <sup>b</sup>	11.58 ± 0.15 <sup>c</sup>	0.24 ± 0.01 <sup>a</sup>	0.2 ± 0.01 <sup>ab</sup>	0.20 ± 0.01 <sup>b</sup>	0.14 ± 0.01	n.d.	n.d.
4,5-Dicaffeoyl-quinic acid	22.24 ± 0.14 <sup>a</sup>	20.74 ± 0.11 <sup>b</sup>	16.28 ± 0.11 <sup>c</sup>	0.08 ± 0.01	n.d.	n.d.	0.26 ± 0.01 <sup>a</sup>	0.13 ± 0.01 <sup>b</sup>	0.09 ± 0.02 <sup>c</sup>
Apigenin	0.16 ± 0.01 <sup>a</sup>	0.09 ± 0.02 <sup>b</sup>	n.d.	0.04 ± 0.01	n.d.	n.d.	0.13 ± 0.01 <sup>c</sup>	0.18 ± 0.01 <sup>b</sup>	0.27 ± 0.01 <sup>a</sup>
Diosmetin	0.95 ± 0.02 <sup>a</sup>	0.94 ± 0.03 <sup>a</sup>	0.94 ± 0.01 <sup>a</sup>	0.89 ± 0.01 <sup>a</sup>	0.66 ± 0.01 <sup>b</sup>	0.41 ± 0.01 <sup>c</sup>	0.40 ± 0.01 <sup>c</sup>	0.79 ± 0.02 <sup>b</sup>	1.53 ± 0.11 <sup>a</sup>
Centaureidin	3.27 ± 0.02 <sup>a</sup>	2.18 ± 0.07 <sup>b</sup>	0.75 ± 0.01 <sup>c</sup>	0.58 ± 0.01 <sup>a</sup>	0.41 ± 0.01 <sup>b</sup>	n.d.	0.48 ± 0.01 <sup>c</sup>	0.84 ± 0.07 <sup>b</sup>	1.01 ± 0.02 <sup>a</sup>
Methoxyacetin	0.05 ± 0.01 <sup>a</sup>	n.d.	n.d.	0.13 ± 0.01 <sup>a</sup>	0.10 ± 0.0 <sup>b</sup>	0.10 ± 0.01 <sup>b</sup>	0.12 ± 0.01 <sup>c</sup>	0.17 ± 0.01 <sup>b</sup>	0.20 ± 0.02 <sup>a</sup>
Casticin	5.17 ± 0.11 <sup>a</sup>	4.44 ± 0.09 <sup>b</sup>	3.73 ± 0.07 <sup>c</sup>	1.87 ± 0.01 <sup>a</sup>	1.53 ± 0.01 <sup>b</sup>	1.08 ± 0.01 <sup>c</sup>	1.77 ± 0.02 <sup>c</sup>	2.3 ± 0.02 <sup>b</sup>	3.43 ± 0.06 <sup>a</sup>

<sup>a, b, c</sup> Different letters denote statistical differences within a line according to Fisher's least significant difference (LSD) procedure ( $p < 0.05$ ). n.d.: not detected.

The amounts of 3,4-DCQA and 3,5-DCQA detected in the basolateral compartment after 2 and 4 h of incubation were quite smaller with respect to their amounts in the apical side, showing a  $P_{app}$  calculated values (at 4 h) of  $1.0 \pm 0.1 \times 10^{-6} \text{ cm s}^{-1}$  for 3,4-DCQA and  $2.2 \pm 0.1 \times 10^{-6} \text{ cm s}^{-1}$  for 3,5-DCQA. Similarly, Zhou et al. [33] indicated that DCQAs showed, after 4 h,  $P_{app}$  values of approx.  $2.5 \times 10^{-6} \text{ cm s}^{-1}$ . However, at 6 h, unexpectedly no DCQAs isomers were detected in basolateral fraction (Table 4). In consistence with this result, D'Antuono et al. [26], did not also detect any DCQAs isomer in the basolateral side, but coumaric and caffeic acids were found in this fraction, suggesting a cellular metabolism activity. However, in our results neither caffeic nor coumaric acids were found in the basolateral fraction at detectable amounts with the analytical technique employed. Regarding Caco-2 transport, Zhou et al. [33] described DCQAs absorption mainly by passive diffusion via paracellular pathways, although some interactions of DCQAs with certain transporters were also reported in vitro [34]. In that context, when evaluating the absorption of a complex plant-extract, we would have to consider that certain phenolics may act like substrates or inhibitors of some transporters expressed in Caco-2 cells, thus, they could act as permeability modifiers for other compounds [35].

### 2.3. Anti-Inflammatory Activity of Caco-2 Cells Basolateral Fraction

Basolateral fraction recovered at 6 h was used to carry out the anti-inflammatory assays, using THP-1 macrophages (stimulated via LPS) to quantify the pro-inflammatory cytokines secretion in the medium. In addition, the basolateral fraction from control digestion (digestion fluids without extract) was also tested. These results are shown in Figure 1. As can be observed, after 24 h the stimulated macrophages (positive control) revealed a significant release of the three pro-inflammatory cytokines, TNF- $\alpha$ , IL-1 $\beta$  and IL-6, compared to non-stimulated cells (negative control). Previous experiments to assess the cytotoxicity of the basolateral fraction indicated that 20  $\mu\text{L/mL}$  did not compromise the macrophages viability (data not shown). Thus, when THP-1 macrophages were incubated with LPS in presence of 10 and 20  $\mu\text{L/mL}$  of the basolateral media, TNF- $\alpha$  secretion was not modified, compared with the levels obtained in absence of the extracts (Figure 1A). In contrast, a significant reduction of IL-1 $\beta$  secreted was observed in presence of both concentrations of basolateral fraction, approx. 30% and 40% for 10 and 20  $\mu\text{L/mL}$  (Figure 1B). The IL-6 release was also suppressed approx. 25% when applied 20  $\mu\text{L/mL}$  of basolateral fraction (Figure 1C).

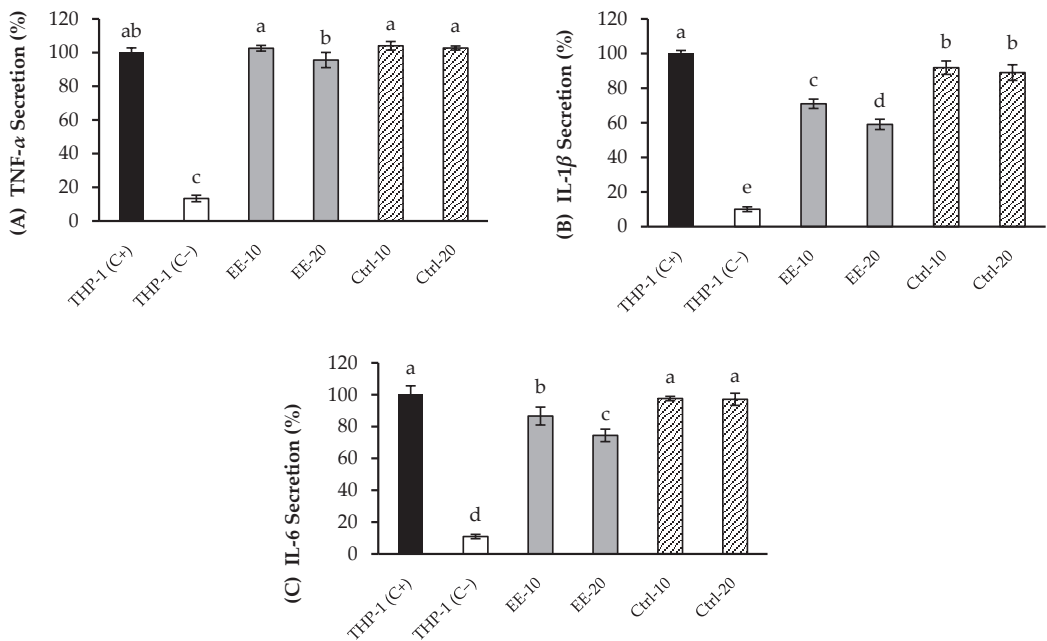


**Figure 1.** Levels of TNF- $\alpha$  (A), IL-1 $\beta$  (B) and IL-6 (C) secreted by THP-1 macrophages activated with LPS, in presence of 10  $\mu$ L/mL (EE-10) and 20  $\mu$ L/mL (EE-20) of basolateral fraction from yarrow enriched-extract (EE). Positive control (THP-1 C+), cells stimulated with LPS without basolateral sample. Negative control (THP-1 C-), cells stimulated with LPS in contact just with RPMI medium. Control digestion (Ctrl) represents the basolateral supernatant from digested fluids without extract at 10  $\mu$ L/mL (Ctrl-10) and 20  $\mu$ L/mL (Ctrl-20). Each bar is the mean of three determinations  $\pm$  S.D. a, b, c, d, e Different letters indicate statistical differences among samples ( $p < 0.05$ ) according to Fisher's least significant difference (LSD) procedure.

Thus, the basolateral fraction from EE exhibited a moderate inhibition of IL-1 $\beta$  and IL-6 cytokines. Considering that this fraction was mainly composed by casticin, diosmetin and centaureidin, these flavonoids could be related, at least partially, with the anti-inflammatory activity. Casticin was shown to decrease the production of pro-inflammatory cytokines, such as IL-1 $\beta$ , IL-6, and TNF- $\alpha$  in RAW 264.7 cells treated with LPS [36]. Moreover, diosmetin also reduced the generation of pro-inflammatory mediators like NO, TNF- $\alpha$  in adipocytes and macrophages, and IL-1 $\beta$  e IL-6 in rheumatoid arthritis fibroblast [37]. Finally, centaureidin has been also effectively inhibited expression of COX-1 and COX-2 enzymes related with the inflammatory response [38]. Nevertheless, the influence of other compounds, including those found in minor concentrations or even those non-detected metabolites of phenolic compounds, cannot be ruled out.

### 3. Materials and Methods

#### 3.1. Yarrow Extract and Yarrow Phenolic Compounds-Enriched Extract Obtention

Upper-dried inflorescences of yarrow were obtained from a local supplier (Plantafarm S.A., León, Spain). The sample was ground (Premill 250, Leal S.A., Granollers, Spain) and sieved to diminish its particle size (<500  $\mu$ m). YE was obtained by ultrasound assisted extraction according to Villalva et al. [23]. Briefly, the ground yarrow was soaked with pure ethanol (plant/solvent 1:10,  $w/v$ ) and conducted to extraction (30 min,  $\leq 40$   $^{\circ}$ C) in a Branson 450 ultrasonic device (Branson Ultrasonics, Danbury, CT, USA). The solvent was removed in a vacuum rotary evaporator (35  $^{\circ}$ C) (IKA RV 10, VWR, Madrid, Spain) to obtain a dry extract.

In order to obtain the EE, a fractionation process was conducted using XAD-7HP macroporous resins (Sigma-Aldrich, St. Louis, MO, USA) packed in a glass column (bed volume, BV, 225 mL) and a mixture of ethanol:water (80:20, *v/v*) as elution solvent. A volume (70 mL) of YE (15 mg/mL final concentration) was placed in the column. After 1 h to allowing the absorption equilibrium, a water-washing step was required (2 BV) to later recover the phenolic compounds using 80% ethanol (3 BV at 2 BV/h). At the end, the ethanol was evaporated in a rotary evaporator and freeze-dried to remove the water. The extracts were kept at  $-20\text{ }^{\circ}\text{C}$  until analysis. All experiments were done by triplicate.

A graphical flowchart summarizing the main steps of the experimental procedure applied is provided in Figure 2.

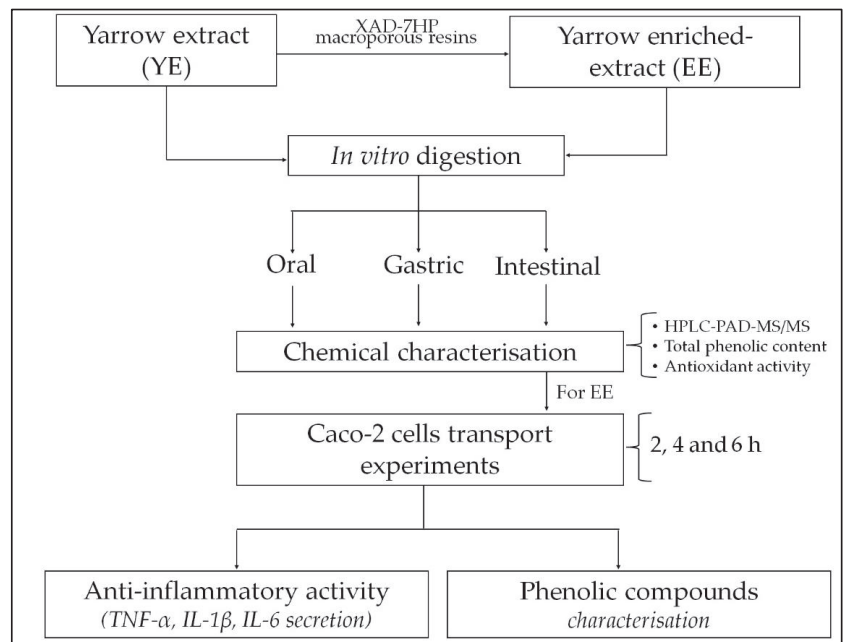


**Figure 2.** Flowchart summarizing the main experimental procedures for the bioavailability assessment of yarrow phenolic compounds.

### 3.2. HPLC-PAD Phenolic Compounds Analysis

Phenolic compounds analysis was performed using an HPLC 1260 Infinity series system with a photodiode-array detector (PAD) (Agilent Technologies Inc., Santa Clara, CA, USA). Both YE and EE dried extracts were dissolved in ethanol or ethanol:water (50:50, *v/v*), filtered (PVDF, 0.45  $\mu\text{m}$ ) and analysed by HPLC-PAD. Chromatographic separation was carried out with a reverse phase ACE Excel SuperC18 column (ACT, Aberdeen, Scotland), equipped with a guard-column of the same material, according to the methodologic conditions described by Villalva et al. (2018) [22]. Identification of phenolic compounds was based on HPLC-PAD-ESI-QTOF-MS/MS analysis by following the Villalva et al. (2021) [23] procedure. Quantification was performed by HPLC-DAD according to the calibration curve established of each authentic phenolic standard (HPLC purity  $\geq 95\%$ ). Calibration curves were also used for the quantification of phenolic compounds with unavailable commercial standard, following their chemical similarity, e.g., apigenin 7-O-glucoside was used for apigenin derivative, and chlorogenic acid curve for caffeoylquinic acid isomers.



### 3.3. Determination of Total Phenolic Content (TPC) and Antioxidant Activity

Total phenolic content was determined by Folin-Ciocalteu reagent as described by Singleton et al. [39]. The results were expressed as mg of gallic acid equivalents (GAE)/g extract. DPPH (2,2-diphenyl-1-picrylhydrazyl, Sigma-Aldrich, Madrid, Spain) free radical methodology was used to evaluate the antioxidant activity according to Brand-Williams et al. [40]. The results were expressed as TEAC value (mmol Trolox/g of extract or mmol Trolox/L of digested extract). All analyses were done in triplicate.

### 3.4. In Vitro Gastrointestinal Digestion

YE and EE were subjected to a three steps digestion process [22]. Briefly, 5 mL of extract solution (20 mg/mL) with 0.1 mL  $\alpha$ -amylase from human saliva (9.3 mg in  $\text{Cl}_2\text{Ca}$  1 mM) (Type XIII-A, Sigma-Aldrich, St. Louis, MO, USA) were stirred for 2 min in a titrator Titrino Plus 877 at 37 °C (Methrom AG, Herisau, Switzerland) (oral phase). Then, 25 mL of a gastric solution (pH 2.0  $\pm$  0.5) containing 127 mg of pepsin from porcine gastric mucosa (536 U/mg, Sigma-Aldrich, St. Louis, MO, USA) was added and incubated for 1 h (gastric phase). After gastric digestion, pH was adjusted to 7.5  $\pm$  0.5 by addition of 10 mL intestinal solution composed by 5.3% (*v/v*) of NaOH 0.1 M, 1.4% (*v/v*) of NaCl 3.25 M, 0.5% of  $\text{CaCl}_2$  325 mM and 2.8% (*v/v*) of a pancreatic-bile extract solution (9.3 mg pancreatin (4  $\times$  USP) and 115.7 mg bile salts in 10 mM trizma-maleate buffer), allowing stirring for 2 h to simulate intestinal phase. When digestion finished, the solutions were immediately cooled and filtered (0.45  $\mu\text{m}$ , PVDF) to conduct the HPLC-PAD analysis, TPC and antioxidant activity assays. Additionally, digestion steps, without yarrow sample addition, were also carried out as control digestion.

### 3.5. Caco-2 Cells Culture and Transport Experiments

Maintenance conditions for Caco-2 cell line (ATCC, Manassas, VA, USA), as well as the cell viability experiments, were followed as previously described by Villalva et al. [22]. To assess the transport assays, Caco-2 cells (density  $3 \times 10^5$  cells/insert) were seeded in polyester Transwell® inserts (24 mm diameter, 0.4  $\mu\text{m}$  pore size, Corning Life Science) and cultured for 21 days at 37 °C (5%  $\text{CO}_2$ ). The day of the transport experiments, the inserts were carefully washed with Phosphate Buffer Solution (PBS) (Gibco, Paisley, UK) and filled with 1.5 mL (apical) and 2.6 mL (basolateral) of pre-warmed Dulbecco's Modified Eagle's Medium (DMEM) (Lonza, Basel, Switzerland) without phenol red, and a specific volume of digested yarrow extract was added in the apical compartment (extract final dilution 1:25, *v/v*). At the end of 2, 4 and 6 h of incubation apical and basolateral supernatants were collected, freeze-dried and stored ( $-20$  °C) until analysis. Cell monolayer integrity was measured before and after the transport assays using an EVOM2 epithelial volt-ohm meter (World Precision Instruments, Hitchin, UK) and only inserts with transepithelial electric resistance (TEER) values  $> 700 \Omega\text{cm}^2$  were used. In addition, lucifer yellow (Sigma-Aldrich, Madrid, Spain) permeation was determined to validate the integrity of cell barrier, according to Uchida et al. [41]. To performed the HPLC-PAD analysis, lyophilized samples from apical and basolateral sides, were conducted to extraction with 60:40 ethanol:water (*v/v*) (150  $\mu\text{L}$  and 175  $\mu\text{L}$ , respectively) followed by centrifugation (15,000 RPM, 5 min). The supernatants were filtered (0.45  $\mu\text{m}$ , PVDF filters) before HPLC analysis.

Cell monolayers were washed with cold PBS, followed by 500  $\mu\text{L}$  pure ethanol addition. After incubation (4 °C, 30 min), cells were scraped off the membrane, sonicated (5 min) and centrifuged (4500 RPM, 15 min) to recover the supernatant. This process was repeated three times, and finally all supernatants were evaporated until dryness with pure  $\text{NO}_2$ . The final residue was re-dissolved in 60:40 ethanol:water (*v/v*) (100  $\mu\text{L}$ ) and filtered prior HPLC injection.

The apparent permeability coefficient ( $P_{app}$ ,  $\text{cm s}^{-1}$ ) of each compound detected in the basolateral supernatant was determined according to D'Antuono et al. [26] with the following equation:

$$P_{app} = \frac{(dC/dt) V}{C_o A} \quad (1)$$

where  $dC/dt$  is the apparent rate of polyphenols transported to the basolateral compartment over the time ( $\mu\text{g L}^{-1} \text{s}^{-1}$ ),  $V$  is the volume of the basolateral compartment ( $\text{cm}^3$ );  $C_o$  is the initial concentration in the apical compartment ( $\mu\text{g L}^{-1}$ ) and  $A$  is the surface area of the membrane ( $\text{cm}^2$ ).

### 3.6. Anti-Inflammatory Assays of Basolateral Fraction from Caco-2 Experiments

Differentiated macrophages from the human monocyte THP-1 cell line (ATCC, Manassas, VA, USA) was used to conduct anti-inflammatory assays according to Villalva et al. [22] with minor modifications. Briefly, THP-1 cells were seeded in 24 well-plate ( $5 \times 10^5$  cells/mL) and differentiated with 100 ng/mL of phorbol 12-myristate 13-acetate (PMA) (Sigma-Aldrich, Madrid, Spain) maintained for 48 h ( $37^\circ\text{C}$ , 5%  $\text{CO}_2$ ). The cytotoxic effect of the basolateral supernatants from Caco-2 over THP-1 macrophages, was determined by the 3-(4,5-dimethylthiazol-2-yl)-2,5-diphenyl tetrazolium bromide assay (MTT) (Sigma-Aldrich, Madrid, Spain). Afterwards, the macrophages were washed and filled with serum-free RPMI medium (Gibco, Paisley, UK) along with a non-toxic concentration of basolateral supernatants and 0.05  $\mu\text{g/mL}$  of bacterial lipopolysaccharide (LPS) (*E. coli* O55:B5, Sigma-Aldrich, Madrid, Spain). After 24 h incubation, the medium was collected and the release of pro-inflammatory cytokines, TNF- $\alpha$ , IL-1 $\beta$ , and IL-6, was measured by an enzyme-linked immunosorbent assay (ELISA) (BD Biosciences, Aalst, Belgium) according to the manufacturer protocol. Cells with LPS but without basolateral sample, represented the positive control of the immunomodulatory assay; negative control was the non-stimulated cells in absence of basolateral sample. Results were expressed as mean of three determinations  $\pm$  standard deviation.

### 3.7. Statistical Analysis

Experimental results are expressed as means  $\pm$  standard deviation (SD). Variance one-way analysis (ANOVA) followed by Fisher's least significance differences (LSD) test were used to distinguish differences between means at  $p < 0.05$ . Statgraphics Centurion XVI software (Version 16, Statpoint Technologies Inc., Warrenton, VA, USA) was used for that purpose.

## 4. Conclusions

Phenolic compounds from yarrow showed a great stability at oral step during the simulated digestion, however gastric and intestinal phases caused important modifications. Mostly CGA and DCQAs suffered an isomerization effect after intestinal step. Besides flavonoids, either in their glycosylated or aglycone form, were also reduced after intestinal phase. Casticin, diosmetin and centaureidin were the most abundant compounds found in the basolateral fraction after Caco-2 experiments at 6 h. This fraction also exhibited a certain inhibition of the pro-inflammatory cytokines IL-1 $\beta$  and IL-6. Thus, the phenolic composition found in this fraction, mainly methoxylated flavonoids, could be related with the observed bioactivity. Although in vitro results cannot be directly extrapolated to human in vivo conditions, our findings exhibit a potential bioavailability of phenolic compounds present in yarrow extracts.

**Supplementary Materials:** The following supporting information can be downloaded at: <https://www.mdpi.com/article/10.3390/molecules27238254/s1>, Table S1: Phenolic compounds identified in yarrow samples by using HPLC-PAD-ESI-QTOF-MS/MS in negative ionization mode. Figure S1: HPLC-PAD base peak chromatogram ( $\lambda = 320$  nm) of yarrow enriched-extract before (red line) and after (blue line) simulated in vitro digestion process. n.i.: non-identified compound.

**Author Contributions:** Conceptualization, S.S., L.J. and M.V.; methodology, S.S., L.J. and M.V.; validation, S.S. and M.V.; formal analysis, S.S., L.J. and M.V.; investigation, M.d.I.N.S.-S. and M.V.; resources, L.J. and S.S.; data curation, S.S., L.J. and M.V.; writing—original draft preparation, S.S. and M.V.; visualization, S.S. and M.V.; writing—review and editing, S.S., L.J. and M.V.; supervision, S.S., L.J. and M.V.; project administration, S.S. and L.J.; funding acquisition, S.S. and L.J. All authors have read and agreed to the published version of the manuscript.

**Funding:** This research was carried out by Spanish Government (Project: PID2019-110183RB-C22/AEI//10.13039/501100011033) and Comunidad Autónoma de Madrid (ALIBIRD2020-CM, project: S2018/BAA-4343).

**Institutional Review Board Statement:** Not applicable.

**Informed Consent Statement:** Not applicable.

**Data Availability Statement:** The data presented in this study are available in this manuscript.

**Conflicts of Interest:** The authors declare no conflict of interest.

## References

- Barda, C.; Grafakou, M.E.; Tomou, E.M.; Skaltsa, H. Phytochemistry and Evidence-Based Traditional Uses of the Genus *Achillea* L.: An Update (2011–2021). *Sci. Pharm.* **2021**, *89*, 50. [\[CrossRef\]](#)
- Mohammadhosseini, M.; Sarker, S.D.; Akbarzadeh, A. Chemical composition of essential oils and extracts of *Achillea* species and their biological activities: A review. *J. Ethnopharmacol.* **2017**, *199*, 257–315. [\[CrossRef\]](#)
- Tadić, V.; Arsić, I.; Zvezdanović, J.; Zugić, A.; Cvetković, D.; Pavkov, S. The estimation of the traditionally used yarrow (*Achillea millefolium* L. Asteraceae) oil extracts with anti-inflammatory potential in topical application. *J. Ethnopharmacol.* **2017**, *199*, 138–148. [\[CrossRef\]](#)
- Trumbeckaite, S.; Benetis, R.; Bumblauskie, L.; Burdulis, D.; Janulis, V.; Toleikis, A.; Viskelis, P.; Jakstas, V. *Achillea millefolium* L. sl herb extract: Antioxidant activity and effect on the rat heart mitochondrial functions. *Food Chem.* **2011**, *127*, 1540–1548. [\[CrossRef\]](#)
- Pereira, J.M.; Peixoto, V.; Teixeira, A.; Sousa, D.; Barros, L.; Ferreira, I.C.F.R.; Vasconcelos, M.H. *Achillea millefolium* L. hydroethanolic extract inhibits growth of human tumor cells lines by interfering with cell cycle and inducing apoptosis. *Food Chem. Toxicol.* **2018**, *118*, 635–644. [\[CrossRef\]](#)
- Zaidi, S.F.; Muhammad, J.S.; Shahryar, S.; Usmanghani, K.; Gilani, A.H.; Jafri, W.; Sugiyama, T. Anti-inflammatory and cytoprotective effects of selected Pakistani medicinal plants in *Helicobacter pylori*-infected gastric epithelial cells. *J. Ethnopharmacol.* **2012**, *141*, 403–410. [\[CrossRef\]](#) [\[PubMed\]](#)
- Abdossi, V.; Kazemi, M. Bioactivities of *Achillea millefolium* essential oil and its main terpenes from Iran. *Int. J. Food Prop.* **2016**, *19*, 1798–1808. [\[CrossRef\]](#)
- Dias, M.I.; Morales, P.; Barreira, J.C.; Oliveira, M.B.P.; Sánchez-Mata, M.C.; Ferreira, I.C. Minerals and vitamin B9 in dried plants vs. infusions: Assessing absorption dynamics of minerals by membrane dialysis tandem in vitro digestion. *Food Biosci.* **2016**, *13*, 9–14. [\[CrossRef\]](#)
- Goulas, V.; Hadjisolomou, A. Dynamic changes in targeted phenolic compounds and antioxidant potency of carob fruit (*Ceratonia siliqua* L.) products during in vitro digestion. *LWT* **2019**, *101*, 269–275. [\[CrossRef\]](#)
- Lima, K.; Silva, O.; Figueira, M.E.; Pires, C.; Cruz, D.; Gomes, S.; Mauricio, E.M.; Duarte, M.P. Influence of the in vitro gastrointestinal digestion on the antioxidant activity of *Artemisia gorgorum* Webb and *Hyptis pectinata* (L.) Poit. Infusions from Cape Verde. *Food Res. Int.* **2019**, *115*, 150–159. [\[CrossRef\]](#)
- Arranz, E.; Corredig, M.; Guri, A. Designing food delivery systems: Challenges related to the in vitro methods employed to determine the fate of bioactives in the gut. *Food Funct.* **2016**, *7*, 3319–3336. [\[CrossRef\]](#)
- Lingua, M.S.; Theumer, M.G.; Kruzynski, P.; Wunderlin, D.A.; Baroni, M.V. Bioaccessibility of polyphenols and antioxidant properties of the white grape by simulated digestion and Caco-2 cell assays: Comparative study with its winemaking product. *Food Res. Int.* **2019**, *122*, 496–505. [\[CrossRef\]](#)
- Ortega-Vidal, J.; Ruíz-Riaguas, A.; Fernández-de Córdova, M.L.; Ortega-Barrales, P.; Llorent-Martínez, E.J. Phenolic profile and antioxidant activity of *Jasania glutinosa* herbal tea. Influence of simulated gastrointestinal in vitro digestion. *Food Chem.* **2019**, *287*, 258–264. [\[CrossRef\]](#)
- Spínola, V.; Llorent-Martínez, E.J.; Castillo, P.C. Antioxidant polyphenols of Madeira sorrel (*Rumex maderensis*): How do they survive to in vitro simulated gastrointestinal digestion? *Food Chem.* **2018**, *259*, 105–112. [\[CrossRef\]](#)
- Bowles, S.L.; Ntamo, Y.; Malherbe, C.J.; Kappo, A.M.; Louw, J.; Muller, C.J. Intestinal transport and absorption of bioactive phenolic compounds from a chemically characterized aqueous extract of *Athrixia phylicoides*. *J. Ethnopharmacol.* **2017**, *200*, 45–50. [\[CrossRef\]](#) [\[PubMed\]](#)

16. Wu, T.; Grootaert, C.; Voorspoels, S.; Jacobs, G.; Pitart, J.; Kamiloglu, S.; Possemiens, S.; Heinonen, M.; Kardum, N.; Glibetic, M.; et al. Aronia (*Aronia melanocarpa*) phenolics bioavailability in a combined in vitro digestion/Caco-2 cell model is structure and colon region dependent. *J. Funct. Foods* **2017**, *38*, 128–139. [[CrossRef](#)]
17. Xu, C.; Kong, L.; Tian, Y. Investigation of the Phenolic Component Bioavailability Using the In Vitro Digestion/Caco-2 Cell Model, as well as the Antioxidant Activity in Chinese Red Wine. *Foods* **2022**, *11*, 3108. [[CrossRef](#)]
18. Goltz, C.; Avila, S.; Barbieri, J.B.; Igarashi-Mafra, L.; Mafra, M.R. Ultrasound-assisted extraction of phenolic compounds from Macela (*Achyrocline satueioides*) extracts. *Ind. Crops Prod.* **2018**, *115*, 227–234. [[CrossRef](#)]
19. Irakli, M.; Chatzopoulou, P.; Ekateriniadou, L. Optimization of ultrasound-assisted extraction of phenolic compounds: Oleuropein, phenolic acids, phenolic alcohols and flavonoids from olive leaves and evaluation of its antioxidant activities. *Ind. Crops Prod.* **2018**, *124*, 382–388. [[CrossRef](#)]
20. Corbin, C.; Fidel, T.; Leclerc, E.A.; Barakzoy, E.; Sagot, N.; Falguières, A.; Renouard, S.; Blondeau, J.P.; Ferroud, C.; Doussot, J.; et al. Development and validation of an efficient ultrasound assisted extraction of phenolic compounds from flax (*Linum usitatissimum* L.) seeds. *Ultrason. Sonochem.* **2015**, *26*, 176–185. [[CrossRef](#)] [[PubMed](#)]
21. Pérez-Larrán, P.; Díaz-Reinoso, B.; Moure, A.; Alonso, J.L.; Domínguez, H. Adsorption technologies to recover and concentrate food polyphenols. *Curr. Opin. Food Sci.* **2018**, *23*, 165–172. [[CrossRef](#)]
22. Villalva, M.; Jaime, L.; Aguado, E.; Nieto, J.A.; Reglero, G.; Santoyo, S. Anti-inflammatory and antioxidant activities from the basolateral fraction of Caco-2 cells exposed to a rosmarinic acid enriched extract. *J. Agric. Food Chem.* **2018**, *66*, 1167–1174. [[CrossRef](#)] [[PubMed](#)]
23. Villalva, M.; Santoyo, S.; Salas-Perez, L.; Siles-Sanchez, M.N.; García-Risco, M.R.; Formari, T.; Reglero, G.; Jaime, L. Sustainable extraction techniques for obtaining antioxidant and anti-inflammatory compounds from the *Lamiaceae* and *Asteraceae* species. *Foods* **2021**, *10*, 2067. [[CrossRef](#)]
24. Bouayed, J.; Deuber, H.; Hoffmann, L.; Bohn, T. Bioaccessible and dialyzable polyphenols in selected apple varieties following in vitro digestion vs. native patterns. *Food Chem.* **2012**, *131*, 1466–1742. [[CrossRef](#)]
25. Yu, Y.; Zhang, B.; Xia, Y.; Li, H.; Shi, X.; Wang, J.; Deng, Z. Bioaccessibility and transformation pathways of phenolics compounds in processed mulberry (*Morus alba* L.) leaves after in vitro gastrointestinal digestion and faecal fermentation. *J. Funct. Foods* **2019**, *60*, 103406. [[CrossRef](#)]
26. D’Antuono, I.; Garbetta, A.; Linsalata, V.; Minervini, F.; Cardinali, A. Polyphenols from artichoke heads (*Cynara cardunculus* (L.) subsp. *scolymus* Hayek): In vitro bio-accessibility, intestinal uptake and bioavailability. *Food Funct.* **2015**, *6*, 1268–1277. [[CrossRef](#)]
27. Gutiérrez-Grijalva, E.P.; Angulo-Escalante, M.A.; León-Félix, J.; Heredia, B. Effect of in vitro digestion on the total antioxidant capacity and phenolic content of 3 species of oregano (*Hedeoma patens*, *Lippia graveolens*, *Lippia palmeri*). *J. Food Sci.* **2017**, *82*, 2832–2839. [[CrossRef](#)]
28. Song, Y.S.; Park, C.M. Luteolin and luteolin-7-O-glucoside strengthen antioxidative potential through the modulation of Nrf2/MAPK mediated HO-1 signaling cascade in RAW 264.7 cells. *Food Chem. Toxicol.* **2014**, *65*, 70–75. [[CrossRef](#)]
29. Shang, Y.F.; Kim, S.M.; Song, D.-G.; Pan, C.-H.; Lee, W.J.; Um, B.H. Isolation and identification of antioxidant compounds from *Ligularia fischeri*. *J. Food Sci.* **2010**, *75*, 530–535. [[CrossRef](#)] [[PubMed](#)]
30. Piazzini, V.; Monteforte, E.; Lucei, C.; Bigagli, E.; Bilia, A.R.; Bergonzi, M.C. Nanoemulsion for improving solubility and permeability of *Vitex agnus-castus* extract: Formulation and in vitro evaluation using PAMPA and Caco-2 approaches. *Drug Deliv.* **2017**, *24*, 380–390. [[CrossRef](#)] [[PubMed](#)]
31. Chen, Z.; Chen, M.; Pan, H.; Sun, S.; Li, L.; Zeng, S.; Jiang, H. Role of catechol-O-methyltransferase in the disposition of luteolin in rats. *Drug Metab. Dispos.* **2011**, *39*, 667–674. [[CrossRef](#)]
32. Čvorović, J.; Ziberna, L.; Fornasaro, S.; Tramer, F.; Passamonti, S. Bioavailability of Flavonoids: The Role of Cell Membrane Transporters. In *Polyphenols: Mechanisms of Action in Human Health and Disease*; Watson, R.R., Preedy, V.R., Zibadi, S., Eds.; Academic Press: Cambridge, MA, USA, 2018; pp. 295–320.
33. Zhou, W.; Shan, J.; Wang, S.; Cai, B.; Di, L. Trans epithelial transport of phenolic acids in *Flos lonicerae japonicae* in intestinal Caco-2 cell monolayers. *Food Funct.* **2015**, *6*, 3072–3080. [[CrossRef](#)] [[PubMed](#)]
34. Farrell, T.L.; Ellam, S.L.; Forreli, T.; Williamson, G. Attenuation of glucose transport across Caco-2 cell monolayers by a polyphenol-rich herbal extract: Interactions with SGLT1 and GLUT2 transporters. *Biofactors* **2013**, *39*, 448–456. [[CrossRef](#)] [[PubMed](#)]
35. Velderrain-Rodríguez, G.R.; Palafox-Carlos, H.; Wall-Medrano, A.; Ayala-Zavala, J.F.; Chen, C.O.; Robles-Sánchez, M.; Astiazaran-García, H.; Alvarez-Parrilla, E.; González-Aguilar, G.A. Phenolic compounds: Their journey after intake. *Food Funct.* **2014**, *5*, 189–197. [[CrossRef](#)]
36. Chan, E.W.C.; Wong, S.K.; Chan, H.T. Casticin from *Vitex* species: A short review on its anticancer and anti-inflammatory properties. *J. Integr. Med.* **2018**, *16*, 147–152. [[CrossRef](#)]
37. Garg, M.; Chaudhary, S.K.; Goyal, A.; Sarup, P.; Kumari, S.; Garg, N.; Vaid, L.; Shiveena, B. Comprehensive review on therapeutic and phytochemical exploration of diosmetin: A promising moiety. *Phytomed. Plus* **2022**, *2*, 100179. [[CrossRef](#)]
38. Gubbiaveranna, V.; Nagaraju, S. Ethnomedicinal, phytochemical constituents and pharmacological activities of *Tridax procumbens*: A review. *Int. J. Pharm. Pharm. Sci.* **2016**, *8*, 1–7.
39. Singleton, V.L.; Orthofer, R.; Lamuela-Reventos, R.M. Analysis of total phenols and other oxidation substrates and antioxidants by means of Folin-Ciocalteu reagent. *Methods Enzymol.* **1999**, *299*, 152–178.

40. Brand-Willians, W.; Cuvelier, M.E.; Berset, C. Use of a free radical method to evaluate antioxidant activity. *Lebensm. Wiss. Technol.* **1995**, *28*, 25–30. [[CrossRef](#)]
41. Uchida, M.; Fukazawa, T.; Yamazaki, Y.; Hashimoto, H.; Miyamoto, Y. A modified fast (4 day) 96-well plate Caco-2 permeability assay. *J. Pharmacol. Toxicol. Methods* **2009**, *59*, 39–43. [[CrossRef](#)]

## Article

# Resveratrol Inhibits Proliferation and Induces Autophagy by Blocking SREBP1 Expression in Oral Cancer Cells

Masakatsu Fukuda <sup>1,\*</sup>, Yudai Ogasawara <sup>2</sup>, Hiroyasu Hayashi <sup>2</sup>, Katsuyuki Inoue <sup>2</sup> and Hideaki Sakashita <sup>2</sup>

<sup>1</sup> Division of Biochemistry, Department of Oral Biology and Tissue Engineering, Meikai University School of Dentistry, Saitama 350-0283, Japan

<sup>2</sup> Division of Oral and Maxillofacial Surgery, Department of Diagnostic and Therapeutic Sciences, Meikai University School of Dentistry, Saitama 350-0283, Japan

\* Correspondence: fukudam@dent.meikai.ac.jp; Tel.: +81-49-285-5511; Fax: +81-49-285-6036

**Abstract:** Resveratrol is a polyphenolic antioxidant found in grapes, red wine, and peanuts and has been reported to have anti-neoplastic effects on various cancer types. However, the exact mechanism of its anti-cancer effects in oral cancer is not fully understood and remains controversial. Resveratrol exhibits strong hypolipidemic effects; therefore, we examined its effect on lipid metabolism in oral cancer. Resveratrol significantly reduced cell viability and induced autophagic cell death in oral cancer cells but not in normal cells. This selective effect was accompanied by significantly reduced lipogenesis, which is caused by downregulation of the transcription factor sterol regulatory element-binding protein 1 (SREBP1) gene, followed by downregulation of the epidermal fatty acid-binding protein (E-FABP). It was strongly suggested that resveratrol-induced autophagy resulted from the inhibition of SREBP1-mediated cell survival signaling. Luciferase reporter assay further indicated that resveratrol has a potent and specific inhibitory effect on SREBP1-dependent transactivation. Importantly, resveratrol markedly suppressed the growth of oral cancer cells in an animal xenograft model, without exhibiting apparent cytotoxicity. In conclusion, resveratrol induces autophagy in oral cancer cells by suppressing lipid metabolism through the regulation of SREBP1 expression, which highlights a novel mechanism of the anti-cancer effect of resveratrol.

**Keywords:** sterol regulatory element-binding protein 1; human oral squamous cell carcinoma; resveratrol; autophagy; epidermal fatty acid-binding protein

**Citation:** Fukuda, M.; Ogasawara, Y.; Hayashi, H.; Inoue, K.; Sakashita, H. Resveratrol Inhibits Proliferation and Induces Autophagy by Blocking SREBP1 Expression in Oral Cancer Cells. *Molecules* **2022**, *27*, 8250. <https://doi.org/10.3390/molecules27238250>

Academic Editor: Nour Eddine Es-Safi

Received: 17 October 2022

Accepted: 23 November 2022

Published: 26 November 2022

**Publisher's Note:** MDPI stays neutral with regard to jurisdictional claims in published maps and institutional affiliations.



**Copyright:** © 2022 by the authors. Licensee MDPI, Basel, Switzerland. This article is an open access article distributed under the terms and conditions of the Creative Commons Attribution (CC BY) license (<https://creativecommons.org/licenses/by/4.0/>).

## 1. Introduction

Human oral squamous cell carcinoma (HOSCC) is the most common oral mucosa cancer. According to the GLOBOCAN 2018, the number of incident cases for lip and oral cancer in the world was estimated at 354,864, with an age-standardized incidence rate of 5.8 for men and 2.3 for women per 100,000. GLOBOCAN also estimated 177,384 deaths, with an age-standardized mortality rate of 2.8 for men and 1.2 for women per 100,000 [1]. Lip and oral cancer are rated the fourth most common malignancy occurring worldwide in men (8.7 per 100,000) [1]. It is an aggressive malignant neoplasm that is difficult to cure using conventional approaches including radio-, chemo-, and surgical therapies. Since surgical treatment often profoundly affects the quality of life and daily activities of patients with HOSCC, the use of novel therapeutic strategies is desirable along with other conventional treatments.

One other thing to note here is that it is an energy metabolism on oral cancer. Energy metabolism, a phenomenon in which cancer cells meet the fuel requirements for proliferation and invasion in a severe tumor microenvironment, is a pivotal feature of cancers [2]. In addition to alterations in glucose metabolism, commonly termed the Warburg effect, cancer cells undergo a wide range of changes in other metabolic pathways, including mitochondrial biogenesis, macromolecule biosynthesis, pentose phosphate pathway, and

lipid metabolism [3–6]. Owing to their critical roles in tumor initiation, development, and metastasis, alterations in lipid metabolism, specifically fatty acid synthase (FAS), have been extensively studied in recent years [7,8]. FAS is a key enzyme involved in the synthesis of fatty acids (FAs) from acetyl-CoA, which is abundantly expressed in the liver and adipose tissue [9]. FAS has been reported to be overexpressed in several human cancers, including those of the lung, melanoma, prostate, breast, and oral cavity, and is associated with poor prognosis [10,11]. Furthermore, FAs are required for cancer cell proliferation to provide new phospholipids for cytomembranes [12]. FAs are intracellularly translocated through FA transporters, such as caveolin-1, fatty acid translocase (FAT/CD36), fatty acid transport proteins (FATP), and fatty acid-binding proteins (FABPs) [12]. FABPs can bind long-chain FAs and comprise a family of cytosolic proteins with over 10 isoforms [13]. Specifically, epidermal FABP (E-FABP) was first isolated from the epidermis, and is expressed in tissues throughout the body [14,15]. Additionally, E-FABP is associated with malignant neoplasms [16]. Studies suggest that cancer cells exhibit a unique behavior in lipid metabolism; for example, while most normal mature cells acquire FAs from the bloodstream, neoplasm cells exhibit increased de novo FA biosynthesis, most of which is modulated by sterol regulatory element-binding protein 1 (SREBP1) [17,18]. SREBP is a transcription factor and a master regulator of genes involved in regulating FA synthesis and uptake [19].

Over the last two decades, preclinical, epidemiological, and early phase clinical trials have shown a promising role of selected dietary constituents in decreasing the incidence of multiple cancers [20–22]. Considering the potential of such phytochemicals, it is essential to identify and develop new broad-spectrum chemopreventive agents that can be used either alone or in combination against cancer. Phytochemicals from natural sources, such as resveratrol, have recently gained interest as anticancer drugs with fewer side effects in patients with oral cancer [23].

Resveratrol (3,4',5-trihydroxy-trans-stilbene) is a polyphenolic compound found abundantly in food and plants [23–25]. It has a wide spectrum of pharmacological bioactivities, including suppression of lipid metabolism as well as anti-inflammatory, anti-atherosclerotic, antioxidant, and antitumor properties [23,26]. Many preclinical studies have shown that resveratrol induces cancer cell death through apoptosis and autophagy [27–29], thereby exerting both preventive and therapeutic effects on cancers. Although resveratrol modulates various steps of carcinogenesis and development, the underlying mechanisms of its anti-cancer effects leading to apoptosis and autophagy are unclear in human oral cancer cells. Therefore, the present study aimed to elucidate the fundamental mechanism of the anti-cancer effects of resveratrol on oral cancer cells through modulation of lipid metabolism and, consequently, clarify a potential target for chemoprevention of oral cancer, in vitro and in vivo.

## 2. Results

### 2.1. Gene Expression Levels of E-FABP and SREBP1 in HOSCC Cell Lines

E-FABP acts as a transporter of FAs which are required for cancer cell proliferation to provide new phospholipids for cytomembranes and that SREBP is a master regulator of genes involved in regulating FA synthesis and uptake. Then, differences in E-FABP and SREBP1 gene expression levels in HOSCC cell lines (HSC-2, HSC-3, HSC-4, Ca9-22, and SAS) were firstly analyzed by qRT-PCR. The results showed that Ca9-22 cells had the highest levels of E-FABP and SREBP1 mRNA expression among the HOSCC cell lines (Figure 1).

### 2.2. Expression of E-FABP and SREBP1 Protein in HOSCC Cell Lines

SDS-solubilized extracts of HOSCC cell lines were subjected to immunoblot analysis to determine E-FABP and SREBP1 protein expression and quantity. Results revealed that all the HOSCC cell lines expressed E-FABP and SREBP1, with the highest levels in Ca9-22

cells (Figure 2). Based on these results, Ca9-22 cells derived from gingival cancer were used to further study the cellular mechanisms.

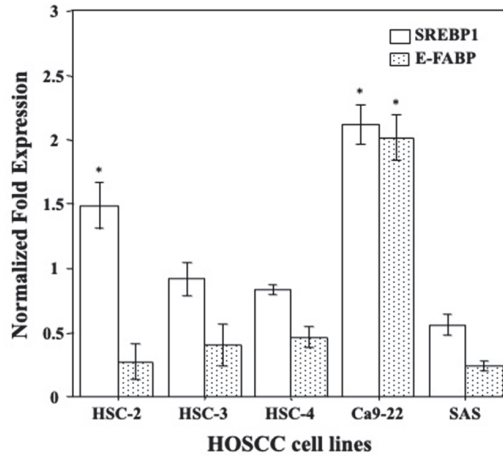


**Figure 1.** Differences in the levels of SREBP1 and E-FABP mRNA expression in HOSCC cell lines. Ca9-22 cells had the highest levels of SREBP1 and E-FABP mRNA expression. Each column and error bar represent the mean values  $\pm$  SD of three independent experiments. All *p*-values: \* *p* < 0.05 compared to relative internal control.

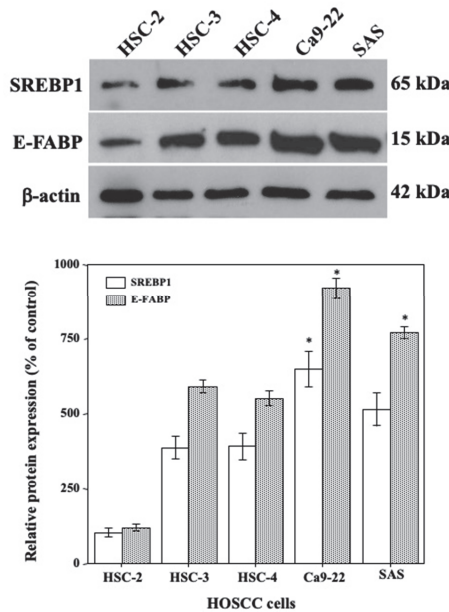


**Figure 2.** Expression profiles of E-FABP and SREBP1 proteins in HOSCC cell lines. SREBP1 and E-FABP are expressed in all HOSCC cells as 65 and 15 kDa peptides, respectively, with the highest expression levels in Ca9-22 cells. Blots are representative of *n* = 3 biological replicates. *p*-values: \* *p* < 0.05 compared to  $\beta$ -actin control.



### 2.3. Impact of Resveratrol on Tumor Cell Growth

We performed a cell viability assay to examine whether resveratrol induced cell death in the Ca9-22 cells. As shown in Figure 3A, cell viability showed a significant time- and dose-dependent reduction in Ca9-22 cells upon treatment with resveratrol. Additionally, we compared the effects of resveratrol on Ca9-22 and NGE cells after 24 h of treatment with 0 and 50  $\mu\text{M}$  resveratrol (Figure 3B). The results showed that Ca9-22 cells underwent morphological changes unlike NGE cells. Moreover, resveratrol treatment had a cytotoxic effect on the Ca9-22 cells. To confirm whether Ca9-22 cell death resulted from apoptosis, the levels of procaspase cleavage to active caspase-8, -9, and -3/7 (markers of apoptotic activity) were analyzed. The results demonstrated decreased levels of all markers in response to resveratrol for 24 h in a dose-dependent manner, indicating that resveratrol did not cause apoptosis in Ca9-22 cells (Figure 3C). We suspected that cell death was caused by other mechanisms, such as autophagy.

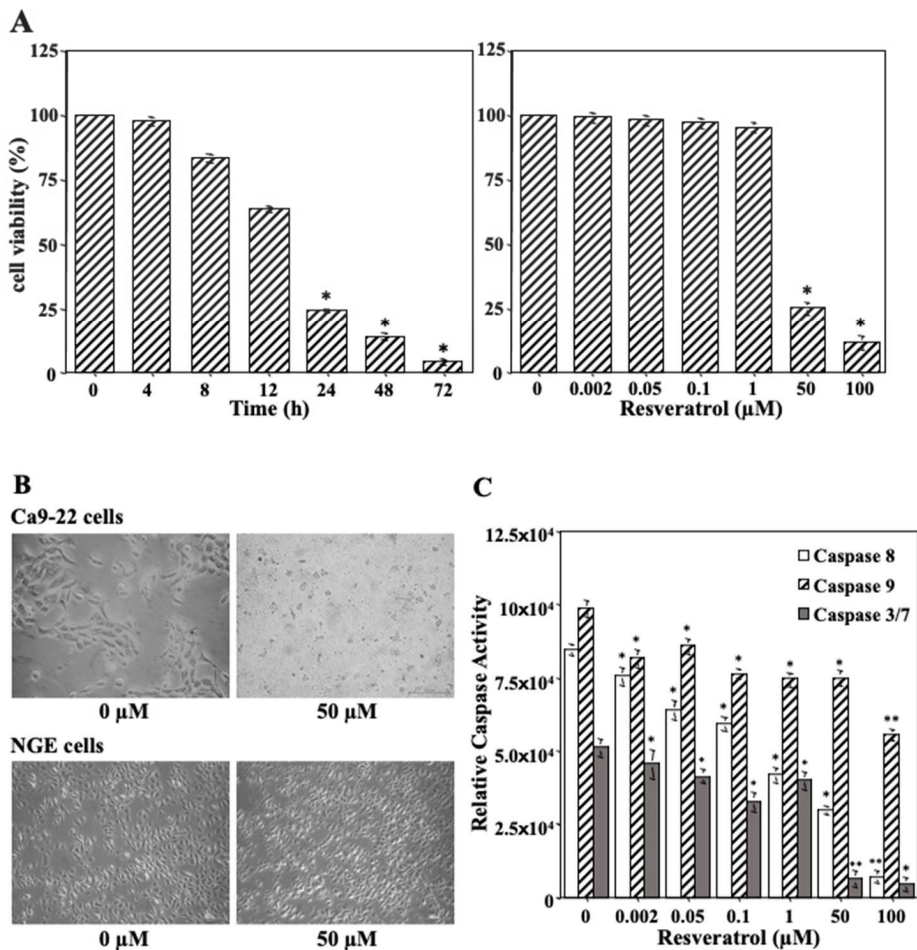


**Figure 3.** Effect of resveratrol on cell viability, morphological characteristics, and apoptotic cell death in Ca9-22 cell line. (A) Cell viability showed a significant time- and dose-dependent reduction in Ca9-22 cells upon treatment with 50  $\mu\text{M}$  of resveratrol for various hours and with various concentrations

of resveratrol for 24 h. Each column and error bar represent the mean values  $\pm$  SD of three independent experiments. \*  $p < 0.05$  compared to untreated control. (B) Ca9-22 cells treated with 50  $\mu$ M of resveratrol for 24 h and observed for the morphological changes. (C) Levels of all markers were decreased in response to resveratrol for 24 h in a dose-dependent manner, indicating that resveratrol did not cause apoptosis in Ca9-22 cells. Each column and error bar represent the mean values  $\pm$  SD of three independent experiments. All  $p$ -values: \*  $p < 0.05$ , \*\*  $p < 0.01$  compared to untreated control. NGE cells: normal gingival epithelial cells.

#### 2.4. Resveratrol-Mediated Induction of Autophagic Death in Ca9-22 Cells

To investigate the effect of resveratrol on the expression of autophagy-related markers (p62, Beclin1, and LC3) in oral cancer cells, proteins extracted from Ca9-22 cell cultures were treated with various non-cytotoxic concentrations (2–100  $\mu$ M) of resveratrol and for various time periods (0, 4, 8, 12, 24, 48, and 72 h) that were quantified using immunoblot analysis. The relative levels of p62, Beclin1, and LC3-II gradually increased after treatment with resveratrol for 24 h in a dose-dependent manner (Figure 4A). A time-course analysis of these markers in Ca9-22 cells treated with 50  $\mu$ M resveratrol (Figure 4B) revealed that p62, Beclin1, and LC3-II proteins were constitutively induced in Ca9-22 cells with a gradual increase in their relative quantities in a time-dependent manner, showing the highest levels at 24 h, followed by a gradual decrease up to 72 h. These findings strongly suggested that resveratrol induces autophagy in Ca9-22 cells in a dose-dependent manner.

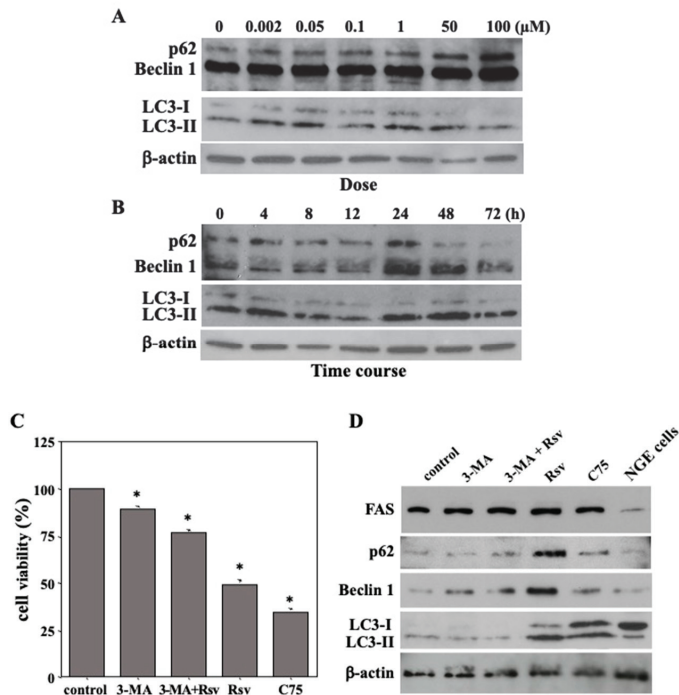
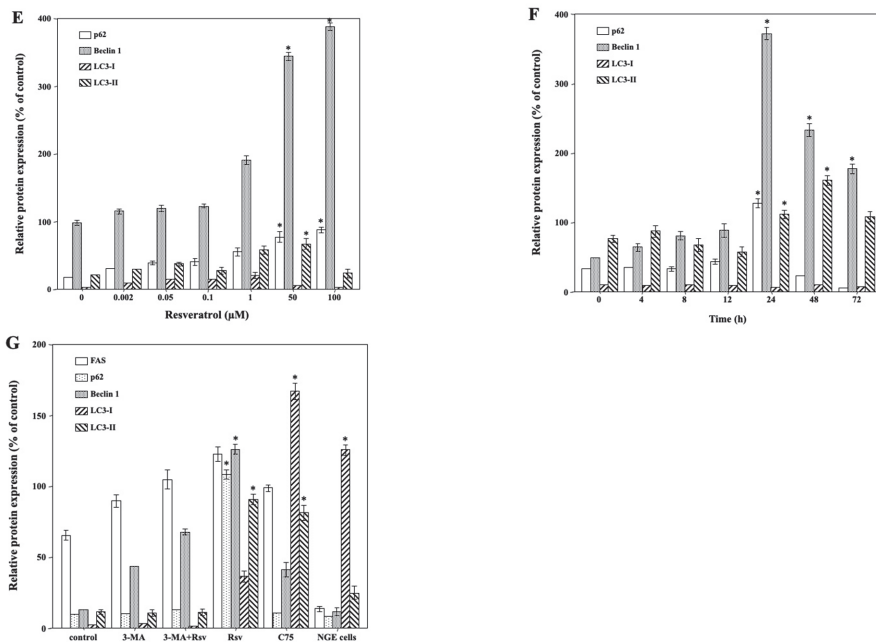


Figure 4. Cont.



**Figure 4.** Resveratrol-induced autophagic cell death in Ca9-22 cells. (A) Relative levels of p62, Beclin1, and LC3-II gradually increased in a dose-dependent manner after treatment with various concentrations (0, 2 nM, 50 nM, 100 nM, 1 μM, 50 μM, and 100 μM) of resveratrol for 24 h. (B) Relative levels of p62, Beclin1, and LC3-II proteins were gradually increased after treatment with 50 μM of resveratrol for various time periods (0, 4, 8, 12, 24, 48, and 72 h) in Ca9-22 cells in a time-dependent manner, showing the highest levels at 24 h, followed by a gradual decrease up to 72 h. (C) Cells were treated with 50 μM of resveratrol, 2 mM of 3-MA or C75 for 24 h. Cell viability was reduced in response to resveratrol; however, pre-treatment with 3-MA inhibited resveratrol-induced cell death. Each column and error bar represent the mean values  $\pm$  SD of three independent experiments. \*  $p < 0.05$  compared to untreated control. (D) Although autophagy-related proteins were markedly increased by resveratrol treatment, 3-MA pretreatment almost completely blocked their expression in Ca9-22 cells. (E) The band intensities of (A) are graphically represented as the relative expressions of p62, Beclin1, and LC3-I,II/ $\beta$ -actin. (F) The band intensities of (B) are graphically represented as the relative expressions of p62, Beclin1, and LC3-I,II/ $\beta$ -actin. (G) The band intensities of (D) are graphically represented as the relative expressions of p62, Beclin1, and LC3-I,II/ $\beta$ -actin. Immunoblots are representative of  $n = 3$  biological replicates. All  $p$ -values: \*  $p < 0.05$  compared to  $\beta$ -actin control. 3-MA: 3-Methyladenine; Rsv: resveratrol; C75: fatty acid synthase (FAS) inhibitor; NGE cells: normal gingival epithelial cells.

To confirm whether resveratrol induced specifically autophagic cell death in Ca9-22 cells, an inhibition assay was performed. Ca9-22 cells were pretreated with 2 mM 3-MA [30], an autophagy inhibitor, for 1 h before exposure to 50 μM resveratrol, for 24 h. The results showed that cell viability was reduced in response to resveratrol; however, pretreatment with 3-MA inhibited resveratrol-induced cell death (Figure 4C). Moreover, treatment with C75, an FAS inhibitor, caused strong cell death in Ca9-22 cells. Additionally, p62, Beclin1, and LC3 expression levels were evaluated by immunoblot analysis. Although autophagy-related proteins were markedly increased by resveratrol treatment, 3-MA pretreatment almost completely blocked their expression in Ca9-22 cells (Figure 4D). Interestingly, increased levels of autophagy-related markers were not observed in resveratrol-treated NGE cells. Therefore, resveratrol may exert tumor-specific cytotoxic effects. These results indicated that autophagic cell death in Ca9-22 cells was indeed a result of resveratrol treat-

ment. It should be noted that, although C75 treatment reduced FAS expression, resveratrol had no effect on FAS expression, despite inducing autophagic cell death in Ca9-22 cells. Accordingly, we focused on E-FABP as a potential therapeutic target.

### 2.5. SREBP1 Regulated E-FABP Expression in Ca9-22 Cells

To investigate the regulatory mechanism of proliferative activity in Ca9-22 cells, we analyzed SREBP1 and E-FABP expression levels in cells treated with TNF- $\alpha$  or resveratrol by immunoblot analysis. The results revealed that the levels of SREBP1 and E-FABP proteins were up- and down-regulated, respectively, in response to TNF- $\alpha$  and resveratrol, compared to those in the control cells (Figure 5A). Hence, we speculated that SREBP1, a nuclear transcription factor related to lipid metabolism, regulates E-FABP expression in Ca9-22 cells. We examined this hypothesis via inhibition of SREBP1 expression of using siRNA. SREBP1 knockdown was confirmed by immunoblot analysis (Figure 5B). Subsequently, we assessed the effect of SREBP1 knockdown on E-FABP expression and found that its protein levels were greatly reduced in SREBP1-knockdown Ca9-22 cells compared to those in control-siRNA transfected or control cells (Figure 5B). Simultaneously, the results of E-FABP knockdown demonstrated that it did not lead to downregulation of SREBP1 expression (Figure 5C) or Ca9-22 cell death (Figure 5D). Collectively, these data indicate that the downregulation of E-FABP is induced via suppression of SREBP1 activity by resveratrol. In other words, resveratrol downregulated SREBP1, which, in turn, regulated E-FABP expression and induced autophagic cell death in Ca9-22 cells.

### 2.6. Resveratrol Inhibits TNF- $\alpha$ -Mediated SREBP1 Activation in Ca9-22 Cells

To examine the TNF- $\alpha$ -mediated regulation of SREBP1 expression in Ca9-22 cells, we performed immunoblotting followed by densitometric analyses. The results revealed that SREBP1 protein initially localized in the cytoplasm of control (untreated) Ca9-22 cells (Figure 6A), then it was transported to the nucleus upon stimulation with TNF- $\alpha$  for 30 min (Figure 6B). However, the time-course analysis of SREBP1 protein expression up to 24 h demonstrated a gradual decrease in nuclear translocation. The regulation of SREBP1 expression in Ca9-22 cells after resveratrol treatment was also analyzed. SREBP1 was primarily localized in the cytoplasm, with small quantities detected in the cell membrane and nucleus upon stimulation with resveratrol for 30 min (Figure 6C). We examined the effect of resveratrol on TNF- $\alpha$ -induced nuclear translocation of SREBP1 by immunoblot analysis. SREBP1 translocation to the nucleus was detected in Ca9-22 cells stimulated with TNF- $\alpha$  (10 ng/mL) and resveratrol (50  $\mu$ M) for 30 min (Figure 6D); however, it was markedly inhibited, compared to that in cells treated with TNF- $\alpha$  alone. Collectively, these results showed inhibition of the nuclear translocation of SREBP1 in resveratrol-treated Ca9-22 cells.

To investigate the effects of TNF- $\alpha$  and resveratrol on SREBP1-dependent transcriptional activity in Ca9-22 cells, a luciferase reporter assay was performed. The results revealed strong luciferase activity induced by TNF- $\alpha$  (Figure 6E). Additionally, the maximum SRE-dependent transcription was observed after treatment with 10 ng/mL of TNF- $\alpha$ , at 4 h (without further increase thereafter), which induced a five-fold increase in luciferase activity compared to that in cells without TNF- $\alpha$ . Meanwhile, the LDLR-Luc reporter construct with a single nucleotide mutation within SRE did not respond to TNF- $\alpha$  (Figure 6F), suggesting that the increase in luciferase activity was completely dependent on the presence of SRE sites. Moreover, luciferase activity in Ca9-22 cells decreased with time after 1 h of resveratrol (50  $\mu$ M) treatment (Figure 6E), with the maximum inhibition (10-fold) at 24 h. In addition, resveratrol inhibited luciferase activity induced by TNF- $\alpha$  in a time-dependent manner (Figure 6E). Similarly, the level of luciferase activity was dependent on the presence of SRE sites, as mentioned above, as the LDLR-Luc reporter construct with a single nucleotide mutation within the SRE did not respond to resveratrol (Figure 6F). Collectively, these data indicated that resveratrol has a specific and potent inhibitory effect on SREBP1-dependent transactivation.

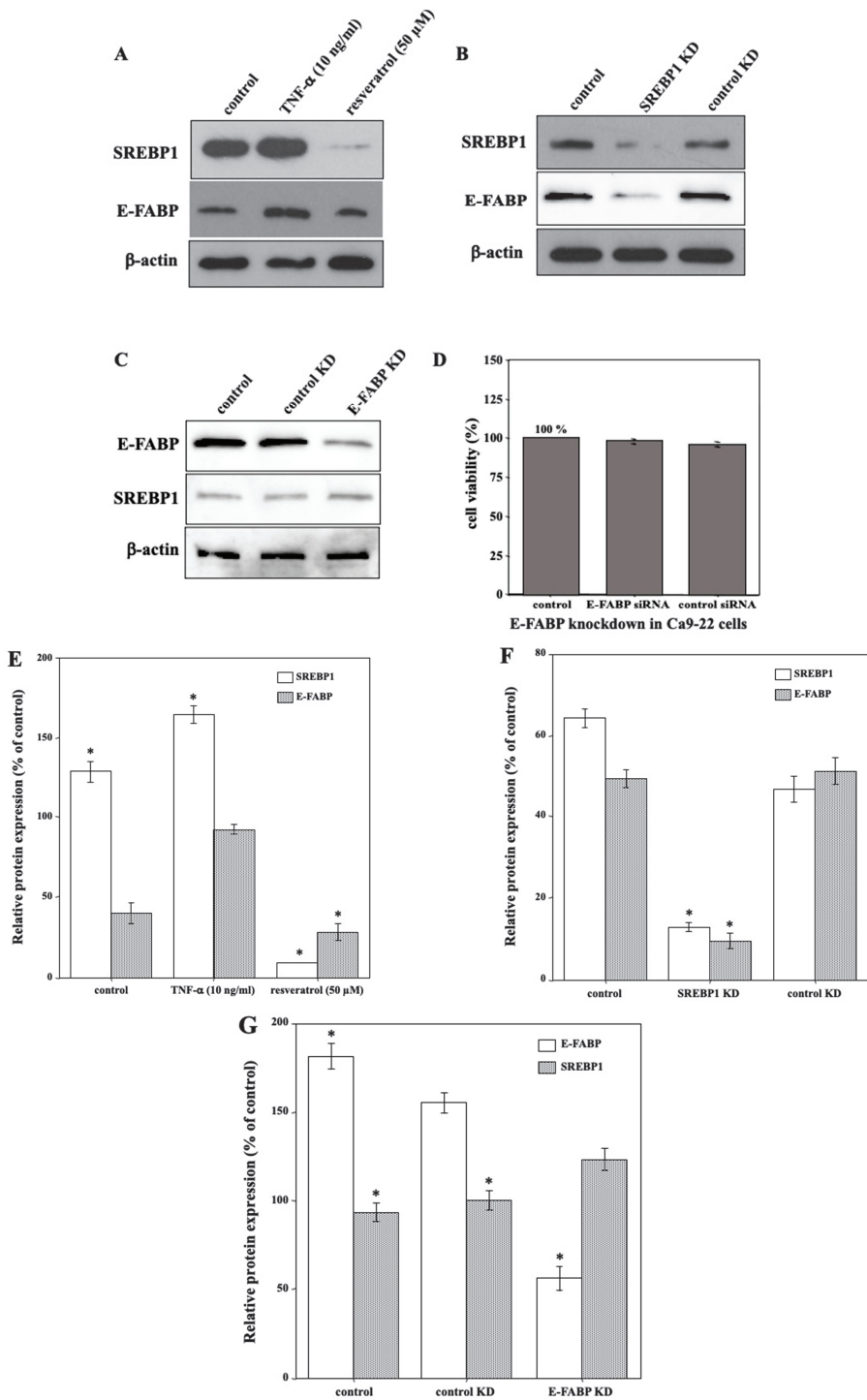
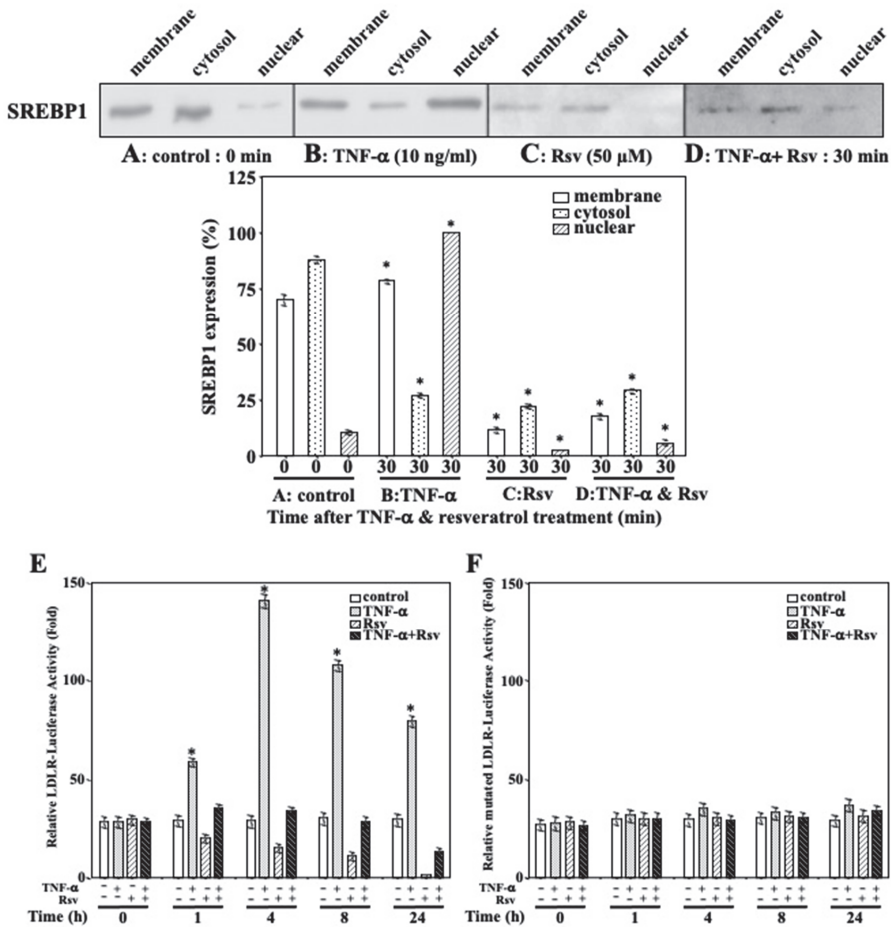


Figure 5. SREBP1 regulates E-FABP expression in Ca9-22 cells. (A) The levels of SREBP1 and E-FABP

proteins were upregulated in response to 10 ng/mL TNF- $\alpha$ , and they were downregulated in response to 50  $\mu$ M resveratrol for 24 h, respectively, compared to those in the control cells. (B) SREBP1 and E-FABP protein levels were markedly reduced by siRNA in Ca9-22 cells compared to those in control siRNA-transfected or control cells. (C) E-FABP knockdown did not lead to downregulation of SREBP1 expression. (D) E-FABP knockdown did not induce Ca9-22 cell death either. (E) The band intensities of (A) are graphically represented as the relative expressions of SREBP1, and E-FABP/ $\beta$ -actin. (F) The band intensities of (B) are graphically represented as the relative expressions of SREBP1, and E-FABP/ $\beta$ -actin. (G) The band intensities of (C) are graphically represented as the relative expressions of E-FABP, and SREBP1/ $\beta$ -actin. Each column and error bar represent the mean values  $\pm$  SD of three independent experiments. Immunoblots are representative of  $n = 3$  biological replicates. All  $p$ -values: \*  $p < 0.05$  compared to  $\beta$ -actin control.

### 2.7. Suppression of Tumor Growth, Inhibition of SREBP1 and E-FABP mRNA Expression, and Induction of Autophagy in the Tumor Mass of Resveratrol-Treated Nude Mice

We examined the effects of resveratrol on tumor development *in vivo*, using a nude mouse model. Mice were injected subcutaneously with Ca9-22 ( $1 \times 10^6$  cells; Figure 7A–C), and the effects of resveratrol on the extent of Ca9-22 tumor mass were evaluated after 8 weeks. The mice were euthanized, and the tumor mass was histopathologically examined. As demonstrated in Table 1, resveratrol not only prevented tumor growth, but also reduced tumor volume in a dose-dependent manner. One mouse from the control group (1/10) died unexpectedly. As shown in Figure 7D, histopathological findings revealed that the tumor mass was composed of various stratified squamous tumor cells arranged as islands with different shapes and sizes, with keratinous pearls inside. Additionally, some of the cells were acidophilic with pyknotic nuclei and karyolysis, while the rest had nuclei of different shapes and sizes, larger than the nuclei of the normal epithelium. Infiltration of inflammatory small round cells was also observed in the peritumoral stroma. After treatment with 50  $\mu$ M resveratrol, the Ca9-22 tumor mass in 6 out of 10 mice was resolved. Although a tumor mass was observed in the remaining 4 mice, a clear regression of the Ca9-22 tumor mass with marked morphological changes, including autophagic vacuoles of cancer tissue (Figure 7E,F), was evident (Table 1). At the highest dose of resveratrol (100  $\mu$ M per day), the Ca9-22 tumor mass was completely resolved when  $1 \times 10^6$  Ca9-22 cells were injected subcutaneously (none of the 10 mice showed a detectable tumor mass; Table 1 and Figure 7G). Moreover, injecting a higher number of Ca9-22 cells ( $1 \times 10^7$ ) resulted in similar effects as resveratrol on the prevention of tumor growth. Next, the mRNA expression of SREBP1, E-FABP, and p62/SQSTM1 was evaluated by RNAscope ISH in the Ca9-22 tumor mass. While SREBP1 and E-FABP mRNAs were widely expressed with similar distribution patterns (Figure 8A,B), p62/SQSTM1 mRNA showed modest expression (Figure 8C) in the tumor mass without resveratrol treatment. In contrast, Ca9-22 tumor masses treated with 50  $\mu$ M resveratrol showed markedly reduced expression of SREBP1 and E-FABP mRNAs (Figure 8E,F), whereas p62 mRNA was expressed only slightly (Figure 8G). To further confirm whether this reduction in cancer tissue was caused by autophagic cell death, the protein expression level of p62/SQSTM1, an autophagy-specific substrate, was examined using immunohistochemistry. We observed high levels of p62 immunoreactivity in the control mice without resveratrol treatment (Figure 8D), whereas it was almost completely absent in Ca9-22 tumor masses treated with 50  $\mu$ M resveratrol (Figure 8H). These findings indicate that resveratrol effectively reduced SREBP1 and E-FABP expression and induced autophagic cell death in Ca9-22 tumor masses in nude mice.



**Figure 6.** Effect of resveratrol on TNF- $\alpha$ -mediated SREBP1 activation in Ca9-22 cells. SREBP1 protein expression in the different cellular fractions was tested with immunoblotting in control (untreated) Ca9-22 cells (A), cells treated with 10 ng/mL TNF- $\alpha$  for 30 min (B), Ca9-22 cells stimulated with 50  $\mu$ M resveratrol for 30 min (C), and Ca9-22 cells stimulated with TNF- $\alpha$  (10 ng/mL) and resveratrol (50  $\mu$ M) for 30 min (D). Immunoblots are representative of  $n = 3$  biological replicates. Each column and error bar represent the mean values  $\pm$  SD of three independent experiments. \*  $p < 0.05$  compared to untreated control. (E) Maximum SRE-dependent transcription was observed with 10 ng/mL of TNF- $\alpha$  at 4 h, which induced a five-fold increase in luciferase activity compared with that in cells without TNF- $\alpha$ . Moreover, luciferase activity in Ca9-22 cells decreased with time after one hour of resveratrol (50  $\mu$ M) treatment, with maximum inhibition (10-fold) at 24 h. Additionally, resveratrol inhibited luciferase activity induced by TNF- $\alpha$  in a time-dependent manner. (F) the LDLR-Luc reporter construct with a single nucleotide mutation within SRE did not respond to TNF- $\alpha$  and/or resveratrol. Each column and error bar represent the mean values  $\pm$  SD of three independent experiments. All  $p$ -values: \*  $p < 0.05$  compared to untreated control.

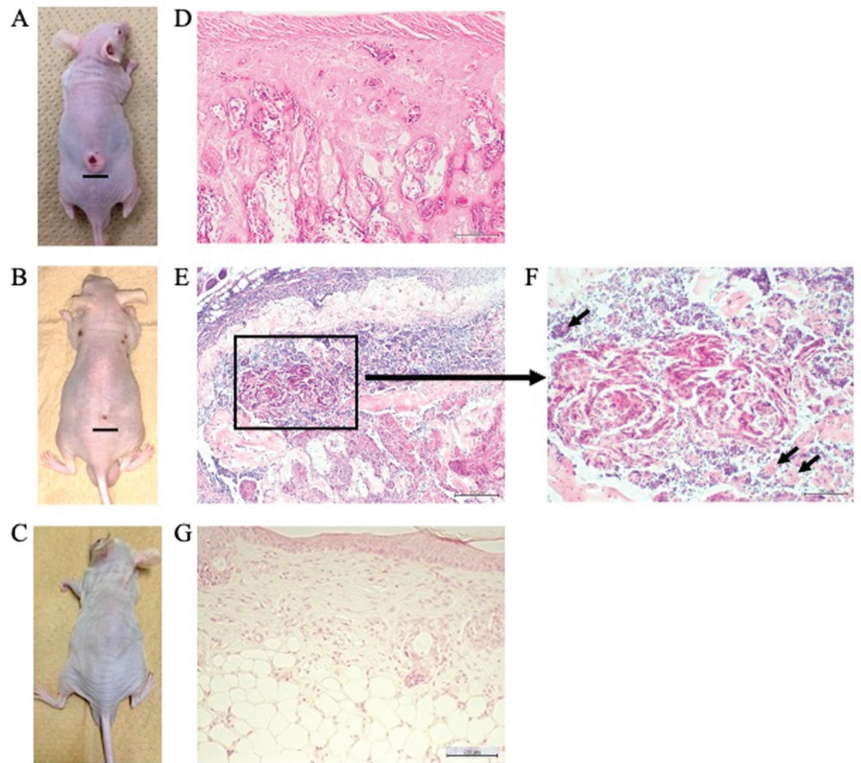


**Figure 7.** Suppression of growth in the Ca9-22 tumor mass of resveratrol-treated nude mice. Tumor appearance in mice after eight weeks of Ca9-22 cell inoculation, and five weeks of saline (control) administration (A), 50  $\mu\text{M}$  of resveratrol (B) or 100  $\mu\text{M}$  of resveratrol (C) administration. Scale bar = 10 mm. (D) Histopathological findings revealed that the tumor mass was composed of various stratified squamous tumor cells, arranged as islands with different shapes and sizes, with keratinous pearls inside (Hematoxylin and eosin (H-E) stain; scale bar = 200  $\mu\text{m}$ , original magnification  $\times 40$ ). (E) Treatment with 50  $\mu\text{M}$  of resveratrol resulted in marked morphological changes in which Ca9-22 tumor masses had formed (H-E stain; scale bar = 200  $\mu\text{m}$ , original magnification  $\times 40$ ). (F) Marked morphological changes were observed, including formation of autophagic vacuoles in Ca9-22 tumor mass indicated by arrows (H-E stain; scale bar, 200  $\mu\text{m}$ , original magnification  $\times 100$ ). (G) At the highest dose of resveratrol (100  $\mu\text{M}/\text{day}$ ), the Ca9-22 tumor mass is completely resolved when  $1 \times 10^6$  Ca9-22 cells were injected subcutaneously (H-E stain; scale bar = 200  $\mu\text{m}$ , original magnification  $\times 40$ ).

**Table 1.** Effect of resveratrol at 8 weeks after subcutaneous inoculation of Ca9-22 cells ( $1 \times 10^6$  cells) in nude mice.

	Control (Saline)	Resveratrol ( $\mu\text{M}/\text{Day}$ )	
		50	100
Animals with tumor formation, n (%)	9/10 (90%)	4/10 (40%)	* 0/10 (0%) **
Tumor volume #, $\text{mm}^3$	$608.9 \pm 11.82$ (100%)	$55.28 \pm 2.87$ (9.08%)	* 0 (0%) **

A mouse in the control group (1/10) died unexpectedly. # Tumor volume was calculated as  $\text{width}^2 \times \text{length} \times 0.5$  and values represent mean  $\pm$  SD (% relative to control). \*  $p < 0.05$ , \*\*  $p < 0.001$  (compared to the control).



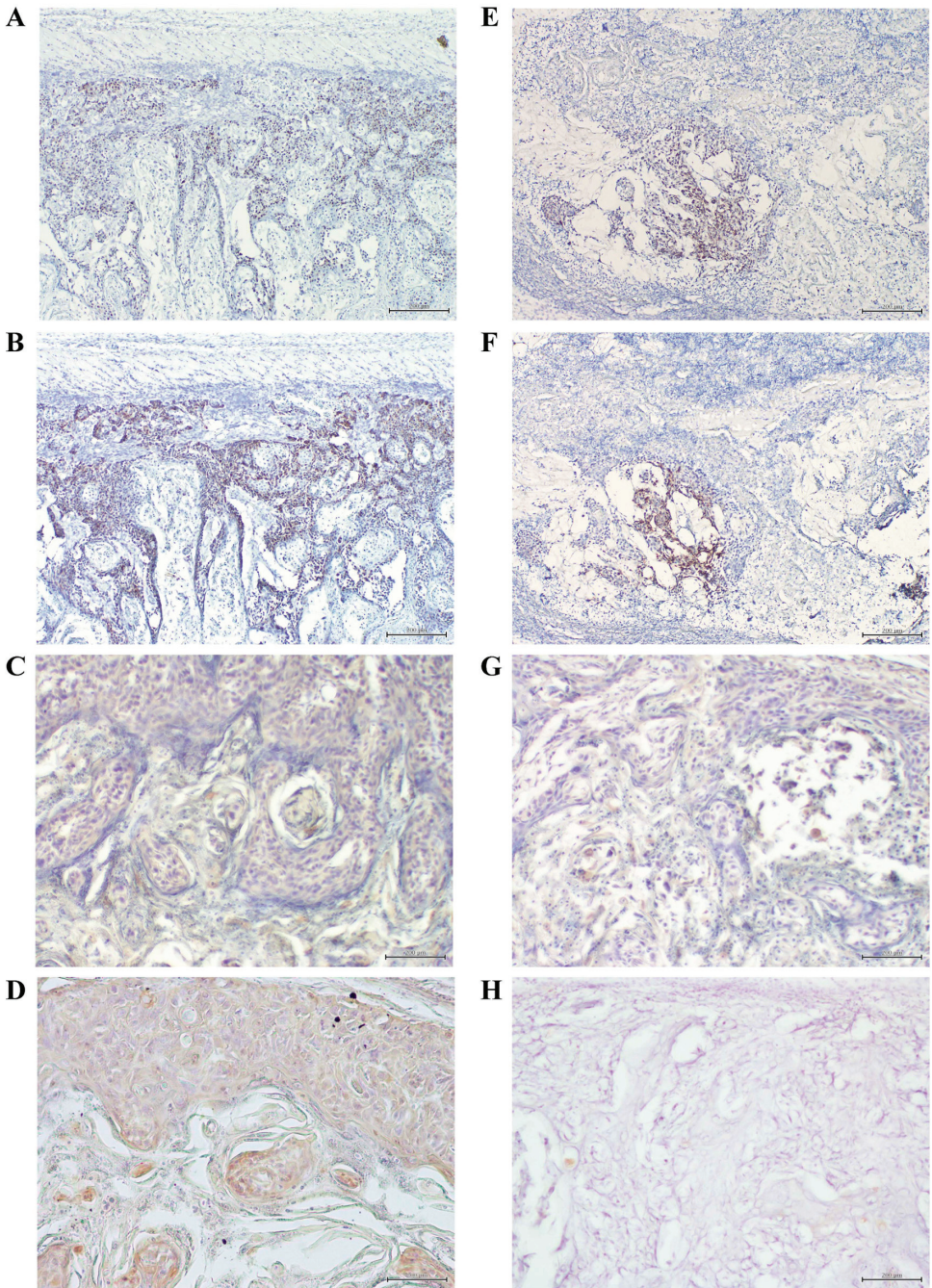
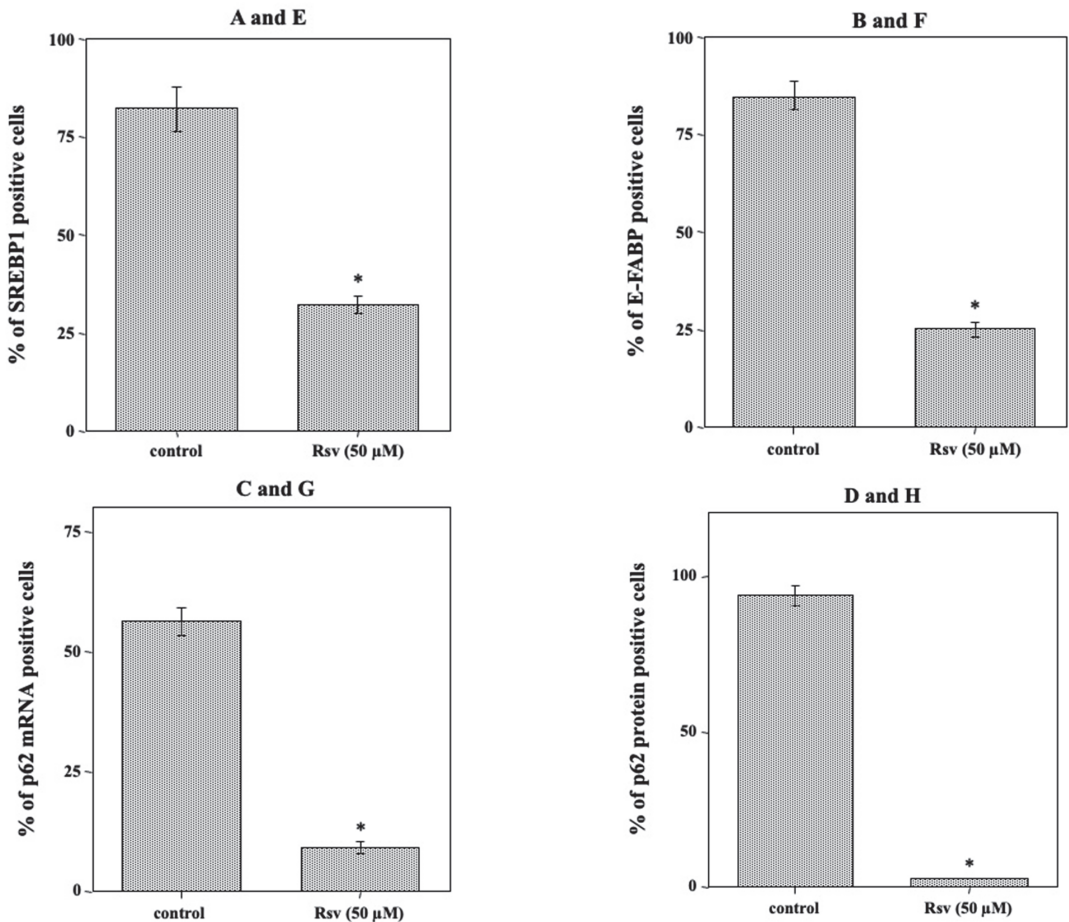


Figure 8. Cont.



**Figure 8.** Inhibition of SREBP1 and E-FABP mRNA expression and induction of autophagy in the Ca9-22 tumor mass of resveratrol-treated nude mice. Expressions of both SREBP1 (A) and E-FABP (B) mRNAs were extensively detected with higher levels in Ca9-22 tumor mass by RNAscope ISH (Scale bar = 200 μm, original magnification ×40) in control (not exposed to resveratrol). In Ca9-22 tumor treated with 50 μM of resveratrol, expressions of both SREBP1 (E) and E-FABP (F) mRNAs were extremely restricted (Scale bar = 200 μm, original magnification ×40). ISH revealed slight expression of p62 mRNA in resveratrol-treated tumor (G), compared to that in the control (C) (Scale bar = 200 μm, original magnification ×40). Immunohistochemistry revealed high levels of p62 immunoreactivity in untreated control (D), compared with that in Ca9-22 tumor mass treated with 50 μM of resveratrol (H) (Scale bar = 200 μm, original magnification ×40). Image analyses of SREBP1, E-FABP and p62 expression in resveratrol-treated Ca9-22 tumor mass was determined using ImageJ program. All *p*-values: \* *p* < 0.05 compared to untreated control.

### 3. Discussion

Resveratrol is a multifunctional polyphenol with various biological activities [28,29]. It is well documented that resveratrol can suppress the expression of genes related to lipid metabolism [31,32] and induce both autophagy and apoptosis in human cancer cells [27–29]. Although SREBPs are well known as master regulators of lipid metabolism [24], it is unclear whether resveratrol inhibits the action of SREBP in human oral cancer cells.

In the present study, we highlighted the SREBP1-associated effect of resveratrol on tumor growth and invasion in oral cancer using an *in vitro* cell culture and an *in vivo* nude mouse cancer model. First, our results indicate that resveratrol induced autophagic cell death, but not apoptosis, in Ca9-22 cells. Therefore, the results of our study are inconsistent with previous findings. Moreover, our results showed that the expression of FAS was not downregulated in resveratrol-treated Ca9-22 cells; therefore, we changed the target from FAS to E-FABP. In addition, resveratrol was highly selective for cancer cells. The cause of this selective cytotoxic effect of resveratrol on cancer cells, but not against NGE cells, remains elusive. Despite an extensive review of the available literature, we found no precise explanation for the mechanism underlying this selective effect exerted by resveratrol on non-cancer cells. We hypothesized that NGE cells do not undergo rigorous lipid metabolism, unlike cancer cells, and have low expression levels of SREBP1, E-FABP, and FAS; therefore, they do not serve as appropriate targets for resveratrol-mediated antioxidative activity.

According to previous studies, SREBPs serve as a key link between lipid metabolism and inflammation, energy stress, cell growth, nutrition, and other pathological and physiological processes [33]. Moreover, TNF- $\alpha$  stimulates SREBP1 activation via a caspase-dependent pathway in HepG2 cells derived from hepatocellular carcinoma [34]. In the present study, we used TNF- $\alpha$  to activate SREBP1 in Ca9-22 cells, to mimic the local inflammatory response in the invasive front of cancer, as some tumor cells were reported to produce TNF- $\alpha$  [35]. The results demonstrated that TNF- $\alpha$ -mediated activation of SREBP1 regulates E-FABP expression, as evidenced by the increased E-FABP expression in TNF- $\alpha$ -stimulated Ca9-22 cells and decreased E-FABP expression after SREBP1 knockdown. Additionally, it is known that nuclear translocation of the E-FABP protein mediated by lipid ligands can activate transcription factors, including SREBPs and PPARs, to initiate proliferative signaling in several cancer models [36]. Therefore, we examined SREBP1 expression in response to E-FABP knockdown in the Ca9-22 cells. These results indicated that SREBP1 expression remained unaffected, and cell death was not induced. Collectively, these findings are consistent with those of previous reports and validate our data. There are several reports available on SREBP1-mediated regulation of FAS expression [8,19]; however, we did not find sufficient reports highlighting the regulation of E-FABP expression by SREBP1. This is the first report of SREBP1-mediated regulation of E-FABP expression. We further found that TNF- $\alpha$ -mediated SREBP1 activation was blocked by resveratrol, suggesting that resveratrol interferes with the TNF- $\alpha$  signal transduction cascade at the initial step. Resveratrol treatment also inhibits the translocation of SREBP1 to the nucleus. Thus, two separate lines of evidence allowed us to conclude that resveratrol is a specific and potent inhibitor of SREBP1 activation in Ca9-22 cells: (a) resveratrol inhibited TNF- $\alpha$ -induced nuclear transactivation of SREBP1, and (b) resveratrol suppressed SREBP1-dependent transcription. Indeed, it has been described that SREBP1 regulates the expression of genes associated with lipid metabolism, including FASN, acetyl-CoA carboxylase 1 (ACC1), SCD1, and LDLR [37]. However, we believe that E-FABP may be an additional SREBP target. Therefore, downregulation of SREBP1 could result in the suppression of crucial effects on lipid metabolism. This study suggests that in oral cancers, resveratrol has suppressive effects of lipid metabolism and anti-cancer activities but that these results need to be confirmed using more cell lines as well as other animal models.

## 4. Materials and Methods

### 4.1. Reagents

Immunoblot analysis of E-FABP was performed using a mouse anti-human E-FABP monoclonal antibody (Mab E-FABP, #sc-365236; Santa Cruz Biotechnology, Santa Cruz, CA, USA) as the primary antibody. Rabbit anti-human p62 polyclonal antibody (Pab p62, #PM045Y), rabbit anti-human Beclin1 polyclonal antibody (Pab Beclin1, #PD017Y), and mouse anti-human LC3 monoclonal antibody (Mab LC3, #M186-3Y) were procured from Medical and Biological Laboratories (Nagoya, Japan). Rabbit anti-human sterol regulatory element-binding protein 1 monoclonal antibody (Mab SREBP1, #NB600-582) was procured

from Novus Biologicals (Centennial, CO, USA). Mouse anti-human fatty acid synthase (FAS) monoclonal antibody (Mab FAS, #10038) was procured from Immuno-Biological Laboratories Co., Ltd. (Fujioka, Japan). The rabbit anti-human  $\beta$ -actin monoclonal antibody (Mab  $\beta$ -actin, #4970) was obtained from Cell Signaling Technology (Tokyo, Japan). Resveratrol (3, 4', 5-trihydroxy-trans-stilbene) and 3-methyladenine (3-MA; PI3K class III inhibitor) were procured from Sigma-Aldrich (St. Louis, MO, USA). Recombinant human TNF- $\alpha$  (R&D Systems, Inc., Minneapolis, MN, USA) was used to stimulate the Ca9-22 cells. For in situ hybridization, probes against human SREBP1 (ACD# 469871), human p62/SQSTM1 (ACD# 415881), and human E-FABP (ACD# 566111-C3) were procured from Advanced Cell Diagnostics Inc. (ACD; Newark, CA, USA).

#### 4.2. Cell Culture

HOSCC cell lines (HSC-2, HSC-3, HSC-4, Ca9-22, and SAS; Japanese Cancer Research Resources Bank, Osaka, Japan) mycoplasma testing has been carried out, and cell lines were cultured independently in 25 cm<sup>2</sup> culture flasks with RPMI-1640 medium containing 10% heat-inactivated fetal bovine serum and 1% antibiotic-antimycotic (Life Technologies, Tokyo, Japan). Cells were grown to confluency, at 37 °C, in an atmosphere of 5% CO<sub>2</sub>. Normal human gingival progenitor (NHGP) cells (CELLnTEC advanced cell systems, Bern, Switzerland) were maintained in gingival progenitor cell maintenance medium (CELLnTEC advanced cell systems) without antibiotics on 10 cm<sup>2</sup> polyethyleneimine-coated glass plates until differentiation into normal gingival epithelial (NGE) cells.

#### 4.3. RNA Extraction and Quantitative Reverse Transcription-Polymerase Chain Reaction (qRT-PCR)

Total RNA was extracted from monolayered HOSCC cells ( $1 \times 10^6$  cells/mL) using the AGPC method, as described previously [38]. The expression patterns of E-FABP and SREBP1 were confirmed by qRT-PCR analyses using a Bio-Rad iCycler system (Bio-Rad, Tokyo, Japan) and the iScript One-Step RT-PCR kit with SYBR Green I (Bio-Rad), according to the manufacturer's instructions and a previously described method [38]. The PCR primers were designed and synthesized by Sigma-Aldrich, Inc. (Ishikari, Japan) with the following primer sequences:

E-FABP: forward, 5'-GCC GCC GTT ATA AAG CAG CC-3'; E-FABP reverse, 5'-GCA AAG CTA TTC CCA CTC CTA GC-3'; SREBP1 forward, 5'-AAT CTG GGT TTT GTG TCT TC-3'; SREBP1 reverse, 5'-AAA AGT TGT GTA CCT TGT GG-3'; GAPDH forward, 5'-CAG CCT CAA GAT CAT CAG CA-3'; and GAPDH reverse, 5'-ACA GTC TTC TGG GTG GCA GT-3'. GAPDH mRNA with previously described primer sequences was used (set at 1) as an internal control [38].

#### 4.4. Immunoblot Analysis

Proteins were extracted from monolayered HOSCC cells ( $1 \times 10^6$  cells/mL) and quantified as previously described [38]. Immunoblot analysis was performed as previously described [38]. MAbs E-FABP (1:1000), PAb SREBP1 (1:1000), PAb p62 (1:1000), PAb Beclin1 (1:1000), MAb LC3 (1:1000), and MAb FAS (1:1000) were used as primary antibodies. Horseradish peroxidase (HRP)-labeled goat anti-rabbit IgG (H + L) or anti-mouse IgG (H + L) antibody (1:25,000) (GE Healthcare, Piscataway, NJ, USA) was used as the secondary antibody. MAb  $\beta$ -actin (1:5000) was used as the internal control. Ca9-22 cells were grown as monolayer culture, and treated with 10 ng/mL TNF- $\alpha$  and/or 50  $\mu$ M resveratrol for 24 h followed by immunoblot analysis for the detection of SREBP1 and E-FABP.

#### 4.5. Cell Viability Assay

The assay was performed as previously described method [38]. Briefly, Ca9-22 cells ( $2 \times 10^4$  cells/100  $\mu$ L/well) were plated in a 96-microwell plate. Subsequently, the cells were treated with or without 2 nM, 50 nM, 100 nM, 1  $\mu$ M, 50  $\mu$ M, and 100  $\mu$ M resveratrol for 24 h. WST-8/ECS solution (10  $\mu$ L; Dojindo Laboratories, Tokyo, Japan) was then added to each well and incubated, at 37 °C, in a 5% CO<sub>2</sub> incubator for 4 h. The cells were oscillated

for 1 min, and absorbance was measured at 450 nm using a microplate reader (Bio-Rad). Next, inhibition assay against autophagy was performed. Ca9-22 cells were individually pretreated with 2 mM 3-MA (an autophagy inhibitor) for 1 h, followed by treatment with or without 50  $\mu$ M resveratrol for 24 h. Thereafter, cell viability assay and immunoblot analysis were performed as described above. Cellular autophagic vacuole morphology was examined and photographed using a phase-contrast microscope (Olympus, Tokyo, Japan).

#### 4.6. Apoptosis Detection Assay

The assay was performed as previously described method [38]. Briefly, Ca9-22 cells ( $5 \times 10^3$  cells/100  $\mu$ L/well) were plated in white-walled 96-well tissue culture plates and incubated for 24 h. The cells were treated with or without 2 nM, 50 nM, 100 nM, 1  $\mu$ M, 50  $\mu$ M, and 100  $\mu$ M resveratrol for 24 h. Thereafter, the activities of caspase-3/7, -8, and -9 were determined using Caspase-Glo<sup>®</sup> 3/7, 8, and 9 assays (Promega, Madison, WI, USA) according to the manufacturer's instructions. Subsequently, 50  $\mu$ L of Caspase-Glo reagent was added to each well and incubated for 30 min, followed by the measurement of luminescence as relative light units (RLUs) using a Veritas Microplate Luminometer (Promega).

#### 4.7. RNA-Mediated Interference

Small interfering RNAs (siRNAs) specific for human E-FABP, SREBP1, and scrambled (control) siRNAs were synthesized by Sigma-Aldrich (St. Louis, MO, USA). The sense and antisense strand sequences of the oligonucleotides were as follows: E-FABP siRNA sense, UGU ACC CUG GGA GAG AAG U; antisense, ACU UCU CUC CCA GGG UAC A; control siRNA sense, GAU CAU GAG CGG UGC GUA A; antisense, UUA CGC ACC GCU CAU GAU C; SREBP1 siRNA sense, GAG GCA AGA CCG AAG UAA A; antisense, UUU ACU UCG GUC UUG CCU C; and control siRNA, MISSION<sup>®</sup> siRNA universal negative control. Before transfection, FuGENE HD transfection reagent (Promega) was mixed with 100 nM E-FABP and 100 nM SREBP1 or 100 nM control siRNA (3:3.4  $\mu$ L) in serum-free medium to a total volume of 500  $\mu$ L followed by incubation for 30 min, at room temperature (RT). For SREBP1 or E-FABP knockdown, Ca9-22 cells (derived from gingival cancer;  $1 \times 10^5$  cells/mL) were seeded on 24-well plates and rinsed with serum-free medium, and transfected with either an SREBP1, an E-FABP siRNA duplex, or a control siRNA using FuGENE HD transfection reagents for 48 h, at 37 °C. The cells were then subjected to cell viability assay, apoptosis detection assay, and immunoblot analysis.

#### 4.8. Analysis of SREBP1 Translocation

To examine SREBP1 translocation to the nucleus, we used a subcellular proteome extraction kit (S-PEK; Calbiochem, Darmstadt, Germany) according to the manufacturer's instructions to extract cytoplasm, cell membrane and nucleus fractions of Ca9-22 cells. Ca9-22 cells were treated with 10 ng/mL of TNF- $\alpha$  and/or 50  $\mu$ M resveratrol. Then, the assay was subsequently performed as previously described method [39]. Thereafter, each sample was subjected to immunoblot analysis followed by densitometric analyses. Filters were scanned and computer-generated images were analyzed with the ImageJ program to obtain densitometric values. For each series of samples (cytoplasm, cell membrane and nucleus), the relative density of each image was calculated and expressed as a percentage of the value (arbitrarily set at 100) indicated by a sharp sign.

#### 4.9. Plasmids

The pGL4 firefly luc2 plasmid and hRLuc-TK-renilla were procured from Promega. The low-density lipoprotein receptor plasmid (pLDLR)-Luc construct (also known as pES7, Addgene plasmid #14940), harboring the SREBP-responsive Sterol Responsive Element (SRE) sequence (ATCACCCAC), and the pLDLR-Luc mutSRE construct (LDLR-Luc MUT, Addgene plasmid #14945), harboring an SREBP-unresponsive mutant SRE (ATAACCCAC) were obtained from Addgene (Watertown, MA, USA). A PCR fragment containing nu-

cleotides 335–3 of the human LDL receptor gene was cloned into the SmaI site of pGL2-basic to generate pLDLR-Luc.

#### 4.10. Transfection of Ca9-22 Cells with Plasmids and Luciferase Reporter Assay

Ca9-22 cells ( $1 \times 10^5$  cells/mL) were cultured for 12 h in 24-well culture plates containing RPMI1640 medium supplemented with 10% FBS. Cells were transiently transfected with pLDLR-Luc, pLDLR-Luc mutSRE, and pGL4-basic plasmids (firefly) as control and hRluc-TK reference Renilla luciferase plasmids (Promega) using FuGENE HD transfection reagents (Roche, Nutley, NJ, USA), according to the manufacturer's instructions. After 24 h of transfection, cells were treated with 10 ng/mL TNF- $\alpha$  and/or 50  $\mu$ M resveratrol for 24 h. Subsequently, cells were lysed, and firefly and Renilla luciferase activities were analyzed using the Dual-Luciferase System (Promega) according to the manufacturer's instructions. To standardize transfection efficiencies, luciferase activity from pLDLR-Luc and pLDLR-Luc mutSRE was normalized to Renilla luciferase activity.

#### 4.11. Nude Mouse Model of Ca9-22 Tumor Mass

All experimental procedures were performed with approval from the Animal Experimentation Committee of our university. Specific pathogen-free athymic four-week-old BALB/c female mice were kept under sterile conditions in a laminar flow room in cages with filter bonnets and fed a sterilized mouse diet and water. Mice were anesthetized with Isoflurane. Mice were subcutaneously injected with Ca9-22 cells ( $1 \times 10^6$  cells in 100  $\mu$ L of PBS) into the back using a 27-gauge needle. Tumor size was measured using calipers daily in all mice, and movable and elastic-hard Ca9-22 tumor masses grew to approximately 10 mm in diameter after three weeks of Ca9-22 cell inoculation. To examine the effects of polyphenols, the mice were treated with 50 and 100  $\mu$ M/day of resveratrol and PBS (control), respectively, by intratumoral injection for seven consecutive days after the Ca9-22 tumor mass had reached approximately 10 mm in diameter. Subsequently, resveratrol or PBS (control) was administered once a week for an additional five weeks (a total of eight weeks after Ca9-22 cell implantation).

#### 4.12. Quantification of Tumor Mass in Nude Mice

After eight weeks of Ca9-22 cell implantation, the mice were euthanized, and the tumor mass status was evaluated quantitatively (Table 1). Animals were transcardially perfused with 200 mL of 0.9% saline containing heparin (10,000 U/l), followed by 200 mL of phosphate-buffered 4% paraformaldehyde. The tumor volume ( $V$ , mm<sup>3</sup>) was calculated as  $0.5 \times L \times W^2$ , where  $L$  and  $W$  refer to the length and width (in mm), respectively. The percentage of tumor growth inhibition is expressed as the mean value ( $\pm$ SD) of tumor volumes (calculated for all groups with 10 mice each) relative to the volume of tumors injected with control PBS. The back skin was excised and the tumor tissue was post-fixed in 4% paraformaldehyde for 18–24 h. Post-fixation, the tumor was equilibrated to 15% and 30% sucrose and then cut into 10–15  $\mu$ m-thick sections on a freezing, sliding stage microtome. Sections were stored at  $-80$  °C until processed for RNAscope in situ hybridization (ISH) and immunohistochemistry (IHC).

#### 4.13. RNAscope ISH

Detection of SREBP1, p62/SQSTM1, and E-FABP mRNAs by RNA ISH was performed on frozen slices using the RNAscope 2.5 HD Reagent Kit-Brown (ACD) according to the manufacturer's instructions. The positive and negative control probes were used in this study. Briefly, frozen slides were dried in an oven, at 60 °C, for 30 min prior to incubation in cold 4% PFA for 15 min. The slides were then dehydrated using 50%, 70%, and 100% ethanol for 5 min each at RT, followed by H<sub>2</sub>O<sub>2</sub> addition and incubation for 10 min at RT. For antigen retrieval, the sections were boiled (98–102 °C) in a target retrieval solution (ACD) for 5 min. After washing the slides with pure H<sub>2</sub>O twice for 30 s each, at RT, they were dehydrated using 100% ethanol for 3 min and air-dried for 5 min, at RT. The slides were

then baked, at 60 °C, for 30 min, and a hydrophobic barrier was formed around the tissue using ImmEdge Hydrophobic Barrier Pen (ACD), followed by protein digestion using protease III treatment for 30 min, at 40 °C. Frozen sections were washed twice with pure H<sub>2</sub>O for 1 min each. Next, the target probes were added and allowed to hybridize at 40 °C, for 2 h. The detection kit was used as follows: amplification steps 1–4 were performed, at 40 °C (AMP1 30 min, AMP2 15 min, AMP3 30 min, and AMP4 15 min), followed by steps 5–6, at RT (AMP5 30 min and AMP6 15 min). Sections were then incubated with diaminobenzidine (DAB) for 10 min, counterstained with Gill’s hematoxylin for 30 s, and incubated for 2 min, at RT. Washing steps between the addition of reagents were performed on an automated platform, at RT. Finally, the slides were removed, immersed in deionized water, dehydrated, cleared, and mounted. Brown punctate signals colocalized with nuclei and/or the cytoplasm of tumor cells were designated as positive.

#### 4.14. Immunohistochemistry

p62 immunostaining was performed as described previously [38]. Diluted MAb p62 (1:1000) and goat anti-rabbit IgG (H + L) antibodies for p62 (1:200) were used as the primary and secondary antibodies, respectively.

#### 4.15. Statistical Analysis

Results were compared between different groups using two-tailed Student’s *t*-test. Differences were considered statistically significant at *p*-values < 0.05. All analyses were performed using StatView statistical software (version 5.0; SAS Institute Inc., Cary, NC, USA). Each column and error bar represent the mean values ± SD of three independent experiments (*n* = 3 experiments; mean values ± SD).

## 5. Conclusions

Resveratrol inhibits the transactivation of SREBP1 with subsequent downregulation of E-FABP expression. Resveratrol blocked Ca9-22 cell proliferation, ultimately inducing autophagic cell death and preventing the growth of Ca9-22 tumor masses in nude mice. This molecular cascade may provide the mechanism by which resveratrol suppresses the development of oral squamous cell carcinomas. Our data also suggest that the anti-cancer activity of resveratrol may rely on the inhibition of SREBP1. However, the mechanism by which resveratrol interferes with SREBP1 activation remains unclear. Further investigation into the role of SREBP1 will help unfold lipid metabolism-mediated cancer proliferation and establish a resveratrol-based therapeutic strategy for oral cancer.

**Author Contributions:** The manuscript consists of contributions of all the aforementioned authors. Conceptualization, M.F. and H.S.; methodology, M.F.; software, M.F.; validation, M.F., K.I. and H.S.; formal analysis, M.F.; investigation, M.F., Y.O. and H.H.; resources, M.F.; data curation, M.F.; writing—original draft preparation, review and editing, M.F., Y.O., H.H., K.I. and H.S.; visualization, M.F.; supervision, M.F.; project administration, M.F.; funding acquisition, M.F. All authors have read and agreed to the published version of the manuscript.

**Funding:** This work was supported by a Grant-in-Aid for scientific research from the Ministry of Education, Science, and Culture of Japan (grant No.: 18K09822).

**Institutional Review Board Statement:** The study was conducted according to the guidelines of the Declaration of Helsinki, and approved by the Research Ethics Committee of Meikai University School of Dentistry, Saitama, Japan (approval number: A1809; date of approval: 15th June 2018). All animal work was carried out in strict accordance with the institutional guidelines for the use and care of laboratory animals. The study protocol was approved by the ethics committee of Meikai University (approval number: A2134; date of approval: 27 October 2021).

**Informed Consent Statement:** Not applicable.

**Data Availability Statement:** The data presented in this study are available on request from the corresponding author.

**Conflicts of Interest:** The authors declare no conflict of interest.

**Sample Availability:** Not applicable.

## References

- Nagao, T.; Warnakulasuriya, S. Screening for oral cancer: Future prospects, research and policy development for Asia. *Oral Oncol.* **2020**, *105*, 104632. [[CrossRef](#)] [[PubMed](#)]
- Tan, Y.T.; Lin, J.F.; Li, T.; Li, J.J.; Xu, R.H.; Ju, H.Q. LncRNA-mediated posttranslational modifications and reprogramming of energy metabolism in cancer. *Cancer Commun.* **2021**, *41*, 109–120. [[CrossRef](#)] [[PubMed](#)]
- Ward, P.S.; Thompson, C.B. Metabolic reprogramming: A cancer hallmark even Warburg did not anticipate. *Cancer Cell* **2012**, *21*, 297–308. [[CrossRef](#)]
- Sun, L.; Suo, C.; Li, S.T.; Zhang, H.; Gao, P. Metabolic reprogramming for cancer cells and their microenvironment: Beyond the Warburg effect. *Biochim. Biophys Acta Rev. Cancer* **2018**, *1870*, 51–66. [[CrossRef](#)] [[PubMed](#)]
- Daye, D.; Wellen, K.E. Metabolic reprogramming in cancer: Unraveling the role of glutamine in tumorigenesis. *Semin. Cell Dev. Biol.* **2012**, *23*, 362–369. [[CrossRef](#)]
- Icard, P.; Shulman, S.; Farhat, D.; Steyaert, J.M.; Alifano, M.; Lincet, H. How the Warburg effect supports aggressiveness and drug resistance of cancer cells? *Drug Resist. Updat.* **2018**, *38*, 1–11. [[CrossRef](#)]
- Currie, E.; Schulze, A.; Zechner, R.; Walther, T.C.; Farese, R.V., Jr. Cellular fatty acid metabolism and cancer. *Cell Metab.* **2013**, *18*, 153–161. [[CrossRef](#)]
- Wu, S.; Näär, A.M. SREBP1-dependent de novo fatty acid synthesis gene expression is elevated in malignant melanoma and represents a cellular survival trait. *Sci. Rep.* **2019**, *9*, 10369. [[CrossRef](#)]
- Wallace, M.; Green, C.R.; Roberts, L.S.; Lee, Y.M.; McCarville, J.L.; Sanchez-Gurmaches, J.; Meurs, N.; Gengatharan, J.M.; Hover, J.D.; Phillips, S.A.; et al. Enzyme promiscuity drives branched-chain fatty acid synthesis in adipose tissues. *Nat. Chem. Biol.* **2018**, *14*, 1021–1031. [[CrossRef](#)]
- Migita, T.; Ruiz, S.; Fornari, A.; Fiorentino, M.; Priolo, C.; Zadra, G.; Inazuka, F.; Grisanzio, C.; Palescandolo, E.; Shin, E.; et al. Fatty acid synthase: A metabolic enzyme and candidate oncogene in prostate cancer. *J. Natl. Cancer Inst.* **2009**, *101*, 519–532. [[CrossRef](#)]
- Carvalho, M.A.; Zecchin, K.G.; Seguin, F.; Bastos, D.C.; Agostini, M.; Rangel, A.L.C.A.; Veiga, S.S.; Raposo, H.F.; Oliveira, H.C.F.; Loda, M.; et al. Fatty acid synthase inhibition with orlistat promotes apoptosis and reduces cell growth and lymph node metastasis in a mouse melanoma model. *Int. J. Cancer* **2008**, *123*, 2557–2565. [[CrossRef](#)] [[PubMed](#)]
- Paul, B.; Lewinska, M.; Andersen, J.B. Lipid alterations in chronic liver disease and liver cancer. *JHEP Rep.* **2022**, *4*, 100479. [[CrossRef](#)] [[PubMed](#)]
- McKillop, I.H.; Girardi, C.A.; Thompson, K.J. Role of fatty acid binding proteins (FABPs) in cancer development and progression. *Cell Signal.* **2019**, *62*, 109336. [[CrossRef](#)] [[PubMed](#)]
- Li, B.; Hao, J.; Zeng, J.; Sauter, E.R. SnapShot: FABP Functions. *Cell* **2020**, *182*, 1066–1066.e1. [[CrossRef](#)]
- Dallaglio, K.; Marconi, A.; Truzzi, F.; Lotti, R.; Palazzo, E.; Petrachi, T.; Saltari, A.; Coppini, M.; Pincelli, C. E-FABP induces differentiation in normal human keratinocytes and modulates the differentiation process in psoriatic keratinocytes *in vitro*. *Exp. Dermatol.* **2013**, *22*, 255–261. [[CrossRef](#)] [[PubMed](#)]
- Tölle, A.; Suhail, S.; Jung, M.; Jung, K.; Stephan, C. Fatty acid binding proteins (FABPs) in prostate, bladder and kidney cancer cell lines and the use of IL-FABP as survival predictor in patients with renal cell carcinoma. *BMC Cancer* **2011**, *11*, 302. [[CrossRef](#)] [[PubMed](#)]
- Jafari, N.; Drury, J.; Morris, A.J.; Onono, F.O.; Stevens, P.D.; Gao, T.; Liu, J.; Wang, C.; Lee, E.Y.; Weiss, H.L.; et al. De novo fatty acid synthesis-driven sphingolipid metabolism promotes metastatic potential of colorectal cancer. *Mol. Cancer Res.* **2019**, *17*, 140–152. [[CrossRef](#)]
- Mashima, T.; Seimiya, H.; Tsuruo, T. De novo fatty-acid synthesis and related pathways as molecular targets for cancer therapy. *Br. J. Cancer* **2009**, *100*, 1369–1372. [[CrossRef](#)]
- Ye, J.; DeBose-Boyd, R.A. Regulation of Cholesterol and Fatty Acid Synthesis. *Cold Spring Harb. Perspect. Biol.* **2011**, *3*, a004754. [[CrossRef](#)] [[PubMed](#)]
- Zaidi, N.; Lupien, L.; Kuemmerle, N.B.; Kinlaw, W.B.; Swinnen, J.V.; Smans, K. Lipogenesis and lipolysis: The pathways exploited by the cancer cells to acquire fatty acids. *Prog. Lipid. Res.* **2013**, *52*, 585–589. [[CrossRef](#)] [[PubMed](#)]
- Wen, Y.A.; Xiong, X.; Zaytseva, Y.Y.; Napier, D.L.; Vallee, E.; Li, A.T.; Wang, C.; Weiss, H.L.; Evers, B.M.; Gao, T. Downregulation of SREBP inhibits tumor growth and initiation by altering cellular metabolism in colon cancer. *Cell Death Dis.* **2018**, *9*, 265. [[CrossRef](#)] [[PubMed](#)]
- Johnson, J.J.; Mukhtar, H. Curcumin for chemoprevention of colon cancer. *Cancer Lett.* **2007**, *255*, 170–181. [[CrossRef](#)]
- Varoni, E.M.; Lo Faro, A.F.; Sharifi-Rad, J.; Iriti, M. Anticancer molecular mechanisms of resveratrol. *Front. Nutr.* **2016**, *3*, 8. [[CrossRef](#)] [[PubMed](#)]
- Marques, F.Z.; Markus, M.A.; Morris, B.J. Resveratrol: Cellular actions of a potent natural chemical that confers a diversity of health benefits. *Int. J. Biochem. Cell Biol.* **2009**, *41*, 2125–2128. [[CrossRef](#)] [[PubMed](#)]



25. Galiniak, S.; Aebisher, D.; Bartusik-Aebisher, D. Health benefits of resveratrol administration. *Acta Biochim. Pol.* **2019**, *66*, 13–21. [[CrossRef](#)] [[PubMed](#)]
26. Dandawate, P.R.; Subramaniam, D.; Jensen, R.A.; Anant, S. Targeting cancer stem cells and signaling pathways by phytochemicals: Novel approach for breast cancer therapy. *Semin. Cancer Biol.* **2016**, *40–41*, 192–208. [[CrossRef](#)] [[PubMed](#)]
27. Lang, F.; Qin, Z.; Li, F.; Zhang, H.; Fang, Z.; Hao, E. Apoptotic cell death induced by resveratrol is partially mediated by the autophagy pathway in human ovarian cancer cells. *PLoS ONE* **2015**, *10*, e0129196. [[CrossRef](#)]
28. Zhu, Y.; He, W.; Gao, X.; Li, B.; Mei, C.; Xu, R.; Chen, H. Resveratrol overcomes gefitinib resistance by increasing the intracellular gefitinib concentration and triggering apoptosis, autophagy and senescence in PC9/G NSCLC cells. *Sci. Rep.* **2015**, *5*, 17730. [[CrossRef](#)]
29. Selvaraj, S.; Sun, Y.; Sukumaran, P.; Singh, B.B. Resveratrol activates autophagic cell death in prostate cancer cells via downregulation of STIM1 and the mTOR pathway. *Mol. Carcinog.* **2016**, *55*, 818–831. [[CrossRef](#)]
30. Button, R.W.; Vincent, J.H.; Strang, C.J.; Luo, S. Dual PI-3 kinase/mTOR inhibition impairs autophagy flux and induces cell death independent of apoptosis and necroptosis. *Oncotarget* **2016**, *7*, 5157–5175. [[CrossRef](#)]
31. Baur, J.A.; Sinclair, D.A. Therapeutic potential of resveratrol: The in vivo evidence. *Nat. Rev. Drug Discov.* **2006**, *5*, 493–506. [[CrossRef](#)] [[PubMed](#)]
32. Szkudelska, K.; Nogowski, L.; Szkudelski, T. Resveratrol, a naturally occurring diphenolic compound, affects lipogenesis, lipolysis and the antilipolytic action of insulin in isolated rat adipocytes. *J. Steroid. Biochem. Mol. Biol.* **2009**, *13*, 17–24. [[CrossRef](#)] [[PubMed](#)]
33. Shimano, H.; Sato, R. SREBP-regulated lipid metabolism: Convergent physiology-divergent pathophysiology. *Nat. Rev. Endocrinol* **2017**, *13*, 710–730. [[CrossRef](#)]
34. Pastorino, J.G.; Shulga, N. Tumor necrosis factor-alpha can provoke cleavage and activation of sterol regulatory element-binding protein in ethanol-exposed cells via a caspase-dependent pathway that is cholesterol insensitive. *J. Biol. Chem.* **2008**, *283*, 25638–25649. [[CrossRef](#)] [[PubMed](#)]
35. Kusnadi, A.; Park, S.H.; Yuan, R.; Pannellini, T.; Giannopoulou, E.; Oliver, D.; Lu, T.; Park-Min, K.H.; Ivashkiv, L.B. The cytokine TNF promotes transcription factor SREBP activity and binding to inflammatory genes to activate macrophages and limit tissue repair. *Immunity* **2019**, *51*, 241–257.e9. [[CrossRef](#)]
36. Eberle, D.; Hegarty, B.; Bossard, P.; Ferre, P.; Fufelle, F. SREBP transcription factors: Master regulators of lipid homeostasis. *Biochimie* **2004**, *86*, 839–848. [[CrossRef](#)]
37. Bertolio, R.; Napoletano, F.; Mano, M.; Maurer-Stroh, S.; Fantuz, M.; Zannini, A.; Bicciato, S.; Sorrentino, G.; Del Sal, G. Sterol regulatory element binding protein 1 couples mechanical cues and lipid metabolism. *Nat. Commun.* **2019**, *10*, 1326. [[CrossRef](#)] [[PubMed](#)]
38. Fukuda, M.; Sakashita, H.; Hayashi, H.; Shiono, J.; Miyake, G.; Komine, Y.; Taira, F.; Sakashita, H. Synergism between  $\alpha$ -mangostin and TRAIL induces apoptosis in squamous cell carcinoma of the oral cavity through the mitochondrial pathway. *Oncol. Rep.* **2017**, *38*, 3439–3446. [[CrossRef](#)]
39. Fukuda, M.; Ehara, M.; Suzuki, S.; Ohmori, Y.; Sakashita, H. IL-23 promotes growth and proliferation in human squamous cell carcinoma of the oral cavity. *Int. J. Oncol.* **2010**, *36*, 1355–1365. [[CrossRef](#)]

Article

# Selection of Enzymatic Treatments for Upcycling Lentil Hulls into Ingredients Rich in Oligosaccharides and Free Phenolics

Sara Bautista-Expósito <sup>1</sup>, Albert Vandenberg <sup>2</sup>, Montserrat Dueñas <sup>3</sup>, Elena Peñas <sup>1</sup>, Juana Frias <sup>1</sup> and Cristina Martínez-Villaluenga <sup>1,\*</sup>

<sup>1</sup> Department of Technological Processes and Biotechnology, Institute of Food Science Technology and Nutrition (ICTAN-CSIC), José Antonio Novais 10, 28040 Madrid, Spain

<sup>2</sup> Department of Plant Sciences, University of Saskatchewan, Saskatoon, SK S7N 5A2, Canada

<sup>3</sup> Research Group in Polyphenols, Unidad de Nutrición y Bromatología, Facultad de Farmacia, University of Salamanca, Miguel de Unamuno Campus, 37007 Salamanca, Spain

\* Correspondence: c.m.villaluenga@csic.es; Tel.: +34-91-393-99-27

**Abstract:** In this study, the comprehensive chemical characterization of red lentil hulls obtained from the industrial production of football and split lentils was described. The lentil hulls were rich in dietary fiber (78.43 g/100 g dry weight with an insoluble to soluble fiber ratio of 4:1) and polyphenols (49.3 mg GAE/g dry weight, of which 55% was bound phenolics), which revealed the suitability of this lentil by-product as a source of bioactive compounds with recognized antioxidant and prebiotic properties. The release of oligosaccharides and phenolic compounds was accomplished by enzymatic hydrolysis, microwave treatment and a combination of both technologies. The key role played by the selection of a suitable enzymatic preparation was highlighted to maximize the yield of bioactive compounds and the functional properties of the lentil hull hydrolysates. Out of seven commercial preparations, the one with the most potential for use in a commercial context was Pectinex<sup>®</sup> Ultra Tropical, which produced the highest yields of oligosaccharides (14 g/100 g lentil hull weight) and free phenolics (45.5 mg GAE/100 g lentil hull weight) and delivered a four-fold increase in terms of the original antioxidant activity. Finally, this enzyme was selected to analyze the effect of a microwave-assisted extraction pretreatment on the yield of enzymatic hydrolysis and the content of free phenolic compounds and oligosaccharides. The integrated microwave and enzymatic hydrolysis method, although it increased the solubilization yield of the lentil hulls (from 25% to 34%), it slightly decreased the content of oligosaccharides and proanthocyanidins and reduced the antioxidant activity. Therefore, the enzymatic hydrolysis treatment alone was more suitable for producing a lentil hull hydrolysate enriched in potential prebiotics and antioxidant compounds.

**Keywords:** lentil hull; enzymatic hydrolysis; microwave-assisted extraction; phenolic compounds; oligosaccharides; antioxidant activity

**Citation:** Bautista-Expósito, S.; Vandenberg, A.; Dueñas, M.; Peñas, E.; Frias, J.; Martínez-Villaluenga, C. Selection of Enzymatic Treatments for Upcycling Lentil Hulls into Ingredients Rich in Oligosaccharides and Free Phenolics. *Molecules* **2022**, *27*, 8458. <https://doi.org/10.3390/molecules27238458>

Academic Editor: Nour Eddine Es-Safi

Received: 4 November 2022

Accepted: 29 November 2022

Published: 2 December 2022

**Publisher's Note:** MDPI stays neutral with regard to jurisdictional claims in published maps and institutional affiliations.



**Copyright:** © 2022 by the authors. Licensee MDPI, Basel, Switzerland. This article is an open access article distributed under the terms and conditions of the Creative Commons Attribution (CC BY) license (<https://creativecommons.org/licenses/by/4.0/>).

## 1. Introduction

Lentil, a pulse crop ranking fourth in terms of global grain legume production, is a dietary source of protein, starch, fiber and micronutrients that are important to human nutrition [1]. The growing demand for plant-based proteins, combined with the existing knowledge of the potential health effects of increased pulse dietary intake, have raised the production of lentil products [1]. Dehulling is a primary process for producing dehulled lentil seeds or split lentils, lentil flour and fractionated protein and fiber ingredients [2]. By-products generated from dehulling are mainly hulls (8–16% of dry seed weight), embryonic axes (1–3% of dry seed weight) and broken cotyledons [2]. As a consequence, the dehulling industry generates a large amount of lower-value by-product, representing 20–28% of the total lentil amount processed [2]. The primary markets for lentil hulls are of low value and have very limited use in human nutrition. Therefore, this by-product not only

represents a low-value disposal problem for millers but also wastes a potential source of novel, nutritious and health-promoting food ingredients.

Lentil hulls are a promising source of nutrients that generally contain 60–90% dietary fiber, 2–8% protein, 3% ash and 1–3% lipids [2]. Lentil dietary fiber consist of cellulose, pectin, xylans and mannans, which can be considered as sources of prebiotics [3]. Moreover, lentil hulls have large amounts of extractable phenolics (procyanidins being the major group followed by phenolic acids and flavonols) and considerable levels of conjugated and bound phenolic acid derivatives linked to cell wall components (proteins, cellulose, hemicellulose and pectin) [4]. Besides the well-documented physiological benefits of dietary fiber [5], the phenolic compounds of lentil hulls provide potential for various physiological benefits such as those related to antioxidant and anti-inflammatory activities [6–8]. These findings represent a good foundation for further investigation into the value-added use of these by-products, particularly in functional foods and nutraceutical products that improve health. Some challenges in the development of functional ingredients from lentil hulls include the compact inner insoluble food matrix, which may be a physical barrier to the release and absorption of phytochemicals and may contribute to a loss of efficacy in maintaining health and reducing the risk of disease [9]. It often seems to be the case that although polysaccharides are fermented by the colonic microbiota, the selectivity for health-promoting bacterial groups is increased by partial hydrolysis [10]. As the bioavailability of bioactive compounds plays an important role in the health benefits of lentil hulls, the health-outcome-oriented hydrolysis of the food matrix using physical, chemical or enzymatic methods are promising strategies for the better exploitation of this byproduct as a functional food ingredient.

Earlier research has demonstrated that the use of commercial enzymes increases the amounts of free phenolics in bran/hull byproducts obtained from certain cereals as well as causing a concurrent increase in their radical scavenging and anti-inflammatory activities [11,12]. The synergy between different feruloyl esterases, pectinases, cellulases, hemicellulases and proteases present in commercial enzymatic preparations is crucial in breaking the bonds among cell-wall polysaccharides, proteins and polyphenols [13]. Differences in the enzymatic profile of commercial enzymatic preparations make the screening and selection of enzymes a key step in the development of functional ingredients from agro-industrial by-products. The integration of physical processing methods has resulted an adequate approach towards a higher solubilization efficiency of bioactive compounds [14]. In recent years, microwave-assisted extraction (MAE) has received considerable attention because it is a green (low energy consumption, non-thermal technology) and appealing technological alternative to conventional chemical extraction processes. The high temperature and pressure involved in the process facilitate the destruction of material surfaces, which in turn results in an increased area and increased amounts of compounds that are released into the solvent [15]. Microwave treatment has been widely studied to enhance the extractability of various components such as protein, oil and bioactive components from agro-industrial byproducts, but there have been no studies that have dealt with the use of MAE for the extraction of phenolics and oligosaccharides from legume seed coats.

In this study, we hypothesized that lentil hulls could be valorized through the extraction of oligosaccharides and phenolic compounds with a high added value due to their potential biological properties. We conducted a comprehensive chemical characterization of red lentil hulls resulting from the industrial processing of red football and split lentils. Likewise, the successful extraction of oligosaccharides and phenolic compounds from the lentil hull by-products through microwave treatment, enzymatic treatment and a combination of the two was accomplished, and their potential as functional food ingredients was accordingly discussed. Seven different commercially available food-grade enzyme preparations, designed to break down plant cell walls (Novozymes A/S), were screened for their ability to increase the extraction yield of bioactive compounds and antioxidant activity.

## 2. Materials and Methods

### 2.1. Materials

Hulls from an industrial de-hulling process that produces red football and split lentils were kindly provided by Prairie Pulse Inc. (Vanscoy, Saskatchewan, SK, Canada) in May 2019. Hulls were ground into a fine powder with a mixer mill (MM 400, Retsch, Haan, Germany) for approximately 3 min at maximum speed and stored in sealed plastic bags at 4 °C. Ultraflo XL, Ultraflo Max, Ultimase BWL 40, Viscozyme L, Celluclast 1.5 L, Pectinex<sup>®</sup> Ultra Tropical and Shearzyme Plus 2X were obtained from Novozymes (Bagsvaerd, Denmark). Fast Blue BB (FBBB) [4-benzoylamino-2,5-dimethoxybenzenediazonium] chloride hemi-(zinc chloride), 2,2'-azinobis 3-ethylbenzothiazoline-6-sulfonic acid (ABTS), 2,2'-diazobis-(2-aminodipropane)-di-hydrochloride (AAPH) and fluorescein were purchased from Sigma-Aldrich Co. (St. Louis, MO, USA). Standards such as (+)-catechin, *trans-p*-coumaric acid, quercetin 3-*O*-rutinoside, quercetin 3-*O*-glucoside and kaempferol 3-*O*-rutinoside were provided by Extrasynthese (Lyon, Genay Cedex, France). Standards of 6-hydroxy-2,5,7,8-tetramethyl-2-carboxylic acid (Trolox), D-glucose, glycerol and gallic acid were acquired from Sigma-Aldrich Co. (St. Louis, MO, USA).

### 2.2. Enzymatic Treatments

Enzymatic extractions were performed using seven commercial glucanases: Ultraflo XL, Ultraflo Max, Ultimase BWL 40, Viscozyme L, Celluclast 1.5L, Pectinex Ultra Tropical and Shearzyme Plus 2X (Novozymes, Bagsvaerd, Denmark). Enzymatic treatments (100 mL) were performed in water at a solid-to-solvent ratio of 1:20 (*w:v*) in accordance with previous studies [11]. Reaction mixtures consisted of a 1% enzyme-to-lentil hull ratio (*w:w*) according to the manufacturer's recommendations and were processed at 40 °C for 3 h in a Thermomixer C shaker (Eppendorf Ibérica, Madrid, Spain) at 2000 rpm. The reaction with Pectinex<sup>®</sup> Ultra Tropical was monitored at selected times (0, 0.5, 1, 1.5, 2, 2.5, 3, 3.5 and 4 h) by taking 2 mL aliquots. Enzymes were deactivated at 95 °C in a water bath for 5 min.

### 2.3. Comparison of Microwave, Enzymatic and Sequential Microwave–Enzymatic Treatments of Lentil Hull

Microwave extraction was performed using a lentil-hull-to-solvent ratio of 1:20 (*w:v*) in a Pyrex bottle, to which 20 mL of bi-distilled water was added. Microwaves were applied at 700 W and 85 °C for 1 min using a JMO01138 microwave (Jocel, Argemil, Portugal) equipped with a rotating plate. The tested power settings were selected according to previous research designed to extract bioactive compounds from fruit peels and pomaces [16,17]. The extracted samples were cooled in an ice water bath for 10 min. For the sequential microwave–enzymatic extractions, the microwave-treated lentil hulls were mixed (step 1) with Pectinex<sup>®</sup> Ultra Tropical (1% enzyme-to-lentil-hull weight ratio) (step 2). The reaction mixtures with a lentil-hull-to-solvent ratio of 1:20 (*w/v*) were incubated for 3 h at 40 °C in a thermomixer C (Eppendorf Ibérica, Madrid, Spain). Enzymes were deactivated by boiling in a water bath for 5 min.

For the three lentil hull treatments, samples were centrifuged for 10 min at 10,000 × *g* in a microcentrifuge (Eppendorf AG, Hamburg, Germany), and the weight of the supernatant was recorded and subsequently freeze-dried to gravimetrically determine the dried water-soluble fraction weight.

### 2.4. Determination of Total Dietary Fiber (TDF), Insoluble Dietary Fiber (IDF) and Soluble Dietary Fiber (SDF) Fractions

The total (TDF), insoluble (IDF) and high-molecular-weight soluble dietary fiber (HMW-SDF) content in the lentil hulls was determined by enzymatic and gravimetric methods using a Rapid Integrated Total Dietary Fiber Assay Kit (K-RINTDF, Megazyme, Wicklow, Ireland). TDF, IDF and HMW-SDF were expressed as g/100 g dry lentil hull weight (DW).

Low-molecular-weight soluble dietary fiber (LMW-SDF), which represents non-digestible oligosaccharides of a degree of polymerization  $\geq 3$ , was determined by size exclusion chromatography following the K-RINTDF protocol ([https://www.megazyme.com/documents/Assay\\_Protocol/K-RINTDF\\_DATA.pdf](https://www.megazyme.com/documents/Assay_Protocol/K-RINTDF_DATA.pdf), accessed on 10 January 2022). Dried lentil hulls and hydrolysates were dissolved in 600  $\mu\text{L}$  of double-distilled water, and glycerol was added as an internal standard at a final concentration of 10 mg/mL. A high-resolution liquid chromatograph (HPLC) Alliance Separation Module 2695 (Waters, Milford, MA, USA) equipped with a 2414 refractive index detector (Waters, Milford, MA, USA) maintained at 50 °C was used. The sample injection volume was 50  $\mu\text{L}$ . Separation was performed in the isocratic mode using microfiltered distilled water as the solvent, two TSKgel® G2500 PWXL columns (7.8 mm id  $\times$  30; Tosoh Co., Tokyo, Japan) connected in series at a flow rate of 0.5 mL/min and at a temperature of 80 °C were used, and a run time of 60 min was used to ensure the column was cleaned out. The LMW-SDF content was expressed as g/100 g DW using the equation (1):

$$\text{Oligosaccharides (g/100g)} = [(Rf \times W_{\text{IS}} \times PA_{\text{LMW-SDF}}/PA_{\text{IS}}) \times (100/M)]/1000 \quad (1)$$

where Rf is the D-glucose response factor (ratio of peak area of D-glucose/peak area of glycerol to the ratio of the mass of D-glucose/mass of glycerol);  $W_{\text{IS}}$  is the amount of internal standard contained in 1 mL of glycerol internal standard solution pipetted into the sample before filtration in mg;  $PA_{\text{LMW-SDF}}$  is the peak area of the LMW-SDF fraction;  $PA_{\text{IS}}$  is the peak area of the glycerol internal standard; and M is the test portion mass in grams of the sample analyzed by HPLC.

#### 2.5. Determination of Total Protein and Starch

The total protein content of lentil hulls (0.5 g) was determined by the Dumas combustion method using a Trumac nitrogen analyzer (Leco Corporation, St Joseph, MI, USA). A conversion factor of 6.25 was used to convert the nitrogen values to protein content. The results were expressed as g/100 g DW.

Total starch was determined by an enzymatic–colorimetric method using a K-TSTA-100A Total Starch Assay Kit (Megazyme, Wicklow, Ireland). A Synergy HT microplate reader (BioTek Instruments, Winooski, VT, USA) was used to read the absorbance at 510 nm. The results were expressed as g/100 g DW.

#### 2.6. Determination of Anti-Nutrients

Trypsin inhibitory activity (TIA) was determined as previously reported [18]. Briefly, samples (100 mg) were extracted in 5 mL of 0.01 M NaOH (pH 8.4–10.0) and shaken for 3 h at 20 °C in a Thermomixer C (Eppendorf, Thermo Fisher Scientific, Waltham, MA, USA) at 2000 rpm. Extract volumes were adjusted to 10 mL with distilled water, shaken for 1 min at 2000 rpm and left standing for 15 min. Aliquots of 1 mL were withdrawn and diluted to produce a 40–60% inhibition of the trypsin activity. TIA was expressed as trypsin inhibitory units (TIU)/mg DW.

Phytic acid content was determined by an enzymatic–colorimetric method using a K-PHYT Phytic Acid (Phytate)/Total Phosphorus Assay kit (Megazyme, Wicklow, Ireland). Absorbance was read at 655 nm using a Synergy HT microplate reader (BioTek Instruments, Winooski, VT, USA). Phytic acid content was expressed as g/100 g DW.

Condensed tannins were determined as described previously [18]. Briefly, 200 mg of the sample was hydrolyzed with 10 mL of hydrochloric acid (HCl)/n-butanol (5:95, v:v) containing 0.7 g/L of ferric (III) chloride ( $\text{FeCl}_3$ ) at 100 °C for 1 h. Samples were centrifuged (14,000  $\times$  g for 10 min), and the supernatants were washed two times with 10 mL of n-butanol:HCl: $\text{FeCl}_3$ . After adjusting the final volume to 25 mL, absorbance was measured at 550 nm in a Synergy HT microplate reader (BioTek Instruments, Winooski, VT, USA). The condensed tannin content was expressed as mg catechin equivalents (CAE)/g DW using a catechin calibration curve.

### 2.7. Extraction of Free and Insoluble Phenolic Compounds

Extraction of the free phenolic compounds of the lentil hulls was performed according to a previously described method [19] with some modifications. Lentil hull dry powder (1 g) was extracted with 20 mL of 80% ethanol, vortexed for 30 s by an IKA Vortex 3 (IKA<sup>®</sup>-Werke GmbH & Co, Staufen, Germany) and shaken for 10 min at 4 °C and 1500 rpm in a Thermomixer C (Eppendorf, Hamburg, Germany). The extract was centrifuged (Centrifuge 5424 R; Eppendorf AG, Hamburg, Germany) at 2500 × g and 4 °C for 10 min, and the supernatant was transferred into a new labeled tube. The residue was submitted to a second cycle of extraction in the same conditions. The combined supernatant containing free phenolic compounds was evaporated by a rotary vacuum evaporator at 40 °C (Rotavapor<sup>®</sup> R-300, Büchi Labortechnik AG, Flawil, Switzerland) and re-suspended in 2 mL of absolute methanol.

The dry residue remaining (1 g) after the removal of free phenolics was subjected to alkaline and acid hydrolysis. The residue was re-suspended in 12 mL of 2 M NaOH, vortexed for 30 s and stirred overnight at room temperature. The hydrolysate was acidified with 6 N HCl to pH 2, and the released phenolics were extracted with 7 mL of ethyl acetate three times and centrifuged at 10,000 × g and 4 °C for 10 min. The remaining aqueous layer was subsequently hydrolysed with 2.5 mL of 6 N HCl and incubated at 85 °C for 30 min. After cooling down on ice for 5 min, hydrolysates were repartitioned with ethyl acetate three times. The organic layers of alkaline and acid hydrolysates were evaporated by a rotary vacuum evaporator at 40 °C (Rotavapor<sup>®</sup> R-300, Büchi Labortechnik AG, Flawil, Switzerland), reconstituted in 5 mL of 70% methanol and filtered using 0.22 µm syringe filters prior to analysis.

### 2.8. Determination of Total Free and Insoluble Phenolic Content

The free and insoluble phenolic content was determined by the FBBB reaction according to [20]. Briefly, 1 mL of lentil extract or standard was mixed with 100 µL of freshly prepared FBBB reagent (0.1% in distilled water) and vortexed for 1 min. Immediately, the extract or standard solutions were shaken after adding 100 µL of 5% NaOH and allowed to react for 120 min at room temperature. Finally, 200 µL of the reaction mixture was placed in a 96-well plate, and the absorbance was measured at 420 nm using a Synergy HT (BioTek Instruments, Winooski, VT, USA) microplate reader. Quantification of the polyphenol content was performed using a gallic acid calibration curve (0–225 µg/mL, R<sup>2</sup> > 0.99). All analyses were performed in duplicate. The data were expressed as mg of gallic acid equivalents (GAE)/g DW.

### 2.9. Analysis of Phenolic Profile by HPLC-DAD-ESI-MS<sup>2</sup>

The identification and quantification of free phenolic compounds was performed according to a previously described method [21]. First, purification of the phenolic extracts was carried out by solid-phase extraction using C18 Sep-Pak cartridges (Waters, Milford, MA, USA), which were previously activated with methanol (2 mL), followed by distilled water (3 mL). Purified sample extracts were injected onto a Hewlett–Packard 1100-diode array detector (DAD) liquid chromatograph (Agilent Technologies, Palo Alto, CA, USA) including a quaternary pump. The mobile phases utilized were 0.1% formic acid in water (solvent A) and 100% acetonitrile (solvent B). The elution gradient employed was 15% B for 5 min, 15–20% B for 5 min, 20–25% B for 10 min, 25–35% B for 10 min, 35–50% B for 10 min and column re-equilibration. The chromatographic separation of the phenolic compounds was conducted at a flow rate of 0.5 mL/min at 35 °C in a Spherisorb S3 ODS-2 C8 column (Waters, Milford, MA, USA) (3 µm, 150 mm × 4.6 mm i.d.). Based on the different maximum absorbance wavelengths among the phytochemicals, the preferred wavelengths for DAD detection were 280 nm (hydroxybenzoic and hydroxycinnamic acids) and 370 nm (flavonols). The mass spectrometer (MS) was coupled to the HPLC system through the DAD cell output, and the detection was conducted in an API-3200 Qtrap (Applied Biosystems, Darmstadt, Germany) equipped with an ESI source, a triple

quadrupole-ion trap mass analyzer and the Analyst 5.1 software. The phenolic compounds were identified using their retention times, UV and mass spectra, fragmentation patterns and comparison to authentic standards when available. For quantitative analysis, gallic acid and *trans-p*-coumaric derivatives were measured using the calibration curves of the respective free acid. Quercetin derivative was quantified using the respective quercetin-3-*O*-glucoside curve, kaempferol derivatives were quantified using kaempferol 3-*O*-rutinoside and (+)-catechin and proanthocyanidins were quantified using the (+)-catechin curve and (–)-epicatechin was quantified using the (–)-epicatechin curve. The concentrations of each phenolic compound were expressed as  $\mu\text{g/g DW}$ .

#### 2.10. Oxygen Radical Absorption Capacity (ORAC) Assay

An ORAC assay of the lentil hull extracts and hydrolysates was determined following an earlier reported procedure [18]. Briefly, 180  $\mu\text{L}$  of 70 nM fluorescein was mixed with 90  $\mu\text{L}$  of 12 mM AAPH and 30  $\mu\text{L}$  of extract or standard. The reaction mixtures were placed in a black 96-well plate (Fisher Scientific, Waltham, MA, USA), and the fluorescence was measured in a Synergy HT microplate reader (BioTek Instruments, Winooski, VT, USA) every minute at excitation and emission wavelengths of 485 and 520 nm, respectively. An external calibration curve using Trolox as the standard in a linear concentration range from 0 to 160  $\mu\text{M}$  was prepared from a freshly made 1 mM stock solution. The results were expressed as  $\mu\text{mol Trolox equivalents (TE)/g DW}$ .

#### 2.11. ABTS (2,2'-Azinobis 3-ethylbenzothiazoline-6-sulfonic acid) Radical Scavenging Assay

The ABTS radical scavenging activity of the lentil hull extracts and hydrolysates was measured following a previously reported method [22]. Briefly, an ABTS radical ( $\text{ABTS}^{\bullet+}$ ) solution was prepared by mixing 7 mM ABTS with 2.45 mM  $\text{K}_2\text{O}_8\text{S}_2$  at a 1:1 (*v/v*) ratio. The mixture was reacted for 16 h (room temperature, dark conditions). Then, the absorbance at 734 nm of the  $\text{ABTS}^+$  working solution was adjusted to  $0.70 \pm 0.02$  by diluting with phosphate buffer (75 mM, pH 7.4). A volume of 20  $\mu\text{L}$  of the extract or standard was mixed with 200  $\mu\text{L}$  of the  $\text{ABTS}^+$  working solution in a 96-well microplate. The mixtures were reacted for 30 min in darkness at room temperature. The absorbance was read at 734 nm in a Synergy HT microplate reader (BioTek Instruments, Winooski, VT, USA), and a Trolox calibration curve was used in the concentration range from 0 to 800  $\mu\text{M}$ . The results were expressed as  $\mu\text{mol TE/g DW}$ .

#### 2.12. Statistical Analysis

All the replicated chemical composition analyses and the oligosaccharide, phenolic compounds and water-soluble fraction yield assays were repeated twice. The experimental data were expressed as the mean and standard deviation of six values accordingly. Pearson's correlation was performed to elucidate the relationships among the variables. The differences between the experimental groups were compared by one-way analysis of variance (ANOVA) and Bonferroni's post hoc test. Differences with  $p \leq 0.05$  were considered statistically significant. All statistical analyses were conducted using Statgraphics Centurion XVIII (Statgraphics Technologies, The Plains, VA, USA).

### 3. Results

#### 3.1. Red Lentil Hulls Are a Source of Dietary Fiber and Polyphenols, Containing Considerable Amounts of Protein and Trypsin Inhibitors and Minor Amounts of Starch and Phytic Acid

The assessment of the nutritional composition of lentil hulls is essential for the determination of any potential use in the development of value-added products. The chemical composition of the red lentil hulls obtained from an industrial lentil-processing plant is shown in Table 1. Almost 90% of the red lentil hulls were composed of carbohydrates and proteins. Among the carbohydrates, TDF was the main compound, representing 78.4 g/100 g DW, which was a slightly higher value compared to those of earlier studies (73.34 and 71.32 g/100 g DW for red and green lentil hulls, respectively) [23]. Dietary fiber

is an important food ingredient with prebiotic properties. Properly increasing dietary fiber intake can increase gastrointestinal motility, improve the abundance of the beneficial gut microbiota and promote the production of short-chain fatty acids so as to prevent gastrointestinal or related diseases [5]. The results of previous studies revealed that only 3.05%, 3.09%, 4.37% and 2.82% of the TDF in the seed coats of mung bean, fava bean, lentil and pea, respectively, was soluble [24]. This was in agreement with our results, which showed insoluble non-starch polysaccharides as the most abundant dietary fiber components in the red lentil hulls (IDF, 69.3 g/100 g DW) with minor amounts of soluble non-starch polysaccharides (HMW-SDF, 9.11 g/100 g DW, Table 1). The HMW-SDF content in the red lentil hulls reported herein was notably higher than that previously reported for red and green lentil hulls (1.5 and 2.90 g/100 g DW, respectively) [23]. Non-digestible oligosaccharides (LMW-SDF) were not detected in the red lentil hulls (Table 1) in accordance with Zhong et al. [2].

**Table 1.** Nutritional composition and total phenolic content of red lentil hulls from lentil processing industry (Prairie Pulse Inc., Vanscoy, SK, Canada).

Nutritional Parameters	Units	Mean $\pm$ SD <sup>1</sup>
TDF	g/100 g	78.43 $\pm$ 2.13
IDF	g/100 g	69.32 $\pm$ 2.67
HMW-SDF	g/100 g	9.11 $\pm$ 0.55
Oligosaccharides	g/100 g	ND
Protein	g/100 g	9.12 $\pm$ 0.01
Starch	g/100 g	0.13 $\pm$ 0.01
Phytic acid	g/100 g	0.06 $\pm$ 0.00
Trypsin inhibitory activity	TIU/mg	18.26 $\pm$ 1.50
Total phenolic compounds	mg GAE/g	49.76 $\pm$ 4.74
Free phenolic compounds	mg GAE/g	21.44 $\pm$ 0.82
Bound phenolic compound	mg GAE/g	27.45 $\pm$ 2.62
Total Condensed tannins	mg CAE/g	15.83 $\pm$ 1.32

<sup>1</sup> (n = 6). Abbreviations: CAE, catechin equivalents; GAE, gallic acid equivalents; HMW-SDF, high-molecular-weight soluble dietary fiber; IDF, insoluble dietary fiber; SD, standard deviation; TDF, total dietary fiber; ND: non-detected; TIU: trypsin inhibitory units.

The ratio of insoluble and soluble fiber may play an important role in influencing the potential health benefits of products. The IDF:HMW-SDF ratio of the red lentil hulls was 7.6, indicating that only about 14% of the intrinsic dietary fiber in the lentil seed coat was accessible for fermentation by the gut microbiota. This was a relatively low content of microbiota-accessible carbohydrates, compared with the 75–90% value for the intrinsic dietary fiber of fruits and vegetables [5]. Thus, the food processing of lentil seed coats through changing the physical structure of dietary fiber may have great potential for improving the quantity and quality of microbiota-accessible carbohydrates.

Regarding the protein content, the mean value reached 9.12 g/100 g DW, which was very close to the reported values for red (8.64 g/100 g) and green (8.58 g/100 g) lentil hulls [23]. Legume seed coats contain structural proteins such as proteoglycans and glycoproteins in the cell wall, which are used for the aggregation and expansion of cells during growth [5]. Minor amounts of starch were present in the lentil hulls (0.13 g/100 g, Table 1), which was in accordance with the literature that points out that the starch content in lentil hulls is below 10% [24].

The phytic acid content of the red lentil hulls (0.06 g/100 g DW) (Table 1) was similar to the reported values for chickpea hulls (0.08 g/100 g DW) but was markedly lower compared to the previous reports for green lentil, red lentil, fava bean and pea hulls (0.15–0.17 g/100 g) [23]. The variation in the phytic acid content of lentil hulls reported in the literature is attributed to genetic and environmental factors [25]. As compared with dehulled red lentil seeds (1.12 g/100 g DW) [18], the lentil hulls in the current study had a lower phytic acid content. In legume seeds, the majority of the phytic acid (more than 95%)



is stored as globoids, which are compartmentalized in the protein storage vacuoles of the cotyledons [25], which explains the low values observed.

Trypsin inhibitory activity was detected in the red lentil hulls, although the mean values (18.3 TIU/mg DW) were remarkably high when compared to the reported values for dehulled red lentil and the whole seeds of grey zero-tannin lentils, black lentil and fava bean (10–16 TIU/mg) [18]. Typical inhibitors of gastrointestinal proteases are protein molecules such as the Bowman–Birk and Kunitz trypsin inhibitors, which are mainly located in cotyledons; however, it is known that polyphenols also have the ability to inhibit digestive enzymes such as trypsin [26]. The higher abundance of free polyphenols in lentil seed coats and their partial extraction in aqueous solutions [27] could explain the high trypsin inhibitory activity observed for the red lentil hulls obtained in the present study (Table 1).

The total phenolic content obtained as the sum of the free and insoluble phenolic fractions of the red lentil hulls was 49.8 mg GAE/g (Table 1). This high amount of phenolic compounds suggested that this lentil milling by-product was a valuable source of phenolic compounds compared to other agri-food by-products (cranberry pomace: ~13.55–15.17 mg GAE/g DW; grape pomace:  $38.7 \pm 0.36$  mg GAE/g DW; and blueberry pomace: ~17.76–20.82 mg GAE/g DW) [28]. The TPC of the red lentil hulls observed in the present study was in the range reported in the literature (40.8–85.37 mg GAE/g DW) for typical hulls of the red, green and black lentil varieties [4,29]. The free and bound phenolic fractions were evenly distributed in the red lentil seed coats studied, with a slightly higher proportion of the bound (55% of the total phenolic content) as compared to the free phenolic fraction (45% of total phenolic fraction). Similarly, black and green lentil hulls showed a ratio of the free-to-insoluble phenolic fraction of 1:1 and 1:1.7, respectively [29]. Condensed tannins accounted for 15.83 mg CAE/g, suggesting that 75.4% of the free phenolic content in the red lentil hulls were catechins or tannins (Table 1). This finding was in agreement with earlier studies showing that procyanidins were the main phenolic subgroup (73–79%) of the free phenolic fraction of lentil hulls [4]. Regarding the distribution of the free and insoluble fractions in the total phenolic content, a variation depending on the lentil variety was found in the literature.

### *3.2. Free Phenolic Compounds in Lentil Hulls Are Major Contributors to the Antioxidant Activity of Lentil Hulls*

The antioxidant activity of the free, bound and total phenolic fractions was measured by in vitro chemical assays such as ORAC and ABTS assays (Figure 1).

The antioxidant activity, as determined by the ORAC and ABTS assays, was significantly higher in the free phenolic fraction as compared to the bound fraction of the red lentil hulls ( $p \leq 0.05$ ), which was in agreement with earlier investigations. For instance, Sun et al. [4] demonstrated a higher antioxidant capacity, as determined by ORAC, DPPH and FRAP assays, in the free phenolic fraction than in the conjugated and bound phenolic fractions of ADM red, Laird, CDC Greenland and Eston lentil hulls. Similar results were reported by Yeo and Shahidi [6] for CDC Greenland, CDC Invincible (green), 3493–6 (green) and CDC Maxim (red) lentil hulls. The untargeted metabolomics approach performed by [8] for correlating seed coat polyphenol profiles with antioxidant activity concluded that, regardless of the pulse crop, the antioxidant activity was largely attributed to proanthocyanidins (the main phenolic subgroup found in the soluble fraction of lentil hulls, Table 1), although flavan-3-ols were also important. These phenolic compounds form hydrogen bonds with the polar head groups of the liposome phospholipids of liposome membranes, which protect against induced oxidative damage [30].

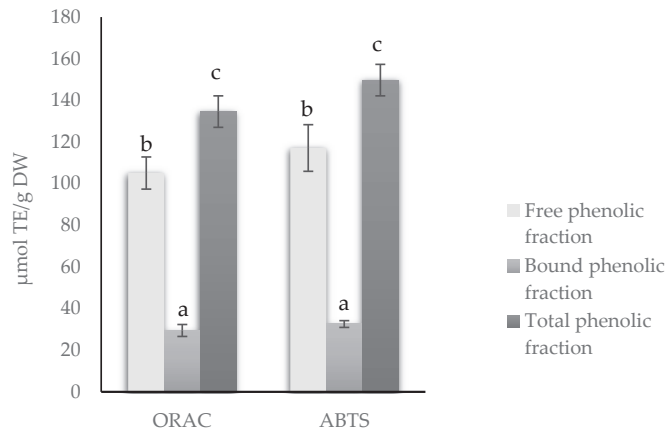


**Figure 1.** Antioxidant activity of free, bound and total phenolic fraction of red lentil hulls. Data are expressed as  $\mu\text{mol}$  Trolox equivalents (TE)/g dry weight. Error bars represent standard deviation ( $n = 6$ ). Different letters denote statistical differences among free, bound and total phenolic fractions ( $p \leq 0.05$ ). Abbreviations: ABTS, 2,2'-azino-bis-3-ethylbenzothiazoline-6-sulfonic acid; ORAC, oxygen radical absorbance capacity; TE: Trolox equivalents; DW: dry weight.

### 3.3. Pectinex<sup>®</sup> Ultra Tropical Released High Amounts of Oligosaccharides and Phenolics from Lentil Hull Food Matrix

To maximize the health benefits of the lentil hulls, enzymatic hydrolysis was explored in the present study as a processing strategy for improving the quantity and quality of microbiota-accessible carbohydrates and phenolics. Increased amounts of accessible oligosaccharides and phenolics in lentil hull hydrolysates can positively influence the regulation of intestinal immunity by directly binding to the toll-like receptors on monocytes, macrophages and intestinal cells in order to modulate cytokine production and immune cell maturation in a microbiota-independent manner [5]. Bioprocessing using enzymes has been used to modify the physical structure of cereal brans and improve the release of bound phenolic acids and soluble carbohydrates [11,20,31]. However, to the best of our knowledge, there have been no studies reporting the release of oligosaccharides and phenolics from lentil hulls by means of enzymatic hydrolysis. In the present study, seven commercial enzyme preparations were used and screened for the release of oligosaccharides and phenolic compounds and their effects on increasing the antioxidant activity of the lentil hulls (Table 2).

Regardless of the enzyme type used, the enzymatic hydrolysis allowed the lentil hulls to be enriched in oligosaccharides compared to the control sample, where these carbohydrates were not detected (Table 2). The enzymatic treatment of the lentil hulls with carbohydrate-hydrolyzing enzymes broke down the cellulose, hemicellulose and pectin in the lentil hulls into smaller poly-, oligo-, di- and monosaccharides, thereby making them water-soluble and subsequently allowing their release from the lentil hull matrix.

The highest oligosaccharide concentration was observed in the hydrolysates obtained using Pectinex<sup>®</sup> Ultra Tropical (14.17 g/100 g DW). Shearzyme<sup>®</sup> Plus 2X (9.79 g/100 g DW) and Viscozyme<sup>®</sup> L (7.54 g/100 g DW) also produced oligosaccharides but to lesser extent than Pectinex<sup>®</sup> Ultra Tropical (Table 2). The rest of the enzymes tested also produced oligosaccharides, although to a lesser extent (1.55–3.57 g/100 g). The enzymatic activities of the tested commercial enzyme preparations were highly variable, and the side activities had a strong impact on the oligosaccharide yields of the hydrolysates. Nevertheless, our results suggested that the greatest increase in the oligosaccharide content of the red lentil hull hydrolysates was determined using the enzyme preparations, which were mainly pectinases. Pectinase<sup>®</sup> Ultra Tropical had pectinase as its main declared activity, and it also had, to lesser extent, cellulase, xylanase and endo-1,4- $\beta$ -glucanase (Table S1). In addition,

compared with the other commercial pectinase preparations, Pectinase<sup>®</sup> Ultra Tropical exhibited the highest pectin-depolymerizing activity [31]. The activity of pectinase is due to a mixture of the following exo- and endo-enzymes: (1) pectinesterases, which catalyze the release of the pectin methyl-ester groups producing polygalacturonic acid and methanol; (2) polymethylgalacturonase and polygalacturonase, which break down pectin  $\alpha$ -1,4-glycosidic linkages; and (3) polymethylgalacturonate lyases and polygalacturonate lyases, which hydrolyze pectin  $\alpha$ -1,4-glycosidic linkages by a *trans*-elimination mechanism [32]. The highest oligosaccharide yield obtained by the Pectinase<sup>®</sup> Ultra Tropical treatment (Table 2) suggested that this enzyme treatment mainly catalyzed the hydrolysis of pectin in the red lentil hulls to release pectin oligosaccharides. Like in other legume seed coats, pectin is a major component of the soluble dietary fiber in lentil, which is characterized as a multi-branched structure composed of linear 1,3- and 1,5-arabinan and linear 1,4-glucan containing arabinose, glucose and galacturonic acid as constituent sugars [33]. The partial hydrolysis of pectin and incomplete monomerization has also been reported during the Pectinex<sup>®</sup> Ultra SPL enzyme-aided cell wall disintegration of carbohydrate-rich byproducts obtained from the production of concentrate soy protein [34].

**Table 2.** Oligosaccharides and soluble phenolic compound release and antioxidant activity in hydrolyzed lentil seed coats treated by seven commercial food-grade enzymes.

Enzymes	OS (g/100 g DW)	SPC (mg GAE/g DW)	SPC Ratio (%)	ORAC ( $\mu$ mol TE/g DW)	ABTS ( $\mu$ mol TE/g DW)
Control	ND	21.45 $\pm$ 2.62	-	105.11 $\pm$ 7.72	117.12 $\pm$ 11.17
Ultraflo <sup>®</sup> XL	3.12 $\pm$ 0.15 a,***	41.04 $\pm$ 1.25 ab,*	71.39 $\pm$ 4.57 ab	451.40 $\pm$ 10.85 b,*	402.01 $\pm$ 37.07 b,*
Ultraflo <sup>®</sup> Max	1.89 $\pm$ 0.01 a	38.29 $\pm$ 1.44 ab,*	61.35 $\pm$ 5.24 ab	399.93 $\pm$ 19.40 a,*	390.82 $\pm$ 18.95 a,*
Ultimase <sup>®</sup> BWL 40	1.55 $\pm$ 0.17 a	40.70 $\pm$ 0.37 ab,*	70.14 $\pm$ 1.34 ab	445.01 $\pm$ 9.79 b,*	417.31 $\pm$ 43.18 b,*
Viscozyme <sup>®</sup> L	7.54 $\pm$ 0.03 b,*	41.44 $\pm$ 0.62 bc,*	72.83 $\pm$ 2.27 bc	421.06 $\pm$ 14.56 b,*	421.55 $\pm$ 34.28 b,*
Celluclast <sup>®</sup> 1.5L	3.57 $\pm$ 0.04 a,***	39.81 $\pm$ 0.97 ab,*	66.92 $\pm$ 3.55 ab	408.08 $\pm$ 11.60 a,*	384.80 $\pm$ 32.34 a,*
Pectinex <sup>®</sup> Ultra Tropical	14.17 $\pm$ 1.41 c,*	45.51 $\pm$ 4.44 c,*	98.59 $\pm$ 0.96 c	442.04 $\pm$ 15.44 b,*	424.06 $\pm$ 29.11 b,*
Shearzyme <sup>®</sup> Plus 2X	9.79 $\pm$ 0.66 b,*	36.18 $\pm$ 0.21 a,*	53.67 $\pm$ 0.75 a	342.17 $\pm$ 34.09 a,*	359.95 $\pm$ 17.17 a,*

Data are the mean  $\pm$  standard deviation (n = 6). Different letters within a column indicate statistical differences among the enzymes ( $p \leq 0.05$  Bonferroni's post hoc test). An asterisk indicates significant differences between control and enzyme treatments (\*  $p \leq 0.000009$ ; \*\*  $p \leq 0.000707$ ; \*\*\*  $p \leq 0.002215$  Dunnett's post hoc test). Abbreviations: ABTS, 2,2'-azino-bis-3-ethylbenzothiazoline-6-sulfonic acid radical scavenging activity; GAE, gallic acid equivalents; ORAC, oxygen radical absorbance capacity; ND, not detected; OS, oligosaccharides; SPC, soluble phenolic compounds; TE, Trolox equivalents; DW: dry weight.

Similarly, the phenolic extraction yield showed a significant variation among the enzymatic treatments that ranged between 54% and 99% of the total bound phenolic content (Table 2). Pectinex<sup>®</sup> Ultra Tropical and Viscozyme<sup>®</sup> L produced the highest concentration of soluble phenolics (45.5 and 41.4 mg GAE/g, respectively), whereas Shearzyme<sup>®</sup> Plus 2X was the least efficient enzymatic treatment in terms of the solubilization of bound phenolics from the red lentil hull food matrix ( $p \leq 0.05$ ). The higher phenolic extraction yield observed when the lentil hulls were treated with Pectinex<sup>®</sup> Ultra Tropical and Viscozyme<sup>®</sup> L might be explained by the enhanced cell-wall structure breakdown as a result of cell-wall component hydrolysis, particularly the glycosidic bonds/linkages between phenolic compounds and cell-wall polysaccharides [16]. Similar results were reported recently by other researchers who treated cranberry pomace (59.93 g/100 g DW of IDF and 12.74 g/100 g of SDF) with different commercial enzymes to modify the dietary fiber composition and technological properties of this by-product [28]. In this previous study, Viscozyme<sup>®</sup> L and Pectinex<sup>®</sup> Ultra Tropical enhanced to a greater extent the yields of oligosaccharides (7.1 and 5.9 g/100 g, respectively, vs. 1.9 g/100 g for the control) and phenolic compounds (7.8 and 7.4 mg GAE/g, respectively, vs. 7.0 mg GAE/g for the control). Moreover, it was demonstrated that water-soluble fractions showed prebiotic activity and enhanced the growth of *Lactobacillus acidophilus* DSM 20,079 and *Bifidobacterium animalis* DSM 20,105 after 24 h of fermentation.

Regardless of the enzyme used, all the lentil hull hydrolysates showed between a three- to four-fold increase in antioxidant activity as compared to the control (105.11 and 117.12  $\mu\text{mol TE/g}$  for the ORAC and ABTS assays, respectively). Pearson's correlation analysis showed a significant positive association between the soluble phenolic content and antioxidant activity of the lentil hull hydrolysates ( $R^2 = 0.64$  and  $0.74$  for the ORAC and ABTS assays, respectively,  $p \leq 0.05$ ). Therefore, the increased antioxidant activity in hydrolysates could be attributed to the enzymatic release of phenolic compounds from the lentil hull food matrix. Moreover, the antioxidant increase could be attributed to the release of oligosaccharides, as previously reported for pectin oligosaccharides [35]. Comparisons among the enzymatic treatments indicated that Ultraflo<sup>®</sup> XL, Ultimase<sup>®</sup> BWL 40, Viscozyme<sup>®</sup> L and Pectinex<sup>®</sup> Ultra Tropical produced lentil hull hydrolysates with a higher antioxidant activity as compared to Ultraflo<sup>®</sup> Max, Celluclast<sup>®</sup> and Shearzyme<sup>®</sup> Plus 2X ( $p \leq 0.05$ ). These results were strongly supported by De Camargo et al. [36] and Gómez-García et al. [37] who studied how enzymatic hydrolysis affected the antioxidant potential of winemaking by-products, in which they found a significant increase in total phenolic compounds and antioxidant activity overall when enzymes such as Viscozyme<sup>®</sup> L, and Pectinex<sup>®</sup> Ultra Tropical were used.

Taking into account all the results from the screening of the seven commercial enzymes, Pectinex<sup>®</sup> Ultra Tropical was selected because it exhibited the highest oligosaccharide and soluble phenolics yield, which was associated to a higher antioxidant activity. To provide insight into the rate at which the release of oligosaccharides and phenolics and the increase in antioxidant activity occurred, the time course of lentil hull hydrolysis by the Pectinex<sup>®</sup> Ultra Tropical treatment is shown in Figure 2.

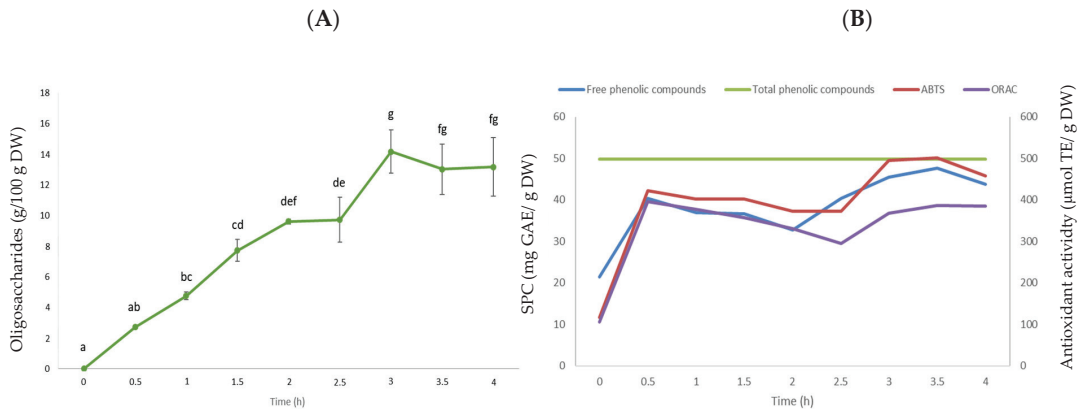


**Figure 2.** Time course of the extraction of oligosaccharides (A) and phenolic compounds and the increase in antioxidant activity as determined by ORAC and ABTS assays (B). Data are the mean  $\pm$  standard deviation ( $n = 6$ ). Different lowercase letters indicate statistical differences among each time ( $p \leq 0.05$  Bonferroni's post hoc test). Green line in panel (B) represents the total phenolic content in untreated lentil hulls. Abbreviations: ABTS, 2,2'-azino-bis-3-ethylbenzothiazoline-6-sulfonic acid radical scavenging activity; ORAC, oxygen radical absorbance capacity; SPC, soluble phenolic compounds; GAE, gallic acid equivalents; TE, Trolox equivalents; DW, dry weight.

The oligosaccharide yield gradually increased in the lentil hull hydrolysates and peaked at 3 h, where the maximum yield was 14 g/100 g lentil hull hydrolysate (Figure 2A). The kinetics of phenolic extraction was much faster (Figure 2B) compared to the behavior of the oligosaccharide extraction yields (Figure 2A). The yield of phenolic compounds increased rapidly up to two-fold in 0.5 h and reached an equilibrium from 0.5 to 2 h, after which it increased again from 2 to 3 h, where the maximum yield was observed. The antioxidant activity, as determined by the ORAC and ABTS assays, showed a similar trend to the phenolic extraction yield. As a result, in this investigation, an enzymatic hydrolysis

endpoint of 3 h was selected as appropriate since a reasonable amount of phenolics was extracted, and maximum oligosaccharide yields and antioxidant activity were achieved.

### 3.4. Pectinex Treatment of Lentil Hull Increased the Bioactive Compounds and Antioxidant Activity to a Greater Extent than Microwaves or Their Combined Treatment

A recent study proved that microwaves (MW) might be considered as an efficient environmentally friendly method for the extraction of phenolic compounds and for the enhancement of the antioxidant activity of pulse extracts [15]. MW technology is advantageous not only due to its quick heating ability for extraction, reduced thermal gradients, higher yield, low usage of solvent, small size of equipment and lower energy but also because of the applicability of water as a green and polar solvent [38]. Moreover, MW technology has already been tested in a semi-industrial scale for the valorization of agro-industrial by-products [39], reducing the environmental and economic impacts and promoting the beneficial effects for human health. In this work, the potential of MW to release oligosaccharides and polyphenols from lentil hulls was tested and compared with the Pectinex® Ultra Tropical (EH-P) treatment and the sequential microwave–enzymatic (MW + EH-P) treatments (Table 3).

**Table 3.** Effect of MW, EH-P and MW + EH-P on oligosaccharides, soluble phenolics, soluble water fraction yields and antioxidant activity of lentil hulls.

Treatment	Oligosaccharides (g/100 g DW)	SPC (mg GAE/g DW)	Water-Soluble Fraction Yield (g/100 g DW)	ORAC (μmol TE/g DW)	ABTS (μmol TE/g DW)
Control	ND	21.45 ± 2.62 <sup>a</sup>	9.58 ± 0.47 <sup>a</sup>	105.11 ± 7.72 <sup>a</sup>	117.12 ± 11.17 <sup>a</sup>
MW	4.65 ± 0.23 <sup>a</sup>	36.28 ± 0.60 <sup>b</sup>	12.59 ± 0.93 <sup>b</sup>	245.60 ± 5.65 <sup>b</sup>	236.97 ± 19.27 <sup>b</sup>
EH-P	14.17 ± 1.41 <sup>c</sup>	45.51 ± 4.44 <sup>d</sup>	24.92 ± 0.25 <sup>c</sup>	442.04 ± 15.44 <sup>d</sup>	424.06 ± 29.11 <sup>d</sup>
MW + EH-P	12.12 ± 0.81 <sup>b</sup>	41.45 ± 0.96 <sup>c</sup>	34.27 ± 0.67 <sup>d</sup>	403.98 ± 20.33 <sup>c</sup>	376.98 ± 15.63 <sup>c</sup>

Data are the mean ± standard deviation (n = 6). Different letters within a column indicate statistical differences ( $p \leq 0.05$  Bonferroni's post hoc test). Abbreviations: GAE, gallic acid equivalents; ND, not detected; MW, microwave; EH-P, enzymatic hydrolysis by Pectinex® Ultra Tropical; MW + EH-P, sequential microwave and enzymatic hydrolysis by Pectinex® Ultra Tropical; ABTS, 2,2'-azino-bis-3-ethylbenzothiazoline-6-sulfonic acid scavenging activity; ORAC, oxygen radical absorbance capacity; SPC, soluble phenolic compounds; TE, Trolox equivalents; GAE, gallic acid equivalents; DW: dry weight.

As compared to the control, the MW treatment significantly increased the amounts of oligosaccharides (4.65 g/100 g DW) and phenolic compounds (36.28 g/100 g DW) and, consequently, the water-soluble yield (12.59 g/100 g DW) in the lentil hulls (Table 3,  $p \leq 0.05$ ). Similarly, Andreani and Karboune [40] reported the microwave-assisted enrichment of extracts from American cranberry pomace with oligosaccharides, with a degree of polymerization yield from 7 to 10. The increased oligosaccharide levels upon the MW treatment of the lentil hull may be explained by the changes in dietary fiber composition as reported previously for whole legume seeds [41]. In black grams, chickpeas, lentils and red and white kidney beans, MW treatment resulted in a reduction in hemicellulose and cellulose content due to their breakdown into low-molecular-weight carbohydrates (oligo-, di- and monosaccharides). Likewise, microwave cooking has been shown to increase the total soluble phenolic content of whole fava bean, lentil and pea seeds [42]. Electromagnetic waves produce dipoles and ion conduction that heat solvent molecules. Microwave heating might cause severe cell rupture due to the thermal expansion of cellular liquid, the denaturation of the cell membrane and through its impact on cell wall components, to which some bioactive compounds (i.e., phenolics) might have been bound to [43].

The higher amounts of bioactive compounds (14.17 g oligosaccharides/100 g DW, 45.51 g GAE/g DW) and the higher water-soluble fraction (24.92 g/100 g DW) and antioxidant activity (424–442 μmol TE/g DW) found in the lentil hull hydrolysates indicated that, in our study, the EH-P treatment was more effective than the MW treatment (Table 3). Our results were supported by the study of Andreani and Karboune [40] who compared enzymatic and microwave extraction approaches for the generation of oligosaccharides from

American cranberry (*Vaccinium macrocarpon*) pomace. In this investigation, higher carbohydrate yields were obtained when the cranberry pomace was treated by multi-enzymatic biocatalysts compared to the microwave-assisted extraction. Moreover, the enrichment of the lentil hulls in terms of soluble phenolic compounds by Pectinex® Ultra Tropical could be explained by the breakdown of pectin into smaller polysaccharides and, to lower extent, cellulose and hemicellulose polymers, thereby allowing the phenolic compounds to be released from the cell wall matrix and increasing the radical scavenging activity. In previous studies, pectinase treatments (Pectinex Yield Mash and Pectinex AFP L-4, to a greater extent) of apple pomace clearly yielded a higher content of soluble phenolics and increased the radical scavenging activity of puree-enriched cloudy apple juices as compared to the untreated control sample [44], which supported our results.

The MW + EH-P treatment led to lower oligosaccharide and phenolic yields in the lentil hulls and decreased the antioxidant activity as compared to the enzyme treatment EH-P (Table 3,  $p \leq 0.05$ ). In contrast, the highest water-soluble fraction yield was observed with the sequential application of MW and EH-P (Table 3). Hence, as the oligosaccharide and phenolic yields could not explain the increasing difference in the solubilization yield as compared to the other treatments, we hypothesized that this increase was due to a higher solubilization of fiber components by the MW pretreatment and the subsequent hydrolysis by Pectinex Ultra Tropical to oligo-, di- and monosaccharides. Some studies have demonstrated that after microwave treatment, the surface area between enzyme and dietary fiber may increase, thus promoting penetration and the release of soluble substances [36]. The decreased yield of total phenolic compounds and antioxidant activity by the microwave pretreatments combined with enzymes (Viscozyme®) might be attributed to the high temperature and microwave radiation affecting the rate of phenolic extraction from the lentil hulls, the enzymatic oxidation and the polymerization processes. Heat from the microwaves causes the structural degradation of phenolic compounds. This results in steric obstruction of the enzyme binding sites to the substrate, which inhibits the degradation of cell-wall components [16].

### 3.5. Pectinex Treatment of Lentil Hull Increased the Content of Extractable Flavan-3-ols to a Greater Extent than Microwaves or Their Combined Treatment

The changes in the level of free phenolic compounds in the lentil hulls before and after the MW, EH-P and MW + EH-P treatments were also measured by HPLC-ESI-MS<sup>2</sup>. The phenolics were identified based on the MS<sup>2</sup> data, UV spectra and retention times (Rt) compared with those of authentic standards, in a database and/or in the literature. A total of 18 compounds were identified or tentatively characterized in the different lentil hull samples. Detailed information of the identified compounds is summarized in Table S2. The main phenolic compounds of the red lentil hulls were (+)-catechin *O*-hexoside (763 µg/g), galloylated dimer I (532 µg/g), procyanidin dimer II (482 µg/g), procyanidin trimer (453 µg/g), prodelfinidin dimer I (446 µg/g), prodelfinidin trimer (390 µg/g) and gallic acid (374 µg/g) (Table 4). (–)-epicatechin, quercetin and kaempferol glucosides and *trans-p*-coumaric acid derivatives were also detected in much lower amounts. The phenolic composition of the red lentil hulls was in accordance with previous studies that characterized the free phenolic profile of hulls from different lentil varieties (CDC Greenland, CDC 3494-6, CDC Invincible, CDC Maxim, Laird and Eston) [4,6]. In these subsets of commercial lentil varieties, the most abundant free phenolics were procyanidins, including monomeric, dimeric and trimeric flavan-3-ols.

**Table 4.** Effect of MW, EH-P and MW + EH-P on individual phenolic compounds ( $\mu\text{g/g}$  DW) of lentil hulls.

Compound	Control	MW	EH-P	MW + EH-P
<i>Phenolic acid</i>				
Gallic acid	373.93 $\pm$ 30.88 <sup>a</sup>	464.02 $\pm$ 10.39 <sup>a</sup>	403.44 $\pm$ 37.10 <sup>a</sup>	507.18 $\pm$ 49.37 <sup>a</sup>
<i>trans-p</i> -coumaric acid derivative I	7.45 $\pm$ 0.96 <sup>b</sup>	7.17 $\pm$ 0.80 <sup>b</sup>	20.98 $\pm$ 2.03 <sup>c</sup>	t <sup>a</sup>
<i>trans-p</i> -coumaric acid derivative II	17.53 $\pm$ 0.96 <sup>c</sup>	15.06 $\pm$ 1.86 <sup>c</sup>	7.84 $\pm$ 0.92 <sup>b</sup>	t <sup>a</sup>
<i>Prodelfphinidin</i>				
Dimer prodelfphinidin I	446.10 $\pm$ 14.92 <sup>a</sup>	517.98 $\pm$ 40.45 <sup>a</sup>	536.34 $\pm$ 15.70 <sup>a</sup>	550.42 $\pm$ 26.96 <sup>a</sup>
Dimer prodelfphinidin II	85.48 $\pm$ 1.69 <sup>a</sup>	156.01 $\pm$ 68.59 <sup>ab</sup>	391.85 $\pm$ 9.99 <sup>c</sup>	243.11 $\pm$ 6.65 <sup>b</sup>
Dimer prodelfphinidin III	51.04 $\pm$ 1.13 <sup>a</sup>	99.98 $\pm$ 14.93 <sup>b</sup>	115.01 $\pm$ 8.83 <sup>b</sup>	116.78 $\pm$ 5.46 <sup>b</sup>
Trimer prodelfphinidin	389.8 $\pm$ 34.42 <sup>a</sup>	525.96 $\pm$ 54.47 <sup>b</sup>	660.25 $\pm$ 15.02 <sup>c</sup>	550.87 $\pm$ 5.96 <sup>bc</sup>
<i>Procyanidin</i>				
Galloylated dimer I	532.8 $\pm$ 49.12 <sup>a</sup>	546.38 $\pm$ 10.02 <sup>a</sup>	955.32 $\pm$ 32.57 <sup>c</sup>	764.40 $\pm$ 43.70 <sup>b</sup>
Galloylated dimer II	100.17 $\pm$ 20.93 <sup>a</sup>	111.31 $\pm$ 30.51 <sup>a</sup>	205.57 $\pm$ 11.87 <sup>b</sup>	159.77 $\pm$ 7.20 <sup>ab</sup>
Dimer procyanidin I	111.70 $\pm$ 21.67 <sup>a</sup>	146.26 $\pm$ 15.28 <sup>a</sup>	263.10 $\pm$ 2.12 <sup>c</sup>	202.29 $\pm$ 16.23 <sup>b</sup>
Dimer procyanidin II	481.45 $\pm$ 1.24 <sup>a</sup>	648.39 $\pm$ 51.75 <sup>b</sup>	760.26 $\pm$ 11.67 <sup>b</sup>	872.67 $\pm$ 4.31 <sup>c</sup>
Trimer procyanidin	452.84 $\pm$ 53.58 <sup>a</sup>	594.95 $\pm$ 53.99 <sup>b</sup>	974.60 $\pm$ 3.86 <sup>c</sup>	912.56 $\pm$ 1.74 <sup>c</sup>
<i>Flavonoid</i>				
(+)-catechin <i>O</i> -hexoside	762.7 $\pm$ 0.12 <sup>a</sup>	799.62 $\pm$ 74.90 <sup>a</sup>	965.40 $\pm$ 1.00 <sup>b</sup>	957.21 $\pm$ 16.46 <sup>b</sup>
(+)-catechin	164.78 $\pm$ 16.53 <sup>a</sup>	553.83 $\pm$ 12.19 <sup>c</sup>	426.83 $\pm$ 22.79 <sup>b</sup>	416.01 $\pm$ 11.33 <sup>b</sup>
(-)-epicatechin	158.28 $\pm$ 11.44 <sup>a</sup>	179.61 $\pm$ 7.32 <sup>a</sup>	211.64 $\pm$ 21.23 <sup>a</sup>	165.27 $\pm$ 23.58 <sup>a</sup>
Quercetin rutinoside hexoside	9.54 $\pm$ 0.35 <sup>c</sup>	9.02 $\pm$ 0.41 <sup>c</sup>	4.89 $\pm$ 0.05 <sup>a</sup>	7.14 $\pm$ 0.63 <sup>b</sup>
Kaempferol dirutinoside	59.62 $\pm$ 2.73 <sup>b</sup>	59.16 $\pm$ 3.57 <sup>b</sup>	20.74 $\pm$ 0.11 <sup>a</sup>	25.88 $\pm$ 1.55 <sup>a</sup>
Kaempferol rutinoside hexoside	58.54 $\pm$ 2.36 <sup>b</sup>	54.55 $\pm$ 0.20 <sup>b</sup>	29.41 $\pm$ 0.48 <sup>a</sup>	32.27 $\pm$ 1.16 <sup>a</sup>

Data are the mean  $\pm$  standard deviation ( $n = 6$ ). Different letters across columns in the same row indicate statistical difference ( $p \leq 0.05$  Bonferroni's post hoc test). Abbreviation: MW, microwaves; EH-P, enzymatic hydrolysis by Pectinex<sup>®</sup> Ultra Tropical; MW + EH-P, sequential microwaves and enzymatic hydrolysis by Pectinex<sup>®</sup> Ultra Tropical; t, traces.

Overall, the MW treatment sharply increased the levels of individual free phenolics such as (+)-catechin (236% vs. control sample) and, to a lesser extent, proanthocyanidins: prodelfphinidin dimer III, procyanidin dimer II and trimers of prodelfphinidin and procyanidin (95%, 35%, 34% and 31% vs. control, respectively) (Table 4). Proanthocyanidins are an important group of bioactive molecules known for their promising benefits to human health [45]. Previous work has been reported on the microwave-assisted extraction of proanthocyanidin yields from seeds, peels, pomaces, leaves and barks of agro-industrial wastes [45,46], although there have been no studies performed for legume seed coats. Generally, in recent studies, higher recovery rates were reported for microwave-assisted extraction as compared with traditional extractions, although the extraction yields may vary depending on the processing conditions.

Compared to the control, EH-P enhanced the release of free phenolic compounds, mainly *trans-p*-coumaric acid derivative I, prodelfphinidins, procyanidins and (+)-catechin (>79% vs. control) and (+)-catechin *O*-hexoside (26.6% vs. control), as shown in Table 4. As discussed in Section 3.3, the enhancement of polyphenols may result from structural changes in the food matrix due to the enzymatic hydrolysis of fibrous polymers in the lentil hull cell walls. Proanthocyanidins are also the main polyphenolic compounds that are retained in apple pomace because they readily bind to cell-wall polysaccharides through hydrogen bonding and/or hydrophobic interactions [47]. Similar to our results, Oszmianski et al. [48] demonstrated that enzymatic preparations containing pectinase (Pectinex Yield Mash, Pectinex Smash XXL and Pectinex XXL) increased the polymeric procyanidin contents in puree-enriched cloudy juices. This was likely due to the enzymatic degradation of both the cell wall and vacuolar membrane that enabled the optimal recovery of these compounds. In another study, the use of a commercial pectinase (Endozym<sup>®</sup> Pectofruit PR) during the maceration of the winemaking process resulted in an increase in the extraction yield and the procyanidin B1 and B2 concentrations of grape juices [49].

The comparison of EH-P and MW indicated that Pectinex<sup>®</sup> Ultra Tropical increased, to a higher extent, the solubilization of most of the phenolic compounds present in the lentil hulls including prodelphinidin dimer II, prodelphinidin trimer, galloylated dimer I, procyanidin dimer I, procyanidin trimer and (+)-catechin *O*-hexoside. Although an overall positive effect was observed in the free phenolic content of the lentil hulls upon enzymatic treatment, some phenolic acids (*trans-p*-coumaric acid derivative II) and flavonoids (quercetin rutinoside hexoside, kaempferol dirutinoside and kaempferol rutinoside hexoside) were significantly lower after the EH-P and EHP+MW treatments than the MW treatment ( $p \leq 0.05$ ). This observation could be due to new interactions between the phenolics (*trans-p*-coumaric acid derivative II, quercetin rutinoside hexoside, kaempferol dirutinoside and kaempferol rutinoside hexoside) and other enzymatic hydrolysis products, particularly oligosaccharides [50]. These results suggested that the hydrolysate matrices of the lentil hulls were enriched mainly in the free proanthocyanidins that prevailed as compared to phenolic acids and flavonoids.

Finally, the MW + EH-P treatment of the lentil hulls showed similar effects in the solubilization of phenolic compounds as compared to the EH-P treatment, although small differences were found between both treatments. MW + EH-P caused a lower extraction of prodelphinidin dimer II, galloylated dimer I and procyanidin dimer I (38, 20 and 23% decrease vs. EH-P, respectively), but slightly higher yields for procyanidin dimer II (15% increase vs. EH-P). Such differences could be explained by thermally induced polyphenol oxidation that may be responsible for the lower antioxidant activity obtained in the lentil hulls after the MW + EH-P treatment (Table 3). Studies have often indicated that some polyphenols are non-stable and sensitive to thermal treatment. Although microwave heating causes a high level of cell disintegration of plant tissues, flavan-3-ols are sensitive to thermal treatments. Fernandes et al. [51] demonstrated that 50% of flavan-3-ols in apple pomace were reduced with hot water extraction.

#### 4. Conclusions

The comprehensive chemical characterization of industrial lentil hulls obtained from the production of football and split lentils reinforced the potential valorization of this underutilized by-product that is typically discarded as waste. Thus, the high content of fibers and total phenolic compounds described in this work warrants further functional studies dealing with the utility of lentil hulls as a human food ingredient. This study also highlighted the key role played by the selection of the commercial enzymatic preparation to streamline the potential food applications of lentil hulls. Thus, the screening of seven commercial enzymatic preparations revealed the suitability of Pectinex<sup>®</sup> Ultra Tropical for releasing oligosaccharides and phenolic compounds from the lentil hull matrix and, consequently, increasing the antioxidant activity in the hydrolysates. The follow-up of the time course of the enzymatic reactions by the Pectinex<sup>®</sup> Ultra Tropical indicated that, after 3 h, the maximum oligosaccharide and phenolic compounds yields as well as the highest antioxidant activity were achieved. The sequential microwave and enzymatic hydrolysis treatment, although it increased the solubilization yield of the lentil hulls, it decreased the content of oligosaccharides and proanthocyanidins and the antioxidant activity. Therefore, the enzymatic hydrolysis treatment alone was more suitable for producing a lentil hull hydrolysate enriched in potential prebiotics and antioxidant compounds. Future research should be focused on the optimization of the process by using different enzymatic hydrolysis parameters (enzyme concentration, enzyme–substrate ratio, pH, temperature, time and stirring speed) in order to establish the full biological potential of lentil hulls.

**Supplementary Materials:** The following supporting information can be downloaded at: <https://www.mdpi.com/article/10.3390/molecules27238458/s1>, Table S1: Origin, working pH and temperature range and declared enzymatic activities of seven commercial glycosidases (Novozymes, Bagsværd, Denmark); Table S2: Retention time (Rt), wavelengths of maximum absorption in the visible region ( $\lambda_{\max}$ ), mass spectral data and tentative identification of phenolic compounds in raw and processed lentil hulls [21,52,53].



**Author Contributions:** Conceptualization, C.M.-V. and A.V.; methodology, S.B.-E., M.D., E.P. and J.F.; software, S.B.-E., M.D. and C.M.-V.; validation, S.B.-E., A.V., M.D., E.P., J.F. and C.M.-V.; formal analysis, S.B.-E., M.D. and C.M.-V.; investigation, S.B.-E., A.V., M.D., E.P., J.F. and C.M.-V.; resources, C.M.-V., M.D. and A.V.; data curation, S.B.-E., M.D. and C.M.-V.; writing—original draft preparation, S.B.-E. and C.M.-V.; writing—review and editing, A.V., M.D., E.P. and J.F.; visualization, S.B.-E., A.V., M.D., E.P., J.F. and C.M.-V.; supervision, C.M.-V., M.D. and A.V.; project administration, C.M.-V. and A.V.; funding acquisition, C.M.-V., J.F. and A.V. All authors have read and agreed to the published version of the manuscript.

**Funding:** This research was funded by the University of Saskatchewan through the SPG-NSERC Industrial Research Chair Program in Lentil Genetic Improvement (Grant No. 20196324), the Escalera de Excelencia CLU-2018-04 cofounded by the P.O. FEDER of Castilla y León 2014–2020 Spain, and by the FEDER/Ministry of Science, Innovation and Universities State Agency of Research (AEI/Spain and FEDER/UE) grant number AGL2017-83718-R. S. Bautista-Expósito is a postdoctoral researcher funded by the University of Saskatchewan through the SPG-NSERC Industrial Research Chair Program in Lentil Genetic Improvement (Grant No. 756 20196324).

**Institutional Review Board Statement:** Not applicable.

**Informed Consent Statement:** Not applicable.

**Data Availability Statement:** Not applicable.

**Acknowledgments:** The authors acknowledge Prairie Pulse Inc. (Vanscoy, SK, Canada) for providing the lentil hulls. Novozymes Ltd. is also acknowledged for kindly donating the food-grade enzymes used in this study and for the scientific and technical advice provided during the study.

**Conflicts of Interest:** The authors declare no conflict of interest.

## References

- Romano, A.; Gallo, V.; Ferranti, P.; Masi, P. Lentil flour: Nutritional and technological properties, in vitro digestibility and perspectives for use in the food industry. *Curr. Opin. Food Sci.* **2021**, *40*, 157–167. [[CrossRef](#)]
- Zhong, L.; Fang, Z.; Wahlqvist, M.L.; Wu, G.; Hodgson, J.M.; Johnson, S.K. Seed coats of pulses as a food ingredient: Characterization, processing, and applications. *Trends Food Sci. Technol.* **2018**, *80*, 35–42. [[CrossRef](#)]
- Tiwari, U.; Cummins, E. Chapter 7—Legume fiber characterization, functionality, and process effects. In *Pulse Foods*, 2nd ed.; Tiwari, B.K., Gowen, A., McKenna, B., Eds.; Academic Press: London, UK, 2021; pp. 147–175. [[CrossRef](#)]
- Sun, Y.; Deng, Z.; Liu, R.; Zhang, H.; Zhu, H.; Jiang, L.; Tsao, R. A comprehensive profiling of free, conjugated and bound phenolics and lipophilic antioxidants in red and green lentil processing by-products. *Food Chem.* **2020**, *325*, 126925. [[CrossRef](#)] [[PubMed](#)]
- Qin, W.; Sun, L.; Miao, M.; Zhang, G. Plant-sourced intrinsic dietary fiber: Physical structure and health function. *Trends Food Sci. Technol.* **2021**, *118*, 341–355. [[CrossRef](#)]
- Yeo, J.; Shahidi, F. Identification and quantification of soluble and insoluble-bound phenolics in lentil hulls using HPLC-ESI-MS/MS and their antioxidant potential. *Food Chem.* **2020**, *315*, 126202. [[CrossRef](#)]
- Peng, L.; Guo, F.; Pei, M.; Tsao, R.; Wang, X.; Jiang, L.; Sun, Y.; Xiong, H. Anti-inflammatory effect of lentil hull (Lens culinaris) extract via MAPK/NF- $\kappa$ B signaling pathways and effects of digestive products on intestinal barrier and inflammation in Caco-2 and Raw264.7 co-culture. *J. Funct. Foods* **2022**, *92*, 105044. [[CrossRef](#)]
- Elessawy, F.M.; Vandenberg, A.; El-Anead, A.; Purves, R.W. An Untargeted Metabolomics Approach for Correlating Pulse Crop Seed Coat Polyphenol Profiles with Antioxidant Capacity and Iron Chelation Ability. *Molecules* **2021**, *26*, 3833. [[CrossRef](#)]
- Yeo, J.; Tsao, R.; Sun, Y.; Shahidi, F. Liberation of insoluble-bound phenolics from lentil hull matrices as affected by *Rhizopus oryzae* fermentation: Alteration in phenolic profiles and their inhibitory capacities against low-density lipoprotein (LDL) and DNA oxidation. *Food Chem.* **2021**, *363*, 130275. [[CrossRef](#)]
- Rastall, R.A.; Diez-Municio, M.; Forssten, S.D.; Hamaker, B.; Meynier, A.; Moreno, F.J.; Respondek, F.; Stah, B.; Venema, K.; Wiese, M. Structure and function of non-digestible carbohydrates in the gut microbiome. *Benef. Microbes* **2022**, *13*, 95–168. [[CrossRef](#)]
- Bautista-Expósito, S.; Tomé-Sánchez, I.; Martín-Diana, A.B.; Frias, J.; Peñas, E.; Rico, D.; Casas, M.J.G.; Martínez-Villaluenga, C. Enzyme Selection and Hydrolysis under Optimal Conditions Improved Phenolic Acid Solubility, and Antioxidant and Anti-Inflammatory Activities of Wheat Bran. *Antioxidants* **2020**, *9*, 984. [[CrossRef](#)]
- Jiménez-Pulido, I.J.; Rico, D.; Martínez-Villaluenga, C.; Pérez-Jiménez, J.; Luis, D.D.; Martín-Diana, A.B. Sprouting and Hydrolysis as Biotechnological Tools for Development of Nutraceutical Ingredients from Oat Grain and Hull. *Foods* **2022**, *11*, 2769. [[CrossRef](#)]
- Radenkovs, V.; Juhnevica-Radenkova, K.; Górnas, P.; Seglina, D. Non-waste technology through the enzymatic hydrolysis of agro-industrial by-products. *Trends Food Sci. Technol.* **2018**, *77*, 64–76. [[CrossRef](#)]

14. Martín-Diana, A.B.; Tomé-Sánchez, I.; García-Casas, M.J.; Martínez-Villaluenga, C.; Frias, J.; Rico, D. A Novel Strategy to Produce a Soluble and Bioactive Wheat Bran Ingredient Rich in Ferulic Acid. *Antioxidants* **2021**, *10*, 969. [[CrossRef](#)] [[PubMed](#)]
15. İşçimen, E.M.; Hayta, M. Microwave-assisted aqueous two-phase system based extraction of phenolics from pulses: Antioxidant properties, characterization and encapsulation. *Ind. Crops Prod.* **2021**, *173*, 114144. [[CrossRef](#)]
16. Singla, M.; Singh, A.; Sit, N. Effect of microwave and enzymatic pretreatment and type of solvent on kinetics of ultrasound assisted extraction of bioactive compounds from ripe papaya peel. *J. Food Process Eng.* **2022**, e14119. [[CrossRef](#)]
17. Peng, G.; Gan, J.; Dong, R.; Chen, Y.; Xie, J.; Huang, Z.; Gu, Y.; Huang, D.; Yu, Q. Combined microwave and enzymatic treatment improve the release of insoluble bound phenolic compounds from the grapefruit peel insoluble dietary fiber. *LWT* **2021**, *149*, 111905. [[CrossRef](#)]
18. Bautista-Expósito, S.; Vandenberg, A.; Peñas, E.; Frias, J.; Martínez-Villaluenga, C. Lentil and Fava Bean With Contrasting Germination Kinetics: A Focus on Digestion of Proteins and Bioactivity of Resistant Peptides. *Front. Plant Sci.* **2021**, *12*, 754287. [[CrossRef](#)] [[PubMed](#)]
19. Dinelli, G.; Segura-Carretero, A.; Di Silvestro, R.; Marotti, I.; Arráez-Román, D.; Benedettelli, S.; Ghiselli, L.; Fernandez-Gutierrez, A. Profiles of phenolic compounds in modern and old common wheat varieties determined by liquid chromatography coupled with time-of-flight mass spectrometry. *J. Chromatogr. A* **2011**, *1218*, 7670–7681. [[CrossRef](#)] [[PubMed](#)]
20. Tomé-Sánchez, I.; Martín-Diana, A.B.; Peñas, E.; Frias, J.; Rico, D.; Jiménez-Pulido, I.; Martínez-Villaluenga, C. Bioprocessed Wheat Ingredients: Characterization, Bioaccessibility of Phenolic Compounds, and Bioactivity During in vitro Digestion. *Front. Plant Sci.* **2021**, *12*, 790898. [[CrossRef](#)] [[PubMed](#)]
21. Bautista-Expósito, S.; Peñas, E.; Dueñas, M.; Silván, J.M.; Frias, J.; Martínez-Villaluenga, C. Individual contributions of Savinase and Lactobacillus plantarum to lentil functionalization during alkaline pH-controlled fermentation. *Food Chem.* **2018**, *257*, 341–349. [[CrossRef](#)]
22. Re, R.; Pellegrini, N.; Proteggente, A.; Pannala, A.; Yang, M.; Rice-Evans, C. Antioxidant activity applying an improved ABTS radical cation decolorization assay. *Free Radic. Biol. Med.* **1999**, *26*, 1231–1237. [[CrossRef](#)]
23. Kaya, E.; Tuncel, N.B.; Yilmaz Tuncel, N. The effect of ultrasound on some properties of pulse hulls. *J. Food Sci. Technol.* **2017**, *54*, 2779–2788. [[CrossRef](#)]
24. Hou, D.; Feng, Q.; Tang, J.; Shen, Q.; Zhou, S. An update on nutritional profile, phytochemical compounds, health benefits, and potential applications in the food industry of pulses seed coats: A comprehensive review. *Crit. Rev. Food Sci. Nutr.* **2022**, 1–23. [[CrossRef](#)]
25. Tripathi, A.; Iswarya, V.; Singh, N.; Rawson, A. Chapter 4—Chemistry of pulses—Micronutrients. In *Pulse Foods*, 2nd ed.; Tiwari, B.K., Gowen, A., McKenna, B., Eds.; Academic Press: London UK, 2021; pp. 61–86. [[CrossRef](#)]
26. Sreerama, Y.N.; Neelam, D.A.; Sashikala, V.B.; Pratapa, V.M. Distribution of Nutrients and Antinutrients in Milled Fractions of Chickpea and Horse Gram: Seed Coat Phenolics and Their Distinct Modes of Enzyme Inhibition. *J. Agric. Food Chem.* **2010**, *58*, 4322–4330. [[CrossRef](#)]
27. Galgano, F.; Tolve, R.; Scarpa, T.; Caruso, M.C.; Lucini, L.; Senizza, B.; Condelli, N. Extraction Kinetics of Total Polyphenols, Flavonoids, and Condensed Tannins of Lentil Seed Coat: Comparison of Solvent and Extraction Methods. *Foods* **2021**, *10*, 1810. [[CrossRef](#)]
28. Jagelaviciute, J.; Basinskiene, L.; Cizeikiene, D.; Syrpas, M. Technological Properties and Composition of Enzymatically Modified Cranberry Pomace. *Foods* **2022**, *11*, 2321. [[CrossRef](#)]
29. Paranavitana, L.; Oh, W.Y.; Yeo, J.; Shahidi, F. Determination of soluble and insoluble-bound phenolic compounds in dehulled, whole, and hulls of green and black lentils using electrospray ionization (ESI)-MS/MS and their inhibition in DNA strand scission. *Food Chem.* **2021**, *361*, 130083. [[CrossRef](#)]
30. Verstraeten, S.V.; Keen, C.L.; Schmitz, H.H.; Fraga, C.G.; Oteiza, P.I. Flavan-3-ols and procyanidins protect liposomes against lipid oxidation and disruption of the bilayer structure. *Free Radic. Biol. Med.* **2003**, *34*, 84–92. [[CrossRef](#)]
31. Escarnot, E.; Aguedo, M.; Paquot, M. Enzymatic hydrolysis of arabinoxylans from spelt bran and hull. *J. Cereal Sci.* **2012**, *55*, 243–253. [[CrossRef](#)]
32. Ben-Othman, S.; Rinken, T. Immobilization of Pectinolytic Enzymes on Nylon 6/6 Carriers. *Appl. Sci.* **2021**, *11*, 4591. [[CrossRef](#)]
33. Babbar, N.; Dejonghe, W.; Gatti, M.; Sforza, S.; Elst, K. Pectic oligosaccharides from agricultural by-products: Production, characterization and health benefits. *Crit. Rev. Biotechnol.* **2016**, *36*, 594–606. [[CrossRef](#)]
34. Nomura, K.; Sakai, M.; Ohboshi, H.; Nakamura, A. Extraction of a water-soluble polysaccharide fraction from lentils and its potential application in acidified protein dispersions. *Food Hydrocoll.* **2021**, *117*, 106740. [[CrossRef](#)]
35. Agrawal, R.M.; Miller, M.J.; Singh, V.; Stein, H.H.; Takhar, P.S. Enzymatic hydrolysis and fermentation of soy flour to produce ethanol and soy protein concentrate with increased polyphenols. *J. Am. Oil Chem. Soc.* **2022**, *99*, 379–391. [[CrossRef](#)]
36. Peng, D.; Zhao-Peng, S.; Jing-liang, Z.; Guo-Xia, L.; Guo-Shao, W.; Xiao-Lu, J. Study on preparation of pectic oligosaccharides from blackberry by enzymatic hydrolysis and its antioxidant activities. *Sci. Technol. Food Ind.* **2016**, 76–79.
37. de Camargo, A.C.; Regitano-d’Arce, M.A.; Biasoto, A.C.; Shahidi, F. Enzyme-assisted extraction of phenolics from winemaking by-products: Antioxidant potential and inhibition of alpha-glucosidase and lipase activities. *Food Chem.* **2016**, *212*, 395–402. [[CrossRef](#)]
38. Gómez-García, R.; Martínez-Ávila, G.C.G.; Aguilar, C.N. Enzyme-assisted extraction of antioxidative phenolics from grape (*Vitis vinifera* L.) residues. *3 Biotech* **2012**, *2*, 297–300. [[CrossRef](#)]

39. Motikar, P.D.; More, P.R.; Arya, S.S. A novel, green environment-friendly cloud point extraction of polyphenols from pomegranate peels: A comparative assessment with ultrasound and microwave-assisted extraction. *Sep. Sci. Technol.* **2021**, *56*, 1014–1025. [[CrossRef](#)]
40. Périno, S.; Pierson, J.T.; Ruiz, K.; Cravotto, G.; Chemat, F. Laboratory to pilot scale: Microwave extraction for polyphenols lettuce. *Food Chem.* **2016**, *204*, 108–114. [[CrossRef](#)]
41. Spadoni Andreani, E.; Karboune, S. Comparison of enzymatic and microwave-assisted alkaline extraction approaches for the generation of oligosaccharides from American Cranberry (*Vaccinium macrocarpon*) Pomace. *J. Food Sci.* **2020**, *85*, 2443–2451. [[CrossRef](#)]
42. Rehinan, Z.-U.; Rashid, M.; Shah, W.H. Insoluble dietary fibre components of food legumes as affected by soaking and cooking processes. *Food Chem.* **2004**, *85*, 245–249. [[CrossRef](#)]
43. Liu, Y.; Ragae, S.; Marcone, M.F.; Abdel-Aal, E.-S.M. Composition of Phenolic Acids and Antioxidant Properties of Selected Pulses Cooked with Different Heating Conditions. *Foods* **2020**, *9*, 908. [[CrossRef](#)]
44. Sharma, M.; Dash, K.K. Microwave and ultrasound assisted extraction of phytochemicals from black jamun pulp: Kinetic and thermodynamics characteristics. *Innov. Food Sci. Emerg. Technol.* **2022**, *75*, 102913. [[CrossRef](#)]
45. Oszmiański, J.; Wojdyło, A.; Kolniak, J. Effect of pectinase treatment on extraction of antioxidant phenols from pomace, for the production of pure-enriched cloudy apple juices. *Food Chem.* **2011**, *127*, 623–631. [[CrossRef](#)]
46. Valencia-Hernandez, L.J.; Wong-Paz, J.E.; Ascacio-Valdés, J.A.; Chávez-González, M.L.; Contreras-Esquivel, J.C.; Aguilar, C.N. Procyanidins: From Agro-Industrial Waste to Food as Bioactive Molecules. *Foods* **2021**, *10*, 3152. [[CrossRef](#)]
47. Peng, M.; Jiang, C.; Jing, H.; Du, X.; Fan, X.; Zhang, Y.; Wang, H. Comparison of different extraction methods on yield, purity, antioxidant, and antibacterial activities of proanthocyanidins from chokeberry (*Aronia melanocarpa*). *J. Food Meas. Charact.* **2022**, *16*, 2049–2059. [[CrossRef](#)]
48. Renard, C.M.; Baron, A.; Guyot, S.; Drilleau, J.-F. Interactions between apple cell walls and native apple polyphenols: Quantification and some consequences. *Int. J. Biol. Macromol.* **2001**, *29*, 115–125. [[CrossRef](#)]
49. Oszmiański, J.; Wojdyło, A.; Kolniak, J. Effect of Enzymatic Mash Treatment and Storage on Phenolic Composition, Antioxidant Activity, and Turbidity of Cloudy Apple Juice. *J. Agric. Food Chem.* **2009**, *57*, 7078–7085. [[CrossRef](#)]
50. Lima, M.d.S.; da Conceição Prudêncio Dutra, M.; Toaldo, I.M.; Corrêa, L.C.; Pereira, G.E.; de Oliveira, D.; Bordignon-Luiz, M.T.; Ninow, J.L. Phenolic compounds, organic acids and antioxidant activity of grape juices produced in industrial scale by different processes of maceration. *Food Chem.* **2015**, *188*, 384–392. [[CrossRef](#)]
51. Fernandes, P.A.R.; Le Bourvellec, C.; Renard, C.M.G.C.; Nunes, F.M.; Bastos, R.; Coelho, E.; Wessel, D.F.; Coimbra, M.A.; Cardoso, S.M. Revisiting the chemistry of apple pomace polyphenols. *Food Chem.* **2019**, *294*, 9–18. [[CrossRef](#)]
52. Dueñas, M.; Sun, B.; Hernández, T.; Estrella, I.; Spranger, M.I. Proanthocyanidin composition in the seed coat of lentils (*Lens culinaris* L.). *J. Agric. Food Chem.* **2003**, *51*, 7999–8004. [[CrossRef](#)]
53. Aguilera, Y.; DUEÑAS, M.; Estrella, I.; Hernandez, T.; Benitez, V.; Esteban, R.M.; Martin-Cabrejas, M.A. Evaluation of phenolic profile and antioxidant properties of Pardina lentil as affected by industrial dehydration. *J. Agric. Food Chem.* **2010**, *58*, 10101–10108. [[CrossRef](#)]

## Article

# Metabolite Profiling of *Alocasia gigantea* Leaf Extract and Its Potential Anticancer Effect through Autophagy in Hepatocellular Carcinoma

Hend Okasha <sup>1</sup>, Tarek Aboushousha <sup>2</sup>, Manuel A. Coimbra <sup>3</sup>, Susana M. Cardoso <sup>3,\*</sup> and Mosad A. Ghareeb <sup>4,\*</sup>

<sup>1</sup> Department of Biochemistry and Molecular Biology, Theodor Bilharz Research Institute, Kornaish El Nile, Warrak El-Hadar, Imbaba, P.O. Box 30, Giza 12411, Egypt

<sup>2</sup> Department of Pathology, Theodor Bilharz Research Institute, Kornaish El Nile, Warrak El-Hadar, Imbaba, P.O. Box 30, Giza 12411, Egypt

<sup>3</sup> LAQV-REQUIMTE, Department of Chemistry, University of Aveiro, 3810-193 Aveiro, Portugal

<sup>4</sup> Department of Medicinal Chemistry, Theodor Bilharz Research Institute, Kornaish El Nile, Warrak El-Hadar, Imbaba, P.O. Box 30, Giza 12411, Egypt

\* Correspondence: susanacardoso@ua.pt (S.M.C.); m.ghareeb@tbri.gov.eg (M.A.G.);

Tel.: +351-234-370-360 (S.M.C.); +20-(02)-01012346834 (M.A.G.);

Fax: +351-234-370-084 (S.M.C.); +20-(02)-35408125 (M.A.G.)

**Abstract:** Hepatocellular carcinoma (HCC) is a poor-prognosis type of cancer with high resistance to chemotherapy, making the search for safe drugs a mandatory issue. Plant-derived products have potential to reduce negative side effects of cancer treatments. In this work, ability of a defatted methanolic extract of *Alocasia gigantea* leaves to fight HCC was evaluated in an animal model. Overall, treatment of HCC-induced mice with the methanolic extract at 150 mg/kg body weight for four consecutive weeks caused induction of autophagy through silencing of the relative expression of autophagy suppressor (mTOR) and inducement of autophagy markers (AMPK, Beclin-1, and LC-3). Moreover, it improved preservation of the hepatic histological architecture of the animals, with minor hepatocytic changes but scattered foci of hepatocytic apoptosis. Chemical profiling of the methanolic extract via ultra-high-performance liquid chromatography coupled to a diode array detector and an electrospray mass spectrometer (UHPLC–DAD–ESI–MS/MS) allowed identification of di-C-glycosyl flavones, mostly represented by 6-C-hexosyl-8-C-pentosyl apigenin isomers, which may possibly be associated with inducement of the autophagy pathway in HCC. Overall, these outcomes gave an initial visualization of the operative effect of some compounds in *A. gigantea* leaves that are potential treatment for HCC.

**Keywords:** *Alocasia gigantea*; hepatocellular carcinoma; autophagy; histopathology; UHPLC–DAD–ESI–MS/MS; phenolic compounds

**Citation:** Okasha, H.; Aboushousha, T.; Coimbra, M.A.; Cardoso, S.M.; Ghareeb, M.A. Metabolite Profiling of *Alocasia gigantea* Leaf Extract and Its Potential Anticancer Effect through Autophagy in Hepatocellular Carcinoma. *Molecules* **2022**, *27*, 8504. <https://doi.org/10.3390/molecules27238504>

Academic Editor: Nour Eddine Es-Safi

Received: 31 October 2022

Accepted: 29 November 2022

Published: 3 December 2022

**Publisher's Note:** MDPI stays neutral with regard to jurisdictional claims in published maps and institutional affiliations.



**Copyright:** © 2022 by the authors. Licensee MDPI, Basel, Switzerland. This article is an open access article distributed under the terms and conditions of the Creative Commons Attribution (CC BY) license (<https://creativecommons.org/licenses/by/4.0/>).

## 1. Introduction

Hepatocellular carcinoma (HCC) is the world's sixth most common cancer, with increasing incidence. Over the years, there has been significant variation in prevalence of risk factors for HCC around the world, such as control of viral hepatitis in developing countries and fatty liver disease in the developed world. Trends in these risk factors are related to changing epidemiology of HCC [1]. HCC accounts for more than 500 to 600 thousand deaths per year worldwide [2].

In recent decades, significant progress has been made in understanding the complex role of autophagy (i.e., the cellular process that eliminates molecules and subcellular elements via lysosome-mediated degradation) in cancer regulation, including in HCC. Despite controversy, it is generally accepted that this cellular process can be overactivated, dysregulated, or suppressed in cancer cells, and its roles in regulating cancer are dependent on different stages of tumorigenesis [3]. In particular, autophagy is recognized to prevent

chronic cellular damage and delay cancer-initiation cells in early stages through elimination of toxic unfolded proteins, oncogenic protein substrates, and damaged organelles, and to contribute to immunosurveillance maintenance [4,5]. Conversely, after malignant cells are established in advanced stages, enhancement of autophagy promotes tumor-cell survival and growth [6,7].

Herbal medicine uses natural ingredients that can serve a variety of treatment purposes, including for cancer [8]. The genus *Alocasia* (family: Araceae) consists of more than 100 species, including herbaceous, perennial, and large plants, that grow in subtropical and tropical regions around the world, such as Asia, the Western Pacific, and Eastern Australia [9]. Distinct parts of plants in the *Alocasia* species are commonly used in traditional medicine to treat coughs, toothache, malaria, and abscesses, and as nyctalopic agents for people who are unable to see clearly in low light [10]. Moreover, several studies have demonstrated potential of *Alocasia* plants to serve as anticancer agents. In particular, it was reported that the butanol extract of *A. cucullata* demonstrates a potent antitumor effect both in vitro and in vivo via antiproliferation of G0/G1 arrest and cell pro-apoptosis, including the PI-3 K/Akt pathway, ERK activity, stimulated cytochrome C release, and caspase 3/7 activity, along with an increase in Bax/Bcl-2 ratio [11]. Additionally, the aqueous extract of *A. macrorrhiza* exhibits anticancer action against hepatic cancer through suppression of proliferation and influences apoptosis in human hepatocellular carcinoma cells, both in vitro and in vivo [12]. Moreover, it has been shown that a 50% ethanolic extract of *A. cucullata* displays in both in vitro and in vivo anti-malignant melanoma activity through alteration of the phosphatase and tensin homolog/phosphoinositide 3-kinase/AKT pathways [13]. Additionally, the water extract of *A. cucullata* roots shows an antitumor effect via activation of antitumor immunity. In terms of its mode of action, the extract strongly stimulated THP-1 differentiation into macrophage-like cells.

*A. gigantea* is one important species of the *Alocasia* genus, commonly known as “Giant Elephant Ear” or “Giant Taro”, and it is widespread in tropical zones, such as Southeast Asia [14]. To the best of our knowledge, phytochemical profiles and bioactive properties of this species remain unknown. Taking this into consideration, this study intends to elucidate phytochemical constituents of a defatted methanolic extract of *A. gigantea* leaves (DefMeOH-E) and simultaneously evaluate *A. gigantea*'s in vivo anticancer activity, particularly via inducement of autophagy in hepatocellular carcinoma.

## 2. Results and Discussion

### 2.1. Phenolic Profile of *A. gigantea* Defatted Methanolic Extract

The total phenolic compounds in the defatted methanol extract of *A. gigantea* represented 293.02 mg GAE/g dry extract, which, based on the UHPLC–DAD–ESI–MS/MS analysis, was identified as di-C-glycosyl flavones (Figure S1, Table 1), particularly from apigenin (peaks 3–7;  $UV_{max}$  271, 334). These compounds were detected in the MS spectrum as  $[M-H]^-$  at  $m/z$  563 and, as represented in Figure 1, showed fragment ions that corresponded to aglycone apigenin plus the residues of the sugar, i.e., at  $m/z$  383  $[Apigenin + 113]^-$  and at  $m/z$  353  $[Apigenin + 83]^-$ , as well as those resultant from sugar breakage (i.e., at  $m/z$  545  $[(M-H)-18]^-$ ,  $m/z$  503  $[(M-H)-60]^-$ ,  $m/z$  473  $[(M-H)-90]^-$ , and  $m/z$  443  $[(M-H)-120]^-$ ) assigned to 6-C-pentosyl-8-C-hexosyl apigenin or 6-C-hexosyl-8-C-pentosyl apigenin derivatives [15,16]. As C-6-isomers are easier to fragment than are C-8-isomers [17], and the ion  $[(M-H)-60]^-$  (characteristic of pentose derivatives) was much less abundant in compounds eluted in peaks 3, 5, and 7 compared to its abundance in compounds from peaks 4, 6, and 8, this data also allowed us to conclude that 6-C-hexosyl-8-C-pentosyl apigenin derivatives were the predominant isomers in DefMeOH-E. The most common sugars involved in the glycosylated flavonoids are the hexoses glucose and galactose, the deoxyhexose rhamnose, and the pentoses arabinose and xylose [18]. In addition to di-C-glycosyl apigenin isomers, two 6-C-hexosyl-8-C-pentosyl luteolin derivatives were detected as minor components in DefMeOH-E (peaks 1 and 2;  $UV_{max}$  271, 346–348;  $[M-H]^-$  at  $m/z$  579→561, 519, 489, 459, 399, 369). Metabolite profiling of the *Colocasia esculenta* species,

which belongs to its closest genus *Colocasia*, via HPLC–DAD–ESI/MS led to identification of 30 glycosylated flavonoids—among them flavone mono-C-glycosides and flavone di-C-glycosides—in which luteolin-6-C-hexoside was the predominant identified compound. The obtained results are in full agreement with our current findings [17].

**Table 1.** Phenolic compounds detected in *A. gigantea* leaves defatted methanolic extract via UHPLC–DAD–ESI–MS/MS analysis.

Peak	RT (min)	$\lambda_{\max}$ (nm)	$m/z$	ESI–MS <sup>2</sup>	Compound
1	9.4	271, 348	579	561, 519, 489, 459, 399, 369	6-C-hexosyl-8-C-pentosyl luteolin (isom 1)
2	9.7	271, 346	579	561, 519, 489, 459, 399, 369	6-C-hexosyl-8-C-pentosyl luteolin (isom 2)
3	10.1	271, 333	563	545, 503, 473, 443, 413, 383, 353	6-C-hexosyl-8-C-pentosyl apigenin (isom 1)
4	10.4	271, 333	563	545, 503, 473, 443, 383, 353	8-C-hexosyl-6-C-pentosyl apigenin (isom 1)
5	10.7	271, 333	563	545, 503, 473, 443, 383, 353	6-C-hexosyl-8-C-pentosyl apigenin (isom 2)
6	11.0	271, 333	563	545, 503, 473, 443, 383, 353	8-C-hexosyl-6-C-pentosyl apigenin (isom 2)
7	10.4	271, 333	563	545, 503, 473, 443, 383, 353	6-C-hexosyl-8-C-pentosyl apigenin (isom 3)
8	11.9	271, 333	563	545, 503, 473, 443, 383, 353	8-C-hexosyl-6-C-pentosyl apigenin (isom 3)

Isom: Isomer.

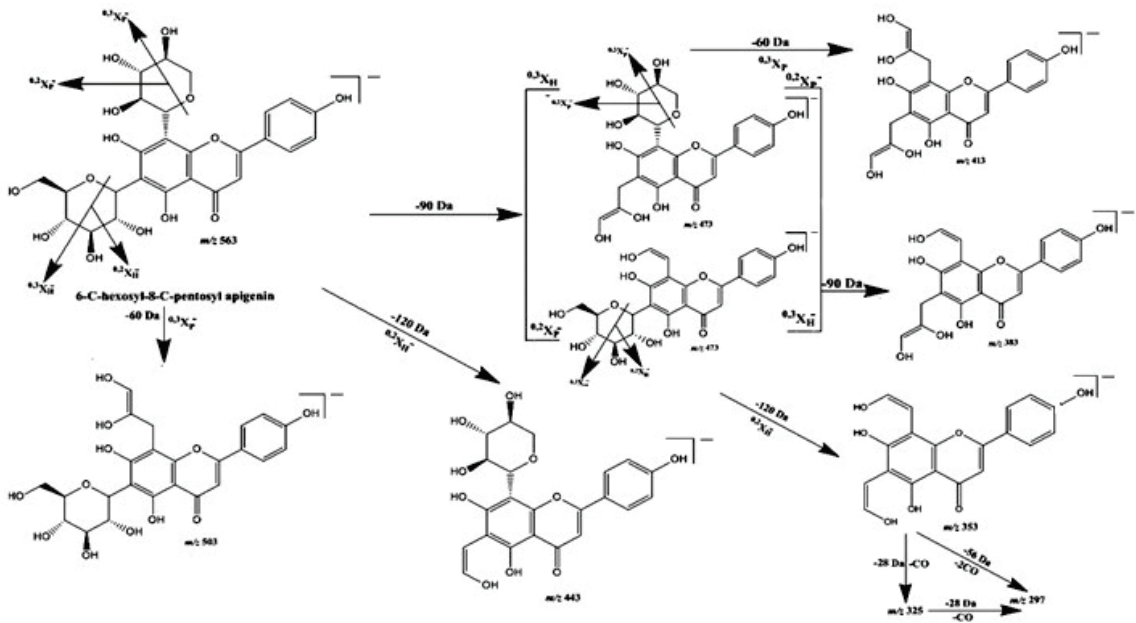


**Figure 1.** Proposed fragmentation pattern of 6-C-hexosyl-8-C-pentosyl apigenin in negative ion mode.

## 2.2. Anticancer Potential of *A. gigantea* Leaf Defatted Methanolic Extract

### 2.2.1. In Vitro Cytotoxic Activity on HCC Cell Line

Anticancer activity of DefMeOH-E was tested first on a hepatic cancer line, HepG2 cell, using a crystal violet assay to determine cells' vitality [19]. As shown in Figure 2, exposure of those cells to increasing concentrations of the extract (in the range of 25 and 100  $\mu\text{g}/\text{mL}$ ) enhanced cytotoxic activity to an  $\text{IC}_{50}$  value of 76.33  $\mu\text{g}/\text{mL}$ . A previous study on another species of *Alocasia*, namely *A. macrorrhiza*, exhibited proliferation inhibition and apoptosis effects on human hepatocellular carcinoma cells in vitro as well as inhibiting hepatoma growth with an  $\text{IC}_{50}$  value of 414  $\mu\text{g}/\text{mL}$  [12]. This result suggests that DefMeOH-E of *A. gigantea* origin has potential anticancer activity against HCC.

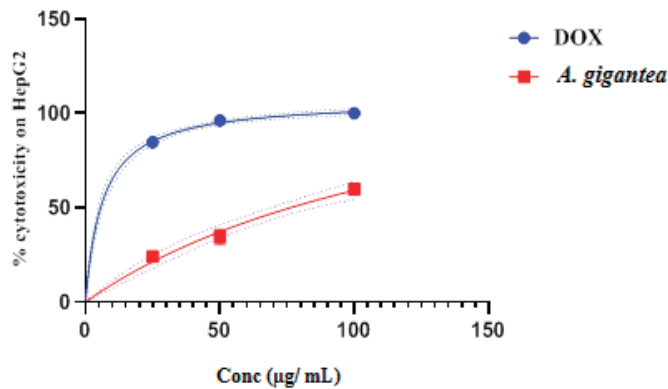


**Figure 2.** *In vitro* cytotoxic activity of *A. gigantea* leaf defatted methanolic extract at different concentrations (100, 50, and 25 µg/mL) in comparison to standard drug doxorubicin.

### 2.2.2. In Vivo Acute Toxicity

The first step in determining *in vivo* toxicity of a plant extract is to conduct an acute oral toxicity test [20]. Therefore, animals were fed with DefMeOH-E at a dose of 2000 mg/kg after a fasting period of 12 h and only allowed to drink water, followed by monitoring of clinical and behavioral signs in the first 4 h, at 72 h, and after 7 days. No mortality or clinical signs of toxicity were observed. Additionally, after 7 days of observation, no mortality was detected. Based on these results, DefMeOH-E was considered non-toxic. For chemical substances and mixtures, the globally harmonized classification system (GHS) of the Organization for Economic Cooperation (OECD) classifies substances with  $LD_{50} > 2-5$  g/kg as unclassified or category 5. This implies that the plant's oral  $LD_{50}$  of 2–5 g/kg may be safe [21].

### 2.2.3. In Vivo Body and Liver Weight and Biochemical Parameters

Animal models of HCC include xenograft models, genetically modified mouse models, and chemically induced models [22]. In the past few years, diethylnitrosamine (DEN) has been widely applied as an “initiating agent” within a myriad of protocols in mice and rats for HCC development [23,24]. It is known to cause changes in enzymes required in DNA repair replication and is regularly utilized as a cancer-causing agent to prompt liver carcinogenesis in mouse models. In this case, it was given as an intraperitoneal injection: a common technique that safely delivers a substance into the peritoneal cavity but can induce high stress in animals [24]. Overall, 48 animals were divided into four groups (12 mice/group), and this study lasted 12 weeks, with normal conditions set for Group I (Gp-I), in which mice were intraperitoneally administered a saline solution once a week, while Group III (Gp-III, *A. gigantea*) was orally administered the plant extract twice a week at 150 mg/kg body weight (BW). In turn, animals in Group II (Gp-II, DEN) were HCC-induced by an intraperitoneal injection of DEN at 3.5 µL/mg BW twice a week, and Group IV (Gp-IV, DEN/*A. gigantea*) was also given DEN twice a week for 12 weeks, combined with an oral treatment of DefMeOH-E at 150 mg/kg in the final four consecutive weeks.

As observed in Figure 3, body weight (BW) of animals just before termination (12 weeks) was different from that registered at the initial point ( $T_0$ ). It increased in Gp-I and Gp-III, while the opposite trend was noticed in Gp-II, which registered 25.45% weight loss ( $p = 0.0012$ ). Notably, this was reversed in part by the *A. gigantea* treatment, as animals in Gp-IV registered a lower decrement in BW compared to those of Gp-II. Liver weight (LW) just before termination was nearly the same in Gp-I (BW =  $31.65 \pm 5.76$ ; LW =  $1.59 \pm 0.39$ ) and Gp-III (BW =  $30.85 \pm 4.64$ ; LW =  $1.51 \pm 0.83$ ). A decrease in LW was detected in Gp-II (BW =  $19.9 \pm 2.03$ ; LW =  $1.075 \pm 0.31$ ), which was related to BW loss in that group. Gp-IV showed a slight increase in LW compared to Gp-II (BW =  $22.68 \pm 1.97$ ; LW =  $1.2 \pm 0.29$ ).

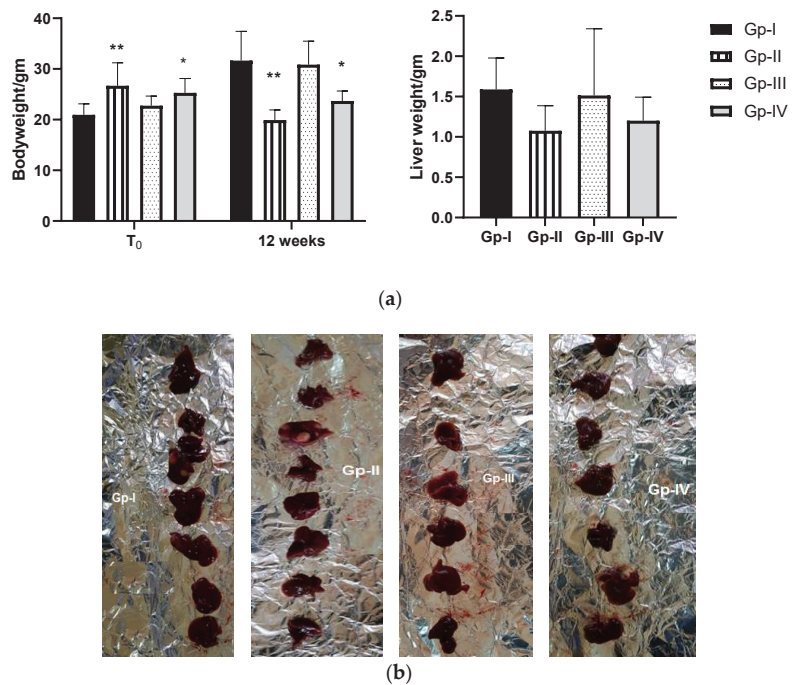


**Figure 3.** (a) Effect of *A. gigantea* leaf defatted methanolic extract on body weight (at initial time and 12 weeks) and liver weight (at 12 weeks) of different mouse groups. Gp-I: Group I, normal group; Gp-II: Group II, treated with DEN; Gp-III: Group III, treated with *A. gigantea*; Gp-IV: Group IV, treated with DEN combined with plant extract. Data represent the mean  $\pm$  SEM. \*  $p < 0.05$ , \*\*  $p < 0.01$  indicate significant differences compared to Gp-I. (b) This photo represents liver mass between different groups.

The liver function was evaluated through examination of the liver enzymes alkaline phosphatase (ALP), alanine transaminase (ALT), and aspartate aminotransferase (AST), as well as the liver waste product total bilirubin (TBILR). Results in Table 2 show that all tested parameters in Gp-II (DEN) were significantly higher when compared to Gp-I (normal group) ( $p < 0.0001$ ). In addition, treatment with DefMeOH-E in Gp-IV caused a remarkable decrease in all liver function parameters compared with the HCC group (Gp-II) ( $p < 0.0001$ ). Overall, these results indicate that serum transaminase ALT, AST, and TBILR activities increased significantly after DEN induction. Overproduction of these proteins in tumor cells is caused by DEN-induced changes in permeability of the cell membrane, resulting in protein leakage into serum [25,26]. In turn, treatment with *A. gigantea* extract in Gp-IV caused reduction in elevated activities of these proteins, which may be due to effective compounds in *A. gigantea* maintaining parenchymal cell recovery in the liver, leading to a decrease in enzymatic leakage [27].



**Table 2.** Serum-liver-function parameters for each animal group used in this study.

Liver Markers	Gp-I	Gp-II	Gp-III	Gp-IV
TBILR	0.22 ± 0.18	1.27 ± 0.12 <sup>c</sup>	0.16 ± 0.07	0.60 ± 0.14 <sup>b</sup>
ALP	8.95 ± 1.75	24.99 ± 2.4 <sup>c</sup>	12.39 ± 2.1 <sup>c</sup>	14.66 ± 1.22 <sup>c</sup>
ALT	7.45 ± 1.86	35.83 ± 3.7 <sup>c</sup>	10.25 ± 1.8 <sup>a</sup>	21.88 ± 5.89 <sup>c</sup>
AST	112.51 ± 8.1	148.62 ± 5.4 <sup>c</sup>	93.99 ± 22.59 <sup>a</sup>	116.52 ± 27.25

Results are expressed in mg/dL (for total direct bilirubin) and international unit per liter (IU/L) for alkaline phosphatase (ALP), alanine transaminase (ALT), and aspartate aminotransferase (AST). Gp-I: Group I, normal group; Gp-II: Group II, treated with diethylnitrosamine; Gp-III: Group III, treated with *A. gigantea*; Gp-IV: Group IV, treated with diethylnitrosamine combined with plant extract. In each line, different letters represent significant differences compared to Gp-I: a— $p < 0.05$ , b— $p < 0.01$ , c— $p < 0.001$ .

The majority of *Alocasia* species research focuses on hepatoprotection, mostly performed with *Alocasia indica* (Roxb.), showing that the ethanolic *A. indica* leaf extract reduces hepatotoxicity [28]. The hepatoprotective effect of the *Alocasia indica* tuber extract has also been demonstrated on albino Wistar rats with CCl<sub>4</sub>-induced liver injury, particularly in ethanolic extract given at 200 mg/kg for 7 days [29]. In addition, *Alocasia macrorrhiza* was also employed in trials as a hepatoprotective agent, reducing leakage of AST, ALT, and ALP in rats with CCl<sub>4</sub>- and Tylenol-induced liver injury [28]. *Alocasia macrorrhiza* also has an anticancer effect on various cell lines, inhibiting growth of hepatoma in vivo [12].

#### 2.2.4. Histopathological Examinations

Histopathological images are represented in Figure 4. Hepatocytes with granular cytoplasm that occupied the acidophilic stain, as well as centrally located nuclei, were seen in the histology of both the Gp-I (normal) and the Gp-III (*A. gigantea*) group. With hematoxylin and eosin (H&E) staining, the central vein and bile ducts could be seen. In the histology of Gp-II (DEN), distorted architecture, focal HCC, and dysplasia were seen, as well as areas of necrosis, cholestasis, bile duct proliferation, and lymphatic dilatation. However, in Gp-IV (DEN/*A. gigantea*), hepatic architecture was more preserved, with minor hepatocytic changes but scattered foci of hepatocytic apoptosis. On the other hand, Gp-III (*A. gigantea*) showed preserved hepatic lobular architecture with no histopathological changes. Dysplastic foci are homogeneous lesions that can be distinguished from the surrounding liver tissue by their distinctive morphology, cytoplasmic staining, nuclear size, and cellular atypia. Due to their elevated proliferation index and poor apoptosis rate, they are additionally regarded as premalignant lesions [30]. Another histological HCC marker is cholestasis, which is almost always extracellular, localized at the biliary pole of the tumor hepatocytes [31].

Despite the absence of studies with *A. gigantea*, a preservative effect on normal morphology, in addition to antitumor properties against tumoral hepatic cells, has been demonstrated for other *Alocasia* species: in particular, hepatotoxic protective effects of *A. indica* tuber extract in alcohol-intoxicated rats, where recovery from ethanol-induced liver damage was observed, with fewer micro-vesicular steatoses, hepatocytes necrosis features, and absence of fat droplets [29]. *A. indica* leaf extract has also been shown to reduce inflammation, degenerative changes, and steatosis in liver tissue treated with CCl<sub>4</sub> and paracetamol [28].

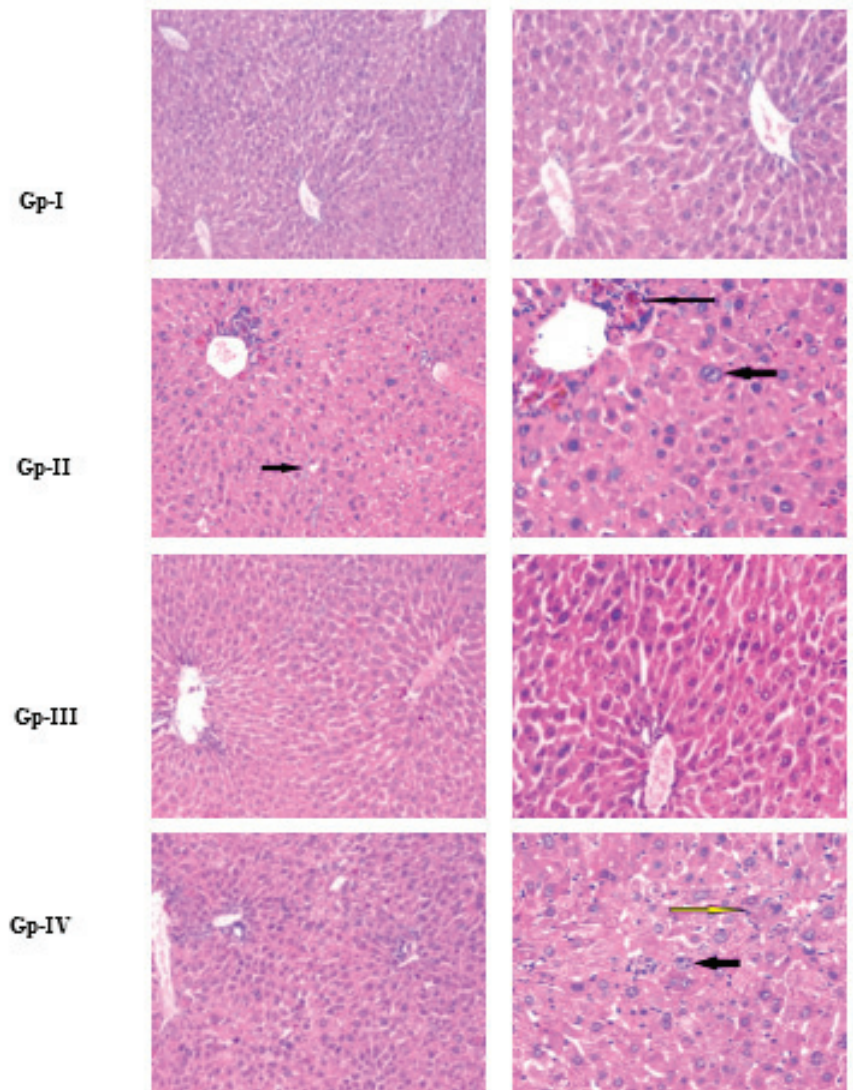


**Figure 4.** Histopathology using hematoxylin and eosin (H&E) staining of the liver, isolated from each animal group used in this study. For each group, the photo on the right side is a zoom-in taken from the photo on the left. Gp-I: Group I, normal group; Gp-II: Group II, treated with diethylnitrosamine; Gp-III: Group III, treated with *A. gigantea*; Gp-IV: Group IV, treated with diethylnitrosamine combined with plant extract. Thick and thin black arrows in Gp-II indicate HCC with focal acinar formation and bizarre-shaped hyperchromatic nuclei and focal cholestasis, respectively. Thin yellow and black arrows in Gp-IV indicate focal hepatocellular dysplasia with focal cholestasis and few apoptotic figures, respectively.

#### 2.2.5. In Vivo Antitumoral Effects through Induction of Autophagy

One of the characteristics of cancer is alteration in cell death; these cells are under survival pressure. They alter as a result of failure of apoptosis, which causes genetic harm [32]. Mutational and expressional alterations of apoptosis genes such as Fas and caspase are abundant in different types of human cancer [33,34]. However, compared to

apoptosis, information on autophagy genes and their function in cancer is significantly limited [6,35]. With this in mind, this study focused on autophagy in HCC, which is a topic under debate.

Table 3 summarizes the results of the relative expression of serum tumor necrosis factor-alpha (TNF- $\alpha$ ) and alfa-fetoprotein (AFP), which are central inflammatory and tumor markers, respectively. Overall, the gathered data indicate that treatment with DefMeOH-E did not induce inflammatory or tumorigenic effects in animals (Gp-III). Conversely, injection of DEN in Gp-II caused a large increase in animals' serum levels of TNF- $\alpha$  and AFP genes, which was significantly reversed by the *A. gigantea* treatment in Gp-IV (DEN/*A. gigantea*). Accordingly, a previous study concluded that combined use of TNF- $\alpha$  and AFP increases sensitivity and specificity for early diagnosis of HCC, as their increased expression is related to HCC [36].

**Table 3.** Effect of *A. gigantea* leaf defatted methanolic extract on TNF- $\alpha$  and AFP relative expression in each animal group.

Serum Markers	Gp-I	Gp-II	Gp-III	Gp-IV
TNF- $\alpha$	0.068 $\pm$ 0.024	322.24 $\pm$ 11.2 <sup>c</sup>	4.25 $\pm$ 2.1 <sup>c</sup>	194.54 $\pm$ 15.92 <sup>c</sup>
AFP	0.98 $\pm$ 0.299	4.48 $\pm$ 1.15 <sup>c</sup>	0.65 $\pm$ 0.25 <sup>a</sup>	2.9 $\pm$ 0.97 <sup>c</sup>

Results are expressed in relative quantification (RQ) for TNF- $\alpha$  (tumor necrosis factor-alpha) and AFP (alfa-fetoprotein). Gp-I: Group I, normal group; Gp-II: Group II, treated with diethylnitrosamine; Gp-III: Group III, treated with *A. gigantea*; Gp-IV: Group IV, treated with diethylnitrosamine combined with plant extract. In each line, different letters represent significant differences compared to Gp-I: a— $p < 0.05$ , b— $p < 0.01$ , c— $p < 0.001$ .

Generally, the process of autophagy entails formation of a double-membrane vesicle that encloses cytoplasm, abnormal proteins, long-lived proteins, and organelles before joining with lysosomes for breakdown. The molecular mechanism of autophagy is complex and involves distinct autophagy-related (Atg) proteins. In this study, the effect of *A. gigantea* extract on autophagy was evaluated through monitoring of autophagy gene markers involved in the initiation step of autophagy: namely adenosine monophosphate-activated protein kinase (AMPK) and mammalian target of rapamycin complex 1 (mTORC1) complexes, the Beclin-1-class III phosphatidylinositol 3-kinase (PI3K) complex (which mediates nucleation of the phagophore to form autophagosome), and LC3 (considered the mature autophagosome marker) [37].

As represented in Figure 5, tumor marker BCL-2 was higher in Gp-II than in the other groups. In addition, mTOR, an autophagy suppressor, was significantly lower in Gp-IV when compared to Gp-II ( $p < 0.0001$ ). In accordance, autophagy markers (AMPK, Beclin-1, and LC-3) also displayed markedly increased expression in Gp-IV ( $p < 0.0001$ ). Taken together, the data collected indicate that combined treatment of DEN with *A. gigantea* extract promoted autophagy and decreased tumor markers in animals.

Previous studies proved that polyphenolic compounds displayed anti-HCC effects through autophagy via interference with canonical (Beclin-1-dependent) and non-canonical (Beclin-1-independent) pathways [38]. Moreover, apigenin has been shown to exhibit anti-cancer properties in various types of cancer, including breast, liver, prostate, lung, and colon cancer, in addition to anti-inflammatory and antioxidant effects [39]. The anti-HCC effect of apigenin through down-regulation of the NF- $\kappa$ B pathway has been shown [40]. Considering the results from our study, it is possible to suggest that apigenin derivatives, i.e., the main phenolic compounds in the *A. gigantea* extract, may play a relevant role in apigenin's antitumoral effect; however, this hypothesis must be further consolidated.

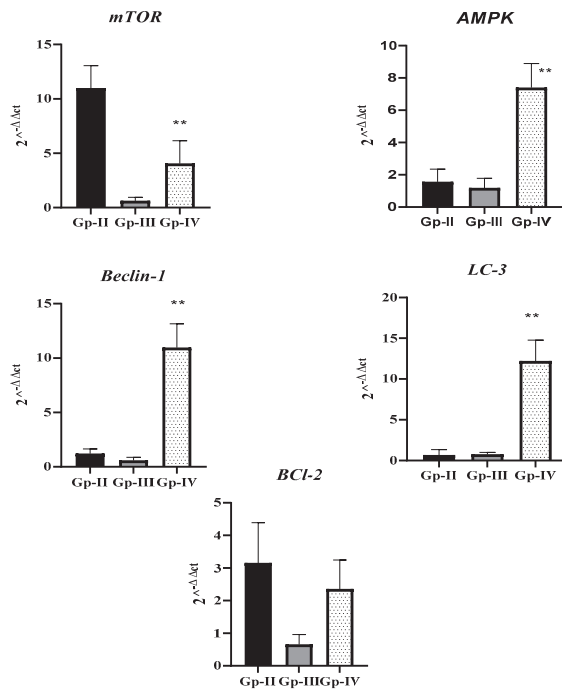


**Figure 5.** Relative quantification ( $RQ = 2^{-\Delta\Delta ct}$ ) of tumor marker BCL-2 and autophagy markers (mTOR, AMPK, Beclin-1, and LC-3) in different animal groups, in relation to Gp-II (DEN group). Gp-II: Group II, treated with diethylnitrosamine; Gp-III: Group III, treated with *A. gigantea*; Gp-IV: Group IV, treated with diethylnitrosamine combined with plant extract. Data represent the mean  $\pm$  SEM. \*\*  $p < 0.01$  indicates significant differences from the DEN group.

### 3. Materials and Methods

#### 3.1. Plant Material

*Alocasia gigantea* leaves were collected after permission and in compliance with relevant international guidelines and legislation from Experimental Plants Station, Faculty of Pharmacy, Cairo University, Giza, Egypt, during April 2020. Identification and authentication of the plant material were achieved by Dr. Tearse Labib, consultant of taxonomy at the Ministry of Agriculture and former director of El-Orman Botanical Garden, Giza, Egypt. A voucher specimen (No. A.g/1/2020) is kept in the herbarium of the Medicinal Chemistry Department at Theodor Bilharz Research Institute.

#### 3.2. Extraction and Defatting

Dry powdered leaves of *A. gigantea* (1100 g) were extracted four times with methanol via maceration (4 L) at room temperature. The combined extracts were filtered and evaporated under vacuum using a rotatory evaporator (Buchi, Flawil, Switzerland) at  $40 \pm 2$  °C to afford a methanol extract of 120.25 g (10.93%). The dried methanol extract was defatted using petroleum ether (60–80 °C), followed by dichloromethane in order to remove undesirable compounds [41], affording 30.87 g (2.81%), 11.29 g (1.03%), and 76.09 g (6.92%), respectively, for petroleum ether, dichloromethane, and defatted methanol extracts. Next, the defatted methanol extract (DefMeOH-E) was stored for further chemical and biological investigations.

### 3.3. Determination of Total Phenolic Content (TPC)

Total phenolic content of each extract was determined using the Folin–Ciocalteu reagent according to the reported procedure of Prior et al. (2019), with gallic acid as a standard [42]. The reaction mixture was composed of 50  $\mu$ L extract (500  $\mu$ g/mL), 250  $\mu$ L Folin–Ciocalteu reagent, and 0.75 mL sodium carbonate (20%). The mixture was shaken, and completed to 5 mL using distilled water. The mixture was allowed to stand for 2 h; then absorbance was measured at 765 nm using a spectrophotometer (UV-vis; Milton Roy 601, Co., Houston, TX, USA). All determinations were carried out in triplicate. Total phenolic content was expressed as mg gallic acid equivalent (GAE) per g extract.

### 3.4. UHPLC–DAD–ESI–MS/MS Analysis

This analysis was performed on an Ultimate 3000 (Dionex Co., San Jose, CA, USA) apparatus equipped with an ultimate 3000 Diode Array Detector (Dionex Co., USA) and coupled to a mass spectrometer, following the general procedure previously described [43]. The chromatographic apparatus consisted of an autosampler/injector, a binary pump, a column compartment and an ultimate 3000 Diode Array Detector (Dionex Co., San Jose, CA, USA), coupled to a Thermo LTQ XL (Thermo Scientific, San Jose, CA, USA) ion trap mass spectrometer equipped with an ESI source. The LC separation was carried out in a Hypersil Gold (ThermoScientific, San Jose, CA, USA) C<sub>18</sub> column (100 mm length; 2.1 mm i.d.; 1.9  $\mu$ m particle diameter; end-capped) maintained at 30 °C and a binary solvent system composed of (A) acetonitrile and (B) 0.1% formic acid (*v/v*). The solvent gradient started with 5–40% of solvent (A) over 14.72 min, at 40–100% over 1.91 min and remaining at 100% for 2.19 more min before returning to initial conditions. The flow rate was 0.2 mL/min, and UV-vis spectral data for all peaks were accumulated in the range of 200–700 nm while chromatographic profiles were recorded at 280 nm. Control and data acquisition of MS were carried out with the Thermo Xcalibur Qual Browser data system (ThermoScientific, San Jose, CA, USA). Nitrogen above 99% purity was used, and the gas pressure was 520 kPa (75 psi). The instrument was operated in negative mode, with the ESI needle voltage set at 5.00 kV and an ESI capillary temperature of 275 °C. The full scan covered the mass range from *m/z* 100 to 2000. CID–MS/MS experiments were performed for precursor ions, using helium as the collision gas, with a collision energy of 25–35 arbitrary units.

### 3.5. In-Vitro Study on HCC Cell Line

The Department of Cell Culture (Vacsera, Egypt) provided the HepG2 cell line. The cells were cultured in a PYR-free 1640 RPMI medium (Thermo Fisher Scientific). The medium was made up of 10% FBS, 1% HEPES, and 1% antibiotic/antimycotic combination (LONZA). Different quantities (500, 250, and 125 g/mL) of the *A. gigantea* extract and doxorubicin (DOX) (as a standard drug) were applied following attachment of the cells (7000 cells/well) on 96 tissue culture plates. The plates were then incubated at 37 °C in 5% CO<sub>2</sub> for 24 h. Cell viability was detected using a crystal violet assay following the general procedure previously described [19].

### 3.6. Animals

All animal experiments were carried out under Institutional Ethical Committee rules for care and use of experimental animals, authorized by Theodor Bilharz Research Institute's Animal Ethics Committee in Giza, Egypt (PT (583)/FWA 00010609). Theodor Bilharz Research Institute's animal house provided a total of 48 male Swiss albino mice (6–7 weeks old) weighing 23  $\pm$  5 g. The animals were given a week to acclimate. Throughout the experiment, all animals were kept in standardized hygienic conditions, including a temperature of 21–22 °C, a humidity of 55%, a standard 12 h light–dark cycle, and food and water accessibility.

### 3.7. Assessment of *A. gigantea* Acute Toxicity

The first step in determining toxicity of a plant extract is to conduct an acute oral toxicity test. The animals were starved for 12 h and only allowed to drink water. They were then weighed after the fasting period, and a test extract was given orally at a dose of 2000 mg/kg. Food was withheld from the animals for 2 h after the test extract was administered. In the first instance, mortality; clinical signs, such as changes in the skin, fur, eyes, and mucous membranes; and behavioral signs, as diarrhea, lethargy, sleep, or tremors were tracked for the first 4 h, then at 72 h and at 7 days after the test extract was administered [44,45].

### 3.8. In Vivo Experimental Design

To reach HCC, diethylnitrosamine (DEN) was used as an inducer. Intraperitoneal injection is a common technique that safely delivers a substance into the peritoneal cavity but can induce high stress in animals. Therefore, we depended on it to deliver HCC [46]. Mice were divided into 4 groups (12 mice/group) that were administered for 12 weeks. Gp-I (normal), a control group, was given a saline solution intraperitoneally (i.p.) (3.5 µL/mg BW); Gp-II (positive) was given diethylnitrosamine (DEN) twice a week i.p. (3.5 µL/mg BW); Gp-III (*A. gigantea*) was given plant extract (150 mg/kg BW) orally twice a week; and Gp-IV (DEN/*A. gigantea*) was also given DEN twice a week i.p. (3.5 µL/mg BW). At the end of 8 weeks, Gp-IV was treated with plant extract (150 mg/kg) orally twice a week for 4 consecutive weeks in combination with DEN.

After the required time was reached, scarification was performed. Euthanasia was chosen to minimize animal pain and distress consistent with the needs of the research protocol. Euthanasia was performed via inhalation of CO<sub>2</sub> from a pressurized tank in a rodent cage that contained up to 5 adult mice, followed by cervical dislocation and decapitation. CO<sub>2</sub> (30–70% displacement per minute depending on cage size) gas flow was slow and neither hissed nor overpowered and frightened the mice [47].

### 3.9. Body and Liver Weight and Biochemical Parameters

Body weight for each group was registered at the beginning of this study and before termination. Liver weight for each group was detected after scarification. The mice fasted overnight after the last treatment. Collected blood samples were centrifuged at 2000 rpm for 10 min. A liver function test was monitored using a serum aspartate aminotransferase (AST) and alanine transaminase (ALT) kit (Sclavo Diagnostics Internationals), an alkaline phosphatase (ALP) kit (N.S. BIO-TEC), and a total direct bilirubin (TBILR) kit (Sclavo Diagnostics Internationals).

### 3.10. Histopathological Examinations

The isolated livers were fixed in 10% buffered formalin. The liver was routinely processed into paraffin blocks. On positively charged glass slides, 4–5 µm thick sections were cut. Sections were then stained with hematoxylin and eosin (H&E) for light microscopic histopathological examination of hepatic architecture, inflammation, dysplasia, and carcinogenesis. The Masson trichrome stain was used to assess tissue fibrosis. Liver histology of different groups was compared using a Zeiss Axio microscope, and photos were taken with the attached digital Mrc5 camera (Zeiss).

### 3.11. Inflammatory, Tumoral, and Autophagy Markers

A commercially available kit was used to isolate total RNA from serum and liver tissues (Biovision, Inc., Milpitas, CA, USA). To detect gene expression of tumor and autophagy markers, quantitative PCR (qPCR) was performed using isolated RNA (1 µg), a cDNA synthesis kit (Biovision, Inc.), and SYBR green master mix (Thermo Fisher Scientific). Each primer's sequence was designed as shown in Table 4. The mean with SD of each detected marker in each group was used to describe relative expression, using the following equation:  $RQ = 2^{-\Delta\Delta Ct}$ .

**Table 4.** Primer sequences for gene expression analysis using qPCR.

Gene	Primer Sequence	Reference
$\beta$ -actin	Sense: GGGAATGGGTCAGAAGGACT Antisense: CTTCTCCATGTCGTCCCAGT	[48]
BCI-2	Sense: ATGCCTTTGTGGAACATATAGGC Antisense: GGTATGCACCCAGAGTGATGC	[49]
mTOR	Sense: GGCCAAAAGGCAGGTGGCT Antisense: ATGTTCACTTTGTGCTTGTA	This study
AMPK	Sense: GGAGAATAATGAATGAAGCC Antisense: CACCTTGGTGTGGATTTC	This study
Beclin-1	Sense: GAGAGACCCAGGAGGAAG Antisense: GGCCCGACATGATGTCAA	This study
LC-3	Sense: CCCGGTGATCATCGAGCGCT Antisense: GAAGGCCTGCGTGGGGTT	This study
AFP	Sense: CTACATTTGCTGCGTCCAA Antisense: CAGCCAACACATCGCTAGTC	This study
TNF- $\alpha$	Forward: ACCCTCACACTCACAAACCA Reverse: GGCAGAGAGGAGGTGACTT	[50]

### 3.12. Statistical Analysis

Data in treatment groups were presented as mean with SD, and statistical analysis was performed using GraphPad Prism 8 (San Diego, CA, USA). One-way or two-way ANOVA was followed by a post-hoc Tukey multiple comparison test.  $p < 0.05$  was determined to be statistically significant.

## 4. Conclusions

Chemical characterization of the defatted methanol extract of *A. gigantea* using UHPLC–DAD–ESI–MS/MS analysis led to identification of eight di-C-glycosyl flavone isomers of apigenin and luteolin. Moreover, the conducted study allowed conclusion that the extract of *A. gigantea* has potential anti-HCC effects via modulation of the autophagy pathway. The outcomes reached give an initial visualization of the operative effect of some compounds, paving the way to extensive study on isolation and activity of individual compounds.

**Supplementary Materials:** The following supporting information can be downloaded at: <https://www.mdpi.com/article/10.3390/molecules27238504/s1>, Figure S1: UHPLC chromatogram (at 280 nm) of *A. gigantea* defatted methanolic extract. Peak numbers correspond to those in Table 1.

**Author Contributions:** H.O.: conceptualization; formal analysis; data curation; visualization; investigation; methodology; writing—original draft, review, and editing. T.A.: investigation (histopathological study); writing—original draft, review, and editing. M.A.C.: investigation (phytochemical analysis); writing and editing. S.M.C.: investigation (phytochemical analysis); supervision; writing—original draft, review, and editing. M.A.G.: conceptualization; formal analysis; data curation; visualization; plant collection; extraction; fractionation; phytochemical analysis; writing—original draft, review, and editing. All authors have read and agreed to the published version of this manuscript.

**Funding:** This research was partially financed by University of Aveiro, FCT/MEC for the financial support to the LAQV-REQUIMTE (UIDB/50006/2020), through national funds, and, where applicable, co-financed by the FEDER, within the PT2020 Partnership.

**Institutional Review Board Statement:** All animal experiments were carried out under Institutional Ethical Committee rules for care and use of experimental animals, authorized by Theodor Bilharz Research Institute’s Animal Ethics Committee in Giza, Egypt (PT (583)/FWA 00010609).

**Informed Consent Statement:** Not applicable.

**Data Availability Statement:** Data are contained within the article.

**Conflicts of Interest:** The authors declare that there are no conflict of interest.

**Sample Availability:** Not applicable.

## References

- Samant, H.; Amiri, H.S.; Zibari, G.B. Addressing the Worldwide Hepatocellular Carcinoma: Epidemiology, Prevention and Management. *J. Gastrointest. Oncol.* **2021**, *12*, S361–S373. [CrossRef] [PubMed]
- Okasha, H. Interferon and P53 Tumor Suppressor Marker in Hepatocellular Carcinoma. *Int. J. Pharm. Res.* **2020**, *12*, 11–14. [CrossRef]
- Mulcahy Levy, J.M.; Thorburn, A. Autophagy in Cancer: Moving from Understanding Mechanism to Improving Therapy Responses in Patients. *Cell Death Differ.* **2020**, *27*, 843–857. [CrossRef] [PubMed]
- Rao, S.; Tortola, L.; Perlot, T.; Wirnsberger, G.; Novatchkova, M.; Nitsch, R.; Sykacek, P.; Frank, L.; Schramek, D.; Komnenovic, V.; et al. A Dual Role for Autophagy in a Murine Model of Lung Cancer. *Nat. Commun.* **2014**, *5*, 3056. [CrossRef] [PubMed]
- White, E. Deconvoluting the Context-Dependent Role for Autophagy in Cancer. *Nat. Rev. Cancer* **2012**, *12*, 401–410. [CrossRef]
- Amaravadi, R.; Kimmelman, A.C.; White, E. Recent Insights into the Function of Autophagy in Cancer. *Genes Dev.* **2016**, *30*, 913–930. [CrossRef]
- Yao, D.; Wang, P.; Zhang, J.; Fu, L.; Ouyang, L.; Wang, J. Deconvoluting the Relationships between Autophagy and Metastasis for Potential Cancer Therapy. *Apoptosis* **2016**, *21*, 683–698. [CrossRef]
- Sayed, A.M.; El-Hawary, S.S.; Abdelmohsen, U.R.; Ghareeb, M.A. Antiproliferative potential of *Physalis peruviana*-derived magnolin against pancreatic cancer: A comprehensive in vitro and in silico study. *Food Funct.* **2022**, *13*, 733–11743. [CrossRef]
- Moon, J.M.; Lee, B.K.; Chun, B.J. Toxicities of Raw *Alocasia odora*. *Hum. Exp. Toxicol.* **2011**, *30*, 1720–1723. [CrossRef]
- Ongpoy, R.C., Jr. The Medicinal Properties of the *Alocasia* Genus: A Systematic Review. *JAASP Res. Pap.* **2017**, *6*, 25–33.
- Wei, P.; Zhiyu, C.; Xu, T.; Xiangwei, Z. Antitumor Effect and Apoptosis Induction of *Alocasia cucullata* (Lour.) G. Don in Human Gastric Cancer Cells In Vitro and In Vivo. *BMC Complement. Altern. Med.* **2015**, *15*, 33. [CrossRef] [PubMed]
- Fang, S.; Lin, C.; Zhang, Q.; Wang, L.; Lin, P.; Zhang, J.; Wang, X. Anticancer Potential of Aqueous Extract of *Alocasia macrorrhiza* against Hepatic Cancer In Vitro and In Vivo. *J. Ethnopharmacol.* **2012**, *141*, 947–956. [CrossRef] [PubMed]
- Fang, M.; Zhu, D.; Luo, C.; Li, C.; Zhu, C.; Ou, J.; Li, H.; Zhou, Y.; Huo, C.; Liu, W.; et al. In Vitro and In Vivo Anti-Malignant Melanoma Activity of *Alocasia cucullata* via Modulation of the Phosphatase and Tensin Homolog/Phosphoinositide 3-Kinase/AKT Pathway. *J. Ethnopharmacol.* **2018**, *213*, 359–365. [CrossRef] [PubMed]
- Alocasia gigantea*, Giant Elephant Ear in GardenTags Plant Encyclopedia. Available online: <https://www.gardentags.com/plant-encyclopedia/Alocasia-gigantea/35606> (accessed on 25 October 2022).
- Li, S.S.; Wu, J.; Chen, L.G.; Du, H.; Xu, Y.J.; Wang, L.J.; Zhang, H.J.; Zheng, X.C.; Wang, L.S. Biogenesis of C-Glycosyl Flavones and Profiling of Flavonoid Glycosides in Lotus (*Nelumbo nucifera*). *PLoS ONE* **2014**, *9*, e108860. [CrossRef]
- Kachlicki, P.; Piasecka, A.; Stobiecki, M.; Marczak, L. Structural Characterization of Flavonoid Glycoconjugates and Their Derivatives with Mass Spectrometric Techniques. *Molecules* **2016**, *21*, 1494. [CrossRef]
- Ferreira, F.; Gonçalves, R.F.; Gil-Izquierdo, A.; Valentão, P.; Silva, A.M.S.; Silva, J.B.; Santos, D.; Andrade, P.B. Further Knowledge on the Phenolic Profile of *Colocasia esculenta* (L.) Shott. *J. Agric. Food Chem.* **2012**, *60*, 7005–7015. [CrossRef]
- Cao, J.; Yin, C.; Qin, Y.; Cheng, Z.; Chen, D. Approach to the Study of Flavone Di-C-Glycosides by High Performance Liquid Chromatography-Tandem Ion Trap Mass Spectrometry and Its Application to Characterization of Flavonoid Composition in Viola Yedoensis. *J. Mass Spectrom.* **2014**, *49*, 7005–7015. [CrossRef]
- Morsi, E.A.; Ahmed, H.O.; Abdel-Hady, H.; El-Sayed, M.; Shemis, M.A. GC-Analysis, and Antioxidant, Anti-Inflammatory, and Anticancer Activities of Some Extracts and Fractions of *Linum usitatissimum*. *Curr. Bioact. Compd.* **2020**, *16*, 1306–1318. [CrossRef]
- Ibrahim, M.B.; Sowemimo, A.A.; Sofidiya, M.O.; Badmos, K.B.; Fageyinbo, M.S.; Abdulkareem, F.B.; Odukoya, O.A. Sub-Acute and Chronic Toxicity Profiles of *Markhamia tomentosa* Ethanolic Leaf Extract in Rats. *J. Ethnopharmacol.* **2016**, *193*, 68–75. [CrossRef]
- Test No. 425: *Acute Oral Toxicity: Up-and-Down Procedure*; OECD Guidelines for the Testing of Chemicals, Section 4; OECD: Paris, France, 2022; ISBN 9789264071049.
- Zhang, H.E.; Henderson, J.M.; Gorrell, M.D. Animal Models for Hepatocellular Carcinoma. *Biochim. Biophys. Acta-Mol. Basis Dis.* **2019**, *1865*, 993–1002. [CrossRef]
- Tolba, R.; Kraus, T.; Liedtke, C.; Schwarz, M.; Weiskirchen, R. Diethylnitrosamine (DEN)-Induced Carcinogenic Liver Injury in Mice. *Lab. Anim.* **2015**, *49*, 59–69. [CrossRef] [PubMed]
- Schulien, I.; Hasselblatt, P. Diethylnitrosamine-Induced Liver Tumorigenesis in Mice. *Methods Cell Biol.* **2021**, *163*, 137–152. [CrossRef] [PubMed]
- Ramakrishnan, G.; Raghavendran, H.R.B.; Vinodhkumar, R.; Devaki, T. Suppression of N-Nitrosodiethylamine Induced Hepatocarcinogenesis by Silymarin in Rats. *Chem. Biol. Interact.* **2006**, *161*, 104–114. [CrossRef]
- Singh, B.N.; Singh, B.R.; Sarma, B.K.; Singh, H.B. Potential Chemoprevention of N-Nitrosodiethylamine-Induced Hepatocarcinogenesis by Polyphenolics from *Acacia nilotica* Bark. *Chem. Biol. Interact.* **2009**, *181*, 20–28. [CrossRef] [PubMed]
- Jadon, A.; Bhadauria, M.; Shukla, S. Protective Effect of *Terminalia belerica* Roxb. and Gallic Acid against Carbon Tetrachloride Induced Damage in Albino Rats. *J. Ethnopharmacol.* **2007**, *109*, 214–218. [CrossRef] [PubMed]
- Mulla, W.A.; Salunkhe, V.R.; Bhise, S.B. Hepatoprotective Activity of Hydroalcoholic Extract of Leaves of *Alocasia indica* (Linn.). *Indian J. Exp. Biol.* **2009**, *47*, 816–821. [PubMed]
- Pal, S.; Bhattacharjee, A.; Mukherjee, S.; Bhattacharya, K.; Mukherjee, S.; Khowala, S. Effect of *Alocasia indica* Tuber Extract on Reducing Hepatotoxicity and Liver Apoptosis in Alcohol Intoxicated Rats. *BioMed Res. Int.* **2014**, *2014*, 349074. [CrossRef]



30. Zimmermann, A. Immunohistochemistry of Hepatocellular Carcinoma. In *Tumors and Tumor-like Lesions of the Hepatobiliary Tract*; Springer: Cham, Switzerland, 2016; pp. 1–27. [[CrossRef](#)]
31. Zimmermann, A. Tumors and Tumor-Like Lesions of the Hepatobiliary Tract. In *Tumors and Tumor-like Lesions of the Hepatobiliary Tract*; Springer: Cham, Switzerland, 2016. [[CrossRef](#)]
32. Wong, R.S.Y. Apoptosis in Cancer: From Pathogenesis to Treatment. *J. Exp. Clin. Cancer Res.* **2011**, *30*, 87. [[CrossRef](#)]
33. Abrahams, V.M.; Kamsteeg, M.; Mor, G. The Fas/Fas Ligand System and Cancer: Immune Privilege and Apoptosis. *Mol. Biotechnol.* **2003**, *25*, 19–30. [[CrossRef](#)]
34. Olsson, M.; Zhivotovsky, B. Caspases and Cancer. *Cell Death Differ.* **2011**, *18*, 1441. [[CrossRef](#)]
35. Elrabat, A.; Eletreby, S.; Zaid, A.M.A.; Zaghoul, M.H.E. Tumor Necrosis Factor-Alpha and Alpha-Fetoprotein as Biomarkers for Diagnosis and Follow-up of Hepatocellular Carcinoma before and after Interventional Therapy. *Egypt. J. Intern. Med.* **2019**, *31*, 840–848. [[CrossRef](#)]
36. Lee, Y.J.; Jang, B.K. The Role of Autophagy in Hepatocellular Carcinoma. *Int. J. Mol. Sci.* **2015**, *16*, 26629–26643. [[CrossRef](#)] [[PubMed](#)]
37. Kiruthiga, C.; Devi, K.P.; Nabavi, S.M.; Bishayee, A. Autophagy: A Potential Therapeutic Target of Polyphenols in Hepatocellular Carcinoma. *Cancers* **2020**, *12*, 562. [[CrossRef](#)] [[PubMed](#)]
38. Yan, X.; Qi, M.; Li, P.; Zhan, Y.; Shao, H. Apigenin in Cancer Therapy: Anti-Cancer Effects and Mechanisms of Action. *Cell Biosci.* **2017**, *7*, 50. [[CrossRef](#)] [[PubMed](#)]
39. Qin, Y.; Zhao, D.; Zhou, H.; Wang, X.-H.; Zhong, W.; Chen, S.; Gu, W.; Wang, W.; Zhang, C.-H.; Liu, Y.-R.; et al. Apigenin Inhibits NF-KB and Snail Signaling, EMT and Metastasis in Human Hepatocellular Carcinoma. *Oncotarget* **2016**, *7*, 41421–41431. [[CrossRef](#)]
40. Ghareeb, M.A.; Sobeh, M.; El-Maadawy, W.H.; Mohammed, H.S.; Khalil, H.; Botros, S.; Wink, M. Chemical Profiling of Polyphenolics in *Eucalyptus globulus* and Evaluation of Its Hepato-Renal Protective Potential against Cyclophosphamide Induced Toxicity in Mice. *Antioxidants* **2019**, *8*, 415. [[CrossRef](#)]
41. Mohammed, H.S.; Ghareeb, M.A.; Aboushousha, T.; Heikal, E.A.; Abu El wafa, S.A. An appraisal of *Luffa aegyptiaca* extract and its isolated triterpenoidal saponins in *Trichinella spiralis* murine models. *Arab. J. Chem.* **2022**, *15*, 104258. [[CrossRef](#)]
42. Prior, R.L.; Wu, X.; Schaich, K. Standardized Methods for the Determination of Antioxidant Capacity and Phenolics in Foods and Dietary Supplements. *J. Agric. Food Chem.* **2005**, *53*, 4290–4302. [[CrossRef](#)]
43. Afonso, A.F.; Pereira, O.R.; Neto, R.T.; Silva, A.M.S.; Cardoso, S.M. Health-Promoting Effects of *Thymus herba-barona*, *Thymus pseudolanuginosus*, and *Thymus caespitosus* Decoctions. *Int. J. Mol. Sci.* **2017**, *18*, 1879. [[CrossRef](#)]
44. Abid, R.; Mahmood, R. Acute and Sub-Acute Oral Toxicity of Ethanol Extract of *Cassia fistula* Fruit in Male Rats. *Avicenna J. Phytomed.* **2019**, *9*, 117–125.
45. Anisuzzman, M.; Hasan, M.M.; Acharzo, A.K.; Das, A.K.; Rahman, S. In Vivo and in Vitro Evaluation of Pharmacological Potentials of Secondary Bioactive Metabolites of *Dalbergia candanensis* Leaves. *Evid.-Based Complement. Altern. Med.* **2017**, *2017*, 5034827. [[CrossRef](#)] [[PubMed](#)]
46. Shirakami, Y.; Gottesman, M.E.; Blaner, W.S. Diethylnitrosamine-Induced Hepatocarcinogenesis Is Suppressed in Lecithin:Retinol Acyltransferase-Deficient Mice Primarily through Retinoid Actions Immediately after Carcinogen Administration. *Carcinogenesis* **2012**, *33*, 268. [[CrossRef](#)] [[PubMed](#)]
47. Baek, J.M.; Kwak, S.C.; Kim, J.Y.; Ahn, S.J.; Jun, H.Y.; Yoon, K.H.; Lee, M.S.; Oh, J. Evaluation of a Novel Technique for Intraperitoneal Injections in Mice. *Lab Anim.* **2015**, *44*, 440–444. [[CrossRef](#)] [[PubMed](#)]
48. Lei, Y.; Wang, S.; Ren, B.; Wang, J.; Chen, J.; Lu, J.; Zhan, S.; Fu, Y.; Huang, L.; Tan, J. CHOP Favors Endoplasmic Reticulum Stress-Induced Apoptosis in Hepatocellular Carcinoma Cells via Inhibition of Autophagy. *PLoS ONE* **2017**, *12*, e0183680. [[CrossRef](#)]
49. Xu, H.; Gao, Y.; Shu, Y.; Wang, Y.; Shi, Q. EPHA3 Enhances Macrophage Autophagy and Apoptosis by Disrupting the MTOR Signaling Pathway in Mice with Endometriosis. *Biosci. Rep.* **2019**, *39*, BSR20182274. [[CrossRef](#)]
50. Zhang, H.; Shang, C.; Tian, Z.; Amin, H.K.; Kassab, R.B.; Abdel Moneim, A.E.; Zhang, Y. Diallyl Disulfide Suppresses Inflammatory and Oxidative Machineries Following Carrageenan Injection-Induced Paw Edema in Mice. *Mediat. Inflamm.* **2020**, *2020*, 8508906. [[CrossRef](#)]

## Article

# Salvianolic Acid B Strikes Back: New Evidence in the Modulation of Expression and Activity of Matrix Metalloproteinase 9 in MDA-MB-231 Human Breast Cancer Cells

Andrea Ianni <sup>1</sup>, Pierdomenico Ruggeri <sup>2</sup>, Pierangelo Bellio <sup>2</sup>, Francesco Martino <sup>3</sup>, Giuseppe Celenza <sup>2</sup>, Giuseppe Martino <sup>1</sup> and Nicola Franceschini <sup>2,\*</sup>

<sup>1</sup> Department of BioScience and Technology for Food, Agriculture and Environment, University of Teramo, Via Renato Balzarini 1, 64100 Teramo, Italy

<sup>2</sup> Department of Biotechnological and Applied Clinical Sciences, University of L'Aquila, Via Vetoio 1, 67100 L'Aquila, Italy

<sup>3</sup> Department of Cardiovascular, Respiratory, Nephrological, Anaesthetic and Geriatric Sciences, "La Sapienza" University of Rome, Policlinico Umberto I, 00185 Rome, Italy

\* Correspondence: nicola.franceschini@univaq.it; Tel.: +39-0862-433456

**Citation:** Ianni, A.; Ruggeri, P.; Bellio, P.; Martino, F.; Celenza, G.; Martino, G.; Franceschini, N. Salvianolic Acid B Strikes Back: New Evidence in the Modulation of Expression and Activity of Matrix Metalloproteinase 9 in MDA-MB-231 Human Breast Cancer Cells. *Molecules* **2022**, *27*, 8514. <https://doi.org/10.3390/molecules27238514>

Academic Editor: Nour Eddine Es-Safi

Received: 13 October 2022

Accepted: 1 December 2022

Published: 3 December 2022

**Publisher's Note:** MDPI stays neutral with regard to jurisdictional claims in published maps and institutional affiliations.



**Copyright:** © 2022 by the authors. Licensee MDPI, Basel, Switzerland. This article is an open access article distributed under the terms and conditions of the Creative Commons Attribution (CC BY) license (<https://creativecommons.org/licenses/by/4.0/>).

**Abstract:** Salvianolic acid B (SalB) is a bioactive compound from *Salviae miltiorrhizae*, one of the most important traditional herbal medicines widely used in several countries for the treatment of cardiovascular diseases. The aim of this study was to evaluate the in vitro effect of SalB on the expression and the activity of matrix metalloproteinase 9 (MMP-9), a zinc-dependent proteolytic enzyme, in human MDA-MB-231 breast cancer cells. This cellular model is characterized by a marked invasive phenotype, supported by a high constitutive expression of MMPs, especially gelatinases. SalB was first of all evaluated by in silico approaches primarily aimed at predicting the main pharmacokinetic parameters. The most favorable interaction between the natural compound and MMP-9 was instead tested by molecular docking analysis that was subsequently verified by an enzymatic inhibition assay. MDA-MB-231 cells were treated with SalB 5  $\mu$ M and 50  $\mu$ M for 24 h and 48 h. The conditioned media obtained from treated cells were then analyzed by gelatin zymography and reverse zymography to, respectively, evaluate the MMP-9 activity and the presence of TIMP-1. The expression of the enzyme was then evaluated by Western blot on conditioned media and by analysis of transcripts through reverse transcriptase-polymerase chain reaction (RT-PCR). The in silico approach showed the ability of SalB to interact with the catalytic zinc ion of the enzyme, with a plausible competitive mode of action. The analysis of conditioned culture media showed a reduction in MMP-9 activity and the concomitant decrease in the enzyme concentration, partially confirmed by analysis of transcripts. SalB showed the ability to modulate the function of MMP-9 in MDA-MB-231 cells. To our knowledge, this is the first time in which the role of SalB on MMP-9 in a highly invasive cellular model is investigated. The obtained results impose further and more specific evaluations in order to obtain a better understanding of the biochemical mechanisms that regulate the interaction between this natural compound and the MMP-9.

**Keywords:** Salvianolic acid B; matrix metalloproteinase 9; gelatinase B; MDA-MB-231 human breast cancer cells; TIMP-1

## 1. Introduction

The MMP-9/Gelatinase B belongs to the wide family of zinc dependent endopeptidases named matrix metalloproteinases (MMPs). MMPs are involved in the physiological degradation of the extracellular matrix (ECM), a fundamental process for tissue development, morphogenesis, remodeling and repair [1]. Due to their important physiological role,

MMPs are tightly regulated: their expression is transcriptionally influenced by growth factors, hormones and cytokines, while their activity is tuned by the activation of propeptides (zymogens) and by inhibition of the enzymatic activity mediated by endogenous tissue inhibitors (TIMPs) [2].

Disturbances of this complex network hindering the normal MMPs function are known to be associated with the development of pathological events related to excessive or insufficient ECM turnover: arthritis, wound healing disorders, fibrotic diseases and cancer [3].

Regarding cancer, it is known that the proteolytic activity which contributes to the degradation of ECM and basal membrane represents a key step in cell invasion, metastasis and angiogenesis [4]. Moreover, several studies have posed evidence of the crucial role of gelatinases in numerous invasive cancers, such as breast cancer [5,6]. Recent observations also provide evidence that MMPs modulate various aspects of inflammation, some of which seem to be essential for the suppression of innate immune response against tumor cells; in this context, MMPs may exert an immune regulatory function in tumor microenvironment, helping cancer cells to escape immune surveillance [7]. It is easy to understand that the identification of MMP inhibitors (MMPi) today represents an important opportunity for the treatment and prevention of numerous chronic and life-threatening diseases. For these reasons, MMPs inhibitor drug discovery has emerged as an important area of research in many fields of medical sciences as also attested by the discovery or repositioning of several MMPs inhibitors [8–10].

In the last decade, great interest was generated in the characterization and use of natural compounds credited with high bioactive potential, including anti-inflammatory, antibacterial, antioxidant, anti-cancer and anti-diabetic properties [11–13]. Into this scenario fits the interest in the identification of natural compounds capable of controlling the expression and activity of MMPs. Specifically, flavonoids have been found to influence MMPs levels in different ways. In many cell types, flavonoids have been described to down-regulate MMPs biosynthesis. Quercetin, for instance, was reported to inhibit the invasivity of murine melanoma cells by decreasing pro-MMP-9 via PKC pathway [14]. It is also known that certain MMPs can be activated by oxidative stress and the antioxidative effect of flavonoids may influence this mechanism [15].

*Salvia miltiorrhiza*, also known as red sage or Chinese sage, is one of the most widely used traditional herb medicines recommended for the treatment of a variety of diseases, such as cardiovascular diseases, hepatitis, hepatocirrhosis, chronic renal failure and dysmenorrhea. In *S. miltiorrhiza*, two pharmacologically active fractions were identified: lipophilic diterpenoids transhinones and water-soluble phenolic acids [16]. In recent years, research has been focused on the phenolic acid fraction where twenty-five phenolic acid compounds have been isolated and identified. Specifically, Salvianolic acid B (SalB) represents the most abundant compound, accounting for 3–5% of total dried weight [17]. To date, SalB has been identified as an agent which may be useful in controlling the expression of MMP-2 and MMP-9 in pathological conditions involving the cardiovascular system. In this context, we should cite the inhibition of MMP-2 upregulation in human aortic smooth muscle cells via suppression of NAD(P)H oxidase-derived reactive oxygen species [18], the prevention of the infarct-induced cardiac remodeling through competitive inhibition of MMP-9 [19] and the attenuation of cardiac fibroblast migration, collagen and cytokine secretion through the in vitro inhibition of the catalytic domain of MMP-9 [20]. However, little attention has been paid to the role of SalB in tumor cell lines characterized by high invasivity potential, in which MMPs play a leading role. The aim of this work is therefore to verify the effect of SalB in regulating the in vitro function of MMP-9 in MDA-MB-231 human breast cancer cells. The only studies that involved the treatment of MDA-MB-231 cells with SalB focused attention on different biochemical and molecular aspects. For example, the work published by Sha et al. [21] analyzed the effects induced by the natural compound on the cell viability, cell cycle and apoptosis of triple-negative MDA-MB-231 cells with the hormone receptor-positive MCF-7 cells as the control. The main finding of the work was specifically related to

SalB ability to enhance the cell apoptosis and decrease cell proliferation by regulating the ceramide glycosylation enzymes. Overall, most of the studies performed on human breast cancer cells involved the use of non-invasive phenotypes (MCF-7 cells), confirming the role of SalB in cell proliferation, migration and invasion abilities, without specific assessments on the gelatinases function [22].

## 2. Results

### 2.1. In Silico Evaluations and In Vitro Analysis of the Interaction between Salvianolic Acid B and MMP-9

The SwissADME (absorption, distribution, metabolism and excretion) web tool was exploited with the aim to obtain a prediction concerning the pharmacokinetic properties of SalB. The main information of the analysis is reported in Table 1, and indicate low absorption from the gastrointestinal (GI) tract and the inability to permeate the blood–brain barrier (BBB). Furthermore, SalB seems unable to inhibit the activity of cytochrome P450 isoforms (CYP1A2, CYP2C19, CYP2C9, CYP2D6, CYP3A4), whose function is associated with drug elimination through metabolic biotransformation. In Figure 1, the bioavailability radar that gives a first glance on the drug-likeness of the compound is instead reported, considering a total of six physicochemical properties: lipophilicity, size, polarity, solubility, flexibility and saturation. From this point of view, SalB showed itself to be a good candidate with reference to lipophilicity and solubility, while the report highlighted values outside the physicochemical range in the case of size, polarity, flexibility and saturation.

In order to predict the most probable binding conformations between SalB and MMP-9, a preliminary in silico study was performed. The most favorable docking is associated with a  $\Delta G$  value equal to  $-14.786$  kcal/mol; in this condition (Figure 2A), SalB is able to approach the active site of the enzyme, placing its carboxylic group close to the catalytic zinc ion. In addition to this, the distance between the O6 SalB carboxylic oxygen and the catalytic zinc ion is  $2.2$  Å (Figure 2B), suggesting the plausible existence of a non-covalent interaction.

**Table 1.** SwissADME (absorption, distribution, metabolism and excretion) parameters attributed to SalB.

Properties	Parameters	SalB
Physicochemical Properties	MW	718.61 g/mol
	Rotatable bonds	14
	HBA	16
	HBD	9
	Molar refractivity	178.07
	TPSA	278.04 Å
Lipophilicity (Log $P_{o/w}$ )	iLOGP	2.10
	XLOGP3	3.98
	WLOGP	2.90
	MLOGP	0.25
	SILICOS-IT	2.57
	Consensus estimation	2.36
Pharmacokinetics	GI absorption	Low
	BBB permeant	No
	P-gp substrate	No
	CYP1A2 inhibitor	No
	CYP2C19 inhibitor	No
	CYP2C9 inhibitor	No
	CYP2D6 inhibitor	No
	CYP3A4 inhibitor	No
Log $K_p$ (skin permeation)	$-7.86$ cm/s	

MW = molecular weight; HBA = H-bond acceptors; HBD = H-bond donors; TPSA = Topological Polar Surface Area; GI = gastrointestinal; BBB = blood–brain barrier; P-gp = permeability glycoprotein; iLOGP, XLOGP3, WLOGP, MLOGP, SILICOS-IT represent lipophilicity predictive models [Daina et al. 2017]; CYP1A2, CYP2C19, CYP2C9, CYP2D6, CYP3A4 are isoforms of cytochrome P450.

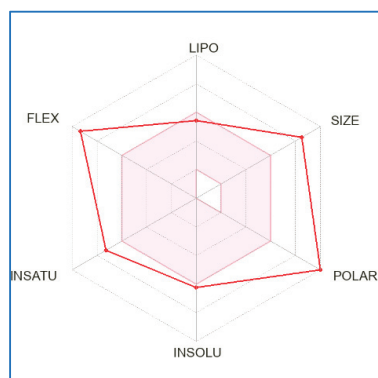


**Figure 1.** Bioavailability radar chart of SalB. The bioavailability radar gives a first glance on the drug-likeness of the compound, considering a total of six physicochemical properties: lipophilicity, size, polarity, solubility, flexibility and saturation. The pink zone represents the physicochemical space for oral bioavailability, and the red line represents the specific oral bioavailability properties associated with the analyzed compound.

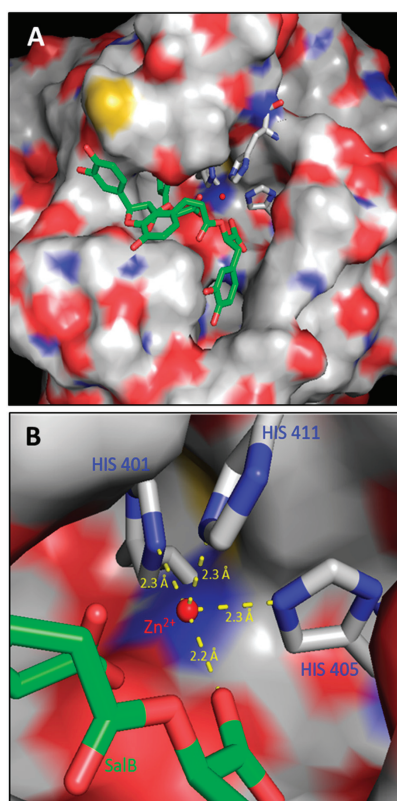


**Figure 2.** Molecular Docking analysis of the interaction between SalB and MMP-9. (A) SalB ability to approach the MMP-9 catalytic pocket. (B) Molecular docking of SalB in the catalytic domain of MMP-9 (PDB code: 1GKC). SalB seems able to interact with the catalytic  $Zn^{2+}$  ion which is coordinated by three histidines (HIS401, HIS405, HIS411). The analysis specifically suggests the existence of a coordinated bond between the catalytic  $Zn^{2+}$  atom and a carboxyl oxygen of SalB structure.

To confirm the computational results, an enzymatic inhibition assay was performed. For this purpose, a recombinant active human MMP-9, composed of the catalytic domain, the gelatin binding domain and the metal binding domain (amino acids 107–457), was used. Increasing the concentrations of SalB ranging from 0  $\mu\text{M}$  to 100  $\mu\text{M}$ , in the presence of different concentrations of substrate (0.375–1.5  $\mu\text{M}$ ), suggested a competitive inhibition of the activity performed by the MMP-9 catalytic domain (CDMMP-9) (Figure 3A), and allowed to define a  $K_i$  value equal to  $57.37 \pm 3.96 \mu\text{M}$  (Figure 3B).

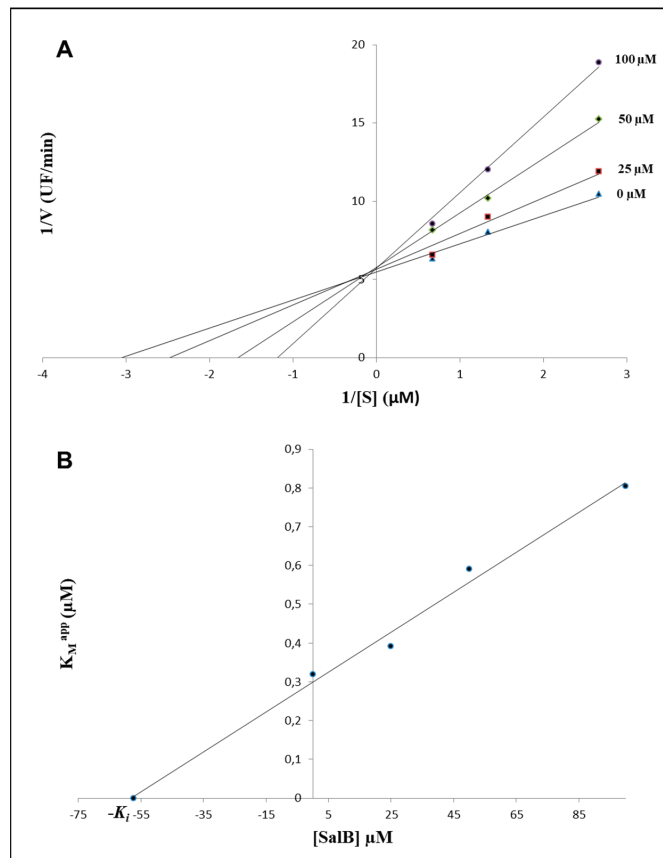


**Figure 3.** Kinetic analysis of SalB against the catalytic domain of MMP-9. (A) Double reciprocal plots of  $1/V$  versus  $1/[S]$  suggest the competitive inhibition of the activity performed by the catalytic domain of MMP-9 (CDMMP-9). (B) Secondary plot of  $K_M^{\text{app}}$  versus different SalB concentrations. The  $K_i$  value of SalB against CDMMP-9 was calculated to be equal to  $57.37 \mu\text{M}$ .

## 2.2. Evaluation of Gelatinolytic Activity in MDA-MB-231 Cells

The zymographic analysis was performed on conditioned media obtained from MDA-MB-231 cells treated for 24 h and 48 h with SalB 5  $\mu\text{M}$  (SalB-5) and 50  $\mu\text{M}$  (SalB-50). Such analysis was effective in highlighting the gelatinolytic potential attributable to MMP-2 and MMP-9.

As shown in Figure 4A, SalB was able to influence the activity of MMP-9, which was significantly reduced in the presence of the higher concentration of the natural compound (50  $\mu\text{M}$ ), both after 24 h and 48 h of treatment ( $p < 0.05$ ). The analysis also highlighted the activity of the active form of the enzyme, which follows the same pattern observed for the zymogen, with lower ability to hydrolyze gelatin in SalB-50 samples at both treatment times ( $p < 0.05$ ).

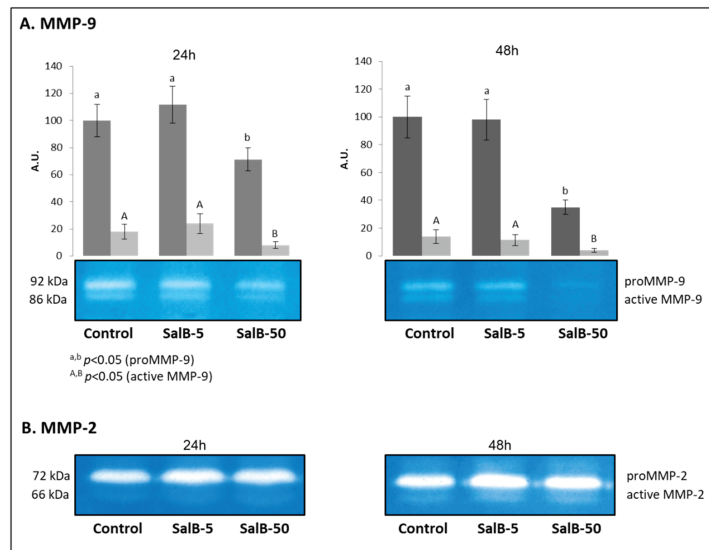


**Figure 4.** Gelatin Zymography for the evaluation of MMP-9 and MMP-2 activity. Zymographic evaluation of MMP-9 (A) and MMP-2 (B) activity in conditioned media obtained from MDA-MB-231 cells treated for 24 h and 48 h with SalB 5 and 50  $\mu$ M.

With regard to MMP-2 (Figure 4B), no significant variations were evidenced, both in relation to the dosage and the timing of the treatment ( $p > 0.05$ ).

### 2.3. Salvanolic Acid B Had no Effects on TIMP-1 Expression in MDA-MB-231 Cells

The potential role of SalB in influencing the endogenous regulation of MMP-9 activity was evaluated by focusing the attention on TIMP-1. Figure 5 shows the results obtained from reverse zymography and Western blot performed on conditioned culture media, and RT-PCR applied on mRNA purified from the corresponding cells. By combining these different approaches, no significant changes ( $p > 0.05$ ) were found in the expression and in the release of TIMP-1 in the extracellular environment.

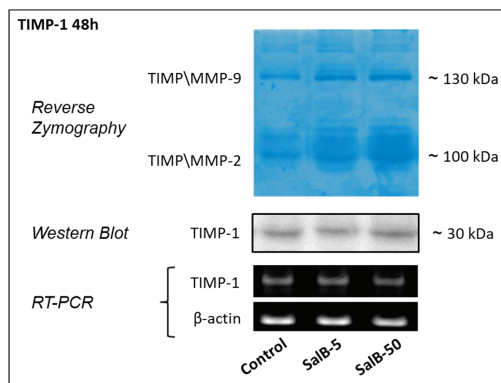


**Figure 5.** Analysis of TIMP-1 through reverse zymography, Western blot and RT-PCR. The role of the tissue inhibitor of metalloproteinases-1 (TIMP-1) has been evaluated through reverse zymography and Western blot that were performed on conditioned media obtained from MDA-MB-231 cells treated for 48 h with SalB 5 and 50  $\mu$ M. In the same sampling were also collected cells for transcripts evaluation by RT-PCR.

#### 2.4. MMP-9 Expression Was Affected in Treated MDA-MB-231 Cells

The samples previously used for the zymographic evaluations, were also subjected to Western blot analysis to verify the relative amount of the enzyme in the conditioned culture media obtained from the various treatments (Figure 6A). In this case, SalB significantly affected the amount of MMP-9 in the conditioned culture medium ( $p < 0.01$ ) only when it was administered at the highest concentration (50  $\mu\text{M}$ ) during 48 h treatment.

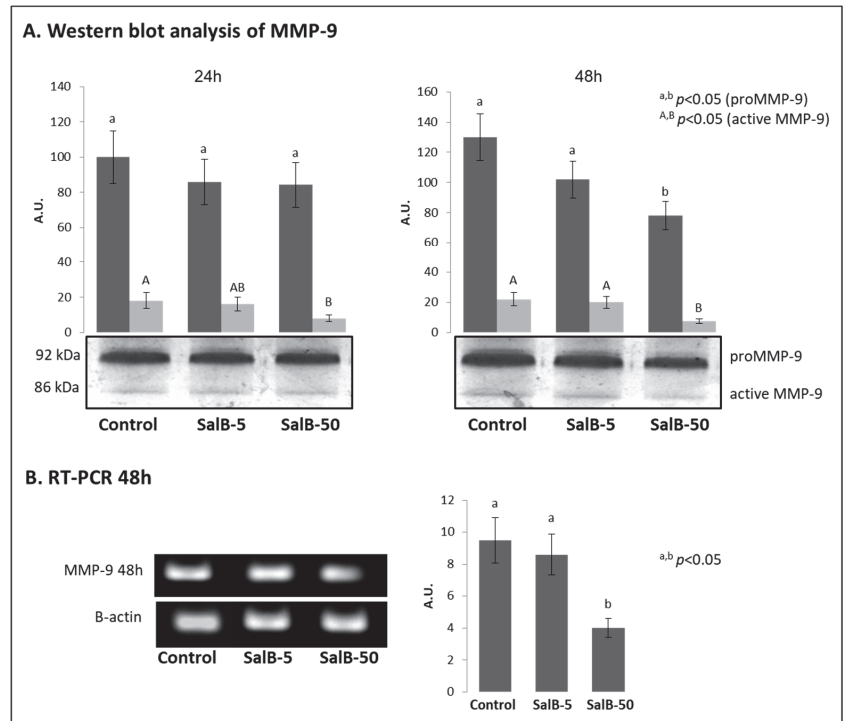


**Figure 6.** Analysis of TIMP-1 through reverse zymography, Western blot and RT-PCR. The Western blot analysis and RT-PCR of MMP-9. (A) The MMP-9 expression was firstly evaluated through Western blot on conditioned media obtained from MDA-MB-231 cells treated for 24 h and 48 h with SalB 5 and 50  $\mu\text{M}$ . Different lower case letters (a,b) indicate significant differences ( $p < 0.05$ ) for the proMMP-9, while different upper case letters indicate significant differences ( $p < 0.05$ ) for the active form of MMP-9. (B) The collection of MDA-MB-231 cells was useful to perform the analysis on MMP-9 transcripts after 48 h treatment with SalB 5 and 50  $\mu\text{M}$ .

In order to verify any changes at the molecular level, the MMP-9 transcripts in cells subjected to 48 h treatment were purified and analyzed. As shown in Figure 6B, a significant reduction in MMP-9 transcript expression ( $p < 0.05$ ) was effectively noted following the treatment with 50  $\mu\text{M}$  SalB, while no variations were evidenced in SalB-5 samples ( $p > 0.05$ ).

### 3. Discussion

Several studies have been conducted to evaluate the ability of SalB to regulate the activity of gelatinases, particularly of MMP-9. To our knowledge this is the first study in which this aspect is evaluated on human MDA-MB-321 breast cancer cells, a highly invasive cellular model characterized by a marked constitutive expression of MMP-9.

Before the evaluation of SalB effect on the selected cell line, a preliminary *in silico* study was performed for the prediction of the drug-likeness of the natural compound and the most probable binding conformations between SalB and MMP-9. The SwissADME web



tool represents an informative approach in order to obtain a prediction about the biotransformation of specific compounds into drugs. First of all, this evaluation evidenced for SalB low absorption from the gastrointestinal tract and the inability to permeate the blood–brain barrier (BBB). In particular, this last aspect argues in favor of the fact that SalB should not induce adverse effects at the level of the central nervous system. Besides this, SalB does not represent a substrate of the permeability glycoprotein (P-gp) that was suggested to be one of the most relevant members among the ATP-binding transporters, responsible for limiting the oral bioavailability of drugs that act as its substrates [23]. In the sphere of pharmacokinetic parameters, the finding concerning the interaction of the natural compound with cytochromes P450 is also relevant, which is actively involved in the processes of drug elimination through metabolic biotransformation [24]. SalB does not represent an inhibitor of these factors, an aspect of considerable importance considering that the inhibition of these isoenzymes was reported to be one of the main causes of pharmacokinetics-related drug–drug interactions, leading to toxic or other unwanted adverse effects due to the lower clearance and accumulation of the drug or its metabolites [25]. The bioavailability radar generated by the web tool, that gives a first glance on the drug-likeness of the compound, showed overall good attitudes for SalB with reference to lipophilicity and solubility, while conditions outside the physicochemical range were evidenced in the case of size, polarity, flexibility and saturation. This finding testifies to the fact that in the pharmaceutical field it could be more plausible for the use of specific structural domains of the natural compound, rather than the molecule in its entirety.

With reference to the specific interaction between SalB and MMP-9, molecular docking evaluations were performed. Specifically, the most favorable docking is associated with a  $\Delta G$  value equal to  $-14.786$  kcal/mol; in this condition SalB is able to approach the active site of the enzyme, placing its carboxylic group close to the catalytic zinc ion. In this conformation, a distance of  $2.2 \text{ \AA}$  was calculated between the SalB carboxylic oxygen and the catalytic zinc atom, suggesting the possible onset of a non-covalent interaction between SalB and MMP-9, in addition to the three coordination interactions between zinc and the catalytic histidines (HIS401, HIS405 and HIS411). Such geometrical constraints are therefore compatible with a tetracoordinated chelation model of the catalytic zinc ion as also suggested by Jacobsen et al. [9] who inserted the carboxylic residue in the list of the “zinc binding domains”.

In order to confirm the computational results, an enzymatic inhibition assay was performed by using a recombinant active human MMP-9. The calculated  $K_i$  value was equal to  $57.37 \pm 3.96 \text{ \mu M}$ , a finding in full agreement with what has been previously reported by Jiang et al. [19], who found a  $K_i$  value of  $79.2 \text{ \mu M}$ , by using a similar analytical strategy.

The encouraging data obtained by the *in silico* analysis confirmed by the enzymatic inhibition assay, provided a rationale for the *in vitro* investigation on human MDA-MB-231 breast cancer cells, characterized by a marked invasive phenotype, supported by a high constitutive expression of several MMPs, especially MMP-9 [26].

In order to define the best experimental conditions for cell treatment with SalB, an MTT cell viability assay was performed, allowing us to define the range of concentrations of SalB and the time of exposure in which the cytotoxic effect does not exceed 10% of cell mortality with respect to untreated cells. In our intention, this was performed to make sure that the treated cells maintain the same vitality as the control cells, in order to ensure that any variations in the expression of MMP-9 were to be totally attributed to the effect of SalB and not simply to a reduction in cell viability. Through this preliminary approach, we believe we have given greater strength to the considerations made on the specific effect of the natural compound on the MMP-9 function. Cells were then treated with two concentrations of SalB,  $5 \text{ \mu M}$  (SalB-5) and  $50 \text{ \mu M}$  (SalB-50), for 24 h and 48 h, respectively.

The zymographic analysis of the conditioned media showed the ability of SalB to inhibit the activity of MMP-9. The analysis also highlighted the activity of the active form of the enzyme, which follows the same pattern observed for the zymogen. This observation suggests that the relation between the two forms remains unchanged under

all the experimental conditions and testifies to the fact that SalB had no effect on the pro-enzyme activation mechanism. The observed reduction in activity may therefore depend on a competitive inhibition model based on the prevalent interaction of SalB with the catalytic domain of the enzyme. This hypothesis finds support in the results obtained from the *in silico* investigation and is in agreement with what was previously observed by Jiang et al. [19] who hypothesized a competitive inhibition of MMP-9 by the SalB. In the same zymograms, the activity of MMP-2 was also visualized. In this case, the SalB did not induce significant variations; a behavior already highlighted in a previous study in which no significant regulation of SalB on MMP-2 activity was found, suggesting that the natural compound was more specific on MMP-9 than on MMP-2 [19]. However, it must be reported that in other studies conducted on murine models or alternative cell lines, a drastic reduction in MMP-2 activity was reported as a consequence of the ability of SalB to interact with mediators of gelatinase expression. One of the best characterized mechanisms concern the inhibition of the tumor necrosis factor- $\alpha$  (TNF- $\alpha$ )-induced MMP-2 upregulation in human aortic smooth muscle cells via suppression of the NAD(P)H oxidase-derived reactive oxygen species [18,27].

It is known that the MMP activity in the extracellular environment is finely regulated by specific endogenous inhibitors (TIMPs) which interact with the enzyme in a stoichiometric 1:1 ratio. For this reason, in the next phase of the study, the role of TIMP-1, which possesses a prevailing selectivity for gelatinases, was evaluated in order to better understand the effect of SalB treatment on MDA-MB-231 cells, and in particular on MMP-9 function. By combining different approaches, no significant changes were found in the expression and in the release of TIMP-1 in the extracellular environment, a fact that confers additional strength to the SalB ability to act as an MMP-9 inhibitor. Concerning the relationship between SalB and TIMPs, no specific studies have been conducted. However, the study performed by Dai et al. [28] must be taken into consideration. They investigated the antifibrotic activity of the active compounds of *Salviae miltiorrhizae* on mice oral mucosal fibroblasts and reported the ability of tanshinone IIA, salvianolic acid A and SalB to reduce TIMP-1 and TIMP-2 expression, a phenomenon that predisposes an increase in gelatinases activity. In agreement with what has been described, it should be also reported that other studies highlighted that flavonoids generally have the ability to influence the expression of TIMPs, with even quite marked effects on the ECM remodeling processes. These are evidence observed in cell lines and *in vivo* models in which, contextually to the effect on TIMPs, perturbations were also monitored for the expression and activity of other factors involved in crucial signaling pathways such as focal adhesion kinase (FAK), phosphatidylinositol-3-kinase (PI3K)-Akt, signal transducer and activator of transcription 3 (STAT3), nuclear factor  $\kappa$ B (NF $\kappa$ B), and mitogen-activated protein kinase (MAPK) [29].

The same samples used for the zymographic evaluations were also subjected to Western blot analysis to verify the amount of the enzyme in the conditioned culture media obtained from the various treatments. In this case, SalB seems to be able to affect the amount of MMP-9 in the conditioned culture medium only if administered at the highest concentration for relatively longer time intervals. This may be due both to a direct effect of SalB in the reduction of gene expression, but also to the ability of the natural compound to interfere with the release of the zymogen from the cytosol to the extracellular environment. For this reason, the MMP-9 transcripts from cells subjected to 48 h treatment with SalB were purified and analyzed in order to highlight any changes in their expression. A significant reduction in MMP-9 expression was effectively noted following the treatment with 50  $\mu$ M SalB. This therefore confirmed SalB tendency to reach the cytoplasm and interfere with the biochemical mechanisms responsible for regulating the gene expression. In this regard, Lin et al. [27] discussed the ability of SalB to inhibit MMP-2 and MMP-9 expression in LPS-stimulated human aortic smooth muscle cells (HASMCs) advancing the hypothesis of a mechanism based on the suppression of JNK and ERK phosphorylation. This is the first time, in our knowledge, that this aspect is highlighted in invasive tumor cells. Therefore, the specific biochemical mechanisms involved require further and more specific evaluations.

## 4. Materials and Methods

### 4.1. Reagents

The Salvianolic acid B (SalB), dimethyl sulfoxide (DMSO), MTT [3-(4,5-dimethylthiazol-2-yl)-2,5-diphenyltetrazolium bromide], trypan blue, Triton X-100, Tween 20 and type B gelatin were purchased from Sigma-Aldrich Chemical Co. (Milan, Italy). Dulbecco's modified Eagle's medium (DMEM), foetal bovine serum (FBS), penicillin, streptomycin, glutamine and trypsin were purchased from Euroclone S.p.A. (Milan, Italy). Human recombinant catalytic domain of MMP-9 was obtained from Vinci Biochem S.r.l. (Firenze, Italy). All other chemicals were reagent grade. Stock solution of SalB (50 mM) was prepared in DMSO and stored in the dark at  $-20\text{ }^{\circ}\text{C}$ .

### 4.2. ADME Analysis and Modelling of the Enzyme-Inhibitor Interaction

When the condition of developing a new drug is expected, it is essential to carry out evaluations that can give preliminary information on the compound being studied, with particular regard to absorption, distribution, metabolism and excretion (ADME). For this purpose, we used the web service SwissADME (<http://www.swissadme.ch/index.php>, accessed on 16 November 2022) [30,31] which was made available by the Swiss Institute of Bioinformatics.

The evaluation of the interactions between SalB and MMP-9 was performed by using the web service (SwissDock) developed by the Swiss Institute of Bioinformatics in order to predict the most favorable binding modes that may occur between a target protein and a small molecule. This web tool exploits the docking software EADock DSS [32] and the CHARMM force field method for calculation [33]. As a model was used, the crystal structure of MMP-9 complexed with a reverse hydroxamate inhibitor (PDB code: 1GKC), and the docking clusters related to the most favorable interactions with SalB (ZINC entry: 49538628) were visualized and analyzed by using PyMOL Molecular Graphics System.

### 4.3. Fluorometric Inhibition Assay of MMP-9 Activity

The *in vitro* ability of SalB to influence MMP-9 activity was performed through a fluorometric inhibition assay. For this purpose, we used the recombinant catalytic domain of MMP-9 (CDMMP-9) which represents the 39 kDa active site of the protein (aa 107–457 + NT His Tag). The enzymatic residue was supplied as lyophilized powder which was reconstituted following manufacturer's instructions with pre-chilled 30% glycerol solution to 10 U/ $\mu\text{L}$ . The rapid and sensitive determination of CDMMP-9 proteolytic potential in the presence of increasing concentrations of SalB (from 5  $\mu\text{M}$  to 100  $\mu\text{M}$ ) was evaluated with a spectrofluorimetric method, as previously reported [10]. Briefly, the methodology is based on monitoring the ability of the enzyme to specifically cleave the self-quenched synthetic substrate MOCac-Pro-Leu-Gly-Leu-A2pr(Dnp)-Ala-Arg-NH<sub>2</sub> (Peptide Institute INC, Osaka, Japan).

The apparent Michaelis constant ( $K_M^{\text{app}}$ ) values for the interaction between the enzyme and different SalB concentrations were calculated by using the double reciprocal plots of  $1/V$  versus  $1/[S]$ . Such parameters were then used to draw a secondary plot for the determination of the apparent inhibition constant ( $K_i$ ).

### 4.4. Identification of the Experimental Conditions and Cell Culture

The MDA-MB-231 human breast cancer cells were obtained from the American Type Culture Collection (ATCC) and maintained in exponential growth in DMEM supplemented with 10% heat-inactivated FBS, 100 U/mL penicillin, 100 mg/mL streptomycin and 2 mM glutamine, and kept in a humidified atmosphere with 5% CO<sub>2</sub> at 37  $^{\circ}\text{C}$ . Cellular viability was determined by trypan blue exclusion assay.

The concentration range and the timing of the cellular treatment with the SalB have been defined through the MTT colorimetric approach which measures viable cells by assessing the conversion of MTT into formazan crystals by mitochondrial activity [34]. Exponentially growing cells were plated in 96-well plates and after 24 h, the medium was

replaced with fresh medium and cells were treated with SalB in the range of concentration from 5  $\mu\text{M}$  to 100  $\mu\text{M}$  for 12 h, 24 h, 48 h and 72 h. Negative controls received the same amount of DMSO (in the ratio 1:1000 in the culture medium) used to solubilize the SalB administered in the other wells. At the end of each incubation period, MTT was added to each well at the final concentration of 0.5 mg/mL and incubated at 37 °C for 3 h. The reaction responsible for the formazan release was stopped by the addition of 0.04 N isopropanol, the absorbance was measured at 570 nm in a microplate reader (Biorad, Hercules, CA, USA).

After defining the parameters for cell treatment with SalB, cells were seeded in six well culture dishes at a density of  $5 \times 10^4$  cells/well. After 24 h, the medium was replaced with fresh medium and cells were treated with 5  $\mu\text{M}$  (Sal-5) and 50  $\mu\text{M}$  (Sal-50) of SalB. Control cells (CTR) received DMSO in a concentration equal to that used for the solubilization of Sal-5 and Sal-50. After 24 h and 48 h, conditioned media were collected, aliquoted and stored at  $-20$  °C until analysis.

#### 4.5. Evaluation of Gelatinases Activity by Zymography and Determination of TIMPs Expression by Reverse Zymography

Protein concentration in conditioned media was determined by Bradford protein concentration assay. Volumes of each sample corresponding to 10  $\mu\text{g}$  of total proteins were diluted in a non-reducing sample buffer without heating and resolved by 8% SDS-PAGE containing 0.3 mg/mL type B gelatin. The gels were then incubated for 45 min in a renaturation buffer (50 mM Tris-HCl pH 8.0, containing 2.5% Triton X-100) to remove SDS. Subsequently, a 24 h incubation in the developing buffer (50 mM Tris-HCl pH 8.0, containing 5 mM  $\text{CaCl}_2$ , 200 mM NaCl and 0.02% Brij 35) was performed to allow enzyme renaturation and activity. Gels were then stained in a 0.1% solution of Coomassie Blue R250 in 40% (*v/v*) methanol and 10% (*v/v*) acetic acid. This analysis was preceded by preliminary evaluations, in which the supernatant of HT1080 fibrosarcoma cells was used as a reference standard for both MMP-2 and MMP-9, as recommended by Toth et al. [35]. Furthermore, in order to verify the metallo-protease nature of the activity displayed, were carried out tests in which the incubation of the zymographic gels was performed in a developing buffer in which a chelating agent (EDTA 100 mM) was added (in this condition no degradation of the substrate was found). Quantitative analysis of visualized spots was performed by using ImageJ software [36].

To reveal the presence of TIMPs in collected samples, reverse zymography was performed as previously described with a modification [37]. Briefly, a cell conditioned medium rich in gelatinases able to degrade gelatin during the incubation in the developer buffer was added to the gel. The presence of TIMPs was visualized as dark bands in which the TIMP bound to the enzyme inhibits its gelatinolytic activity.

#### 4.6. Western Blotting Analysis of MMP-9 and TIMP-1

Samples of conditioned media containing 40  $\mu\text{g}$  of total proteins, were mixed with a reducing sample buffer and subjected to 10% SDS-PAGE. Separated proteins were then trans-blotted onto polyvinylidene difluoride (PVDF) transfer membranes. The non-specific protein binding site on membranes was blocked by incubation in a solution containing 5% non-fat dry milk (Biorad, Milan, Italy) in TBS 0.1% Tween 20 (TBS-T) for 1 h, and then incubated overnight at 4 °C with the primary antibodies for human MMP-9 and TIMP-1 diluted in 1% non-fat dry milk in TBS-T. Membranes were then washed in TBS-T, incubated for 1 h with secondary HRP-conjugated antibody diluted in blocking solution, and the immunoreactive bands were detected by inducing a chemiluminescence reaction through the ECL chemiluminescent reagent (GE Healthcare, Little Chalfont, England). Quantitative analysis of immunoreactive spots was performed by using ImageJ software [36].

#### 4.7. RNA Purification and Reverse Transcriptase Polymerase Chain Reaction (RT-PCR)

Total RNA was extracted from treated cells with EUROGOLD Total RNA Mini kit (EuroClone, Milan, Italy) and 1 µg of each sample was subjected to retrotranscriptase reaction and PCR amplification in the same tube using the Hyperscript™ One-step RT-PCR Premix (TEMA RICERCA, Bologna, Italy) and following manufacturer's indications. Expression levels of MMP-9 and TIMP-1 were normalized to the expression levels of the housekeeping β-actin gene. PCR was performed by using the following oligonucleotides: MMP-9 (sense 5'-CGC AGA CAT CGT CAT CCA GT-3', anti-sense 5'-GGA TTG GCG TTG GAA GAT GA-3'), TIMP-1 (sense 5'-CTG TTG TTG CTG TGG CTG ATA-3', antisense 5'-CCG TCC ACA AGC AAT GAG T-3') and β-actin (sense 5'-ATG ATG ATA TCG CCG CGC TCG-3', antisense 5'-GCG CTC GGT GAG GAT CTT CA-3'). The RT-PCR products were resolved by 1.5% agarose gel electrophoresis.

#### 4.8. Statistical Analysis

Data were statistically analyzed by using SigmaPlot 12.0 software (Systat software, Inc., San Jose, CA, USA) for Windows operating system. Differences between means were evaluated by Student's t-test with confidence levels set at 95% ( $p < 0.05$ ) and 99% ( $p < 0.01$ ).

### 5. Conclusions

In the present research, for the first time to our knowledge, the ability of salvianolic acid B, an active compound of *Salviae miltiorrhizae*, to modulate the function of MMP-9 in human MDA-MB-231 breast cancer cells was demonstrated in an in vitro model characterized by a high invasive potential. Particularly, we found a marked tendency of the natural compound to interact with the catalytic domain of MMP-9 with the consequent inhibition of its activity, presumably reducing the ability of the enzyme to interact with the substrate. Furthermore, an inhibitory effect on the enzyme expression was observed. From this point of view, more specific studies will have to be conducted in order to characterize the biochemical mechanisms that oversee this phenomenon.

**Author Contributions:** Conceptualization, A.I. and N.F.; methodology, P.R., P.B., F.M. and G.C.; investigation, A.I. and P.R.; resources, N.F.; data curation, A.I. and G.C.; writing—original draft preparation, A.I.; writing—review and editing, G.M. and N.F.; supervision, G.M. and N.F.; project administration, A.I. and N.F.; funding acquisition, N.F. All authors have read and agreed to the published version of the manuscript.

**Funding:** This research received no external funding.

**Institutional Review Board Statement:** Not applicable.

**Informed Consent Statement:** Not applicable.

**Data Availability Statement:** The datasets used and/or analyzed during the current study are available from the corresponding author on reasonable request.

**Acknowledgments:** Authors are grateful to Dr. Mariolina Angelini for the kind cooperation.

**Conflicts of Interest:** The authors declare no conflict of interest. The funders had no role in the design of the study; in the collection, analyses, or interpretation of data; in the writing of the manuscript; or in the decision to publish the results.

### References

1. Nagase, H.; Visse, R.; Murphy, G. Structure and function of matrix metalloproteinases and TIMPs. *Cardiovasc. Res.* **2006**, *69*, 562–573. [[CrossRef](#)] [[PubMed](#)]
2. Brew, K.; Dinakarandian, D.; Nagase, H. Tissue inhibitors of metalloproteinases: Evolution, structure and function. *Biochim. et Biophys. Acta (BBA) Protein Struct. Mol. Enzym.* **2000**, *1477*, 267–283. [[CrossRef](#)]
3. Klein, T.; Bischoff, R. Physiology and pathophysiology of matrix metalloproteases. *Amino Acids* **2011**, *41*, 271–290. [[CrossRef](#)]
4. Stamenkovic, I. Matrix metalloproteinases in tumor invasion and metastasis. *Semin. Cancer Biol.* **2000**, *10*, 415–433. [[CrossRef](#)] [[PubMed](#)]

5. Merdad, A.; Karim, S.; Schulten, H.J.; Dallol, A.; Buhmeida, A.; Al-Thubaity, F.; Gari, M.A.; Chaudhary, A.G.; Abuzenadah, A.M.; Al-Qahtani, M.H. Expression of matrix metalloproteinases (MMPs) in primary human breast cancer: MMP-9 as a potential biomarker for cancer invasion and metastasis. *Anticancer. Res.* **2014**, *34*, 1355–1366. [[PubMed](#)]
6. Giusti, I.; D'Ascenzo, S.; Millimaggi, D.; Taraboletti, G.; Carta, G.; Franceschini, N.; Pavan, A.; Dolo, V. Cathepsin B mediates the pH-dependent proinvasive activity of tumor-shed microvesicles. *Neoplasia* **2008**, *10*, 481. [[CrossRef](#)] [[PubMed](#)]
7. Nissinen, L.; Kähäri, V.M. Matrix metalloproteinases in inflammation. *Biochim. Biophys. Acta, Gen. Subj.* **2014**, *1840*, 2571–2580. [[CrossRef](#)]
8. Lee, M.; Celenza, G.; Boggess, B.; Blasé, J.; Shi, Q.; Toth, M.; Margarida Bernardo, M.; Wolter, W.R.; Suckow, M.A.; Heseck, D.; et al. A Potent Gelatinase Inhibitor with Anti-Tumor-Invasive Activity and its Metabolic Disposition. *Chem. Biol. Drug Des.* **2009**, *73*, 189–202. [[CrossRef](#)]
9. Jacobsen, J.A.; Jourden, J.L.M.; Miller, M.T.; Cohen, S.M. To bind zinc or not to bind zinc: An examination of innovative approaches to improved metalloproteinase inhibition. *Biochim. Biophys. Acta, Mol. Cell Res.* **2010**, *1803*, 72–94. [[CrossRef](#)]
10. Ianni, A.; Celenza, G.; Franceschini, N. Oxaprozin: A new hope in the modulation of matrix metalloproteinase 9 activity. *Chem. Biol. Drug Des.* **2019**, *93*, 811–817. [[CrossRef](#)] [[PubMed](#)]
11. Huneif, M.A.; Alqahtani, S.M.; Abdulwahab, A.; Almedhesh, S.A.; Mahnashi, M.H.; Riaz, M.; Ur-Rahman, N.; Jan, M.S.; Ullah, F.; Aasim, M.; et al.  $\alpha$ -Glucosidase,  $\alpha$ -Amylase and Antioxidant Evaluations of Isolated Bioactives from Wild Strawberry. *Molecules* **2022**, *27*, 3444. [[CrossRef](#)]
12. Al-Joufi, F.A.; Jan, M.; Zahoor, M.; Nazir, N.; Naz, S.; Talha, M.; Sadiq, A.; Nawaz, A.; Khan, F.A. *Anabasis articulata* (Forssk.) Moq: A Good Source of Phytochemicals with Antibacterial, Antioxidant, and Antidiabetic Potential. *Molecules* **2022**, *27*, 3526. [[CrossRef](#)]
13. Majid, M.; Farhan, A.; Asad, M.I.; Khan, M.R.; Hassan, S.S.U.; Haq, I.U.; Bungau, S. An Extensive Pharmacological Evaluation of New Anti-Cancer Triterpenoid (Nummularic Acid) from *Ipomoea batatas* through In Vitro, In Silico, and In Vivo Studies. *Molecules* **2022**, *27*, 2474. [[CrossRef](#)] [[PubMed](#)]
14. Ende, C.; Gebhardt, R. Inhibition of matrix metalloproteinase-2 and-9 activities by selected flavonoids. *Planta Med.* **2004**, *70*, 1006–1008. [[CrossRef](#)] [[PubMed](#)]
15. Rice-Evans, C. Flavonoids and isoflavones: Absorption, metabolism, and bioactivity. *Free Radic. Biol. Med.* **2004**, *7*, 827–828. [[CrossRef](#)] [[PubMed](#)]
16. Wang, B.Q. *Salvia miltiorrhiza*: Chemical and pharmacological review of a medicinal plant. *J. Med. Plants Res.* **2010**, *4*, 2813–2820.
17. Zhao, G.R.; Zhang, H.M.; Ye, T.X.; Xiang, Z.J.; Yuan, Y.J.; Guo, Z.X.; Zhao, L.B. Characterization of the radical scavenging and antioxidant activities of danshensu and salvianolic acid B. *Food Chem. Toxicol.* **2008**, *46*, 73–81. [[CrossRef](#)]
18. Zhang, H.S.; Wang, S.Q. Salvianolic acid B from *Salvia miltiorrhiza* inhibits tumor necrosis factor- $\alpha$  (TNF- $\alpha$ )-induced MMP-2 upregulation in human aortic smooth muscle cells via suppression of NAD(P)H oxidase-derived reactive oxygen species. *J. Mol. Cell. Cardiol.* **2006**, *41*, 138–148. [[CrossRef](#)]
19. Jiang, B.; Chen, J.; Xu, L.; Gao, Z.; Deng, Y.; Wang, Y.; Xu, F.; Shen, X.; Guo, D.A. Salvianolic acid B functioned as a competitive inhibitor of matrix metalloproteinase-9 and efficiently prevented cardiac remodeling. *BMC Pharmacol.* **2010**, *10*, 10. [[CrossRef](#)]
20. Wang, Y.; Xu, F.; Chen, J.; Shen, X.; Deng, Y.; Xu, L.; Yin, J.; Chen, H.; Teng, F.; Liu, X.; et al. Matrix metalloproteinase-9 induces cardiac fibroblast migration, collagen and cytokine secretion: Inhibition by salvianolic acid B from *Salvia miltiorrhiza*. *Phytomedicine* **2011**, *19*, 13–19. [[CrossRef](#)]
21. Sha, W.; Zhou, Y.; Ling, Z.Q.; Xie, G.; Pang, X.; Wang, P.; Gu, X. Antitumor properties of Salvianolic acid B against triple-negative and hormone receptor-positive breast cancer cells via ceramide-mediated apoptosis. *Oncotarget* **2018**, *9*, 36331. [[CrossRef](#)] [[PubMed](#)]
22. Katary, M.A.; Abdelsayed, R.; Alhashim, A.; Abdelhasib, M.; Elmarakby, A.A. Salvianolic acid B slows the progression of breast cancer cell growth via enhancement of apoptosis and reduction of oxidative stress, inflammation, and angiogenesis. *Int. J. Mol. Sci.* **2019**, *20*, 5653. [[CrossRef](#)] [[PubMed](#)]
23. Varma, M.V.; Sateesh, K.; Panchagnula, R. Functional role of P-glycoprotein in limiting intestinal absorption of drugs: Contribution of passive permeability to P-glycoprotein mediated efflux transport. *Mol. Pharm.* **2005**, *2*, 12–21. [[CrossRef](#)] [[PubMed](#)]
24. Testa, B.; Kraemer, S.D. The Biochemistry of Drug Metabolism—An Introduction. *Chem. Biodivers* **2007**, *4*(3), 257–405. [[CrossRef](#)]
25. Kirchmair, J.; Göller, A.H.; Lang, D.; Kunze, J.; Testa, B.; Wilson, I.D.; Glen, R.C.; Schneider, G. Predicting drug metabolism: Experiment and/or computation? *Nat. Rev. Drug. Discov.* **2015**, *14*, 387–404. [[CrossRef](#)]
26. Liu, Q.; Loo, W.T.; Sze, S.C.W.; Tong, Y. Curcumin inhibits cell proliferation of MDA-MB-231 and BT-483 breast cancer cells mediated by down-regulation of NF $\kappa$ B, cyclinD and MMP-1 transcription. *Phytomedicine* **2009**, *16*, 916–922. [[CrossRef](#)]
27. Lin, S.J.; Lee, I.T.; Chen, Y.H.; Lin, F.Y.; Sheu, L.M.; Ku, H.H.; Shiao, M.S.; Chen, J.W.; Chen, Y.L. Salvianolic acid B attenuates MMP-2 and MMP-9 expression in vivo in apolipoprotein-E-deficient mouse aorta and in vitro in LPS-treated human aortic smooth muscle cells. *J. Cell. Biochem.* **2007**, *100*, 372–384. [[CrossRef](#)]
28. Dai, J.P.; Zhu, D.X.; Sheng, J.T.; Chen, X.X.; Li, W.Z.; Wang, G.F.; Li, K.S.; Su, Y. Inhibition of tanshinone IIA, salvianolic acid A and salvianolic acid B on areca nut extract-induced oral submucous fibrosis in vitro. *Molecules* **2015**, *20*, 6794–6807. [[CrossRef](#)]
29. Cayetano-Salazar, L.; Nava-Tapia, D.A.; Astudillo-Justo, K.D.; Arizmendi-Izazaga, A.; Sotelo-Leyva, C.; Herrera-Martinez, M.; Villegas-Comonfort, S.; Navarro-Tito, N. Flavonoids as regulators of TIMPs expression in cancer: Consequences, opportunities, and challenges. *Life Sci.* **2022**, *308*, 120932. [[CrossRef](#)]

30. Hassan, S.S.U.; Abbas, S.Q.; Ali, F.; Ishaq, M.; Bano, I.; Hassan, M.; Jin, H.Z.; Bungau, S.G. A Comprehensive in silico exploration of pharmacological properties, bioactivities, molecular docking, and anticancer potential of vieloplain F from *Xylopia vielana* Targeting B-Raf Kinase. *Molecules* **2022**, *27*, 917. [[CrossRef](#)]
31. Daina, A.; Michielin, O.; Zoete, V. SwissADME: A free web tool to evaluate pharmacokinetics, drug-likeness and medicinal chemistry friendliness of small molecules. *Sci. Rep.* **2017**, *7*, 1–13. [[CrossRef](#)]
32. Grosdidier, A.; Zoete, V.; Michielin, O. SwissDock, a protein-small molecule docking web service based on EADock DSS. *Nucleic Acids Res.* **2011**, *39*, 270–277. [[CrossRef](#)] [[PubMed](#)]
33. Vanommeslaeghe, K.; Hatcher, E.; Acharya, C.; Kundu, S.; Zhong, S. CHARMM general force field: A force field for drug-like molecules compatible with the CHARMM all-atom additive biological force fields. *J. Comput. Chem.* **2010**, *31*, 671–690. [[CrossRef](#)] [[PubMed](#)]
34. Mosmann, T. Rapid colorimetric assay for cellular growth and survival: Application to proliferation and cytotoxicity assays. *J. Immunol. Met.* **1983**, *65*, 55–63. [[CrossRef](#)] [[PubMed](#)]
35. Toth, M.; Sohail, A.; Fridman, R. Assessment of gelatinases (MMP-2 and MMP-9) by gelatin zymography. In *Metastasis Research Protocols*; Humana Press: Totowa, NJ, USA, 2012; pp. 121–135. [[CrossRef](#)]
36. Rasband, W.S. *ImageJ software*; National Institutes of Health: Bethesda, MD, USA, 2012.
37. Hawkes, S.P.; Li, H.; Taniguchi, G.T. Zymography and reverse zymography for detecting MMPs and TIMPs. In *Matrix Metalloproteinase Protocols*; Humana Press: Totowa, NJ., USA, 2010; pp. 257–269. [[CrossRef](#)]

Review

# Recent Advances in Natural Polyphenol Research

Irene Dini \* and Lucia Grumetto \*

Department of Pharmacy, University of Naples Federico II, Via Domenico Montesano 49, 80131 Napoli, Italy

\* Correspondence: irdini@unina.it (I.D.); lucia.grumetto@unina.it (L.G.)

**Abstract:** Polyphenols are secondary metabolites produced by plants, which contribute to the plant's defense against abiotic stress conditions (e.g., UV radiation and precipitation), the aggression of herbivores, and plant pathogens. Epidemiological studies suggest that long-term consumption of plant polyphenols protects against cardiovascular disease, cancer, osteoporosis, diabetes, and neurodegenerative diseases. Their structural diversity has fascinated and confronted analytical chemists on how to carry out unambiguous identification, exhaustive recovery from plants and organic waste, and define their nutritional and biological potential. The food, cosmetic, and pharmaceutical industries employ polyphenols from fruits and vegetables to produce additives, additional foods, and supplements. In some cases, nanocarriers have been used to protect polyphenols during food processing, to solve the issues related to low water solubility, to transport them to the site of action, and improve their bioavailability. This review summarizes the structure-bioactivity relationships, processing parameters that impact polyphenol stability and bioavailability, the research progress in nanocarrier delivery, and the most innovative methodologies for the exhaustive recovery of polyphenols from plant and agri-waste materials.

**Keywords:** antioxidant; circular economy; agri-food wastes; sustainability; flavonoids; polyphenols bioavailability; polyphenols activity; functional food; nutraceuticals; cosmeceuticals; nano-delivery; bioavailability; health

**Citation:** Dini, I.; Grumetto, L.Recent Advances in Natural Polyphenol Research. *Molecules* **2022**, *27*, 8777. <https://doi.org/10.3390/molecules27248777>

Academic Editor: Nour Eddine Es-Safi

Received: 12 November 2022

Accepted: 9 December 2022

Published: 11 December 2022

**Publisher's Note:** MDPI stays neutral with regard to jurisdictional claims in published maps and institutional affiliations.



**Copyright:** © 2022 by the authors. Licensee MDPI, Basel, Switzerland. This article is an open access article distributed under the terms and conditions of the Creative Commons Attribution (CC BY) license (<https://creativecommons.org/licenses/by/4.0/>).

## 1. Introduction

Natural polyphenols are secondary metabolites of plants, vegetables, cereals, fruits, coffee, tea, and other plants. The exceptional functionality and biocompatibility of the polyphenols have stimulated the interest of researchers to use them as building blocks in functional foods, supplements, cosmetics, and drugs [1,2]. They have a phenolic ring, a basic monomer responsible for the protective action against oxidative injury [3]. Polyphenolic compounds can moderate oxidative stress and prevent or even inhibit oxidation by chelating iron and scavenging reactive radicals [4,5]. Dietary polyphenols can act as antioxidants, anti-inflammatory, and antiallergic compounds, decrease and prevent age-related diseases, can help against cardiovascular events (i.e., through their hypocholesterolemic, anti-thrombotic, antihypertensive, and anti-atherogenic), cancer, osteoporosis, diabetes, and neurodegenerative diseases [6]. The dietary polyphenols' bioavailability depends on the chemical and physical characteristics of the natural matrix that contains them, the stability during the digestive process, the intestinal enzymes' metabolization, and intestinal microbiota [7]. The gut microflora can modify the polyphenols' bioactivity and bioavailability [8]. Their bioaccessibility can be affected by preservation and processing methods, the interaction with the matrix components, and the fluids and enzymes secreted during digestion [9]. Physical, chemical, and enzymatic treatments can alter their properties. The preservation and processing can determine damage to the native polyphenol molecules and the production of new "process-derived" compounds [10]. Nanodelivery technology can improve polyphenols' absorption, bioavailability, functional quality, and performance [11–15].



This review summarizes the natural polyphenols classes, the extraction and methods performed to isolate them from natural sources and agro-waste, the factors that affect their bioavailability, and the application and development of nanodelivery systems.

## 2. Polyphenols in Nature

Polyphenols are involved in plant defense against pathogens and ultraviolet radiation [16]. The plants' outer layers contain higher phenolics [17]. Insoluble phenolics are in cell walls, while soluble phenolics are in the plant cell vacuoles [18]. The degree of ripeness during harvest time, pedoclimatic conditions, infections, processing, and storage can affect the polyphenolic content [19]. The phenolic acids (e.g., derivatives of cinnamic acid and benzoic acid), flavonoids (e.g., flavonols, flavanones, flavones, flavanols, isoflavones, and anthocyanins), lignans, and stilbenes are the most naturally occurring classes of compounds (Figure 1). The shikimate pathway produces the phenolic acids. The phenylpropanoids pathway forms lignans, lignins, flavonoids, and stilbenes [20,21]. The biosynthesis of complex polyphenols is linked to primary metabolism: the flavonoids' ring B and the chromane ring originate from the amino acid phenylalanine, obtained from the shikimate pathway, whereas ring A is formed from three malonyl-CoA units added through sequential decarboxylation condensation reactions [22]. In food, polyphenolic compounds can impact astringency, bitterness, flavor, color, and oxidative stability [19].

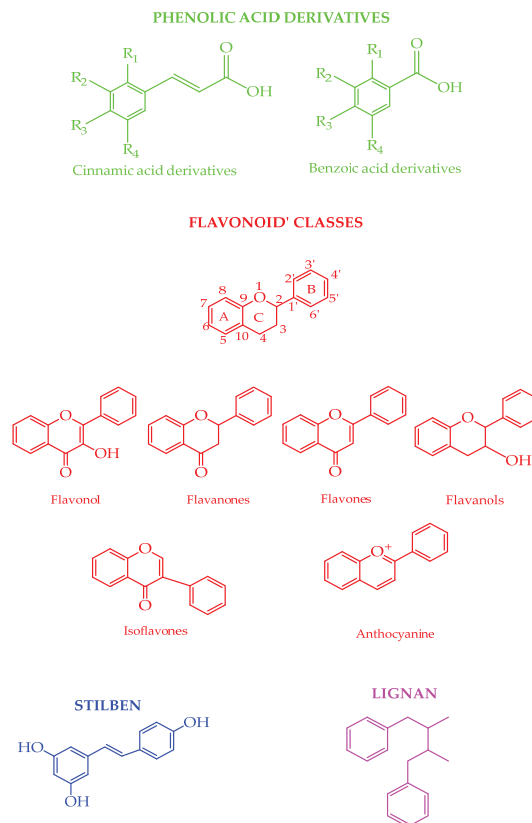


**Figure 1.** Chemical structures of the different polyphenol classes. The colors indicate the sub-class. The numbers indicate the positions in the nomenclature.

### 3. Polyphenols Bioavailability

There is no relation between the concentration of polyphenols in food and their bioavailability in the human body. The polyphenols, after ingestion, pass through the gastrointestinal epithelium and enter the circulatory vessels to reach the site of action. In food, polyphenols can exist as aglycon, glycosides, esters, or polymers.

The polyphenols' chemical structure limits the rate, absorption, and metabolites circulating in the plasma. The polyphenolic compounds with hydroxyl groups can be modified by methylation, glucuronidation, or sulfation enzymatic reactions. The 5–10% of total polyphenolic compounds may be metabolized in the small intestine. The rest of the polyphenols accumulate in the large intestine and are evacuated in the feces [23]. The conjugated polyphenols must be hydrolyzed by colonic microflora or intestinal enzymes (i.e.,  $\beta$ -glucosidases and lactase-phlorizin hydrolase) before absorption [24]. During the absorption process, they are transformed into oligomeric phenols by gastric acid in the stomach, and glycosidic polyphenols are cleaved by cytosolic glucosidase and lactase in the small intestine into aglycon and glycoside(s) (e.g., glucose, xylose, and galactose) radicals [25]. Finally, intestinal bacterial enzymes can metabolize the remaining aglycone fraction. In the intestinal and colonic epithelium, polyphenols can be involved in conjugation reactions with methyl, glucuronide, or sulfate groups, making the identification of the metabolites in the blood and tissue complex [26]. The glycosides of quercetin and the isoflavones (genistein and daidzein) are not recovered in plasma or urine [27–29]. Instead, anthocyanins glycosides are the most representative circulating forms [30,31]. Experimental studies showed that quercetin, without glycosides, is absorbed at the gastric level [32], anthocyanins in the stomach [33,34], and proanthocyanidins [33,35] and hydroxycinnamic acids are absorbed by the small intestine [36]. The remaining polyphenols are hydrolyzed in the colon by microflora enzymes into aglycones that are metabolized into benzoic acid derivatives [37,38].

The polyphenols' digestibility affects their biological properties [39]. Soluble polyphenols have more evident responses during gastrointestinal digestion since the cell wall does not protect them. Unfortunately, human enzymes cannot digest some cell wall materials.

The flavonoids linked to other macromolecules cannot exert their beneficial actions [37]. The heat and pressure application (processing parameters) can facilitate the disruption of the cell wall and their release improving their bioactivity [38].

The pH and number of OH groups in benzene rings can affect phenolic stability. Conjugated nonphenolic aromatic acids, such as trans-cinnamic acid, are stable at high pH. The aromatic acids with a single OH group (e.g., ferulic acid) are stable at high pH because they do not form quinone oxidation products. The aromatic acids, with two phenolic OH groups (e.g., caffeic acid) or three (e.g., gallic acid), are unstable at pH 7–11. The changes are ascribable to the two adjacent phenolic OH groups attached to the benzene ring. Flavonoid molecules (e.g., rutin) that have a wholly conjugated aromatic structure are influenced by pH because the spatial arrangement between the  $\pi$ -electron system and an OH group controls the extent of  $\pi$ -orbital overlap and susceptibilities to the chemical change. The flavonoids in which the first benzene ring is located in the meta-position (e.g., catechin, epicatechin) do not have planar structures. Therefore, the  $\pi$ -electrons of the two benzene rings cannot cooperate via conjugation and are less susceptible at high pH [40,41].

In plant-based food, polyphenols and cell wall polysaccharides co-exist, and their affinity may influence foods' physicochemical and nutritional properties during processing and digestion. The affinity of cell wall polysaccharides with polyphenols depends on their structures, concentrations, temperature, pH, ionic strength, and the presence of proteins [42].

The enzyme concentrations, solubility, pH, digestion time [43], and processing methods (e.g., washing, refrigerating, fermentation, grain milling, roasting, juicing, blanching, and thermal processing) impact polyphenols' bioaccessibility and absorption [9].

Cooking and freezing processes positively impact the polyphenols' bioaccessibility since they soften the cell wall. The cooking medium also influences their bioaccessibility [44,45].

Pasteurization affects the polyphenols' bioaccessibility in the function of the heat treatment intensity, steps involved in processing, and type of food, decreasing the adverse processing effects on small bioactive compounds and even increasing polyphenols content [46]. Pasteurization can enhance food polyphenols extraction since the temperature softens the cell wall [47].

Finally, the interactions between macronutrients, micronutrients, and other phytochemicals, in finished products may also impact polyphenols' stability [48].

#### 4. Polyphenols & Microbiota

Gut microbiota can break the flavonoid C-ring in different positions, producing simple phenolics from the A and B rings. Most of these metabolites are acid or aldehyde phenolics with 1, 2, and (or) 3 hydroxyl and methyl ester radicals. Non-flavonoid phenolics (e.g., hydrolyzable tannins, stilbenes, lignans, and hydroxy-benzoic acid derivatives) are absorbed in the small intestine based on their chemical complexity. The gut bacteria can hydrolyze the ester bonds in tannins, dehydroxylate, and decarboxylate, the gallic acid [49], and reduce the resveratrol and its precursors [50].

The role of polyphenols and their metabolites on the gut microbiota is not elucidated. They probably have a prebiotic-like effect [51], since they can modulate the gut microbial profile. [52,53].

The polyphenols' prebiotic effect is associated mainly with the promotion of probiotics (e.g., Bifidobacteriaceae and Lactobacillaceae) or the inhibition of pathogenic bacteria (i.e., *E. coli*, *Clostridium perfringens*, and *Helicobacter pylori* [52]) resulting in reduced proinflammatory immune response and decreased risk of colon cancer, gastroenteritis, inflammatory bowel disease, and metabolic syndrome [54,55].

Some polyphenols prevent bacterial growth, binding the cell membranes in a concentration-dependent manner. Catechins can change the microbial (i.e., *Bordetella bronchiseptica*, *Klebsiella pneumoniae*, *E. coli*, *Pseudomonas aeruginosa*, *Serratia marcescens*, *Bacillus subtilis* *Salmonella cholerae*s, and *Staphylococcus aureus*) cell membrane permeability by producing H<sub>2</sub>O<sub>2</sub> [56]. In Gram-positive bacteria, polyphenolic compounds can delay the oligopeptides autoinducers that sense the bacterial quorum sensing. In Gram-negative bacteria, they can prevent the bacteria-acylated homoserine lactones autoinducers [57].

#### 5. Effects of the Food-Processing Techniques on Polyphenol Levels and Bioavailability

The heat treatments (e.g., boiling, steaming, frying, stewing, baking, roasting, ovens, steam, and microwave) and the transformation food processing (e.g., roasting, toasting, drying, pasteurization, canning, and sterilization), can affect the polyphenols' bioavailability. The heat breaks cell walls, mobilizes the phenolic compounds, improves their availability, enhances their oxidation processes, and degrades them based on their thermostability. Domestic cooking and industrial thermal processes can cause losses in polyphenols, with significant variability depending on the nature of food matrices [58].

Boiling produces the most harmful polyphenol composition changes. Instead, steaming and frying can preserve them since the polar media (water) can extract higher levels of polyphenol than nonpolar media (oil) [59]. During boiling, heat decomposes the tissues, and the phenolics leak into the water [60]. Water volume can impact the polyphenol alteration during the heat process: small water volumes produce lower phenolic extraction than larger volumes [61]. Diverse boiling times produce different polyphenol profiles in foods, and a long time can cause more severe damage than a short one [62]. The type of heat treatment affects the polyphenol bioavailability. Steaming is the best heat method to preserve phenolic fractions since they are indirectly exposed to water [63]. The form in which phenolics are present also affects bioavailability [64].

Canning, a process employed to produce sterilized and microbiologically safe food products by applying heat treatment, can decrease phenolic compound levels [65] because they migrate into the surrounding medium [66].

Drying, the preservation process that aims to decrease the moisture content of food by using heat and mass transfer, can affect the phenolic levels in the function of the temperature regime. Freeze-drying is the most efficient method to preserve phenolic content, while hot-air-drying is the least. The vast variety of chemical polyphenol classes also influences the variability in the effects caused by drying [67]. Oven-dried processes produce higher levels of bioaccessible phenolics than other drying processes [68–70]. Slow freezing enhances the bioavailability of the phenolic compounds since it forms ice crystals that favor the polyphenols extraction, oxidation, and degradation, during digestion [71].

Peeling fruits and vegetables determines the loss of high amounts of bioactive compounds since they are contained in the peel and external parts of the plants at higher levels than other parts [72]. Grinding, the technique that reduces the size of solid particles using mechanical forces, enhances the polyphenols extractions as a function of the particle size [73]. The ultrasound treatments pulsed electric field, high-pressure, and pulsed-light processing enhance polyphenols digestion, bioaccessibility, and bioavailability [74].

## 6. Polyphenol Biological Activities

Epidemiological studies have shown an inverse association between a polyphenolic-rich diet and the risk of chronic human diseases. Polyphenolic compound-rich foods and beverages can have antioxidant, anti-inflammatory, anticancer, and anti-aging properties and reduce the risk of degenerative diseases such as cardiovascular, diabetes mellitus, and neuronal diseases.

### 6.1. Antioxidant Activity

Experimental evidence showed that polyphenols protect cell constituents against oxidative damage and degenerative diseases associated with oxidative stress [75]. The polyphenol-rich foods can improve plasma antioxidant capacity by scavenging radical species (e.g., ROS, RNS) or repressing radicals' formation by inhibiting the activities of the oxido-reductive enzymes' and/or chelating the metals that intercept free radical production. Their phenolic groups can accept an electron to form phenoxy radicals, interrupting chain oxidation reactions, and conjugated aromatic systems can delocalize an unpaired electron [76]. Polyphenols reduce the oxidation of lipids and other molecules by donating hydrogen to radicals (R). The resonance makes PO· (phenoxy radical) relatively stable (new chain reactions are not started) and acts as terminators of the propagation route when reacting with other free radicals (Figure 2).

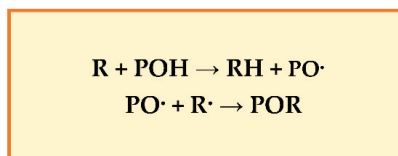


Figure 2. Reactions between lipids and phenols.

The reduction activity of phenolic acids and their derivatives depends on the free hydroxyl groups in the molecule [77]. The hydroxycinnamic acids show better antioxidant activity than hydroxybenzoic acid equivalents due to the aryloxy-radical stabilizing effect of the  $-\text{CH}=\text{CH}-\text{COOH}$  linked to the phenyl ring by resonance [78]. The phenolic acids' antioxidant activity of free, esterified, glycosylated, and nonglycosylated phenolics is mainly ascribed to radical scavenging via the hydrogen atom donation mechanism [78,79].

The flavonoids' radical scavenging depends on the ortho-dihydroxy structure in the B ring, which allows higher stability to the radical form and participates in electron delocalization of the 2,3-double bond with a 4-oxo function in the C ring [77].

The chemical electron deficiency of anthocyanins is particularly reactive toward ROS/RNS.

The polyphenolic compounds with dihydroxy groups prevent metals-induced free radical formation by conjugating the transition metals that interact with hydrogen peroxide ( $\text{H}_2\text{O}_2$ ) through the Fenton reaction to form hydroxyl radicals ( $\cdot\text{OH}$ ).

Phenolic compounds with catecholate and gallate groups can stop metal-induced oxygen radicals by improving metal ion autoxidation or forming an inactive complex with weaker interaction [79].

The metal ions can attack the flavonoids into positions 3' and 4' (B ring), 3 and 4, 3 and 5, 4-keto and 3-hydroxy, and 4-keto and 5-hydroxy (C ring) [80].

Moreover, polyphenols can improve cellular antioxidant activity by regulating Nrf2, which controls some detoxifying enzymes (SOD, GSH, GPx1, NADP(H) quinone oxidoreductase, HO-1, and GST) [77]. Finally, polyphenols can influence microRNAs [81].

MicroRNAs are a class of small, endogenous, noncoding RNAs. Some microRNAs (i.e., miR-21, miR-125, and miR-146) are involved in vascular inflammation and diseases [82–84]. Dietary polyphenols can influence the microRNAs' expression and biogenesis [30]. For example, curcuminoids can act as anti-atherosclerosis agents by upregulating miR-126 expression [85]. Resveratrol can act as a cardioprotective molecule by improving the mRNA activating SIRT1, and enhancing the SOD' levels [86–89].

Gallic acid can decelerate atherosclerosis progression by upregulating miR-145 and downregulating miR-21 expression [90].

Under certain conditions, the polyphenolic compounds can initiate an autoxidation process and perform as prooxidants. In these cases, the phenoxy radicals can interact with oxygen to make quinones and superoxide anions [91]. pH, high concentrations of transition metal ions, and oxygen molecules can induce the autoxidation of polyphenols [92]. Quercetin and gallic acid can have prooxidant activity; instead, the hydrolyzable tannins have little or no prooxidant activity [93].

### 6.2. Anti-Inflammatory Activity

Plant polyphenols can decrease the effect of the cytokine, affecting their receptors or reducing their secretion processes [94].

Phenolic compounds can suppress the binding of proinflammatory mediators, control eicosanoid synthesis, prevent stimulated resistant units, and impede the activity of COX-2 and NO synthase, acting on NF- $\kappa$ B [95]. Some phenolic acids, such as rosmarinic acid and isosalvianolic acid, can reduce the production of IL-6, TNF- $\alpha$ , and IL-1 $\beta$  at the gene and protein levels [30].

The catechols' enzymatic activity depends on the structure of the B ring and needs nucleophilic additions [96]. The procyanidins decrease the concentrations of NO, prostaglandin E2, and ROS [97].

The flavonoids (e.g., flavones) regulate IL-6 in the blood [98]. The flavonoids' anti-inflammatory mechanism is related to the unsaturation in the C ring that affects the strength of binding interactions by resonance [99].

### 6.3. Anticancer Activity

Cancer development consists of initiation, promotion, progression, invasion, and metastasis [100]. Genetic mutations occur when DNA damage is not repaired, and a clone of mutated cells is reproduced during mitosis. Tumor promotion is a reversible and long-term process in which a selective clonal expansion of the cells forms a population of aggressively proliferating multi-cellular cells (pre-malignant tumor). Clonal expansion determines the development of the pre-malignant cells into tumors (tumor progression phase). Finally, some tumor cells may be cut off from the primary tumor mass, migrate toward blood vessels or lymphatic vessels and produce a second lesion (invasion and metastasis phases). The natural phenolic compounds can induce cell cycle arrest at G1, S, S-G2, and G2 phases by down-regulating cyclins and cyclins-dependent kinases or producing the expression of p21, p53, and p27 genes [80].

Polyphenols can act against tumor initiation and promotion, changing the redox status and affecting essential cellular functions (i.e., cell cycle, apoptosis, angiogenesis, inflammation, invasion, and metastasis) [101]. Oxidative damage can cause cancer since ROSs can damage the DNA and affect cell replication and signal transduction [102].

The flavonoid anticancer effects are related to their antioxidant and pro-oxidant activities [103,104]. The flavonol kaempferol can induce apoptosis and arrest in the S-phase of cancerous cells by modulating ROS levels [105]. When it acts as pro-oxidants it decreases NF- $\kappa$ B levels and produces cyclooxygenase-2 (COX) overexpression, inducing apoptosis, and cell-cycle arrest [106].

Some flavonoids and resveratrol can affect the procarcinogens' activation by impeding phase I metabolizing enzymes (e.g., cytochrome P450) [107–110]. They can help carcinogens' detoxification and removal inducing the phase II metabolizing enzymes (e.g., glutathione S-transferase, UDP-glucuronyl-transferase, and NAD(P)H quinone oxidoreductase) [111].

The polyphenols can produce apoptosis-inducing cell cycle arrest inhibiting the extracellular regulated kinase, c-Jun N-terminal kinase, and P38 mitogen-activated protein kinase pathway, transcription factors, NF- $\kappa$ B, activator protein-1 (AP1), protein kinase C (PKC), and growth factor-mediated pathways. The apigenin inhibits the growth of human thyroid carcinoma cells, probably by decreasing the phosphorylation of MAPK and by activating the protein kinases, and scavenging H<sub>2</sub>O<sub>2</sub> [112].

The 3,4 dihydroxybenzoic acid stimulates apoptosis, in human gastric carcinoma cells, by ROS overproduction which can activate JNK/p38 MAPKs [113].

The polyphenolic compounds can negatively affect some factors involved in the inflammatory processes, such as the NF- $\kappa$ B, proinflammatory cytokines release, COX-2, lipoxygenases, inducible nitric oxide synthase, and MAPK-mediated pathway [80]. For example, Epigallocatechin gallate can block NF- $\kappa$ B activation in human epithelial cells and downregulate the expression of inducible nitric oxide synthase and nitric oxide production in macrophages [114]. Finally, the kaempferol can counteract malignant cell invasion and metastasis, down-regulating the matrix metalloproteinases (MMP-2 and MMP-9), urokinase-plasminogen activator (uPA), and uPA receptor expression [115,116].

#### 6.4. Cardiovascular Protective Activity

Cardiovascular (CVD) pathologies are the primary cause of morbidity and mortality (ischemic heart disease and stroke contribute 85%) [117]. Oxidative stress and inflammatory processes are considered promoters of endothelial dysfunction [118,119]. Polyphenols have antioxidant, anti-inflammatory abilities and can modulate lipid metabolism [120]. They (mainly quercetin and resveratrol) can decrease LDL oxidation [121], cholesterol synthesis, improve LDL receptor expression and activity [122,123], and the cholesterol transporters expression [124]. The anthocyanins and resveratrol can improve fecal cholesterol elimination [125,126] and decrease the triglyceride plasma level, decreasing the apolipoprotein B48 and apolipoprotein B100 production in the liver and intestine [127] or the lipoprotein lipase expression [128]. Flavonoids can also reduce blood pressure ameliorating flow-mediated dilation in humans (by improving the NO synthase activity) [129,130] and influencing the renin-angiotensin system [131,132]. Moreover, they can prevent platelet aggregation, decreasing the activity of cyclooxygenase 1, and thromboxane A2 that act as a vasoconstrictor and platelet aggregation's inducer, respectively [133]. Finally, the polyphenols' prebiotic-like activity can account for the amelioration of markers of CVD [124].

#### 6.5. Antidiabetic Activity

There are two main types of diabetes (diabetes-1 and diabetes-2). Diabetes type-2 or diabetes mellitus is due to damage in glucose metabolism and advancing insulin resistance that leads to hyperglycemia. The leading causes of hyperglycemia are dietary carbohydrates' digestion and absorption, glycogen storage reduction,  $\beta$ -cell dysfunction, peripheral tissue insulin resistance, deficiency in insulin signaling pathways, and improved gluconeogenesis and production of hepatic glucose [134]. Polyphenols can decrease the intestinal absorption

of carbohydrates, control the enzymes that regulate glucose metabolism, and increase the  $\beta$ -cell functionality, insulin secretion, and the anti-inflammatory and antioxidant properties of these components (Figure 3).

The phenolic acids, flavonoids, and tannins can regulate the key enzymes responsible for the digestion of carbohydrates ( $\alpha$ -glucosidase and  $\alpha$ -amylase) [135]. The catechin, epicatechins, and chlorogenic, caffeic, ferulic, and tannic acids can decrease the glucose transporters  $\text{Na}^+$ -dependent (SGLT1 and SGLT2) [136]. The coffee phenols, anthocyanin, and curcumin can regulate postprandial glycemia and decrease the progression of glucose intolerance by a simplified insulin response and improved secretion of glucagon-like polypeptide-1 (GLP-1) and glucose-dependent insulinotropic polypeptide (GIP) [137]. Ferulic acid can decrease blood glucose by improving glucokinase activity and glycogen production in the liver [138]. Catechins and epicatechins can decrease hyperglycemia and hepatic glucose output, downregulating the expression of liver glucokinase, and upregulating the glucose-6-phosphatase and phosphoenolpyruvate carboxykinase [139].

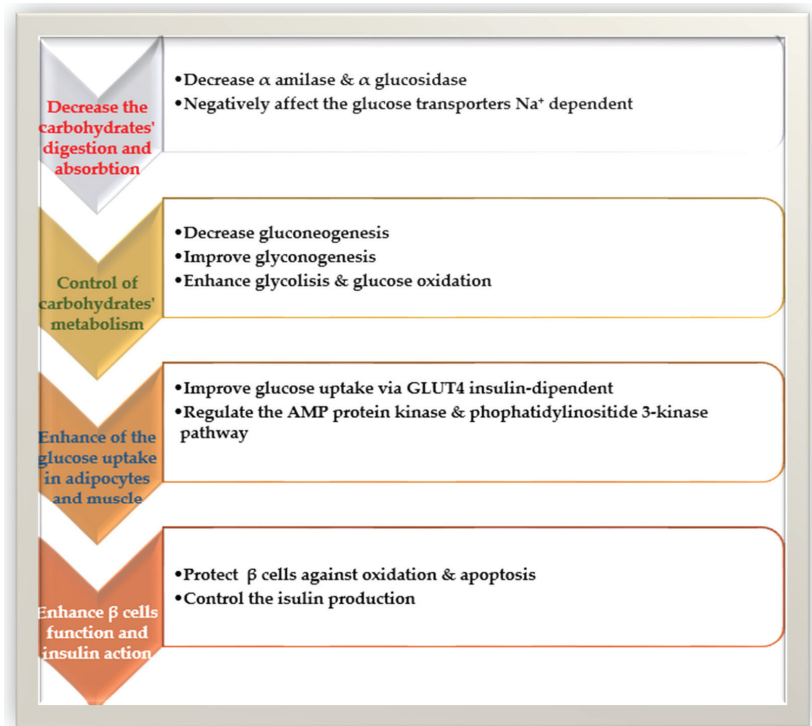


**Figure 3.** The polyphenols' effects on glucose homeostasis and insulin resistance.

#### 6.6. Neurodegenerative Protection

Neurodegenerative diseases are due to the deterioration of neurons' structure and/or function. Reactive oxygen and reactive nitrogen species can determine neuronal cell dysfunction and death. The phenolic compounds can interact with the amino acid residues of acetylcholinesterase's (AChE) active site, making hydrogen bonds and hydrophobic and  $\pi$ - $\pi$  interactions. Multiple hydroxyl groups can improve the inhibition of AChE, increasing the binding capacity [30]. Resveratrol can protect against microglia-dependent  $\beta$ -amyloid toxicity by decreasing the nuclear factor  $\kappa\text{B}$  [140]. Some polyphenols protect against Parkinson's disease by scavenging the neurotoxin N-methyl-4-phenyl-1,2,3,6-tetrahydropyridine (MPTP)-mediated radical formation [141] or decreasing free radicals' formation by chelating iron [142].

### 6.7. Anti-Aging Action

Aging determines detrimental changes in the cells and tissues. The cosmetic industry constantly strives in product development and reformulation to meet consumers' preferences. Today, nature-derived products are in demand on the market. Some botanical preparations that contain polyphenols (e.g., flavonoids, phenolic acids, and stilbenes) are employed in the composition of anti-aging products [143]. Free radicals and oxidative stress are the major contributors to aging damage. The phenolic hydroxyl groups on polyphenol molecules can scavenge ROS [144]. The polyphenolic compounds can regulate the production of oxidase enzymes (sodium oxide dismutase 1 in the cytosol, sodium oxide dismutase 2 in the mitochondria), and endogenous antioxidants [145–149] can improve the transcriptional factor Nrf2 DNA-binding activity and regulate protein expression [150–152]. Anti-aging formulations contain botanicals metabolites able to protect DNA, regulate the enzymes' action, decrease inflammation, and alter hormone imbalance [143].

The epigallocatechin-3-gallate in green tea decreases the UVB-induced hydrogen peroxide release from normal epidermal keratinocytes, MAPK phosphorylation, and inflammation by activating NFκB. The flavins in black tea decrease UVB-induced AP-1 induction, prevent UVB-induced phosphatidylinositol 3-kinase activation, decrease the amount of ROS in the skin, and offer photoprotection by reducing local and systemic immunosuppression UVB-induced [153]. Resveratrol is employed to reduce hydrogen peroxide, improve lipid peroxidation, and decrease the levels of COX-2 and ornithine decarboxylase. Moreover, it can decrease UVA-induced oxidative stress in human keratinocytes since it controls the Keap1-a protein that acts on Nrf2 [153]. Curcuminoids (found in Turmeric spice) can decrease inflammation by inhibiting the MAPK and NFκB signaling pathways and decreasing nitric oxide levels and COX2. Moreover, in keratinocytes and fibroblasts, curcuminoids can decrease UVB-induced TNF mRNA expression and matrix metalloproteinase-1 expression [154].

### 6.8. Antiallergic Action

Allergic diseases happen when an organism becomes sensitive to an innocuous allergen and releases many allergy-related intermediaries. Polyphenols limit the production of IgE, the release of allergic mediators, and allergy symptoms. Polyphenols can control hypersensitivity by regulating oxidation and interacting with inflammatory mediators [155]. Catechins can decrease Th2 cytokine production and T cell activation and proliferation. Caffeic, chlorogenic, and ferulic acids can irreversibly bind peanut allergens (Ara h1 and Ara h2), reducing their allergenicity [156]. Punicalagin, phloridzin, and rutin can improve the growth of probiotics such as *Lactobacillus* and *Bifidobacterium*, which positively impact food allergies [157].

### 6.9. Antiosteoporotic Action

Osteoporosis causes the loss of bone mineral density, decreased bone mass, and microstructural deterioration. Flavonoids and stilbenes can improve osteogenesis by controlling the bone morphogenetic protein, NF-κB, IGF, and MAPK, and can inhibit the osteoclastogenesis pathways through epigenetic regulations. They can activate SIRT-1 (histone deacetylase) and modify the NAD<sup>+</sup>/NADH ratio [158–160].

### 6.10. Antimicrobial Action

Some plant extracts rich in polyphenols can decrease the growth of fungi and bacteria (i.e., *Listeria monocytogenes*, *Salmonella* spp., and *Escherichia coli*) [161,162], minimize the exposure of humans to resistant bacteria [163], and can have a synergic action with other antimicrobials. These findings have suggested a potential use of polyphenol-rich extracts as food preservatives and in the pharmaceutical industry to improve efficacy and decrease antibiotic side effects, such as repressing antibiotic-resistant bacteria [164]. The polyphenol-rich extracts can be placed on the food surface by spraying, dipping, brushing, or mixing with other ingredients [165]. Unfortunately, in some cases, the interaction with



food components can cause a lack of antimicrobial efficacy. Therefore, it was thought to encapsulate them in carriers to increase their distribution in the food and reduce contact with food matrix molecules that reduce their effectiveness [166]. The mechanisms of antibacterial action are not yet entirely deciphered. However, it is known that many sites of action at the cellular level are involved. Polyphenols can modify the cell membrane permeability, destroy the cell wall integrity and change intracellular functions by binding some enzymes [167].

### 7. Polyphenols Potentialities in the Nutraceutical Era

Today, consumers include a high level of bioactive compounds in their standard diet, preferably derived from natural sources such as plants and fruits, in the hope of giving more life to the years by preventing disabling pathologies that decrease the skills that allow living life in all its manifestations [168]. Food and pharmaceutical companies develop nutraceutical foods and supplements that contain botanical extracts and metabolites alone or combined with other ingredients [169–171].

Numerous studies strongly suggested that including polyphenols or polyphenol-rich extracts in supplements or foods may protect the body tissues against oxidative stress and aging [172,173].

The primary issue in using plant extracts is that fungi, which can produce toxins, can contaminate the extracts (e.g., *Aspergillus* section *Nigri* that produces Ochratoxin A, a carcinogenic, teratogenic, nephrotoxic, neurotoxic, and immunotoxic toxin) [174]. The research should implement efforts to develop analytical controls that safeguard consumer safety.

### 8. Polyphenols Extraction

Extraction plays a pivotal role in the purification of polyphenols from foodstuffs. Extraction techniques can employ traditional or “conventional” such as percolation, maceration, and Soxhlet extraction, and modern methods, such as ultrasound or microwave, the latter is most extensively used (Figure 4). In both cases, extraction efficiency depends on various factors such as the nature of the solvent, solvent–solid ratio, temperature, and particle size. Polyphenol can be extracted from fresh, frozen, or dried plant samples. The extracts can be added to an organic solvent, such as methanol or ethanol, with low viscosity to accelerate mass transfer [175]. Before extraction, the pretreatment of the plant matrices (e.g., cleaning, washing, milling, grinding, drying, homogenizing) is crucial.

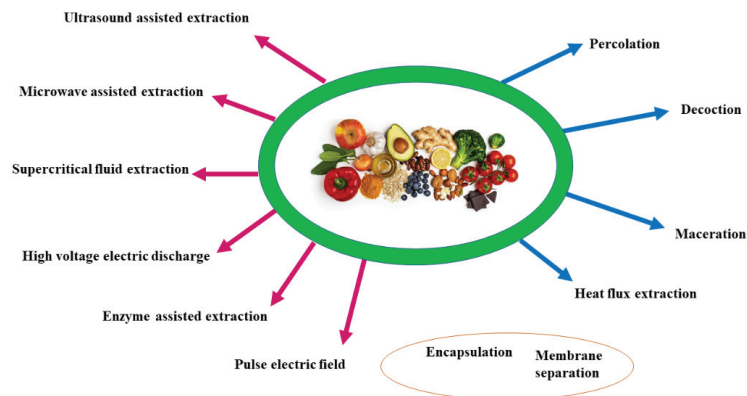


**Figure 4.** The polyphenols’ traditional and modern extraction methods. Blue arrows: traditional extraction methods; red arrows: modern methods; in the orange circle: techniques used to improve polyphenol management.

Percolation extraction uses water as a solvent. It takes a long time to obtain the pure extract to be concentrated [176].

The maceration is a solid-liquid extraction method using different solvents depending on the target compounds' physical and chemical properties. It has low efficiency and extraction yield and employs a large volume of solvents compared to non-conventional techniques such as ultrasound-assisted extraction (UAE) [177]. A higher ratio of solid/solvent increases polyphenols recovery [178].

Decoction extracts plant materials by boiling. It is inefficient for heat and light-sensitive compounds [179]. The decoction of Citrus fruits produces by-products of Citrus peels with high concentration levels of polyphenol fraction [180].

Heat reflux extraction is a solid-liquid extraction method performed with repeated solvent evaporation and condensation at a constant temperature. It requires less extraction time and solvent than percolation or maceration and allows for a greater extraction yield [181]. Polyphenols from wastes of *Vitis vinifera* were extracted by Moldovan et al. by using heat reflux extraction [182].

The solid-phase extraction (SPE) method is considered quick and easy to extract polyphenols from vegetable oils. According to the experimental needs, different stationary phases were used (e.g., C8 cartridges, octadecyl C18, diol-bonded phase cartridges, amino-phase cartridges, and octadecyl C18EC) [6]. The non-conventional techniques employ supercritical fluid, high-voltage electric discharge, and enzyme-assisted extraction. It is preferable to extract the bound polyphenols, also referred to as non-extractable polyphenols (NEP), from plant sources using one or more combinations of modern technology rather than conventional methods. A comparison between traditional and SFE extraction performed on black tea leftovers showed that SPE technique gives the best performance in extraction of phenolic compounds (SPE gives 521 mg GAE/g; traditional gives 283 mg GAE/g) [183].

The extraction with supercritical fluids such as CO<sub>2</sub>, propane, argon, and SF<sub>6</sub> allows for an easy penetration inside plant materials and high solvents. Power-pulsed electric fields (PEF) perform a gentle extraction due to the electroporation of cell membranes. It has been applied to exotic fruits, grapes, and oil crop components [184]. Microwave-assisted extraction (MAE) is an eco-friendly technique with higher efficiency in the recovery of polyphenols from waste products if compared to that of extracts prepared by ultrasound-assisted extraction (UAE) and conventional methods such as maceration [185].

Fruit skins, stem barks, grain seed coats, brans, and pods, are generally considered agro-waste, but they are essential resources for NEP recovery [186–188]. Table 1 reports conventional and non-conventional techniques applied to extract polyphenols from organic waste.

**Table 1.** Extraction of free and bound polyphenols.

Conventional Extraction Methods	Matrix	Extraction Solvent/Membrane Separation Type	Higher % of Recovery Compared to Traditional Method	Reference
Percolation	<i>Vernonia cinerea leaves</i>	Ethanol 60%		[188]
Decoction	<i>Citrus peels</i>	Ethanol 75%		[180]
Heat reflux extraction	<i>Pleioblastus amarus</i>	Ethanol 75%		[189]
Maceration	<i>Citrus peel</i>	Ethanol 80%		[180]
<b>Non- Conventional methods</b>				
Ultrasound assisted	<i>Olive pomace</i>	water	58%	[190]
Microwave assisted	<i>Blackcurrant By-Products</i>	water	25%	[191]
Supercritical fluid	<i>Lees Vitis vinifera grapes</i>	CO <sub>2</sub>	−35%	[192]
High voltage electric discharge	<i>Spent coffee grounds</i>	24% ethanol	20.03%	[193]
Pulse electric field	<i>Vitis vinifera, Sideritis scardica and Crocus sativus</i>	water	44.36–49.15%	[194]
Enzyme assisted	<i>Green yerba mate</i>	water	38.67–52.08%	[195]
Membrane assisted pre-purification	<i>Winery and olive mill wastes</i>	NF270 membrane	95% for polyphenol compounds removal	[196]

## 9. Polyphenol Nano Delivery Systems

The potential of antioxidative and repair pathways decreases with age, causing several adverse effects such as the risk of neurodegenerative diseases such as Parkinson's disease, memory loss, Alzheimer's disease, atherosclerosis, and cancers due to the accumulation of reactive oxygen species. Polyphenols, due to their oxidizing ability, can protect from the damaging effects of ROS. Therefore, they can be used as active compounds in several formulations preventing oxidative stress [197,198]. The loading of polyphenols into lipid nanocarriers (NCs) is an essential tool for increasing bioavailability, reducing degradation, and protecting antioxidant polyphenols' activity. The NCs are biodegradable and have no significant toxicity. The nanoemulsion, liposome, phytosome, solid lipid nanoparticles (SLNs), nanostructured lipid carrier (NLCs), and lipid-polymer hybrid nanoparticles (LPHNs) can encapsulate polyphenols to improve their biophysiological target [199]. Nanoparticles (NPs) have diameters as small as 1–100 nm. They can enhance polyphenols delivery and promote their absorption and bioavailability [200]. The transcellular pathway is a route for the NPs transportation (via endocytosis or macropinocytosis mechanisms) and subjected to the degradative microenvironment of the cellular lysosome environment in the acidic endosomal lumen [201]. Carbohydrate-based delivery systems, such as mono, oligo, and polysaccharide, are employed to encapsulate polyphenols due to their abundance and low cost; for example, curcumin was encapsulated in chitosan using an injection-gelation method to increase its bioavailability, antioxidant properties, and to improve stability and effects on tumor cells [202].

Protein-based systems have been employed to prepare nanoparticles for carrying polyphenols. The proteins act as "host" and polyphenols as "guest" molecules. The polyphenols bind specific regions on the protein surfaces through hydrogen and/or hydrophobic non-covalent bounds. The  $\beta$ -lactoglobulin nano delivery was used to increase the water solubility 3-fold at pH 7 of the epigallocatechin-3-gallate and naringenin [203]. Finally, polyphenols are used to design polyphenol-based nanomaterials for biomedical applications. For example, the polyphenol-grafted polymers are used as antidiabetic agents [204], the curcumin encapsulated in chitosan and polyglycolic acid (PGA) particles for wound healing [205], and the polyphenol-loaded electrospun nanofibers to improve the remineralization and regeneration of bone [206].

## 10. Polyphenols in Active Packaging

In recent years, packaging technology has evolved, including intelligent or smart packaging. Biodegradable, active, and bioactive packaging are new trends in food packaging research. Food contact materials (FCM) are engineered to protect foods, and improve their shelf-life [207]. Plastic packaging materials, such as polycarbonate, polyethylene, and polyethylene terephthalate, widely used in food packaging, are nonbiodegradable and disadvantageous to the environment and human health [208–210]. To date, natural and biodegradable biopolymer-based packaging films and edible coatings represent the alternative to plastic packaging materials [211]. Natural biopolymers, including proteins, polysaccharides, and lipids, have been used in packaging manufacturing [212]. Fruit industrial manufacture generates large amounts of waste that harm the environment and causes considerable treatment expense [213]. Nevertheless, these by-products are rich in bioactive compounds [214], some of which can be incorporated into biodegradable plastics for food packaging to protect the polymeric matrix against thermal [162,213], photo-induced degradation, and preserve the food freshness and quality [215]. The solvent-based impregnation of biodegradable polymers with extracts of *Cistus linnaeus* is used to improve the polymers' thermal stability [216]. Chemically-synthesized and biomass-derived biodegradable polymers have been used as matrices to protect food during transportation, storage, and sale. Polyphenols are employed in the so-called "leaching systems" that are active-releasing systems able to release actives by direct contact between food and packaging material. For this purpose, the propolis is mixed with biopolymers, plasticizers, and reinforcing agents to produce active packaging and edible coatings [213,216].

Biopolymers can be dissolved in solvents depending on their hydrophilicity. Hydrophilic biopolymers, such as gelatin,  $\kappa$ -carrageenan, alginate, and agar in water, chitosan, can be dissolved in acidic solutions [217], while organic solvents, chloroform, and ethyl acetate can be employed for hydrophobic biopolymer such as polylactic acid (PLA) [218]. For example, the ethanolic propolis extract, and propolis in powder, together with plasticizers such as glycerol and (PEG) polyethylene glycol, have been added to biopolymeric solutions [219]. Tea polyphenols (TP) are employed as an active component in biopolymer materials for active food packaging. Shao et al. have incorporated TP into pullulan-carboxymethylcellulose sodium (Pul-CMC) solutions on electrospun nanofiber films [220].

## 11. Conclusions

Polyphenols are secondary plant metabolites that can benefit human health and preserve food. The use of polyphenols as supplements, antibiotic drugs, cosmetics, and natural food preservatives is a promising trend in the industry because of the growing interest in natural products and the multiple biological activities of these products.

The great demand for polyphenols and the small quantity produced by the plants have determined the need to use extraction techniques that allow exhaustive extraction even when it is necessary to recover them from non-traditional sources such as organic waste. For this purpose, unconventional techniques such as supercritical fluid, high-voltage electric discharge, and enzyme-assisted extraction must be optimized.

The polyphenols' low oral bioavailability and interactions with other molecules negatively impact the possible industrial application. Therefore, different nanocarriers have been developed to protect, improve bioavailability, ensure achievement to the active site, and improve their effectiveness. It is essential to underline that polyphenols are commonly present in plant-based foods such as fruits and vegetables.

Guidelines for their consumption and supplementation should be provided by regulatory bodies to make consumers safe and informed.

**Author Contributions:** Conceptualization, writing—original draft preparation I.D. and L.G. All authors have read and agreed to the published version of the manuscript.

**Funding:** This research received no external funding.

**Data Availability Statement:** Not applicable.

**Conflicts of Interest:** The authors declare no conflict of interest.

## References

- Li, Y.; Chemat, F. (Eds.) Food, Cosmetics and Drugs. In *Plant Based "Green Chemistry 2.0": Moving from Evolutionary to Revolutionary*; Springer: Singapore, 2019; pp. 197–235.
- Becker, L.; Zaiter, A.; Petit, J.; Karam, M.-C.; Sudol, M.; Baudelaire, E.; Scher, J.; Dicko, A. How do grinding and sieving impact on physicochemical properties, polyphenol content, and antioxidant activity of *Hieracium pilosella* L. powders? *J. Funct. Foods* **2017**, *35*, 666–672. [[CrossRef](#)]
- Olszowy, M. What is responsible for antioxidant properties of polyphenolic compounds from plants? *Plant Physiol. Biochem.* **2019**, *144*, 135–143. [[CrossRef](#)] [[PubMed](#)]
- Dini, I.; Izzo, L.; Graziani, G.; Ritieni, A. The Nutraceutical Properties of "Pizza Napoletana TSG" a Traditional Food Rich in Bioaccessible Antioxidants. *Antioxidants* **2021**, *10*, 495. [[CrossRef](#)] [[PubMed](#)]
- Dini, I. Spices and herbs as therapeutic foods. In *Food Quality: Balancing Health and Disease*; Holban, A.M., Grumezescu, A.M., Eds.; Academic Press Elsevier: London, UK, 2018; pp. 433–469.
- Dini, I.; Seccia, S.; Senatore, A.; Coppola, D.; Morelli, E. Development and Validation of an Analytical Method for Total Polyphenols Quantification in Extra Virgin Olive Oils. *Food Anal. Methods* **2020**, *13*, 457–464. [[CrossRef](#)]
- Bertelli, A.; Biagi, M.; Corsini, M.; Baini, G.; Cappellucci, G.; Miraldi, E. Polyphenols: From Theory to Practice. *Foods* **2021**, *10*, 2595. [[CrossRef](#)] [[PubMed](#)]
- Pasinetti, G.M.; Singh, R.; Westfall, S.; Herman, F.; Faith, J.; Ho, L. The Role of the Gut Microbiota in the Metabolism of Polyphenols as Characterized by Gnotobiotic Mice. *J. Alzheimers Dis.* **2018**, *63*, 409–421. [[CrossRef](#)]
- Wojtunik-Kulesza, K.; Oniszczuk, A.; Oniszczuk, T.; Combrzyński, M.; Nowakowska, D.; Matwijczuk, A. Influence of In Vitro Digestion on Composition, Bioaccessibility and Antioxidant Activity of Food Polyphenols—A Non-Systematic Review. *Nutrients* **2020**, *12*, 1401. [[CrossRef](#)]

10. Debelo, H.; Li, M.; Ferruzzi, M.G. Processing influences on food polyphenol profiles and biological activity. *Curr. Opin. Food Sci.* **2020**, *32*, 90–102. [[CrossRef](#)]
11. Milinčić, D.D.; Popović, D.A.; Lević, S.M.; Kostić, A.; Tešić, Ž.L.; Nedović, V.A.; Pešić, M.B. Application of Polyphenol-Loaded Nanoparticles in Food Industry. *Nanomaterials* **2019**, *9*, 1629. [[CrossRef](#)]
12. Hu, B.; Liu, X.; Zhang, C.; Zeng, X. Food macromolecule based nanodelivery systems for enhancing the bioavailability of polyphenols. *J. Food Drug Anal.* **2017**, *25*, 3–15. [[CrossRef](#)]
13. Hu, B.; Ting, Y.; Zeng, X.; Huang, Q. Cellular uptake and cytotoxicity of chitosan-caseinophosphopeptides nanocomplexes loaded with epigallocatechin gallate. *Carbohydr. Polym.* **2012**, *89*, 362–370. [[CrossRef](#)] [[PubMed](#)]
14. Homayouni, H.; Kavoosi, G.; Nassiri, S.M. Physicochemical, antioxidant and antibacterial properties of dispersion made from tapioca and gelatinized tapioca starch incorporated with carvacrol. *LWT* **2017**, *77*, 503–509. [[CrossRef](#)]
15. Serpa Guerra, A.M.; Gómez Hoyos, C.; Velásquez-Cock, J.A.; Vélez Acosta, L.; Gañán Rojo, P.; Velásquez Giraldo, A.M.; Zuluaga Gallego, R. The nanotech potential of turmeric (*Curcuma longa* L.) in food technology: A review. *Crit. Rev. Food Sci. Nutr.* **2020**, *60*, 1842–1854. [[CrossRef](#)]
16. Fereidoon, S.; Vamadevan, V.; Won Young, O.; Han, P. Phenolic compounds in agri-food by-products, their bioavailability and health effects. *J. Food Bioact.* **2019**, *5*, 57–119. [[CrossRef](#)]
17. Tzima, K.; Brunton, N.P.; Lyng, J.G.; Frontuto, D.; Rai, D.K. The effect of Pulsed Electric Field as a pretreatment step in Ultrasound Assisted Extraction of phenolic compounds from fresh rosemary and thyme by-products. *Innov. Food Sci. Emerg. Technol.* **2021**, *69*, 102644. [[CrossRef](#)]
18. Zhang, B.; Zhang, Y.; Li, H.; Deng, Z.; Tsao, R. A review on insoluble-bound phenolics in plant-based food matrix and their contribution to human health with future perspectives. *Trends Food Sci. Technol.* **2020**, *105*, 347–362. [[CrossRef](#)]
19. Pino, C.; Sepúlveda, B.; Tapia, F.; Saavedra, J.; García-González, D.L.; Romero, N. The Impact of Mild Frost Occurring at Different Harvesting Times on the Volatile and Phenolic Composition of Virgin Olive Oil. *Antioxidants* **2022**, *11*, 852. [[CrossRef](#)] [[PubMed](#)]
20. Chen, Z.; Wu, J.; Ma, Y.; Wang, P.; Gu, Z.; Yang, R. Biosynthesis, metabolic regulation and bioactivity of phenolic acids in plant food materials. *Shipin Kexue/Food Sci.* **2018**, *39*, 321–328.
21. Petersen, M.; Hans, J.; Matern, U. Biosynthesis of Phenylpropanoids and Related Compounds. In *Annual Plant Reviews Volume 40: Biochemistry of Plant Secondary Metabolism*; Wiley-Blackwell: Hoboken, NJ, USA, 2010; pp. 182–257.
22. Liu, W.; Feng, Y.; Yu, S.; Fan, Z.; Li, X.; Li, J.; Yin, H. The Flavonoid Biosynthesis Network in Plants. *Int. J. Mol. Sci.* **2021**, *22*, 12824. [[CrossRef](#)]
23. Chen, L.; Cao, H.; Xiao, J. *Polyphenols: Absorption, Bioavailability, and Metabolomics*; Woodhead Publishing: Cambridge, UK, 2018; pp. 45–67.
24. Brown, N.M.; Lydeking-Olsen Grgić, J.; Šelo, G.; Planinić, M.; Tišma, M.; Bucić-Kojić, A. Role of the Encapsulation in Bioavailability of Phenolic Compounds. *Antioxidants* **2020**, *9*, 923. [[CrossRef](#)]
25. Del Rio, D.; Rodriguez-Mateos, A.; Spencer, J.P.; Tognolini, M.; Borges, G.; Crozier, A. Dietary (poly)phenolics in human health: Structures, bioavailability, and evidence of protective effects against chronic diseases. *Antioxid Redox Signal* **2013**, *18*, 1818–1892. [[CrossRef](#)] [[PubMed](#)]
26. Cipolletti, M.; Solar Fernandez, V.; Montalesi, E.; Marino, M.; Fiochetti, M. Beyond the Antioxidant Activity of Dietary Polyphenols in Cancer: The Modulation of Estrogen Receptors (ERs) Signaling. *Int. J. Mol. Sci.* **2018**, *19*, 2624. [[CrossRef](#)] [[PubMed](#)]
27. Kumar, S.; Pandey, A.K. Chemistry and biological activities of flavonoids: An overview. *Sci. World J.* **2013**, *2013*, 162750. [[CrossRef](#)] [[PubMed](#)]
28. Sesink, A.L.; O’Leary, K.A.; Hollman, P.C. Quercetin glucuronides but not glucosides are present in human plasma after consumption of quercetin-3-glucoside or quercetin-4’-glucoside. *J. Nutr.* **2001**, *131*, 1938–1941. [[CrossRef](#)] [[PubMed](#)]
29. Setchell, K.D.; Brown, N.M.; Lydeking-Olsen, E. The clinical importance of the metabolite equol—a clue to the Effectiveness of soy and its isoflavones. *J. Nutr.* **2002**, *132*, 3577–3584. [[CrossRef](#)]
30. Rahman, M.M.; Rahaman, M.S.; Islam, M.R.; Rahman, F.; Mithi, F.M.; Alqahtani, T.; Almikhlaifi, M.A.; Alghamdi, S.Q.; Alruwaili, A.S.; Hossain, M.S.; et al. Role of Phenolic Compounds in Human Disease: Current Knowledge and Future Prospects. *Molecules* **2021**, *27*, 233. [[CrossRef](#)]
31. Felgines, C.; Talavera, S.; Gonthier, M.P.; Texier, O.; Scalbert, A.; Lamaison, J.L.; Remesy, C. Strawberry anthocyanins are recovered in urine as glucuro- and sulfoconjugates in humans. *J. Nutr.* **2003**, *133*, 1296–1301. [[CrossRef](#)]
32. Crespy, V.; Morand, C.; Besson, C.; Manach, C.; Demigne, C.; Remesy, C. Quercetin, but not Its Glycosides, Is Absorbed from the Rat Stomach. *J. Agric. Food Chem.* **2002**, *50*, 618–621. [[CrossRef](#)]
33. Filesi, C.; Giovannini, C.; Masella, R. Polyphenols, dietary sources and bioavailability. *Ann. Ist. Super. Sanita* **2007**, *43*, 348–361.
34. Passamonti, S.; Vrhovsek, U.; Vanzo, A.; Mattivi, F. Fast Access of Some Grape Pigments to the Brain. *J. Agric. Food Chem.* **2005**, *53*, 7029–7034. [[CrossRef](#)]
35. Halliwell, B.; Zhao, K.; Whiteman, M. The gastrointestinal tract: A major site of antioxidant action? *Free Radic. Res.* **2000**, *33*, 819–830. [[CrossRef](#)] [[PubMed](#)]
36. Clifford, M.N. Chlorogenic acids and other cinnamates—nature, occurrence and dietary burden. *J. Sci. Food Agric.* **1999**, *79*, 362–372. [[CrossRef](#)]

37. Kuhnau, J. Flavonoids. A class of semi-essential food components: Their role in human nutrition. *World Rev. Nutr. Diet.* **1976**, *24*, 117–191. [[PubMed](#)]
38. Nunes, M.C.; Graça, C.; Vlaisavljević, S.; Tenreiro, A.; Sousa, I.; Raymundo, A. Microalgal cell disruption: Effect on the bioactivity and rheology of wheat bread. *Algal Res.* **2020**, *45*, 101749. [[CrossRef](#)]
39. Bohn, T.; McDougall, G.J.; Alegria, A.; Alminger, M.; Arrigoni, E.; Aura, A.M.; Brito, C.; Cilla, A.; El, S.N.; Karakaya, S.; et al. Mind the gap-deficits in our knowledge of aspects impacting the bioavailability of phytochemicals and their metabolites—A position paper focusing on carotenoids and polyphenols. *Mol. Nutr. Food Res.* **2015**, *59*, 1307–1323. [[CrossRef](#)]
40. Friedman, M.; Jürgens, H.S. Effect of pH on the stability of plant phenolic compounds. *J. Agric. Food Chem.* **2000**, *48*, 2101–2110. [[CrossRef](#)]
41. Williams, A.W.; Boileau, T.W.M.; Erdman, J.W. Factors Influencing the Uptake and Absorption of Carotenoids. *Proc. Soc. Exp. Biol. Med.* **1998**, *218*, 106–108. [[CrossRef](#)]
42. Zhu, F. Interactions between cell wall polysaccharides and polyphenols. *Crit. Rev. Food Sci. Nutr.* **2018**, *58*, 1808–1831. [[CrossRef](#)]
43. Diep, T.T.; Yoo, M.J.Y.; Rush, E. Effect of In Vitro Gastrointestinal Digestion on Amino Acids, Polyphenols and Antioxidant Capacity of Tamarillo Yoghurts. *Int. J. Mol. Sci.* **2022**, *23*, 2526. [[CrossRef](#)]
44. Palermo, M.; Pellegrini, N.; Fogliano, V. The effect of cooking on the phytochemical content of vegetables. *J. Sci. Food Agric.* **2014**, *94*, 1057–1070. [[CrossRef](#)]
45. Dalmau, M.E.; Llabrés, P.J.; Eim, V.S.; Rosselló, C.; Simal, S. Influence of freezing on the bioaccessibility of beetroot (*Beta vulgaris*) bioactive compounds during in vitro gastric digestion. *Sci. Food Agric. J.* **2019**, *99*, 1055–1065. [[CrossRef](#)] [[PubMed](#)]
46. Lorenzo, J.M.; Estevez, M.; Barba, F.J.; Thirumdas, R.; Franco, D.; Munekata, P.E.S. *Polyphenols: Bioaccessibility and Bioavailability of Bioactive Components*; Woodhead Publishing Series in Food Science; Elsevier: Amsterdam, The Netherlands, 2019; pp. 309–332.
47. Barba, F.J.; Terefe, N.S.; Buckow, R.; Knorr, D.; Orlien, V. New opportunities and perspectives of high pressure treatment to improve health and safety attributes of foods. A review. *Food Res. Int.* **2015**, *77*, 725–742. [[CrossRef](#)]
48. Ho, K.; Redan, B.W. Impact of thermal processing on the nutrients, phytochemicals, and metal contaminants in edible algae. *Crit. Rev. Food Sci. Nutr.* **2022**, *62*, 508–526. [[CrossRef](#)] [[PubMed](#)]
49. Tomás-Barberán, F.A.; Gonzalez-Sarrias, A.; García-Villalba, R.; Núñez-Sánchez, M.Á.; Selma, M.V.; García-Conesa, M.T.; Espín, J.C. Urolithins, the rescue of “old” metabolites to understand a “new” concept: Metabotypes as a nexus among phenolic metabolism, microbiota dysbiosis, and host health status. *Mol. Nutr. Food Res.* **2017**, *61*, 1500901. [[CrossRef](#)]
50. Bode, L.M.; Bunzel, D.; Huch, M.; Cho, G.S.; Ruhland, D.; Bunzel, M.; Bub, A.; Franz, C.M.; Kulling, S.E. In vivo and in vitro metabolism of trans-resveratrol by human gut microbiota. *Am. J. Clin. Nutr.* **2013**, *97*, 295–309. [[CrossRef](#)]
51. Filosa, S.; Di Meo, F.; Crispi, S. Polyphenols-gut microbiota interplay and brain neuromodulation. *Neural Regen. Res.* **2018**, *13*, 2055–2059. [[CrossRef](#)]
52. Alves-Santos, A.M.; Sugizaki, C.S.A.; Lima, G.C.; Naves, M.M.V. Prebiotic effect of dietary polyphenols: A systematic review. *J. Funct. Foods* **2020**, *74*, 104169. [[CrossRef](#)]
53. Moorthy, M.; Chaiyakunapruk, N.; Jacob, S.A.; Palanisamy, U.D. Prebiotic potential of polyphenols, its effect on gut microbiota and anthropometric/clinical markers: A systematic review of randomised controlled trials. *Trends Food Sci. Technol.* **2020**, *99*, 634–649. [[CrossRef](#)]
54. Roberfroid, M.; Gibson, G.R.; Hoyles, L.; McCartney, A.L.; Rastall, R.; Rowland, I.; Wolvers, D.; Watzl, B.; Szajewska, H.; Stahl, B.; et al. Prebiotic effects: Metabolic and health benefits. *Br. J. Nutr.* **2010**, *104* (Suppl. S2), S1–S63. [[CrossRef](#)]
55. Morais, C.A.; de Rosso, V.V.; Estadella, D.; Pisani, L.P. Anthocyanins as inflammatory modulators and the role of the gut microbiota. *J. Nutr. Biochem.* **2016**, *33*, 1–7. [[CrossRef](#)]
56. Wu, M.; Brown, A.C. Applications of Catechins in the Treatment of Bacterial Infections. *Pathogens* **2021**, *10*, 546. [[CrossRef](#)] [[PubMed](#)]
57. Bouyahya, A.; Dakka, N.; Et-Touys, A.; Abrini, J.; Bakri, Y. Medicinal plant products targeting quorum sensing for combating bacterial infections. *Asian Pac. J. Trop. Med.* **2017**, *10*, 729–743. [[CrossRef](#)] [[PubMed](#)]
58. Rothwell, J.A.; Medina-Remón, A.; Pérez-Jiménez, J.; Neveu, V.; Knaze, V.; Slimani, N.; Scalbert, A. Effects of food processing on polyphenol contents: A systematic analysis using Phenol-Explorer data. *Mol. Nutr. Food Res.* **2015**, *59*, 160–170. [[CrossRef](#)] [[PubMed](#)]
59. Farooq, S.; Abdullah; Zhang, H.; Weiss, J. A comprehensive review on polarity, partitioning, and interactions of phenolic antioxidants at oil-water interface of food emulsions. *Compr. Rev. Food Sci. Food Saf.* **2021**, *20*, 4250–4277. [[CrossRef](#)] [[PubMed](#)]
60. Igor Otavio, M.; Cristine Vanz, B.; Maria Izabela, F.; Hector Alonzo Gomez, G.; Chung-Yen Oliver, C.; Giuseppina Pace Pereira, L. Phenolic Compounds: Functional Properties, Impact of Processing and Bioavailability. In *Phenolic Compounds*; Marcos, S.-H., Mariana, P.-T., Maria del Rosario, G.-M., Eds.; IntechOpen: Rijeka, Croatia, 2017; p. Ch. 1.
61. Gil-Martín, E.; Forbes-Hernández, T.; Romero, A.; Cianciosi, D.; Giampieri, F.; Battino, M. Influence of the extraction method on the recovery of bioactive phenolic compounds from food industry by-products. *Food Chem.* **2022**, *378*, 131918. [[CrossRef](#)]
62. Wołosiak, R.; Drużyńska, B.; Piecyk, M.; Majewska, E.; Worobiej, E. Effect of Sterilization Process and Storage on the Antioxidative Properties of Runner Bean. *Molecules* **2018**, *23*, 1409. [[CrossRef](#)]
63. de Lima, A.C.S.; da Rocha Viana, J.D.; de Sousa Sabino, L.B.; da Silva, L.M.R.; da Silva, N.K.V.; de Sousa, P.H.M. Processing of three different cooking methods of cassava: Effects on in vitro bioaccessibility of phenolic compounds and antioxidant activity. *LWT—Food Sci. Technol.* **2017**, *76*, 253–258. [[CrossRef](#)]

64. Kurilich, A.C.; Clevidence, B.A.; Britz, S.J.; Simon, P.W.; Novotny, J.A. Plasma and urine responses are lower for acylated vs nonacylated anthocyanins from raw and cooked purple carrots. *J. Agric. Food Chem.* **2005**, *53*, 6537–6542. [[CrossRef](#)]
65. Wani, S.M.; Masoodi, F.A.; Yousuf, S.; Dar, B.N.; Rather, S.A. Phenolic compounds and antiproliferative activity of apricots: Influence of canning, freezing, and drying. *J. Food Process. Preserv.* **2020**, *44*, e14887. [[CrossRef](#)]
66. Chaovanalikit, A.; Wrolstad, R.E. Anthocyanin and Polyphenolic Composition of Fresh and Processed Cherries. *J. Food Sci.* **2004**, *69*, FCT73–FCT83. [[CrossRef](#)]
67. Arfaoui, L. Dietary Plant Polyphenols: Effects of Food Processing on Their Content and Bioavailability. *Molecules* **2021**, *26*, 2959. [[CrossRef](#)] [[PubMed](#)]
68. Kamiloglu, S.; Demirci, M.; Selen, S.; Toydemir, G.; Boyacioglu, D.; Capanoglu, E. Home processing of tomatoes (*Solanum lycopersicum*): Effects on in vitro bioaccessibility of total lycopene, phenolics, flavonoids, and antioxidant capacity. *J. Sci. Food Agric.* **2014**, *94*, 2225–2233. [[CrossRef](#)] [[PubMed](#)]
69. Kamiloglu, S.; Capanoglu, E. Investigating the in vitro bioaccessibility of polyphenols in fresh and sun-dried figs (*Ficus carica* L.). *Int. J. Food Sci. Technol.* **2013**, *48*, 2621–2629. [[CrossRef](#)]
70. Aydin, E.; Gocmen, D. The influences of drying method and metabisulfite pretreatment on the color, functional properties and phenolic acids contents and bioaccessibility of pumpkin flour. *LWT—Food Sci. Technol.* **2015**, *60*, 385–392. [[CrossRef](#)]
71. Yanat, M.; Baysal, T. Effect of freezing rate and storage time on quality parameters of strawberry frozen in modified and home type freezer. *Hrvat. Časopis Za Prehrambenu Tehnol. Biotehnol. I Nutr.* **2018**, *13*, 154–158. [[CrossRef](#)]
72. Rafiq, S.; Kaul, R.; Sofi, S.A.; Bashir, N.; Nazir, F.; Ahmad Nayik, G. Citrus peel as a source of functional ingredient: A review. *J. Saudi Soc. Agric. Sci.* **2018**, *17*, 351–358. [[CrossRef](#)]
73. Derossi, A.; Ricci, I.; Caporizzi, R.; Fiore, A.; Severini, C. How grinding level and brewing method (Espresso, American, Turkish) could affect the antioxidant activity and bioactive compounds in a coffee cup. *J. Sci. Food Agric.* **2018**, *98*, 3198–3207. [[CrossRef](#)]
74. Li, S.; Zhang, R.; Lei, D.; Huang, Y.; Cheng, S.; Zhu, Z.; Wu, Z.; Cravotto, G. Impact of ultrasound, microwaves and high-pressure processing on food components and their interactions. *Trends Food Sci. Technol.* **2021**, *109*, 1–15. [[CrossRef](#)]
75. Leyane, T.S.; Jere, S.W.; Houreld, N.N. Oxidative Stress in Ageing and Chronic Degenerative Pathologies: Molecular Mechanisms Involved in Counteracting Oxidative Stress and Chronic Inflammation. *Int. J. Mol. Sci.* **2022**, *23*, 7273. [[CrossRef](#)]
76. Gulcin, İ. Antioxidants and antioxidant methods: An updated overview. *Arch. Toxicol.* **2020**, *94*, 651–715. [[CrossRef](#)]
77. Luo, J.; Si, H.; Jia, Z.; Liu, D. Dietary Anti-Aging Polyphenols and Potential Mechanisms. *Antioxidants* **2021**, *10*, 283. [[CrossRef](#)] [[PubMed](#)]
78. Rice-Evans, C.A.; Miller, N.J.; Paganga, G. Structure-antioxidant activity relationships of flavonoids and phenolic acids. *Free Radic. Biol. Med.* **1996**, *20*, 933–956. [[CrossRef](#)] [[PubMed](#)]
79. Chalas, J.; Claise, C.; Edeas, M.; Messaoudi, C.; Vergnes, L.; Abella, A.; Lindenbaum, A. Effect of ethyl esterification of phenolic acids on low-density lipoprotein oxidation. *Biomed. Pharmacother.* **2001**, *55*, 54–60. [[CrossRef](#)] [[PubMed](#)]
80. Dai, J.; Mumper, R.J. Plant Phenolics: Extraction, Analysis and Their Antioxidant and Anticancer Properties. *Molecules* **2010**, *15*, 7313–7352. [[CrossRef](#)] [[PubMed](#)]
81. Gandhi, S.U.; Kim, K.; Larsen, L.; Rosengren, R.J.; Safe, S. Curcumin and synthetic analogs induce reactive oxygen species and decreases specificity protein (Sp) transcription factors by targeting microRNAs. *BMC Cancer* **2012**, *12*, 564. [[CrossRef](#)] [[PubMed](#)]
82. Urbich, C.; Kuehbachner, A.; Dimmeler, S. Role of microRNAs in vascular diseases, inflammation, and angiogenesis. *Cardiovasc. Res.* **2008**, *79*, 581–588. [[CrossRef](#)]
83. Cheng, H.S.; Sivachandran, N.; Lau, A.; Boudreau, E.; Zhao, J.L.; Baltimore, D.; Delgado-Olguin, P.; Cybulsky, M.; Fish, J.E. MicroRNA-146 represses endothelial activation by inhibiting pro-inflammatory pathways. *EMBO Mol. Med.* **2013**, *5*, 1017–1034. [[CrossRef](#)]
84. Li, D.; Yang, P.; Xiong, Q.; Song, X.; Yang, X.; Liu, L.; Yuan, W.; Rui, Y.C. MicroRNA-125a/b-5p inhibits endothelin-1 expression in vascular endothelial cells. *J. Hypertens.* **2010**, *28*, 1646–1654. [[CrossRef](#)]
85. Cione, E.; La Torre, C.; Cannataro, R.; Caroleo, M.C.; Plastina, P.; Gallelli, L. Quercetin, Epigallocatechin Gallate, Curcumin, and Resveratrol: From Dietary Sources to Human MicroRNA Modulation. *Molecules* **2019**, *25*, 63. [[CrossRef](#)]
86. Li, Y.; Tian, L.; Sun, D.; Yin, D. Curcumin ameliorates atherosclerosis through upregulation of miR-126. *J. Cell. Physiol.* **2019**, *234*, 21049–21059. [[CrossRef](#)]
87. Tanno, M.; Kuno, A.; Yano, T.; Miura, T.; Hisahara, S.; Ishikawa, S.; Shimamoto, K.; Horio, Y. Induction of manganese superoxide dismutase by nuclear translocation and activation of SIRT1 promotes cell survival in chronic heart failure. *J. Biol. Chem.* **2010**, *285*, 8375–8382. [[CrossRef](#)] [[PubMed](#)]
88. Huang, J.P.; Hsu, S.C.; Li, D.E.; Chen, K.H.; Kuo, C.Y.; Hung, L.M. Resveratrol Mitigates High-Fat Diet-Induced Vascular Dysfunction by Activating the Akt/eNOS/NO and Sirt1/ER Pathway. *J. Cardiovasc. Pharmacol.* **2018**, *72*, 231–241. [[CrossRef](#)] [[PubMed](#)]
89. Fourny, N.; Lan, C.; Sérére, E.; Bernard, M.; Desrois, M. Protective Effect of Resveratrol against Ischemia-Reperfusion Injury via Enhanced High Energy Compounds and eNOS-SIRT1 Expression in Type 2 Diabetic Female Rat Heart. *Nutrients* **2019**, *11*, 105. [[CrossRef](#)]
90. Chung, D.J.; Wu, Y.L.; Yang, M.Y.; Chan, K.C.; Lee, H.J.; Wang, C.J. Nelumbo nucifera leaf polyphenol extract and gallic acid inhibit TNF- $\alpha$ -induced vascular smooth muscle cell proliferation and migration involving the regulation of miR-21, miR-143 and miR-145. *Food Funct.* **2020**, *11*, 8602–8611. [[CrossRef](#)] [[PubMed](#)]

91. Shubina, V.S.; Kozina, V.I.; Shatalin, Y.V. Comparison of Antioxidant Properties of a Conjugate of Taxifolin with Glyoxylic Acid and Selected Flavonoids. *Antioxidants* **2021**, *10*, 1262. [[CrossRef](#)]
92. Eghbaliferiz, S.; Iranshahi, M. Prooxidant Activity of Polyphenols, Flavonoids, Anthocyanins and Carotenoids: Updated Review of Mechanisms and Catalyzing Metals. *Phytother Res.* **2016**, *30*, 1379–1391. [[CrossRef](#)]
93. Velderrain-Rodríguez, G.R.; Torres-Moreno, H.; Villegas-Ochoa, M.A.; Ayala-Zavala, J.F.; Robles-Zepeda, R.E.; Wall-Medrano, A.; González-Aguilar, G.A. Gallic Acid Content and an Antioxidant Mechanism Are Responsible for the Antiproliferative Activity of ‘Ataulfo’ Mango Peel on LS180 Cells. *Molecules* **2018**, *23*, 695. [[CrossRef](#)]
94. Zhang, Z.; Li, X.; Sang, S.; McClements, D.J.; Chen, L.; Long, J.; Jiao, A.; Jin, Z.; Qiu, C. Polyphenols as Plant-Based Nutraceuticals: Health Effects, Encapsulation, Nano-Delivery, and Application. *Foods* **2022**, *11*, 2189. [[CrossRef](#)]
95. de la Lastra, C.A.; Villegas, I. Resveratrol as an anti-inflammatory and anti-aging agent: Mechanisms and clinical implications. *Mol. Nutr. Food Res.* **2005**, *49*, 405–430. [[CrossRef](#)]
96. Lobo, A.; Liu, Y.; Song, Y.; Liu, S.; Zhang, R.; Liang, H.; Xin, H. Effect of procyanidins on lipid metabolism and inflammation in rats exposed to alcohol and iron. *Heliyon* **2020**, *6*, e04847. [[CrossRef](#)]
97. Zhang, P.; Mak, J.C.; Man, R.Y.; Leung, S.W. Flavonoids reduces lipopolysaccharide-induced release of inflammatory mediators in human bronchial epithelial cells: Structure-activity relationship. *Eur. J. Pharmacol.* **2019**, *865*, 172731. [[CrossRef](#)]
98. Liu, H.; Ma, S.; Xia, H.; Lou, H.; Zhu, F.; Sun, L. Anti-inflammatory activities and potential mechanisms of phenolic acids isolated from *Salvia miltiorrhiza* f. *alba* roots in THP-1 macrophages. *J. Ethnopharmacol.* **2018**, *222*, 201–207. [[CrossRef](#)] [[PubMed](#)]
99. Wang, T.Y.; Li, Q.; Bi, K.S. Bioactive flavonoids in medicinal plants: Structure, activity and biological fate. *Asian J. Pharm. Sci.* **2018**, *13*, 12–23. [[CrossRef](#)] [[PubMed](#)]
100. Asif, P.J.; Longobardi, C.; Hahne, M.; Medema, J.P. The Role of Cancer-Associated Fibroblasts in Cancer Invasion and Metastasis. *Cancers* **2021**, *13*, 4720. [[CrossRef](#)]
101. Kampa, M.; Nifli, A.P.; Notas, G.; Castanas, E. Polyphenols and cancer cell growth. *Rev. Physiol. Biochem. Pharmacol.* **2007**, *159*, 79–113. [[CrossRef](#)] [[PubMed](#)]
102. Vaidya, F.U.; Chhipa, A.S.; Sagar, N.; Pathak, C. Oxidative Stress and Inflammation Can Fuel Cancer. In *Role of Oxidative Stress in Pathophysiology of Diseases*; Maurya, P.K., Dua, K., Eds.; Springer: Singapore, 2020; pp. 229–258.
103. Oliveira-Marques, V.; Marinho, H.S.; Cyrne, L.; Antunes, F. Modulation of NF-kappaB-dependent gene expression by H2O2: A major role for a simple chemical process in a complex biological response. *Antioxid. Redox Signal.* **2009**, *11*, 2043–2053. [[CrossRef](#)]
104. Valko, M.; Leibfritz, D.; Moncol, J.; Cronin, M.T.; Mazur, M.; Telser, J. Free radicals and antioxidants in normal physiological functions and human disease. *Int. J. Biochem. Cell Biol.* **2007**, *39*, 44–84. [[CrossRef](#)]
105. Norris, L.E.; Collene, A.L.; Asp, M.L.; Hsu, J.C.; Liu, L.F.; Richardson, J.R.; Li, D.; Bell, D.; Osei, K.; Jackson, R.D.; et al. Comparison of dietary conjugated linoleic acid with safflower oil on body composition in obese postmenopausal women with type 2 diabetes mellitus. *Am. J. Clin. Nutr.* **2009**, *90*, 468–476. [[CrossRef](#)]
106. Shirakami, Y.; Sakai, H.; Kochi, T.; Seishima, M.; Shimizu, M. Catechins and Its Role in Chronic Diseases. *Adv. Exp. Med. Biol.* **2016**, *929*, 67–90.
107. Miron, A.; Aprotosoia, A.C.; Trifan, A.; Xiao, J. Flavonoids as modulators of metabolic enzymes and drug transporters. *Ann. NY Acad. Sci.* **2017**, *1398*, 152–167. [[CrossRef](#)]
108. Guthrie, A.R.; Chow, H.H.S.; Martinez, J.A. Effects of resveratrol on drug- and carcinogen-metabolizing enzymes, implications for cancer prevention. *Pharmacol. Res. Perspect.* **2017**, *5*, e00294. [[CrossRef](#)]
109. Truong, V.-L.; Jeong, W.-S. Cellular Defensive Mechanisms of Tea Polyphenols: Structure-Activity Relationship. *Int. J. Mol. Sci.* **2021**, *22*, 9109. [[CrossRef](#)] [[PubMed](#)]
110. Abulnaja, K.; Bakkar, A.; Kannan, K.; Al-Manzlawi, A.M.; Kumosani, T.; Qari, M.; Moselhy, S. Olive leaf (*Olea europaea* L. folium) extract influences liver microsomal detoxifying enzymes in rats orally exposed to 2-amino-1-methyl-6-phenyl-imidazo pyridine (PhIP). *Environ. Sci. Pollut. Res.* **2022**, *2022*, 1–9. [[CrossRef](#)] [[PubMed](#)]
111. Majidinia, M.; Bishayee, A.; Yousefi, B. Polyphenols: Major regulators of key components of DNA damage response in cancer. *DNA Repair* **2019**, *82*, 102679. [[CrossRef](#)] [[PubMed](#)]
112. Yin, F.; Giuliano, A.E.; Van Herle, A.J. Signal pathways involved in apigenin inhibition of growth and induction of apoptosis of human anaplastic thyroid cancer cells (ARO). *Anticancer Res.* **1999**, *19*, 4297–4303.
113. Chen, C.; Yu, R.; Owuor, E.D.; Kong, A.N. Activation of antioxidant-response element (ARE), mitogen-activated protein kinases (MAPKs) and caspases by major green tea polyphenol components during cell survival and death. *Arch. Pharmacol. Res.* **2000**, *23*, 605–612. [[CrossRef](#)]
114. Yahfoufi, N.; Alsadi, N.; Jambi, M.; Matar, C. The Immunomodulatory and Anti-Inflammatory Role of Polyphenols. *Nutrients* **2018**, *10*, 1618. [[CrossRef](#)]
115. Talib, W.H.; Abuawad, A.; Thiab, S.; Alshweiat, A.; Mahmod, A.I. Flavonoid-based nanomedicines to target tumor microenvironment. *OpenNano* **2022**, *8*, 100081. [[CrossRef](#)]
116. Chen, H.J.; Lin, C.M.; Lee, C.Y.; Shih, N.C.; Peng, S.F.; Tsuzuki, M.; Amagaya, S.; Huang, W.W.; Yang, J.S. Kaempferol suppresses cell metastasis via inhibition of the ERK-p38-JNK and AP-1 signaling pathways in U-2 OS human osteosarcoma cells. *Oncol. Rep.* **2013**, *30*, 925–932. [[CrossRef](#)]



117. Ke, C.; Gupta, R.; Xavier, D.; Prabhakaran, D.; Mathur, P.; Kalkonde, Y.V.; Kolpak, P.; Suraweera, W.; Jha, P. Divergent trends in ischaemic heart disease and stroke mortality in India from 2000 to 2015: A nationally representative mortality study. *Lancet Glob. Health* **2018**, *6*, e914–e923. [[CrossRef](#)]
118. Koenig, W. Inflammation Revisited: Atherosclerosis in The Post-CANTOS Era. *Eur. Cardiol.* **2017**, *12*, 89–91. [[CrossRef](#)] [[PubMed](#)]
119. Hurtubise, J.; McLellan, K.; Durr, K.; Onasanya, O.; Nwabuko, D.; Ndisang, J.F. The Different Facets of Dyslipidemia and Hypertension in Atherosclerosis. *Curr. Atheroscler. Rep.* **2016**, *18*, 82. [[CrossRef](#)] [[PubMed](#)]
120. Zanutti, I.; Dall’Asta, M.; Mena, P.; Mele, L.; Bruni, R.; Ray, S.; Del Rio, D. Atheroprotective effects of (poly)phenols: A focus on cell cholesterol metabolism. *Food Funct.* **2015**, *6*, 13–31. [[CrossRef](#)] [[PubMed](#)]
121. Elejalde, E.; Villarán, M.C.; Alonso, R.M. Grape polyphenols supplementation for exercise-induced oxidative stress. *J. Int. Soc. Sport. Nutr.* **2021**, *18*, 3. [[CrossRef](#)] [[PubMed](#)]
122. Chambers, K.F.; Day, P.E.; Aboufarrag, H.T.; Kroon, P.A. Polyphenol Effects on Cholesterol Metabolism via Bile Acid Biosynthesis, CYP7A1: A Review. *Nutrients* **2019**, *11*, 2588. [[CrossRef](#)] [[PubMed](#)]
123. Yang, D.; Wang, T.; Long, M.; Li, P. Quercetin: Its main pharmacological activity and potential application in clinical medicine. *Oxidative Med. Cell. Longev.* **2020**, *2020*, 8825387. [[CrossRef](#)]
124. Potì, F.; Santi, D.; Spaggiari, G.; Zimetti, F.; Zanotti, I. Polyphenol Health Effects on Cardiovascular and Neurodegenerative Disorders: A Review and Meta-Analysis. *Int. J. Mol. Sci.* **2019**, *20*, 351. [[CrossRef](#)]
125. Kobayashi, S. The Effect of Polyphenols on Hypercholesterolemia through Inhibiting the Transport and Expression of Niemann-Pick C1-Like 1. *Int. J. Mol. Sci.* **2019**, *20*, 4939. [[CrossRef](#)]
126. Huang, J.; Hao, Q.; Wang, Q.; Wang, Y.; Wan, X.; Zhou, Y. Supplementation with green tea extract affects lipid metabolism and egg yolk lipid composition in laying hens. *J. Appl. Poult. Res.* **2019**, *28*, 881–891. [[CrossRef](#)]
127. Pang, J.; Xu, H.; Wang, X.; Chen, X.; Li, Q.; Liu, Q.; You, Y.; Zhang, H.; Xu, Z.; Zhao, Y.; et al. Resveratrol enhances trans-intestinal cholesterol excretion through selective activation of intestinal liver X receptor alpha. *Biochem. Pharmacol.* **2021**, *186*, 114481. [[CrossRef](#)]
128. Azorin-Ortuño, M.; Yáñez-Gascón, M.J.; González-Sarriás, A.; Larrosa, M.; Vallejo, F.; Pallarés, F.J.; Lucas, R.; Morales, J.C.; Tomás-Barberán, F.A.; García-Conesa, M.T.; et al. Effects of long-term consumption of low doses of resveratrol on diet-induced mild hypercholesterolemia in pigs: A transcriptomic approach to disease prevention. *J. Nutr. Biochem.* **2012**, *23*, 829–837. [[CrossRef](#)] [[PubMed](#)]
129. Mozos, I.; Flangea, C.; Vlad, D.C.; Gug, C.; Mozos, C.; Stoian, D.; Luca, C.T.; Horbańczuk, J.O.; Horbańczuk, O.K.; Atanasov, A.G. Effects of Anthocyanins on Vascular Health. *Biomolecules* **2021**, *11*, 811. [[CrossRef](#)] [[PubMed](#)]
130. Sultana, R.; Alashi, A.M.; Islam, K.; Saifullah, M.; Haque, C.E.; Aluko, R.E. Inhibitory Activities of Polyphenolic Extracts of Bangladeshi Vegetables against  $\alpha$ -Amylase,  $\alpha$ -Glucosidase, Pancreatic Lipase, Renin, and Angiotensin-Converting Enzyme. *Foods* **2020**, *9*, 844. [[CrossRef](#)] [[PubMed](#)]
131. Abbaszadeh, H.; Keikhaei, B.; Mottaghi, S. A review of molecular mechanisms involved in anticancer and antiangiogenic effects of natural polyphenolic compounds. *Phytother. Res.* **2019**, *33*, 2002–2014. [[CrossRef](#)]
132. Yang, T.; Chen, Y.Y.; Liu, J.R.; Zhao, H.; Vaziri, N.D.; Guo, Y.; Zhao, Y.Y. Natural products against renin-angiotensin system for antifibrosis therapy. *Eur. J. Med. Chem.* **2019**, *179*, 623–633. [[CrossRef](#)] [[PubMed](#)]
133. Meng, T.; Xiao, D.; Muhammed, A.; Deng, J.; Chen, L.; He, J. Anti-Inflammatory Action and Mechanisms of Resveratrol. *Molecules* **2021**, *26*, 229. [[CrossRef](#)] [[PubMed](#)]
134. DeFronzo, R.A.; Ferrannini, E.; Groop, L.; Henry, R.R.; Herman, W.H.; Holst, J.J.; Hu, F.B.; Kahn, C.R.; Raz, I.; Shulman, G.I.; et al. Type 2 diabetes mellitus. *Nat. Rev. Dis. Prim.* **2015**, *1*, 15019. [[CrossRef](#)] [[PubMed](#)]
135. Bahadoran, Z.; Mirmiran, P.; Azizi, F. Dietary polyphenols as potential nutraceuticals in management of diabetes: A review. *J. Diabetes Metab Disord* **2013**, *12*, 43. [[CrossRef](#)]
136. Hanhineva, K.; Törrönen, R.; Bondia-Pons, I.; Pekkinen, J.; Kolehmainen, M.; Mykkänen, H.; Poutanen, K. Impact of Dietary Polyphenols on Carbohydrate Metabolism. *Int. J. Mol. Sci.* **2010**, *11*, 1365–1402. [[CrossRef](#)]
137. Dao, T.M.; Waget, A.; Klopp, P.; Serino, M.; Vachoux, C.; Pechere, L.; Drucker, D.J.; Champion, S.; Barthélemy, S.; Barra, Y.; et al. Resveratrol increases glucose induced GLP-1 secretion in mice: A mechanism which contributes to the glycemic control. *PLoS ONE* **2011**, *6*, e20700. [[CrossRef](#)]
138. Wang, Y.; Alkhalidi, H.; Liu, D. The Emerging Role of Polyphenols in the Management of Type 2 Diabetes. *Molecules* **2021**, *26*, 703. [[CrossRef](#)] [[PubMed](#)]
139. Li, X.; Wu, J.; Xu, F.; Chu, C.; Li, X.; Shi, X.; Zheng, W.; Wang, Z.; Jia, Y.; Xiao, W. Use of Ferulic Acid in the Management of Diabetes Mellitus and Its Complications. *Molecules* **2022**, *27*, 6010. [[CrossRef](#)] [[PubMed](#)]
140. Markus, M.A.; Morris, B.J. Resveratrol in prevention and treatment of common clinical conditions of aging. *Clin. Interv. Aging* **2008**, *3*, 331–339.
141. Aquilano, K.; Baldelli, S.; Rotilio, G.; Ciriolo, M.R. Role of nitric oxide synthases in Parkinson’s disease: A review on the antioxidant and anti-inflammatory activity of polyphenols. *Neurochem. Res.* **2008**, *33*, 2416–2426. [[CrossRef](#)]
142. Nebrisi, E.E. Neuroprotective Activities of Curcumin in Parkinson’s Disease: A Review of the Literature. *Int. J. Mol. Sci.* **2021**, *22*, 11248. [[CrossRef](#)] [[PubMed](#)]
143. Ferreira, M.S.; Magalhães, M.C.; Oliveira, R.; Sousa-Lobo, J.M.; Almeida, I.F. Trends in the Use of Botanicals in Anti-Aging Cosmetics. *Molecules* **2021**, *26*, 3584. [[CrossRef](#)]

144. Gasmı, A.; Mujawdiya, P.K.; Noor, S.; Lysiuk, R.; Darmohray, R.; Piscopo, S.; Lenchyk, L.; Antonyak, H.; Dehtiarova, K.; Shanaida, M.; et al. Polyphenols in Metabolic Diseases. *Molecules* **2022**, *27*, 6280. [\[CrossRef\]](#)
145. Yang, X.H.; Li, L.; Xue, Y.B.; Zhou, X.X.; Tang, J.H. Flavonoids from *Epimedium pubescens*: Extraction and mechanism, antioxidant capacity and effects on CAT and GSH-Px of *Drosophila melanogaster*. *PeerJ* **2020**, *8*, e8361. [\[CrossRef\]](#)
146. Zheng, Y.; Liu, Y.; Ge, J.; Wang, X.; Liu, L.; Bu, Z.; Liu, P. Resveratrol protects human lens epithelial cells against H<sub>2</sub>O<sub>2</sub>-induced oxidative stress by increasing catalase, SOD-1, and HO-1 expression. *Mol. Vis.* **2010**, *16*, 1467–1474.
147. Yang, Y.; Wu, Z.Z.; Cheng, Y.L.; Lin, W.; Qu, C. Resveratrol protects against oxidative damage of retinal pigment epithelium cells by modulating SOD/MDA activity and activating Bcl-2 expression. *Eur. Rev. Med. Pharmacol. Sci.* **2019**, *23*, 378–388. [\[CrossRef\]](#)
148. Uygur, R.; Yagmurca, M.; Alkoc, O.A.; Genc, A.; Songur, A.; Ucok, K.; Ozen, O.A. Effects of quercetin and fish n-3 fatty acids on testicular injury induced by ethanol in rats. *Andrologia* **2014**, *46*, 356–369. [\[CrossRef\]](#) [\[PubMed\]](#)
149. Roy, S.; Sannigrahi, S.; Vaddepalli, R.P.; Ghosh, B.; Pusp, P. A novel combination of methotrexate and epigallocatechin attenuates the overexpression of proinflammatory cartilage cytokines and modulates antioxidant status in adjuvant arthritic rats. *Inflammation* **2012**, *35*, 1435–1447. [\[CrossRef\]](#) [\[PubMed\]](#)
150. Hussain, Y.; Khan, H.; Alsharif, K.F.; Hayat Khan, A.; Aschner, M.; Saso, L. The Therapeutic Potential of Kaemferol and Other Naturally Occurring Polyphenols Might Be Modulated by Nrf2-ARE Signaling Pathway: Current Status and Future Direction. *Molecules* **2022**, *27*, 4145. [\[CrossRef\]](#) [\[PubMed\]](#)
151. Kobayashi, M.; Yamamoto, M. Molecular mechanisms activating the Nrf2-Keap1 pathway of antioxidant gene regulation. *Antioxid. Redox Signal.* **2005**, *7*, 385–394. [\[CrossRef\]](#)
152. Kim, J.Y.; Park, Y.K.; Lee, K.P.; Lee, S.M.; Kang, T.W.; Kim, H.J.; Dho, S.H.; Kim, S.Y.; Kwon, K.S. Genome-wide profiling of the microRNA-mRNA regulatory network in skeletal muscle with aging. *Aging* **2014**, *6*, 524–544. [\[CrossRef\]](#)
153. Hoang, H.T.; Moon, J.-Y.; Lee, Y.-C. Natural Antioxidants from Plant Extracts in Skincare Cosmetics: Recent Applications, Challenges and Perspectives. *Cosmetics* **2021**, *8*, 106. [\[CrossRef\]](#)
154. Xue, N.; Liu, Y.; Jin, J.; Ji, M.; Chen, X. Chlorogenic Acid Prevents UVA-Induced Skin Photoaging through Regulating Collagen Metabolism and Apoptosis in Human Dermal Fibroblasts. *Int. J. Mol. Sci.* **2022**, *23*, 6941. [\[CrossRef\]](#)
155. Oršolić, N. Allergic Inflammation: Effect of Propolis and Its Flavonoids. *Molecules* **2022**, *27*, 6694. [\[CrossRef\]](#)
156. Shakoar, H.; Feehan, J.; Apostolopoulos, V.; Platat, C.; Al Dhaheer, A.S.; Ali, H.I.; Ismail, L.C.; Bosevski, M.; Stojanovska, L. Immunomodulatory Effects of Dietary Polyphenols. *Nutrients* **2021**, *13*, 728. [\[CrossRef\]](#)
157. Loo, Y.T.; Howell, K.; Chan, M.; Zhang, P.; Ng, K. Modulation of the human gut microbiota by phenolics and phenolic fiber-rich foods. *Compr. Rev. Food Sci. Food Saf.* **2020**, *19*, 1268–1298. [\[CrossRef\]](#)
158. Lee, J.S.; Lee, M.S.; An, S.; Yang, K.; Lee, K.; Yang, H.S.; Lee, H.; Cho, S.-W. Plant Flavonoid-Mediated Multifunctional Surface Modification Chemistry: Catechin Coating for Enhanced Osteogenesis of Human Stem Cells. *Chem. Mater.* **2017**, *29*, 4375–4384. [\[CrossRef\]](#)
159. Yu, T.; Wang, Z.; You, X.; Zhou, H.; He, W.; Li, B.; Xia, J.; Zhu, H.; Zhao, Y.; Yu, G.; et al. Resveratrol promotes osteogenesis and alleviates osteoporosis by inhibiting p53. *Aging* **2020**, *12*, 10359–10369. [\[CrossRef\]](#) [\[PubMed\]](#)
160. Bellavia, D.; Caradonna, F.; Dimarco, E.; Costa, V.; Carina, V.; De Luca, A.; Raimondi, L.; Fini, M.; Gentile, C.; Giavaresi, G. Non-flavonoid polyphenols in osteoporosis: Preclinical evidence. *Trends Endocrinol. Metab.* **2021**, *32*, 515–529. [\[CrossRef\]](#) [\[PubMed\]](#)
161. Tomadoni, B.; Viacava, G.; Cassani, L.; Moreira, M.R.; Ponce, A. Novel biopreservatives to enhance the safety and quality of strawberry juice. *J. Food Sci. Technol.* **2016**, *53*, 281–292. [\[CrossRef\]](#)
162. Dini, I. Chapter 14—Use of Essential Oils in Food Packaging. In *Essential Oils in Food Preservation, Flavor and Safety*; Preedy, V.R., Ed.; Academic Press: San Diego, CA, USA, 2016; pp. 139–147.
163. Gupta, P.D.; Birdi, T.J. Development of botanicals to combat antibiotic resistance. *J. Ayurveda Integr. Med.* **2017**, *8*, 266–275. [\[CrossRef\]](#)
164. Olszewska, M.A.; Gėdas, A.; Simões, M. Antimicrobial polyphenol-rich extracts: Applications and limitations in the food industry. *Food Res. Int.* **2020**, *134*, 109214. [\[CrossRef\]](#)
165. Villalobos-Delgado, L.H.; Nevárez-Moorillon, G.V.; Caro, I.; Quinto, E.J.; Mateo, J. 4—Natural antimicrobial agents to improve foods shelf life. In *Food Quality and Shelf Life*; Galanakis, C.M., Ed.; Academic Press: Cambridge, MA, USA, 2019; pp. 125–157.
166. Martinengo, P.; Arunachalam, K.; Shi, C. Polyphenolic Antibacterials for Food Preservation: Review, Challenges, and Current Applications. *Foods* **2021**, *10*, 2469. [\[CrossRef\]](#)
167. Bouarab-Chibane, L.; Forquet, V.; Lantėri, P.; Clément, Y.; Léonard-Akkari, L.; Oulahal, N.; Degraeve, P.; Bordes, C. Antibacterial Properties of Polyphenols: Characterization and QSAR (Quantitative Structure-Activity Relationship) Models. *Front. Microbiol.* **2019**, *10*, 829. [\[CrossRef\]](#)
168. Dini, I.; Laneri, S. Spices, Condiments, Extra Virgin Olive Oil and Aromas as Not Only Flavorings, but Precious Allies for Our Wellbeing. *Antioxidants* **2021**, *10*, 868. [\[CrossRef\]](#)
169. Dini, I. Contribution of Nanoscience Research in Antioxidants Delivery Used in Nutricosmetic Sector. *Antioxidants* **2022**, *11*, 563. [\[CrossRef\]](#)
170. Dini, I. The Potential of Dietary Antioxidants. *Antioxidants* **2021**, *10*, 1752. [\[CrossRef\]](#)
171. Cavallo, P.; Dini, I.; Sepe, I.; Galasso, G.; Fedele, F.L.; Sicari, A.; Bolletti Censi, S.; Gaspari, A.; Ritieni, A.; Lorito, M.; et al. An Innovative Olive Pâté with Nutraceutical Properties. *Antioxidants* **2020**, *9*, 581. [\[CrossRef\]](#) [\[PubMed\]](#)

172. Dini, I.; Laneri, S. The New Challenge of Green Cosmetics: Natural Food Ingredients for Cosmetic Formulations. *Molecules* **2021**, *26*, 3921. [[CrossRef](#)] [[PubMed](#)]
173. Dini, I.; Laneri, S. Nutricosmetics: A brief overview. *Phytother. Res.* **2019**, *33*, 3054–3063. Dini, I. Bio Discarded from Waste to Resource. *Foods* **2021**, *10*, 2652. [[CrossRef](#)]
174. Fanelli, F.; Cozzi, G.; Raiola, A.; Dini, I.; Mulè, G.; Logrieco, A.F.; Ritieni, A. Raisins and Currants as Conventional Nutraceuticals in Italian Market: Natural Occurrence of Ochratoxin A. *J. Food Sci.* **2017**, *82*, 2306–2312. [[CrossRef](#)]
175. Ajila, C.M.; Brar, S.K.; Verma, M.; Tyagi, R.D.; Godbout, S.; Valéro, J.R. Extraction and analysis of polyphenols: Recent trends. *Crit. Rev. Biotechnol.* **2011**, *31*, 227–249. [[CrossRef](#)]
176. Sridhar, A.; Ponnuchamy, M.; Kumar, P.S.; Kapoor, A.; Vo, D.V.N.; Prabhakar, S. Techniques and Modeling of Polyphenol Extraction from Food: A Review. *Environ. Chem. Lett.* **2021**, *19*, 3409–3443. [[CrossRef](#)]
177. Safdar, M.N.; Kausar, T.; Jabbar, S.; Mumtaz, A.; Ahad, K.; Saddozai, A.A. Extraction and quantification of polyphenols from kinnow (*Citrus reticulata* L.) peel using ultrasound and maceration techniques. *J. Food Drug Anal.* **2017**, *25*, 488–500. [[CrossRef](#)]
178. Čujić, N.; Šavikin, K.; Janković, T.; Pljevljakušić, D.; Zdunić, G.; Ibrić, S. Optimization of polyphenols extraction from dried chokeberry using maceration as traditional technique. *Food Chem.* **2016**, *194*, 135–142. [[CrossRef](#)]
179. Sharma, K.; Ko, E.Y.; Assefa, A.D.; Ha, S.; Nile, S.H.; Lee, E.T.; Park, S.W. Temperature-dependent studies on the total phenolics, flavonoids, antioxidant activities, and sugar content in six onion varieties. *J. Food Drug Anal.* **2015**, *23*, 243–252. [[CrossRef](#)]
180. Reynoso-Camacho, R.; Rodríguez-Villanueva, L.D.; Sotelo-González, A.M.; Ramos-Gómez, M.; Pérez-Ramírez, I.F. Citrus decoction by-product represents a rich source of carotenoid, phytosterol, extractable and non-extractable polyphenols. *Food Chem.* **2021**, *350*, 129239. [[CrossRef](#)] [[PubMed](#)]
181. Moldovan, M.L.; Iurian, S.; Puscas, C.; Silaghi-Dumitrescu, R.; Hanganu, D.; Bogdan, C.; Vlase, L.; Oniga, I.; Benedec, D. A Design of Experiments Strategy to Enhance the Recovery of Polyphenolic Compounds from *Vitis vinifera* By-Products through Heat Reflux Extraction. *Biomolecules* **2019**, *9*, 529. [[CrossRef](#)]
182. Zhang, Q.W.; Lin, L.G.; Ye, W.C. Techniques for extraction and isolation of natural products: A comprehensive review. *Chin. Med.* **2018**, *13*, 20. [[CrossRef](#)]
183. Mushtaq, M.; Sultana, B.; Akram, S.; Anwar, F.; Adnan, A.; Rizvi, S.S.H. Enzyme-assisted supercritical fluid extraction: An alternative and green technology for non-extractable polyphenols. *Anal. Bioanal. Chem.* **2017**, *409*, 3645–3655. [[CrossRef](#)] [[PubMed](#)]
184. Siddeeg, A.; Faisal Manzoor, M.; Haseeb Ahmad, M.; Ahmad, N.; Ahmed, Z.; Kashif Iqbal Khan, M.; Aslam Maan, A.; Mahr-Un-Nisa; Zeng, X.-A.; Ammar, A.-F. Pulsed Electric Field-Assisted Ethanolic Extraction of Date Palm Fruits: Bioactive Compounds, Antioxidant Activity and Physicochemical Properties. *Processes* **2019**, *7*, 585. [[CrossRef](#)]
185. da Rosa, G.S.; Vanga, S.K.; Gariepy, Y.; Raghavan, V. Comparison of microwave, ultrasonic and conventional techniques for extraction of bioactive compounds from olive leaves (*Olea europaea* L.). *Innov. Food Sci. Emerg. Technol.* **2019**, *58*, 102234. [[CrossRef](#)]
186. Zagklis, D.P.; Paraskeva, C.A. Isolation of organic compounds with high added values from agro-industrial solid wastes. *J. Environ. Manag.* **2018**, *216*, 183–191. [[CrossRef](#)]
187. Tapia-Quirós, P.; Montenegro-Landívar, M.F.; Reig, M.; Vecino, X.; Saurina, J.; Granados, M.; Cortina, J.L. Integration of membrane processes for the recovery and separation of polyphenols from winery and olive mill wastes using green solvent-based processing. *J. Environ. Manag.* **2022**, *307*, 114555. [[CrossRef](#)]
188. Alara, O.R.; Abdurahman, N.H.; Ukaegbu, C.I. Soxhlet extraction of phenolic compounds from *Vernonia cinerea* leaves and its antioxidant activity. *J. Appl. Res. Med. Aromat. Plants* **2018**, *11*, 12–17.
189. Ma, Y.; Meng, A.; Liu, P.; Chen, Y.; Yuan, A.; Dai, Y.; Ye, K.; Yang, Y.; Wang, Y.; Li, Z. Reflux Extraction Optimization and Antioxidant Activity of Phenolic Compounds from *Pleioblastus amarus* (Keng) Shell. *Molecules* **2022**, *27*, 362. [[CrossRef](#)]
190. Rodríguez, Ó.; Bona, S.; Stäbler, A.; Rodríguez-Turienzo, L. Ultrasound-Assisted Extraction of Polyphenols from Olive Pomace: Scale up from Laboratory to Pilot Scenario. *Processes* **2022**, *10*, 2481. [[CrossRef](#)]
191. Alchera, F.; Ginepro, M.; Giacalone, G. Microwave-Assisted Extraction of Polyphenols from Blackcurrant By-Products and Possible Uses of the Extracts in Active Packaging. *Foods* **2022**, *11*, 2727. [[CrossRef](#)] [[PubMed](#)]
192. Farias-Campomanes, A.M.; Rostagno, M.A.; Coaquira-Quispe, J.J.; Meireles, M.A.A. Supercritical fluid extraction of polyphenols from lees: Overall extraction curve, kinetic data and composition of the extracts. *Bioresour. Bioprocess.* **2015**, *2*, 45. [[CrossRef](#)]
193. Yong, D.; Ting, J.; Jun, X. Circulating Polyphenols Extraction System with High-Voltage Electrical Discharge: Design and Performance Evaluation. *Sustain. Chem. Eng.* **2018**, *6*, 15402–15410.
194. Lakka, A.; Bozinou, E.; Makris, D.P.; Lalas, S.I. Evaluation of Pulsed Electric Field Polyphenol Extraction from *Vitis vinifera*, *Sideritis scardica* and *Crocus sativus*. *ChemEngineering* **2021**, *5*, 25. [[CrossRef](#)]
195. Heemann, A.C.W.; Heemann, R.; Kalegari, P.; Spier, M.R.; Santin, E. Enzyme-assisted extraction of polyphenols from green yerba mate. *Braz. J. Food Technol.* **2019**, *22*, e2017222. [[CrossRef](#)]
196. Meini, M.-R.; Cabezudo, I.; Boschetti, C.E.; Romanini, D. Recovery of phenolic antioxidants from Syrah grape pomace through the optimization of an enzymatic extraction process. *Food Chem.* **2019**, *283*, 257–264. [[CrossRef](#)]
197. Ciccone, L.; Piragine, E.; Brogi, S.; Camodeca, C.; Fucci, R.; Calderone, V.; Nencetti, S.; Martelli, A.; Orlandini, E. Resveratrol-like Compounds as SIRT1 Activators. *Int. J. Mol. Sci.* **2022**, *23*, 15105. [[CrossRef](#)]

198. Rudrapal, M.; Khairnar, S.J.; Khan, J.; Dukhyil, A.B.; Ansari, M.A.; Alomary, M.N.; Alshabrm, F.M.; Palai, S.; Deb, P.K.; Devi, R. Dietary Polyphenols and Their Role in Oxidative Stress-Induced Human Diseases: Insights into Protective Effects, Antioxidant Potentials and Mechanism(s) of Action. *Front. Pharm.* **2022**, *13*, 806470. [[CrossRef](#)]
199. Pimentel-Moral, S.; Verardo, V.; Robert, P.; Segura-Carretero, A.; Martínez-Férez, A. 13—Nanoencapsulation strategies applied to maximize target delivery of intact polyphenols. In *Encapsulations*; Grumezescu, A.M., Ed.; Academic Press: Cambridge, MA, USA, 2016; pp. 559–595.
200. Ivanov, M.; Novović, K.; Malešević, M.; Dinić, M.; Stojković, D.; Jovčić, B.; Soković, M. Polyphenols as Inhibitors of Antibiotic Resistant Bacteria-Mechanisms Underlying Rutin Interference with Bacterial Virulence. *Pharmaceuticals* **2022**, *15*, 385. [[CrossRef](#)]
201. Acosta, E. Bioavailability of nanoparticles in nutrient and nutraceutical delivery. *Curr. Opin. Colloid Interface Sci.* **2009**, *14*, 3–15. [[CrossRef](#)]
202. Wang, J.; Byrne, J.D.; Napier, M.E.; DeSimone, J.M. More Effective Nanomedicines through Particle Design. *Small* **2011**, *7*, 1919–1931. [[CrossRef](#)] [[PubMed](#)]
203. Mohammadian, M.; Salami, M.; Momen, S.; Alavi, F.; Emam-Djomeh, Z. Fabrication of curcumin-loaded whey protein microgels: Structural properties, antioxidant activity, and in vitro release behavior. *LWT* **2019**, *103*, 94–100. [[CrossRef](#)]
204. Caballero, S.; Li, Y.O.; McClements, D.J.; Davidov-Pardo, G. Encapsulation and delivery of bioactive citrus pomace polyphenols: A review. *Crit. Rev. Food Sci. Nutr.* **2022**, *62*, 8028–8044. [[CrossRef](#)] [[PubMed](#)]
205. Pandey, K.B.; Rizvi, S.I. Role of red grape polyphenols as antidiabetic agents. *Integr. Med. Res.* **2014**, *3*, 119–125. [[CrossRef](#)] [[PubMed](#)]
206. Lin, Y.-H.; Lin, J.-H.; Hong, Y.-S. Development of chitosan/poly- $\gamma$ -glutamic acid/pluronic/curcumin nanoparticles in chitosan dressings for wound regeneration. *J. Biomed. Mater. Res. Part B Appl. Biomater.* **2017**, *105*, 81–90. [[CrossRef](#)]
207. Raja, I.S.; Preeth, D.R.; Vedhanayagam, M.; Hyon, S.-H.; Lim, D.; Kim, B.; Rajalakshmi, S.; Han, D.-W. Polyphenols-loaded electrospun nanofibers in bone tissue engineering and regeneration. *Biomater. Res.* **2021**, *25*, 29. [[CrossRef](#)]
208. Drago, E.; Campardelli, R.; Pettinato, M.; Perego, P. Innovations in Smart Packaging Concepts for Food: An Extensive Review. *Foods* **2020**, *9*, 1628. [[CrossRef](#)]
209. García Ibarra, V.; Rodríguez Bernaldo de Quirós, A.; Paseiro Losada, P.; Sendón, R. Non-target analysis of intentionally and non intentionally added substances from plastic packaging materials and their migration into food simulants. *Food Packag. Shelf Life* **2019**, *21*, 100325. [[CrossRef](#)]
210. Pilevar, Z.; Bahrami, A.; Beikzadeh, S.; Hosseini, H.; Jafari, S.M. Migration of styrene monomer from polystyrene packaging materials into foods: Characterization and safety evaluation. *Trends Food Sci. Technol.* **2019**, *91*, 248–261. [[CrossRef](#)]
211. Yildirim, S.; Röcker, B.; Pettersen, M.K.; Nilsen-Nygaard, J.; Ayhan, Z.; Rutkaite, R.; Radusin, T.; Suminska, P.; Marcos, B.; Coma, V. Active Packaging Applications for Food. *Compr. Rev. Food Sci. Food Saf.* **2018**, *17*, 165–199. [[CrossRef](#)] [[PubMed](#)]
212. Hassan, B.; Chatha, S.A.S.; Hussain, A.I.; Zia, K.M.; Akhtar, N. Recent advances on polysaccharides, lipids and protein based edible films and coatings: A review. *Int. J. Biol. Macromol.* **2018**, *109*, 1095–1107. [[CrossRef](#)] [[PubMed](#)]
213. Fierascu, R.C.; Sieniawska, E.; Ortan, A.; Fierascu, I.; Xiao, J. Fruits By-Products—A Source of Valuable Active Principles. A Short Review. *Front. Bioeng. Biotechnol.* **2020**, *8*, 319. [[CrossRef](#)] [[PubMed](#)]
214. Chaouch, M.A.; Benvenuti, S. The Role of Fruit by-Products as Bioactive Compounds for Intestinal Health. *Foods* **2020**, *9*, 1716. [[CrossRef](#)]
215. Vasile, C.; Baican, M. Progresses in Food Packaging, Food Quality, and Safety-Controlled-Release Antioxidant and/or Antimicrobial Packaging. *Molecules* **2021**, *26*, 1263. [[CrossRef](#)]
216. Yong, H.; Liu, J. Active packaging films and edible coatings based on polyphenol-rich propolis extract: A review. *Compr. Rev. Food Sci. Food Saf.* **2021**, *20*, 2106–2145. [[CrossRef](#)]
217. Latos-Brozio, M.; Masek, A. Effect of Impregnation of Biodegradable Polyesters with Polyphenols from *Cistus linnaeus* and *Juglans regia* Linnaeus Walnut Green Husk. *Polymers* **2019**, *11*, 669. [[CrossRef](#)]
218. Shahbazi, Y.; Shavisi, N. A novel active food packaging film for shelf-life extension of minced beef meat. *J. Food Saf.* **2018**, *38*, e12569. [[CrossRef](#)]
219. Mascheroni, E.; Guillard, V.; Nalin, F.; Mora, L.; Piergiovanni, L. Diffusivity of propolis compounds in Poly(lactic acid) polymer for the development of anti-microbial packaging films. *J. Food Eng.* **2010**, *98*, 294–301. [[CrossRef](#)]
220. Shao, P.; Niu, B.; Chen, H.; Sun, P. Fabrication and characterization of tea polyphenols loaded pullulan-CMC electrospun nanofiber for fruit preservation. *Int. J. Boil. Macromol.* **2018**, *107*, 1908–1914. [[CrossRef](#)]



Review

# Dihydrochalcones in Sweet Tea: Biosynthesis, Distribution and Neuroprotection Function

Yong-Kang Wang<sup>1</sup>, Si-Yi Hu<sup>1</sup>, Feng-Yi Xiao<sup>1</sup>, Zhan-Bo Dong<sup>2</sup>, Jian-Hui Ye<sup>1</sup>, Xin-Qiang Zheng<sup>1</sup>, Yue-Rong Liang<sup>1</sup> and Jian-Liang Lu<sup>1,\*</sup><sup>1</sup> Tea Research Institute, Zhejiang University, Hangzhou 310058, China<sup>2</sup> Agricultural and Rural Bureau of Pingyang County, Wenzhou 325499, China

\* Correspondence: jllu@zju.edu.cn; Tel./Fax: +86-571-88982704

**Abstract:** Sweet tea is a popular herbal drink in southwest China, and it is usually made from the shoots and tender leaves of *Lithocarpus litseifolius*. The sweet taste is mainly attributed to its high concentration of dihydrochalcones. The distribution and biosynthesis of dihydrochalcones in sweet tea, as well as neuroprotective effects in vitro and in vivo tests, are reviewed in this paper. Dihydrochalcones are mainly composed of phloretin and its glycosides, namely, trilobatin and phloridzin, and enriched in tender leaves with significant geographical specificity. Biosynthesis of the dihydrochalcones follows part of the phenylpropanoid and a branch of flavonoid metabolic pathways and is regulated by expression of the genes, including *phenylalanine ammonia-lyase*, *4-coumarate: coenzyme A ligase*, *trans-cinnamic acid-4-hydroxylase* and *hydroxycinnamoyl-CoA double bond reductase*. The dihydrochalcones have been proven to exert a significant neuroprotective effect through their regulation against A $\beta$  deposition, tau protein hyperphosphorylation, oxidative stress, inflammation and apoptosis.

**Keywords:** *Lithocarpus litseifolius*; trilobatin; phloridzin; phloretin; metabolic pathway; bioactivity

**Citation:** Wang, Y.-K.; Hu, S.-Y.; Xiao, F.-Y.; Dong, Z.-B.; Ye, J.-H.; Zheng, X.-Q.; Liang, Y.-R.; Lu, J.-L.

Dihydrochalcones in Sweet Tea: Biosynthesis, Distribution and Neuroprotection Function. *Molecules* **2022**, *27*, 8794. <https://doi.org/10.3390/molecules27248794>

Academic Editor: Nour Eddine Es-Safi

Received: 19 November 2022

Accepted: 9 December 2022

Published: 12 December 2022

**Publisher's Note:** MDPI stays neutral with regard to jurisdictional claims in published maps and institutional affiliations.



**Copyright:** © 2022 by the authors. Licensee MDPI, Basel, Switzerland. This article is an open access article distributed under the terms and conditions of the Creative Commons Attribution (CC BY) license (<https://creativecommons.org/licenses/by/4.0/>).

## 1. Introduction

Tea is one of the most popular beverages worldwide. In addition to the traditional tea made from the leaves of *Camellia sinensis* (L.) O. Kuntze, herbal teas are regionally consumed and usually made from the leaves or other tissues of multifarious plants, such as sweet tea (*Lithocarpus litseifolius*), camomile (*Chrysanthemum lavandulifolium*), jasmine (*Jasminum sambac*), *Dracocephalum rupestre*, honeysuckle (*Lonicera japonica*) and *Litsea coreana* var. *lanuginosa*. The *Lithocarpus litseifolius* has usually been called sweet tea or sweet leaf tree by the local residents since the products made from its leaves taste quite sweet. In China, the plucked shoots and tender leaves are often manufactured according to protocols similar to green tea or black tea, the annual output of the sweet tea product is estimated to exceed 2000 t, and these products are commonly consumed by local people in some provinces along the Yangtze River, such as Sichuan, Chongqing, Hunan and Jiangxi. The sweet tea has attracted much more attention recently because of its unique taste and health benefits, which are attributed to dihydrochalcones (DHCs) such as trilobatin, phloridzin and phloretin. DHCs are a class of flavonoids characterized by a basic C<sub>6</sub>-C<sub>3</sub>-C<sub>6</sub> backbone structure and the absence of a heterocyclic C ring. DHCs are considered to be the primary precursors and represent important intermediates in the synthesis of flavonoids [1,2]. DHCs, especially phloretin, phloridzin and trilobatin, have a variety of health effects, like antioxidant activity [3], anti-inflammation [4,5], antidiabetic activity [6,7], cardioprotection [8], intestinal protection [9], hepatoprotective effect [10], anticancer activity [11] and neuroprotection [12]. With an increase in the population aging, the incidence of neurodegenerative diseases has increased dramatically [13]. Neurodegenerative diseases mainly include Alzheimer's disease (AD), Parkinson's disease (PD), stroke and so on. In folk experience, drinking sweet tea can often be used to prevent and treat neurodegenerative diseases, which might be attributed to the effect of DHCs. Nowadays, DHCs have been

well studied in *Malus pumila* Mill., being 25.6–113.7 mg/g DW in leaves [14] and 99.9 mg/g DW in immature fruits. These are natural sources for the DHCs' separation and utilization. However, the sweet tea can also be considered as an alternative source of the DHCs because of its high level of these compounds. This review introduces the physiological and biochemical characteristics of the sweet tea, summarizes the DHCs biosynthesis and the influencing factors, and finally elaborates on the neuroprotection of the sweet tea and its related mechanisms.

## 2. Physio-Biochemical Characteristics of the Sweet Tea

### 2.1. Morphological Characteristics

*Lithocarpus polystachyus* or *Lithocarpus litseifolius* have been used to refer to the sweet tea tree in published reports. According to WFO ([www.worldfloraonline.org](http://www.worldfloraonline.org) (accessed on 1 January 2020)), *Lithocarpus polystachyus* is an evergreen arbor in the genus *Lithocarpus* of the family *Fagaceae*. It was first reported as *Quercus polystachya* Wall. ex A. DC. in 1864, then renamed as *Pasania polystachya* (Wall. ex A. DC.) Oerst. in 1871 and *Synaedrys polystachya* (Wall. ex A. DC.) Koidz. in 1916. Later, it was finally designated as *Lithocarpus polystachyus* (Wall. ex A. DC.) Rehder in 1919. *Lithocarpus litseifolius* is also a species belonging to the genus *Lithocarpus* in the family *Fagaceae*. This species was first reported as *Quercus litseifolia* Hance in 1884, then renamed as *Pasania litseifolia* (Hance) Schottky in 1912 and *Synaedrys litseifolia* (Hance) Koidz. in 1916, and finally designated as *Lithocarpus litseifolius* (Hance) Chun in 1928. However, according to FOC ([www.eFloras.org](http://www.eFloras.org), (accessed on 2 March 2021)), these two species are synonyms and belong to the same variety of *Lithocarpus litseifolius*, namely, *Lithocarpus litseifolius* var. *Litseifolius*, as shown in Figure 1, because of their similar morphological characteristics and overlapping geographical distributions. This variety mainly distributes in south China, Laos, northeast Myanmar, northern Vietnam and India [15,16]. In addition to the var. *litseifolius*, another var. *pubescens* Huang has also been found and identified in dense forests of Tian'e County, Guangxi, China. Main morphological differences have been screened out from these two varieties, i.e., the branchlets and infructescences rachis, the cupule size and the fruit ripening time. Glabrous branchlets, sparsely pubescent infructescences rachis, 0.8–1.4 cm cupule diameter and fruit ripening in Jun–Oct has been observed in the former, while puberulent branchlets and infructescences rachis, relatively big cupule (1.2–1.5 cm in diameter) and early fruit ripening time (in April–May) have been witnessed in the latter. In this review, *Lithocarpus litseifolius* is used to refer to all the sweet tea, including the two varieties and the synonymous plants. The sweet tea is a common light-loving and drought-tolerant tree species in the mountain area and usually possesses big elliptic leaves around 8–18 cm in length and 3–8 cm in broadness, ~25 cm male inflorescences in a panicle and ~35 cm female inflorescences with two to six spikes. Its tender leaves or shoots can be picked two to three times a year, but leaf-picking is quite difficult because the tree can grow up to 20 m under natural conditions; therefore, pruning usually has been performed to control the height of the tree below 1.5 m for improving the picking efficiency. Up to now, products in the market are mainly harvested from wild resources since this plant has not been popularly cultivated. Although sweet tea can be propagated through cuttings and seeds similar to the *Camellia sinensis*, sexual propagation through seeds is mainly adopted, which will lead to production difficulties because of the mixed genetic background of the trees.

### 2.2. Concentration of the DHCs and Influence Factors

The sweet tea contains diverse secondary metabolites. Eighteen terpenoids have been identified from cupules [17,18] and 35 flavonoids, including flavones, flavonols, dihydroflavones, isoflavones and DHCs, are detected in stems [19]. Meanwhile, seven triterpenoids are isolated from the leaves and twigs [20], 268 volatiles are identified from young leaves [21] and 68 phenolic compounds have been quantified and quantified from leaves [22]. In this respect, the leaves are the main economic parts of the sweet tea. Among these metabolites, DHCs are the most abundant component in sweet tea. Research showed that the content and composition of the DHCs are influenced by many factors, such as geographical distribution of the trees, leaf maturity and harvest time (Table 1). Yang et al. reported that the abundance of the DHCs is significantly correlated with latitude negatively

as well as temperature and soil organic matter and nitrogen content positively [23]. With the decline of latitude, the growth and development of the sweet tea tree will be positively stimulated by an increase in the average annual temperature and rainfall; therefore, increased leaf area, broadened vein distance and accelerated growth rate of the trees have usually been observed in the low latitude area [24–28]. In the sweet tea, trilobatin, phloridzin and phloretin are the main DHCs. The content of these compounds varies with the tissues and organs of the sweet tea tree. With an increase in the maturity of leaves, the phloridzin level increases, and trilobatin decreases [26]; meanwhile, the level of phloretin is relatively low and changes little. Thus, a high level of trilobatin is usually observed in the tender leaves, with a content of about 14–28%, while accumulated phloridzin is witnessed in the mature and old leaves [25]. For the same plant, the content of the three DHCs in tender leaves fluctuates with the harvest time. The content of trilobatin peaks in April, and the phloridzin peaks in April and August [24]. This implies that the DHCs may possess important biological functions for the growth and development of the plant. When the phloridzin biosynthesis was blocked through transgenic operation, the genetically modified ‘Royal Gala’ apple showed a series of severe phenotypic changes, including stunted growth, reduced internode length, narrowed leaf, increased lateral branches and weakened adventitious roots [29]. Exogenous supplementation of phloridzin to the genetically modified apple tree would enhance axial leaf growth and partially restore the leaf to a ‘normal’ shape [30]. Moreover, phloridzin biosynthesis would promote photosynthetic carbon accumulation but limit nitrogen accumulation via the shoot-dependent nitrogen assimilation pathway in apples [31]. In general, high-level phloridzin in mature leaves may help to maintain the morphological and physiological functions of the leaves by regulating photosynthesis and resistance. However, the exact physiological effect has not been clearly revealed till now, and much more research needs to be carried out to elucidate the accumulation mechanism and physiological roles of the DHCs, especially in sweet tea trees. The processing method will remarkably affect the composition and content of the DHCs in the sweet tea. At present, the harvested leaves of the sweet tea have usually been made into “green tea” and “black tea” by adopting traditional tea processing technologies. Fixation, as a characteristic step of green tea processing, can denature the enzymes of fresh leaves and maximally maintain the color and composition of the raw materials through heating at high temperatures in a short time. Four fixation styles, including roller-fixation, microwave-fixation, steam-fixation and fry-fixation, were tested, and the results showed that retention of the different DHCs changed with the fixation styles. The content of the phloretin in products followed the order: fry-fixation > roller-fixation > microwave-fixation > steam-fixation. The level of the phloridzin was highest in products through microwave-fixation, a medium through steam-fixation and roller-fixation, and lowest through fry-fixation. The highest trilobatin was observed in roller-fixation treated products, medium in microwave-fixation and fry-fixation treated products and lowest in steam-fixation treated products [32]. This indicated that the different DHCs might possess various thermal sensitivities and could transform among them during heat treatment. Fermentation is the key step of black tea processing. After fermentation, the contents of total polyphenols, trilobatin and phloridzin in the sweet tea were decreased by 26.36%, 10.24% and 39.37%, respectively [33]. This suggested that the redox activity of meta hydroxyls is higher than that of para hydroxyls. In addition, the level of phloridzin extracted from the sweet tea leaves fermented with *Saussurea* bacteria is much higher than that of the naturally fermented and unfermented leaves [34]. Studies also showed that the drying method would impact the level of phenolics in sweet tea, and freeze-drying could retain the highest level of phenolics [35].



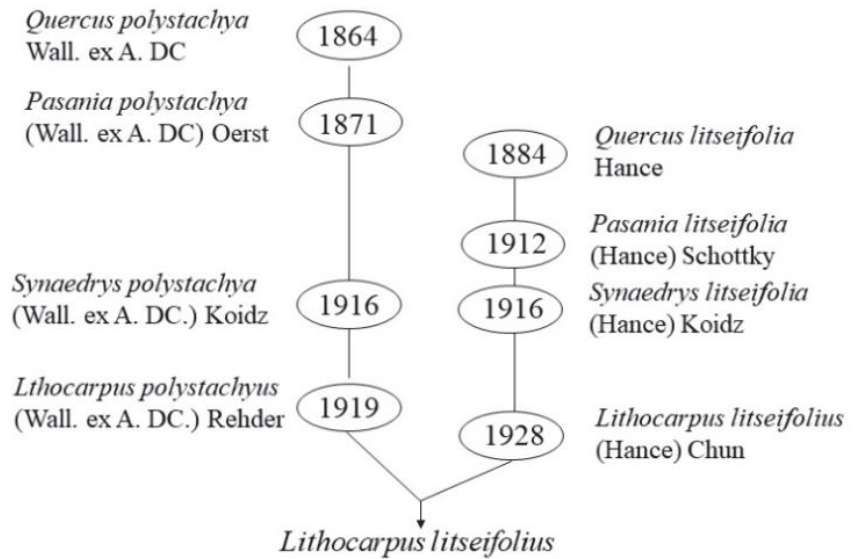


Figure 1. The change of scientific name of the sweet tea.

Table 1. Effect of the location, picking time and leaf maturity on the content of DHCs in the sweet tea.

Influencing Factors	Content (mg/g)			Reference
	Trilobatin	Phloridzin	Phloretin	
<b>Picking time</b>				
April	257.52–279.74	11.44–22.34	0.13–0.55	[24,26]
November	30.94–33.59	143.12–208.31	0.11–0.44	
<b>Leaf maturity</b>				
Tender leaf	82.90–279.74	9.30–57.40	1.90–2.50	[24,36,37]
Old leaf	19.30–128.80	144.60–208.31	3.60–4.30	
<b>Location</b>				
Sichuan	73.32–278.15	4.89–62.87	0.08–1.25	[24–26,33,36,37]
Chongqing	41.87–133.98	14.90–31.69	0.10–1.39	
Guangxi	0.90–198.70	4.80–144.60	4.98	
Hunan	171.95–272.35	8.35–19.25	0.18–1.01	
Jiangxi	69.56–183.84	11.58–49.84	0.27–4.16	
Guizhou	161.42–176.90	5.26–7.46	0.36–0.38	
Yunnan	4.87–264.60	0.61–208.29	0.27–1.55	
Guangdong	0.44–60.62	20.29–57.33	Not mentioned	
Fujian	185.47–244.56	7.83–19.24	0.48–1.19	

### 3. DHCs Biosynthesis and Its Regulation

Trilobatin and phloridzin, being positional isomers of the glycosidically bound phloretin, are produced through a side branch of the phenylpropanoids and flavonoids pathways (Figure 2) [38] which is initiated from cleavage of phenylalanine catalyzed by phenylalanine ammonia-lyase (PAL). The first committed step of the DHCs biosynthesis is the conversion of p-dihydrocoumaryl-CoA from p-coumaryl-CoA, which can be catalyzed by a hydroxycinnamoyl-CoA double bond reductase (HCDBR) [39]. Then phloretin will be produced from the p-dihydrocoumaryl-CoA and

three units of malonyl-CoA through decarboxylative condensation and cyclization mediated by chalcone synthase (CHS) [40]. Finally, biosynthesis of phloridzin and trilobatin requires the action of UDP-glycosyltransferases (UGTs), also called phloretin-2'-O-glycosyltransferase (P2'GT) and phloretin-4'-O-glycosyltransferase (P4'GT), to attach a glucose moiety at either 2' or 4' positions of the phloretin A-ring [1,41]. UGTs catalyze glycosylation of the flavonoids in the plant, and members of the *UGT88Fs* subfamily encode P2'GT and P4'GT, which are responsible for the glycosylation of phloretin in apples [41–45]. *UGT88F1* was the firstly cloned gene encoding the P2'GT in apples [42]. The exogenously expressed P2'GT by *UGT88F1* can specifically glycosylate the phloretin in the presence of UDP-glucose, UDP-xylose and UDP-galactose, but not toward caffeic acid, chlorogenic acid, coumaric acid, cyanidin, 3,4-dihydroxyhydrocinnamic acid, 3-hydroxybenzoic acid, naringenin, 3,4-dihydroxybenzoic acid, catechin, epicatechin, quercetin and rutin. Reports showed that the enzymes encoded by *UGT71A15* and *UGT71K1* of apple can also convert phloretin into phloridzin in vitro [45], while *UGT75L17* of apple encodes P4'GT which catalyzes the 4' position glycosylation of phloretin to produce the trilobatin in the presence of UDP-glucose [41]. Overexpression of the *UGT75L17* in *Escherichia coli* can be used for efficiently producing trilobatin from phloretin [46]. *UGT71A16*, *UGT71K2* and *UGT88F2* isolated from pear, the relative homolog of *UGT71A15*, *UGT71K1* and *UGT88F1* in apple, can encode the enzymes to synthesize phloridzin from phloretin [45]. This indicated that the biosynthesis limitation of phloridzin and analogs in pear is due to unable formation of phloretin or its precursor(s) rather than a lack of glycosyltransferases. Studies also revealed that trilobatin can be produced through the hydrogenation of the naringin and then hydrolysis with  $\alpha$ -L-rhamnosidase in aqueous medium [47]; however, this pathway might not exist under physiological conditions. In the sweet tea tree, *chalcone isomerase* (*CHI*), *leucoanthocyanidin reductase* (*LAR*), *flavone 3-hydroxylase* (*F3H*) and *4-coumarate: coenzyme A ligase* (*4CL*) have been cloned, and expression of the *LAR* and *4CL* is positively correlated with DHCs content significantly [48–51].

The biosynthesis of phloridzin is mainly influenced by light quality, light intensity and photoperiod. The phloridzin content in the sweet tea leaves decreases in the red or blue light treatment and increases in the green light treatment compared with natural light. The content increases with prolonging the illumination time from 8 h to 14 h and with increasing the intensity from 12.5 to 37.5  $\mu\text{mol}\cdot\text{m}^{-2}\cdot\text{s}^{-1}$  in the white light treatment. The change in the phloridzin level is consistent with the expression of *PAL* and *4CL* genes [15]. Thus, the effect of the light on the phloridzin accumulation is mainly regulated by the expression of the genes involved in the early steps of the phenylpropanoid pathway, which might be used to explain the fluctuation of the DHCs along with the change of the season and latitude. In addition, DHCs biosynthesis may also be modulated by hormone level and development status because the accumulation of phloridzin and trilobatin regularly changes with the increase of leaf maturity.

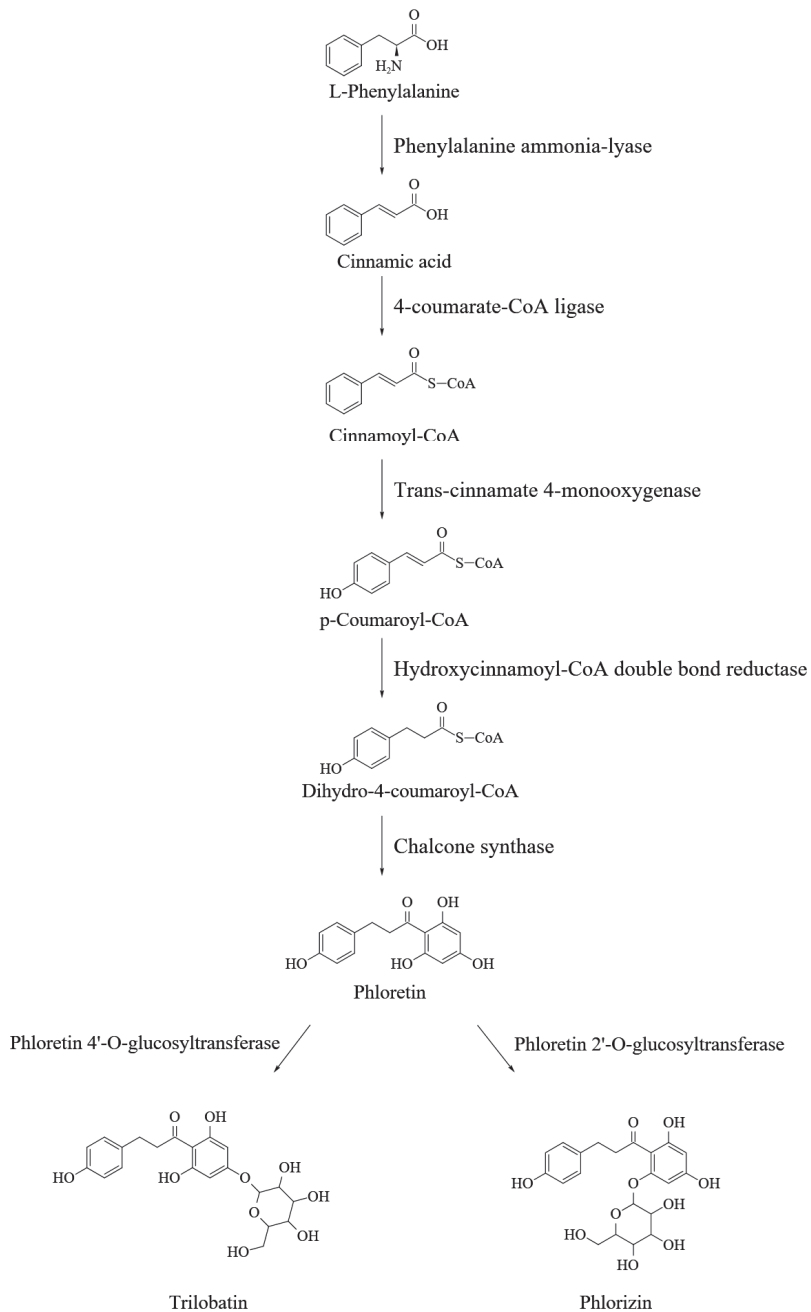


**Figure 2.** Biosynthesis pathway of the DHCs.

#### 4. Neuroprotective Effects of the DHCs

AD, PD and stroke are the main neurological disorders. The pathogenesis of AD is related to amyloid  $\beta$ -protein ( $A\beta$ ) deposition, formation of nerve fiber tangles (NFTs) through abnormal phosphorylation of tubulin-associated unit (Tau) protein, and synaptic dysfunction. PD syndrome is characterized by the degenerative death of dopaminergic

neurons in the midbrain substantia nigra, decreased dopamine concentration in the striatum, and the formation of a Lewy body. The DHCs might exert their neuroprotective effects either directly by inhibiting or alleviating the neurological damage or indirectly by preventing the nervous tissue from oxidative stress, inflammation and apoptosis (Table 2).

**Table 2.** Neuroprotective effects of the DHCs.

Compound and Effects	Treatment	Model	Reference
<b>Trilobatin</b>			
Decrease the phosphorylation of p38	12.5, 25, and 50 $\mu$ M	A $\beta$ <sub>25–35</sub> -induced HT22 cells	[52]
Reduce the production of A $\beta$ by decreasing the BACE1 levels	10 or 20 mg/kg	3 $\times$ FAD AD model mice	[53]
Activate the AMPK signaling pathway to respond the oxidative stress	15, 30 and 60 $\mu$ M	H <sub>2</sub> O <sub>2</sub> -induced injury PC12 cells	[12]
Increase <i>Sirt3</i> expression and activity	5, 10 and 20 mg/kg	MCAO-induced focal cerebral ischemia rats	[54]
Activate the Nrf2/ARE pathway	10, 20, and 40 $\mu$ M	Isoflurane-induced HT22 cells	[55]
<b>Phloretin</b>			
Protect synaptophysin and improve neuron cells	5 mg/kg	A $\beta$ <sub>1–42</sub> -injected male Wistar rats	[56]
Inhibit the A $\beta$ accumulation through antioxidation and anti-inflammation	2.5 and 5 mg/kg	A $\beta$ <sub>25–35</sub> -induced sporadic Alzheimer’s disease rats	[57]
Inhibit the activation of microglia and astrocytes	5 mg/kg	MPTP-induced Parkinson’s disease mice	[58]
Improve the activity of neuron cells via normalizing the AChE activity and alleviating reactive gliosis	2.5, 5 and 10 mg/kg	Scopolamine induced amnesia mice	[59]
Up-regulate the transcription and translation of <i>Nrf2</i>	40 and 80 mg/kg	Cerebral ischemia/reperfusion rats	[60]
<b>Phloridzin</b>			
Normalize neural signaling and exhibit anti-inflammatory effect	10 or 20 mg/kg	Lipopolysaccharide-induced cognitive impairment mice	[61]

#### 4.1. Prevention and Treatment of Neurological Diseases

Under normal physiological conditions, amyloid precursor protein (APP) can be digested by  $\alpha$ -secretase to produce soluble  $\alpha$ -APP fragment (sAPP $\alpha$ ) and 83-amino-acid membrane-bound C-terminal fragment (C83), and then the C83 is cleaved by  $\gamma$ -secretase to produce non-toxic fragments. However, when the APP is cleaved by  $\beta$ -secretase, soluble  $\beta$ -APP (sAPP $\beta$ ) and 99-amino-acid C-terminal (C99) fragments will be generated, and then the C99 will be digested by  $\gamma$ -secretase to produce a variety of A $\beta$  peptides containing 39–42 amino acid residues. The A $\beta$  monomers can spontaneously aggregate and deposit into oligomers, fibrils and senile plaques, which then induce oxidative injury, microglial and astrocytic activity as well as alter kinase/phosphatase activity, eventually leading to neuronal death and AD [62]. Recent reports showed that trilobatin and phloretin can decrease A $\beta$  deposition by down-regulating the expression of *beta-site APP cleaving enzyme 1 (BACE1)* and consequentially decreasing the  $\beta$ -secretase [53]. Oral administration with 20 mg/kg trilobatin could protect 3  $\times$  FAD (familial Alzheimer’s disease) mice from neurological damage by alleviating A $\beta$  deposition, synaptic degeneration, astrocytosis and microgliosis activation, neuronal loss and cognitive deficits [53]. Phloretin could also suppress A $\beta$  aggregation in the dentate gyrus and CA1 (Cornu Ammonis region 1) regions of the hippocampus in the A $\beta$ -induced AD rats [57]. Furthermore, the A $\beta$ <sub>1–42</sub> impaired plasticity at the neuronal and presynaptic levels could be restored to normal value by phloretin treatment [56].

Tau is a main microtubule-associated protein of neurons and plays a critical role in microtubule assembly and stability maintenance. Abnormal hyperphosphorylation of tau neutralizes the basic inhibitory domains and enables tau–tau interaction, resulting in the formation of NFTs in nerve cells, consequently causing the disintegration of tubulins and collapse of the delivery system, eventually leading to the death of the nerve cell. At present, it is well known that glycogen synthase kinase-3 $\beta$  (GSK-3 $\beta$ ) and protein phosphatase 2A

(PP2A) are the two most important enzymes which can regulate the phosphorylation of tau protein. In mice, treatment of trilobatin can directly inhibit the hyperphosphorylation of tau at Ser396 and Ser202 sites and indirectly alleviate the phosphorylation of tau through suppressing the hyperphosphorylation of GSK-3 $\beta$  which acts as a Tau kinase [53], as shown in Figure 3.

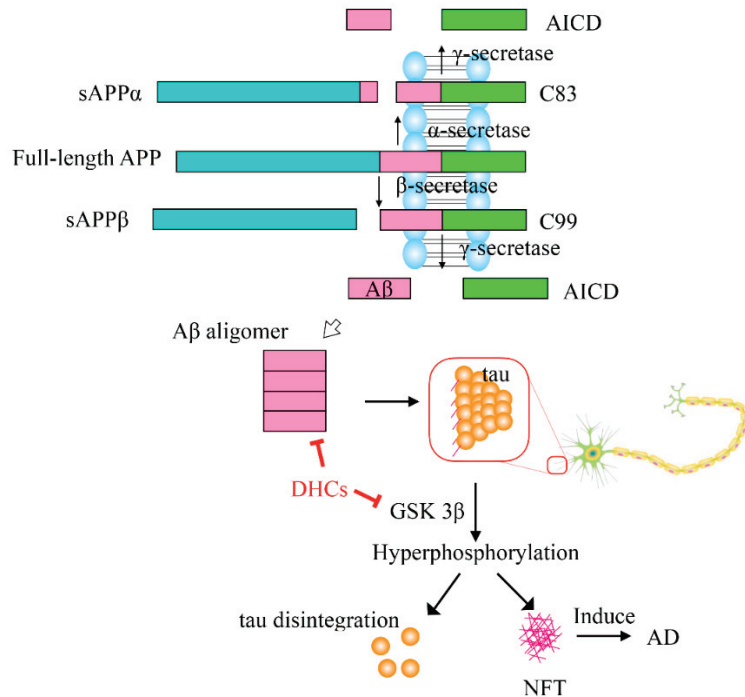


**Figure 3.** Directly neuroprotective effects of the DHCs. APP, amyloid precursor protein; sAPP $\alpha$ , soluble  $\alpha$ -APP fragment; C83, 83-amino-acid membrane-bound C-terminal fragment; AICD, APP intracellular domain; sAPP $\beta$ , soluble  $\beta$ -APP; C99, 99-amino-acid C-terminal; A $\beta$ , amyloid  $\beta$ -protein; GSK 3 $\beta$ , glycogen synthase kinase 3 $\beta$ ; NFT, Nerve Fiver Tangles. Arrow ( $\rightarrow$ ) indicates activation, and the blunt arrow ( $-$ ) indicates inhibition.

#### 4.2. Antioxidative Effect

It is widely presumed that excessive radical oxygen species (ROS) would lead to a variety of neurological diseases. Trilobatin is able to maintain mitochondrial ROS homeostasis by inhibiting overproduction and promoting the elimination of ROS. Regulation of trilobatin against ROS might carry out mainly by influencing the oxidative stress signal transduction (Figure 4). Pretreatment with trilobatin can stimulate AMP-activated protein kinase (AMPK) phosphorylation which will consequently trigger activation of peroxisome proliferators activated receptor- $\gamma$  coactivator-1 $\alpha$  (PGC-1 $\alpha$ ) and estrogen-related receptor  $\alpha$  (ERR $\alpha$ ), and then the activated ERR $\alpha$  will bind to the ERR $\alpha$  response element (ERRE) of sirtuin 3 (*Sirt3*) promoter to activate the transcription of *Sirt3* which encodes a major mitochondria NAD $^{+}$ -dependent deacetylase, or the activated PGC-1 $\alpha$  will accelerate the disassociation of complex Kelch-like ECH-associated protein 1 (Keap-1)/Nuclear respiratory factor 2 (Nrf2) to provoke translocation of the key transcript factor Nrf2 from the cytoplasm into nucleus which can activate the transcription of *Sirt3* through recognizing and binding to antioxidant response element (ARE) of the *Sirt3* promoter. The elevated *Sirt3* will promote superoxide dismutase 2 (SOD2) deacetylation, which can boost ROS scavenging. It was confirmed that trilobatin protected HT22 cells against isoflurane-induced neurotoxicity mainly via activating the Nrf/ARE pathway [55], and phloretin

could also eliminate the oxidative stress of the cerebral ischemia/reperfusion rats mainly through activating the Nrf2 defense pathway [60]. The study also showed that trilobatin could reverse the cytotoxicity of HT22 cells induced by the A $\beta_{25-35}$  treatment partially by inhibiting the oxidative injury mediated by mitogen-activated protein kinase p38 (p38)/Sirt3 pathway [52]. In addition, trilobatin can exert antioxidant capacity by improving the activities of NADH-ubiquinone oxidoreductase and ATPase and balancing the NAD<sup>+</sup>/NADH ratio [12]. However, the antioxidative effects of phloretin and phloridzin cannot be achieved by increasing the activity of enzymes such as SOD or catalase (CAT). However, they can directly scavenge the superoxide anions generated from both the electron transfer chain reactions of NADH-ubiquinone oxidoreductase /FMN/Fe-S clusters (complex I) and ubiquinone-cytochrome c oxidoreductase/cytochrome b/ Fe-S clusters (complex III) in human SH-SY5Y neuronal-like cells treated with inducer rotenone [63].

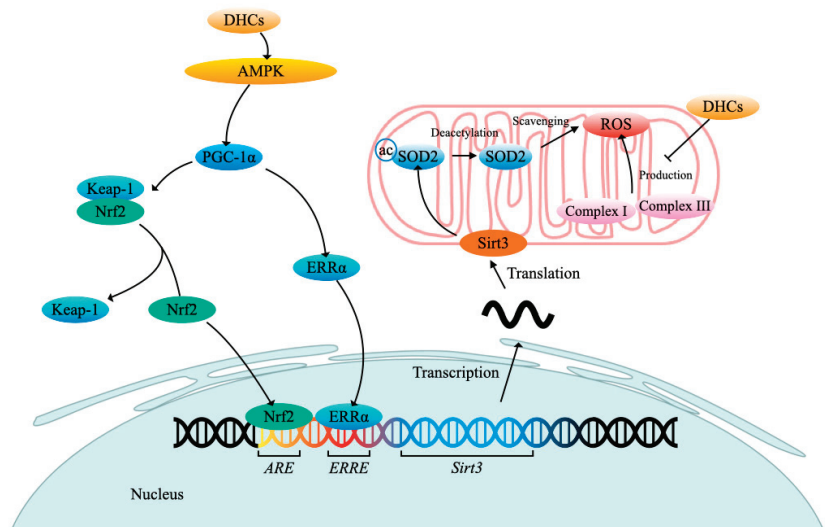


**Figure 4.** DHCs exert neuroprotection through their antioxidative effect. DHCs, dihydrochalcones; AMPK, AMP-activated protein kinase; PGC-1 $\alpha$ , peroxisome proliferators activated receptor- $\gamma$  coactivator-1 $\alpha$ ; Keap-1, Kelch-like ECH-associated protein 1; Nrf2, Nuclear respiratory factor 2; ARE, antioxidant response element; ERR $\alpha$ , estrogen-related receptor  $\alpha$ ; ERRE, ERR $\alpha$  response element; Sirt3, sirtuin 3; SOD2, superoxide dismutase 2; ac, acetylation; ROS, radical oxygen species. Arrow ( $\rightarrow$ ) indicates activation, and the blunt arrow ( $-$ ) indicates inhibition.

#### 4.3. Anti-Neuroinflammation and Anti-Apoptosis

Neuroinflammation is critical damage resulting in neurological diseases. It has been proved that trilobatin could inhibit the inflammation in middle cerebral artery occlusion (MCAO)-induced cerebral I/R injury rats by suppressing the toll-like receptor 4 (TLR4)/myeloid differentiation factor 88 (MyD88)/tumor necrosis factor (TNF) receptor-associated factor 6 (TRAF6) signaling pathway, and down-regulating the phosphorylation level of NF- $\kappa$ Bp65 which will restrain the release of proinflammatory factors, including IL-1 $\beta$ , IL-6, TNF- $\alpha$  and inducible nitric oxide synthase (iNOS) [54], as shown in Figure 5. Pretreatment with phloretin could also inhibit the activation of the glial cell and suppress the inflammatory responses [58].

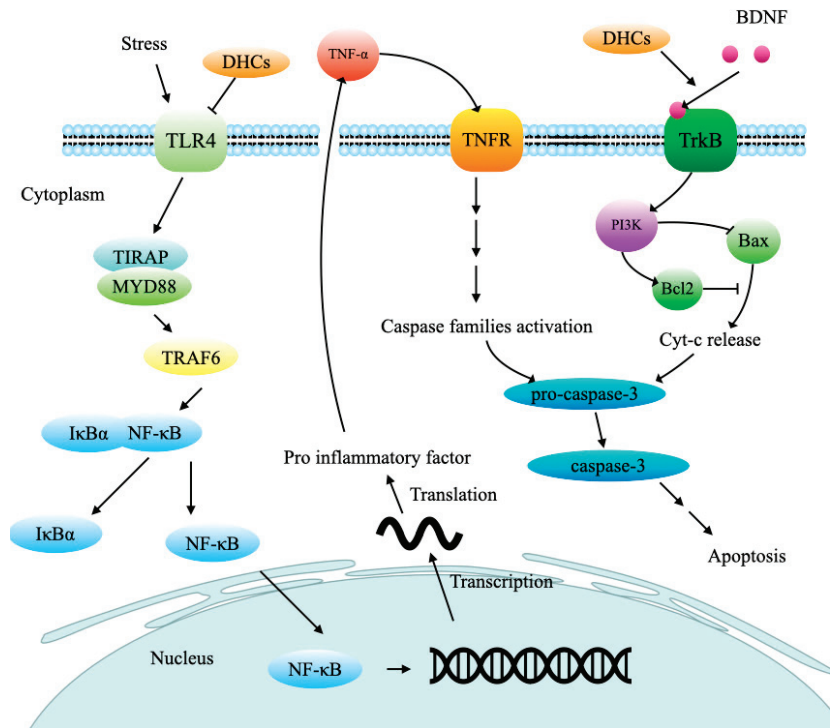


**Figure 5.** DHCs exert neuroprotective effects through their anti-inflammation and anti-apoptosis. TLR4, Toll-like receptor 4; TIRAP, toll/interleukin 1 receptor domain-containing adaptor protein; MYD88, myeloid differentiation factor 88; TRAF6, TNF receptor-associated factor 6; IκBα, inhibitor of NF-κB; NF-κB, nuclear factor κ-B; TNF-α, tumor necrosis factor α; TNFR, tumor necrosis factor receptor; BDNF, brain-derived neurotrophic factor; Trk B, tyrosine kinase receptor B; PI3K, phosphatidylinositol 3- kinase. Arrow (→) indicates activation, and the blunt arrow (–) indicates inhibition.

The experiment showed phloridzin could significantly elevate the brain-derived neurotrophic factor (BDNF) level and reduce the acetylcholinesterase (AChE) activity in the hippocampus and cortex of the lipopolysaccharide (LPS)-treated mice [61]. BDNF can bind to tyrosine receptor kinase B (Trk B), which activates phosphatidylinositol 3-kinase (PI3K), and then spurs the anti-apoptosis and protein synthesis [64]. AChE can degrade acetylcholine and terminate the excitatory effect of neurotransmitters on the postsynaptic membrane, and reduced AChE levels can inhibit neuron damage and prevent AD formation. A large amount of AChE was expressed when cells were in the state of apoptosis. The increased AChE protein can not only inhibit cell growth but also enter the nucleus and participate in the formation of apoptotic bodies and promote apoptosis [65]. Another research confirmed that inhibition of AChE activity through pretreatment and treatment with phloretin could improve spatial memory formation during the Morris water maze (MWM) test in scopolamine-induced amnesia mice [59]. Tests also showed that trilobatin could prevent HT22 cells from the injury induced by the Aβ<sub>25–35</sub> treatment via suppression of the caspase-3-dependent apoptosis pathway. Caspase-3, the most important terminal cleavage enzyme in the process of apoptosis, can be activated by TNF, cyt-c and other caspase families. The activated caspase-3 further enlarges the cascading effects and finally leads to cell death [66].

## 5. Conclusions

The shoots and leaves of *Lithocarpus litseifolius* are rich in DHCs, which taste sweet and possess a variety of physiological effects. Phloretin, trilobatin and phloridzin are the main components of the DHCs. The level of these compounds usually fluctuates along with leaf maturity and distribution location, but some contradictory results have been reported because many samples usually have been collected without uniform picking standards from natural growth trees instead of cultivated plants. The biosynthesis of the DHCs begins with the phenylpropanoid pathway and turns to a branch of the flavonoid pathway at the step from p-coumarinyl CoA to dihydro-4-coumaroyl CoA rather than directly to naringenin chalcone. It has been speculated that the accumulation of the DHCs might be regulated at the transcriptional level at the early steps of the pathway. The DHCs can prevent the neuron tissues from damage by directly inhibiting A $\beta$  deposition and tau hyperphosphorylation as well as indirectly eliminating oxidative stress, inflammation and apoptosis. However, up to now, many issues are not clear, especially why the *Lithocarpus litseifolius* accumulates high levels of DHCs in their leaves, what is the exact biological function of these compounds for the trees and how these compounds are synthesized and metabolized precisely. Meanwhile, many more studies need to be approached for better utilizing the *Lithocarpus litseifolius*, such as collection and improvement of the germplasm, technology development of standardization cultivation, optimization of the processing system and new biological function extension and its mechanism elaboration of the DHCs.

**Author Contributions:** Data curation: Y.-K.W. and Z.-B.D.; visualization: Y.-K.W. and S.-Y.H.; validation: F.-Y.X. and J.-H.Y.; formal analysis: F.-Y.X. and Z.-B.D.; writing—original draft: Y.-K.W. and S.-Y.H.; supervision: X.-Q.Z. and Y.-R.L.; writing—review and editing: J.-H.Y. and J.-L.L.; funding acquisition: X.-Q.Z. and J.-L.L.; project administration: Y.-R.L.; conceptualization: J.-L.L. All authors have read and agreed to the published version of the manuscript.

**Funding:** This work was financially supported by the Zhejiang Science and Technology Major Program on Agricultural New Variety Breeding—Tea Plant (No. 2021C02067-6), the National Natural Science Foundation of China (No. 32272763) and China Agriculture Research System of MOF and MARA.

**Data Availability Statement:** Not applicable.

**Conflicts of Interest:** The authors declare no competing financial interests.

## References

- Gosch, C.; Halbwirth, H.; Kuhn, J.; Miosic, S.; Stich, K. Biosynthesis of phloridzin in apple (*Malus × domestica* Borkh.). *Plant Sci.* **2009**, *176*, 223–231. [[CrossRef](#)]
- Barreca, D.; Bellocco, E.; Laganà, G.; Ginestra, G.; Bisignano, C. Biochemical and antimicrobial activity of phloretin and its glycosylated derivatives present in apple and kumquat. *Food Chem.* **2014**, *160*, 292–297. [[CrossRef](#)] [[PubMed](#)]
- Li, X.; Chen, B.; Xie, H.; He, Y.; Zhong, D.; Chen, D. Antioxidant structure-activity relationship analysis of five dihydrochalcones. *Molecules* **2018**, *23*, 1162. [[CrossRef](#)] [[PubMed](#)]
- Chang, W.; Huang, W.; Liou, C. Evaluation of the anti-inflammatory effects of phloretin and phlorizin in lipopolysaccharide-stimulated mouse macrophages. *Food Chem.* **2012**, *134*, 972–979. [[CrossRef](#)] [[PubMed](#)]
- Fan, X.; Zhang, Y.; Dong, H.; Wang, B.; Ji, H.; Liu, X. Trilobatin attenuates the LPS-mediated inflammatory response by suppressing the NF- $\kappa$ B signaling pathway. *Food Chem.* **2015**, *166*, 609–615. [[CrossRef](#)]
- Dong, H.; Li, M.; Zhu, F.; Liu, F.; Huang, J. Inhibitory potential of trilobatin from *Lithocarpus polystachyus* Rehd against  $\alpha$ -glucosidase and  $\alpha$ -amylase linked to type 2 diabetes. *Food Chem.* **2012**, *130*, 261–266. [[CrossRef](#)]
- Londzin, P.; Siudak, S.; Cegiela, U.; Pytlak, M.; Janas, A.; Waligora, A.; Folwarczna, J. Phloridzin, an apple polyphenol, exerted unfavorable effects on bone and muscle in an experimental model of type 2 diabetes in rats. *Nutrients* **2018**, *10*, 1701. [[CrossRef](#)]
- Li, C.; Wang, L.; Dong, S.; Hong, Y.; Zhou, X.; Zheng, W.; Zheng, C. Phlorizin exerts direct protective effects on palmitic acid (PA)-induced endothelial dysfunction by activating the PI3K/AKT/eNOS signaling pathway and increasing the levels of nitric oxide (NO). *Med. Sci. Monit. Basic Res.* **2018**, *24*, 1. [[CrossRef](#)]
- Lu, Y.; Liang, J.; Chen, S.; Wang, B.; Yuan, H.; Li, C.; Wu, Y.; Wu, Y.; Shi, X.; Gao, J.; et al. Phloridzin alleviate colitis in mice by protecting the intestinal brush border and improving the expression of sodium glycogen transporter 1. *J. Funct. Foods* **2018**, *45*, 348–354. [[CrossRef](#)]
- Zuo, A.; Yu, Y.; Shu, Q.; Zheng, L.; Wang, X.; Peng, S.; Xie, Y.; Cao, S. Hepatoprotective effects and antioxidant, antityrosinase activities of phloretin and phloretin isonicotinyl hydrazone. *J. Chin. Med. Assoc.* **2014**, *77*, 290–301. [[CrossRef](#)]



11. Yang, K.; Tsai, C.; Wang, Y.; Wei, P.; Lee, C.; Chen, J.; Wu, C.; Ho, Y. Apple polyphenol phloretin potentiates the anticancer actions of paclitaxel through induction of apoptosis in human hep G2 cells. *Mol. Carcinog.* **2009**, *48*, 420–431. [[CrossRef](#)] [[PubMed](#)]
12. Gao, J.; Liu, S.; Xu, F.; Liu, Y.; Lv, C.; Deng, Y.; Shi, J.; Gong, Q. Trilobatin protects against oxidative injury in neuronal PC12 cells through regulating mitochondrial ROS homeostasis mediated by AMPK/Nrf2/Sirt3 signaling pathway. *Front. Mol. Neurosci.* **2018**, *11*, 267. [[CrossRef](#)]
13. Hou, Y.; Dan, X.; Babbar, M.; Wei, Y.; Hasselbalch, S.G.; Croteau, D.L.; Bohr, V.A. Ageing as a risk factor for neurodegenerative disease. *Nat. Rev. Neurol.* **2019**, *15*, 565–581. [[CrossRef](#)] [[PubMed](#)]
14. Gutierrez, B.; Zhong, G.; Brown, S. Genetic diversity of dihydrochalcone content in *Malus* germplasm. *Genet. Resour. Crop Evol.* **2018**, *65*, 1485–1502. [[CrossRef](#)]
15. Zhang, Y.; Lin, L.; Long, Y.; Guo, H.; Wang, Z.; Cui, M.; Huang, J.; Xing, Z. Comprehensive transcriptome analysis revealed the effects of the light quality, light intensity, and photoperiod on phlorizin accumulation in *Lithocarpus polystachyus* Rehd. *Forests* **2019**, *10*, 995. [[CrossRef](#)]
16. Cheng, J.; Lyu, L.; Shen, Y.; Li, K.; Liu, Z.; Wang, W.; Xie, L. Population structure and genetic diversity of *Lithocarpus litseifolius* (Fagaceae) assessed using microsatellite markers. *Nord. J. Bot.* **2016**, *34*, 752–760. [[CrossRef](#)]
17. Wang, H.; Ning, R.; Shen, Y.; Chen, Z.; Li, J.; Zhang, R.; Leng, Y.; Zhao, W. Lithocarpic acids A-N, 3,4-seco-cycloartane derivatives from the cupules of *Lithocarpus polystachyus*. *J. Nat. Prod.* **2014**, *77*, 1910–1920. [[CrossRef](#)] [[PubMed](#)]
18. Ning, R.; Wang, H.; Shen, Y.; Chen, Z.; Zhang, R.; Leng, Y.; Zhao, W. Lithocarpic acids O-S, five homo-cycloartane derivatives from the cupules of *Lithocarpus polystachyus*. *Bioorg. Med. Chem. Lett.* **2014**, *24*, 5395–5398. [[CrossRef](#)]
19. Liu, L.; Peng, J.; Shi, S.; Li, K.; Xiong, P.; Cai, W. Characterization of flavonoid constituents in stems of *Lithocarpus litseifolius* (Hance) Chun by UHPLC-Q-exactive orbitrap MS. *Curr. Anal. Chem.* **2021**, *17*, 521–527. [[CrossRef](#)]
20. Cheng, Y.; Liu, F.; Wang, C.; Hwang, T.; Tsai, Y.; Yen, C.; Wang, H.; Tseng, Y.; Chien, C.; Chen, Y.; et al. Bioactive triterpenoids from the leaves and twigs of *Lithocarpus litseifolius* and *L. corneus*. *Planta Med.* **2018**, *84*, 49–58. [[CrossRef](#)]
21. Liu, H.; Liu, Y.; Li, M.; Mai, Y.; Guo, H.; Wadood, S.; Raza, A.; Wang, Y.; Zhang, J.; Li, H.; et al. The chemical, sensory, and volatile characteristics of instant sweet tea (*Lithocarpus litseifolius* [Hance] Chun) using electronic nose and GC-MS-based metabolomics analysis. *LWT-Food Sci. Technol.* **2022**, *163*, 113518. [[CrossRef](#)]
22. Zhao, Y.; Li, X.; Zeng, X.; Huang, S.; Hou, S.; Lai, X. Characterization of phenolic constituents in *Lithocarpus polystachyus*. *Anal. Methods* **2014**, *6*, 1359–1363. [[CrossRef](#)]
23. Yang, X.; Yang, Z.; Wang, Y. Active component content in different *Lithocarpus litseifolius* populations related to meteorologic and soil factors. *J. Cent. South Univ. For. Technol.* **2021**, *41*, 34–41. (In Chinese) [[CrossRef](#)]
24. Yang, J.; Huang, Y.; Yang, Z.; Zhou, C.; Hu, X. Identification and quantitative evaluation of major sweet ingredients in sweet tea (*Lithocarpus polystachyus* Rehd.) based upon location, harvesting time, leaf age. *J. Chem. Soc. Pak.* **2018**, *40*, 158–164.
25. Wei, M.; Tuo, Y.; Zhang, Y.; Deng, Q.; Shi, C.; Chen, X.; Zhang, X. Evaluation of two parts of *Lithocarpus polystachyus* Rehd. from different Chinese areas by multicomponent content determination and pattern recognition. *J. Anal. Methods Chem.* **2020**, *2020*, 8837526. [[CrossRef](#)]
26. He, C.; Peng, Y.; Xiao, W.; Hu, Y.; Xiao, P. Quick determination of five sweet constituents in Duosuike Tiancha by RSLC. *China J. Chin. Mater. Med.* **2012**, *37*, 961–965. (In Chinese)
27. Huang, X.; Liang, W.; Li, B.; Wang, K.; Chen, J.; Li, K. On leaf morphological and venation of *Lithocarpus polystachyus* from different provenances. *J. Beihua. Univ. Nat. Sci.* **2019**, *20*, 237–243. (In Chinese)
28. Huang, X.; Wang, K.; Li, B.; Liang, W.; Chen, J.; Lan, J.; Li, K. Variation comparison of seedling growth and physiological characteristics of different provenances of *Lithocarpus polystachyus*. *Guangxi For. Sci.* **2018**, *47*, 409–414. (In Chinese) [[CrossRef](#)]
29. Zhou, K.; Hu, L.; Li, Y.; Chen, X.; Zhang, Z.; Liu, B.; Li, P.; Gong, X.; Ma, F. MdUGT88F1-mediated phloridzin biosynthesis regulates apple development and *Valsa* canker resistance. *Plant Physiol.* **2019**, *180*, 2290–2305. [[CrossRef](#)]
30. Dare, A.; Yauk, Y.; Tomes, S.; McGhie, I.; Rebstock, R.; Cooney, J.; Atkinson, R. Silencing a phloretin-specific glycosyltransferase perturbs both general phenylpropanoid biosynthesis and plant development. *Plant J.* **2017**, *91*, 237–250. [[CrossRef](#)]
31. Zhou, K.; Hu, L.; Yue, H.; Zhang, Z.; Zhang, J.; Gong, X.; Ma, F. MdUGT88F1-mediated phloridzin biosynthesis coordinates carbon and nitrogen accumulation in apple. *J. Exp. Bot.* **2021**, *73*, 886–902. [[CrossRef](#)] [[PubMed](#)]
32. Li, H.; Yang, J.; Wang, Y.; Yao, X.; Lv, L. Effects of different processing methods on active ingredients in the sweet tea. *Spec. Wild Econ. Anim. Plant Res.* **2021**, *43*, 75–82+92. (In Chinese) [[CrossRef](#)]
33. Liu, Y.; Huang, W.; Li, C.; Liu, A.; Wang, T.; Tang, T. Active components and hypoglycemic activities of the whole fermentation tea of *Lithocarpus litseifolius*. *Food Ferment. Ind.* **2020**, *46*, 53–60. (In Chinese) [[CrossRef](#)]
34. Sun, Z.; Liu, J.; Wang, H.; Yang, C. The influence on the yield of phlorizin in *Lithocarpus polystachyus* Rehd fermented by *Saureurea bacteria*. *Guangzhou Chem. Ind.* **2014**, *42*, 116–118. (In Chinese)
35. Liu, H.; Liu, Y.; Mai, Y.; Guo, H.; He, X.; Xia, Y.; Li, H.; Zhuang, Q.; Gan, R. Phenolic content, main flavonoids, and antioxidant capacity of instant sweet tea (*Lithocarpus litseifolius* Hance Chun) prepared with different raw materials and drying methods. *Foods* **2021**, *10*, 1930. [[CrossRef](#)] [[PubMed](#)]
36. Sun, Y.; Li, W.; Liu, Z. Preparative isolation, quantification and antioxidant activity of dihydrochalcones from Sweet Tea (*Lithocarpus polystachyus* Rehd.). *J. Chromatogr. B Analyt. Technol. Biomed. Life Sci.* **2015**, *1002*, 372–378. [[CrossRef](#)] [[PubMed](#)]
37. Wang, K.; Li, K.; Chen, J.; Huang, J.; Ma, J. Determination and variation trends of main active constituents in wild *Lithocarpus polystachyus*. *Non-Wood For. Res.* **2016**, *34*, 96–100+122. (In Chinese) [[CrossRef](#)]

38. Gosch, C.; Halbwirth, H.; Stich, K. Phloridzin: Biosynthesis, distribution and physiological relevance in plants. *Phytochemistry* **2010**, *71*, 838–843. [[CrossRef](#)]
39. Ibdah, M.; Berim, A.; Martens, S.; Valderrama, A.; Palmieri, L.; Lewinsohn, E.; Gang, D. Identification and cloning of an NADPH-dependent hydroxycinnamoyl-CoA double bond reductase involved in dihydrochalcone formation in *Malus × domestica* Borkh. *Phytochemistry* **2014**, *107*, 24–31. [[CrossRef](#)]
40. Feinbaum, R.; Ausubel, F. Transcriptional regulation of the *Arabidopsis thaliana* chalcone synthase gene. *Mol. Cell Biol.* **1988**, *8*, 1985–1992.
41. Yahyaa, M.; Davidovich-Rikanati, R.; Eyal, Y.; Sheachter, A.; Marzouk, S.; Lewinsohn, E.; Ibdah, M. Identification and characterization of UDP-glucose:Phloretin 4'-O-glycosyltransferase from *Malus × domestica* Borkh. *Phytochemistry* **2016**, *130*, 47–55. [[CrossRef](#)]
42. Jugdé, H.; Nguy, D.; Moller, I.; Cooney, J.; Atkinson, R. Isolation and characterization of a novel glycosyltransferase that converts phloretin to phlorizin, a potent antioxidant in apple. *FEBS J.* **2008**, *275*, 3804–3814. [[CrossRef](#)] [[PubMed](#)]
43. Zhang, T.; Liang, J.; Wang, P.; Xu, Y.; Wang, Y.; Wei, X.; Fan, M. Purification and characterization of a novel phloretin-2'-O-glycosyltransferase favoring phloridzin biosynthesis. *Sci. Rep.* **2016**, *6*, 35274. [[CrossRef](#)] [[PubMed](#)]
44. Gosch, C.; Flachowsky, H.; Halbwirth, H.; Thill, J.; Mjka-Wittmann, R.; Treutter, D.; Richter, K.; Hanke, M.; Stich, K. Substrate specificity and contribution of the glycosyltransferase UGT71A15 to phloridzin biosynthesis. *Trees-Struct. Funct.* **2012**, *26*, 259–271. [[CrossRef](#)]
45. Gosch, C.; Halbwirth, H.; Schneider, B.; Hoelscher, D.; Stich, K. Cloning and heterologous expression of glycosyltransferases from *Malus × domestica* and *Pyrus communis*, which convert phloretin to phloretin 2'-O-glucoside (phloridzin). *Plant Sci.* **2010**, *178*, 299–306. [[CrossRef](#)]
46. Nawade, B.; Yahyaa, M.; Davidovich-Rikanati, R.; Lewinsohn, E.; Ibdah, M. Optimization of culture conditions for the efficient biosynthesis of trilobatin from phloretin by engineered *Escherichia coli* harboring the apple phloretin-4'-O-glycosyltransferase. *J. Agric. Food Chem.* **2020**, *68*, 14212–14220. [[CrossRef](#)]
47. Lei, L.; Hu, B.; Liu, A.; Lu, Y.; Zhou, J.; Zhang, J.; Wong, W. Enzymatic production of natural sweetener trilobatin from citrus flavanone naringin using immobilised  $\alpha$ -L-rhamnosidase as the catalyst. *Int. J. Food Sci. Technol.* **2018**, *53*, 2097–2103. [[CrossRef](#)]
48. Zhu, J.; Wang, Z.; Wang, Z.; Zhang, Y.; Huang, J.; Xing, Z. Cloning and expression of LAR gene and its correlation with phloridzin content in *Lithocarpus polystachyus*. *Chin. Traditional. Herb. Drugs* **2020**, *51*, 3292–3297. (In Chinese)
49. Lin, L.; Long, Y.; Feng, R.; Yin, F.; Huang, J.; Xing, Z. Cloning and bioinformatic analysis of chalcone isomerase gene in *Lithocarpus polystachyus*. *Chin. Traditional. Herb. Drugs* **2017**, *48*, 5080–5084. (In Chinese)
50. Yin, F.; Long, Y.; Feng, R.; Lin, L.; Huang, J.; Xing, Z. Cloning of flavanone 3-hydroxylase gene from *Lithocarpus polystachyus* and its sequence analysis. *Chin. Traditional. Herb. Drugs* **2017**, *48*, 5085–5089. (In Chinese)
51. Xing, Z.; Feng, R.; Wang, Z.; Zhang, Y.; Wang, Z.; Huang, J.; Long, Y. Cloning and expression analysis on 4-coumarate-CoA ligase gene in *Lithocarpus polystachyus*. *Non-Wood For. Res.* **2019**, *37*, 16–21. (In Chinese) [[CrossRef](#)]
52. Chen, N.; Wang, J.; He, Y.; Xu, Y.; Zhang, Y.; Gong, Q.; Yu, C.; Gao, J. Trilobatin protects against A $\beta$ <sub>25–35</sub>-induced hippocampal HT22 cells apoptosis through mediating ROS/p38/Caspase 3-dependent pathway. *Front. Pharmacol.* **2020**, *11*, 584. [[CrossRef](#)] [[PubMed](#)]
53. Ding, J.; Huang, J.; Yin, D.; Liu, T.; Ren, Z.; Hu, S.; Ye, Y.; Le, C.; Zhao, N.; Zhou, H.; et al. Trilobatin alleviates cognitive deficits and pathologies in an Alzheimer's Disease mouse model. *Oxid. Med. Cell. Longev.* **2021**, *2021*, 3298400. [[CrossRef](#)] [[PubMed](#)]
54. Gao, J.; Chen, N.; Li, N.; Xu, F.; Wang, W.; Lei, Y.; Shi, J.; Gong, Q. Neuroprotective effects of trilobatin, a novel naturally occurring Sirt3 agonist from *Lithocarpus polystachyus* Rehd., mitigate cerebral ischemia/reperfusion injury: Involvement of TLR4/NF-kappa B and Nrf2/Keap-1 signaling. *Antioxid. Redox Signal.* **2020**, *33*, 117–143. [[CrossRef](#)] [[PubMed](#)]
55. Shen, T.; Shang, Y.; Wu, Q.; Ren, H. The protective effect of trilobatin against isoflurane-induced neurotoxicity in mouse hippocampal neuronal HT22 cells involves the Nrf2/ARE pathway. *Toxicology* **2020**, *442*, 152537. [[CrossRef](#)] [[PubMed](#)]
56. Ghumatkar, P.; Peshattiwari, V.; Patil, S.; Muke, S.; Whitfield, D.; Howlett, D.; Francis, P.; Sathaye, S. The effect of phloretin on synaptic proteins and adult hippocampal neurogenesis in A $\beta$ <sub>1–42</sub>-injected male Wistar rats. *J. Pharm. Pharmacol.* **2018**, *70*, 1022–1030. [[CrossRef](#)]
57. Ghumatkar, P.; Patil, S.; Peshattiwari, V.; Vijaykumar, T.; Dighe, V.; Vanage, G.; Sathaye, S. The modulatory role of phloretin in A $\beta$ <sub>25–35</sub> induced sporadic Alzheimer's disease in rat model. *Naunyn Schmiedebergs Arch. Pharmacol.* **2019**, *392*, 327–339. [[CrossRef](#)]
58. Zhang, G.; Yang, G.; Liu, J. Phloretin attenuates behavior deficits and neuroinflammatory response in MPTP induced Parkinson's disease in mice. *Life Sci.* **2019**, *232*, 116600. [[CrossRef](#)]
59. Ghumatkar, P.; Patil, S.; Jain, P.; Tambe, R.; Sathaye, S. Nootropic, neuroprotective and neurotrophic effects of phloretin in scopolamine induced amnesia in mice. *Pharmacol. Biochem. Behav.* **2015**, *135*, 182–191. [[CrossRef](#)]
60. Liu, Y.; Zhang, L.; Liang, J. Activation of the Nrf2 defense pathway contributes to neuroprotective effects of phloretin on oxidative stress injury after cerebral ischemia/reperfusion in rats. *J. Neurol. Sci.* **2015**, *351*, 88–92. [[CrossRef](#)]
61. Kamdi, S.; Raval, A.; Nakhate, K. Phloridzin attenuates lipopolysaccharide-induced cognitive impairment via antioxidant, anti-inflammatory and neuromodulatory activities. *Cytokine* **2021**, *139*, 155408. [[CrossRef](#)] [[PubMed](#)]
62. Liu, W.; Sun, Y. Research progress on amyloid  $\beta$ -protein aggregation and its regulation. *CIESC J.* **2022**, *73*, 2381–2396. (In Chinese)

63. Barreca, D.; Curro, M.; Bellocco, E.; Ficarra, S.; Lagana, G.; Tellone, E.; Giunta, M.; Visalli, G.; Caccamo, D.; Galtieri, A.; et al. Neuroprotective effects of phloretin and its glycosylated derivative on rotenone-induced toxicity in human SH-SY5Y neuronal-like cells. *Biofactors* **2017**, *43*, 549–557. [[CrossRef](#)]
64. Wang, K.; Ren, J. Research progress of brain-derived neurotrophic factor in treatment of cerebral infarction. *Med. Recapitul.* **2020**, *26*, 2151–2155. (In Chinese)
65. Wu, H.; Li, T.; Gao, F.; Qian, Y.; Wang, X. Advances of acetylcholinesterase and its traditional Chinese medicine inhibitors. *Pharm. Biotechnol.* **2015**, *22*, 362–365. (In Chinese) [[CrossRef](#)]
66. Yu, F.; Xu, Y. Research progress of caspase-3. *Chin. J. Cell Biol.* **2020**, *42*, 2072–2078. (In Chinese)

Article

# Enhancement of the Functional Properties of Mead Aged with Oak (*Quercus*) Chips at Different Toasting Levels

Juciane Prois Fortes<sup>1,2</sup>, Fernanda Wouters Franco<sup>1,2</sup>, Julia Baranzelli<sup>1,2</sup>, Gustavo Andrade Ugalde<sup>3</sup>, Cristiano Augusto Ballus<sup>1</sup>, Eliseu Rodrigues<sup>4</sup>, Márcio Antônio Mazutti<sup>5</sup>, Sabrina Somacal<sup>1,2,\*</sup> and Claudia Kaehler Sautter<sup>1,2</sup>

<sup>1</sup> Graduate Program on Food Science and Technology, Center of Rural Sciences, Federal University of Santa Maria, Santa Maria, RS 97105-900, Brazil

<sup>2</sup> Integrated Centre for Laboratory Analysis Development (NIDAL), Department of Food Technology and Science, Center of Rural Sciences, Federal University of Santa Maria, Santa Maria, RS 97105-900, Brazil

<sup>3</sup> Graduate Program on Pharmaceutical Sciences, Center of Health Sciences, Federal University of Santa Maria, Santa Maria, RS 97105-900, Brazil

<sup>4</sup> Department of Food Science, Federal University of Rio Grande do Sul, Porto Alegre, RS 91501-970, Brazil

<sup>5</sup> Department of Chemical Engineering, Federal University of Santa Maria, Santa Maria, RS 97105-900, Brazil

\* Correspondence: [sabrina.somacal@ufsm.br](mailto:sabrina.somacal@ufsm.br)

**Abstract:** Consumers increasingly prefer and seek functional beverages, which, given their characteristics, provide important bioactive compounds that help prevent and treat chronic diseases. Mead is a traditional fermented alcoholic beverage made from honey solution. The aging process of mead with oak chips is innovative and bestows functional characteristics to this beverage. Thus, in this study, we sought to develop and characterize a novel functional beverage by combining the health benefits of honey with the traditional aging process of alcoholic beverages in wood. Phenolic compounds, flavonoids, and antioxidant capacity were analyzed in mead using oak chips at different toasting levels and aged for 360 days. LC-ESI-QTOF-MS/MS was used to analyze the chemical profile of different meads. Over time, the aging process with oak chips showed a higher total phenolic and flavonoid content and antioxidant capacity. Eighteen compounds belonging to the classes of organic acids, phenolic acids, flavonoids, and tannins were identified in meads after 360 days. Our findings revealed that the addition of oak chips during aging contributed to *p*-coumaric, ellagic, abscisic, and chlorogenic acids, and naringenin, vanillin, and tiliroside significantly impacted the functional quality of mead.

**Keywords:** polyphenols; honey; functional beverage; characterization; alcoholic beverage; fermented beverage; phenolic compounds; antioxidant; functional foods; beneficial effects

**Citation:** Fortes, J.P.; Franco, F.W.; Baranzelli, J.; Ugalde, G.A.; Ballus, C.A.; Rodrigues, E.; Mazutti, M.A.; Somacal, S.; Sautter, C.K. Enhancement of the Functional Properties of Mead Aged with Oak (*Quercus*) Chips at Different Toasting Levels. *Molecules* **2023**, *28*, 56. <https://doi.org/10.3390/molecules28010056>

Academic Editor: Nour Eddine Es-Safi

Received: 15 November 2022  
Revised: 7 December 2022  
Accepted: 14 December 2022  
Published: 21 December 2022



**Copyright:** © 2022 by the authors. Licensee MDPI, Basel, Switzerland. This article is an open access article distributed under the terms and conditions of the Creative Commons Attribution (CC BY) license (<https://creativecommons.org/licenses/by/4.0/>).

## 1. Introduction

The increased prevalence of noncommunicable diseases in recent years has made consumers increasingly aware of healthy and natural diets [1]. Consequently, the food and beverages industry faces new challenges in designing functional foods. Among the different types of functional foods, beverages are the most acceptable due to logistic facilities, their distribution, and the ease of incorporating bioactive compounds as functional ingredients [2]. Furthermore, functional beverages have gained more market shares over the last decade [3].

Recently, wine and beer, two of the most popular alcoholic beverages, have been identified as functional beverages, and the benefits of their moderate consumption have been widely supported by the scientific community [4]. The main source of the beneficial potential of consuming these beverages is phenolic compounds. After consuming phenolic-compound-rich foods, such as functional beverages, the colon is the leading site of microbial fermentation. Intestinal microbiota transforms phenolic compounds into phenolic acids or

lactone structures, which produce metabolites with biological and antioxidant activity, and evidence suggests that these metabolites have health benefits for humans [3,5,6].

Mead or honey wine is a beverage traditionally produced by diluting honey in water and yeast and may present some variations through the addition of fruit or fruit juice, herbs, or spices [7]. Fermentation and maturation/aging are the two most time-consuming processes in mead production, often lasting a few days to months [8]. The final composition of the mead will depend on the type of honey used, the ingredients added, and the fermentation and storage conditions [9]. Mead has been produced since ancient times, especially in Eastern European countries; however, it is currently not as popular as other alcoholic beverages, highlighting the need for further research on this beverage and its potential functionality [10].

Honey is widely known for its health-promoting biological characteristics such as its anti-inflammatory, antiviral, antifungal, and antitumor properties [11]. Among the bioactive descriptors in honey, phenolic compounds, organic acids, carbohydrates, amino acids, proteins, minerals, vitamins, and lipids stand out [11,12], which directly influence the chemical and sensory characteristics of the mead [8,9,12]. Nevertheless, the composition of honey is quite variable and relies on the floral source and seasonal and environmental conditions, in addition to the processing and storage techniques used [9,11].

The aging process of alcoholic beverages in wood provides various changes in the composition and concentration of compounds in beverages [13,14]. Such modifications may be noticeable by changes in the beverages' taste, color, and aroma. In addition to sensory changes, many phenolic compounds are acquired or elevated during maturation [13,15]. Martínez et al. (2008) tested different quenching methods on the chemical composition of American (*Quercus alba*) and French (*Quercus petraea*) oak, and their findings showed the evolution of ellagitannins, a low molecular weight phenolic compound, and volatile compounds regarding oak species and the tempering method [16]. The natural process in the open air was considered superior to the artificial and mixed drying methods, as it showed greater effectiveness in reducing excess ellagitannins. In addition, the evolution of the aromatic potential of the wood was more positive, reaching higher concentrations of compounds such as volatile phenols, phenolic aldehydes, furanic compounds, and *cis*- and *trans*-methyl- $\gamma$ -octalactones. The wood toasting process takes place after tempering, where the wood is subjected to temperatures in the range of 150–240 °C for a certain period, according to the desired toasting level. In this step, thermal degradation reactions occur, transforming nonvolatile precursors into active aromatic volatile compounds [17].

Due to technological advances in the maturation/aging area of alcoholic beverages, alternative systems using wooden barrels to carry out this process have emerged. Staves, chips, shavings, and other alternative sources of extraction of compounds from oak or other species of forest wood have become common for the maturation and aging process of alcoholic beverages, generating a new use of wood residues in the cooperage [15,18].

Thus, this study aimed to develop a functional mead with multifloral honey and submit it to the aging process with oak chips (*Quercus*), a wood commonly used for the maturation and aging of alcoholic beverages that can provide bioactive compounds. In addition, we sought to evaluate the phenolic compounds content and antioxidant capacity after fermentation and identify the phytochemical compounds in mead aged with oak chips at two toasting levels.

## 2. Results and Discussion

Functional beverages can be a valuable component of the human diet given their ability to provide essential hydration and important bioactive compounds for maintaining health and/or contributing to preventing and treating chronic diseases [1,2,5,6]. Mead is a beverage that has been gaining more and more notoriety over time, although there are few studies on it; hence, this study is unprecedented as it presents data from meads aged with oak chips, a process so far only used for other types of alcoholic beverages [13] and which can improve the functionality of this beverage. In this study, the antioxidant capacity,

total phenolic and flavonoid content, and characterization of phytochemical compounds of meads subjected to a 360-day aging period with oak chips (*Quercus*) at different toasting levels were determined.

Honey is a source of numerous biologically active compounds, including phenolic and volatile compounds, peptides, proteins, amino acids, enzymes, and minerals, which can be transferred to the mead during production [12]. Among all the substances, our attention was given to the phenolic compounds, which contribute to the mead functional quality. This phytochemical group includes flavonoids, tannins, and phenolic acids, which are natural antioxidants that play significant roles in the human body due to their capability to inhibit free radicals, which may cause cell damage, leading to chronic diseases [2,3,19]. Beverages are considered good dietary sources of phenolic compounds; moreover, the phenolic compounds in beverages are highly bioaccessible because they pass directly into intestinal fluids [5], making this study highly innovative in carrying out the aging process of mead with oak chips and monitoring it over time.

At time zero, all elaborated meads had a similar content of phenolic compounds, which came from the honey used (Figure 1). In the base mead (BM), these values remained constant for up to 180 days and then decreased with advancing maturation time. Meads with chips addition showed higher total phenolic compound levels until the aging period of 180 days. This increase may be related to the extraction of phenolic compounds from oak into mead throughout the maturation process. Canas et al. (2019) observed higher total phenolic compounds in wine spirits aged for 180 days with oak staves [20]. This increase was due to the combination of the thermal degradation of lignin and increased wood permeability during thermal treatment. Mead is still poorly studied, although due to its characteristics similar to young white wines, aging time may have provided oxidative reactions and/or condensation between the mead compounds with some wood molecules, reducing the phenolic compounds after 270 days of aging.

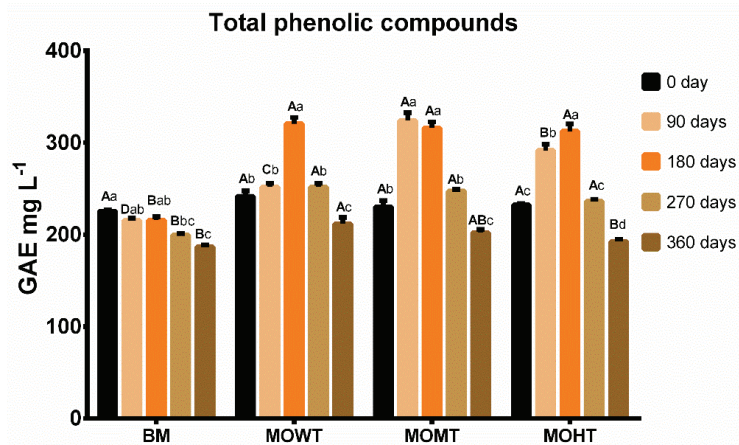


**Figure 1.** Composition of total phenolics (mg GAE L<sup>-1</sup>) of meads aged with oak (*Quercus*) chips. Data are presented as means  $\pm$  SEM ( $n = 5$ ). Lowercase letters indicate significant differences over time within the same experimental group ( $p \leq 0.05$ ). Capital letters indicate significant differences between experimental groups within the same time ( $p \leq 0.05$ ). GAE: gallic acid equivalent; BM: base mead; MOWT: mead aged with oak chips without toasting; MOMT: mead aged with oak chips at medium toasting; MOHT: mead aged with oak chips at high toasting.

Furthermore, flavonoids gradually increased in meads with oak chips throughout the aging period, with a maximum content at 270 days (Figure 2). We observed that the concentration of this class of phenolic compounds varied from 10.6 mg to 20.5 mg CAE L<sup>-1</sup>. Regardless of the toasting degree, the oak chips increased the mead flavonoids concentra-

tions, which may have contributed to increasing the antioxidant capacity throughout the aging process (Figure 3) since these compounds have high free radical scavenging potential, as described elsewhere [8,19].

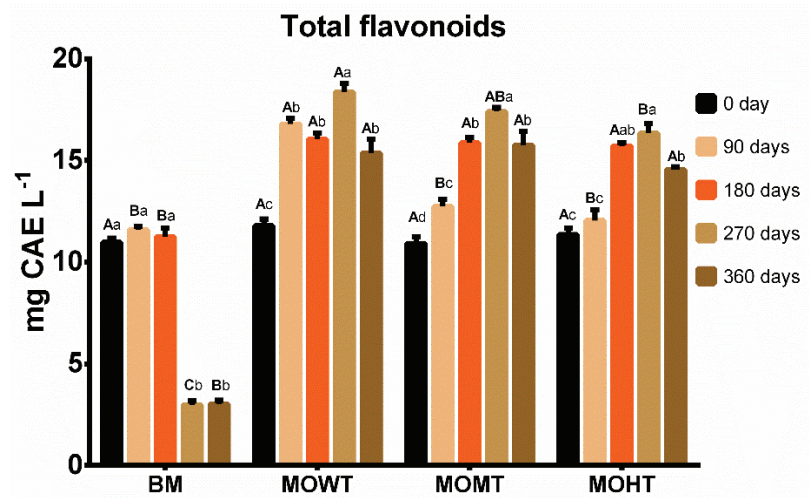


**Figure 2.** Composition of total flavonoids ( $\text{mg CAE L}^{-1}$ ) of meads aged with oak (*Quercus*) chips. Data are presented as means  $\pm$  SEM ( $n = 5$ ). Lowercase letters indicate significant differences over time within the same experimental group ( $p \leq 0.05$ ). Capital letters indicate significant differences between experimental groups within the same time ( $p \leq 0.05$ ). CAE: catechin equivalent; BM: base mead; MOWT: mead aged with oak chips without toasting; MOMT: mead aged with oak chips at medium toasting; MOHT: mead aged with oak chips at high toasting.

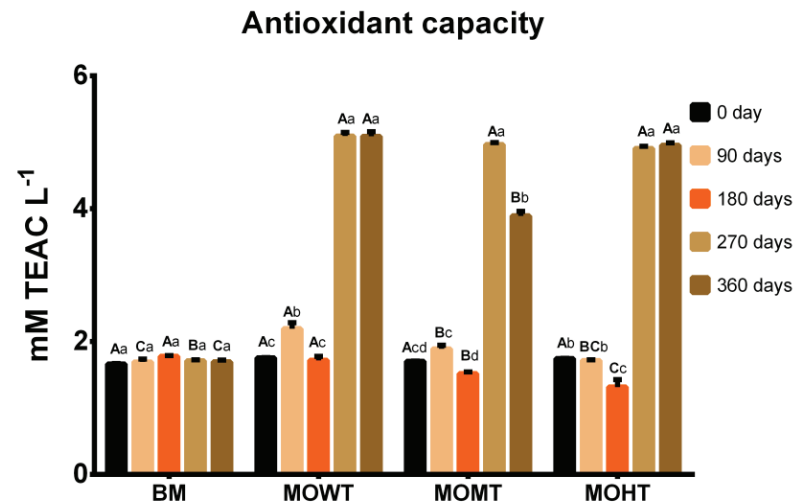


**Figure 3.** Antioxidant capacity ( $\text{mM TEAC L}^{-1}$ ) of meads aged with oak (*Quercus*) chips. Data are presented as means  $\pm$  SEM ( $n = 5$ ). Lowercase letters indicate significant differences over time within the same experimental group ( $p \leq 0.05$ ). Capital letters indicate significant differences between experimental groups within the same time ( $p \leq 0.05$ ). TEAC: Trolox equivalent antioxidant capacity; BM: base mead; MOWT: mead aged with oak chips without toasting; MOMT: mead aged with oak chips at medium toasting; MOHT: mead aged with oak chips at high toasting.

The antioxidant capacity of meads depends on the raw material's chemical composition, the environmental factors that directly affect the honey production process, and the technologies used to process it [8,9]. Apart from technological processes such as fermentation and aging, these beverages' antioxidant properties and chemical composition are determined by the additives used in their manufacturing [8]. In this investigation, the antioxidant capacity was determined with a 2,2'-azino-bis (3-ethylbenzothiazoline) 6-sulfonic acid (ABTS) assay and varied from 1.31 to 5.06 mM of Trolox equivalent antioxidant capacity per liter (TEAC L<sup>-1</sup>), showing a significant increase after 270 days of aging in meads with the addition of the oak chips (Figure 3). In meads, the antioxidant capacity is related to the presence of phenolic compounds, and the diversity of these compounds is directly linked to the honey used [8]. Hence, meads that only use honey and water in their composition tend to have lower compound diversity.

Nevertheless, meads with the addition of fruit juices or herbal extracts have a wider range of these phytochemicals [12]. The profile of the antioxidant capacity is a concomitant event to the behavior of the flavonoid content over time (Figures 2 and 3), especially at 270 days. A similar behavior was observed in unripened meads and other wood-aged beverages [10,21]. However, one cannot rule out the possibility that other bioactive compounds, in addition to flavonoids, contributed to the antioxidant capacity observed in the final aging period of meads with oak chips in this investigation. Phenolic compounds are found in plants as they come from their secondary metabolism. Bees, by collecting pollen, transfer many of these compounds to the honey; consequently, these phytochemicals will be present in the mead, even in smaller amounts [9,11]. The Brazilian flora is vast, generating honeys with various phenolic compounds, with a predominance of many phenolic acids such as 3,4-dihydroxybenzoic, salicylic, caffeic, chlorogenic, *p*-coumaric, ferulic, gallic, syringic acids, and flavonoids including isorhamnetin, kaempferol, luteolin, naringenin, pinobanksin, quercetin, and rutin [22].

In this study, the phenolic compounds in the meads at the end of 360 days of aging were identified through MS/MS mass spectrometry analysis by combining the chromatographic behavior and collision spectra with compounds already described in the literature. Eighteen compounds belonging to the classes of organic acids, phenolic acids, flavonoids, and tannins were tentatively identified and are listed in Table 1 and in the Supplementary Material (Figure S1).

Among the compounds identified are citric acid, protocatechuic acid, sinapyl alcohol, syringic acid, ethylvanillin, 1-(2-hydroxy-4,6-dimethoxyphenyl)-ethanone, sebacic acid, and quercetin in all samples, which are therefore compounds from the honey used in the beverage's elaboration. Adding oak chips during aging, regardless of the toasting, contributed to vanillin, *p*-coumaric acid, ellagic acid, abscisic acid, and naringenin. However, chlorogenic acid and tiliroside were only present in the meads aged with oak chips without toasting (MOWT) and meads aged with oak chips at high toasting (MOHT). Various studies have demonstrated that chlorogenic acids are partially bioavailable and potentially beneficial to human health [6]. The antioxidant and anti-inflammatory effects of coffee chlorogenic acids are responsible for, at least to a certain extent, the association between coffee consumption and the lower incidence of various degenerative and nondegenerative diseases, in addition to higher longevity [6]. 2,3-Dihydroxy-1-guaiacylpropanone was only found in the BM, and the 3-hydroxy-3-(3-hydroxyphenyl) propionic acid was found in the BM and mead aged with oak chips without toasting (MOWT).



Table 1. Phytochemical compounds detected in mead produced with multifloral honey aged with oak (*Quercus*) chips.

Tentative Identification	RT (min)	Molecular Formula	Molecular Weight	Theoretical (m/z)	Observed (m/z)	Fragmentation Ion (m/z)	BM	MOWT	MOMT	MOHT	Reference
Citric acid	2.1	C <sub>6</sub> H <sub>8</sub> O <sub>7</sub>	192.0270	191.0197	191.0368	111.0205	X	X	X	X	[12]
3-Hydroxy-3-(3-hydroxyphenyl)propionic acid	9.0	C <sub>9</sub> H <sub>10</sub> O <sub>4</sub>	182.0579	181.0506	181.0533	121.0420/122.0480	X	X			[23]
2,3-Dihydroxy-1-guaiacylpropanone	9.2	C <sub>10</sub> H <sub>12</sub> O <sub>5</sub>	212.0685	211.0612	211.0789	134.0499/150.0450	X				[23]
Chlorogenic acid	9.2	C <sub>16</sub> H <sub>18</sub> O <sub>9</sub>	354.0951	353.0878	353.0899	191.0574	X	X	X	X	[22]
Protocatechuic acid	9.3	C <sub>7</sub> H <sub>6</sub> O <sub>4</sub>	154.0266	153.0193	153.0335	109.0376	X	X	X	X	[12]
Butanedioic acid	10.6	C <sub>8</sub> H <sub>14</sub> O <sub>5</sub>	190.0841	189.0768	189.0791	129.0680/127.0878/99.0934	X	X	X	X	[24]
Vanillin	10.7	C <sub>8</sub> H <sub>8</sub> O <sub>3</sub>	152.0475	151.0403	151.0414	108.0181	X	X	X	X	[12]
Sinapyl alcohol	10.7	C <sub>11</sub> H <sub>14</sub> O <sub>4</sub>	210.0892	209.0819	209.0996	137.0266	X	X	X	X	[25]
Syringic acid	10.8	C <sub>9</sub> H <sub>10</sub> O <sub>5</sub>	198.0528	197.0455	197.0477	111.0182/125.0360/140.0247	X	X	X	X	[22]
Ethylvanillin	11.0	C <sub>9</sub> H <sub>10</sub> O <sub>3</sub>	166.0630	165.0557	165.0583	119.0514/117.0355	X	X	X	X	[12]
<i>p</i> -Coumaric	11.1	C <sub>9</sub> H <sub>8</sub> O <sub>3</sub>	164.0473	163.0401	163.0401	119.0518	X	X	X	X	[10]
1-(2-hydroxy-4,6-dimethoxyphenyl)-ethanone	11.4	C <sub>10</sub> H <sub>12</sub> O <sub>4</sub>	196.0736	195.0663	195.0690	117.0337/134.0387	X	X	X	X	[26]
Ellagic acid	11.6	C <sub>14</sub> H <sub>6</sub> O <sub>8</sub>	302.0063	300.9990	301.0017	229.0170/301.0018	X	X	X	X	[27]
Abscisic acid	17.1	C <sub>15</sub> H <sub>20</sub> O <sub>4</sub>	264.1362	263.1289	263.1313	136.0543/203.1091	X	X	X	X	[22]
Sebacic acid	17.5	C <sub>10</sub> H <sub>18</sub> O <sub>4</sub>	202.1205	201.1132	201.1302	183.1170/139.1259	X	X	X	X	[28]
Quercetin	17.7	C <sub>15</sub> H <sub>12</sub> O <sub>5</sub>	302.0427	301.0354	301.0584	151.0175/107.0253/116.0828/121.0426	X	X	X	X	[22]
Naringenin	18.5	C <sub>15</sub> H <sub>10</sub> O <sub>7</sub>	272.0685	271.0612	271.0632	125.0266/197.0639/225.0540/253.0480	X	X	X	X	[10]
Tiliroside	20.7	C <sub>30</sub> H <sub>26</sub> O <sub>13</sub>	594.1373	593.1301	593.1326	121.0298/209.0480/417.0965	X	X	X	X	[29]

BM: base mead (only honey); MOWT: mead aged with oak chips without toast; MOMT: mead aged in oak chips in medium toast; MOHT: mead aged in oak chips in high toast.

During the aging process, the transformations of lignin, present in woods such as French oak, are among the most important factors that affect the quality of beverages aged in contact with this material. Lignin is a polymer that undergoes thermal degradation during the manufacturing of barrels or by hydrolysis and ethanololysis during the aging of wines and alcoholic beverages [30]. The lignin macromolecule has ramifications of coniferyl alcohols (guaiacyl compounds) and sinapyl (syringyl compounds). Coniferyl alcohol generates coniferylaldehydes, which are converted into vanillin, while sinapyl alcohol gives rise to sinapaldehyde, which is transformed into syringaldehyde and later oxidized to syringic acid. Other compounds, such as hydrolyzable tannins, present in French oak, are more soluble in hydroalcoholic solutions; its transformation into ellagic acid is very common [31], corroborating the identification of this compound only in meads with the addition of oak chips.

In the present investigation, meads aged with oak chips showed a higher phenolic compound content and diversity. It is known that these compounds may be related to physicochemical and sensory characteristics in foods [8,12]. Thus, the sensory evaluation of meads is important to know the impact of compounds on sensory aspects, including color, flavor, and astringency. The absence of a sensory evaluation of different meads is one of the limitations of this study. These analyses were scheduled to be carried out in 2020–2021, and the study had already been approved by the institutional ethics committee (CAAE no. 58889316.3.0000.5346). Unfortunately, given the restrictions imposed by the SARS-CoV-2 pandemic, it was impossible to carry out the analyses. Until now, the classic wood-aging method employed in numerous alcoholic beverages has not yet been tested in mead. Hence, despite the absence of a sensory evaluation, this study is pioneering and can contribute to essential elucidations in the field of functional beverages.

Mead is a traditional alcoholic beverage obtained by the fermentation of mead wort and popularly produced at home and in small meaderies. Different types of mead can be distinguished based on the honey-to-water ratio, the addition of spices and/or fruits, and the method of wort preparation [8,10,12]. The consumption of mead has gained popularity given the presence of its natural and high-quality bioactive compounds. As a result, mead production and consumption have remarkably increased during the past years [8]. The regular consumption of foods and beverages rich in bioactive compounds has been associated with a series of beneficial health effects [1,2], although, in the case of mead, in addition to these compounds, this beverage also has a considerable alcohol content (8–18%) [8,10,12]. The excessive and prolonged use of alcoholic beverages is significantly linked to mild symptoms such as fatigue, difficulty walking, fainting, and behavioral changes. In addition, long-term consumption is responsible for serious health problems such as depression, anxiety, impaired cognitive performance, and liver diseases (e.g., alcoholic hepatitis and liver cirrhosis), which is considered one of the main causes of death and functional disability in the world [32,33]. Given the above, the moderate consumption of mead and other alcoholic beverages is suggested.

### 3. Materials and Methods

#### 3.1. Analytical Reagents

HPLC-grade methanol used for the mobile phase was obtained from Merck (Darmstadt, Germany). HPLC-grade acetonitrile and formic acid used for the mobile phase were obtained from Sigma-Aldrich (St. Louis, MO, USA). HPLC-grade water was obtained from a Milli-Q system (Millipore, Bedford, MA, USA). ABTS (2,2'-azino-bis(3-ethylbenzothiazoline) 6-sulfonic acid) was obtained from Sigma-Aldrich (St. Louis, MO, USA).

#### 3.2. Experimental Design

The experimental design was completely randomized with four treatments and five sampling units for each treatment (Table 2).

**Table 2.** Coding and characterization of treatments used in this study.

Code	Treatment
BM	Base mead—not aged with oak chips
MOWT	Mead aged with oak chips without toasting
MOMT	Mead aged with oak chips at medium toasting (170 °C for 35 min)
MOHT	Mead aged with oak chips at high toasting (200 °C for 45 min)

### 3.3. Samples Acquisition

To produce the mead we used multifloral honey from an apiary located in Santiago city (29.1991393' S and 54.8644842' W, 467 m) in the central region of Rio Grande do Sul, Southern Brazil. It has an area of 2,413 km<sup>2</sup> of foraging, and the climate is classified as humid subtropical, with an annual average temperature of between 18 and 20 °C and an average annual rainfall of 359 mm. For the aging of mead, we utilized oak chips (*Quercus*) purchased from WE Consultoria (Porto Alegre, Rio Grande do Sul, Brazil).

The mead was prepared with multifloral honey and water until it reached 21° Brix; then, it was inoculated with 20 hg L<sup>-1</sup> of the *Saccharomyces baianus* yeast strain and 30 hg L<sup>-1</sup> of nutrients (Nutrystart). Fermentation was carried out in a glass fermenter with a capacity of 30 L with the system maintained under anaerobic conditions through the water seal at a constant temperature of 20 °C, and it was monitored daily by measuring the total soluble solids content and initial and final density. The end of the fermentation process occurred at 27 days with the cessation of carbon dioxide evolution followed by the stabilization of total soluble solids and the stabilization of density. The mead was then stabilized for 15 days at 16 °C. The time between fermentation and the beginning of aging was 45 days. In the last step, the mead was sulfited at 50 ppm and bottled in 300 mL bottles with the addition of 2 g L<sup>-1</sup> of oak chips (*Quercus*) followed by the aging process. Aliquots were taken every 90 days for up to 360 days to analyze the content of the total phenolic compounds, total flavonoids, and antioxidant capacity. At the end of the 360 days of aging, the phenolic compounds in the different meads were identified.

### 3.4. Total Phenolic Content

The total phenolic compounds in each mead sample were quantified with spectrophotometry through the redox reaction with the Folin–Ciocalteu reagent [34]. The readings of the samples were performed in triplicate of the absorbances in a UV–visible spectrophotometer (FEMTO 600 plus) at a wavelength of 765 nm after they were left to rest for two hours at room temperature. The phenolic compounds content was calculated by interpolating the absorbance of the samples against the calibration curve constituted with a standard of gallic acid (0–80 mg L<sup>-1</sup>), and the results are expressed in milligrams of gallic acid equivalent per liter (mg GAE L<sup>-1</sup>).

### 3.5. Flavonoids Content

Flavonoid compound determination was performed according to the method of Zhishen, Mengcheng, and Jianming (1999) [35]. The absorbance readings were performed in triplicate with a UV–visible spectrophotometer (FEMTO 600 plus) at 550 nm. The flavonoid concentration in the meads was calculated by interpolating the data with the calibration curve constituted with the catechin standard (0–250 mg L<sup>-1</sup>), and the results were expressed in milligrams of catechin equivalent per liter (mg CAE L<sup>-1</sup>).

### 3.6. Antioxidant Capacity Determination

The antioxidant capacity of meads was determined with the ABTS method using the method described by Re et al. (1999) [36]. The absorbance readings of the samples were taken 6 min after the reaction in a UV–visible spectrophotometer (FEMTO® 600 plus) at 750 nm. The ABTS concentration was calculated from a calibration curve using Trolox as

the standard (0–0.2 mM TEAC L<sup>-1</sup>). Readings were performed in triplicate, and the results are expressed as mM of Trolox equivalent antioxidant capacity per liter (mM TEAC L<sup>-1</sup>).

### 3.7. Purification Procedure in SPE C18

Samples were purified prior to performing the LC-ESI-QTOF-MS/MS analysis. Sample purification was performed according to the method described by Rodriguez-Saona and Wrolstad (2001) with adaptations [37,38]. The mead samples (6 mL) were placed in a rotary evaporator (Büchi, Essen, Germany) at 35 °C for five minutes to remove the alcohol present in the sample. Afterward, the sample was loaded into C-18 solid phase extraction (SPE) cartridges (cartridges SPE-C18, Strata C18-E, Phenomenex), previously activated with methanol and conditioned with acidified water (0.1% *v/v* formic acid). The polar compounds were washed with two volumes of aqueous formic acid solution (0.1% *v/v*). Fewer polar phenolic compounds were eluted with two volumes of ethyl acetate (3 mL). The ethyl acetate fraction was dried on a rotary evaporator and made up to a known volume (1 mL) with acidified methanol (0.1% *v/v* formic acid) and acidified water (0.1% *v/v* formic acid) (200 + 800 µL). All fractions were analyzed directly as purified fractions in a chromatograph.

### 3.8. Phenolic Compound Identification by LC-ESI-QTOF-MS/MS

The method to identify the phenolic compounds was based on Quatrin et al. (2019) [39]. The liquid chromatography (LC) instrument (Shimadzu, Kyoto, Japan) was connected in series to a DAD detector (SPD-M20A) and a mass spectrometer (MS) with a Quadrupole-Time-of-Flight (QTOF) analyzer and an electrospray ionization source (ESI) (Bruker Daltonics, micrOTOF-Q III, Bremen, Germany). A 20 µL sample was injected into a reversed-phase column (C-18 Hypersil Gold, 5 µm particle size, 150 mm, 4.6 mm; Thermo Fisher Scientific, Waltham, MA, USA). Mobile phase A for this method consisted of ultrapure water with formic acid acidified methanol (95:5:0.1 *v/v*); mobile phase B was acetonitrile and formic acid (99.9:0.1 *v/v*). The ESI conditions were a capillary voltage of −4500 V (negative), nebulizer gas pressure at 30 psi, dry gas at 11 mL min<sup>-1</sup>, and gas temperature at 310 °C. The MS/MS experiments were performed in a full scan range of 100–1800 *m/z* of all fragments formed from 3 major parent ions per second. The LC solutions software (Version 3, Shimadzu, Kyoto, Japan) was used to process the data obtained. The tentative identification of compounds was based on the combined information of elution order, ultraviolet–visible (UV–Vis) spectra, and mass spectrometry fragmentation patterns. These data were compared to literature data and public databases (PubChem, KEGG, MassBank of North America (MoNA), ChemSpider, Phenol-Explorer, and FooDB).

### 3.9. Statistical Analysis

All analytical results were selected for an analysis of variance (ANOVA). The comparison of posthoc mean analysis was performed with a Tukey's test at 5% error probability using Statistica 9.0 software (StatSoft, Tulsa, OK, USA); the graphs were made using the GraphPad Prism 6.0 software (Dotmatics, San Diego, CA, USA).

## 4. Conclusions

The highly innovative process of using oak chips to improve mead characteristics has not yet been described in the literature. Oak chips increase phenolic compound variability in mead, their flavonoid content, and their antioxidant capacity over storage time. Our findings revealed that mead aged with oak chips as a beverage has more potential for beneficial biological activity due to the higher phenolic compound content than mead without oak chips. Therefore, the use of oak chips in the mead aging process, regardless of toasting levels, improved the functional quality of the beverage.

**Supplementary Materials:** The following supporting information can be downloaded at: <https://www.mdpi.com/article/10.3390/molecules28010056/s1>, Figure S1: Representative chromatogram of mead aged with oak chips.

**Author Contributions:** Conceptualization, J.P.F. and C.K.S.; data curation, J.P.F., S.S. and C.K.S.; formal analysis, J.P.F., F.W.F., J.B. and G.A.U.; funding acquisition, E.R., M.A.M. and C.K.S.; investigation, J.P.F., F.W.F., J.B. and S.S.; methodology, J.P.F., F.W.F., J.B., G.A.U., C.A.B. and M.A.M.; project administration, C.K.S.; supervision, C.A.B., E.R., S.S. and C.K.S.; validation, F.W.F., E.R. and M.A.M.; writing—original draft, J.P.F.; writing—review and editing, S.S. and C.K.S. All authors have read and agreed to the published version of the manuscript.

**Funding:** This study was financed in part by Conselho Nacional de Desenvolvimento Científico e Tecnológico (CNPq, Brazil) [grant number 475597/2010-9], Coordenação de Aperfeiçoamento de Pessoal de Nível Superior (CAPES, Brazil) [finance code 001], and Fundação de Amparo à Pesquisa do Estado do Rio Grande do Sul (FAPERGS, RS, Brazil) [grant number 17/2551-0000949-5].

**Institutional Review Board Statement:** Not applicable.

**Data Availability Statement:** The data presented in this study are openly available in the Harvard Dataverse at doi: 10.7910/DVN/MBWA4J.

**Conflicts of Interest:** The authors declare no conflict of interest.

**Sample Availability:** All meads samples are available from the authors.

## References

- Sethi, G.; Vidyalaya, K.M.; Raina, A.; Vidyalaya, K.M. Consumers' Awareness about Nutritional Aspects of Healthy Food: A Qualitative Study. *Universe Int. J. Interdiscip. Res.* **2020**, *2020*, 438–443.
- Zaidel, D.N.A.; Muhamad, I.I.; Hashim, Z.; Jusoh, Y.M.M.; Salleh, E. Innovation and Challenges in the Development of Functional and Medicinal Beverages. In *Functional Foods and Nutraceuticals for Human Health*; Apple Academic Press: Boca Raton, FL, USA, 2021; pp. 137–198.
- Cong, L.; Bremer, P.; Miroso, M. Functional Beverages in Selected Countries of Asia Pacific Region: A Review. *Beverages* **2020**, *6*, 21. [[CrossRef](#)]
- Radonjić, S.; Maraš, V.; Raičević, J.; Košmerl, T. Wine or Beer? Comparison, Changes and Improvement of Polyphenolic Compounds during Technological Phases. *Molecules* **2020**, *25*, 4960. [[CrossRef](#)] [[PubMed](#)]
- Cantele, C.; Rojo-Poveda, O.; Bertolino, M.; Ghirardello, D.; Cardenia, V.; Barbosa-Pereira, L.; Zeppa, G. In Vitro Bioaccessibility and Functional Properties of Phenolic Compounds from Enriched Beverages Based on Cocoa Bean Shell. *Foods* **2020**, *9*, 715. [[CrossRef](#)]
- Farah, A.; dePaula Lima, J. Consumption of Chlorogenic Acids through Coffee and Health Implications. *Beverages* **2019**, *5*, 11. [[CrossRef](#)]
- Kahoun, D.; Řezková, S.; Královský, J. Effect of Heat Treatment and Storage Conditions on Mead Composition. *Food Chem.* **2017**, *219*, 357–363. [[CrossRef](#)]
- Starowicz, M.; Granvogl, M. Trends in Food Science & Technology an Overview of Mead Production and the Physicochemical, Toxicological, and Sensory Characteristics of Mead with a Special Emphasis on Flavor. *Trends Food Sci. Technol.* **2020**, *106*, 402–416. [[CrossRef](#)]
- Akalın, H.; Bayram, M.; Anlı, R.E. Determination of Some Individual Phenolic Compounds and Antioxidant Capacity of Mead Produced from Different Types of Honey. *J. Inst. Brew.* **2017**, *123*, 167–174. [[CrossRef](#)]
- Bednarek, M.; Szwengiel, A. Distinguishing between Saturated and Unsaturated Meads Based on Their Chemical Characteristics. *LWT* **2020**, *133*, 109962. [[CrossRef](#)]
- Cianciosi, D.; Forbes-Hernández, T.; Afrin, S.; Gasparrini, M.; Reboredo-Rodríguez, P.; Manna, P.; Zhang, J.; Bravo Lamas, L.; Martínez Flórez, S.; Agudo Toyos, P.; et al. Phenolic Compounds in Honey and Their Associated Health Benefits: A Review. *Molecules* **2018**, *23*, 2322. [[CrossRef](#)]
- Švecová, B.; Bordovská, M.; Kalvachová, D.; Hájek, T. Analysis of Czech Meads: Sugar Content, Organic Acids Content and Selected Phenolic Compounds Content. *J. Food Compos. Anal.* **2015**, *38*, 80–88. [[CrossRef](#)]
- Rubio-Bretón, P.; Garde-Cerdán, T.; Martínez, J. Use of Oak Fragments during the Aging of Red Wines. Effect on the Phenolic, Aromatic, and Sensory Composition of Wines as a Function of the Contact Time with the Wood. *Beverages* **2018**, *4*, 102. [[CrossRef](#)]
- Martínez-Gil, A.M.; del Alamo-Sanza, M.; del Barrio-Galán, R.; Nevares, I. Alternative Woods in Oenology: Volatile Compounds Characterisation of Woods with Respect to Traditional Oak and Effect on Aroma in Wine, a Review. *Appl. Sci.* **2022**, *12*, 2101. [[CrossRef](#)]
- Fernández de Simón, B.; Cadahía, E.; del Álamo, M.; Nevares, I. Effect of Size, Seasoning and Toasting in the Volatile Compounds in Toasted Oak Wood and in a Red Wine Treated with Them. *Anal. Chim. Acta* **2010**, *660*, 211–220. [[CrossRef](#)]

16. Martínez, J.; Cadahía, E.; Fernández de Simón, B.; Ojeda, S.; Rubio, P. Effect of the Seasoning Method on the Chemical Composition of Oak Heartwood to Cooperage. *J. Agric. Food Chem.* **2008**, *56*, 3089–3096. [[CrossRef](#)]
17. Farrell, R.R.; Wellinger, M.; Gloess, A.N.; Nichols, D.S.; Breadmore, M.C.; Shellie, R.A.; Yeretzyan, C. Real-Time Mass Spectrometry Monitoring of Oak Wood Toasting: Elucidating Aroma Development Relevant to Oak-Aged Wine Quality. *Sci. Rep.* **2015**, *5*, 17334. [[CrossRef](#)]
18. Fernández de Simón, B.; Muiño, I.; Cadahía, E. Characterization of Volatile Constituents in Commercial Oak Wood Chips. *J. Agric. Food Chem.* **2010**, *58*, 9587–9596. [[CrossRef](#)]
19. Sharifi-Rad, M.; Anil Kumar, N.V.; Zucca, P.; Varoni, E.M.; Dini, L.; Panzarini, E.; Rajkovic, J.; Tsouh Fokou, P.V.; Azzini, E.; Peluso, L.; et al. Lifestyle, Oxidative Stress, and Antioxidants: Back and Forth in the Pathophysiology of Chronic Diseases. *Front. Physiol.* **2020**, *11*, 694. [[CrossRef](#)]
20. Canas, S.; Caldeira, I.; Anjos, O.; Belchior, A.P. Phenolic Profile and Colour Acquired by the Wine Spirit in the Beginning of Ageing: Alternative Technology Using Micro-Oxygenation vs Traditional Technology. *LWT* **2019**, *111*, 260–269. [[CrossRef](#)]
21. Laqui-Estaña, J.; López-Solis, R.; Peña-Neira, Á.; Medel-Marabolí, M.; Obrique-Slier, E. Wines in Contact with Oak Wood: The Impact of the Variety (Carmènère and Cabernet Sauvignon), Format (Barrels, Chips and Staves), and Aging Time on the Phenolic Composition. *J. Sci. Food Agric.* **2019**, *99*, 436–448. [[CrossRef](#)]
22. Seraglio, S.K.T.; Valese, A.C.; Daguer, H.; Bergamo, G.; Azevedo, M.S.; Gonzaga, L.V.; Fett, R.; Costa, A.C.O. Development and Validation of a LC-ESI-MS/MS Method for the Determination of Phenolic Compounds in Honeydew Honeys with the Diluted-and-Shoot Approach. *Food Res. Int.* **2016**, *87*, 60–67. [[CrossRef](#)] [[PubMed](#)]
23. Ma, C.; Dunshea, F.R.; Suleria, H.A. LC-ESI-QTOF/MS Characterization of Phenolic Compounds in Palm Fruits (Jelly and Fishtail Palm) and Their Potential Antioxidant Activities. *Antioxidants* **2019**, *8*, 483. [[CrossRef](#)] [[PubMed](#)]
24. Xu, S.; Zhu, J.; Zhao, Q.; Hardie, J.; Hu, B. Changes in the Profile of Aroma Compounds in *Vitis vinifera* L. cv Merlot from Grapes to Wine. *Bangladesh J. Bot.* **2017**, *46*, 1089–1098.
25. Simonelt, B.R.T.; Rogge, W.F.; Mazurek, M.A.; Standley, L.J.; Hildemann, L.M.; Cass, G.R. Lignin Pyrolysis Products, Lignans, and Resin Acids as Specific Tracers of Plant Classes in Emissions from Biomass Combustion. *Environ. Sci. Technol.* **1993**, *27*, 2533–2541. [[CrossRef](#)]
26. Abdulsallam, B.; Ohood Hasan, A.; Nael Abu, T.; Ali, A.-R.; Sachil, K. Chemical Composition of Propolis from the Baha Region in Saudi Arabia. *Czech J. Food Sci.* **2018**, *36*, 109–118. [[CrossRef](#)]
27. Maia, I.R.D.O.; Trevisan, M.T.S.; Silva, M.G.D.V.; Breuer, A.; Owen, R.W. Characterization and Quantitation of Polyphenolic Compounds in *Senna macranthera* Var *Pudibunda* from the Northeast of Brazil. *Nat. Prod. Commun.* **2019**, *14*, 1934578X1985170. [[CrossRef](#)]
28. Isidorov, V.A.; Czyżewska, U.; Jankowska, E.; Bakier, S. Determination of Royal Jelly Acids in Honey. *Food Chem.* **2011**, *124*, 387–391. [[CrossRef](#)]
29. Lucas, C.I.S.; Ferreira, A.F.; Costa, M.A.P.D.C.; Silva, F.D.L.; Estevinho, L.M.; Carvalho, C.A.L.D. Phytochemical Study and Antioxidant Activity of *Dalbergia ecastaphyllum*. *Rodriguésia* **2020**, *71*, 1–15. [[CrossRef](#)]
30. Le Floch, A.; Jourdes, M.; Teissedre, P.-L. Polysaccharides and Lignin from Oak Wood Used in Cooperage: Composition, Interest, Assays: A Review. *Carbohydr. Res.* **2015**, *417*, 94–102. [[CrossRef](#)]
31. Mosedale, J.; Puech, J.-L. Wood Maturation of Distilled Beverages. *Trends Food Sci. Technol.* **1998**, *9*, 95–101. [[CrossRef](#)]
32. Niemelä, O.; Aalto, M.; Bloigu, A.; Bloigu, R.; Halkola, A.S.; Laatikainen, T. Alcohol Drinking Patterns and Laboratory Indices of Health: Does Type of Alcohol Preferred Make a Difference? *Nutrients* **2022**, *14*, 4529. [[CrossRef](#)]
33. Wang, S.-C.; Chen, Y.-C.; Chen, S.-J.; Lee, C.-H.; Cheng, C.-M. Alcohol Addiction, Gut Microbiota, and Alcoholism Treatment: A Review. *Int. J. Mol. Sci.* **2020**, *21*, 6413. [[CrossRef](#)]
34. Singleton, V.L.; Rossi, J.A. Colorimetry of Total Phenolics with Phosphomolybdic-Phosphotungstic Acid Reagents. *Am. J. Enol. Vitic.* **1965**, *16*, 144–158.
35. Zhishen, J.; Mengcheng, T.; Wu, J. The Determination of Flavonoid Contents in Mulberry and Their Scavenging Effects on Superoxide Radicals. *Food Chem.* **1999**, *64*, 555–559. [[CrossRef](#)]
36. Re, R.; Pellegrini, N.; Proteggente, A.; Pannala, A.; Yang, M.; Rice-Evans, C. Antioxidant Activity Applying an Improved ABTS Radical Cation Decolorization Assay. *Free Radic. Biol. Med.* **1999**, *26*, 1231–1237. [[CrossRef](#)]
37. Rodríguez-Saona, L.E.; Wrolstad, R.E. Extraction, Isolation, and Purification of Anthocyanins. *Curr. Protoc. Food Anal. Chem.* **2001**, F1.1.1–F1.1.11. [[CrossRef](#)]
38. Bochi, V.C.; Barcia, M.T.; Rodrigues, D.; Speroni, C.S.; Giusti, M.M.; Godoy, H.T. Polyphenol Extraction Optimisation from Ceylon Gooseberry (*Dovyalis hebecarpa*) Pulp. *Food Chem.* **2014**, *164*, 347–354. [[CrossRef](#)]
39. Quatrin, A.; Pauletto, R.; Maurer, L.; Minuzzi, N.; Nichelle, S.; Carvalho, J.; Maróstica Junior, M.; Rodrigues, E.; Bochi, V.; Emanuelli, T. Characterization and Quantification of Tannins, Flavonols, Anthocyanins and Matrix-Bound Polyphenols from Jaboticaba Fruit Peel: A Comparison between *Myrciaria trunciflora* and *M. jaboticaba*. *J. Food Compos. Anal.* **2019**, *78*, 59–74. [[CrossRef](#)]

**Disclaimer/Publisher’s Note:** The statements, opinions and data contained in all publications are solely those of the individual author(s) and contributor(s) and not of MDPI and/or the editor(s). MDPI and/or the editor(s) disclaim responsibility for any injury to people or property resulting from any ideas, methods, instructions or products referred to in the content.



Review

# Treatment of High-Polyphenol-Content Waters Using Biotechnological Approaches: The Latest Update

Barbara Muñoz-Palazon <sup>1,2,3</sup>, Susanna Gorrasi <sup>1</sup>, Aurora Rosa-Masegosa <sup>2,3</sup>, Marcella Pasqualetti <sup>1,4</sup>,  
Martina Braconcini <sup>1</sup> and Massimiliano Fenice <sup>1,5,\*</sup>

<sup>1</sup> Department of Ecological and Biological Sciences (DEB), University of Tuscia, Largo dell'Università snc, 01100 Viterbo, Italy

<sup>2</sup> Institute of Water Research, University of Granada, C/Ramón y Cajal, 4, 18071 Granada, Spain

<sup>3</sup> Faculty of Pharmacy, University of Granada, Campus de Cartuja, s/n, 18071 Granada, Spain

<sup>4</sup> Laboratory of Ecology of Marine Fungi, CoNISMa, Department of Ecological and Biological Sciences (DEB), University of Tuscia, Largo dell'Università snc, 01100 Viterbo, Italy

<sup>5</sup> Laboratory of Applied Marine Microbiology, CoNISMa, Department of Ecological and Biological Sciences (DEB), University of Tuscia, Largo dell'Università snc, 01100 Viterbo, Italy

\* Correspondence: fenice@unitus.it; Tel.: +39-0761-357318

**Abstract:** Polyphenols and their intermediate metabolites are natural compounds that are spread worldwide. Polyphenols are antioxidant agents beneficial for human health, but exposure to some of these compounds can be harmful to humans and the environment. A number of industries produce and discharge polyphenols in water effluents. These emissions pose serious environmental issues, causing the pollution of surface or groundwater (which are used to provide drinking water) or harming wildlife in the receiving ecosystems. The treatment of high-polyphenol-content waters is mandatory for many industries. Nowadays, biotechnological approaches are gaining relevance for their low footprint, high efficiency, low cost, and versatility in pollutant removal. Biotreatments exploit the diversity of microbial metabolisms in relation to the different characteristics of the polluted water, modifying the design and the operational conditions of the technologies. Microbial metabolic features have been used for full or partial polyphenol degradation since several decades ago. Nowadays, the comprehensive use of biotreatments combined with physical-chemical treatments has enhanced the removal rates to provide safe and high-quality effluents. In this review, the evolution of the biotechnological processes for treating high-polyphenol-content water is described. A particular emphasis is given to providing a general concept, indicating which bioprocess might be adopted considering the water composition and the economic/environmental requirements. The use of effective technologies for environmental phenol removal could help in reducing/avoiding the detrimental effects of these chemicals. In addition, some of them could be employed for the recovery of beneficial ones.

**Citation:** Muñoz-Palazon, B.; Gorrasi, S.; Rosa-Masegosa, A.; Pasqualetti, M.; Braconcini, M.; Fenice, M. Treatment of High-Polyphenol-Content Waters Using Biotechnological Approaches: The Latest Update. *Molecules* **2023**, *28*, 314. <https://doi.org/10.3390/molecules28010314>

Academic Editor: Nour Eddine Es-Safi

Received: 2 December 2022

Revised: 26 December 2022

Accepted: 28 December 2022

Published: 30 December 2022



**Copyright:** © 2022 by the authors. Licensee MDPI, Basel, Switzerland. This article is an open access article distributed under the terms and conditions of the Creative Commons Attribution (CC BY) license (<https://creativecommons.org/licenses/by/4.0/>).

**Keywords:** polyphenols; biological treatment; bioreactors; water; aerobic granular sludge; conventional active ted sludge; biofilter; photobioreactor; membrane bioreactor; bio-electrochemical systems

## 1. Introduction

Water is a renewable natural resource, but its inappropriate use has become a problem due to its excessive exploitation caused by the demographic explosion and industrial demands [1]. Environmental pollution is a problem, especially when industrial effluents are discharged into natural water bodies. Most wastes from industries containing organic and inorganic pollutants are easily drawn into wastewater. Many of these pollutants suppose a risk to wildlife species, ecological niches, and ultimately to human health.

Phenol (C<sub>6</sub>H<sub>5</sub>OH) or phenic acid is an organic compound that consists of a phenyl group (-C<sub>6</sub>H<sub>5</sub>) bearing a single hydroxyl group (OH<sup>-</sup>) [1]. Polyphenols are an enormous group of secondary plant metabolites characterized by two or more phenolic rings



in their chemical structure [2]. Polyphenols could be mainly classified as flavonoids and nonflavonoids, or according to their complexity, as monomeric and polymeric compounds [3]. However, the principal polyphenolic compounds are grouped into phenolic acids, flavonoids, lignans, and stilbenes [4], characterized by complex chemical structures and the presence of diversified functional groups (Figure 1). For instance, flavonoids are essential bioactive compounds in various biological processes, including nitrogen fixation, photosynthesis, or energy transfer [5,6], while lignans have high pharmacological activities, such as antiviral, antitumoral, and antimicrobial properties [7,8]. Some phenolic compounds have been described as “priority substances” in the field of water policy by the European Water Framework Directive, the Environmental Protection Agency of the United States, and the National Pollutant Release Inventory of Canada [9,10], with 11 out of 126 undesirable chemicals [11]. Phenolic compounds are among the most prevalent water organic contaminants, showing toxicity even at low concentrations and affecting the taste and odor of the drinking water [1]. They are the main substances in the wastewater effluents of several industries, such as pharmaceutical, agricultural, petrochemical, pulp and paper, organic chemicals, and plastic manufacturing [12]. Furthermore, they may lead to water pollution via natural occurrences. In humans, short-term exposure to polyphenol concentrations in the range of 9–25 mg·L<sup>-1</sup> can cause irritation to the skin and mucous membranes, while long-term exposure may cause lung problems, muscle weakness, tremors, coma, metabolic diseases, and respiratory arrest at lethal doses [10,13]. Actually, it has been described that 50 mg·kg<sup>-1</sup>day<sup>-1</sup> of bisphenol A is sufficient for human fatality [11].

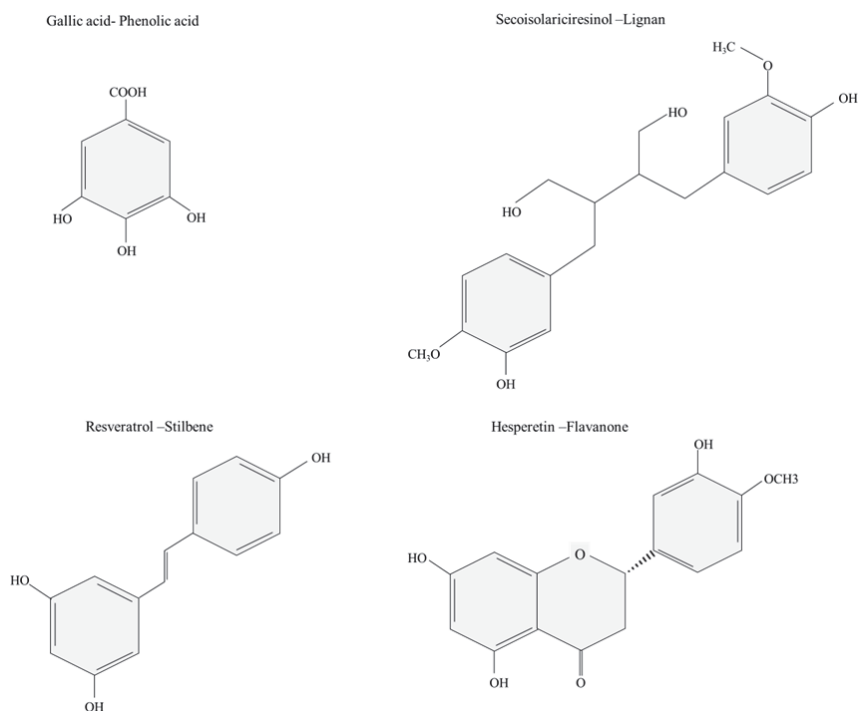


**Figure 1.** Examples of principal polyphenolic compounds clustered in phenolic acids (gallic acid) [14], lignans (secoisolariciresinol) [3], stilbenes (resveratrol) [15], and hesperetin (flavanone) [3].

On the other hand, there is enough evidence that polyphenols and the other bioactive compounds found in widely consumed products (e.g., tea, red wine, cocoa, fruits, fruit juices, and olive oil) have a potentially positive impact on the prevention of a wide range

of degenerative and age-related diseases, such as carcinogenesis and tumor development at the cellular level [11,15,16]. For years, polyphenols have been associated with their antioxidant activity, which has been widely verified *in vitro*. The antioxidant function of polyphenols is provided by their reducing properties, which allow them to act as free radical scavengers [17]. On the other hand, their activity *in vivo* depends on the bioavailability, the structures of compounds, and the composition and metabolic features of the human gut microbiota. In addition to antioxidant capacity, polyphenols have potential healthy properties for humans as anti-inflammatory, antiallergic, antihypertensive, neuropreventive, analgesic, antiviral, and antimicrobial agents [16,18,19]. These compounds are employed as effective antimicrobial agents in healthcare as an alternative to other treatments and in food preservation [20,21]. For example, the antibiotic activity of phenolic compounds is due to the modification of the bacterial structure, the pathogenic traits, or the changes in metabolism. In particular, tannins and flavonoids are able to inactivate membrane adhesins, enzymes, and transport proteins [22].

Despite the toxic effect of polyphenols on the aquatic environment and wildlife, the benefits are principally related to their consumption which allows for the prevention of diseases in humans and food preservation. This makes it essential to know the right approach for selecting and extracting the polyphenol of interest from the various effluents. These waters will be later treated by biological technologies to remove the remaining pollutants, giving the place a sustainable and circular economy, recovering the added-value compounds, and discharging high-quality waters into natural water bodies.

## 2. Polluted Waters as Sources of Phenolic Compounds: The Challenge of Their Profitability in the Circular Economy

The presence of polyphenols in water could be due to natural or anthropogenic sources. The decomposition of vegetal material (fruits, vegetables, or resins) contributes to the phenolic concentration in natural waters due to their water solubility. In drinking waters, the pollution is mainly due to the lixiviation of residues, while in lakes and other water bodies, this occurs by *in situ* decay. However, the water quality is primarily injured by the pressure exerted by the discharge of industrial wastewater. Polyphenols are present in the effluents from several industrial activities, such as pharmaceuticals, plastics, paint, pulp and paper, agrofood manufacturing, petrochemical, and wood products [3]. In fact, their concentration reaches 3900 mg·L<sup>-1</sup> in coking operations, 6800 mg·L<sup>-1</sup> in coal processing, 1220 mg·L<sup>-1</sup> in the petrochemical industry, 500 mg·L<sup>-1</sup> in refineries, or 1000 mg·L<sup>-1</sup> in the agrofood industry (e.g., in olive washing waters) [23–25]. Table 1 shows some effluents containing polyphenols from some industries.

**Table 1.** Phenol levels in industrial wastewaters [1,14,26–28].

Type of Industry	Range of Total Phenol Concentration (mg·L <sup>-1</sup> )
Rubber	3–10
Leather	4–6
Ferrous	5–9
Pulp and paper	22
Fiberglass	40–2564
Petroleum-processing plant	40–185
Wood Preserving	50–953
Fabric	100–150
Petrochemical	200–1200
Coke ovens (without dephenolization)	300–3900
Olive washing	400–1120
Agri-food (winery, oil)	400–10,700
Phenolic resins	1270–1345
Coal conversion	1700–7000

The presence of polyphenols in industrial wastewater effluents represents a major environmental problem related to the toxic effects on microorganisms, plants, and animals in the trophic chain [29]. However, the management of these harmful compounds could become a challenge for their valorization within a circular economy. Interesting sources of polyphenols are the wastes and byproducts from the agrifood production processes that could be employed in the food preservation, cosmetic, and pharmaceutical industries, supposing a new sustainable way to obtain the functional compounds could be found [17,30]. Therefore, the recovery of these substances from wastewater meets the two-fold objective: biodegradability improvement and byproduct valorization [31].

For example, the production of olive oil and wine is one of the most important economic activities in Mediterranean countries. These activities generate large amounts of solid and liquid wastes containing high levels of polyphenols [24,32]. Therefore, their recovery from these wastes provides an opportunity to obtain valuable biomolecules with a concomitant reduction in environmental toxicity issues [29,32]. In olive mill wastewater (OMW), polyphenols are partitioned between the water and oil phases, but the major fraction is retained in the wastewater due to the high solubility in water. Polyphenol extraction from OMW is very promising since these compounds are potent antioxidants. Among them, hydroxytyrosol and tyrosol are postulated as the most economically relevant phenolic components in the cosmetics, food preservation, and pharmaceutical industries [29,33].

### 3. Recovery of Polyphenols from Wastewater

Phenol recovery is necessary and useful but difficult, especially when unknown interactions with other pollutants in wastewater may occur [34]. However, this procedure offers a great economic advantage and makes these wastewaters less hazardous and easier to treat using biological methods [33]. Therefore, extensive research efforts have been directed toward the recovery of polyphenols from some agrofood industries (such as OMW or wineries) wastewaters [31,33].

The recovery of polyphenols is mostly performed by membrane processes, liquid-liquid extraction, which is often assisted by surfactants, or solid phase extraction using diverse resins for their recovery [29]. For example, the use of membrane processes requires small areas, and the separation of specific compounds could also facilitate the subsequent biological wastewater treatment [31,35]. The diverse membrane characteristics (ultrafiltration, nanofiltration, and reverse osmosis) could allow for the retention of solutes on the membrane surface, resulting in material accumulation (biofouling) that interferes with the concentration polarization, reducing the membrane lifetime [31]. Another example is the solid-phase extraction procedure for the recovery of phenolic compounds using several resins. The results of these studies highlighted how the desorption process is difficult because the solvents have low selectivity for specific polyphenols, and polyphenol ionization limits the removal performance [34].

Nowadays, much effort is put into the search for more efficient alternatives to extract the most interesting polyphenols for the cosmetic, pharmaceutical, and food industries. Currently, the adsorption process on suitable materials is postulated as an efficient method to recover specific polyphenols from aqueous solutions [36]. A large selection of synthetic polymeric adsorbents (such as polystyrene-divinylbenzene or divinylbenzene-ethylvinylbenzene copolymers) is available for carrying out an optimal process [36]. The adsorption on resins is a common separation technology, as the relatively inexpensive resins are lasting and chemically stable. In addition, these technologies include liquid extraction with a deep eutectic solvent, deionized water, or aqueous solutions of cyclodextrins using a semiautomatic extractor and multielement mixed micelle. The adsorption system is considered an economical, simple, and reversible method which avoids the use of toxic solvents. One of the most interesting and well-known materials used for adsorption is activated carbon [37,38]. The technique with activated carbon has been tested with several sorbents, including methylene blue and manganese oxide [39,40]. However, the

latest research employed animal proteins as coating biopolymers, avoiding environmental problems [33].

#### 4. Technologies to Remove Phenolic Compounds from Water Sources

Considering the harmful effects of some polyphenols and their derivatives on human health and natural environments, the removal of these compounds from water and wastewater is a great challenge for human and environmental safety, and the search and recognition of effective tools for their treatment, degradation, and removal are worthwhile [2,11]. Accordingly, great efforts have been spent, using physical, chemical, and biological methods to develop and optimize techniques for finding a sustainable solution to this problem. Undoubtedly, physicochemical technologies are more expensive than biological ones, and sometimes they are not completely effective because undesirable compounds are often produced as intermediates [41].

Among the physical-chemical methods, conventional processes have been applied for phenolic compound removal, such as distillation, adsorption, solid-phase extraction, liquid-liquid extraction, and catalytic and wet air oxidation. Furthermore, the last decade has been characterized by the development of phenolic acid degradation technologies. Some of these technologies are based on advanced oxidation, membrane filtration, heterogeneous photocatalysis, ozonization, enzymatic treatment, and the Fenton reaction [1,4]. However, these technologies have serious disadvantages, which are mainly related to their economical cost (e.g., the high energy consumption) and environmental unsustainability due to the production of secondary pollutants [42]. For these reasons, the search for biological alternatives for the treatment of effluents polluted with phenols is a challenge of great biotechnological interest.

The biological technologies for degrading and removing phenolic compounds are considered to represent a promising alternative because their main advantage is phenol degradation into nontoxic products, or even mineralization, accompanied by lower exploitation expenses [23]. Hence, there is a vast demand to develop economical, green, and sustainable technologies, in particular for rural areas with low income and highly impacted by agrofood industries [24] and/or in petrochemical, paper, and pharmaceutical factories [10,43].

It is very attention-grabbing to observe that the main development of biological technologies to remove phenolic compounds was based on aerobic conditions [43,44]. However, in recent years more attention has been paid to the development of anaerobic systems due to their tolerance to high organic loading rates (ORL), lower sludge excess production, and the valorization of methane generation [45,46]. Moreover, one of the most relevant advantages of anaerobic processes is robustness and resilience against changes in the influent composition [47].

The biological treatment of wastewater with high polyphenol content could be seriously compromised, especially when industrial discharges contain flavan-3-ols, flavonols, and tannins due to their wide spectrum of antimicrobial activities [48]. Although biological treatments are described as affordable, efficient, and environmentally friendly processes, the stability of the process could be compromised by the high load of phenolic compounds and their inherent toxicity [24]. Thus, it is crucial to develop technologies adapted to water composition and origin. In addition, it is important to allow for the adaptation of the initial biomass (inoculum) because microbiota with high activity and robustness are essential for achieving the efficient removal of recalcitrant compounds, mitigating the effect of wastewater discharges into natural environments [49].

#### 5. Feasible Biological Technologies for the Removal of Phenolic Compounds from Waters

The optimization of biological processes poses attractive alternatives to be implemented, because they are usually eco-friendly and economical, minimizing the generation of subproducts while being generally easy to operate. The microorganisms used in

biological technologies may promote the degradation of several organic and inorganic contaminants found in wastewater. The biodegradation could be mediated by extracellular or intracellular enzymes, and the pollutants could be removed by extracellular biosorption or active uptake and then incorporated and bioaccumulated [50–52]. Biological treatment could encounter difficulties in removing recalcitrant products, but the removal of polyphenols from water using many technologies has been reported [53]. The most useful technologies for the degradation of phenolic compounds based on biological treatments are discussed hereafter (Figure 2).

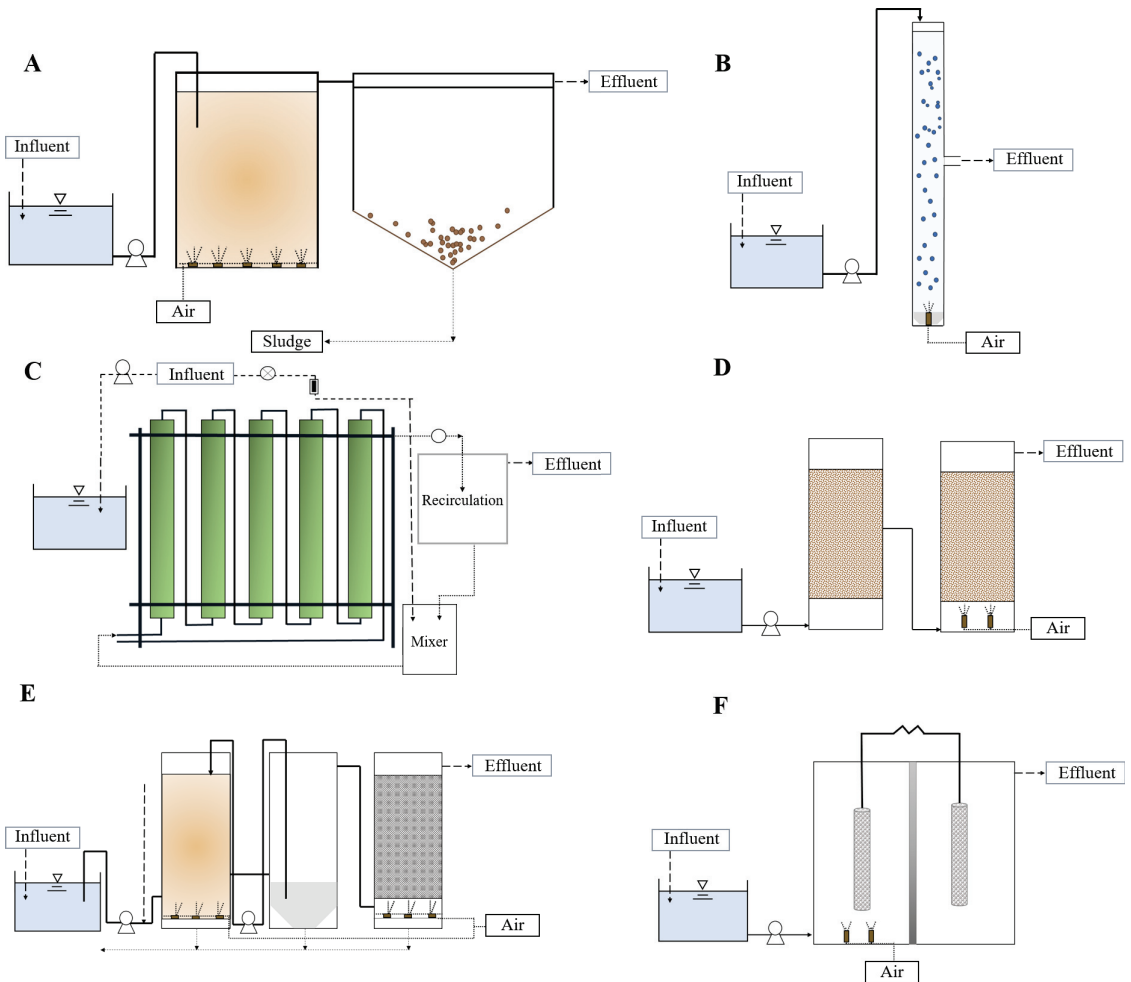


**Figure 2.** Diagram of biological water technologies for removing phenolic compounds from water: conventional activated sludge (A); aerobic granular sludge (B); photobioreactor (C); biofilter (D); membrane bioreactor (E); microbial fuel cell (F).

### 5.1. Conventional Activated Sludge

Conventional activated sludge (CAS) is a biological technology that has been used for treating wastewater for more than 100 years [54]. In the ‘classical’ context, CAS is a process performed by a suspended microbial biomass under aerobic conditions; the cells in contact with polluted water oxidize the compounds within an aerated chamber, and the biomass-liquid phases are then separated into a second chamber that acts as a

settler. The biomass of the activated sludge is composed of large flocs with filamentous microorganisms [55].

The activated sludge-based technology is the most diffused wastewater treatment worldwide [56]; thus, it is essential to understand which effects (on the global process) are exerted by the presence of phenolic compounds on raw water (inlet) in order to comprise the feasibility of their application to high-polyphenol-content waters. Siripattanakul-Ratpukdi et al. [57] investigated CAS system inhibition due to the high presence of phenolic compounds using synthetic wastewater supplemented with phenol as the sole carbon source to simulate the contaminated wastewater. The results pointed out that the system was able to completely remove the phenol in the case of low–moderate contamination ( $10 \text{ mg}\cdot\text{L}^{-1}$  phenol), whereas a low phenol removal ratio was observed in the highly contaminated scenario ( $100 \text{ mg}\cdot\text{L}^{-1}$ ) due to the inhibition caused by its recalcitrant nature. Moreover, the authors highlighted that phenol adsorption might also occur due to physical-chemical properties, such as the porous floc structure, which increases the surface area in contact with the wastewater and facilitates the adsorption process [58].

More recent studies reported the effective treatment of olive oil mill wastewater (OOMW) with a total phenol concentration of  $\sim 8730 \text{ mg}\cdot\text{L}^{-1}$  using CAS, but only after a dilution of up to  $128 \text{ mg}\cdot\text{L}^{-1}$  of polyphenols, obtaining a chemical oxygen demand (COD) and polyphenols removal ratio of 90% and 92%, respectively [59]. However, it is worth noting that various local and or international regulations do not permit effluent dilution [60,61].

However, CAS showed several disadvantages in comparison to novel technologies, such as the production of excess sludge, the big surface needed, or the low biomass retention time [62,63].

In recent years, the CAS configuration has been improved to overcome the technology's weaknesses. For instance, integrated fixed-film activated sludge (IFAS) is one of the most promising recent CAS configurations for its advantages, such as longer solids retention time, nutrient removal, complete nitrification, and lower carbon footprint [64]. Ahmed et al. [65] designed a kinetic model to evaluate the IFAS efficiency in petrochemical wastewater treatment and demonstrated that this technology is a viable bioprocess but is sensitive in non–steady states. Similarly, Lin et al. [66] carried out a phenol biodegradation experiment using a biofilm reactor, obtaining removal rates of 94–96% at different hydraulic retention times (HRT); moreover, they corroborated the results with their own mathematical model.

## 5.2. Aerobic Granular Sludge

Aerobic granular sludge (AGS) is a recent biological technology characterized by the immobilization of cells embedded in a tridimensional polymeric matrix with a spherical shape. AGS is usually operated in aerated cylindrical columns to promote the compactness and density of the granules, allowing for high biomass retention and resistance against toxic compounds. In fact, toxic compounds do not affect the single cells because a gradient is generated from the external to the internal layers, permitting high resilience against recalcitrant pollutants [63]. Several researchers have focused on the treatment of phenol [67], *p*-nitrophenol [68], halogenated phenols [69,70], and phenolic acids [24]. The microbial consortia used in the process were able to degrade the toxic compounds by diverse metabolic pathways, although it has been demonstrated that a preliminary adaptation of the granular sludge in the presence of phenols improves the removal performance [68].

The successful application of AGS for degrading phenolic compounds has been extensively demonstrated during the last decade [24]. Firstly, Liu et al. [71] and Jiang et al. [72] cultivated granular biomasses in presence of phenols to establish their degradation rate and toxicity at different levels/concentrations. Liu et al. [71] concluded that, despite the damage that polyphenols could cause to the granular biomass, the polyphenol removal activity of granular sludge was positively correlated with higher biomass concentration (Mix Liquor Suspended Solids, MLSS). For the first time, Jiang et al. [72] demonstrated

the capability of aerobic granules to provide stable and efficient phenol biodegradation, remarking that the granules represent an excellent immobilization strategy and biofilm functional structure, overcoming the inhibition effect of phenols on microbial growth and biodegradation activity. Undoubtedly, this research reported that the phenol concentration affects the selection of the phenol-degrading microorganisms within the granular biomass and directly impacts the robustness of the system and, consequently, the ability to achieve high performance.

Later research described several operational conditions and designs to optimize the removal of phenolic compounds. For instance, one research revealed that *p*-nitrophenol could be successfully removed; even an increase in *p*-nitrophenol concentration led to an increase in the performance rate (operating with values up to  $40.1 \text{ mg}\cdot\text{L}^{-1}$ ) [68]. Concomitantly, the start-up and optimization of AGS technology for operation in continuous flows posed a challenge for overcoming the possible disadvantages that batch-flow operations can entail at the industrial level. Jemaat et al. [44] investigated the response of AGS in a continuous-flow treatment of industrial wastewater in sequentially alternating pollutant scenarios using *p*-nitrophenol, phenol, and 2-chlorophenol with a concentration of  $15 \text{ mg}\cdot\text{L}^{-1}$ . Although these loads were lower than those used by Suja et al. ( $25\text{--}200 \text{ mg}\cdot\text{L}^{-1}$ ) [68] and Wang et al. ( $10\text{--}50 \text{ mg}\cdot\text{L}^{-1}$ ) [69], the difficulties involved in the continuous flow and the need to degrade *o*-cresol generated greater complications for the steady-state of granular biomasses. The results showed that AGS, in a continuous flow, was able to remove phenol and *p*-nitrophenol. During the first months of operation, the HPLC analysis did not detect *p*-nitrophenol in the effluent, but *p*-nitrocatechol (an intermediate of the aerobic degradation pathway) was found. Nonetheless, after this period, *p*-nitrophenol and *p*-nitrocatechol were below the detection limit of HPLC, and the nitrogen and *o*-cresol removals were almost complete. During the last stage, the system showed notable flaws, such as the serious damage to biomass conformation, a reduction in organic matter removal, the detection of intermediate compounds, and the accumulation of 2-chlorophenol. These issues suggested a need for further research to solve the inefficiency of AGS in continuous flow [44].

In addition, some authors tested a strategy based on the use of easily degradable carbon sources as co-substrates to hardly biodegradable polyphenols to ensure the stable biodegradation of these xenobiotics. Wang et al. used glucose as a co-substrate of 2,4-dichlorophenol to promote granule formation, obtaining successful polyphenol removal and biomass stability for long-term operations [69]. Ho et al. [67] reported that, in the presence of co-substrates as an additional carbon source, phenols at concentrations up to  $3000 \text{ mg}\cdot\text{L}^{-1}$  were removed with minimal lag time, while at  $5000 \text{ mg}\cdot\text{L}^{-1}$  phenol concentration, the granular biomass exhibits a longer lag time (20 h). In addition, this research demonstrated that granular sludge systems had weaker inhibition than CAS systems for treating phenol-rich wastewater.

The improvement of AGS technology for treating phenolic compounds has greatly increased during the last decade, driven by a greater knowledge of how to promote the metabolic pathways of the microorganisms of interest. Muñoz-Palazon et al. [24] operated AGS in sequential batch reactors with a mix of phenolic acids at concentrations from 50 to  $300 \text{ mg}\cdot\text{L}^{-1}$ , achieving excellent removal performance. Furthermore, the authors noted that higher concentrations ( $600\text{--}1000 \text{ mg}\cdot\text{L}^{-1}$ ) meant a strong detriment for the physical-chemical and polyphenolic removal rate (ranging from 30–60%). In this sense, despite the presence of the co-substrate as an alternative carbon source, it was observed that the proliferation of filamentous microorganisms promoted the breakage and disintegration of granules, resulting in floc-biomass formation and the destabilization of the steady state.

### 5.3. Photobioreactors

Photobioreactor technology represents a potentially viable strategy for removing pollutants from sewage, producing, at the same time, microalgal biomasses that are considered valuable products [73]. This process has demonstrated high photosynthetic efficiency and a low footprint, offering an environmentally sustainable alternative versus physical-chemical

technologies that produce chemical waste or sludge as byproducts [73,74]. This technology is based on the growth of microalgae in illuminated reactors, which could effectively transform the inorganic nutrients into organic compounds by means of photosynthesis [73]. Microalgae can be co-cultivated with bacteria to optimize phenolic compound removal; microalgae produce the oxygen required by bacteria to mineralize the organic pollutants, and the carbon dioxide produced by bacteria is, in turn, used by the microalgae [75]. Therefore, the photosynthetically produced oxygen avoids the insufflation (in the reactor) of the air needed to support the bacterial metabolic processes [76]. Biofilm photobioreactors involve microalgae–bacteria consortia and show several advantages, such as high biomass concentration, high biodegradation ratios, and resistance against toxic compounds [76]. Likewise, the biofilm promotes mass transfer from the external to the internal layer, providing hypoxic niches for the growth of facultative or strict anaerobic microorganisms [77]. The photobioreactor design needs to be adapted to the composition of wastewater and the operational conditions. For instance, Muñoz et al. [75] tested different photobioreactor configurations in order to achieve maximum efficiency in polyphenol removal. The reactors were based on four designs: a flat plate and a tubular packed-bed photobioreactor with the algal-bacterial biofilm attached to a glass material; a flat plate and tubular photobioreactor with the biofilm attached to the bioreactor walls; an algal-turf reactor open pond with biofilm attached on the reactor base, and a column photobioreactor with suspended biomass. All of them operated under a continuous illumination irradiance at  $180 \mu\text{E}\cdot\text{m}^{-2}\text{s}^{-1}$ . Muñoz et al. [75] indicated that photobioreactors involving biofilms presented two limitations that caused operational problems: photoinhibition, by the high density of the photon flux density, and the potential risk of clogging due to the excess biomass. In addition, the bioreactors with a suspended biomass and biofilms achieved similar removal efficiencies, but the latter promoted better biomass settleability than the suspended cultures.

Maza-Márquez et al. [77] described the treatment of real olive-washing wastewater (OWW) using a photobioreactor designed as a semi-open system consisting of a mixing tank, a tubular photobioreactor (composed of five-column tubes), a recirculation tank, and a collector tank. In this study, the average light intensity was  $450 \pm 50 \mu\text{E}\cdot\text{m}^{-2}$  at the outer layer, but the dark color of the OWW reduced the light transmission and may have inhibited the growth of the microalgae. Even so, the concentration of the polyphenols was drastically reduced (90.6%), revealing that the algae–bacteria consortium improves the metabolisms responsible for phenolic compound degradation, which was also corroborated by Chan et al. [76]. Moreover, the biological oxygen demand (BOD<sub>5</sub>) was completely removed in all scenarios. Therefore, this research supported the fact that microalgae provide enough oxygen for the bacterial degradation of polyphenols.

The previously described photobioreactor was implemented at full-scale [78], highlighting the success of the technology for removing COD and BOD<sub>5</sub> from OWW. Further, the results of spectrophotometric analysis by Folin–Ciocalteu showed the almost complete removal of the phenolic compounds, which was related to the microalgae–bacteria consortia composed of *Rhodospseudomonas* and *Azotobacter* bacteria and *Sphaeropleales* microalgae [78].

#### 5.4. Biofilters

Biofilter technology is one of the most important biological processes that is used for the removal of organic pollutants. In fact, biofilter technologies are widely employed for providing drinking water [79]. Biofilters are mostly characterized by the ability to separate the particulate matter and biomass from the aqueous phase, reducing the natural organic matter and several compounds. Biofilter performance allows for a reduction in the taste and odor of water, as well as removing the micropollutants involved in environmental concerns and human health [80]. Any type of support material that allows biomass immobilization could be used in biofilters. Nowadays, several materials of both natural (rock, slugs, sand, anthracite, and granular activated carbon) and artificial (membranes and plastics) origin are used as carriers [81–83]. However, the ‘classical’ biofilter technology is based on the



use of filter sand of different particle diameters from a rapid-rate to a slow-rate [84]. In addition, the biofilter process is very attractive because it significantly reduces the chlorine demand [79]. Usually, the proliferation of microbiota within an immobilized biofilm depends on the influent composition, inoculum origin, material support, and operational conditions. The versatility of this technology makes it difficult to define a universal reactor design since an effective design requires deep initial knowledge and the characterization of all the parameters to be considered (inlet water characterization and the required quality). Current molecular biological techniques have allowed for the promotion of microorganisms of interest to degrade target pollutants [79].

Although biofilter technology is not so widely used for the treatment of high-polyphenol-content waters, Huang et al. [49] have tested the treatment of wastewater with high content of a complex mixture of polyphenols (2,5-diethylphenol, trimethylphenol, ethylphenol, 2-(1-methylpropyl)-phenol, 2-ethyl-6-methylphenol, and 1-ethyl-4-methoxyphenol). The composition of the influent water was even more complex due to the presence of other kinds of biorefractory compounds widely found in coking wastewater, which implied more difficulties for polyphenol removal by biological treatment. The results revealed that after anaerobic filtration treatment, the phenols were quite degraded, and the achieved removal rates were 92.31% for *p*-diphenol and 53% for 2,5-diethylphenol. Additionally, the chromatography analyses showed that new compounds (such as dihydroxybenzene and cyclohexanone) were produced during the bioprocess, indicating the presence of intermediate molecules or simple compounds obtained from the full or partial degradation of the polyphenols. The different heights along the biofilter generated a gradient of pollutants, subproducts, and oxygen conditions that affected the microbial community structure responsible for the biotransformation and biodegradation processes [49,82].

### 5.5. Various Treatments Combined with Biofilters

#### 5.5.1. Conventional Activated Sludge Coupled with an Immobilized Biological Filter

As mentioned before, CAS technology is the most implemented biological technology for treating urban wastewater [85]. CAS includes an aeration chamber and a secondary clarifier; in the first chamber, the raw wastewater is mixed with the floc microorganisms, where the aerobic niche promotes the fast degradation of organic matter. Then, the water is transported to the secondary clarifier, where the floc-forming bacteria and the particulate matter are settled in order to provide a clear effluent. However, CAS efficiency for the removal of suspended particulate matter in the secondary settler is quite limited; thus, the coupling of CAS with a subsequent biofilter could improve the retention of the suspended solids and the solid-water phase separation. Additionally, the water streamflow through the reactor allows for the removal of other substances due to the development of different niches along the biofilm that is colonized by microbial communities with different metabolic competencies. The secretion of sticky and negatively charged extracellular polymeric substances by the bacterial biofilm makes it more resistant to toxic compounds; in addition, the biofilm promotes the mass transport and substrate conversion from the external to internal layers [86,87]. Thus, the toxic effect of polyphenolic compounds could be weakened along the depth/height of the immobilized biofilm, and the single cells are not directly affected, as they are embedded in a polysaccharide membrane that protects them. The implementation of conventional biological processes coupled with biofilter technology has been deeply studied for treating industrial wastewater with high-volatile organic compound content, harmful gases, and numerous toxic compounds to avoid the severe contamination produced by these industries [88]. Some microorganisms that form the attached biomass were able to convert target pollutants into intermediate or final products with low or absent harmfulness.

Tong et al. [89] described a pilot-scale CAS process coupled with an immobilized aerated biofilter designed for treating wastewater characterized by a large number of recalcitrant compounds that are generated during the oil extraction process. The carrier employed for the biofiltration process was the polycrylamide urepan, which was designed with

micro- and macropores to immobilize a wide spectrum of microorganisms of several sizes. The treatment train consisted of a CAS system followed by a settling tank; then, the water streamflow was passed through an immobilized biological aerated filter (I-BAF). The composition of the oil wastewater was very complex due to the low organic substrate concentration, the high presence of refractory organic compounds, and a low C:N:P ratio (which was 100:6:0.007, whereas it should be close to 100:5:1 to achieve good performance). Phenolic compounds were the most prominent group (with 15 kinds/species), accounting for ca. 31.5% of the load influent. The results revealed that CAS technology was able to remove all phenolic compounds without the need to pass through an I-BAF. The bacteria consortia identified in the activated sludge were more diverse than those on the biofilm of the I-BAF. Tong et al. [89] highlighted the role of *Pseudomonas* sp., *Planococcus* sp., and *Bacillus* spp. in phenolic compound removal; their role in polyphenol degradation in various natural and engineering environments has been studied in-depth [90–92].

### 5.5.2. Expanded Granular Sludge Bed Coupled with Biofilter

Expanded granular sludge bed (EGSB) technology is considered to represent the third generation of anaerobic reactor technologies. This process is characterized by the expansion of granular sludge and the promotion of the mass transfer between pollutants and microbiota by the high recirculation rate and a high height/diameter ratio ( $\geq 20$ ) [93]. Some authors combined the EGSB with biofilters for the treatment of recalcitrant compounds because the fixed biofilm promotes syntrophic mechanisms and resists and degrades polyphenols and their intermediates of degradation [93,94]. Several strategies for an EGSB coupled with biofilters have been tested. For instance, Wang et al. [93] implemented an aerobic biofiltration system to minimize the surface needed for the implementation of the treatment, but the exploitation cost increased due to the requirement of air insufflation. Rintala and Puhakka [95] reported the effectiveness of the EGSB coupled with an aerobic biofilter for chlorophenols degradation, demonstrating that the molecules are anaerobically attacked and dechlorinated, allowing for their mineralization in the subsequent aerobic biotreatment step. However, Collins et al. [94] highlighted the economical disadvantages related to this system (operations carried out under aerobic and mesophilic conditions). Therefore, these authors operated the EGSB combined with an anaerobic biofilter (ABF) at lower temperatures (15 °C). This system had a long start-up period, but once the steady-state was achieved, no trichlorophenols or 2,4 dichlorophenols were found in the effluent, evidencing the successful dehalogenation and a split reductive dichlorination pathway. In the subsequent scenarios, Collins et al. [94] added a higher polyphenol concentration to the influent, and they observed a similar trend. The HPLC results revealed the absence of the phenols and the presence of unidentified compounds possibly correlated with 4-hydroxybenzoic acid or other intermediate degradation products [96].

### 5.5.3. Membrane Bioreactor Technology

Membrane bioreactor (MBR) technology combines the activated sludge process with a membrane to separate the solid-liquid phases, avoiding the need for a secondary settler [97]. The configuration of the MBR has been developed and optimized in order to increase performance and removal efficiency. Depending on the required quality of the effluent, the employed membrane can be of nanofiltration, microfiltration, or ultrafiltration [98]. In the 'classical' MBR design, the configuration can generally have a submerged or side-stream membrane using external recirculation. Currently, novel changes have been implemented in the classical MBR designs to adhere to more restrictive legislation [99–101]. There are several ways to remove the phenolic compounds contained in wastewater by diverse membrane bioreactor configurations [11], including the moving-bed bioreactor (MBBR) [100,102], the anaerobic–anoxic–oxic (A<sup>2</sup>O) membrane reactor [25], the two-phase partitioning membrane bioreactor [101], or the few novel designs with photocatalysis, using material coupled to the MBBR [103].

During the last two decades, the interest aroused by membrane technologies led to the development of many novel configurations optimized for obtaining maximum polyphenol removal yields. Hosseini et al. [102] used the MBBR for treating phenolic compounds at concentrations in the range 200–800 mg·L<sup>-1</sup>, with HRT from 8 to 24 h. The results suggested that, regardless of the HRT, the ratio of phenolic COD:total COD should be close to 0.6 to achieve successful removal. The authors emphasized that MBBR technology was able to remove 480 mg·L<sup>-1</sup> phenol COD in short cycles (8–12 h), and the biomass exhibited low sensitivity against toxic load [102]. On the contrary, the A<sup>2</sup>O MBR system used to treat coal gasification wastewater had strong and negative effects caused by changes in HRT. The water inlet had high phenolic (1000 to 1600 mg·L<sup>-1</sup>) and COD (2000 to 4200 mg·L<sup>-1</sup>) concentrations. The real origin of the wastewater made the composition highly variable, with poor biodegradability due to the presence of refractory compounds [25]. Even so, the technology was able to remove almost all COD and ammonium (97% and 92%, respectively), as well as the total phenolic compounds (from the initial concentration of 776 to 2.32 mg·L<sup>-1</sup>). The authors described that the refractory compounds were converted into biodegradable substances in the anaerobic chamber and, subsequently, microbial activity notably reduced the compound toxicity in the anoxic and oxic chambers. In this case, if it was mandatory to meet a requirement for nitrogen discharges into water bodies; A<sup>2</sup>O MBR could be an optimal option for such implementations.

More recent advances have been achieved by combining the membrane bioreactors with other technologies. Mancuso et al. [103] coupled a TiO<sub>2</sub>-based-photocatalyst that was doped with Fe and/or Cr with an MBBR. They emphasized the difficulties arising from OMWW treatment using only MBR technology due to the short membrane lifetimes, biofouling clogging, and high operational costs [99,104]. Therefore, they proposed a preliminary photocatalysis treatment driven by solar UV in presence of a TiO<sub>2</sub> semiconductor and metal elements to save energy and solve the limitations given by the energy required for the operation. The results highlighted high polyphenol removal efficiency (close to 97%), as well as a notable increase in the biodegradability of these compounds in the presence of H<sub>2</sub>O<sub>2</sub> and the consequent improvement in the capability of treating larger wastewater flows.

Most of the industries related to chemical and agrifood factories produce effluents with high levels of salinity (representing 5% of the total industrial wastewater production), which directly affects biological processes due to osmotic pressure damaging the cells. Few studies have investigated the impact of salinity fluctuations on various aerobic processes in membrane technologies [105]. Muñoz Sierra et al. [46,106] particularized the lack of knowledge about the anaerobic MBR treatment of wastewaters with high polyphenols content and variable salinity. The research demonstrated an efficiency of 86–98% in terms of total phenolic compound removal in the presence of 18–37 gNa<sup>+</sup>·L<sup>-1</sup>. At these salinity concentrations, the biomass showed robustness and resilience against adverse conditions, but at higher concentrations, methanogenic activity and cell membrane integrity were compromised. Besides, an extractive membrane bioreactor (EMB) was implemented to treat landfill leachate effluent with a high phenolic concentration (150–200 mg·L<sup>-1</sup> [107]. The technology was able to reduce the phenolic fraction by ~98%; in addition, the HPLC analysis corroborated the absence of polyphenols and intermediate metabolites [107].

### 5.6. Microbial Bio-electrochemical Technology

Microbial bio-electrochemical technology (MET) is a growing biotechnological tool that combines electrochemistry, material science, and microbiology with the aim of generating energy [108].

The most used configuration of MET is the microbial fuel cell (MFC) technology based on converting the chemical energy of microbial metabolism into electricity during water treatment [109]. The process consists of an anode chamber and a cathode chamber separated by a proton exchange membrane or a salt bridge [110]. In the anode, microorganisms oxidize the substrates and produce electrons and protons. The protons are conducted to the

cathode through the exchange membrane, and the electrons are transported to the external circuit [110]. The membrane prevents the transfer of bacteria from the anode to the cathode and limits oxygen diffusion in the opposite direction [111]. Although the MFC is the most well-known design in METs, currently, the optimization and development of METs, combining catalytic redox activity with different abiotic electrochemical parameters and physic conditions, is in continuous expansion [112,113]. The versatility of the designs and the operational conditions, the consumption of several biodegradable substrates, and the production of energy make this technology one of the greenest for water treatment [114].

Friman et al. [115] implemented a bio-electrochemical cell technology to degrade phenols, operating similarly to MFCs, but with a constant external voltage applied between the electrodes. The phenol removal rate was ~80%, and the authors observed that it was not proportional to the time of contact between the pollutants and biomass, but higher biomass concentration was supposed to increase phenol removal efficiency. Hedbavna et al. [116] described how phenolic compounds found in the groundwater (caused by refinery industry lixivate) could serve as electron donors for voltage production, while the microorganisms found in the anode could be electron acceptors. The MFC systems were tested using phenolic compounds and acetate as electron donors, with closed and open circuits, and the results were similar for both the MFCs, with a polyphenolic reduction > 86% (from 1440 to >200  $\mu\text{M}$ ). During the initial phase, 4-hydroxy-3-methylbenzoic acid and 4-hydroxybenzoic acid (two metabolites of phenols) were detected at high concentrations in the anode chamber (108  $\mu\text{M}$  and 104  $\mu\text{M}$ , respectively). However, after stabilization, the values began to gradually decrease, indicating an increment in intermediate metabolite degradation.

The phenols were able to relatively inhibit electricity production (35–65%), but the robustness of the technology demonstrated high degradation rates for phenolic compounds such as 4-hydroxybenzoic, syringic, and vanillic acids, and their intermediate metabolites (despite the inherent toxicity of polyphenols) [117]. Li et al. [117] reported that the absence of additional electron donors improved the removal efficiency of phenolic compounds, as the microbiota was driven to use them as carbon sources. The research demonstrated that the removal of the phenolic compounds was driven by the degradation process rather than the adsorption process and that the microorganisms used intermediate metabolites for energy production and voltage generation instead of the parent phenolic compounds [117]. Li et al. [117] established that the fermentative process was not inhibited by high concentrations of phenolic acids; in addition, the main biotransformation of syringic acids gave rise to 3,4-dihydroxy-5-methoxybenzoic acid, which was subsequently converted into gallic acid and pyrogallol acid [118].

## 6. Microorganisms and Their Products Involved in Phenolic Biodegradation

Microorganisms are responsible for the suitable performance of all biological technologies described previously. A high number of microorganisms are able to degrade polyphenols in aquatic environments, including bacteria, fungi, and protozoa. Efficient biodegradation could be carried out by a single species [119,120] or microbial consortia [24,77]. During the design of a bioprocess, the selection of microorganisms or microbial consortia according to the nature of the water and the target pollutants is essential. The ability to achieve high performance will depend on the contaminant nature and the metabolic possibilities of the biomass in the bioreactor [91]. However, some drawbacks are found in urban or industrial wastewater, given the complexity of the matrices. Therefore, the microbial consortia employed as inoculum are generally selected by the technology configuration and influent composition since some microorganisms have competitive advantages in consuming, digesting, or degrading compounds under different abiotic and biotic parameters.

Given that phenol is widespread, some microorganisms have developed metabolic pathways for using it as carbon and/or energy source in several environments [1]. Undoubtedly, some microbial groups are more resistant to phenolic compounds. The microorganisms that are able to degrade polyphenols have been recognized in both the *Bacteria*

and *Eukarya* domains. Among the best-known microorganisms that can successfully carry out phenol biodegradation, there are bacteria such as *Bacillus*, *Pseudomonas*, *Flavobacterium*, and *Alcaligenes*, as well as fungal representatives, such as *Trichosporon*, *Aspergillus*, *Trametes*, and the yeast *Candida tropicalis* [24,121].

Aerobic bacteria transform phenol into nontoxic intermediate compounds that enter into the tricarboxylic acid cycle through ortho- or meta-pathways of degradation (Figure 3) [12]. In both pathways, phenol is firstly converted into catechol by the monohydroxylation of the C<sub>6</sub> ring at the *o*-position, which is catalyzed by phenol hydroxylase [91]. Phenol hydroxylase catalyzes the attachment of a hydroxyl group at the ortho-position of the aromatic ring, and then phenol is converted into catechol. This reaction is carried out by NADP-dependent flavin mono-oxygenase enzyme [12]. All mono-oxygenases include one atom of molecular oxygen in the corresponding substrate, while the other oxygen atom is reduced to H<sub>2</sub>O by a hydrogen donor, which is different for each enzyme. In addition to the hydroxylation of phenol, which is the preferred substrate of the phenol hydroxylase, this enzyme can catalyze the hydroxylation of hydroxyl-, amino-, halogen-, or methyl-substituted phenols [12]. Chlorophenol and (chloromethyl) phenol hydroxylases are employed to convert the substrates into chlorinated catechols or chloromethylcatechols, which play a key role in ortho- or meta-pathways. Phenol hydroxylase also catalyzes the conversion of alkylphenols into alkylcatechols. The aromatic ring of catechol is further opened by catechol 1,2-dioxygenase, leading to the formation of succinyl-CoA and acetyl CoA, or by catechol 2,3-dioxygenase, leading to the formation of pyruvate and acetaldehyde. Moreover, long-chain alkylphenols, nitrophenols, chloronitrophenols, and bisphenols require specific peripheral degradation pathways [91]. The bacterial degradation of nitrophenols can start with mono-oxygenation (a mono-oxygenase catalyzes the nitro groups elimination as a nitrite ion by adding an oxygen atom), the reduction of the nitro group (a nitroreductase catalyzes the nitrogen group reduction into amino groups or hydroxylamine), reductive dehalogenation from halonitrophenol compounds (a reductive dehalogenase removes the halogen atom, following the oxidative removal of the nitro group), and dioxygenation (insertion of two hydroxyl groups with the removal of the nitro group as nitrite ion) [122–124].

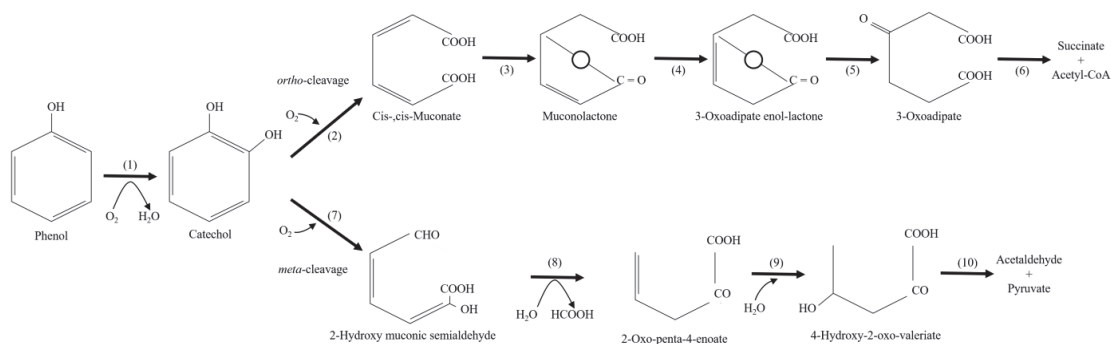


**Figure 3.** Aerobic phenol biodegradation pathways. (1) phenol monooxygenase, (2) catechol 1,2-dioxygenase, (3) muconate lactonizing enzyme, (4) muconolactone isomerase, (5) oxoadipate enol-lactone hydrolase, (6) oxoadipate succinyl-CoA transferase, (7) catechol 2,3-dioxygenase, (8) hydroxy-muconic semialdehyde hydrolase, (9) 2-oxopent-4-enoic acid hydrolase, (10) 4-hydroxy-2-oxoalder aldolase [125].

Some nitrophenol-degrading bacteria have been isolated by utilizing media enriched in mononitrophenols, halonitrophenols, or polynitrophenols. Among the isolated strains were *Arthrobacter nitrophenolicus* sp. [126], *Burkholderia* sp. RKJ [127], *Pseudomonas* sp. [122], *Rhodotorula glutinis* [128], *Sphingomonas* sp. [122], and *Paraburkholderia* [129].

In Mediterranean countries, OWW has been widely studied due to its recalcitrant nature that is related to high polyphenol content. For example, Maza-Marquez et al. [26] demonstrated that the phenolic pollutants found in an OWW storage basin could be treated using specific bacterial taxa, such as *Firmicutes* and *Clostridiales*. Muñoz-Palazon et al. [24] observed that the microbial communities in AGS reactors treating high polyphenol concentrations were dominated by *Lamprospedia*, *Acinetobacter*, *Arenimonas*, *Pseudomonas*, and *Corynebacterium*.

*Eukarya* microorganisms are widespread in environmental and engineering niches and play an essential role in the bioremediation field. Many studies have focused on phenolic compound degradation by fungi due to their ability to use organic pollutants as substrates for their growth. Some *Ascomycota* members have been isolated in systems designed for the treatment of OMWW with polyphenols as the sole carbon source, including *Aspergillus niger*, *Penicillium* sp., *Fusarium* sp., and *Alternaria* sp. [59]. The *Basidiomycota* phylum is the major fungal group that has members able to degrade toxic compounds due to their rich production of tyrosinases, laccases, and peroxidases [130]. Tyrosinases oxidate both monophenols and 1,2-diphenols (catechols) to quinones; laccases of a low-molecular-weight use 1,4-diphenols as substrate, which acts as monophenols and polyphenols; peroxidases are oxidoreductases that catalyze peroxide reduction and the concomitant oxidation of various substrates, including phenols [131,132]. These fungal enzymes are widely employed in industrial processes due to their role in improving organoleptic properties. For this reason, some authors highlighted the need for improved knowledge about the employment of wild-type and bioengineered fungi to obtain these enzymes of industrial interest [130,133].

In addition to bacteria and fungi, microalgae have also been recognized for their high capability to resist toxic compounds due to their extraordinary ability to produce extracellular laccases that allow for the biodegrading and transforming of aromatic compounds [134,135]. Microalgae can biotransform, mineralize, and remove compounds under phototrophic or mixotrophic conditions. Some phylotypes, such as *Chlorella* sp., can remove polyphenols under light or dark conditions [136,137]; moreover, it has been reported that *Scenedesmus quadricauda* and *Ankistrodesmus braunii* biotransform polyphenols in simpler compounds [138].

The immense diversity of the metabolic pathways and resistance of prokaryotic and eukaryotic microorganisms allows for the development of various strategies for biotechnological tools in order to provide a high-quality water effluent. However, further combined efforts among chemical, engineering, and microbiological areas have to be made to obtain higher yields via the microorganisms dwelling in engineering systems.

## 7. Conclusions

The biological treatment field has made immeasurable efforts to improve the feasibility and efficiency of the best available techniques for treating contaminated waters with high polyphenol content. From a classical engineering perspective, water treatment has always been more effective using physical-chemical technologies than biological approaches. However, this review provides a comprehensive reading on the success of combining biological, chemical, and engineering aspects to achieve polyphenol removal in water bodies. The main cause of inefficiency in biological water treatment lies in the lack of knowledge about (a) the characteristics of the influent, (b) the selection of the best fit technology, and (c) the optimum operational parameters to promote the biochemical processes. This review emphasizes the important role of microorganisms in these biotechnological processes, discarding the concept of reactors as ‘black boxes’, which exclusively evaluate the mass balance. Biotechnological approaches operated in a precise direction might improve the quality of the treated water in an economically and environmentally sustainable context.

The most decisive parameters for selecting the optimum biological technology for degrading pollutants and amending contaminated water are reported hereafter:

- (a) The concentration and nature of the polyphenols (variability of composition);
- (b) The presence of other toxic and recalcitrant compounds in the raw water matrix;
- (c) The carbon, nitrogen, and phosphorous concentration;

- (d) The water quality requirements for the treated water;
- (e) Logistics: the operational and economic possibilities for its implementation.

**Author Contributions:** All authors contributed significantly to the paper review. Conceptualization, data acquisition, resources, and writing of the original draft were carried out by B.M.-P., S.G., A.R.-M. and M.F.; review, and editing were carried out by B.M.-P., S.G., A.R.-M., M.P., M.B. and M.F. All authors have read and agreed to the published version of the manuscript.

**Funding:** This research received no external funding.

**Institutional Review Board Statement:** Not applicable.

**Informed Consent Statement:** Not applicable.

**Data Availability Statement:** Not applicable.

**Acknowledgments:** Barbara Muñoz-Palazon is supported by a grant from the University of Granada, the Ministerio de Universidades (Spain's Government), and the European Union-NextGenerationEU funds. Aurora Rosa-Masegosa is supported by grants from the Ministerio de Universidades and Ministerio de Educacion y Formacion Profesional (Spain's Government).

**Conflicts of Interest:** The authors declare no conflict of interest.

## References

1. Mohd, A. Presence of Phenol in Wastewater Effluent and Its Removal: An Overview. *Int. J. Environ. Anal. Chem.* **2022**, *102*, 1362–1384. [[CrossRef](#)]
2. Peeters, K.; Višnjevec, A.M.; Esakkimuthu, E.S.; Schwarzkopf, M.; Tavzes, Č. The Valorisation of Olive Mill Wastewater from Slovenian Istria by Fe<sub>3</sub>O<sub>4</sub> Particles to Recover Polyphenolic Compounds for the Chemical Specialties Sector. *Molecules* **2021**, *26*, 6946. [[CrossRef](#)] [[PubMed](#)]
3. de la Rosa, L.A.; Moreno-Escamilla, J.O.; Rodrigo-García, J.; Alvarez-Parrilla, E. *Phenolic Compounds*; Elsevier Inc.: Amsterdam, The Netherlands, 2018; ISBN 9780128132784.
4. Cladis, D.P.; Weaver, C.M.; Ferruzzi, M.G. (Poly)Phenol Toxicity in Vivo Following Oral Administration: A Targeted Narrative Review of (Poly)Phenols from Green Tea, Grape, and Anthocyanin-Rich Extracts. *Phytother. Res.* **2022**, *36*, 323–335. [[CrossRef](#)]
5. Bernini, R.; Pasqualetti, M.; Provenzano, G.; Tempesta, S. Ecofriendly Synthesis of Halogenated Flavonoids and Evaluation of Their Antifungal Activity. *New J. Chem.* **2015**, *39*, 2980–2987. [[CrossRef](#)]
6. Bernini, R.; Mincione, E.; Provenzano, G.; Fabrizi, G.; Tempesta, S.; Pasqualetti, M. Obtaining New Flavanones Exhibiting Antifungal Activities by Methyltrioxorhenium-Catalyzed Epoxidation-Methanolysis of Flavones. *Tetrahedron* **2008**, *64*, 7561–7566. [[CrossRef](#)]
7. Durazzo, A.; Lucarini, M.; Camilli, E.; Marconi, S.; Gabrielli, P.; Lisciani, S.; Gambelli, L.; Aguzzi, A.; Novellino, E.; Santini, A.; et al. Dietary Lignans: Definition, Description and Research Trends in Databases Development. *Molecules* **2018**, *23*, 3251. [[CrossRef](#)]
8. Andargie, M.; Vinas, M.; Rathgeb, A.; Möller, E.; Karlovsky, P. Lignans of Sesame (*Sesamum Indicum* L.): A Comprehensive Review. *Molecules* **2021**, *26*, 883. [[CrossRef](#)]
9. Singh, A.; Kumar, V.; Srivastana, J. Assessment of Bioremediation of Oil and Phenol Contents in Refinery Waste Water via Bacterial Con-Sortium. *J. Pet. Environ. Biotechnol.* **2013**, *4*, 1–4. [[CrossRef](#)]
10. Villegas, L.G.C.; Mashhadi, N.; Chen, M.; Mukherjee, D.; Taylor, K.E.; Biswas, N. A Short Review of Techniques for Phenol Removal from Wastewater. *Curr. Pollut. Rep.* **2016**, *2*, 157–167. [[CrossRef](#)]
11. Raza, W.; Lee, J.; Raza, N.; Luo, Y.; Kim, K.H.; Yang, J. Removal of Phenolic Compounds from Industrial Waste Water Based on Membrane-Based Technologies. *J. Ind. Eng. Chem.* **2019**, *71*, 1–18. [[CrossRef](#)]
12. Krastanov, A.; Alexieva, Z.; Yemendzhiev, H. Microbial Degradation of Phenol and Phenolic Derivatives. *Eng. Life Sci.* **2013**, *13*, 76–87. [[CrossRef](#)]
13. Gasmí, A.; Mujawdiya, P.K.; Noor, S.; Lysiuk, R.; Darmohray, R.; Piscopo, S.; Lenchyk, L.; Antonyak, H.; Dehtiarova, K.; Shanida, M.; et al. Polyphenols in Metabolic Diseases. *Molecules* **2022**, *27*, 6280. [[CrossRef](#)] [[PubMed](#)]
14. Cañadas, R.; González-Miquel, M.; González, E.J.; Díaz, I.; Rodríguez, M. Hydrophobic Eutectic Solvents for Extraction of Natural Phenolic Antioxidants from Winery Wastewater. *Sep. Purif. Technol.* **2021**, *254*, 117590. [[CrossRef](#)]
15. Froldi, G.; Ragazzi, E. Selected Plant-Derived Polyphenols as Potential Therapeutic Agents for Peripheral Artery Disease: Molecular Mechanisms. *Molecules* **2022**, *27*, 7110. [[CrossRef](#)]
16. Santos-Buelga, C. Polyphenols and Human Beings: From Epidemiology to Molecular Targets. *Molecules* **2021**, *26*, 4218. [[CrossRef](#)] [[PubMed](#)]
17. Zillich, O.V.; Schweiggert-Weisz, U.; Eisner, P.; Kerscher, M. Polyphenols as Active Ingredients for Cosmetic Products. *Int. J. Cosmet. Sci.* **2015**, *37*, 455–464. [[CrossRef](#)]

18. Sahiner, M.; Sanem Yilmaz, A.; Gungor, B.; Ayoubi, Y.; Sahiner, N. Therapeutic and Nutraceutical Effects of Polyphenolics from Natural Sources. *Molecules* **2022**, *27*, 6225. [[CrossRef](#)]
19. Gorrasi, S.; Pasqualetti, M.; Muñoz-palazon, B.; Novello, G.; Mazzucato, A.; Campiglia, E.; Fenice, M. Comparison of the Peel-Associated Epiphytic Bacteria of Anthocyanin-Rich “Sun Black” and Wild-Type Tomatoes under Organic and Conventional Farming. *Microorganisms* **2022**, *10*, 2240. [[CrossRef](#)]
20. Manso, T.; Lores, M.; de Miguel, T. Antimicrobial Activity of Polyphenols and Natural Polyphenolic Extracts on Clinical Isolates. *Antibiotics* **2022**, *11*, 46. [[CrossRef](#)]
21. Gutiérrez-Del-Río, I.; López-Ibáñez, S.; Magadán-Corpas, P.; Fernández-Calleja, L.; Pérez-Valero, Á.; Tuñón-Granda, M.; Miguélez, E.M.; Villar, C.J.; Lombó, F. Terpenoids and Polyphenols as Natural Antioxidant Agents in Food Preservation. *Antioxidants* **2021**, *10*, 1264. [[CrossRef](#)]
22. Laganà, P.; Anastasi, G.; Marano, F.; Piccione, S.; Singla, R.K.; Dubey, A.K.; Delia, S.; Coniglio, M.A.; Facciola, A.; di Pietro, A.; et al. Phenolic Substances in Foods: Health Effects as Anti-Inflammatory and Antimicrobial Agents. *J. AOAC Int.* **2019**, *102*, 1378–1387. [[CrossRef](#)]
23. Mohammadi, S.; Kargari, A.; Sanaeepur, H.; Abbassian, K.; Najafi, A.; Mofarrah, E. Phenol Removal from Industrial Wastewaters: A Short Review. *Desalination Water Treat* **2015**, *53*, 2215–2234. [[CrossRef](#)]
24. Muñoz-Palazon, B.; Rodríguez-Sánchez, A.; Hurtado-Martinez, M.; de Castro, I.M.; Juárez-Jimenez, B.; Gonzalez-Martinez, A.; Gonzalez-Lopez, J. Performance and Microbial Community Structure of an Aerobic Granular Sludge System at Different Phenolic Acid Concentrations. *J. Hazard. Mater.* **2019**, *376*, 58–67. [[CrossRef](#)] [[PubMed](#)]
25. Wang, Z.; Xu, X.; Gong, Z.; Yang, F. Removal of COD, Phenols and Ammonium from Lurgi Coal Gasification Wastewater Using A2O-MBR System. *J. Hazard. Mater.* **2012**, *235–236*, 78–84. [[CrossRef](#)]
26. Maza-Márquez, P.; Martínez-Toledo, M.V.; González-López, J.; Rodelas, B.; Juárez-Jiménez, B.; Fenice, M. Biodegradation of Olive Washing Wastewater Pollutants by Highly Efficient Phenol-Degrading Strains Selected from Adapted Bacterial Community. *Int. Biodeterior. Biodegrad.* **2013**, *82*, 192–198. [[CrossRef](#)]
27. Cifuentes-Cabezas, M.; Carbonell-Alcaina, C.; Vincent-Vela, M.C.; Mendoza-Roca, J.A.; Álvarez-Blanco, S. Comparison of Different Ultrafiltration Membranes as First Step for the Recovery of Phenolic Compounds from Olive-Oil Washing Wastewater. *Process Saf. Environ. Prot.* **2021**, *149*, 724–734. [[CrossRef](#)]
28. Tundis, R.; Conidi, C.; Loizzo, M.R.; Sicari, V.; Romeo, R.; Cassano, A. Concentration of Bioactive Phenolic Compounds in Olive Mill Wastewater by Direct Contact Membrane Distillation. *Molecules* **2021**, *26*, 1808. [[CrossRef](#)]
29. Bertin, L.; Ferri, F.; Scoma, A.; Marchetti, L.; Fava, F. Recovery of High Added Value Natural Polyphenols from Actual Olive Mill Wastewater through Solid Phase Extraction. *Chem. Eng. J.* **2011**, *171*, 1287–1293. [[CrossRef](#)]
30. Nabavi, S.F.; di Lorenzo, A.; Izadi, M.; Sobarzo-Sánchez, E.; Daglia, M.; Nabavi, S.M. Antibacterial Effects of Cinnamon: From Farm to Food, Cosmetic and Pharmaceutical Industries. *Nutrients* **2015**, *7*, 7729–7748. [[CrossRef](#)]
31. Giacobbo, A.; Bernardes, A.M.; Rosa, M.J.F.; de Pinho, M.N. Concentration Polarization in Ultrafiltration/Nanofiltration for the Recovery of Polyphenols from Winery Wastewaters. *Membranes* **2018**, *8*, 46. [[CrossRef](#)]
32. Tapia-Quirós, P.; Montenegro-Landívar, M.F.; Reig, M.; Vecino, X.; Cortina, J.L.; Saurina, J.; Granados, M. Recovery of Polyphenols from Agri-Food By-Products: The Olive Oil and Winery Industries Cases. *Foods* **2022**, *11*, 362. [[CrossRef](#)] [[PubMed](#)]
33. Yangui, A.; Abderrabba, M. Towards a High Yield Recovery of Polyphenols from Olive Mill Wastewater on Activated Carbon Coated with Milk Proteins: Experimental Design and Antioxidant Activity. *Food Chem.* **2018**, *262*, 102–109. [[CrossRef](#)] [[PubMed](#)]
34. Cui, P.; Chen, B.; Yang, S.; Qian, Y. Optimal Design of an Efficient Polyphenols Extraction Process for High Concentrated Phenols Wastewater. *J. Clean. Prod.* **2017**, *165*, 1395–1406. [[CrossRef](#)]
35. Mudimu, O.A.; Peters, M.; Brauner, F.; Braun, G. Overview of Membrane Processes for the Recovery of Polyphenols from Olive Mill Wastewater Olive Mill Wastewater. *Am. J. Environ. Sci.* **2012**, *8*, 195–201. [[CrossRef](#)]
36. Hellwig, V.; Gasser, J. Polyphenols from Waste Streams of Food Industry: Valorisation of Blanch Water from Marzipan Production. *Phytochem. Rev.* **2020**, *19*, 1539–1546. [[CrossRef](#)]
37. Thue, P.S.; Adebayo, M.A.; Lima, E.C.; Sieliechi, J.M.; Machado, F.M.; Dotto, G.L.; Vaghetti, J.C.P.; Dias, S.L.P. Preparation, Characterization and Application of Microwave-Assisted Activated Carbons from Wood Chips for Removal of Phenol from Aqueous Solution. *J. Mol. Liq.* **2016**, *223*, 1067–1080. [[CrossRef](#)]
38. Kumar, A.; Jena, H.M. Removal of Methylene Blue and Phenol onto Prepared Activated Carbon from Fox Nutshell by Chemical Activation in Batch and Fixed-Bed Column. *J. Clean. Prod.* **2016**, *137*, 1246–1259. [[CrossRef](#)]
39. Zhang, X.; Cheng, L.; Wu, X.; Tang, Y.; Wu, Y. Activated Carbon Coated Polygorskite as Adsorbent by Activation and Its Adsorption for Methylene Blue. *J. Environ. Sci.* **2015**, *33*, 97–105. [[CrossRef](#)]
40. Lee, M.E.; Park, J.H.; Chung, J.W.; Lee, C.Y.; Kang, S. Removal of Pb and Cu Ions from Aqueous Solution by Mn<sub>3</sub>O<sub>4</sub>-Coated Activated Carbon. *J. Ind. Eng. Chem.* **2015**, *21*, 470–475. [[CrossRef](#)]
41. Hasan, M.; Hakim, A.; Iqbal, A.; Bhuiyan, F.R.; Begum, M.K.; Sharmin, S.; Abir, R.A. Computational Study and Homology Modeling of Phenol Hydroxylase: Key Enzyme for Phenol Degradation. *Int. J. Comput. Bioinform. Silico Model.* **2015**, *4*, 691–698.
42. Xiao, J.; Xie, Y.; Han, Q.; Cao, H.; Wang, Y.; Nawaz, F.; Duan, F. Superoxide Radical-Mediated Photocatalytic Oxidation of Phenolic Compounds over Ag<sup>+</sup>/TiO<sub>2</sub>: Influence of Electron Donating and Withdrawing Substituents. *J. Hazard. Mater.* **2016**, *304*, 126–133. [[CrossRef](#)]



43. Vashi, H.; Iorhemen, O.T.; Tay, J.H. Aerobic Granulation: A Recent Development on the Biological Treatment of Pulp and Paper Wastewater. *Environ. Technol. Innov.* **2018**, *9*, 265–274. [[CrossRef](#)]
44. Jemaat, Z.; Suárez-Ojeda, M.E.; Pérez, J.; Carrera, J. Sequentially Alternating Pollutant Scenarios of Phenolic Compounds in a Continuous Aerobic Granular Sludge Reactor Performing Simultaneous Partial Nitritation and O-Cresol Biodegradation. *Bioresour. Technol.* **2014**, *161*, 354–361. [[CrossRef](#)] [[PubMed](#)]
45. Shi, X.; Leong, K.Y.; Ng, H.Y. Anaerobic Treatment of Pharmaceutical Wastewater: A Critical Review. *Bioresour. Technol.* **2017**, *245*, 1238–1244. [[CrossRef](#)] [[PubMed](#)]
46. Muñoz Sierra, J.D.; Oosterkamp, M.J.; Wang, W.; Spanjers, H.; van Lier, J.B. Comparative Performance of Upflow Anaerobic Sludge Blanket Reactor and Anaerobic Membrane Bioreactor Treating Phenolic Wastewater: Overcoming High Salinity. *Chem. Eng. J.* **2019**, *366*, 480–490. [[CrossRef](#)]
47. Muñoz Sierra, J.D.; Oosterkamp, M.J.; Wang, W.; Spanjers, H.; van Lier, J.B. Impact of Long-Term Salinity Exposure in Anaerobic Membrane Bioreactors Treating Phenolic Wastewater: Performance Robustness and Endured Microbial Community. *Water Res.* **2018**, *141*, 172–184. [[CrossRef](#)]
48. Daglia, M. Polyphenols as Antimicrobial Agents. *Curr. Opin. Biotechnol.* **2012**, *23*, 174–181. [[CrossRef](#)]
49. Huang, Y.; Hou, X.; Liu, S.; Ni, J. Correspondence Analysis of Bio-Refractory Compounds Degradation and Microbiological Community Distribution in Anaerobic Filter for Coking Wastewater Treatment. *Chem. Eng. J.* **2016**, *304*, 864–872. [[CrossRef](#)]
50. More, T.T.; Yadav, J.S.S.; Yan, S.; Tyagi, R.D.; Surampalli, R.Y. Extracellular Polymeric Substances of Bacteria and Their Potential Environmental Applications. *J. Environ. Manag.* **2014**, *144*, 1–25. [[CrossRef](#)]
51. Vashi, H.; Iorhemen, O.T.; Tay, J.H. Extensive Studies on the Treatment of Pulp Mill Wastewater Using Aerobic Granular Sludge (AGS) Technology. *Chem. Eng. J.* **2019**, *359*, 1175–1194. [[CrossRef](#)]
52. Gupta, S.; Nayak, A.; Roy, C.; Yadav, A.K. An Algal Assisted Constructed Wetland-Microbial Fuel Cell Integrated with Sand Filter for Efficient Wastewater Treatment and Electricity Production. *Chemosphere* **2021**, *263*, 128132. [[CrossRef](#)] [[PubMed](#)]
53. Rengaraj, S.; Moon, S.H.; Sivabalan, R.; Arabindoo, B.; Murugesan, V. Agricultural Solid Waste for the Removal of Organics: Adsorption of Phenol from Water and Wastewater by Palm Seed Coat Activated Carbon. *Waste Manag.* **2002**, *22*, 543–548. [[CrossRef](#)] [[PubMed](#)]
54. Edward, A.; William, T.L. Experiments on the Oxidation of Sewage without the Aid of Filters. *J. Soc. Chem. Ind.* **1914**, *33*, 523–539.
55. Koivuranta, E.; Stoor, T.; Hattunieni, J.; Niinimäki, J. On-Line Optical Monitoring of Activated Sludge Flocc Morphology. *J. Water Process. Eng.* **2015**, *5*, 28–34. [[CrossRef](#)]
56. Abdel Wahaab, R.; Mahmoud, M.; van Lier, J.B. Toward Achieving Sustainable Management of Municipal Wastewater Sludge in Egypt: The Current Status and Future Prospective. *Renew. Sustain. Energy Rev.* **2020**, *127*, 109880. [[CrossRef](#)]
57. Siripattanakul-Ratpukdi, S. Phenolic Based Pharmaceutical Contaminated Wastewater Treatment Kinetics by Activated Sludge Process. *J. Clean Energy Technol.* **2014**, *2*, 150–153. [[CrossRef](#)]
58. Mandal, A.; Das, S.K. Phenol Adsorption from Wastewater Using Clarified Sludge from Basic Oxygen Furnace. *J. Environ. Chem. Eng.* **2019**, *7*, 103259. [[CrossRef](#)]
59. Elmansour, T.E.; Mandi, L.; Ahmali, A.; Elghadraoui, A.; Aziz, F.; Hejjaj, A.; Del Bubba, M.; Ouazzani, N. Effect of Polyphenols on Activated Sludge Biomass during the Treatment of Highly Diluted Olive Mill Wastewaters: Biomass Dynamics and Purifying Performances. *Water Sci. Technol.* **2020**, *82*, 1416–1429. [[CrossRef](#)]
60. Schellenberg, T.; Subramanian, V.; Ganeshan, G.; Tompkins, D.; Pradeep, R. Wastewater Discharge Standards in the Evolving Context of Urban Sustainability—The Case of India. *Front. Environ. Sci.* **2020**, *8*, 30. [[CrossRef](#)]
61. Center, Regional Environmental. Regional Environmental Center Section 5 Water Protection Legislation. In *Handbook on the Implementation of EC Environmental Legislation*; Publication office: European Commission: Brussels, Belgium, 2008; pp. 613–733.
62. Fang, F.; Qiao, L.L.; Ni, B.J.; Cao, J.S.; Yu, H.Q. Quantitative Evaluation on the Characteristics of Activated Sludge Granules and Flocs Using a Fuzzy Entropy-Based Approach. *Sci. Rep.* **2017**, *7*, srep42910. [[CrossRef](#)]
63. Rosa-Masegosa, A.; Muñoz-Palazon, B.; Gonzalez-Martinez, A.; Fenice, M.; Gorrasi, S.; Gonzalez-Lopez, J. New Advances in Aerobic Granular Sludge Technology Using Continuous Flow Reactors: Engineering and Microbiological Aspects. *Water* **2021**, *13*, 1792. [[CrossRef](#)]
64. Waqas, S.; Bilal, M.R.; Man, Z.; Wibisono, Y.; Jaafar, J.; Indra Mahlia, T.M.; Khan, A.L.; Aslam, M. Recent Progress in Integrated Fixed-Film Activated Sludge Process for Wastewater Treatment: A Review. *J. Environ. Manag.* **2020**, *268*, 110718. [[CrossRef](#)] [[PubMed](#)]
65. Ahmed, M.E.; Abusam, A.; Mydlarczyk, A. Kinetic Modeling of GAC-IFAS Chemostat for Petrochemical Wastewater Treatment. *J. Water Resour. Hydraul. Eng.* **2017**, *6*, 27–33. [[CrossRef](#)]
66. Lin, Y.H.; Hsien, T.Y. Kinetics of Biodegradation of Phenolic Wastewater in a Biofilm Reactor. *Water Sci. Technol.* **2009**, *59*, 1703–1711. [[CrossRef](#)] [[PubMed](#)]
67. Ho, K.L.; Chen, Y.Y.; Lin, B.; Lee, D.J. Degrading High-Strength Phenol Using Aerobic Granular Sludge. *Appl. Microbiol. Biotechnol.* **2010**, *85*, 2009–2015. [[CrossRef](#)]
68. Suja, E.; Nancharaiyah, Y.V.; Venugopalan, V.P. P-Nitrophenol Biodegradation by Aerobic Microbial Granules. *Appl. Biochem. Biotechnol.* **2012**, *167*, 1569–1577. [[CrossRef](#)]
69. Wang, S.G.; Liu, X.W.; Zhang, H.Y.; Gong, W.X.; Sun, X.F.; Gao, B.Y. Aerobic Granulation for 2,4-Dichlorophenol Biodegradation in a Sequencing Batch Reactor. *Chemosphere* **2007**, *69*, 769–775. [[CrossRef](#)]

70. Duque, A.F.; Bessa, V.S.; Carvalho, M.F.; de Kreuk, M.K.; van Loosdrecht, M.C.M.; Castro, P.M.L. 2-Fluorophenol Degradation by Aerobic Granular Sludge in a Sequencing Batch Reactor. *Water Res.* **2011**, *45*, 6745–6752. [[CrossRef](#)]
71. Liu, Y.; Woon, K.H.; Yang, S.F.; Tay, J.H. Influence of Phenol on Cultures of Acetate-Fed Aerobic Granular Sludge. *Let. Appl. Microbiol.* **2002**, *35*, 162–165. [[CrossRef](#)]
72. Jiang, H.L.; Tay, J.H.; Tay, S.T.L. Aggregation of Immobilized Activated Sludge Cells into Aerobically Grown Microbial Granules for the Aerobic Biodegradation of Phenol. *Let. Appl. Microbiol.* **2002**, *35*, 439–445. [[CrossRef](#)]
73. Gao, F.; Li, C.; Yang, Z.H.; Zeng, G.M.; Feng, L.J.; Liu, J.-Z.; Liu, M.; Cai, H.W. Continuous Microalgae Cultivation in Aquaculture Wastewater by a Membrane Photobioreactor for Biomass Production and Nutrients Removal. *Ecol. Eng.* **2016**, *92*, 55–61. [[CrossRef](#)]
74. Luo, Y.; Le-Clech, P.; Henderson, R.K. Simultaneous Microalgae Cultivation and Wastewater Treatment in Submerged Membrane Photobioreactors: A Review. *Algal. Res.* **2017**, *24*, 425–437. [[CrossRef](#)]
75. Muñoz, R.; Köllner, C.; Guieysse, B. Biofilm Photobioreactors for the Treatment of Industrial Wastewaters. *J. Hazard. Mater.* **2009**, *161*, 29–34. [[CrossRef](#)] [[PubMed](#)]
76. Chan, S.S.; Khoo, K.S.; Chew, K.W.; Ling, T.C.; Show, P.L. Recent Advances Biodegradation and Biosorption of Organic Compounds from Wastewater: Microalgae-Bacteria Consortium—A Review. *Bioresour. Technol.* **2022**, *344*, 126159. [[CrossRef](#)] [[PubMed](#)]
77. Maza-Márquez, P.; González-Martínez, A.; Martínez-Toledo, M.V.; Fenice, M.; Lasserrot, A.; González-López, J. Biotreatment of Industrial Olive Washing Water by Synergetic Association of Microalgal-Bacterial Consortia in a Photobioreactor. *Environ. Sci. Pollut. Res.* **2017**, *24*, 527–538. [[CrossRef](#)]
78. Maza-Márquez, P.; González-Martínez, A.; Rodelas, B.; González-López, J. Full-Scale Photobioreactor for Biotreatment of Olive Washing Water: Structure and Diversity of the Microalgal-Bacteria Consortium. *Bioresour. Technol.* **2017**, *238*, 389–398. [[CrossRef](#)]
79. Kirisits, M.J.; Emelko, M.B.; Pinto, A.J. Applying Biotechnology for Drinking Water Biofiltration: Advancing Science and Practice. *Curr. Opin. Biotechnol.* **2019**, *57*, 197–204. [[CrossRef](#)]
80. Lewandowski, Z.; Boltz, J.P. Biofilms in Water and Wastewater Treatment. *Treatise Water Sci.* **2011**, *4*, 529–570. [[CrossRef](#)]
81. González-Martínez, A.; Muñoz-Palazon, B.; Kruglova, A.; Vilpanen, M.; Kuokkanen, A.; Mikola, A.; Heinonen, M. Performance and Microbial Community Structure of a Full-Scale ANITATMMox Bioreactor for Treating Reject Water Located in Finland. *Chemosphere* **2021**, *271*, 129526. [[CrossRef](#)]
82. Garcia-Ruiz, M.J.; Muñoz-Palazon, B.; Gonzalez-Lopez, J.; Osorio, F. Performance and Microbial Community Structure of an Anammox Biofilter Treating Real Wastewater from a Sludge Return. *J. Environ. Chem. Eng.* **2021**, *9*, 105211. [[CrossRef](#)]
83. Hella, M.S.; Abou-Elela, S.I.; Aly, O.H. Potential of Using Nonwoven Polyester Fabric (NWPFF) as a Packing Media in Multistage Passively Aerated Biological Filter for Municipal Wastewater Treatment. *Water Environ. J.* **2020**, *34*, 247–258. [[CrossRef](#)]
84. Zhu, I.X.; Getting, T.; Bruce, D. Review of Biologically Active Filters in Drinking Water Applications. *J. Am. Water Work. Assoc.* **2010**, *102*, 67–77. [[CrossRef](#)]
85. Orhon, D.; Sözen, S. Reshaping the Activated Sludge Process: Has the Time Come or Passed? *J. Chem. Technol. Biotechnol.* **2020**, *95*, 1632–1639. [[CrossRef](#)]
86. Mohapatra, R.K.; Behera, S.S.; Patra, J.K.; Thatoi, H.; Parhi, P.K. *Potential Application of Bacterial Biofilm for Bioremediation of Toxic Heavy Metals and Dye-Contaminated Environments*; Elsevier: Amsterdam, The Netherlands, 2019; ISBN 9780444642790.
87. Muffler, K.; Ulber, R. *Productive Biofilms*; Springer: Cham, Switzerland, 2014; Volume 146, ISBN 978-3-319-09694-0.
88. Hou, J.; Yu, C.; Meng, F.; He, X.; Wang, Y.; Chen, W.; Li, M. Succession of the Microbial Community during the Process of Mechanical and Biological Pretreatment Coupled with a Bio-Filter for Removal of VOCs Derived from Domestic Waste: A Field Study. *RSC Adv.* **2021**, *11*, 39924–39933. [[CrossRef](#)] [[PubMed](#)]
89. Tong, K.; Zhang, Y.; Liu, G.; Ye, Z.; Chu, P.K. Treatment of Heavy Oil Wastewater by a Conventional Activated Sludge Process Coupled with an Immobilized Biological Filter. *Int. Biodeterior. Biodegrad.* **2013**, *84*, 65–71. [[CrossRef](#)]
90. Hasan, S.A.; Jabeen, S. Degradation Kinetics and Pathway of Phenol by Pseudomonas and Bacillus Species. *Biotechnol. Biotechnol. Equip.* **2015**, *29*, 45–53. [[CrossRef](#)]
91. Prasad, R.; Aranda, E. *Approaches in Bioremediation: The New Era of Environmental Microbiology and Nanobiotechnology*; Springer: Cham, Switzerland, 2018; ISBN 978-3-030-02368-3.
92. Wang, J.; Wang, X.; Yu, Z.; Huang, S.; Yao, D.; Xiao, J.; Chen, W.; Wang, Z.; Zan, F. Using Algae Bacteria Consortia to Effectively Treat Coking Wastewater: Performance, Microbial Community, and Mechanism. *J. Clean. Prod.* **2022**, *334*, 130269. [[CrossRef](#)]
93. Wang, Y.; Yan, G.; Wang, Q.; Chen, C.; Li, M.; Guo, S. Refining Wastewater Treatment Using EGSB-BAF System. *Desalination Water Treat* **2015**, *53*, 2808–2815. [[CrossRef](#)]
94. Collins, G.; Foy, C.; McHugh, S.; O’Flaherty, V. Anaerobic Treatment of 2,4,6-Trichlorophenol in an Expanded Granular Sludge Bed-Anaerobic Filter (EGSB-AF) Bioreactor at 15 °C. *FEMS Microbiol. Ecol.* **2005**, *53*, 167–178. [[CrossRef](#)]
95. Rintala, J.A.; Puhakka, J.A. Anaerobic Treatment in Pulp- and Paper-Mill Waste Management: A Review. *Bioresour. Technol.* **1994**, *47*, 1–18. [[CrossRef](#)]
96. Song, J.; Zhao, Q.; Guo, J.; Yan, N.; Chen, H.; Sheng, F.; Lin, Y.; An, D. The Microbial Community Responsible for Dechlorination and Benzene Ring Opening during Anaerobic Degradation of 2,4,6-trichlorophenol. *Sci. Total Environ.* **2019**, *651*, 1368–1376. [[CrossRef](#)] [[PubMed](#)]

97. Melin, T.; Jefferson, B.; Bixio, D.; Thoeye, C.; De Wilde, W.; De Koning, J.; van der Graaf, J.; Wintgens, T. Membrane Bioreactor Technology for Wastewater Treatment and Reuse. *Desalination* **2006**, *187*, 271–282. [[CrossRef](#)]
98. Koyuncu, I.; Sengur, R.; Turken, T.; Guclu, S.; Pasaoglu, M.E. *Advances in Water Treatment by Microfiltration, Ultrafiltration, and Nanofiltration*; Woodhead Publishing: Oxford, UK, 2015; Volume 2019, ISBN 9781782421269.
99. Rodriguez-Sanchez, A.; Leyva-Diaz, J.C.; Muñoz-Palazon, B.; Rivadeneyra, M.A.; Hurtado-Martinez, M.; Martin-Ramos, D.; Gonzalez-Martinez, A.; Poyatos, J.M.; Gonzalez-Lopez, J. Biofouling Formation and Bacterial Community Structure in Hybrid Moving Bed Biofilm Reactor-Membrane Bioreactors: Influence of Salinity Concentration. *Water* **2018**, *10*, 1133. [[CrossRef](#)]
100. Liu, C.; Olivares, C.I.; Pinto, A.J.; Lauderdale, C.V.; Brown, J.; Selbes, M.; Karanfil, T. The Control of Disinfection Byproducts and Their Precursors in Biologically Active Filtration Processes. *Water Res.* **2017**, *124*, 630–653. [[CrossRef](#)] [[PubMed](#)]
101. Praveen, P.; Loh, K.C. Phenolic Wastewater Treatment through Extractive Recovery Coupled with Biodegradation in a Two-Phase Partitioning Membrane Bioreactor. *Chemosphere* **2015**, *141*, 176–182. [[CrossRef](#)]
102. Hosseini, S.H.; Borghei, S.M. The Treatment of Phenolic Wastewater Using a Moving Bed Bio-Reactor. *Process. Biochem.* **2005**, *40*, 1027–1031. [[CrossRef](#)]
103. Mancuso, A.; Morante, N.; De Carluccio, M.; Sacco, O.; Rizzo, L.; Fontana, M.; Esposito, S.; Vaiano, V.; Sannino, D. Solar Driven Photocatalysis Using Iron and Chromium Doped TiO<sub>2</sub> Coupled to Moving Bed Biofilm Process for Olive Mill Wastewater Treatment. *Chem. Eng. J.* **2022**, *450*, 138107. [[CrossRef](#)]
104. Rodríguez-Calvo, A.; Gonzalez-Lopez, J.; Ruiz, L.M.; Gómez-Nieto, M.Á.; Muñoz-Palazon, B. Effect of Ultrasonic Frequency on the Bacterial Community Structure during Biofouling Formation in Microfiltration Membrane Bioreactors for Wastewater Treatment. *Int. Biodeterior. Biodegrad.* **2020**, *155*, 105102. [[CrossRef](#)]
105. Rodriguez-Sanchez, A.; Leyva-Diaz, J.C.; Muñoz-Palazon, B.; Gonzalez-Lopez, J.; Poyatos, J.M. Effect of Variable Salinity Wastewater on Performance and Kinetics of Membrane-Based Bioreactors. *J. Chem. Technol. Biotechnol.* **2019**, *94*, 3236–3250. [[CrossRef](#)]
106. Muñoz Sierra, J.D.; Oosterkamp, M.J.; Spanjers, H.; van Lier, J.B. Effects of Large Salinity Fluctuations on an Anaerobic Membrane Bioreactor Treating Phenolic Wastewater. *Chem. Eng. J.* **2021**, *417*, 129263. [[CrossRef](#)]
107. Mosca Angelucci, D.; Donati, E.; Tomei, M.C. Extractive Membrane Bioreactor to Detoxify Industrial/Hazardous Landfill Leachate and Facilitate Resource Recovery. *Sci. Total Environ.* **2022**, *806*, 150892. [[CrossRef](#)] [[PubMed](#)]
108. Hassan, R.Y.A.; Febbraio, F.; Andreescu, S. Microbial Electrochemical Systems: Principles, Construction and Biosensing Applications. *Sensors* **2021**, *21*, 1279. [[CrossRef](#)] [[PubMed](#)]
109. Rahimnejad, M.; Adhami, A.; Darvari, S.; Zirepour, A.; Oh, S.E. Microbial Fuel Cell as New Technology for Bioelectricity Generation: A Review. *Alex. Eng. J.* **2015**, *54*, 745–756. [[CrossRef](#)]
110. Ghasemi, M.; Wan Daud, W.R.; Ismail, M.; Rahimnejad, M.; Ismail, A.F.; Leong, J.X.; Miskan, M.; Ben Liew, K. Effect of Pre-Treatment and Biofouling of Proton Exchange Membrane on Microbial Fuel Cell Performance. *Int. J. Hydrogen Energy* **2013**, *38*, 5480–5484. [[CrossRef](#)]
111. Ditzig, J.; Liu, H.; Logan, B.E. Production of Hydrogen from Domestic Wastewater Using a Bioelectrochemically Assisted Microbial Reactor (BEAMR). *Int. J. Hydrogen Energy* **2007**, *32*, 2296–2304. [[CrossRef](#)]
112. Santoro, C.; Arbizzani, C.; Erable, B.; Ieropoulos, I. Microbial Fuel Cells: From Fundamentals to Applications. A Review. *J. Power Sources* **2017**, *356*, 225–244. [[CrossRef](#)]
113. Wang, X.; Aulenta, F.; Puig, S.; Esteve-Núñez, A.; He, Y.; Mu, Y.; Rabaey, K. Microbial Electrochemistry for Bioremediation. *Environ. Sci. Ecotechnology* **2020**, *1*, 100013. [[CrossRef](#)]
114. Maddalwar, S.; Kumar Nayak, K.; Kumar, M.; Singh, L. Plant Microbial Fuel Cell: Opportunities, Challenges, and Prospects. *Bioresour. Technol.* **2021**, *341*, 125772. [[CrossRef](#)]
115. Friman, H.; Schechter, A.; Nitzan, Y.; Cahan, R. Phenol Degradation in Bio-Electrochemical Cells. *Int. Biodeterior. Biodegrad.* **2013**, *84*, 155–160. [[CrossRef](#)]
116. Hedbavna, P.; Rolfe, S.A.; Huang, W.E.; Thornton, S.F. Biodegradation of Phenolic Compounds and Their Metabolites in Contaminated Groundwater Using Microbial Fuel Cells. *Bioresour. Technol.* **2016**, *200*, 426–434. [[CrossRef](#)]
117. Li, B.; Liu, X.N.; Tang, C.; Zhou, J.; Wu, X.Y.; Xie, X.X.; Wei, P.; Jia, H.H.; Yong, X.Y. Degradation of Phenolic Compounds with Simultaneous Bioelectricity Generation in Microbial Fuel Cells: Influence of the Dynamic Shift in Anode Microbial Community. *Bioresour. Technol.* **2019**, *291*, 121862. [[CrossRef](#)] [[PubMed](#)]
118. Zeng, X.; Collins, M.A.; Borole, A.P.; Pavlostathis, S.G. The Extent of Fermentative Transformation of Phenolic Compounds in the Bioanode Controls Exoelectrogenic Activity in a Microbial Electrolysis Cell. *Water Res.* **2017**, *109*, 299–309. [[CrossRef](#)] [[PubMed](#)]
119. Juárez-Jiménez, B.; Manzanera, M.; Rodelas, B.; Martínez-Toledo, M.V.; González-López, J.; Crognale, S.; Pesciaroli, C.; Fenice, M. Metabolic characterization of a strain (BM90) of *Delftia tsuruhatensis* showing highly diversified capacity to degrade low molecular weight phenols. *Biodegradation* **2010**, *21*, 475–489. [[CrossRef](#)]
120. Juárez Jimenez, B.; Reboleiro Rivas, P.; Gonzalez Lopez, J.; Pesciaroli, C.; Barghini, P.; Fenice, M. Immobilization of *Delftia Tsuruhatensis* in Macro-Porous Cellulose and Biodegradation of Phenolic Compounds in Repeated Batch Process. *J. Biotechnol.* **2012**, *157*, 148–153. [[CrossRef](#)] [[PubMed](#)]
121. Satish, K.; Neeraj; Viraj, K.M.; Santosh, K.K. Biodegradation of Phenol by Free and Immobilized *Candida Tropicalis* NPD1401. *Afr. J. Biotechnol.* **2018**, *17*, 57–64. [[CrossRef](#)]

122. Arora, P.K.; Srivastava, A.; Singh, V.P. Bacterial Degradation of Nitrophenols and Their Derivatives. *J. Hazard. Mater.* **2014**, *266*, 42–59. [[CrossRef](#)] [[PubMed](#)]
123. Arora, P.K.; Srivastava, A.; Garg, S.K.; Singh, V.P. Recent Advances in Degradation of Chloronitrophenols. *Bioresour. Technol.* **2018**, *250*, 902–909. [[CrossRef](#)]
124. Arora, P.K.; Sasikala, C.; Ramana, C.V. Degradation of Chlorinated Nitroaromatic Compounds. *Appl. Microbiol. Biotechnol.* **2012**, *93*, 2265–2277. [[CrossRef](#)]
125. Singh, T.; Bhatiya, A.K.; Mishra, P.K.; Srivastava, N. An effective approach for the degradation of phenolic waste. In *Abatement of Environmental Pollutants*; Singh, P., Kumar, A., Borthaku, A., Eds.; Elsevier: Amsterdam, The Netherlands, 2020; pp. 203–243. [[CrossRef](#)]
126. Arora, P.K.; Jain, R.K. *Arthrobacter Nitrophenolicus* Sp. Nov. a New 2-Chloro-4-Nitrophenol Degrading Bacterium Isolated from Contaminated Soil. *3 Biotech* **2013**, *3*, 29–32. [[CrossRef](#)]
127. Arora, P.K.; Jain, R.K. Metabolism of 2-Chloro-4-Nitrophenol in a Gram Negative Bacterium, *Burkholderia* Sp. RKJ 800. *PLoS ONE* **2012**, *7*, e38676. [[CrossRef](#)]
128. Dulak, K.; Sordon, S.; Matera, A.; Kozak, B.; Huszcza, E.; Popłoński, J. Novel Flavonoid C-8 Hydroxylase from *Rhodotorula glutinis*: Identification, Characterization and Substrate Scope. *Microb. Cell Fact.* **2022**, *21*, 175. [[CrossRef](#)] [[PubMed](#)]
129. Wilhelm, R.C.; Cyle, K.T.; Martinez, C.E.; Karasz, D.C.; Newman, J.D.; Buckley, D.H. *Paraburkholderia solitsugae* Sp. Nov. and *Paraburkholderia elongata* Sp. Nov., Phenolic Acid-Degrading Bacteria Isolated from Forest Soil and Emended Description of *Paraburkholderia madseniana*. *Int. J. Syst. Evol. Microbiol.* **2020**, *70*, 5093–5105. [[CrossRef](#)] [[PubMed](#)]
130. Martínková, L.; Kotik, M.; Marková, E.; Homolka, L. Biodegradation of Phenolic Compounds by Basidiomycota and Its Phenol Oxidases: A Review. *Chemosphere* **2016**, *149*, 373–382. [[CrossRef](#)] [[PubMed](#)]
131. Baldrian, P. Fungal Laccases—Occurrence and Properties. *FEMS Microbiol. Rev.* **2006**, *30*, 215–242. [[CrossRef](#)]
132. Ikehata, K.; Buchanan, I.D.; Smith, D.W. Recent Developments in the Production of Extracellular Fungal Peroxidases and Laccases for Waste Treatment. *J. Environ. Eng. Sci.* **2004**, *3*, 1–19. [[CrossRef](#)]
133. Shukla, A.C. *Applied Mycology Entrepreneurship with Fungi*; Springer: Cham, Switzerland, 2022; ISBN 9783030906481.
134. Otto, B.; Schlosser, D. First Laccase in Green Algae: Purification and Characterization of an Extracellular Phenol Oxidase from *Tetracystis aerea*. *Planta* **2014**, *240*, 1225–1236. [[CrossRef](#)]
135. Lindner, A.V.; Pleissner, D. Utilization of Phenolic Compounds by Microalgae. *Algal. Res.* **2019**, *42*, 101602. [[CrossRef](#)]
136. Wang, L.; Xue, C.; Wang, L.; Zhao, Q.; Wei, W.; Sun, Y. Strain Improvement of *Chlorella* Sp. for Phenol Biodegradation by Adaptive Laboratory Evolution. *Bioresour. Technol.* **2016**, *205*, 264–268. [[CrossRef](#)]
137. Di Caprio, F.; Scarponi, P.; Altimari, P.; Iaquaniello, G.; Pagnanelli, F. The Influence of Phenols Extracted from Olive Mill Wastewater on the Heterotrophic and Mixotrophic Growth of *Scenedesmus* sp. *J. Chem. Technol. Biotechnol.* **2018**, *93*, 3619–3626. [[CrossRef](#)]
138. Pinto, G.; Pollio, A.; Previtiera, L.; Stanzione, M.; Temussi, F. Removal of Low Molecular Weight Phenols from Olive Oil Mill Wastewater Using Microalgae. *Biotechnol. Lett.* **2003**, *25*, 1657–1659. [[CrossRef](#)]

**Disclaimer/Publisher’s Note:** The statements, opinions and data contained in all publications are solely those of the individual author(s) and contributor(s) and not of MDPI and/or the editor(s). MDPI and/or the editor(s) disclaim responsibility for any injury to people or property resulting from any ideas, methods, instructions or products referred to in the content.



## Article

# Comparative Effects of Two Forms of Chitosan on Selected Phytochemical Properties of *Plectranthus amboinicus* (Lour.)

Maria Stasińska-Jakubas <sup>1</sup>, Barbara Hawrylak-Nowak <sup>1,\*</sup>, Magdalena Wójciak <sup>2</sup> and Sławomir Dresler <sup>2,3</sup>

<sup>1</sup> Department of Botany and Plant Physiology, Faculty of Environmental Biology, University of Life Sciences in Lublin, Akademicka 15, 20-950 Lublin, Poland

<sup>2</sup> Department of Analytical Chemistry, Medical University of Lublin, Chodźki 4a, 20-093 Lublin, Poland

<sup>3</sup> Department of Plant Physiology and Biophysics, Institute of Biological Science, Maria Curie-Skłodowska University, 20-033 Lublin, Poland

\* Correspondence: barbara.nowak@up.lublin.pl

**Abstract:** In response to stress factors, plants produce a wide range of biologically active substances, from a group of secondary metabolites, which are applied in medicine and health prophylaxis. Chitosan is a well-known elicitor affecting secondary metabolism in plants, but its effect on the phytochemical profile of *Plectranthus amboinicus* has not been assessed yet. In the present experiment, the effectiveness of the foliar application of two forms of chitosan (chitosan suspension or chitosan lactate) was compared in order to evaluate their potential to induce the accumulation of selected polyphenolic compounds in the aboveground parts of *P. amboinicus*. It was shown that chitosan lactate had substantially higher elicitation efficiency, as the use of this form exerted a beneficial effect on the analysed quality parameters of the raw material, especially the content of selected polyphenolic compounds (total content of polyphenols, flavonols, anthocyanins, and caffeic acid derivatives) and the free radical-scavenging activity of extracts from elicited plants. Concurrently, it had no phytotoxic effects. Hence, chitosan lactate-based elicitation can be an effective method for optimisation of the production of high-quality *P. amboinicus* raw material characterised by an increased concentration of health-promoting and antioxidant compounds.

**Keywords:** chitosan; Indian borage; phenolic compounds; biotic elicitor; secondary metabolites

**Citation:** Stasińska-Jakubas, M.; Hawrylak-Nowak, B.; Wójciak, M.; Dresler, S. Comparative Effects of Two Forms of Chitosan on Selected Phytochemical Properties of *Plectranthus amboinicus* (Lour.). *Molecules* **2023**, *28*, 376. <https://doi.org/10.3390/molecules28010376>

Academic Editor: Nour Eddine Es-Safi

Received: 10 December 2022

Revised: 27 December 2022

Accepted: 29 December 2022

Published: 2 January 2023



**Copyright:** © 2023 by the authors. Licensee MDPI, Basel, Switzerland. This article is an open access article distributed under the terms and conditions of the Creative Commons Attribution (CC BY) license (<https://creativecommons.org/licenses/by/4.0/>).

## 1. Introduction

The current trends in the promotion of a healthy lifestyle and the simultaneous increase in the prevalence of lifestyle diseases have contributed to the growing interest of many industries in both high-quality herbal raw materials and the contents of health-enhancing substances in plants, especially those with antioxidant properties [1]. Those plant chemical compounds have the ability to protect the body against the harmful effects of oxidative stress and prevent the risk of different cardiovascular, metabolic, and degenerative diseases, cancers, or premature aging [2,3]. For this reason, it is important not only to search for solutions to stimulate the production of desired secondary metabolites but also to investigate the chemical composition and properties of plant species that have not been used on a larger scale so far [3].

One of the effective methods for enhancement of the phytoaccumulation of bioactive compounds and thus improvement of the quality of raw materials involves elicitation with various types of substances and factors used as the so-called elicitors of plant defence reactions [4]. As indicated in current literature reports, elicitors stimulate receptors on the surface of the cytoplasmic membrane and activate a number of plant defence mechanisms, leading to the stimulation of secondary metabolism pathways and production of compounds that contribute to plant survival in stress conditions [5,6]. An increasingly frequently used biotic elicitor is chitosan, which can potentially be applied for the optimisation of plant production due to its natural origin, favourable physicochemical properties, and

high biological activity, with the most important antioxidant and antimicrobial effects, as well as the regulation of plant growth, development, and resistance. Chitosan is a polysaccharide biopolymer derived from the partial deacetylation of chitin, obtained most often from marine-processing waste and from insect exoskeletons and fungal cell walls [7–9]. Additionally, an important issue in the context of elicitation is that the use of chitosan helps to improve the yield of many phytochemical antioxidant compounds, e.g., substances from the group of polyphenols, terpenoids, naphthoquinones, and alkaloids [7,10].

Polyphenolic compounds constitute a large group of secondary metabolites comprising over 8000 substances, with phenolic acids, flavonoids, isoflavonoids, stilbenes, and lignans as the most important compounds. In plants, these substances perform important protective functions against unfavourable biotic and abiotic environmental factors [11–13]. However, most polyphenols also exert a beneficial effect on the human organism through their antioxidant, anti-inflammatory, antiviral, anti-proliferative, hepatoprotective, nephroprotective, antidepressant, immunomodulatory, and anticancer activity. They can be effective e.g., in the treatment of cardiovascular diseases, skin diseases, diabetes, cancer, and neurodegenerative diseases, especially for the prophylaxis and treatment of Alzheimer's disease [11,14–17]. Additionally, polyphenols can modulate energy metabolism, thereby exerting a positive effect on general well-being, delaying the aging process, and reducing the risk of age-related diseases [18]. These compounds play a significant role not only for plants that produce them, but also for people who use their health-beneficial properties. The importance of polyphenols and their connection with plant stress responses and secondary resistance in animals is often emphasised in the literature as xenohormesis hypothesis. It assumes that some plant chemical compounds are able to allow heterotrophs to adapt to changing environmental conditions by inducing biological responses. Therefore, xenohormesis is in fact the final pharmacological effect initiated by plant adaptation [19–21]. Given the wide spectrum of activity and the high abundance of this group of compounds in the chemical composition of *Plectranthus amboinicus* (Lour.) plants, the phytochemical analyses performed in this study focused on the effect of two forms of chitosan (chitosan suspension or chitosan lactate) on the total content of polyphenolic compounds and the level of some representatives of this group, i.e., flavonoids, anthocyanins, and caffeic acid derivatives.

*P. amboinicus* (some common names include Indian borage, Mexican mint, Cuban oregano, French thyme, Spanish thyme) is a perennial plant from the family Lamiaceae. The leaf raw material of this species is most often used for medicinal purposes, as it contains more than 100 substances with health-promoting properties: phenolic acids (rosmarinic acid, chlorogenic acid, caffeic acid, hydroxycinnamic acid, p-coumaric acid), flavonoids (quercetin, luteolin, apigenin, genquanine), carotenoids, steroidal glycosides, alkaloids, saponins, tannins, and phytosterols. This species also provides raw material for the extraction of essential oil, for which the chemical composition comprises germacrene,  $\beta$ -caryophyllene, carvacrol, thymol, camphene, zingiberene, chavicol, nerol, linalool,  $\delta$ -cadinene, p-cymene,  $\alpha$ -humulene,  $\gamma$ -terpinene,  $\alpha$ -terpineol, and  $\beta$ -selinene. The presence of these compounds determines the wide spectrum of activity and application of fresh *P. amboinicus* leaves, as well as oils and extracts [22–27].

In folk medicine, formulations made from *P. amboinicus* leaves are used in the treatment of various ailments, e.g., cough, nasal congestion, oral diseases, colic, indigestion, hepatopathy, headaches, fever, convulsions, epilepsy, nephrolithiasis, gallstones, or rheumatism. Fresh leaves of this plant are also collected to prepare remedies for external use to soothe burns or insect and arachnid bites and to treat skin inflammation, hard-to-heal wounds, and urinary infections. Moreover, due to its high content of minerals (iron, calcium, potassium, magnesium, zinc), this plant can be consumed as a food with pro-health properties or in combination with probiotic products to restore the normal intestinal microflora [22,24,26–28]. The long-term use of this species in natural medicine in many countries is supported by numerous scientific studies reporting strong antibacterial, fungistatic, fungicidal, anthelmintic, diuretic, antioxidant, antimutagenic, and anticancer

properties of this plant species [23–25,28]. Additionally, aqueous *P. amboinicus* extracts exert anti-inflammatory and analgesic effects [29], and ethanol extracts have anxiolytic and antiepileptic properties [30]. It has also been found that essential oil extracted from this species may potentially be used as a natural repellent or an agent for the control of mosquito populations [31]. However, due to the high variability of its chemical composition, further research on the biological activity and potential applications of this species is required [26].

Given the information presented above and the lack of literature reports on the potential use of chitosan for stimulation of the biosynthesis of secondary metabolites in *P. amboinicus*, the present study was carried out to compare the effectiveness of the application of a chitosan suspension and a chitosan lactate solution (differing in solubility and deacetylation degree) in the elicitation of selected phenolic compounds in the aboveground parts of this species. The hypothesis that the two forms of chitosan vary in their eliciting effects and differently influence the accumulation of phenolic compounds in *P. amboinicus* was tested. This study, for the first time, provides insight into the effect of the foliar application of chitosan on the basic physiology and chemical composition of this interesting and pharmaceutically important species.

## 2. Results

### 2.1. Content of Polyphenolic Compounds and Antioxidant Activity after Application of Chitosan

The total content of polyphenolic compounds in the extracts from *P. amboinicus* leaves and stems was found to depend on the form of chitosan. Only the CHL foliar application caused a significant increase in the concentration of this group of compounds in the leaves (by 43% compared to that in the control) (Figure 1a). In comparison with the control plants, the leaves of the CHT- or CHL-treated plants showed an increase in the level of flavonols (by 8% and 11%, respectively) and anthocyanins (by 30% and 51%, respectively) (Figure 1b,c). In contrast, the level of anthocyanins in the stems declined after the application of both chitosan forms (Figure 1c). The application of chitosan did not influence the total content of phenolic compounds and flavonols in the stems (Figure 1a,b). Additionally, the extracts from the CHL-treated *P. amboinicus* leaves exhibited an increased ability to reduce DPPH radicals. However, the application of the CHT solution resulted in a decrease in the free radical-scavenging activity (FRSA) of the stems, compared to that in the control (Figure 1d).

Given the general content of phenolic compounds and flavonols, as well as the varied response of leaf and stem tissues to chitosan application, only the *P. amboinicus* leaf extracts were subjected to further detailed analyses. All extracts had a similar qualitative profile of polyphenols, and sixteen components were identified based on mass data [m/z-H] and UV-Vis spectra obtained in the range of 200–400 nm (Table 1; Figure 2). The mass data and chromatographic parameters were compared with available standards, or the components were tentatively identified based on literature. No peaks from the new compounds were observed under the influence of CHT or CHL. The caffeic acid derivatives were predominant (Figure 2), and therefore, they were determined quantitatively.

The effect of the chitosan application on the concentration of individual caffeic acid derivatives is shown in Figure 3. Among the analysed compounds, the highest concentrations were determined in the case of rosmarinic acid, for which the level additionally increased significantly after the application of CHL (by 55% versus the control plants) but not CHT. Similarly, rosmarinic acid glucoside constituted a significant fraction of the phenolic metabolites present in the *P. amboinicus* leaves; however, its accumulation did not increase after the application of CHL but was even reduced by the CHT treatment. After the application of CHL, the level of chlorogenic and neochlorogenic acids increased by 42% and 37%, respectively, compared to that of the control. The CHT spraying treatment resulted in a 16% increase in the neochlorogenic acid level as well. The concentration of caffeoylglucose I and caffeoylglucose III increased after treatments with both forms of chitosan, whereas an increase in the caffeoylglucose II level was only observed after the application of CHL. In addition, the level of some metabolites (rosmarinic acid glucoside, salvianolic acid B) was found to decline with the CHT treatment. In general, the accumulation of most of the



analysed compounds increased in plants treated with the chitosan foliar application, and CHL turned out to be a much more effective inducer of the biosynthesis and accumulation of these compounds than CHT (Figure 3).

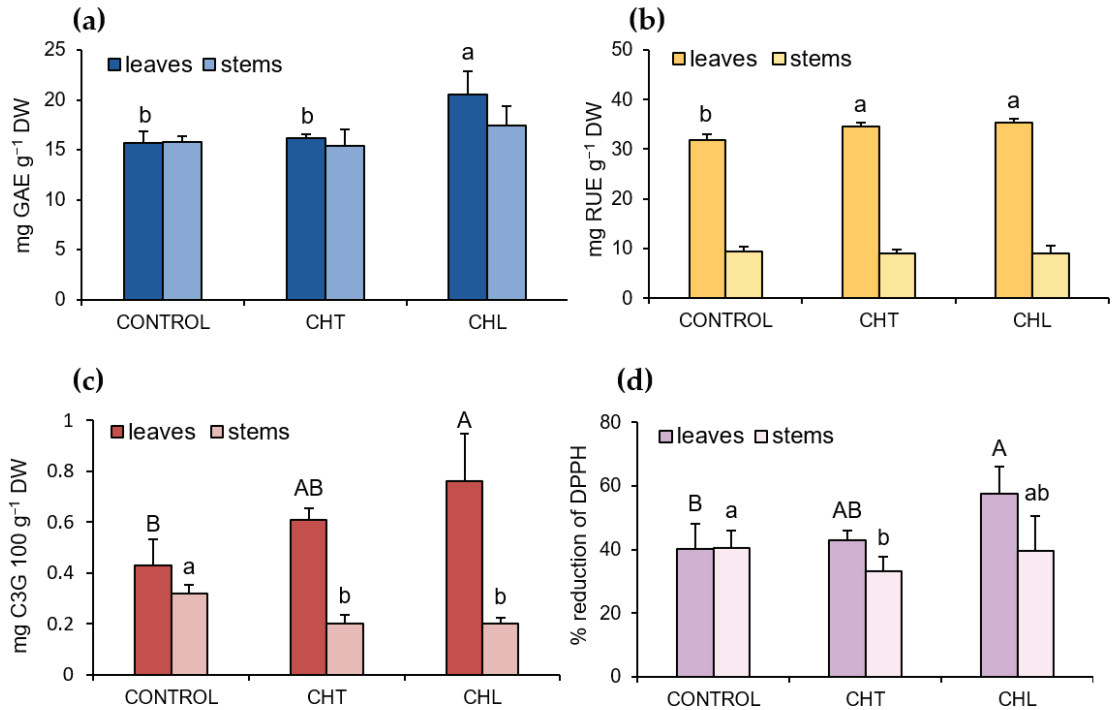


**Figure 1.** Total content of phenolics (a), flavonols (b), and anthocyanins as cyanidin 3-glycoside, C3G (c) and free radical scavenging activity (d) of *P. amboinicus* leaf and stem extracts, depending on the form of chitosan in the solution used for spraying the plants (CHT—chitosan suspension; CHL—chitosan lactate). Mean values ( $\pm$ standard deviation;  $n = 3$ ) marked with different letters were statistically significantly different ( $p < 0.05$ ). The absence of a letter designation means the absence of statistically significant differences.

**Table 1.** MS data of components identified in the *P. amboinicus* leaf samples in negative ionisation mode.

Peak	RT [min]	[M – H] <sup>-</sup> (Fragments)	$\Delta$ ppm	Formula	Identified	References
1	1.54	191.05648	1.92	C <sub>7</sub> H <sub>12</sub> O <sub>6</sub>	Quinic acid	Standard
2	6.64	315.07341 (153)	3.97	C <sub>13</sub> H <sub>16</sub> O <sub>9</sub>	Dihydroxybenzoic acid hexoside	[32]
3	7.89	153.01942	0.57	C <sub>7</sub> H <sub>6</sub> O <sub>4</sub>	Dihydroxybenzoic acid	[33]
4	10.28	353.08901 (191, 179, 135)	3.40	C <sub>16</sub> H <sub>18</sub> O <sub>9</sub>	Neochlorogenic acid	Standard
5	10.99	341.08831 (179, 135, 221)	1.47	C <sub>15</sub> H <sub>18</sub> O <sub>9</sub>	Caffeoylglucose I	[33]
6	11.32	297.06176 (179, 135, 117)	0.59	C <sub>13</sub> H <sub>14</sub> O <sub>8</sub>	Caffeic acid derivative I	[34]

Table 1. Cont.

Peak	RT [min]	[M – H] <sup>−</sup> (Fragments)	Δppm	Formula	Identified	References
7	12.37	297.06282 (179, 135, 117)	4.12	C <sub>13</sub> H <sub>14</sub> O <sub>8</sub>	Caffeic acid derivative II	[34]
8	13.00	341.08791 (179, 135, 221)	0.30	C <sub>15</sub> H <sub>18</sub> O <sub>9</sub>	Caffeoylglucose II	[33]
9	14.60	341.08911 (179, 135, 221)	3.81	C <sub>15</sub> H <sub>18</sub> O <sub>9</sub>	Caffeoylglucose III	[33]
10	15.43	353.08921 (191, 179, 135)	3.97	C <sub>16</sub> H <sub>18</sub> O <sub>9</sub>	Chlorogenic acid	Standard
11	16.05	179.03556	3.21	C <sub>9</sub> H <sub>8</sub> O <sub>4</sub>	Caffeic acid	Standard
12	17.66	297.06259 (179, 135, 117)	3.35	C <sub>13</sub> H <sub>14</sub> O <sub>8</sub>	Caffeic acid derivative III	[34]
13	32.49	521.13221 (359, 341, 179)	4.11	C <sub>24</sub> H <sub>26</sub> O <sub>13</sub>	Rosmarinic acid glucoside	[33]
14	38.52	359.07791 (179, 161)	1.86	C <sub>18</sub> H <sub>16</sub> O <sub>8</sub>	Rosmarinic acid	Standard [33]
15	46.41	717.14781 (519, 321, 339)	2.37	C <sub>36</sub> H <sub>30</sub> O <sub>16</sub>	Salvianolic acid B	[33,35]
16	49.43	503.08523 (285, 443)	4.20	C <sub>23</sub> H <sub>20</sub> O <sub>13</sub>	Luteolin 30-(4''-acetylglucuronide)	[33]

Caffeoylglucose and caffeic acid derivatives were quantified using a calibration curve for caffeic acid.

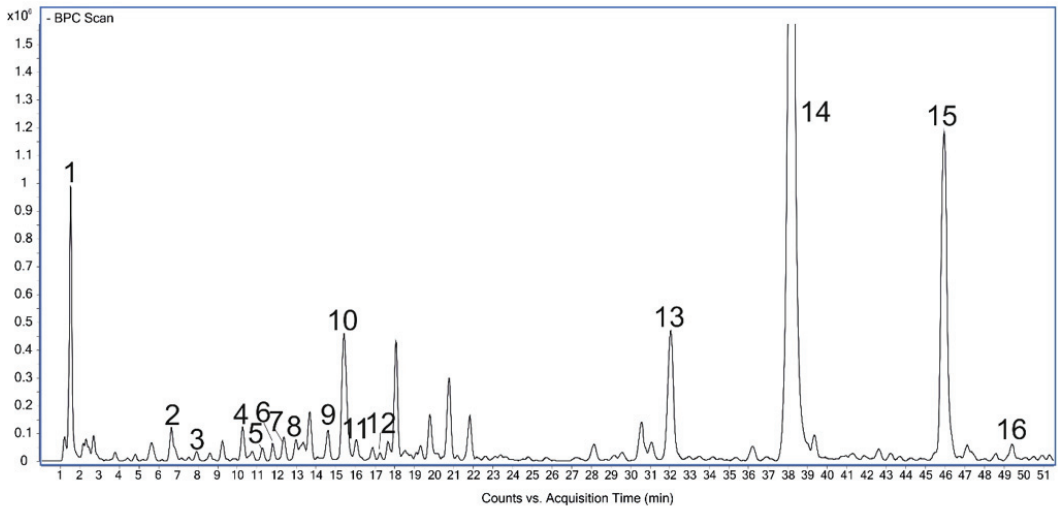


**Figure 2.** Chromatogram of *P. amboinicus* leaf extract with peaks identified via UHPLC-MS. (1) quinic acid; (2) dihydroxybenzoic acid hexoside; (3) dihydroxybenzoic acid; (4) neochlorogenic acid; (5) caffeoylglucose I; (6) caffeic acid derivative I; (7) caffeic acid derivative II; (8) caffeoylglucose II; (9) caffeoylglucose III; (10) chlorogenic acid; (11) caffeic acid; (12) caffeic acid derivative III; (13) rosmarinic acid glucoside; (14) rosmarinic acid; (15) salvianolic acid B; (16) luteolin 30-(4''-acetylglucuronide).

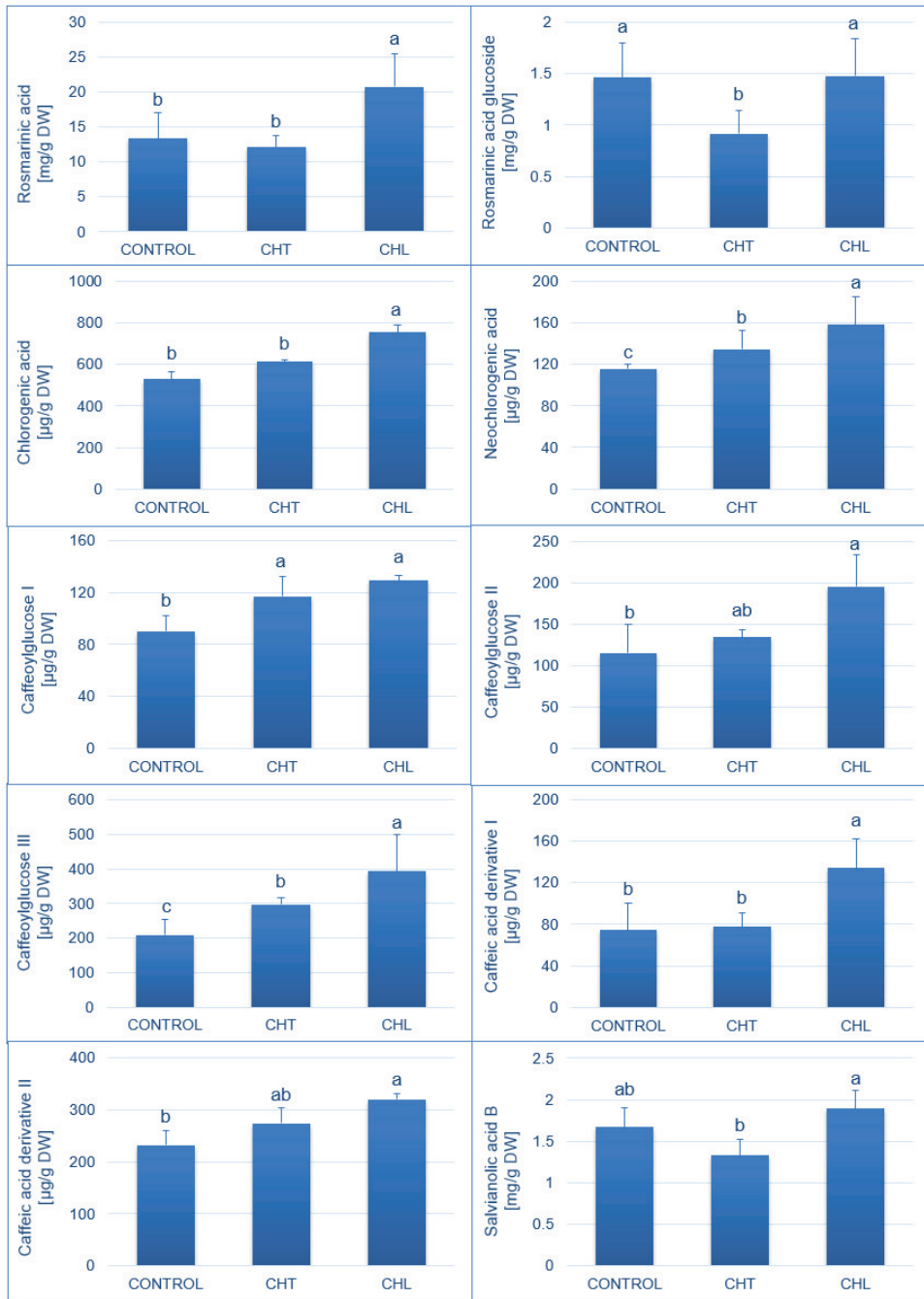


**Figure 3.** Content of selected phenolic compounds in *P. amboinicus* leaf extracts, depending on the form of chitosan used in the solutions for spraying the plants (CHT—chitosan suspension; CHL—chitosan lactate). Mean values ( $\pm$ standard deviation;  $n = 3$ ) marked with different letters were statistically significantly different ( $p < 0.05$ ).

## 2.2. Principle Component Analysis

The PCA of the accumulation of secondary metabolites and antioxidant capacity of the tested *P. amboinicus* leaves clearly grouped the samples into three groups according to the chitosan treatment (Figure 4). The first and second factors explained almost 84% of total variability; however, the first component defined 71% of total variability and showed negative loading by all evaluated variables. This component facilitated separation of the CHL samples from the control and partially from the CHT individuals. In turn, the second component explained approx. 14% of the total variance and was mostly positively correlated with salvianolic acid B and rosmarinic acid glucoside, but negatively correlated with TFC and caffeoylglucose I. The second component was responsible for separation of the control from the CHT individuals.

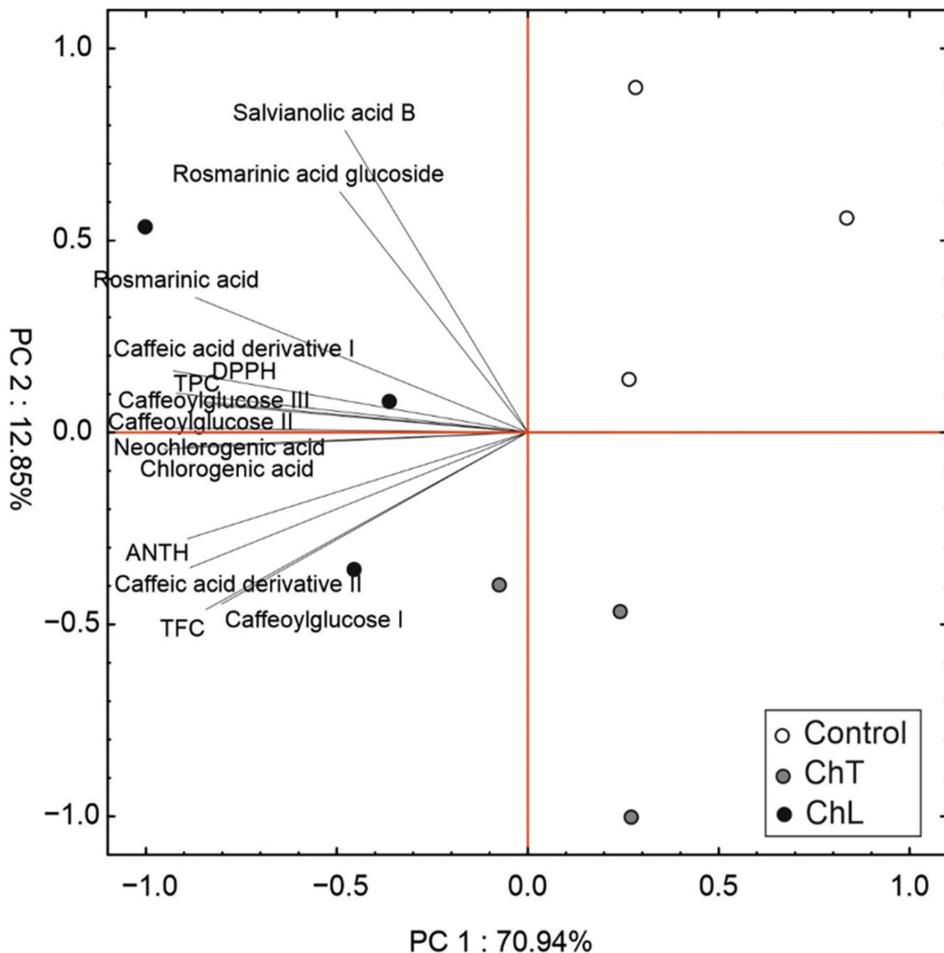


**Figure 4.** Scaled scatter plot of the principal component analysis (PCA) of selected secondary metabolites and antioxidant capacity (ANTH—anthocyanins; CHT—chitosan suspension, CHL—chitosan lactate, DPPH—antioxidant capacity, TPC—total phenolic content; TFC—total flavonol content). The length of the lines expresses the correlation between the original data and the factor axes.

### 2.3. Dry Weight of Aboveground Parts and Selected Parameters of Chlorophyll a Fluorescence after Application of Chitosan

The results indicated slight differences in the effect of both forms of chitosan on the dry weight of *P. amboinicus* organs. The dry weight of the stems was higher (by 15%) compared to that of the control plants only with the CHL treatment. No such relationship was observed for the leaves (Figure 5a).

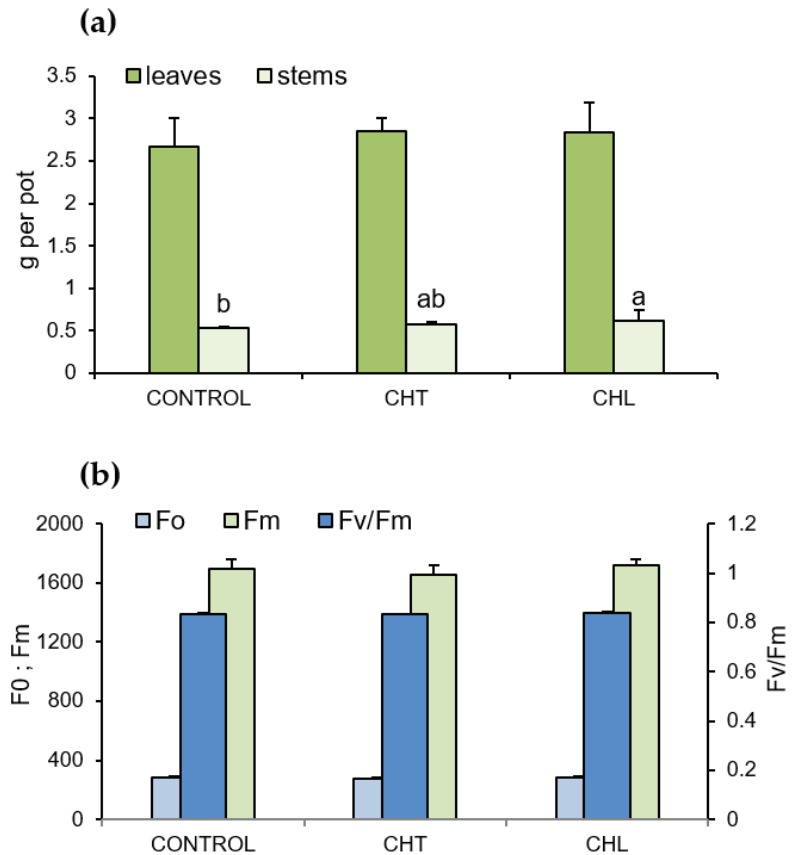


**Figure 5.** Dry matter yield of the aboveground parts (a) and selected chlorophyll a fluorescence indices (b) in *P. amboinicus* leaves, depending on the chitosan form in the solution used for spraying the plants (CHT—chitosan suspension; CHL—chitosan lactate). Mean values ( $\pm$ standard deviation;  $n_{(A)} = 3$ ,  $n_{(B)} = 10$ ) marked with different letters were statistically significantly different ( $p < 0.05$ ). The absence of letter designation means the absence of statistically significant differences.

The analysis of the results of the measurement of selected chlorophyll a fluorescence indices (minimum fluorescence—F0, maximum fluorescence—Fm, and the ratio of variable to minimum fluorescence—Fv/Fm) in the *P. amboinicus* leaves showed no significant differences in the effect of chitosan on the photosynthetic apparatus functioning in the plants (Figure 5b). No visual signs of phytotoxicity of the compound were observed either.

### 3. Discussion

The progressive development of lifestyle diseases and the growing demand of pharmaceutical, food, and cosmetic industries for high-quality raw materials of plant origin have encouraged research aimed at the optimisation of plant production and analysis of bioactive compounds contained in less-common plant species. Elicitation, which involves

plant defence reactions enhancing the biosynthesis and accumulation of secondary metabolites, is one of the tools used for improvements of the quality of raw materials. Chitosan is increasingly being used as a biotic elicitor in plant production. The object of the present study was *P. amboinicus*, which is highly valued in Indian, African, and Asian medicine due to its numerous pharmacological properties associated with the relatively high content of polyphenols [26]. The aim of the present study was to compare the effectiveness of the use of a chitosan suspension and chitosan lactate in the elicitation of this group of compounds in the studied species. The elicitor exhibits high biological activity, biodegradability, and non-toxicity [9], which is in line with the current environment protection trends. Moreover, the presence of the primary amino group in the chitosan molecule allows for a wide range of chemical modifications changing its solubility, charge, chelating activities, and thus biological properties [36].

In our experiment, we investigated the effect of the CHT and CHL solutions on plant growth and the function of the photosynthetic apparatus in *P. amboinicus*. The analysed parameters (biomass, chlorophyll *a* fluorescence) did not indicate a negative impact of both chitosan forms on plant growth and photosynthesis efficiency. Similarly, our previous study showed that foliar applications of CHL (100 mg/L or 500 mg/L) did not have a significant effect on the photosynthesis in *Ocimum basilicum* or slightly stimulated this process in *Melissa officinalis* [37]. Other studies not only confirmed the absence of phytotoxic effects but also indicated a beneficial effect of chitosan on photosynthesis effectiveness. As demonstrated in an experiment conducted by Xu and Mou [38], the application of moderate concentrations of chitosan (0.2% or 0.3%) to the soil improved photosynthesis parameters in lettuce. In turn, Khan et al. [39] reported an improvement in the net photosynthesis efficiency in corn and soybean leaves several days after the application of chitosan. Chitosan nanoparticles (10 ppm) were also found to increase the intensity of photosynthesis in *Coffea canephora* in greenhouse conditions [40].

Polyphenolic compounds are a large group of secondary metabolites with documented health-promoting properties. Given the wide spectrum of activity and the high abundance of this group of compounds in the chemical composition of *Plectranthus amboinicus* (Lour.) plants, our phytochemical analyses focused on the impact of both chitosan forms on the total polyphenol content and the level of some compounds from this group. The efficacy of elicitation was found to be largely dependent not only on the chitosan form and solubility but also on the plant organ. The foliar application of the CHL solution resulted in an increase in the total concentration of phenolic compounds (by 43% versus that in the control) in the *P. amboinicus* leaf extracts. Both chitosan forms were characterised by similar effectiveness in the induction of the accumulation of soluble flavonols in the leaves, whereas CHL increased the anthocyanin concentration more potently than CHT.

The concentration of caffeic acid derivatives in *P. amboinicus* leaves depended on the chitosan form applied. The treatment with CHL induced a significant 55%, 42%, and 37% increase in the concentration of rosmarinic, chlorogenic, and neochlorogenic acids in the leaves, respectively, relative to that in the control. In turn, the CHT foliar treatment caused a significant increase only in the concentration of neochlorogenic acid, whereas both forms of chitosan led to an increase in the level of caffeoylglucose I and caffeoylglucose III. Other studies reported the effectiveness of chitosan in the stimulation of the biosynthesis of both total polyphenols and individual compounds from this group present in herbal plants. For example, the application of 50 ppm or 200 ppm of chitosan increased the total content of phenolic compounds by 38% and 29%, respectively, in *Origanum vulgare* ssp. *hirtum* [41]. Similar results were obtained in experiments on *Ocimum basilicum* and *Melissa officinalis* treated with CHL solutions at concentrations of 100 mg/L or 500 mg/L [37]. The study showed that single spraying with a solution containing a lower CHL amount increased the concentration of rosmarinic acid in the analysed species most effectively. Moreover, the application of both 100 mg/L and 500 mg/L of CHL increased the total accumulation of polyphenols and anthocyanins in the lemon balm raw material. A study conducted by Fooladi Vanda et al. [42] showed the highest increase in the total content of

phenolic compounds in shoot cultures of lemon balm after treatment with 100 mg/L of chitosan. However, the induction of rosmarinic acid biosynthesis did not depend on the chitosan concentration (50, 100, 150 mg/L). The effectiveness of chitosan in the elicitation of flavonoids was also demonstrated in *Isatis tinctoria* root hair cultures [43]. Similarly, studies conducted on herbal plants in greenhouse conditions indicated the effectiveness of chitosan in the stimulation of the biosynthesis of phenolic compounds and flavonoids in sage [44] and peppermint [45]. Chitosan was also reported to increase the pro-health value of fruits, e.g., apricots [46], strawberries [47], or tomatoes [48], via the stimulation of the biosynthesis of phenolic compounds. The high biological activity of chitosan and its derivatives in the stimulation of stress responses may be related to the presence of acid pectins in plant cell walls, as these compounds can bind calcium and form chain dimers. Cationic chitosan can interact with negatively charged pectin and pectin dimers modifying their supramolecular arrangement. This in turn alarms the cells of cell wall degradation, e.g., by pathogens [49], the activation of signal transduction pathways, and the initiation of a cascade of plant biochemical defence mechanisms associated with e.g., the accumulation of secondary metabolites. Moreover, chitosan can interfere positively with complex cellular networks, including cellular signalling, redox homeostasis, and transcription processes, thereby modifying plant metabolic activities [50].

Taking into account the antioxidant properties of phenolic compounds, the effect of chitosan on the FRSA of the extracts of *P. amboinicus* leaves and stems was analysed as well. The treatment with CHL, but not CHT, increased the FRSA in the leaf extracts. Similarly, chitosan was reported to increase the antioxidant activity in peppermint [45], basil [51], or sage [44] raw materials. The increase in the FRSA of extracts is most probably associated with an increase in the content of polyphenolic compounds, of which the redox properties play an important role in quenching and neutralising ROS [52].

One of the determinants of the success of the elicitation process is the selection of an elicitor that will be appropriate for a given plant species, as well as its concentration and exposure time [53], as the absence of phytotoxic effects is as important as the expected effectiveness. The present analyses showed that the foliar application of both chitosan forms had no negative effects on the dry weight of *P. amboinicus* organs. An exception was the CHL solution, which induced an increase in the dry weight of the stems.

The results of many studies have confirmed the effectiveness of chitosan as a plant growth-stimulating substance not only in the production of medicinal and seasoning raw materials but also in the production of fruits and vegetables. The use of this polymer was shown to have a beneficial effect on the fruit yield in e.g., haskap berries [54], strawberries [55,56], or soybeans [57]. Moreover, different concentrations of chitosan oligosaccharides were effective in stimulating the growth of *Origanum vulgare* ssp. *hirtum* in field conditions [34]. Studies carried out on okra demonstrated that the foliar application of this polymer had a positive effect on the growth and morphological features of this plant both in field conditions and in pot cultivation [58]. Similar results were obtained in experiments conducted with the use of chitosan solutions in the cultivation of other seasoning and medicinal species, i.e., *Curcuma longa* [59], *Sylibum marianum* [60], or three basil cultivars [61].

## 4. Materials and Methods

### 4.1. Experimental Design and Conditions

*Plectranthus amboinicus* (Lour.) seeds (Vilmorin Garden Company, Komorniki, Poland) were sown into 0.5 L plastic pots (20 seeds in each) filled with a potting mix, sprayed with water abundantly, and allowed to germinate. The Kronen substrate, intended for sowing seeds, transplanting seedlings, and rooting plants, was used in the experiment. The substrate contained a fine fraction of weakly and strongly decomposed high peat (pH = 6.0–6.8). The seed germination and plant growth were observed in controlled laboratory conditions, i.e., in an air-conditioned phytotron equipped with fluorescent lamps with a 14 h photoperiod, a temperature of 27 °C during the day and 23 °C at night,

and 60–65% relative humidity. The surface photon flux density in the photosynthetically active range was  $170\text{--}200\ \mu\text{mol m}^{-2}\ \text{s}^{-1}$  at the level of plant tops.

On day 42 after sowing the seeds, the plants were assigned to three experimental treatment groups. Two of the groups were sprayed with aqueous solutions containing two forms of chitosan (traditional chitosan suspension—CHT or chitosan lactate—CHL) at a concentration of 200 mg/L of CHT and a dose of 10 mL per pot. The control plants received the same volume of distilled water. The spraying solutions were enriched with a 0.02% surface tension-reducing agent, Tween<sup>®</sup> 20 (Sigma-Aldrich, St. Louis, MO, USA). The volume used for spraying ensured the optimal saturation of the leaves with the solutions. The chitosan forms were produced from shrimp shells; they differed substantially in their water solubility. CHL (Heppes Medical Chitosan GmbH; deacetylation degree of 80–95%) exhibited considerably higher solubility than CHT (Sigma-Aldrich; deacetylation degree of  $\geq 75\%$ ), which formed a suspension. A varied spraying scheme was applied twice at three-day intervals. In total, 20 mL of chitosan solutions per pot was added to each experimental series. On day 10 day after the application of the first dose of the solutions, the dry matter yield of the aboveground parts was determined, the measurements of chlorophyll *a* fluorescence were carried out, and phytochemical analyses were performed.

## 4.2. Methods of Plant Material Analysis

### 4.2.1. Preparation of Methanol Extracts

The dried plant material was ground in an electric mill. Next, 0.1 g of the raw material was mixed with 5 mL of an 80% methanol aqueous solution (*v/v*) and placed in an ultrasonic bath at room temperature for 30 min. The extracts were then centrifuged (5 min; 6000 rpm).

### 4.2.2. Determination of Total Soluble Phenolic Compounds

The total content of phenolic compounds in the extracts of *P. amboinicus* leaves and stems was determined with the spectrophotometric method [62] using the Folin-Ciocalteu reagent (Chempur, Piekary Śląskie, Poland). Here, 1.9 mL of distilled water, 1 mL of F-C reagent, and 100  $\mu\text{L}$  of the extract were pipetted into test tubes. The reaction mixture was shaken using an ML-962 microshaker (JWElectronics, Warsaw, Poland). After 5 min, 3 mL of a saturated  $\text{Na}_2\text{CO}_3$  solution (POCH, Gliwice, Poland) was added and mixed, and the mixture was incubated at 40 °C. After 30 min, absorbance was measured spectrophotometrically at 756 nm (Cecil CE 9500, Cecil Instruments, Cambridge, UK). The total phenolic content was read from a standard curve prepared for gallic acid (Sigma-Aldrich, St. Louis, MO, USA).

### 4.2.3. Determination of Total Soluble Flavonols

The content of flavonols in the extracts was determined with the simplified Christ-Müller method [63], which is based on the ability of flavonols to form complexes with aluminium ions. For this, 450  $\mu\text{L}$  of 80% methanol, 750  $\mu\text{L}$  of 2%  $\text{AlCl}_3$  (Acros Organics, Geel, Belgium), and 300  $\mu\text{L}$  of the sample were pipetted into Eppendorf tubes. The mixture was shaken using an ML-692 microshaker (JWElectronics, Warsaw, Poland) and placed in a shaded place at room temperature for 30 min. After this time, the absorbance of the solutions was read at 425 nm (Cecil CE 9500, Cecil Instruments, Cambridge, UK). An aqueous solution of 80% methanol was the control sample (A0). The concentration of flavonols was read from the standard curve prepared for rutin (Sigma-Aldrich, St. Louis, MO, USA).

### 4.2.4. Determination of Total Soluble Anthocyanins

The content of anthocyanins in the aboveground parts of *P. amboinicus* was determined using the spectrophotometric differential pH method [64]. Anthocyanins were extracted from 0.2 g of the plant material with 7 mL of 80% methanol (*v/v*) acidified to pH = 2.0 using an ultrasonic bath (25 °C, 30 min.). Next, the extracts were centrifuged (10 min; 6000 rpm). Two samples of each extract were prepared. Then, 1 mL of the analysed extract was pipetted



into test tubes; next, 4 mL of buffer with pH = 1.0 was added to one of the samples, and the other sample was supplemented with 4 mL of buffer with pH = 4.5. Absorbance was read at 520 nm and 700 nm (Cecil CE 9500, Cecil Instruments, Cambridge, UK) using appropriate buffers as reagent samples. The absorbance of the analysed solutions was calculated with the following formula:

$$A = (A_{520\text{nm pH}1.0} - A_{700\text{nm pH}1.0}) - (A_{520\text{nm pH}4.5} - A_{700\text{nm pH}4.5})$$

where:

A—absorbance of the solution at a specific wavelength

The final calculations of the content of anthocyanins in the plant material, expressed in mg of cyanidin-3-glucoside (C3G) per 100 g DW, were made taking into account the molar absorption coefficient and the molecular mass of C3G, as well as the sample dilution factor.

#### 4.2.5. Determination of Free Radical-Scavenging Activity with the DPPH Method

The free radical-scavenging activity (FRSA) of the analysed extracts was determined using the synthetic free radical DPPH (1,1-diphenyl-2-picrylhydrazyl; Sigma-Aldrich, USA). Here, 2 mL of a methanolic DPPH solution (200  $\mu\text{M}$ ) and 50  $\mu\text{L}$  of the extract were pipetted into spectrophotometric cuvettes. Then, 15 min after the addition of the plant extract, the extinction was read at a wavelength of 517 nm (Cecil CE 9500, Cecil Instruments, UK). The DPPH solution supplemented with 50  $\mu\text{L}$  of 80% methanol was the control (A0). The FRSA of the analysed extracts was calculated using the following formula [65]:

$$\% \text{ reduction of DPPH} = 100 \times (A_0 - A_{15}) / A_0$$

where:

A0—absorbance of the control sample

A15—absorbance 15 min after addition of the analysed sample.

#### 4.2.6. UHPLC-MS Analysis

All standards, formic acid, and MS-grade acetonitrile were obtained from Sigma-Aldrich (St. Louis, MO, USA). The extract was analysed using an ultra-high performance liquid chromatograph (UHPLC) Infinity Series II coupled with a DAD detector and an Agilent 6224 ESI/TOF mass detector (Agilent Technologies, Santa Clara, CA, USA) on an RP18 Titan column (Supelco, Sigma-Aldrich, St. Louis, MO, USA) (10 cm  $\times$  2.1 mm, 1.9  $\mu\text{m}$ ). The thermostat temperature was 30  $^{\circ}\text{C}$ , and the flow rate of the mobile phase was 0.2 mL/min. Water with 0.05% of formic acid (solvent A) and acetonitrile with 0.05% of formic acid (solvent B) were used as components of the mobile phase. The gradient elution program was as follows: 0–8 min from 98% A to 93% A (from 2% to 7% B), 8–15 min from 93% A to 88% A (from 7% to 12% B), 15–29 min from 88% A to 85% A (from 12% to 15% B), 29–40 min from 85% A to 80% A (from 15% B to 20% B), and 40–60 min from 80% A to 65% A (from 20% B to 35% B). Chromatograms were collected from 200 to 400 nm. The ion source operating parameters in the LC–MS analysis were as follows: drying gas temperature, 325  $^{\circ}\text{C}$ ; drying gas flow, 8 L  $\text{min}^{-1}$ ; nebuliser pressure, 30 psi; capillary voltage, 3500 V; and skimmer, 65 V. The voltage on the fragmentator was 180 V. Ions were acquired in the range from 100 to 1300 m/z. Quantification was based on calibration curves obtained using methanol standard solutions (Sigma-Aldrich, St. Louis, MO, USA) of the identified compounds.

#### 4.2.7. Biometric Parameters

To determine the plant dry matter, the aboveground parts were cut off from the roots at a height of several millimetres above the substrate surface. The dry matter yield was determined after drying the plant material to a constant weight at 60  $^{\circ}\text{C}$  and expressed in grams per pot.

#### 4.2.8. Measurement of Selected Parameters of Chlorophyll a Fluorescence

The parameters of chlorophyll a fluorescence were measured using a Handy-PEA portable fluorimeter (Hansatech Instruments, Pentney, UK). The following chlorophyll a fluorescence indices were determined:  $F_0$ —minimum fluorescence,  $F_m$ —maximum fluorescence, and  $F_v/F_m$ —ratio of variable to maximum fluorescence ( $F_v = F_m - F_0$ ), which is regarded as the most reliable and non-invasive indicator of the maximum quantum efficiency of photosystem PSII after dark adaptation [66]. Fragments of leaf blades were shaded for 15 min using special clips, and then, the measurements were carried out.

#### 4.3. Statistical Analysis

Statistical processing of numerical data provided by the laboratory analyses was carried out using Statistica ver. 13.3 (TIBCO Software Inc. 2017, Palo Alto, CA, USA). One-way analysis of variance (ANOVA) was performed, and Tukey's post-hoc test was used to determine the significance of differences between pairs of means at the significance level  $\alpha = 0.05$ .

### 5. Conclusions

The comparison of the efficiency of elicitation of *P. amboinicus* with the analysed forms of chitosan showed higher bioactivity of the CHL solution than that of CHT, which was probably associated with the substantially better solubility, and thus bioavailability, of CHL and its higher deacetylation degree. The application of CHL led to a significant increase in the total content of polyphenols, soluble flavonols, anthocyanins, and most of the caffeic acid derivatives (including rosmarinic and chlorogenic acids). The changes in the level of polyphenolic compounds induced by CHT were much less pronounced; however, this chitosan form caused a significant increase in the content of caffeoylglucose I and caffeoylglucose III and a decrease in the level of rosmarinic acid glucoside. In general, despite the tendency to induce polyphenol biosynthesis by CHT, its elicitation efficiency was significantly lower than that of CHL. The CHL treatment also enhanced the FRSA of the leaf extracts, whereas the CHT treatment reduced this parameter in the stem extracts. Therefore, the foliar application of CHL solutions can be a simple, effective, inexpensive, and eco-friendly approach for optimisation of the production of *P. amboinicus* raw material in pots, yielding increased contents of certain health-promoting and antioxidant polyphenolic compounds. The present results indicate the most relevant recommendations for the practical use of chitosan as an elicitor in *P. amboinicus* cultivation and the production of plant material with increased nutraceutical value.

**Author Contributions:** M.S.-J. and B.H.-N., project designation, cultivation of the plants; M.S.-J., analysis of growth parameters, chlorophyll fluorescence, total phenolics, soluble flavonols, and FRSA; S.D. and M.W., HPLC-UV-MS analysis and data interpretation; B.H.-N. and S.D., statistical analysis and data visualisation; M.S.-J., B.H.-N. and S.D., original manuscript draft; M.W., critical revision of the manuscript. All authors have read and agreed to the published version of the manuscript.

**Funding:** This research received no external funding.

**Institutional Review Board Statement:** Not applicable.

**Informed Consent Statement:** Not applicable.

**Data Availability Statement:** The data presented in this study are available on request from the corresponding author.

**Acknowledgments:** Special thanks for technical support and help with the experiments are extended to Weronika Woch, MSc.

**Conflicts of Interest:** The authors declare no conflict of interest.

**Sample Availability:** Samples of the compounds are not available from the authors.

## References

1. Fierascu, R.C.; Fierascu, I.; Baroi, A.M.; Ortan, A. Selected aspects related to medicinal and aromatic plants as alternative sources of bioactive compounds. *Int. J. Mol. Sci.* **2021**, *22*, 1521. [[CrossRef](#)] [[PubMed](#)]
2. Souiri, E.; Amin, G.; Farsam, H.; Jalalizadeh, H.; Barezi, S. Screening of thirteen medicinal plant extracts for antioxidant activity. *Iran. J. Pharm. Res.* **2022**, *7*, 128584. [[CrossRef](#)]
3. Shakya, A.K. Medicinal plants: Future source of new drugs. *Int. J. Herb. Med.* **2016**, *4*, 59–64. [[CrossRef](#)]
4. Gorelick, J.; Bernstein, N. Elicitation: An underutilized tool in the development of medicinal plants as a source of therapeutic secondary metabolites. *Adv. Agron.* **2014**, *124*, 201–230. [[CrossRef](#)]
5. Baenas, N.; Garcia-Viguera, C.; Moreno, D.A. Elicitation: A tool for enriching the bioactive composition of foods. *Molecules* **2014**, *19*, 13541–13563. [[CrossRef](#)]
6. Thakur, M.; Bhattacharya, S.; Khosla, P.K.; Puri, S. Improving production of plant secondary metabolites through biotic and abiotic elicitation. *J. Appl. Res. Med. Arom.* **2019**, *12*, 1–12. [[CrossRef](#)]
7. Amborabe, B.-E.; Bonmort, J.; Fleurat-Lessard, P.; Roblin, G. Early events induced by chitosan on plant cells. *J. Exp. Bot.* **2008**, *59*, 2317–2324. [[CrossRef](#)]
8. Wang, W.; Xue, C.; Mao, X. Chitosan: Structural modification, biological activity and application. *Int. J. Biol. Macromol.* **2020**, *164*, 4532–4546. [[CrossRef](#)]
9. Stasińska-Jakubas, M.; Hawrylak-Nowak, B. Protective, biostimulating, and eliciting effects of chitosan and its derivatives on crop plants. *Molecules* **2022**, *27*, 2801. [[CrossRef](#)]
10. Ferri, M.; Tassoni, A. Chitosan as elicitor of health beneficial secondary metabolites in in vitro plant cell cultures. In *Handbook of Chitosan Research and Applications*; Mackay, R.G., Tait, J.M., Eds.; Nova Science Publishers Inc.: Hauppauge, NY, USA, 2011; pp. 389–414.
11. Stiller, A.; Garrison, K.; Gurdyumov, K.; Kenner, J.; Yasmin, F.; Yates, P.; Song, B.-H. From Fighting Critters to Saving Lives: Polyphenols in Plant Defense and Human Health. *Int. J. Mol. Sci.* **2021**, *22*, 8995. [[CrossRef](#)]
12. Šamec, D.; Karalija, E.; Šola, I.; Vujčić, B.; Salopek-Sondi, B. The Role of Polyphenols in Abiotic Stress Response: The Influence of Molecular Structure. *Plants* **2021**, *10*, 118. [[CrossRef](#)] [[PubMed](#)]
13. Froidi, G.; Ragazzi, E. Selected plant-derived polyphenols as potential therapeutic agents for peripheral artery disease: Molecular mechanisms, efficacy and safety. *Molecules* **2022**, *27*, 7110. [[CrossRef](#)]
14. Chen, Z.; Farag, M.; Zhong, Z.; Zhang, C.; Yang, Y.; Shengpeng, W.; Wang, Y. Multifaceted role of phyto-derived polyphenols in nanodrug delivery systems. *Adv. Drug Deliv. Rev.* **2021**, *176*, 113870. [[CrossRef](#)] [[PubMed](#)]
15. Zhang, Y.; Cai, P.; Cheng, G.; Zhang, Y. A brief review of phenolic compounds identified from plants: Their extraction, analysis, and biological activity. *Nat. Prod. Commun.* **2022**, *17*, 1–14. [[CrossRef](#)]
16. Noor, S.; Mohammad, T.; Rub, M.A.; Raza, A.; Azum, N.; Yadav, D.K.; Hassan, M.I.; Asiri, M.A. Biomedical features and therapeutic potential of rosmarinic acid. *Arch. Pharm. Res.* **2022**, *45*, 205–228. [[CrossRef](#)] [[PubMed](#)]
17. Albuquerque, B.R.; Heleno, S.A.; Oliveira, B.; Barros, L.; Ferreira, I.C.F.R. Phenolic compounds: Current industrial applications, limitations and future challenges. *Food Funct.* **2021**, *12*, 14–29. [[CrossRef](#)]
18. Luo, J.; Si, H.; Jia, Z.; Liu, D. Dietary Anti-Aging Polyphenols and Potential Mechanisms. *Antioxidants* **2021**, *10*, 283. [[CrossRef](#)]
19. Agathokleous, E.; Kitao, M.; Calabrese, E.J. Hormesis: A compelling platform for sophisticated plant science. *Trends Plant Sci.* **2019**, *24*, 318–327. [[CrossRef](#)]
20. Fernández-Calvet, A.; Euba, B.; Caballero, L.; Díez-Martínez, R.; Menéndez, M.; Ortiz de Solórzano, C.; Leiva, J.; Micol, V.; Barrajón-Catalán, E.; Garmendia, J. Preclinical evaluation of the antimicrobial-immunomodulatory dual action of xenohormetic molecules against *Haemophilus influenzae* respiratory infection. *Biomolecules* **2019**, *19*, 891. [[CrossRef](#)]
21. Suter, S.; Lucock, M. Xenohormesis: Applying evolutionary principles to contemporary health issues. *Explor. Res. Hypothesis Med.* **2017**, *2*, 79–85. [[CrossRef](#)]
22. Kaliappan, N.D.; Viswanathan, P.K. Pharmacognostical studies on the leaves of *Plectranthus amboinicus* (Lour) Spreng. *Int. J. Green Pharm.* **2008**, *2*, 182–184. [[CrossRef](#)]
23. Murthy, P.S.; Ramalakshmi, K.; Srinivas, P. Fungitoxic activity of Indian borage (*Plectranthus amboinicus*) volatiles. *Food Chem.* **2009**, *114*, 1014–1018. [[CrossRef](#)]
24. Erny Sabrina, M.N.; Razali, M.; Mirfat, A.H.S.; Mohd Shukri, M.A. Antimicrobial activity and bioactive evaluation of *Plectranthus amboinicus* essential oil. *Am. J. Res. Commun.* **2014**, *2*, 121–127.
25. Aguiar, J.J.S.; Sousa, C.P.B.; Araruna, M.K.A.; Silva, M.K.N.; Portelo, A.C.; Lopes, J.C.; Carvalho, V.R.A.; Figueredo, F.G.; Bitu, V.C.N.; Coutinho, H.D.M.; et al. Antibacterial and modifying-antibiotic activities of the essential oils of *Ocimum gratissimum* L. and *Plectranthus amboinicus* L. *Eur. J. Integr. Med.* **2015**, *7*, 151–156. [[CrossRef](#)]
26. Arumugam, G.; Swamy, M.K.; Sinniah, U.R. *Plectranthus amboinicus* (Lour.) Spreng: Botanical, phytochemical, pharmacological and nutritional significance. *Molecules* **2016**, *21*, 369. [[CrossRef](#)]
27. Wadikar, D.D.; Patki, P.E. *Coleus aromaticus*: A therapeutic herb with multiple potentials. *J. Food Sci. Technol.* **2016**, *53*, 2895–2901. [[CrossRef](#)]
28. Patel, R.D.; Mahobia, N.K.; Singh, M.P.; Singh, A.; Sheikh, N.W.; Alam, G.; Singh, S.K. Antioxidant potential of leaves of *Plectranthus amboinicus* (Lour) Spreng. *Der Pharm. Lett.* **2010**, *2*, 240–245.

29. Chiu, Y.J.; Huang, T.H.; Chiu, C.S.; Lu, T.C.; Chen, Y.W.; Peng, W.H.; Chen, C.Y. Analgesic and antiinflammatory activities of the aqueous extract from *Plectranthus amboinicus* (Lour.) Spreng. Both in vitro and in vivo. *Evid. Based Complement. Altern. Med.* **2012**, *1*, 1–11. [[CrossRef](#)]
30. Bhattacharjee, P.; Majumder, P. Investigation of phytochemicals and anti-convulsant activity of the plant *Coleus amboinicus* (lour.). *Int. J. Green Pharm.* **2013**, *7*, 211–215. [[CrossRef](#)]
31. Lalthazuali; Mathew, N. Mosquito repellent activity of volatile oils from selected aromatic plants. *Parasitol Res.* **2017**, *116*, 821–825. [[CrossRef](#)]
32. Zhao, Y.; Lu, H.; Wang, Q.; Liu, H.; Shen, H.; Xu, W.; Ge, J.; He, D. Rapid qualitative profiling and quantitative analysis of phenolics in *Ribes meyeri* leaves and their antioxidant and antidiabetic activities by HPLC-QTOF-MS/MS and UHPLC-MS/MS. *J. Sep. Sci.* **2021**, *44*, 1404–1420. [[CrossRef](#)] [[PubMed](#)]
33. Ślusarczyk, S.; Cieślak, A.; Yanza, Y.R.; Szumacher-Strabel, M.; Varadyova, Z.; Stafiniak, M.; Wojnicz, D.; Matkowski, A. Phytochemical profile and antioxidant activities of *Coleus amboinicus* Lour. cultivated in Indonesia and Poland. *Molecules* **2021**, *26*, 2915. [[CrossRef](#)] [[PubMed](#)]
34. Formato, M.; Piccolella, S.; Zidorn, C.; Pacifico, S. UHPLC-HRMS analysis of *Fagus sylvatica* (Fagaceae) leaves: A renewable source of antioxidant polyphenols. *Antioxidants* **2021**, *10*, 1140. [[CrossRef](#)] [[PubMed](#)]
35. Cheng, T.; Ye, J.; Li, H.; Dong, H.; Xie, N.; Mi, N.; Zhang, Z.; Zou, J.; Jin, H.; Zhang, W. Hybrid multidimensional data acquisition and data processing strategy for comprehensive characterization of known, unknown and isomeric compounds from the compound Dan Zhi Tablet by UPLC-TWIMS-QTOFMS. *RSC Adv.* **2019**, *9*, 8714–8727. [[CrossRef](#)]
36. Varlamov, V.P.; Il'ina, A.V.; Shagdarova, B.T.; Lunkov, A.P.; Mysyakina, I.S. Chitin/chitosan and its derivatives: Fundamental problems and practical approaches. *Biochemistry (Moscow)* **2020**, *85*, S154–S176. [[CrossRef](#)]
37. Hawrylak-Nowak, B.; Dresler, S.; Rubiniowska, K.; Matraszek-Gawron, R. Eliciting effect of foliar application of chitosan lactate on the phytochemical properties of *Ocimum basilicum* L. and *Melissa officinalis* L. *Food Chem.* **2021**, *342*, 128358. [[CrossRef](#)]
38. Xu, C.; Mou, B. Chitosan as soil amendment affects lettuce growth, photochemical efficiency, and gas exchange. *HortTechnology* **2018**, *28*, 476–480. [[CrossRef](#)]
39. Khan, W.M.; Prithiviraj, B.; Smith, D.L. Effect of foliar application of chitin and chitosan oligosaccharides on photosynthesis of maize and soybean. *Photosynthetica* **2002**, *40*, 621–624. [[CrossRef](#)]
40. Van, S.N.; Minh, H.D.; Anh, D.N. Study on chitosan nanoparticles on biophysical characteristics and growth of *Robusta coffee* in green house. *Biocatal. Agric. Biotechnol.* **2013**, *2*, 289–294. [[CrossRef](#)]
41. Yin, H.; Frette, X.C.; Christensen, L.P.; Grevsen, K. Chitosan oligosaccharides promote the content of polyphenols in Greek oregano (*Origanum vulgare* ssp. *hirtum*). *J. Agric. Food Chem.* **2012**, *60*, 136–143. [[CrossRef](#)]
42. Fooladi Vanda, G.; Shabani, L.; Razavizadeh, R. Chitosan enhances rosmarinic acid production in shoot cultures of *Melissa officinalis* L. through the induction of methyl jasmonate. *Bot. Stud.* **2019**, *60*, 26. [[CrossRef](#)] [[PubMed](#)]
43. Jiao, J.; Gai, Q.-Y.; Wang, X.; Qin, Q.-P.; Wang, Z.-Y.; Liu, J.; Fu, Y.-J. Chitosan elicitation of *Isatis tinctoria* L. hairy root cultures for enhancing flavonoid productivity and gene expression and related antioxidant activity. *Ind. Crop. Prod.* **2018**, *124*, 28–35. [[CrossRef](#)] [[PubMed](#)]
44. Vosoughi, N.; Gomarian, M.; Pirbalouti, A.G.; Khaghani, S.; Malekpoor, F. Essential oil composition and total phenolic, flavonoid contents, and antioxidant activity of sage (*Salvia officinalis* L.) extract under chitosan application and irrigation frequencies. *Ind. Crop. Prod.* **2018**, *117*, 366–374. [[CrossRef](#)]
45. Salimgandomi, S.; Shabrangy, A. The effect of chitosan on antioxidant activity and some secondary metabolites of *Mentha piperita* L. *J. Pharm. Health Sci.* **2016**, *4*, 135–142.
46. Ghasemnezhad, M.; Shiri, M.A.; Sanavi, M. Effect of chitosan coatings on some quality indices of apricot (*Prunus armeniaca* L.) during cold storage. *Casp. J. Environ. Sci.* **2010**, *8*, 25–33.
47. He, Y.; Bose, S.K.; Wang, W.; Jia, X.; Lu, H.; Yin, H. Pre-harvest treatment of chitosan oligosaccharides improved strawberry fruit quality. *Int. J. Mol. Sci.* **2019**, *19*, 2194. [[CrossRef](#)]
48. Badawy, M.E.I.; Rabea, E.I. Potential of the biopolymer chitosan with different molecular weights to control postharvest gray mold of tomato fruit. *Postharvest Biol. Technol.* **2009**, *51*, 110–117. [[CrossRef](#)]
49. Cabrera, J.C.; Boland, A.; Cambier, P.; Frettinger, P.; Van Cutsem, P. Chitosan oligosaccharides modulate the supramolecular conformation and the biological activity of oligogalacturonides in *Arabidopsis*. *Glycobiology* **2010**, *20*, 775–786. [[CrossRef](#)]
50. Farooq, T.; Akram, M.N.; Hameed, A.; Ahmed, T.; Hameed, A. Nanoprimer-mediated memory imprints reduce salt toxicity in wheat seedlings by modulating physiobiochemical attributes. *BMC Plant Biol.* **2022**, *22*, 540. [[CrossRef](#)]
51. Kim, H.; Chen, F.; Wang, X.; Rajapakse, N.C. Effect of chitosan on the biological properties of sweet basil (*Ocimum basilicum* L.). *J. Agric. Food Chem.* **2005**, *53*, 3696–3701. [[CrossRef](#)]
52. Zheng, W.; Wang, S.Y. Antioxidant activity and phenolic compounds in selected herbs. *J. Agric. Food Chem.* **2001**, *49*, 5165–5170. [[CrossRef](#)] [[PubMed](#)]
53. Bhaskar, R.; Xavier, L.S.E.; Udayakumaran, G.; Kumar, D.S.; Venkatesh, R.; Nagella, P. Biotic elicitors: A boon for the in-vitro production of plant secondary metabolites. *Plant Cell Tissue Organ Cult.* **2022**, *149*, 7–24. [[CrossRef](#)]
54. Poterańska, N.; Mijowska, K.; Ochmian, I. The influence of foliar calcium fertilizers and bio-stimulators on bushes growth, yield and fruit quality of blue honeysuckle (*Lonicera caerulea* L.) Czarna cultivar. In *Research and Development of Young Scientists in Poland–Life Sciences*; Young Scientists: Szczecin, Poland, 2015; pp. 132–138. (In Polish)

55. El-Miniawy, S.M.; Ragab, M.E.; Youssef, S.M.; Metwally, A.A. Response of strawberry plants to foliar spraying of chitosan. *Res. J. Agric. Biol. Sci.* **2013**, *9*, 366–372.
56. Rahman, M.; Mukta, J.A.; Sabir, A.A.; Gupta, D.R.; Mohi-Ud-Din, M.; Hasanuzzaman, M.; Miah, M.G.; Rahman, M.; Islam, M.T. Chitosan biopolymer promotes yield and stimulates accumulation of antioxidants in strawberry fruit. *PLoS ONE* **2018**, *13*, e0203769. [[CrossRef](#)] [[PubMed](#)]
57. Zeng, D.; Luo, X.; Tu, R. Application of bioactive coatings based on chitosan for soybean seed protection. *Int. J. Carbohydr. Chem.* **2012**, *2012*, 104565. [[CrossRef](#)]
58. Mondal, M.; Malek, M.; Puteh, A.; Ismail, M.; Ashrafuzzaman, M.; Naher, L. Effect of foliar application of chitosan on growth and yield in okra. *Aust. J. Crop. Sci.* **2012**, *6*, 918–921.
59. Sathiyarayanan, A.; Sathiyabama, M. Effect of chitosan on growth, yield and curcumin content in turmeric under field condition. *Biocatal. Agric. Biotechnol.* **2016**, *6*, 102–106. [[CrossRef](#)]
60. Safikhan, S.; Khoshbakht, K.; Chaichi, M.R.; Amini, A.; Motesharezadeh, B. Role of chitosan on the growth, physiological parameters and enzymatic activity of milk thistle (*Silybum marianum* (L.) Gaertn.) in a pot experiment. *J. Appl. Res. Med. Aromat. Plants* **2018**, *10*, 49–58. [[CrossRef](#)]
61. Mathew, R.; Sankar, P.D. Effect of methyl jasmonate and chitosan on growth characteristics of *Ocimum basilicum* L., *Ocimum sanctum* L. and *Ocimum gratissimum* L. cell suspension cultures. *Afr. J. Biotechnol.* **2012**, *11*, 4759–4766. [[CrossRef](#)]
62. Wang, C.; Lu, J.; Zhang, S.; Wang, P.; Hou, J.; Qian, J. Effects of Pb stress on nutrient uptake and secondary metabolism in submerged macrophyte *Vallisneria spiralis*. *Ecotoxicol. Environ. Saf.* **2011**, *74*, 1297–1303. [[CrossRef](#)]
63. *Polish Pharmacopoeia V*; Polish Pharmaceutical Society: Warsaw, Poland, 1999; pp. 56–57. (In Polish)
64. Giusti, M.M.; Wrolstad, R.E. Characterization and measurement of anthocyanins by UV-visible spectroscopy. *Curr. Protoc. Food Anal. Chem.* **2001**, *F.1.2.*, 1–13. [[CrossRef](#)]
65. Molyneux, P. The use of the stable free radical diphenylpicrylhydrazyl (DPPH) for estimating antioxidant activity. *Songklanakarin J. Sci. Technol.* **2004**, *26*, 211–219.
66. Murchie, E.H.; Lawson, T. Chlorophyll fluorescence analysis: A guide to good practice and understanding some new applications. *J. Exp. Bot.* **2013**, *64*, 3983–3998. [[CrossRef](#)] [[PubMed](#)]

**Disclaimer/Publisher’s Note:** The statements, opinions and data contained in all publications are solely those of the individual author(s) and contributor(s) and not of MDPI and/or the editor(s). MDPI and/or the editor(s) disclaim responsibility for any injury to people or property resulting from any ideas, methods, instructions or products referred to in the content.

Review

# Edible Insects an Alternative Nutritional Source of Bioactive Compounds: A Review

Donatella Aiello <sup>1</sup>, Marcella Barbera <sup>2</sup>, David Bongiorno <sup>3</sup>, Matteo Cammarata <sup>2</sup>, Valentina Censi <sup>2</sup>, Serena Indelicato <sup>3</sup>, Fabio Mazzotti <sup>1</sup>, Anna Napoli <sup>1,\*</sup>, Daniela Piazzese <sup>2,\*</sup> and Filippo Saiano <sup>4</sup>

<sup>1</sup> Department of Chemistry and Chemical Technologies, University of Calabria, 87036 Arcavacata di Rende, Italy

<sup>2</sup> Department of Earth and Marine Sciences, University of Palermo, 90123 Palermo, Italy

<sup>3</sup> Department of Biological, Chemical and Pharmaceutical Science and Technology (STEBICEF), University of Palermo, 90123 Palermo, Italy

<sup>4</sup> Department Agricultural Food and Forestry Sciences, University of Palermo, 90128 Palermo, Italy

\* Correspondence: amc.napoli@unical.it (A.N.); daniela.piazzese@unipa.it (D.P.)

**Abstract:** Edible insects have the potential to become one of the major future foods. In fact, they can be considered cheap, highly nutritious, and healthy food sources. International agencies, such as the Food and Agriculture Organization (FAO), have focused their attention on the consumption of edible insects, in particular, regarding their nutritional value and possible biological, toxicological, and allergenic risks, wishing the development of analytical methods to verify the authenticity, quality, and safety of insect-based products. Edible insects are rich in proteins, fats, fiber, vitamins, and minerals but also seem to contain large amounts of polyphenols able to have a key role in specific bioactivities. Therefore, this review is an overview of the potential of edible insects as a source of bioactive compounds, such as polyphenols, that can be a function of diet but also related to insect chemical defense. Currently, insect phenolic compounds have mostly been assayed for their antioxidant bioactivity; however, they also exert other activities, such as anti-inflammatory and anticancer activity, antityrosinase, antigenotoxic, and pancreatic lipase inhibitory activities.

**Keywords:** insect-based foods; polyphenols; Folin–Ciocalteu method; phenols and flavonoids; polyphenols bioactivity

**Citation:** Aiello, D.; Barbera, M.; Bongiorno, D.; Cammarata, M.; Censi, V.; Indelicato, S.; Mazzotti, F.; Napoli, A.; Piazzese, D.; Saiano, F. Edible Insects an Alternative Nutritional Source of Bioactive Compounds: A Review. *Molecules* **2023**, *28*, 699. <https://doi.org/10.3390/molecules28020699>

Academic Editor: Nour Eddine Es-Safi

Received: 15 December 2022

Revised: 4 January 2023

Accepted: 7 January 2023

Published: 10 January 2023



**Copyright:** © 2023 by the authors. Licensee MDPI, Basel, Switzerland. This article is an open access article distributed under the terms and conditions of the Creative Commons Attribution (CC BY) license (<https://creativecommons.org/licenses/by/4.0/>).

## 1. Introduction

The consumption of edible insects has been a food habit for thousands of years and is common in 120 countries around the world [1,2]. Around 2000 edible insect species raw or processed are consumed across Asia, Australia, Africa, and Central and South America, while insect consumption is uncommon in Western societies [3,4]. The most widespread insect species in the world are beetles followed in descending order by caterpillars; ants, bees, and wasps; grasshoppers and locusts; true bugs; dragonflies; termites; flies; and cockroaches [3,5]. Due to the wide range of edible insect species, their nutritional value is highly variable: A summary of the nutrient composition of more than 200 edible insects (based on dry matter) is shown in Figure 1 [6]. It is possible to observe that the composition of edible insects is generally subject to great variation even within the same species. For example, the species of the order Orthoptera, including crickets, grasshoppers, and locusts, have an average protein content of 61% with variations ranging from 6 to 77%. This suggests that this variation not only result from differences between species and developmental stages but also from different feed and geographical origins, as well as differences in measuring methods. However, globally, the most common edible insects are rich in protein, mono- and polyunsaturated fats, and fiber [6–8].

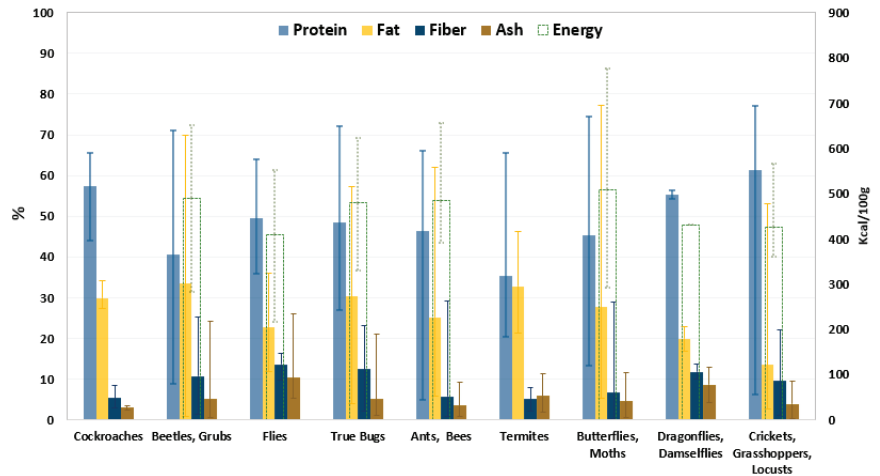


**Figure 1.** Nutritional composition [%] and energy content [kcal/100 g] of edible insects. Data are reported as average value of dry matter and the error bars indicate the maximum and minimum value determined [6].

This aspect leads several international agencies, such as the Food and Agriculture Organization (FAO), to consider insects as cheap, highly nutritious, and healthy food sources [9,10]. In addition, insects have become important in traditional Oriental medicine as a regular treatment for gastritis, fever, cough, asthma, arthritis, rheumatism, and diabetes [6,11–13]. Due to their recognized pharmacological properties, scientific research has focused on the beneficial properties of insects for human health. Recent studies report that edible insects can provide bioactive compounds, such as phenolic compounds and flavonoids [7,12,14–17], acting as antioxidant, anti-inflammatory, anticancer, antimicrobial, and antibacterial inhibitors of the pancreatic lipase enzyme, insulin regulators, and glycaemic inhibitors [13,18–23]. Although beneficial effects are often due to the synergy of different components, several studies report the key role of polyphenolic content concerning specific bioactive activities. For instance, experimental *in vitro* studies demonstrated the antioxidant effect of polyphenolic compounds derived from the extracts of house crickets (*Acheta domesticus*), mealworms (*Tenebrio molitor*) [24], and dark black chafer beetles (*Holotrichia parallela*) [14]. An *in vivo* study performed in mice [25] proved the antioxidant effects of phenolic compounds in a vegetal tea and an insect tea (*Hydrillodes repugnalis*). They found that mice treated with insect tea showed higher superoxide dismutase, glutathione peroxidase, glutathione activities, and lower nitric oxide and malonaldehyde activities than control group mice. In addition to antioxidant properties, it has been reported that polyphenols from the hydroethanolic extracts of the edible insect *Polyrhachis vicina* may act as pancreatic lipase inhibitors [22]. Moreover, other authors [26] reported that hydroxytyrosol dimers isolated from *Brynhoptera rynchopetera* exhibited selective cytotoxicity and good inhibitory activity on mouse melanoma proliferation. In addition to the nutritional benefits, a new global interest in edible insects and invertebrates has recently emerged as the imbalance between the production and consumption of animal-origin food is increasing. This is creating various socioeconomic concerns, exacerbated by climate change [10,27]. From an environmental and ecological point of view, insects represent a highly sustainable replacement for meat and animal products. Their farming results in lower greenhouse gas emissions, requires less water and land, represents a much lower economic investment compared to livestock, and also can limit deforestation for pasture use (Table 1) [28].

**Table 1.** Environmental impact of mealworms and cricket compared to other animal products.

	Chicken	Pork	Beef	Insects	Reference
Water L/kg meat	2300	3500–22,000	43,000	40	[8,29]
Feed kg/kg live animal	2.5	5	10	1.7	[30]
Land ha/kg protein	2–3.5	2–3.5	10	1	[31]
CH <sub>4</sub> emissions g/kg biomass	n.r. <sup>1</sup>	1.9	114	0.1	[32,33]
CO <sub>2</sub> emissions g/kg biomass	n.r. <sup>1</sup>	79.6	285	7.6	[32,33]

<sup>1</sup> n.r.: not reported.

From a social and economic perspective, the insect market offers livelihood and entrepreneurial development opportunities for farmers in rural communities, thus improving the quality of life in poor and developing countries [9,34–37]. Furthermore, primary production and processing of edible insects are expected to increase in Western countries, resulting in new commercial opportunities and new sources of income [6,10,38]. Despite all these favorable aspects, the consumption of edible insects has been associated with several risk factors, including biological, toxicological, and allergenic risks [8,10,39–42]. Molds and yeasts with mycotoxigenic potential can affect edible insects causing adverse reactions in humans [8,43,44]. The presence of tropomyosin in insects, a fibrous protein also found in crustaceans and arthropods, can cause allergic reactions in consumers [45,46]. Microbial contamination can also affect insects, but with a higher risk for wild ones [47]. Further, standards or criteria that determine guidelines for management and hygiene are still fragmented, increasing consumer mistrust, especially in Western countries where entomophagy is not fully accepted [10,42,48]. Globally, rules and regulations, both at the national and international level, on the production, storage, and consumption of insects as food/feed ingredients are often absent or, at best, nonexhaustive [4,28,42,49]. Although cultural barriers and legislative deficits related to entomophagy still exist, the human consumption of insects is becoming strategic due to their health properties, high nutritional values, and environmental sustainability [10,38]. Currently, research trends and food innovations focus on food fortification with alternative, sustainable, and functional food to improve the nutritional value of food by correcting nutrient or minerals deficiencies or enhancing health-promoting properties [50–58]. In this contest, insects represent one of the most valuable functional ingredients and interesting solutions for the food industry [13,59–63]. Insect powder can be a valuable ingredient to supplement deficiencies in food, such as in gluten-free products. For example, the enrichment of gluten-free bread with 10% of cricket powder significantly increased the nutritional value, with protein content exceeding seven-fold the reference bread [64]. Moreover, cricket powder addition resulted in an increase of the total polyphenolic compound content from 1.9 mg/g in control bread to 6.2 mg/g in insect-enriched bread; likewise, the total antioxidant capacity before digestion increased about fourfold and after digestion about sixfold without affecting either beneficial or pathogenic microflora. Zielinska et al. [65] tested the effect of adding cricket (*Gryllos sigillatus*) and mealworm (*T. molitor*) flours to muffins. In muffins enriched with insect flour, they found an increase in protein content, a decrease in carbohydrate content, and a reduction in the glycemic index. In addition, the antioxidant capacity, as well as total phenolic content, increased correspondingly as the percentage of insect flour in the muffins increased. Additionally, enriched muffins were accepted by consumers. The researcher also reported that the use of appropriate processes in food technology can ensure high retention of nutrients and bioactive compounds in food, enhancing its health properties [66]. For instance, Gaglio et al. [67] investigated in vitro the antioxidant potential of bread added with mealworm and buffalo worm before and after gastrointestinal digestion in comparison with insect-free bread. The authors found that replacing semolina with buffalo and mealworm powder increased the antioxidant capacity of the bread before digestion by three- and four-fold, respectively. After gastrointestinal digestion, all samples (bread with insects and control bread) showed a higher antioxidant capacity value than that measured before digestion. This may be explained because phenolic antioxidants can be released from the wheat during digestion, increasing the antioxidant potential of the digested bread [67]. Interesting to note



is that, in other studies, fortification of bread with plant-based additives, such as Saskatoon berry powder or grape pomace, resulted in a similar increase in the antioxidant potential of the product [68–70]). The increased polyphenol content in fermented samples could be explained because, during the fermentation process, bacteria may remove sugar moieties, hydrolyze galloyl moieties, and release free phenolic compounds [71,72]. Nevertheless, insect studies on polyphenol compounds are mainly related to the total content, and interference caused by proteins, amino acids, and peptides could cause an overestimation of these compounds [73,74]. Among other factors, both the total polyphenol content and quality profiles are highly variable between insect species (Tables 2 and 3).

**Table 2.** Total Polyphenol Index (TPI) expressed as gGAE/100 g (GAE, Gallic acid equivalent).

Insects	gGAE/100 g	Reference
Stink bugs ( <i>Encosternum delegorguei</i> )	3.6	[17,75]
Cricket ( <i>Henicus whellani</i> )	0.08	[17]
Cricket ( <i>Henicus whellani</i> )	0.77	[27]
Beetle ( <i>Eulepida mashona</i> )	0.08	[76]
Ground cricket ( <i>Henicus whellani</i> )	0.77	[77]
Stinkbugs ( <i>Encosternum delegorguei</i> )	3.6	[17,75]
House cricket ( <i>Acheta domestica</i> )	0.3–5.0	[24]
Chafer beetles ( <i>Holotrichia parallela</i> )	5 g	[14]
Beetle ( <i>Eulepida mashona</i> )	0.08	[27]
Rhinoceros beetle ( <i>Allomyrina dichotoma</i> )	0.13	[78]
Mealworm beetle ( <i>Tenebrio molitor</i> )	0.26	[78]
Scarabaeidae ( <i>Protaetia brevitarsis</i> )	1.18	[78]
Cricket ( <i>Gryllus bimaculatus</i> )	1.56	[78]
Cricket ( <i>Teleogryllus emma</i> )	1.55	[78]
Bee ( <i>Apis mellifera</i> )	1.24	[78]

**Table 3.** Polyphenolic compounds in different species of insects.

Family/Species	Polyphenolic Compounds	Reference
Black ant		
<i>Polyrhachis vicina</i>	Salicylic acid, trans-cinnamic acid, vanillic acid, isoferulic acid, gallic acid, 3,4-dihydroxybenzoic acid, formononetin, liquiritigenin, quercetin, caffeic acid, naringenin, catechin, sakuranetin, and L-epicatechin.	[22]
Acrididae		
<i>Acheta domestica</i>	Quinic acid, gallic acid, 4-hydroxybenzoic acid, chlorogenic acid, caffeic acid, syringic acid, <i>p</i> -coumaric acid, ferulic acid, sinapic acid, 2-hydroxybenzoic acid, daidzein, quercetin, naringenin, and apigenin	[16]
<i>Dissoteira carolina</i>	Quercetin (3,3',4',5,7-pentahydroxyflavone) and quercetin- $\beta$ -3-O-glucoside	[79]
<i>Schistocerca americana</i>	Luteolin (3',4',5,7-tetrahydroxyflavone) and $\beta$ -3-O-glucoside	[80]
Beetle		
<i>Holotrichia parallela</i>	Resveratrol, 4-hydroxyacetophenone, protocathechualdehyde, ferulic acid, gallic acid, protocatechuic acid, epicatechin, quercetin, and catechin	[14]
Caterpillar		
<i>Rondotia menciana</i>	Quercetin-glycosides and kaempferol-glycosides	[81]
Silkworm		
<i>Bombyx mori</i>	Quercetin, kaempferol, and quercetin-glycosides	[82,83]

Table 3. Cont.

Family/Species	Polyphenolic Compounds	Reference
Butterfly		
<i>Antheraea pernyi</i>	Hyperoside (quercetin 3-O-glucoside), isoquercitroside, tricin 7-O-hexoside, hesperetin 5-O-glucoside, protocatechuic acid, luteolin 7-O-glucoside (cynaroside), kaempferol 3-O-glucoside (astragalol), C-hexosyl-luteolin O-p-coumaroylhexoside, luteolin 6-C-glucoside, tricin 4'-O-( $\beta$ -guaiacylglyceryl) ether O-hexoside, orientin, luteolin C-hexoside, kaempferol 3-O-galactoside (trifolin), and tricin 4'-O-( $\beta$ -guaiacylglyceryl) ether 7-O-hexoside <sup>1</sup>	[84]
<i>Melanargia galathea</i>	Tricin (4',5,7-trihydroxy-3',5'-dimethoxyflavone), apigenin (4,5,7-trihydroxyflavone), tricin 7-glucoside, orientin (8-glucosylluteolin), luteolin 7-diglucoiside, orientin 7-glucoside, vitexin 7-glucoside, isoorientin (luteolin 6-C-glucoside), isovitexin (6-C-glucosylapigenin), and tricin 4'-conjugate	[85]
<i>Coenonympha pamphilus</i>	Tricin (4',5,7-trihydroxy-3',5'-dimethoxyflavone)	[86]
<i>Lysandra coridon</i> Poda	Kaempferol-glycosides	[87]
<i>Polyommatus icarus</i>	Quercetin, kaempferol, and quercetin-glycosides and kaempferol-glycosides	[88]
<i>Pieris brassicae</i>	Kaempferol glycosides and ferulic and sinapic acids	[79]
<i>Melanargia galathea</i>	Glycosides of tricin (tricin-glycosides), lutexin, and tricin (4',5,7-trihydroxy-3',5'-dimethoxyflavone)	[89]
Hymenoptera		
<i>Amauronematus amplus</i> , <i>Arge</i> sp., <i>Nematus bre-vivalvis</i> , <i>Nematus pravus</i> , <i>Nematus viridis</i> , <i>Nematus alpestris</i> , <i>Trichiosoma scalesii</i>	Quercetin-glycosides, kaempferol-glycosides	[90]
<i>Neodiprion sertifer</i>	(+)-Catechin 7-O- $\beta$ -glucoside, isorhamnetin 3,7,4'-tri-O- $\beta$ -glucosid, kaempferol 3,7, 4'-tri-O- $\beta$ -glucoside, kaempferol 3,7, 4'-tri-O- $\beta$ -glucoside, and quercetin 3,7,4'-tri-O- $\beta$ -glucoside	[91]

<sup>1</sup> More abundant out of a total of 225 identified compounds.

Even though little investigation has been conducted up to now, the presence of phenolic compounds in insects has been associated with their diet and with the ability of insects to synthesize phenolic compounds through the sclerotization process [16]. The influence of various feeds on the production of bioactive substances, such as polyphenols and flavonoids in *Protaetia brevitarsis* larvae, has been investigated [92]. The primary larvae feed (oak-fermented sawdust) was supplemented with fruits and vegetal (aloe, apple, banana, sweet persimmon, and sweet pumpkin). The authors found that compared with the mean total polyphenol content of the control group (19.2 mgGAE/g), the total polyphenol content of larvae receiving supplementary feeds was always higher; the combined mean from all groups receiving supplementary feed was 25.5 mg/g (the highest polyphenol content was observed in larvae receiving sweet pumpkin, 30.4 mg/g), whereas the total flavonoid contents in groups receiving supplemental feed do not vary significantly concerning control group. This suggests that diet can affect the uptake of polyphenols in insects as early as the larval stage [16]. In this study, the insects appear to have a selective uptake of flavonoids, mainly kaempferol and quercetin, as well as flavones, such as tricine and isovitexin. Most of these compounds have been identified in their glycosylated form with glucose, rhamnose, or galactose. Flavonols and flavones synthesized by the host plant are metabolized or absorbed by the insect. An understanding of an insect's phenolic profile can provide indications of their possible use as functional foods.

## 2. Identification and Characterization of Phenolic Compounds in Insects

The European community categorizes insect-based food as "novel food" according to Reg. 2015/2283 [93]. A starting list of 12 species of insects is under evaluation; however,

the first focus interest of the European Food Safety Authority (EFSA) is the risk control of edible insects. To date, only three insects (the house cricket *A. domesticus*, yellow mealworm *T. molitor*, and migratory locust *Locusta migratoria*) are officially retained edible insects; their trade has been approved by the European Commission after the positive scientific opinion of the EFSA [94–96]. Since regulation (EU) No. 2017/2470 allows the trade of insect-based products (either whole or in the form of a powder) (EU 217/2470) [97], the FAO recommended the development of analytical methods to verify the authenticity, quality, and safety of products of insect powders [10,98]. No specific indications are officially reported regarding the detection and assay of polyphenols; however, research of phenolic compounds derived from insect diets gained interest, especially combined with the exploration of insects' feeding habits [17].

Literature data report the use of larvae or adult insects instead; pupae are rarely used [99,100]). When necessary (i.e., for crickets, locusts, and grasshoppers), wings, legs, and antennae are removed, while in scorpions, the stingers are eliminated [15]. Several procedures provide freeze-drying of insects followed by grinding them into powder before processing [22,99]. Sometimes, powdered insects are defatted with hexane washing, and the lipid-free solids are used for the extraction of water-soluble extracts [101]. In other cases, the defatting step is performed by microwave-assisted extraction (MAE) with petroleum ether, and the residues are collected for the next extraction step in alcoholic (methanol, ethanol) or alcoholic/aqueous solutions at a fixed temperature and time [14,16]. Ssepuyua et al. [15] report a study on the suitable conditions for the extraction of antioxidant compounds from *Ruspolia differens* and prove that the defatting step affects the amount of the antioxidant compounds. The antioxidants are predominately found in the apolar nonfat phase, and the highest concentration of antioxidant compounds is obtained after sonication for 60 min. Moreover, the authors demonstrated that the amounts of total phenols and flavonoids are relatively higher and comparable to those of many fruits and vegetables. Different, but at the same time very interesting, is the method proposed by Vasconcelos dos Santos et al. [102] that makes use of the crude oil (SRO) extracted from *Speciomerus ruficornis* larvae. The artisanal extraction provides that entire and wet larvae are directly placed on heat (150 °C) in a sealed stainless-steel pan until the oil flows out from the bugs, and the total polyphenol content is analyzed from SRO.

The quantification of bioactive compounds has obtained a great interest in food products, especially as relevant to preservation or to the prevention of deterioration by oxidation. Some antioxidants, such as polyphenols (e.g., caffeic acid, tannic acid, ferulic acid, ascorbic acid, and quercetin), became key compounds for neutralizing the damaging effects of oxidation [103]. A common methodology used for the quantification of antioxidant capacities is the Folin–Ciocalteu (FC) colorimetric method, which is based on the single electron-transfer (SET) reaction [41,78,104]. This assay was also adopted to evaluate the total polyphenol amount in edible insects or insect meal powder. However, the action mechanism of FC assay is centered on oxidation/reduction reaction, and it is prejudiced by the presence of other nonphenolic compounds, such as ascorbic acid, other enediols, and oleic acid [104]. This means that the total polyphenol content evaluated through FC assay reflects the oxidizing capacity of several different compounds together. Some researchers [101] reported the total polyphenol index (TPI) of water-soluble extracts of twelve commercially available edible insects and two invertebrates. Results are expressed as milligrams of gallic acid equivalents (GAE) per 100 g of defatted sample.

Crickets, grasshoppers, silkworms, African caterpillars, and evening cicadas displayed values of antioxidant capacity two- or three-fold higher in vitro than orange juice or olive oil [101]. However, the phenolic content of analyzed samples, as determined by TPI following a procedure modified by Giacintucci et al. [105], showed higher values only for grasshoppers compared to fresh orange juice. The authors suggested that the observed antioxidant capacity was not only due to the polyphenol compounds but also to the proteins, which is in agreement with the literature data [18,106].

Analytical instrumental techniques are currently adopted to identify and characterize peptides, proteins, or lipids differently extracted from insects [98], insect organs [84], or hemolymph [107]. Indeed, it is well-known that standard analytical techniques are generally used for the identification and quantitative determination of phenolic compounds in several food matrices and also in insect meal powder. The coupling of liquid chromatography (LC) to mass spectrometry (LC-MS) facilitates metabolite identification and quantitation by reducing sample complexity and allowing analyte separation before detection [108]. Mass spectrometry has proven to be a very capable technique in flavonoid analysis because of its high sensitivity and signal reproducibility; moreover, the ability to couple with chromatographic techniques leads to both qualitative and quantitative determinations [109–116]. LC-MS and MS/MS are becoming the methods of choice for detecting analytes in complex samples. Seventeen phenolic compounds in edible *A. domesticus* were characterized and determined by HPLC-MS [16]. The authors have investigated the content of phenolic compounds in a commercial and organic sample, and major compounds identified in both extracts correspond to 4-hydroxybenzoic acid, *p*-coumaric acid, ferulic acid, and syringic acid. Several bioactive compounds, including phenolic acids and flavonoids, have been detected in the extract from the edible insect *P. vicina* [22]. The characterization of these components was carried out by HPLC-MS/MS. The most abundant identified antioxidant compounds are salicylic acid, gallic acid, liquiritigenin, and naringenin. The same authors also report the antioxidant activity of the analyzed extract and the characterization and quantification of fatty acids. Again, by mass spectrometry but with the help of other spectroscopic techniques, such as NMR, used to gain structural information for different classes of compounds [117–120], hydroxytyrosol derivatives were identified in the edible *Blaps rynchopetera* [26]. The insect *Blaps japonensis* is employed as an ethnomedicine in China for the treatment of several disorders, such as cancer and inflammation [121]. The authors analyzed the extract obtained from these insects and identified eight phenolic compounds, two of which were already known. The characterization was carried out by spectroscopic studies, such as NMR and high-resolution mass spectrometry. Liu et al. [14] investigated the antioxidant activity of an ethanolic extract of *H. parallela* Motschulsky a black beetle, a common crop pest in China. The authors characterized the extract by liquid chromatography and used it for identification of a standard solution of phenolic compounds: gallic acid, quercetin, catechin, protocatechuic acid, epicatechin, protocatechualdehyde, resveratrol, ferulic acid, and 4-hydroxyacetophenone [14]. Using a metabolomics approach, Fu et al. have identified more than 200 flavonoid metabolites in *Antheraea pernyi*, an edible insect; the study was conducted by LC-MS/MS in positive and negative modes. These flavonoid metabolites came from eight subclasses, including flavones, flavonols, flavonoids, flavanones, polyphenols, isoflavones, anthocyanins, and proanthocyanidins. The most abundant identified compounds are: hyperoside, isoquercitroside, tricine 7-*O*-hexoside, hesperetin 5-*O*-glucoside, and protocatechic acid [84].

### 3. Insects' Bioactive Compounds as a Function of Diet

Polyphenols are vastly acknowledged as healthy substances, able to exert diverse bioactivities linked to chronic diseases, such as antioxidant, anti-inflammatory, and anti-cancer activity. Insects, however, are not capable to produce polyphenols de-novo and achieve them from their diet. Since the early 20th century, several studies have tried to relate insects' herbivore feeding to their polyphenol content [17,77,88,122–125]. A recent study by Yoon et al. [92] also evidenced a similar aspect. Indeed, the authors ascertained that the content of nutrients and polyphenols of *P. brevitarsis* larvae could be tailored by supplementing auxiliary feeds, including aloe, apple, banana, sweet persimmon (*S. persimmon*), and sweet pumpkin (*S. pumpkin*). The feed and the breeding environment modification can be used to alter *P. brevitarsis* larvae's capacity to serve as a healthy functional food. Haber et al. [99] report a study on the nutritional characterization of bees as a function of diet. They introduced two different diets: (i) bees fed only in nature, collecting pollen and nectar (natural diet) and (ii) bees fed in nature with the addition of a sucrose solution,

as usually is performed by beekeepers during the winter. Total polyphenolic content is determined according to Musundire et al. [75] using the Folin–Ciocalteu assay. Reported data demonstrate that the nutritional value is found to differ between larvae and pupae, whereas antioxidant properties changed only between the different diets. *A. domesticus* was also subjected to study to verify the effect of diet on polyphenol content. In particular, the objective of Nino and coworkers' study [16] was to elucidate the phenolic composition of farmed *A. domesticus* consuming two different diets (organic and commercial) and evaluate their potential in vitro antioxidant activity. The content of total phenolic compounds, determined by FC assay, revealed a high phenols content that cannot be attributed only to the phenolic compounds present in the sample but also to other components that are able to react with the Folin–Ciocalteu reagent. For example, the cricket extracts contained unsaturated fatty acids, vitamins, and free amino acids that have shown reactivity with the FC reagent in previous studies [74]. The confirmation of the presence of phenolic compounds in insects has been previously reported for a variety of species, mainly Lepidoptera (e.g., butterflies and moths) and also in this case, the main assumption is that these compounds are directly correlated with the insects' diet [126].

#### 4. Biological Activity of Polyphenols Extracts Obtained from Insects

##### 4.1. Antioxidant Bioactivity

Currently, insect phenolics have mostly been assayed for their antioxidant bioactivity. However, kaempferol and quercetin found in insects can lead to other biological activities. Phenolic compounds decompose peroxide species, neutralize free radicals [127], and they can be able to bind to metal ions when the number and the specific location of hydroxyl groups in the molecule allow for it [128]. To investigate the antioxidant activity of phenolic compounds in insects, Liu et al. [14] evaluated the water extracts (WE) and ethanol extracts (EE) obtained from dark black chafer beetle (*H. parallela*). The EE had a superior activity compared to the butyl hydroxytoluene (BHT) standard, showing a better peroxidation inhibition activity. The WE revealed a higher reducing power than EE. Both extracts also proved to be a better chelating agent concerning ethylenediaminetetraacetic acid (EDTA) in sequestering the iron ions. In EE, the authors also found a substantial catechin concentration ( $7.66 \pm 0.05$  mg/g extract).

Ethanol extracts obtained from house cricket (*A. domesticus*) and mealworm (*T. molitor*) showed an in vitro antioxidant activity evaluated with the 1,1-diphenyl 2-picrylhydrazyl (DPPH) assay with around 80% inhibition [24].

Ssepunya and coworkers [15] in recent research also evaluated the effects of the defatting procedure on *R. differens* (grasshopper) pastes. It has been found that the antioxidant activity of the nondefatted samples was similar to that of the defatted ones, suggesting that antioxidant compounds are located within the polar components of the pastes. This implies that the defatting step is not necessary to obtain a more active dietary supplement.

Pyo et al. [78] evaluated the bioactivities of six Korean edible insects (*Allomyrina dichotoma*-AD, *Tenebrio molitor*-TM, *Protaetia brevitarsis*-PB, *Gryllus bimaculatus*-GB, *Teleogryllus emma*-TE, and *Apis mellifera*-AM) to develop functional food ingredients. Ethanol extracts of AD were considered for antioxidation capacity, PB and AM for nitrite scavenging, and TE for anticoagulation, antioxidation, and hemolysis. Experimental data collected employing in vitro experimental tests showed the polyphenolic and flavonoidic content is not related to the measured antioxidant activity. Interestingly, even if not reported in the text, the major content of polyphenols has been found in GB and TE extracts. These were the only species fed by vegetable supplements.

Silkworm pupae (SWP) are another type of industry byproduct that can be recovered to exploit its nutritional properties to enhance the human diet. Sadat et al. [23], in their minireview, resume all the bioactive compounds so far identified in SWP methanolic extracts. It has been evidenced the presence of several polyphenols, including quercetin, resveratrol, kaempferol, myricetin, and naringenin. All these substances are accredited with strong antioxidant activities. This is also evident for the extracts of SWP (*Bombyx*

*mori*, *Antheraea assamensis*, and *Antheraea mylitta*) that possess high ROS scavenging activity shown through by DPPH [129] (2,20-azino-bis-3-ethyl-benzothiazoline)-6-sulfonic acid (ABTS) and ferric reducing antioxidant power (FRAP) essays [130].

#### 4.2. Other Biological Effects

Several biological effects linked to the presence of active substances have been evaluated in the literature (Table 4).

**Table 4.** Biological activity of insect extracts.

Insect Species	Most Abundant Molecules	Activity	References
<i>P. vicina</i>	salicylic acid, gallic acid, liquiritigenin	PL inhibitory activity	Zhang et al. [22]
<i>A. assamensis</i>	not specified	antityrosinase activity	Deori et al. [131]
<i>B. mori</i>	not specified	antigenotoxic activity	Deori et al. [131]
<i>B. japonensis</i>	blapsins	anticancer activity, inhibitory activities versus the JAK3 family genes; oncological, cardiovascular, and neurological disorders, organ transplantation, and autoimmune diseases	Yan et al. [121]
<i>Macrotermes facilger</i>	polyphenols	antioxidant and antimicrobial properties;	Kunatsa et al. [41]
<i>Macrotermes facilger</i>	oxalates, tannins, and cyanogenic glycosides	antinutritional properties	Kunatsa et al. [41]
<i>Henicus whellani</i>	polyphenols	antioxidant and antimicrobial properties;	Kunatsa et al. [41]
<i>Henicus whellani</i>	oxalates, tannins, and cyanogenic glycosides	antinutritional properties	Kunatsa et al. [41]

Zhang et al. [22] prepared a hydroethanolic extract of *P. vicina* to characterize its bioactivity. In particular, the pancreatic lipase (PL) inhibitory activity antioxidant activity and total flavonoid and total polyphenol contents of *P. vicina* extract have been tested in vitro. Phenolic acids such as salicylic acid and gallic acid and flavonoids such as liquiritigenin and naringenin were found. These constituted the major polyphenols in the *P. vicina* extracts. Docking studies evidenced an interaction of these four major constituents of the polyphenolic fraction with PL. Based on the measured antioxidant and PL inhibitory activities of this extract, a nutraceutical application to treat obesity and reduce oxidative stress-induced diseases can be advised.

Deori and coworkers [130] also evidenced that methanolic extracts of *A. assamensis* showed stronger antityrosinase activity of SWP as compared to kojic acid, while *B. mori* SWP extracts were characterized by antigenotoxic activity.

*B. japonensis* was the subject of a characterization study by Yan et al., [121]. This research group individuated new compounds called Blapsins (C to J) involved in several interesting bioactivities. Each compound was tested against cancer cells (A549, Huh-7, K562) and the COX-2 isoenzyme, ROCK1, and JAK3 genes. It was shown that the Blapsins (C to J) all have anticancer activity; in addition, Blapsin C, D, and F possess ROCK1 inhibitory activity, and Blapsins (C to G) have selective inhibitory activities versus the JAK3 family genes. All these activities show the possible beneficial effects of *B. japonensis* extract for the treatment of oncological, cardiovascular, and neurological disorders, organ transplantation, and autoimmune diseases. The study evidence that these results somewhat justify Chinese ethnomedicine.

Most of the reported studies evaluated the possible positive effects of the insect extracts on the human diet, often ignoring their adverse effects. However, it must be considered that these extracts can also contain anti-nutrients that should be removed or reduced. Kunatsa and coworkers [41] conducted a qualitative–quantitative screening of two edible insects: *Macrotermes facilger* and *Henicus whellani*. The extracts were characterized by antioxidant and antimicrobial properties, attributed to the polyphenolic content. However, oxalates, tannins, and cyanogenic glycosides were also found. These might have antinutritional

properties; therefore, the authors suggest, food processing, such as boiling and cooking, to reduce antinutrient concentrations to safe levels before insect consumption.

#### 4.3. Phenols' Internal Synthesis and Immune Defences

On the other hand, some nondietary phenolic compounds that are found in insects' bodies are derived from a chemical mechanism of sclerotization that leads to the phenols synthesized through the phenoloxidase enzyme [17,132].

In insects, melanins (eumelanin and pheomelanin) are synthesized for several purposes. These include color patterning, cuticle sclerotization, organogenesis, clot formation, and innate immunity. Traditional views of insect immunity detail the storage of prophenoloxidases inside specialized blood cells (hemocytes) and their release upon recognition of foreign bodies [133].

The pathway called the prophenoloxidase activating (proPO) system represents a defense and/or recognition system at first proposed for arthropods [134,135]. The proenzyme is converted to its active form, phenoloxidase, by proteolytic cleavage, and the resulting enzyme catalyzes both the o-hydroxylation of monophenols and the oxidation of diphenols to quinones. In turn, these quinones are polymerized nonenzymatically to melanin. This pigment is ubiquitous throughout the animal kingdom, and melanization supports hemocyte reactivity to foreign agents. Activation depends upon a cascade of serine proteases and other factors in the hemolymph, and some of these factors are sensitive to  $\beta$ -1,3-glucans, lipopolysaccharides (LPS), or other carbohydrates derived from bacteria or from microbial cell walls; therefore, there are certain biochemical and functional similarities to the alternative pathway of complement. Phagocytosis, encapsulation, clotting, microbial killing, and wound repair are defense responses in which the component proteins of the proPO system are involved [135].

Reactive forms of oxygen, such as superoxide anion, hydroxyl radical, and hydrogen peroxide anion, have been implicated as components of vertebrate and invertebrate [136–138] cytotoxic mechanisms. The propensity of quinones for redox cycling makes these eumelanin precursors potential sources of the reactive forms of oxygen [139–141]. It has been demonstrated [142] that phenolic compounds exhibit cytotoxic activity toward human melanoma cells since they can be converted into toxic products by tyrosinase. Thus, the proPO system produces several molecules, including polyphenols and melanin capable of having a key role in specific bioactivities in insects, but their real beneficial impact on health has yet to be evaluated [143,144].

## 5. Final Remarks

This review shows the potential of insects as providers of a wide variety of bioactive compounds, such as polyphenols, which are widely recognized as health substances. Polyphenols are represented in insects because they may function as pigment and chemical defense. Insects can selectively absorb and accumulate the flavonoids in their body from the larval stage via their host plant; therefore, the diet is the determinant for the type and amount of polyphenols present. They also may synthesize and store nondietary phenolic compounds through the sclerotization process. Currently, insect phenolics have mostly been assayed for their antioxidant bioactivity; however, they also exert other bioactivities, such as antiinflammatory and anticancer activity, antityrosinase, antigenotoxic, and pancreatic lipase inhibitory activities. Although several studies have been conducted on the use of insects, both whole and in flour form, as food supplements and as extracts in the treatment of acute diseases, there are few reports on the identification and characterization of the polyphenol profile. This is due to the most common adoption of unselective colorimetric methods as FC, and this may lead to an overestimation of phenolic content. Although an increasing number of studies focus on polyphenol profiling using mass spectrometry (LC-MS and MS/MS) techniques, to date, only fragmented data are available on only a few edible insect species.

Based on recent scientific developments on this topic, future research aims to encourage an investigation of new different classes of insects and polyphenols to evaluate their real beneficial health impact.

Despite these gaps, the high nutritional value as well as the presence of bioactive compounds associated with their undoubtedly ecological properties suggest insects as having a role in sustainable and functional foods. To date, only a few studies have evaluated biological, chemical, and allergenic risks and the presence of antinutrients. It should also be reminded that insects are typically processed by roasting, freezing, extrusion, and blanching, among other methods. Even if these processes do not significantly affect the total phenolic content in processed fruits and plants [17], up to date, there are not enough studies to describe the effects of such processing methods on insects. While actual knowledge could suggest that mild processing can maintain the functionality of these compounds, it is strongly advisable that processing time and temperatures should be evaluated and optimized. It is paramount to define standards, criteria, or guidelines for the management of insect-derived products. Indeed, legal regulations are the key prerequisite for the correct development of insect farming and the effective marketing of insect-based foods.

**Author Contributions:** Conceptualization, writing and original draft preparation, D.A., M.B., D.B., M.C., V.C., S.I. and F.M.; conceptualization, review, and editing, F.S.; review, editing, and supervision A.N. and D.P. All authors have read and agreed to the published version of the manuscript.

**Funding:** This research received no external funding.

**Institutional Review Board Statement:** Not applicable.

**Informed Consent Statement:** Not applicable.

**Data Availability Statement:** Not applicable.

**Conflicts of Interest:** The authors declare no conflict of interest.

**Sample Availability:** Not applicable.

## References

1. Tang, C.; Yang, D.; Liao, H.; Sun, H.; Liu, C.; Wei, L.; Li, F. Edible insects as a food source: A review. *Food Prod. Process. Nutr.* **2019**, *1*, 1–13. [CrossRef]
2. Wendin, K.; Olsson, V.; Langton, M. Mealworms as food ingredient sensory investigation of a model system. *Foods* **2019**, *8*, 319. [CrossRef] [PubMed]
3. Jongema, Y. *List of Edible Insects of the World (1 April 2017)*; Wageningen UR: Wageningen, The Netherlands, 2017. Available online: <https://www.wur.nl/en/Research-Results/Chair-groups/Plant-Sciences/Laboratory-of-Entomology/Edible-insects/Worldwide-species-list.htm> (accessed on 3 November 2021).
4. Żuk-Golaszewska, K.; Gałęcki, R.; Obremski, K.; Smetana, S.; Figiel, S.; Gołaszewski, J. Edible Insect Farming in the Context of the EU Regulations and Marketing An Overview. *Insects* **2022**, *13*, 446. [CrossRef] [PubMed]
5. El Hajj, R.; Mhemdi, H.; Besombes, C.; Allaf, K.; Lefrançois, V.; Vorobiev, E. Edible Insects' Transformation for Feed and Food Uses An Overview of Current Insights and Future Developments in the Field. *Processes* **2022**, *10*, 970. [CrossRef]
6. Sun-Waterhouse, D.; Waterhouse, G.I.; You, L.; Zhang, J.; Liu, Y.; Ma, L.; Gao, J.; Dong, Y. Transforming insect biomass into consumer wellness foods: A review. *Food Res. Int.* **2016**, *89*, 129–151. [CrossRef] [PubMed]
7. Da Silva Lucas, A.J.; de Oliveira, L.M.; Da Rocha, M.; Prentice, C. Edible insects: An alternative of nutritional, functional and bioactive compounds. *Food Chem.* **2020**, *311*, 126022. [CrossRef]
8. Ordoñez-Araque, R.; Egas-Montenegro, E. Edible insects: A food alternative for the sustainable development of the planet. *Int. J. Gastron. Food Sci.* **2021**, *23*, 100304. [CrossRef]
9. Hanboonsong, Y.; Jamjanya, T.; Durst, P.B. Six-legged livestock: Edible insect farming, collection and marketing in Thailand. *RAP Publ.* **2013**, *3*, 8–21.
10. Food and Agriculture Organization of the United Nations. *Looking at Edible Insects from a Food Safety Perspective*; Challenges and Opportunities for the Sector; FAO: Rome, Italy, 2021. [CrossRef]
11. Dobermann, D.; Swift, J.A.; Field, L.M. Opportunities and hurdles of edible insects for food and feed. *Nutr. Bull.* **2017**, *42*, 293–308. [CrossRef]
12. Lee, J.H.; Kim, T.K.; Jeong, C.H.; Yong, H.I.; Cha, J.Y.; Kim, B.K.; Choi, Y.S. Biological activity and processing technologies of edible insects: A review. *Food Sci. Biotechnol.* **2021**, *30*, 1003–1023. [CrossRef]



13. Escobar-Ortiz, A.; Hernández-Saavedra, D.; Lizardi-Mendoza, J.; Pérez-Ramírez, I.F.; Mora-Izaguirre, O.; Ramos-Gómez, M.; Reynoso-Camacho, R. Consumption of cricket *Acheta domestica* flour decreases insulin resistance and fat accumulation in rats fed with high-fat and-fructose diet. *J. Food Biochem.* **2022**, *46*, e14269. [[CrossRef](#)] [[PubMed](#)]
14. Liu, S.; Sun, J.; Yu, L.; Zhang, C.; Bi, J.; Zhu, F.; Qu, M.; Yang, Q. Antioxidant activity and phenolic compounds of *Holotrichia parallela* Motschulsky extracts. *Food Chem.* **2012**, *134*, 1885–1891. [[CrossRef](#)] [[PubMed](#)]
15. Ssepuyya, G.; Kagulire, J.; Katongole, J.; Kabbo, D.; Claes, J.; Nakimbugwe, D. Suitable extraction conditions for determination of total anti-oxidant capacity and phenolic compounds in *Ruspolia differens* Serville. *J. Insects Food Feed* **2021**, *7*, 205–214. [[CrossRef](#)]
16. Nino, M.C.; Reddivari, L.; Ferruzzi, M.G.; Liceaga, A.M. Targeted phenolic characterization and antioxidant bioactivity of extracts from edible *Acheta domestica*. *Foods* **2021**, *10*, 2295. [[CrossRef](#)]
17. Nino, M.C.; Reddivari, L.; Osorio, C.; Kaplan, I.; Liceaga, A.M. Insects as a source of phenolic compounds and potential health benefits. *J. Insects Food Feed* **2021**, *7*, 1077–1087. [[CrossRef](#)]
18. Zielinska, E.; Baraniak, B.; Karaś, M. Antioxidant and anti-inflammatory activities of hydrolysates and peptide fractions obtained by enzymatic hydrolysis of selected heat-treated edible insects. *Nutrients* **2017**, *9*, 970. [[CrossRef](#)]
19. David-Birman, T.; Raftan, G.; Lesmes, U. Effects of thermal treatments on the colloidal properties, antioxidant capacity and in-vitro proteolytic degradation of cricket flour. *Food Hydrocoll.* **2018**, *79*, 48–54. [[CrossRef](#)]
20. Issaoui, M.; Delgado, A.M.; Caruso, G.; Micali, M.; Barbera, M.; Atrous, H.; Ouslati, A.; Chammem, N. Phenols, flavors, and the Mediterranean diet. *J. AOAC Int.* **2020**, *103*, 915–924. [[CrossRef](#)]
21. Nardini, M. Phenolic compounds in food: Characterization and health benefits. *Molecules* **2022**, *27*, 783. [[CrossRef](#)]
22. Zhang, Z.; Chen, S.; Wei, X.; Xiao, J.; Huang, D. Characterization, Antioxidant Activities, and Pancreatic Lipase Inhibitory Effect of Extract From the Edible Insect *Polyrhachis vicina*. *Front. Nutr.* **2022**, *9*, 860174. [[CrossRef](#)]
23. Sadat, A.; Biswas, T.; Cardoso, M.H.; Mondal, R.; Ghosh, A.; Dam, P.; Nesa, J.; Chakraborty, J.; Bhattacharjya, D.; Franco, O.L.; et al. Silkworm pupae as a future food with nutritional and medicinal benefits. *Curr. Opin. Food Sci.* **2022**, *44*, 100818. [[CrossRef](#)]
24. Del Hierro, J.N.; Gutiérrez-Docio, A.; Otero, P.; Reglero, G.; Martín, D. Characterization, antioxidant activity, and inhibitory effect on pancreatic lipase of extracts from the edible insects *Acheta domestica* and *Tenebrio molitor*. *Food Chem.* **2020**, *309*, 125742. [[CrossRef](#)] [[PubMed](#)]
25. Zhao, X.; Song, J.L.; Yi, R.; Li, G.; Sun, P.; Park, K.Y.; Suo, H. Comparison of antioxidative effects of Insect tea and its raw tea Kuding tea polyphenols in Kunming mice. *Molecules* **2018**, *23*, 204. [[CrossRef](#)]
26. Pang, X.Q.; Wu, X.M.; Wang, Q.; Meng, D.; Huang, Y.M.; Xu, J.L.; Li, Y.; Liu, H.; Xiao, H.; Ding, Z.T. Hydroxytyrosol Dimers from Medicinal Insect *Blaps Rynchopetera* and the in Vitro Cytotoxic Activity. *Nat. Prod. Commun.* **2022**, *17*, 1–8. [[CrossRef](#)]
27. Giampieri, F.; Alvarez-Suarez, J.M.; Machì, M.; Cianciosi, D.; Navarro-Hortal, M.D.; Battino, M. Edible insects: A novel nutritious, functional, and safe food alternative. *Food Front.* **2022**, *3*, 358–365. [[CrossRef](#)]
28. Van Huis, A.; Van Itterbeeck, J.; Klunder, H.; Mertens, E.; Halloran, A.; Muir, G.; Vantomme, P. *Edible Insects: Future Prospects for Food and Feed Security*; FAO Forestry Paper No. 171; FAO: Rome, Italy, 2013.
29. Pimentel, D.; Berger, B.; Filiberto, D.; Newton, M.; Wolfe, B.; Karabinakis, E.; Clark, S.; Poon, E.; Abbet, E.; Nandagopal, S. Water resources: Agricultural and environmental issues. *BioScience* **2004**, *54*, 909–918. [[CrossRef](#)]
30. Van Huis, A. Potential of insects as food and feed in assuring food security. *Annu. Rev. Entomol.* **2013**, *58*, 563–583. [[CrossRef](#)]
31. Oonincx, D.G.; De Boer, I.J. Environmental impact of the production of mealworms as a protein source for humans—A life cycle assessment. *PLoS ONE* **2012**, *7*, e51145. [[CrossRef](#)]
32. Oonincx, D.G.; Van Itterbeeck, J.; Heetkamp, M.J.; Van Den Brand, H.; Van Loon, J.J.; Van Huis, A. An exploration on greenhouse gas and ammonia production by insect species suitable for animal or human consumption. *PLoS ONE* **2010**, *5*, e14445. [[CrossRef](#)]
33. Mason, J.B.; Black, R.; Booth, S.L.; Brentano, A.B.; Broadbent, B.C.; Connolly, P.; Finley, J.; Goldin, J.; Griffin, T.; Hagen, K.; et al. Fostering strategies to expand the consumption of edible insects: The value of a tripartite coalition between academia, industry, and government. *Curr. Dev. Nutr.* **2018**, *2*, nzy056. [[CrossRef](#)]
34. Halloran, A.; Hanboonsong, Y.; Roos, N.; Bruun, S. Life cycle assessment of cricket farming in north-eastern Thailand. *J. Clean. Prod.* **2017**, *156*, 83–94. [[CrossRef](#)]
35. Halloran, A.; Roos, N.; Hanboonsong, Y. Cricket farming as a livelihood strategy in Thailand. *Geogr. J.* **2017**, *183*, 112–124. [[CrossRef](#)]
36. Kozanayi, W.; Frost, P. *Marketing of Mopane Worm in Southern Zimbabwe*; Institute of Environmental Studies: Harare, Zimbabwe, 2002; pp. 1–31.
37. Imathiu, S. Benefits and food safety concerns associated with consumption of edible insects. *NFS J.* **2020**, *18*, 1–11. [[CrossRef](#)]
38. Derrien, C.; Bocconi, A. Current status of the insect producing industry in Europe. In *Edible Insects in Sustainable Food Systems*; Halloran, A., Flore, R., Vantomme, P., Roos, N., Eds.; Springer International Publishing: Cham, Switzerland, 2018; pp. 471–479.
39. Gezondheidsraad, H. *Common Advice SciCom 14-2014 and SHC Nr. 9160—Subject: Food Safety Aspects of Insects Intended for Human Consumption*; FASFC: Brussels, Belgium, 2014.
40. Poma, G.; Cuykx, M.; Amato, E.; Calaprice, C.; Focant, J.F.; Covaci, A. Evaluation of hazardous chemicals in edible insects and insect-based food intended for human consumption. *Food Chem. Toxicol.* **2017**, *100*, 70–79. [[CrossRef](#)] [[PubMed](#)]
41. Kunatsa, Y.; Chidewe, C.; Zvidzai, C.J. Phytochemical and anti-nutrient composite from selected marginalized Zimbabwean edible insects and vegetables. *J. Agric. Food Res.* **2020**, *2*, 100027. [[CrossRef](#)]

42. Acosta-Estrada, B.A.; Reyes, A.; Rosell, C.M.; Rodrigo, D.; Ibarra-Herrera, C.C. Benefits and challenges in the incorporation of insects in food products. *Front. Nutr.* **2021**, *8*, 687712. [\[CrossRef\]](#)
43. Stoops, J.; Crauwels, S.; Waud, M.; Claes, J.; Lievens, B.; Van Campenhout, L. Microbial community assessment of mealworm larvae *Tenebrio molitor* and grasshoppers *Locusta migratoria migratorioides* sold for human consumption. *Food Microbiol.* **2016**, *53*, 122–127. [\[CrossRef\]](#)
44. Leoni, C.; Volpicella, M.; Dileo, M.C.; Gattulli, B.A.; Ceci, L.R. Chitinases as food allergens. *Molecules* **2019**, *24*, 2087. [\[CrossRef\]](#)
45. De Gier, S.; Verhoeckx, K. Insect food allergy and allergens. *Mol. Immunol.* **2018**, *100*, 82–106. [\[CrossRef\]](#)
46. Jeong, K.Y.; Park, J.W. Insect allergens on the dining table. *Curr. Protein Pept. Sci.* **2020**, *21*, 159–169. [\[CrossRef\]](#)
47. Caparros Megido, R.; Desmedt, S.; Blecker, C.; Béra, F.; Haubruge, É.; Alabi, T.; Francis, F. Microbiological load of edible insects found in Belgium. *Insects* **2017**, *8*, 12. [\[CrossRef\]](#) [\[PubMed\]](#)
48. Lombardi, A.; Vecchio, R.; Borrello, M.; Caracciolo, F.; Cembalo, L. Willingness to pay for insect-based food: The role of information and carrier. *Food Qual. Prefer.* **2019**, *72*, 177–187. [\[CrossRef\]](#)
49. Grabowski, N.T.; Tchibozo, S.; Abdulmawjood, A.; Acheuk, F.; M’Saad Guerfali, M.; Sayed, W.A.; Plötz, M. Edible insects in Africa in terms of food, wildlife resource, and pest management legislation. *Foods* **2020**, *9*, 502. [\[CrossRef\]](#) [\[PubMed\]](#)
50. Allen, L.H.; de Benoist, B.; Dary, O.; Hurrell, R. *Guidelines on Food Fortification with Micronutrients*; World Health Organization, Department of Nutrition for Health and Development: Geneva, Switzerland, 2006.
51. Alfonzo, A.; Martorana, A.; Guarrasi, V.; Barbera, M.; Gaglio, R.; Santulli, A.; Settanni, L.; Galati, A.; Moschetti, G.; Francesca, N. Effect of the lemon essential oils on the safety and sensory quality of salted sardines (*Sardina pilchardus* Walbaum 1792). *Food Control* **2017**, *73*, 1265–1274. [\[CrossRef\]](#)
52. Alfonzo, A.; Gaglio, R.; Barbera, M.; Francesca, N.; Moschetti, G.; Settanni, L. Evaluation of the fermentation dynamics of commercial baker’s yeast in presence of pistachio powder to produce lysine-enriched breads. *Ferment* **2019**, *6*, 2. [\[CrossRef\]](#)
53. Barbera, M. Reuse of food waste and wastewater as a source of polyphenolic compounds to use as food additives. *J. AOAC Int.* **2020**, *103*, 906–914. [\[CrossRef\]](#)
54. Gaglio, R.; Alfonzo, A.; Barbera, M.; Franciosi, E.; Francesca, N.; Moschetti, G.; Settanni, L. Persistence of a mixed lactic acid bacterial starter culture during lysine fortification of sourdough breads by addition of pistachio powder. *Food Microbiol.* **2020**, *86*, 103349. [\[CrossRef\]](#)
55. Gaglio, R.; Restivo, I.; Barbera, M.; Barbaccia, P.; Ponte, M.; Tesoriere, L.; Bonanno, A.; Attanzio, A.; Di Grigoli, A.; Francesca, N.; et al. Effect on the antioxidant, lipoperoxyl radical scavenger capacity, nutritional, sensory and microbiological traits of an ovine stretched cheese produced with grape pomace powder addition. *Antioxidants* **2021**, *10*, 306. [\[CrossRef\]](#)
56. Gaglio, R.; Barbaccia, P.; Barbera, M.; Restivo, I.; Attanzio, A.; Maniaci, G.; Di Grigoli, A.; Francesca, N.; Tesoriere, L.; Bonanno, A.; et al. The use of winery by-products to enhance the functional aspects of the fresh ovine “primosale” cheese. *Foods* **2021**, *10*, 461. [\[CrossRef\]](#)
57. Barbaccia, P.; Busetta, G.; Barbera, M.; Alfonzo, A.; Garofalo, G.; Francesca, N.; Moschetti, G.; Settanni, L.; Gaglio, R. Effect of grape pomace from red cultivar ‘Nero d’Avola’ on the microbiological, physicochemical, phenolic profile and sensory aspects of ovine Vastedda-like stretched cheese. *J. Appl. Microbiol.* **2022**, *133*, 130–144. [\[CrossRef\]](#)
58. Busetta, G.; Ponte, M.; Barbera, M.; Alfonzo, A.; Ioppolo, A.; Maniaci, G.; Guarcella, R.; Francesca, N.; Palazzolo, E.; Bonanno, A.; et al. Influence of Citrus Essential Oils on the Microbiological, Physicochemical and Antioxidant Properties of Primosale Cheese. *Antioxidants* **2022**, *11*, 2004. [\[CrossRef\]](#) [\[PubMed\]](#)
59. Adeboye, A.O.; Bolaji, T.A.; Fatola, O.L. Nutritional composition and sensory evaluation of cookies made from wheat and palm weevil larvae flour blends. *Annu. Food Sci. Technol.* **2016**, *17*, 543–547.
60. Kim, H.W.; Setyabrata, D.; Lee, Y.J.; Jones, O.G.; Kim, Y.H.B. Pre-treated mealworm larvae and silkworm pupae as a novel protein ingredient in emulsion sausages. *Innov. Food Sci. Emerg. Technol.* **2016**, *38*, 116–123. [\[CrossRef\]](#)
61. De Oliveira, L.M.; da Silva Lucas, A.J.; Cadaval, C.L.; Mellado, M.S. Bread enriched with flour from cinereous cockroach *Nauphoeta cinerea*. *Innov. Food Sci. Emerg. Technol.* **2017**, *44*, 30–35. [\[CrossRef\]](#)
62. González, C.M.; Garzón, R.; Rosell, C.M. Insects as ingredients for bakery goods. A comparison study of *H. illucens*, *A. domestica* and *T. molitor* flours. *Innov. Food Sci. Emerg. Technol.* **2019**, *51*, 205–210. [\[CrossRef\]](#)
63. Vasilica, B.T.B.; Chis, M.S.; Alexa, E.; Pop, C.; Păucean, A.; Man, S.; Igual, M.; Haydee, K.M.; Dalma, K.E.; Stanila, S. The Impact of Insect Flour on Sourdough Fermentation-Fatty Acids, Amino-Acids, Minerals and Volatile Profile. *Insects* **2022**, *13*, 576. [\[CrossRef\]](#) [\[PubMed\]](#)
64. Kowalczewski, P.L.; Gumienna, M.; Rybicka, I.; Górna, B.; Sarbak, P.; Dziejdz, K.; Kmiecik, D. Nutritional value and biological activity of gluten-free bread enriched with cricket powder. *Molecules* **2021**, *26*, 1184. [\[CrossRef\]](#)
65. Zielinska, E.; Pankiewicz, U.; Sujka, M. Nutritional, physicochemical, and biological value of muffins enriched with edible insects flour. *Antioxidants* **2021**, *10*, 1122. [\[CrossRef\]](#)
66. Mendoza-Salazar, A.; Santiago-López, L.; Torres-Llanaez, M.J.; Hernández-Mendoza, A.; Vallejo-Cordoba, B.; Liceaga, A.M.; González-Córdova, A.F. In Vitro Antioxidant and Antihypertensive Activity of Edible Insects Flours Mealworm and Grasshopper Fermented with *Lactococcus lactis* Strains. *Ferment* **2021**, *7*, 153. [\[CrossRef\]](#)
67. Gaglio, R.; Barbera, M.; Tesoriere, L.; Osimani, A.; Busetta, G.; Matraxia, M.; Attanzio, A.; Restivo, I.; Aquilanti, L.; Settanni, L. Sourdough “ciabatta” bread enriched with powdered insects: Physicochemical, microbiological, and simulated intestinal digesta functional properties. *Innov. Food Sci. Emerg. Technol.* **2021**, *72*, 102755. [\[CrossRef\]](#)

68. Szawara-Nowak, D.; Bączek, N.; Zieliński, H. Antioxidant capacity and bioaccessibility of buckwheat-enhanced wheat bread phenolics. *J. Food Sci. Technol.* **2016**, *53*, 621–630. [CrossRef] [PubMed]
69. Hayta, M.; Özüğür, G.; Etlü, H.; Şeker, İ.T. Effect of Grape *Vitis vinifera* L. Pomace on the Quality, Total Phenolic Content and Anti-Radical Activity of Bread. *J. Food Process. Preserv.* **2014**, *38*, 980–986. [CrossRef]
70. Lachowicz, S.; Świeca, M.; Pejcz, E. Biological activity, phytochemical parameters, and potential bioaccessibility of wheat bread enriched with powder and microcapsules made from Saskatoon berry. *Food Chem.* **2021**, *338*, 128026. [CrossRef]
71. Parkar, S.G.; Trower, T.M.; Stevenson, D.E. Fecal microbial metabolism of polyphenols and its effects on human gut microbiota. *Anaerobe* **2013**, *23*, 12–19. [CrossRef] [PubMed]
72. Zhao, D.; Shah, N.P. Lactic acid bacterial fermentation modified phenolic composition in tea extracts and enhanced their antioxidant activity and cellular uptake of phenolic compounds following in vitro digestion. *J. Funct. Foods* **2016**, *20*, 182–194. [CrossRef]
73. Ikawa, M.; Schaper, T.D.; Dollard, C.A.; Sasner, J.J. Utilization of Folin–Ciocalteu phenol reagent for the detection of certain nitrogen compounds. *J. Agric. Food Chem.* **2003**, *51*, 1811–1815. [CrossRef]
74. Everette, J.D.; Bryant, Q.M.; Green, A.M.; Abbey, Y.A.; Wangila, G.W.; Walker, R.B. Thorough study of reactivity of various compound classes toward the Folin–Ciocalteu reagent. *J. Agric. Food Chem.* **2010**, *58*, 8139–8144. [CrossRef]
75. Musundire, R. Bio-active compounds composition in edible stinkbugs consumed in South-Eastern districts of Zimbabwe. *Int. J. Biol.* **2014**, *6*, 36–45. [CrossRef]
76. Musundire, R.; Zvidzai, C.J.; Chidewe, C.; Ngadze, R.T.; Macheka, L.; Manditsera, F.A.; Mubaiwa, J.; Masheka, A. Nutritional and bioactive compounds composition of *Eulepida mashona*, an edible beetle in Zimbabwe. *J. Insects Food Feed* **2016**, *2*, 179–187. [CrossRef]
77. Musundire, R.; Zvidzai, C.J.; Chidewe, C.; Samende, B.K.; Manditsera, F.A. Nutrient and anti-nutrient composition of *Henicus whellani* Orthoptera: Stenopelmatidae, an edible ground cricket, in south-eastern Zimbabwe. *Int. J. Trop. Insect Sci.* **2014**, *34*, 223–231. [CrossRef]
78. Pyo, S.J.; Kang, D.G.; Jung, C.; Sohn, H.Y. Anti-thrombotic, anti-oxidant and haemolysis activities of six edible insect species. *Foods* **2020**, *9*, 401. [CrossRef]
79. Hopkins, T.L.; Ahmad, S.A. Flavonoid wing pigments in grasshoppers. *Experientia* **1991**, *47*, 1089–1091. [CrossRef]
80. Bernays, E.A.; Howard, J.J.; Champagne, D.; Estes, B.J. Rutin: A phagostimulant for the polyphagous acridid *Schistocerca americana*. *Entomol. Exp. Appl.* **1991**, *60*, 19–28. [CrossRef]
81. Hirayama, C.; Ono, H.; Meng, Y.; Shimada, T.; Daimon, T. Flavonoids from the cocoon of *Rondotia menciiana*. *Phytochem* **2013**, *94*, 108–112. [CrossRef] [PubMed]
82. Kurioka, A.; Yamazaki, M. Purification and identification of flavonoids from the yellow green cocoon shell Sasamayu of the silkworm, *Bombyx mori*. *Biosci. Biotechnol. Biochem.* **2002**, *66*, 1396–1399. [CrossRef] [PubMed]
83. Tamura, Y.; Nakajima, K.I.; Nagayasu, K.I.; Takabayashi, C. Flavonoid 5-glucosides from the cocoon shell of the silkworm, *Bombyx mori*. *Phytochemistry* **2002**, *59*, 275–278. [CrossRef]
84. Fu, X.; Chai, C.L.; Li, Y.P.; Li, P.; Luo, S.H.; Li, Q.; Li, M.W.; Liu, Y.Q. Metabolomics reveals abundant flavonoids in edible insect *Antheraea pernyi*. *J. Asia Pac. Entomol.* **2021**, *24*, 711–715. [CrossRef]
85. Wilson, A. Flavonoid pigments in marbled white butterfly *Melanargia galathea* are dependent on flavonoid content of larval diet. *J. Chem. Ecol.* **1985**, *11*, 1161–1179. [CrossRef]
86. Morris, S.J.; Thomson, R.H. The flavonoid pigments of the small heath butterfly, *Coenonympha pamphilus* L. *J. Insect Physiol.* **1964**, *10*, 377–383. [CrossRef]
87. Wilson, A. Flavonoid pigments in chalkhill blue *Lysandra coridon* Poda and other lycaenid butterflies. *J. Chem. Ecol.* **1987**, *13*, 473–493. [CrossRef]
88. Burghardt, F.; Fiedler, K.; Proksch, P. Uptake of flavonoids from *Vicia villosa* Fabaceae by the lycaenid butterfly, *Polyommatus icarus* Lepidoptera: Lycaenidae. *Biochem. Syst. Ecol.* **1997**, *25*, 527–536. [CrossRef]
89. Morris, S.J.; Thomson, R.H. Flavonoid pigments in the marbled white butterfly (*Melanargia Galathea* Seitz). *Tetrahedron Lett.* **1963**, *4*, 101–104. [CrossRef]
90. Vihakas, M.A.; Kapari, L.; Salminen, J.P. New types of flavonol oligoglycosides accumulate in the hemolymph of birch-feeding sawfly larvae. *J. Chem. Ecol.* **2010**, *36*, 864–872. [CrossRef] [PubMed]
91. Vihakas, M.; Tähtinen, P.; Ossipov, V.; Salminen, J.P. Flavonoid metabolites in the hemolymph of European pine sawfly *Neodiprion sertifer* larvae. *J. Chem. Ecol.* **2012**, *38*, 538–546. [CrossRef]
92. Yoon, C.H.; Jeon, S.H.; Ha, Y.J.; Kim, S.W.; Bang, W.Y.; Bang, K.H.; Gal, S.W.; Kim, I.S.; Cho, Y.S. Functional chemical components in *Protaetia brevitarsis* larvae: Impact of supplementary feeds. *Food Sci. Anim. Resour.* **2020**, *40*, 461–473. [CrossRef]
93. EU Regulation 2015/2283 on Novel Foods, Amending Regulation (EU) No 1169/2011 of the European Parliament and the Council and Repealing Regulation (EC) No 258/97 of the European Parliament and the Council and Commission Regulation (EC) No 1852/2001. Available online: <https://eur-lex.europa.eu/legal-content/IT/TXT/?uri=CELEX:32015R2283> (accessed on 3 November 2021).
94. Turck, D.; Bohn, T.; Castenmiller, J.; De Henauw, S.; Hirsch-Ernst, K.I.; Knutsen, H.K. Safety of partially defatted house cricket (*Acheta domesticus*) powder as a novel food pursuant to Regulation (EU) 2015/2283. *EFSA J.* **2022**, *20*, e07258.

95. Turck, D.; Castenmiller, J.; De Henauw, S.; Hirsch-Ernst, K.I.; Kearney, J.; Maciuk, A.; Knutsen, H.K. Safety of dried yellow mealworm (*Tenebrio molitor* larva) as a novel food pursuant to Regulation (EU) 2015/2283. *EFSA J.* **2021**, *19*, e06343.
96. Turck, D.; Castenmiller, J.; De Henauw, S.; Hirsch-Ernst, K.I.; Kearney, J.; Knutsen, H.K. Safety of frozen and dried formulations from migratory locust (*Locusta migratoria*) as a Novel food pursuant to Regulation (EU) 2015/2283. *EFSA J.* **2021**, *19*, e06667.
97. EU Implementing Regulation 2017/2470. Commission Implementing Regulation (EU) 2017/2470 of 20 December 2017 Establishing the Union List of Novel Foods in Accordance with Regulation (EU) 2015/2283 of the European Parliament and the Council on Novel Foods. Available online: [https://eur-lex.europa.eu/eli/reg\\_impl/2017/2470/oj](https://eur-lex.europa.eu/eli/reg_impl/2017/2470/oj) (accessed on 3 November 2021).
98. Tata, A.; Massaro, A.; Marzoli, F.; Miano, B.; Bragolusi, M.; Piro, R.; Belluco, S. Authentication of Edible Insects' Powders by the Combination of DART-HRMS Signatures: The First Application of Ambient Mass Spectrometry to Screening of Novel Food. *Foods* **2022**, *11*, 2264. [[CrossRef](#)]
99. Haber, M.; Mishyna, M.; Itzhak Martinez, J.J.; Benjamin, O. Edible larvae and pupae of honey bee (*Apis mellifera*): Odor and nutritional characterization as a function of diet. *Food Chem.* **2019**, *292*, 197–203. [[CrossRef](#)]
100. Schiel, L.; Wind, C.; Krueger, S.; Braun, P.G.; Koethe, M. Applicability of analytical methods for determining the composition of edible insects in German Food Control. *J. Food Compos. Anal.* **2022**, *112*, 104676. [[CrossRef](#)]
101. Di Mattia, C.; Battista, N.; Sacchetti, G.; Serafini, M. Antioxidant activities in vitro of water and Liposoluble Extracts obtained by different species of edible insects and invertebrates. *Front. Nutr.* **2019**, *6*, 106. [[CrossRef](#)] [[PubMed](#)]
102. Vasconcelos dos Santos, O.; Sodré Dias, P.C.; Dias Soares, S.; Vieira da Conceição, L.R.; Teixeira-Costa, B.E. Artisanal oil obtained from insects' larvae (*Speciomerus ruficornis*): Fatty acids composition, physicochemical, nutritional and antioxidant properties for application in food. *Eur. Food Res. Technol.* **2021**, *247*, 1803–1813. [[CrossRef](#)]
103. Huang, D.; Ou, B.; Prior, R.L. The chemistry behind antioxidant capacity assays. *J. Agric. Food Chem.* **2005**, *53*, 1841–1856. [[CrossRef](#)] [[PubMed](#)]
104. Prior, R.L.; Wu, X.; Schaich, K. Standardized methods for the determination of antioxidant capacity and phenolics in foods and dietary supplements. *J. Agric. Food Chem.* **2005**, *53*, 4290–4302. [[CrossRef](#)] [[PubMed](#)]
105. Giacintucci, V.; Di Mattia, C.; Sacchetti, G.; Neri, L.; Pittia, P. Role of olive oil phenolics in physical properties and stability of mayonnaise-like emulsions. *Food Chem.* **2016**, *213*, 369–377. [[CrossRef](#)]
106. Hall, F.; Johnson, P.E.; Liceaga, A. Effect of enzymatic hydrolysis on bioactive properties and allergenicity of cricket (*Grylodes sigillatus*) protein. *Food Chem.* **2018**, *262*, 39–47. [[CrossRef](#)]
107. Aiello, D.; Giglio, A.; Talarico, F.; Vommaro, M.L.; Tagarelli, A.; Napoli, A. Mass Spectrometry-Based Peptide Profiling of Haemolymph from *Pterostichus melas* Exposed to Pendimethalin Herbicide. *Molecules* **2022**, *27*, 4645. [[CrossRef](#)]
108. Bongiorno, D.; Di Stefano, V.; Indelicato, S.; Avellone, G.; Ceraulo, L. Bio-phenols determination in olive oils: Recent mass spectrometry approaches. *Mass Spectrom. Rev.* **2021**, e21744. [[CrossRef](#)]
109. Indelicato, S.; Bongiorno, D.; Indelicato, S.; Drahos, L.; Turco Liveri, V.; Turiák, L.; Vekey, K.; Ceraulo, L. Degrees of freedom effect on fragmentation in tandem mass spectrometry of singly charged supramolecular aggregates of sodium sulfonates. *J. Mass Spectrom.* **2013**, *48*, 379–383. [[CrossRef](#)]
110. Bongiorno, D.; Indelicato, S.; Giorgi, G.; Scarpella, S.; Liveri, V.T.; Ceraulo, L. Electrospray ion mobility mass spectrometry of positively charged sodium bis(2-ethylhexyl)sulfosuccinate aggregates. *Eur. J. Mass Spectrom.* **2014**, *20*, 169–175. [[CrossRef](#)] [[PubMed](#)]
111. Francesca, N.; Barbera, M.; Martorana, A.; Saiano, F.; Gaglio, R.; Aponte, M.; Moschetti, G.; Settanni, L. Optimised method for the analysis of phenolic compounds from caper (*Capparis spinosa* L.) berries and monitoring of their changes during fermentation. *Food Chem.* **2016**, *196*, 1172–1179. [[CrossRef](#)] [[PubMed](#)]
112. Bongiorno, D.; Ceraulo, L.; Indelicato, S.; Turco Liveri, V.; Indelicato, S. Charged supramolecular assemblies of surfactant molecules in gas phase. *Mass Spectrom. Rev.* **2016**, *35*, 170–187. [[CrossRef](#)] [[PubMed](#)]
113. Di Donna, L.; Bartella, L.; De Vero, L.; Gullo, M.; Giuffrè, A.M.; Zappia, C.; Capocasale, M.; Poiana, M.; D'Urso, S. Vinegar production from Citrus bergamia by-products and preservation of bioactive compounds. *Eur. Food Res. Technol.* **2020**, *246*, 1981–1990. [[CrossRef](#)]
114. Mazzotti, F.; Bartella, L.; Talarico, I.R.; Napoli, A.; Di Donna, L. High-throughput determination of flavanone-O-glycosides in citrus beverages by paper spray tandem mass spectrometry. *Food Chem.* **2021**, *360*, 130060. [[CrossRef](#)]
115. Bartella, L.; Mazzotti, F.; Talarico, I.R.; De Luca, G.; Santoro, I.; Prejanò, M.; Riccioni, C.; Marino, T.; Di Donna, L. Structural Characterization of Peripolin and Study of Antioxidant Activity of HMG Flavonoids from Bergamot Fruit. *Antioxidants* **2022**, *11*, 1847. [[CrossRef](#)]
116. Argo, A.; Bongiorno, D.; Bonifacio, A.; Pernice, V.; Liotta, R.; Indelicato, S.; Zerbo, S.; Fleres, P.; Ceraulo, L.; Procaccianti, P. A fatal case of a paint thinner ingestion: Comparison between toxicological and histological findings. *Am. J. Forensic Med. Pathol.* **2010**, *31*, 186–191. [[CrossRef](#)]
117. Pérez-Trujillo, M.; Gómez-Caravaca, A.M.; Segura-Carretero, A.; Fernández-Gutiérrez, A.; Parella, T. Separation and identification of phenolic compounds of extra virgin olive oil from *Olea europaea* L. by HPLC-DAD-SPE-NMR/MS. Identification of a new diastereoisomer of the aldehydic form of oleuropein aglycone. *J. Agric. Food Chem.* **2010**, *58*, 9129–9136. [[CrossRef](#)]
118. Castiglione, F.; Appetecchi, G.B.; Passerini, S.; Panzeri, W.; Indelicato, S.; Mele, A. Multiple points of view of heteronuclear NOE: Long range vs short range contacts in pyrrolidinium based ionic liquids in the presence of Li salts. *J. Mol. Liq.* **2015**, *210*, 215–222. [[CrossRef](#)]

119. Domínguez-Rodríguez, G.; Marina, M.L.; Plaza, M. Strategies for the extraction and analysis of non-extractable polyphenols from plants. *J. Chromatogr. A* **2017**, *1514*, 1–15. [[CrossRef](#)]
120. Sugiki, T.; Furuita, K.; Fujiwara, T.; Kojima, C. Current NMR techniques for structure-based drug discovery. *Molecules* **2018**, *23*, 148. [[CrossRef](#)] [[PubMed](#)]
121. Yan, Y.M.; Zhu, H.J.; Zhou, F.J.; Tu, Z.C.; Cheng, Y.X. Phenolic compounds from the insect *Blaps japonensis* with inhibitory activities towards cancer cells, COX-2, ROCK1 and JAK3. *Tetrahedron* **2019**, *75*, 1029–1033. [[CrossRef](#)]
122. Harborne, J.B. Flavonoid pigments. In *Herbivores: Their Interactions with Secondary Plant Metabolites*, 2nd ed.; Rosenthal, G.A., Berenbaum, M.R., Eds.; Academic Press: San Diego, CA, USA, 1991; pp. 389–429.
123. Schittko, U.; Burghardt, F.; Fiedler, K.; Wray, V.; Proksch, P. Sequestration and distribution of flavonoids in the common blue butterfly *Polyommatus icarus* reared on *Trifolium repens*. *Phytochemistry* **1999**, *51*, 609–614. [[CrossRef](#)]
124. Salminen, J.P.; Lempa, K. Effects of hydrolysable tannins on a herbivorous insect: Fate of individual tannins in insect digestive tract. *Chemecology* **2002**, *12*, 203–211. [[CrossRef](#)]
125. Ferreres, F.; Fernandes, F.; Oliveira, J.M.; Valentão, P.; Pereira, J.A.; Andrade, P.B. Metabolic profiling and biological capacity of *Pieris brassicae* fed with kale (*Brassica oleracea* L. var. acephala). *Food Chem. Toxicol.* **2009**, *47*, 1209–1220. [[CrossRef](#)] [[PubMed](#)]
126. Burghardt, F.; Proksch, P.; Fiedler, K. Flavonoid sequestration by the common blue butterfly *Polyommatus icarus*: Quantitative intraspecific variation in relation to larval hostplant, sex and body size. *Biochem. Syst. Ecol.* **2001**, *29*, 875–889. [[CrossRef](#)]
127. Sang, S.; Lapsley, K.; Jeong, W.-S.; Lachance, P.A.; Ho, C.T.; Rosen, R.T. Antioxidative phenolic compounds isolated from almond skins (*Prunus amygdalus* Batsch). *J. Agric. Food Chem.* **2002**, *50*, 2459–2463. [[CrossRef](#)]
128. Shahidi, F.; Ambigaipalan, P. Phenolics and polyphenolics in foods, beverages and spices: Antioxidant activity and health effects—A review. *J. Funct. Foods* **2015**, *18*, 820–897. [[CrossRef](#)]
129. Ghosh, A.; Ray, M.; Gangopadhyay, D. Evaluation of proximate composition and antioxidant properties in silk-industrial byproduct. *Food Sci. Technol.* **2020**, *132*, 109900. [[CrossRef](#)]
130. Wannee, S.; Luchai, B. 1-Deoxynojirimycin and polyphenolic composition and antioxidant activity of different native Thai silkworm (*Bombyx mori*) larvae. *J. King Saud Univ. Sci.* **2020**, *32*, 2762–2766. [[CrossRef](#)]
131. Deori, M.; Boruah, D.C.; Devi, D.; Devi, R. Antioxidant and antigenotoxic effects of pupae of the MUGA silkworm *Antheraea assamensis*. *Food Biosci.* **2014**, *5*, 108–114. [[CrossRef](#)]
132. Sugumaran, M. Chemistry of cuticular sclerotization. *Adv. Insect Physiol.* **2010**, *39*, 151–209.
133. Whitten, M.M.A.; Coates, C.J. Re-evaluation of insect melanogenesis research: Views from the dark side. *Pigment Cell Melanoma Res.* **2017**, *30*, 386–401. [[CrossRef](#)] [[PubMed](#)]
134. Söderhäll, K. Prophenoloxidase activating system and melanization—A recognition mechanism of arthropods? A review. *Dev. Comp. Immunol.* **1982**, *6*, 601–611. [[PubMed](#)]
135. Cerenius, L.; Söderhäll, K. Immune properties of invertebrate phenoloxidases. *Dev. Comp. Immunol.* **2021**, *122*, 104098. [[CrossRef](#)]
136. Bell, K.; Smith, V.J. In vitro superoxide production by hyaline cells of the shore crab *Carcinus maenas* (L.). *Dev. Comp. Immunol.* **1993**, *17*, 211–219. [[CrossRef](#)]
137. Anderson, R.S. Hemocyte-derived reactive oxygen intermediate production in four bivalve mollusks. *Dev. Comp. Immunol.* **1994**, *18*, 89–96. [[CrossRef](#)]
138. Valembois, P.; Lassègues, M. In vitro generation of reactive oxygen species by free coelomic cells of the annelid *Eisenia fetida andrei*: An analysis by chemiluminescence and nitro blue tetrazolium reduction. *Dev. Comp. Immunol.* **1995**, *19*, 195–204. [[CrossRef](#)]
139. Riley, P.A. Radicals in melanin biochemistry. *Ann. N. Y. Acad. Sci.* **1988**, *551*, 111–119. [[CrossRef](#)]
140. Salvatore, L.; Gallo, N.; Aiello, D.; Lunetti, P.; Barca, A.; Blasi, L.; Madaghiele, M.; Bettini, S.; Giancane, G.; Hasan, M.; et al. An Insight on Type I Collagen from Horse Tendon for the Manufacture of Implantable Devices. *Int. J. Biol. Macromol.* **2020**, *154*, 291–306. [[CrossRef](#)]
141. O'Brien, P.J. Molecular mechanisms of quinone cytotoxicity. *Chem. Biol. Interact.* **1991**, *80*, 1–41. [[CrossRef](#)] [[PubMed](#)]
142. Smit, N.P.M.; Peters, K.; Menko, W.; Westerhof, W.; Pavel, S.; Riley, P.A. Cytotoxicity of a selected series of substituted phenols towards cultured melanoma cells. *Melanoma Res.* **1996**, *2*, 295–304. [[CrossRef](#)] [[PubMed](#)]
143. Nappi, A.J.; Vass, E. Melanogenesis and the generation of cytotoxic molecules during insect cellular immune reactions. *Pigment Cell Res.* **1993**, *6*, 117–126. [[CrossRef](#)] [[PubMed](#)]
144. Cotelle, N.; Moreau, S.; Cotelle, P.; Catteau, J.P.; Bernier, J.L.; Henicart, J.P. Generation of free radicals by simple prenylated hydroquinone derivativs, natural antitumor agents from the marine urochordate *Aplidium californicum*. *Chem. Res. Toxicol.* **1991**, *4*, 300–305. [[CrossRef](#)] [[PubMed](#)]

**Disclaimer/Publisher's Note:** The statements, opinions and data contained in all publications are solely those of the individual author(s) and contributor(s) and not of MDPI and/or the editor(s). MDPI and/or the editor(s) disclaim responsibility for any injury to people or property resulting from any ideas, methods, instructions or products referred to in the content.

Article

# Grain Germination Changes the Profile of Phenolic Compounds and Benzoxazinoids in Wheat: A Study on Hard and Soft Cultivars

Julia Baranzelli <sup>1</sup>, Sabrina Somacal <sup>1</sup>, Camila Sant'Anna Monteiro <sup>1</sup>, Renius de Oliveira Mello <sup>1</sup>, Eliseu Rodrigues <sup>2</sup>, Osmar Damian Prestes <sup>3</sup>, Rosalía López-Ruiz <sup>4</sup>, Antonia Garrido Frenich <sup>4</sup>, Roberto Romero-González <sup>4</sup>, Martha Zavariz de Miranda <sup>5</sup> and Tatiana Emanuelli <sup>1,\*</sup>

<sup>1</sup> Department of Food Technology and Science, Center of Rural Sciences, Federal University of Santa Maria, Santa Maria 97105-900, Rio Grande do Sul, Brazil

<sup>2</sup> Department of Food Science, Federal University of Rio Grande do Sul, Porto Alegre 91501-970, Rio Grande do Sul, Brazil

<sup>3</sup> Department of Chemistry, Center of Natural and Exact Sciences, Federal University of Santa Maria, Santa Maria 97105-900, Rio Grande do Sul, Brazil

<sup>4</sup> Research Group 'Analytical Chemistry of Contaminants', Department of Chemistry and Physics, Research Center for Mediterranean Intensive Agrosystems and Agri-Food Biotechnology (CIAIMBITAL), University of Almeria, 04120 Almeria, Spain

<sup>5</sup> Grain Quality Laboratory, Brazilian Agricultural Research Corporation-Embrapa Trigo, Passo Fundo 99050-970, Rio Grande do Sul, Brazil

\* Correspondence: tatiana.emanuelli@ufsm.br

**Citation:** Baranzelli, J.; Somacal, S.; Monteiro, C.S.; Mello, R.d.O.; Rodrigues, E.; Prestes, O.D.; López-Ruiz, R.; Garrido Frenich, A.; Romero-González, R.; Miranda, M.Z.d.; et al. Grain Germination Changes the Profile of Phenolic Compounds and Benzoxazinoids in Wheat: A Study on Hard and Soft Cultivars. *Molecules* **2023**, *28*, 721. <https://doi.org/10.3390/molecules28020721>

Academic Editor: Nour Eddine Es-Safi

Received: 13 December 2022

Revised: 4 January 2023

Accepted: 7 January 2023

Published: 11 January 2023



**Copyright:** © 2023 by the authors. Licensee MDPI, Basel, Switzerland. This article is an open access article distributed under the terms and conditions of the Creative Commons Attribution (CC BY) license (<https://creativecommons.org/licenses/by/4.0/>).

**Abstract:** Pre-harvest sprouting is a frequent problem for wheat culture that can be simulated by laboratory-based germination. Despite reducing baking properties, wheat sprouting has been shown to increase the bioavailability of some nutrients. It was investigated whether wheat cultivars bearing distinct grain texture characteristics (BRS Guaraim, soft vs. BRS Marcante, hard texture) would have different behavior in terms of the changes in phytochemical compounds during germination. Using LC-Q-TOF-MS, higher contents of benzoxazinoids and flavonoids were found in the hard cultivar than in the soft one. Free phytochemicals, mainly benzoxazinoids, increased during germination in both cultivars. Before germination, soft and hard cultivars had a similar profile of matrix-bound phytochemicals, but during germination, these compounds have been shown to decrease only in the hard-texture cultivar, due to decreased levels of phenolic acids (*trans*-ferulic acid) and flavonoids (apigenin) that were bound to the cell wall through ester-type bonds. These findings confirm the hypothesis that hard and soft wheat cultivars have distinct behavior during germination concerning the changes in phytochemical compounds, namely the matrix-bound compounds. In addition, germination has been shown to remarkably increase the content of benzoxazinoids and the antioxidant capacity, which could bring a health-beneficial appeal for pre-harvested sprouted grains.

**Keywords:** cereal; pre-harvest sprouting; bioactive compounds

## 1. Introduction

Wheat (*Triticum aestivum* L.) is among the most-produced cereals in the world. Wheat production is affected by climate changes [1]. Under conditions of high humidity and temperature, cereal crops suffer a process of natural germination before harvest. This process, which is known as pre-harvest sprouting, reduces grain quality and generates economic losses worldwide [1]. Sprouted wheat is usually discarded due to the loss of its baking properties [2–4] or it can be destined for uses other than baking [5,6], such as for feed or industrial uses (production of starch, vital gluten, furfural, ethanol, etc.).

In contrast, grain germination has been also used as a natural method of biological processing to improve the nutritional, functional and sensory properties of grains along

with increasing micronutrient content [7]. Grain germination can increase the content of health-beneficial phytochemicals, such as phenolic compounds [8,9] and benzoxazinoids [10]. Phenolic compounds have antioxidant, antidiabetic and antitumor properties, and have been shown to prevent cardiovascular diseases [11]. Benzoxazinoids exhibit antimicrobial properties, act as central nervous system stimulators, immunoregulators, appetite inhibitors and body weight reducers [10].

Phenolic compounds are found in the form of glycosides linked to different sugar fractions, or in other forms linked to organic acids, amines, lipids, carbohydrates and other phenols, mainly phenolic acids [12]. Cereal phenolic acids occur in free (~25%) or bound (~75%) forms [13], being linked through ester or ether bonds to cell wall polysaccharides [14].

Benzoxazinoids are a class of natural products that are widely distributed in cereals, being concentrated in the cover layer of grains (pericarp) [15]. They can be divided into three groups, namely hydroxamic acids, lactams and benzoxazolinones [16], and have been shown to be increased during the germination of some cereal grains [17], but their behavior during wheat germination remains unknown.

The phytochemical compounds found in the free state are easily extracted with conventional organic solvents [18], whereas those linked to sugars and proteins, or cell wall structures, require very hard conditions for their extraction, such as acid or alkaline hydrolysis [19,20]. Grain germination is a physiological process that can trigger both the hydrolysis of matrix-bound phytochemical compounds and the formation of new compounds [3,21,22].

Therefore, wheat that is naturally germinated before harvest could have a higher content of phytochemical compounds, which would improve its functional quality and, thus, add value to this product. In fact, germination can increase the bioavailability of nutrients, such as vitamins, bioelements and other biologically active substances, due to the partial hydrolysis of starch, proteins, hemicelluloses and celluloses. In this process, hydrolytic enzymes are activated (endohydrolase such as  $\alpha$  and  $\beta$ -amylases, proteases, diphenoloxidase and catalase) that break down starch, fibers and proteins, and lead to an increase in the number of digestible compounds along with an improvement in functional properties [23]. Laboratory-based germination that simulates field humidity and temperature conditions can be used as a model to study the influence of pre-harvest sprouting on wheat grain properties [2,5,6].

Another important property beneficial to health is the antioxidant capacity of cereals. Antioxidant compounds protect cells against oxidative stress caused by reactive species [23]. The main compounds responsible for such effects in cereals are vitamins, sterols, and phenolic compounds. They all contribute to some extent to the antioxidant properties and are affected in different ways by germination. Phenolic acids have potential antioxidant properties due to the presence of an aromatic phenolic ring. Its antioxidant properties are explained by the donation of electrons and the transfer of the hydrogen atom to free radicals. They act as free radical scavengers, reducing agents and inhibitors of singlet oxygen formation. Benzoxazinoids also exhibit antioxidant properties that are related to the presence of a hydroxyl group attached to the heterocyclic nitrogen atom, mainly in hydroxamic acids [24].

Wheat cultivars exhibit physiological differences and can be classified according to the grain hardness (method 55-31.01, AACCI, [25]). Wheat grains cultivated in Brazil are similar to the hard red spring wheat from the United States, but wheat production occurs only in the winter. BRS Marcante is a Brazilian wheat cultivar that has hard texture and exhibits high values of grain hardness index (GHI > 67), gluten strength ( $W > 275 \times 10^{-4}$  J) [26], dough development time (DDT > 21.5 min) and stability (>30.2 min) [2], being indicated mainly to produce different kinds of bread and pasta. In contrast, BRS Guaraim has much lower values for these markers, exhibiting a soft grain texture (GHI < 46),  $W (< 206 \times 10^{-4}$  J) and DDT (<4.1 min) [27] and is more suitable for cake and cookie production.

The hypothesis of this study is that wheat cultivars bearing distinct wheat grain texture characteristics would have different behavior in terms of the changes in phytochemical

compounds during germination. In this sense, the objective of this study was to investigate the effect of germination on the profile of phytochemical compounds and antioxidant capacity of Brazilian wheat cultivars that have soft or hard grain texture.

## 2. Results and Discussion

### 2.1. Grain Characteristics, Alveography and Germination Follow-Up in Wheat Cultivars

The wheat cultivars selected for the study have different technological characteristics. BRS Marcante cultivar presents higher values for grain texture (GHI), GFN, hectoliter weight and thousand kernel weight compared to BRS Guaraim (111%, 62%, 8% and 12% higher, respectively; Supplementary materials, Table S1). Additionally, the alveograph data were also higher for BRS Marcante cultivar, as observed for gluten strength, tenacity and tenacity/extensibility ratio parameters (164%, 101% and 49% higher, respectively; Supplementary materials, Table S1), in relation to BRS Guaraim cultivar.

Grain hardness is the single most important trait in determining technological properties and end-use quality of wheat products. Hard-textured wheats have more glutenins, whereas soft-textured wheats have more gliadins [28]. The greater content of glutenins leads to increased gluten strength, elasticity and extensibility of the dough.

The germination process conditions used in this study resulted in small sprouts at 24 h (Supplementary materials, Table S2). From 48 h onwards, the grains began to emit small rootlets that became larger at 72 h, but the emergence of the seedling did not occur (Supplementary materials, Table S2). Germination is characterized by the activation of enzymes, including  $\alpha$ -amylase, which is responsible for the degradation of starch into sugars that provide energy for the embryo's growth [29]. GFN was assessed to characterize changes in amylase activity during wheat germination (Table 1). Before germination, GFN was higher for BRS Marcante than BRS Guaraim ( $p < 0.05$ ; Table 1), indicating lower amylase activity for BRS Marcante.

**Table 1.** Germination follow-up through grain falling number values (GFN, expressed in seconds) of wheat cultivars from soft (BRS Guaraim) and hard (BRS Marcante) texture.

Germination Time	BRS Guaraim	BRS Marcante	Time Mean
0 h	352 ± 12 <sup>aB</sup>	389 ± 6 <sup>aA</sup>	370 ± 8
24 h	216 ± 7 <sup>bA</sup>	162 ± 7 <sup>bB</sup>	189 ± 9
48 h	96 ± 5 <sup>cA</sup>	69 ± 2 <sup>cB</sup>	82 ± 4
72 h	62 ± 0 <sup>dA</sup>	62 ± 0 <sup>cA</sup>	62 ± 0
Cultivar mean	181 ± 21	171 ± 24	

Means ± standard error of mean were reported (n = 6). Values that have no common superscript letter are significantly different ( $p < 0.05$ ) within the same row (uppercase letters) or within the same column (lowercase letter).

As expected, the germination process decreased GFN, indicating increased amylolytic activity, which reduces starch content and gelatinization capacity [30]. The increase in amylolytic activity was faster for BRS Marcante than BRS Guaraim, as indicated by the lower GFN values at 24 and 48 h ( $p < 0.05$ ; Table 1). The increase in grain moisture during germination causes a gradual decrease in the falling number and in the grain hardness index [31]. This causes the texture of the durum wheat grain to become softer after germination, possibly due to a decrease in the starch crystallinity [32]. This alteration facilitates the enzymatic attack and decrease of GFN with the advance of germination.

### 2.2. Tentative Identification of Phytochemical Compounds

Thirty-two phytochemical compounds, comprising amino acids, phenolic acids, flavonoids and benzoxazinoids, were identified in BRS Marcante and BRS Guaraim wheat cultivars based on the data provided by LC-Orbitrap-MS and LC-Q-TOF-MS analysis (Supplementary materials, Figure S1 and Table S3). Eighteen compounds were in the free state, whereas fourteen compounds were extracted only after alkaline hydrolysis (eight compounds), indicating that they were linked to the cell wall or simple sugars



through ester-type bonds, or after acid hydrolysis (six compounds), indicating that they were linked to polysaccharides through ether-type glycosidic bonds [14]. Previous studies have already reported the presence of phenolic compounds and flavonoids [33–36], amino acids [37] and benzoxazinoids [36,38,39] in wheat.

The greatest diversity of compounds was identified in the free phytochemical fraction. Amino acids were identified in LC-Q-TOF-MS analysis in the positive ionization mode. Phenylalanine (RT 6.3 min) showed a protonated MS spectrum  $[M + H]^+$  at  $m/z$  166 and  $MS^2$  fragments at  $m/z$  120 and 103. The main fragmentation pathway of phenylalanine starts from the loss of  $H_2O + CO$  to form a fragment ion at  $m/z$  120.0851, and a fragment ion at  $m/z$  103.0590 was formed by the additional loss of  $NH_3$ . Tryptophan showed a protonated MS spectrum  $[M + H]^+$  at  $m/z$  205 and  $MS^2$  fragments at  $m/z$  118, 143, 146, 144 and 115. The fragmentation product  $m/z$  146.0636 was obtained after the loss of  $NH_3$  and  $CH_2CO$ . This fragment further dissociated to form the fragmented ion at  $m/z$  118.0717 after the loss of  $CO$ . The fragment at  $m/z$  144.0827 was formed after the loss of  $NH_3$  and  $CO_2$ , and the dissociation of  $\bullet H$  forms the fragment  $m/z$  143.0776. The fragmented ion at  $m/z$  115.0588 was formed after the sequential losses of  $NH_3$ ,  $H_2O$ ,  $CO$  and  $HCN$ . In addition, amino acids showed MS spectrum and  $MS^2$  fragmentation patterns similar to previously reported data [37].

Among benzoxazinoids, two compounds that belong to the hydroxamic acids subclass were identified, namely DIBOA-hex-hex and DIMBOA-hex-hex. At 17.2 min, the compound was tentatively identified as DIBOA-hex-hex (MW = 505). In the negative ionization mode, the MS spectrum showed the deprotonated molecule  $[M-H]^-$  at  $m/z$  504 and  $MS^2$  fragment at  $m/z$  162  $[M-H-342]^-$ , corresponding to the loss of two hexose molecules ( $C_{12}H_{22}O_{11}$ ), and at  $m/z$  134  $[M-H-370]^-$ , corresponding to the sequential loss of  $CO$ . At 24.3 min, the compound was tentatively identified as DIMBOA-hex-hex (MW = 535). In the negative ionization mode, the MS spectrum showed the deprotonated molecule  $[M-H]^-$  at  $m/z$  534 and  $MS^2$  fragment at  $m/z$  192  $[M-H-342]^-$ , corresponding to the loss of two hexose molecules, at  $m/z$  164  $[M-H-370]^-$ , corresponding to the sequential loss of  $CO$ , and at  $m/z$  149  $[M-H-385]^-$ , corresponding to the sequential loss of  $\bullet CH_3$ . In addition, benzoxazinoids exhibited MS spectrum and  $MS^2$  fragmentation patterns similar to previously reported data [36,39].

Phenolic acids and some flavonoids from the free fraction were identified by comparison with standards and confirmed using LC-Orbitrap-MS. Four apigenin derivatives were identified using LC-Q-TOF-MS in the negative ionization mode. Compounds eluted at 38.5 and 42.8 min were identified as apigenin-hex-pent I e II (MW = 564). The MS spectrum showed the deprotonated molecule  $[M-H]^-$  at  $m/z$  563 and fragment in  $MS^2$  at  $m/z$  443  $[M-H-120]^-$ , corresponding to the loss of  $C_4H_8O_4$ , at  $m/z$  353  $[M-H-210]^-$ , corresponding to the loss of  $C_7H_{14}O_7$ , and at  $m/z$  383  $[M-H-90]^-$ , corresponding to the loss of  $C_8H_{14}O_6$ . Moreover, the MS spectrum and  $MS^2$  fragmentation patterns were similar to previously reported data [40]. The compounds eluted at 52.4 and 53.1 min were identified as apigenin-hex-hex-hex I e II (MW = 770). In the negative ionization mode, the MS spectrum showed the deprotonated molecule  $[M-H]^-$  at  $m/z$  769 and fragment in  $MS^2$  at  $m/z$  425  $[M-H-344]^-$ , corresponding to the loss of a molecule of  $C_6H_{10}O_7$  (194) and a molecule of  $C_5H_{10}O_5$  (150), and the dissociation of  $\bullet H$  forms the fragment  $m/z$  426.0868. At  $m/z$  545  $[M-H-224]^-$ , corresponding to the loss of  $C_9H_{12}O_3$  (168) and two molecules of  $CO$  (56), the dissociation of  $\bullet H$  forms the fragment  $m/z$  546.1238. Moreover, MS spectrum and  $MS^2$  fragmentation patterns were similar to previously reported data for apigenin-hex-hex-hex [41,42].

The fraction of phytochemicals extracted through alkaline and acid hydrolysis, which comprises matrix-bound compounds, showed less diversity compared to the free fraction, being composed mainly of phenolic acids and a flavonoid. All compounds were identified by comparison to an authentic standard using LC-Orbitrap-MS analysis. The presence of p-coumaric acid, *trans* and *cis*-ferulic acid were also confirmed using LC-Q-TOF-MS analysis.

The compound eluted at 27.8 min was tentatively identified as *p*-coumaric acid (MW = 164). In the negative ionization mode, the MS spectrum showed the deprotonated molecule  $[M-H]^-$  at  $m/z$  163 and fragment in  $MS^2$  at  $m/z$  119  $[M-H-44]^-$ , corresponding to the loss of  $CO_2$ . Moreover, the MS spectrum and  $MS^2$  fragmentation patterns were similar to previously reported data for *p*-coumaric acid [36].

The compounds eluted at 35.7 and 36.7 min were tentatively identified as *trans* and *cis*-ferulic acid (MW = 194). In the negative ionization mode, the MS spectrum showed the deprotonated molecule  $[M-H]^-$  at  $m/z$  193. Ferulic acid produces a typical negative fragment in  $MS^2$  at  $m/z$  133  $[M-H-60]^-$  from demethylation and decarboxylation, corresponding to the loss of  $C_2H_4O_2$ , and the dissociation of  $\bullet H$  forms the fragment  $m/z$  134.0368 [36].

Some peaks could not be identified, but one of them, which was the most abundant in the extract obtained after acid hydrolysis (Figure S1c), had MS characteristics that are not compatible with phenolic or benzoxazinoid compounds.

### 2.3. Changes in the Phytochemical Profile of Wheat during Germination

The phytochemical profiles of BRS Guaraim and BRS Marcante across 72 h of germination are shown in Tables 2 and 3. Before germination, most phytochemicals of BRS Guaraim and BRS Marcante cultivars were bound to the grain matrix (64% released by alkaline hydrolysis and 8% released by acid hydrolysis), being composed mainly of phenolic acids, followed by flavonoids (Table 3). *Trans*-Ferulic acid was the major single compound found in the wheat grains (46–48% of the total phytochemicals) before germination followed by *p*-coumaric acid (9–12% of total phytochemicals), as previously reported [22,43,44]. The fraction of free phytochemicals amounted to 28% of total phytochemicals from wheat, and was mainly composed of flavonoids, followed by benzoxazinoids and a minor content of phenolic acids (Table 2). Flavonoids mainly occur in C-glycoside forms [42], and glycosylated apigenins were the main flavonoid structures found (Tables 2 and 3). Benzoxazinoids amounted to almost 10% of free phytochemicals and DIBOA-hex-hex was the predominant form of benzoxazinoids in the wheat (Table 2), as previously reported [45,46].

**Table 2.** Changes in free phytochemical compounds (mg·100 g<sup>-1</sup> whole wheat flour d.b.) of wheat grains according to the germination time (G) and cultivar (C).

Cultivar (C)	Germination Time (G)				Mean	<i>p</i> -Value			
	0 h	24 h	48 h	72 h		C	G	C × G	
	Vanillic acid						0.1977	0.0233	0.0035
BRS Guaraim	0.18 <sup>Aa</sup>	0.00 <sup>b</sup>	0.00 <sup>b</sup>	0.00 <sup>b</sup>	0.04				
BRS Marcante	0.00 <sup>B</sup>	0.00	0.00	0.06	0.02				
Mean	0.09	0.00	0.00	0.03			SEM =	0.01330	
	DIBOA-hex-hex *						0.0006	0.0001	0.7841
BRS Guaraim	1.39	1.50	4.09	10.28	4.31 <sup>B</sup>				
BRS Marcante	3.97	3.97	8.66	14.63	7.81 <sup>A</sup>				
Mean	2.68 <sup>c</sup>	2.73 <sup>c</sup>	6.37 <sup>b</sup>	12.45 <sup>a</sup>			SEM =	0.79561	
	DIMBOA-hex-hex *						0.7277	0.0001	0.8312
BRS Guaraim	0.69	0.54	3.64	7.61	3.12				
BRS Marcante	0.79	0.95	2.75	7.23	2.93				
Mean	0.74 <sup>c</sup>	0.74 <sup>c</sup>	3.19 <sup>b</sup>	7.42 <sup>a</sup>			SEM =	0.47198	
	Apigenin-hex-pent I <sup>#</sup>						0.048	0.0159	0.0414

Table 2. Cont.

Cultivar (C)	Germination Time (G)				Mean	p-Value		
	0 h	24 h	48 h	72 h		C	G	C × G
BRS Guaraim	4.05 <sup>a</sup>	2.29 <sup>Bb</sup>	4.06 <sup>a</sup>	4.62 <sup>a</sup>	3.75			
BRS Marcante	4.16	4.25 <sup>A</sup>	4.38	4.47	4.31			
Mean	4.10	3.27	4.22	4.54		0.0001	SEM = 0.8075	0.16399
		Sinapic acid						0.9454
BRS Guaraim	0.50	0.49	0.52	0.47	0.49 <sup>B</sup>			
BRS Marcante	0.92	0.93	0.89	0.85	0.89 <sup>A</sup>			
Mean	0.71	0.71	0.70	0.66		0.0001	SEM = 0.937	0.03594
		Apigenin-hex-pent II <sup>#</sup>						0.3065
BRS Guaraim	6.27	6.49	6.37	6.79	6.48 <sup>B</sup>			
BRS Marcante	7.77	7.75	7.63	7.43	7.65 <sup>A</sup>			
Mean	7.02	7.12	7.00	7.11		0.0001	SEM = 0.0347	0.11631
		Apigenin-hex-hex-hex I <sup>#</sup>						0.5372
BRS Guaraim	4.11	4.22	4.75	4.49	4.39 <sup>B</sup>			
BRS Marcante	5.14	5.19	5.38	5.23	5.23 <sup>A</sup>			
Mean	4.62 <sup>b</sup>	4.70 <sup>ab</sup>	5.06 <sup>a</sup>	4.86 <sup>ab</sup>		0.0001	SEM = 0.101	0.08466
		Apigenin-hex-hex-hex II <sup>#</sup>						0.2309
BRS Guaraim	5.20	5.53	5.44	6.48	5.66 <sup>B</sup>			
BRS Marcante	8.38	8.60	8.92	8.70	8.65 <sup>A</sup>			
Mean	6.79	7.06	7.18	7.59		0.8968	SEM = 0.0001	0.25354
		Apigenin <sup>#</sup>						0.9937
BRS Guaraim	3.89	3.99	1.94	3.83	3.41			
BRS Marcante	3.91	3.83	1.92	3.86	3.38			
Mean	3.90 <sup>a</sup>	3.91 <sup>a</sup>	1.93 <sup>b</sup>	3.84 <sup>a</sup>		0.0001	SEM = 0.3897	0.18772
		Sum of free phenolic acids						0.4308
BRS Guaraim	0.68	0.49	0.52	0.47	0.54 <sup>B</sup>			
BRS Marcante	0.92	0.93	0.89	0.91	0.91 <sup>A</sup>			
Mean	0.8	0.71	0.7	0.69		0.022	SEM = 0.0001	0.03671
		Sum of free benzoxazinoids						0.9849
BRS Guaraim	2.08	2.03	7.72	17.88	7.43 <sup>B</sup>			
BRS Marcante	4.76	4.92	11.41	21.86	10.74 <sup>A</sup>			
Mean	3.42 <sup>c</sup>	3.48 <sup>c</sup>	9.56 <sup>b</sup>	19.87 <sup>a</sup>		0.0001	SEM = 0.0368	1.22276
		Sum of free flavonoids						0.2241
BRS Guaraim	23.5	22.5	22.6	26.2	23.7 <sup>B</sup>			
BRS Marcante	29.4	29.6	28.2	29.7	29.2 <sup>A</sup>			
Mean	26.4 <sup>ab</sup>	26.1 <sup>ab</sup>	25.4 <sup>b</sup>	27.9 <sup>a</sup>		0.0001	SEM = 0.0001	0.53165
		Sum of free phytochemical compounds						0.9583
BRS Guaraim	26.3	25.0	30.8	44.5	31.7 <sup>B</sup>			
BRS Marcante	35.0	35.5	40.5	52.4	40.9 <sup>A</sup>			
Mean	30.7 <sup>c</sup>	30.2 <sup>c</sup>	35.7 <sup>b</sup>	48.5 <sup>a</sup>			SEM = 1.55007	

Means (n = 6) followed by different capital letters within the same column and different small letters within the same row differ ( $p < 0.05$ ), respectively, between cultivars and germination times using the Student–Newman–Keuls test. \* Benzoxazinoids were quantified as equivalent to 2H-1,4-benzoxazin-3(H)-one; # Flavonoids were quantified as equivalent to quercetin. DIBOA: 2,4-dihydroxy-1,4-benzoxazin-3-one; DIMBOA: Dihydroxy-7-methoxy-1,4-benzoxazin-3-one; hex: hexoside; pent: pentoside; LoQ: limit of quantification; SEM: standard error of mean. Vanillic acid LoQ: 0.025 ppm; 2H-1,4-benzoxazin-3(H)-one LoQ: 0.106 ppm; Quercetin LoQ: 0.444 ppm; Sinapic acid LoQ: 0.258 ppm.

**Table 3.** Changes in bound phytochemical compounds (mg·100 g<sup>-1</sup> whole wheat flour d.b.) of wheat grains according to the germination time (G) and cultivar (C).

Cultivar (C)	Germination Time (G)				Mean	<i>p</i> -Value		
	0 h	24 h	48 h	72 h		C	G	C × G
Bound phytochemical compounds—Alkaline hydrolysis								
4-Hydroxybenzoic acid								
BRS Guaraim	0.27	0.61	1.03 <sup>B</sup>	1.64 <sup>A</sup>	0.89	0.489	0.0008	0.003
BRS Marcante	0.00 <sup>b</sup>	0.00 <sup>b</sup>	2.71 <sup>Aa</sup>	0.00 <sup>Bb</sup>	0.68			
Mean	0.14	0.30	1.87	0.82				
Vanillic acid								
BRS Guaraim	0.00 <sup>b</sup>	0.00 <sup>b</sup>	0.09 <sup>Aa</sup>	0.00 <sup>b</sup>	0.02	0.029	SEM =	0.19072
BRS Marcante	0.00	0.00	0.00 <sup>B</sup>	0.00	0.00			
Mean	0.00	0.00	0.05	0.00				
<i>p</i> -Coumaric acid								
BRS Guaraim	2.85	2.97	3.03	2.76	2.90	0.317	SEM =	0.00673
BRS Marcante	3.24	2.93	3.04	2.78	3.00			
Mean	3.04	2.95	3.04	2.77				
<i>trans</i> -Ferulic acid								
BRS Guaraim	44.2	45.7	50.9 <sup>A</sup>	43.9	46.2	0.61	SEM =	0.2318
BRS Marcante	56.5 <sup>a</sup>	50.8 <sup>a</sup>	27.9 <sup>Bb</sup>	40.9 <sup>ab</sup>	44.0			
Mean	50.3	48.3	39.4	42.4				
Sinapic acid								
BRS Guaraim	3.80	4.70	5.82	4.24	4.64 <sup>B</sup>	0.046	SEM =	0.0143
BRS Marcante	5.68	5.44	6.15	4.30	5.39 <sup>A</sup>			
Mean	4.74 <sup>ab</sup>	5.07 <sup>ab</sup>	5.99 <sup>a</sup>	4.27 <sup>b</sup>				
Apigenin <sup>#</sup>								
BRS Guaraim	11.0	11.0	11.1	10.8 <sup>A</sup>	11.0	0.016	SEM =	0.0015
BRS Marcante	11.0 <sup>a</sup>	10.8 <sup>a</sup>	11.0 <sup>a</sup>	5.4 <sup>Bb</sup>	9.5			
Mean	11.0	10.9	11.0	8.1				
Sum of bound phenolic acids—Alkaline hydrolysis								
BRS Guaraim	51.1	54.0	60.9 <sup>A</sup>	52.5	54.6	0.734	SEM =	0.461
BRS Marcante	65.4 <sup>a</sup>	59.2 <sup>ab</sup>	39.8 <sup>Bb</sup>	48.0 <sup>ab</sup>	53.1			
Mean	58.2	56.6	50.4	50.2				
Sum of bound flavonoids—Alkaline hydrolysis								
BRS Guaraim	11.0	11.0	11.1	10.8 <sup>A</sup>	11.0	0.016	SEM =	0.0002
BRS Marcante	11.0 <sup>a</sup>	10.8 <sup>a</sup>	11.0 <sup>a</sup>	5.4 <sup>Bb</sup>	9.5			
Mean	11.0	10.9	11.0	8.1				
Sum of bound phytochemical compounds—Alkaline hydrolysis								
BRS Guaraim	62.1	65.0	72.0 <sup>A</sup>	63.3	65.6	0.522	SEM =	0.309
BRS Marcante	76.4 <sup>a</sup>	70.0 <sup>ab</sup>	50.8 <sup>Bb</sup>	53.3 <sup>b</sup>	62.6			
Mean	69.2	67.5	61.4	58.3				
Bound phytochemical compounds—Acid hydrolysis								
<i>p</i> -Coumaric acid								
BRS Guaraim	8.56	7.47 <sup>B</sup>	9.39	8.72	8.53	0.9534	SEM =	0.5427
BRS Marcante	7.73	9.36 <sup>A</sup>	8.11	9.04	8.56			
Mean	8.14	8.41	8.75	8.88				

Means (n = 6) followed by different capital letters within the same column and different small letters within the same row differ ( $p < 0.05$ ), respectively, between cultivars and germination times using the Student–Newman–Keuls test. # Flavonoids were quantified as equivalent to quercetin. LoQ: limit of quantification; SEM: standard error of mean. 4-Hydroxybenzoic acid LoQ: 0.062; Vanillic acid LoQ: 0.025 ppm; *p*-Coumaric acid LoQ: 0.029 ppm; *trans*-Ferulic acid LoQ: 0.033 ppm; Sinapic acid LoQ: 0.258 ppm; Quercetin LoQ: 0.444 ppm.

Free phenolic compounds are generally synthesized in the endoplasmic reticulum and stored in the vacuole of plant cells [19]. Looking at the sum of free phenolic acids, BRS Marcante had the highest levels ( $p < 0.05$ ), but no changes were detected during germination regardless of the cultivar (Table 2). Sinapic acid was the major free phenolic acid being found at higher levels in BRS Marcante than BRS Guaraim (82% higher,  $p < 0.05$ ),

and its content was not altered during germination (Table 2). Before germination, vanillic acid was found only in BRS Guaraim, but decreased with the advance of germination, while in BRS Marcante, it showed a trend of increasing (Table 2).

DIBOA-hex-hex was the major benzoxazinoid in both cultivars and was 1.8-fold higher in BRS Marcante than in BRS Guaraim, whereas DIMBOA-hex-hex did not differ between cultivars (Table 2). Previous studies have already reported DIBOA dihexoside as the main benzoxazinoid found in wheat [41,45,47], but benzoxazinoid behavior during wheat germination was still unknown. Benzoxazinoids increased with the advance of germination (Table 2), reaching the highest levels at 72 h (480% higher value than at 0 h; Table 2). This finding is in line with previous reports showing the highest levels of benzoxazinoids in the sprouts of other cereals such as rye [17]. Benzoxazinoids are concentrated in the bran and germ [10], fractions which are mainly involved in germination.

Flavonoids were the major class of compounds in the free phytochemical fraction (~73% of free phytochemicals). Apigenins hex-pent II, hex-hex-hex I and hex-hex-hex II were higher in BRS Marcante than in BRS Guaraim, and this made the sum of flavonoids also higher in BRS Marcante (23% higher). Although most free flavonoids did not change during germination, apigenin (aglycone form) showed a U-shaped behavior that was not affected by cultivar, being decreased up to 48 h, followed by an increase at 72 h of germination (Table 2). BRS Guaraim showed a similar U-shaped behavior for apigenin hex-pent I that was not found in BRS Marcante ( $p < 0.05$ ; Table 2). The cause of these changes may be related to the binding of apigenin aglycone with other structures, even forming glycosylated apigenins, or the release of cell wall bound apigenins or sugars and proteins [48]. De novo synthesis may also contribute to some of these changes [47]. The sum of free phytochemical compounds, which was 1.3-fold higher in BRS Marcante than BRS Guaraim, was remarkably increased during germination (48 h onwards,  $p < 0.05$ ; Table 2).

Concerning the bound phytochemical compounds that are released by alkaline hydrolysis, there was no difference between cultivars in the sum of bound phenolic acids, but the content of sinapic acid released by alkaline hydrolysis was higher in BRS Marcante than BRS Guaraim (16% higher content, Table 3). Independent of the cultivar, there was a bell-shaped behavior for sinapic acid content during germination, with peak values at 48h of germination. Bound 4-hydroxybenzoic acid released by alkaline hydrolysis was linearly increased with the advance of germination in BRS Guaraim, while BRS Marcante showed a bell-shaped behavior with peak values at 48 h of germination ( $p < 0.05$ ; Table 3). Bound vanillic acid released by alkaline hydrolysis, which was not detected in any wheat cultivar before germination, was found only in germinated grains of BRS Guaraim and exhibited a bell-shaped behavior with peak values at 48 h (Table 3). In the free fraction of this cultivar, it appeared only before germination. Free vanillic acid of BRS Guaraim may have been linked to complex cell wall structures through ester-type bonds during the beginning of germination, explaining the disappearance of the free form and its appearance after 48 h in the fraction released after alkaline hydrolysis [14]. Bound *p*-coumaric acid that was released by alkaline hydrolysis did not differ between cultivars or germination times (Table 3). *trans*-Ferulic acid was the major component (70%) among the bound phytochemicals released after alkaline hydrolysis (Table 3). *trans*-Ferulic acid and the sum of phenolic acids released by alkaline hydrolysis had a U-shaped behavior throughout germination in BRS Marcante, but not in BRS Guaraim (Table 3). The lowest content of *trans*-ferulic acid and of the sum of phenolic acids was found for BRS Marcante at 48 h, resulting in 1.8-fold lower content than BRS Guaraim.

Apigenin was the only flavonoid quantified in the bound fraction released after alkaline hydrolysis. In BRS Marcante, apigenin underwent a significant decrease at 72 h of germination (Table 3), which was not observed in BRS Guaraim.

Although there was no difference in the sum of bound phytochemicals released by alkaline hydrolysis between cultivars, the level of this group of compounds decreased in BRS Marcante from 48 h onwards, resulting in lower levels than BRS Guaraim (41% lower levels, Table 3). One explanation for this behavior is the release of compounds bound

to the cell wall during germination, which increases the content of free compounds [48]. Accordingly, the sum of free phenolic compounds increased during germination.

In the fraction of bound compounds that were released by acid hydrolysis, only *p*-coumaric acid was identified (Table 3). There was a significant cultivar vs. germination time interaction in the levels of *p*-coumaric acid released by acid hydrolysis, resulting in higher levels for BRS Marcante than BRS Guaraim at 24 h of germination (25% higher levels,  $p < 0.05$ ). However, no marked changes were observed in the content of this phenolic acid throughout germination. Kim, Kwak and Kim [44] found gallic, 4-hydroxybenzoic, vanillic, caffeic, syringic, ferulic and *p*-coumaric acids in the free and bound fractions of germinated and not-germinated wheat. Initially, they observed low levels followed by an increase with the advance of germination, and the highest levels were found at 72 h and 96 h of germination. Ferulic and vanillic acid had the highest increase with values up to 1.5-fold higher in germinated than in not-germinated grains. Most phenolic acids in wheat occur in the bound form and have been shown to increase with advancing germination, i.e., *p*-coumaric, ferulic and sinapic acids, likely through the decomposition of lignin and other chemical reactions [43,44].

#### 2.4. Multivariate Analysis of Phytochemical Changes in during Wheat Germination

MANOVA using the likelihood ratio test (Wilks), Pillai, Hotelling–Lawley and Roy tests revealed that, when all dependent variables (phytochemical compounds) were combined in the analysis, there was a significant interaction effect of wheat cultivar vs. germination time (Supplementary materials, Table S4). This finding confirms the hypothesis that the soft and hard wheat cultivars evaluated showed distinct changes in free and bound phytochemical compounds during germination, and qualifies the data for the Principal Component Analysis (PCA).

Cluster analysis further confirmed the distinct behavior of BRS Guaraim and BRS Marcante concerning the changes in phytochemicals during germination. Cluster analysis revealed that wheat cultivars were grouped into three groups according to the free phytochemical variables during germination (Figure 1(a1)), explaining 63.3% of the data variation. BRS Marcante was grouped into a single group regardless of the germination time (M-0 h, -24 h, -48 h and -72 h), whereas BRS Guaraim was divided into two groups: one for 0 and 24 h (G-0 h and -24 h) and the other for 48 h and 72 h (G-48 h and -72 h). Cluster analysis of the free phytochemical variables (Figure 1(a2)) also revealed three groups, which were able to explain 73% of the data variation. One of these groups included vanillic acid and DIBOA-hex-hex, another group was composed of DIMBOA-hex-hex, apigenin-hex-pent I and II and sinapic acid, and the last one was composed of apigenins hex-hex-hex I, II and aglycone.

The cluster analysis of wheat cultivars during germination according to the bound phytochemicals that were released after alkaline hydrolysis divided samples into three groups (57.1%) (Figure 1(b1)). The first group included BRS Guaraim 0, 24 and 72 h (G-0 h, -24 h and -72 h) and BRS Marcante 24 and 72 h (M-24 h and -72 h), the second group included BRS Guaraim 48 h and BRS Marcante 0 h (G-48 h and M-0 h) and the third group was represented only by BRS Marcante 48 h (M-48 h). The dependent variables (bound phytochemical compounds) of this analysis, in turn, were only divided into two groups (54.2%), one comprising *p*-coumaric, sinapic, *trans*-ferulic and vanillic acid, and the other comprising 4-hydroxybenzoic acid and apigenin (Figure 1(b2)).

PCA was used as an exploratory analysis to verify if changes in the phytochemical compounds of free or bound fractions would allow the discrimination of wheat cultivars during germination (Figure 2). A biplot (cultivar and germination time vs. content of free phytochemicals, Figure 2a) confirmed the findings of cluster analysis and increased the proportion of explained variance to 86.6% using the first three principal components. Another biplot (cultivar and germination time vs. content of bound phytochemicals released after alkaline hydrolysis, Figure 2b) confirmed the findings of cluster analysis and increased the proportion of explained variance to 84.5% using the first three principal components.

BRS Marcante before germination and up to 24 h of germination was associated with high levels of some free phytochemicals, namely sinapic acid, apigenin and apigenin hex-pent II, and apigenin hex-hex-hex I and II (Figure 2a, green circle). With the progression of germination, BRS Marcante changed the profile of free phytochemical compounds, becoming associated with high levels of vanillic acid, apigenin hex-pent I and DIBOA hex-hex after 72 h of germination (Figure 2a, pink circle). On the other hand, BRS Guaraim was already associated with high levels of vanillic acid, apigenin hex-pent I and DIBOA hex-hex before germination (Figure 2a, pink circle), which were changed to a free phenolic profile associated with DIMBOA hex-hex after 72 h of germination (Figure 2a, blue circle).

Bound phenolic compounds are located mainly in the cell wall and are formed through the conjugation of free phenolic compounds with macromolecules such as cellulose and proteins [22]. Concerning the profile of bound phytochemicals that were released after alkaline hydrolysis, there was an association between BRS Guaraim and BRS Marcante samples at the start (0 and 24 h) and in the end of germination (72 h) (Figure 2b, green circle). However, at 48 h of germination there was a distinct profile of bound phytochemicals between cultivars. While BRS Marcante was associated with high levels of 4-hydroxybenzoic acid (pink circle), BRS Guaraim was associated with high levels of vanillic acid and *trans*-ferulic acid (blue circle; Figure 2b).

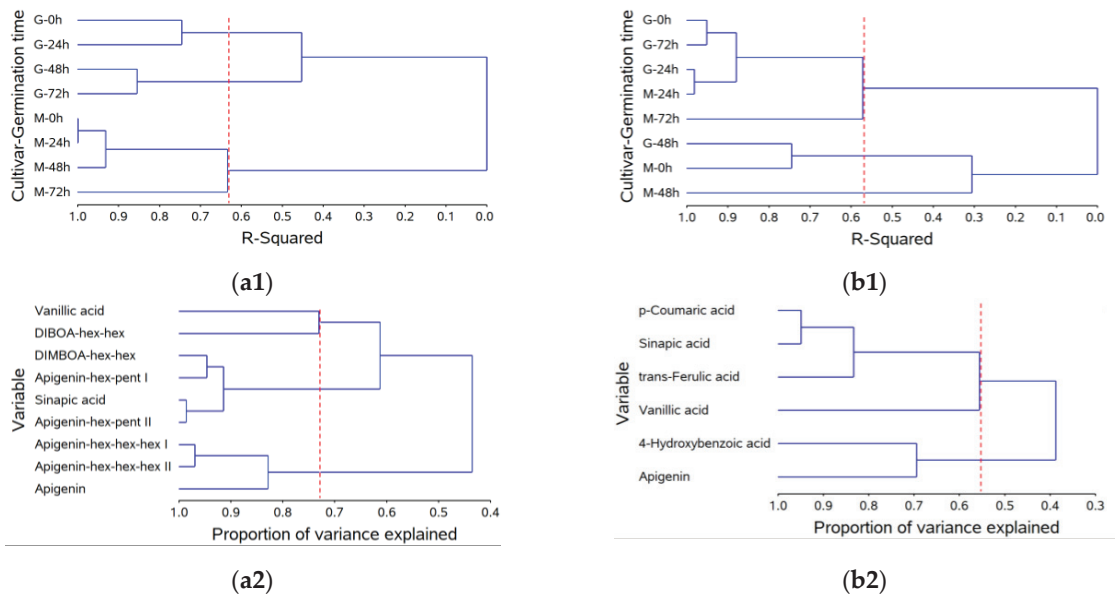


**Figure 1.** Dendrogram of wheat cultivars (G = Guaraim, M = Marcante) under different germination times (0, 24, 48 and 72 h; ordinate axis) in relation to the coefficient of determination ( $r^2$ , abscissa axis) using Euclidean distance as a measure of dissimilarity and Ward's agglomerative hierarchical algorithm as a clustering method for the free phytochemical fraction (a1) and for the bound phytochemical fraction that was released after alkaline hydrolysis (b1); and dendrogram of phytochemical content (mg/100 g, ordinate axis) in relation to the coefficient of determination ( $r^2$ , abscissa axis) using the correlation matrix as a measure of similarity and the principal component as a clustering method for the free phytochemical fraction (a2) and for the bound phytochemical fraction that was released after alkaline hydrolysis (b2). a1 = 63.3% and a2 = 73.0%; b1 = 57.1% and b2 = 54.2%.

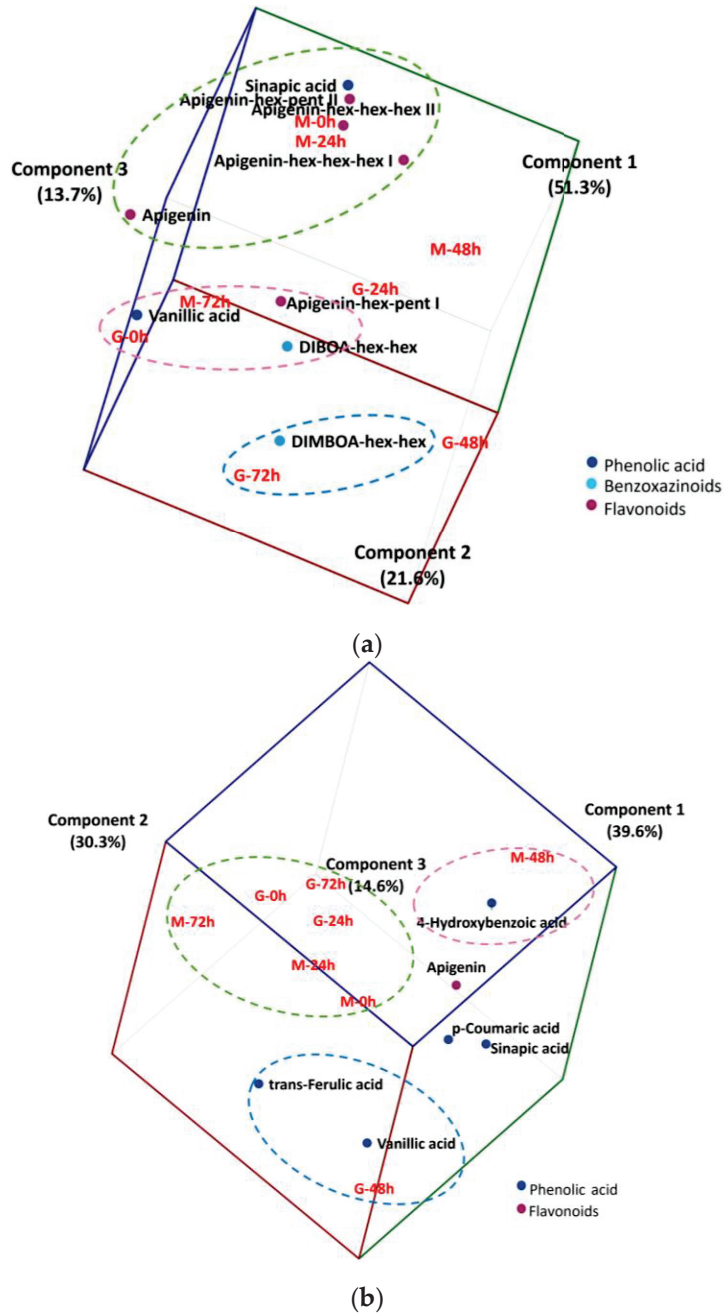


**Figure 2.** Three-dimensional biplot of wheat cultivars (G = Guaraim, M = Marcante) at different germination times (0, 24, 48 and 72 h) (scores) versus phytochemicals (loadings) in relation to the main components of principal component analysis for the free phytochemical fraction (a) and for the bound phytochemical fraction that was released after alkaline hydrolysis (b); a = 86.6% and b = 84.5%. Colored dashed ellipses indicate the proximity among samples and variables.



### 2.5. Antioxidant Capacity of Wheat Cultivars during Germination

During germination, in addition to the hydrolysis of macronutrients such as protein [49] and starch (Table 1), phytochemical compounds may be synthesized, released or conjugated, which may result in changes in the antioxidant capacity (Figure 3). The antioxidant capacity is associated with the ability to scavenge free radicals, break radical chain reactions and chelate metals [50]. The oxygen radical absorbance assay was used to evaluate the antioxidant capacity of wheat grains. The antioxidant capacity was assessed only in the extract containing the free phytochemicals, which is expected to be solubilized during digestion and available for intestinal absorption. Although bound phytochemicals, namely bound phenolic compounds, have already been demonstrated to exert antioxidant effects *in vivo* [51,52], such effects depend on their interaction and biotransformation by gut microbiota, which was not investigated in the present study.

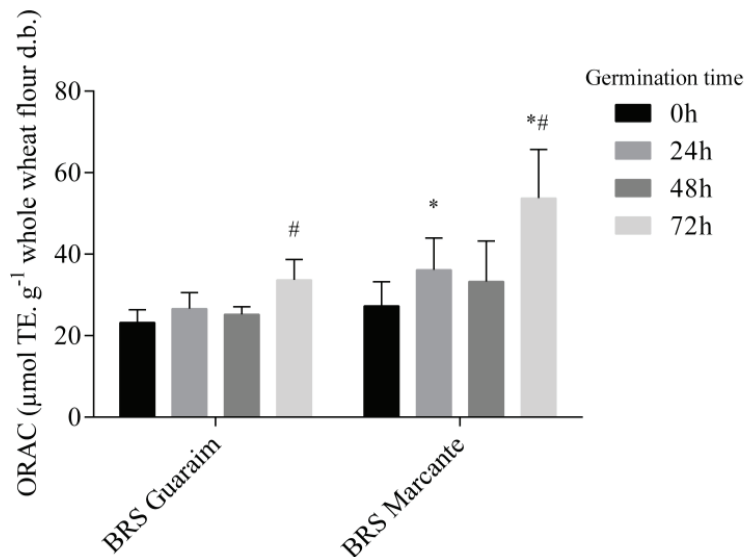


**Figure 3.** Changes in the oxygen radical absorbance capacity (ORAC) of the free phytochemical fraction of germinated wheat. # Significantly different ( $p < 0.05$ ) from the same cultivar at 0 h. \* Significantly different ( $p < 0.05$ ) from BRS Guaraim at the same germination time.  $n = 6$ .

Although BRS Marcante had a higher content of free phytochemical compounds than BRS Guaraim (Table 2), the peroxy radical scavenging capacity of both cultivars was similar before germination (Figure 3). The compounds that most contribute to this antioxidant activity are phenolic acids and flavonoids [53]. In both cultivars, there was an increase in the antioxidant capacity after 72 h of germination ( $p < 0.05$ ), and this increase was higher for BRS Marcante, which had a higher antioxidant capacity than BRS Guaraim at 24 h (58% higher) and 72 h (41% higher;  $p < 0.05$ ).

Many studies demonstrate increased antioxidant capacity in sprouted wheat [54–58] and generally attribute this to the release of bound phytochemicals. In contrast to the free phytochemical compounds that are soluble in conventional organic solvent, most phytochemical compounds of wheat are bound to cell wall components or sugars. These matrix-bound phytochemical compounds (BPC) are insoluble and, therefore, will not contribute to the antioxidant capacity assessed in the extracts of wheat grain. However, during food digestion, BPC will reach the colon, where they can be fermented by gut microbiota and exert nutraceutical properties [59]. In addition, BPC could be a substrate for metabolic transformation during grain germination. The diverse and complex structure of BPC makes it difficult to analyze these compounds. For this reason, alkaline and acid

hydrolysis were used to release the small units of phytochemical compounds and obtain some insight into the type of chemical bonds responsible for their linkage to the food matrix. The total concentration of phytochemicals bound to the cell wall (ester-type bonds, alkaline hydrolysis) was 2.1- and 1.5-fold higher for BRS Guaraim and BRS Marcante, respectively, than the total concentration of free phytochemicals. Phytochemicals linked to simple sugars (ether-type glycosidic bonds, acid hydrolysis) were 3.6- and 4.5-fold lower, respectively. Of the total phytochemical compounds found in wheat, approximately 70% and 64% correspond to the total bound fraction, respectively, for BRS Guaraim and BRS Marcante. Our result agrees with [13], which says that 60% to 90% of the phytochemical compounds in cereals occur in a bound form.

### 3. Materials and Methods

#### 3.1. Wheat Samples

Wheat (*T. aestivum* L.) grains of BRS Marcante and BRS Guaraim cultivars were obtained in the experimental fields of the Brazilian Agricultural Research Corporation (Embrapa Trigo) in Passo Fundo, RS state, Brazil (geographical coordinates: 28°15'46"S; 52°24'24"W; 687 m), in two crop seasons.

#### 3.2. Samples Characterization

The GHI (method 55-31.01, AACCI [25], Perten Instruments, Springfield, IL, USA), grain falling number, (GFN, method 56-81.03, AACCI [25], Perten Instruments, Springfield, IL, USA), hectoliter weight (method 55-10.01, AACCI [25] with results expressed in kg·hL<sup>-1</sup>) and thousand kernel weight [60] were assessed to characterize the grains. The technological quality of wheat cultivars was evaluated according to AACCI [25] and included alveography (method 54-30.02, AACCI [25], Chopin Alveograph, Villeneuve-la-Garenne, France) of whole wheat flours, considering the parameters gluten strength (W), tenacity (P) and tenacity/extensibility ratio (P/L).

#### 3.3. Germination

Wheat grain germination was performed as described by Baranzelli et al. [2] with some modification. Wheat grains were germinated in triplicate under controlled lighting conditions (12 h day/12 h night), relative humidity (80%), grain moisture (30%) and temperature (25 °C day/15 °C night) for 0, 24, 48, and 72 h. Germination temperatures were selected according to the average of the maximum (day) and minimum (night) temperatures of the years 2014, 2015 and 2016 in Passo Fundo during the wheat crop season (September to November). This region is among the major Brazilian wheat producers.

#### 3.4. Grain Milling

The whole wheat grains were first ground in a knife mill (Marconi, Piracicaba, SP, Brazil), followed by grinding in a hammer mill (Perten Instruments, Springfield, IL, USA) with a 0.8 mm sieve.

#### 3.5. Germination Marker

The GFN was evaluated according to method 56–81.03 (AACCI [25], Perten Instruments, Springfield, IL, USA) with altitude correction (Passo Fundo, RS, Brazil = 687 m).

#### 3.6. Extraction of Free and Matrix-Bound Phytochemical Compounds

Free phytochemical compounds (FPC) were extracted from 0.25 g of whole wheat flour diluted in 2.5 mL of acetone/water (80:20, *v/v*) solution acidified with 0.1% formic acid. Samples were vortex-mixed for 2 min, centrifuged at 1500 × *g* for 3 min and the supernatant was collected. Extraction was repeated three times, the supernatants were pooled and 6 mL of extract was concentrated in a rotary evaporator at 38 °C.

Matrix-bound phytochemical compounds (BPC) were extracted through alkaline and acid hydrolysis according to Zhang et al. [61] with adaptations. For alkaline hydrolysis,

2.0 mL of distilled water and 1.5 mL of 3 mol·L<sup>-1</sup> NaOH were added to the residue remaining after FPC extraction. Samples were shaken for 16 h at 20 °C and then had the pH adjusted to ~2.0. Phytochemical compounds released were extracted three times with 15 mL of diethyl ether/ethyl acetate solution (1:1, *v/v*). The supernatants were mixed, and 40 mL was dried in a rotary evaporator at 38 °C. The acid hydrolysis was carried out by adding 1.5 mL of 6 mol·L<sup>-1</sup> HCl to the residue remaining after alkaline hydrolysis. Samples were incubated at 85 °C for 30 min and, thereafter, had the pH adjusted to ~2.0. The extraction followed the same steps as described for alkaline hydrolysis.

Extracts of FPC and BPC obtained through alkaline and acidic hydrolysis were resuspended in 1.2 mL of acidified water/methanol solution (1:0.2 *v/v*, 0.1% formic acid) and stored at -20 °C until further analysis.

### 3.7. Phytochemical Compounds Identification

The phytochemical compounds of wheat extracts were identified using two different sets of liquid chromatograph (LC) equipment. The first exploratory analysis was conducted using an LC system connected to a mass spectrometer (MS) that had a hybrid Orbitrap analyzer and an electrospray ionization source (ESI, Q-Exactive™, Thermo Fisher Scientific, Bremen, Germany), using the chromatographic conditions previously described by Astudillo-Pascual et al. [62].

Thereafter, compound identification was accomplished using an LC-MS equipped with a quadrupole-time-of flight (Q-TOF) analyzer and an electrospray ionization source (ESI) (Bruker Daltonics, micrOTOF-Q III model, Bremen, Germany). Chromatographic parameters were set according to Quatrin et al. [63] and Q-TOF-MS parameters were set according to Mallmann et al. [64].

The identification of phytochemical compounds was based on the retention time and order of elution in the reverse phase column, maximum absorption wavelength (UV-vis) and characteristics of the MS spectrum compared to authentic standards analyzed under the same conditions or with literature data. For the reliable identification of compounds, comparison was made with analytical standards and databases, based on neutral mass isotope distribution, retention time and MS/MS fragments using the customized database of polyphenols from PubChem (<https://pubchem.ncbi.nlm.nih.gov/>) (accessed on 20 July 2020)) and other metabolites from KEGG (<http://www.genome.jp/kegg/>) (accessed on 23 July 2020)), MoNA: MassBank of North America (<https://mona.fiehnlab.ucdavis.edu/>) (accessed on 3 August 2020)), FooDB (<https://foodb.ca>) (accessed on 12 August 2020)) and ReSpect for Phytochemicals (<http://spectra.psc.riken.jp/menta.cgi/respect/index>) (accessed on 13 August 2020)). For the non-targeted identification, the parameters generated by the software were applied in descending order of importance: precursor exact mass error and fragment mass error (<10 ppm); isotopic similarity (>80%) and highest fragmentation score (score > 30).

### 3.8. Quantification of Phytochemical Compounds

The quantification of free and matrix-bound phytochemical compounds of germinated wheat samples was performed according to Quatrin et al. [63].

Absorption spectra were recorded from 200 to 800 nm, and chromatograms for the quantification of phytochemical compounds were obtained at 280, 320 and 360 nm. Results were expressed as mg·100 g<sup>-1</sup> of whole wheat flour on dry basis. The quantification conditions were validated in our laboratory (Nidal-UFSM) (Supplementary materials, Box S1 and Table S5) following the International Conference on Harmonization Guidelines.

### 3.9. Oxygen Radical Absorbance Capacity (ORAC)

The oxygen radical absorbance capacity (ORAC) of FPC was determined according to the method described by Ou, Hampsch-woodill and Prior [65]. Values were expressed as μmol of Trolox equivalents·g<sup>-1</sup> sample on dry basis.

### 3.10. Statistical Analysis

The results of germination markers and ORAC were analyzed using 2-way analysis of variance (ANOVA, 2 cultivars  $\times$  4 germination times) with six replicates ( $n = 6$ , where three replicates each were provided from two different crop seasons), followed by Tukey's test for mean comparison at a level of 5% significance. Statistica software (version 9.0, StatSoft Inc., Tulsa, OK, USA) was used to perform this statistical analysis.

For the results of the phytochemical quantification, the experimental design was randomized into blocks in a  $2 \times 4$  factorial scheme (2 wheat cultivars  $\times$  4 germination times), totaling eight (8) treatments with six replicates each ( $n = 6$ ). Data were submitted to ANOVA using the GLM procedure, their means were adjusted using the ordinary least squares method with the LSMEANS command and compared using the Student–Newman–Keuls (SNK) test.

Then, multivariate analysis of variance (MANOVA) was performed, in which the matrices of sums of squares and products were obtained. To test the hypothesis that the treatment means vectors were null, the Wilks ( $\lambda$ ), Pillai ( $V$ ), Hotelling–Lawley ( $U$ ) and Roy ( $F_0$ ) tests were performed. Additionally, cluster analysis was performed for treatments using the DISTANCE, CLUSTER and TREE procedures, using the average Euclidean distance as a dissimilarity measure and Ward as the clustering method. A cluster analysis of the dependent variables was also performed using the VARCLUS and TREE procedures, using the correlation matrix as input. Principal component analysis was performed using the PRINQUAL, PRINCOMP and FACTOR procedures (Ravindra Khattree and Dayanand N. Naik 2000). Statistical analyses were performed on the SAS<sup>®</sup> System for Windows<sup>™</sup> version 9.4 (SAS Institute Inc., Cary, NC, USA), at a 5% significance level.

Chromatogram figures were obtained from the LabSolutions software, dendrogram figures were obtained from the SAS<sup>®</sup> software, PCA figures were produced using Microsoft Excel and the antioxidant capacity figure was produced using GraphPad Prism version 6 for Windows (GraphPad Software, San Diego, CA, USA).

## 4. Conclusions

Germination proved to be a good tool to increase and diversify the content of bioactive compounds in wheat, as indicated by the increase in the content of benzoxazinoids and antioxidant capacity. Changes in the profile of phytochemical compounds during germination were different between the soft- and hard-texture cultivars, and the hard-texture cultivar had the greatest increase in antioxidant capacity after germination. Before germination, the hard-texture cultivar, BRS Marcante, had a higher content of total benzoxazinoids and flavonoids than the soft-texture cultivar, BRS Guaraim, including DIBOA-hex-hex, free and bound sinapic acid, and apigenins hex-pent II, and hex-hex-hex I and II. On the other hand, the soft-texture cultivar, BRS Guaraim, had a greater content of DIMBOA-hex-hex. Free phytochemical compounds, mainly benzoxazinoids, increased during germination in both cultivars. Before germination, few differences were observed between the soft and hard cultivar concerning the profile of matrix-bound phytochemicals, which comprise the major group of phenolic compounds in wheat. During germination, the levels of this group of compounds have been shown to decrease only in the hard-texture cultivar, due to decreased levels of phenolic acids (*trans*-ferulic acid) and flavonoids (apigenin) that were bound to the cell wall through ester-type bonds. These findings confirm the hypothesis that hard and soft wheat cultivars have distinct behavior during germination concerning the changes in phytochemical compounds, namely the matrix-bound compounds. In addition, germination has been shown to remarkably increase the content of benzoxazinoids, and the antioxidant capacity of the free phytochemical fraction of wheat, which could bring a health-beneficial appeal for pre-harvested sprouted grains that have lost their baking properties.

**Supplementary Materials:** The following supporting information can be downloaded at: <https://www.mdpi.com/article/10.3390/molecules28020721/s1>. Table S1. Technological characteristics of two Brazilian wheat cultivars bearing soft (BRS Guaraim) and hard (BRS Marcante) texture grains. Table S2. Grain images during germination. Figure S1. Representative LC-PDA chromatograms of phytochemicals extracted from wheat grains. Free compounds (a) and bound compounds obtained by alkaline (b) and acid (c) hydrolysis. Table S3. Tentative identification of wheat phytochemicals by LC-Q-TOF-MS and LC-Orbitrap-MS. Table S4. Results of multivariate analysis of variance (MANOVA) for phytochemical compounds from wheat cultivars (C) under different germination times (T), using likelihood ratio test (Wilks) and Pillai, Hotelling-Lawley and Roy's tests. Box S1. Validation data for the analysis of benzoxazinone and phenolic compounds. Table S5. Accuracy test for the analysis of phenolic and benzoxazinoid compounds in wheat grains.

**Author Contributions:** Conceptualization, J.B. and T.E.; data curation, R.d.O.M., E.R. and O.D.P.; formal analysis, J.B., C.S.M., R.d.O.M., E.R., O.D.P., R.L.-R., A.G.F., R.R.-G. and M.Z.d.M.; funding acquisition, T.E.; investigation, S.S., M.Z.d.M. and T.E.; methodology, J.B., S.S., C.S.M., R.d.O.M., E.R., O.D.P. and M.Z.d.M.; project administration, M.Z.d.M. and T.E.; resources, T.E.; supervision, S.S., M.Z.d.M. and T.E.; validation, J.B. and S.S.; writing—original draft, J.B.; writing—review and editing, J.B., S.S., M.Z.d.M. and T.E. All authors have read and agreed to the published version of the manuscript.

**Funding:** This research was funded by CAPES (Coordenação de Aperfeiçoamento Pessoal de Nível Superior), grant number 001 and CNPq (National Council of Scientific and Technological Development) grant numbers 435932/2018-7 and 309604/2021-4.

**Data Availability Statement:** The data presented in this study are available on request from the corresponding author.

**Acknowledgments:** We thank Enio Marchesan and his team from the Phytotechnics Department of the Federal University of Santa Maria for loaning the germination chambers.

**Conflicts of Interest:** The authors declare no conflict of interest.

## References

- Li, C.; Nonogaki, H.; Barrero, J. *Seed Dormancy, Germination and Pre-Harvest Sprouting*; Balestrazzi, A., Ed.; University of Pavia: Pavia, Italy, 2019; Volume 9, ISBN 9782889457625.
- Baranzelli, J.; Kringel, D.H.; Colussi, R.; Paiva, F.F.; Aranha, B.C.; de Miranda, M.Z.; Zavareze, E.d.R.; Dias, A.R.G. Changes in Enzymatic Activity, Technological Quality and Gamma-Aminobutyric Acid (GABA) Content of Wheat Flour as Affected by Germination. *LWT-Food Sci. Technol.* **2018**, *90*, 483–490. [[CrossRef](#)]
- Olaerts, H.; Courtin, C.M. Impact of Preharvest Sprouting on Endogenous Hydrolases and Technological Quality of Wheat and Bread: A Review. *Compr. Rev. Food Sci. Food Saf.* **2018**, *17*, 698–713. [[CrossRef](#)] [[PubMed](#)]
- Olaerts, H.; Roye, C.; Derde, L.J.A.; Sinnaeve, G.; Meza, W.R.; Bodson, B.; Courtin, C.M. Impact of Preharvest Sprouting of Wheat (*Triticum aestivum*) in the Field on Starch, Protein and Arabinoxylan Properties. *J. Agric. Food Chem.* **2016**, *64*, 8324–8332. [[CrossRef](#)] [[PubMed](#)]
- Baranzelli, J.; Kringel, D.H.; Mallmann, J.F.; Bock, E.; el Halal, S.L.M.; Prietto, L.; Zavareze, E.d.R.; de Miranda, M.Z.; Dias, A.R.G. Impact of Wheat (*Triticum aestivum* L.) Germination Process on Starch Properties for Application in Films. *Starch/Staerke* **2019**, *71*, 1800262. [[CrossRef](#)]
- Kringel, D.H.; Baranzelli, J.; Schöffner, J.D.N.; el Halal, S.L.M.; de Miranda, M.Z.; Dias, A.R.G.; Zavareze, E.D.R. Germinated Wheat Starch as a Substrate to Produce Cyclodextrins: Application in Inclusion Complex to Improve the Thermal Stability of Orange Essential Oil. *Starch/Staerke* **2020**, *72*, 1–7. [[CrossRef](#)]
- Hefni, M.; Witthöft, C.M. Increasing the Folate Content in Egyptian Baladi Bread Using Germinated Wheat Flour. *LWT-Food Sci. Technol.* **2011**, *44*, 706–712. [[CrossRef](#)]
- Sibian, M.S.; Saxena, D.C.; Riar, C.S. Effect of Germination on Chemical, Functional and Nutritional Characteristics of Wheat, Brown Rice and Triticale: A Comparative Study. *J. Sci. Food Agric.* **2017**, *97*, 4643–4651. [[CrossRef](#)]
- Nelson, K.; Mathai, M.L.; Ashton, J.F.; Donkor, O.N.; Vasiljevic, T.; Mamilla, R.; Stojanovska, L. Effects of Malted and Non-Malted Whole-Grain Wheat on Metabolic and Inflammatory Biomarkers in Overweight/Obese Adults: A Randomised Crossover Pilot Study. *Food Chem.* **2016**, *194*, 495–502. [[CrossRef](#)]
- Adhikari, K.B.; Tanwir, F.; Gregersen, P.L.; Steffensen, S.K.; Jensen, B.M.; Poulsen, L.K.; Nielsen, C.H.; Høyer, S.; Borre, M.; Fomsgaard, I.S. Benzoxazinoids: Cereal Phytochemicals with Putative Therapeutic and Health-Protecting Properties. *Mol. Nutr. Food Res.* **2015**, *59*, 1324–1338. [[CrossRef](#)]
- Kadiri, O. A Review on the Status of the Phenolic Compounds and Antioxidant Capacity of the Flour: Effects of Cereal Processing. *Int. J. Food Prop.* **2017**, *20*, S798–S809. [[CrossRef](#)]

12. Călinoiu, L.F.; Vodnar, D.C. Whole Grains and Phenolic Acids: A Review on Bioactivity, Functionality, Health Benefits and Bioavailability. *Nutrients* **2018**, *10*, 1615. [[CrossRef](#)] [[PubMed](#)]
13. Lemmens, E.; Moroni, A.v.; Pagand, J.; Heirbaut, P.; Ritala, A.; Karlen, Y.; Lê, K.-A.; van den Broeck, H.C.; Brouns, F.J.P.H.; de Brier, N.; et al. Impact of Cereal Seed Sprouting on Its Nutritional and Technological Properties: A Critical Review. *Compr. Rev. Food Sci. Food Saf.* **2019**, *18*, 305–328. [[CrossRef](#)]
14. Acosta-Estrada, B.A.; Gutiérrez-Urbe, J.A.; Serna-Saldívar, S.O. Bound Phenolics in Foods, a Review. *Food Chem.* **2014**, *152*, 46–55. [[CrossRef](#)]
15. Kowalska, I.; Jędrejek, D. Benzoxazinoid and Alkylresorcinol Content, and Their Antioxidant Potential, in a Grain of Spring and Winter Wheat Cultivated under Different Production Systems. *J. Cereal Sci.* **2020**, *95*, 103063. [[CrossRef](#)]
16. de Bruijn, W.J.C.; Gruppen, H.; Vincken, J.P. Structure and Biosynthesis of Benzoxazinoids: Plant Defence Metabolites with Potential as Antimicrobial Scaffolds. *Phytochemistry* **2018**, *155*, 233–243. [[CrossRef](#)] [[PubMed](#)]
17. Tanwir, F.; Dionisio, G.; Adhikari, K.B.; Fomsgaard, I.S.; Gregersen, P.L. Biosynthesis and Chemical Transformation of Benzoxazinoids in Rye during Seed Germination and the Identification of a Rye Bx6-like Gene. *Phytochemistry* **2017**, *140*, 95–107. [[CrossRef](#)]
18. Lattanzio, V. Phenolic Compounds: Introduction. In *Natural Products: Phytochemistry, Botany and Metabolism of Alkaloids, Phenolics and Terpenes*; Merillon, J.-M., Ramawat, K.G., Eds.; Springer: Berlin/Heidelberg, Germany, 2014; Volume 1, pp. 1543–1580, ISBN 9783642221446.
19. Saura-Calixto, F. Concept and Health-Related Properties of Nonextractable Polyphenols: The Missing Dietary Polyphenols. *J. Agric. Food Chem.* **2012**, *60*, 11195–11200. [[CrossRef](#)] [[PubMed](#)]
20. Wang, Z.; Li, S.; Ge, S.; Lin, S. Review of Distribution, Extraction Methods, and Health Benefits of Bound Phenolics in Food Plants. *J. Agric. Food Chem.* **2020**, *68*, 3330–3343. [[CrossRef](#)] [[PubMed](#)]
21. Benincasa, P.; Falcinelli, B.; Lutts, S.; Stagnari, F.; Galieni, A. Sprouted Grains: A Comprehensive Review. *Nutrients* **2019**, *11*, 421. [[CrossRef](#)]
22. Gan, R.Y.; Lui, W.Y.; Wu, K.; Chan, C.L.; Dai, S.H.; Sui, Z.Q.; Corke, H. Bioactive Compounds and Bioactivities of Germinated Edible Seeds and Sprouts: An Updated Review. *Trends Food Sci. Technol.* **2017**, *59*, 1–14. [[CrossRef](#)]
23. Singh, A.; Sharma, S. Bioactive Components and Functional Properties of Biologically Activated Cereal Grains: A Bibliographic Review. *Crit. Rev. Food Sci. Nutr.* **2017**, *57*, 3051–3071. [[CrossRef](#)]
24. Makowska, B.; Bakera, B.; Rakoczy-Trojanowska, M. The Genetic Background of Benzoxazinoid Biosynthesis in Cereals. *Acta Physiol. Plant* **2015**, *37*, 176. [[CrossRef](#)]
25. AACCI. *American Association of Cereal Chemists*, 11th ed.; Approved Methods of the AACCI International: St. Paul, MI, USA, 2010.
26. Caierão, E.; e Silva, M.S.; Scheeren, P.L.; de Castro, R.L.; Eichelberger, L.; do Nascimento Junior, A.; Guarienti, E.M.; de Miranda, M.Z.; Pires, J.L.F.; Maciel, J.L.N.; et al. Resultados Agronômicos e Qualitativos Da Nova Cultivar de Trigo ‘BRS Marcante’. *Ciência Rural* **2015**, *45*, 644–646. [[CrossRef](#)]
27. Scheeren, P.L.; Caierão, E.; e Silva, M.S.; de Castro, R.L.; Caetano, V.d.R.; Bassoi, M.C.; Pires, J.L.F.; Eichelberger, L.; de Miranda, M.Z.; Guarienti, E.M.; et al. BRS-Guaraim-Cultivar de Trigo Brando e Farinha Branqueadora. *XI Reun. Comissão Bras. Pesqui. Trigo Triticale* **2017**, *11*, 1–5.
28. Sharma, S.; Katyal, M.; Singh, N.; Singh, A.M.; Ahlawat, A.K. Comparison of Effect of Using Hard and Soft Wheat on the High Molecular Weight-Glutenin Subunits Profile and the Quality of Produced Cookie. *J. Food Sci. Technol.* **2022**, *59*, 2545–2561. [[CrossRef](#)] [[PubMed](#)]
29. Nonogaki, M.; Nonogaki, H. Germination. In *Encyclopedia of Applied Plant Sciences*; Thomas, B., Ed.; Academic Press: Salem, OR, USA, 2017; Volume 1, pp. 509–512, ISBN 9780123948083.
30. Olaerts, H.; Roye, C.; Derde, L.J.A.; Sinnaeve, G.; Meza, W.R.; Bodson, B.; Courtin, C.M. Evolution and Distribution of Hydrolytic Enzyme Activities during Preharvest Sprouting of Wheat (*Triticum aestivum*) in the Field. *J. Agric. Food Chem.* **2016**, *64*, 5644–5652. [[CrossRef](#)]
31. Miã, Â.A.; Grundas, S. Wheat Grain Hardness Modified by the Laboratory Sprouting Test. *Int. Agrophys.* **2012**, *16*, 283–288.
32. You, S.-Y.; Oh, S.-G.; Han, H.M.; Jun, W.; Hong, Y.-S.; Chung, H.-J. Impact of Germination on the Structures and in vitro Digestibility of Starch from Waxy Brown Rice. *Int. J. Biol. Macromol.* **2016**, *82*, 863–870. [[CrossRef](#)] [[PubMed](#)]
33. Zilic, S. Phenolic Compounds of Wheat. Their Content, Antioxidant Capacity and Bioaccessibility. *MOJ Food Process. Technol.* **2016**, *2*, 37. [[CrossRef](#)]
34. Gammoh, S.; Alu’datt, M.H.; Alhamad, M.N.; Rababah, T.; Ereifej, K.; Almajwal, A.; Ammari, Z.A.; al Khateeb, W.; Hussein, N.M. Characterization of Phenolic Compounds Extracted from Wheat Protein Fractions Using High-Performance Liquid Chromatography/Liquid Chromatography Mass Spectrometry in Relation to Anti-Allergenic, Anti-Oxidant, Anti-Hypertension, and Anti-Diabetic Propertie. *Int. J. Food Prop.* **2017**, *20*, 2383–2395. [[CrossRef](#)]
35. Sharma, M.; Rahim, M.S.; Kumar, P.; Mishra, A.; Sharma, H.; Roy, J. Large-Scale Identification and Characterization of Phenolic Compounds and Their Marker–Trait Association in Wheat. *Euphytica* **2020**, *216*, 127. [[CrossRef](#)]
36. Koistinen, V.M.; Hanhineva, K. Mass Spectrometry-Based Analysis of Whole-Grain Phytochemicals. *Crit. Rev. Food Sci. Nutr.* **2017**, *57*, 1688–1709. [[CrossRef](#)]

37. Zhang, P.; Chan, W.; Ang, I.L.; Wei, R.; Lam, M.M.T.; Lei, K.M.K.; Poon, T.C.W. Revisiting Fragmentation Reactions of Protonated  $\alpha$ -Amino Acids by High-Resolution Electrospray Ionization Tandem Mass Spectrometry with Collision-Induced Dissociation. *Sci. Rep.* **2019**, *9*, 6453. [[CrossRef](#)] [[PubMed](#)]
38. Hanhineva, K.; Keski-Rahkonen, P.; Lappi, J.; Katina, K.; Pekkinen, J.; Savolainen, O.; Timonen, O.; Paananen, J.; Mykkänen, H.; Poutanen, K. The Postprandial Plasma Rye Fingerprint Includes Benzoxazinoid-Derived Phenylacetamide Sulfates. *J. Nutr.* **2014**, *144*, 1016–1022. [[CrossRef](#)] [[PubMed](#)]
39. de Bruijn, W.J.C.; Vincken, J.P.; Duran, K.; Gruppen, H. Mass Spectrometric Characterization of Benzoxazinoid Glycosides from Rhizopus-Elicited Wheat (*Triticum aestivum*) Seedlings. *J. Agric. Food Chem.* **2016**, *64*, 6267–6276. [[CrossRef](#)]
40. Santos, M.C.B.; Lima, L.R.d.S.; Nascimento, F.R.; do Nascimento, T.P.; Cameron, L.C.; Ferreira, M.S.L. Metabolomic Approach for Characterization of Phenolic Compounds in Different Wheat Genotypes during Grain Development. *Food Res. Int.* **2018**, *124*, 118–128. [[CrossRef](#)] [[PubMed](#)]
41. Pihlala, J.-M.; Hellstrom, J.; Kurtelius, T.; Mattila, P. Flavonoids, Anthocyanins, Phenolamides, Benzoxazinoids, Lignans and Alkylresorcinols in Rye (*Secale cereale*) and Some Rye Products. *J. Cereal Sci.* **2018**, *79*, 183–192. [[CrossRef](#)]
42. Zhu, Y.; Sang, S. Phytochemicals in Whole Grain Wheat and Their Health-Promoting Effects. *Mol. Nutr. Food Res.* **2017**, *61*, 1600852. [[CrossRef](#)]
43. Tian, C.; Wang, Y.; Yang, T.; Sun, Q.; Ma, M.; Li, M. Evolution of Physicochemical Properties, Phenolic Acid Accumulation, and Dough-Making Quality of Whole Wheat Flour During Germination Under UV-B Radiation. *Front. Nutr.* **2022**, *1*, 877324. [[CrossRef](#)]
44. Kim, M.J.; Kwak, H.S.; Kim, S.S. Effects of Germination on Protein,  $\gamma$ -Aminobutyric Acid, Phenolic Acids, and Antioxidant Capacity in Wheat. *Molecules* **2018**, *23*, 2244. [[CrossRef](#)]
45. Tanwir, F.; Fredholm, M.; Gregersen, P.L.; Fomsgaard, I.S. Comparison of the Levels of Bioactive Benzoxazinoids in Different Wheat and Rye Fractions and the Transformation of These Compounds in Homemade Foods. *Food Chem.* **2013**, *141*, 444–450. [[CrossRef](#)] [[PubMed](#)]
46. Dihm, K.; Lind, M.V.; Sundén, H.; Ross, A.; Savolainen, O. Quantification of Benzoxazinoids and Their Metabolites in Nordic Breads. *Food Chem.* **2017**, *235*, 7–13. [[CrossRef](#)] [[PubMed](#)]
47. Hanhineva, K.; Rogachev, I.; Aura, A.M.; Aharoni, A.; Poutanen, K.; Mykkänen, H. Qualitative Characterization of Benzoxazinoid Derivatives in Whole Grain Rye and Wheat by LC-MS Metabolite Profiling. *J. Agric. Food Chem.* **2011**, *59*, 921–927. [[CrossRef](#)] [[PubMed](#)]
48. Nkhata, S.G.; Ayua, E.; Kamau, E.H.; Shingiro, J.-B. Fermentation and Germination Improve Nutritional Value of Cereals and Legumes through Activation of Endogenous Enzymes. *Food Sci. Nutr.* **2018**, *6*, 2446–2458. [[CrossRef](#)] [[PubMed](#)]
49. Xu, M.; Rao, J.; Chen, B. Phenolic Compounds in Germinated Cereal and Pulse Seeds: Classification, Transformation, and Metabolic Process. *Crit. Rev. Food Sci. Nutr.* **2020**, *60*, 740–759. [[CrossRef](#)]
50. Zilic, S.; Basic, Z.; Sukalovic, V.H.-T.; Maksimovic, V.; Jankovic, M.; Filipovic, M. Can the Sprouting Process Applied to Wheat Improve the Contents of Vitamins and Phenolic Compounds and Antioxidant Capacity of the Flour? *Int. J. Food Sci. Technol.* **2014**, *49*, 1040–1047. [[CrossRef](#)]
51. Maurer, L.H.; Cazarin, C.B.B.; Quatrin, A.; Nichelle, S.M.; Minuzzi, N.M.; Teixeira, C.F.; da Cruz, I.B.M.; Júnior, M.R.M.; Emanuelli, T. Dietary Fiber and Fiber-Bound Polyphenols of Grape Peel Powder Promote GSH Recycling and Prevent Apoptosis in the Colon of Rats with TNBS-Induced Colitis. *J. Funct. Foods* **2020**, *64*, 103644. [[CrossRef](#)]
52. Maurer, L.H.; Cazarin, C.B.B.; Quatrin, A.; Minuzzi, N.M.; Nichelle, S.M.; Lamas, C.d.A.; Cagnon, V.H.A.; Morari, J.; Velloso, L.A.; Júnior, M.R.M.; et al. Grape Peel Powder Attenuates the Inflammatory and Oxidative Response of Experimental Colitis in Rats by Modulating the NF-KB Pathway and Activity of Antioxidant Enzymes. *Nutr. Res.* **2020**, *76*, 52–70. [[CrossRef](#)]
53. Vuolo, M.M.; Lima, V.S.; Junior, M.R.M. Phenolic Compounds: Structure, Classification, and Antioxidant Power. In *Bioactive Compounds: Health Benefits and Potential Applications*; Elsevier: Amsterdam, The Netherlands, 2019; Volume Chapter 2, pp. 33–50, ISBN 9780128147757.
54. Naumenko, N.; Potoroko, I.; Kalinina, I. Stimulation of Antioxidant Activity and  $\gamma$ -Aminobutyric Acid Synthesis in Germinated Wheat Grain *Triticum Aestivum* L. by Ultrasound: Increasing the Nutritional Value of the Product. *Ultrason. Sonochem.* **2022**, *86*, 106000. [[CrossRef](#)]
55. Miyahira, R.F.; Pena, F.d.L.; Fabiano, G.A.; Lopes, J.d.O.; Ponte, L.G.S.; da Cunha, D.T.; Bezerra, R.M.N.; Antunes, A.E.C. Changes in Phenolic Compound and Antioxidant Activity of Germinated Broccoli, Wheat, and Lentils during Simulated Gastrointestinal Digestion. *Plant Foods Hum. Nutr.* **2022**, *77*, 233–240. [[CrossRef](#)]
56. Yang, B.; Yin, Y.; Liu, C.; Zhao, Z.; Guo, M. Effect of Germination Time on the Compositional, Functional and Antioxidant Properties of Whole Wheat Malt and Its End-Use Evaluation in Cookie-Making. *Food Chem.* **2021**, *349*, 129125. [[CrossRef](#)]
57. Dhillon, B.; Choudhary, G.; Sodhi, N.S. A Study on Physicochemical, Antioxidant and Microbial Properties of Germinated Wheat Flour and Its Utilization in Breads. *J. Food Sci. Technol.* **2020**, *57*, 2800–2808. [[CrossRef](#)]
58. Chen, Z.; Wang, P.; Weng, Y.; Ma, Y.; Gu, Z.; Yang, R. Comparison of Phenolic Profiles, Antioxidant Capacity and Relevant Enzyme Activity of Different Chinese Wheat Varieties during Germination. *Food Biosci.* **2017**, *20*, 159–167. [[CrossRef](#)]
59. Maurer, L.H.; Cazarin, C.B.B.; Quatrin, A.; Minuzzi, N.M.; Costa, E.L.; Morari, J.; Velloso, L.A.; Leal, R.F.; Rodrigues, E.; Bochi, V.C.; et al. Grape Peel Powder Promotes Intestinal Barrier Homeostasis in Acute TNBS-Colitis: A Major Role for Dietary Fiber and Fiber-Bound Polyphenols. *Food Res. Int.* **2019**, *123*, 425–439. [[CrossRef](#)]

60. Brasil, M.A.P.A. *Regras Para Análise de Sementes*; Ministério da Agricultura Pecuária e Abastecimento: Brasília, Brazil, 2009; Volume 1, ISBN 1932-6203.
61. Zhang, Y.; Wang, L.; Yao, Y.; Yan, J.; He, Z. Phenolic Acid Profiles of Chinese Wheat Cultivars. *J. Cereal Sci.* **2012**, *56*, 629–635. [[CrossRef](#)]
62. Astudillo-Pascual, M.; Domínguez, I.; Aguilera, P.A.; Frenich, A.G. New Phenolic Compounds in Posidonia Oceanica Seagrass: A Comprehensive Array Using High Resolution Mass Spectrometry. *Plants* **2021**, *10*, 864. [[CrossRef](#)]
63. Quatrin, A.; Pauletto, R.; Maurer, L.H.; Minuzzi, N.; Nichelle, S.M.; Carvalho, J.F.C.; Maróstica, M.R.; Rodrigues, E.; Bochi, V.C.; Emanuelli, T. Characterization and Quantification of Tannins, Flavonols, Anthocyanins and Matrix-Bound Polyphenols from Jaboticaba Fruit Peel: A Comparison between *Myrciaria Trunciflora* and *M. Jaboticaba*. *J. Food Compos. Anal.* **2019**, *78*, 59–74. [[CrossRef](#)]
64. Mallmann, L.P.; Tischer, B.; Vizzotto, M.; Rodrigues, E.; Manfroi, V. Comprehensive Identification and Quantification of Unexploited Phenolic Compounds from Red and Yellow Araçá (*Psidium cattleianum* Sabine) by LC-DAD-ESI-MS/MS. *Food Res. Int.* **2020**, *131*, 108978. [[CrossRef](#)] [[PubMed](#)]
65. Ou, B.; Hampsch-woodill, M.; Prior, R.L. Development and Validation of an Improved Oxygen Radical Absorbance Capacity Assay Using Fluorescein as the Fluorescent Probe. *J. Agric. Food Chem.* **2001**, *49*, 4619–4626. [[CrossRef](#)] [[PubMed](#)]

**Disclaimer/Publisher’s Note:** The statements, opinions and data contained in all publications are solely those of the individual author(s) and contributor(s) and not of MDPI and/or the editor(s). MDPI and/or the editor(s) disclaim responsibility for any injury to people or property resulting from any ideas, methods, instructions or products referred to in the content.





Article

# Evaluation of Antioxidant and Anticancer Activity of Mono- and Polyfloral Moroccan Bee Pollen by Characterizing Phenolic and Volatile Compounds

Volkan Aylanc<sup>1,2,3</sup>, Samar Larbi<sup>1,2,4</sup>, Ricardo Calhella<sup>1,2</sup>, Lillian Barros<sup>1,2</sup>, Ferial Rezouga<sup>4</sup>, María Shantal Rodríguez-Flores<sup>5</sup>, María Carmen Seijo<sup>5</sup>, Asmae El Ghouzi<sup>6</sup>, Badiaa Lyoussi<sup>6</sup>, Soraia I. Falcão<sup>1,2,\*</sup> and Miguel Vilas-Boas<sup>1,2,\*</sup>

- <sup>1</sup> Centro de Investigação de Montanha (CIMO), Instituto Politécnico de Bragança, Campus de Santa Apolónia, 5300-253 Bragança, Portugal
  - <sup>2</sup> Laboratório Associado para a Sustentabilidade e Tecnologia em Regiões de Montanha (SusTEC), Instituto Politécnico de Bragança, Campus de Santa Apolónia, 5300-253 Bragança, Portugal
  - <sup>3</sup> Departamento de Química e Bioquímica, Faculdade de Ciências, Universidade do Porto, 4169-007 Porto, Portugal
  - <sup>4</sup> Département de Génies Biologique et Agroalimentaire, Université Libre de Tunis, 30 Avenue Kheireddine Pacha, Tunis 1002, Tunisia
  - <sup>5</sup> Facultad de Ciencias, Universidad de Vigo, Campus as Lagoas, 36310 Vigo, Pontevedra, Spain
  - <sup>6</sup> Laboratory Physiology-Pharmacology and Environmental Health, Faculty of Sciences Dhar El Mehraz, University Sidi Mohammed Ben Abdallah, Fez 30050, Morocco
- \* Correspondence: sfalcao@ipb.pt (S.I.F.); mvboas@ipb.pt (M.V.-B.); Tel.: +351-273303401 (S.I.F.); +351-273303309 (M.V.-B.)

**Abstract:** Bee pollen is frequently characterized as a natural source of bioactive components, such as phenolic compounds, which are responsible for its pharmaceutical potential and nutritional properties. In this study, we evaluated the bioactive compound contents of mono- and polyfloral bee pollen samples using spectroscopic and chromatographic methods and established links with their antioxidant and antitumor activity. The findings demonstrated that the botanical origin of bee pollen has a remarkable impact on its phenolic (3–17 mg GAE/g) and flavonoid (0.5–3.2 mg QE/g) contents. Liquid chromatography–mass spectrometry analysis revealed the presence of 35 phenolic and 13 phenylamide compounds in bee pollen, while gas chromatography–mass spectrometry showed its richness in volatiles, such as hydrocarbons, fatty acids, alcohols, ketones, etc. The concentration of bioactive compounds in each sample resulted in a substantial distinction in their antioxidant activity, DPPH (EC<sub>50</sub>: 0.3–0.7 mg/mL), ABTS (0.8–1.3 mM Trolox/mg), and reducing power (0.03–0.05 mg GAE/g), with the most bioactive pollens being the monofloral samples from *Olea europaea* and *Ononis spinosa*. Complementarily, some samples revealed a moderate effect on cervical carcinoma (GI<sub>50</sub>: 495 µg/mL) and breast adenocarcinoma (GI<sub>50</sub>: 734 µg/mL) cell lines. This may be associated with compounds such as quercetin-*O*-diglucoside and kaempferol-3-*O*-rhamnoside, which are present in pollens from *Olea europaea* and *Coriandrum*, respectively. Overall, the results highlighted the potentiality of bee pollen to serve health-promoting formulations in the future.

**Keywords:** antiradical capacity; antitumor activity; bee products; bioactive compounds; phenolic compounds; phenylamides

**Citation:** Aylanc, V.; Larbi, S.; Calhella, R.; Barros, L.; Rezouga, F.; Rodríguez-Flores, M.S.; Seijo, M.C.; El Ghouzi, A.; Lyoussi, B.; Falcão, S.I.; et al. Evaluation of Antioxidant and Anticancer Activity of Mono- and Polyfloral Moroccan Bee Pollen by Characterizing Phenolic and Volatile Compounds. *Molecules* **2023**, *28*, 835. <https://doi.org/10.3390/molecules28020835>

Academic Editor: Nour Eddine Es-Safi

Received: 13 December 2022

Revised: 9 January 2023

Accepted: 9 January 2023

Published: 13 January 2023



**Copyright:** © 2023 by the authors. Licensee MDPI, Basel, Switzerland. This article is an open access article distributed under the terms and conditions of the Creative Commons Attribution (CC BY) license (<https://creativecommons.org/licenses/by/4.0/>).

## 1. Introduction

The major product of beekeeping activities is known as honey. However, honey bees, the golden insects of nature, can provide a much wider range of products with enormous potential, such as bee pollen, bee bread, propolis, royal jelly, bee venom, and beeswax [1]. This great variety of natural products has been intensively researched and employed in different industries for various purposes [2–4]. For example, propolis and bee venom are

the subjects of important research in the field of pharmacy due to their strong biological activities [5,6], while honey, bee pollen, and bee bread are considered important products as functional foods due to their nutritional values and remarkable biological activities [7–9].

Essentially, bee pollen is the male gametophyte of the plant. Worker bees collect these pollen grains from flowers and mix them with their own secretions, turning them into moist pellets. These pellets then stick to the pollen basket on the hind legs of the bees and begin their journey toward the hive [1]. Reaching the hive, the bees are forced to trespass an apparatus placed at the entrance of the hive, pollen traps, where the pellets are forced to detach from the bees' legs, following in the trap. The chemical composition and biological activity of bee pollen exhibit significant changes from pollen to pollen [1,7], depending on the type of plant from which this pollen originates, geographical conditions, collection season, as well as storage and processing factors [4,10].

With the development of analytical instruments and methods, the number of studies demonstrating that bee pollen is a natural source of bioactive compounds and micro- and macronutrients has progressed [3,7,10]. These advances have encouraged researchers to evaluate bee pollen, especially for the food sector. For example, there is an intense effort to fabricate functional foods with enhanced nutritional values and more potent biological activities by incorporating bee pollen in different food products, such as bread [11], biscuits [12], and meat [13]. Additionally, several studies stated that bee pollen samples from different geographical locations around the world are a great source of aldehydes, alcohols, fatty acids, phenolic compounds, terpenes, and esters that—when combined—potentiate the pharmaceutical properties of bee pollen, such as antioxidant, anti-inflammation, anticancer, and antidiabetic properties [1,7,14]. Such potential health benefits of bee pollen are particularly linked to the presence of phenolic compounds [1,15]. Studies analyzing the chemical composition of bee pollen verify that it contains several flavonoids (e.g., kaempferol, quercetin, and isorhamnetin,) and flavonoid glycosides among other simple phenolics [4,10,16,17]. Even though this class of compounds is mostly non-nutritive in the diet for humans, there is some evidence to suggest that modest consumption in the long term may reduce the incidence of certain cancers and chronic diseases [18]. Reactive oxygen (ROS) and nitrogen species (RNS) produced owing to the metabolic activity of cells or due to environmental factors can damage biological molecules, such as DNA, enzymes, and cells, and possibly contribute to cellular dysfunction and disease [19,20]. Phenolic compounds have the potential to reduce the adverse effects of ROS and RNS based on various antioxidant action mechanisms. For example, the binding of metal ions needed for catalysis of ROS generation, the scavenging of ROS and RNS or their precursors, the upregulation of endogenous antioxidant enzymes, or the repair of oxidative damage to biomolecules [20]. Additionally, some phenolic compounds react directly with free radicals, quenching them without reacting with other cell components [19–21].

It is obvious that more research is needed to reveal food and pharmacological characteristics of bee pollen, leading us to categorize them as mono- and polyfloral and determine the properties of each botanical origin accurately. Even though some countries established standards for bee pollen according to their own national regulations [1], this natural product lacks international standardization. Indeed, it has been emphasized in numerous studies that there is a requirement for more research based on the chemical composition of different bee pollens by referring to their botanical origins [1,2,7,14].

To fulfill this lack, we aimed to understand the link between the antioxidant and anti-tumor potentials of mono- and polyfloral bee pollen samples from Morocco depending on the type and abundance of bioactive compounds evaluated by liquid chromatography coupled to diode array detection and electrospray ionization tandem mass spectrometry (LC/DAD/ESI-MS<sup>n</sup>) and gas chromatography–mass spectrometry (GC-MS). In particular, the number of studies that associate the presence of volatile compounds and phenylamides, which represents a significant amount of the bioactive content of bee pollen, with the biological activities is still very limited.

## 2. Results and Discussion

### 2.1. Color and Palynological Assessment

Color and palynological analytical results of bee pollen samples are given in Table 1. Visual inspection of bee pollen loads revealed diversity in color, including light purple, light yellow, orange, yellow, and dark yellow. A notable particularity among the samples was that between BP7 and BP8, the samples had slightly different colors even though they came from the same pollen species. This could most likely be explained by the presence of minor pollen species. However, the oxidation of the samples by exposure to air or light [22] cannot be dismissed.

**Table 1.** Geographical location, codes, colors, and botanical origin of bee pollen samples.

Geographical Location	Sample Code	Visual Color	Family	Relative Frequency (%) of Pollen Types	Classification
Larache, MR	BP1	Light purple	Apiaceae	<i>Coriandrum</i> and <i>Daucus</i> sp. (100%)	Monofloral
Khenichat, MR	BP2	Yellow	Brassicaceae	<i>Brassica</i> sp. (60%), <i>Sinapis</i> sp. (30%) and <i>Tamarix</i> sp. (<10%) <i>Carduus</i> / <i>Galactites</i> sp. (35%), <i>Taraxacum</i> sp. (17%), <i>Scorzonera</i> / <i>Lactuca</i> sp. (8%), <i>Bellis</i> sp. (8%), <i>Olea europaea</i> (8%) and <i>Echium</i> sp. (6%), <i>Eucalyptus</i> sp. (3%)	Polyfloral
Had Kourt, MR	BP3	Orange	Asteraceae	<i>Olea europaea</i> (>85%), <i>Tamarix</i> sp. (<5%)	Polyfloral
Kenitra, MR	BP4	Dark yellow	Oleaceae	<i>Raphanus</i> sp. (>80%) and <i>Sinapis</i> sp. (<10%)	Monofloral
Fez, MR	BP5	Dark yellow	Brassicaceae	<i>Helianthemum</i> sp. (>70%) and <i>Anthemis</i> sp. (<10%), <i>Lhytrum</i> sp. (<5%)	Polyfloral
Sefrou, MR	BP6	Orange	Cistaceae	<i>Ononis spinosa</i> / <i>Astragalus</i> sp. (>90%), <i>Lhytrum</i> sp. and <i>Quercus</i> sp. (<10%)	Monofloral
Arfoud, MR	BP7	Light yellow	Fabaceae	<i>Ononis spinosa</i> / <i>Astragalus</i> sp. (>90%), <i>Lhytrum</i> sp. and <i>Quercus</i> sp. (<10%)	Monofloral
Taza, MR	BP8	Yellow	Fabaceae	<i>Ononis spinosa</i> / <i>Astragalus</i> sp. (>90%), <i>Lhytrum</i> sp. and <i>Quercus</i> sp. (<10%)	Monofloral

MR: Morocco, BP: bee pollen.

The botanical origin of the bee pollen samples was easily distinguished under the light microscope according to the morphology of the pollen grains, although, it was challenging to distinguish the species of some pollen grains from the same type because of the high morphological similarity. In these cases, only the genus name was indicated, as in *Coriandrum*, *Carduus*, or *Ononis*. The sample was considered monofloral when the relative frequency of pollen species was  $\geq 80\%$  [23]. The results allowed the classification of five samples as monofloral and three samples as polyfloral. BP1, BP2, BP4, BP5, and BP8 bee pollen samples were assigned to the monofloral classes originated from *Coriandrum* (100%), *Brassica* (90%), *Olea europaea* (100%), *Raphanus* (>80%), and *Ononis* (>95%), respectively. Other samples exhibited pollen species of various botanical origins at different relative frequencies, as in Table 1. These pollens are common to other previously identified in Moroccan bee products, particularly in honeydew honey [24] and bee bread samples (natural fermented bee pollen observed inside the hive) [25]. Evidently, it is quite possible that the harvested bee pollen samples in the same or nearby geographic areas may reveal different botanical origins, as this may vary in line with the dominant flora in the area where the apiaries are located as well as honeybee preference [1].

## 2.2. Total Phenolic and Flavonoid Content

As shown in Figure 1a, the hydroethanolic bee pollen extracts resulted in a wide range of total phenolic content. The values ranged between  $2.7 \pm 0.6$  and  $16.8 \pm 1.1$  mg of gallic acid equivalents per g of bee pollen (mg GAE/g), with more than six-fold variation. Three extracts exhibited relatively high phenolic contents ( $>10$  mg GAE/g): BP7 ( $16.8 \pm 1.1$  mg GAE/g), BP5 ( $12.1 \pm 0.3$  mg GAE/g), and BP4 ( $10.3 \pm 0.7$  mg GAE/g). In contrast, BP8 and BP1 presented the lowest phenolic contents, with values of  $2.7 \pm 0.6$  and  $3.7 \pm 0.1$  mg GAE/g, respectively. The most notable point among the results was that the samples with the highest and lowest phenolic contents had the same main pollen type, *Ononis*, as given in Table 1. However, while sample BP8 is monofloral with *Ononis* ( $>95\%$ ), sample BP7 is polyfloral and contains other pollen types, such as *Lythrum* or *Acacia*, which may be responsible for the increment in the phenolic content.

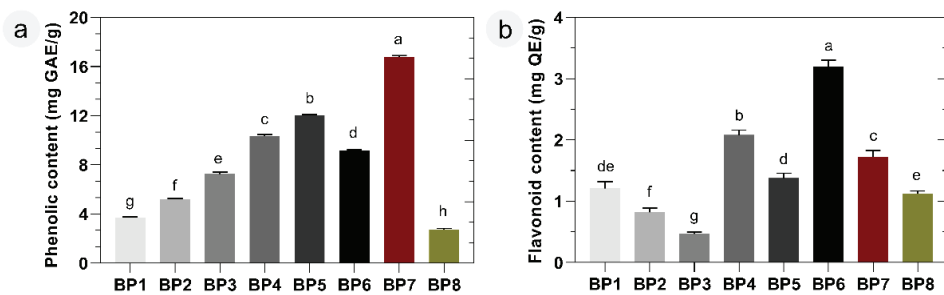


**Figure 1.** (a) Phenolic content and (b) flavonoid content of mono- and polyfloral bee pollen samples. Different letters (a–h) indicate significant differences on the phenolic content ( $p < 0.05$ ).

The flavonoid content of bee pollen samples was measured by the aluminum chloride method, which is commonly employed to determine the amount of flavonoids, and the results were illustrated in Figure 1b. The highest flavonoid content was recorded in the BP6 extract ( $3.2 \pm 0.1$  mg of quercetin equivalents per g of bee pollen (mg QE/g), which was dominated by *Helianthemum* ( $>78\%$ ) from the Cistaceae family. The BP6 was followed by BP4, BP7, and BP5 extracts, with values of  $2.1 \pm 0.1$ ,  $1.7 \pm 0.2$ , and  $1.4 \pm 0.2$  mg QE/g, respectively. Among the analyzed samples, these three samples demonstrated the highest values of total phenolic compounds with a positive correlation. Concerning samples BP1, BP2, and BP3, a decrease in the flavonoid content was observed in contrast with the increase in the total phenolic content, Figure 1a,b. The findings revealed that high phenolic content may not always correlate with high flavonoid content, as stated by some authors before [26].

The total phenolic or flavonoid values of the tested bee pollen were significantly ( $p < 0.05$ ) different from each other in multiple comparisons, with one exception (BP1–BP8 in flavonoid content). Our trends are similar to the findings of Morais et al. [27] and Araújo et al. [28], who stated that the total phenolic (from 10.5 to 16.8 mg GAE/g;  $n = 5$ ) and flavonoid content of bee pollen samples (from 1.4 to 9.1 mg QE/g;  $n = 9$ ) could lead to variable values depending on the pollen species. Additionally, the present results are also consistent with other studies previously reported for bee pollen at different geographic locations [12,17,29].

## 2.3. LC/DAD/ESI-MS<sup>n</sup> Bioactive Compounds Analysis

The optimized chromatographic conditions provided the identification and quantification of the bioactive compounds in the Moroccan bee pollen samples. The ESI source in negative ion mode was chosen for the assessment of the compounds, and the most intense peak in MS was selected as the precursor ion ( $m/z$ ). The compound identification was performed according to the detected precursor ion and MS/MS fragmentation by comparison with standards and reported data in the literature. When this information was

not available, the MS data were validated by combining the described UV (ultraviolet) spectra and retention time data available in the literature. The quantification was performed through the chromatogram at 280 nm and using the calibration curves of the phenolic compound with the closest structural similarity.

The chromatographic profile allowed the identification of a total of 48 bioactive compounds in the bee pollen samples, of which 31 were flavonoids, mostly flavonol glycosides; 13 were phenylamide compounds; and 4 were phenolic acids, as in Tables 2 and S1.

Myricetin, quercetin, isorhamnetin, kaempferol, and herbacetin glycosides were the most abundant flavonoids identified, consistent with previous studies reporting them as the main phytochemical compounds in bee pollen of various botanical origins [1,4,14].

Bee pollen flavonol aglycones presented a series of losses associated to different sugar moieties, such as pentosides, hexosides, deoxyhexosides, and deoxyhexosyl-hexosides. The peaks corresponding to acetyl glycosides and malonyl glycosides were observed in several compounds. Peak 6 presented a pseudomolecular ion  $[M-H]^-$  at  $m/z$  667, releasing an  $MS^2$  fragment at  $m/z$  316 ( $[M-H-350]^-$ , loss of an acetyl deoxyhexosyl-hexoside moiety), corresponding to myricetin, as in Figures 2 and 3a. Additionally, Peak 14 was identified as a myricetin derivate with a  $[M-H]^-$  at  $m/z$  565 and presented a fragmentation pattern with an  $MS^2$  with an ion at  $m/z$  521 formed by the loss of a carboxyl group ( $-44u$ ). The following  $MS^3$  spectrum indicated a loss of an acetyl hexoside moiety ( $-204u$ ). The compound was tentatively identified as myricetin-*O*-malonyl hexoside, as in Figures 2 and 3b. A similar fragmentation pattern was observed for other flavonol glycoside derivatives, such as quercetin-*O*-malonyl deoxyhexosyl-hexoside (peak 20,  $m/z$  695), isorhamnetin-*O*-malonyl pentosyl-hexoside (peak 25,  $m/z$  695), 3',4',5',3,5,6,7-heptahydroxy-flavonol-*O*-malonyl hexoside (peak, 27,  $m/z$  579), and kaempferol-*O*-malonyl rutinoides (peak 31,  $m/z$  533), as in Figure 2 and Tables 2 and S1.

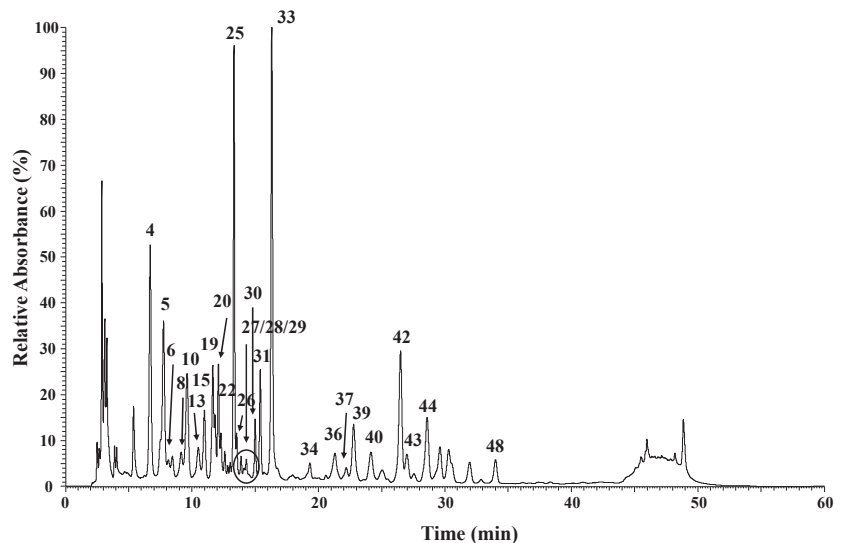


Figure 2. Chromatographic profile at 280 nm for BP6 phenolic extract.

Table 2. Phenolic and phenylamide profile of Moroccan bee pollen samples. The values are expressed as mg of each compound/g of bee pollen.

Peak	Proposed Compound	BP1	BP2	BP3	BP4	BP5	BP6	BP7	BP8
1	Caffeic acid hexoside	0.36 ± 0.40	nd	nd	nd	0.14 ± 0.00	nd	nd	nd
2	Caffeic acid	nd	nd	nd	nd	nd	nd	nd	0.15 ± 0.00
3	<i>p</i> -coumaric acid hexoside	0.22 ± 0.02	0.16 ± 0.00	nd	nd	nd	nd	nd	nd
4	Myricetin-3- <i>O</i> -rutinoside	nd	nd	0.17 ± 0.00	nd	nd	0.80 ± 0.01	nd	nd
5	Quercetin- <i>O</i> -diglucoside	0.98 ± 0.02	1.77 ± 0.01	0.20 ± 0.00	3.30 ± 0.12	1.15 ± 0.10	0.53 ± 0.21	0.74 ± 0.00	0.43 ± 0.00
6	Myricetin- <i>O</i> -acetyl deoxyhexosyl-hexoside	nd	nd	nd	nd	nd	0.18 ± 0.01	nd	nd
7	Methylherbacetin- <i>O</i> -dihexoside	nd	0.17 ± 0.00	0.18 ± 0.01	nd	nd	nd	nd	nd
8	Myricetin- <i>O</i> -hexoside	nd	nd	nd	nd	nd	0.20 ± 0.01	nd	nd
9	Quercetin- <i>O</i> -pentosyl-hexoside	nd	nd	nd	nd	nd	nd	nd	0.17 ± 0.00
10	Quercetin-3- <i>O</i> -rutinoside	nd	nd	0.21 ± 0.00	0.38 ± 0.01	0.33 ± 0.06	0.48 ± 0.02	nd	nd
11	Kaempferol- <i>O</i> -diglucoside	nd	0.74 ± 0.00	nd	nd	0.83 ± 0.01	nd	0.30 ± 0.04	0.22 ± 0.00
12	Isorhamnetin- <i>O</i> -deoxyhexosyl- <i>O</i> -hexoside	nd	nd	nd	0.24 ± 0.01	nd	nd	nd	nd
13	Myricetin- <i>O</i> -malonyl hexoside	nd	nd	nd	nd	nd	0.24 ± 0.00	nd	nd
14	Methylherbacetin-3- <i>O</i> -rutinoside	nd	nd	0.18 ± 0.00	nd	nd	nd	nd	0.17 ± 0.00
15	Kaempferol- <i>O</i> -deoxyhexosyl- <i>O</i> -hexoside	nd	nd	nd	nd	0.22 ± 0.01	0.32 ± 0.01	nd	nd
16	Isorhamnetin- <i>O</i> -pentosyl-hexoside	nd	nd	0.18 ± 0.01	nd	nd	nd	0.17 ± 0.00	0.17 ± 0.00
17	Isorhamnetin- <i>O</i> -pentosyl-hexoside (isomer)	nd	nd	nd	nd	nd	nd	nd	0.20 ± 0.00
18	<i>p</i> -coumaric acid	0.20 ± 0.00	nd	nd	nd	nd	nd	nd	nd
19	Quercetin- <i>O</i> -malonyl deoxyhexosyl-hexoside	nd	nd	nd	nd	nd	0.23 ± 0.03	nd	nd
20	Kaempferol-3- <i>O</i> -rutinoside	nd	nd	0.17 ± 0.01	nd	0.30 ± 0.05	0.29 ± 0.00	0.23 ± 0.01	0.18 ± 0.00
21	Isorhamnetin-3- <i>O</i> -hexosyl-deoxyhexoside	nd	nd	nd	nd	nd	nd	nd	0.81 ± 0.20
22	Quercetin-3- <i>O</i> -glucoside	nd	nd	nd	0.35 ± 0.00	nd	0.19 ± 0.00	nd	nd
23	Isorhamnetin- <i>O</i> -malonyl rutinoside	nd	nd	0.21 ± 0.00	nd	nd	nd	nd	nd
24	Isorhamnetin- <i>O</i> -malonyl pentosyl-hexoside	nd	nd	0.28 ± 0.00	nd	nd	nd	nd	nd
25	Quercetin- <i>O</i> -malonyl hexoside	nd	nd	0.22 ± 0.00	nd	nd	0.84 ± 0.00	nd	nd
26	3',4',5',3',5',6,7-heptahydroxyflavonol- <i>O</i> -malonyl hexoside	nd	nd	nd	nd	nd	0.18 ± 0.00	nd	nd
27	Quercetin- <i>O</i> -malonyl hexoside (isomer)	nd	nd	nd	nd	nd	0.17 ± 0.00	nd	nd
28	Quercetin-3- <i>O</i> -rhamnoside	0.20 ± 0.01	nd	nd	nd	nd	1.19 ± 0.00	nd	nd
29	Isorhamnetin-3- <i>O</i> -glucoside	nd	nd	0.20 ± 0.00	nd	nd	0.20 ± 0.00	nd	0.16 ± 0.00
30	Kaempferol- <i>O</i> -malonyl rutinoside	nd	nd	0.19 ± 0.01	nd	nd	0.25 ± 0.01	nd	nd

Table 2. Cont.

Peak	Proposed Compound	BP1	BP2	BP3	BP4	BP5	BP6	BP7	BP8
31	Isorhamnetin- <i>O</i> -malonyl hexoside	nd	nd	0.26 ± 0.00	nd	nd	0.37 ± 0.01	nd	nd
32	Kaempferol-3- <i>O</i> -rhamnoside	1.60 ± 0.01	nd	0.21 ± 0.01	0.38 ± 0.03	nd	nd	nd	0.17 ± 0.00
33	Quercetin-3- <i>O</i> -rhamnoside	0.20 ± 0.01	nd	nd	nd	nd	1.19 ± 0.00	nd	nd
34	<i>N</i> <sup>1</sup> - <i>p</i> -coumaroyl- <i>N</i> <sup>5</sup> , <i>N</i> <sup>10</sup> -dicaffeoylspermidine	nd	nd	nd	nd	0.24 ± 0.06	0.16 ± 0.00	0.36 ± 0.01	nd
35	<i>N</i> <sup>1</sup> , <i>N</i> <sup>5</sup> , <i>N</i> <sup>10</sup> - <i>tri-p</i> -coumaroylspermidine	nd	nd	0.15 ± 0.00	nd	0.18 ± 0.00	nd	nd	nd
36	Kaempferol	nd	nd	nd	nd	nd	0.30 ± 0.00	2.80 ± 0.03	0.42 ± 0.00
37	Isorhamnetin	nd	nd	nd	nd	nd	0.19 ± 0.00	1.57 ± 0.08	0.15 ± 0.00
38	<i>N</i> <sup>1</sup> , <i>N</i> <sup>5</sup> - <i>di-p</i> -coumaroyl- <i>N</i> <sup>10</sup> -caffeoylspermidine	nd	nd	nd	nd	nd	nd	0.51 ± 0.02	nd
39	<i>N</i> <sup>10</sup> - <i>tri-p</i> -coumaroylspermidine (isomer)	nd	nd	nd	nd	0.25 ± 0.00	0.23 ± 0.00	2.48 ± 0.01	0.24 ± 0.00
40	<i>N</i> <sup>10</sup> - <i>tri-p</i> -coumaroylspermidine (isomer)	nd	nd	nd	nd	0.19 ± 0.02	0.19 ± 0.00	1.61 ± 0.01	0.17 ± 0.00
41	<i>N</i> <sup>1</sup> , <i>N</i> <sup>5</sup> , <i>N</i> <sup>10</sup> - <i>tri-p</i> -coumaroylspermidine (isomer)	nd	nd	nd	nd	nd	nd	0.61 ± 0.02	0.15 ± 0.00
42	<i>N</i> <sup>10</sup> - <i>tri-p</i> -coumaroylspermidine (isomer)	nd	nd	0.19 ± 0.06	nd	0.32 ± 0.00	0.34 ± 0.00	10.52 ± 0.11	0.22 ± 0.00
43	Tetracoumaroyl spermine	nd	nd	0.20 ± 0.04	nd	nd	0.15 ± 0.01	nd	nd
44	Tetracoumaroyl spermine (isomer)	nd	nd	0.23 ± 0.06	nd	nd	0.22 ± 0.04	nd	nd
45	Tetracoumaroyl spermine (isomer)	nd	nd	0.14 ± 0.00	nd	nd	nd	nd	nd
46	Tetracoumaroyl spermine (isomer)	nd	nd	0.17 ± 0.01	nd	nd	nd	nd	nd
47	Tetracoumaroyl spermine (isomer)	nd	nd	0.16 ± 0.02	nd	nd	nd	nd	nd
48	Tetracoumaroyl spermine (isomer)	nd	nd	0.16 ± 0.02	nd	nd	0.16 ± 0.01	nd	nd
	Total phenolic acids (mg/g)	0.78	0.16	—	—	0.14	—	—	0.15
	Total flavonoids (mg/g)	2.98	2.68	2.86	4.65	2.83	8.82	5.81	3.25
	Total phenylamide derivatives (mg/g)	—	—	1.40	—	1.18	1.45	16.09	0.78



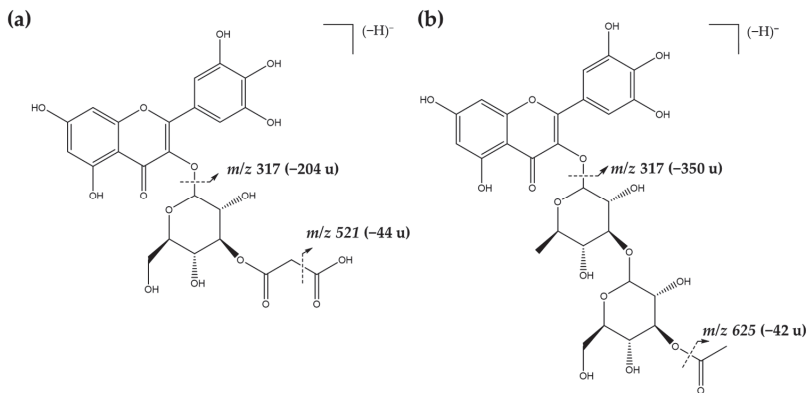


**Figure 3.** Mass fragmentation pattern for the tentative identification of (a) myricetin-*O*-acetyl deoxyhexosyl-hexoside and (b) myricetin-*O*-malonyl hexoside present in sample BP6.

Compounds such as quercetin-*O*-diglucoside, kaempferol-*O*-diglucoside, and kaempferol-3-*O*-rutinoside—assigned to the precursor ions  $[M-H]^-$  at  $m/z$  625,  $m/z$  609, and  $m/z$  593—were the most common flavonoid glycosides within all samples. These compounds have been reported in Portuguese bee pollen, which had predominantly *Plantago* sp., *Crepis capillaris*, and *Cytisus striatus* pollen species [10].

Comparing the samples individually, BP6 exhibited a profile with more diversity of phenolic compounds and the highest total concentration (8.8 mg/g), which was in accordance with the previous results in the flavonoid content of it. A similar situation was observed for the BP3 sample concerning the diversity of compounds. This could be related to the polyfloral nature of BP3 and BP6, for which different plant sources contribute to the high diversity of compounds. On the other hand, BP2, with 60% *Brassica* pollen, was the poorest in terms of compounds. Chromatographic results also revealed that Moroccan bee pollen samples contained four phenolic acids—caffeic acid ( $m/z$  179), caffeic acid hexoside ( $m/z$  341), *p*-coumaric acid ( $m/z$  163), and *p*-coumaric acid hexoside ( $m/z$  325)—at low concentrations in BP1, BP2, BP5, and BP8. Such phenolic acids have a wide distribution in the plant kingdom, and their presence has been associated with biological activities such as antiproliferative, antioxidant, and antimicrobial activities [30,31].

The employed chromatographic method allowed the identification of another group of chemical compounds, phenylamides. Even though these compounds have not been the subject of research often, they are responsible for some functions in plants. Phenylamides exist in high concentrations in higher plants, especially on the surface of male reproductive organs, namely pollen [32]. The reason for this is still a mystery, yet some researchers have stated that these compounds may be related to the protection of plant genetic material inside pollen grains from UV light [32]. Regardless, these compounds are obviously a major component of pollen grains, including bee pollen [4,17]. Phenylamides are molecular products chemically formed via covalent bonds between the carboxylic groups of hydroxycinnamic acids (e.g., coumaric acid, ferulic acid, and caffeic acid) and amine groups of aliphatic di- and polyamines or aromatic monoamines [33].

Phenylamide compounds were not detected in samples BP1, BP2, and BP4, as shown in Table 2, which can be due to the low concentration of these compounds in the samples or be related to the applied extraction method. The rigid pollen double-layer can have meaningful effects on the recovery of compounds as previously discussed when applying different extraction techniques [17]. Among the peaks detected in bee pollen phenolic extracts, all phenylamides showed specific UV spectra with a UVmax at around 298 and 310 nm, [4], as in Table 2 and Table S1.

Confirmed with: <sup>a</sup> MS<sup>n</sup> fragmentation; <sup>b</sup> Standard; References: <sup>c</sup> Kang et al. [34]; <sup>d</sup> El Ghouizi et al. [4]; <sup>e</sup> Aylanc et al. [10]; <sup>f</sup> Sobral et al. [35]; <sup>g</sup> Llorach et al. [36]; <sup>h</sup> Falcão et al. [37]; <sup>i</sup> Mihajlovic et al. [38]. BP: bee pollen. nd: not detected.

Moroccan bee pollen contained several phenylamides, such as *N*<sup>1</sup>-*p*-coumaroyl-*N*<sup>5</sup>; *N*<sup>10</sup>-dicaffeoylspermidine (*m/z* 614); *N*<sup>1</sup>, *N*<sup>5</sup>, *N*<sup>10</sup>-tri-*p*-coumaroylspermidine (*m/z* 582) and its four isomers; *N*<sup>1</sup>, *N*<sup>5</sup>-di-*p*-coumaroyl-*N*<sup>10</sup>-caffeoylspermidine (*m/z* 598); and tetra-coumaroyl spermine (*m/z* 785) and its five isomers. *N*<sup>1</sup>, *N*<sup>5</sup>, *N*<sup>10</sup>-tri-*p*-coumaroylspermidine was the most common compound among the samples, with a concentration of 10.5 ± 0.1 mg/g in BP7, implying approximately a 10-fold difference compared to the average of other samples. Previously [17], this phenylamide was described in high concentrations in bee pollen samples containing mainly *Jasione montana* (Campanulaceae family), *Eucalyptus* (Myrtaceae), and *Rubus* (Rosaceae). Another common compound in the bee pollen samples was the tetracoumaroyl spermine and its isomers, present in BP3 and BP6 samples with concentrations ranging from 0.14–0.23 mg/g.

#### 2.4. Volatile Compounds Profiling

Mono and polyfloral bee pollen volatile compounds were extracted using the solid phase microextraction (SPME) technique followed by GC-MS analysis. The quantification was obtained directly from the total ion chromatogram (TIC) and expressed as a relative percentage. Linear retention indices (LRI) were calculated for each component detected. The list of volatile compounds with the calculated LRI and relative concentration (R%) is given in Table 3 and Table S2. Moroccan bee pollen presented a wide variety of volatile compounds, with a total of 47 compounds identified, which included 13 aldehydes, 12 esters, 5 hydrocarbons, 5 ketones, 5 terpenes (3 oxygen-containing monoterpenes, 1 monoterpene hydrocarbon, and 1 sesquiterpene hydrocarbon), 4 carboxylic acids, and 1 ether. The great diversity in the composition is due to the different botanical origins, but may also be influenced by the harvesting time, conservation methods, and extraction methodology [39].

Generally, the most common and abundant compounds were hexanal, ranging from 5.3 to 59.8%, and 3,5-octadien-2-one and its isomer, with a concentration ranging from 2.6 to 27.5%. Additionally, octanoic acid was present in all samples in a range from 1.9 to 7.7%, with the exception of the BP8 sample. 3,5-octadien-2-one (22.9%) and octanal (16.6%) were the most dominant compounds in *Coriandrum* monofloral bee pollen (BP1). In total, six volatile organic compounds were identified in BP2, and 2,4-heptadienal (33.6%) and hexanal (14.9%) from the aldehyde group were detected in high percentages. Additionally, 3,5-octadien-2-one (27.5%) from the ketone group and eucalyptol (10.6%) from the oxygen-containing monoterpenes were found in high concentrations. Volatile compounds, such as hexanal and octanal, were previously identified as being common in different bee pollen samples from Croatia [40], and the presence of eucalyptol was also detected at a relatively low rate (1.9%) in bee pollen samples from Latvia [29]. BP3 sample showed a rich profile in fatty acids and their esters, including hexanoic acid (20.3%), ethyl decanoate (16.7%), ethyl octanoate (14.8%), and methyl octanoate (11.5%). Various organic compounds from different classes were present in the BP4 and BP5 samples, in which methyl octanoate (13.1%) and hexanoic acid (20.5%) were the main compounds in each sample, respectively. Volatile organic compound results reported for polyfloral bee pollen samples (*n* = 16) in a study conducted by Prudun et al. [40] revealed the presence of these two compounds, and yet the samples had different botanical origins than those described in the current study. As previously described for the other samples, BP6 and BP7 presented high concentrations of 3,5-octadiene-2-one, with values of 12.4% and 23.9%, respectively. Hexanal was also identified as one of the main compounds in BP6 (12.3%), BP7 (21.0%), and BP8, which showed a relative percentage of 59.8%. This revealed that *Ononis* bee pollen is a good source of aldehydes. Some authors previously stated that hexanal is biologically active, emphasizing its significant effect on the inhibition of microbiological contaminants [41].

**Table 3.** Identification and quantification of volatile compounds in Moroccan bee pollen samples. The values are expressed as the relative percentage (R%).

Peak	Compound	BP1	BP2	BP3	BP4	BP5	BP6	BP7	BP8
1	2-propenylidene-cyclobutene	nd	nd	nd	nd	4.3 ± 0.7	nd	nd	4.7 ± 1.5
2	Hexanal	5.3 ± 0.8	14.92 ± 2.5	nd	nd	nd	12.3 ± 1.4	21.0 ± 2.3	59.8 ± 5.9
3	2-hexenal	2.2 ± 0.7	nd	nd	nd	nd	nd	5.5 ± 0.3	8.5 ± 2.4
4	Heptanal	nd	nd	nd	nd	nd	nd	nd	6.2 ± 0.3
5	2,5-dimethyl-pyrazine	3.9 ± 1.8	nd	nd	nd	nd	nd	nd	nd
6	1,2-cyclopentanediol	nd	nd	nd	0.9 ± 0.0	nd	nd	nd	nd
7	2,4-heptadienal	8.5 ± 2.9	33.6 ± 12.1	nd	nd	nd	nd	11.5 ± 1.2	nd
8	Ethyl hexanoate	nd	nd	nd	nd	nd	5.0 ± 0.8	nd	nd
9	Octanal	16.6 ± 1.3	nd	nd	nd	nd	nd	nd	nd
10	2,4-heptadienal (isomer)	9.2 ± 0.3	nd	nd	nd	nd	nd	nd	nd
11	Hexanoic acid	nd	nd	20.3 ± 3.4	nd	20.5 ± 2.3	nd	nd	nd
12	Eucalyptol	nd	10.6 ± 1.6	nd	nd	nd	6.4 ± 0.5	nd	nd
13	3,5-octadien-2-one	22.9 ± 2.1	27.5 ± 1.8	nd	nd	2.6 ± 1.2	12.4 ± 1.3	23.9 ± 3.4	nd
14	2,6,6-trimethylbicyclo [3.1.1]hept-3-ylamine	5.9 ± 1.0	nd	nd	nd	nd	nd	nd	nd
15	3,5-octadien-2-one (isomer)	12.7 ± 3.6	nd	nd	nd	nd	nd	25.6 ± 1.0	nd
16	Nonanal	1.9 ± 0.6	nd	nd	1.3 ± 0.1	nd	nd	1.7 ± 0.2	5.1 ± 1.1
17	Cis-β-terpineol	nd	nd	nd	nd	8.3 ± 0.8	nd	nd	nd
18	Methyl octanoate	nd	nd	nd	nd	nd	nd	1.4 ± 0.1	nd
19	Lilac aldehyde D	1.4 ± 0.1	nd	nd	nd	nd	nd	nd	nd
20	2,6-nonadienal	nd	nd	nd	nd	nd	nd	nd	nd
21	Isopinocarveol	nd	nd	nd	nd	nd	nd	nd	3.0 ± 0.3
22	Octanoic acid	4.3 ± 0.1	7.4 ± 0.6	2.9 ± 0.7	5.2 ± 1.4	7.5 ± 1.4	7.7 ± 0.8	1.3 ± 0.5	nd
23	Ethyl octanoate	nd	5.9 ± 2.0	14.8 ± 2.7	3.3 ± 0.2	nd	nd	1.9 ± 0.4	nd
24	Lilac alcohol D	3.8 ± 0.7	nd	nd	nd	nd	nd	1.2 ± 0.4	nd
25	β-cyclocitral	nd	nd	nd	nd	2.7 ± 0.6	nd	nd	nd
26	Methyl 7-hexanoate	nd	nd	nd	nd	nd	1.4 ± 0.4	nd	nd
27	Methyl nonanoate	nd	nd	nd	nd	nd	nd	1.5 ± 0.5	nd
28	Anisaldehyde	nd	nd	nd	5.7 ± 1.4	nd	nd	nd	nd
29	Geranyl vinyl ether	nd	nd	0.5 ± 0.0	nd	nd	nd	nd	nd
30	3-cyclohex-1-enyl-prop-2-enal	1.3 ± 0.2	nd	nd	nd	nd	nd	nd	nd
31	2-methyl-1-nonene-3-ine	nd	nd	nd	nd	nd	nd	nd	3.0 ± 0.2

Table 3. Cont.

Peak	Compound	BP1	BP2	BP3	BP4	BP5	BP6	BP7	BP8
32	Ethyl nonanoate	nd	nd	3.1 ± 1.2	3.3 ± 0.2	7.41 ± 2.00	nd	1.2 ± 0.8	nd
33	Nonanoic acid	nd	nd	nd	nd	8.22 ± 2.50	nd	1.6 ± 0.2	nd
34	Methyl 8-methyl-nonanoate	nd	nd	nd	nd	nd	nd	0.7 ± 0.1	nd
35	3-methyl-2-pent-2-enyl-cyclopent-2-enone	nd	nd	nd	2.4 ± 0.7	nd	nd	nd	nd
36	Ethyl decanoate	nd	nd	nd	nd	nd	10.9 ± 2.5	nd	nd
37	Methyl octanoate	nd	nd	11.5 ± 3.0	13.1 ± 2.3	nd	11.8 ± 2.1	nd	nd
38	Caryophyllene	nd	nd	nd	3.8 ± 0.3	nd	nd	nd	nd
39	Decanoic acid	nd	nd	nd	nd	nd	22.8 ± 1.3	nd	nd
40	6,10-dimethyl-5,9-undecadien-2-one	nd	nd	nd	8.4 ± 1.4	17.6 ± 2.8	nd	nd	nd
41	4,6-dimethyl-(Z)-5,9-undecadien-2-one	nd	nd	5.7 ± 0.2	nd	nd	nd	nd	nd
42	β-ionone	nd	nd	nd	nd	1.6 ± 0.3	nd	nd	nd
43	β-ionone epoxide	nd	nd	nd	nd	11.7 ± 0.1	nd	nd	nd
44	10-methyl-methyl undecanoate	nd	nd	1.1 ± 0.5	nd	nd	nd	nd	nd
45	Ethyl decanoate	nd	nd	16.7 ± 4.3	1.4 ± 0.4	nd	nd	nd	nd
46	Ethyl dodecanoate	nd	nd	nd	nd	7.4 ± 1.8	nd	nd	nd
47	5-(1-piperidyl)-furan-2-carboxaldehyde	nd	nd	2.7 ± 1.4	nd	nd	nd	nd	nd

Although volatile compounds are not frequently associated with properties such as antioxidant and antitumor, which we discuss in the next section, they are known to have some biological activities, and revealing their presence may significantly affect consumers' preferences due to factors such as taste and aroma when bee pollen is used as a food supplement and food ingredient [29,40]. It is therefore important to identify the compounds present by referring to the botanical origin of bee pollen.

## 2.5. Biological Activity

### 2.5.1. Antioxidant Capacity

The antioxidant capacities of mono- and polyfloral Moroccan bee pollen samples were measured by DPPH (2,2-diphenyl-1-picrylhydrazyl), ABTS [2,2'-azinobis-(3-ethyl-benzothiazoline-6-sulfonic acid)], and reducing power assays and the results are shown in Figure 4a–c.

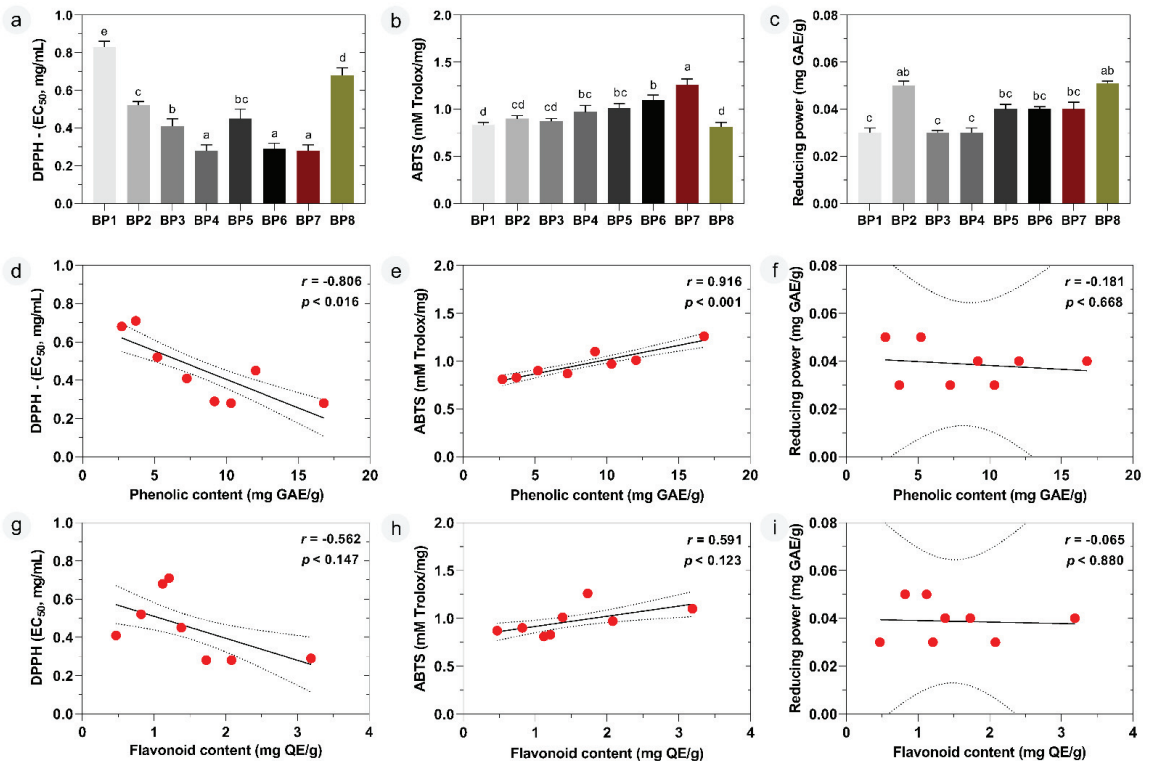


**Figure 4.** Antioxidant activity of mono- and polyfloral bee pollen samples. (a) DPPH free radical scavenging activity; (b) ABTS free radical scavenging activity; (c) reducing power activity and correlation of (d,g) DPPH; (e,h) ABTS; and (f,i) reducing power activity with phenolic content and flavonoid, respectively. Different letters (a–e) mean significant differences ( $p < 0.05$ ).  $r$ : Pearson's correlation coefficient.

DPPH radical scavenging activities ranged from EC<sub>50</sub> 0.71 mg/mL to EC<sub>50</sub> 0.28 mg/mL, which indicates a 2.5-fold change. Here, a low EC<sub>50</sub> value indicates high radical scavenging activity. The monofloral sample BP7 exhibited the highest antioxidant activity (0.28 mg/mL) together with *Olea europaea* monofloral bee pollen (BP4), followed by BP6 (0.29 mg/mL), BP3 (0.41 mg/mL), BP5 (0.45 mg/mL), and BP2 (0.52 mg/mL).

In the ABTS assay, the radical scavenging values ranged between 0.81 and 1.26 mM Trolox equivalents per mg of bee pollen, which represent a lower (approximately 1.6-fold) variation compared to the DPPH. As in the DPPH assay, here the BP7 sample showed the highest antioxidant activity with a value of 1.26 mM Trolox/mg, followed by BP6 (1.10 mM Trolox/mg), BP5 (1.01 mM Trolox/mg) and BP4 (0.97 mM Trolox/mg). Along with this, BP1 and BP8, representing monofloral bee pollen samples of *Coriandrum* and *Ononis*, respectively, had the lowest activity in both radical scavenging tests.

The results of the reducing power assay to measure the reduction potential ( $\text{Fe}^{3+} \rightarrow \text{Fe}^{2+}$ ) of bioactive compounds in bee pollen samples were slightly different from the other two antioxidant assay findings. Among the samples, high reducing power activity was measured as 0.05 mg GAE/g in BP2 and BP8, while the lowest value was measured as 0.03 mg GAE/g in BP1, BP3 and BP4. The remaining samples showed an antioxidant capacity of 0.04 mg GAE/g.

Researchers agree that a single method is often not sufficient to quantify the potential activities of antioxidants, so employing antioxidant quantification assays based on different working principles is a necessary method of comprehensively evaluating the material under analysis [17,31,42]. Antioxidant results obtained from the current study demonstrated that some samples, such as BP4, BP5, BP6, and BP7, contain pollen species with potent free radical scavengers with minor reducing power activity. The antioxidant potential of the samples could be attributed to their total bioactive compound content, especially to the phenolics [10,29]. The phenolic and flavonoid contents and the calculated total amount of phenolic compounds from the LC-DAD-ESI-MS<sup>n</sup> analysis were highest in the BP4, BP5, BP6, and BP7 bee pollen samples, which were those that exhibited higher radical scavenging profiles in the DPPH and ABTS assays. This situation indicated the existence of a correlation between the amount of phenolic compounds and antioxidant capacity, with a strong relationship between radical scavenging activity and total phenolic content (Figure 4d,e), as well as a moderate correlation with flavonoid content (Figure 4g,h). Dudonné et al. [42] previously highlighted that the phenolic content determined using Folin–Ciocalteu analysis correlated with DPPH and ABTS, showing stronger free radical inhibition values in parallel with the increase in phenolic content. Our results are also consistent with those previously reported for the antioxidant activities of bee pollen from various geographical locations, such as Brazil, Poland, Lithuania, and China [12,28,29]. The high correlation found may be due to the presence of several flavonols, such as quercetin, kaempferol, and myricetin derivatives, with a planar structure caused by the hydroxyl group in position 3 that promotes a higher radical capture due to easier conjugation and electron delocalization. The high number of hydroxyl groups is another factor contributing for the potency of those compounds as electron scavengers. It should be noted that the negative correlation of phenolic and flavonoid content with DPPH was due to the expression of DPPH as EC<sub>50</sub>, where a low value corresponds to a high radical scavenging activity.

On the other hand, both mono- and polyfloral bee pollen did not exhibit any appreciable antioxidant activity in the reducing power test, although there were statistically significant ( $p < 0.05$ ) differences among their phenolic compound concentration, as in Figure 1. In the correlation analysis, there is no significant ( $p > 0.05$ ) link between the phenolic/flavonoid content and reducing power, as shown in Figure 4f,i. This could be due to the stronger activity of individual compounds present in the sample rather than being related to the high phenolic content.

### 2.5.2. Antitumor Activity

Each bee pollen extract was screened for potential in vitro cytotoxicity activity against human-cancer-derived cell lines, such as stomach gastric adenocarcinoma (AGS), epithelial colorectal adenocarcinoma (CaCo2), cervical carcinoma (HeLa), breast adenocarcinoma (MCF-7), and non-small-cell lung cancer (NCI-H460) as well as a non-tumor cell line, human fetal osteoblastic (hFOB). The growth inhibition (GI) of the cells was not significant in most

of the samples ( $GI_{50} > 1000$ ,  $\mu\text{g/mL}$ ). BP1 ( $734 \pm 7$   $\mu\text{g/mL}$ ) and BP4 ( $495 \pm 6$   $\mu\text{g/mL}$ ) showed cytotoxicity effects exclusively against MCF-7 and HeLa, respectively, Figure 5.

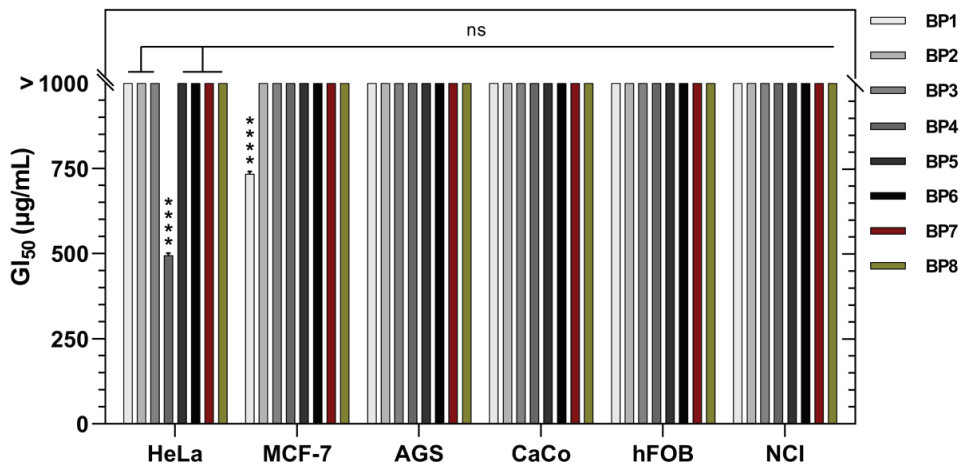


Figure 5. Cytotoxicity activity of the Moroccan bee pollen samples. \*\*\*\*:  $p < 0.0001$ .

The cytotoxic activities of plant-based materials are generally associated with the presence of phenolic compounds in their chemical composition. Along with this, it is known that the types and concentrations of these natural compounds have a determinative role in the inhibition of growth, proliferation, and invasion of cancer cells in different pathways. Ravishankar et al. [43] mentioned the ability of quercetin in the downregulation of oncogene expression as well as the upregulation of tumor suppressor genes. Regarding BP1, the detected compound at a distinctive concentration was kaempferol-3-*O*-rhamnoside (1.60 mg/g), and this flavonol was previously reported by Lee et al. [44] to suppress the protein expression and metastasis-promoting markers of MCF-7 breast cancer cells, thereby reducing their migration and invasion ability to the level of control. BP4 showed cytotoxic activity against the HeLa cell line with a higher inhibition rate than BP1. Even though the monofloral BP4 from *Olea europaea* species did not actually show a remarkable profile in terms of bioactive compound diversity, the chromatographic result revealed its richness in quercetin-*O*-diglucoside ( $3.3 \pm 0.1$  mg/g) compound, which might have determined its main action against the HeLa cancer cell line, as referred to in a previous study above. Additionally, none of the tested bee pollen fractions exhibited any cytotoxic activity against hFOB employed as the normal cell line.

### 3. Materials and Methods

#### 3.1. Collection and Preparation of Bee Pollen

Bee pollen samples were collected by local beekeepers between 2015 and 2017 from different locations in Morocco, Table 1, and stored in the freezer ( $-20$  °C) until further analysis.

#### 3.2. Palynological Analysis

Palynological analysis was performed according to a method previously described [45]. Accordingly, 10 mL of distilled water was added to 1 g of bee pollen samples and vortexed vigorously. Then, a 100  $\mu\text{L}$  aliquot was placed on a slide, and after drying, one drop of glycerin jelly was added for permanent preparation. Pollen grain identification was performed by optical microscope. A reference collection from the botanical laboratory of the University of Vigo, Spain, and different pollen morphology guides were used for the identification of pollen types. The relative frequency of each pollen type was calculated by counting a minimum of 500 pollen grains per slide.

### 3.3. Extraction of Phenolic Compounds

Aliquots of 2 g bee pollen samples were accurately ground and weighed into a centrifuge tube and extracted with 15 mL of ethanol/water (70:30, *v/v*) at 70 °C for 30 min, in a water bath at 100× *g*. The mixture was vacuum filtered, and the derived extract was stored at −20 °C until further analysis.

### 3.4. Total Phenolic and Flavonoid Content

The total phenolic compounds in the bee pollen samples were quantified spectrophotometrically according to a previously reported method [10]. Briefly, 0.5 mL of the extract (5 mg/mL) was mixed with Folin–Ciocalteu’s reagent (0.25 mL). After 3 min, 1 mL of 20% sodium carbonate was added to the mixture, and the volume was made up to 5 mL with distilled water. The solution was kept at 70 °C for 10 min and then cooled in the dark at room temperature for 20 min. Subsequently, the mixture was centrifuged for 10 min at 5000× *g*, and the absorbance was measured at 760 nm (Analytikjena 200–2004 spectrophotometer, Analytik Jena, Jena, Germany). The total phenolic content was expressed as mg GAE/g bee pollen (GAE—gallic acid equivalents).

The aluminum chloride method was carried out to determine the total flavonoid content [10]. An aliquot of 0.2 mL of sample solution (5 mg/mL) was mixed with 0.2 mL of aluminum chloride solution (2%  $\text{AlCl}_3$  in acetic acid/methanol, 5/95, *v/v*). Following this, 2.8 mL of methanol with 5% glacial acetic acid was added. The mixture was then incubated in the dark at room temperature for 30 min, and the absorbance was measured at 415 nm using a spectrophotometer. The total flavonoid content was expressed as mg QE/g bee pollen (QE—quercetin equivalents).

### 3.5. LC/DAD/ESI-MS<sup>n</sup> Analysis

The samples for analysis were prepared according to the method previously described [17]. Briefly, 20 mg of bee pollen extract was dissolved in 2 mL of 80% ethanol, filtered through a 0.22 μm membrane, and kept in the freezer at −32 °C until analysis.

A Dionex UltiMate 3000 ultra-pressure liquid chromatography instrument connected to a diode array and attached to a mass detector was used for LC/DAD/ESI-MS<sup>n</sup> analyses (Thermo Fisher Scientific, San Jose, CA, USA). LC was run in a Macherey–Nagel Nucleosil C18 column (250 mm × 4 mm id; particles diameter of 5 μm, end-capped), and its temperature was kept constant at 30 °C. The conditions applied in the liquid chromatography were based on previous work [4]; the flow rate was 1 mL/min, and the injection volume was 10 μL. The final spectra data were accumulated in the wavelength interval of 190–600 nm. The results were expressed as mg/g of pollen. The mass spectrometer was operated in the negative ion mode using Linear Ion Trap LTQ XL mass spectrometer (Thermo Scientific, CA, USA) equipped with an ESI source. The source’s voltage was 5 kV, in addition to −20 V and −65 V for the capillary and the tube lens, respectively. The capillary’s temperature was fixed to 325 °C. Both sheath and auxiliary gas ( $\text{N}_2$ ) flows were fixed to 50 and 10 (arbitrary units). Mass spectra were acquired by full range acquisition covering 100–1000 *m/z*. For the fragmentation study, a data-dependent scan was performed by deploying collision-induced dissociation (CID). The normalized collision energy of the CID cell was set at 35 (arbitrary units). Data acquisition was carried out with the Xcalibur<sup>®</sup> data system (Thermo Scientific, San Jose, CA, USA).

Quantification was achieved using calibration curves for *p*-coumaric acid (0.00925–0.4 mg/mL;  $y = 2.06 \times 10^7 x - 3.5 \times 10^5$ ;  $R^2 = 0.973$ ), kaempferol (0.037–1.6 mg/mL;  $y = 4.27 \times 10^6 x + 1.98 \times 10^5$ ;  $R^2 = 0.983$ ), chrysin (0.0185–0.8 mg/mL;  $y = 1.20 \times 10^7 x - 5.83 \times 10^4$ ;  $R^2 = 0.999$ ), quercetin (0.037–1.6 mg/mL;  $y = 3.9 \times 10^6 x + 4.65 \times 10^5$ ;  $R^2 = 0.937$ ), naringenin (0.0185–0.8 mg/mL;  $y = 7.85 \times 10^6 x - 3.04 \times 10^5$ ;  $R^2 = 0.978$ ). When the standard was not available, the compound quantification was expressed in the equivalent of the structurally closest compound. The results were expressed as mg/g of pollen.



### 3.6. Volatile Compounds Analysis

#### 3.6.1. Solid Phase Microextraction

Preliminary optimization of the extraction time and the addition of saline solution led to specific extraction conditions. Approximately 2.5 g of ground bee pollen was mixed with 2.5 mL of a 30% sodium chloride solution in a glass bottle until homogenization. The vial was sealed with a predrilled septum and placed in a thermostatic bath at 50 °C. Headspace sampling was performed using a manual SPME holder equipped with a 65 µm polydimethylsiloxane/divinylbenzene (PDMS/DVB) StableFlex fiber (Supelco, Bellefonte, PA, USA). Sampling of the volatile bee pollen compounds was achieved by inserting the fiber through the septum and exposing it to the headspace for 60 min with continuous stirring. The fiber was then retracted and transferred to the injector port of the gas chromatograph where the compounds were desorbed for 5 min.

#### 3.6.2. GC-MS Profiling and Quantification

The volatile compounds analysis was carried out according to a previously reported method with some modifications [46]. The GC-MS unit consisted of a Perkin Elmer system (GC Clarus® 580 GC module and Clarus® SQ 8 S MS module) gas chromatograph equipped with DB-5 MS fused-silica column (30 m × 0.25 mm i.d., film thickness 0.25 µm; J & W Scientific, Inc.) and interfaced with a Perkin-Elmer Turbomass mass spectrometer (software version 6.1, Perkin Elmer, Shelton, CT, USA). The SPME fiber was desorbed at 250 °C for 5 min. The oven temperature was programmed as 40–170 °C, at 3 °C/min, subsequently at 25 %/min up to 290 °C, and then held isothermal for 15 min. The transfer line temperature was 280 °C; ion source temperature, 230 °C; carrier gas, helium, adjusted to a linear velocity of 40 cm/s; ionization energy, 70 eV; scan range, 40–300 u; scan time, 1s. Identifications were based on the comparison of the obtained spectra with those of the NIST mass spectral library and were confirmed using linear retention indices determined from the retention times of an *n*-alkane (C<sub>7</sub>–C<sub>36</sub>) (Supelco, Bellefonte, PA, USA) mixture analyzed under identical conditions. They were compared to published data and, when possible, to commercial standard compounds. Quantitation (average value for three replicates per sample) was carried out using relative values directly obtained from peak TIC.

### 3.7. Antioxidant Capacity of Bee Pollen

Three different assays based on different working mechanisms were employed to measure the antioxidant capacity of bee pollen samples.

#### 3.7.1. DPPH Free Radical Scavenging Activity

DPPH free radical scavenging activity of bee pollen was performed according to Aylanc et al. [10]. A volume of 0.15 mL of the phenolic extract solutions, with concentrations ranging from 0.034 to 0.5 mg/mL were mixed with 0.15 mL of DPPH (0.024 mg/mL) and the absorbance was read at 515 nm using an ELX800 Microplate Reader (Bio-Tek Instruments, Inc., Winooski, VT, USA). The percentage of radical inhibition was calculated using the following equation:

$$\% \text{ Inhibition} = [(A_{DPPH} - A_{Sample}) / A_{DPPH}] \times 100 \quad (1)$$

The amount of antioxidant required to decrease the initial DPPH concentration by 50% (EC<sub>50</sub>) was achieved by plotting the inhibition percentage against the extract concentration.

#### 3.7.2. ABTS Free Radical Scavenging Activity

The ABTS assay was carried out to determine the ability of bee pollen samples to scavenge the ABTS radical cation using Trolox as the standard, according to the previously described method with modifications [47]. Stock ABTS<sup>+</sup> solution was prepared from 7 mM ABTS and 2.45 mM sodium persulfate in deionized water. The ABTS<sup>+</sup> solution was diluted with distilled water to obtain an absorbance of 0.700 (±0.020) at 734 nm. Bee pollen

extract (5mg/mL, 0.04 mL) was added to the diluted ABTS<sup>+</sup> solution (0.96 mL) and mixed immediately. The mixture was incubated for 10 min in the dark, and the absorbance was determined at 734 nm. The percentage of inhibition was calculated by the formula:

$$\% \text{ Inhibition} = \frac{(1 - A_{\text{Sample}})}{A_{\text{Control}}} \times 100 \quad (2)$$

$A_{\text{Sample}}$  is the absorbance of ABTS<sup>+</sup> solution with sample, and  $A_{\text{Control}}$  is the absorbance of ABTS<sup>+</sup> solution without sample. The Trolox equivalent antioxidant capacity of the bee pollen samples (mM Trolox/mg bee pollen extract) was calculated using the calibration curve as follows:

$$\text{TEAC (mM } \frac{\text{Trolox}}{\text{mg}} \text{ bee pollen extract)} = \frac{(\% \text{ Inhibition Sample} - b)}{a} \times \frac{\text{aliquot volume (mL)}}{\text{bee pollen weight (mg)}} \quad (3)$$

where  $a$  and  $b$  are the slope and the intercept of the calibration curve, respectively.

### 3.7.3. Reducing Power

The reducing power assay was performed according to a previously reported method [10]. Bee pollen extract (5 mg/mL, 0.25 mL) was mixed with sodium phosphate buffer (pH = 6.6, 1.25 mL). Potassium ferricyanide (1%, 1.25 mL) was added, and the mixture was incubated at 50 °C for 20 min. Then, trichloroacetic acid (10%, 1.25 mL) was added. The mixture was centrifuged at 3000×  $g$  for 10 min, and 1.25 mL was removed from the top to a new tube. Following, 1.25 mL of water and 0.25 mL of 0.1% ferric chloride were added, and the absorbance was read at 700 nm. The values were expressed as mg GAE/g bee pollen.

### 3.8. Cytotoxic Activity

To evaluate the cytotoxic activity of bee pollen extract with the Sulforhodamine B (SRB) colorimetric assay [48], 5 human tumor cell lines were used: AGS, CaCo2, HeLa, MCF-7, and NCI-H460 as well as hFOB a non-tumor cell line. The treatment solution was prepared from a 20 mg/mL hydroethanolic bee pollen extract, which was freeze-dried and then diluted to various concentrations (125 µg/mL to 2000 µg/mL).

The cell lines subcultures were performed in RPMI-1640 medium enriched with 2 mM glutamine, 100 U/mL penicillin, 100 µg/mL streptomycin, 10% FBS and kept in a humidified air incubator containing 5% CO<sub>2</sub> at 37 °C. After 24 h of incubation, the attached cells were treated with different extract concentrations and incubated again for 48 h. Afterward, the adherent cells were fixed with cold trichloroacetic acid (TCA 10%, 100 µL) and incubated at 4 °C for 1 h. Subsequently, the cells were washed with deionized water and dried. SRB solution (SRB 0.1% in 1% acetic acid, 100 µL) was added to each plate well and incubated for 30 min at room temperature. The unbound SRB was removed with 1% acetic acid, and the plates were air-dried. The bound SRB was solubilized with Tris (10 mM, 200 µL). To measure the absorbance at 540 nm, an ELX800 microplate reader (Bio-Tek Instruments, Inc; Winooski, VT, USA) was used. Elicipticine was used as a positive control, and the results were expressed as GI<sub>50</sub> values in µg/mL (sample concentration that inhibited 50% of the net cell growth).

### 3.9. Statistical Analysis

All analyses were performed in triplicate, and the results were denoted as mean ± standard deviation (SD). The obtained data were analyzed using GraphPad Prism version 9.4 (San Diego, CA, USA). One-way analysis of variance, followed by Tukey's multiple comparison test, was conducted to see whether there is statistical significance.  $p < 0.05$  was considered significant. Additionally, Pearson's correlation coefficients were calculated to ascertain the relationship between the tested parameters.

#### 4. Conclusions

Herein, Moroccan mono- and polyfloral bee pollen samples were subjected to different tests to determine their antioxidant and antitumor potential after evaluating the individual volatile compounds and their amounts as well as the phenolic and flavonoid contents of the samples. Several differences were found between monofloral and polyfloral bee pollen samples in terms of both diversity and concentration of bioactive compounds. Regardless of mono- and polyfloral classes, all bee pollen samples showed significant activities in free radical scavenging tests, but they did not show significant performance in reducing power and antitumor tests, except with some minor activities. The monofloral samples BP4 from *Olea europaea* and BP7 from *Ononis spinose* showed the highest radical scavenging activity against DPPH and ABTS, respectively, while BP2 and BP8 equally showed the highest reducing power activity. Moreover, among the samples tested, only BP1 (against MCF-7) and BP4 (against HeLa) showed cytotoxicity activity, which may be linked to the presence of specific flavonoids such as quercetin-*O*-diglucoside and kaempferol-3-*O*-rhamnoside. The antioxidant action of bee pollen samples and their cytotoxic effects on some cancer cells may be summed concisely as a combination of their phenolic, phenylamide, and volatile compounds content. Overall, the findings of our study contribute to establishing quality standards for Moroccan bee pollen and promoting the consumption of this natural beehive product, with potential evidence for the prevention or reduction of some health problems in which free radicals play major roles.

**Supplementary Materials:** The following supporting information can be downloaded at: <https://www.mdpi.com/article/10.3390/molecules28020835/s1>; Table S1: Phenolic and phenylamide profile of bee pollen samples; Table S2: Identification of volatile compounds in bee pollen samples.

**Author Contributions:** Conceptualization, M.V.-B. and S.I.F.; methodology, V.A., S.L., S.I.F., R.C., M.S.R.-F. and F.R.; software, V.A., S.L. and S.I.F.; validation, M.V.-B., S.I.F., M.C.S. and L.B.; formal analysis, V.A., A.E.G. and M.V.-B.; investigation, V.A., S.L. and R.C.; resources, M.V.-B. and B.L.; data curation, V.A., S.I.F. and M.V.-B.; writing—original draft preparation, V.A. and S.I.F.; writing—review and editing, V.A., S.I.F., L.B., M.C.S. and M.V.-B.; visualization, V.A. and S.I.F.; supervision, M.V.-B., S.I.F. and F.R.; project administration, M.V.-B.; funding acquisition, M.V.-B. All authors have read and agreed to the published version of the manuscript.

**Funding:** The authors are grateful to the Foundation for Science and Technology (FCT, Portugal) for financial support through national funds FCT/MCTES (PIDDAC); to CIMO (UIDB/00690/2020 and UIDP/00690/2020) and SusTEC (LA/P/0007/2021), Ph.D. research grant (2021.07764.BD) for Volkan Aylanc; and contracts through the individual and institutional scientific employment program—contract for Lillian Barros, Soraia I. Falcão, and Ricardo Calhella. Thanks to the Project PDR2020-1.0.1-FEADER-031734: “DivInA-Diversification and Innovation on Beekeeping Production”. Finally, this work was funded by the European Regional Development Fund (ERDF) through the Regional Operational Program North 2020 within the scope of Project GreenHealth-Digital strategies in biological assets to improve well-being and promote green health, Norte-01-0145-FEDER-000042.

**Data Availability Statement:** Data is contained within the article and Supplementary Materials.

**Conflicts of Interest:** The authors declare no conflict of interest.

#### References

1. Aylanc, V.; Falcão, S.I.; Ertosun, S.; Vilas-Boas, M. From the hive to the table: Nutrition value, digestibility and bioavailability of the dietary phytochemicals present in the bee pollen and bee bread. *Trends Food Sci. Technol.* **2021**, *109*, 464–481. [[CrossRef](#)]
2. Camacho-Bernal, G.I.; Cruz-Cansino, N.D.S.; Ramírez-Moreno, E.; Delgado-Olivares, L.; Zafra-Rojas, Q.Y.; Castañeda-Ovando, A.; Suárez-Jacobo, Á. Addition of Bee Products in Diverse Food Sources: Functional and Physicochemical Properties. *Appl. Sci.* **2021**, *11*, 8156. [[CrossRef](#)]
3. Kurek-Górecka, A.; Górecki, M.; Rzepecka-Stojko, A.; Balwierz, R.; Stojko, J. Bee Products in Dermatology and Skin Care. *Molecules* **2020**, *25*, 556. [[CrossRef](#)] [[PubMed](#)]
4. El-Ghouzi, A.; El-Menyiy, N.; Falcão, S.I.; Vilas-Boas, M.; Lyoussi, B. Chemical composition, antioxidant activity, and diuretic effect of Moroccan fresh bee pollen in rats. *Vet. World* **2020**, *13*, 1251. [[CrossRef](#)] [[PubMed](#)]

5. Touzani, S.; Al-Wailib, N.; Imtara, H.; Aboulghazia, A.; Hammad, N.; Falcão, S.; Vilas-Boas, M.; El Arabi, I.; Al-Waili, W.; Lyoussi, B. Arbutus Unedo Honey and Propolis Ameliorate Acute Kidney Injury, Acute Liver Injury, and Proteinuria via Hypoglycemic and Antioxidant Activity in Streptozotocin-Treated Rats. *Cell. Physiol. Biochem.* **2022**, *56*, 66–81.
6. El Mehdi, I.; Falcão, S.I.; Harandou, M.; Boujraf, S.; Calhelha, R.C.; Ferreira, I.C.F.R.; Anjos, O.; Campos, M.G.; Vilas-Boas, M. Chemical, cytotoxic, and anti-inflammatory assessment of honey bee venom from *Apis mellifera intermissa*. *Antibiotics* **2021**, *10*, 1514. [[CrossRef](#)]
7. Kieliszek, M.; Piwowarek, K.; Kot, A.M.; Błażej, S.; Chlebowska-Śmigiel, A.; Wolska, I. Pollen and bee bread as new health-oriented products: A review. *Trends Food Sci. Technol.* **2018**, *71*, 170–180. [[CrossRef](#)]
8. Mutlu, C.; Tontul, S.A.; Erbaş, M. Production of a minimally processed jelly candy for children using honey instead of sugar. *LWT* **2018**, *93*, 499–505. [[CrossRef](#)]
9. Pelka, K.; Bucekova, M.; Godocikova, J.; Szweida, P.; Majtan, J. Glucose oxidase as an important yet overlooked factor determining the antibacterial activity of bee pollen and bee bread. *Eur. Food Res. Technol.* **2022**, *248*, 2929–2939. [[CrossRef](#)]
10. Aylanc, V.; Tomás, A.; Russo-Almeida, P.; Falcão, S.I.; Vilas-Boas, M. Assessment of bioactive compounds under simulated gastrointestinal digestion of bee pollen and bee bread: Bioaccessibility and antioxidant activity. *Antioxidants* **2021**, *10*, 651. [[CrossRef](#)]
11. Conte, P.; del Caro, A.; Balestra, F.; Piga, A.; Fadda, C. Bee pollen as a functional ingredient in gluten-free bread: A physical-chemical, technological and sensory approach. *LWT* **2018**, *90*, 1–7. [[CrossRef](#)]
12. Krystyan, M.; Gumul, D.; Ziobro, R.; Korus, A. The fortification of biscuits with bee pollen and its effect on physicochemical and antioxidant properties in biscuits. *LWT* **2015**, *63*, 640–646. [[CrossRef](#)]
13. Turhan, S.; Saricaoglu, F.T.; Mortas, M.; Yazici, F.; Gencelep, H. Evaluation of Color, Lipid Oxidation and Microbial Quality in Meatballs Formulated with Bee Pollen During Frozen Storage. *J. Food Process. Preserv.* **2017**, *41*, e12916. [[CrossRef](#)]
14. Rzepecka-Stojko, A.; Stojko, J.; Kurek-Górecka, A.; Górecki, M.; Kabała-Dzik, A.; Kubina, R.; Moździerz, A.; Buszman, E.; Iriti, M. Polyphenols from Bee Pollen: Structure, Absorption, Metabolism and Biological Activity. *Molecules* **2015**, *20*, 21732–21749. [[CrossRef](#)] [[PubMed](#)]
15. Mohamed, N.A.; Ahmed, O.M.; Hozayen, W.G.; Ahmed, M.A. Ameliorative effects of bee pollen and date palm pollen on the glycemic state and male sexual dysfunctions in streptozotocin-induced diabetic wistar rats. *Biomed. Pharmacother.* **2018**, *97*, 9–18. [[CrossRef](#)] [[PubMed](#)]
16. Anjos, O.; Fernandes, R.; Cardoso, S.M.; Delgado, T.; Farinha, N.; Paula, V.; Estevinho, L.M.; Carpes, S.T. Bee pollen as a natural antioxidant source to prevent lipid oxidation in black pudding. *LWT* **2019**, *111*, 869–875. [[CrossRef](#)]
17. Aylanc, V.; Ertosun, S.; Russo-Almeida, P.; Falcão, S.I.; Vilas-Boas, M. Performance of green and conventional techniques for the optimal extraction of bioactive compounds in bee pollen. *Int. J. Food Sci. Technol.* **2022**, *57*, 3490–3502. [[CrossRef](#)]
18. Khan, H.Y.; Mohammad, R.M.; Azmi, A.S.; Hadi, S.M. *Functional Foods in Cancer Prevention and Therapy*; Academic Press: Cambridge, MA, USA, 2020; pp. 221–236.
19. Rice-Evans, C.A.; Miller, N.J.; Paganga, G. Structure-antioxidant activity relationships of flavonoids and phenolic acids. *Free Radic. Biol. Med.* **1996**, *20*, 933–956. [[CrossRef](#)]
20. Morton, L.W.; Caccetta, R.A.A.; Puddey, I.B.; Croft, K.D. Chemistry And Biological Effects Of Dietary Phenolic Compounds: Relevance To Cardiovascular Disease. *Clin. Exp. Pharmacol. Physiol.* **2000**, *27*, 152–159. [[CrossRef](#)]
21. Aylanc, V.; Eskin, B.; Zengin, G.; Dursun, M.; Cakmak, Y.S. In vitro studies on different extracts of fenugreek (*Trigonella spruneriana* BOISS.): Phytochemical profile, antioxidant activity, and enzyme inhibition potential. *J. Food Biochem.* **2020**, *44*, e13463. [[CrossRef](#)]
22. Barth, O.M.; Freitas, A.S.; Oliveira, É.S.; Silva, R.A.; Maester, F.M.; Andrella, R.R.S.; Cardozo, G.M.B.Q. Evaluation of the botanical origin of commercial dry bee pollen load batches using pollen analysis: A proposal for technical standardization. *An. Acad. Bras. Cienc.* **2010**, *82*, 893–902. [[CrossRef](#)] [[PubMed](#)]
23. Campos, M.G.R.; Bogdanov, S.; de Almeida-Muradian, L.B.; Szczesna, T.; Mancebo, Y.; Frigerio, C.; Ferreira, F. Pollen composition and standardisation of analytical methods. *J. Apic. Res.* **2008**, *47*, 154–161. [[CrossRef](#)]
24. Díez, M.J.; Andrés, C.; Terrab, A. Physicochemical parameters and pollen analysis of Moroccan honeydew honeys. *Int. J. Food Sci. Technol.* **2004**, *39*, 167–176. [[CrossRef](#)]
25. Bakour, M.; Fernandes, Â.; Barros, L.; Sokovic, M.; Ferreira, I.C.F.R.; Lyoussi, B. Bee bread as a functional product: Chemical composition and bioactive properties. *LWT* **2019**, *109*, 276–282. [[CrossRef](#)]
26. Aryal, S.; Baniya, M.K.; Danekhu, K.; Kunwar, P.; Gurung, R.; Koirala, N. Total Phenolic Content, Flavonoid Content and Antioxidant Potential of Wild Vegetables from Western Nepal. *Plants* **2019**, *8*, 96. [[CrossRef](#)]
27. Morais, M.; Moreira, L.; Feás, X.; Estevinho, L.M. Honeybee-collected pollen from five Portuguese Natural Parks: Palynological origin, phenolic content, antioxidant properties and antimicrobial activity. *Food Chem. Toxicol.* **2011**, *49*, 1096–1101. [[CrossRef](#)]
28. Araújo, J.S.; Chambó, E.D.; Costa, M.A.P.d.C.; da Silva, S.M.P.C.; de Carvalho, C.A.L.; Estevinho, L.M. Chemical Composition and Biological Activities of Mono- and Heterofloral Bee Pollen of Different Geographical Origins. *Int. J. Mol. Sci.* **2017**, *18*, 921. [[CrossRef](#)]
29. Kaškonienė, V.; Ruočkusienė, G.; Kaškonas, P.; Akuneca, I.; Maruška, A. Chemometric Analysis of Bee Pollen Based on Volatile and Phenolic Compound Compositions and Antioxidant Properties. *Food Anal. Methods* **2015**, *8*, 1150–1163. [[CrossRef](#)]

30. Kahraman, H.A.; Tutun, H.; Kaya, M.M.; Usluer, M.S.; Tutun, S.; Yaman, C.; Sevin, S.; Keyvan, E. Ethanol extract of Turkish bee pollen and propolis: Phenolic composition, antiradical, antiproliferative and antibacterial activities. *Biotechnol. Biotechnol. Equip.* **2022**, *36*, 44–55. [[CrossRef](#)]
31. Gercek, Y.C.; Celik, S.; Bayram, A.S. Screening of Plant Pollen Sources, Polyphenolic Compounds, Fatty Acids and Antioxidant/Antimicrobial Activity from Bee Pollen. *Molecules* **2021**, *27*, 117. [[CrossRef](#)]
32. Vogt, T. Unusual spermine-conjugated hydroxycinnamic acids on pollen: Function and evolutionary advantage. *J. Exp. Bot.* **2018**, *69*, 5311–5315. [[CrossRef](#)] [[PubMed](#)]
33. Edreva, A.M.; Velikova, V.B.; Tsonev, T.D. Phenylamides in plants. *Russ. J. Plant Physiol.* **2007**, *54*, 287–301. [[CrossRef](#)]
34. Kang, J.; Price, W.E.; Ashton, J.; Tapsell, L.C.; Johnson, S. Identification and characterization of phenolic compounds in hydromethanolic extracts of sorghum wholegrains by LC-ESI-MS<sup>n</sup>. *Food Chem.* **2016**, *211*, 215–226. [[CrossRef](#)]
35. Sobral, F.; Calhelha, R.C.; Barros, L.; Dueñas, M.; Tomás, A.; Santos-Buelga, C.; Vilas-Boas, M.; Ferreira, I.C.F.R. Flavonoid composition and antitumor activity of bee bread collected in northeast Portugal. *Molecules* **2017**, *22*, 248. [[CrossRef](#)] [[PubMed](#)]
36. Llorach, R.; Gil-Izquierdo, A.; Ferreres, F.; Tomás-Barberán, F.A. HPLC-DAD-MS/MS ESI Characterization of Unusual Highly Glycosylated Acylated Flavonoids from Cauliflower (*Brassica oleracea* L. var. *botrytis*) Agroindustrial Byproducts. *J. Agric. Food Chem.* **2003**, *51*, 3895–3899. [[CrossRef](#)] [[PubMed](#)]
37. Falcão, S.I.; Vale, N.; Gomes, P.; Domingues, M.R.M.; Freire, C.; Cardoso, S.M.; Vilas-Boas, M. Phenolic profiling of Portuguese propolis by LC-MS spectrometry: Uncommon propolis rich in flavonoid glycosides. *Phytochem. Anal.* **2012**, *24*, 309–318. [[CrossRef](#)]
38. Mihajlovic, L.; Radosavljevic, J.; Burazer, L.; Smiljanic, K.; Velickovic, T.C. Composition of polyphenol and polyamide compounds in common ragweed (*Ambrosia artemisiifolia* L.) pollen and sub-pollen particles. *Phytochemistry* **2015**, *109*, 125–132. [[CrossRef](#)]
39. Lima Neto, J.D.S.; Lopes, J.A.D.; Moita Neto, J.M.; de Lima, S.G.; da Luz, C.F.P.; Cító, A.M.D.G.L. Volatile compounds and palynological analysis from pollen pots of stingless bees from the mid-north region of Brazil. *Braz. J. Pharm. Sci.* **2017**, *53*, 14093. [[CrossRef](#)]
40. Prdun, S.; Svečnjak, L.; Valentić, M.; Marijanović, Z.; Jerković, I. Characterization of Bee Pollen: Physico-Chemical Properties, Headspace Composition and FTIR Spectral Profiles. *Foods* **2021**, *10*, 2103. [[CrossRef](#)]
41. Utto, W.; Mawson, A.J.; Bronlund, J.E. Hexanal reduces infection of tomatoes by *Botrytis cinerea* whilst maintaining quality. *Postharvest Biol. Technol.* **2008**, *47*, 434–437. [[CrossRef](#)]
42. Dudonné, S.; Vitrac, X.; Coutière, P.; Woillez, M.; Mérillon, J.M. Comparative Study of Antioxidant Properties and Total Phenolic Content of 30 Plant Extracts of Industrial Interest Using DPPH, ABTS, FRAP, SOD, and ORAC Assays. *J. Agric. Food Chem.* **2009**, *57*, 1768–1774. [[CrossRef](#)]
43. Ravishankar, D.; Rajora, A.K.; Greco, F.; Osborn, H.M.I. Flavonoids as prospective compounds for anti-cancer therapy. *Int. J. Biochem. Cell Biol.* **2013**, *45*, 2821–2831. [[CrossRef](#)]
44. Lee, G.A.; Choi, K.C.; Hwang, K.A. Kaempferol, a phytoestrogen, suppressed triclosan-induced epithelial-mesenchymal transition and metastatic-related behaviors of MCF-7 breast cancer cells. *Environ. Toxicol. Pharmacol.* **2017**, *49*, 48–57. [[CrossRef](#)] [[PubMed](#)]
45. Louveaux, J.; Maurizio, A.; Vorwohl, G. Methods of Melissopalynology. *Bee World* **2015**, *59*, 139–157. [[CrossRef](#)]
46. Rodríguez-Flores, M.S.; Falcão, S.I.; Escuredo, O.; Seijo, M.C.; Vilas-Boas, M. Description of the volatile fraction of *Erica* honey from the northwest of the Iberian Peninsula. *Food Chem.* **2021**, *336*, 127758. [[CrossRef](#)] [[PubMed](#)]
47. Bicudo de Almeida-Muradian, L.; Monika Barth, O.; Dietemann, V.; Eyer, M.; Freitas, A.d.S.d.; Martel, A.C.; Marcazzan, G.L.; Marchese, C.M.; Mucignat-Caretta, C.; Pascual-Maté, A.; et al. Standard methods for *Apis mellifera* honey research. *J. Apic. Res.* **2020**, *59*, 1–62. [[CrossRef](#)]
48. Abreu, R.M.V.; Ferreira, I.C.F.R.; Calhelha, R.C.; Lima, R.T.; Vasconcelos, M.H.; Adegas, F.; Chaves, R.; Queiroz, M.J.R.P. Anti-hepatocellular carcinoma activity using human HepG2 cells and hepatotoxicity of 6-substituted methyl 3-aminothieno[3,2-b]pyridine-2-carboxylate derivatives: In vitro evaluation, cell cycle analysis and QSAR studies. *Eur. J. Med. Chem.* **2011**, *46*, 5800–5806. [[CrossRef](#)]

**Disclaimer/Publisher’s Note:** The statements, opinions and data contained in all publications are solely those of the individual author(s) and contributor(s) and not of MDPI and/or the editor(s). MDPI and/or the editor(s) disclaim responsibility for any injury to people or property resulting from any ideas, methods, instructions or products referred to in the content.

Article

# A Comparative UHPLC-Q-Trap-MS/MS-Based Metabolomics Analysis to Distinguish *Foeniculum vulgare* Cultivars' Antioxidant Extracts

Maria Assunta Crescenzi <sup>1,2</sup>, Gilda D'Urso <sup>1</sup>, Sonia Piacente <sup>1</sup> and Paola Montoro <sup>1,\*</sup><sup>1</sup> Department of Pharmacy, University of the Study of Salerno, Via Giovanni Paolo II 132, I-84084 Fisciano, Italy<sup>2</sup> Ph.D. Program in Drug Discovery & Development, Department of Pharmacy, University of the Study of Salerno, Via Giovanni Paolo II 132, I-84084 Fisciano, Italy

\* Correspondence: pmontoro@unisa.it

**Abstract:** Among the environmental factors, seasonality is the one which most affects the metabolome of a plant. Depending on the harvest season, the plant may have a variable content of certain metabolites and thus may have different biological properties. *Foeniculum vulgare* is an annual plant whose cultivation creates large amounts of waste rich in bioactive compounds. The present investigation was performed with the aim of determining the amount of biologically active compounds in *F. vulgare* wastes obtained from varieties of different seasonality. Ten polyphenolic compounds were quantified in the little stems and leaves of Tiziano, Pegaso, and Preludio cultivars by ultra performance liquid chromatography (UPLC) hyphenated to QTRAP mass spectrometry by using the MRM (multiple reaction monitoring) method. The antioxidant activity of hydroalcoholic extracts was then evaluated using TEAC and DPPH spectrophotometric assays, followed by a multivariate statistical analysis to determine the correlation between metabolite expression and antioxidant activity. The Preludio variety, grown in summer, showed a higher content of bioactive compounds, which guarantees it a better antioxidant power; kaempferol 3-O-glucuronide, quercetin 3-O-glucuronide, and quercetin 3-O-glucoside are the polyphenolic compounds that could be mainly responsible for the antioxidant effect of fennel. The PLS chemometric model, which correlated quantitative data obtained by a sensitive and selective LC-ESI-QTrap-MS/MS analysis of antioxidant activity, resulted in a selective tool to detect the compounds responsible for the activity shown by the extracts in chemical tests.

**Keywords:** metabolomics; antioxidant activity; multivariate statistical analysis

**Citation:** Crescenzi, M.A.; D'Urso, G.; Piacente, S.; Montoro, P. A Comparative UHPLC-Q-Trap-MS/MS-Based Metabolomics Analysis to Distinguish *Foeniculum vulgare* Cultivars' Antioxidant Extracts. *Molecules* **2023**, *28*, 900. <https://doi.org/10.3390/molecules28020900>

Academic Editor: Nour Eddine Es-Safi

Received: 18 November 2022

Revised: 9 January 2023

Accepted: 13 January 2023

Published: 16 January 2023



**Copyright:** © 2023 by the authors. Licensee MDPI, Basel, Switzerland. This article is an open access article distributed under the terms and conditions of the Creative Commons Attribution (CC BY) license (<https://creativecommons.org/licenses/by/4.0/>).

## 1. Introduction

Fennel (*Foeniculum vulgare* Mill) is one of the most used plants in traditional medicine, showing a high number of pharmaceutical applications [1–3]. In vitro and in vivo studies [4] have shown several pharmacological activities of fennel including antimicrobial [5], antiviral [6], anti-inflammatory [7], apoptotic [8], cardiovascular [9], and antitumor [10,11].

Fennel, grown mainly in the Mediterranean area, is an annual species. The part of fennel that is sold and most frequently used in food market is the soft white bulb [12]. The remaining parts of the plant such as the leaves, and stems represent a waste product that is, however, rich in bioactive compounds [1,13,14].

Previous studies from our research group, through the metabolite profiling of fennel waste, highlighted that the little stems and leaves are the richest parts in terms of secondary metabolites containing important antioxidants such as phenolic acids, glycosylated flavonoids, and iridoids [15,16].

Antioxidants are molecules capable of reducing oxidation reactions in the human body and in food products [17,18]. Therefore, these compounds, in addition to being used as natural antioxidants in food preservation to extend food stability and storage life, can eliminate the free radicals generated by oxidation reactions in the human body that damage

cells [19]. The abundance of free radicals is associated with the onset of chronic diseases; therefore, the daily intake of antioxidant compounds can play an important role in the prevention and/or treatment of these diseases [20,21].

It is widely known that environmental factors, among them seasonality, can qualitatively and quantitatively affect the occurrence of metabolites in plants [22]. Different varieties of the same plant could have an increase or a reduction of some compounds according to the season in which they grow. The variability in the content of secondary metabolites could also determine a variability in their biological activities, such as the antioxidant activity [23,24].

Quantitative plant metabolomics is a tool to improve the understanding of plant biochemistry and metabolism by providing accurate measurements of the concentrations of known metabolites occurring in various plant samples prior to statistical and bioinformatic analysis [25]. Targeted approaches focus on the analysis of specific groups of metabolites associated with specific metabolic pathways or classes of compounds. The complexity and dynamics of metabolism require multiple analytical platforms to cover the full spectrum of metabolites. Among them, mass spectrometry MS/MS provides a highly sensitive and selective quantitative analysis of metabolites and has the ability to identify metabolites. Meanwhile multifunctional mass analyzers operating in integrated, or hybrid configurations can further facilitate metabolite identification by obtaining high-resolution and accurate MS/MS spectra. Among them, triple quadrupole (QqQ) is considered a reference tool for the absolute quantification of small molecules due to its sensitivity and specificity using multiple reaction monitoring (MRM): the first quadrupole (Q1) of the MS selects and transmits the precursor ions to the second quadrupole (Q2) for further fragmentation [26]. Therefore, this research was aimed at quantifying some metabolites in three varieties of different seasonality of *F. vulgare*, Tiziano (winter cultivar), Pegaso (spring cultivar), and Preludio (summer cultivar). Hydro-alcoholic extracts of the little stems and leaves were analyzed through UPLC-ESI-QTRAP-MS/MS analysis in MRM.

The antioxidant activity of fennel waste was evaluated by two spectrophotometric assays, specifically DPPH (1,1-diphenyl-2-picrylhydrazyl radical) and TEAC (Trolox equivalent antioxidant capacity). The content of flavonoids was also assessed using an allumine chloride colorimetric assay. Using these assays, the antioxidant activities of the spring (Pegaso) and summer (Preludio) fennel variety extracts were compared with those of the winter variety (Tiziano), whose results were previously reported [15].

PLS (Partial least squares (PLS) analysis, a multivariate data analysis projection method, can classify samples according to their properties, identified as a Y variable in a correlation plot. By using PLS analysis, the metabolomic quantitative data were correlated to specific assay results. Thus, in the present work the most important metabolites involved in the antioxidant activity were identified.

The study confirmed that seasonality can alter the metabolome of plants; in fact, the Preludio variety, grown in the summer period, has a higher content of bioactive compounds such as quercetin 3-O-glucoside, quercetin 3-O-glucuronide, and feruloylquinic acid.

## 2. Results and Discussion

### 2.1. UPLC-ESI-QTRAP-MS/MS Quantitative Analysis

Ten known metabolites were quantified in fennel waste obtained from different cultivars by UPLC-ESI-QTRAP-MS/MS analysis. Data obtained from the Tiziano variety have already been published previously [16], they are reported for a comparison with the other two varieties of different seasonality.

The mass spectral parameters of each compound were optimized according to standard methods, as shown in Table 1, along with a precursor/production transition selected to apply an MRM method for revealing them (Figure 1).

**Table 1.** Mass spectral parameters and precursor/product MRM transitions of standard compounds measured using a UHPLC system interfaced with an ABSciex Q-Trap 6500 instrument in MRM mode (UPLC-ESI-QTRAP-MS/MS).

	Compounds	DP	EP	CE	CXP	PI	DI
1	neochlorogenic acid	−60	−4	−24	−17	353	191
2	dicafeoylquinic acid	−61	−4	−24	−38	515	353
3	quercetin 3-O-glucoside	−138	−9	−28	−32	463	301
4	feruloylquinic acid	−89	−4	−33	−21	367	191
5	quercetin 3-O-glucuronide	−52	−8	−35	−30	477	301
6	isorhamnetin 3-O-glucuronide	−52	−8	−35	−30	491	315
7	kaempferol 3-O-glucuronide	−59	−8	−35	−30	461	285
8	dicafeoylquinic acid malonyl *	−61	−4	−24	−38	601	395
9	kaempferol 3-O-rutinoside **	−81	−4	−35	−30	593	285
10	kaempferol 3-O-glucoside **	−81	−4	−25	−30	447	285

DP, declustering potential; EP, entrance potential; CE, collision energy; CXP, collision cell exit potential; PI, product ion; DI, daughter ion. \* Compound quantified on the dicafeoylquinic acid curve. \*\* Compounds quantified on the kaempferol 3-O-glucuronide curve.

For both the Tiziano and Pegaso varieties, the leaves showed a higher concentration of the quantified compounds (Table 2). On the contrary for the Preludio variety, the little stems were the richest source of bioactive compounds (Figure 2A).

Neochlorogenic acid (1) and quercetin 3-O-glucoside (3) were abundant in the leaf of the spring variety, Pegaso, with concentrations of 192.67 and 90.36 mg, respectively. Additionally, this variety showed the greatest concentration of isorhamnetin 3-O-glucuronide (6) (888.86 mg) (Figure 2B). Kaempferol 3-O-rutinoside (9) and kaempferol 3-O-glucoside (10) were detected only in the fennel waste from the Preludio variety. A higher concentration of bioactive compounds was found in the little stem of this variety of fennel. In fact, it was rich in glucuronate flavonoids such as quercetin 3-O-glucuronide (5) and kaempferol 3-O-glucuronide (7). These flavonoids were present at 1611.00 and 562.50 mg concentrations, respectively. In the little stem of Preludio fennel, grown during the summer, the highest concentrations of feruloylquinic acid (4) and quercetin 3-O-glucoside (3) were detected, with concentrations of 310.50 and 264.60 mg respectively in 100 g of dried plant material.

## 2.2. Method Validation

According to EMA guidelines, the UPLC-ESI-QTRAP-MS/MS method has been validated as previously described [16,27]. Each standard solution was analyzed in triplicate to assess a calibration curve by plotting the area of the external standard alongside each metabolite concentration. The linearity was evaluated considering the correlation coefficients of each calibration curve obtained for standard compounds. The correlation values obtained were in the range of 0.997–0.999.

A signal-to-noise ratio (S/N) of 3:1 and 10:1 was obtained by serially diluting the standard compounds under optimized conditions in order to determine, respectively, the limit of detection (LOD) and the limit of quantification (LOQ). Therefore, the developed method demonstrated good sensitivity with a LOD between 0.002 and 0.010 mg/L and a LOQ between 0.002 and 0.08 mg/L.

A sample was analyzed three times on the same day and three times over three consecutive days, in order to evaluate the precision of the method; the value was expressed as a percentage relative standard deviation (RSD). The RSD value for any analyte was in the range of 2–4%. Using the optimized parameters, we performed recovery experiments to evaluate the extraction efficiency.

At three concentration levels (high, middle, and low), UPLC-ESI-QTRAP-MS/MS experiments were performed in triplicate at each concentration level for three standard



solutions. The recovery and precision were appreciable, with recovery rates ranging from 95% to 105% on the same day.

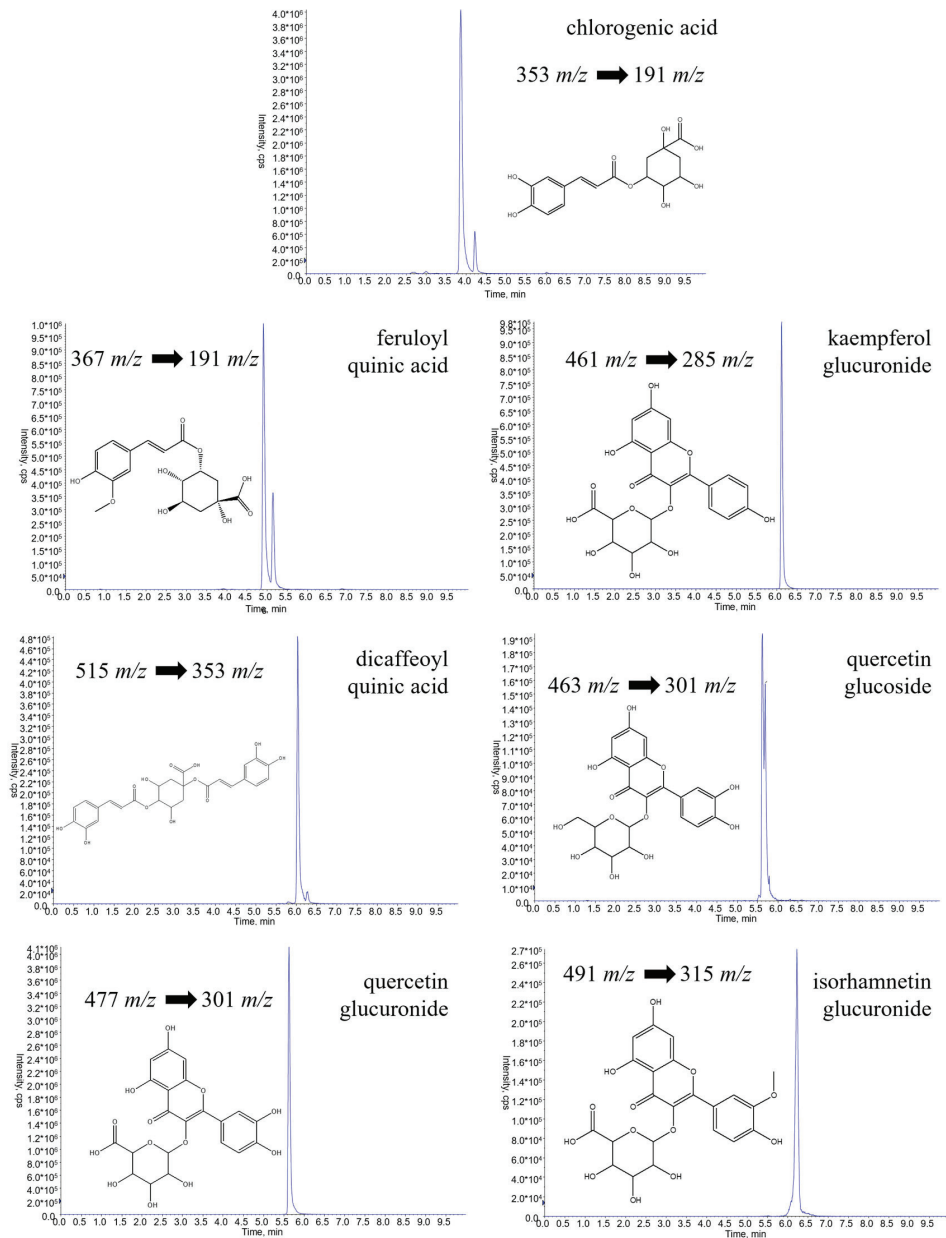


**Figure 1.** Q1/Q3 mass transitions for chlorogenic acid, quercetin glucoside, quercetin glucuronide, kaempferol glucuronide, isorhamnetin glucuronide, feruloylquinic acid, and dicaffeoylquinic acid obtained by UHPLC-ESI-QTRAP-MS/MS analysis and selected for MRM analysis of a standard mix.

**Table 2.** Quantitative results obtained from the analyses of selected phenolic compounds in the *F. vulgare* waste of different cultivars using UHPLC-ESI-QTRAP-MS/MS analyses in MRM mode.

	Compounds	FVLS-T	FVLE-T	FVLS-PE	FVLE-PE	FVLS-PR	FVLE-PR
1	neochlorogenic acid	6.80 ± 0.06	17.10 ± 0.86	28.84 ± 0.65	192.67 ± 3.34	151.74 ± 2.50	82.12 ± 2.63
2	dicafeoylquinic acid	11.15 ± 0.21	41.17 ± 0.00	0.82 ± 0.02	1.71 ± 0.11	89.37 ± 2.42	22.88 ± 3.52
3	quercetin 3-O-glucoside	3.16 ± 0.67	50.85 ± 0.00	3.24 ± 0.05	90.36 ± 0.59	264.60 ± 3.09	81.60 ± 6.25
4	feruloylquinic acid	42.47 ± 0.00	46.77 ± 1.20	9.58 ± 0.36	103.13 ± 2.09	310.50 ± 5.91	185.60 ± 1.28
5	quercetin 3-O-glucuronide	1.14 ± 0.11	163.76 ± 2.61	11.14 ± 0.23	427.88 ± 8.36	1611.00 ± 16.11	872.00 ± 4.67
6	isorhamnetin 3-O-glucuronide	0.89 ± 0.13	257.90 ± 4.23	9.98 ± 1.02	888.86 ± 10.76	12.29 ± 1.07	5.26 ± 0.70
7	kaempferol 3-O-glucuronide	0.14 ± 0.00	37.84 ± 1.28	19.42 ± 0.26	238.76 ± 6.69	562.50 ± 10.73	366.40 ± 5.40
8	dicafeoylquinic acid malonyl *	19.98 ± 1.01	48.18 ± 4.65	nd	0.61 ± 0.00	147.97 ± 5.46	107.72 ± 2.49
9	kaempferol 3-O-rutinoside **	nd	nd	nd	nd	16.92 ± 0.87	8.09 ± 1.13
10	kaempferol 3-O-glucoside **	nd	nd	nd	nd	15.24 ± 1.69	6.64 ± 0.75

Mean in mg/100 g dried weight with standard deviation. FVLS-T, *Foeniculum vulgare* little stem Tiziano variety; FVLE-T, *Foeniculum vulgare* leaf Tiziano variety; FVLS-PE, *Foeniculum vulgare* little stem Pegaso variety; FVLE-PE, *Foeniculum vulgare* leaf Pegaso variety; FVLS-PR, *Foeniculum vulgare* little stem Preludio variety; FVLE-PR, *Foeniculum vulgare* leaf Preludio variety. \* Compound quantified on the dicafeoylquinic acid curve. \*\* Compounds quantified on the kaempferol 3-O-glucuronide curve. nd, not detected.

### 2.3. Antioxidant Activity and Content of Flavonoid

Flavonoids are phenolic compounds which are very abundant in fennel waste. These compounds exert antioxidant, antimicrobial, photoreceptor, feeding, and light-screening functions in plants [28]. Research shows that flavonoids also have antiallergenic, antiviral, anti-inflammatory, antioxidant, and vasodilating properties in the human organism [29]. Due to the presence of glycosylated flavonoids in fennel waste, the flavonoid content and antioxidant activities of extracts were chemically tested using spectrophotometric methods (Table 3).

There was a higher flavonoid content in the leaves than in the little stems of all the varieties tested. In particular, the leaves of the summer variety, Preludio, presented the richest source of flavonoid compounds with a concentration of 1.497 mg. Although each extract showed good antioxidant activity, by comparing the results with those obtained for the two positive controls (quercetin 3-O-glucoside and vitamin C), the leaves in general, compared to the little stems, were shown to be more active. Specifically, according to the data from the quantitative analysis, the Pegaso and Preludio varieties exerted the highest antioxidant activity-reaching TEAC values (equivalent antioxidant capacity in TROLOX expressed in mg/mL) of 1.501 for FVLE-PR and 1.676 for FVLE-PE and, respectively, an IC<sub>50</sub> for DPPH (expressed in mg/mL) of 0.010 for FVLE-PR and 0.634 for FVLE-PE.

### 2.4. Multivariate Data Analysis

Quantitative data obtained for biological triplicates of the various samples were used to apply a multivariate statistical analysis with a targeted approach.

A data matrix was created where the rows (variables) were the quantities of each metabolite analyzed by LC-ESI-QTRAP-MS/MS (Table 2) and the columns were the various samples, each in triplicate, and represented the observations. This matrix was the X-block for the PLS-based approach, which is a regression technique applied to examine the relationship between two blocks of data, called X- and Y-block. The Y-block is the antioxidant activity, expressed as a % of inhibition of TEAC or DPPH. A score scatter plot

generated by PLS highlights the extracts with the greatest antioxidant activity, evaluating their proximity to the Y-block. Additionally, a loading scatter plot shows the variables closest to the Y-block, which correspond to the variables that had a greater impact on antioxidant activity.

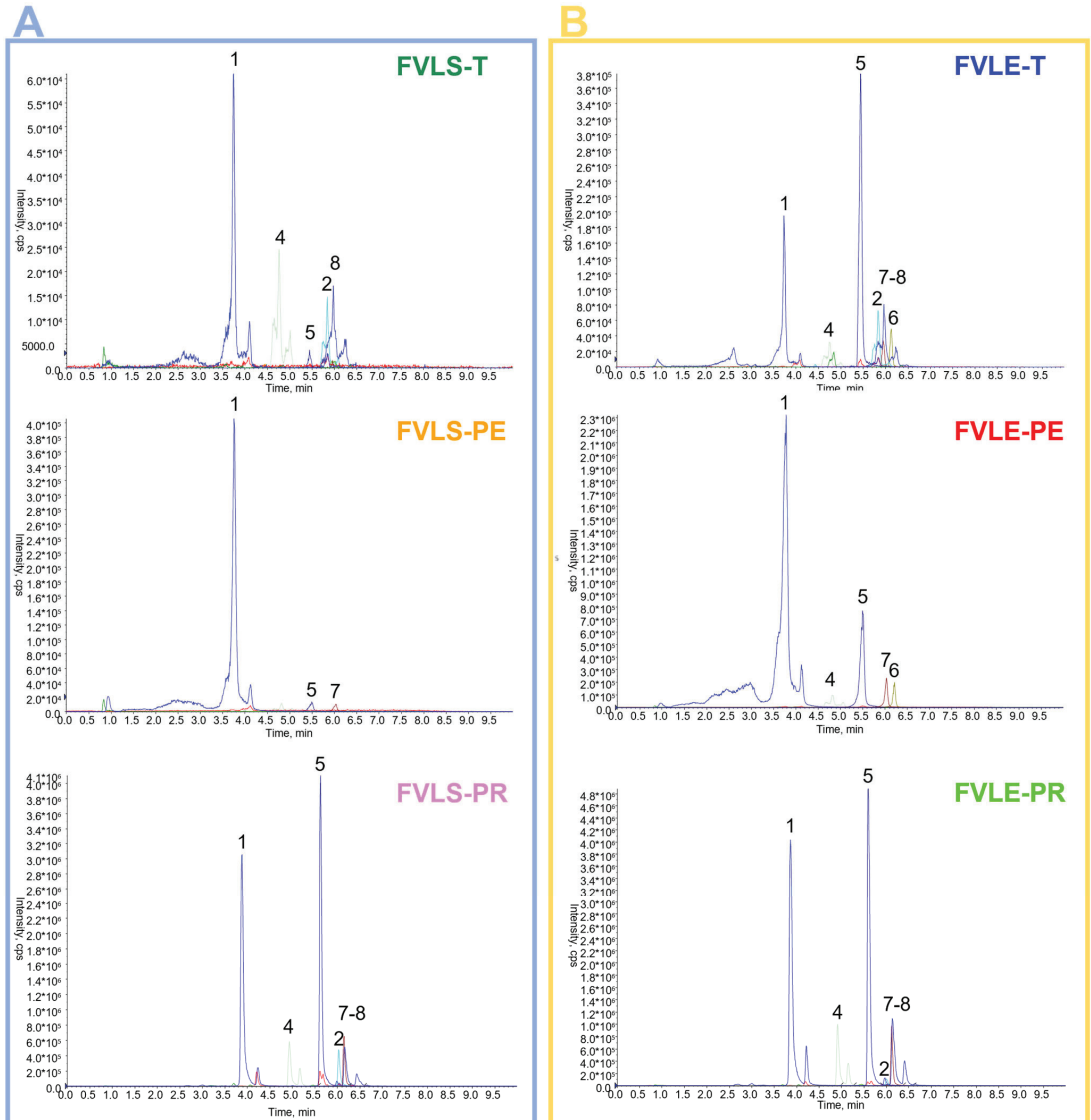


**Figure 2.** UHPLC-ESI-QTRAP-MS/MS profiles of hydroalcoholic extracts of the little stems (A) and leaves (B) of three varieties of *F. vulgare*. FVLS-T, *Foeniculum vulgare* little stem Tiziano variety; FVLS-PE, *Foeniculum vulgare* little stem Pegaso variety; FVLS-PR, *Foeniculum vulgare* little stem Preludio variety; FVLE-T, *Foeniculum vulgare* leaf Tiziano variety; FVLE-PE, *Foeniculum vulgare* leaf Pegaso variety; FVLE-PR, *Foeniculum vulgare* leaf Preludio variety.

**Table 3.** Antioxidant activity of extracts of *F. vulgare* evaluated by TEAC and DPPH, Radical scavenging activity assays, and the total amount of plant flavonoids of fennel.

<i>F. vulgare</i> Extracts	TEAC [mg/mL $\pm$ SD <sup>a</sup> ] <sup>b</sup>	DPPH [IC <sub>50</sub> (mg/mL) $\pm$ SD <sup>a</sup> ]	Total Flavonoids [mg/g Plant Extract (in RE) $\pm$ SD <sup>a</sup> ] <sup>c</sup>
FVLS-T	0.375 $\pm$ 0.006	5.782 $\pm$ 0.001	ND
FVLE-T	0.823 $\pm$ 0.008	0.342 $\pm$ 0.002	0.206 $\pm$ 0.006
FVLS-PE	0.448 $\pm$ 0.006	3.280 $\pm$ 0.002	0.083 $\pm$ 0.001
FVLE-PE	1.676 $\pm$ 0.010	0.634 $\pm$ 0.006	1.331 $\pm$ 0.002
FVLS-PR	0.509 $\pm$ 0.004	1.109 $\pm$ 0.002	0.309 $\pm$ 0.001
FVLE-PR	1.501 $\pm$ 0.009	0.010 $\pm$ 0.002	1.497 $\pm$ 0.002
quercetin 3-O-glucoside vitamin C	1.813 $\pm$ 0.007 / /	/ / 0.270 $\pm$ 0.006	/ / /

SD <sup>a</sup>, standard deviation of three independent experiments; <sup>b</sup>, antioxidant activity determined by TEAC assay, and expressed as the antioxidant capacity equivalent in TROLOX in mg/mL; <sup>c</sup>, flavonoid content evaluated by aluminum chloride assay and expressed as mg of rutin equivalents (RE) in grams of extract.

Figure 3 shows the score scatter plot of the PLS analysis for DPPH (panel A) and the loading scatter plot (panel B). The first component explains the 62% of variance, while the second explains the 23% of variance. The most active samples are located on the right side of the plot and are the leaves of all the varieties of fennel and the little stems of the Preludio summer variety. The loading scatter plot has an outlier, the isorhamnetin 3-O-glucuronide, which was eliminated to obtain a new loading scatter plot with the regression line (Figure 4A). The variables with the greatest antioxidant power are those positioned in the upper right part of the plot, the flavonoids quercetin 3-O-glucuronide, quercetin 3-O-glucoside, and kaempferol 3-O-glucuronide.

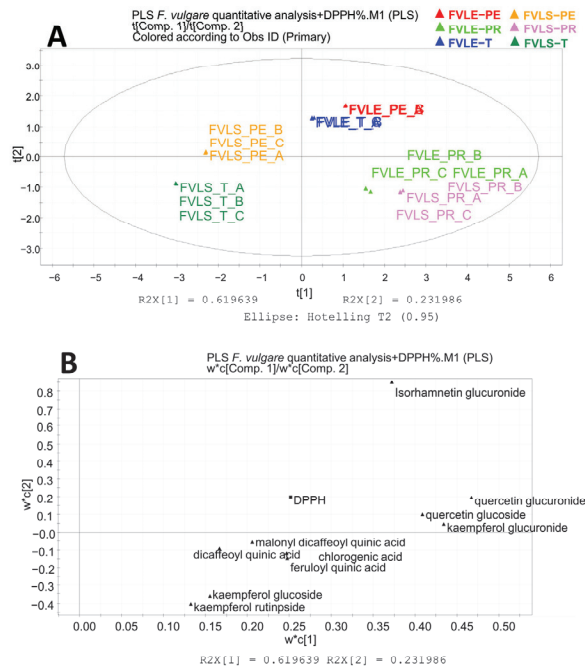


**Figure 3.** Partial least square analysis: quantitative results related to the antioxidant activity (DPPH) of the ethanolic extracts of *F. vulgare* waste. (A) Score scatter plot; (B) loading plot. FVLE-T, *Foeniculum vulgare* leaf Tiziano variety; FVLE-PE, *Foeniculum vulgare* leaf Pegaso variety; FVLE-PR, *Foeniculum vulgare* leaf Preludio variety.

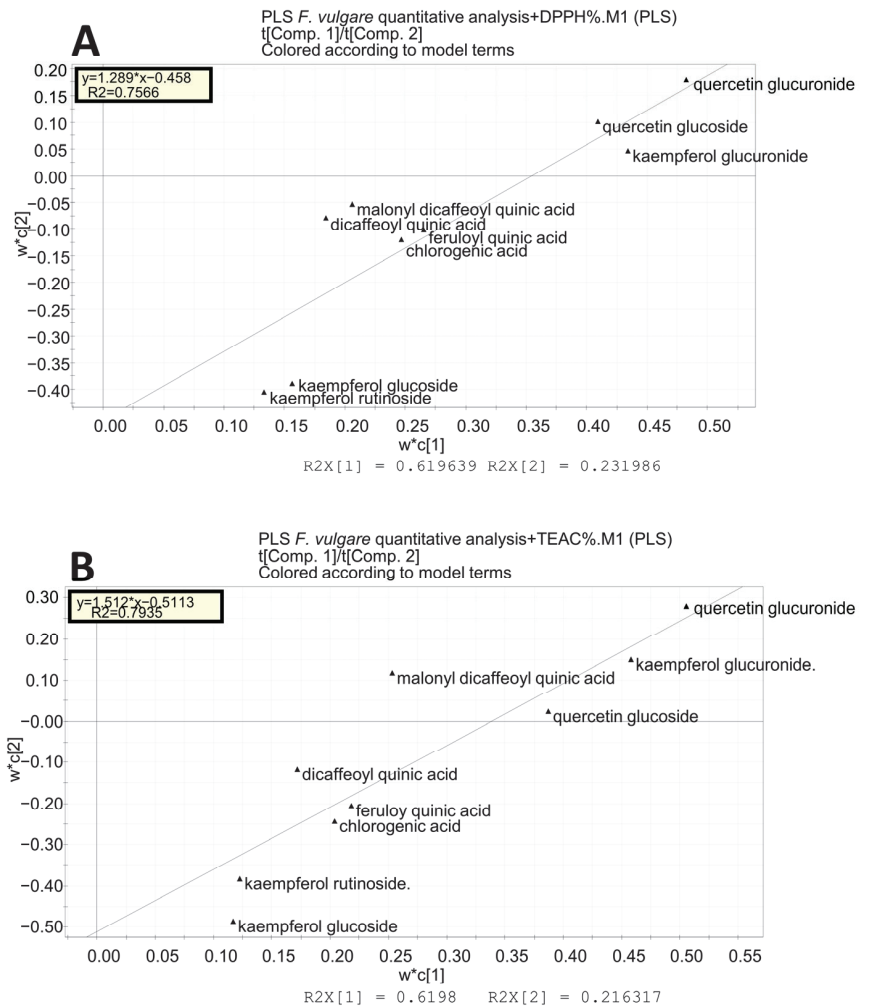


**Figure 4.** Partial least square analysis: loading scatter plots obtained from a targeted data analysis excluding the outlier isorhamnetin glucuronide. (A) Loading scatter plot with regression line with the Y-block as the DPPH value; (B) loading scatter plot with regression line with the Y-block as the TEAC value.

A PLS analysis with TEAC inhibition as the Y-block is represented by Figure 5. The first component explains the 62% of variance, while the second explains the 22% of variance. The results of the score scatter plot are the same as obtained with the DPPH, thus confirming that Preludio leaves and little stems are the parts of fennel waste with the greatest antioxidant activity. Again, the isorhamnetin 3-O-glucuronide is an outlier and was eliminated. The variables that are responsible for the antioxidant power are confirmed as quercetin 3-O-glucuronide, quercetin 3-O-glucoside, kaempferol 3-O-glucuronide, and also malonyl dicaffeoylquinic acid (Figure 4B).

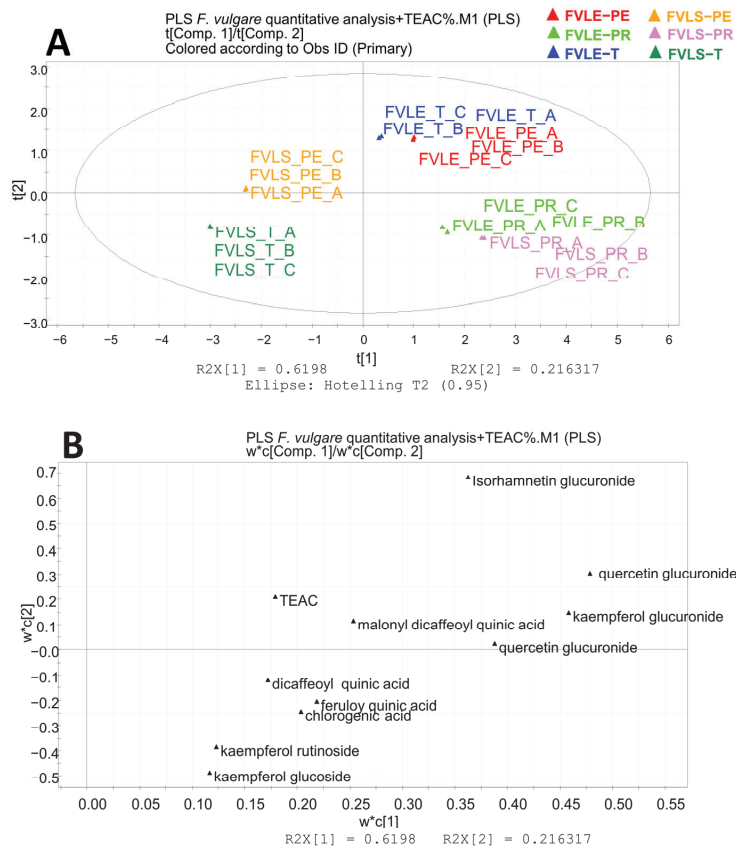


**Figure 5.** Partial least square analysis: quantitative results related to the antioxidant activity (TEAC) of the ethanolic extracts of *F. vulgare* waste. (A) Score scatter plot; (B) loading plot. FVLE-T, *Foeniculum vulgare* leaf Tiziano variety; FVLE-PE, *Foeniculum vulgare* leaf Pegaso variety; FVLE-PR, *Foeniculum vulgare* leaf Preludio variety.

### 3. Materials and Methods

#### 3.1. Raw Materials

A company specialized in the production and marketing of fennel, Paolillo (Eboli, Salerno, Italy), provided the by-products of *F. vulgare*. As part of the processing, the waste of fennel was recovered from the Tiziano variety harvested in December 2019 and from the Pegaso variety harvested in April 2021, both of which were grown in Campomarino in Molise, and from the Preludio variety harvested in July 2021, cultivated in Avezzano in Abruzzo. Superficial leaves and smaller stems of fennel were collected. The samples were classified into the following groups: FVLS-T (*F. vulgare* little stems of the Tiziano variety), FVLE-T (*F. vulgare* leaves of the Tiziano variety), FVLS-PE (*F. vulgare* little stems of the Pegaso variety), FVLE-PE (*F. vulgare* leaves of the Pegaso variety), FVLS-PR (*F. vulgare* little stems of the Preludio variety), and FVLE-PR (*F. vulgare* leaves of the Preludio variety).

#### 3.2. Chemicals

The ethanol and water used for the extractions were bought from VWR (Milan, Italy). Acetonitrile (ACN), formic acid, water, and methanol of LC-MS grade were provided by Romil (Milan, Italy). The standards used for the optimization of the method—neochlorogenic acid, dicaffeoylquinic acid, quercetin 3-O-glucoside, feruloylquinic acid, quercetin 3-O-glucuronide,

isorhamnetin 3-*O*-glucuronide, and kaempferol 3-*O*-glucuronide—were purchased from Sigma-Aldrich (Milan, Italy). Trolox (6-hydroxy-2, 5, 7, 8-tetramethylchroman-2-carboxylic acid), DPPH (2, 2-Diphenyl-1-picrylhydrazyl), K<sub>2</sub>S<sub>2</sub>O<sub>8</sub> (potassium persulfate), PBS (Phosphate Buffered Saline), and ABTS (2, 2'-azino-bis-(3-ethylbenzothiazoline-6-sulfonic acid) were bought from Sigma-Aldrich (Milan, Italy).

### 3.3. Sample Preparation

Before freeze-drying, the fennel waste was separated into different parts and stored at  $-80$  °C. The classes of samples were FVLS-T (*F. vulgare* little stems of the Tiziano variety), FVLE-T (*F. vulgare* leaves of the Tiziano variety), FVLS-PE (*F. vulgare* little stems of the Pegaso variety), FVLE-PE (*F. vulgare* leaves of the Pegaso variety), FVLS-PR (*F. vulgare* little stems of the Preludio variety), and FVLE-PE (*F. vulgare* leaves of the Preludio variety).

The freeze-dried plant materials were extracted by ultrasound assisted extraction as previously described [15]. For the sonication of the FVBU and FVST samples, 1 g of dried drugs were extracted with 20 mL ethanol/water (80:20) for 15 min in an ultrasonic bath. In contrast, the extraction of the FVLS and FVLE samples required 40 mL for 1 g of the matrix. The extraction was repeated three times and the extracts were filtered with filter paper 67 g/m<sup>2</sup> (530-16100-Aptaca). For LC-MS analysis, the combined extracts, dried under a nitrogen stream, were dissolved in methanol with a final concentration of 1 mg/mL.

### 3.4. Quantitative Analysis

#### 3.4.1. ESI-QTRAP-MS and ESI-QTRAP-MS/MS Analyses

The standard samples were analyzed using an ABSciex 6500 QTRAP spectrometer (Foster City, CA, USA) using ESI-QTRAP-MS/MS with full-scan and collision-induced dissociation (CID) analyses.

Flow rates of 10  $\mu$ L/min were used to infuse a standard solution of each metabolite (1  $\mu$ g/mL in methanol) into the source to optimize the analytical parameters. The data were acquired using the negative ion MS and MS/MS mode.

#### 3.4.2. UPLC-ESI-QTRAP-MS/MS Analyses in MRM (Multiple Reaction Monitoring) Mode

The bioactive compounds of fennel waste were analyzed quantitatively using a Shimadzu Nexera LC system in line with a Sciex 6500 QTRAP MS equipped with an Omega C18 column (Phenomenex, Aschaffenburg, Germany) (100  $\times$  2.1 mm i.d., 1.6  $\mu$ m). The mobile phases used were water + 0.1% formic acid (A) and acetonitrile + 0.1% formic acid (B). The gradient used at a flow rate of 0.300 mL/min, using the following increasing linear gradient (*v/v*) of solvent B was: 0.1–2.13 min, from 5% to 15%; 2.13–6.40 min, from 15% to 35%; 6.40–8.53, from 35% to 80%, and then back to 5% for 1.53 min. The ion mode was negative, and 5  $\mu$ L of each sample was used for injection. The 6500 QTRAP was set up for IonSpray operation, and compounds were detected using multiple reaction monitoring (MRM). The mass spectrometry source parameters were set as follows: curtain gas (CUR) = 35; collision gas (CAD) = medium; ion spray voltage (IS) =  $-4500$ ; temperature (TEM) = 350; ion source gas 1 (GS1) = 25; ion source gas 2 (GS2) = 25. [16]. The transitions of each analyzed metabolite are listed in Table 1 with the following parameters: declustering potential (DP), entrance potential (EP), collision energy (CE), collision cell exit potential (CXP). The dwell time for each analyte was 20 ms. There were typically 14 points across all chromatographic peaks with a total cycle time of 0.3 s. Analyst software 1.6.2 was used for the data acquisition and processing (ABSciex, Foster City, CA, USA).

#### 3.4.3. Method Validation

The UPLC-ESI-QTRAP-MS/MS method was validated according to the European Medicines Agency guidelines (EMA quality guidelines ICH Q2) to validate the analytical methods following the procedure of the previous work [16,27].

### 3.5. DPPH Radical Scavenging Activity

The antiradical activity against 1,1-diphenyl-2-picrylhydrazyl radical (DPPH•) was evaluated in the stems and leaves of the three varieties of *F. vulgare*.

Extracts with antioxidant activity can reduce DPPH• to DPPH-H. As a result, there is a decrease in absorbance at 517 nm and it was measured on a UV-visible spectrophotometer (Spectrophotometer Multiskan Go, Thermo Scientific). The procedure of the assay was previously described [30]. The fennel extracts were tested with the following concentrations: 0.625–1.25–2.5 and 5 mg/mL, and the assay was performed in triplicate. The antioxidant power of vitamin C was evaluated as a positive control. The percentage of the radical inhibition of DPPH was calculated by the following Equation (1):

$$\% \text{ Inhibition DPPH}\bullet = \left( 1 - \frac{A_{\text{treated}} - A_{\text{blank}}}{A_{\text{control}}} \right) \times 100 \quad (1)$$

where  $A_{\text{control}}$  is the average absorption of DPPH, while  $A_{\text{treated}}$  is the average absorption of the extract with DPPH, and  $A_{\text{blank}}$  is the average absorption of the extract solution only. The concentration of an extract that provides 50% DPPH inhibition ( $IC_{50}$ ) was calculated by plotting the inhibition (%) against each extract concentration.

### 3.6. Trolox Equivalent Antioxidant Capacity (TEAC) Assay

In line with previous works [15,31], the antioxidant capacity of the extracts was measured using the Trolox equivalent antioxidant capacity assay.

The TEAC value shows the ability of the antioxidant to scavenge the radical cation 2,2'-azinobis (3-ethylbenzothiazoline-6-sulfonate) ABTS<sup>•+</sup> by spectrophotometric analysis. The ABTS<sup>•+</sup> solution was prepared by mixing 7 mM ABTS in H<sub>2</sub>O with 2.45 mM potassium persulfate, and was stored in the dark at room temperature for 12 h. Subsequently, it was diluted with PBS (phosphate saline buffer, pH = 7.4), until an absorbance of 0.7 was reached at 734 nm and equilibrated at 30 °C.

The fennel extracts were diluted with methanol/water producing solutions at concentrations of 250, 500, 750, and 1000 mg/mL, respectively. A 96-well plate was used for the assay, containing 15 µL of each sample and 150 µL of ABTS. The absorbance was measured immediately at 734 nm. Triplicates of all the experiments were conducted.

As a function of the concentration of 6-hydroxy-2,5,7,8-tetramethylchroman-2-carboxylic acid (Trolox), the percentage decrease in absorbance was calculated for each concentration relative to a blank absorbance (methanol/water).

As a measure of antioxidant activity, the TEAC values were calculated from the concentration of a standard Trolox solution having the same antioxidant capacity as 1 mg/mL of the tested extract. As a reference compound, quercetin 3-O-glucoside was used.

### 3.7. Total Flavonoid Assay

An allumine chloride colorimetric assay was used to measure the total flavonoid content utilizing rutin as a standard according to the procedure previously described [15,32]. In a 10 mL volumetric flask, 1 mL (1 mg/mL) of each sample was mixed with 4 mL of water. The flask was then filled with 0.3 mL of 5% NaNO<sub>2</sub>. After 5 min, 0.3 mL of 10% AlCl<sub>3</sub> was added. After 6 min, 2 mL of 1 M NaOH was added, and finally the solution was made up to a volume of 10 mL with water. The absorbances of the samples and the blank were measured at 510 nm in a UV-Vis spectrophotometer. According to Equation (2), the flavonoid content in different extracts is rutin equivalent (RE):

$$\text{Flavonoid amount} = \frac{A * m_0 * 10}{A_0 * m} \quad (2)$$

The flavonoid content RE is expressed as mg/g plant extracts. In the equation,  $A$  is the average of the absorbance of the extract in three samples,  $A_0$  is the average of the



absorbance of the rutin standard solution in three samples,  $m$  is the weight of the analyzed plant extract in g, and  $m_0$  is the weight of the rutin in the solution in g.

### 3.8. Multivariate Data Analysis

A multivariate statistical analysis was applied with a targeted approach to better understand the relationship between the amount of bioactive compounds most expressed in fennel extracts and their antioxidant activity [33]. A data matrix was created in which the rows represented the different samples analyzed and the columns represented the content of the different metabolites quantified by LC-ESI-QTrap-MS/MS analysis. Another column was created, used as component Y, in which the antioxidant activity, expressed as a percentage of inhibition, was added for each sample calculated by either DDPH assay or TEAC assay.

PLS is a regression technique used to relate two sets of data [34]. The dataset was processed using SIMCAP+ 12.0 software (Umetrix AB, Umea, Sweden) for PLS, an approach for modeling the covariance structures between two spaces to find the fundamental relationships between two matrices; X is the amount of bioactive compounds in fennel extracts and Y is the antioxidant activity. Before performing the multivariate data analysis, Pareto scaling was applied to normalize the data. The PLS method was validated through Hotelling's permutation test and the T2 test. The significance of the mode was confirmed by the Q2 values of 0.8 and 0.4, respectively, in the models with DPPH and TEAC as Y-blocks.

## 4. Conclusions

The differences in the quantitative content of flavonoids in fennel varieties characterized by different seasonality showed an interesting variability in terms of flavonoids and phenylpropanoids, for example for neochlorogenic acid, quercetin 3-O-glucuronide, and dicaffeoylquinic acid malonyl.

The chemometric model obtained by the correlation of quantitative data, obtained by sensitive and selective LC-ESI-QTrap-MS/MS analysis of antioxidant activities with a PLS regression model proved to be a selective tool to detect the compounds involved in the antioxidant activities demonstrated by the extracts in chemical tests. The study allowed the identification of quercetin-3-O-glucuronide and kaempferol-3-O-glucuronide as the compounds that better contribute to the evaluated activity, independent of the extract under investigation. Similar correlation methods, based on multivariate data analysis and LC-MS, can be applied to better define the metabolites involved in the bioactivity of extracts of other plants with an interesting nutraceutical potential.

**Author Contributions:** Conceptualization, M.A.C., G.D. and P.M.; data curation, M.A.C., G.D. and P.M.; funding acquisition, S.P. and P.M.; investigation, M.A.C. and G.D.; methodology, M.A.C. and G.D.; project administration, P.M.; resources, S.P. and P.M.; software, M.A.C. and G.D.; supervision, P.M.; validation, M.A.C., G.D. and P.M.; visualization, S.P. and P.M.; writing—original draft, M.A.C., G.D. and P.M.; writing—review and editing, M.A.C., G.D., S.P. and P.M. All authors have read and agreed to the published version of the manuscript.

**Funding:** This research received no external funding.

**Institutional Review Board Statement:** Not applicable.

**Informed Consent Statement:** Not applicable.

**Data Availability Statement:** The data presented in this study is contained within the article.

**Acknowledgments:** The materials used for experiments were provided by "Società agricola Paolillo s.r.l.", via Ilaria Alpi lo. Cioffi, Eboli (SA), Italy.

**Conflicts of Interest:** The authors declare no conflict of interest.

**Sample Availability:** Samples of the compounds are available from the Pharmaceutical Biology Laboratory, Department of Pharmacy, University of Salerno, Via Giovanni Paolo II 132, I-84084 Fisciano, Italy.

## References

- Badgular, S.B.; Patel, V.V.; Bandivdekar, A.H. *Foeniculum vulgare* Mill: A review of its botany, phytochemistry, pharmacology, contemporary application, and toxicology. *Biomed. Res. Int.* **2014**, *2014*, 842674. [[CrossRef](#)] [[PubMed](#)]
- Feroli, F.; Giambanelli, E.; D'Antuono, L.F. Fennel (*Foeniculum vulgare* Mill. subsp. piperitum) florets, a traditional culinary spice in Italy: Evaluation of phenolics and volatiles in local populations, and comparison with the composition of other plant parts. *J. Sci. Food Agric.* **2017**, *97*, 5369–5380. [[CrossRef](#)] [[PubMed](#)]
- Jahan, A. Fennel (*Foeniculum vulgare*). *Plants Med. Values* **2019**, *32*.
- Islam, M.; Srivastava, A.; Kumar, S.; Verma, N. Chemical and pharmacological properties of *Foeniculum vulgare* Mill: A review. *WJPLS* **2022**, *7*, 48–56.
- Esquivel-Ferríño, P.; Favela, J.M.d.J.H.; Garza Gonzalez, E.; Torres, N.; Rios Gomez, Y.; Del, M.; Camacho-Corona, M.d.R. Antimycobacterial Activity of Constituents from *Foeniculum vulgare* Var. Dulce Grown in Mexico. *Molecules* **2012**, *7*, 8471–8482. [[CrossRef](#)]
- Yakut, H.I.; Koyuncu, E.; Cakir, U.; Tayman, C.; Koyuncu, İ.; Taskin Turkmenoglu, T.; Cakir, E.; Ozyazici, A.; Aydogan, S.; Zenciroglu, A. Preventative and therapeutic effects of fennel (*Foeniculum vulgare*) seed extracts against necrotizing enterocolitis. *J. Food Biochem.* **2020**, *44*, e13284. [[CrossRef](#)]
- Choi, E.M.; Hwang, J.K. Antiinflammatory, analgesic and antioxidant activities of the fruit of *Foeniculum vulgare*. *Fitoterapia* **2004**, *75*, 557–565. [[CrossRef](#)]
- Bogucka-Kocka, A.; Smolarz, H.D.; Kocki, J. Apoptotic activities of ethanol extracts from some *Apiaceae* on human leukaemia cell lines. *Fitoterapia* **2008**, *79*, 487–497. [[CrossRef](#)]
- Tognolini, M.; Ballabeni, V.; Bertoni, S.; Bruni, R.; Impicciatore, M.; Barocelli, E. Protective effect of *Foeniculum vulgare* essential oil and anethole in an experimental model of thrombosis. *Pharmacol. Res.* **2007**, *56*, 254–260. [[CrossRef](#)]
- Mohamad, R.H.; El-Bastawesy, A.M.; Abdel-Monem, M.G.; Noor, A.M.; Al-Mehdar, H.A.; Sharawy, S.M.; El-Merzabani, M.M. Antioxidant and anticarcinogenic effects of methanolic extract and volatile oil of fennel seeds (*Foeniculum vulgare*). *J. Med. Food* **2011**, *14*, 986–1001. [[CrossRef](#)]
- Kaur, B.; Rolta, R.; Salaria, D.; Kumar, B.; Fadare, O.A.; da Costa, R.A.; Ahmad, A.; Al-Rawi, M.B.A.; Raish, M.; Rather, I.A. An in silico Investigation to Explore Anti-Cancer Potential of *Foeniculum vulgare* Mill. Phytoconstituents for the Management of Human Breast Cancer. *Molecules* **2022**, *27*, 4077. [[CrossRef](#)] [[PubMed](#)]
- Rather, M.A.; Dar, B.A.; Sofi, S.N.; Bhat, B.A.; Qurishi, M.A. *Foeniculum vulgare*: A comprehensive review of its traditional use, phytochemistry, pharmacology, and safety. *Arab. J. Chem.* **2016**, *9*, S1574–S1583. [[CrossRef](#)]
- Parejo, I.; Jauregui, O.; Sánchez-Rabeneda, F.; Viladomat, F.; Bastida, J.; Codina, C. Separation and characterization of phenolic compounds in fennel (*Foeniculum vulgare*) using liquid chromatography-negative electrospray ionization tandem mass spectrometry. *J. Agric. Food Chem.* **2004**, *52*, 3679–3687. [[CrossRef](#)]
- Piccaglia, R.; Marotti, M. Characterization of some Italian types of wild fennel (*Foeniculum vulgare* Mill.). *J. Agric. Food Chem.* **2001**, *49*, 239–244. [[CrossRef](#)] [[PubMed](#)]
- Crescenzi, M.A.; D'Urso, G.; Piacente, S.; Montoro, P. LC-ESI/LTQOrbitrap/MS Metabolomic Analysis of Fennel Waste (*Foeniculum vulgare* Mill.) as a Byproduct Rich in Bioactive Compounds. *Foods* **2021**, *10*, 1893. [[CrossRef](#)] [[PubMed](#)]
- Crescenzi, M.A.; D'Urso, G.; Piacente, S.; Montoro, P. UPLC-ESI-QTRAP-MS/MS Analysis to Quantify Bioactive Compounds in Fennel (*Foeniculum vulgare* Mill.) Waste with Potential Anti-Inflammatory Activity. *Metabolites* **2022**, *12*, 701. [[CrossRef](#)]
- Sonia, N.S.; Chandran, M.; Geethalekshmi, P. Vegetable peels as natural antioxidants for processed foods—A review. *Agric. Rev.* **2016**, *37*, 35–41. [[CrossRef](#)]
- Wang, H.; Liu, X.; Tu, M.; Xu, X.; Yang, S.; Chen, D. Current sample preparation methods and analytical techniques for the determination of synthetic antioxidants in edible oils. *J. Sep. Sci.* **2022**, *45*, 3874–3886. [[CrossRef](#)]
- Saini, A.; Panesar, P.S.; Bera, M.B. Valorization of fruits and vegetables waste through green extraction of bioactive compounds and their nanoemulsions-based delivery system. *Bioresour. Bioprocess.* **2019**, *6*, 26. [[CrossRef](#)]
- Zhou, D.A.-O.X.; Luo, M.A.-O.; Shang, A.A.-O.X.; Mao, Q.A.-O.; Li, B.A.-O.; Gan, R.A.-O.; Li, H.A.-O. Antioxidant Food Components for the Prevention and Treatment of Cardiovascular Diseases: Effects, Mechanisms, and Clinical Studies. *Oxidative Med. Cell. Longev.* **2021**, *2021*, 6627355. [[CrossRef](#)]
- Castaldo, L.; Izzo, L.; De Pascale, S.; Narváez, A.; Rodriguez-Carrasco, Y.; Ritieni, A. Chemical Composition, in vitro Bioaccessibility and Antioxidant Activity of Polyphenolic Compounds from Nutraceutical Fennel Waste Extract. *Molecules* **2021**, *26*, 1968. [[CrossRef](#)] [[PubMed](#)]
- Ribeiro, D.A.; Camilo, C.J.; de Fátima Alves Nonato, C.; Rodrigues, F.F.G.; Menezes, I.R.A.; Ribeiro-Filho, J.; Xiao, J.; de Almeida Souza, M.M.; da Costa, J.G.M. Influence of seasonal variation on phenolic content and in vitro antioxidant activity of *Secondatia floribunda* A. DC. (*Apocynaceae*). *Food Chem.* **2020**, *315*, 126277. [[CrossRef](#)] [[PubMed](#)]
- Aoussar, N.; Rhallabi, N.; Ait Mhand, R.; Manzali, R.; Bouksaim, M.; Douira, A.; Mellouki, F. Seasonal variation of antioxidant activity and phenolic content of *Pseudevernia furfuracea*, *Evernia prunastri* and *Ramalina farinacea* from Morocco. *J. Saudi Soc. Agric. Sci.* **2020**, *19*, 1–6. [[CrossRef](#)]
- Shi, B.; Zhang, W.; Li, X.; Pan, X. Seasonal variations of phenolic profiles and antioxidant activity of walnut (*Juglans sigillata* Dode) green husks. *Int. J. Food Prop.* **2017**, *20*, S2635–S2646. [[CrossRef](#)]

25. Jorge, T.F.; Mata, A.T.; António, C.A.-O. Mass spectrometry as a quantitative tool in plant metabolomics. *Philos. Trans. A Math. Phys. Eng. Sci.* **2016**, *374*, 20150370. [[CrossRef](#)]
26. Xiao, J.F.; Zhou, B.; Resson, H.W. Metabolite identification and quantitation in LC-MS/MS-based metabolomics. *Trends Analyt. Chem.* **2012**, *32*, 1–14. [[CrossRef](#)]
27. European Medicines Agency. ICH Guideline Q2(R2) on Validation of Analytical Procedures. Available online: [european.eu](http://european.eu) (accessed on 3 March 2022).
28. Pietta, P.G. Flavonoids as antioxidants. *J. Nat. Prod.* **2000**, *63*, 1035–1042. [[CrossRef](#)]
29. Olivares-Vicente, M.; Barrajon-Catalan, E.; Herranz-Lopez, M.; Segura-Carretero, A.; Joven, J.; Encinar, J.A.; Micol, V. Plant-Derived Polyphenols in Human Health: Biological Activity, Metabolites and Putative Molecular Targets. *Curr. Drug Metab.* **2018**, *19*, 351–369. [[CrossRef](#)]
30. Masullo, M.; Cerulli, A.; Mari, A.; de Souza Santos, C.C.; Pizza, C.; Piacente, S. LC-MS profiling highlights hazelnut (*Nocciola di Giffoni* PGI) shells as a byproduct rich in antioxidant phenolics. *Food Res. Int.* **2017**, *101*, 180–187. [[CrossRef](#)]
31. Kılınç, H.; Masullo, M.; D’Urso, G.; Karayildirim, T.; Alankus, O.; Piacente, S. Phytochemical investigation of *Scabiosa sicula* guided by a preliminary HPLC-ESIMS. *Phytochemistry* **2020**, *174*, 112350. [[CrossRef](#)]
32. Dobravalskytė, D.; Venskutonis, P.R.; Talou, T. Antioxidant properties and essential oil composition of *Calamintha grandiflora* L. *Food Chem.* **2012**, *135*, 1539–1546. [[CrossRef](#)] [[PubMed](#)]
33. D’Urso, G.; Pizza, C.; Piacente, S.; Montoro, P. Combination of LC-MS based metabolomics and antioxidant activity for evaluation of bioactive compounds in *Fragaria vesca* leaves from Italy. *J. Pharm. Biomed. Anal.* **2018**, *150*, 233–240. [[CrossRef](#)] [[PubMed](#)]
34. Montoro, P.; D’Urso, G.; Kowalczyk, A.; Tuberoso, C.I.G. LC-ESI/LTQ-Orbitrap-MS Based Metabolomics in Evaluation of Bitter Taste of *Arbutus unedo* Honey. *Molecules* **2021**, *26*, 2765. [[CrossRef](#)] [[PubMed](#)]

**Disclaimer/Publisher’s Note:** The statements, opinions and data contained in all publications are solely those of the individual author(s) and contributor(s) and not of MDPI and/or the editor(s). MDPI and/or the editor(s) disclaim responsibility for any injury to people or property resulting from any ideas, methods, instructions or products referred to in the content.

## Article

# Brain Targeting by Intranasal Drug Delivery: Effect of Different Formulations of the Biflavone “Cupressuflavone” from *Juniperus sabina* L. on the Motor Activity of Rats

El-Sayed Khafagy<sup>1,2,\*</sup>, Gamal A. Soliman<sup>3,4</sup>, Ahmad Abdul-Wahhab Shahba<sup>5</sup>, Mohammed F. Aldawsari<sup>1</sup>, Khalid M. Alharthy<sup>3</sup>, Maged S. Abdel-Kader<sup>6,7</sup> and Hala H. Zaatout<sup>7</sup>

<sup>1</sup> Department of Pharmaceutics, College of Pharmacy, Prince Sattam bin Abdulaziz University, Al-kharj 11942, Saudi Arabia

<sup>2</sup> Department of Pharmaceutics and Industrial Pharmacy, Faculty of Pharmacy, Suez Canal University, Ismailia 41522, Egypt

<sup>3</sup> Department of Pharmacology, College of Pharmacy, Prince Sattam Bin Abdulaziz University, P.O. Box 173, Al-Kharj 11942, Saudi Arabia

<sup>4</sup> Department of Pharmacology, College of Veterinary Medicine, Cairo University, Giza 12211, Egypt

<sup>5</sup> Kayyali Chair for Pharmaceutical Industries, Department of Pharmaceutics, College of Pharmacy, King Saud University, P.O. Box 2457, Riyadh 11451, Saudi Arabia

<sup>6</sup> Department of Pharmacognosy, College of Pharmacy, Prince Sattam Bin Abdulaziz University, P.O. Box 173, Al-Kharj 11942, Saudi Arabia

<sup>7</sup> Department of Pharmacognosy, Faculty of Pharmacy, Alexandria University, Alexandria 21215, Egypt

\* Correspondence: e.khafagy@psau.edu.sa

**Citation:** Khafagy, E.-S.; Soliman, G.A.; Shahba, A.A.-W.; Aldawsari, M.F.; Alharthy, K.M.; Abdel-Kader, M.S.; Zaatout, H.H. Brain Targeting by Intranasal Drug Delivery: Effect of Different Formulations of the Biflavone “Cupressuflavone” from *Juniperus sabina* L. on the Motor Activity of Rats. *Molecules* **2023**, *28*, 1354. <https://doi.org/10.3390/molecules28031354>

Academic Editor: Nour Eddine Es-Safi

Received: 30 November 2022

Revised: 16 January 2023

Accepted: 27 January 2023

Published: 31 January 2023



**Copyright:** © 2023 by the authors. Licensee MDPI, Basel, Switzerland. This article is an open access article distributed under the terms and conditions of the Creative Commons Attribution (CC BY) license (<https://creativecommons.org/licenses/by/4.0/>).

**Abstract:** The polar fractions of the *Juniperus* species are rich in bioflavonoid contents. Phytochemical study of the polar fraction of *Juniperus sabina* aerial parts resulted in the isolation of cupressuflavone (CPF) as the major component in addition to another two bioflavonoids, amentoflavone and robustaflavone. Biflavonoids have various biological activities, such as antioxidant, anti-inflammatory, antibacterial, antiviral, hypoglycemic, neuroprotective, and antipsychotic effects. Previous studies have shown that the metabolism and elimination of biflavonoids in rats are fast, and their oral bioavailability is very low. One of the methods to improve the bioavailability of drugs is to alter the route of administration. Recently, nose-to-brain drug delivery has emerged as a reliable method to bypass the blood–brain barrier and treat neurological disorders. To find the most effective CPF formulation for reaching the brain, three different CPF formulations (A, B and C) were prepared as self-emulsifying drug delivery systems (SEDDS). The formulations were administered via the intranasal (IN) route and their effect on the spontaneous motor activity in addition to motor coordination and balance of rats was observed using the activity cage and rotarod, respectively. Moreover, pharmacokinetic investigation was used to determine the blood concentrations of the best formulation after 12 h. of the IN dose. The results showed that formulations B and C, but not A, decreased the locomotor activity and balance of rats. Formula C at IN dose of 5 mg/kg expressed the strongest effect on the tested animals.

**Keywords:** *Juniperus sabina*; cupressuflavone; intranasal; pharmacokinetic; motor coordination

## 1. Introduction

The frequency of neurological illnesses has been rising over the past few years. A billion people worldwide may suffer from neurological illnesses, according to a 2020 World Health Organization (WHO) assessment [1]. Based on this fact, neurological illnesses are regarded as one of the leading causes of disability and fatalities globally [1,2]. Despite the fact that the majority of novel entities never make it to clinical trials, scientific efforts are continuous to find and create new and effective neuropharmaceuticals.

In fact, successful medications should be able to pass via absorptive membranes, escape the hepatic first-pass effect, and then cross the blood–brain barrier (BBB) unaltered to reach the brain [3,4]. The drug molecule must be lipophilic, with low molecular weight (400 Da), and nonionizable at physiological pH in the absence of the active efflux transporter mechanism to pass through the BBB [3,5]. The lack of such characters reduces the drug bioavailability by limiting the solubility and absorption rate leading to diminished effectiveness [6,7]. Therefore, substantial dosages must be administered to reach minimal effective blood concentrations [8].

Alternative formulations have been created to address the issues, with lipidic nanosystems garnering greater attention recently as nanoemulsions, solid lipid nanoparticles, nano-lipid carriers, and self-emulsifying drug delivery systems (SEDDS) [6]. These systems' major objective is to maintain lipophilic chemicals in solution following contact with aqueous environments, such as those found in the nasal mucosa or gastrointestinal (GI) tract [6]. Lipophilic BCS class II and IV medicines can be included into self-emulsifying drug delivery systems (SEDDS), a form of lipidic nanosystem that is well known for this property [6,7]. The oral route has been the focus of the majority of SEDDS research up until this point [9].

Other delivery methods, however, may be of significant interest for SEDDS, especially if they enhance brain targeting of CNS-active medications. In this situation, it might be advantageous to investigate the intranasal (IN) administration of medications included in lipidic SEDDS. The nasal cavity is the only anatomical region that directly connects the central nervous system (CNS) with the outside world, which is the fundamental justification. Because medicines can partially cross the BBB and enter the brain directly, this mode of delivery becomes particularly appealing for treating neurological illnesses [10,11]. Drugs delivered through the nasal cavity can also pass through the bloodstream to the brain. As a result, there is no GI passage, no hepatic first-pass effect, and granting systemic drug absorption [10,12,13]. Combining the IN route as a potential conduit for nose-to-brain administration with the development of neurotherapeutics in SEDDS form can lead to a considerable rise in brain bioavailability, and an advancement in patient therapeutic management may be anticipated. In addition, numerous long-term side effects of illnesses and non-adherence to medication may be prevented in this way [8].

Genus *Juniperus* is a member of the cypress family (Cupressaceae). The genus comprises more than 65 species widely distributed in the Northern Hemisphere [14]. Members of the genus are evergreen shrubs or trees with needle- or scale-like leaves [15]. Previous phytochemical studies of the *Juniperus* species resulted in the isolation of diterpenes, sesquiterpenoids, lignans, phenylpropanoid, flavonoids, and coumarins [16–18]. Several biflavonoids including amentoflavone, cupressuflavone, robustaflavone, hinokiflavone, and mono-O-methylhinokiflavone were isolated from the polar fractions of the leaf extract of *J. phoenicea* [19–21].

Amentoflavone and related bioflavonoids were reported as potent psychoactive drug leads. Their effect is due to the interactions with CNS receptors and biogenic amine transporters. Biflavonoids such as amentoflavone and dihydroamentoflavone showed the strongest binding activity to rBZP, GABAA receptor, and NET [22]. Biflavonoids including cupressuflavone demonstrated neuroprotective effects via the inhibition of  $\beta$ -secretase and cyclin-dependent kinases (CDKs) [23]. Naturally occurring biflavonoids were also effective against oxidative stress-induced and amyloid  $\beta$ -peptide-induced cell death in neuronal cells [24]. Amentoflavone and ginkgetin from the leaves of *Chamaecyparis obtusa* significantly protected HT22 cells against glutamate-induced oxidative stress [25].

Accordingly, the aim of the current study is to formulate cupressuflavone in a self-nanoemulsifying drug delivery system (CPF-SNEDDS) for IN administration to achieve combined enhancement of drug solubility and cross the BBB to improve CNS bioavailability. The drug was initially incorporated in an optimized SNEDDS formulation, which was then evaluated in vivo to estimate the pharmacological and pharmacokinetic parameters.

## 2. Results and Discussion

### 2.1. Characterization of the Isolated Compounds

HRESIMS of the three isolated compounds (Figures S6, S14 and S24) showed  $(M+H)^+$  at  $m/z$  539.0972, 539.0981, and 539.0973 for **1**, **2**, and **3**, respectively, all represented the molecular formula  $C_{30}H_{18}O_{11}$ . The UV data of **1–3** was diagnostic for the 5, 7, 4'-trihydroxy flavone skeleton [26]. The  $^1H$ - and  $^{13}C$ -NMR (Tables S1 and S2; Figures S1–S5) of **1** showed a set of signals for one apigenin skeleton lacking the H-8 resonance [27]. The MS and NMR data of **1** were diagnostic for symmetric biflavone. Literature data and direct comparison with a previously isolated sample enabled the identification of **1** as cupressuflavone (Figure 1) [21,28].

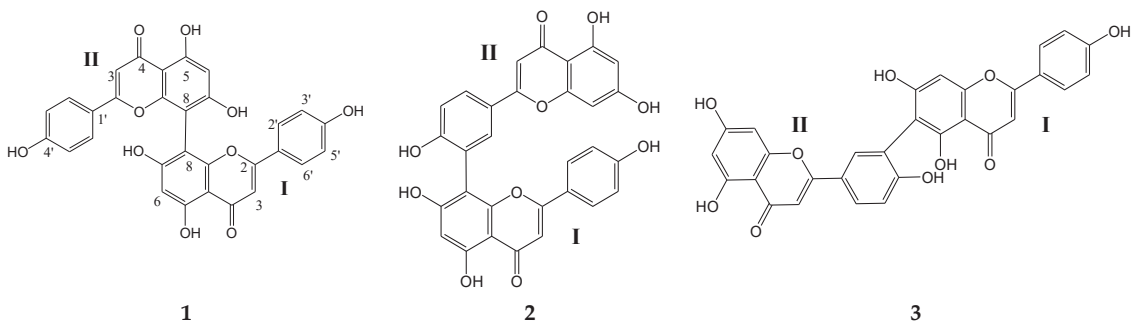


**Figure 1.** Chemical structure of the isolated biflavones.

Compounds **2** and **3** showed signals for two flavonoidal skeletons indicating asymmetric dimeric structures. The  $^1H$ -NMR of **2** and **3** (Figures S7–S13 and S15–S23) showed ABX coupling systems at  $\delta_H$  8.32 (d,  $J = 1.8$  Hz), 6.86 (d,  $J = 8.6$  Hz), and 7.87 (dd,  $J = 1.8, 8.6$  Hz) and 8.18 (bs), 6.79 (d,  $J = 8.3$  Hz), 7.66 (bd,  $J = 8.3$  Hz) assigned for disubstituted ring-B in part II of **2** and **3**, respectively. The values of the carbon chemical shifts of C-3' and C-4' at  $\delta_C$  124.3, 160.8 and 119.9, 158.5 ppm in **2** and **3**, respectively, indicated that C-3' is not oxygenated and it is the point of connection with part I of the two compounds. Both **2** and **3** lack either H-6 or H-8 signal of part I in the  $^1H$ -NMR. The data of **2** were identical with those reported for amentoflavone (Figure 1) [28,29] with connection to part II via C-8. Compound **3** was confirmed as the skeleton where connection to part II took place via C-6. The data of **3** enable its identification as robustaflavone (Figure 1) [29,30].

### 2.2. Excipients Selection and Formulation Optimization

The preliminary precipitation-based solubility study showed that CPF is highly soluble in DMSO while it showed poor solubility in several other excipients with diverse chemical compositions ranging from medium to long chain, monoglycerides/triglycerides/free fatty acids along with several co-solvents and surfactants (Table 1). These findings reflect the challenging physicochemical properties of CPF that limit its efficient formulation. According to these findings, DMSO was selected as an essential excipient within all the selected formulations. On the other hand, Pluronic F127 and Cremophor El were selected to formulate CPF due to their emulsification capabilities along with their potential role in nose-to-brain delivery, as previously demonstrated [31–33].

**Table 1.** Estimated apparent solubility of CPF in various excipients.

Excipient	Role	Estimated Apparent Solubility
Miglyol 810	Oil (medium chain triglycerides)	<2% w/w
Capmul MCM	Oil (medium chain monoglycerides)	<2% w/w
Soybean oil	Oil (long chain triglycerides)	<2% w/w
Maisine 35-1	Oil (long chain monoglycerides)	<2% w/w
Caprylic acid c8	Oil (medium chain free fatty acid)	<2% w/w
Oleic acid	Oil (long chain free fatty acid)	<2% w/w
PG	Co-solvent	<2% w/w
PEG 400	Co-solvent	<2% w/w
Transcutol HP	Co-solvent	<2% w/w
DMSO	Co-solvent	20–24% w/w
Imwitor 988	Co-surfactant	<2% w/w
Imwitor 308	Co-surfactant	<2% w/w
Cremophor EL	Surfactant	<2% w/w
Cremophor RH40	Surfactant	<2% w/w
Tween 85	Surfactant	<2% w/w
HCO-30	Surfactant	<2% w/w

The self-emulsifying nature of the various formulations upon aqueous dispersion showed different degrees of transparency ranging from a clear to whitish milky suspension. The formulations were optimized based on their self-emulsification efficiencies. The compositions of the optimized formulations are presented in Table 2. The most interesting formulation system (formula C) was able to produce nanoemulsions (SNEDDS) (Table 2). Components were developed using water-soluble surfactants and co-solvents.

**Table 2.** The composition (%w/w) of formulations.

Excipients	Formulations		
	A	B	C
CPF	0.5	0.5	0.5
Pluronic F-127	-	9.5	9.5
DMSO	99.5	90	30
Kolliphor EL	-	-	10
Distilled water ad to	-	-	100

### 2.3. Formulation Characterization

Both formulations B and C showed (<200 nm) nano-scale particle size upon aqueous dilution. However, formulation C showed significantly lower droplet size and polydispersity index (PDI) compared to formulation B ( $p < 0.05$ ) (Figure 2A,B). Formulation C showed an average of 37 nm droplet size and 0.2 PDI which suggests the ultimate efficiency of the self-nanoemulsification process and could be attributed to the presence of the highly hydrophilic surfactant (Cr-EL) in the formulation. Several previous studies confirmed the crucial effect of hydrophilic surfactants (high HLB) on the droplet size and self-emulsification efficiency of SNEDDSs [34,35].

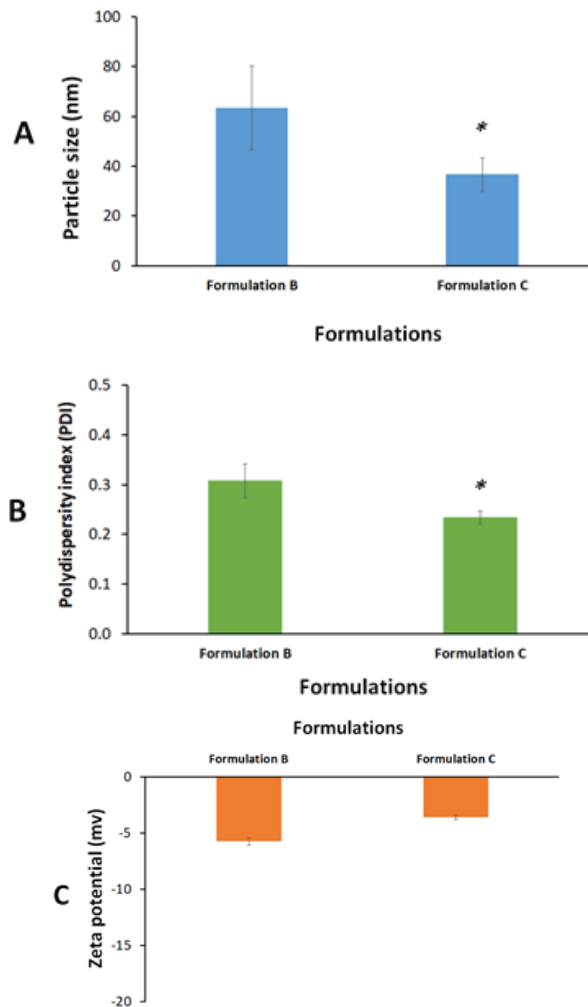


**Figure 2.** Graphical representations of (A) particle size, (B) polydispersity index, and (C) zeta potential of the diluted formulations. Data were expressed as mean  $\pm$  SE. \* denotes significant difference ( $p < 0.05$ ) between the formulations.

On the other hand, both formulations B and C showed low zeta potential values ( $-6$  and  $-4$  mV, respectively) (Figure 2C). Zeta potential is an important parameter that could be linked with nanoemulsion stability. Colloids with low zeta potential absolute values (negative or positive) are prone to the risk of particle agglomeration and physical instability upon storage. Accordingly, formulation C was designed to be prepared and stored in an anhydrous form while it was mixed with water only prior to intranasal administration to avoid undesirable changes in formulation stability upon storage.

#### 2.4. Effect on Spontaneous Motor Activity

Figure 3 shows the effect of Chlorpromazine (CPZ), and A, B, and C formulae on the spontaneous motor activity as vertical and horizontal beam breaks by the rats. Horizontal activity measures exploratory activities at the floor level of the activity cage and small body movement activity such as grooming. On the other hand, vertical activity measures rearing and elevated sniffing movements. Within 10 min observation, the horizontal and vertical



activities of rats treated with CPZ, formula B, and C were significantly decreased relative to the NC rats. Further, there were no significant differences in the horizontal and vertical activities between the formula A-treated group and NC rats. The effects of formula C on the horizontal and vertical activities of rats were 2.43- and 2.27-fold, respectively, lower than those observed in the NC group.

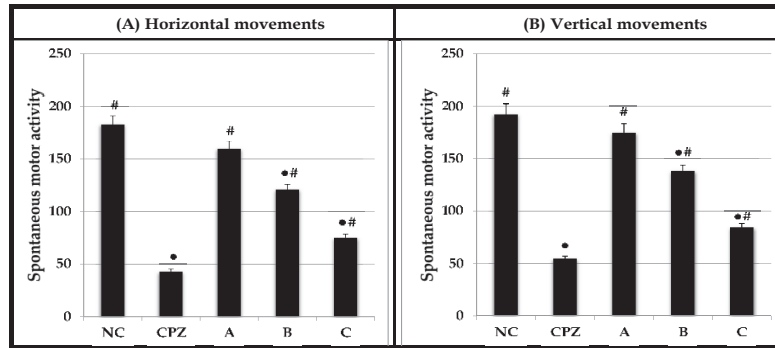


**Figure 3.** Effect of CPZ and A, B, and C formulae on spontaneous motor activity of rats for 10 min using activity cage. Values are expressed as mean  $\pm$  SEM,  $n = 6$  rats/ group. • Significant change at  $p \leq 0.05$  with respect to negative control (NC) rats. # Significant change at  $p \leq 0.05$  with respect to CPZ-treated rats.

### 2.5. Effect on Motor Coordination and Balance

The effects of CPZ, A, B, and C formulae on the motor coordination and balance of rats using the accelerating rotarod test are displayed in Figure 4. Based on this test, we observed no significant difference in latency to fall between the A-treated rats ( $259.2 \pm 9.57$  s) and NC group ( $286.5 \pm 9.84$  s). However, the motor performance declined in rats exposed to CPZ and formula B and C in comparison with the NC group. Rats treated with C formula fell off the rotarod faster ( $115.8 \pm 5.22$  s) than those treated with formula A ( $259.2 \pm 9.57$  s) and B ( $194.6 \pm 6.36$  s). Moreover, formula C showed a 2.47-fold decrease in motor coordination and balance compared to the NC group.

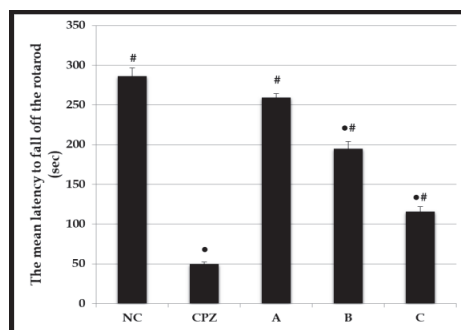


**Figure 4.** Effect of CPZ and A, B, and C formulae on motor coordination and balance in rats using accelerating rotarod. Values are expressed as mean  $\pm$  SEM,  $n = 6$  rats/ group. • Significant change at  $p \leq 0.05$  with respect to negative control (NC) rats. # Significant change at  $p \leq 0.05$  with respect to CPZ-treated rats.

### 2.6. Systemic Absorption of CPF after Intranasal Administration

Biflavonoids and flavonoids may be transported from the systemic blood to the brain through the BBB with possible CNS activation [36,37]. Rats that had undergone

Hirai's surgical procedure were given the drug solution and its optimized formula via the intranasal route to assess the systemic absorption of CPF. Figure 5 shows the time profiles of systemic absorption of CPF after the intranasal administration of drug and its optimized formula C. CPF was slightly absorbed after the nasal administration in the form of solution. The intranasal administration of CPF-optimized formula C significantly increased the nasal absorption and the plasma concentration that was elevated at 15 min post intranasal administration.

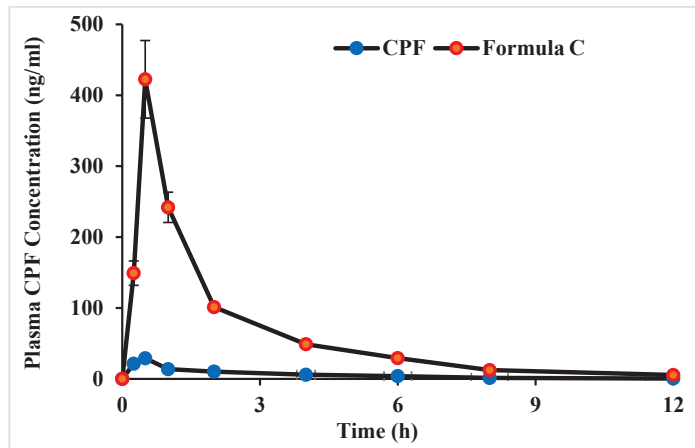


**Figure 5.** Time profiles of plasma CPF concentration (1 mg/kg) after intranasal administration of CPF solution and formula C to rats. Each data value represents the mean  $\pm$  SEM of  $n = 3$ .

Table 3 provides a statistical summary of the pharmacokinetic parameters for the CPF-optimized formula and CPF solution. The CPF level reached its maximal concentration in the plasma after 0.5 h following the intranasal administration of both the drug solution and the CPF-optimized formula, according to the pharmacokinetics results (formula C). This  $T_{max}$  might be attributed to the fast absorption through the intranasal route. The plasma  $C_{max}$  of the intranasal CPF formula was  $422.5 \pm 54.71$  ng/mL, and the intranasal solution was  $29.16 \pm 3.56$  ng/mL. The  $AUC_{0-12}$  was  $263.02 \pm 62.29$  ng.h/mL for the CPF solution and  $29,274.87 \pm 4,855.87$  ng.h/mL for the optimized CPF formula. Statistics indicated that these pharmacokinetic parameter changes were significant. This implied that the systemic absorption of CPF following intranasal delivery was optimal with CPF formula C.

**Table 3.** Pharmacokinetic parameters following intranasal administration of CPF and formula C of CPF.

Pharmacokinetic Parameters	CPF Solution	Formula C
$C_{max}$ (ng/mL)	$29.16 \pm 3.56$	$422.5 \pm 54.71$ **
$T_{max}$ (h)	$0.5 \pm 0.0$	$0.5 \pm 0.0$
$AUC_{0-12}$ (ng.h/mL)	$263.02 \pm 62.29$	$29,274.87 \pm 4,855.87$ **
$AUC_{0-\infty}$ (ng.h/mL)	$265.39 \pm 61.72$	$29,297.89 \pm 4,848.26$ **
$t_{1/2}$ (h)	$2.63 \pm 0.35$	$2.7 \pm 0.41$
$K$ ( $h^{-1}$ )	$0.27 \pm 0.4$	$0.26 \pm 0.3$

Each data value represents the mean  $\pm$  SEM of  $n = 3$ ; \*\*  $p < 0.01$ , significantly different from control (CPF solution).

### 2.7. In Vivo Brain Distribution of CPF after an Intranasal Administration

Considering that CPF is known to cross the BBB, a rise in plasma levels of the substance could lead to its distribution into the brain. We showed that giving the improved formula via the intranasal route enhanced the body's absorption of CPF (Figure 4 and Table 3), encouraging further estimation of the CPF amount in the brain.

The CPF formula was validated via the brain concentration of CPF at 15 min after intranasal injection (Figure 6). The findings imply that intranasal delivery of the CPF formula tended to improve the distribution of CPF into the brain. The optimized formula preferentially enhanced the brain concentration of CPF. These results may be due to making direct transportation of CPF from the nasal cavity to the brain easier. The findings thus revealed that intranasal administration of the formula could enhance the transfer of CPF to the brain. In accordance, previous studies revealed that the addition of a hydrophilic emulsifying agent such as Cremophor RH40 increased fluorescein isothiocyanate brain uptake [36]. Pluronic block copolymers such as Pluronic® P85 showed the ability to increase the blood–brain barrier permeability of several drugs [32]. In addition, Pluronic® F127 was reported to enhance the mucus penetration of nanoparticles for nose-to-brain delivery [33].

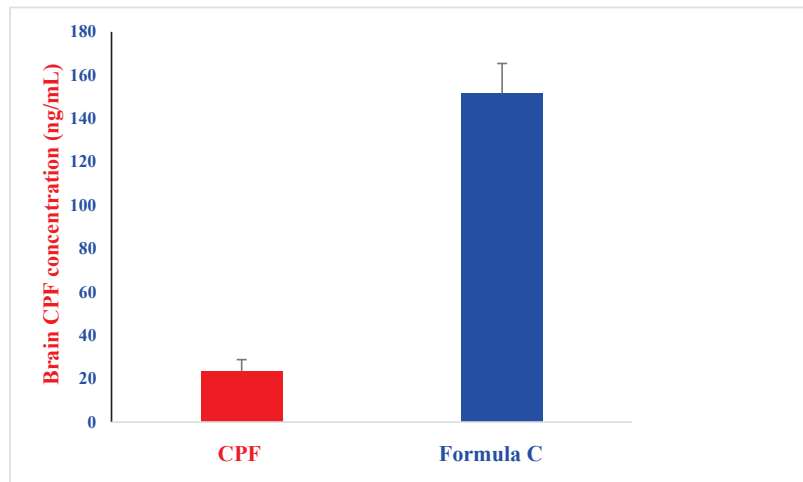


**Figure 6.** Distribution of CPF (1 mg/kg) in the brain at 15 min after intranasal administration of CPF solution and formula C to rats. Each data value represents the mean  $\pm$  SEM of  $n = 3$ .

### 3. Materials and Methods

#### 3.1. General

Melting points were measured using open capillary tubes *Thermosystem FP800 Mettler FP80* central processor supplied with *FP81 MBC* cell apparatus and were uncorrected. Ultra-violet absorptions were obtained using a Unicam Heyios a UV–Visible spectrophotometer.  $^1\text{H}$ -,  $^{13}\text{C}$ -NMR, and 2D-NMR experiments were collected using UltraShield Plus 500 MHz (Bruker, Billerica, MA, USA) (NMR Unite at the College of Pharmacy, Prince Sattam Bin Abdulaziz University) spectrometer operating at 500 MHz for protons and 125 MHz for carbon atoms, respectively. Chemical shift values are reported in  $\delta$  (ppm) relative to the residual solvent peak, and the coupling constants ( $J$ ) are reported in Hertz (Hz). HRMS were determined by direct injection using Thermo Scientific UPLC RS Ultimate 3000—Q Exactive hybrid quadrupole-Orbitrap mass spectrometer combining high performance quadrupole precursor selection with high resolution, accurate-mass (HR/AM) Orbitrap™ detection. Direct infusion of isocratic elution acetonitrile/methanol (70:30) with 0.1% formic acid was used to flush the samples. Runtime was 1 min using nitrogen as auxiliary gas with flow rate 5  $\mu\text{L}/\text{min}$ . Scan range from 160–1500  $m/z$  was used. Resolving power was adjusted to 70,000 @  $m/z$  200. Detection was in both positive and negative modes separately. Calibration was conducted using Thermo Scientific Pierce™ LTQ Velos ESI Positive Ion Calibration Solution including Caffeine, Met-Arg-Phe-Ala (MRFA), Ultramark 1621, *n*-Butyl-amine components, and Pierce™ LTQ Velos ESI. Negative Ion Calibration Solution includes sodium dodecyl sulphate (SDS), sodium taurocholate, Ultramark 1621 components. Capillary temperature set at 320 °C and capillary voltage at 4.2 Kv. Sephadex

LH-20 (Amersham Biosciences, Uppsala, Sweden), silica gel 60/230–400 mesh (EM Science, Swedesboro, NJ, USA), RP C-18 silica gel 40–63/230–400 mesh (Fluka) was used for column chromatography. The thin layer chromatography (TLC) analysis was performed on Kiesel gel 60 F254 and RP-18 F254 (Merck, Rahway, NJ, USA) plates. A UV lamp (entela Model UVGL-25) operated at 254 nm was used for detecting spots on the TLC plates.

### 3.2. Plant Materials

Aerial parts of *Juniperus sabina* L. (Cupressaceae) were described earlier [38].

### 3.3. Extraction, Fractionation and Purification

The dried ground aerial parts (1000 g) were extracted till exhaustion by percolation at room temperature with 95% ethanol (10 L). The resulted extract was concentrated in vacuo to leave dark green viscous residue with aromatic odor. Approximately 200 g of the total extract were dissolved in 1200 mL of 20% aqueous ethanol and fractionated with petroleum ether (500 mL  $\times$  3) to yield 45.86 g petroleum ether soluble fraction. The aqueous ethanol fraction was diluted with water to increase water content to 40% and the resulted solution was fractionated with chloroform (500 mL  $\times$  3) to yield 44.93 g of chloroform soluble fraction, while the remaining aqueous ethanol soluble layer was lyophilized to produce 98.54 g.

The lyophilized aqueous ethanol fraction was reconstituted in water and filtered to yield 37.54 g of water insoluble fraction. Part of the water insoluble fraction (20 g) was purified over Sephadex LH-20 column (300 g, 5 cm id) eluting with methanol. Fractions of 20 mL each were collected, screened with TLC and similar fractions were pooled. Fractions 14–28 provided 435 mg of **1**. Fractions 36–42 yielded 174 mg of **2**, while fractions 50–52 afforded 8 mg of **3**.

### 3.4. Characterization of the Isolated Compounds

**Cupressuflavone (1)**: Yellow powder; mp 392 °C Decomp.; UV  $\lambda_{\max}$  (MeOH) 329, 276, and 226 nm;  $^1\text{H}$ - and  $^{13}\text{C}$ -NMR ( $\text{CD}_3\text{OD}$ ,  $\delta$ ): Tables S1 and S2. HRESIMS:  $m/z$  539.0972 (Cal. 539.0978 for  $\text{C}_{30}\text{H}_{18}\text{O}_{11}$ ) (100,  $[\text{M}+\text{H}]^+$ ).

**Amentoflavone (2)**: Yellow powder; mp 260 °C; UV ( $\lambda_{\max}$ , MeOH): 335, 271, 224 nm;  $^1\text{H}$ - and  $^{13}\text{C}$ -NMR ( $\text{CD}_3\text{OD}$ ,  $\delta$ ): Tables S1 and S2. HRESIMS:  $m/z$  539.0981 (Cal. 539.0978 for  $\text{C}_{30}\text{H}_{18}\text{O}_{11}$ ) (100,  $[\text{M}+\text{H}]^+$ ).

**Robustaflavone (3)**: Yellow powder; mp 351 °C; UV ( $\lambda_{\max}$ , MeOH): 333, 268, 225 nm;  $^1\text{H}$ - and  $^{13}\text{C}$ -NMR ( $\text{CD}_3\text{OD}$ ,  $\delta$ ): Tables S1 and S2. HRESIMS:  $m/z$  539.0973 (Cal. 539.0978 for  $\text{C}_{30}\text{H}_{18}\text{O}_{11}$ ) (100,  $[\text{M}+\text{H}]^+$ ).

### 3.5. Estimation of Apparent Drug Solubility

Several excipients including oils, co-solvents, co-surfactants, and surfactants were preliminarily screened for their suitability for CPF formulation based on their estimated apparent drug solubility. The apparent solubility was indirectly estimated by evaluating drug precipitation-tendency in each excipient. Approximately 1–2  $w/w\%$  CPF was added to each excipient, vortexed to achieve maximum solubilization, and then centrifuged to assess drug precipitation tendency. Excipients that were able to maintain the initial drug amount solubilized were subjected to additional drug loadings until precipitation was observed.

### 3.6. Preparation of CPF Formulations for Intranasal Delivery

Three cupressuflavone (CPF) formulations were prepared to deliver the drug intranasally, namely the drug solution, Microwave Irradiation Solid Dispersion (MW-SD), and self-nanoemulsifying drug delivery system (SNEDDS).

### 3.6.1. Drug Solution

Pure CPF (5 mg) was dissolved in dimethyl sulfoxide (DMSO) to achieve a final CPF concentration of 0.5% *w/w*. The mixture was initially heated at 60 °C, and vortexed to ensure complete homogenization (formulation A).

### 3.6.2. Microwave Irradiation Solid Dispersion (MW-SD)

MW-SD was prepared using domestic MW irradiation (Samsung Model ME0113M1). Pure CPF was blended with Pluronic F-127 at 1:19 *w/w* ratio (Table 1). A precise amount of the drug and the carrier were gently mixed for approx. 1 min. The MW power was set at power 900 W and the samples were subjected to MW irradiation for 7.5 min. The samples were allowed to cool, solidify, and subsequently pulverized to obtain uniform powder. The prepared MW-SD was then mixed with DMSO, heated at 60 °C, and vortexed to ensure complete homogenization (formulation B). (Table 1) [39].

### 3.6.3. Solid-Dispersion Loaded Self-Nano Emulsifying Drug Delivery System (SNEDDS)

A predetermined amount of CPF-loaded MW-SD was mixed with DMSO and Koliphor El, heated at 60 °C, and vortexed to ensure complete homogenization. Prior to assessing the formulation, a precise amount of distilled water was added to the anhydrous formulation as given in Table 1 (formulation C). The mixture was then vortexed for 2 min at ambient temperature to form homogenous mixture [40].

## 3.7. Formulation Characterization

### Particle Size, Polydispersity Index (PDI), and Zeta Potential

Formulation B and formulation C (anhydrous) were dispersed in Milli-Q water at a ratio of 1:9 *w/w*, vortexed for 2 min, and sonicated to ensure uniform formulation dispersion. The diluted formulations were then characterized in terms of the average particle size and polydispersity index (PDI) using a Zetasizer Nano ZS (Malvern Panalytical Ltd., Malvern, UK). Zeta potential was evaluated by laser doppler velocimetry (LDV) mode using the same Nano ZS. Samples were analyzed as triplicates where each replicate was subjected to 3 consecutive measurements (6 runs each).

## 3.8. Experimental Animals

Adult male Sprague Dawley rats with weights ranging from 260 to 280 g were used in this study. Animals were obtained from the lab animal unit at the College of Pharmacy, Prince Sattam bin Abdulaziz University. Animals were kept in ventilated cages; 3–4 rats per cage (IVC Blue Line, Techniplast, Buguggiate VA, Italy). Rats were maintained in controlled laboratory situations ( $24 \pm 0.5$  °C and 12 h/12 h dark/light cycle) with feed and water *ad libitum*. The supervision and dealing with rats were in accordance with the international guidelines for use of animals [41]. The study complied with the regulations of the Standing Committee of Bioethics Research at Prince Sattam bin Abdulaziz University which follow the National Regulations on Animal Welfare and Institutional Animal Ethical Committee under the approval number SCBR-048-2022.

## 3.9. Intranasal Delivery of Cupressuflavone Formulations to Rats

Intranasal (IN) delivery of CPF formulations was carried out as described earlier [42]. Briefly, rats were hand-restrained, placed in a supine position, and given the vehicle, chlorpromazine (CPZ), or formulations by IN administration through a micropipette (Pipetman P-20, Gilson Inc., Middleton, WI, USA) in a constant volume of 50  $\mu$ L [43]. Rats were held in a supine position for 5–10 s after administration to increase the chance for the drug to reach the olfactory region or the nasal cavity with direct access to the brain [44].

## 3.10. Assessment of Spontaneous Motor Activity Using Activity Cage

The activity cage (Model No. 47.420, Ugo Basile S.R.L., Italy) was a Plexiglas box  $41 \times 41 \times 33$  (h) cm with 16 infrared (IR) light beams (2.5 cm above the floor level) on the

horizontal x- and y-axes, producing a network of perpendicular light beams covering the bottom of the cage for assessment of the horizontal activity. Another set of 16 horizontal IR light beams was elevated 5 cm over the floor plane for measurement of the vertical activity (rearing). The beam interruptions were counted and recorded by an electronic unit connected to the activity cage. The day before measurement of the motor activity, animals were allowed to adapt to the cage apparatus for 60 min.

On the test day, rats were allowed to further habituate for 30 min, after which IN administrations were delivered. Five groups of 6 rats each were used for the study. The 1st group, which served as a negative control (NC), received the vehicle (saline). The 2nd group received the standard drug, chlorpromazine (CPZ), at a dose of 1 mg/kg and served as a reference group (REF). The test groups (Groups 3, 4, and 5) were given A, B, or C formula, respectively, at 5 mg/kg.

Thirty min after administration, each animal was placed into the activity cage apparatus for 10 min [45,46]. During the experimental period, silent environment was strongly maintained. Spontaneous motor activity was measured by 2 parameters: (a) horizontal activity equivalent to exploratory activities at the floor level of the activity cage and small movement performance (e.g., grooming) and (b) vertical activity measured rearing and high sniffing activities. At the end of the 10 min session, each animal was returned from the activity cage apparatus to its home cage. The inner walls of the activity cage were wiped out with ethyl alcohol (70%) between sessions to block olfactory cues.

### 3.11. Assessment of Motor Coordination and Balance Using Accelerating Rotarod

Motor coordination and balance of the rats were evaluated with the rotarod apparatus (Model No. 7750; Ugo Basile, Italy) following the method reported by Abada et al. [47]. All animals were trained for 3 consecutive days (4 sessions per day). Each session consisted of 4 attempts lasting 300 s with an inter-attempts period of 30 min. During that period, rats were trained to maintain balance against the motion of a rotating rod that increased from 4 to 40 rotations per minute (rpm). Failure of a rat to maintain balance suggests a neurological deficit. Animals that were able to keep their balance on the bar for 180 s were selected and randomly assigned to five groups such as those used in the activity cage test.

After 30 min of IN administration, each rat was tested 3 times using accelerating speeds of the rotating cylinder of 4 to 40 rpm for 5 min with a 10 min intertrial interval. The device was wiped with ethyl alcohol (70%) and dried prior to each attempt. The mean latency to fall off the rotating cylinder was determined and animals remaining on the rod for more than 300 s were eliminated and their time scored as 300 s.

### 3.12. In Vivo CPF Pharmacokinetic and Biodistribution Study

Rats were confined in a supine position and given an intraperitoneal (i.p.) injection of sodium pentobarbital (50 mg/kg; Nembutal<sup>®</sup>; Abbott Laboratories, Chicago, IL, USA) to induce anesthesia. To keep the anesthetic going, more sodium pentobarbital (12.5 mg/kg) i.p. injections were administered every hour. To close the nasal cavity, surgery was conducted as explained by Hirai et al. [48]. An incision was made in the neck. In order to keep the solutions in the nasal cavity and to maintain respiration, the trachea and esophagus were subsequently cannulated with polyethylene tubing. The nasopalatine ducts were plugged with a medical super glue to stop nasal cavity solutions from draining into the mouth cavity. Rats were given 40  $\mu$ L (20  $\mu$ L /nostril) of CPF solution or the chosen formula intranasally using a micropipette (Pipetman P-20, Gilson Inc., Middleton, WI, USA) at a dose of 1 mg/kg body weight (1 mg/mL). Before and 0.25, 0.5, 1, 2, 4, 6, 8, and 12 h after dosage, blood samples (0.25 mL) were obtained from the jugular vein. Heparin was used to heparinize a 1 mL tuberculin syringe by aspirating heparin to cover the syringe wall and then depressing the plunger to the needle hub to release the remaining heparin. The plasma was extracted from the blood by centrifugation at  $5400 \times g$  for 15 min. The plasma sample was stored until analysis at  $-80$  °C in the freezer.

The right jugular vein was used to collect 0.2 mL of blood at predetermined intervals (0.5 h) after injection. The rat's head was swiftly severed, and the entire brain was carefully isolated, and PBS-cleansed until it was ice cold (pH 7.4). The brain samples were weighed after the water content was removed. The brain samples were homogenized in a homogenizer with two times the volume of ice-cold PBS (pH 7.4) (Heidolph DIAX 900, Chicago, IL, USA). The concentration of CPF was determined using the plasma and supernatant produced after centrifuging the blood sample and brain homogenate at 4 °C and 5400 × g for 15 min. Until analysis, samples were stored at −80 °C.

### 3.13. LC-MS/MS

Plasma and brain samples were analyzed using UHPLC instrument, equipped with a Quaternary pump, a degasser, and autosampler (Dionex UltiMate 3000, Thermo Fisher Scientific®, Waltham, MA, USA). The system is coupled with diode array detector (DAD—3000; Thermo Fisher Scientific®). Separation was performed on RP18 HPLC column (150 mm × 4.6 mm i.d., particle size 5 µm, Dionex, Thermo Fisher Scientific®), and the column oven was maintained at room temperature. The used mobile phase was composed of ultrapure water (A) and acetonitrile (B), each acidified with 1% acetic acid, under 1.0 mL/min flow rate. An isocratic system composed of 80% A and 20% B run for 20 min was selected for the separation. Concentrations were determined based on isolated CPF detected at 340 nm. From each dilution, a sample of 25 µL was injected using the autosampler. The peak representing CPF was detected at RT = 10.27 ± 0.01.

### 3.14. Pharmacokinetic Parameters

The individual plasma concentration–time curves were used to calculate the maximum plasma drug concentration ( $C_{max}$ , ng/mL), the time to attain  $C_{max}$  ( $T_{max}$ , h), and the elimination half-life ( $t_{1/2}$ , h). The area under the curve (AUC) from zero to twelve hours ( $AUC_{0-12}$ , ng·h/mL) and from zero to infinity ( $AUC_{0-\infty}$ , ng·h/mL) were both determined using the trapezoidal rule approach.

### 3.15. Data and Statistical Analysis

All values were expressed as mean ± standard error of mean (S.E.M.). Statistical analysis was performed using one-way ANOVA with post hoc 't' test. The statistical analysis was performed using GraphPad Software, San Diego, CA, USA (version 4). Regarding the droplet size, PDI, and zeta potential data, SPSS (version 28) software was utilized to perform the descriptive statistics, identify, and remove the detected outliers. The significance of the data was analyzed by independent *t*-test where *p* values of less than 0.05 were considered as statistically significant.

## 4. Conclusions

Phytochemical study of the polar fraction of *J. sabina* aerial parts extract resulted in the isolation of three known biflavones: cupressuflavone (CPF), amentoflavone, and robustaflavone. The structures were elucidated using spectroscopic methods including UV, 1D, and 2D NMR as well as HRESIMS. The effect of the major component, CPF, on the CNS was demonstrated. For this purpose, three formulae of the compound were developed for intranasal administration as SNEDDSs. The best formulae were developed using a water-soluble surfactant, and co-solvent based on the formulations design of SNEDDSs. In the *in vivo* evaluation, the rats treated with formula C expressed a decrease in horizontal and vertical movement when tested with the activity cage, and they were unable to maintain their balance when tested with the rotarod apparatus compared to the control group. These findings confirmed the ability of formula C to cause a significant decrease in the motor activity, coordination, and balance of rats after IN administration. Distribution of CPF in the brain and plasma followed the intranasal administration of the developed formula. The pharmacokinetic parameter changes were statistically significant. The data revealed that the optimal CPF formulation involved systemic absorption of CPF after IN administration. The

optimized formula boosted the concentration of CPF preferentially, which might indicate the possible direct transport of CPF from the nasal cavity to the brain.

**Supplementary Materials:** The following supporting information can be downloaded at: <https://www.mdpi.com/article/10.3390/molecules28031354/s1>. Spectrum and datas of Compound 1, 2 and 3.

**Author Contributions:** Conceptualization, E.-S.K., G.A.S. and M.S.A.-K.; methodology, E.-S.K., G.A.S., K.M.A. and H.H.Z.; software, K.M.A. and H.H.Z.; validation, H.H.Z., M.F.A., K.M.A. and A.A.-W.S.; formal analysis, A.A.-W.S., K.M.A. and H.H.Z.; investigation, E.-S.K., A.A.-W.S., G.A.S., M.S.A.-K. and H.H.Z.; resources, M.F.A. and M.S.A.-K.; data curation, K.M.A. and H.H.Z.; writing—original draft preparation, K.M.A., M.F.A. and H.H.Z.; writing—review and editing, E.-S.K., G.A.S. and M.S.A.-K.; visualization, E.-S.K., K.M.A. and H.H.Z.; project administration, G.A.S. and M.S.A.-K. All authors have read and agreed to the published version of the manuscript.

**Funding:** The project was funded by the Deputyship for Research & Innovation, Ministry of Education in Saudi Arabia via project number (IF-PSAU-2022/03/23340).

**Institutional Review Board Statement:** The study was conducted in accordance with the Declaration of Helsinki and approved by the Standing Committee of Bioethics Research at Prince Sattam Bin Abdulaziz University under the approval number SCBR-048-2022.

**Informed Consent Statement:** Not applicable.

**Data Availability Statement:** Not applicable.

**Conflicts of Interest:** The authors declare no conflict of interest.

**Sample Availability:** Sample of the compounds 1 are available from the authors.

## References

- World Health Organization. Neurological Disorders Affect Millions Globally: WHO Report. Available online: <https://www.who.int/news/item/27-02-2007-neurological-disorders-affect-millions-globally-who-report> (accessed on 2 May 2022).
- Pandey, M.; Jain, N.; Kanoujia, J.; Hussain, Z.; Gorain, B. Advances and Challenges in Intranasal Delivery of Antipsychotic Agents Targeting the Central Nervous System. *Front. Pharmacol.* **2022**, *13*, 904. [CrossRef] [PubMed]
- Zhou, X.; Smith, Q.R.; Liu, X. Brain penetrating peptides and peptide–drug conjugates to overcome the blood–brain barrier and target CNS diseases. *Rev. Nanomed. Nanobiotech.* **2021**, *13*, e1695. [CrossRef] [PubMed]
- Chen, Y.S.; Chiu, Y.H.; Li, Y.S.; Lin, E.Y.; Hsieh, D.K.; Lee, C.H.; Huang, M.H.; Chuang, H.M.; Lin, S.Z.; Harn, H.J.; et al. Integration of PEG 400 into a self-nanoemulsifying drug delivery system improves drug loading capacity and nasal mucosa permeability and prolongs the survival of rats with malignant brain tumors. *Int. J. Nanomed.* **2019**, *14*, 3601–3613. [CrossRef] [PubMed]
- Nagaraja, S.; Basavarajappa, G.M.; Karnati, R.K.; Bakir, E.M.; Pund, S. Ion-triggered In Situ gelling nanoemulgel as a platform for nose-to-brain delivery of small lipophilic molecules. *Pharmaceutics* **2021**, *13*, 1216. [CrossRef] [PubMed]
- Rajpoot, K.; Tekade, M.; Pandey, V.; Nagaraja, S.H.; Youngren-Ortiz, S.R.; Tekade, R.K. *Self-Microemulsifying Drug-Delivery System: Ongoing Challenges and Future Ahead*; Elsevier: Amsterdam, The Netherlands, 2019; ISBN 9780128145081.
- Buya, A.B.; Belouqui, A.; Memvanga, P.B.; Pr at, V. Self-nano-emulsifying drug-delivery systems: From the development to the current applications and challenges in oral drug delivery. *Pharmaceutics* **2020**, *12*, 1194. [CrossRef]
- Pires, P.C.; Santos, A.O. Nanosystems in nose-to-brain drug delivery: A review of non-clinical brain targeting studies. *J. Control. Release* **2018**, *270*, 89–100. [CrossRef]
- Froelich, A.; Osmalek, T.; Jadach, B.; Puri, V.; Michniak-Kohn, B. Microemulsion-based media in nose-to-brain drug delivery. *Pharmaceutics* **2021**, *13*, 201. [CrossRef]
- Keller, L.A.; Merkel, O.; Popp, A. Intranasal drug delivery: Opportunities and toxicologic challenges during drug development. *Drug Deliv. Transl. Res.* **2021**, *12*, 735–757. [CrossRef]
- Kapoor, M.; Cloyd, J.C.; Siegel, R.A. A review of intranasal formulations for the treatment of seizure emergencies. *J. Control. Release* **2016**, *237*, 147–159. [CrossRef] [PubMed]
- Costa, C.; Moreira, J.N.; Amaral, M.H.; Sousa Lobo, J.M.; Silva, A.C. Nose-to-brain delivery of lipid-based nanosystems for epileptic seizures and anxiety crisis. *J. Control. Release* **2019**, *295*, 187–200. [CrossRef]
- Oliveira, P.; Fortuna, A.; Alves, G.; Falc o, A. Drug-metabolizing Enzymes and Efflux Transporters in Nasal Epithelium: Influence on the Bioavailability of Intranasally Administered Drugs. *Curr. Drug Metab.* **2016**, *17*, 628–647. [CrossRef]
- Hampe, A.; Petit, R.J. Cryptic forest refugia on the ‘Roof of the World’. *New Phytol.* **2010**, *185*, 5–7. [CrossRef]
- Ogren, T.L. *The Allergy-Fighting Garden: Stop Asthma and Allergies with Smart Landscaping*; Ten Speed Press: Berkeley, CA, USA, 2015; pp. 131–133.



16. Inatomi, Y.; Murata, H.; Inada, A.; Nakanishi, T.; Lang, F.A.; Murata, J.; Iinuma, M. New glycosides of acetophenone derivatives and phenylpropanoids from *Juniperus occidentalis*. *J. Nat. Med.* **2013**, *67*, 359–368. [CrossRef]
17. Seca, A.M.L.; Silva, A.M.S. A new 4',7'-epoxy-8,3'-oxyneolignan from the acetone extract of *Juniperus brevifolia* leaves. *Phytochem. Lett.* **2010**, *3*, 126–128. [CrossRef]
18. Abdel-Kader, M.S.; Hamad, A.M.; Alanazi, M.T.; Alanazi, A.H.; Ali, R.; Foudah, A.I.; Alqarni, M.H. Characterization and hepatoprotective evaluation of sesquiterpenes and diterpenes from the aerial parts of *Juniperus sabina* L. *Saudi Pharm J.* **2019**, *27*, 920–929. [CrossRef]
19. Fatma, W.; Taufeeq, H.M.; Shaida, W.A.; Rahman, W. Biflavonoids from *Juniperus macropoda* Boiss and *Juniperus phoenicea* Linn. (Cupressaceae). *Indian J. Chem. Sect. B Org. Chem. Incl. Med. Chem.* **1979**, *17B*, 193–194.
20. Alqasoumi, S.I.; Abdel-Kader, M.S. Terpenoids from *Juniperus procera* with hepatoprotective activity. *Pak. J. Pharm. Sci.* **2012**, *25*, 315–322.
21. Alqasoumi, S.I.; Farraj, A.I.; Abdel-Kader, M.S. Study of the hepatoprotective effect of *Juniperus phoenicea* constituents. *Pak. J. Pharm. Sci.* **2013**, *26*, 999–1008.
22. Moawad, A.; Hifnawy, M. Flavonoids and Biflavonoids of Amentoflavone Class as Potential Psychoactive Drug Leads. *J. Complement. Altern. Med. Res.* **2017**, *2*, 1–9. [CrossRef]
23. Shrestha, S.; Park, J.H.; Lee, D.Y.; Cho, J.G.; Seo, W.D.; Kang, H.C.; Baek, N.I.; Yoo, K.-H.; Chung, I.-S.; Jeon, J.-I.; et al. Cytotoxic and neuroprotective biflavonoids from the fruit of *Rhus parviflora*. *J. Korean Soc. Appl. Biol. Chem.* **2012**, *55*, 557–562. [CrossRef]
24. Kang, S.S.; Lee, J.Y.; Choi, Y.K.; Song, S.S.; Kim, J.S.; Jeon, S.J.; Han, Y.N.; Son, K.H.; Han, B.H. Neuroprotective effects of naturally occurring biflavonoids. *Bioorg. Med. Chem. Lett.* **2005**, *15*, 3588–3591. [CrossRef]
25. Jeong, E.J.; Hwang, L.; Lee, M.; Lee, K.Y.; Ahn, M.-J.; Sung, S.H. Neuroprotective biflavonoids of *Chamaecyparis obtusa* leaves against glutamate-induced oxidative stress in HT22 hippocampal cells. *Food Chem. Toxicol.* **2014**, *64*, 397–402. [CrossRef] [PubMed]
26. Mabry, T.J.; Markham, K.R.; Thomas, M.B. *The Systemic Identification of Flavonoids*; Springer: Berlin/Heidelberg, Germany, 1970.
27. Ersöz, T.; Harput, Ü.Ş.; Saracoğlu, İ.; Çaliş, İ.; Ogihara, Y. Phenolic Compounds from *Scutellaria pontica*. *Turk. J. Chem.* **2002**, *26*, 16. Available online: <https://journals.tubitak.gov.tr/chem/vol26/iss4/16> (accessed on 30 January 2023).
28. Wollenweber, E.; Kraut, L.; Mues, R. External Accumulation of Biflavonoids on *Gymnosperm* Leaves. *Z. Nat. C* **1998**, *53*, 946–950. [CrossRef]
29. Geiger, H.; Seeger, T.; Hahn, H.; Zinsmeister, H.D.; Markham, K.R.; Wong, H. <sup>1</sup>HNMR Assignments in Biflavonoid Spectra by Proton-Detected C-H Correlation. *Z. Nat. C* **1993**, *48*, 821–826. [CrossRef]
30. Jo, A.; Yoo, H.J.; Lee, M. Robusta flavone Isolated from *Nandina domestica* Using Bioactivity-Guided Fractionation Downregulates Inflammatory Mediators. *Molecules* **2019**, *24*, 1789. [CrossRef]
31. Dhuria, S.V.; Hanson, L.R.; Frey, W.H. Intranasal delivery to the central nervous system: Mechanisms and experimental considerations. *J. Pharm. Sci.* **2010**, *99*, 1654–1673. [CrossRef]
32. Chen, Y.; Liu, L. Modern methods for delivery of drugs across the blood–brain barrier. *Adv. Drug Deliv. Rev.* **2012**, *64*, 640–665. [CrossRef]
33. Sonvico, F.; Clementino, A.; Buttini, F.; Colombo, G.; Pescina, S.; Stanişcuaski Guterres, S.; Raffin Pohlmann, A.; Nicoli, S. Surface-Modified Nanocarriers for Nose-to-Brain Delivery: From Bioadhesion to Targeting. *Pharmaceutics* **2018**, *10*, 34. [CrossRef]
34. Pouton, C.; Porter, C. Formulation of lipid-based delivery systems for oral administration: Materials, methods and strategies. *Adv. Drug Deliv. Rev.* **2008**, *60*, 625–637. [CrossRef]
35. Shahba, A.A.; Mohsin, K.; Alanazi, F.K. The studies of phase equilibria and efficiency assessment for self-emulsifying lipid-based formulations. *AAPS Pharm. Sci. Technol.* **2012**, *13*, 522–533. [CrossRef] [PubMed]
36. Veronika, B.; Tobias, B.; Brigitte, K.; Werner, W.; Hilke, W. Long-term effects of St. John's wort and hypericin on monoamine levels in rat hypothalamus and hippocampus. *Brain Res.* **2002**, *930*, 21–29.
37. Oliver, G.; Jie, W.; McGregor, G.P.; Veronika, B. Anxiolytic activity of a phytochemically characterized *Passiflora incarnata* extract is mediated via the GABAergic system. *Planta Med.* **2008**, *74*, 1769–1773.
38. Abdel-Kader, M.S.; Alanazi, M.T.; Saeedan, A.S.B.; Al-Saikhan, F.I.; Hamad, A.M. Hepatoprotective and nephroprotective activities of *Juniperus sabina* L. aerial parts. *J. Pharm. Pharmacogn. Res.* **2017**, *5*, 29–39.
39. Shahba, A.A.; Tashish, A.Y.; Alanazi, F.K.; Kazi, M. Combined Self-Nanoemulsifying and Solid Dispersion Systems Showed Enhanced Cinnarizine Release in Hypochlorhydria/Achlorhydria Dissolution Model. *Pharmaceutics* **2021**, *13*, 627. [CrossRef]
40. El-Laithy, H.M.; Basalious, E.B.; El-Hoseiny, B.M.; Adel, M.M. Novel self-nanoemulsifying self-nanosuspension (SNESNS) for enhancing oral bioavailability of diacerein: Simultaneous portal blood absorption and lymphatic delivery. *Int. J. Pharm.* **2015**, *490*, 146–154. [CrossRef]
41. Committee for the Update of the Guide for the Care and Use of Laboratory Animals. *Guide for the Care and Use of Laboratory Animals*, 8th ed.; Institute for Laboratory Animal Research: Washington, DC, USA, 2011.
42. Marks, D.R.; Tucker, K.; Cavallin, M.A.; Mast, T.G.; Fadool, D.A. Awake intranasal insulin delivery modifies protein complexes and alters memory, anxiety, and olfactory behaviors. *J. Neurosci.* **2009**, *29*, 6734–6751. [CrossRef]
43. Westin, U.; Piras, E.; Jansson, B.; Bergström, U.; Dahlin, M.; Brittebo, E.; Björk, E. Transfer of morphine along the olfactory pathway to the central nervous system after nasal administration to rodents. *Eur. J. Pharm. Sci.* **2005**, *24*, 565–573. [CrossRef]
44. Erdo, F.; Bors, L.; Farkas, D.; Bajza, A.; Gizurarson, S. Evaluation of intranasal delivery route of drug administration for brain Targeting. *Brain Res. Bull.* **2018**, *143*, 155–170. [CrossRef]

45. Stevens, J.; Suidgeest, E.; Van Der Graaf, P.; Danhof, M.; De Lange, E. A new minimal-stress freely-moving rat model for preclinical studies on intranasal administration of CNS drugs. *Pharm. Res.* **2009**, *26*, 1911–1917. [[CrossRef](#)]
46. Wambebe, C.; Gamaniel, K.; Akah, P.; Kapu, S.D.; Samson, A.; Orisadipe, A.T.; Okogun, J.I. Central and uterotonic effects of cycleanine. *Indian J. Pharmacol.* **1997**, *29*, S366–S372.
47. Abada, Y.K.; Nguyen, H.P.; Schreiber, R.; Ellenbroek, B. Assessment of motor function, sensory motor gating and recognition memory in a novel BACHD transgenic rat model for Huntington disease. *PLoS ONE* **2013**, *8*, e68584. [[CrossRef](#)] [[PubMed](#)]
48. Hirai, S.; Yashiki, T.; Matsuzawa, T.; Mima, H. Absorption of drugs from the nasal mucosa of rat. *Int. J. Pharm.* **1981**, *7*, 317–325.

**Disclaimer/Publisher’s Note:** The statements, opinions and data contained in all publications are solely those of the individual author(s) and contributor(s) and not of MDPI and/or the editor(s). MDPI and/or the editor(s) disclaim responsibility for any injury to people or property resulting from any ideas, methods, instructions or products referred to in the content.



Article

# Ultrasound-Assisted Extraction of Total Phenolic Compounds and Antioxidant Activity Evaluation from Oregano (*Origanum vulgare* ssp. *hirtum*) Using Response Surface Methodology and Identification of Specific Phenolic Compounds with HPLC-PDA and Q-TOF-MS/MS

Afroditi Michalaki <sup>1,\*</sup>, Haralabos C. Karantonis <sup>1,\*</sup>, Anastasia S. Kritikou <sup>2</sup>, Nikolaos S. Thomaidis <sup>2</sup> and Marilena E. Dasenaki <sup>3</sup>

<sup>1</sup> Laboratory of Food Chemistry, Biochemistry and Technology, Department of Food Science and Nutrition, School of the Environment, University of The Aegean, 81400 Lemnos, Greece

<sup>2</sup> Laboratory of Analytical Chemistry, Department of Chemistry, National and Kapodistrian University of Athens, 15771 Athens, Greece

<sup>3</sup> Laboratory of Food Chemistry, Department of Chemistry, National and Kapodistrian University of Athens, 15771 Athens, Greece

\* Correspondence: fnsd20011@fns.aegean.gr (A.M.); chkarantonis@aegean.gr (H.C.K.); Tel.: +30-225408311 (H.C.K.)

**Citation:** Michalaki, A.; Karantonis, H.C.; Kritikou, A.S.; Thomaidis, N.S.; Dasenaki, M.E. Ultrasound-Assisted Extraction of Total Phenolic Compounds and Antioxidant Activity Evaluation from Oregano (*Origanum vulgare* ssp. *hirtum*) Using Response Surface Methodology and Identification of Specific Phenolic Compounds with HPLC-PDA and Q-TOF-MS/MS. *Molecules* **2023**, *28*, 2033. <https://doi.org/10.3390/molecules28052033>

Academic Editor: Lucia Panzella

Received: 14 December 2022

Revised: 15 February 2023

Accepted: 15 February 2023

Published: 21 February 2023



**Copyright:** © 2023 by the authors. Licensee MDPI, Basel, Switzerland. This article is an open access article distributed under the terms and conditions of the Creative Commons Attribution (CC BY) license (<https://creativecommons.org/licenses/by/4.0/>).

**Abstract:** Oregano is native to the Mediterranean region and it has been reported to contain several phenolic compounds particularly flavonoids that have been related with multiple bioactivities towards certain diseases. Oregano is cultivated in the island of Lemnos where the climate promotes its growth and thus it could be further used in promoting local economy. The aim of the present study was to establish a methodology for the extraction of total phenolic content along with the antioxidant capacity of oregano by using response surface methodology. A Box–Behnken design was applied to optimize the extraction conditions with regard to the extraction time, temperature, and solvent mixture with the use of ultrasound-assisted extraction. For the optimized extracts, identification of the most abundant flavonoids (luteolin, kaempferol, and apigenin) was performed with an analytical HPLC-PDA and UPLC-Q-TOF MS methodology. The predicted optimal conditions of the statistical model were identified, and the predicted values confirmed. The linear factors evaluated, temperature, time, and ethanol concentration, all showed significant effect ( $p < 0.05$ ), and the regression coefficient ( $R^2$ ) presented a good correlation between predicted and experimental data. Actual values under optimum conditions were  $362.1 \pm 1.8$  and  $108.6 \pm 0.9$  mg/g dry oregano with regard to total phenolic content and antioxidant activity based on 2,2-Diphenyl-1-picrylhydrazyl (DPPH) assay, respectively. Additionally, further antioxidant activities by 2,2'-azino-bis(3-ethylbenzothiazoline-6-sulfonic acid) (ABTS) ( $115.2 \pm 1.2$  mg/g dry oregano), Ferric Reducing Antioxidant Power (FRAP) ( $13.7 \pm 0.8$  mg/g dry oregano), and Cupric Reducing Antioxidant Capacity (CUPRAC) ( $1.2 \pm 0.2$  mg/g dry oregano) assays were performed for the optimized extract. The extract acquired under the optimum conditions contain an adequate quantity of phenolic compounds that could be used in the production of functional foods by food enrichment procedure.

**Keywords:** oregano; box–behnken; phenolics; antioxidants; HPLC-PDA analysis; UPLC-Q-TOF MS

## 1. Introduction

Oregano (*Origanum vulgare* ssp. *hirtum*) is an aromatic herb that mainly comes from *Lamiaceae* and *Verbenaceae* families, which are the most world's commercially traded culinary herbs that has been used long as a condiment and spice for food, salads, meat, etc. [1,2]. *Origanum vulgare* L. originally came from warm climates in western and southwestern

Eurasia and the Mediterranean region. It is a perennial plant that has the characteristics of an herb, green, and leaflike, with round shaped leaves. It is split into four main groups: Turkish oregano (*Origanum onites*), Spanish oregano (*Coridohymus capitatu*), Greek oregano (*Origanum vulgare*), and Mexican oregano (*Lippia graveolens*). The most studied oregano species is the Greek oregano (*Origanum vulgare*), with many studies explaining the potential as antioxidant, antimicrobial, antifungal, anti-inflammatory, and skin defensive auxiliaries with all these capacities to be associated with its rich polyphenolic content [3]. Oregano has been traditionally used in folk medicine for the treatment of general infections, inflammation-related illnesses, asthma, indigestion, stomachache, bronchitis, coughs, diarrhea, menstrual disorders, and diabetes [4,5]. Previous studies on the chemical composition of oregano have revealed the presence of phenolic acids and flavonoids. These compounds can potentially prevent the oxidating stress [6,7]. High antioxidant capacity is an important factor for the delay or the prevention of several diseases, such as heart diseases, neurodegenerative diseases, cancer, and of the aging process [8].

Oregano is known to contain a high quantity of phenolic acids and especially flavonoids. Among others, apigenin, luteolin, and kaempferol have been studied for its presence in oregano extracts [9,10]. Despite the well-known antioxidant properties of apigenin, this molecule has been also reported for the potential benefits on the immune system, sleep, testosterone production, blood sugar levels, and several types of cancer [11]. Furthermore, luteolin and kaempferol have been studied for the anti-oxidative, anti-tumor, and anti-inflammatory properties, but also for their potential anticancer properties [12–14]. In addition, oregano and its extracts are used to treat various illnesses, such as Alzheimer's and cardiovascular diseases, but also are employed to help people with thrombosis problems and strokes [15].

Considering the health benefits of specific oregano constituents, it is of high interest to evaluate and optimize a procedure that will properly extract the compounds of interest in order to further utilize the extracts. Taking into consideration that the extraction step is of highest importance to acquire the compounds of interest; there is growing interest in evaluating the proper extraction techniques and optimize the respective process parameters.

Several new extraction techniques have been developed in the frame of green extraction, such as microwave extraction (ME), supercritical fluid extraction (SFE), and ultrasonic-assisted extraction (UAE). Special interest has been given in ultrasound assisted extraction due to its positive impact on bioactive compounds extraction process, such as higher product yields, shorter extraction time, and lower costs in contrast with other extraction techniques [16,17].

*Origanum vulgare* ssp. *hirtum* is cultivated on the island of Lemnos and is a crop important for the economic viability of the island. The study and highlighting of important bioactivities, such as its antioxidant activity, could lead to its further use as a raw material for the development of new functional foods. The goal of promoting innovation and entrepreneurship in the context of the agri-food sector is served within this study performed. The exploitation of the local herbs, such as *Origanum vulgare* ssp. *hirtum*, which is abundant in the island of Lemnos, could lead to the production of new functional foods or the further development of already existing traditional products. Increased consumer demand for such foods will in turn lead to more sustainable conditions in the future for local communities in these areas. Additionally, the increased consumer demand for such products would assist local economies in these locations by helping them establish a more solid economic basis for the future. At the same time, research in this area will continue to contribute towards this direction.

Thus, the aim of the present study was to identify the optimum extraction conditions of Oregano (*Origanum vulgare* ssp. *hirtum*) cultivated in the Greek island of Lemnos with regard to total phenolic compounds and the antioxidant activities of the extracts by using a response surface methodology. Additionally, for the extracts acquired under the optimum conditions, the existence of apigenin, kaempferol, and luteolin by HPLC-PDA and HPLC-QTOF-MS methodology was evaluated.

## 2. Results and Discussion

### 2.1. Model Fitting

The optimization of the extraction procedure by ultrasound assisted extraction (UAE) of total phenolic compounds and antioxidant activity evaluation by DPPH assay from oregano was carried out by response surface methodology. More specifically, a Box–Behnken Design (BBD) was used to find out the combined effect between the factors of extraction temperature (40 °C, 60 °C, and 80 °C) ( $X_1$ ), extraction time (20 min, 30 min, and 40 min) ( $X_2$ ), and ethanol concentration (60%, 70%, and 80% *v/v*) ( $X_3$ ).

The experimental design matrix produced based on BBD consisted of 15 combinations, including three center points, resulting in a randomizing run order to reduce impact of variation on response values owing to the external factors. The results obtained are shown in Table 1. The experimental values varied from 25.0 mg to 250.0 mg gallic acid equivalent/g dry oregano regarding the total phenolic compounds and 22.2 mg to 95.6 mg Trolox equivalent/g dry oregano regarding the DPPH assay (Table 1).

**Table 1.** Coded and actual values of BBD design, and the results of experiments for total phenolic compounds and antioxidant activity evaluation by DPPH assay from oregano.

Run	Independent Factors			Dependent Factors			
	$X_1$ Temperature (°C)	$X_2$ Time(min)	$X_3$ Ethanol (% <i>v/v</i> )	Experimental Values		Predicted Values	
				TPC (mg/g) <sup>1</sup>	DPPH (mg/g) <sup>1</sup>	TPC (mg/g) <sup>1</sup>	DPPH (mg/g) <sup>1</sup>
1	60 (0)	20 (−1)	80 (+1)	80.0	30.4	77.2	30.8
2	40 (−1)	30 (0)	80 (+1)	25.0	22.2	23.8	20.3
3	80 (+1)	30 (0)	80 (+1)	95.0	41.3	103.6	43.9
4	60 (0)	30 (0)	70 (0)	73.3	46.8	78.1	38.8
5	80 (+1)	20 (−1)	70 (0)	180.0	71.7	194.4	78.4
6	40 (−1)	20 (−1)	70 (0)	30.9	39.3	31.5	36.2
7	60 (0)	40 (+1)	80 (+1)	64.7	27.7	67.4	28.2
8	40 (−1)	30 (0)	60 (−1)	25.0	26.2	28.3	30.6
9	80 (+1)	30 (0)	60 (−1)	205.0	75.2	150.7	66.4
10	60 (0)	40 (+1)	60 (−1)	134.8	55.9	141.4	55.2
11	40 (−1)	40 (+1)	70 (0)	40.9	42.2	36.6	43.0
12	60 (0)	30 (0)	70 (0)	69.5	31.6	78.1	38.8
13	80 (+1)	40 (+1)	70 (0)	250.0	95.6	289.3	93.2
14	60 (0)	20 (−1)	60 (−1)	75.0	36.5	71.9	35.8
15	60 (0)	30 (0)	70 (0)	95.0	39.6	78.1	38.8

<sup>1</sup> DPPH (2,2-diphenyl-1-picrylhydrazyl): Results are presented as mg of Trolox equivalents (TE) per g of dry oregano; TPC: Total phenolic content presented as mg of Gallic acid equivalents per g of dry oregano.

The fitting of the full quadratic approximation of the BBD response surface model was estimated by the analysis of variance (ANOVA). The F-values and relevant *p*-values were used to examine the significance of each source of terms, that is, linear, two-factor interaction, quadratic, and the regression coefficients of the fitted models. Terms with *p*-value lower than 0.05 at the 95% confidence interval were identified as statistically significant.

A multiple regression analysis was employed to fit the response value and the experiment data. Model reduction was carried out, excluding a lower-order term that did not affect the model hierarchy to further refine full quadratic response surface model by removing the insignificant terms with a significance level greater than 5% ( $p > 0.05$ ). To further refine full quadratic response surface model, due to the existence of non-significance effect of factors, transformation of the data, and exclusion of time\*temperature term was performed.

The results of the analysis of variance (ANOVA), after data transformation and model reduction, that was used to determine the degree to which the quadratic approximation of the BBD response surface reduced models fitted the data are presented in Table 2.

**Table 2.** Results of the analysis of the variance (ANOVA) for transformed data concerning the fitting of reduced response surface model for UAE extraction of total phenolic content (TPC) and antioxidant activity evaluation (DPPH assay).

Source	2 DF	1 TPC		DF	1 DPPH	
		F-Value	p-Value		F-Value	p-Value
Model	8	80.68	0.000	8	17.30	0.001
Linear	3	194.68	0.000	3	31.87	0.000
Time	1	10.83	0.017	1	3.55	0.108
Temperature	1	550.09	0.000	1	71.62	0.000
EtOH Conc	1	23.13	0.003	1	20.45	0.004
Square	3	11.30	0.007	3	11.98	0.006
Time*Time	1	17.93	0.005	1	8.37	0.028
Temperature*Temperature	1	5.74	0.054	1	9.58	0.021
EtOH Conc*EtOH Conc	1	7.68	0.032	1	15.50	0.008
2-Way Interaction	2	13.74	0.006	2	3.43	0.102
Time*Temperature	1	-	-	1	-	-
Time*EtOH Conc	1	14.24	0.009	1	4.05	0.091
Temperature*EtOH Conc	6	13.24	0.011	6	2.81	0.145
Error	4			4		
Lack-of-Fit	2	0.10	0.973	2	0.14	0.953
Pure Error	14			14		
R <sup>2</sup>		0.9772		0.9390		
Adjusted R <sup>2</sup>		0.9544		0.8780		
Predicted R <sup>2</sup>		0.9108		0.8084		

<sup>1</sup>: Box-Cox data transformation was performed using optimal  $\lambda = -0.12$  for TPC, and  $\lambda = 0.23$  for DPPH. Reduction in the models was performed with the exclusion of temperature\*time term without affecting the hierarchy model.  
<sup>2</sup>: DF stands for Degree of freedom.

The ANOVA results (Table 2) suggested that the refined second-order models were statistically significant for TPC and DPPH, since the F-values of 80.68 and 17.30 have a zero % and 0.001 % chance, respectively to occur due to noise.

Table 2 also indicates the linear, quadratic, and interaction terms that are significant for the models concerning the two tests performed, total phenolic content, and antioxidant activity evaluation. Concerning the linear terms temperature ( $X_1$ ), time ( $X_2$ ), and ethanol concentration ( $X_3$ ), they all showed significant effect ( $p < 0.05$ ). Temperature, time, and ethanol as solvent have been previously shown to be factors of interest when optimization of phenolic compound green extraction is studied [18,19].

In addition to the linear source, quadratic terms indicated statistically significant effects. Quadratic term of temperature ( $X_1^2$ ), time ( $X_2^2$ ), and ethanol concentration ( $X_3^2$ ) indicated statistically significant effects on both models ( $p < 0.05$ ).

Moreover, concerning the interaction coefficient that exert statistically significant effects on the models, the interaction of time and ethanol concentration ( $X_1X_3$ ), and temperature and ethanol ( $X_2X_3$ ), showed statistically significant effect on the model of total phenolic compounds ( $p < 0.05$ ).

The regression coefficient ( $R^2$ ) was also evaluated, results are presented in Table 2, indicating a good correlation between predicted and experimental data.

Depending on the substance and the molecules extracted, variations in ethanol may alter solution polarity, which could be extremely important for extraction by impacting phenolic solubility. On the other hand, high ethanol concentrations can result in pectin dehydration and protein denaturation, which prevent phenolics from diffusing through the matrix of plant material into the solution. Additionally, the right amount of water in the solution may cause the dry matter of plants to swell, expanding the contact surface between the solvent and the solute, performing a positive effect on the extraction [20]. More specifically, the amount of 60% ethanol has been successfully studied for its capacity to optimum extract phenolics from oregano [21].

Furthermore, in order to increase the mass transfer rate, cavitation effect, but also the solubility of phenolic compounds, solvent extraction is often carried out at relatively high temperatures, but high temperatures may also cause phenolic deterioration [22]. However, flavonoids degradation at high temperatures (greater than 150 °C) have been reported in prolonged extraction time (greater than 201 min) [23]. In the study performed by Oreopoulou et al., lower quantities of total phenolics were obtained compared to the quantity obtained in the present study. The immersion of oregano to water–steam distillation for 6 h, is possible to lead to degradation of some phenolics. Increased temperature improves the extraction efficiency of phenolics because it increases their solubility and diffusivity, which in turn improves the mass transfer. However, heat may be able to lessen the severity of cavitation bubbles collapsing by reducing the variations in vapor pressure between the interior and exterior of the bubbles. When the temperature of the extracted material is raised, the surface tension decreases, reducing the sheer force of the popping bubbles.

Extracting at the lowest possible cost is largely dependent on how quickly the procedure can be completed. Typically, better extraction efficiency may be seen during the first time periods owing to the steep gradient solvent slope, which gradually diminishes with time. In addition, short extraction times are achieved as a result of cavitation, thermal, and physical phenomena induced at the extracted material's surface [24].

The lack of fit was also not significant ( $p > 0.05$ ) for the models of TPC and antioxidant activity evaluation implying that the models fit the data and each model may give accurate predictions.

Significant linear, quadratic, and interaction terms lead to the predictive equations (Equations (1) and (2)) as presented in Table 3. Positive and negative signs, of its coefficient in its equation of the quadratic models, indicate, respectively, positive or negative effect on the extraction efficiency of the studied phenolics.

**Table 3.** Quadratic models of polynomial predictive equations of response surface total phenolic content (TPC) and antioxidant activity evaluation (DPPH assay) from oregano.

<sup>1</sup> Predictive Equations		
TPC	(Equation (1))	$-TPC^{-0.5} - 1.013 - 0.00053 X_2 + 0.00852 X_1 + 0.01692 X_3 + 0.000142 X_2^2 - 0.000049 X_1^2 - 0.000104 X_3^2 - 0.000105 X_2 X_3$
DPPH	(Equation (2))	$\ln(DPPH) = -8.39 - 0.0171X_2 - 0.0431X_1 + 0.389X_3 + 0.001946 X_2^2 + 0.000520 X_1^2 - 0.002647 X_3^2 - 0.001301 X_2X_3$

<sup>1</sup> DPPH: Results are presented as mg of Trolox equivalents (TE) per g of dry oregano; TPC: Total phenolic content presented as mg of Gallic acid equivalents per g of dry oregano.  $X_1$ : Temperature (T) in °C;  $X_2$ : Time in min,  $X_3$ : Ethanol concentration (% *v/v*).

## 2.2. Optimization of the Extraction Conditions

Response surface methodology was employed to evaluate the combined effect of the three factors to maximize the extraction of the total phenolic compounds and the antioxidant activity of the extracts as per the DPPH assay. The three-dimensional response surface plots that describe the interactive effect of the independent factors on the quantity of phenolics that were extracted by UAE are presented, for all three factors which were shown to be significant, in Figures 1–6.

The response surface methodology holds an important role in the exploration of the optimum conditions of independent variables that can contribute to achieve a maximum response [25,26]. Response surface plots are useful for establishing the response values and operation conditions as required. Additionally, they can provide a method to visualize the results and help in processing the experimental levels of each variable and the type of interactions between [27].



Total phenolic compounds surface plot

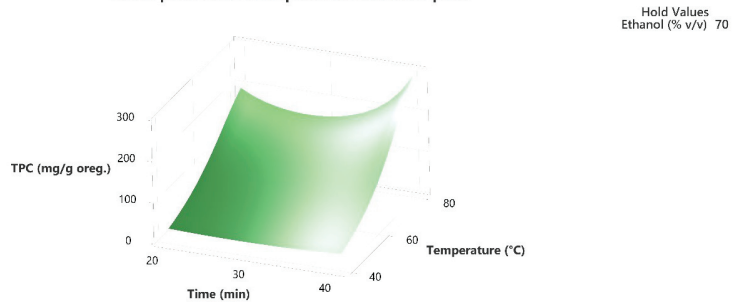


**Figure 1.** Three-dimensional response surface plot of the TPC (response variable) in mg of gallic acid equivalent/g of dry matter (DM) of oregano as a function of Time ( $X_2$ ) in min. and Temperature ( $X_1$ ) in Celsius degrees (°C) while holding ethanol at 70% ( $v/v$ ).

Total phenolic compounds surface plot

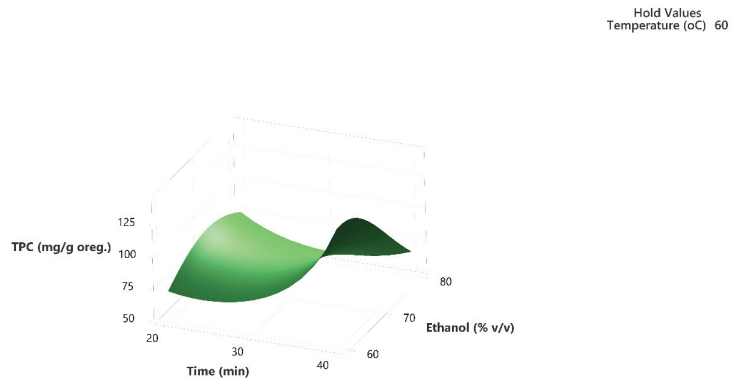


**Figure 2.** Three-dimensional response surface plot of the TPC (response variable) in mg of gallic acid equivalent/g of dry matter (DM) of oregano as a function of Time ( $X_2$ ) in min. and Ethanol % $v/v$  ( $X_3$ ) while holding temperature at 60 °C.

Total phenolic compounds surface plot

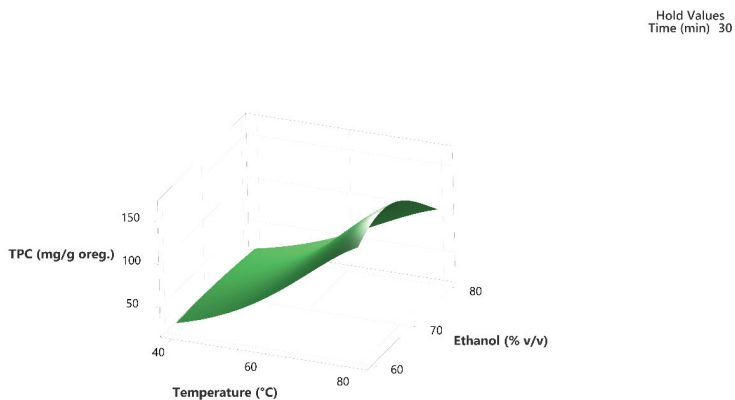


**Figure 3.** Three-dimensional response surface plot of the TPC (response variable) in mg of gallic acid equivalent/g of dry matter (DM) of oregano as a function of temperature ( $X_2$ ) in °C and Ethanol % $v/v$  ( $X_3$ ) while holding time at 30 min.

Antioxidant capacity evaluation surface plot

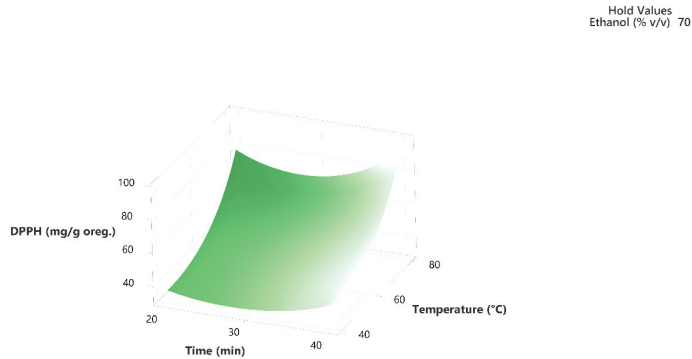


**Figure 4.** Three-dimensional response surface plot of the antioxidant capacity evaluation-DPPH assay (response variable) in mg of Trolox equivalent/g of dry matter (DM) oregano as a function of Time ( $X_2$ ) in min. and Temperature ( $X_1$ ) in Celsius degrees ( $^{\circ}\text{C}$ ) while holding ethanol at 70% ( $v/v$ ).

Antioxidant capacity evaluation surface plot

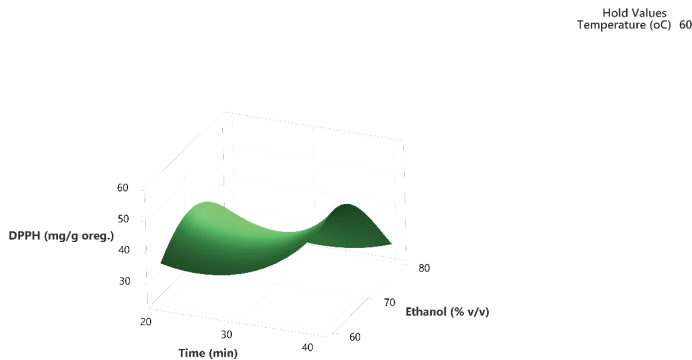


**Figure 5.** Three-dimensional response surface plot of the antioxidant capacity evaluation-DPPH assay (response variable) in mg of Trolox equivalent/g of dry matter (DM) of oregano as a function of Time ( $X_2$ ) in min. and Ethanol % $v/v$  ( $X_3$ ) while holding temperature at 60  $^{\circ}\text{C}$ .

Antioxidant capacity evaluation surface plot

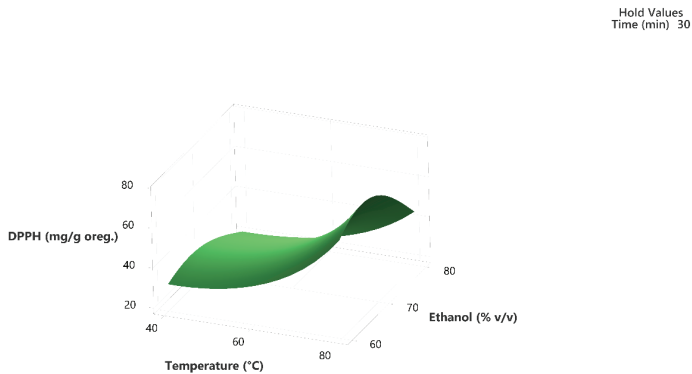


**Figure 6.** Three-dimensional response surface plot of the antioxidant capacity evaluation-DPPH assay (response variable) in mg of Trolox equivalent/g of dry matter (DM) of oregano as a function of temperature ( $X_2$ ) in Celsius degrees ( $^{\circ}\text{C}$ ) and Ethanol % $v/v$  ( $X_3$ ) while holding time at 30 min.

The 3D response surface plots in Figures 3 and 6 show that extraction both for total phenolic compounds and the evaluation of antioxidant activity are favored in high values of ethanol in solvent ( $X_3$ ), and high values of temperature ( $T$ ;  $X_1$ ). On the other hand, negative effect seems to have for both models the long experiment duration ( $X_2$ ) and high values of temperature ( $T$ ;  $X_1$ ) as Figures 1 and 4 indicate.

Based on the experimental results of the total phenolic content and the antioxidant activity evaluation, the extracted amounts shown in Table 4 of the specific combination of the three factors lead to maximum extraction. A temperature of 80 °C, time of 40 min, and ethanol of 60% ( $v/v$ ) results in a maximum extraction of  $362.1 \pm 1.8$  mg GAE/g DM with regard to the total phenolic content and  $108.6 \pm 0.9$  mg TE/g DM with regard to the DPPH assay.

**Table 4.** Solution for maximum extraction of total phenolic content (TPC) and antioxidant activity evaluation (DPPH assay) from oregano.

Independent Factors <sup>1</sup>	Predicted Values <sup>1</sup>	Experimental Values	Desirability <sup>2</sup>
TPC (mg/gDM)	363.0 <sup>a</sup>	$362.1 \pm 1.8$ <sup>a</sup>	1.0000
DPPH (mg/gDM)	108.5 <sup>a</sup>	$108.6 \pm 0.9$ <sup>a</sup>	1.0000

<sup>1</sup>: Independent factors were set at 80 °C ( $X_1$ ), 40 min DM ( $X_2$ ), and 60% ( $v/v$ ) ( $X_3$ ) both for TPC and antioxidant activity evaluation (DPPH assay). Same letters in rows denote values of not statistically significant difference.  
<sup>2</sup> Both individual and composite desirability for maximum total phenolic content and antioxidant activity based on DPPH assay.

The optimal conditions were calculated with the response optimizer of the Minitab<sup>®</sup> statistical software, and the results are presented in Table 4.

### 2.3. Verification of the Models

The validity of the predictive model was confirmed comparing the predicted and the experimental values at optimal conditions. The values predicted by the model at optimal conditions were 363.0 mg gallic acid equivalent per g of oregano, and 108.5 mg Trolox equivalent per g of dry oregano for total phenolic compounds and antioxidant capacity evaluation with regard to the DPPH assay, respectively, and the actual experimental values were  $362.1 \pm 1.8$  and  $108.6 \pm 0.9$  mg/g dry oregano. No significant differences were found between the predicted and the actual values ( $p > 0.05$ ) indicating high accuracy of response optimization.

The desirability value may define the ideal solution's degree of precision. The closer the desirability value is to 1, the greater the optimization precision. Therefore, the model validation and response values are not substantially different from the predictions under ideal circumstances.

### 2.4. Antioxidant Activity Evaluation and Total Phenolic Determination

The antioxidant activity evaluation by the DPPH, ABTS, FRAP, and CUPRAC assays, and total phenolic content (TPC) of oregano optimized extracts are reported in Table 5.

Both ABTS and DPPH tests measure the ability of compounds to scavenge free radicals. Small differences between the DPPH and ABTS values of the optimized extract indicated that the phenolic compounds contributing to the free radical scavenging activity were compounds with comparable hydrophilicity as the ABTS assay is applicable to both hydrophilic and lipophilic antioxidant systems, whereas the DPPH assay is only applicable to hydrophobic antioxidant systems [28]. On the other hand, the FRAP and CUPRAC tests assess the sample's capacity to reduce using ferric and cupric ions, respectively.

The results are promising since the higher amount of total phenolic compounds were extracted compared to studies that have been performed in the past, taking into consideration the advantage of the results obtained in this study, which concerns the green extraction perspective that was employed [29,30].

**Table 5.** Antioxidant activities of oregano optimized extract.

<sup>1</sup> Parameters	Oregano Optimized Extract	Calibration Curve
DPPH (mg TE/g)	108.6 ± 0.9	$y = -0.0849x + 0.625$
ABTS (mg TE/g)	115.2 ± 1.2	$y = -97.31x + 67.084$
FRAP (mg TE/g)	13.7 ± 0.8	$y = 58.018x - 2.944$
CUPRAC (mg TE/g)	1.2 ± 0.2	$y = 161.7x + 0.7858$
TPC (mg GAE/g)	362.1 ± 1.8	$y = 0.018x + 0.102$

<sup>1</sup> DPPH, ABTS, FRAP, and CUPRAC: Results are presented as mg of Trolox equivalents (TE) per g of dry oregano; TPC: Total phenolic content presented as mg of Gallic acid equivalents per g of dry oregano. Results are expressed as mean ± SD in final reported results between the three replicates of the optimized extracts acquired. For the calibration curves presented, y is referred to the concentration of Trolox or gallic acid obtained, and x is referred to the absorbance acquired during the experimental procedure of each assay.

Antioxidants are used in foods to delay or prevent the oxidation of molecules. Natural and synthetic antioxidants are both viable options. Some synthetic antioxidants, such as butylated hydroxy-anisole (BHA) and butylated hydroxytoluene (BHT), have been banned due to their carcinogenicity. As a result, phenolic compounds and other naturally occurring antioxidants are receiving more attention for potential application in the food enrichment process. Therefore, it is of significant importance to create natural antioxidants from plant matrices for nutritional reasons, and to enhance the nutritional profile of the goods [31].

### 2.5. Determination and Identification of Phenolic Compounds in Oregano Samples by HPLC-PDA and UHPLC-QTOF-MS

For the optimized extracts, identification and determination of apigenin, luteolin, and kaempferol were performed in oregano ultrasound assisted extract obtained with ethanol/water 60/40 (v/v) as a solvent for 40 min extraction duration and temperature was set at 80 °C.

Determination of phenolic compounds performed with the validated analytical method of HPLC-PDA. Figures 7–9 show the profile of the phenolic compounds under evaluation for the standard and sample solution at the 340 nm. Luteolin, apigenin, and kaempferol were quantitatively determined at  $1.30 \pm 0.05$ ,  $1.43 \pm 0.06$ , and  $0.40 \pm 0.03$  mg/g dry oregano, respectively.

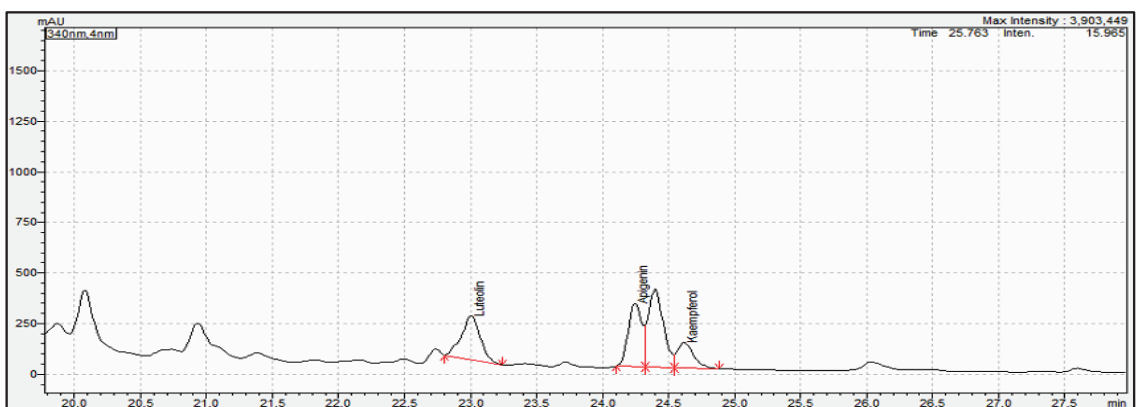


**Figure 7.** Representative chromatogram acquired for oregano sample extract at 340 nm. Red line in figure shows the integration area for the quantification of each compound.

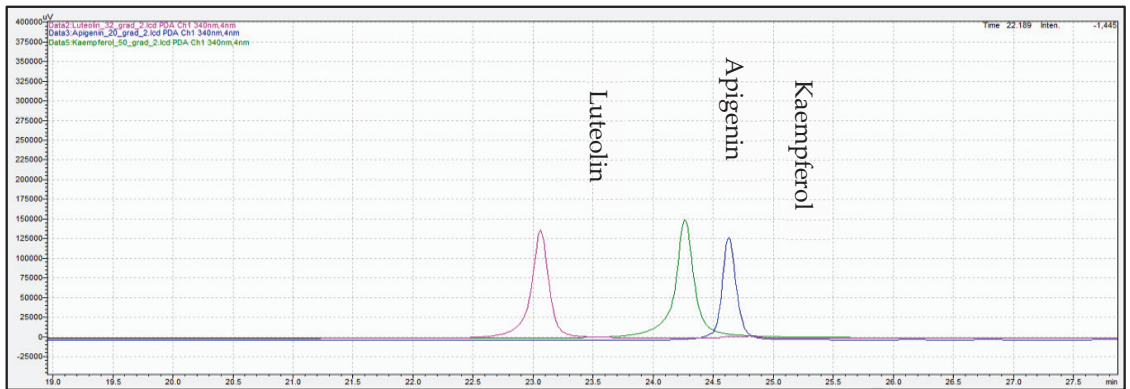


**Figure 8.** Overlay representative chromatogram acquired for standard solution of (pink color), apigenin (green color), and kaempferol (blue color) at 340 nm.

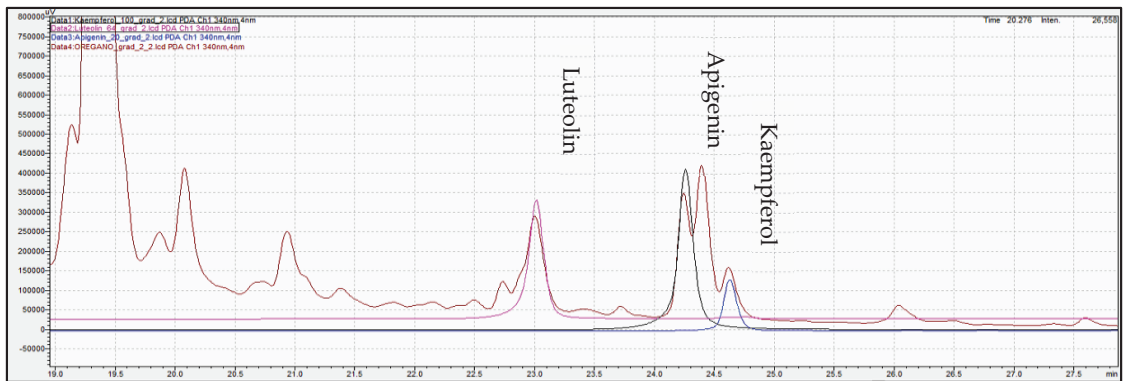


**Figure 9.** Overlay chromatogram acquired for standard solution of luteolin (pink color), apigenin (black color), kaempferol (blue color), and oregano extract (brown color) at 340 nm.

The oregano extracts also analyzed with the use of UHPLC-QTOF-MS for confirmatory purposes, and the respective mass spectrums are presented at Figure 10. Precursor ions were obtained, and the identification performed with validated methodology along with the software library for the three phenolic compounds.

Identification of apigenin, luteolin, and kaempferol was based on the accurate mass measurements of the molecular ion  $[M-H]^-$  along with the fragmentation patterns of each molecule, the UV-Vis data and the comparison with the commercial standards that were available for these specific phenolic compounds.

Phenolic compounds have attracted attention with respect to their applications in foods and pharmaceutical matrices, especially considering the bioactive potential of these molecules [32]. The health advantages of apigenin, kaempferol, and luteolin have been extensively researched [33,34]; therefore, it would be of great interest to enrich foods with extracts containing an adequate amount of these phenolics, and further assess their properties. Due to the use of human-friendly solvents, these extracts may be used in the process of food enrichment to improve their nutritional profile. However, there are some variables that must be considered before going with oregano extract food fortification. One critical characteristic is the stability of the extracts and the examination of approaches to increase stability, such as the encapsulation of the extracts' components of interest [35].

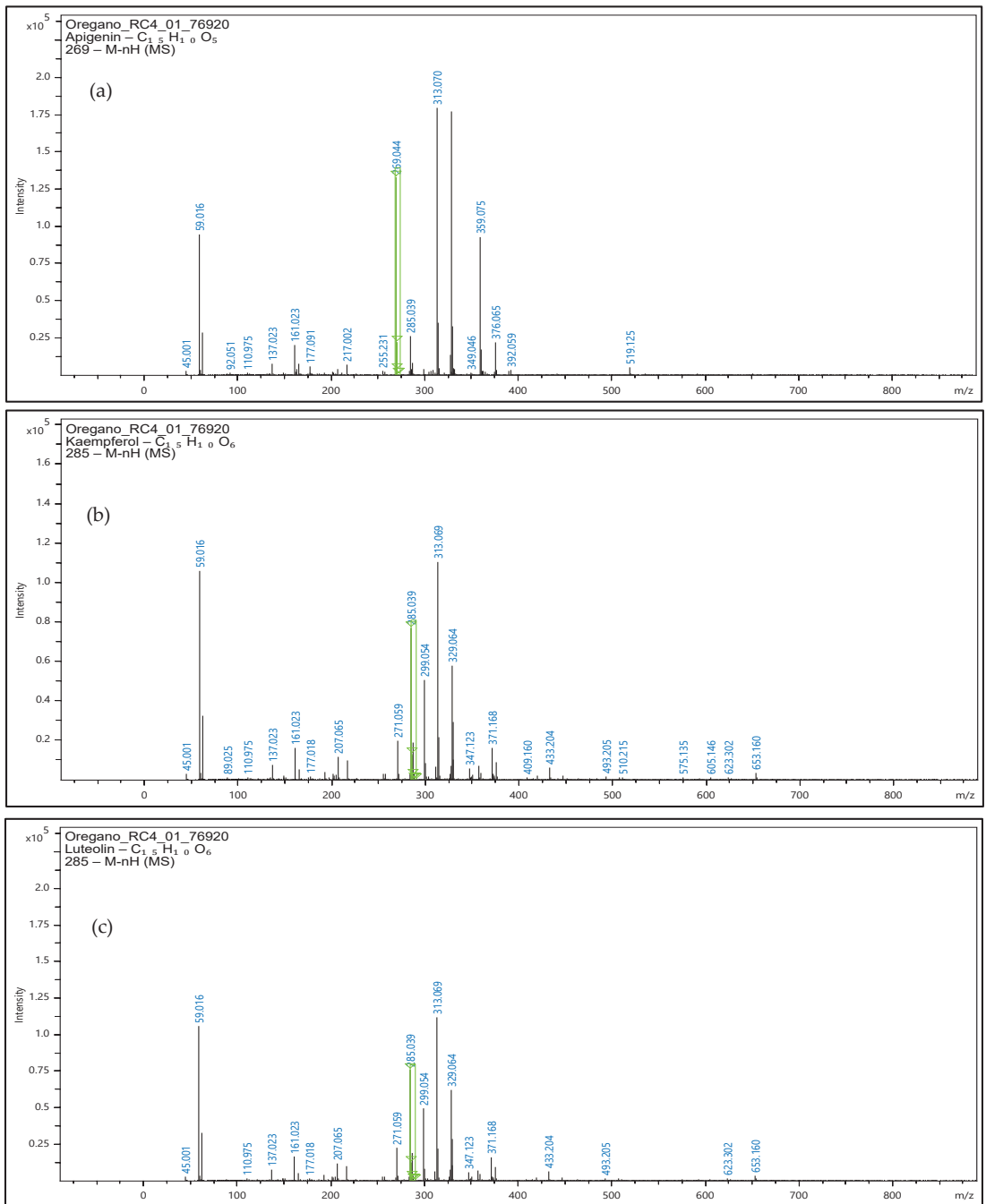


**Figure 10.** Mass spectrum of oregano extract samples at negative ionization were the precursor ion of apigenin- m/z 269 (a), kaempferol- m/z 285 (b), and luteolin- m/z 285 (c) are obtained. Green line in figure denotes the m/z value for each precursor ion.

### 3. Materials and Methods

#### 3.1. Chemicals and Reagents

Organic oregano (*Origanum vulgare* ssp. *hirtum*), native in the Greek island of Lemnos (39°55' N 25°15' E) and harvested during May of 2022, used in the experiments was kindly offered by Aegean Organics Ltd. (Lemnos, Greece). Oregano leaves were used. The reagents Folin–Ciocalteu, Trolox (6-hydroxy-2,5,7,8-tetremethychroman-2-carboxylic acid) and anhydrous sodium carbonate were purchased from SDS (Peypin, France). DPPH (1, 1-Diphenyl-2-picryl-hydrazyl), caffeic acid, luteolin, and apigenin were purchased from Sigma–Aldrich (St. Louis, MO, USA). Methanol, acetic acid HPLC water, and acetoni-trile were purchased from Thermo-Fisher scientific (Nepean, ON, Canada). Neocuproine was purchased from Acros Organics (Fair Lawn, NJ, USA). Ammonium acetate, sodium chloride, sodium dihydrogen phosphate dehydrate, and copper chloride dihydrate were all purchased from Penta (CZ Ltd., Chrudim, Czech Republic). ABTS (2,20 -Azino-bis-(3-ethylbezothiazoline-6-sulphonic acid) was purchased from Applichem (Darmstadt, Germany). Potassium persulfate was purchased from Chem-Lab (Zedelgem, Belgium).

#### 3.2. Preparation of the Samples

For the preparation of the oregano samples, the already dried oregano (moisture < 10%) was processed for one minute in a laboratory grinder, IKA A 10 basic (IKA Works, Wilmington, DE, USA), to get a sample of fine powder.

#### 3.3. Ultrasound-Assisted Extraction (UAE)

The phenolic compounds extraction from oregano samples performed with the use of a threaded end of 1.000 mL maximum volume cup-horn of 750 Watt ultrasonic processor VCX-750 equipped with a sealed converter (Sonics & Materials, Inc. Newtown, CT, USA). A one-to-one pulse in seconds was applied combined with a 60% amplitude, while several temperatures were applied for 25 °C to 80 °C for the preliminary experiments. With regard to the sample preparation, 0.25 g of dried samples were weighed in a 10-mL tube. The tube was filled up to 5.0 mL with Purified water, ethanol, or ethanol/water in various ratios. After extraction, samples were centrifuged for 5 min at 3000× g and supernatants were filtered in HPLC vials through 0.20-µm RC (regenerated cellulose) filters before the analysis.

#### 3.4. Evaluation of Antioxidant Activity

The antioxidant activities of the extracts, obtained at optimized conditions, were evaluated by the DPPH, ABTS, FRAP, and CUPRAC assays. Each sample was examined in triplicate. Trolox solutions were prepared in appropriate concentrations for quantitation purposes and the results expressed as Trolox equivalents in mg per g of oregano for all the antioxidant tests performed.

The capacity of extracts to scavenge the free radical of DPPH was evaluated by the method of Brand-Williams et al. [36] [NO\_PRINTED\_FORM] with minor modifications. An aliquot of the extract (2 to 10), or an appropriate standard solution of Trolox was diluted with methanol up to 0.9 mL. Then, 0.1 mL of 0.6 mM DPPH reagent in methanol was added, followed by vigorous stirring. After 15.0 min in the dark, the absorbance was measured at 515 nm against a reference sample containing methanol.

Determination of ABTS radical scavenging activity of samples was performed by the method of Miller et al. [37] with minor modifications. ABTS radical cation (ABTS<sup>•+</sup>) was produced by the oxidation of ABTS with potassium persulfate (K<sub>2</sub>S<sub>2</sub>O<sub>8</sub>). The ABTS<sup>•+</sup> was generated by reacting 7 mmol/L stock solution of ABTS with potassium persulphate in a final concentration equal to 2.45 mmol/L. The ABTS<sup>•+</sup> working solution was prepared by dilution of the stock solution using distilled water to give an absorbance of 0.700 at 734 nm. Aliquots of parsley extracts (2 to 10 µL), or appropriate amounts of Trolox standards were diluted to 1.0 mL with working ABTS<sup>•+</sup> solution and were vigorously stirred. Samples remained for 15.0 min in the dark at ambient temperature and the absorbance was measured

at 734 nm. The ability of the extracts to scavenge the ABTS<sup>•+</sup> was evaluated relative to a reference sample that did not contain any quantity of extract.

The reducing potential of the samples was determined using the FRAP assay as described by Benzie and Strain [38]. The method is based on the reduction in the Fe<sup>3+</sup>—tripiryridyl triazine complex to its ferrous-colored form at low pH in the presence of antioxidants. The FRAP reagent was freshly prepared and contained 0.2 mL of a 10 mM TPTZ (2,4,6-tripyridyl-s-triazine) solution in 40 mM HCl plus 0.2 mL of 20 mM FeCl<sub>3</sub>•6H<sub>2</sub>O plus 0.2 mL of 3.0 M acetate buffer, pH 3.6. Aliquots of extracts (2 to 10 µL) were transferred in test tubes, and dissolved up of 900 µL with distilled water, followed by addition of 300 µL of FRAP solution and vigorous stirring. The samples were incubated for 10 min in a 37 °C water bath, and the absorbance was measured at 593 nm.

The reducing capacity of the samples was also determined using the CUPRAC assay according to Özyürek et al. [39]. Aliquots of parsley extracts (2 to 10 µL) were transferred in test tubes and diluted with 300 µL of 10 mM CuCl<sub>2</sub>•2H<sub>2</sub>O, 7.5 mM neocuproine, and 1 mM CH<sub>3</sub>COONH<sub>4</sub> buffer solution with pH = 7.0, followed by the addition of distilled water up to the volume of 1200 µL. The samples were well stirred and remained at room temperature for 30 min. The absorbance of the samples was then measured at 450 nm.

### 3.5. Determination of Phenolic Compounds

The total content of phenolics in oregano extracts obtained at optimized conditions were measured in triplicate by using a modified version of Singleton and Rossi's technique and was determined using the Folin–Ciocalteu's method with some modifications [40] using a spectrophotometer Lambda 25 (Perkin Elmer, Norwalk, CT, USA). The experiment was carried out by combining 1 to 10 µL of oregano extracts with 1.8 mL of distilled water and 0.1 mL of Folin–Ciocalteu reagent. The materials were then rapidly mixed and incubated in the dark for two minutes. After adding 0.3 mL of 20% (*w/v*) aqueous Na<sub>2</sub>CO<sub>3</sub>, the samples were rapidly agitated and incubated at 40 °C in a water bath for 30 min. Absorbance was measured spectrophotometrically at 765 nm, by a Spectrophotometer Lambda 25 (Perkin Elmer, Norwalk, CA, USA). Gallic acid was used to develop a standard curve. The final findings were expressed as equivalent concentrations of gallic acid (mg GAE per g oregano).

### 3.6. Determination of Phenolic Compounds with HPLC-PDA

For the determination of phenolic compounds during preliminary experiments, but also during the analysis of the optimized extracts produced in the frame of experimental design, a Shimadzu HPLC 2030C prominence-i system was used, equipped with a binary pump, a degasser, an autosampler, a column heater, and a PDA detector. A Phenomenex Luna C18(2) analytical column (4.6 mm × 250 mm, particle size 5.0 µm) was used for the separation of the phenolic compounds under evaluation. The elution was performed using water acidified with 0.2% formic acid (mobile phase A) and methanol (mobile phase B). The adopted elution gradient was applied as follows: 0 min, 5% mobile phase B; 1 min, 5% mobile phase B; 30 min, 95% mobile phase B; 30.1 min, 5% mobile phase B; and 33 min, 5% mobile phase B. The injection volume was 20 µL, UV-vis spectra were recorded from 190 to 800 nm, while the chromatograms were registered at 280 and 340 nm. The analytical methodology was successfully validated in terms of linearity, accuracy, stability, limit of quantitation, and precision (system precision and reproducibility) for each phenolic compound under evaluation [41]. Quantification and identification performed with the use of commercial standards that were available for the phenolic compounds under evaluation.

### 3.7. Identification of Phenolic Compounds with HPLC-QTOF-MS

An UHPLC system with an HPG-3400 pump (Dionex UltiMate 3000 RSLC, Thermo Fisher Scientific, Germany) coupled to a QTOF mass spectrometer (Maxis Impact, Bruker Daltonics, Bremen, Germany) was used for the analysis. Negative electrospray ionization mode was applied. Separation was carried out using an Acclaim RSLC C18 column



(2.1 × 100 mm, 2.2 μm) purchased from Thermo Fisher Scientific (Driesch, Germany) with a pre-column of ACQUITY UPLC BEH C18 (1.7 μm, VanGuard Pre-Column, Waters (Waters Corporation®), Wexford, Ireland). Column temperature was set at 30 °C. The solvents used consisted of (A) 90% H<sub>2</sub>O, 10% methanol, and 5 mM CH<sub>3</sub>COONH<sub>4</sub> (Mobile phase A), and 100% methanol and 5 mM CH<sub>3</sub>COONH<sub>4</sub> (Mobile phase B). The adopted elution gradient started with 1% of organic phase B with flow rate 0.2 mL min<sup>-1</sup> during 1 min, gradually increasing to 39% for the next 2 min, then increasing to 99.9% and flow rate 0.4 mL min<sup>-1</sup> for the following 11 min. These almost pure organic conditions were kept constant for 2 min (flow rate 0.48 mL min<sup>-1</sup>), then initial conditions (1% B–99% A) were restored within 0.1 min (flow rate decreased to 0.2 mL min<sup>-1</sup>) to re-equilibrate the column for the next injection.

The QTOF-MS system was equipped with an electrospray ionization interface (ESI), operating in negative mode with the following settings: capillary voltage of 3500 V, end plate off-set of 500 V, nebulizer pressure of 2 bar (N<sub>2</sub>), drying gas of 8 L min<sup>-1</sup> (N<sub>2</sub>), and drying temperature of 200 °C. A QTOF external calibration was daily performed with sodium formate (cluster solution), and a segment (0.1–0.25 min) in every chromatogram was used for internal calibration, using calibrant injection at the beginning of each run. The sodium formate calibration mixture consisted of 10 mM sodium formate in a mixture of H<sub>2</sub>O/isopropanol (1:1). Full scan mass spectra were recorded over the range of 50–1000 m/z, with a scan rate of 2 Hz. MS/MS experiments were conducted using AutoMS data-dependent acquisition mode based on the fragmentation of the five most abundant precursor ions per scan. The instrument provided a typical resolving power (FWHM) between 36,000 and 40,000 at m/z 226.1593, 430.9137, and 702.8636, respectively. Identification was performed with the use of commercial standards that were available for the phenolic compounds under evaluation along with the fragmentation patterns of each molecule.

### 3.8. Experimental Design

The Box–Behnken design (BBD), a standard RSM design, is highly suited to fitting a quadratic surface, which is often used for process optimization, was selected to identify the optimum extraction conditions for total phenolic compounds and antioxidant activity measurements. The three independent factors were temperature (X<sub>1</sub>), time (X<sub>2</sub>), and ethanol concentration (X<sub>3</sub>).

Each factor was coded to three levels: −1, 0, and +1. One replicate experiment was performed. The factors and their corresponding levels, both coded and actual, chosen in the three-factor-three-level BBD were based on preliminary one-factor-at-a-time experiments, literature research, and instrumental specifications, and are presented in Table 6.

**Table 6.** Independent factors and their levels in the Box–Behnken Experimental Design.

Factors	Codes	Factor Levels and Range		
		−1	0	1
Temperature (°C)	X <sub>1</sub>	40	60	80
Time (min)	X <sub>2</sub>	20	30	40
Ethanol (% v/v)	X <sub>3</sub>	60	70	80

RSM was used to fit a complete second-order polynomial equation to the design points and experiment data. The following quadratic response surface model equation (a) for four components was fitted:

$$Y = \beta_0 + \sum_{i=1}^3 \beta_i X_i + \sum_i \beta_{ii} X_i^2 + \sum_{i=1}^2 \sum_{j=i+1}^3 \beta_{ij} X_i X_j + \epsilon \quad (3)$$

In Equation (3), Y corresponds to the response variable expressed by mg GAE/g and mg TE/g for TPC and DPPH, respectively, for both tests performed (total phenolic content

and antioxidant evaluation).  $X_i$  and  $X_j$  are the independent factors affecting the response (Table 1). The terms  $\beta_0$ ,  $\beta_i$ ,  $\beta_{ij}$ , and  $\beta_{ij}$  are the regression coefficients of the model (intercept, linear, quadratic, and interaction term), and  $\varepsilon$  corresponds to the random error term.

Analysis of variance (ANOVA) was used to estimate the fitting of the entire quadratic approximation of the BBD response surface model. The significance of each source of terms (linear, two-factor interaction, and quadratic), and the regression coefficients of the fitted model were examined using the F-values and pertinent  $p$ -values. Statistically significant terms were those whose probability ( $p$ -value) at the 95% confidence level fell below 0.05.

### 3.9. Verification of the Statistical Model

Optimum extraction conditions of the total phenolic content and antioxidant activity evaluation of oregano samples based on the evaluation for extraction temperature, and time and solvent composition were obtained using the predictive equations of RSM. The obtained concentration was determined after extraction of phenolic compounds under optimal conditions. The experimental and predicted values were compared to determine the validity of the model.

### 3.10. Statistical Analysis

Data presented as mean  $\pm$  standard deviation ( $m \pm SD$ ) for triplicate measurements. The response values of the RSM model for one replication with three center points were analyzed by Minitab<sup>®</sup> trial version statistical software (Minitab Ltd., Coventry, UK). SPSS V 28.0.10 software (IBM Corp., Armonk, NY, USA) was used for one-sample t-test analysis for the verification of the model. Statistical significance was defined at  $<0.05$ .

## 4. Conclusions

In this study, a Box–Behnken Box–Behnken design (BBD), along with Box–Cox transformation of the data and model reduction, have been developed to optimize the extraction conditions for maximum total phenolic extractions and antioxidant activity based on DPPH assay from Oregano (*Origanum vulgare* ssp. *hirtum*) cultivated in Lemnos.

For the optimized extracts, the antioxidant activity was also measured with ABTS, FRAP, and CUPRAC assays. Then, luteolin, kaempferol, and apigenin were determined by HPLC–DAD and identified by UHPLC–Q–TOF–MS in extracts obtained by UAE from oregano sample.

The adequacy of the predictive model and the verification of the model were confirmed. Optimal conditions were calculated and found the same both for total phenolic contain, and antioxidant activity evaluation (DPPH assay). Using a concentration of ethanol equal to 60% ( $v/v$ ), a temperature of 80 °C, and a time period of 40 min, the predictive and the actual values along with the desirability were equal to 363.0, 362.1  $\pm$  1.8, and 1.000 for TPC; and 108.5, 108.6  $\pm$  0.9, and 1.000 for DPPH.

High values of total phenolic compounds equal to 362.1  $\pm$  1.8 mg GAE per g of oregano were determined in the optimized extract, and high antioxidant capacities that ranged from 1.2 mg to 115.2 mg Trolox equivalent per g of oregano with respect to DPPH, ABTS, FRAP, and CUPRAC assays, respectively, were obtained (Table 5). Additionally, luteolin, apigenin, and kaempferol were quantitatively determined at 1.30  $\pm$  0.05, 1.43  $\pm$  0.06, and 0.40  $\pm$  0.03 mg/g dry oregano, respectively.

With these findings, an adequate amount of the phenolic compounds under consideration were extracted from Oregano, specifically apigenin, luteolin, and kaempferol (1.30 0.05, 1.43 0.06, and 0.40 0.03 mg/g dry oregano, respectively) using ultrasound-assisted extraction and green solvents, such as ethanol/water mixture. It is important to highlight the fact that the results are obtained under the green extraction rules, which means that the extracts can further be used in food enrichment procedures.

However, there are several factors that must be considered before the commercial implementation of the recovery of value-added chemicals from natural products. The bioavailability, but also the metabolism of phenolic compounds are important parameters

that is necessary to be investigated in order to better understand the biological mechanisms, which will empower the development of better applications for the phenolic compounds. The considerable total phenolic content of oregano extracts presents an opportunity for the creation of novel functional foods or the refinement of current traditional products with superiority in consumer health protection. The results indicate that oregano extract could be the subject of a mixture design for the formulation of new enriched healthy animal or plant food products, such as meat products, dairy products, bakery snacks, traditional pasta, spread products, beverages, etc. The result of the study highlights the nutraceutical potential of extracts from oregano (*Origanum vulgare* ssp. *hirtum*) cultivated in Lemnos. Oregano is a widespread cultivation aromatic herb, and considerable amount is easily accessible for the creation of novel functional foods or the refinement of current traditional products with shown superiority in consumer health protection.

**Author Contributions:** Conceptualization, H.C.K.; methodology, H.C.K., A.M., A.S.K., N.S.T. and M.E.D.; software, H.C.K. and A.M.; validation, H.C.K. and A.M.; investigation, H.C.K., A.M. and A.S.K.; resources, H.C.K., N.S.T. and M.E.D.; data curation, H.C.K. and A.M.; writing—original draft preparation, A.M.; writing—review and editing, H.C.K.; supervision, H.C.K.; project administration, H.C.K.; funding acquisition, H.C.K. All authors have read and agreed to the published version of the manuscript.

**Funding:** This research was funded by EPAnEk -NRSF 2014–2020; Operational Program “Competitiveness, Entrepreneurship and Innovation”, Call 111 “Support of Regional Excellence” in the context of the implementation of the program: AGRICA II: AGRifood Research and Innovation Network of Excellence of the Aegean, which is co-financed by the European Regional Development Fund (ERDF), MIS code: 5046750.

**Institutional Review Board Statement:** Not applicable.

**Informed Consent Statement:** Not applicable.

**Data Availability Statement:** Not applicable.

**Acknowledgments:** Special thanks to Nikolaos Paterakis and Aegean Organics Ltd. (<https://aegeanorganics.com/>) for the kind offer of the oregano sample used in the experiments.

**Conflicts of Interest:** The authors declare no conflict of interest. The funders had no role in the design of the study; in the collection, analyses, or interpretation of data; in the writing of the manuscript; or in the decision to publish the results.

## References

1. Majeed, M.; Hussain, A.I.; Chatha, S.A.S.; Khosa, M.K.K.; Kamal, G.M.; Kamal, M.A.; Zhang, X.; Liu, M. Optimization Protocol for the Extraction of Antioxidant Components from *Origanum vulgare* Leaves Using Response Surface Methodology. *Saudi J. Biol. Sci.* **2016**, *23*, 389–396. [[CrossRef](#)] [[PubMed](#)]
2. Bautista-Hernández, I.; Aguilar, C.N.; Martínez-ávila, G.C.G.; Torres-León, C.; Iliina, A.; Flores-Gallegos, A.C.; Kumar Verma, D.; Chávez-González, M.L. Mexican Oregano (*Lippia graveolens* Kunth) as Source of Bioactive Compounds: A Review. *Molecules* **2021**, *26*, 5156. [[CrossRef](#)] [[PubMed](#)]
3. Gutiérrez-Grijalva, E.P.; Antunes-Ricardo, M.; Acosta-Estrada, B.A.; Gutiérrez-Urbe, J.A.; Basilio Heredia, J. Cellular Antioxidant Activity and in Vitro Inhibition of  $\alpha$ -Glucosidase,  $\alpha$ -Amylase and Pancreatic Lipase of Oregano Polyphenols under Simulated Gastrointestinal Digestion. *Food Res. Int.* **2019**, *116*, 676–686. [[CrossRef](#)] [[PubMed](#)]
4. Gutiérrez-Grijalva, E.P.; Picos-Salas, M.A.; Leyva-López, N.; Criollo-Mendoza, M.S.; Vazquez-Olivo, G.; Heredia, J.B. Flavonoids and Phenolic Acids from Oregano: Occurrence, Biological Activity and Health Benefits. *Plants* **2018**, *7*, 2. [[CrossRef](#)] [[PubMed](#)]
5. Singh, N.; Yadav, S.S. A Review on Health Benefits of Phenolics Derived from Dietary Spices. *Curr. Res. Food Sci.* **2022**, *5*, 1508–1523. [[CrossRef](#)]
6. Mar, P.D.; el Khalfi, B.; Soukri, A. Protective Effect of Oregano and Sage Essentials Oils against the Effect of Extracellular H<sub>2</sub>O<sub>2</sub> and SNP in *Tetrahymena thermophila* and *Tetrahymena pyriformis*. *J. King Saud Univ. Sci.* **2020**, *32*, 279–287. [[CrossRef](#)]
7. Shirvani, H.; Bazgir, B.; Shamsoddini, A.; Saeidi, A.; Tayebi, S.M.; Escobar, K.A.; Laher, I.; VanDusseldorp, T.A.; Weiss, K.; Knechtle, B.; et al. Oregano (*Origanum vulgare*) Consumption Reduces Oxidative Stress and Markers of Muscle Damage after Combat Readiness Tests in Soldiers. *Nutrients* **2023**, *15*, 137. [[CrossRef](#)]
8. Zhang, H.; Tsao, R. Dietary Polyphenols, Oxidative Stress and Antioxidant and Anti-Inflammatory Effects. *Curr. Opin. Food Sci.* **2016**, *8*, 33–42. [[CrossRef](#)]

9. Jafari Khorsand, G.; Morshedloo, M.R.; Mumivand, H.; Emami Bistgani, Z.; Maggi, F.; Khademi, A. Natural Diversity in Phenolic Components and Antioxidant Properties of Oregano (*Origanum vulgare* L.) Accessions, Grown under the Same Conditions. *Sci. Rep.* **2022**, *12*, 5813. [CrossRef]
10. Kruma, Z.; Andjelkovic, M.; Verhe, R.; Kreicbergs, V. PHENOLIC COMPOUNDS IN BASIL, OREGANO AND THYME. 2008. Available online: <https://lluflb.llu.lv/conference/foodbalt/2008/Foodbalt-Proceedings-2008-99-103.pdf> (accessed on 17 April 2008).
11. Salehi, B.; Venditti, A.; Sharifi-Rad, M.; Kregiel, D.; Sharifi-Rad, J.; Durazzo, A.; Lucarini, M.; Santini, A.; Souto, E.B.; Novellino, E.; et al. The Therapeutic Potential of Apigenin. *Int. J. Mol. Sci.* **2019**, *20*, 1305. [CrossRef]
12. Cizmarova, B.; Hubkova, B.; Bolerazska, B.; Marekova, M.; Birkova, A. Caffeic Acid: A Brief Overview of Its Presence, Metabolism, and Bioactivity. *Bioact. Compd. Health Dis* **2020**, *3*, 74–81. [CrossRef]
13. Lin, Y.; Shi, R.; Wang, X.; Shen, H.-M. Luteolin, a Flavonoid with Potential for Cancer Prevention and Therapy. *Curr. Cancer Drug Targets* **2008**, *8*, 634–646. [CrossRef]
14. Luo, Y.; Shang, P.; Li, D. Luteolin: A Flavonoid That Has Multiple Cardio-Protective Effects and Its Molecular Mechanisms. *Front Pharm.* **2017**, *8*, 692. [CrossRef]
15. Aranha, C.P.M.; Jorge, N. Antioxidant Potential of Oregano Extract (*Origanum vulgare* L.). *Br. Food J.* **2012**, *114*, 954–965. [CrossRef]
16. Wen, C.; Zhang, J.; Zhang, H.; Dzah, C.S.; Zandile, M.; Duan, Y.; Ma, H.; Luo, X. Advances in Ultrasound Assisted Extraction of Bioactive Compounds from Cash Crops—A Review. *Ultrason. Sonochem.* **2018**, *48*, 538–549. [CrossRef]
17. Alara, O.R.; Abdurahman, N.H.; Ukaegbu, C.I. Extraction of Phenolic Compounds: A Review. *Curr. Res. Food Sci.* **2021**, *4*, 200–214. [CrossRef] [PubMed]
18. Vo, T.P.; Nguyen, L.N.H.; Le, N.P.T.; Mai, T.P.; Nguyen, D.Q. Optimization of the Ultrasonic-Assisted Extraction Process to Obtain Total Phenolic and Flavonoid Compounds from Watermelon (*Citrullus lanatus*) Rind. *Curr. Res. Food Sci.* **2022**, *5*, 2013–2021. [CrossRef]
19. Rao, M.V.; Sengar, A.S.; C K, S.; Rawson, A. Ultrasonication—A Green Technology Extraction Technique for Spices: A Review. *Trends Food Sci. Technol.* **2021**, *116*, 975–991. [CrossRef]
20. Muñoz-Márquez, D.B.; Martínez-Ávila, G.C.; Wong-Paz, J.E.; Belmares-Cerda, R.; Rodríguez-Herrera, R.; Aguilar, C.N. Ultrasound-Assisted Extraction of Phenolic Compounds from *Laurus nobilis* L. and Their Antioxidant Activity. *Ultrason. Sonochem.* **2013**, *20*, 1149–1154. [CrossRef] [PubMed]
21. Oreopoulou, A.; Goussias, G.; Tsimogiannis, D.; Oreopoulou, V. Hydro-Alcoholic Extraction Kinetics of Phenolics from Oregano: Optimization of the Extraction Parameters. *Food Bioprod. Process.* **2020**, *123*, 378–389. [CrossRef]
22. Kumar, K.; Srivastav, S.; Sharanagat, V.S. Ultrasound Assisted Extraction (UAE) of Bioactive Compounds from Fruit and Vegetable Processing by-Products: A Review. *Ultrason. Sonochem.* **2021**, *70*, 105325. [CrossRef] [PubMed]
23. Casazza, A.A.; Aliakbarian, B.; Sannita, E.; Perego, P. High-Pressure High-Temperature Extraction of Phenolic Compounds from Grape Skins. *Int. J. Food Sci. Technol.* **2012**, *47*, 399–405. [CrossRef]
24. Mahindrakar, K.V.; Rathod, V.K. Ultrasonic Assisted Aqueous Extraction of Catechin and Gallic Acid from *Syzygium Cumini* Seed Kernel and Evaluation of Total Phenolic, Flavonoid Contents and Antioxidant Activity. *Chem. Eng. Process. —Process Intensif.* **2020**, *149*, 107841. [CrossRef]
25. Zhang, L.-L.; Xu, M.; Wang, Y.-M.; Wu, D.-M.; Chen, J.-H. Optimizing Ultrasonic Ellagic Acid Extraction Conditions from Infructescence of *Platycarya Strobilacea* Using Response Surface Methodology. *Molecules* **2010**, *15*, 7923–7932. [CrossRef]
26. Silva, E.M.; Rogez, H.; Larondelle, Y. Optimization of Extraction of Phenolics from *Inga Edulis* Leaves Using Response Surface Methodology. *Sep. Purif Technol.* **2007**, *55*, 381–387. [CrossRef]
27. Zhong, K.; Wang, Q. Optimization of Ultrasonic Extraction of Polysaccharides from Dried Longan Pulp Using Response Surface Methodology. *Carbohydr Polym.* **2010**, *80*, 19–25. [CrossRef]
28. Kim, D.-O.; Lee, K.W.; Lee, H.J.; Lee, C.Y. Vitamin C Equivalent Antioxidant Capacity (VCEAC) of Phenolic Phytochemicals. *J. Agric. Food Chem.* **2002**, *50*, 3713–3717. [CrossRef]
29. Liberal, Á.; Fernandes, Á.; Polyzos, N.; Petropoulos, S.A.; Dias, M.I.; Pinela, J.; Petrović, J.; Soković, M.; Ferreira, I.C.F.R.; Barros, L. Bioactive Properties and Phenolic Compound Profiles of Turnip-Rooted, Plain-Leafed and Curly-Leafed Parsley Cultivars. *Molecules* **2020**, *25*, 5606. [CrossRef]
30. Tang, E.L.-H.; Rajarajeswaran, J.; Fung, S.; Kanthimathi, M.S. *Petroselinum Crispum* Has Antioxidant Properties, Protects against DNA Damage and Inhibits Proliferation and Migration of Cancer Cells. *J. Sci. Food Agric.* **2015**, *95*, 2763–2771. [CrossRef]
31. Shi, J.; Nawaz, H.; Pohorly, J.; Mittal, G.; Kakuda, Y.; Jiang, Y. Extraction of Polyphenolics from Plant Material for Functional Foods—Engineering and Technology. *Food Rev. Int.* **2005**, *21*, 139–166. [CrossRef]
32. Rocchetti, G.; Gregorio, R.P.; Lorenzo, J.M.; Barba, F.J.; Oliveira, P.G.; Prieto, M.A.; Simal-Gandara, J.; Mosele, J.I.; Motilva, M.J.; Tomas, M.; et al. Functional Implications of Bound Phenolic Compounds and Phenolics–Food Interaction: A Review. *Compr. Rev. Food Sci. Food Saf.* **2022**, *21*, 811–842. [CrossRef] [PubMed]
33. Ali, F.; Rahul; Naz, F.; Jyoti, S.; Siddique, Y.H. Health Functionality of Apigenin: A Review. *Int. J. Food Prop.* **2017**, *20*, 1197–1238. [CrossRef]
34. Taheri, Y.; Sharifi-Rad, J.; Antika, G.; Yilmaz, Y.B.; Tumer, T.B.; Abuhamdah, S.; Chandra, S.; Saklani, S.; Kiliç, C.S.; Sestito, S.; et al. Paving Luteolin Therapeutic Potentialities and Agro-Food-Pharma Applications: Emphasis on in Vivo Pharmacological Effects and Bioavailability Traits. *Oxid. Med. Cell Longev.* **2021**, *2021*, 1987588. [CrossRef] [PubMed]

35. Vinceković, M.; Viskiđ, M.; Jurić, S.; Giacometti, J.; Bursać Kovačević, D.; Putnik, P.; Donsi, F.; Barba, F.J.; Režek Jambrak, A. Innovative Technologies for Encapsulation of Mediterranean Plants Extracts. *Trends Food Sci. Technol.* **2017**, *69*, 1–12. [[CrossRef](#)]
36. Brand-Williams, W.; Cuvelier, M.E.; Berset, C. Use of a Free Radical Method to Evaluate Antioxidant Activity. *LWT—Food Sci. Technol.* **1995**, *28*, 25–30. [[CrossRef](#)]
37. Miller, N.J.; Rice-Evans, C.; Davies, M.; Gopinathan, V.; Milner, A. A Novel Method for Measuring Antioxidant Capacity and Its Application to Monitoring the Antioxidant Status in Premature Neonates. *Clin. Sci.* **1993**, *84*, 407–412. [[CrossRef](#)]
38. Benzie, I.F.F.; Strain, J.J. The Ferric Reducing Ability of Plasma (FRAP) as a Measure of “Antioxidant Power”: The FRAP Assay. *Anal. Biochem.* **1996**, *239*, 70–76. [[CrossRef](#)]
39. Özyürek, M.; Güçlü, K.; Apak, R. The Main and Modified CUPRAC Methods of Antioxidant Measurement. *TrAC—Trends Anal. Chem.* **2011**, *30*, 652–664. [[CrossRef](#)]
40. Singleton, V.L.; Orthofer, R.; Lamuela-Raventós, R.M. Analysis of Total Phenols and Other Oxidation Substrates and Antioxidants by Means of Folin-Ciocalteu Reagent. *Methods Enzymol.* **1999**, *299*, 152–178.
41. ICH Topic Q 2 (R1) Validation of Analytical Procedures: Text and Methodology Step 5 Note for Guidance on Validation of Analytical Procedures: Text and Methodology (CPMP/ICH/381/95) Approval by CPMP November 1994 Date for Coming into Operation. 1995. Available online: <https://www.fda.gov/media/152208/download> (accessed on 17 November 2005).

**Disclaimer/Publisher’s Note:** The statements, opinions and data contained in all publications are solely those of the individual author(s) and contributor(s) and not of MDPI and/or the editor(s). MDPI and/or the editor(s) disclaim responsibility for any injury to people or property resulting from any ideas, methods, instructions or products referred to in the content.

Article

# Characterization and Biological Activities of In Vitro Digested Olive Pomace Polyphenols Evaluated on Ex Vivo Human Immune Blood Cells

Claudio Alimenti <sup>1,†</sup>, Mariacaterina Lianza <sup>2,†</sup>, Fabiana Antognoni <sup>2</sup>, Laura Giusti <sup>3</sup>, Onelia Bistoni <sup>4</sup>, Luigi Liotta <sup>5</sup>, Cristina Angeloni <sup>2</sup>, Giulio Lupidi <sup>3,‡</sup> and Daniela Beghelli <sup>1,\*,‡</sup>

<sup>1</sup> School of Biosciences and Veterinary Medicine, University of Camerino, 62032 Camerino, Italy

<sup>2</sup> Department for Life Quality Studies, Alma Mater Studiorum, University of Bologna, 47921 Rimini, Italy

<sup>3</sup> School of Pharmacy, University of Camerino, 62032 Camerino, Italy

<sup>4</sup> Rheumatology Unit, Department of Medicine, University of Perugia, 06126 Perugia, Italy

<sup>5</sup> Department of Veterinary Science, University of Messina, 98168 Messina, Italy

\* Correspondence: daniela.beghelli@unicam.it

† These authors contributed equally to this work.

‡ These authors contributed equally to this work.

**Abstract:** Olive pomace (OP) represents one of the main by-products of olive oil production, which still contains high quantities of health-promoting bioactive compounds. In the present study, three batches of sun-dried OP were characterized for their profile in phenolic compounds (by HPLC-DAD) and in vitro antioxidant properties (ABTS, FRAP and DPPH assays) before (methanolic extracts) and after (aqueous extracts) their simulated in vitro digestion and dialysis. Phenolic profiles, and, accordingly, the antioxidant activities, showed significant differences among the three OP batches, and most compounds showed good bioaccessibility after simulated digestion. Based on these preliminary screenings, the best OP aqueous extract (OP-W) was further characterized for its peptide composition and subdivided into seven fractions (OP-F). The most promising OP-F (characterized for its metabolome) and OP-W samples were then assessed for their potential anti-inflammatory properties in ex vivo human peripheral mononuclear cells (PBMCs) triggered or not with lipopolysaccharide (LPS). The levels of 16 pro- and anti-inflammatory cytokines were measured in PBMC culture media by multiplex ELISA assay, whereas the gene expressions of interleukin-6 (IL-6), IL-10 and TNF- $\alpha$  were measured by real time RT-qPCR. Interestingly, OP-W and OP-F samples had a similar effect in reducing the expressions of IL-6 and TNF- $\alpha$ , but only OP-W was able to reduce the release of these inflammatory mediators, suggesting that the anti-inflammatory activity of OP-W is different from that of OP-F.

**Keywords:** olive pomace; PBMC; cytokines; immune gene expression; HPLC-DAD; antioxidants; inflammation; metabolome; phenolic bioaccessibility

**Citation:** Alimenti, C.; Lianza, M.; Antognoni, F.; Giusti, L.; Bistoni, O.; Liotta, L.; Angeloni, C.; Lupidi, G.; Beghelli, D. Characterization and Biological Activities of In Vitro Digested Olive Pomace Polyphenols Evaluated on Ex Vivo Human Immune Blood Cells. *Molecules* **2023**, *28*, 2122. <https://doi.org/10.3390/molecules28052122>

Academic Editor: Nour Eddine Es-Safi

Received: 28 January 2023

Revised: 17 February 2023

Accepted: 21 February 2023

Published: 24 February 2023



**Copyright:** © 2023 by the authors. Licensee MDPI, Basel, Switzerland. This article is an open access article distributed under the terms and conditions of the Creative Commons Attribution (CC BY) license (<https://creativecommons.org/licenses/by/4.0/>).

## 1. Introduction

Climate change, loss of biodiversity and environmental pollution increase are challenges that must be faced by improving the relationship between humans and ecosystems. With this aim, EU environmental policy and legislation strongly encourages the reuse and recycling of waste, a reduction in harmful chemicals, and the use of environmentally friendly compounds that are also technologically satisfactory and economically convenient.

Agri-food industries are among the principal producers of waste and by-products in the world [1]. The European Union alone produces about 90 million tons of food by-products every year, with an impressively negative effect on the environment [2]. For these reasons, researchers are paying more and more attention to these wastes not only as a potential source of energy, but also as a source of bioactive molecules. In recent years,

agri-food by-products have been increasingly considered for the extraction of bioactive compounds such as antioxidants, vitamins, minerals, dietary fiber, essential fatty acids, oligosaccharides and oligopeptides [3,4]. In the Mediterranean area, a huge amount of waste is generated during the olive oil production process [5].

The Mediterranean basin contains approximately 98% of the planted olive (*Olea europaea* L.) trees, and together with other European countries, produces 80% of the world's olive oil [6]. Consequently, the olive oil industry generates significant amounts of olive oil by-products (olive pomace, olive leaves and olive mill wastewater), which need to be managed by these countries according to strategies aimed toward reducing the impact on the environment through the sustainable re-use of agri-food waste.

Olive pomace (OP) is an olive oil by-product rich in high-value compounds (e.g., polyphenols, dietary fiber, unsaturated fatty acids, antioxidants and minerals) and, in the context of a sustainable economy, the interest in recovering and utilizing bioactive compounds to add health benefits to the diet has increased during recent years [7].

Currently, there is indeed a wide bibliography in favor of the beneficial health effects of extra virgin olive oil, as well as on the possibility of obtaining valuable bioactive compounds from the waste products of the olive oil processing process (olive pomace and olive mill wastewater). A search in PubMed using the terms “olive oil AND health” or “olive by-products AND health” produced 3073 and 85 results, respectively (updated on 2 January 2023). Indeed, besides the well-recognized healthy effects of extra virgin olive oil [8–10], beneficial properties have also been demonstrated for processing by-products (leaves and olive mill wastewaters) including anti-cancer [11], prevention against age-related diseases [12], cardioprotective, anti-diabetic [13] and anti-inflammatory [14], among others [7,15–17]. In a recent study by Markhali et al. [18], oleuropein, one of the most common bioactive compounds in olive oil by-products, was found to be effectively capable of rebuilding the tissue damage caused by cisplatin in the stomach and the lungs, whereas Žugčić et al. showed that the compounds found in olive leaves exerted positive effects on gut microbiota [19].

The health-promoting effects of OP have mainly been associated with the presence of antioxidants, especially those belonging to plant-specialized metabolites, attributable to five classes of polyphenols (biophenols) identified as secoiridoids, simple phenols, flavonoids, phenolic acids, and lignans [20]. Interestingly, OP extract has been demonstrated to ameliorate lipid accumulation and lipid-dependent oxidative imbalance [21]. However, high amounts of  $\alpha$ -tocopherol (2.63 mg/100 g) and fatty acids have also been identified as bioactive compounds in OP by Nunes et al. [22], and a relevant contribution to the reported beneficial effects of OP in preventing cardiovascular and gut diseases has been attributed not only to polyphenols, but also to sugars and minerals present in the pomace by Ribeiro et al. [23].

Di Nunzio et al. [24] demonstrated that an aqueous OP extract was able to significantly reduce IL-8 secretion, one of the main proinflammatory cytokines, in Caco-2 cells in both basal and inflamed conditions, suggesting OP as a potential low-cost, high added-value ingredient for the formulation of functional and innovative food [24,25].

With a view to a potential use of OP in the formulation of innovative and functional foods or nutraceuticals, in this study we evaluated the prospective anti-inflammatory properties of OP compounds following digestion in the gastrointestinal (GI) compartments and passing the mucosal and intestinal barriers. Indeed, it has been observed that the bioavailability of polyphenols greatly changes during digestion, due to their different degrees of absorption, stability, solubility, and permeability [15,23,26].

To this purpose, three batches of sun-dried OP were characterized for their profiles in phenolic compounds and in vitro antioxidant properties before (methanolic extracts) and after (aqueous extracts) their simulated in vitro digestion and dialysis. The most promising aqueous extract, selected based on its composition of bioactive compounds, was further characterized and tested for its anti-inflammatory potential using PBMC cells.

PBMC cells were chosen because, circulating in the blood stream throughout the body, they represent not only the first systemic cell lines acting in the innate and adaptative immune responses, but also one of the two most represented cell categories (leukocytes vs. red blood cells) of the first tissue in which these bioactive compounds enter the body.

## 2. Results

A preliminary characterization of the three different OP batches (OP1, OP2, and OP3) was carried out to identify the OP batch with the highest potential biological properties before and after *in vitro* digestion. Only the OP extract with the highest potential biological properties was used for the subsequent experiments.

### 2.1. Total Phenol Content (TPC) and Phenolic Characterization of OP Extracts

The total phenol content and the individual phenolic characterization of each OP extract obtained from the three different batches of OP was determined before (methanol extracts) and after (aqueous extracts) the simulated *in vitro* digestion.

#### 2.1.1. Total Phenol Content (TPC) and Phenolic Characterization of Methanolic OP Extracts

In addition to the evaluation of the total content of phenolic compounds (TPC), a targeted HPLC-DAD analysis was carried out on the three methanolic OP extracts to identify and quantify some of the characteristic compounds of OP belonging to different chemical classes, such as secoiridoids, catechols, diterpens, flavonoids, hydroxycinnamic and phenolic acids (Table 1). Significant differences in the phenolic content were found among the three extracts, with OP1 being the richest for most metabolites. The most abundant compound was luteolin; its highest concentration was found in OP1. The biggest differences among the extracts were found for hydroxytyrosol and tyrosol, which were in the ranges of 4.9–224.6  $\mu\text{g}$  and 8.2–223.0  $\mu\text{g}/\text{g}$ , respectively, with OP1 showing the maximum level, and OP3 the minimum level. Regarding hydroxycinnamic acids, caffeic and chlorogenic acids were detected in all extracts. OP2 showed the highest content of caffeic acid, while OP1 was the richest in chlorogenic acid. Gallic acid levels were below the limit of quantification (LOQ) in all samples. Considering the total targeted metabolite index (TTMI), which represents the sum of the identified compounds, its value was significantly higher in OP1 than both OP2 and OP3 (Table 1).

**Table 1.** Phenolic composition ( $\mu\text{g}/\text{g}$  dry weight) and TPC (mg of GAE/g extract) of the three OP batches.

Sample	Ht	T	Ole	Lig	Pin	Myr	Lut	Api	CA	ChlA	GA	TTMI	TPC
OP1	224.6 ± 0.4 <sup>a</sup>	222.9 ± 1.8 <sup>a</sup>	128.9 ± 1.9 <sup>a</sup>	103.7 ± 0.5 <sup>a</sup>	36.9 ± 0.9 <sup>a</sup>	91.9 ± 0.5 <sup>a</sup>	599.9 ± 2.7 <sup>a</sup>	221.5 ± 5.5 <sup>a</sup>	7.8 ± 1.1 <sup>a</sup>	48.4 ± 4.3 <sup>a</sup>	nd	1686.5 <sup>a</sup>	99.8 ± 8.5 <sup>A</sup>
OP2	36.9 ± 0.5 <sup>b</sup>	46.7 ± 2.5 <sup>b</sup>	44.9 ± 1.7 <sup>b</sup>	27.1 ± 0.1 <sup>b</sup>	24.0 ± 1.3 <sup>b</sup>	70.8 ± 1.2 <sup>b</sup>	474.1 ± 1.7 <sup>b</sup>	175.5 ± 0.2 <sup>b</sup>	9.8 ± 0.1 <sup>b</sup>	28.9 ± 3.2 <sup>b</sup>	nd	938.7 <sup>b</sup>	26.3 ± 3.9 <sup>B</sup>
OP3	4.9 ± 0.3 <sup>c</sup>	8.2 ± 0.5 <sup>c</sup>	29.4 ± 0.1 <sup>c</sup>	24.1 ± 0.6 <sup>c</sup>	17.8 ± 0.7 <sup>c</sup>	72.9 ± 1.1 <sup>b</sup>	354.7 ± 3.2 <sup>c</sup>	129.9 ± 1.1 <sup>c</sup>	7.5 ± 0.5 <sup>a</sup>	11.4 ± 1.5 <sup>c</sup>	nd	660.8 <sup>c</sup>	14.5 ± 2.4 <sup>C</sup>

Ht = hydroxytyrosol, T = tyrosol, Ole = oleuropein, Lig = ligstroside, Pin = pinosresinol, Myr = myricetin, Lut = luteolin, Api = apigenin, CA = caffeic acid, ChlA = chlorogenic acid, GA = gallic acid, TTMI = total targeted metabolite index, TPC = total phenolic content, nd = not detected. Superscript letters <sup>A,B,C,a,b,c</sup> within the same column refer to statistical analysis, and different letters indicate significant differences for  $p < 0.0001$  and 0.5, respectively.

#### 2.1.2. Total Phenol Quantification (TPC) and Phenolic Characterization of Aqueous OP Extracts

Table 2 reports the phenolic compositions and TPC of the two types of aqueous extracts (< or >3.5 kDa) obtained from the three OP batches after *in vitro* digestion and dialysis.



**Table 2.** Phenolic composition (total µg in the dialyzed samples) and TPC (mg of GAE/g extract) of the digested OP batches. See Table 1 for abbreviations.

Sample	Ht	T	Ole	Lig	Pin	Myr	Lut	Api	CA	ChlA	GA	TTMI	TPC
OP1-W n.a.	138.8 ± 0.4 <sup>A</sup>	241.6 ± 6.7 <sup>A</sup>	41.7 ± 3.0 <sup>A</sup>	28.2 ± 2.2	50.6 ± 0.8 <sup>A</sup>	201.0 ± 0.1 <sup>A</sup>	212.2 ± 1.9 <sup>A</sup>	nd	30.5 ± 2.8 <sup>A</sup>	32.7 ± 1.3 <sup>A</sup>	76.2 ± 1.4 <sup>A</sup>	1053.5	127.9 ± 4.1 <sup>A</sup>
OP2-W n.a.	59.4 ± 1.1 <sup>B</sup>	101.0 ± 4.5 <sup>B</sup>	37.8 ± 1.2 <sup>B</sup>	nd	46.8 ± 3.4 <sup>B</sup>	188.7 ± 2.1 <sup>B</sup>	197.5 ± 1.6 <sup>B</sup>	nd	24.8 ± 0.6 <sup>B</sup>	28.9 ± 3.0 <sup>A</sup>	93.8 ± 1.3 <sup>B</sup>	778.7	96.8 ± 10.6 <sup>B</sup>
OP3-W n.a.	nd	nd	12.8 ± 1.0 <sup>C</sup>	nd	48.1 ± 1.3 <sup>AB</sup>	183.0 ± 2.3 <sup>B</sup>	192.2 ± 1.0 <sup>B</sup>	nd	18.0 ± 1.2 <sup>C</sup>	18.4 ± 1.1 <sup>B</sup>	295.4 ± 2.1 <sup>C</sup>	767.9	88.5 ± 21.7 <sup>B</sup>
OP1-W	386.7 ± 3.1 <sup>a</sup>	627.8 ± 3.4 <sup>a</sup>	129.8 ± 4.8 <sup>a</sup>	23.9 ± 1.3 <sup>a</sup>	41.4 ± 1.7 <sup>a</sup>	161.6 ± 1.5 <sup>a</sup>	168.4 ± 1.0 <sup>a</sup>	nd	36.2 ± 0.5 <sup>a</sup>	57.5 ± 2.1 <sup>a</sup>	56.0 ± 0.6 <sup>a</sup>	1527.7	96.1 ± 3.0 <sup>a</sup>
OP2-W	62.5 ± 1.4 <sup>b</sup>	77.7 ± 1.8 <sup>b</sup>	13.1 ± 1.1 <sup>b</sup>	15.4 ± 0.9 <sup>b</sup>	28.7 ± 0.8 <sup>b</sup>	118.9 ± 0.3 <sup>b</sup>	124.4 ± 0.7 <sup>b</sup>	nd	14.1 ± 0.8 <sup>b</sup>	26.9 ± 1.4 <sup>b</sup>	34.9 ± 0.7 <sup>b</sup>	516.6	72.4 ± 13.9 <sup>b</sup>
OP3-W	nd	nd	23.9 ± 1.1 <sup>c</sup>	20.7 ± 1.7 <sup>a</sup>	26.3 ± 1.8 <sup>b</sup>	100.5 ± 0.3 <sup>c</sup>	105.1 ± 0.1 <sup>c</sup>	nd	12.8 ± 1.7 <sup>b</sup>	15.0 ± 1.3 <sup>c</sup>	34.1 ± 3.1 <sup>b</sup>	338.4	68.5 ± 7.6 <sup>b</sup>

Superscript letters within the same column refer to statistical analysis. Uppercase letters <sup>A,B,C</sup> refer to non-absorbable aqueous digested samples (OP-W n.a.); lowercase letters <sup>a,b,c</sup> refer to absorbable aqueous digested samples (OP-W). Different letters indicate significant differences for  $p < 0.05$ .

The aqueous OP extracts, characterized by the presence of bioavailable compounds (serum available) with a molecular weight (m.w.) <3.5 kDa after dialysis [23] were indicated as OP-W (1, 2 or 3); whereas the non-available digested aqueous extracts were indicated as OP-W n.a. (1, 2 or 3; m.w. > 3.5 kDa).

The distribution of the detected metabolites in the bioavailable and non-bioavailable aqueous extracts obtained after the in vitro digestion varied, depending on the molecule type (Table 2). As a general trend, most metabolites detected in the pomace were also found in the absorbable fraction, with a different percentage of recovery, depending on samples. Only apigenin was not found, neither in the non-absorbable or the absorbable samples.

The bioaccessibility index, calculated as the percentage of the bioactive compound which was solubilised after the intestinal dialysis in reference to its total content in the undigested food, is reported in Table 3. A high bioaccessibility (more than 80%) was found for hydroxytyrosol and tyrosol in OP1 and OP2, while undetectable levels of both metabolites were present in OP3, probably due to their low levels in the original pomace extract (Table 2). Similar values were found for myricetin and caffeic acid, while the bioaccessibility of pinoreosin and chlorogenic acid were slightly lower, in the range of 46–70%. Oleuropein and ligstroside were found in the absorbable fraction at percentages ranging from 14 to 50% for the former, and 11 to 43% for the latter. A lower bioaccessibility was observed for luteolin, with a percentage of about 14%, with no differences among the three samples.

**Table 3.** Bioaccessibility index (%) of metabolites in the absorbable aqueous-digested OP samples (OP-W). See Table 1 for abbreviations.

Sample	Ht	T	Ole	Lig	Pin	Myr	Lut	Api	CA	ChlA	GA
OP1-W	86.1	140.8	50.3	11.5	56.1	87.9	14.0	-	231.2	59.4	-
OP2-W	84.5	83.2	14.6	28.3	60.0	84.0	13.1	-	71.5	46.6	-
OP3-W	-	-	40.7	43.0	74.0	68.9	14.8	-	84.9	66.1	-

## 2.2. Antioxidant Properties and Reducing Power of OP Extracts

The antioxidant potential and reducing power of each OP extract obtained from the three different batches of OP before and after the simulated in vitro digestion were evaluated by three different spectrophotometric assays.

### 2.2.1. Antioxidant Properties and Reducing Power (ABTS, DPPH and FRAP Assays) of Methanolic OP Extracts

Table 4 reports the antioxidant properties and reducing powers evaluated in the methanolic extracts obtained from the three crude OP batches (1, 2, and 3). In accordance with the different results obtained for the phenolic content and TTMI index, OP1 methanolic extracts showed the highest antioxidant activity of all the antioxidant assays utilized, whereas OP2 resulted in an intermediate position between the other two extracts. Therefore, the trends of antioxidant responses resembled the trends of TPC found in the three different OP batches.

**Table 4.** The radical scavenging activity of methanolic extracts obtained from the three crude OP1, OP2 and OP3 batches. Values are reported as Trolox equivalent ( $\mu\text{g TE}/\text{mg dry extract}$ ).

Samples	Radical Scavenging Assays		
	ABTS	DPPH	FRAP
	Trolox Equivalent $\pm$ SD	Trolox Equivalent $\pm$ SD	Trolox Equivalent $\pm$ SD
OP1	124.6 $\pm$ 4.2 <sup>a</sup>	44.5 $\pm$ 2.5 <sup>a</sup>	74.6 $\pm$ 3.5 <sup>a</sup>
OP2	55.6 $\pm$ 4.1 <sup>b</sup>	19.6 $\pm$ 2.4 <sup>b</sup>	31.5 $\pm$ 1.5 <sup>b</sup>
OP3	19.5 $\pm$ 1.2 <sup>c</sup>	9.22 $\pm$ 0.7 <sup>c</sup>	6.3 $\pm$ 0.07 <sup>c</sup>

<sup>a,b,c</sup> different letters mean significant differences;  $p < 0.05$ .

### 2.2.2. Antioxidant Properties and Reducing Power (ABTS, and FRAP Assays) of Aqueous OP-W n.a. and OP-W Extracts after In Vitro Digestion and Dialysis

Table 5 reports the results of the radical scavenging assays evaluated in the aqueous extracts obtained from the in vitro digestion and dialysis of the three OP batches (1, 2, and 3). All the digested OP samples conserved their own antioxidant properties proportionally to the content of the original bioactive compounds, therefore, the OP1 samples, both absorbable and not, showed the highest antioxidant activity when compared with the other two OP samples.

**Table 5.** The radical scavenging activity of aqueous OP extracts after in vitro digestion and dialysis. Values are reported as Trolox equivalent ( $\mu\text{g TE}/\text{mg dry extract}$ ).

Samples	ABTS	FRAP
	Trolox Equivalent $\pm$ SD	Trolox Equivalent $\pm$ SD
OP-W n.a. <sup>1</sup>		
1	127.3 $\pm$ 7.4 <sup>a</sup>	88.3 $\pm$ 3.1 <sup>a</sup>
2	79.5 $\pm$ 6.5 <sup>b</sup>	45.1 $\pm$ 2.2 <sup>b</sup>
3	74.3 $\pm$ 10.5 <sup>b</sup>	40 $\pm$ 0.1 <sup>b</sup>
OP-W <sup>2</sup>		
1	82.5 $\pm$ 4.5 <sup>a</sup>	44.8 $\pm$ 0.8 <sup>a</sup>
2	68.9 $\pm$ 3.0 <sup>b</sup>	22.7 $\pm$ 0.6 <sup>b</sup>
3	73.6 $\pm$ 2.2 <sup>b</sup>	14.4 $\pm$ 1.0 <sup>c</sup>

<sup>1</sup> OP-W n.a. (samples 1, 2 and 3): not absorbable aqueous extracts (m.w. > 3.5 kDa). <sup>2</sup> OP-W (samples 1, 2 and 3): absorbable aqueous extracts (m.w. < 3.5 kDa). <sup>a,b,c</sup>: different letters mean significant differences at  $p < 0.05$ .

### 2.2.3. Antioxidant Property (ABTS) and TPC of Aqueous OP-W Fractions (OP-F)

Based on the previous results, OP-W1 was selected as the most promising extract, and further fractionated using reverse-phase chromatography (HPLC-DAD) on a semipreparative C18 column. Figure 1 shows the seven different major chromatographic peaks obtained. All these peaks were characterized by low hydrophobicity, as suggested by the fact that they eluted at a low concentration of acetonitrile (10–20%).

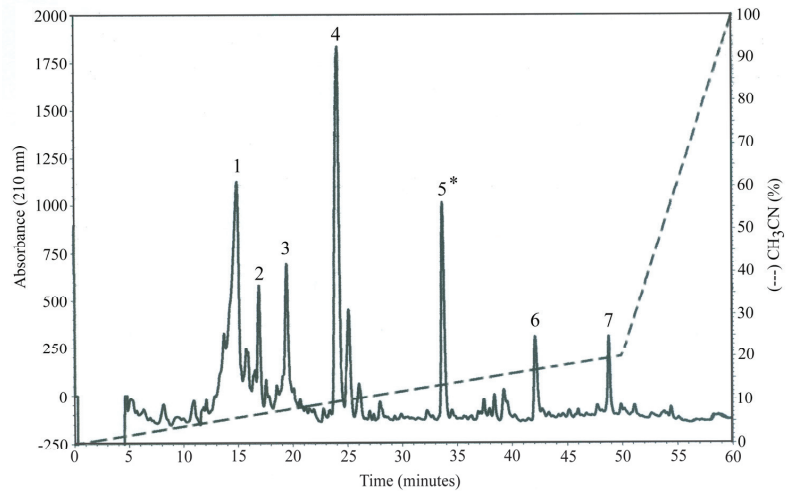


**Figure 1.** Major chromatographic peaks (n.7) obtained from OP-W1. The most bioactive aqueous adsorbable extract result was the fifth one (\*), by HPLC-DAD.

The material was selectively eluted at each peak and then tested for its radical scavenging activity (ABTS assay) and TPC (Table 6). The fifth peak resulted as the most biologically active (\*).

**Table 6.** The radical scavenging activity of the seven fractions obtained from OP-W1, the aqueous adsorbable OP extract (OP-F) characterized by the highest antioxidant properties. Values are reported as Trolox equivalent ( $\mu\text{g TE}/\text{mg dry extract}$ ).

OP-F	ABTS	TPC
	Trolox Equivalent $\pm$ SD	mg of GAE/g Extract $\pm$ SD
1	$63.3 \pm 5.3$ <sup>AB</sup>	$156.7 \pm 0.7$ <sup>A</sup>
2	$26.5 \pm 0.6$ <sup>A</sup>	$127.3 \pm 3.1$ <sup>A</sup>
3	$369.7 \pm 4.0$ <sup>C</sup>	$719.5 \pm 10.9$ <sup>B</sup>
4	$342.2 \pm 5.8$ <sup>C</sup>	$761.8 \pm 10.0$ <sup>B</sup>
5	$1036.7 \pm 35.5$ <sup>D</sup>	$1199.4 \pm 69.9$ <sup>C</sup>
6	$76.5 \pm 3.2$ <sup>BE</sup>	$197.4 \pm 9.7$ <sup>A</sup>
7	$253.7 \pm 8.3$ <sup>F</sup>	$450.5 \pm 28.6$ <sup>D</sup>

Different capital letters mean significant differences;  $p < 0.0001$ .

### 2.3. OP-W Peptide Identification and Possible Bioactivity

The peptide content of OP-W was detected by mass spectrometry. After digestion, we obtained 78 and 93, or 96 and 112 peptides (before and after further trypsinization) and some of them permitted the identification of 13 and 14 proteins specific to *Olea europaea* olive or to saprophytic microorganisms of the olive tree plant, respectively. Tables 7 and 8 report the number of peptides identified in the OP-W1 samples, and the corresponding proteins were searched in both “Olea” and “Olea Europea” protein databases. Some of these

proteins, such as 50S ribosomal protein L16, amine oxidase, pectinesterase, 2, profilin-1, 4-coumarate-CoA ligase, and putative geraniol 10 hydroxylase, as expected, were derived from *Olea europaea*; whereas, others from *Pseudomonas* (sp. PIC125 and PIC 141) belonged to bacteria with potential as a biocontrol tool against pathogenic microorganisms (i.e., *Verticillium dahlia* Kleb.) of olive plants [27].

**Table 7.** List of identified OP-W1 peptides and corresponding proteins by LC-MS/MS analysis. The databases consulted were FASTA-file *Olea* and *Olea europaea* (common olive).

OP-W1 Proteins				
ID	Protein	Organism	MW	Peptides
J9XLG0	Putative polyphenol oxidase	<i>Olea europaea</i>	53658	2
E3TJS3	50S ribosomal protein L16	<i>Olea europaea</i>	15346	2
A0A0N9LRR6	Amine oxidase	<i>Olea europaea</i>	87207	4
B2VPR8	Pectin esterase 2	<i>Olea europaea</i>	39856	2
A0A0G3FBC7	LIP (fragment)	<i>Olea europaea</i>	11938	2
A4GE45	Profilin-1	<i>Olea europaea</i>	14520	2
A0A649ZUF2	4-coumarate-CoA ligase	<i>Olea europaea</i>	59898	3
Q5DTB7	Ole e 3 allergen	<i>Olea europaea</i>	5795	2
J9XH65	Putative geraniol 10-hydroxylase	<i>Olea europaea</i>	46724	5
A0A126X2X6	Putative LOV domain-containing	<i>Olea europaea</i>	70139	2
A0A7G7YFM0	Ribulose biphosphate carboxylase	<i>Olea europaea</i>	53072	2
Q1W4C7	Hexosyltransferase	<i>Olea europaea</i>	31071	2
J9XLE5	Isopentenyl-diphosphate Delta-isomerase	<i>Olea europaea</i>	25822	2
A0A1B1V5C3	Putative transcriptional corepressor	<i>Olea europaea</i>	54598	2

**Table 8.** List of identified peptides and corresponding proteins from organisms in the OP-W1 sample by LC-MS/MS analysis. The databases consulted were FASTA-file *Olea* and *Olea europaea* (common olive).

Proteins from Organisms in OP-W1 Sample				
ID	Protein	Organism	MW	Peptides
A0A2A2DN42	Chemotaxis protein	<i>Pseudomonas</i> sp. PIC141	57171	2
A0A2A2DPP3	Short chain dehydrogenase	<i>Pseudomonas</i> sp. PIC 125	28887	3
A0A2A2E801	Poly(A) polymerase	<i>Pseudomonas</i> sp. PIC 125	53512	2
A0A2A2DPY9	PhoH family protein	<i>Pseudomonas</i> sp. PIC 141	38446	2
A0A2A2E7V3	UvrABC system protein C	<i>Pseudomonas</i> sp. PIC125	67237	2
A0A2A2E543	Amine oxidase	<i>Pseudomonas</i> sp. PIC141	62484	2
A0A2A2DX44	Serine hydrolase	<i>Pseudomonas</i> sp. PIC141	40686	2
A0A2A2DU16	Haemagglutinin	<i>Pseudomonas</i> sp. PIC125.	9783	2
A0A2A2DPN3	DUF1329 domain	<i>Pseudomonas</i> sp. PIC125	50476	2
A0A2A2DJ68	TonB-dep. siderophore receptor	<i>Pseudomonas</i> sp. PIC125	78117	3
A0A2A2EB40	Tail-specific protease	<i>Pseudomonas</i> sp. PIC125	77756	3
A0A2A2E740	RNA helicase	<i>Pseudomonas</i> sp. PIC125	48800	3
A0A2A2E9Q7	Coproporphyrinogen-III oxidase	<i>Pseudomonas</i> sp. PIC125	53148	2

The profile of these peptides was checked in the open-access tool PeptideRanker (a score higher than 0.6 was considered as potentially “bioactive”) to forecast the eventuality of biological activity of a peptide sequence [28], and two or five peptides of the *Olea europaea* olive received a score between 0.66 and 0.79, or 0.63 and 0.68, before and after trypsinization, respectively. These peptides were in reference to two or four proteins, respectively (putative geraniol 10-hydroxylase, hexosyltransferase or amine oxidase, pectin esterase 2, putative geraniol 10-hydroxylase, and putative LOV domain-containing, respectively). Subsequently,

the best scored peptides were submitted to BIOPEP search (accessed on 15 February 2023, h <http://www.uwm.edu.pl/biochemia/index.php/pl/biopep/>) to hypothesize their possible bioactivities [29], but, so far, no bioactivity has been detected for these peptides.

Furthermore, nine and six peptides (before and after trypsinization, respectively) attributable to *Pseudomonas* sp. PIC25 resulted in a score higher than 0.6, but none of these were recognized in the proteins identified in Table 8; neither were they present in the BIOPEP database.

#### 2.4. Untargeted Metabolomics of the Most Bioactive OP-F

Table 9 reports the percentages of different metabolites identified in the fifth OP1-F sample by GCMS analysis. Among these metabolites, a high percentage (about 25%) were represented by antioxidant compounds such as tyrosol and 4 hexylphenol, probably responsible for the highest antioxidant activity observed in the fifth peak (Table 6). Of interest was the 7.6% presence of glutamic acid, which is known to help in maintaining the integrity of the intestinal barrier, as it is incorporated into proteins during their synthesis by the “good” bacteria of the intestinal microbiota, thus, favoring their development [30,31].

**Table 9.** List of identified metabolites (expressed in percentage) recognized in the fifth OP-F sample by GCMS analysis.

Metabolites	%
Trietanolamine	3.07
Propanamine,N(2fluorophenyl)3(4morpholyl)	0.18
Glycerol	3.2
Ciclopentylamine	2.26
1 propanamine N,N diproyl	2.26
Cystathionine	1.04
Tris,N-acetyl	1.08
Homocysteine	7.1
Tyrosol	20.49
Glutamic acid	7.61
4 Hexylphenol	4.52
Phenol,3 butanol	0.58
Bis oxyethylthiosulfide	2.74
Linoleic acid	0.23
Sugar	3.25

#### 2.5. Cellular Anti-Inflammatory Activities

To better clarify, at a molecular level, whether OP-W and OP-F aqueous extracts were able to modulate the expression of pro-inflammatory (IL-6 and TNF- $\alpha$ ) and anti-inflammatory (IL-10) genes, a real time RT-PCR analysis was carried out on RNA of human PBMCs, which were previously in vitro supplemented, or not supplemented (CTRL), with the aqueous OP extracts (OP-W and OP-F; 2.5  $\mu$ g/mL of extracts for 24 h) and then stimulated (s.) or not stimulated (n.s.) with LPS (100 ng/mL for 2.5 h). The mRNA expression levels of cytokines in OP-W s. and OP-F s. samples showed significant reductions for IL-6 (in both OP-W s. and OP-F s. cells;  $p < 0.05$ ), IL-10 ( $p < 0.01$  and  $< 0.05$ , respectively), and TNF- $\alpha$  ( $p < 0.01$  and  $< 0.05$ , respectively), when compared with not supplemented cells (CTRL s.) (Figure 2).

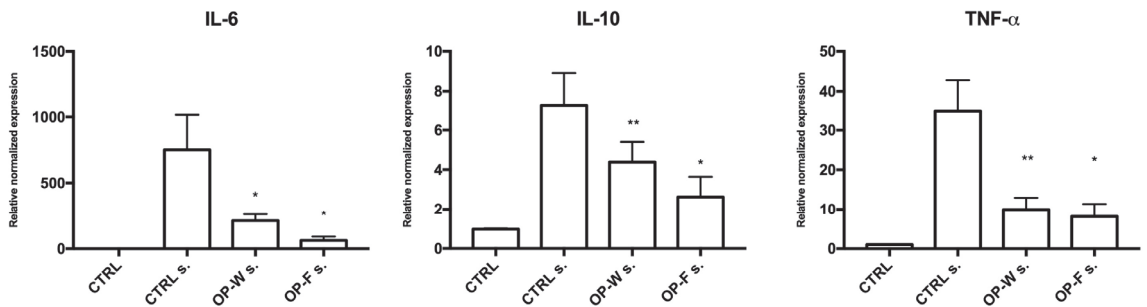


**Figure 2.** Real time PCR relative quantification of mRNAs encoding IL-6, IL-10, and TNF- $\alpha$  ( $\pm$  S.E.M.), evaluated in human PBMCs after stimulation (s) or not (n.s.) with LPS for 2 h in an incubator at 37 °C, 5% CO<sub>2</sub>. Blood cells were previously cultured in presence or not (CTRL) of aqueous extracts obtained from OP (OP-W and OP-F) after in vitro digestion and dialysis. \*  $p < 0.05$ , \*\*  $p < 0.01$ .

### 2.6. Cytokines Concentrations in Conditioned Medium

To confirm the anti-inflammatory effect of OP aqueous extracts (OP-W and OP-F) in LPS stimulated cells, the concentration of a panel of 16 cytokines (of IL-1 $\alpha$ , IL-1 $\beta$ , IL-2, IL-4, IL-5, IL-6, IL-8, IL-10, IL-12, IL-13, IL-15, IL-17, IL-23, IFN $\gamma$ , TNF- $\alpha$  and TNF- $\beta$ ) in PBMC culture supernatants was measured by a multiplex ELISA assay. Only the cytokines IL-6, IL-8 and TNF- $\alpha$  resulted as detectable (the remaining were below the detection levels) and, among these, both IL-6 and TNF- $\alpha$  resulted as significantly reduced by the OP-W extracts ( $p < 0.05$ ) (Figure 3). Interestingly, the only cytokine that resulted as detectable also in the conditioned medium of cells not stimulated by LPS was IL-8 (means  $\pm$  S.E.M. were  $57.8 \pm 13.1$ ,  $68.3 \pm 16.2$ ,  $100.6 \pm 54.5$  pg/mL in CTRL n.s., OP-W n.s. and OP-F n.s. cells, respectively;  $p =$  n.s.).

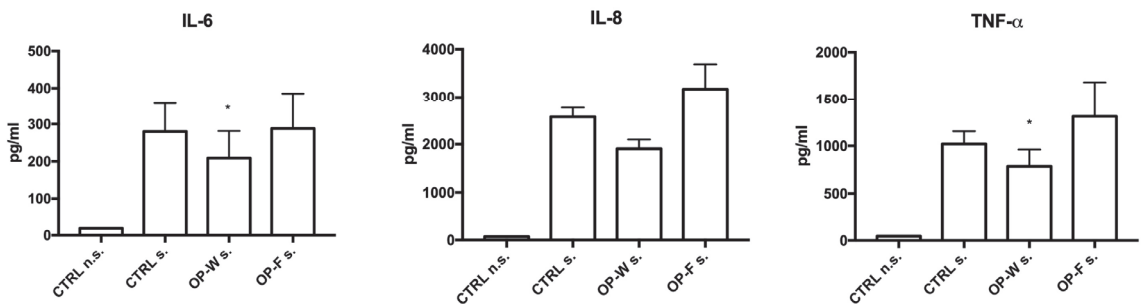


**Figure 3.** Cytokine concentrations evaluated in the culture medium of human PBMCs after stimulation (s), or not (n.s.), with LPS for 2 h in an incubator at 37 °C, 5% CO<sub>2</sub>. Blood cells were previously cultured in presence, or not (CTRL), of aqueous extracts obtained from OP after in vitro digestion and dialysis. \*  $p < 0.05$ .

### 3. Discussion

Our results regarding the phenolic composition of olive pomace extracts confirm that this by-product retains most bioactive compounds present in the fruit, despite the complex chemical transformations occurring during the fruit processing and pomace storage stages.

The chemical profile of this by-product has been widely described by several authors [32,33] and our results allow the conclusion that, despite a huge variability due to the impact of both endogenous (i.e., varieties) and exogenous (i.e., agro-pedoclimatic) factors [34,35], olive pomace represents a good source of natural health-promoting compounds in concentrations much higher than virgin olive oil [36,37]. In the present study too, the evaluation of three

different olive pomace samples confirmed the presence of beneficial health compounds in all the batches investigated. These OP samples, although belonging to the same cultivar planted in the same territory, were different in terms of the period of olive harvest and, consequently, their ripening state.

The main phenolic compounds identified in the three pomace samples included hydroxytyrosol, tyrosol, oleuropein, ligstroside, pinoresinol, flavonoids, and hydroxycinnamic acids, and big differences were observed among samples [36]. OP1, the sample characterized by the highest content of unripened olives, was also the sample with the highest levels of target phenols, and with the highest antioxidant activity, based on the three in vitro tests used. Indeed, the ripening state strongly influences the phenolic content and antioxidant properties, that decrease along olive maturation [38].

This OP sample also conserved its highest antioxidant properties in both the aqueous absorbable and not absorbable digested extracts (OP-W n.a. and OP-W, Table 4), being the target phenols here mainly represented. Furthermore, the fifth fraction (OP-F; Table 5), obtained by the same OP1-W sample, also conserved a very high antioxidant property. This was probably due to the high content of tyrosol (20.49%) and 4-hexylphenol (4.52%), that together represented more than 25% of the total OP1-F sample, as testified by the metabolomic analysis (Table 8). Indeed, the free radical scavenging and metal-chelator properties of hydroxytyrosol and secoiridoid derivatives have been well recognized [39], and the high antioxidant efficiency has been attributed to the presence of the *O*-dihydroxymethyl moiety in the molecule, which mainly acts as a chain breaker by donating a hydrogen atom to peroxy-radicals (ROO<sup>\*</sup>). However, it has been proposed that hydroxytyrosol may confer an antioxidant protection by also reinforcing the endogenous defence systems against oxidative stress, by boosting different cellular signalling pathways [40]. A good antioxidant capacity has also been demonstrated for the 4-*O*-monohydroxy compounds ligstroside and tyrosol [41], and several interesting functional properties have been reported for oleuropein, including antioxidant, anti-inflammatory, anti-atherogenic, anti-cancer, and anti-microbial activities, among others [42]. Luteolin and apigenin have been confirmed as relevant components of olive pomace, as previously reported by Peralbo-Molina et al. [33], and are known to exert a protective effect against the deleterious effects of reactive oxygen [43].

However, in order to exert beneficial health effects, phenolic compounds in OP samples must be bioaccessible and bioavailable [44]. Bioaccessibility, which is defined as the release of a compound from its natural matrix to be available for intestinal absorption, is the first limiting factor for bioavailability. Ahmad-Qasen et al. [45] demonstrated that, after ingestion, the bioaccessibility of total phenolic compounds decreased during the first hour of the digestion process due to the degradation of the bioactive compounds following the pH variation and enzymatic activity, whereas for the rest of the digestion process, a constant value of TPC reached the duodenum. Furthermore, Ribeiro et al., 2020 [23], showed that after gastrointestinal digestion, more than 50% of the water-soluble compounds remained bioaccessible, especially hydroxytyrosol and potassium.

Bioavailability represents the ability of a nutrient or food bioactive to be efficiently digested, absorbed and distributed to provide its beneficial effect to the organism, participating in its physiological processes and storage [46].

Despite the huge research on the biological properties of olive phenolic compounds, information relative to their bioavailability, that strongly influences the pharmacological function, is limited. Recently, however, excellent reviews on the bioavailability of bisphenols and their metabolism have been proposed [46–49]. It has been shown that after oral administration, hydroxytyrosol is dose-dependently absorbed until the saturation of the phase I metabolic processes of intestinal transporters is reached. Thereafter, the absorption stops and hydroxytyrosol seems to undergo a rapid and intense metabolism [48,50], so that only a small fraction of free (unchanged) hydroxytyrosol is detectable in plasma. Indeed, the biological role of many bioactive compounds in the human organism is attributed to their metabolites, and the intestine represents the main site where it occurs for orally administered compounds [51]. In most human studies, the hydroxytyrosol absorption rate

ranges from 55 to 90%, circulating bound to lipoproteins, reaching its maximal concentration after 1–2 h following its administration, then the molecule rapidly becomes undetectable. As proof of its absorption, the feces and urinary excretion of hydroxytyrosol and its metabolic derivatives have usually been adopted, with excretion rates resulting as maximum at 0–4 h [52,53].

Tyrosol has generally fewer studies due to its lower bioactivity, and also lower metabolites, according to the available information [46,51].

Our results showed that most phenolic compounds present in the olive pomace extracts were still detected at high levels in the absorbable fraction obtained after *in vitro* digestion, indicating in most cases a very high bioaccessibility. Hydroxytyrosol, for instance, showed bioaccessibility indexes higher than 80% in two out of three samples, and similar values were found for tyrosol in OP2. These results were in accordance with data reported by Ribeiro et al. [23], who obtained very similar values (82 and 77%, for hydroxytyrosol and tyrosol, respectively), demonstrating that they were the most bioaccessible compounds present in olive pomace. In a previous investigation, Seiquer et al. [54] also reported that the most bioaccessible and stable compounds after *in vitro* digestion of olive oil were tyrosol and hydroxytyrosol, and specifically, these compounds were absorbed in the intestine by passive diffusion as a result of their polar structure, thus, also demonstrating a good bioavailability, even though dissimilar to each other [47]. The passive diffusion of these compounds in the small intestine was recently confirmed by Sakavitsi et al. [51] who also observed a passive diffusion of caffeic acid, homovanillic acid, HT-3-*O*-sulphate, and 3,4-dihydroxyphenylacetic acid [48] as the main metabolites of hydroxytyrosol.

In OP1, the bioaccessibility index of tyrosol was higher than 100%, and the same was observed for caffeic acid. This was not surprising, suggesting that these molecules may be released from the food matrix and/or metabolized from other phenolic compounds with more complex structures [55].

Furthermore, bioavailability studies in the human body have demonstrated that absorbed oleuropein and tyrosol can be metabolized into free hydroxytyrosol, thus, increasing the concentration of HT in circulation [48,56].

However, potential beneficial effects have also been demonstrated for other compounds present in OP such as mineral, proteins and sugars [23]. In this study, the effects of sugars and minerals were not evaluated, while the possible presence of interesting peptides (after digestion of proteins) for their biological effects was investigated.

Mass spectrometry analysis of OP1-W peptide hydrolysates allowed the identification of 13 and 14 proteins specific to *Olea europaea* olive or to saprophytic microorganisms of the olive tree plant, respectively. The profile of these peptides was checked in the open-access PeptideRanker and BIOPEP tools. Overall, seven peptides of *Olea europaea* olive received a significant score. These peptides were referable to putative geraniol 10-hydroxylase, hexosyltransferase or amine oxidase, pectin esterase 2, putative geraniol 10-hydroxylase, and putative LOV domain-containing. However, none of the best scored peptides matched with the BIOPEP database.

Even if the presence of *Pseudomonas* sp. in OP samples could not be reconducted to any beneficial health effects for “consumers”, it was interesting to find traces of how plants and microorganisms join forces to address environmental pitfalls. Indeed, these strains of *Pseudomonas* spp. (PICF141 and PIC25) have shown high *in vitro* inhibition ability of pathogens’ growth such as *V. dahliae*, responsible for Verticillium wilt of olive [27]. Furthermore, fifteen peptides attributable to *Pseudomonas* sp. PIC25 showed a best score, but none were recognized in the proteins identified in Table 8, neither were they present in the BIOPEP database.

Finally, we tested, *ex vivo*, the effects of OP1-W and OP1-F extracts on cells present in the blood, the first tissue with which these extracts come into contact as soon as they are absorbed by the intestinal wall, even before they undergo phase I and II metabolism that favors their urinary excretion [57].



To date, no data exist on the effects of predigested phenols obtained from olive by-products, neither on human blood immune cells (PBMC) withdrawn from healthy individuals, or on in vitro cell cultures.

We found that the digested absorbable OP1-W extract showed significant anti-inflammatory activity on the ex vivo human PBMC stimulated by LPS. This finding was testified by the significant reduction in pro-inflammatory cytokines IL-6 and TNF- $\alpha$  in conditioned medium ( $p < 0.05$ ; Figure 3) and by a lowering trend of IL-8 together with a significantly lower expression of mRNAs encoding IL-6 and TNF- $\alpha$  ( $p < 0.5$  and  $p < 0.01$ , respectively; Figure 2).

Furthermore, in the ex vivo evaluations, a significant down-regulation of IL-10, a typical anti-inflammatory gene, was also observed. Even if this finding seems in contrast with the previous results, we assumed that it was due to a reduced triggering of the inflammatory process (and its subsequent cascade of pro- and anti-inflammatory signals) in PBMC pre-treated with OP-W (for 22 h) in response to a pro-inflammatory stimulus (LPS), rather than to a lower ability to induce the IL-10 gene to turn off an inflammation fully triggered. This finding was in accordance with results reported by Camargo et al. [14], who observed that the dietary assumption of high-phenol virgin olive oil in patients suffering metabolic syndrome, by switching the activity of peripheral blood mononuclear cells to a less deleterious inflammatory profile, was able to repress the inflammatory process, even if it occurred because of the addition of a stimulus of inflammation (i.e., LPS).

Indeed, LPS normally acts by activating the nuclear factor-kappa B (NF- $\kappa$ B) and mitogen-activated protein kinase (MAPK) pathways, causing the overexpression of various inflammatory mediators, such TNF- $\alpha$ , IL-1 $\beta$ , IL-6, nitric oxide (NO) and prostaglandin E2 (PGE2) [58,59]. However, Camargo et al. [14] found a chemokine repression as a direct consequence of phenols interaction with NF- $\kappa$ B/MAPK/AP-1 inflammation signaling pathways.

Recent research has found evidence of the ability of the phenols of several plants to induce cellular, biochemical, and epigenetic modifications, resulting in modulation of the homeostasis of key cellular processes such as the control of oxidative stress, inflammatory response, and gene expression, among others [57]. Wang et al. [60] recently showed that pretreatment with tyrosol markedly inhibited the activation of NF- $\kappa$ B and apolipoprotein-1 (AP-1) in LPS-induced A549 cells.

In the present study, the fifth absorbable OP1-F aqueous extract, which was constituted of more than 20% of tyrosol and utilized at the same concentration of OP-W, significantly reduced the expression of mRNAs encoding IL-6, IL-10, and TNF- $\alpha$  ( $p < 0.05$ ); however, it was not able to significantly reduce the cytokine levels in the conditioned medium. Indeed, an increasing trend was observed, although not statistically significant, for all three detectable cytokines. We supposed that the lack of ability of the OP1-F extract (used at the same concentration of OP-W) vs. OP1-W sample to reduce the concentration of cytokines IL-8 and TNF- $\alpha$  was due to a too-high concentration of tyrosol (by using the OP1-F extract at the same concentration of OP1-W extract, the tyrosol level resulted as much higher) or to the presence, in the OP1-W extract, of other compounds eliciting a synergistic effect with tyrosol in quenching the inflammatory response elicited by LPS stimulus.

Indeed, we supposed that a too-high level of tyrosol could induce a sort of paradoxical effect [61,62] as seems stated by the higher IL-8 level in PBMC supplemented with OP1-F aqueous extract, but not triggered by LPS. Indeed, in the present study, as observed by other authors [24], in Caco-2 cell culture maintained at basal condition (control), the only interleukin detectable in the basal medium was IL-8. However, while in the presence of the extract OP1-W extract, the interleukin IL-8 showed a decreasing trend; in the presence of OP1-F extract, the trend was the opposite.

Various reports have stated that diets with high contents of polyphenols are associated with a reduced production of these inflammatory cytokines and a consequent improvement of inflammation [10]. In the present study, for the first time, similar results exerted by digested phenols derived from olive pomace on the ex vivo cultured human (healthy) PBMCs have been demonstrated.

Interestingly, the concentration of phenols in the dose of OP-W extract here adopted on cells was in the order of nanogram. Even if it was quite difficult to find and compare data relative to the bioavailability of oil phenols or phenols of olive by-products orally administered in human in vivo studies [46,47,53], in blood, what was possible to infer from the literature was that it is not impossible to reach this nanogram concentration, although for a very short time, by ingesting, for example, a quantity corresponding to 10 g of olives. Therefore, these preliminary results relative to the anti-inflammatory properties exerted by the mixture of phenols present in the in vitro absorbable digested olive pomace seem promising and worthy of further investigation.

An expanding body of literature has shown that, through increasingly eco-friendly and cost-effective extraction processes applied to olive oil processing by-products [63,64], it is possible to obtain high quantities of bioactive compounds which have been proven to be effective in exerting beneficial effects on health. Our data further demonstrate that olive pomace can, therefore, become a valuable raw material that can be used not only in the energy sectors, food, cosmetic and animal feed [7,65], but also in the nutraceutical field.

## 4. Materials and Methods

### 4.1. Chemicals and Reagents

All reagents were of analytical purity. The 2,2-diphenyl-1-picrylhydrazyl (DPPH), ABTS diammonium salt (2,2-azinobis-3-ethylbenzothiazoline-6-sulphonic acid), Folin-Ciocalteu's reagent, standards of Trolox and gallic acid were purchased from Sigma-Aldrich Corp. (Milan, Italy). Bile salts were from Oxoid™ (Hampshire, U.K.). Spectrapor 3 45 MM/15 M membrane (cut-off 3.5 kDa) was purchased from Fischer Scientific (Milan, Italy). Pancreatin (from porcine pancreas: P3292-100G), pepsin (from pig gastric mucosa: ≈2500 units/mg protein), α-amylase from human saliva (A0521-500 units/mg), formic acid, potassium sorbate, sodium carbonate, trifluoroacetic acid (TFA), and peptidyl-dipeptidase were purchased from Sigma-Aldrich Corp. (Milan, Italy).

Hydroxytyrosol, tyrosol, oleuropein, apigenin, luteolin and myricetin were purchased from Extrasynthese (Lyon, France); caffeic acid, chlorogenic acid, pinosresinol, and ligstroside were purchased from Sigma-Aldrich Corp. (Milan, Italy). Acetonitrile was purchased from Pai Acs, Panreac. All other chemicals and solvents were of the highest analytical grade from Sigma-Aldrich Co. (St. Louis, MO, USA).

### 4.2. Olive Pomace Methanolic Extracts

Three batches of sun-dried OP were gently provided by Oil Mill Industry Consoli (Adrano, Catania, Italy) and transported to the laboratory where they were packed in polyethylene bags and kept in a freezer at −80 °C until analysis. OP1 was collected in September, OP2 in October, and OP3 in November/December, thus, the ripening state increased with each harvest of olives. These OP samples were stratified (and stabilized with Consoli's patent), one batch on top of the other, in a unique big pool, and stabilized with Consoli's patent (Consoli's patent 0001428707). The pool was well covered until the following summer season, when the pool was opened, and the OP was dried under the sun. Olive pomace samples were collected from the bottom of the pool at the end of June (OP1), July (OP2), and August (OP3). These OP samples were composed mainly of the olive cultivar *Olea europaea* L. (*Nocellara etnea* as main cultivar) and the proximate composition as reported in Chiofalo et al. [66].

From each OP sample (OP1, OP2 and OP3; 5 g/batch), methanolic extracts were obtained by using a Soxhlet apparatus for 5 h to fall and 200 mL of pure methanol. The obtained solutions were then evaporated with a Rotavapor (Buchi B-490) to collect the OP extracts for further characterization. The crude extracts (methanolic OP extracts) were then weighed (1.228 g, 0.967 g, and 1.004 g, respectively) and the yield calculated (24.6%, 19.34%, and 20.1%, respectively).

#### 4.2.1. Radical Scavenging Activity Assays in Methanolic OP Extracts

By using the 1,1-diphenyl-2-picrylhydrazyl (DPPH) method, the radical scavenging activity of the methanolic OP1, OP2 and OP3 extracts was measured [67]. In a 96-multiwell plate, 50  $\mu$ L aliquot of each OP extract (0–2 mg/mL) or of the standard Trolox (0–100 mg/mL), in triplicate, was added to 200  $\mu$ L of DPPH solution (0.1 mM in methanol). After incubation in darkness for 30 min at 37 °C, the absorbance was measured at 490 nm using a UV–VIS microplate reader (FLUOstar Optima, BMG Labtech, Ortenberg, Germany) against DPPH solution as a blank. Values were expressed as Trolox equivalent ( $\mu$ g TE/mg dry extract).

The radical cation scavenging activity of each extract was measured using the 2,2'-azino-bis (3-ethylbenzo-thiazoline-6-sulphonate) diammonium salt (ABTS) method [68]. In a 96-multiwell plate, 50  $\mu$ L aliquot of sample (0–5 mg/mL) was added to 200  $\mu$ L of ABTS solution (5 mM). ABTS solution was derived by oxidizing ABTS with  $MnO_2$  in distilled water for 30 min in the dark, and then the solution was filtered through filter paper. After 20 min incubation in darkness at room temperature, the absorbance was read at 734 nm using a UV–VIS microplate reader (FLUOstar Optima, BMG Labtech, Ortenberg, Germany) against ABTS solution as a blank. Values were expressed as Trolox equivalent ( $\mu$ g TE/mg dry extract).

#### 4.2.2. Ferric Reducing Antioxidant Power (FRAP) Assay in Methanolic OP Extracts

The reducing power of methanolic OP1, OP2 and OP3 extracts was evaluated according to a ferric reducing antioxidant power (FRAP) assay [69]. In a 96-multiwell plate, 25  $\mu$ L aliquot of sample (0–2 mg/mL) or of standard Trolox (0–100  $\mu$ g/mL) was added to 175  $\mu$ L of FRAP working solution containing 20 mmol/L ferric chloride, 300 mmol/L acetate buffer (pH 3.6), and 10 mmol/L TPTZ (2,4,6-tri(2-pyridyl)—S-triazine) made up in 40 mmol/L HCl. The three solutions were mixed at a 10:1:1 ratio (*v:v:v*). The mixture was incubated in darkness for 30 min at 37 °C and then the absorbance was determined using a UV–VIS microplate reader (FLUOstar Optima, BMG Labtech, Ortenberg, Germany) at 593 against FRAP solution as a blank. Values were expressed as Trolox equivalent ( $\mu$ g TE/mg dry extract).

#### 4.2.3. TPC of Methanolic OP Extracts

The Folin–Ciocalteu method was used to determine TPC [70]. Briefly, 25  $\mu$ L aliquots of OP1, OP2 and OP3 extracts (5 mg/mL) were incubated for 5 min with 125  $\mu$ L of 10% (*w/v*) Folin–Ciocalteu reagent. After the addition of 125  $\mu$ L of  $Na_2CO_3$  (10% *w/v*) and incubation for 30 min in darkness at room temperature, the absorbance was read using a UV–VIS microplate reader (FLUOstar Optima, BMG Labtech, Ortenberg, Germany) at 320 nm. The results were derived from a gallic acid calibration curve (0–1000  $\mu$ g/mL) prepared from a stock solution (1 mg/mL in ethanol). Values were expressed as mg of gallic acid equivalents (GAE) per gram of dried weight extract (mg of GAE/g extract).

#### 4.3. OP In Vitro Digestion and OP Aqueous Extracts

To mimic the in vitro oral, gastric and intestinal digestion of OP samples, the procedure indicated by Diab et al. [26] was followed. Briefly, 5 g of each OP batch were mixed with 25 mL SSF and 3 mL (stock 75 U/mL)  $\alpha$ -salivary amylase (from human saliva), 5.8 mL distilled  $H_2O$ , and 0.2 mL  $CaCl_2$ , and then incubated on a magnetic stirrer for 2 min at 37 °C (oral digestion). For the gastric digestion, 40 mL SGF, 7 mL pepsin (stock 25,000 U/mL), 3 mL distilled  $H_2O$ , and 0.03 mL  $CaCl_2$  were added to the oral outcome and the pH was lowered to 3.0 by HCl; the mixture was incubated for 2 h at 37 °C on a magnetic stirrer, and the pH was checked regularly. Finally, 50 mL of gastric outcome was mixed with 20 mL of pancreatin (stock 100 U/mL), 50 mL of SIF, 6 mL distilled  $H_2O$ , 10 mL bile salt (stock 10 mM), 0.024 mL  $CaCl_2$ , and 0.7 mL of 1 M HCl to neutralize the pH to 7.0 to simulate the intestinal digestion.

At the end of this process, the obtained mixture was incubated on a magnetic stirrer for 2 h at 37 °C. Then, to inactivate the enzymes used in the digestion process, the mixture was heated to 90 °C for 10 min. Eventually, the mixture was dialyzed with membrane cut-off 3.5 kDa (Spectra/Por molecular porous membrane tubing, Thermo Fisher Scientific, Milan, Italy) against 250 mL of water for 24 h at 4 °C to separate the high molecular weight (mw) fraction (>3.5 kDa, inside the dialysis membrane) from the low mw fraction (<3.5 kDa, outside the dialysis membrane). At the end of the incubation process, the solution outside the dialysis tubing (OP-W) represented the aqueous OP sample that was available for absorption (whole serum-available sample) and the solution that had not managed to diffuse through the dialysis tubing (OP-W n.a.) represented the whole non-absorbable sample (colon-available) [23]. The dialyzed digested OP-W and OP-W n.a. extracts were then lyophilized, obtaining the OP digested aqueous extracts that were further characterized for their bioactive properties.

#### 4.3.1. Radical Scavenging Activity Assays in Aqueous OP-W n.a. and OP-W Extracts

The ABTS and DPPH assays described at Section 4.2.1. were utilized to determine the radical scavenging activities of the three aqueous OP-W n.a. and OP-W (5 mg/mL) extracts.

#### 4.3.2. Ferric Reducing Antioxidant Power (FRAP) Assay in Aqueous OP-W n.a. and OP-W Extracts

The FRAP assay described at Section 4.2.2. was utilized to determine the ferric reducing antioxidant powers of the OP-W n.a. and OP-W (5 mg/mL).

#### 4.3.3. TPC in OP-W n.a., OP-W

The TPC assay described at Section 4.2.3. was utilized to evaluate the total phenolic contents in the OP-W n.a. and OP-W samples.

#### 4.3.4. HPLC-DAD Analysis of Methanolic and Aqueous OP Extracts

The analysis of phenolic compounds in methanolic and aqueous OP samples were carried out with a Jasco (Tokyo, Japan) HPLC-DAD system, consisting of a PU-4180 pump, a MD-4015 PDA detector, and an AS-4050 autosampler. An Agilent Zorbax Eclipse Plus C18 reverse-phase column (Agilent, Santa Clara, CA, USA.) (4.6 × 100 mm I.D, 3.5 µm) was used as a stationary phase. Two different methods, modified from that of Peršurić et al. [71], were applied for the separation and identification of the analytes in the mixture, both employing water adjusted to pH 2.5 with orto-phosphoric acid (Solvent A) and acetonitrile (Solvent B) as the mobile phase. For the identification and quantification of hydroxytyrosol, tyrosol, oleuropein, apigenin, luteolin, myricetin, ligstroside, and pinosresinol, the following step gradient was used: 90 to 72% A for 10 min, 72% for 15 min, 72 for 70% for 10 min, 70% for 10 min, 70 to 5% for 10 min, and kept constant for 5 min. The gradient was restored to initial conditions and kept constant for 20 min for re-equilibration. The flow rate was 0.5 mL/min, the injection volume for both reference standards and samples was 50 µL, and the detection wavelengths were set at 280 and 360 nm.

For the identification and quantification of phenolic acids (gallic, caffeic, and chlorogenic acid) a different step gradient was used: 97% A for 6 min, 97 to 85% for 11 min, 85 to 82.8% for 10 min, 82.8 to 50% for 13 min, back to initial conditions for 3 min, and constant for 13 min for re-equilibration. The injection volume was 20 µL, the flow rate was 0.7 mL/min, and the PDA wavelengths were set at 280, 329 and 360 nm.

To quantify the analytes, calibration curves were constructed for each standard by injecting six different concentrations (50 ppm, 25 ppm, 12.5 ppm, 6.25 ppm, 3.12 ppm and 1.56 ppm) in duplicate. Stock solutions of hydroxytyrosol, tyrosol, oleuropein, apigenin, luteolin, myricetin, ligstroside, and pinosresinol were prepared with DMSO/acetonitrile (20/80) mixture at a concentration of 2 mg/mL. The dilutions were then carried out with water adjusted to pH 2.5 with orto-phosphoric acid to ensure greater stability of the analytes.

Gallic acid was dissolved in water, while caffeic and chlorogenic acid were dissolved in methanol and further diluted with the mobile phase.

The bioaccessibility index was calculated as the percentage of the compound detected in the digested and lyophilized samples, with reference to the undigested sample.

#### 4.3.5. HPLC-DAD Fractioning of OP-W (OP-F)

The most bioactive OP-W extract (about 8 mg), based on its antioxidant properties, was further purified using reversed-phase high-performance chromatography on a 10-mm × 250 mm semipreparative C18 column (Supelco, Bellefonte, PA, U.S.A.), equilibrated in water and eluted at a flow rate of 2 mL/min with a discontinuous gradient of acetonitrile. In this way, seven OP-W fractions (OP-F) were obtained, and the ABTS and TCP were determined on those OP-Fs.

#### 4.3.6. LC-MS/MS Peptide Profiling of OP-W

The most bioactive OP-W extract was resuspended in 50 mM ammonium bicarbonate, pH 8.0, reduced with 10 mM DTT at 56 °C for 45 min, and alkylated with a 55 mM solution of iodoacetamide for 30 min at room temperature in the dark and then desalted by a SEP-PAK chromatography. The main fraction was manually collected and lyophilized. An aliquot of the sample was directly analyzed by LC-MS/MS for protein identification. The remaining portion of the lyophilized fraction was resuspended in 50 mM ammonium bicarbonate, pH 8.0, and incubated with trypsin in a 1/50 ratio (*w/w*) at 37 °C for 2 h. The sample was acidified with a final concentration of 0.2% trifluoroacetic acid. The peptide mixture was first concentrated and desalted by C18 zip-tip and then was lyophilized. The lyophilized fraction was resuspended in 0.2% HCOOH and analyzed by LC-MS/MS, using a 6530 Q-TOF LC/MS (Agilent) system equipped with a nano-HPLC. After loading, peptide mixtures were first concentrated and desalted on the pre-column. For protein identification, the raw data obtained from the LC-MS/MS analysis were used to search both “Olea” and “Olea Europea” protein databases by an in-house version of the Mascot software.

#### 4.3.7. Search of Potential Biological Activities and Peptide Ranking

The potential bioactivities of OP-W peptides were predicted using the open access tool PeptideRanker (accessed on 15 February 2023, <http://bioware.ucd.ie/compass/biowareweb/>) [72], a web-based tool used to predict the probability of biological activity of peptide sequences. PeptideRanker provides peptide scores in the range of 0–1. The maximum scores indicate the most active peptides, whereas the minimum scores denote the least active peptides. Here, only those peptides with a score higher than 0.6 were considered as potentially “bioactive”. Subsequently, the lists of best-ranked peptides were submitted to the web-available database BIOPEP (accessed on 15 February 2023, <http://www.uwm.edu.pl/biochemia/index.php/pl/biopep/>) which contains collected data relative to peptides with a recognized bioactivity.

#### 4.3.8. Untargeted Metabolomics of OP-F by GCMS Analysis

Due to the small quantity of each of the seven separated OP-F, only the most promising fraction (the fifth fraction), based on ABTS and TPC results, was referred to untargeted metabolomics by GCMS Analysis. GC/MS analysis was performed by a 7820A (Agilent Technologies, Santa Clara, CA, USA) with a HB-5 ms capillary column (30 m × 0.25 mm × 0.25 µm film thickness) (Agilent Technologies). The injector, ion source, quadrupole, and GC/MS interface temperature were 230, 230, 150, and 280 °C, respectively. The flow rate of helium carrier gas was kept at 1 mL/min. An amount of 1 µL of derivatized sample was injected with a 3 min solvent delay time and split ratio of 10:1. The initial column temperature was 40 °C and held for 2 min, ramped to 150 °C at a rate of 15 °C/min, and held 1 min, and then finally increased to 280 °C, at a rate of 30 °C/min, and kept at this temperature for 5 min. The ionization was carried out in the electron impact (EI) mode at 70 eV. The MS data were acquired in full scan mode from *m/z* 40–400 with an acquisition frequency of 12.8 scans

per second. Compound identification was confirmed by injection of pure standards and comparison of the retention time and corresponding EI MS spectra.

#### 4.4. Human PBMC Culture, Supplementation and RNA Extraction

Human peripheral blood mononuclear cells were isolated from fresh heparinized blood samples (20 mL) obtained from five healthy donors. Cells were separated by gradient centrifugation and then the number of live mononuclear cells, suspended in complete medium containing RPMI 1640 Medium (Thermo Fischer Scientific, Waltham, MA, USA) with 10% heat inactivated fetal bovine serum (Gibco™, Thermo Fischer Scientific, Waltham, MA, U.S.A.), 100 µg/mL streptomycin (Biochrom<sup>AG</sup>, Berlin, Germany), 2 mM L-glutamine (Euroclone<sup>®</sup>, Milan, Italy) and 100 units/mL penicillin (Biochrom<sup>AG</sup>, Berlin, Germany), was determined using a counting chamber and the Trypan blue dye exclusion procedure [70]. The final number of live cells was adjusted to  $4 \times 10^6$ /well (2 mL) and blood cells of each donor were cultured in triplicate at 37 °C in 5% CO<sub>2</sub>, supplemented or not (CTRL) with OP-W and OP-F aqueous extracts (final concentration of 2.5 µg/mL) that were previously filtered on 0.22 µm acetate cellulose filters. The aqueous extract concentrations were chosen after preliminary tests and, based on the yield obtained after dialysis (8.9%), the OP-W extract contained 0.87, 1.4, 0.3, 0.36, and 0.38 µg/mg of hydroxytyrosol, tyrosol, oleuropein, myricetin, and luteolin, respectively.

After 24 h of incubation, one half of cells/donor (CTRL, OP-W and OP-F cells/donor) was triggered (stimulated: s.) or not (n.s.) with LPS (100 ng/mL) for 2.5 h. Later, cells were transferred in Eppendorf vials (2 mL) and centrifugated ( $\times 300$  g) to separate the conditioned media for cytokine measurements. Finally, the residual cells were washed twice with phosphate-buffered saline (Gibco™, Thermo Fischer Scientific, Waltham, MA, USA) and finally stored at  $-80$  °C until RNA extraction by Mini Kit (QIAGEN GmbH, Hilden, Germany).

A NanoVue Spectrophotometer (GE Healthcare, Milano, Italy) was used to measure RNA yield and purity. Only samples with A260/A280 ratio > 1.8 were used.

#### 4.5. Analysis of mRNA Levels by Real Time Reverse Transcriptase-Polymerase Chain Reaction (Real Time RT-PCR)

To obtain cDNA, 1 µg of RNA for each sample was reverse transcribed using an iScript cDNA Synthesis Kit (Bio-Rad Laboratories, Hercules, CA, U.S.A.). The subsequent PCR was performed in a total volume of 10 µL containing 2.5 µL (12.5 ng) of cDNA, 2 µL of RNAsi free dH<sub>2</sub>O, 5 µL SsoAdvanced Universal SYBR Green Supermix (Bio-Rad Laboratories), and 0.5 µL (500 nM) of each primer. The investigated genes were IL-6, IL-10, and TNF $\alpha$ . All primers (listed in Table 10) were purchased from Sigma-Aldrich Life Science Co. LLC (USA) and were intended for human cells. The 18S gene was used as the reference gene.

**Table 10.** List of primers (Sigma-Aldrich Life Science Co. LLC., U.S.A.) utilized in the present study.

Gene	5'-Forward-3'	5'-Reverse-3'
IL-6	GCAGAAAAAGGCAAAGAATC	CTACATTGCCCGAAGAGC
IL-10	GCCTTTAATAAGCTCCAAGAG	ATCTTCATTGTCATGTAGGC
TNF- $\alpha$	AGGCAGTCAGATCATCTTC	TTATCTTCAGCTCCACG
18S	GTAACCCGTTGAACCCCAT	CCATCCAATCGGTAGTAGCC

#### 4.6. Measurement of PBMC Cytokines in Conditioned Medium

The pro- and anti-inflammatory cytokines IL-1 $\alpha$ , IL-1 $\beta$ , IL-2, IL-4, IL -5, IL-6, IL-8, IL-10, IL-12, IL-13, IL-15, IL-17, IL-23, IFN $\gamma$ , TNF- $\alpha$  and TNF- $\beta$  were estimated in the culture conditioned medium of human PBMC, by using multiplex immunoassay (Q-Plex Human Cytokine—Screen 16-plex, Quansys Biosciences, Technogenetics Srl., Milan, Italy), Q-View Imager LS, Q-View software, and following the manufacturer's instructions. The culture medium was obtained from PBMC previously cultured or not with OP-W and OP-F (2.5 µg/mL for 24 h) and then stimulated (s.) or not (n.s.) by LPS (100 ng/mL for 2.5 h).

#### 4.7. Statistical Analysis

Data relative to real time RT-PCR and cytokine concentrations were analyzed by using the two-tailed paired *t*-test, whereas one-way ANOVA with Tukey's multiple comparison test was adopted for data relative to radical scavenging activities and phenolic characterization (Prism 7, GraphPad Software Inc., San Diego, U.S.A.) considering significant differences for  $p < 0.05$ . Values were expressed as mean (S.D.) unless otherwise stated.

#### 5. Conclusions

In recent years, there has been growing interest in natural substances as possible sources of active compounds for disease prevention and/or health benefits. The greater awareness of the need to reduce environmental impact and to better exploit resources still available, has led researchers to focus their efforts on the possibility of identifying beneficial molecules for the organism from by-products of the food chain. In this context of a circular economy, the olive processing cycle could provide an example of reuse of waste products. The pomace and vegetative waters are, in fact, rich with very interesting molecules, among which are luteolin, with known anti-tumoral properties; hydroxytyrosol, having hypocholesterolemic action; and tyrosyl, ligstroside, and oleuropein.

In the present research, the phenolic composition and antioxidant activities of three batches of olive pomaces, differing by ripening state, and evaluated both before and after an *in vitro* simulation of the digestive process, revealed very different contents of phenols (hydroxytyrosol, tyrosol, oleuropein, ligstroside, pinoresinol, flavonoids, and hydroxycinnamic acids) and antioxidant properties, thus, confirming the great influence of the ripening stage and storage conditions on phenolic composition.

Although only part of ingested phenolics can pass the gut barrier, it was noteworthy that these nutraceutical compounds were still present in the digested absorbable aqueous extract of olive pomace and were able to exert an interesting anti-inflammatory activity both at transcriptional level and in the supernatants of human *ex vivo* PBMC cultures. The data here presented were in line with the *in vivo* repression of several pro-inflammatory genes observed in the only other work found in the literature that used PBMC cells from patients with metabolic syndrome [14].

However, further studies are necessary to determine the cause of the lower anti-inflammatory response obtained with OP-F, compared with the OP-W sample. Indeed, it could be connected to a higher bioactivity orchestrated by the entire phyto complex (synergistic effect) present in the OP-W sample, probably able to involve different pathways/mechanisms, or conversely, to an excessively high dose of tyrosol in OP-F. Nature and/or evolution could have determined the fast ability to metabolize and eliminate the excessive ingestion of phenols just to reduce deleterious effects when too concentrated in circulation.

The *in vitro* experiments represent a consistent approach to evaluating the health effect of new functional ingredients, but despite the inherent "défaillance" in *in vitro* simulation of digestion which is a rather complex physiological process, we believe that compounds under *in vitro* testing should always undergo a preventive *in vitro* digestion before their evaluation in cell cultures. Undoubtedly, the *in vitro* digestion represents one of the experimental approaches to encompass the open questions of bioavailability and metabolism food bioactives, particularly of phenols.

In the present research, however, it was not considered whether, and to what extent, the microbiota could affect digestion and bioavailability of the not absorbable olive pomace extract which, therefore, could also contribute to the increased bioavailability of bioactive compounds.

Furthermore, in the digested and absorbable sample used for cell testing, potentially bioactive peptides were also identified. Those resulting peptides have not yet been described, and they will be further investigated together with the characterization of polysaccharides and minerals, which are also potentially bioactive.

In the future, we would like to evaluate the potential immunomodulatory activity of these aqueous extracts, and, for this purpose, we believe that PBMCs taken from patients with autoimmune diseases could represent a consistent *ex vivo* model that could provide interesting outcomes.

The results herein reported clearly evidence the anti-inflammatory effect of digested aqueous OP extract and pave the way to an exploitation of the olive pomace by-product as a functional ingredient or as a nutraceutical.

**Author Contributions:** All authors contributed to this work significantly. Conceptualization, D.B., F.A. and G.L.; methodology, M.L., D.B., L.L., C.A. (Claudio Alimenti), F.A., L.G., G.L. and O.B.; software, C.A. (Claudio Alimenti), L.G.), F.A.; validation, C.A. (Claudio Alimenti), L.G. and F.A.; formal analysis, M.L., C.A. (Claudio Alimenti), D.B., G.L. and O.B.; resources, D.B. and L.L.; data curation, C.A. (Claudio Alimenti), L.G., M.L., F.A. and D.B.; writing—original draft preparation, D.B., M.L., F.A.; writing—review and editing, L.G., C.A. (Cristina Angeloni), L.L. and G.L. All authors have read and agreed to the published version of the manuscript.

**Funding:** This research was partially funded by P.O. Fesr Sicilia 2014/2020. OT1—Specific Objective 1.1—Action 1.1.5—BIOTRAK Project. Grant number 08SR1091000150-CUP G69J18001000007.

**Institutional Review Board Statement:** The study was approved by the local ethical committee (CEAS) in accordance with the Declaration of Helsinki (study registration number 2050/12).

**Informed Consent Statement:** Informed consent was obtained from all subjects involved in the study.

**Data Availability Statement:** Data supporting the results of this study are available from authors and are available on request.

**Acknowledgments:** The authors wish to thank Feed Manufacturing Industry Dipasquale Srl. (Avola, SR, IT) and Oil Mill Industry Consoli (Adrano, Catania, IT) for providing the olive pomace batches.

**Conflicts of Interest:** The authors declare no conflict of interest. The funding sponsors had no role in the design of the study; in the collection, analysis, or interpretation of data; in the writing of the manuscript, and in the decision to publish the results.

## References

1. Kaza, S.; Yao, L.; Bhada-Tata, P.; Van Woerden, F.; Lonkova, K.; Morton, J.; Poveda, R.A.; Sarraf, M.; Malkawi, F.; Harinath, A.S.; et al. *What a Waste 2.0: A Global Snapshot of Solid Waste Management to 2050*; Urban Development Series; World Bank Group: Washington, DC, USA, 2018; ISBN 978-1-4648-1347-4.
2. Tapia-Quirós, P.; Montenegro-Landívar, M.F.; Reig, M.; Vecino, X.; Cortina, J.L.; Saurina, J.; Granados, M. Recovery of Polyphenols from Agri-Food By-Products: The Olive Oil and Winery Industries Cases. *Foods* **2022**, *11*, 362. [[CrossRef](#)] [[PubMed](#)]
3. Fava, F.; Zanolari, G.; Vannini, L.; Guerzoni, E.; Bordoni, A.; Viaggi, D.; Robertson, J.; Waldron, K.; Bald, C.; Esturo, A.; et al. New Advances in the Integrated Management of Food Processing By-Products in Europe: Sustainable Exploitation of Fruit and Cereal Processing by-Products with the Production of New Food Products (NAMASTE EU). *New Biotechnol.* **2013**, *30*, 647–655. [[CrossRef](#)] [[PubMed](#)]
4. Difonzo, G.; Gennaro, G.; Pasqualone, A.; Caponio, F. Potential Use of Plant-based By-products and Waste to Improve the Quality of Gluten-free Foods. *J. Sci. Food Agric.* **2022**, *102*, 2199–2211. [[CrossRef](#)] [[PubMed](#)]
5. Malekjani, N.; Jafari, S.M. Valorization of Olive Processing By-Products via Drying Technologies: A Case Study on the Recovery of Bioactive Phenolic Compounds from Olive Leaves, Pomace, and Wastewater. *Crit. Rev. Food Sci. Nutr.* **2022**, *1–19*. [[CrossRef](#)]
6. Baniias, G.; Achillas, C.; Vlachokostas, C.; Moussiopoulos, N.; Stefanou, M. Environmental Impacts in the Life Cycle of Olive Oil: A Literature Review: Environmental Impacts in the Life Cycle of Olive Oil. *J. Sci. Food Agric.* **2017**, *97*, 1686–1697. [[CrossRef](#)] [[PubMed](#)]
7. Mallamaci, R.; Budriesi, R.; Clodoveo, M.L.; Biotti, G.; Micucci, M.; Ragusa, A.; Curci, F.; Muraglia, M.; Corbo, F.; Franchini, C. Olive Tree in Circular Economy as a Source of Secondary Metabolites Active for Human and Animal Health Beyond Oxidative Stress and Inflammation. *Molecules* **2021**, *26*, 1072. [[CrossRef](#)] [[PubMed](#)]
8. Barbalace, M.C.; Zallocco, L.; Beghelli, D.; Ronci, M.; Scortichini, S.; Digiaco, M.; Macchia, M.; Mazzoni, M.R.; Fiorini, D.; Lucacchini, A.; et al. Antioxidant and Neuroprotective Activity of Extra Virgin Olive Oil Extracts Obtained from Quercetano Cultivar Trees Grown in Different Areas of the Tuscany Region (Italy). *Antioxidants* **2021**, *10*, 421. [[CrossRef](#)]
9. Cicerale, S.; Lucas, L.; Keast, R. Antimicrobial, Antioxidant and Anti-Inflammatory Phenolic Activities in Extra Virgin Olive Oil. *Curr. Opin. Biotechnol.* **2012**, *23*, 129–135. [[CrossRef](#)]
10. Marcelino, G.; Hiane, P.A.; Freitas, K.d.C.; Santana, L.F.; Pott, A.; Donadon, J.R.; de Cássia Avellaneda, G.R. Effects of Olive Oil and Its Minor Components on Cardiovascular Diseases, Inflammation, and Gut Microbiota. *Nutrients* **2019**, *11*, 1826. [[CrossRef](#)]



11. Bassani, B.; Rossi, T.; De Stefano, D.; Pizzichini, D.; Corradino, P.; Macrì, N.; Noonan, D.M.; Albin, A.; Bruno, A. Potential Chemopreventive Activities of a Polyphenol Rich Purified Extract from Olive Mill Wastewater on Colon Cancer Cells. *J. Funct. Foods* **2016**, *27*, 236–248. [\[CrossRef\]](#)
12. Omar, S.; Scott, C.; Hamlin, A.; Obied, H. Olive Biophenols Reduces Alzheimer’s Pathology in SH-SY5Y Cells and APP<sup>swe</sup> Mice. *Int. J. Mol. Sci.* **2018**, *20*, 125. [\[CrossRef\]](#) [\[PubMed\]](#)
13. Guasch-Ferré, M.; Hruby, A.; Salas-Salvadó, J.; Martínez-González, M.A.; Sun, Q.; Willett, W.C.; Hu, F.B. Olive Oil Consumption and Risk of Type 2 Diabetes in US Women. *Am. J. Clin. Nutr.* **2015**, *102*, 479–486. [\[CrossRef\]](#) [\[PubMed\]](#)
14. Camargo, A.; Ruano, J.; Fernandez, J.M.; Parnell, L.D.; Jimenez, A.; Santos-Gonzalez, M.; Marin, C.; Perez-Martinez, P.; Uceda, M.; Lopez-Miranda, J.; et al. Gene Expression Changes in Mononuclear Cells in Patients with Metabolic Syndrome after Acute Intake of Phenol-Rich Virgin Olive Oil. *BMC Genom.* **2010**, *11*, 253. [\[CrossRef\]](#) [\[PubMed\]](#)
15. Corona, G.; Spencer, J.; Dessì, M. Extra Virgin Olive Oil Phenolics: Absorption, Metabolism, and Biological Activities in the GI Tract. *Toxicol. Ind. Health* **2009**, *25*, 285–293. [\[CrossRef\]](#) [\[PubMed\]](#)
16. Castrogiovanni, P.; Trovato, F.; Loreto, C.; Nsir, H.; Szychlińska, M.; Musumeci, G. Nutraceutical Supplements in the Management and Prevention of Osteoarthritis. *Int. J. Mol. Sci.* **2016**, *17*, 2042. [\[CrossRef\]](#) [\[PubMed\]](#)
17. Recinella, L.; Chiavaroli, A.; Orlando, G.; Menghini, L.; Ferrante, C.; Di Cesare Mannelli, L.; Ghelardini, C.; Brunetti, L.; Leone, S. Protective Effects Induced by Two Polyphenolic Liquid Complexes from Olive (*Olea Europaea*, Mainly Cultivar Coratina) Pressing Juice in Rat Isolated Tissues Challenged with LPS. *Molecules* **2019**, *24*, 3002. [\[CrossRef\]](#)
18. Markhali, F.S.; Teixeira, J.A.; Rocha, C.M.R. Olive Tree Leaves—A Source of Valuable Active Compounds. *Processes* **2020**, *8*, 1177. [\[CrossRef\]](#)
19. Žugčić, T.; Abdelkebir, R.; Alcantara, C.; Collado, M.C.; García-Pérez, J.V.; Meléndez-Martínez, A.J.; Režek Jambrak, A.; Lorenzo, J.M.; Barba, F.J. From Extraction of Valuable Compounds to Health Promoting Benefits of Olive Leaves through Bioaccessibility, Bioavailability and Impact on Gut Microbiota. *Trends Food Sci. Technol.* **2019**, *83*, 63–77. [\[CrossRef\]](#)
20. Leouifoudi, I.; Harnafi, H.; Ziyad, A. Olive Mill Waste Extracts: Polyphenols Content, Antioxidant, and Antimicrobial Activities. *Adv. Pharmacol. Sci.* **2015**, *2015*, 1–11. [\[CrossRef\]](#)
21. Barbaro, B.; Toietta, G.; Maggio, R.; Arciello, M.; Tarocchi, M.; Galli, A.; Balsano, C. Effects of the Olive-Derived Polyphenol European on Human Health. *Int. J. Mol. Sci.* **2014**, *15*, 18508–18524. [\[CrossRef\]](#)
22. Antónia Nunes, M.; Costa, A.S.G.; Bessada, S.; Santos, J.; Puga, H.; Alves, R.C.; Freitas, V.; Oliveira, M.B.P.P. Olive Pomace as a Valuable Source of Bioactive Compounds: A Study Regarding Its Lipid- and Water-Soluble Components. *Sci. Total Environ.* **2018**, *644*, 229–236. [\[CrossRef\]](#) [\[PubMed\]](#)
23. Ribeiro, T.B.; Oliveira, A.; Campos, D.; Nunes, J.; Vicente, A.A.; Pintado, M. Simulated Digestion of an Olive Pomace Water-Soluble Ingredient: Relationship between the Bioaccessibility of Compounds and Their Potential Health Benefits. *Food Funct.* **2020**, *11*, 2238–2254. [\[CrossRef\]](#) [\[PubMed\]](#)
24. Di Nunzio, M.; Picone, G.; Pasini, F.; Caboni, M.F.; Gianotti, A.; Bordoni, A.; Capozzi, F. Olive Oil Industry By-Products. Effects of a Polyphenol-Rich Extract on the Metabolome and Response to Inflammation in Cultured Intestinal Cell. *Food Res. Int.* **2018**, *113*, 392–400. [\[CrossRef\]](#) [\[PubMed\]](#)
25. Gullón, P.; Gullón, B.; Astray, G.; Carpena, M.; Fraga-Corral, M.; Prieto, M.A.; Simal-Gandara, J. Valorization of By-Products from Olive Oil Industry and Added-Value Applications for Innovative Functional Foods. *Food Res. Int.* **2020**, *137*, 109683. [\[CrossRef\]](#) [\[PubMed\]](#)
26. Diab, F.; Khalil, M.; Lupidi, G.; Zbeeb, H.; Salis, A.; Damonte, G.; Bramucci, M.; Portincasa, P.; Vergani, L. Influence of Simulated In Vitro Gastrointestinal Digestion on the Phenolic Profile, Antioxidant, and Biological Activity of *Thymbra spicata* L. Extracts. *Antioxidants* **2022**, *11*, 1778. [\[CrossRef\]](#)
27. Gómez-Lama Cabanás, C.; Legarda, G.; Ruano-Rosa, D.; Pizarro-Tobías, P.; Valverde-Corredor, A.; Niqui, J.L.; Triviño, J.C.; Roca, A.; Mercado-Blanco, J. Indigenous *Pseudomonas* Spp. Strains from the Olive (*Olea Europaea* L.) Rhizosphere as Effective Biocontrol Agents against *Verticillium Dahliae*: From the Host Roots to the Bacterial Genomes. *Front. Microbiol.* **2018**, *9*, 277. [\[CrossRef\]](#)
28. Bartolomei, M.; Capriotti, A.L.; Li, Y.; Bollati, C.; Li, J.; Cerrato, A.; Cecchi, L.; Pugliese, R.; Bellumori, M.; Mulinacci, N.; et al. Exploitation of Olive (*Olea Europaea* L.) Seed Proteins as Upgraded Source of Bioactive Peptides with Multifunctional Properties: Focus on Antioxidant and Dipeptidyl-Dipeptidase—IV Inhibitory Activities, and Glucagon-like Peptide 1 Improved Modulation. *Antioxidants* **2022**, *11*, 1730. [\[CrossRef\]](#)
29. Aiello, G.; Lammi, C.; Boschin, G.; Zanon, C.; Arnoldi, A. Exploration of Potentially Bioactive Peptides Generated from the Enzymatic Hydrolysis of Hempseed Proteins. *J. Agric. Food Chem.* **2017**, *65*, 10174–10184. [\[CrossRef\]](#)
30. Baj, A.; Moro, E.; Bistoletti, M.; Orlandi, V.; Crema, F.; Giaroni, C. Glutamatergic Signaling Along The Microbiota-Gut-Brain Axis. *Int. J. Mol. Sci.* **2019**, *20*, 1482. [\[CrossRef\]](#)
31. Tomé, D. The Roles of Dietary Glutamate in the Intestine. *Ann. Nutr. Metab.* **2018**, *73*, 15–20. [\[CrossRef\]](#)
32. Araújo, M.; Pimentel, F.B.; Alves, R.C.; Oliveira, M.B.P.P. Phenolic Compounds from Olive Mill Wastes: Health Effects, Analytical Approach and Application as Food Antioxidants. *Trends Food Sci. Technol.* **2015**, *45*, 200–211. [\[CrossRef\]](#)
33. Peralbo-Molina, A.; Priego-Capote, F.; Luque de Castro, M.D. Tentative Identification of Phenolic Compounds in Olive Pomace Extracts Using Liquid Chromatography–Tandem Mass Spectrometry with a Quadrupole–Quadrupole–Time-of-Flight Mass Detector. *J. Agric. Food Chem.* **2012**, *60*, 11542–11550. [\[CrossRef\]](#)

34. Páscoa, R.N.M.J.; Nunes, M.A.; Reszczyński, F.; Costa, A.S.G.; Oliveira, M.B.P.P.; Alves, R.C. Near Infrared (NIR) Spectroscopy as a Tool to Assess Blends Composition and Discriminate Antioxidant Activity of Olive Pomace Cultivars. *Waste Biomass Valor* **2021**, *12*, 4901–4913. [[CrossRef](#)]
35. Ryan, D.; Prenzler, P.D.; Lavee, S.; Antolovich, M.; Robards, K. Quantitative Changes in Phenolic Content during Physiological Development of the Olive (*Olea Europaea*) Cultivar Hardy's Mammoth. *J. Agric. Food Chem.* **2003**, *51*, 2532–2538. [[CrossRef](#)] [[PubMed](#)]
36. Nunes, M.A.; Palmeira, J.D.; Melo, D.; Machado, S.; Lobo, J.C.; Costa, A.S.G.; Alves, R.C.; Ferreira, H.; Oliveira, M.B.P.P. Chemical Composition and Antimicrobial Activity of a New Olive Pomace Functional Ingredient. *Pharmaceuticals* **2021**, *14*, 913. [[CrossRef](#)] [[PubMed](#)]
37. Lesage-Meessen, L.; Navarro, D.; Maunier, S.; Sigoillot, J.-C.; Lorquin, J.; Delattre, M.; Simon, J.-L.; Asther, M.; Labat, M. Simple Phenolic Content in Olive Oil Residues as a Function of Extraction Systems. *Food Chem.* **2001**, *75*, 501–507. [[CrossRef](#)]
38. Navajas-Porras, B.; Pérez-Burillo, S.; Morales-Pérez, J.; Rufián-Henares, J.A.; Pastoriza, S. Relationship of Quality Parameters, Antioxidant Capacity and Total Phenolic Content of EVOO with Ripening State and Olive Variety. *Food Chem.* **2020**, *325*, 126926. [[CrossRef](#)]
39. Visioli, F.; Poli, A.; Gall, C. Antioxidant and Other Biological Activities of Phenols from Olives and Olive Oil. *Med. Res. Rev.* **2002**, *22*, 65–75. [[CrossRef](#)]
40. Bayram, B.; Ozelcik, B.; Grimm, S.; Roeder, T.; Schrader, C.; Ernst, I.M.A.; Wagner, A.E.; Grune, T.; Frank, J.; Rimbach, G. A Diet Rich in Olive Oil Phenolics Reduces Oxidative Stress in the Heart of SAMP8 Mice by Induction of Nrf2-Dependent Gene Expression. *Rejuvenation Res.* **2012**, *15*, 71–81. [[CrossRef](#)]
41. Torres de Pinedo, A.; Peñalver, P.; Morales, J.C. Synthesis and Evaluation of New Phenolic-Based Antioxidants: Structure–Activity Relationship. *Food Chem.* **2007**, *103*, 55–61. [[CrossRef](#)]
42. Haris Omar, S. Oleuropein in Olive and Its Pharmacological Effects. *Sci. Pharm.* **2010**, *78*, 133–154. [[CrossRef](#)]
43. Zhao, G.; Yao-Yue, C.; Qin, G.-W.; Guo, L.-H. Luteolin from Purple Perilla Mitigates ROS Insult Particularly in Primary Neurons. *Neurobiol. Aging* **2012**, *33*, 176–186. [[CrossRef](#)]
44. de Bock, M.; Thorstensen, E.B.; Derraik, J.G.B.; Henderson, H.V.; Hofman, P.L.; Cutfield, W.S. Human Absorption and Metabolism of Oleuropein and Hydroxytyrosol Ingested as Olive (*Olea Europaea* L.) Leaf Extract. *Mol. Nutr. Food Res.* **2013**, *57*, 2079–2085. [[CrossRef](#)] [[PubMed](#)]
45. Ahmad-Qasem, M.H.; Barrajón-Catalán, E.; Micol, V.; Mulet, A.; García-Pérez, J.V. Influence of Freezing and Dehydration of Olive Leaves (Var. Serrana) on Extract Composition and Antioxidant Potential. *Food Res. Int.* **2013**, *50*, 189–196. [[CrossRef](#)]
46. Nikou, T.; Sakavitsi, M.E.; Kalampokis, E.; Halabalaki, M. Metabolism and Bioavailability of Olive Bioactive Constituents Based on In Vitro, In Vivo and Human Studies. *Nutrients* **2022**, *14*, 3773. [[CrossRef](#)] [[PubMed](#)]
47. Galmés, S.; Reynés, B.; Palou, M.; Palou-March, A.; Palou, A. Absorption, Distribution, Metabolism, and Excretion of the Main Olive Tree Phenols and Polyphenols: A Literature Review. *J. Agric. Food Chem.* **2021**, *69*, 5281–5296. [[CrossRef](#)]
48. Bender, C.; Strassmann, S.; Golz, C. Oral Bioavailability and Metabolism of Hydroxytyrosol from Food Supplements. *Nutrients* **2023**, *15*, 325. [[CrossRef](#)]
49. Mechi, D.; Baccouri, B.; Martín-Vertedor, D.; Abaza, L. Bioavailability of Phenolic Compounds in Californian-Style Table Olives with Tunisian Aqueous Olive Leaf Extracts. *Molecules* **2023**, *28*, 707. [[CrossRef](#)]
50. Domínguez-Perles, R.; Auñón, D.; Ferreres, F.; Gil-Izquierdo, A. Gender Differences in Plasma and Urine Metabolites from Sprague–Dawley Rats after Oral Administration of Normal and High Doses of Hydroxytyrosol, Hydroxytyrosol Acetate, and DOPAC. *Eur. J. Nutr.* **2017**, *56*, 215–224. [[CrossRef](#)]
51. Sakavitsi, M.E.; Breyneart, A.; Nikou, T.; Lauwers, S.; Pieters, L.; Hermans, N.; Halabalaki, M. Availability and Metabolic Fate of Olive Phenolic Alcohols Hydroxytyrosol and Tyrosol in the Human GI Tract Simulated by the In Vitro GIDM–Colon Model. *Metabolites* **2022**, *12*, 391. [[CrossRef](#)]
52. Alemán-Jiménez, C.; Domínguez-Perles, R.; Medina, S.; Prgomet, I.; López-González, I.; Simonelli-Muñoz, A.; Campillo-Cano, M.; Auñón, D.; Ferreres, F.; Gil-Izquierdo, Á. Pharmacokinetics and Bioavailability of Hydroxytyrosol Are Dependent on the Food Matrix in Humans. *Eur. J. Nutr.* **2021**, *60*, 905–915. [[CrossRef](#)] [[PubMed](#)]
53. Kountouri, A.M.; Mylona, A.; Kaliora, A.C.; Andrikopoulos, N.K. Bioavailability of the Phenolic Compounds of the Fruits (Drupes) of *Olea Europaea* (Olives): Impact on Plasma Antioxidant Status in Humans. *Phytomedicine* **2007**, *14*, 659–667. [[CrossRef](#)] [[PubMed](#)]
54. Seiquer, I.; Rueda, A.; Olalla, M.; Cabrera-Vique, C. Assessing the Bioavailability of Polyphenols and Antioxidant Properties of Extra Virgin Argan Oil by Simulated Digestion and Caco-2 Cell Assays. Comparative Study with Extra Virgin Olive Oil. *Food Chem.* **2015**, *188*, 496–503. [[CrossRef](#)] [[PubMed](#)]
55. Nørskov, N.P.; Hedemann, M.S.; Lærke, H.N.; Knudsen, K.E.B. Multicompartmental Nontargeted LC–MS Metabolomics: Explorative Study on the Metabolic Responses of Rye Fiber versus Refined Wheat Fiber Intake in Plasma and Urine of Hypercholesterolemic Pigs. *J. Proteome Res.* **2013**, *12*, 2818–2832. [[CrossRef](#)] [[PubMed](#)]
56. Karković Marković, A.; Torić, J.; Barbarić, M.; Jakobušić Brala, C. Hydroxytyrosol, Tyrosol and Derivatives and Their Potential Effects on Human Health. *Molecules* **2019**, *24*, 2001. [[CrossRef](#)] [[PubMed](#)]
57. Bucciantini, M.; Leri, M.; Nardiello, P.; Casamenti, F.; Stefani, M. Olive Polyphenols: Antioxidant and Anti-Inflammatory Properties. *Antioxidants* **2021**, *10*, 1044. [[CrossRef](#)] [[PubMed](#)]

58. Gilmore, T.D. Introduction to NF- $\kappa$ B: Players, Pathways, Perspectives. *Oncogene* **2006**, *25*, 6680–6684. [[CrossRef](#)]
59. Kim, E.K.; Choi, E.-J. Pathological Roles of MAPK Signaling Pathways in Human Diseases. *Biochim. Et Biophys. Acta (BBA) Mol. Basis Dis.* **2010**, *1802*, 396–405. [[CrossRef](#)]
60. Wang, W.; Xia, Y.; Yang, B.; Su, X.; Chen, J.; Li, W.; Jiang, T. Protective Effects of Tyrosol against LPS-Induced Acute Lung Injury via Inhibiting NF- $\kappa$ B and AP-1 Activation and Activating the HO-1/Nrf2 Pathways. *Biol. Pharm. Bull.* **2017**, *40*, 583–593. [[CrossRef](#)]
61. Martín-Peláez, S.; Castañer, O.; Solà, R.; Motilva, M.; Castell, M.; Pérez-Cano, F.; Fitó, M. Influence of Phenol-Enriched Olive Oils on Human Intestinal Immune Function. *Nutrients* **2016**, *8*, 213. [[CrossRef](#)]
62. Bouayed, J.; Bohn, T. Exogenous Antioxidants—Double-Edged Swords in Cellular Redox State: Health Beneficial Effects at Physiologic Doses versus Deleterious Effects at High Doses. *Oxidative Med. Cell. Longev.* **2010**, *3*, 228–237. [[CrossRef](#)] [[PubMed](#)]
63. Cea Pavez, I.; Lozano-Sánchez, J.; Borrás-Linares, I.; Nuñez, H.; Robert, P.; Segura-Carretero, A. Obtaining an Extract Rich in Phenolic Compounds from Olive Pomace by Pressurized Liquid Extraction. *Molecules* **2019**, *24*, 3108. [[CrossRef](#)]
64. Chanioti, S.; Tzia, C. Extraction of Phenolic Compounds from Olive Pomace by Using Natural Deep Eutectic Solvents and Innovative Extraction Techniques. *Innov. Food Sci. Emerg. Technol.* **2018**, *48*, 228–239. [[CrossRef](#)]
65. Bionda, A.; Lopreiato, V.; Crepaldi, P.; Chiofalo, V.; Fazio, E.; Oteri, M.; Amato, A.; Liotta, L. Diet Supplemented with Olive Cake as a Model of Circular Economy: Metabolic and Endocrine Responses of Beef Cattle. *Front. Sustain. Food Syst.* **2022**, *6*, 1077363. [[CrossRef](#)]
66. Chiofalo, B.; Di Rosa, A.R.; Lo Presti, V.; Chiofalo, V.; Liotta, L. Effect of Supplementation of Herd Diet with Olive Cake on the Composition Profile of Milk and on the Composition, Quality and Sensory Profile of Cheeses Made Therefrom. *Animals* **2020**, *10*, 977. [[CrossRef](#)] [[PubMed](#)]
67. Srinivasan, R.; Chandrasekar, M.J.N.; Nanjan, M.J.; Suresh, B. Antioxidant Activity of Caesalpinia Digyna Root. *J. Ethnopharmacol.* **2007**, *113*, 284–291. [[CrossRef](#)] [[PubMed](#)]
68. Re, R.; Pellegrini, N.; Proteggente, A.; Pannala, A.; Yang, M.; Rice-Evans, C. Antioxidant Activity Applying an Improved ABTS Radical Cation Decolorization Assay. *Free Radic. Biol. Med.* **1999**, *26*, 1231–1237. [[CrossRef](#)] [[PubMed](#)]
69. Firuzi, O.; Lacanna, A.; Petrucci, R.; Marrosu, G.; Saso, L. Evaluation of the Antioxidant Activity of Flavonoids by “Ferric Reducing Antioxidant Power” Assay and Cyclic Voltammetry. *Biochim. Et Biophys. Acta (BBA) Gen. Subj.* **2005**, *1721*, 174–184. [[CrossRef](#)] [[PubMed](#)]
70. Nkuimi Wandjou, J.G.; Lancioni, L.; Barbalace, M.C.; Hrelia, S.; Papa, F.; Sagratini, G.; Vittori, S.; Dall’Acqua, S.; Caprioli, G.; Beghelli, D.; et al. Comprehensive Characterization of Phytochemicals and Biological Activities of the Italian Ancient Apple ‘Mela Rosa Dei Monti Sibillini’. *Food Res. Int.* **2020**, *137*, 109422. [[CrossRef](#)]
71. Peršurić, Ž.; Saftić Martinović, L.; Zengin, G.; Šarolić, M.; Kraljević Pavelić, S. Characterization of Phenolic and Triacylglycerol Compounds in the Olive Oil By-Product Pâté and Assay of Its Antioxidant and Enzyme Inhibition Activity. *LWT* **2020**, *125*, 109225. [[CrossRef](#)]
72. Mooney, C.; Haslam, N.J.; Pollastri, G.; Shields, D.C. Towards the Improved Discovery and Design of Functional Peptides: Common Features of Diverse Classes Permit Generalized Prediction of Bioactivity. *PLoS ONE* **2012**, *7*, e45012. [[CrossRef](#)] [[PubMed](#)]

**Disclaimer/Publisher’s Note:** The statements, opinions and data contained in all publications are solely those of the individual author(s) and contributor(s) and not of MDPI and/or the editor(s). MDPI and/or the editor(s) disclaim responsibility for any injury to people or property resulting from any ideas, methods, instructions or products referred to in the content.

Article

# Comparative Methods to Evaluate the Antioxidant Capacity of Propolis: An Attempt to Explain the Differences

Vanessa B. Paula <sup>1,2,\*</sup>, Leticia M. Estevinho <sup>2,3</sup>, Susana M. Cardoso <sup>4</sup> and Luís G. Dias <sup>2,3</sup><sup>1</sup> Doctoral School, University of León (ULE), Campus de Vegazana, 24007 León, Spain<sup>2</sup> Centro de Investigação de Montanha (CIMO), Instituto Politécnico de Bragança, 5300-252 Bragança, Portugal; leticia@ipb.pt (L.M.E.); ldias@ipb.pt (L.G.D.)<sup>3</sup> Laboratório Associado para a Sustentabilidade e Tecnologia em Regiões de Montanha (SusTEC), Instituto Politécnico de Bragança, Campus de Santa Apolónia, 5300-253 Bragança, Portugal<sup>4</sup> Associated Laboratory for Green Chemistry of the Network of Chemistry and Technology LAQV-REQUIMTE, Department of Chemistry, University of Aveiro, 3810-193 Aveiro, Portugal; susanacardoso@ua.pt

\* Correspondence: vanessapaula@ipb.pt

**Abstract:** Propolis is a natural product produced by bees that contains a complex mixture of compounds, including phenolic compounds and flavonoids. These compounds contribute to its biological activities, such as antioxidant capacity. This study analysed the pollen profile, total phenolic content (TPC), antioxidant properties, and phenolic compound profile of four propolis samples from Portugal. The total phenolic compounds in the samples were determined by six different techniques: four different Folin–Ciocalteu (F-C) methods, spectrophotometry (SPECT), and voltammetry (SWV). Of the six methods, SPECT allowed the highest quantification, while SWV achieved the lowest. The mean TPC values for these methods were  $422 \pm 98$  and  $47 \pm 11$  mg GAE/g sample, respectively. Antioxidant capacity was determined by four different methods: DPPH, FRAP, original ferrocyanide (OFec), and modified ferrocyanide (MFec). The MFec method gave the highest antioxidant capacity for all samples, followed by the DPPH method. The study also investigated the correlation between TPC and antioxidant capacity with the presence of hydroxybenzoic acid (HBA), hydroxycinnamic acid (HCA), and flavonoids (FLAV) in propolis samples. The results showed that the concentrations of specific compounds in propolis samples can significantly impact their antioxidant capacity and TPC quantification. Analysis of the profile of phenolic compounds by the UHPLC-DAD-ESI-MS technique identified chrysin, caffeic acid isoprenyl ester, pinocembrin, galangin, pinobanksin-3-*O*-acetate, and caffeic acid phenyl ester as the major compounds in the four propolis samples. In conclusion, this study shows the importance of the choice of method for determining TPC and antioxidant activity in samples and the contribution of HBA and HCA content to their quantification.

**Keywords:** propolis; total phenolic compounds; antioxidant capacity; UHPLC-DAD-ESI-MS

**Citation:** Paula, V.B.; Estevinho, L.M.; Cardoso, S.M.; Dias, L.G. Comparative Methods to Evaluate the Antioxidant Capacity of Propolis: An Attempt to Explain the Differences. *Molecules* **2023**, *28*, 4847. <https://doi.org/10.3390/molecules28124847>

Academic Editor: Armando Zarrelli

Received: 30 April 2023

Revised: 7 June 2023

Accepted: 13 June 2023

Published: 19 June 2023



**Copyright:** © 2023 by the authors. Licensee MDPI, Basel, Switzerland. This article is an open access article distributed under the terms and conditions of the Creative Commons Attribution (CC BY) license (<https://creativecommons.org/licenses/by/4.0/>).

## 1. Introduction

Propolis is a natural mixture of resin from trees or shrubs, buds, leaves, bark, and plant exudates collected by bees, *Apis mellifera* L., to which they add small amounts of secretions from their salivary glands [1,2]. Its composition contains a complex mixture of compounds, including phenolic compounds (hydroxybenzoic and hydroxycinnamic acids) and flavonoids [3,4], which are believed to contribute to its biological activities, such as antibacterial [5], anti-inflammatory [5,6], antitumor [5,7], cytotoxic [8], and antioxidant activities [5], among others.

The determination of TPC is important for the evaluation of antioxidant activities, since studies have shown that there is a direct correlation between antioxidant capacity and the content of total phenolic compounds [9,10].

The most commonly used spectroscopic techniques for the determination of total phenolic content (TPC) are Fourier transform infrared spectroscopy (FT-IR), Raman spec-

troscopy, and the Folin–Ciocalteu (F-C) assay using UV–Vis spectroscopy [11,12]. The F-C method is an easy and economical technique for the measurement of total phenolic compounds and is suitable for routine laboratory use [13]. This colorimetric method requires the use of a reference substance (e.g., gallic acid) to measure the total concentration of phenolic hydroxyl groups in the plant extract [14]. The F-C technique is based on the reaction of phenolic compounds with the F-C reagent which, in the presence of sodium carbonate, forms a blue complex whose intensity is related to the concentration of phenols present in the sample [12,14,15]. In the F-C method, the reagents are prepared in water or polar organic solvents, which only allows the determination of hydrophilic phenols in a sample [13].

The determination of antioxidant capacity uses spectroscopic techniques such as the diphenyl-2-picrylhydrazyl (DPPH) assay, the chemiluminescence assay, the Trolox equivalent antioxidant capacity, the ferric-reducing power antioxidant assay (FRAP), and electron spin resonance (ESPR) [16]. The DPPH method only allows the determination of hydrophobic antioxidants, while FRAP is based on the reduction of transition metal ions, iron, and copper [9].

Alternatives to traditional methods for determining the TPC and antioxidant properties of phenolic compounds are electrochemical methods [3,17]. Cyclic voltammetry (CV), differential pulse voltammetry (DPV), and square wave voltammetry (SWV) techniques have been successfully used to detect phenolic compounds (phenolic acids and flavonoids) in a variety of aqueous and non-aqueous solutions [3,18]. The advantage of electrochemical techniques is that they allow rapid, simple, and inexpensive determinations and, in some cases, allow measurements in the presence of colouring or masking compounds that may interfere with measurements made by other techniques, e.g., spectrophotometry [19,20].

Several analytical methods can be used to characterise and identify the phenols present in propolis. Techniques such as high-performance liquid chromatography (HPLC) [21], capillary electrophoresis (CE) [22], chemiluminescence (CL) [23], ultra-high-resolution liquid chromatography–tandem mass spectrometry (UHPLC-MS/MS) [24], liquid chromatography coupled to mass spectrometry (LC-MS-MS) [25,26], and gas chromatography–mass spectrometry (GC-MS) [26,27] can be used. However, the most widely used is ultra-high-performance liquid chromatography coupled to triple quadrupole mass spectrometry (UHPLC-QqQ-MS/MS) due to its high sensitivity, selectivity, and high throughput [28]. The phenolic compounds detected in propolis samples were hydroxybenzoic acids (HBAs) and hydroxycinnamic acids (HCAs), as well as protocatechic, gentiic, p-coumaric, ferulic, and caffeic acids [3,29]. Flavonoid aglycones of flavones, flavonols, flavonones, and chalcones are also present in propolis extracts, including pinobanksin, quercetin, apigenin, t-cinnamic acid, luteolin, chrysin, pinocembrin, galangin, kaempferol, and pinostrobin [3,30].

The aims of this work were to study the profile of phenolic compounds of four ethanolic propolis extracts collected from different regions of Portugal using the UHPLC-DAD-MS<sup>n</sup> method; comparison of different analytical methods for TPC and antioxidant capacity; correlation of these analytical methods with the content of HBAs, HCAs, and FLAVs quantified in propolis samples; pollen analysis to determine the floral origin of propolis samples. The novelty of this work was the attempt to correlate the methods for quantifying TPC and antioxidant capacity with the HBA, HCA, and FLAV contents quantified in propolis samples, which allowed us to explain the differences between the methods. Besides contributing to standardisation of procedures, this may increase confidence in the assessment of the characteristics of propolis samples, ensuring their quality and efficacy in different applications.

## 2. Results

### 2.1. Pollinic Analysis

The results of the analysis of the pollen profile of propolis allow inferring its floral origin. The main pollen types and the percentage of the number of pollen grains counted in each sample are shown in Table 1. The pollen profile considering the main pollens

included by ten pollen species: *Populus* sp., *Trifolium repens*, *Cistus ladanifer*, *Quercus* sp., *Pinus nigra*, *Leontodon* sp., *Castanea sativa*, *Euphorbia* sp., *Echium vulgare*, and *Olea europaea*. The four propolis samples have quite similar botanical origins. However, the predominant pollen types were different: *Trifolium repens*, Braga sample ( $25.6 \pm 0.1\%$ ), *Populus* sp., Lousã and Macedo samples ( $51.5 \pm 1.5\%$  and  $20.2 \pm 0.2\%$ , respectively), and *Castanea sativa*, Montesinho sample ( $35.0 \pm 2.0\%$ ). All samples have high percentages of *Populus* sp. (percentages ranging from  $51.5 \pm 1.5\%$  to  $20.2 \pm 0.2\%$ ). Only the sample from Lousã had a pollen predominance higher than 45%, which is classified as dominant pollen. All the other samples have only secondary pollen.

**Table 1.** Pollen profile of the propolis samples (% values).

Samples	Braga	Lousã	Macedo	Montesinho
<i>Populus</i> sp.	$21.4 \pm 1.9$	$51.5 \pm 1.5$	$20.2 \pm 0.2$	$27.4 \pm 1.6$
<i>Trifolium repens</i>	$25.6 \pm 0.1$			
<i>Cistus ladanifer</i>	$19.9 \pm 1.5$		$2.80 \pm 0.6$	
<i>Quercus</i> sp.			$19.9 \pm 2.4$	$5.50 \pm 0.6$
<i>Pinus nigra</i>	$18.7 \pm 0.5$			$10.1 \pm 0.3$
<i>Leontodon</i> sp.		$5.50 \pm 0.5$	$11.4 \pm 2.5$	$3.70 \pm 0.4$
<i>Castanea sativa</i>		$11.0 \pm 1.0$	$7.0 \pm 0.4$	$35.0 \pm 2.0$
<i>Euphorbia</i> sp.		$3.50 \pm 0.5$	$10.9 \pm 0.5$	
<i>Echium vulgare</i>	$1.95 \pm 0.15$	$5.50 \pm 0.5$	$3.55 \pm 0.85$	$4.35 \pm 0.55$
<i>Olea europaea</i>			$6.70 \pm 0.9$	$7.55 \pm 0.65$

## 2.2. Total Phenolic Compounds

### 2.2.1. Quantification of Total Phenolic Compounds with Six Methods

The TPC of the samples was determined spectrophotometrically (F-C methods and spectrophotometric method) and electrochemically (square wave voltammetry method). For the determination of total phenolic compounds, a calibration line with gallic acid (GA) as standard was established for each method. For the F-C, spectrophotometric, and SWV methods, the concentrations used for the calibration curve were 10–800, 20–240, and 20–280 mg/L, respectively. Square wave voltammograms were recorded in the range of +0.1 to +0.9 V. The results were expressed as mg gallic acid equivalents per g of sample (mg GAE/g) and are presented in Table 2.

**Table 2.** Total phenolic compounds (mg GAE/g of extract) determined using six different methods.

Samples	F-C1 <sup>c</sup>	F-C2 <sup>b</sup>	F-C3 <sup>b</sup>	F-C4 <sup>c</sup>	SPECT <sup>a</sup>	SWV <sup>d</sup>
Braga <sup>b</sup>	$146 \pm 4$	$220 \pm 7$	$255 \pm 6$	$126 \pm 3$	$460 \pm 8$	$46 \pm 11$
Lousã <sup>c</sup>	$79 \pm 2$	$117 \pm 2$	$105 \pm 6$	$75 \pm 2$	$263 \pm 6$	$43 \pm 1$
Macedo <sup>a</sup>	$168 \pm 3$	$258 \pm 6$	$289 \pm 9$	$156 \pm 7$	$503 \pm 2$	$49 \pm 3$
Montesinho <sup>b</sup>	$147 \pm 5$	$221 \pm 4$	$235 \pm 7$	$139 \pm 27$	$465 \pm 16$	$60 \pm 6$

F-C1 to F-C4, Folin–Ciocalteu colorimetric method; SPECT, spectrophotometric method; SWV, square wave voltammetry method; different letters indicate significant differences.

The Macedo sample had higher levels of TPC, except for the SWV method. The TPC values obtained from the Lousã sample were the lowest for all six quantification methods examined in the study. Among these methods, the SWV method showed the lowest quantification with values ranging from 43 to 60 mg GAE/g extract, while the SPECT method showed the highest with values ranging from 263 to 503 mg GAE/g extract. The mean TPC values obtained by SPECT were approximately 2.8 times higher than those

of the other methods studied. Of the four methods using the F-C reagent, the F-C4 method gave the lowest TPC results, while the F-C3 method gave the highest overall results.

A two-factor ANOVA without interaction was performed to check the differences between propolis samples (factor 1, four samples) and TPC quantification (factor 2, six methods). For both factors (factor 1:  $p$ -value < 0.001; factor 2:  $p$ -value < 0.001) there were significant differences in at least one of the means tested. Overall, the data show homogeneity of variances between factor 1 and factor 2 (Levene test,  $p$ -value = 0.331) and a distribution close to normality (Shapiro–Wilk test,  $p$ -value = 0.047). The ANOVA model was significant ( $p$ -value < 0.001) and has an RSE of 31.94, a DF of 63, and an  $R^2$  of 0.9474, indicating that the model accounts for 94.74% of the variability within the experimental data.

The result of the statistical analysis of the TPC concentration data showed that the samples from Montesinho and Braga were statistically similar ( $210 \pm 133$  and  $209 \pm 135$  mg GAE/g extract, respectively) and different from the samples from Macedo and Lousã, which were statistically different ( $238 \pm 145$  and  $113 \pm 74$  mg GAE/g extract, respectively). As for the methods used for TPC analysis, F-C1 and F-C4 were found to be similar, as were F-C2 and F-C3. Spectrophotometric and voltammetric methods gave statistically different results (MSerror = 1020; DF = 63). The mean TPC values in ascending order for the voltammetric, F-C4, F-C1, F-C2, F-C3, and spectrophotometric methods were  $47 \pm 11$ ,  $123 \pm 33$ ,  $134 \pm 34$ ,  $204 \pm 55$ ,  $221 \pm 73$ , and  $422 \pm 98$  mg GAE/g sample, respectively.

Box plots were made for each sample and the means of each group were compared to see if there were significant differences. The results of these tests are depicted on the plots. This approach provided a clear visualisation of the data, making it easier to draw conclusions about the differences between the samples and the analytical methodologies (Figure 1).

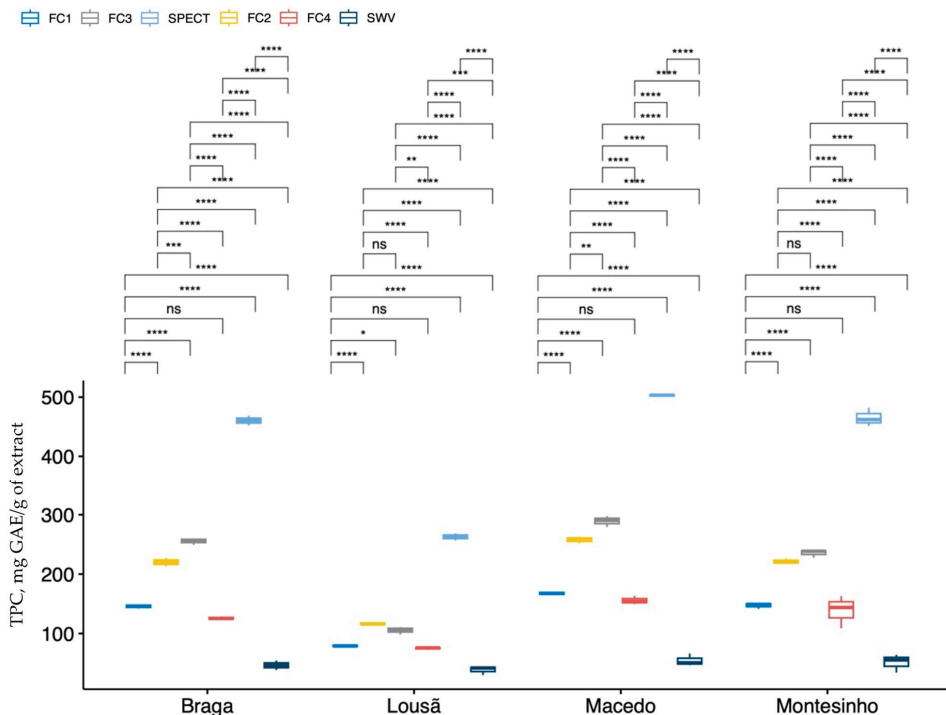


**Figure 1.** Box plots of each propolis sample compared with the means of the TPC methods. ns—not significant; the significance levels are translated by the following symbols: \*\*\*\* ( $p$ -value < 0.0001); \*\*\* ( $p$ -value < 0.001); \*\* ( $p$ -value < 0.01); \* ( $p$ -value < 0.05); ns ( $p$ -value > 0.05).

Figure 1 shows that some TPC methods of analysis were significantly different from each other, confirming the results of the statistical analysis of the ANOVA, which shows that the F-C1 and F-C4 methods were indeed statistically equal, as were F-C2 and F-C3. The SPECT and SWV methods were statistically different, with higher and lower TPC values, respectively, in all samples. Overall, the behaviour of the different methods for the four propolis samples was similar. For the Lousã sample, the four F-C methods and the voltammetric method are close, with the spectrophotometric method standing out with higher values (on average 3.1 times higher than the other methods).

### 2.2.2. Correlation of TPC with HBA, HCA, and FLAV

For the estimation models, the results of independent variables (HBA, HCA, and FLAV) reported in a previous work of our team [31] and the dependent variables (methods of analysis of the concentration of total phenolic compounds) were used in the logarithmic form (results presented in several orders of magnitude). The results of the estimation models obtained, as well as the values of RSE,  $R^2$ , and  $p$ -value of method significance, are presented in Table 3.

Estimation models were of the type:

$$\log([\text{total phenolics}]) = b + a1 \times \log([\text{HBA}]) + a2 \times \log([\text{HCA}]) + a3 \times \log([\text{FLA}]) \quad (1)$$

**Table 3.** Relationship between the results of total phenolics obtained by 6 different methods and the total concentrations of HBA, HCA, and FLAV present in propolis samples.

Method	RSE	$R^2$	$p$ -Value	$b \pm s$	HBA $\pm s$	HCA $\pm s$	FLAV $\pm s$
FC1	0.032	0.9903	<0.001	$-11.3 \pm 0.5$	ns	ns	$3.1 \pm 0.1$
FC2	0.024	0.9960	<0.001	$-10.3 \pm 1.4$	$-0.5 \pm 0.1$	$0.7 \pm 0.2$	$2.7 \pm 0.5$
FC3	0.039	0.9920	<0.001	$-5.8 \pm 0.3$	ns	$2.0 \pm 0.1$	ns
FC4	0.106	0.8907	<0.001	$-10.5 \pm 1.7$	ns	ns	$2.9 \pm 0.3$
SPECT	0.021	0.9944	<0.001	$-8.4 \pm 0.3$	ns	ns	$2.7 \pm 0.1$
SWV					ns	ns	ns

ns—not significant.

Table 3 reveals that the presence of HBA compounds in propolis samples does not have a significant impact on the quantification of TPC; however, it may have a negative influence on the F-C2 method. As for the HCA compounds, only the F-C2 and F-C3 methods showed a positive influence on the quantification of TPC, while the other methods did not show any significance. The presence of flavonoids showed a positive effect on quantifying TPC in four methods, while the F-C3 and SWV methods did not show any significance.

Figure 2 shows, as an example, the plot of the data obtained by the estimation model about the experimental values obtained by the F-C3 method, verifying an acceptable linear fit (significant estimation model,  $p$ -value < 0.001; slope =  $0.992 \pm 0.028$  close to 1; intercept =  $0.04 \pm 0.15$  close to 0;  $R^2 = 0.992$  close to 1), reflected in the low value of the RSE (0.039) and the acceptable closure coefficient (0.9920) obtained in the estimation model.

## 2.3. Antioxidant Capacity

### 2.3.1. Estimation of the Antioxidant Capacity

In this study, four different methods were used to measure the antioxidant capacity of propolis samples collected from different geographical origins and L-ascorbic acid (positive control). The tests performed were a radical scavenging assay (DPPH) and three reducing power assays using iron (III) (FRAP, MFec, and OFec). The results are presented in Table 4 and are expressed in terms of  $EC_{50}$ , units in mg/L.



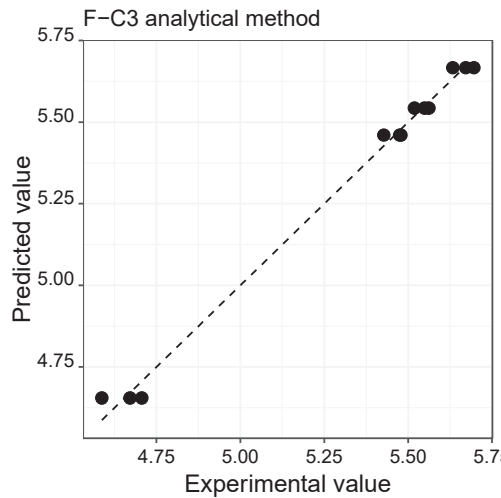


**Figure 2.** Linear relationship between the total phenolic content results (mg GAE/g of extract) obtained from the model estimation and the F-C3 analytical method.

**Table 4.** Antioxidant capacity ( $EC_{50}$ , mg/L) was determined using four different methods.

Samples	DPPH <sup>b</sup>	FRAP <sup>a</sup>	MFec <sup>c</sup>	OFec <sup>a</sup>
Braga <sup>b</sup>	206 ± 6	566 ± 1	115 ± 3	480 ± 12
Lousã <sup>a</sup>	488 ± 2	795 ± 10	332 ± 5	859 ± 6
Macedo <sup>c</sup>	168 ± 5	430 ± 8	94 ± 2	326 ± 10
Montesinho <sup>c</sup>	173 ± 3	445 ± 15	137 ± 2	364 ± 3
L-ascorbic acid	23 ± 0.5	71 ± 0.4	42 ± 3	22 ± 0.1

DPPH, 2,2-diphenyl-1-picrylhydrazyl; FRAP, ferric-reducing antioxidant power; MFec, modified ferricyanide method; OFec, original ferricyanide method; different letters indicate significant differences.

In general, samples showed high antioxidant capacity. The Macedo sample exhibited the highest antioxidant capacity ( $EC_{50}$  values varied between 94 ± 2 and 326 ± 10 mg/L) and the Lousã sample the lowest ( $EC_{50}$  values varied between 332 ± 5 and 859 ± 6 mg/L) for the four methods studied. The MFec method gave the highest antioxidant capacity in all the samples, followed by the DPPH method. FRAP and OFec gave low antioxidant capacity values, with close values between the two. Regarding the antioxidant capacity of ascorbic acid, the DPPH and OFec methods gave lower and similar  $EC_{50}$  values, whereas the FRAP method gave a higher  $EC_{50}$  value. As expected, the propolis samples showed much higher values than the positive control, since it is a purified compound with high antioxidant capacity.

Two-way ANOVA without interaction was performed to test the differences between the propolis samples (factor 1, four samples) and their antioxidant capacity (factor 2, four methods). The ANOVA model was significant ( $p$ -value < 0.001), with an RSE of 7.1 and  $R^2$  of 0.9993, which means that the model explains 99.93% of the variability within the experimental data. Significant differences were found within each of the factors ( $p$ -value < 0.001). The overall data showed normality (Shapiro–Wilk test, with  $p$ -value = 0.292) and homogeneity of the values (Levene test, with  $p$ -value = 0.705).

The Macedo and Montesinho samples were statistically equal (mean  $EC_{50}$  values of 255 ± 138 mg/L and 280 ± 134 mg/L, respectively), while the Braga and Lousã samples are statistically different (mean  $EC_{50}$  values of 342 ± 195 mg/L and 618 ± 227 mg/L, respectively). Among the four methods tested to determine the antioxidant capacity of

propolis samples, we found that the FRAP and OFec methods were statistically equivalent (mean EC<sub>50</sub> values of 559 ± 153 mg/L and 507 ± 220 mg/L, respectively), while the DPPH and MFec methods were statistically different (mean EC<sub>50</sub> values of 259 ± 139 mg/L and 170 ± 99 mg/L, respectively).

To evaluate the antioxidant capacity of different propolis samples, box plots were created for each method employed. These box plots give an overview of the value distribution within each method, enabling simple comparison between samples. To further analyse the data, the means of each method were compared to identify any significant differences. These comparisons are displayed on the box plots, making it easy to identify which methods produced the greatest variation in antioxidant capacity between samples (Figure 3).

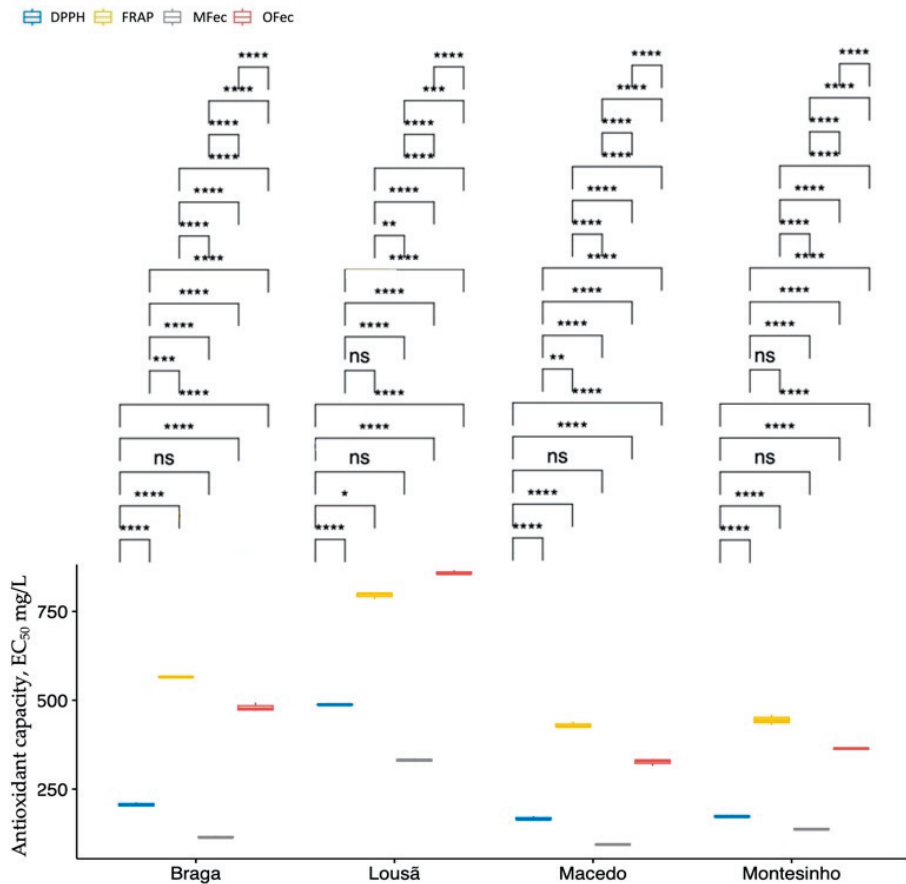


**Figure 3.** Box plots of each method of antioxidant capacity for each propolis sample. ns—not significant; the significance levels are translated by the following symbols: \*\*\*\* ( $p$ -value < 0.0001); \*\*\* ( $p$ -value < 0.001); \*\* ( $p$ -value < 0.01); \* ( $p$ -value < 0.05); ns ( $p$ -value > 0.05).

Figure 3 demonstrates the analytical methods that yielded the highest and lowest quantification of antioxidant capacity. The behaviour of the samples was generally comparable for all methods. In ascending order of EC<sub>50</sub> values, the samples from Macedo, Montesinho, Braga, and finally Lousã showed the highest values. The samples from Macedo and Montesinho exhibited similar levels of antioxidant capacity, which was validated by ANOVA indicating that the samples were statistically equivalent.

### 2.3.2. Correlation of Antioxidant Capacity with HBA, HCA, and FLAV

In evaluating the results of antioxidant capacity, we attempted to obtain estimation models related to the concentrations of HBA, HCA, and FLAV present in the propolis samples (as presented in the study by Paula et al. [31]).

The results of the estimation models obtained, as well as the values of RSE,  $R^2$ , and  $p$ -value of method significance, are presented in Table 5.

Estimate models used:

$$\log([\text{antioxidant}]) = b + a_1 \times \log([\text{HBA}]) + a_2 \times \log([\text{HCA}]) + a_3 \times \log([\text{FLA}]) \quad (2)$$

**Table 5.** Correlation between the antioxidant capacity obtained by 4 different methods and the concentrations of HBA, HCA, and FLAV present in the propolis samples.

Method	RSE	$R^2$	$p$ -Value	$b \pm s$	HBA $\pm s$	HCA $\pm s$	FLAV $\pm s$
DPPH	0.022	0.9981	<0.001	$38.1 \pm 1.2$	ns	$1.6 \pm 0.2$	$-7.9 \pm 0.5$
OFec	0.021	0.9979	<0.001	$43.2 \pm 1.2$	$1.3 \pm 0.1$	$1.9 \pm 0.2$	$-10.3 \pm 0.5$
MFec	0.019	0.9988	<0.001	$18.3 \pm 0.2$	$0.9 \pm 0.1$	$-3.2 \pm 0.1$	ns
FRAP	0.020	0.9956	<0.001	$34.3 \pm 1.2$	$0.9 \pm 0.1$	$1.9 \pm 0.2$	$-8.3 \pm 0.4$

ns—not significant.

From the analysis of Table 5, all the estimation models show an acceptable fit, but with marked differences. The presence of HBA and HCA compounds in propolis samples has an overall positive effect on the quantification of their antioxidant capacity. They only have a negative effect on the MFec method and had no significant effect on the DPPH method. The same cannot be said for flavonoids, as they tend to have a negative effect on antioxidant capacity in all methods except the MFec method, which showed no significant interaction.

Figure 4 shows the relationship between the data obtained by the model estimated in relation to the experimental values obtained with the MFec method, which shows an acceptable linear fit (significant estimation model,  $p$ -value < 0.001; slope =  $0.999 \pm 0.010$  close to 1; intercept =  $0.006 \pm 0.055$  close to 0;  $R^2 = 0.999$  close to 1), which is reflected in the low value of the RSE (0.019) and the acceptable coefficient of determination (0.9988) obtained in the estimation model.

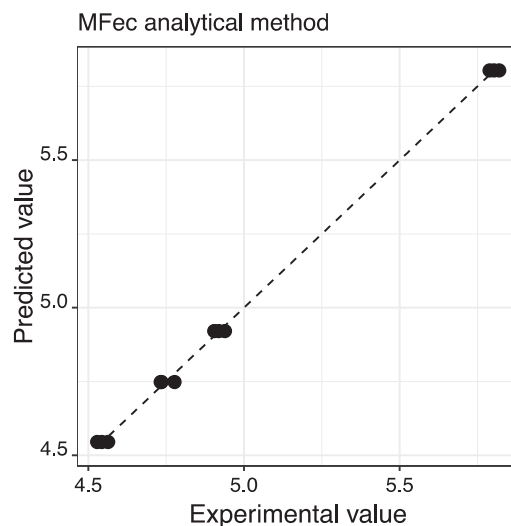


**Figure 4.** Linear relationship between the model estimation results and the MFec analysis method ( $EC_{50}$  mg/L).

#### 2.4. UHPLC-DAD-ESI-MS<sup>n</sup> Analysis

This study was carried out using UHPLC-DAD-ESI-MS<sup>n</sup> in negative ion mode because of its greater sensitivity in analysing the different classes of polyphenols [32]. All the phytochemicals in propolis were characterised by their UV spectra (absorbance at 280 nm), retention time ( $t_R$ ), and MS/MS (MS<sup>2</sup> and MS<sup>3</sup>) data and compared with the literature [33–37] (Supplementary Material).

Of a total of 62 compounds, 56 were identified, including 26 phenolic acids and their derivatives (caffeic acid, *p*-coumaric acid, isoferulic acid, ferulic acid, 3,4-dimethyl-caffeic acid, cinnamic acid, *p*-coumaric acid methyl ester, cinnamylidenacetic acid, caffeic acid isoprenyl ester, caffeic acid isoprenyl ester (isomer), caffeic acid phenylethyl ester, *p*-coumaric acid isoprenyl ester, *p*-coumaric benzyl ester, *p*-coumaric acid isoprenyl ester (isomer), caffeic acid cinnamyl ester (isomer), *p*-coumaric acid derivative, *p*-coumaric cinnamyl ester, caffeic acid derivative, *p*-coumaric acid-4-hydroxyphenylethyl ester dimer, caffeic acid cinnamyl ester (isomer), *p*-methoxy-cinnamic acid cinnamyl ester, *p*-methoxy-cinnamic acid cinnamyl ester (isomer)) and 30 flavonoids and derivatives (quercetin, pinobanksin-5-methyl-ether, quercetin-3-methyl-ether, apigenin, pinobanksin, kaempferol, isorhamnetin, pinocembrin-5-methyl-ether, kaempferol-methyl ether, quercetin-dimethyl-ether, galangin-5-methyl ether, pinobanksin-5-methyl-ether-3-*O*-acetate, rhamnetin, chrysin, acacetin, pinocembrin, galangin, kaempferide, pinobanksin-3-*O*-acetate, chrysoeriol-methyl-ether, pinocembrin-5-*O*-3-hydroxyl-4-methoxyphenylpropionate, pinobanksin-3-*O*-propionate, pinobanksin-5-methyl-ether-3-*O*-pentanoate, pinobanksin-7-methyl-ether-5-*O*-*p*-hydroxyphenylpropionate, pinobanksin-3-*O*-butyrate or isobutyrate, pinobanksin-3-*O*-pentaonate, pinobanksin-3-*O*-pentaonate or 2-methylbutyrate, pinobanksin-*O*-hexanoate, pinobanksin-3-*O*-hexanoate).

Among them, quercetin-3-methyl-ether, acacetin, and chrysoeriol-methyl-ether were only detected in the Lousã sample, while cinnamic acid, pinobankin-*O*-hexanoate, and pinobankin-3-*O*-hexanoate were absent in that sample.

The compounds with a larger peak area (although the concentration response can be different) in the four propolis samples were chrysin, caffeic acid isoprenyl ester, pinocembrin, galangin, pinobanksin-3-*O*-acetate, and caffeic acid phenylethyl ester.

Figure 5 shows the phenolic compounds present in the four propolis samples, their respective retention times, and the quantification of the areas of the chromatographic peaks in log units.

A PCA was performed to analyse the mass spectrometry composition results and the UHPLC-DAD peak areas of each propolis sample. The Yeo–Johnson transformation was used to pre-process the data. With only four principal components, 100% of the variability in the data could be accounted for. Figure 6 shows the two-dimensional space represented by the first two principal components, which account for 99.67% of the variability (PC1: 93.94%; PC2: 5.73%).

PCA highlighted the differences between the samples, showing that the Macedo, Montesinho, and Braga samples were similar (correlation of 0.97), while the Lousã sample was significantly different (correlations of 0.30, 0.32, and 0.37 for the samples from Montesinho, Braga, and Macedo, respectively). The differences evidenced by PCA were high concentrations of the compounds caffeic acid derivative (rt. 40.58, 41.29, 42.72 min), caffeic acid cinnamyl ester (isomer) (rt. 41.16 min), chrysoeriol-methyl-ether (rt. 27.96 min), *p*-coumaric acid isoprenyl ester (isomer) (rt. 31.42 min), kaempferol-methyl ether (rt. 15.15 min), quercetin-3-methyl-ether (rt. 11.38 min), chrysin (rt. 22.80 min), acacetin (rt. 23.53 min), and unknown (rt. 38.42, 45.66, 48.56 min) and low concentration of the compounds cinnamic acid (rt. 11.49 min), cinnamylidenacetic acid (rt. 18.44 min), unknown (rt. 33.86, 43.37 min), pinobanksin-7-methyl-ether-5-*O*-*p*-hydroxyphenylpropionate (rt. 37.05 min), pinobanksin-*O*-hexanoate (rt. 40.41 min), pinobanksin-3-*O*-hexanoate (rt. 42.12 min), and *p*-coumaric acid derivative (rt. 45.67 min).

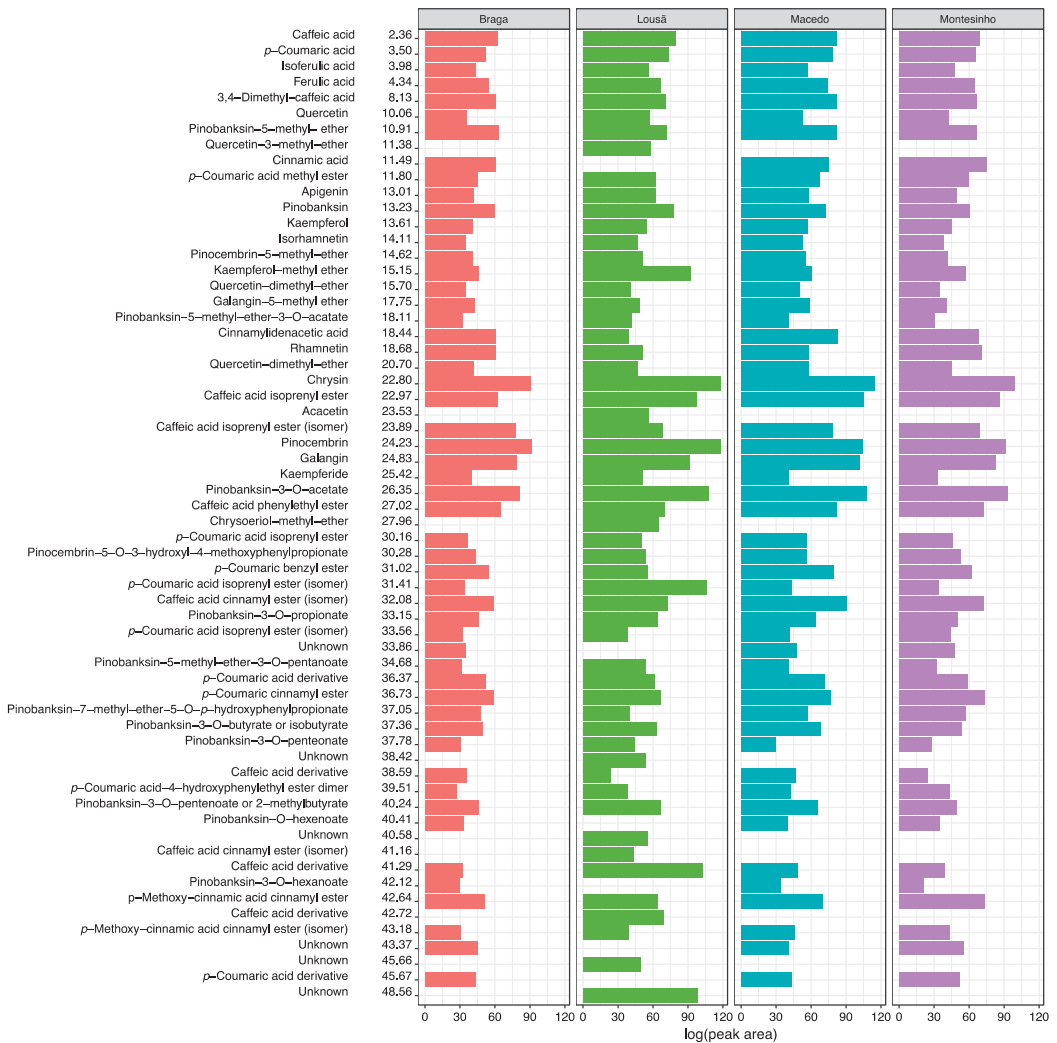


**Figure 5.** Profile of phenolic compounds obtained by UHPLC-DAD-ESI-MS<sup>n</sup> in negative ion mode in the four propolis samples (retention times and peak areas of the chromatogram obtained by diode array detector, in logarithmic units).

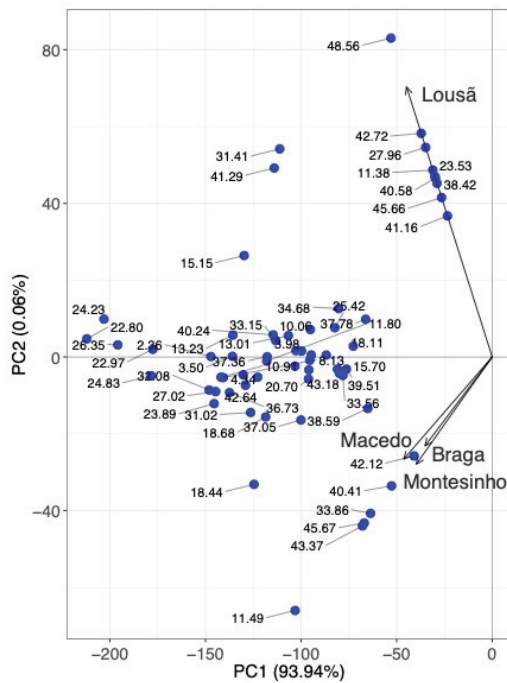


**Figure 6.** Biplot of the principal component analysis of the MS profile of phenolic compounds obtained for the four propolis samples.

### 3. Discussion

#### 3.1. Pollinic Analysis

In temperate regions of the world, *Populus* species have been described as the main source of propolis [38,39]. In this work, the four propolis samples have a high percentage of this pollen. This agrees with the works of Dias et al. [40], which analysed Portuguese propolis samples from different regions, and Falcão et al. [41], which analysed samples from temperate regions, including Portugal. It is stated that propolis derived from *Populus nigra* could be used in the pharmaceutical and/or food industry due to its rich phytochemical composition [42]. However, in this study, the sample with the highest *Populus* sp. content was not the one with the highest biological properties. Therefore, applications based only on pollen analysis are not a satisfactory approach to determine the bioactive properties of this natural product [43]. However, caution should be taken when relating the results to the propolis pollen profile as this may not be an accurate indicator of plant origin and could be dangerously misleading [44].

#### 3.2. Quantification of Total Phenolic Compounds

Six different methods were used to quantify TPC: four spectrophotometric methods based on the F-C reagent and one based on spectra at 280 nm. The sixth method is an electrochemical method using square wave voltammetry. The differences obtained between the six methods for quantification of total phenolic compounds in propolis samples are discussed below.

The F-C method is based on electron transfer in which a mixture of two acids, phosphotungstic and phosphomolybdic, reduces phenols and produces a colour change measured at 765 nm [45,46]. This method is sensitive to pH, temperature, and reaction time [47,48]. The pH at the end of the reaction varies according to the method used, since the final concentrations of the reactants F-C and  $\text{Na}_2\text{CO}_3$  differ between the methods. This explains

the differences between the four F-C methods investigated in this work. According to the result of the ANOVA, the four F-C methods were grouped in pairs: F-C1 and F-C4 methods with high final concentrations of F-C (33 and 50%, respectively) and low concentrations of  $\text{Na}_2\text{CO}_3$  (3.3 and 3.0%, respectively) and F-C2 and F-C3 methods with low concentrations of F-C reagent (5 and 2%, respectively) and  $\text{Na}_2\text{CO}_3$  (3 and 0.8%, respectively). The methods using low concentrations of these reagents allowed higher quantification of TPC due to the lower pH at the end of the reaction. Lawag et al. [49] also concluded that lower pH values allowed higher quantification of TPC in honey samples. As with F-C methods, the spectrophotometric (SPECT) method is based on spectrophotometry and results can be expressed in simple terms as absorbance measured at 280 nm ( $A_{280}$ ) or converted to gallic acid equivalents [45,50]. The SPECT method is a faster and less expensive method for measuring the total phenolic content in samples. The SPECT method requires only one reagent, hydrochloric acid, which is readily available and much less expensive than the reagents used in the F-C method. In addition, SPECT requires no incubation time, making it faster than FC, which requires a long incubation period. The SPECT method gave a higher quantification of TPC compared to F-C and SWV methods. Way et al. [51] also found higher values for total phenolic compounds in cider samples using the spectrophotometric method (Somers) than the F-C method.

In recent years, electrochemical methods have been extensively investigated for the determination of phenolic compounds, mainly due to their simplicity, high sensitivity, rapid response, and low cost [52]. Most of the biological activity of these compounds is due to their ability to donate electrons to a wide range of receptor species. The redox potential of natural phenolic compounds covers a significant range, which is the first source of selection allowing the selective analysis of different electroactive compounds by different voltammetric techniques such as cyclic voltammetry (CV), differential pulse voltammetry (DPV), or square wave voltammetry (SWV) [53].

The SWV technique has several advantages over other voltammetric techniques such as CV and DPV, including the fact that it consumes fewer electroactive species, is faster, is more sensitive, takes much less time to analyse, and has fewer problems with electrode poisoning than other methods [54,55].

The TPC values obtained with the SWV method were lower than those obtained with the F-C and SPECT methods. As reported in previous publications [56,57], the values obtained with the F-C method are generally higher than those obtained with electrochemical analysis. This behaviour is attributed to the different oxidants used, i.e., the chemical reagents used in the F-C method and the potential applied for the oxidation reaction at the electrode surface in electrochemical sensors [58]. In the F-C method, the reagents oxidise not only the phenolic compounds but also other non-phenolic species that may be present in the sample. In the SWV method, only the phenolic compounds are oxidised by the oxidising potentials applied [58,59]. Regarding the correlation between TPC and the different groups of phenolic compounds, the results indicate that the presence of HBA and HCA compounds did not have a significant influence on the quantification of TPC in the majority of the methods tested. However, the HCA content present in the samples has a positive influence on the quantification of TPC in methods F-C2 and F-C3. These methods have higher TPC quantification. On the other hand, the presence of FLAV compounds in propolis samples can positively influence the quantification of TPC in all tested methods. Several works show that there is a positive correlation between TPC and flavonoid content [60,61]. However, no comparative work has been found relating TPC to HBA and HCA content. Therefore, to the authors' knowledge, this is the first work that attempts to evaluate the influence of phenolic groups on the results obtained by different methods for total phenolic content. Overall, this study sheds light on the influence of different groups of phenolic compounds on TPC quantification and highlights the varying effectiveness of different methods in capturing total phenolic content. The results show that the F-C2 method had the strongest correlation with the three groups of phenolic compounds. Conversely, the results of the SPECT method, which measured higher levels of TPC in the samples, only correlated

significantly with FLAV compounds, while the presence of HBA and HCA compounds had no significant effect.

### 3.3. Antioxidant Capacity

In this study, three different reducing power assays (FRAP, MFec, and OFec) and one radical scavenging assay (DPPH) were used to measure the antioxidant capacity of propolis samples from different geographical locations. The DPPH and FRAP methods are the most widely used assays to evaluate the antioxidant capacity of foods and biological extracts [47,62].

The principle of the DPPH method is based on the reaction between the free radical DPPH and antioxidants. The free radical DPPH has a stable deep purple colour. When DPPH radicals are allowed to react with antioxidants, the colour of the solution changes to yellow [47,63].

The FRAP, MFec, and OFec methods are based on the same principle. This is the reduction of ferric ions ( $\text{Fe}^{3+}$ ) to ferrous ions ( $\text{Fe}^{2+}$ ), forming a blue complex [64]. The three methods differ in the reagents used and the pH of the solution. The FRAP assay is a colorimetric method that exploits the ability of antioxidants to reduce the colourless  $[\text{Fe}^{3+}-(2,4,6\text{-tris}(2\text{-pyridyl})\text{-s-triazine})_2]^{3+}$  complex to the intense blue  $[\text{Fe}^{2+}-(\text{TPTZ})_2]^{2+}$  complex in an acidic medium [65]. Such colour changes are measured spectrophotometrically at 593 nm. This method requires specific conditions, including an acidic medium (pH 3.6) to facilitate iron solubility. The low pH decreases the ionisation potential that drives electron transfer and increases the redox potential, causing a shift in the dominant reaction mechanism [66]. In the OFec method, a phosphate buffer at pH 6.6 was used and Prussian blue solution was measured at 700 nm. One of the differences between the OFec and MFec methods is that the modified method does not use pH 6.6 phosphate buffer. There is also no precipitation of the Prussian blue solution due to the stabilising effect of the sodium dodecyl sulphate (SDS) reagent [47,64]. Of the three iron-based methods, FRAP and MFec assays were carried out in acidic solution due to the hydrolysis of the ferric ion at a slightly neutral to acidic pH.

The results obtained by the four methods differed slightly. The MFec method allowed for quantifying higher antioxidant capacity in all the propolis samples, while the OFec and FRAP methods showed the lowest antioxidant capacity. It is natural that the results obtained from different antioxidant assays based on electron transfer give comparable but not identical results for antioxidants. This is due to the diversity of reaction conditions, such as redox potential, pH, and kinetics, of these assays.

Some authors [47,67,68] conclude that the FRAP method has limitations and needs to be modified. The fact that it is based on an aqueous solution (acetate buffer) limits the method to hydrophilic substances, whereas plant essential oils and their antioxidant components (i.e., terpenes) are hydrophobic. The same applies to the OFec method, which is also based on an acetate buffer. Ferricyanide methods can be a cheaper alternative to FRAP under certain conditions, with partially improved molar uptake (and thus sensitivity) of antioxidants, lower intercept values, wider linear range, and better additivity of total antioxidant capacity values of antioxidant components in mixtures.

Overall, the results showed a positive contribution of HBA and HCA content in determining antioxidant capacity. The FRAP and OFec methods showed the greatest contribution of these compounds to the determination of antioxidant capacity. However, the contribution of HCA was greater than that of HBA, which was confirmed by Natella et al. [69], who reported that HCA had stronger antioxidant capacity than HBA when the propenoic side chain was attached instead of the carboxyl group of benzoic acid derivatives. These two groups (HBA and HCA) showed antioxidant properties against different types of free radicals [70–72]. Velika et al. [73] investigated the relationship between HBA and antioxidant capacity and found that there was a positive correlation between them. They concluded that the structure and position of the hydroxyl group is very important for antioxidant capacity. Mazzone et al. [74] confirmed the antioxidant properties of HCA



and derivatives. They indicated that a structural change in the ethylene spacer between the aromatic ring and the carboxyl functionality increases the antioxidant capacity of the derivatives. The antioxidant capacity of phenolic acids is based on the phenolic hydroxyl, so the number and position of phenolic hydroxyls are directly related to their antioxidant capacity [75,76]. In addition, the methoxy and carboxylic acid groups also have important effects on the antioxidant capacity of phenolic acids [76,77]. This may be the reason for the results obtained regarding the contributions of HBA and HCA in the different methods for the determination of antioxidant capacity.

The correlation of antioxidant capacity with FLAV shows that flavonoids contribute negatively to the determination of antioxidant capacity in all tested methods, except in the MFec method. The antioxidant capacity of flavonoids is mainly related to their chemical structure and, as with phenolic acids, is based on the O-H bond dissociation energy value [76,78]. Some authors have also found a negative correlation between flavonoids and antioxidant capacity in propolis extract [10,60,79]. Khiya et al. [80] also found a negative correlation between flavonoids and the DPPH and FRAP methods in leaf extracts of *Salvia officinalis*. The results suggest that the OFec and FRAP methods are most closely related to the three groups of phenolic compounds but did not reveal a higher antioxidant capacity in propolis samples. This suggests that the negative influence of flavonoids may interfere with the determination of the antioxidant capacity of the samples, since the MFec method showed the highest antioxidant capacity.

The effectiveness of antioxidants depends on several factors, the most important of which are structural properties, temperature, properties of the substrate susceptible to oxidation, concentration, the presence of synergistic and pro-oxidant compounds, and the physical state of the system [76]. It should be noted that the methods used to determine antioxidant capacity have different reaction systems. The DPPH assay reacts in an ethanol system whereas the FRAP, OFec, and MFec methods react in a water system. It should also be noted that flavonoids can act as antioxidants by different mechanisms such as hydrogen atom transfer, single electron transfer, and transition metal chelation [76]. Kiokas et al. [81] stated that the strong antioxidant and biochemical potential of these natural products may be linked to the synergistic effect of their individual phenolic compounds. However, antagonistic effects cannot be neglected either. The study highlights the positive correlation between total phenolic compound content and antioxidant capacity, as reported by several authors [60,82,83]. The sample with a higher TPC content also showed higher antioxidant capacity.

### 3.4. UHPLC-DAD-ESI-MS<sup>n</sup> Analysis

The UHPLC-DAD-ESI-MS/MS method was used for the separation and identification by analytical chromatography of 56 compounds from propolis extracts. Characteristic peaks were identified by comparing their chromatographic behaviour, UV spectra, and MS information with those of reference compounds, referring to previous studies [33–37,84].

Only the phenolic compounds HCA and FLAV were detected and identified in the propolis samples. Falcão et al. [35] also identified only these groups of compounds in propolis samples. In the present study, flavonoids identified as chrysin, pinocembrin, galangin, and pi-nobanksin-3-O-acetate were detected in the four propolis extracts with large peak areas, thus suggesting their predominance. Falcão et al. [41] have also identified these four flavonoids as the main compounds in Portuguese propolis extracts. Consistent with this, Yuan et al. [84] and Avula et al. [33] identified these four flavonoids as the most abundant in propolis samples using three extraction methods and in propolis extracts from different geographical locations, respectively. Guzelmeric et al. [43] have also identified pinocembrin, galangin, and chrysin in propolis extracts. In addition, Bhuyan et al. [85] report pinocembrin and galangin as significant components in two propolis samples from Australia.

As for phenolic acids, the largest peak areas were found for caffeic acid derivatives such as isoprenyl ester and phenylethyl ester. These data also agree with literature data, as

caffeic acid derivatives were identified as the main components of the O-subtype of Serbian and Turkish propolis samples [43,86].

Globally, the presence of these compounds (phenolic acids and flavonoids) in propolis samples is characteristic of poplar buds [41,87,87]. This agrees with the analysis of the pollen, which showed that the pollen of the species *Populus* sp. was present in all samples.

#### 4. Materials and Methods

##### 4.1. Chemicals and Reagents

All reagents were of analytical quality and used as purchased. The standard used was gallic acid (1-Hidrate) from Panreac (99%, Barcelona, Spain). As solvents, absolute ethanol (EtOH) was acquired from Panreac (HPLC quality, Spain, 99.9%); diethyl ether from Carlo Erba. Other reagents were hydrochloric acid (HCl) from Carlo Erba (Val-de-Reuil, France, 37% and  $d = 1,18$ ); glacial acetic acid and acetic anhydride from Merck (Darmstadt, Germany); sulphuric acid ( $H_2SO_4$ ) from José Manuel Gomes dos Santos; glycerol from Analar Normapur (VWR Chemicals); potassium hydroxide (KOH), sodium carbonate ( $Na_2CO_3$ ), sodium chloride (NaCl), sodium hydrogen phosphate ( $Na_2HPO_4$ ), and potassium dihydrogen phosphate ( $KH_2PO_4$ ) were acquired from Panreac (Spain); Folin–Ciocalteu reagent and potassium chloride (KCl) were acquired from Scharlau (Spain); potassium hexacyanoferrate(III) ( $K_3Fe(CN)_6$ ), 2,3,5-Triphenyltetrazolium chloride (TPTZ), and ferric chloride hexahydrate ( $FeCl_3 \cdot 6H_2O$ ) were acquired from ACRÖS Organics (Geel, Belgium); potassium hexacyanoferrate(II) trihydrate ( $K_4Fe(CN)_6 \cdot 3H_2O$ ) were from Riedel-de-Haën (Hanover, German); sodium dodecyl sulphate (SDS), sodium acetic acid trihydrate salt ( $CH_3COOH \cdot 3H_2O$ ), and 2,2-diphenyl-1-picrylhydrazyl (DPPH) were from Sigma Aldrich (Darmstadt, Germany); and trichloroacetic acid (TCA) was from Biochem Chemopharma (Cosne-Cours-sur-Loire, France). The deionised water used in all analytical work was of type II.

##### 4.2. Propolis Samples

Propolis samples were collected in three locations in the northern region of Portugal (Montesinho, in the Trás-os-Montes sub-region; Macedo de Cavaleiros, in the Trás-os-Montes sub-region; Braga, Minho sub-region) and one in the central region (Lousã, Baixo Mondego). Samples were prepared by mixing 5 g of raw propolis with absolute ethanol (1:5,  $w/v$ ) and left overnight with stirring (60 rpm). After this step, the solution obtained was filtered (Whatman n 4 filter paper). Two further ethanolic extractions were carried out using the same procedures. The combined ethanolic extracts were stored at low temperatures ( $-18\text{ }^\circ\text{C}$ ) and filtered after 12 h to remove wax; this procedure was repeated two more times. The ethanol was evaporated with a rotary evaporator (IKA model RV8). To the propolis extract obtained, 100 mL of diethyl ether and 100 mL of deionised water were added to obtain two visible phases. The sample was treated with diethyl ether solvent to extract as many phenolic compounds as possible. The supernatant (diethyl ether) was then transferred to a new beaker, and the solvent extraction process was repeated three more times until a transparent area was obtained between the two visible phases. From the resulting extracts (approximate yield of 2 g of purified propolis extract), 0.1 g of extract from each sample was weighed and dissolved in 25 mL of 80% absolute ethanol. This propolis solution was used to determine the total phenolic content using a gallic acid standard calibration line. To determine the antioxidant capacity, different concentrations of propolis (from 12–1200 mg/L) were prepared to calculate the  $EC_{50}$  value in mg/L.

##### 4.3. Pollinic Analysis

Pollen analysis was performed according to the method described by Barth et al. [88]. The pollen collection, within 0.5 g of propolis, was mixed with 15 mL of ethanol for 24 h. After 24 h, the preparation was centrifuged for 15 min at 2200 rpm (Eppendorf centrifuge 5810 R, Hamburg, Germany). To the sediment obtained by centrifugation, 3 mL of 10% ( $w/v$ ) KOH was added and it was placed in a water bath and boiled for 2 min. The

mixture was centrifuged at 2200 rpm for 10 min and, after washing with deionised water, centrifuged again at 2200 rpm for 10 min. The sediment was left overnight in 5 mL glacial acetic acid. This mixture was centrifuged at 2000 rpm for 17 min. Then, 5 mL of the mixture of acetic anhydride and sulphuric acid (9:1 *v/v*) was added and heated in a water bath at 80 °C for 3 min. The mixture was centrifuged at 2000 rpm for 17 min. The resulting sediment was washed with deionised water, centrifuged at 2200 rpm for 10 min, then washed with 50% glycerol–water and centrifuged at 2000 rpm for a further 15 min. The sediment was mounted on glycerol–gelatine.

#### 4.4. Quantification of Phenolic Compounds

Determination of total phenolic content (TPC) in the ethanolic extract of the different propolis was carried out spectrophotometrically (estimated by a colorimetric assay based on four different procedures using Folin–Ciocalteu reagent (F-C reagent) and spectrophotometric method). Phenolic compounds were also determined electrochemically (cyclic voltammetry method). The absorbance was measured in a PC VWR UV–Vis spectrophotometer and the results were expressed as mg of gallic acid equivalents/g of extract.

- F-C1 assay: described by Moreira et al. [89]. The reaction of 0.5 mL propolis extract mixed with 0.5 mL of the F-C reagent and 0.5 mL of 10% sodium carbonate ( $\text{Na}_2\text{CO}_3$ ) was kept in the dark at room temperature for 60 min (final concentrations of F-C and  $\text{Na}_2\text{CO}_3$  in solution, 33% and 3%, respectively), after which the absorbance was read at 700 nm.
- F-C2 assay: described by Obied et al. [90]. Propolis extract (0.1 mL) was added to a 10 mL volumetric flask containing 7 mL water. Then, 0.5 mL of F-C reagent was added and, after 1 min, 1.5 mL of  $\text{Na}_2\text{CO}_3$  (20% *w/v*) was added (final concentrations of F-C and  $\text{Na}_2\text{CO}_3$  in solution, 5% and 3%, respectively). The flask was shaken, and the volume was made up to 10 mL with water. The flask was kept for 60 min in the dark at room temperature. The absorbance was read at 760 nm.
- F-C3 assay: described by Shaghaghi et al. [91]. Aliquots of 0.5 mL of samples were mixed with 2.4 mL of deionised water, 2 mL of 2%  $\text{Na}_2\text{CO}_3$ , and 0.1 mL of F-C reagent (final concentrations of F-C and  $\text{Na}_2\text{CO}_3$  in solution, 2% and 0.8%, respectively). After incubation at room temperature for 60 min, the absorbance of the reaction mixture was measured at 750 nm.
- F-C4 assay: described by Metrouh-Amir et al. [92]. First, 0.2 mL of sample extract was mixed with 1 mL of F-C reagent and 0.8 mL of 7.5% (*w/v*)  $\text{Na}_2\text{CO}_3$  was added (final concentrations of F-C and  $\text{Na}_2\text{CO}_3$  in solution, 50% and 3%, respectively). After incubation for 60 min at room temperature in the dark, the absorbance was measured at 740 nm.
- Spectrophotometry (SPECT): described by Obied et al. [90]. Aqueous ethanol (95% *v/v*; 1 mL) containing 0.1% hydrochloric acid was added to the dilute extract (1 mL) in a 10 mL volumetric flask, and the volume was made up to 10 mL with 2% hydrochloric acid. The absorbance was measured at 280 nm to determine total biophenols using gallic acid as standard.
- Square wave voltammetry (SWV): described by Meirinho et al. [93] with some modifications. Phosphate-buffered saline (PBS) was prepared to contain 137 mM NaCl, 2.7 mM KCl, 8.1 mM  $\text{Na}_2\text{HPO}_4$ , and 1.47 mM  $\text{KH}_2\text{PO}_4$ , with pH adjusted to 7.4. The redox probe was always freshly prepared in order to obtain a solution with concentration of 5 mM of  $\text{K}_3\text{Fe}(\text{CN})_6$  and  $\text{K}_4\text{Fe}(\text{CN})_6$  (1:1) and 10 mM of KCl in 100 mL of PBS, at pH 7.4. Square wave voltammetry (SWV) at a potential range of  $-0.2$  to 1.1 V was used to evaluate the reducing properties of the oxides. The amplitude was set at 100 mV and the frequency at 50 Hz. At the additive level, the step size was set to 5 mV. Platinum electrodes from Micrux Technologies were used for this analysis.

#### 4.5. Antioxidant Capacity

The concentration of propolis corresponding to 0.5 of the absorbance ( $EC_{50}$ ) was calculated from a linear regression analysis of absorbances as a function of extract concentrations in solution using Excel (Microsoft Corporation, Redmond, WA, USA). The  $EC_{50}$  results for the four methods were expressed in mg/L.

##### 4.5.1. 2,2-Diphenyl-1-picrylhydrazyl (DPPH): Described by Hatano et al. [94]

An aliquot of 0.3 mL of propolis extract was mixed with 2.7 mL of DPPH reagent ( $2.0 \times 10^{-4}$  M). The mixture was allowed to stand in the dark for 60 min. The absorbance of the solutions was measured at 517 nm. The inhibitory effect of DPPH was calculated from the percentage of DPPH discoloration using the following equation:

$$\% \text{ inhibition} = [(ADPPH - AS)/ADPPH] \times 100 \quad (3)$$

where AS is the absorbance of the solution when the sample extract was added and ADPPH is the absorbance of the DPPH solution. The concentration of extract giving 50% inhibition ( $EC_{50}$  mg/L) was calculated from the graph of the effect of percentage of removal as a function of the concentration of extract in the solution.

##### 4.5.2. Ferric-Reducing Antioxidant Power Method (FRAP): Described by Berker et al. [64]

The FRAP reagent was prepared using a buffer solution of 0.3 M sodium acetic acid trihydrate salt ( $CH_3COOH \cdot 3H_2O$ ) at pH 3.6 to which glacial acetic acid, a solution of TPTZ dissolved in 96% EtOH ( $1.0 \times 10^{-2}$  M), and  $FeCl_3 \cdot 6H_2O$  solution ( $2.0 \times 10^{-2}$  M) were added in a volume ratio of 10:1:1. The FRAP reagent was prepared and used fresh. Then, 0.1 mL of sample was mixed with 3 mL of FRAP reagent and 0.3 mL of deionised water. After 6 min the absorbance was read at 595 nm.

##### 4.5.3. Original Ferricyanide Method (OFec): Described by Berker et al. [64]

A mixture of 1.0 mL sample, 2.5 mL 0.2 M phosphate buffer (pH 6.6), and 2.5 mL  $K_3Fe(CN)_6$  solution (1%) was incubated for 20 min at 50 °C in a water bath. The incubated mixture was allowed to cool to room temperature and 2.5 mL of TCA (10%) was added. The solution was thoroughly mixed, an aliquot of 2.5 mL was taken, and 2.5 mL of water followed by 0.5 mL of  $FeCl_3 \cdot 6H_2O$  solution (0.1%) was added. Absorbance was measured at 700 nm after 2 min.

##### 4.5.4. Modified Ferricyanide Method (MFec): Described by Berker et al. [64]

The mixture of 1.0 mL of propolis extract, 5 mL of deionised water, 1.5 mL of HCl (1 M), 1.5 mL of ferricyanide solution (1%), 0.5 mL of SDS (1%), and 0.5 mL of  $FeCl_3 \cdot 6H_2O$  (0.2%) was incubated at 50 °C on a water bath for 20 min. After that, it was left to cool to room temperature and the absorbance was measured at 750 nm.

#### 4.6. Quantification of HBA, HCA, and FLAV

The quantification of the levels of HBA, HCA, and FLAV present in the propolis samples was carried out according to the method of Obied et al. [90], and the results cited in this paper were published in the work of Paula et al. [31]. The simultaneous quantification of the three classes of phenolic compounds (HBA, HCA, and FLAV) was carried out using multivariate calibrations obtained with mixed standard solutions of gallic acid, ferulic acid, and quercetin (representative compounds of these classes) and the corresponding UV-Vis spectra.

#### 4.7. Compound Identification by UHPLC-DAD-ESI-MS<sup>n</sup>

The UHPLC-DAD-ESI-MS<sup>n</sup> analyses were performed on a Finnigan Surveyor Plus HPLC instrument equipped with a DAD and coupled to an MS. The chromatographic system consisted of a quaternary pump, an autosampler, a degasser, a photodiode array

detector, and an automatic thermostatic column compartment. The HPLC was run on a Macherey-Nagel Nucleosil C18 column (250 mm<sub>4</sub> mm i.d.; 5 mm particle diameter, end-capped) and the temperature was maintained at 25 °C. The mobile phase consisted of (A) 0.1% (*v/v*) formic acid in water and (B) acetonitrile, previously degassed and filtered. The solvent gradient started with 80% A and 20% B, reached 30% B at 10 min, 40% B at 40 min, 60% B at 60 min, 90% B at 80 min, and returned to the initial conditions. For the HPLC analysis, the propolis extract (0.1 g) was dissolved in 25 mL of 80% ethanol. All samples were filtered through a 0.2 mm nylon membrane (Whatman). The flow rate was 1 mL/min, and 200 mL/min was injected into the MS. Spectral data were collected for all peaks in the 200–600 nm range. The MS used was a Finnigan Surveyor LCQ XP MAX quadrupole ion trap MS equipped with an ESI source. The Thermo Xcalibur Roadmap data system was used for control and data acquisition. Nitrogen of over 99% purity was used and the gas pressure was 520 kPa (75 psi). The instrument was operated in negative ion mode with the ESI needle voltage set at 5.00 kV and the ESI capillary temperature set at 325 °C. The full scan covered the mass range from *m/z* 50 to 1000. MS<sup>n</sup> data were acquired simultaneously for the selected precursor ion. The collision-induced decomposition (CID)-MS-MS and MS<sup>n</sup> experiments were performed using helium as the collision gas with a collision energy of 25–40 eV. The quantification of the areas was carried out and the data for the identification of the phenolic compounds were obtained using the Xcalibur 2.2 software of the Thermo Scientific™ LC-MS systems, which allows data acquisition and processing. The identification of phenolic compounds was based on the interpretation of ultraviolet (UV) spectrophotometry and mass spectrometry (MS and MS/MS) data and comparison with the literature [33–37].

#### 4.8. Statistical Analysis

All assays were performed in triplicate and results are presented as mean ± standard deviation. All statistical analyses were performed using R software (R version 3.3.2, 31 October 2016), a free software environment for statistical computing and graphics. Two-factor ANOVA without interaction was used to evaluate two independent variables (factors) that influence the dependent variable. It was applied to verify the differences between propolis samples (4 samples) and TPC quantification (6 methods), as well as to test the differences between propolis samples (4 samples) and their antioxidant capacity (4 methods). Multiple linear regression models were established between TPC or antioxidant capacity values and HBA, HCA, and FLAV contents. The intercept was removed if it was not significant (*p*-value > 0.05). The results are considered satisfactory when the linear regression parameters are close to the theoretical values [95,96]: ‘zero’ (0) for root-square error (RSE) and intercept; ‘one’ (1) for slope and coefficient of determination (R<sup>2</sup>). Principal component analysis was applied to evaluate the MS data, to understand the variability of the propolis samples, and to define which phenolic compounds contribute to their distinctiveness. PCA (using R software) was performed on the covariance matrix, ignoring the center and scale transformation, with only the pre-treatment with the Yeo–Johnson transformation.

## 5. Conclusions

The pollinic analysis of the propolis samples showed a similar pollen profile, which is in agreement with the results of the GC-MS/MS analysis.

The results of TPC and antioxidant capacity demonstrated the importance of carefully selecting the method for determining these properties in propolis samples, as different methods can yield different results. Based on the linear relationship between the content of HBA, HCA, and FLAV and the results of TPC and antioxidant properties, it was found that the presence of HBA and HCA compounds in propolis samples can have a positive effect on the quantification of TPC and antioxidant capacity, while flavonoids can have a positive effect on the quantification of TPC and a negative effect on antioxidant capacity in most of the methods. The methods that gave the highest values for TPC (SPECT) and antioxidant capacity (MFec) did not correspond to the methods that showed the highest

correlation with the three groups of phenolic compounds (F-C2, OFec, and FRAP). This is due to the fact that the methods correlate differently with the HBA, HCA, and FLAV compounds present in the samples. Therefore, the choice of method depends on the aim of the work and the sample to be analysed. It is important to note that the bioactive effects of propolis are still an active area of research and the specific mechanisms and contributions of each component are not yet fully understood. However, it is widely accepted that the bioactive properties of propolis result from the collective action of its various constituents, including, but not limited to, phenolic compounds.

Using the UHPLC-DAD-ESI-MS<sup>n</sup> technique, most of the compounds present in the propolis samples were identified. The study revealed significant compositional differences between the Lousã sample and the other samples, as well as the variability in chemical composition of propolis samples from different geographical origins. It is noteworthy that the only phenolic acids detected in the four propolis samples were HCAs and their derivatives, which could be related to the fact that only the negative ion mode was used.

To evaluate the potentiality of propolis samples in human health, it is crucial to have analytical data about composition (qualitative and quantitative) and biological properties, as these results are related to the overall synergetic and antagonistic effects. Therefore, research in this area needs to be intensified to develop methods related to each group of phenolic compounds. It is also necessary to identify the remaining groups of compounds (e.g., terpenes) that may interfere with the biological properties of this natural product.

Overall, this study provides valuable insights into the composition and properties of propolis samples from Portugal, which can be useful in developing natural products and supplements and also in studying the performance of different analytical methodologies.

**Supplementary Materials:** The following supporting information can be downloaded at: <https://www.mdpi.com/article/10.3390/molecules28124847/s1>, Table S1. Characterisation of phenolic compounds from Portuguese propolis by UHPLC-DAD-ESI-MS<sup>n</sup>. Figure S1. Chromatograms with UV detector (280 nm) of the four propolis samples.

**Author Contributions:** Conceptualization, investigation, methodology, writing—original draft preparation, V.B.P.; software, formal analysis, L.G.D.; data curation, V.B.P., L.G.D. and S.M.C.; writing—review and editing, L.G.D., S.M.C. and L.M.E.; project administration, funding acquisition, L.M.E. All authors have read and agreed to the published version of the manuscript.

**Funding:** This research was funded by the Project-PHARMAPITOX-Desenvolvimento de um coletor inovador e protocolo para purificação da apitoxina para uso nas indústrias farmacéutica e cosmética. This project was co-financed by the European Regional Development Fund (FEDER), NORTE-01-0247-FEDER-113540, through the Competitiveness and Internationalisation Operational Programme—PORTUGAL2020.

**Institutional Review Board Statement:** The study did not require ethical approval.

**Informed Consent Statement:** No require consent statement.

**Data Availability Statement:** Data available on request.

**Acknowledgments:** The authors are grateful to: Nelson De Moura of the company Ecoapis Unipessoal Lda (<http://www.ecoapis.pt> (accessed on 15 March 2023)) for supplying the propolis samples; Foundation for Science and Technology (FCT, Portugal) for financial support through national funds FCT/MCTES (PIDDAC) to CIMO (UIDB/00690/2020 and UIDP/00690/2020) and SusTEC (LA/P/0007/2020).

**Conflicts of Interest:** The authors declare no conflict of interest.

**Sample Availability:** Samples of the compounds are available from the authors.

## References

- Belfar, M.L.; Lanez, T.; Rebiai, A.; Ghiaba, Z. Evaluation of Antioxidant Capacity of Propolis Collected in Various Areas of Algeria Using Electrochemical Techniques. *Int. J. Electrochem. Sci.* **2015**, *10*, 9641–9651.
- Ristivojević, P.; Trifković, J.; Andrić, F.; Milojković-Opsenica, D. Poplar-type propolis: Chemical composition, botanical origin and biological activity. *Nat. Prod. Commun.* **2015**, *10*, 1934578X1501001117. [[CrossRef](#)]
- Masek, A.; Chrzescijanska, E.; Latos, M.; Kosmalska, A. Electrochemical and spectrophotometric characterization of the propolis antioxidants properties. *Int. J. Electrochem. Sci.* **2019**, *14*, 1231–1247. [[CrossRef](#)]
- Nina, N.; Quispe, C.; Jiménez-Aspee, F.; Theoduloz, C.; Giménez, A.; Schmeda-Hirschmann, G. Chemical profiling and antioxidant activity of Bolivian propolis. *J. Sci. Food Agric.* **2016**, *96*, 2142–2153. [[CrossRef](#)]
- Touzani, S.; Embaslat, W.; Imtara, H.; Kmail, A.; Kadan, S.; Zaid, H.; ElArabi, I.; Badiaa, L.; Saad, B. In vitro evaluation of the potential use of propolis as a multitarget therapeutic product: Physicochemical properties, chemical composition, and immunomodulatory, antibacterial, and anticancer properties. *BioMed Res. Int.* **2019**, *2019*, 4836378. [[CrossRef](#)]
- Sokeng, S.D.; Talla, E.; Sakava, P.; Fokam Tagne, M.A.; Henoumont, C.; Sophie, L.; Mbafor, J.T.; Tchuenguem Fohouo, F.-N. Anti-inflammatory and analgesic effect of arachic acid ethyl ester isolated from propolis. *BioMed Res. Int.* **2020**, *2020*, 8797284. [[CrossRef](#)]
- Sepúlveda, C.; Núñez, O.; Torres, A.; Guzmán, L.; Wehinger, S. Antitumor activity of propolis: Recent advances in cellular perspectives, animal models and possible applications. *Food Rev. Int.* **2020**, *36*, 429–455. [[CrossRef](#)]
- Utispan, K.; Chitkul, B.; Koontongkaew, S. Cytotoxic Activity of Propolis Extracts from the Stingless Bee *Trigona Sirindhornae* Against Primary and Metastatic Head and Neck Cancer Cell Lines. *Asian Pac. J. Cancer Prev.* **2017**, *18*, 1051–1055. [[PubMed](#)]
- Masek, A.; Chrzescijanska, E.; Latos-Brozio, M.; Zaborski, M. Characteristics of juglone (5-hydroxy-1,4-naphthoquinone) using voltammetry and spectrophotometric methods. *Food Chem.* **2019**, *301*, 125279. [[CrossRef](#)]
- Touzani, S.; Imtara, H.; Katekhaye, S.; Mechchate, H.; Ouassou, H.; Alqahtani, A.S.; Noman, O.M.; Nasr, F.A.; Fearnley, H.; Fearnley, J.; et al. Determination of phenolic compounds in various propolis samples collected from an African and an Asian region and their impact on antioxidant and antibacterial activities. *Molecules* **2021**, *26*, 4589. [[CrossRef](#)]
- Okur, İ.; Baltacıoğlu, C.; Ağçam, E.; Baltacıoğlu, H.; Alpas, H. Evaluation of the effect of different extraction techniques on sour cherry pomace phenolic content and antioxidant activity and determination of phenolic compounds by FTIR and HPLC. *Waste Biomass Valorization* **2019**, *10*, 3545–3555. [[CrossRef](#)]
- Tagkouli, D.; Tsiaka, T.; Kritsi, E.; Soković, M.; Sinanoglou, V.J.; Lantzouraki, D.Z.; Zoumpoulakis, P. Towards the optimization of microwave-assisted extraction and the assessment of chemical profile, antioxidant and antimicrobial activity of wine lees extracts. *Molecules* **2022**, *27*, 2189. [[CrossRef](#)] [[PubMed](#)]
- Bastola, K.P.; Guragain, Y.N.; Bhadriraju, V.; Vadlani, P.V. Evaluation of standards and interfering compounds in the determination of phenolics by Folin-Ciocalteu assay method for effective bioprocessing of biomass. *Am. J. Analyt. Chem.* **2017**, *8*, 416–431. [[CrossRef](#)]
- Schofield, P.; Mbugua, D.M.; Pell, A.N. Analysis of condensed tannins: A review. *Anim. Feed. Sci. Technol.* **2001**, *91*, 21–40. [[CrossRef](#)]
- Kupina, S.; Fields, C.; Roman, M.C.; Brunelle, S.L. Determination of total phenolic content using the Folin-C assay: Single-laboratory validation, first action 2017.13. *J. AOAC Int.* **2018**, *101*, 1466–1472. [[CrossRef](#)]
- Amamra, S.; Cartea, M.E.; Belhaddad, O.E.; Soengas, P.; Baghiani, A.; Kaabi, I.; Arrar, L. Determination of total phenolics contents, antioxidant capacity of *Thymus vulgaris* extracts using electrochemical and spectrophotometric methods. *Int. J. Electrochem. Sci.* **2018**, *13*, 7882–7893. [[CrossRef](#)]
- Jara-Palacios, M.J.; Escudero-Gilete, M.L.; Hernández-Hierro, J.M.; Heredia, F.J.; Hernanz, D. Cyclic voltammetry to evaluate the antioxidant potential in winemaking byproducts. *Talanta* **2017**, *165*, 211–215. [[CrossRef](#)]
- Pisoschi, A.; Cimpeanu, C.; Predoi, G. Electrochemical methods for total antioxidant capacity and its main contributors determination: A review. *Open Chem.* **2015**, *13*, 824–856. [[CrossRef](#)]
- Hoyos-Arbeláez, J.; Vázquez, M.; Contreras-Calderón, J. Electrochemical methods as a tool for determining the antioxidant capacity of food and beverages: A review. *Food Chem.* **2017**, *221*, 1371–1381. [[CrossRef](#)]
- Masek, A.; Chrzescijanska, E.; Kosmalska, A.; Zaborski, M. Characteristics of compounds in hops using cyclic voltammetry. UV-VIS. FTIR and GC-MS analysis. *Food Chem.* **2014**, *156*, 353–361. [[CrossRef](#)]
- Wang, Z.; Tang, C.; Dai, F.; Xiao, G.; Luo, G. HPLC determination of phenolic compounds in different solvent extracts of mulberry leaves and antioxidant capacity of extracts. *Int. J. Food Prop.* **2021**, *24*, 544–552. [[CrossRef](#)]
- Peng, Y.; Zhang, Y.; Ye, J. Determination of phenolic compounds and ascorbic acid in different fractions of tomato by capillary electrophoresis with electrochemical detection. *J. Agric. Food Chem.* **2008**, *56*, 1838–1844. [[CrossRef](#)]
- Al Haddabi, B.; Al Lawati, H.A.; Suliman, F.O. A comprehensive evaluation of three microfluidic chemiluminescence methods for the determination of the total phenolic contents in fruit juices. *Food Chem.* **2017**, *214*, 670–677. [[CrossRef](#)]
- Faccin, H.; Loose, R.F.; Viana, C.; Lameira, O.A.; de Carvalho, L.M. Determination of phenolic compounds in extracts of Amazonian medicinal plants by liquid chromatography-electrospray tandem mass spectrometry. *Anal. Methods* **2017**, *9*, 1141–1151. [[CrossRef](#)]
- López-Fernández, O.; Domínguez, R.; Pateiro, M.; Muneke, P.E.; Rocchetti, G.; Lorenzo, J.M. Determination of polyphenols using liquid chromatography–tandem mass spectrometry technique (LC–MS/MS): A review. *Antioxidants* **2020**, *9*, 479. [[CrossRef](#)]

26. Capriotti, A.L.; Cavaliere, C.; Foglia, P.; Piovesana, S.; Ventura, S. Chromatographic methods coupled to mass spectrometry detection for the determination of phenolic acids in plants and fruits. *J. Liq. Chromatogr.* **2015**, *38*, 353–370. [[CrossRef](#)]
27. Viñas, P.; Campillo, N. Gas Chromatography: Mass Spectrometry Analysis of Polyphenols in Foods. *Polyphen. Plants* **2019**, *2019*, 285–316.
28. Andrade, J.K.S.; Denadai, M.; de Oliveira, C.S.; Nunes, M.L.; Narain, N. Evaluation of bioactive compounds potential and antioxidant activity of brown, green and red propolis from Brazilian northeast region. *Food Res. Int.* **2017**, *101*, 129–138. [[CrossRef](#)] [[PubMed](#)]
29. Kumazawa, S.; Ahn, M.R.; Fujimoto, T.; Kato, M. Radical-scavenging activity and phenolic constituents of propolis from different regions of Argentina. *Nat. Prod. Res.* **2010**, *24*, 804–812. [[CrossRef](#)] [[PubMed](#)]
30. Huang, S.; Zhang, C.-P.; Wang, K.; Li, G.Q.; Hu, F.-L. Recent advances in the chemical composition of propolis. *Molecules* **2014**, *19*, 19610–19632. [[CrossRef](#)]
31. Paula, V.B.; Estevinho, L.M.; Dias, L.G. Quantification of three phenolic classes and total phenolic content of propolis extracts using a single UV-vis spectrum. *J. Apic. Res.* **2017**, *56*, 569–580. [[CrossRef](#)]
32. Cuyckens, F.; Claeys, M. Mass spectrometry in the structural analysis of flavonoids. *J. Mass. Spectrom.* **2004**, *39*, 1–15. [[CrossRef](#)]
33. Avula, B.; Sagi, S.; Masoodi, M.H.; Bae, J.Y.; Wali, A.F.; Khan, I.A. Quantification and characterization of phenolic compounds from Northern Indian propolis extracts and dietary supplements. *J. AOAC Int.* **2020**, *103*, 1378–1393. [[CrossRef](#)]
34. Vieira de Moraes, D.; Rosalen, P.L.; Ikegaki, M.; de Souza Silva, A.P.; Massarioli, A.P.; de Alencar, S.M. Active antioxidant phenolics from Brazilian red propolis: An optimization study for their recovery and identification by LC-ESI-QTOF-MS/MS. *Antioxidants* **2021**, *10*, 297. [[CrossRef](#)]
35. Falcão, S.I.; Vale, N.; Gomes, P.; Domingues, M.R.; Freire, C.; Cardoso, S.M.; Vilas-Boas, M. Phenolic profiling of Portuguese propolis by LC-MS spectrometry: Uncommon propolis rich in flavonoid glycosides. *Phytochem. Anal.* **2013**, *24*, 309–318. [[CrossRef](#)]
36. Gardana, C.; Scaglianti, M.; Pietta, P.; Simonetti, P. Analysis of the polyphenolic fraction of propolis from different sources by liquid chromatography tandem mass spectrometry. *J. Pharm. Biomed. Anal.* **2007**, *45*, 390–399. [[CrossRef](#)] [[PubMed](#)]
37. Pellati, F.; Orlandini, G.; Pinetti, D.; Benvenuti, S. HPLC-DAD and HPLC-ESI-MS/MS methods for metabolite profiling of propolis extracts. *J. Pharm. Biomed. Anal.* **2011**, *55*, 934–948. [[CrossRef](#)]
38. Righi, A.A.; Negri, G.; Salatino, A. Comparative Chemistry of Propolis from Eight Brazilian Localities. *Evid. Based Complement. Altern. Med.* **2013**, *2013*, 1–14. [[CrossRef](#)] [[PubMed](#)]
39. Popova, M.P.; Bankova, V.S.; Bogdanov, S.; Tsvetkova, I.; Naydenski, C.; Marcazzan, G.L.; Sabatini, A.-G. Chemical Characteristics of Poplar Type Propolis of Different Geographic Origin. *Apidologie* **2007**, *38*, 306. [[CrossRef](#)]
40. Dias, L.G.; Pereira, A.P.; Estevinho, L.M. Comparative study of different Portuguese samples of propolis: Pollinic, sensorial, physicochemical, microbiological characterization and antibacterial activity. *Food Chem. Toxicol.* **2012**, *50*, 4246–4253. [[CrossRef](#)] [[PubMed](#)]
41. Falcão, S.I.; Tomás, A.; Vale, N.; Gomes, P.; Freire, C.; Vilas-Boas, M. Phenolic quantification and botanical origin of Portuguese propolis. *Ind. Crops Prod.* **2013**, *49*, 805–812. [[CrossRef](#)]
42. Ristivojević, P.; Dimkić, I.; Guzelmeric, E.; Trifković, J.; Knežević, M.; Berić, T.; Yesilada, E.; Milojković-Opsenica, D.; Stanković, S. Profiling of Turkish propolis subtypes: Comparative evaluation of their phytochemical compositions, antioxidant and antimicrobial activities. *LWT* **2018**, *95*, 367–379. [[CrossRef](#)]
43. Guzelmeric, E.; Ristivojević, P.; Trifković, J.; Dastan, T.; Yilmaz, O.; Cengiz, O.; Yesilada, E. Authentication of Turkish propolis through HPTLC fingerprints combined with multivariate analysis and palynological data and their comparative antioxidant activity. *LWT* **2018**, *87*, 23–32. [[CrossRef](#)]
44. Salatino, A.; Teixeira, É.W.; Negri, G. Origin and chemical variation of Brazilian propolis. *Evid. Based Complement. Altern. Med.* **2005**, *2*, 33–38. [[CrossRef](#)] [[PubMed](#)]
45. Aleixandre-Tudo, J.L.; Du Toit, W. The Role of UV-Visible Spectroscopy for Phenolic Compounds Quantification in Winemaking. In *Frontiers and New Trends in the Science of Fermented Food and Beverages*; IntechOpen: London, UK, 2018.
46. Magalhaes, L.M.; Segundo, M.A.; Reis, S.; Lima, J.L. Methodological aspects about in vitro evaluation of antioxidant properties. *Anal. Chim. Acta* **2008**, *613*, 1–19. [[CrossRef](#)]
47. Munteanu, I.G.; Apetrei, C. Analytical methods used in determining antioxidant activity: A review. *Int. J. Mol. Sci.* **2021**, *22*, 3380. [[CrossRef](#)]
48. Blasco, A.J.; Rogerio, M.C.; Gonzalez, M.C.; Escarpa, A. Electrochemical index as a screening method to determine total polyphenolics in foods: A proposal. *Anal. Chim. Acta* **2005**, *539*, 237–244. [[CrossRef](#)]
49. Lawag, I.L.; Nolden, E.S.; Schaper, A.A.; Lim, L.Y.; Locher, C. A Modified Folin-Ciocalteu Assay for the Determination of Total Phenolics Content in Honey. *Appl. Sci.* **2023**, *13*, 2135. [[CrossRef](#)]
50. Bener, M.; Ozyürek, M.; Güçlü, K.; Apak, R. Novel optical fiber reflectometric CUPRAC sensor for total antioxidant capacity measurement of food extracts and biological samples. *J. Agric. Food Chem.* **2013**, *61*, 8381–8388. [[CrossRef](#)]
51. Way, M.L.; Jones, J.E.; Nichols, D.S.; Dambergs, R.G.; Swarts, N.D. A comparison of laboratory analysis methods for total phenolic content of cider. *Beverages* **2020**, *6*, 55. [[CrossRef](#)]



52. Yola, M.L.; Atar, N.; Üstündağ, Z.; Solak, A.O. A novel voltammetric sensor based on p-aminothiophenol functionalized graphene oxide/gold nanoparticles for determining quercetin in the presence of ascorbic acid. *J. Electroanal. Chem.* **2013**, *698*, 9–16. [CrossRef]
53. Bounegru, A.V.; Apetrei, C. Laccase and Tyrosinase Biosensors Used in the Determination of Hydroxycinnamic Acids. *Int. J. Mol. Sci.* **2021**, *22*, 4811. [CrossRef] [PubMed]
54. Bojko, L.; de Jonge, G.; Lima, D.; Lopes, L.C.; Viana, A.G.; Garcia, J.R.; Pessôa, C.A.; Wohnrath, K.; Inaba, J. Porphyrin-capped silver nanoparticles as a promising antibacterial agent and electrode modifier for 5-fluorouracil electroanalysis. *Carbohydr. Res.* **2020**, *498*, 108193. [CrossRef]
55. Newair, E.F.; Kilmartin, P.A.; Garcia, F. Square wave voltammetric analysis of polyphenol content and antioxidant capacity of red wines using glassy carbon and disposable carbon nanotubes modified screen-printed electrodes. *Eur. Food Res. Technol.* **2018**, *244*, 1225–1237. [CrossRef]
56. Ibarra-Escutia, P.; Gómez, J.J.; Calas-Blanchard, C.; Marty, J.L.; Ramírez-Silva, M.T. Amperometric biosensor based on a high resolution photopolymer deposited onto a screen-printed electrode for phenolic compounds monitoring in tea infusions. *Talanta* **2010**, *81*, 1636–1642. [CrossRef] [PubMed]
57. Montereali, M.R.; Della Seta, L.; Vastarella, W.; Pilloton, R. A disposable Laccase–Tyrosinase based biosensor for amperometric detection of phenolic compounds in must and wine. *J. Mol. Catal. B Enzym.* **2010**, *64*, 189–194. [CrossRef]
58. Adam, M.S.S.; Newair, E.F. Square-Wave and Cyclic Voltammetry of Native Proanthocyanidins Extracted from Grapevine (*Vitis vinifera*) on the Glassy Carbon Electrode. *Chemosensors* **2022**, *10*, 429. [CrossRef]
59. Abdel-Hamid, R.; Newair, E.F. Electrochemical behavior of antioxidants: I. Mechanistic study on electrochemical oxidation of gallic acid in aqueous solutions at glassy-carbon electrode. *J. Electroanal. Chem.* **2011**, *657*, 107–112. [CrossRef]
60. Asem, N.; Abdul Gapar, N.A.; Abd Hapit, N.H.; Omar, E.A. Correlation between total phenolic and flavonoid contents with antioxidant activity of Malaysian stingless bee propolis extract. *J. Apic. Res.* **2020**, *59*, 437–442. [CrossRef]
61. Adli, M.A.; Zohdi, R.M.; Othman, N.A.; Amin, N.S.M.; Mukhtar, S.M.; Eshak, Z.; Hazmi, I.R.; Jahrudin, D.H.J. Determination of Antioxidant Activity, Total Phenolic and Flavonoid Contents of Malaysian Stingless Bee Propolis Extracts. *J. Sustain. Sci. Manag.* **2022**, *17*, 132–143. [CrossRef]
62. Moniruzzaman, M.; Khalil, M.I.; Sulaiman, S.A.; Gan, S.H. Advances in the analytical methods for determining the antioxidant properties of honey: A review. *Afr. J. Tradit. Complement. Altern. Med.* **2012**, *9*, 36–42. [CrossRef]
63. Baliyan, S.; Mukherjee, R.; Priyadarshini, A.; Vibhuti, A.; Gupta, A.; Pandey, R.P.; Chang, C.M. Determination of antioxidants by DPPH radical scavenging activity and quantitative phytochemical analysis of *Ficus religiosa*. *Molecules* **2022**, *27*, 1326. [CrossRef] [PubMed]
64. Berker, K.I.; Güçlü, K.; Tor, I.; Apak, R. Comparative evaluation of Fe (III) reducing power-based antioxidant capacity assays in the presence of phenanthroline, batho-phenanthroline, tripyridyltriazine (FRAP), and ferricyanide reagents. *Talanta* **2007**, *72*, 1157–1165. [CrossRef] [PubMed]
65. Benzie, I.F.; Strain, J.J. Ferric reducing/antioxidant power assay: Direct measure of total antioxidant activity of biological fluids and modified version for simultaneous measurement of total antioxidant power and ascorbic acid concentration. In *Methods in Enzymology*; Academic Press: Cambridge, MA, USA, 1999; Volume 299, pp. 15–27.
66. Gulcin, I. Antioxidants and antioxidant methods: An updated overview. *Arch. Toxicol.* **2020**, *94*, 651–715. [CrossRef]
67. Wojtnik-Kulesza, K.A. Approach to Optimization of FRAP Methodology for Studies Based on Selected Monoterpenes. *Molecules* **2020**, *25*, 5267. [CrossRef] [PubMed]
68. Benzie, I.F.; Devaki, M. The ferric reducing/antioxidant power (FRAP) assay for non-enzymatic antioxidant capacity: Concepts, procedures, limitations and applications. In *Measurement of Antioxidant Activity & Capacity: Recent Trends and Applications*; Wiley: Hoboken, NJ, USA, 2018; pp. 77–106.
69. Natella, F.; Nardini, M.; Di Felice, M.; Scaccini, C. Benzoic and cinnamic acid derivatives as antioxidants: Structure–activity relation. *J. Agric. Food Chem.* **1999**, *47*, 1453–1459. [CrossRef]
70. Wang, J.; Jiang, Z. Synthesis, characterisation, antioxidant and antibacterial properties of p-hydroxybenzoic acid-grafted chitosan conjugates. *Int. J. Food Sci. Technol.* **2022**, *57*, 1283–1290. [CrossRef]
71. Teixeira, J.; Gaspar, A.; Garrido, E.M.; Garrido, J.; Borges, F. Hydroxycinnamic acid antioxidants: An electrochemical overview. *BioMed Res. Int.* **2013**, *2013*, 251754. [CrossRef]
72. Razzaghi-Asl, N.; Garrido, J.; Khazraei, H.; Borges, F.; Firuzi, O. Antioxidant properties of hydroxycinnamic acids: A review of structure-activity relationships. *Curr. Med. Chem.* **2013**, *20*, 4436–4450. [CrossRef]
73. Velika, B.; Kron, I. Antioxidant properties of benzoic acid derivatives against superoxide radical. *Free Radic. Antioxid.* **2012**, *2*, 62–67. [CrossRef]
74. Mazzone, G.; Russo, N.; Toscano, M. Antioxidant properties comparative study of natural hydroxycinnamic acids and structurally modified derivatives: Computational insights. *Comput. Theor. Chem.* **2016**, *1077*, 39–47. [CrossRef]
75. Rodriguez-Bonilla, P.; Gandia-Herrero, F.; Matencio, A.; Garcia-Carmona, F.; Lopez-Nicolas, J.M. Comparative study of the antioxidant capacity of four stilbenes using ORAC, ABTS+, and FRAP techniques. *Food Anal. Method.* **2017**, *10*, 2994–3000. [CrossRef]
76. Al-Mamary, M.A.; Moussa, Z. Antioxidant activity: The presence and impact of hydroxyl groups in small molecules of natural and synthetic origin. In *Antioxidants—Benefits, Sources, Mechanisms of Action*; InTech Open: London, UK, 2021; pp. 318–377.

77. Farhoosh, R.; Johnny, S.; Asnaashari, M.; Molaahmadibahraseman, N.; Sharif, A. Structure–AA relationships of o-hydroxyl, o-methoxy, and alkyl ester derivatives of p-hydroxybenzoic acid. *Food Chem.* **2016**, *194*, 128–134. [[CrossRef](#)]
78. Glevitzky, I.; Dumitrele, G.A.; Glevitzky, M.; Pasca, B.; Otrisal, P.; Bungau, S.; Cioca, G.; Pantis, C.; Popa, M.J.R.C. Statistical analysis of the relationship between antioxidant activity and the structure of flavonoid compounds. *Rev. Chim.* **2019**, *70*, 3103–3107. [[CrossRef](#)]
79. Yu, M.; Gouvinhas, I.; Rocha, J.; Barros, A.I. Phytochemical and antioxidant analysis of medicinal and food plants towards bioactive food and pharmaceutical resources. *Sci. Rep.* **2021**, *11*, 10041. [[CrossRef](#)]
80. Khiya, Z.; Oualcadi, Y.; Gamar, A.; Berrekhis, F.; Zair, T.; Hilali, F.E. Correlation of total polyphenolic content with antioxidant activity of hydromethanolic extract and their fractions of the *Salvia officinalis* leaves from different regions of Morocco. *J. Chem.* **2021**, *2021*, 8585313. [[CrossRef](#)]
81. Kiokias, S.; Proestos, C.; Oreopoulou, V. Phenolic acids of plant origin—A review on their antioxidant activity in vitro (o/w emulsion systems) along with their in vivo health biochemical properties. *Foods* **2020**, *9*, 534. [[CrossRef](#)]
82. Socha, R.; Galkowska, D.; Bugaj, M.; Juszcak, L. Phenolic composition and antioxidant activity of propolis from various regions of Poland. *Nat. Prod. Res.* **2015**, *29*, 416–422. [[CrossRef](#)] [[PubMed](#)]
83. Narimane, S.; Demircan, E.; Salah, A.; Salah, R. Correlation between antioxidant activity and phenolic acids profile and content of Algerian propolis: Influence of solvent. *Pak. J. Pharm. Sci.* **2017**, *30*, 1417–1423. [[PubMed](#)]
84. Yuan, Y.; Zheng, S.; Zeng, L.; Deng, Z.; Zhang, B.; Li, H. The phenolic compounds, metabolites, and antioxidant activity of propolis extracted by ultrasound-assisted method. *J. Food Sci.* **2019**, *84*, 3850–3865. [[CrossRef](#)] [[PubMed](#)]
85. Bhuyan, D.J.; Alsherbiny, M.A.; Low, M.N.; Zhou, X.; Kaur, K.; Li, G.; Li, C.G. Broad-spectrum pharmacological activity of Australian propolis and metabolomic-driven identification of marker metabolites of propolis samples from three continents. *Food Funct.* **2021**, *12*, 2498–2519. [[CrossRef](#)]
86. Ristivojević, P.; Andrić, F.L.; Trifković, J.Đ.; Vovk, I.; Stanisavljević, L.Ž.; Tešić, Ž.L.; Milojković-Opsenica, D.M. Pattern recognition methods and multivariate image analysis in HPTLC fingerprinting of propolis extracts. *J. Chromatogr. B* **2014**, *28*, 301–310. [[CrossRef](#)]
87. Alvear, M.; Santos, E.; Cabezas, F.; Pérez-SanMartín, A.; Lespinasse, M.; Veloz, J. Geographic Area of Collection Determines the Chemical Composition and Antimicrobial Potential of Three Extracts of Chilean Propolis. *Plants* **2021**, *10*, 1543. [[CrossRef](#)]
88. Barth, O.M.; Dutra, V.M.L.; Justo, R.L. Análise polínica de algumas amostras de própolis do Brasil Meridional. *Ciência Rural St. Maria* **1999**, *29*, 663–667. [[CrossRef](#)]
89. Moreira, L.; Dias, L.G.; Pereira, J.A.; Estevinho, L. Antioxidant properties, total phenols and pollen analysis of propolis samples from Portugal. *Food Chem. Toxicol.* **2008**, *46*, 3482–3485. [[CrossRef](#)] [[PubMed](#)]
90. Obied, H.K.; Allen, M.S.; Bedgood, D.R.; Prenzler, P.D.; Robards, K. Investigation of Australian olive mill waste for recovery of biophenols. *J. Agric. Food Chem.* **2005**, *53*, 9911–9920. [[CrossRef](#)]
91. Shaghghi, M.; Manzoori, J.L.; Jouyban, A. Determination of total phenols in tea infusions, tomato and apple juice by terbium sensitized fluorescence method as an alternative approach to the Folin–Ciocalteu spectrophotometric method. *Food Chem.* **2008**, *108*, 695–701. [[CrossRef](#)]
92. Metrouh-Amir, H.; Duarte, C.M.; Maiza, F. Solvent effect on total phenolic contents, antioxidant, and antibacterial activities of *Matricaria pubescens*. *Ind. Crops Prod.* **2015**, *67*, 249–256. [[CrossRef](#)]
93. Meirinho, S.G.; Dias, L.G.; Peres, A.M.; Rodrigues, L.R. Development of an electrochemical aptasensor for the detection of human osteopontin. *Procedia Eng.* **2014**, *87*, 316–319. [[CrossRef](#)]
94. Hatano, T.; Kagawa, H.; Yasuhara, T.; Okuda, T. Two new flavonoids and other constituents in licorice root: Their relative astringency and radical scavenging effects. *Chem. Pharm. Bull.* **1988**, *36*, 2090–2097. [[CrossRef](#)]
95. Roig, B.; Thomas, O. Rapid estimation of global sugars by UV photodegradation and UV spectrophotometry. *Anal. Chim. Acta* **2003**, *477*, 325–329. [[CrossRef](#)]
96. Costa Arca, V.; Peres, A.M.; Machado, A.A.S.C.; Bona, E.; Dias, L.G. Sugars’ Quantifications Using a Potentiometric Electronic Tongue with Cross-Selective Sensors: Influence of an Ionic Background. *Chemosensors* **2019**, *7*, 43. [[CrossRef](#)]

**Disclaimer/Publisher’s Note:** The statements, opinions and data contained in all publications are solely those of the individual author(s) and contributor(s) and not of MDPI and/or the editor(s). MDPI and/or the editor(s) disclaim responsibility for any injury to people or property resulting from any ideas, methods, instructions or products referred to in the content.



MDPI  
St. Alban-Anlage 66  
4052 Basel  
Switzerland  
[www.mdpi.com](http://www.mdpi.com)

*Molecules* Editorial Office  
E-mail: [molecules@mdpi.com](mailto:molecules@mdpi.com)  
[www.mdpi.com/journal/molecules](http://www.mdpi.com/journal/molecules)



Disclaimer/Publisher's Note: The statements, opinions and data contained in all publications are solely those of the individual author(s) and contributor(s) and not of MDPI and/or the editor(s). MDPI and/or the editor(s) disclaim responsibility for any injury to people or property resulting from any ideas, methods, instructions or products referred to in the content.





Academic Open  
Access Publishing

[mdpi.com](https://www.mdpi.com)

ISBN 978-3-0365-9077-6